James Weifu Lee *Editor*

Advanced Biofuels and Bioproducts

Volume 1

Springer

Advanced Biofuels and Bioproducts

James Weifu Lee
Editor

Advanced Biofuels and Bioproducts

Springer

Editor
James Weifu Lee
Department of Chemistry and Biochemistry
Old Dominion University
Norfolk, VA, USA

ISBN 978-1-4614-3347-7 ISBN 978-1-4614-3348-4 (eBook)
DOI 10.1007/978-1-4614-3348-4
Springer New York Heidelberg Dordrecht London

Library of Congress Control Number: 2012939845

Printed on acid-free paper

Springer is part of Springer Science+Business Media (www.springer.com)

Preface

The aim of this book is to provide the current status and development in the biomass energy research field and report new and highly innovative technology concepts to provide green/clean energy and control climate change. It will point out the potential benefits of these new technology concepts and the technical challenges that we need to overcome to achieve the mission. This book could be helpful to a wide audience including not only energy and environmental scientists and engineers but also industry and academia, teachers and students, and the general public including the policy makers across the world. The book will address a variety of topics and technology concepts ranging from the latest development in smokeless biomass pyrolysis, Fischer–Tropsch hydrocarbons synthesis for biomass-derived syngas to liquid transportation fuels, catalytic and selective pyrolysis of biomass for production of fuels such as biodiesels and special chemicals such as levoglucosan and phenolic compounds, biomass hydrothermal processing, biomethane and naturally occurring hydrocarbon gas hydrates, to "cellulosic biofuels," "electrofuels," and photobiological production of advanced biofuels (e.g., hydrogen, lipids/biodiesel, ethanol, butanol, and/or related higher alcohols) directly from water and carbon dioxide. Advanced bioproducts such as biochar that could bring significant benefits in helping control climate change and sustainable economic development will also be covered. Each chapter typically will describe a specific technology including its fundamental concept, potential benefits, current status, and technical challenges. Therefore, this BioEnergy sciences book will enable readers to quickly understand the up-to-date technical opportunities/challenges so that the readers may also be able to somehow contribute to this mission, since currently energy and environment (climate change) are such huge and urgent issues to human civilization on Earth. Together, we can help overcome the challenges and build a sustainable future with clean renewable energy of tomorrow.

Norfolk, VA, USA — James Weifu Lee

Acknowledgments

The editor, James Weifu Lee, would like to thank all of the nearly 100 authors and a number of peer reviewers across the world for their wonderful contributions in support of this book project. The editing work of this book series was accomplished using significant amounts of the editor's spare time including his family time. Therefore, the editor also wishes to thank his family for their understanding and wonderful support.

Contents

Part VIII Electrofuels

Part I
Introduction and Brazil's Biofuel Success

Chapter 1
Introduction: An Overview of Advanced Biofuels and Bioproducts

James Weifu Lee

Abstract The field of advanced biofuels and bioproducts may play an increasingly significant role in providing renewable energy and ensuring environmental health for a sustainable future of human civilization on Earth. This chapter as an introduction for the book provides a quick overview of advanced biofuels and bioproducts by highlighting the new developments and opportunities in the bioenergy research & development (R&D) arena in relation to the global energy and environmental challenges. The topics include: (1) Brazil's sugarcane ethanol as an early and still encouraging example of biofuels at a nationally significant scale, (2) smokeless biomass pyrolysis for advanced biofuels production and global biochar carbon sequestration, (3) cellulosic biofuels, (4) synthetic biology for photobiological production of biofuels from carbon dioxide and water, (5) lipid-based biodiesels, (6) life-cycle energy and environmental impact analysis, (7) high-value bioproducts and biomethane, and (8) electrofuels.

1 The Energy and Environment Challenges and Opportunities

The world currently faces a systematic energy and environmental problem of increased CO_2 emissions, decreased soil-carbon content, and global-climate change. To solve the massive global energy and environmental sustainability problem, it likely requires a comprehensive portfolio of R&D efforts with multiple energy technologies.

J.W. Lee (✉)
Department of Chemistry & Biochemistry, Old Dominion University,
Physical Sciences Building, Room 3100B, 4402 Elkhorn Avenue, Norfolk, VA 23529, USA

Johns Hopkins University, Whiting School of Engineering,
118 Latrobe Hall, Baltimore, MD 21218, USA
e-mail: jwlee@odu.edu; JLee349@JHU.edu

J.W. Lee (ed.), *Advanced Biofuels and Bioproducts*, DOI 10.1007/978-1-4614-3348-4_1,

The field of advanced biofuels and bioproducts, such as photosynthetic biomass energy, may represent one of the major R&D areas that have the potential to provide renewable clean energy, in additions to the other renewable energy technologies, including nuclear energy, geothermal, wind, solar, and hydropower. Photosynthesis captures more CO_2 from the atmosphere than any other processes on Earth capture. Each year, land-based green plants capture about 440 gigatons (Gt) CO_2 (equivalent to 120 GtC y^{-1}) from the atmosphere into biomass [1]. That is, about one-seventh of all the CO_2 in the atmosphere (820 GtC) is fixed by photosynthesis (gross primary production) every year. Theoretically, if there is a technology that could translate as small as 7.5% of the annual terrestrial gross photosynthetic products (120 GtC y^{-1}) to a usable biofuel to substitute fossil fuels that would be sufficient to eliminate the entire amount (nearly 9 GtC y^{-1}) of CO_2 emitted into the atmosphere annually from the use of fossil fuels. The success of Brazil's sugarcane ethanol reported in Chap. 2 has demonstrated that with the advancement of science and technology and coupled with proper policy support, it is possible for the field of advanced biofuels and bioproducts to make a significant contribution to enrich the energy market at a national and/or possibly global scale. Presently, ethanol from sugarcane replaces approximately 50% of the gasoline that would be used in Brazil if such an option did not exist. Therefore, Brazil's sugarcane–ethanol success may be regarded as an early but still encouraging example of biofuels at least at a national scale. However, understandably, Brazil's sugarcane–ethanol technology per se may or may not be applicable to the other parts of the world such as the United States because of the differences in climates, crop ecosystems, and various other factors. Development and deployment of other innovative biofuels technologies are essential to achieve the mission of renewable energy production. The following highlights some of the bioenergy R&D areas that may be of special significance.

2 Smokeless Biomass Pyrolysis for Advanced Biofuels Production and Global Biochar Carbon Sequestration

Biomass utilization through smokeless (emission-free, clean, and efficient) pyrolysis is a potentially significant approach for biofuels production and biochar carbon sequestration at gigatons of carbon (GtC) scales. One of the key ideas here is to use a biomass-pyrolysis process to produce certain biofuels and more importantly to "lock" some of the unstable biomass carbon such as dead leaves, waste woods, cornstovers, and rice straws into a stable form of carbon—biochar, which could be used as a soil amendment to improve soil fertility and at the same time, to serve as a carbon sequestration agent, since biochar can be stable in soil for thousands of years and can help retain nutrients in soil to reduce the runoff of fertilizers from agriculture lands that would otherwise pollute the rivers and water bodies. This "carbon negative" approach, which was co-initiated by Danny Day of Eprida Inc. and James Weifu Lee (the Editor) through their joint 2002 U.S. provisional patent application followed by a PCT application [2, 3], is now receiving

increased attention worldwide [4, 5], especially since certain related studies have also indicated the possibility of using biochar as a soil amendment for carbon sequestration [6–9].

Chapter 3 provides an overview of this smokeless biomass-pyrolysis approach for producing biofuels and biochar as a possible arsenal to control climate change. For the immediate future, application of this biochar producing biomass-pyrolysis approach to turn waste biomass into valuable products could likely provide the best economic and environmental benefits. Globally, each year, there are about 6.6 Gt dry matter of biomass (3.3 GtC) such as crop stovers that are appropriated but not used. Development and deployment of the smokeless biomass pyrolysis technology could turn this type of waste biomass into valuable biochar and biofuel products. Even if assuming that only half amount of this waste biomass is utilized by this approach, it would produce 0.825 GtC y^{-1} of biochar and large amounts of biofuel (with a heating value equivalent to that of 3,250 million barrels of crude oil). By storing 0.825 GtC y^{-1} of biochar (equivalent to 3 Gt of CO_2 per year) into soil and/or underground reservoirs alone, it could offset the world's 8.67 GtC y^{-1} of fossil fuel CO_2 emissions by 9.5%, which is still very significant. So far, there are no other technologies that could have such a big (GtC) capacity in effectively capturing and sequestering CO_2 from the atmosphere. Therefore, this is a unique "carbon-negative" bioenergy technology system approach, which in the perspective of carbon management is likely going to be more effective (and better) than the nuclear energy option, since the nuclear-power energy system is merely a carbon-neutral energy technology that could not capture CO_2 from the atmosphere. This is true also in comparing the "carbon-negative" smokeless biomass-pyrolysis approach with any other carbon-neutral energy technologies, including solar photovoltaic electricity, geothermal, wind, and hydropower, and all carbon-neutral biofuel technologies such as cellulosic biofuels, photobiological biofuels from carbon dioxide and water, lipid-based biodiesels, and electrofuels, which are also covered in this book. Consequently, nuclear energy and any other carbon-neutral energy technologies all cannot reverse the trend of climate change; on the other hand, the smokeless biochar-producing biomass-pyrolysis energy system approach, in principle, could not only reduce but also could possibly reverse the climate change. Therefore, this "carbon-negative" smokeless biomass-pyrolysis approach clearly merits serious research and development worldwide to help provide clean energy and control climate change for a sustainable future of human civilization on Earth [10].

Chapter 4 reports an invention on partial oxygenation of biochar for enhanced cation exchange capacity, which is one of the key properties that enable biochar to help retain soil nutrients to reduce fertilizers runoff from agriculture lands and to keep water environment clean. Chapter 5 describes chemical structural characterization of biochars using advanced solid-state ^{13}C nuclear magnetic resonance spectroscopy, which is scientifically important in understanding the chemistry and application of biochar materials. As reported in Chap. 6, one of the ideas is to use biochar particles incorporated with certain fertilizer species such as ammonium bicarbonate and/or urea, hopefully to make a type of slow-releasing fertilizer.

Use of this type of biochar fertilizer would place the biochar carbon into soil to improve soil fertility and, at the same time, store (sequester) carbon into the soil and subsoil earth layers to achieve carbon sequestration. Chapter 7 discusses selection and use of designer biochars to improve characteristics of Southeastern USA Coastal Plain degraded soils while Chap. 8 describes biochar as a co-product to bioenergy from slow-pyrolysis technology.

There are significant progresses and scientific understanding in the arts of biomass pyrolysis. Chapter 9 reports the arts of catalytic pyrolysis of biomass for the production of both biofuels and biochar while Chap. 10 describes the selective fast pyrolysis of biomass to produce fuels and chemicals. As reported in Chap. 11, it is also possible to produce advanced biofuels and biochar through hydrothermo processing of biomass.

To avoid negative impact on air quality with such a large (GtC)-scale operation required to achieve the envisioned global biochar carbon sequestration, the biomass-pyrolysis process technology must be smokeless (emission-free, clean, and efficient). Therefore, it is essential to fully develop a smokeless biomass-pyrolysis process to achieve the mission. One of the possible productive ways to achieve the smokeless (emission-free, clean, and efficient) feature is by converting the pyrolysis syngas "smoke" into clean energy such as liquid transportation fuel. Currently, there are a number of Fischer–Tropsch processing technologies [11, 12] that could be helpful for conversion of biomass-derived syngas into advanced (drop-in-ready) liquid biofuels, such as biodiesel, to replace petroleum-based transportation fuels. Chapter 12 describes the fundamentals of the biomass-to-liquid fuel process technologies via Fischer–Tropsch and related syntheses. Chapter 13 reports Fischer–Tropsch hydrocarbons synthesis from a simulated biosyngas while Chap. 14 describes Fischer–Tropsch synthesis of liquid fuel with Fe catalyst using CO_2-containing syngas that can be produced from biomass pyrolysis.

3 Cellulosic Biofuels

Chapter 15 reports cellulosic butanol production from agricultural biomass and residues: recent advances in technology while Chap. 16 describes the technology concept of consolidated bioprocessing of lignocellulosic biomass for biofuels production. The research opportunity here is the possibility of converting vast amount of lignocellulosic plant biomass materials such as cornstover, wheat straw, switchgrass, and woody plant materials into usable biofuels such as ethanol and/or butanol. Recently, bisabolane has also been identified as a terpene-based advanced biofuel that may be used as an alternative to D2 diesel [13]. This field of cellulosic biofuels has been active for more than 25 years and it still remains a hot topic because of its significant potential. One of the major challenges is known as the "lignocellulosic recalcitrance" which represents a quite formidable technical barrier to the cost-effective conversion of plant biomass to fermentable sugars. That is, because of the

recalcitrance problem, lignocellulosic biomasses (such as cornstover, switchgrass, and woody plant materials) could not be readily converted to fermentable sugars to make ethanol or butanol without certain pretreatment, which is often associated with high processing cost. Despite more than 25 years of R&D efforts in lignocellulosic biomass pretreatment and fermentative processing, the problem of recalcitrant lignocellulosics still remains as a formidable technical barrier that has not yet been fully eliminated so far. This problem is probably rooted from the long history of natural plant evolution; plant biomass has evolved effective mechanisms for resisting assault on its cell-wall structural sugars from the microbial and animal kingdoms. This property underlies a natural recalcitrance, creating roadblocks to the cost-effective transformation of lignocellulosic biomass to fermentable sugars. Therefore, one of the R&D approaches is to unlock the sugars by re-engineering the cell wall structure through molecular genetics. Chapter 17 describes the synthesis, regulation, and modification of plant cell wall carbohydrates (lignocellulosic biomass) as a resource for biofuels and bioproducts while Chap. 18 reports genetic modifications of plant cell walls to increase biomass and bioethanol production. Other approaches include but are not limited to developing more effective pretreatment, enzymes, and microorganisms that could help convert the biomass materials into biofuels. Chapter 19 reviews the structural features of cellulose and cellulose degrading enzymes and describes the technology concept of designer enzymes/cellulosomes for cellulose-based biofuels production.

4 Synthetic Biology for Photobiological Production of Biofuels from Carbon Dioxide and Water

This multidisciplinary R&D area involves synthetic biology and genetic transformation of photosynthetic organisms to create designer transgenic organisms that can photobiologically produce biofuels such as hydrogen, lipids/biodiesel, ethanol, butanol, and/or other related higher alcohols (e.g., pentanol and hexanol), or hydrocarbons directly from water and carbon dioxide. Chapter 20 reports inventions on creating designer algae for photobiological production of hydrogen from water. In wild-type algae, there are four physiological problems associated with the proton gradient across the algal thylakoid membrane, which severely limit algal hydrogen production. These technical issues are: (1) accumulation of a proton gradient across the algal thylakoid membrane, (2) competition from carbon dioxide fixation, (3) requirement for bicarbonate binding at photosystem II (PSII) for efficient photosynthetic activity, and (4) competitive drainage of electrons by molecular oxygen. As reported in Chap. 20 one of the key inventions here is the genetic insertion of a proton channel into the algal thylakoid membrane to simultaneously eliminate all of the four transthylakoid proton gradient-associated technical problems for enhanced photoautotrophic hydrogen production.

In addition to the designer proton-channel algae, Chap. 20 describes a further invention on creating designer switchable PSII algae for robust photobiological production of hydrogen from water splitting, which can eliminate all the following three molecular oxygen (O_2)-associated technical problems: (4) competitive drainage of electrons generated from photosynthetic water splitting by molecular oxygen, (5) oxygen sensitivity of algal hydrogenase, and (6) the H_2–O_2 gas separation and safety issue. Use of the two inventions (two US patents): (I) designer proton-channel algae [14] and (II) designer switchable PSII algae [15], may enable efficient and robust photobiological production of hydrogen with an enhanced yield likely more than ten times better than that of the wild-type.

This designer-algae synthetic biology approach can be applied not only for hydrogen production, but also for the production of other advanced biofuels of choice, such as ethanol and/or butanol, depending on specific metabolic pathway designs [16, 17]. Chapter 21 reports inventions on application of synthetic biology for photobiologically production of ethanol directly from carbon dioxide and water while Chap. 22 describes the methods of creating designer transgenic organisms for photobiological production of butanol and/or related higher alcohols from carbon dioxide and water. One of the key ideas here is to genetically introduce a set of specific enzymes to interface with the Calvin-cycle activity so that certain intermediate product such as 3-phosphoglycerate (3-PGA) of the Calvin cycle could be converted immediately to biofuels such as butanol. The net result of the envisioned total process, including photosynthetic water splitting and proton-coupled electron transport for generation of NADPH and ATP that supports the Calvin cycle and the butanol production pathway is the conversion of CO_2 and H_2O to butanol ($CH_3CH_2CH_2CH_2OH$) and O_2 as shown in (1). Therefore, theoretically, this could be a new mechanism to synthesize biofuels (e.g., butanol) directly from CO_2 and H_2O with the following photosynthetic process reaction:

$$4CO_2 + 5H_2O \rightarrow CH_3CH_2CH_2CH_2OH + 6O_2 \quad (1)$$

This photobiological biofuel production process completely eliminates the problem of recalcitrant lignocellulosics by bypassing the bottleneck problem of the biomass technology. Since this approach could theoretically produce biofuels (such as hydrogen, ethanol, butanol, related higher alcohols, and/or hydrocarbons/biodiesel) directly from water and carbon dioxide with high solar-to-biofuel energy efficiency, it may provide the ultimate green/clean renewable energy technology for the world as a long-term goal. According to a recent study [18] for this type of direct photosynthesis-to-biofuel process, the practical maximum solar-to-biofuel energy conversion efficiency could be about 7.2% while the theoretical maximum solar-to-biofuel energy conversion efficiency is calculated to be 12%.

The designer algae approach may also enable the use of seawater and/or groundwater for photobiological production of biofuels without requiring freshwater or agricultural soil, since the biofuel-producing function can be placed through molecular genetics into certain marine algae and/or cyanobacteria that can use seawater and/or

certain groundwater. They may be used also in a sealed photobioreactor that could be operated on a desert for the production of biofuels with highly efficient use of water since there will be little or no water loss by evaporation and/or transpiration that a common crop system would suffer. That is, this designer algae approach could provide a new generation of renewable energy (e.g., butanol) production technology without requiring arable land or freshwater resources, which may be strategically important to many parts of the world for long-term sustainable development. Recently, certain independent studies [19, 20] have also applied synthetic biology in certain model cyanobacteria, such as *Synecoccus elongatus* PCC7942, for photobiological production of isobutanol and 1-butanol.

Furthermore, the designer algae approach may be applied for enhanced photobiological production of other bioproducts, including (but not limited to) lipids, hydrocarbons, intermediate metabolites, and possibly high-value bioproducts such as docosahexaenoic acid (DHA) omega-3 fatty acid, eicosapentaenoic acid (EPA) omega-3 fatty acid, arachidonic acid (ARA) omega-6 fatty acid, chlorophylls, carotenoids, phycocyanins, allophycocyanin, phycoerythrin, and their derivatives/related product species.

5 Lipid-Based Biodiesels

Biodiesel is a mixture of fatty acid alkyl esters obtained typically by transesterification of triglycerides from vegetable oils, algal lipids, or animal fats. Transesterification of the lipid feedstocks is already a quite well-established chemical engineering process with a multiple-step reaction, including three reversible steps in series, where triglycerides are converted to diglycerides, then diglycerides are converted to monoglycerides, and monoglycerides are then converted to esters (biodiesel) and glycerol (by-product). One of the major challenges is to cost-effectively produce large quantities of lipids that can be readily harvested for biodiesel fuel production.

One of the approaches is to produce vegetable oils through Jatropha plantation. Chapter 23 reports the production of biodiesel and nontoxic jatropha seedcake from *Jatropha curcas*. The highest potential in biodiesel production probably resides in algae. The bio-oil (lipids) content for some of the algae can be upto 30–60% of its dry biomass, which energy density is at least as high as coal. Chapter 24 provides a quite comprehensive review of biofuels from microalgae towards meeting the advanced fuel standards. Chapter 25 discusses the bioprocess engineering aspects of biodiesel and bioethanol production from microalgae while Chap. 26 describes the arts of closed photo-bioreactors as tools for biofuel production. Chapter 27 reports extraction of hydrocarbons from *Botryococcus braunii* while Chap. 28 describes valorization of waste oils and animal fats for biodiesel production. Chapter 29 reports a single-step direct thermo-conversion of algal biomass to biodiesel with the formation of an algal char as potential fertilizer.

6 Life-Cycle Energy and Environmental Impact Analysis

To assess a new energy technology before considering its implementation, it is essential to perform a life-cycle analysis on its total energy efficiency and environment impact, including both its potential benefits and risks. A viable energy technology should have a significant net energy gain or a carbon footprint reduction based on its objective life-cycle analysis. Chapter 30 reports the process economics and greenhouse gas audit for microalgal biodiesel production. Chapter 31 discusses the sustainability considerations about microalgae for biodiesel production while Chap. 32 reports a life-cycle assessment for algae-to-energy systems.

7 High Value Bioproducts and Biomethane

Use of biomass technology can produce high-value products also. For example, certain cyanobacteria and green algae have been used as human foods, sources for vitamins, proteins, fine chemicals, and bioactive compounds. Chapter 33 reports fed-batch cultivation of *Spirulina platensis*, which can be used as high-value health nutrient supplement. Chapter 34 discusses the bioprocess development for Chlorophyll extraction from microalgae while Chap. 35 reports the screening methods for bioactive compounds from algae. Fermentation of biomass for methane production represents another important bioresource for biofuel production and waste management. Chapter 36 provides a comprehensive review on algae/biomethane production. Methane hydrates created from biomass at the bottom of the vast oceans and in certain permafrost regions may represent another significant resource that could hopefully be explored for utilization in the future as well. Chapter 37 reports methane hydrates on its current status, resources, technology, and potential.

8 Electrofuels

Electrofuels is a newly created biofuel technology concept that may have significant potential in producing transportation fuel from non-biomass feedstocks such as CO_2, H_2, and/or electricity. One of its key features is the application of certain chemolithoautotrophic organisms with synthetic biology to synthesize biofuel(s), such as butanol through fixation of CO_2 using H_2 and/or electrons as a source of reductant. Potentially, this approach could become quite attractive for biofuels production, since large quantities of inexpensive electricity (thus H_2 from electrolysis of water) and CO_2 feedstock could foreseeably become available in the near future. With advanced photovoltaic cells, the solar-to-electricity energy conversion efficiency can now reach more than 20%. A solar electricity-based electrofuel process with certain chemolithoautotrophic CO_2 fixation pathways [21] could have a combined solar-to-biofuels energy conversion efficiency higher than that of a

photosynthesis-based biofuel technology. Therefore, the electrofuels approach merits serious exploration also. In 2009, the United States Department of Energy (DOE) Advanced Research Projects Agency-Energy (ARPA-E) created the electrofuels program to explore the potential of non-photosynthetic autotrophic organisms for the conversion of durable forms of energy to energy-dense, infrastructure-compatible liquid fuels. Chapter 38 reports the US DOE/ARPA-E Electrofuels program efforts, including its rationale, approach, potential benefits, and challenges. Chapter 39 discusses the motivations and the methods used to engineer *Ralstonia eutropha* to produce the liquid transportation fuel isobutanol from CO_2, H_2, and O_2; and Chap. 40 reports the development of an integrated Microbial-ElectroCatalytic (MEC) system consisting of *R. eutropha* as a chemolithoautotrophic host for metabolic engineering coupled to a small-molecule electrocatalyst for the production of biofuels from CO_2 and H_2, which extends well beyond biomass-derived substrates.

References

1. Geider RJ, Delucia EH et al (2001) Primary productivity of planet earth: biological determinants and physical constraints in terrestrial and aquatic habitats. Glob Chang Biol 7(8):849–882
2. Day DM, Lee JW (2004) The production and use of a soil amendment made by the combined production of hydrogen, sequestered carbon and utilizing off gases containing carbon dioxide. PCT Int Appl WO 2004037747 A2:58
3. Day DM, Evans RJ, Lee JW, Reicosky D (2005) Economical CO_2, SOx, and NOx capture from fossil-fuel utilization with combined renewable hydrogen production and large-scale carbon sequestration. Energy 30:2558–2579
4. Marris E (2006) Sequestration news feature: black is the new green. Nature 442:624–626
5. Lehmann J (2007) Commentary: a handful of carbon. Nature 447:143–144
6. Gundale MJ, Thomas H, DeLuca TH (2007) Charcoal effects on soil solution chemistry and growth of *Koeleria macrantha* in the ponderosa pine/douglas fir ecosystem. Biol Fertil Soils 43:303–311
7. Solomon D, Lehmann J, Thies J, Schafer T, Liang B, Kinyangi J, Neves E, Petersen J, Luizao F, Skjemstad J (2007) Molecular signature and sources of biochemical recalcitrance of organic C in Amazonian Dark Earths. Geochim Cosmochim Acta 71:2285–2298
8. Lehmann J, Gaunt J, Rondon M (2006) Bio-char sequestration in terrestrial ecosystems: a review. Mitig Adapt Strat Glob Chang 11:403–427
9. Adriana ED, Zwieten LV, Smernik RJ, Morris S, Munroe PR (2011) Terra Preta Australis: reassessing the carbon storage capacity of temperate soils. Agric Ecosyst Environ 140:137–147
10. Lee JW, Hawkins B, Day DM, Reicosky DC (2010) Sustainability: the capacity of smokeless biomass pyrolysis for energy production, global carbon capture and sequestration. Energy Environ Sci 3(11):1695–1705
11. Hamelinck CN, Faaij PC, den Uil H, Boerrigter H (2004) Production of FT transportation fuels from biomass; technical options, process analysis and optimisation, and development potential. Energy 29:1743–1771
12. James OO, Mesubi AM, Ako TC, Maity S (2010) Increasing carbon utilization in Fischer–Tropsch synthesis using H_2-deficient or CO_2-rich syngas feeds. Fuel Process Technol 91:136–144
13. Peralta-Yahya PP, Ouellet M, Chan R, Mukhopadhyay A, Keasling JD, Lee TS (2011) Identification and microbial production of a terpene-based advanced biofuel. Nat Commun. doi:10.1038/ncomms1494
14. Lee JW (2011) Designer proton-channel transgenic algae for photobiological hydrogen production. US Patent No. 7,932,437 B2

15. Lee JW (2010) Switchable photosystem-II designer algae for photobiological hydrogen production. U.S. Patent No. US 7,642,405 B2
16. Lee JW (2011) Designer organisms for photosynthetic production of ethanol from carbon dioxide and water. US Patent No. 7,973,214 B2
17. Lee JW (2009) Designer organisms for photobiological butanol production from carbon dioxide and water. PCT International Publication No. WO 2009/105733 A2
18. Robertson DE, Jacobson SA, Morgan F, Berry D, Church GM, Afeyan NB (2011) A new dawn for industrial photosynthesis. Photosynth Res 107:269–277
19. Lan EI, Liao JC (2011) Metabolic engineering of cyanobacteria for 1-butanol production from carbon dioxide. Metab Eng 13:353–363
20. Atsumi S, Higashide W, Liao JC (2009) Direct photosynthetic recycling of carbon dioxide to isobutyraldehyde. Nat Biotechnol 27(12):1177–1182
21. Berg IA, Kockelkorn D, Ramos-Vera WH, Say RF, Zarzycki J, Hügler M, Alber BE, Fuchs G (2010) Autotrophic carbon fixation in archaea. Nat Rev Microbiol 8:447–460

Chapter 2
Sugarcane Ethanol: Strategies to a Successful Program in Brazil

José Goldemberg

Abstract Presently, ethanol from sugarcane replaces approximately 50% of the gasoline that would be used in Brazil if such an option did not exist. In some aspects, ethanol may represent a better fuel than gasoline and to a great extent a renewable fuel contributing little to greenhouse gas emissions in contrast with fossil-derived fuels. Production of ethanol increase from 0.6 billion liters in 1975/1976 to 27.6 billion liter in 2009/2010. Although production costs in 1975/1976 were three times higher than gasoline prices in the international market, such costs declined dramatically thanks to technological advances and economics of scale becoming full competitive (without subsidies) with gasoline after 2004. This was achieved through appropriate policies of the Brazilian government. These policies and the rationale for them as a strategy to reduce oil imports are discussed here with the possibilities of replication in other countries.

1 Introduction

Sugarcane has been cultivated in Brazil since the sixteenth century and more recently the country became the largest producers of sugar accounting for approximately 25% of the world's production. The production of ethanol has been small but starting in 1931 the Government decided that all the gasoline used in the country (mostly imported) should contain 5% of ethanol from sugarcane. This was done to benefit sugar producing units when faced by declining prices of sugar in the international market which notoriously fluctuate over the years (Fig. 1).

Around 1970 the sugar industry in Brazil was stagnated, processing only 70–80 million tonnes of sugarcane per year mainly due to Government policies of guaranteed prices to producers: when the international price of sugar was low the

J. Goldemberg (✉)
University of São Paulo, Institute of Eletrotechnics and Energy, São Paulo, Brazil
e-mail: goldemb@iee.usp.br

J.W. Lee (ed.), *Advanced Biofuels and Bioproducts*, DOI 10.1007/978-1-4614-3348-4_2,

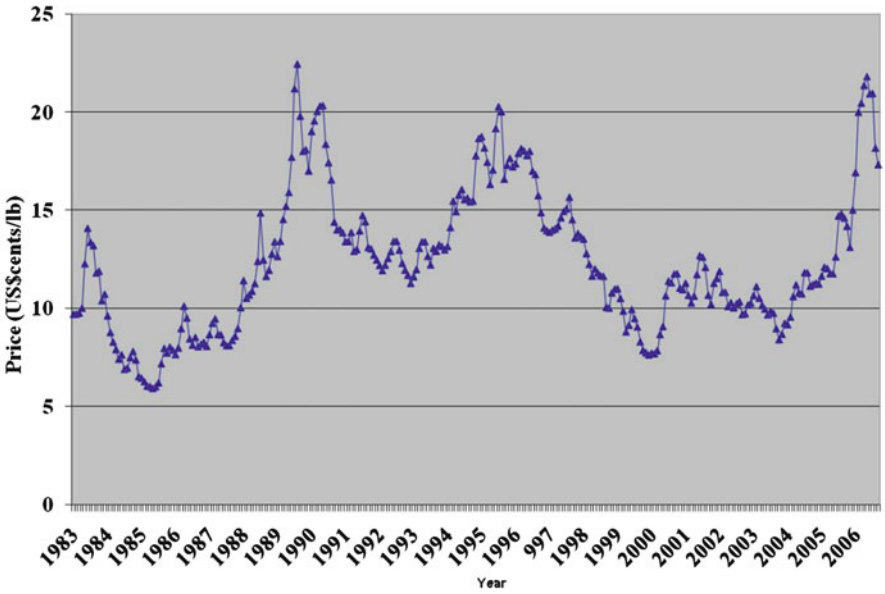

Fig. 1 World refined sugar price—1983/2007

government purchased the sugar at prices that satisfied the producers. Competition and modernization were thus discouraged; each producer had a quota and therefore few concerns about losing money. Sugar producers did not plan in the long run and usually produced strictly what they considered attractive in a given year. Since the price of sugar in the international markets varies significantly over time, as seen in Fig. 1, such lack of planning frequently left them out of the market when prices suffered strong fluctuations [1].

The solution proposed at that time by Ministry of Industry and Commerce [2] was to expand production regardless of the prices of sugar and use the excess production (when prices were low) to produce ethanol which was more expensive to produce than gasoline. One of the drivers for that was the need to eliminate lead components from gasoline (lead tetraethyl) which was imported saving thus foreign currency. Such ideas did not prosper until the oil crisis of 1973: the cost of oil went suddenly from US$ 2.90 per barrel to US$ 11.65 per barrel. The import bill with oil (80% of which was imported) skyrocketed from 600 million dollars in 1973 to 2.5 billion in 1974, approximately 32% of all Brazilian imports and 50% of all the hard currency that the country received from exports.

2 The Expansion of Ethanol Production

Under these conditions the Government decided to accelerate ethanol production thorough decree 76,593 of November 14, 1975 which is really the *birth certificate* of the Brazilian "Alcohol Program." The idea was to reduce gasoline consumption

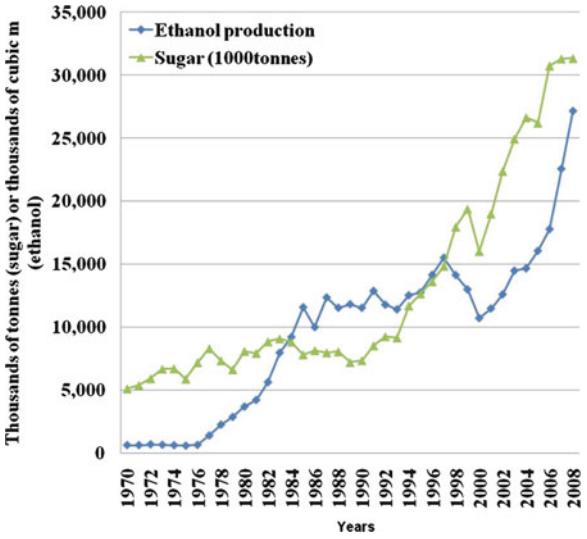

Fig. 2 Ethanol and sugar production—Brazil 1970–2008

and therefore decrease oil imports. Production goals were set at three billion liters of ethanol in 1980 and 10.7 billion liters in 1985.

This decree determined that very generous financing terms were to be offered to entrepreneurs through Government banks[1] and that the price of ethanol should be on a parity with sugar 35% higher than the price of 1 kg of sugar.[2]

The decree made the production of ethanol and the production of sugar equally attractive to the entrepreneurs. This opened the way for the increase in the production of ethanol which happened indeed as seen in Fig. 2.

Production increased from 600 million liters/year in 1975/1976 to 3.4 billion liters per year in 1979/1980. This corresponded to 14% of the gasoline used in 1979.

3 The Expansion of Ethanol Consumption

In principle, therefore the problem of increasing ethanol production was solved. The remaining problem was to make sure that the ethanol produced was consumed.

The Government solved the problem using two instruments [1]:

- Adopting mandates for mixing ethanol to gasoline. Up to 1979, the mixture of ethanol in the gasoline increased gradually to approximately 10% which required small changes in the existing motors. In 1981, ethanol consumption reached 2.5 billion liters.

[1] The interest to be paid on these loans was lower than the rate of inflation which resulted in a negative real interest rate.

[2] Theoretically one can produce 0.684 L of ethanol with 1 kg of sugar which is fairly close to the value established by the decree 76,593.

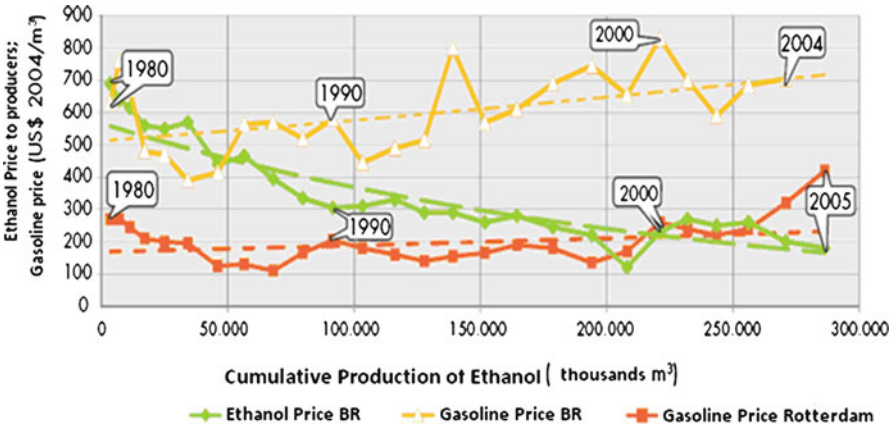

Fig. 3 Learning curve for ethanol production from sugarcane in Brazil. *Source*: Refs. [8, 9]

- Setting the price of ethanol paid to producers at 59% of the selling price of gasoline (which was more than twice the cost of imported gasoline). The high price of gasoline has been used for a long time by the Government as a method of collecting resources to subsidize diesel oil. Parts of such resources were then used to subsidize ethanol.

Subsidies of approximately one billion dollars per year on the average over the 30 years were needed to sustain the program. These subsidies were removed gradually and in 2004 the price paid to ethanol producers was similar to the cost of gasoline in the international market as seen in Fig. 3.

4 Technologies for Ethanol Use

Decree 76,593 and its consequences were adopted purely for economic reasons. Only in 1978 it become evident through work of university groups [2] that ethanol for sugarcane was very close of being a renewable energy source (except for the minor ingredients of pesticides, fertilizers, and some diesel oil needed for its production). All the energy for the process of crushing the sugarcane, fermenting and distillation originated in the bagasse of the sugarcane. The ratio of the energy contained in a 1 L of ethanol to the energy of fossil origin used in the process was approximately 4.53 to 1 when the first evaluation was carried out [3]. Today, evaluations are showing that the rate is even better (8 to 1) due to the significant agricultural and industrial efficiency improvements [4, 5]. Impressive productivity gains of 3% per year over 30 years have been achieved. As an example, Fig. 4 gives the growth of sugarcane agriculture productivity in different regions of Brazil, from 1977 to 2009, indicating an increase of 51% in the period.

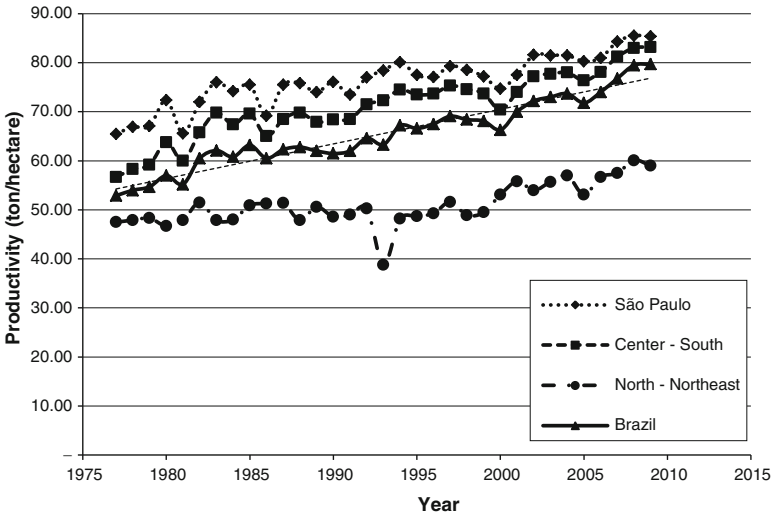

Fig. 4 Evolution of the sugarcane productivity in Brazil. *Source*: Ref. [10]

The second oil shock in 1979 led the Government to the drastic move to introduce cars with motors designed to operate exclusively with hydrated ethanol in order to increase ethanol consumption [2].

A few years earlier President Ernesto Geisel had visited the Air Force Technological Center in São José dos Campos, São Paulo, and was very impressed by the work being done there by engineers, led by Urbano Ernesto Stumpf, on ethanol-fueled cars using hydrated ethanol (95.5% pure ethanol and 4.5% water). Important changes in the engine were needed to use that fuel, which required a compression ratio of 12:1, compared to 8:1 for regular gasoline. The higher compression ratio meant higher efficiency, which partly compensated for ethanol's lower energy content. Combining all these factors, 199 L of pure (anhydrous) ethanol replace one barrel of gasoline (159 L). This change to engines meant a drastic change in auto manufacture, but under Government pressure, local carmakers adapted and nationalistic elements in the Government saw ethanol as an instrument of national independence. In addition to that Brazilian auto manufacturers could no longer export their cars since hydrated ethanol was not available in other countries. It was also a problem to drive Brazilian cars in neighboring countries (and even some states in Brazil) that did not have service stations selling hydrated ethanol. Despite that the production of these cars began in earnest at the end of the decade; between 1979 and 1985, they accounted for 85% of all new car sales [2]. Over this same period, the percentage of ethanol in gasoline reached approximately 20% [1].

Two fleets of automobiles were circulating in the country: some running on gasoline, using a blend of up to 20% anhydrous ethanol and 80% gasoline, and others

running on hydrated ethanol. In 1985, the scenario changed dramatically, as petroleum prices fell and sugar prices recovered on the international market. Subsidies were reduced and ethanol production could not keep up with demand. The production of ethanol leveled off but the total amount being used remained more or less constant because the blend was increased to 25% and more cars were using the blend. Thus, by 1990 a serious supply crises occurred and due to a shortage of the appropriate fuel. The government tried to mitigate the shortage importing ethanol and methanol. Methanol was blended with gasoline and ethanol yielding another fuel that could be used in gasoline cars, freeing more ethanol for the neat ethanol powered ones. But, the shortage crisis lasting 1 year scared consumers and the sales of neat ethanol cars dropped rapidly: by the year 2000, it was lower than 1% of total new cars sold.

Then, after 2003, ethanol consumption rose again, as flexible-fuel engines were introduced in the cars produced in Brazil. These cars are built to use pure ethanol with a high compression ratio (approximately 12:1) but can run with any proportion of ethanol and gasoline, from zero to 100%, as they have sensors that can detect the proportion and adjust the ignition electronically. Flex-fuel cars were an immediate hit; today, they represent more than 95% of all new cars sold because they allow drivers to choose the cheapest blend on any given day. Approximately 50% of the gasoline that would otherwise be used in Brazil today was replaced by ethanol. The production of pure ethanol driven cars is being discontinued because of the success with the flexible-fuel engines.

In the 30 years since 1976 ethanol substituted 1.51 billion barrels of gasoline which correspond to savings of US$ 75 billion (in dollars of 2006) taking into account the amount of gasoline saved each year at the world market price [6].

5 Expansion of the Ethanol Program to Other Countries

To emulate the successful Ethanol Program of Brazil, which is clearly an instrument to reduce CO_2 emissions from gasoline, a number of countries have adopted ethanol mandates to introduce ethanol in their automotive fleets. As a consequence, it is necessary to subsidize producers at a rate of approximately 11 billion dollars per year mainly in the United States where ethanol is produced from corn.

Table 1 shows the existing mandates in a number of countries and projections of the amount of ethanol that will be needed by 2020/2022.

Present gasoline consumption in these countries is 943.2 billion liters, 82% of present gasoline consumption.

The potential demand for 2020/2022 on the basis of existing mandates [7] is 178.7 billion liters.

Clearly, an enormous effort will have to be made to meet the projected demand for 2020 in the basis of either first- or second-generation technologies.

Table 1 Present production and potential demand for ethanol

Country/region	Present gasoline consumption[a] 2007 (billion liters per year)	Present ethanol production[b] 2008 (billion liters per year)	Potential demand resulting from present mandates up to 2020/2022 per year
US	530	34	136
European Union	148	2.3	8.51
China	54	1.9	5.4
Japan	60	0.1	1.8
Canada	39	0.9	1.95
United Kingdom	26	0.03	1.3
Australia	20	0.075	2.0
Brazil	25.2	27	19.6
South Africa	11.3	0.12	0.9
India	13.6	0.3	0.68
Thailand	7.2	0.3	0.7
Argentina	5.0	0.2	0.25
The Philippines	5.1	0.08	0.26
Total	943.2	67.3	178.7

[a]*Source*: From [11]
[b]*Source*: From [7]

6 Summary

A discussion is made of the policies adopted by the Brazilian government in the mid 1970s of last century to increase the production of ethanol from sugarcane. The success of such policies can be assessed by the enormous increase in production (from 0.6 billion liter in 1975/1978 to 27.6 billion in 2009/2010) as well as the sharp decline in production costs which turned this renewable fuel competitive with gasoline.

References

1. Goldemberg J (2009) The Brazilian experience with biofuels. Daedalus 4(4, Fall):91–107
2. Silva O, Frischetti D (2008) Etanol: a revolução verde e amarela. Bizz Comunicação e Produções. 1 ed - São Paulo, Brasil. ISBN 978-85-61163-01-3
3. Silva JG, Serra GE, Moreira JR, Gonçalves JC, Goldemberg J, Goldemberg J (1978) Energy balance for ethyl alcohol production from crops. Science 201:903–906
4. Macedo IC, Leal MRLV, Da Silva JEAR (2004) Assessment of greenhouse gas emissions in the production and use of fuel ethanol in Brazil. Secretariat of the Environment of the State of São Paulo, Brazil, p 32
5. Pacca S, Moreira JR (2009) Historical carbon budget of the Brazilian ethanol program. Energy Policy 37 (2009) 4863–4873
6. BNDES and CGEE (2008) Sugarcane-based bioethanol: energy for sustainable. 1 ed - Rio de Janeiro, Brasil: BNDES, p 304. ISBN: 978-85-87545-27-5

7. REN21 (2009) Renewables Global Status Report: 2009 Update (Paris: REN21 Secretariat)
8. Goldemberg J, Coelho ST, Lucon O, Nastari PM (2004) Ethanol learning curve: the Brazilian experience. Biomass Bioenergy 26:301–304
9. Goldemberg J (2007) Ethanol for a sustainable energy future. Science 315:808–810
10. IBGE (Brazilian Institute of Geography and Statistics) (2010) Pesquisa Agrícola Municipal (Agriculture Municipal Research 2010) Compiled by Center of Sugarcane Technology (CTC). Availableat:http://www.sidra.ibge.gov.br/bda/tabela/listabl.asp?z=t&o=11&i=P&c=99. Accessed 24 June 2010
11. OECD/IEA (2010) IEA Statistics Oil Information, Paris. ISBN 978-92-64-08422-3

Part II
Smokeless Biomass Pyrolysis for Advanced Biofuels Production and Global Biochar Carbon Sequestration

Chapter 3
Smokeless Biomass Pyrolysis for Producing Biofuels and Biochar as a Possible Arsenal to Control Climate Change

James Weifu Lee and Danny M. Day

Abstract Smokeless (emission-free, clean, and efficient) biomass pyrolysis for biochar and biofuel production is a possible arsenal for global carbon capture and sequestration at gigatons of carbon (GtC) scales. The world's annual unused waste biomass, such as crop stovers, is about 3.3 GtC y^{-1}. If this amount of biomass (3.3 GtC y^{-1}) is processed through the smokeless pyrolysis approach, it could produce biochar (1.65 GtC y^{-1}) and biofuels (with heating value equivalent to 3,250 million barrels of crude oil) to help control global warming and achieve energy independence from fossil fuel. By using 1.65 GtC y^{-1} of biochar into soil and/or underground reservoirs alone, it would offset the 8.5 GtC y^{-1} of fossil fuel CO_2 emissions by 19%. The worldwide maximum capacity for storing biochar carbon into agricultural soils is estimated to be about 428 GtC. It may be also possible to provide a global carbon "thermostat" mechanism by creating biochar carbon energy storage reserves. This biomass-pyrolysis "carbon-negative" energy approach merits serious research and development worldwide to help provide clean energy and control climate change for a sustainable future of human civilization on Earth.

J.W. Lee (✉)
Department of Chemistry and Biochemistry, Old Dominion University,
Physical Sciences Building 3100B, 4402 Elkhorn Avenue, Norfolk, VA 23529, USA

Whiting School of Engineering, Johns Hopkins University,
118 Latrobe Hall, Baltimore, MD 21218, USA
e-mail: jlee349@jhu.edu; jwlee@odu.edu

D.M. Day
Eprida Power and Life Sciences, Inc.,
6300 Powers Ferry Road, #307, Atlanta, GA 30339, USA

J.W. Lee (ed.), *Advanced Biofuels and Bioproducts*, DOI 10.1007/978-1-4614-3348-4_3,

1 Introduction

This approach of smokeless (emission-free, clean, and efficient) biomass pyrolysis with biochar application as soil amendment and carbon sequestration agent was initiated through our joint 2002 US provisional patent application followed by a PCT application [1]. One of the key concepts here is to use a biomass-pyrolysis process to produce certain biofuels and more importantly to "lock" some of the unstable biomass carbon, such as dead leaves, waste woods, cornstovers, and rice straws, into a stable form of carbon—biochar, which could be used as a soil amendment to improve soil fertility and at the same time, to serve as a carbon sequestration agent, since biochar can be stable in soil for thousands of years and can help retain nutrients in soil to reduce the runoff of fertilizers from agriculture lands that would otherwise pollute the rivers and water bodies. The general philosophy or the "idea roots" of this approach can trace back to Lee's early work in 1998 at Oak Ridge National Laboratory (ORNL) in developing the method for reducing CO_2, CO, NO_x, and SO_x emissions, which subsequently resulted in a US Patent that laid a framework of solidifying carbon dioxide and placing it into soil and/or subsoil earth layers for win–win benefits on carbon sequestration, environmental health, and agricultural productivity [2, 3]. In 2002, when Day of Eprida visited Lee's lab at ORNL, we shared our visions and together extended this approach with the process of smokeless biomass pyrolysis and using biochar fertilizer as soil amendment and carbon sequestration agent [4, 5].

When this approach of smokeless biomass pyrolysis and using biochar fertilizer as soil amendment for carbon sequestration was first proposed, we encountered various skepticisms from our peers, some of them with very good/tough questions, such as "how stable is biochar when used as carbon sequestration agent in soil?" and "how long would your envisioned biochar fertility effect last in soil?" In our minds, there were no doubts that biochar material and its fertility effects (such as cation exchanging capacity) could be stable for hundreds and perhaps thousands of years. However, to provide an absolutely clear answer to this type of questions, it would require a long-term biochar-soil experiment that lasts hundreds of years, which would be practically impossible to complete in our life time. We presented our findings first at the USDA Carbon Sequestration Conference in November of 2002 and included references to the "black carbon" in the prehistoric (pre-Columbian) "Terra Preta" soils in Amazonia [6, 7]. Subsequently, one of us (Day) organized and sponsored the first two US biochar scientific meetings and held briefings around the world to educate and further the use of biochar. The first US biochar and energy production scientific meeting which was sponsored by Eprida (Day) held in June 2004 at the University of Georgia at Athens with about 60 participants from across the world, including Brazil, Austria, Germany, New Zealand, Japan, and the USA. Since then, the approach of smokeless biomass pyrolysis and biochar soil application gradually became a hot research and development topic across the world.

Because biochar is not completely digestible to microorganisms, a biochar-based soil amendment could serve as a permanent carbon-sequestration agent in soils/subsoil earth layers for thousands of years. As indicated by the recent discovery of

biochar particles in "Terra Preta" soils formed by pre-Columbian indigenous agriculturalists in Amazonia, biochar materials could be stored in soils as a means of carbon sequestration for hundreds and perhaps thousands of years. The longest lifetime of biochar material that has been reported with scientific evidence is about 38,000 years, according to the carbon isotope dating of a prehistoric Cro-Magnon man's charcoal painting discovered in the Grotte Chauvet cave [8]. The black carbon in a "Terra Preta" soil at the Acutuba site has been dated about 6,850 years ago [9]. At the Jaguariuna soil site in Brazil, some high abundance of charcoal found in the summit soil was dated to occur about 9,000 years ago [10]. These carbon-isotope dating results all indicate how stable and permanent the biochar carbon sequestration can be. Through a ^{14}C-labeling study, the mean residence time of pyrogenic carbon in soils has now been estimated in the range of millennia [11].

Here, we must point out that the practice of the pre-Columbian indigenous agriculturalists may or may not be applicable to achieving our envisioned clean energy production and global biochar carbon sequestration, although the discovery of biochar particles in "Terra Preta" soils seems to provide quite nice support for the proposed approach of smokeless biomass pyrolysis using biochar fertilizer for soil amendment and carbon sequestration. First of all, the biochar materials accumulated in the "Terra Preta" soil were probably resulted from some low-tech processes, including (1) "slash and burn," (2) "slash and char," and (3) wild fires. All of these three processes generate large amounts of hazardous smokes that can impact air quality. In the practice of "slash and burn," trees, bushes, and other green plants are cut down and burned in the field to clear the land for cropland. The burning of biomass in open fields creates large amounts of hazardous smoke similar to a wild fire; the biochar formed through the slash-and-burn techniques represents only about 1.7% of the pre-burn biomass [12]. "Slash and char" is a practice to make charcoal from biomass by use of conventional charcoal kilns [11, 13], which is better than the practice of "slash and burn," but would still produce large amount of smoke. Use of conventional charcoal kilns for charcoal production at a gigatons of carbon (GtC) scale would produce large amounts of smoke (pollutants including soot black-carbon particles) that are not acceptable to the environment and air quality, in addition to allowing heat, energy, and valuable chemicals to escape into the atmosphere. A recent study indicates that black-carbon aerosols which can directly absorb solar radiation might have substantially contributed to the rapid Arctic warming during the past 3 decades [14, 15]. Therefore, a smokeless and efficient modern biomass-pyrolysis process is essential to achieve the mission of annually converting gigatons of biomass into biochar and biofuel. Development and deployment of a modern biomass-pyrolysis biofuel/biochar-producing process would enable collecting of the "smoke" (organic volatiles and gases) into the biofuel fraction for clean energy (e.g., hydrogen and/or liquid fuels) production. Therefore, further development and use of this type of smokeless biofuel/biochar-producing biomass-pyrolysis technologies are needed for the envisioned large (GtC) scale mission of mitigating global CO_2 emissions, and, at the same time, ensuring good air quality.

Furthermore, the "Terra Preta" soils in Amazonia rain forest region represent only a tiny spot on Earth. What one may learn from there may or may not be useful

to the rest of the world because of the differences in climates, soil types, crops and ecological systems, and other factors. More importantly, for the envisioned modern application of biochar as a meaningful arsenal for global carbon sequestration to control global warming, it would require an operation of both biochar production and soil application at GtC scales, which have never been done in any human history. Serious studies across the world are needed before this approach could be considered for practical implementation.

Therefore, in the following, we provide a quick overview of the biomass-pyrolysis "carbon-negative" energy approach and discuss its future research and development opportunities.

2 The Biomass-Pyrolysis "Carbon-Negative" Approach

As illustrated in Figs. 1 and 2, photosynthesis captures more CO_2 from the atmosphere than any other process does on Earth. Each year, land-based green plants capture about 440 gigatons (Gt) CO_2 (equivalent to 120 Gt C y^{-1}) from the atmosphere into biomass [16]. However, biomass is not a stable form of carbon material with nearly all returning to the atmosphere in a relatively short time as CO_2. Because of respiration and biomass decomposition, there is nearly equal amount of CO_2 (about 120 GtC y^{-1}) released from the terrestrial biomass system back into the atmosphere each year [17]. As a result, using biomass for carbon sequestration is limited. Any technology that could significantly prolong the lifetime of biomass materials would be helpful to global carbon sequestration. The approach of smokeless biomass pyrolysis can provide such a possible capability to convert the otherwise unstable biomass into biofuels, and, more importantly, biochar which is suitable for use as a soil amendment and serve as a semipermanent carbon-sequestration agent in soils/subsoil earth layers for hundreds and perhaps thousands of years [4].

Biomass pyrolysis is a process in which biomass, such as waste woods and/or crop residues (e.g., cornstover), is heated to about 400°C in the absence of oxygen and converted to biofuels (bio-oils, syngas) and biochar—a stable form of solid black carbon (C) material (Fig. 3). Although its detailed thermochemical reactions are quite complex, the biomass-pyrolysis process can be described by the following general equation:

$$\text{Biomass(e.g., lignin cellulose)} \rightarrow \text{biochar} + H_2O + \text{bio - oils} + \text{syngas}$$

The yield and characteristics of biochar produced varies widely depending on the feedstock properties and pyrolysis conditions, including temperature, heating rate, pressure, moisture, and vapor-phase residence time. Typically, biochar contains mainly carbon (C) with certain amounts of hydrogen (H), oxygen (O), and nitrogen (N) atoms, plus ash. As reported in one of our previous studies [4], a typical composition of biochar on an ash- and nitrogen-free basis can be 82% C, 3.4% H, and 14.6% O. Biochar has been produced throughout recorded history in energy-wasteful earthen pits, kilns, and steel drums releasing smoke. Advances in technology allow the organic volatiles (bio-oils) and syngas (CO, CO_2, and H_2, etc.) from biomass

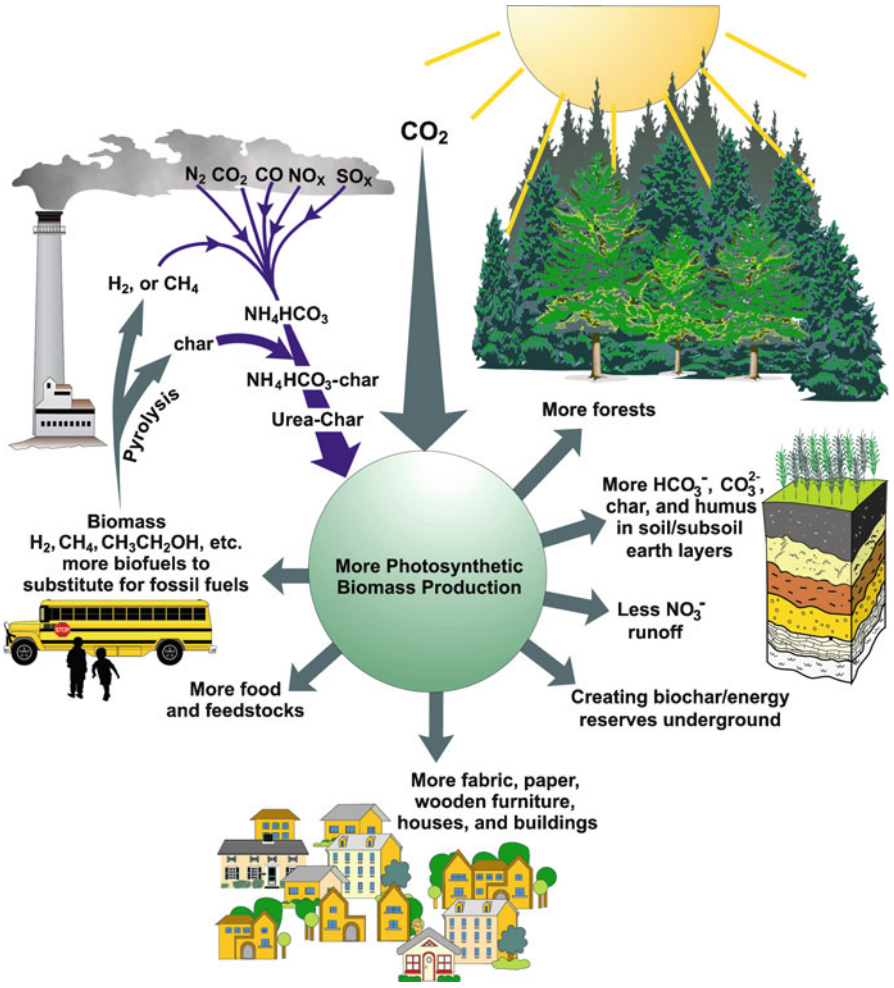

Fig. 1 The potential benefits of smokeless biomass pyrolysis energy technology for carbon dioxide capture and sequestration. As illustrated by the major CO_2 *arrow* pointing from the *top*, photosynthetic biomass production on Earth (*center*) is the biggest process that can take CO_2 from the atmosphere. The biomass pyrolysis process (*upper left*) could convert a fraction of biomass into biochar and biofuels (such as H_2 and CH_4), which could be optionally utilized to make NH_4HCO_3-char and/or urea-char fertilizers. Use of the biochar fertilizers could store carbon into soil and subsoil earth layers, reduce fertilizer (such as NO_3^-) runoff, and improve soil fertility for more photosynthetic biomass production that could further translate to more win–win benefits, including more forest, more fabric and wooden products, more food and feedstocks, and with possibility of creating biochar/energy reverses (*bottom right*) as "global carbon thermostat" to control climate change (reproduced from ref. [5])

pyrolysis to be used as a biofuel for clean energy production. Typically, through a 400°C slow-pyrolysis process, about 50% of the dry biomass C (carbon) can be converted into biochar while the remaining 50% C in the biofuel portion provides part of its energy to sustain the process.

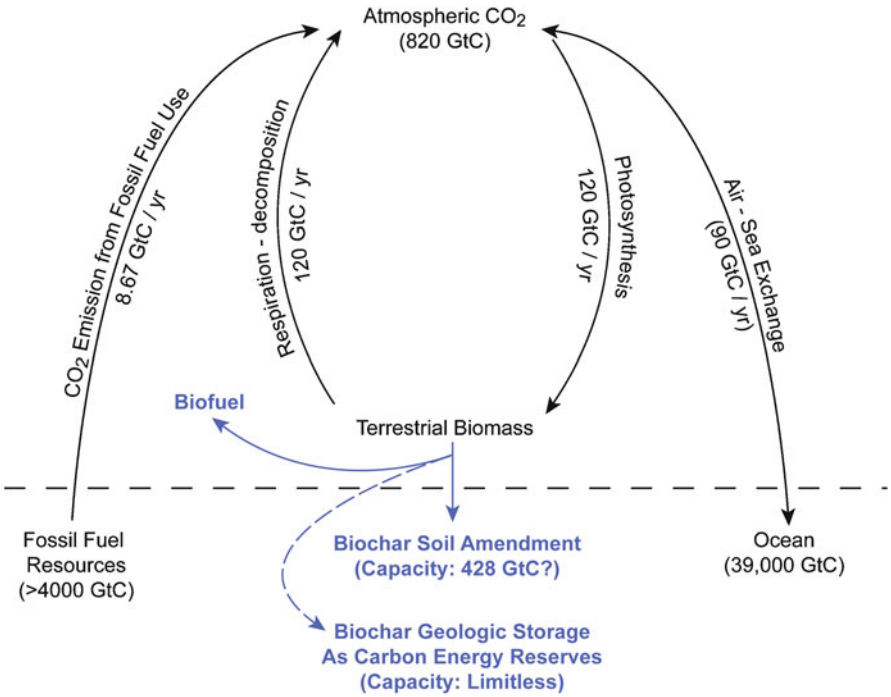

Fig. 2 The global carbon cycle and envisioned "carbon-negative" biomass-pyrolysis energy technology concept for biofuel and biochar production, and carbon dioxide capture and sequestration (reproduced from ref. [5])

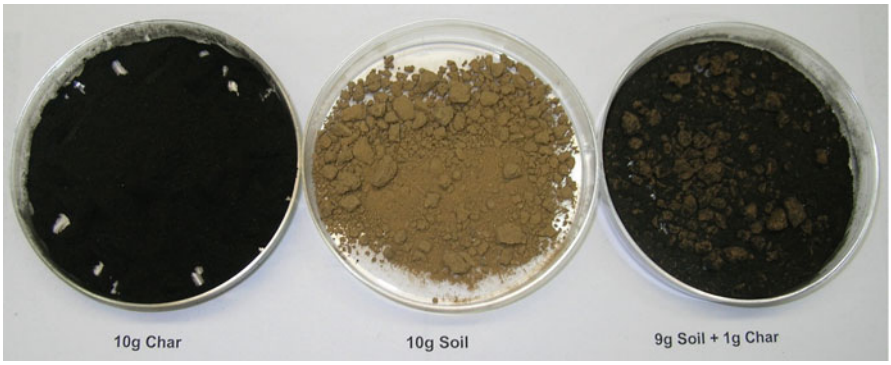

Fig. 3 Photographs showing, from *left* to *right*, 10 g biochar from pyrolysis of cornstover, 10 g soil, and 10 g mixture of biochar (10% W) and soil (90% W). The soil sample shown here is a surface soil from 0 to 15 cm deep at the University of Tennessee's Research and Education Center, Milan, Tennessee, USA (358,560 N latitude, 888,430 W longitude), which is also known as the Carbon Sequestration in Terrestrial Ecosystems site (CSiTE) supported by the US Department of Energy (reproduced from ref. [5])

In perspective of the global carbon cycle, as shown in Fig. 1, this biochar-producing biomass-pyrolysis approach essentially employs the existing natural green-plant photosynthesis on the planet as the first step to capture CO_2 from the atmosphere; then, the use of a pyrolysis process converts biomass materials primarily into biofuel and char—a complex but stable form of solid carbon material that can enhance plant growth when used as soil amendment. The net result is the removal of CO_2 from the atmosphere through the process of capturing CO_2 from the atmosphere and placing it into soils and/or subsoil earth layers as a stable carbon (biochar) while producing significant amount of biofuel energy through biomass pyrolysis. Therefore, this is a "carbon negative" energy production approach.

The world's annual unused waste biomass such as crop stovers is about 6.6 Gt of dry biomass [18], which is equivalent to about 3.3 GtC y^{-1} since dry biomass typically contains C as 50% of its total mass. If this amount of biomass (3.3 GtC y^{-1}) is processed through controlled low-temperature pyrolysis assuming 50% conversion of biomass C to stable biochar C and 35% of the biomass energy to biofuels, it could produce biochar (1.65 GtC y^{-1}) and biofuels (with heating value equivalent to 3,250 million barrels of crude oil) to help control global warming and achieve energy independence from fossil fuel. By using 1.65 GtC y^{-1} of biochar as a beneficial soil amendment, it would offset the 8.5 GtC y^{-1} of fossil fuel CO_2 emissions by 19%. Therefore, the envisioned biochar-producing biomass-pyrolysis approach (Figs. 1 and 2) should be considered as an option to mitigate the problem of global greenhouse-gas emissions.

The capacity of carbon sequestration by the application of biochar fertilizer in soils could be quite significant since the technology could potentially be applied in many land areas, including croplands, grasslands, and also a fraction of forest lands. The maximum capacity of carbon sequestration through biochar soil amendment in croplands alone is estimated to be about 428 GtC for the world. This capacity is estimated according to: (a) the maximal amount of biochar carbon that could be cumulatively placed into soil while still beneficial to soil environment and plant growth; and (b) the arable land area that the technology could potentially be applied through biochar agricultural practice.

Using charcoal collected from a wildfire, Gundale and DeLuca recently showed that the amount of charcoal that can be applied can be as much as 10% of the weight of soil to increase plant *Koeleria macrantha* biomass growth without negative effect [19]. The composition of a biochar material depends on its source biomass material and pyrolysis conditions. Typically, biochar material produced from low-temperature (about 400°C) pyrolysis contains about 70% (w) of its mass as the stable carbon (C) and the remainder as ash content, oxides, and residual degradable carbon (such as bio-oil residue). The density of bulk soil is typically about 1.3 tons m^{-3}. With this preliminary knowledge, we calculated that the maximum theoretical biochar sequestration capacity is about 303.8 ton C per hectare (1 ha = 2.47 acres; 123 ton C per acre) in a 30-cm soil layer alone. From the size of the world's arable land (1,411 million hectares), the worldwide potential capacity for storing biochar carbon in agricultural soils was estimated to be 428 GtC (Table 1). This estimate (428 GtC), which is somewhat higher than that (224 GtC) estimated by Lehman et al. [20],

Table 1 Calculated capacity of biochar carbon sequestration in world agricultural soils (reproduced from ref. [5])

World region	Arable land[a] (million hectares)	Estimated capacity (GtC) of biochar carbon storage in soil[b]
North America	215.5	65.5
Europe	277.5	84.3
Asia	504.5	153.3
Africa	219.2	66.6
Oceania	45.6	13.9
Central America/Caribbean	36.2	10.9
South America	112.5	34.2
Total	1,411	428.7

[a]Arable land area (1 ha = 2.47 acres) from the 2007 database of the Food and Agriculture Organization of the United Nations: http://faostat.fao.org/site/377/default.aspx#ancor

[b]Calculated based on the theoretical biochar carbon(C) storage capacity of 303.8 ton C per hectare for the first 30-cm soil layer alone, assuming average soil density of 1.3 tons m^{-3}, maximally 10% biochar by soil weight, and biochar material containing about 70% (w) of its mass as the stable carbon (C)

probably represents an upper limit value. The maximal amounts of biochar carbon that could be cumulatively placed into soil while still beneficial to soil environment and plant growth are probably dependent on a number of factors, including the specific biochar properties, topography, soil type, weather, and plant species. Worldwide biochar soil field tests are needed to obtain more accurate information on the capacity of biochar carbon sequestration in soils.

3 Future R&D Opportunities

Since this technology concept of smokeless biomass pyrolysis with biochar soil application is still in its early developing stage, much more research and development work is needed before this approach could be considered for practical implementation. To achieve the mission, a number of technical issues still need to be addressed. First, as pointed out previously, the process technology must be smokeless (emission-free, clean, and efficient) to avoid negative impact on air quality with such a large (GtC)-scale operation. Therefore, it is essential to fully develop a smokeless biomass-pyrolysis process to achieve the mission. As illustrated in Fig. 4, one of the possible productive ways to achieve the smokeless (emission-free, clean, and efficient) feature is by converting the pyrolysis syngas "smoke" into clean energy, such as liquid biofuels. Currently, there are a number of Fischer–Tropsch processing technologies that might be helpful for conversion of biomass-derived syngas into advanced (drop-in-ready) liquid biofuels, such as biodiesel, to replace petroleum-based transportation fuels. However, significant R&D efforts are needed to fully develop and demonstrate this approach since the currently existing refinery technologies cannot cost-effectively convert biomass-derived syngas and/or bio-oils into liquid transportation biofuels.

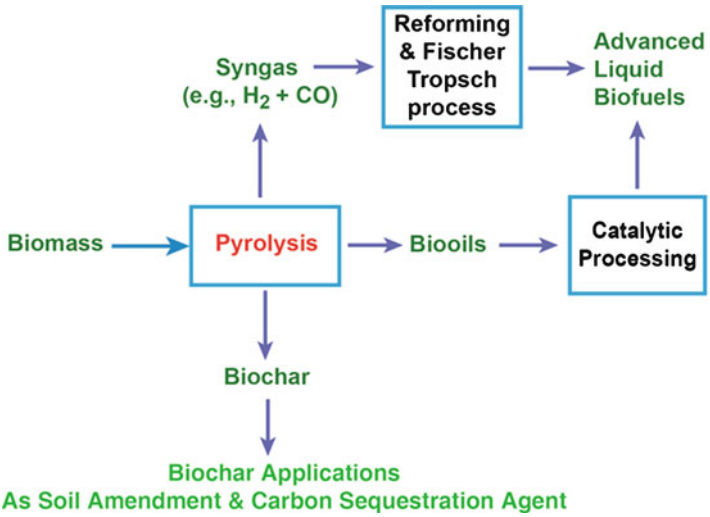

Fig. 4 Illustration of an envisioned emission-free smokeless biomass pyrolysis technology system for advanced biofuels production and biochar carbon sequestration

Second, there are significant R&D opportunities to improve biofuels products in relation to proper utilization of the biomass-pyrolysis-derived syngas and bio-oils that currently cannot be used as a liquid transportation fuel. For example, one of the problems here is that the biofuel fractions (syngas and bio-oils) from biomass pyrolysis are not in a desired form that could be used as a transportation fuel for cars. In other words, although the amounts and the heating value of the syngas and bio-oils from the envisioned biomass pyrolysis approach could potentially be very large (with heating value equivalent to that of about 3,250 million barrels of crude oil for the world), it is not clear how much they could really replace crude oil because the efficiency for conversion of the syngas and bio-oils into the advanced liquid biofuels has not been fully established. Additional refinery technology is needed to convert the biomass-derived syngas and/or bio-oils into certain desirable advanced liquid biofuels such as biodiesel for use in cars in order to replace the petroleum-based transportation fuels. It is possible to catalytically convert the biomass-derived syngas into liquid transportation fuels through the Fischer–Tropsch synthesis of hydrocarbons [21–23]. It is also possible to convert the liquid bio-oils by different refinery processes, such as catalytic processing into biodiesel for use as a transportation fuel. Therefore, it is probably worthwhile to explore the use of a proper refinery process, such as the Fischer–Tropsch process, to couple with a continuous biomass pyrolysis for production of advanced liquid biofuels and biochar. However, since most require expensive catalysts, other viable options (such as using bio-oils as a heating oil and noncatalytic fuel production) remain to be examined to determine trade-off between energy efficiency and costs. Significant research efforts are needed to develop innovative technologies, such as catalytic bio-oils-hydroprocessing and/or an updated Fischer–Tropsch process, to convert the syngas into advanced (drop-in-ready)

liquid biofuels to replace petroleum-based transportation fuels. This also reflects the need of developing tools for optimizing the entire process in relation to feedstock, energy, greenhouse gases, and economics.

Third, significantly more research efforts are needed on the aspects of biochar production and biochar soil applications. Biochar typically is a spectrum of substances produced from biomass pyrolysis. In order for biochar to serve as an effective soil amendment and carbon sequestration agent, the biochar product must possess certain required properties and quality standards, such as its cation exchange capacity and stability. More research is needed to further optimize the biochar cation exchange capacity [24] while still retaining its carbon stability. It has also been reported that biochar occasionally shows inhibitory effects on plant growth, especially, when biochar soil application exceeds about 5–10% by weight [25–27]. So far, very little is known about the true identity of the biochar inhibitory factors. If biochar were to be globally used as a soil amendment and carbon sequestration agent at GtC scales, the release of potentially toxic compounds into soil and associated hydrologic systems might have unpredictable consequences in agroecosystems. These characteristics of biochar, including both its beneficial features (e.g., cation exchange capacity) and possible harmful factors need to be systematically studied, since they are directly related to its application impacts (benefits and risks) on soil and the environment. Rigorous biochar-soil studies at large scales across the world are needed to systematically assess the effects of biochar applications on soil fertility, including plant growth, on soil carbon storage (sequestration) and on the associated soil and hydrological ecosystems. Additional work is needed also on how to employ this approach in helping to utilize various waste biomass materials, including (but not limited to) dead leaves, waste woods, and various agriculture stovers, such as cornstovers and rice straws to produce both biochar and biofuels in a distributed manner across the world. It is also worthwhile to explore beneficial utilization of certain sewage solid waste, such as, on what fraction of sewage sludge could be added to waste biomass to produce a higher nutrient dense slow-release biochar and safely recycle the valuable nutrients currently lost in waste processing. With these studies and added knowledge, it should be possible to produce "fit-for-purpose" biochars to address specific soil and environmental constraints and maximize the benefits of biochar soil application at the national and international scales.

Fourth, systematic lifecycle impact-assessment on energy, carbon, land, water, air, and environmental health, including toxicology and ecology studies, must be carefully conducted to fully evaluate the potential benefits and possible risks in relation to biomass pyrolysis and biochar application as soil amendment for global carbon sequestration at GtC scales.

Furthermore, the maximum capacity of carbon sequestration through biochar soil amendment in world agricultural soils (1,411 million hectares) is estimated to be about 428 GtC, assuming maximally 10% biochar C by soil weight for the first 30-cm soil layer alone. To verify this potential capacity and demonstrate its feasibility, soil pot studies and field trials of biochar applications in relation to soil fertility and carbon sequestration are needed in all of the world regions and different soil types. For the immediate future, biochar should be used to revitalize barren degraded land.

This will improve the world's capacity for growing biomass thus naturally removing more CO_2 from the atmosphere.

Another question to answer is whether it is possible to provide a global carbon "thermostat" mechanism to control the atmospheric CO_2 concentrations by creating large reservoirs underground (and/or above ground) for any biochar not used for soil restoration. Since the capacity of biochar storage reservoirs could be so large (limitless), the envisioned photosynthetic biomass production and biochar-producing biomass-pyrolysis approach (Figs. 1 and 2) could be used for many years to reduce the atmospheric CO_2 concentrations to any desired levels if the world population is mobilized to implement the approach. This is different from the application of biochar as a soil amendment where biochar particles are mixed with soil particles in such a diluted manner (such as 10% by soil weight) that recovering of biochar materials from the mixed soils would be very difficult. The biochar materials in reservoirs are preferably in a pure and concentrated form so that they could be readily retrieved at any time when needed for use of its energy by combustion. Therefore, global use of biochar reservoirs in a regulated manner could provide a global carbon "thermostat" mechanism to control global warming (climate change) in a desirable manner as well.

As a conclusion, this smokeless biomass-pyrolysis "carbon-negative" energy-production approach merits a major program support for serious research and development worldwide. With further research and development, this approach could provide more efficient and cleaner biomass pyrolysis technology for producing biofuels and biochar from biomass as a significant arsenal to help achieve independence from fossil energy and to control climate change for a sustainable future on Earth.

References

1. Day DM, Lee JW (2004) The production and use of a soil amendment made by the combined production of hydrogen, sequestered carbon and utilizing off gases containing carbon dioxide. PCT Int Appl 58pp. WO 2004037747 A2
2. Lee JW Li R (1998) Method for reducing CO_2, CO, NOx, and SOx emissions. ORNL Invention Disclosure. ERID 0631
3. Lee JW Li R (2002) Method for reducing CO_2, CO, NOx, and SOx emissions. United States Patent No. US 6,447,437 B1
4. Day D, Evans RJ, Lee JW, Reicosky D (2005) Economical CO_2, SOx, and NOx capture from fossil-fuel utilization with combined renewable hydrogen production and large-scale carbon sequestration. Energy 30(14):2558–2579
5. Lee JW, Hawkins B, Day DM, Reicosky DC (2010) Sustainability: the capacity of smokeless biomass pyrolysis for energy production, global carbon capture and sequestration. Energy Environ Sci 3(11):1695–1705
6. Denevan WM (1996) A bluff meddle of river in the settlement in prehistoric Amazonia. Ann Assoc Am Geogr 86(4):654–681
7. Woods WI, McCann JM (1999) The anthropogenic origin and persistence of Amazonian Dark Earth. Yearbook, conference of Latin Americanist geographer, vol 25, pp 7–14
8. Bard E (2001) Extending the calibrated radiocarbon record. Science 292:2443–2444

9. German LA (2003) Historical contingencies in the coevolution of environment and livelihood: contributions to the debate on Amazonian Black Earth. Geoderma 111:307–331
10. Gouveia SEM, Pessenda LCR et al (2002) Carbon isotopes in charcoal and soils in studies of paleovegetation and climate changes during the late Pleistocene and the Holocene in the south-east and center west regions of Brazil. Global Planet Change 33(1–2):95–106
11. Kuzyakov Y, Subbotina I, Chen H, Bogomolova I, Xu X (2009) Black carbon decomposition and incorporation into soil microbial biomass estimated by ^{14}C labeling. Soil Biol Biochem 41:210–219
12. Steiner C (2006) Slash and char as alternative to slash and burn. Dissertation, University of Bayreuth, Germany
13. Okimori Y, Ogawa M, Takahashi F (2003) Potential of CO_2 emission reductions by carbonizing biomass waste from industrial tree plantation in South Sumatra, Indonesia. Mitig Adapt Strat Glob Change 8:261–280
14. Shindell D, Faluvegi G (2009) Climate response to regional radiative forcing during the twentieth century. Nat Geosci 2:294–300
15. Kintisch E (2009) Climate change: new push focuses on quick ways to curb global warming. Science 324:323
16. Geider RJ, Delucia EH et al (2001) Primary productivity of planet earth: biological determinants and physical constraints in terrestrial and aquatic habitats. Glob Chang Biol 7(8):849–882
17. Sauerbeck DR (2001) CO_2 emissions and C sequestration by agriculture—perspectives and limitations. Nutr Cycl Agroecosyst 60(1–3):253–266
18. Krausmann F, Erb K, Gingrich S, Lauk C, Haberl H (2008) Global patterns of socioeconomic biomass flows in the year 2000: a comprehensive assessment of supply, consumption and constraints. Ecol Econ 65:471–487
19. Gundale MJ, DeLuca TH (2007) Charcoal effects on soil solution chemistry and growth of *Koeleria macrantha* in the ponderosa pine/Douglas fir ecosystem. Biol Fertil Soils 43:303–311
20. Lehmann J, Gaunt J, Rondon M (2006) Bio-char sequestration in terrestrial ecosystems—a review. Mitig Adapt Strat Glob Change 11:403–427
21. Hamelinck CN, Faaij APC, den Uil H, Boerrigter H (2004) Production of FT transportation fuels from biomass; technical options, process analysis and optimisation, and development potential. Energy 29:1743–1771
22. Demirbas A (2007) Progress and recent trends in biofuels. Prog Energ Combust Sci 33:1–18
23. James OO, Mesubi AM, Ako TC, Maity S (2010) Increasing carbon utilization in Fischer–Tropsch synthesis using H_2-deficient or CO_2-rich syngas feeds. Fuel Process Technol 91: 136–144
24. Lee JW, Kidder M, Evans BR, Paik S, Buchanan AC, Garten C, Brown R (2010) Characterization of biochars produced from cornstover for soil amendment. Environ Sci Technol 44: 7970–7974
25. Rondon MA, Lehmann J, Ramírez J, Hurtado M (2007) Biological nitrogen fixation by common beans (*Phaseolus vulgaris* L.) increases with bio-char additions. Biol Fertil Soils 43:699–708
26. Rillig MC, Wagner M, Salem M, Antunes P, George C, Ramke HG, Titirici MM, Antonietti M (2010) Material derived from hydrothermal carbonization: effects on plant growth and arbuscular mycorrhiza. Appl Soil Ecol 45:238–242
27. Gundale MJ, DeLuca TH (2007) Charcoal effects on soil solution chemistry and growth of *Koeleria macrantha* in the ponderosa pine/Douglas fir ecosystem. Biol Fertil Soils 43: 303–311

Chapter 4
Oxygenation of Biochar for Enhanced Cation Exchange Capacity

James Weifu Lee, A.C. Buchanan III, Barbara R. Evans, and Michelle Kidder

Abstract This chapter reports a technological concept for producing a partially oxygenated biochar material that possesses enhanced cation-exchanging property by reaction of a biochar source with one or more oxygenating compounds in such a manner that the biochar material homogeneously acquires oxygen-containing cation-exchanging groups. This concept is based on our recent experimental finding that the O:C atomic ratio in biochar material correlates with its cation-exchange capacity. The technology is directed at biochar compositions and soil formulations containing the partially oxygenated biochar materials for soil amendment and carbon sequestration.

1 Introduction

Photosynthesis captures more carbon dioxide (CO_2) from the atmosphere than any other process on Earth. Each year, land-based green plants capture about 403 gigatons (Gt) of CO_2 (equivalent to 110 Gt C y^{-1}) from the atmosphere into biomass [1]. However, only about ½ of the primary photosynthesis product (110 Gt C y^{-1}) becomes plant tissue (biomass), the other half is respired directly from photosynthetic sugars; furthermore, since biomass is not a stable form of carbon material,

J.W. Lee (✉)
Formerly, Oak Ridge National Laboratory, P.O. Box 2008, Oak Ridge, TN 37831, USA

Department of Chemistry and Biochemistry, Old Dominion University, Physical Sciences Building 3100B, Norfolk, VA 23529, USA

Whiting School of Engineering, Johns Hopkins University, 118 Latrobe Hall, Baltimore, MD 21218, USA
e-mail: JWLee@odu.edu; JLee349@jhu.edu

A.C. Buchanan III • B.R. Evans • M. Kidder
Oak Ridge National Laboratory, P.O. Box 2008, Oak Ridge, TN 37831, USA

J.W. Lee (ed.), *Advanced Biofuels and Bioproducts*, DOI 10.1007/978-1-4614-3348-4_4,

a substantial portion of the biomass decomposes in a relatively short time to CO_2. As a result, increased biomass production (i.e., by increased tree growth) is of limited utility for carbon sequestration since the resulting biomass soon returns the absorbed CO_2.

Unlike untreated biomass, carbonized biomass (i.e., charcoal or "biochar") contains carbon in a highly stabilized state, i.e., as elemental carbon. The inertness of elemental carbon results in its very slow decomposition to CO_2. Typically, at least several 100 years are necessary for the complete decomposition of biochar to CO_2. Through a ^{14}C labeling study, the mean residence time of pyrogenic carbon in soils has now been estimated in the range of millennia [2]. As a result, there is great interest in producing biochar as a means for mitigating atmospheric CO_2 production. There is particular interest in incorporating produced biochar into soil (i.e., as a soil amendment) where the biochar functions both as a CO_2 sequestrant and as a soil amendment [3].

Biochar production and incorporation into soil has been practiced since ancient times. Of particular relevance is the recent discovery of biochar particles in soils formed by pre-Columbian indigenous agriculturalists in Amazonia, i.e., the so-called Terra Preta soil [4].

The capacity of carbon sequestration by the application of biochar fertilizer is estimated to be quite significant. The amount of biochar materials that could be placed into soil could be as high as 10% by weight of the soil [5]. Accordingly, in the first 30-cm layer of US cropland soil alone, 40 Gt of carbon could be sequestered in the form of biochar particles. The worldwide capacity for storing biochar carbon in agricultural soils could exceed 400 Gt of carbon. A conversion as low as 8% of the annual terrestrial photosynthetic products (110 Gt C y^{-1}) into stable biochar material would be sufficient to offset the entire amount (over 8 Gt C y^{-1}) of CO_2 emitted into the atmosphere annually from the use of fossil fuels.

Significant amounts of biochar are currently being produced as a byproduct in biomass-to-biofuel production processes. The most common biomass-to-biofuel production processes include low temperature and high temperature pyrolysis (i.e., gasification) processes [6, 7]. Pyrolysis operations generally entail combusting biomass in the substantial absence of oxygen. Biofuels commonly produced in low temperature pyrolysis operations include hydrogen, methane, and ethanol. Gasification processes are generally useful for producing syngas (i.e., H_2 and CO).

An important property of biochar is its cation-exchanging ability. The cation-exchanging ability or lack thereof of a biochar is evident by the magnitude of its cation exchange capacity (CEC). It is known that biochar which has an increased CEC generally possesses a greater nutrient retention capability. These biochars with greater CEC generally possess a significant amount of hydrophilic oxygen-containing groups, such as phenolic and carboxylic groups, which impart the greater cation exchange ability [7].

The CEC is defined as the amount of exchangeable cations (e.g., K^+, Na^+, NH_4^+, Mg^{2+}, Ca^{2+}, Fe^{3+}, Al^{3+}, Ni^{2+}, and Zn^{2+}) bound to a sample of soil. CEC is often expressed as centimoles (cmol) or millimoles (mmol) of total or specific cations per kilogram (kg) of soil. A substantial lack of a cation-exchanging property is generally considered to be reflected in a CEC of less than 50 mmol kg^{-1}. A moderate CEC is typically

considered to be within the range of above 50 and at or less than 250 mmol kg^{-1}. An atypical or exceptionally high CEC would be at least 250 mmol kg^{-1}.

Though biochar is generally considered useful for CO_2 sequestration, the types of biochar found in ancient soils or produced as an industrial byproduct are highly variable in their physical and property characteristics, e.g., chemical composition, porosity, charge density, and CEC. One of the most common production processes of biochar is the practice since ancient times of burning biomass in open pits. Such uncontrolled processes generally produce significant quantities of oxide gases of combustion, such as CO_2 and CO, generally in amounts significantly greater than 20% by weight of the carbon content of the biochar source. In addition, the resulting biochar is highly nonuniform in composition, e.g., substantially nonoxygenated portions particularly in the interior portions of the biochar pit and moderately oxygenated portions at the outer peripheral portions of the biochar pit. Furthermore, the uncontrolled process generally results in significant batch-to-batch variability. Moreover, by the uncontrolled process, the characteristics of the resulting biochar are generally unpredictable and not capable of being adjusted or optimized.

Though biochar materials possessing moderate cation exchange capacities are known, such biochar compositions are not typical, and moreover, are found sporadically and in unpredictable locations of the world. Therefore, there is a need for a method that produces oxygenated biochar compositions which have at least a moderate CEC, and more preferably, a CEC significantly higher than found in known soil deposits. Such biochar materials would have the advantage of more effectively retaining soil nutrients, and thus, functioning as superior fertilizing/soil amending materials as well as sequestering carbon.

In order to make such superior biochar materials readily available for widespread soil application, the biochar must be reproducibly manufactured with low batch-to-batch variation in one or more characteristics of the biochar (e.g., CEC, particle size, porosity, C:O ratio, and the like) and should be substantially uniform in its characteristics, such as oxygen-to-carbon ratio, CEC, and chemical composition. Further, the production method needs to able to be appropriately modified in order to obtain adjustment or optimization in one or more properties dependent on desired application and source feed stock. In the remainder of this chapter, we discuss several technology concepts to achieve these goals.

2 Technological Concept to Produce Partially Oxygenated Biochar with Higher Cation Exchange Capacity

The key concept is the production of a partially oxygenated biochar material, which possesses enhanced cation-exchanging property. The technology concept is based on our recent experimental finding that the oxygen (O) to carbon (C) atom (O:C) ratio in biochar material correlates with its cation-exchange capacity [8, 9]. This makes sense, since the cation-exchanging groups are generally oxygen-containing chemical groups, such as hydroxy (–OH) and carboxyl (–COOH) groups. The cation-exchanging

ability of a biochar is known to be predominantly dependent on the density of cation-exchanging groups present in the biochar. This biochar CEC-enhancing technology comprises a series of methods described below.

In one of the proposed methods, a biochar source is reacted with one or more oxygenating compounds in a controlled manner such that the biochar source homogeneously acquires oxygen-containing cation-exchanging groups in an incomplete combustion process. An "incomplete combustion process" means that a significant portion of the total carbon content in the biochar source remains and is not converted to oxide gases of combustion after the oxygenation process is completed. Oxide gases of combustion typically include, for example, CO_2, H_2O, and CO. No more than about 20% by weight of the carbon contained in the biochar source should be lost due to combustion, and preferably, only between 1 and 10% by weight of the carbon contained in the biochar source is converted to combustion gases. The best yield of biochar can be obtained from a combustionless process, in which substantially none (e.g., less than 0.5% by weight) of the carbon content of the biochar source is lost through conversion to oxide gases.

In contrast to the typically used, highly uncontrolled combustion processes, the method described here uses a highly controlled oxygenation process that results in the partial oxidation of biochar material, such that a biochar with a cation exchange property could be produced while advantageously emitting much lower amounts of oxide gases of combustion. Moreover, due in large part to the controlled nature of the oxygenation process, this method produces a substantially uniform and homogeneously oxygenated biochar. In this context, "substantially uniform" means that there is an absence in the oxygenated biochar of regions of nonoxygenated biochar (as commonly found in biochar material formed under uncontrolled conditions, such as in open pits). A substantially uniform oxygenated biochar will possess different macroscopic regions of 100 μm^2 to 1 cm^2 in size that vary by no more than 0.1–10% in at least one characteristic, such as CEC, oxygen to carbon ratio, and/or surface area. The substantial uniformity of the oxygenated biochar advantageously provides a user with a biochar material that gives a consistent result when distributed into soil, either packaged or in the ground. Furthermore, a substantial uniformity of the oxygenated biochar ensures that a tested characteristic of the biochar is indicative of the entire batch of biochar.

This method ensures production of a substantially uniform biochar by an effective level of mixing of the biochar during the oxygenation process. For example, biochar can be agitated, shaken, or stirred either manually or mechanically during the oxygenation process. In another example, the biochar can be reacted in an open or closed container such as a kiln fitted with a tumbling mechanism such that the biochar is tumbled and mixed during the oxygenation reaction.

The biochar source can be any biochar material that could benefit by the oxygenation process of the inventive method. In addition to raw biomass, byproducts of a pyrolysis or gasification process, or material acquired from an existent biochar deposit can be used. Generally, the biochar is plant-derived (i.e., derived from cellulosic biomass or vegetation). The plant-derived biomass materials include: cornstover (e.g., the leaves, husks, stalks, or cobs of corn plants), grasses (e.g., switchgrass,

miscanthus, wheat straw, rice straw, barley straw, alfalfa, bamboo, hemp), sugarcane, hull or shell material (e.g., peanut, rice, and walnut hulls), woodchips, saw dust, paper or wood pulp, food waste, agricultural waste, and forest waste. The biomass material can be in its native form, i.e., unmodified except for natural degradation processes or the biomass material can be modified by adulteration with a non-biomass carbon-based material (e.g., plastic- or rubber-based materials) or by physical modification (e.g., mashing, grinding, compacting, blending, heating, steaming, bleaching, nitrogenating, oxygenating, or sulfurating), before being converted to biochar.

The oxygenating compounds that are used include any general use compounds or materials that tend to be reactive by imparting oxygen atoms into organic materials. Most notable in this regard is oxygen gas, in the form of air. The oxygen gas may also be in an artificial gas mixture, such as an oxygen–nitrogen, oxygen–argon, oxygen–helium, oxygen–steam (H_2O), or oxygen–carbon dioxide mixture. An artificial gas mixture can be advantageous in that the level of oxygen can be precisely controlled, thereby preventing combustion and optimizing the density and kind of oxygen-containing groups in the biochar. Some examples of other oxygenating compounds include the hypohalites (e.g., a hypochlorite salt, such as NaOCl), the halites (e.g., a chlorite or bromite salt, such as NaO_2Cl or NaO_2Br), the halates (e.g., a chlorate or bromate salt, such as NaO_3Cl or NaO_3Br), the perhalates (e.g., a perchlorate, perbromate, or periodate salt, such as NaO_4Cl, NaO_4Br, or NaO_4I), the halogen–oxygen compounds (e.g., ClO_2), the peroxides (e.g., H_2O_2 and urea peroxide), superoxides (e.g., NaO_2 and KO_2), ozone, pyrosulfates (e.g., NaS_2O_7), peroxodisulfates (e.g., $Na_2S_2O_7$, $K_2S_2O_7$, and $(NH_4)_2S_2O_7$), percarboxylic acids (e.g., peracetic acid), percarbonates, and permanganates (e.g., K_2MnO_4). Alternatively, oxygenation can be carried out with two or more chemicals that react with each other to form oxygen gas in situ (e.g., a permanganate salt or hypohalite combined with hydrogen peroxide).

In another version of this method shown in Fig. 1, the biochar source is treated with an oxygen plasma. Any of the oxygen plasma processes, including high and low temperature plasma processes, can be used to introduce oxygen into the biochar materials to increase their O:C ratios, and, concomitantly, their CEC. Thus, the technological concept described here includes oxygen plasma treatment as a treatment that improves CEC by enhanced "partial oxygenation" of the biochar materials.

Preferably, a low temperature oxygen plasma (e.g., 15–30°C), commonly used for surface modification and cleaning, is used. Generally, the plasma process entails subjecting the biochar at reduced pressure (i.e., in a vacuum chamber) to a source of ionized oxygen or oxygen radicals. The ionized source of oxygen is typically produced by exposing oxygen at a reduced pressure of about 0.05–2 Torr to an ionizing source, such as an ionizing microwave, radiofrequency, or current source. Commonly, a radiofrequency source (e.g., of 13.56 MHz at an RF power of about 10–100 W) is used to ionize the oxygen. The particular oxygen plasma conditions depend on several factors, including the type of plasma generator, gas composition, power source capability and characteristics, operating pressure and temperature, the degree of oxygenation required, and characteristics of the particular biochar being treated (i.e., its susceptibility or resistance to oxygenation). Depending on several factors,

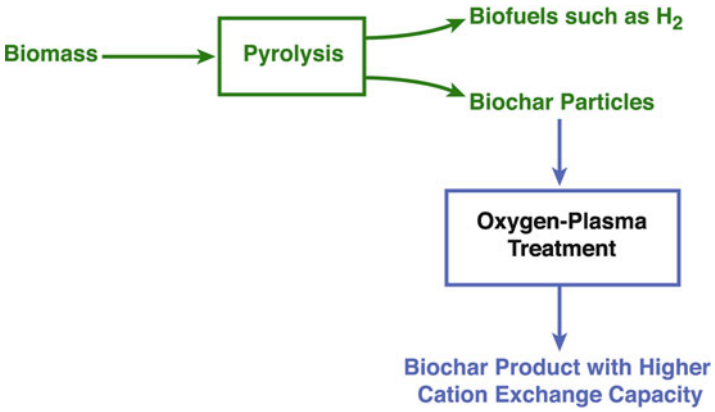

Fig. 1 This figure illustrates the application of oxygen-plasma treatment as an integrated or post-biochar-production processing technology to create biochar product with higher cation-exchange capacity

including those mentioned above, the biochar is typically exposed to the ionized oxygen for at least 0.1–5 min, with times as long as 60 min possible. Though the biochar is typically plasma treated within a temperature range of about 15–30°C, a lower temperature (e.g., less than 15°C) or a higher temperature (e.g., between 30 and 100°C) may be used. Generally, an oxygen plasma process is conducted as a combustionless process, i.e., without producing oxide gases of combustion.

Another possible method is the treatment of a biochar source with one or more oxygenating compounds (typically, oxygen in the form of air) at a temperature at which the oxygenating compound is reactive enough to impart oxygen-containing cation-exchanging groups to the biomass, i.e., at a suitably reactive temperature, wherein the amount of the oxygenating compound and/or time of reaction is appropriately adjusted such that the biochar acquires the cation-exchanging groups in an incomplete combustion process. The reaction can be conducted as a combustionless process. Highly reactive oxygenating compounds can typically function effectively at room temperature (e.g., 15–30°C) or even lower temperatures (e.g., less than 15°C). Moderately reactive oxygenating compounds (e.g., oxygen) can typically function effectively within a temperature range of 100–950°C. Longer reaction times generally yield a more oxygenated biochar whereas shorter reaction times generally yield a less oxygenated biochar. Therefore, a moderately reactive or substantially unreactive oxygenating compound may effectively oxygenate biochar by use of a temperature of or less than 100°C if a sufficient period of time is used, ranging from at least 12 h to as long as 3 months.

Alternatively, an incomplete combustion process is attained by limiting the amount of oxygenating compound to an amount less than that required for complete combustion of the biochar source. A permissible amount of oxygenating compound less than required for complete combustion can be determined based on the amount of carbon contained in the biochar source, from which an amount of oxygenating compound less than required for complete combustion is calculated. The amount of

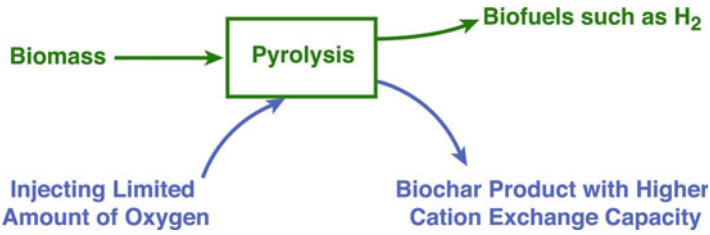

Fig. 2 This figure illustrates a process of injecting a calculated/limited amount of oxygen (O_2) into the biomass-pyrolysis process to achieve partial oxidation of product biochar for enhanced cation-exchange capacity

carbon contained in the biochar sample can be determined by either an accurate measurement (e.g., by elemental analysis) or by an approximation (e.g., by weighing, and assuming nearly all of the weight to be from carbon materials). The amount of oxygenating compound is preferably no more than about 20–30% of the moles of oxygenating compound required for complete combustion of the biochar, and, preferably, in the range of 0.1–15%.

The oxygenating compound can be reacted with biochar in a closed system in order to ensure that the intended amount of oxygenating compound as measured is reacted with the biochar. When an oxygenating solid or liquid oxygenating compound is used, the solid or liquid can be weighed into the closed container along with the biochar source and the contents homogeneously mixed or blended under conditions suitable for oxygenation of the biochar to take place. For example, the temperature of the mixed reactants in the container can be raised along with proper agitation until the solid or liquid becomes suitably vaporized in order to promote uniform reaction with the biochar. When an oxygenating gas is used, a selected volume of the gas corresponding to a calculated weight or moles of the gas can be charged into the closed system along with the biochar source before raising the temperature for more efficient oxygenation of the biochar. This could be applied also as a part of the biomass-pyrolysis process by injecting the calculated, limited amount of oxygen or air into the reactor system as illustrated in Fig. 2. Alternatively, the process is simplified to opening the closed container containing an amount of biochar to cause the container to fill with air, and then closed before proceeding with the heating process, thereby resulting in the addition of a limited amount of air.

Particularly when air or an artificial oxygen-gas mixture is used, the reactants are typically placed in a heatable closed system (i.e., a thermally insulated chamber), such as an oven, kiln, or furnace. The heatable closed system can be any suitable system typically operated or assisted by, for example, a flame (e.g., from a natural gas source), electricity, or microwaves. The kiln can be any of the downdraft, updraft, cross draft, fluid bed, or rotating kilns. The heatable closed system can also be one configured to adjust the moisture level of the biochar. The moisture level can be suitably adjusted to a humidity level anywhere between 1 and 100%. The reactants are heated in the closed chamber to a temperature or temperature range between 100 and 550°C. Heating can advantageously be minimized or altogether dispensed with

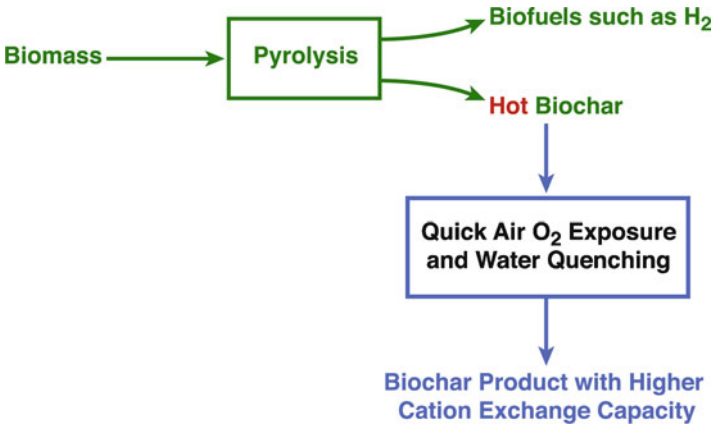

Fig. 3 This figure illustrates a process of quick air O_2 exposure and water quenching of hot biochar as a post-biochar-production processing means to create biochar product with higher cation-exchange capacity

by reacting still hot biochar (i.e., as rendered hot by a biomass-to-biochar production process) under the oxygenating conditions of the invention. In this case, the hot biochar should be at a temperature between 250 and 450°C, or around 400°C.

In another variant of the method, the biochar and one or more oxygenating reactants are reacted for a period of time necessary for substantially all of the oxygenating reactant in a closed container to be consumed. The conditions of temperature and/or time can also be selected such that only a portion of the oxygenating reactant in a closed container is consumed.

An incomplete combustion process is attained by conducting the oxygenation reaction in an open or closed container and rapidly quenching the reaction. As illustrated in Fig. 3, the reaction can be quenched by contacting the reacting biochar with an excessive amount of water and/or an inert substance, preferably when the biochar material is still hot, e.g., at a temperature of 150–450°C, as produced from a biomass-to-biochar process. The inert substance can be carbon dioxide or a form of biomass (e.g., soil, plant-material, or the like). The water and/or inert substance should preferably cover all of the reacting biochar, or alternatively, function as a bulk surface shield of the biochar, with the result that the oxygenating process (including a combustion process, if occurring) is immediately halted due to restricted access of the oxygenating compound to the biochar. If an elevated temperature is being used in the oxygenation process, the quenching step also typically has the effect of rapidly reducing the temperature of the biochar. A quenching step can alternatively be practiced by rapid sealing of an open container in which air-combustion of biochar is taking place.

The method described here can also include one or more preliminary steps for producing biochar (i.e., the biochar source or "produced biochar") from biomass before the biochar is oxygenated. The biomass-to-biochar process can be conducted within any suitable time frame before the produced biochar is oxygenated.

A biomass-to-biochar process can be conducted in a nonintegrated manner with the biochar oxygenation process. In the nonintegrated process, biochar produced by a biomass-to-biochar process is transported to a separate location where the biochar oxygenation process is conducted. The transport process generally results in the cooling of the biochar to ambient temperature conditions (e.g., 15–30°C) before oxygenation occurs. Typically, the produced biochar is packaged and/or stored in the nonintegrated process before oxygenation of the biochar.

A biomass-to-biochar process can be conducted in an integrated manner with a biochar oxygenation process. In the integrated process, biochar produced by a biomass-to-biochar process is oxygenated in situ without first being cooled to ambient temperature. For example, freshly produced biochar can have a temperature in the range of 50–450°C, before it is oxygenated. If desired, the freshly produced biochar can be subjected to additional heating to elevate and/or maintain its temperature before the oxygenation step.

The biochar oxygenation process can be integrated with a biomass-to-fuel process, such as a low temperature or high temperature pyrolysis process. In such processes, typically about 40–60% of the biomass carbon is converted into biochar while the remaining 40–60% of the carbon is converted to fuel, such as H_2 and/or bio-oils. Since it has been found that lower temperature pyrolysis processes generally yield a biochar material with better fertilizer retention properties, the biochar oxygenation process is best integrated with a biomass pyrolysis process conducted at temperatures of 350–450°C.

The integrated process can be configured as a batch process wherein separate batches of produced biochar are oxygenated at different times. The integrated process can also be configured as a continuous process wherein which biochar produced by the biomass-to-biochar process is continuously subjected to an oxygenation process as it is produced. For example, produced biochar can be continuously transported either manually or by an automated conveyor mechanism through a biochar oxygenation zone. The automated conveyor mechanism can be a conveyor belt, gravity-fed mechanism, or air pressure mechanism.

The technology concept is based on the utility of an oxygenated biochar having a particular, exceptional, or optimal set of characteristics, exemplified in the oxygen-to-carbon molar ratio, CEC, surface area, composition, and uniformity in these and other characteristics. The methods described above are particularly suitable for producing these types of biochars.

Dependent upon the reaction conditions, the CEC of the oxygenated biochar is at least moderate, that is, between 50 and 240 mmol kg^{-1}, while preferably the CEC of the oxygenated biochar could be atypically or exceptionally high, in the range of 250–850 mmol kg^{-1}. The CEC value should be substantially uniform throughout the biochar material.

The density of oxygen-containing cation-exchanging groups is typically proportional to the measured oxygen-to-carbon molar ratio of the biochar, wherein the higher the oxygen-to-carbon molar ratio, the greater the density of cation-exchanging groups in the biochar. The oxygen-to-carbon molar ratio of the oxygenated biochar is preferably adjusted within a range of 0.1:1–0.4:1 that is substantially uniform throughout the biochar material.

The oxygenated biochar should have a suitable specific surface area (SSA), as commonly determined by BET analysis, typically within the range 10–65 $m^2\ g^{-1}$ and suitable pore size up to 100,000 nm. The oxygenated biochar has a suitable charge density in the range of 1–75 mmol m^{-2}. It can have any suitable carbon, nitrogen, oxygen, hydrogen, phosphorous, calcium, sulfur, ash, and volatile matter content. The carbon content is typically 20–95 mol%, the nitrogen content 0.1–8.0 mol%, the oxygen content 1–30 mol%, and the hydrogen content 1–30 mol%. The phosphorus and calcium content can range from 5 to 25,000 mg kg^{-1} while the sulfur content is in the range of 50–2,000 ppm. The ash content ranges from 1 to 70% and the volatile matter content 1–40%.

The particle size of the oxygenated biochar should range between 50 and 5,000 μm. For certain applications for which it is important to ensure that the biochar materials are resistant to becoming airborne, such as use in windy and/or desert areas, larger biochar particle sizes, such as 6,000–50,000 μm, or even up to 100,000 μm will be desirable. The biochar materials may also be in the form of an agglomeration, compaction, or fusion of biochar particles (e.g., pellets or cakes) for this type of application as well.

Soil-fertilizing compounds or materials can be mixed with the oxygenated biochar to enrich it. Suitable soil-fertilizing compounds include nitrogen-based (e.g., ammonium-based), carbonate-based (e.g., $CaCO_3$), phosphate-based (e.g., the known phosphate minerals, such as in rock phosphate or triple superphosphate), and potassium-based (e.g., KCl). Typically, the added compounds or materials would include at least one nitrogen source, usually NH_4^+-containing compound or material. Some examples of such nitrogen-containing fertilizing compounds or materials are $(NH_4)_2CO_3$, NH_4HCO_3, NH_4NO_3, $(NH_4)_2SO_4$, $(NH_2)_2CO$, biuret, triazine-based materials (e.g., melamine or cyanuric acid), urea–formaldehyde resin, and polyamine or polyamide polymers. Organic fertilizers can be mixed with the biochar. Some examples of organic fertilizer materials include peat moss, manure, insect material, seaweed, sewage, and guano. The biochar material can be combined with a fertilizer by any of a number of commonly used methods. For example, the biochar material can be saturated with a gas stream of hydrated ammonia to saturate the biochar material. Fertilizer compounds may also be applied as a coating to the biochar material, utilizing standard formulations for time-release of the fertilizer if desired.

Obviously, soil will be admixed with any of the various biochar compositions described above. The oxygenated biochar can potentially be used to improve soil of any type and composition and should be compatible with common soil components, such as clay, sand, silt, plant matter containing lignin and cellulose, peat, and humic substances.

In summary, this technology comprises a series of proposed methods to produce partially oxygenated biochar products with enhanced CEC properties for applications as a soil amendment and carbon sequestration agent. A further detailed description of the technology concept can be found in our recent US Patent application [10]. Application of biochar as soil amendment is potentially a revolutionary approach in achieving carbon sequestration globally at Gt C scales [11]. An improved biochar soil amendment material with enhanced CEC properties is beneficial to helping

retain soil nutrients, reduce fertilizer run off, and ensure the associated soil and hydrologic environmental health. Therefore, this biochar CEC-enhancing technology could play a significant role in helping achieve this mission.

Acknowledgments This technology concept was funded through a subcontract from Iowa State University under USDA Grant No. 68-3A75-5-233 at Oak Ridge National Laboratory, managed by UT-Battelle, LLC, for DOE under contract No. DE-AC05-00OR22725. MKK and ACB were funded in part by the Division of Chemical Sciences, Geosciences and Biosciences, Office of Basic Energy Sciences, US Department of Energy.

References

1. Geider RJ, Delucia EH et al (2001) Primary productivity of planet earth: biological determinants and physical constraints in terrestrial and aquatic habitats. Glob Chang Biol 7(8):849–882
2. Kuzyakov Y, Subbotina I, Chen H, Bogomolova I, Xu X (2009) Black carbon decomposition and incorporation into soil microbial biomass estimated by ^{14}C labeling. Soil Biol Biochem 41:210–219
3. Day D, Evans RJ, Lee JW, Reicosky D (2005) Economical CO_2, SOx, and NOx capture from fossil-fuel utilization with combined renewable hydrogen production and large-scale carbon sequestration. Energy 30:2558–2579
4. Liang B, Lehmann J, Solomon D, Kinyangi J, Grossman J, O'Neill B, Skjemstad JO, Thies J, Luizão FJ, Peterson J, Neves EG (2006) Black carbon increases cation exchange capacity in soils. Soil Sci Soc Am J 70:1719–1730
5. Gundale MJ, DeLuca TH (2007) Charcoal effects on soil solution chemistry and growth of Koeleria macrantha in the ponderosa pine/Douglas fir ecosystem. Biol Fertil Soils 43:303–311
6. Antal MJ, Gronli M (2003) The art, science, and technology of charcoal production. Ind Eng Chem Res 42(8):1619–1640
7. Das KC, Singh K, Adolphson R, Hawkins B, Oglesby R, Lakly D, Day D (2010) Steam pyrolysis and catalytic steam reforming of biomass for hydrogen and biochar production. Appl Eng Agric 26(1):137–146
8. Lee JW, Kidder M, Evans BR, Paik S, Buchanan AC III, Garten CT, Brown RC (2010) Characterization of biochars produced from cornstovers for soil amendment. Environ Sci Technol 44:7970–7974
9. Lee JW, Kidder M, Evans BR, Li X, Paik S, Buchanan AC, Garten CT, Hawkins B, Day D (2012) Characterization of biochars produced from peanut hulls and pine wood in relation to soil amendment and carbon sequestration. In prep for submission to Energ Environ Sci
10. Lee JW, Buchanan AC, Kidder M, Evans R (2010) Enhancing cation-exchange capacity of biochar for soil amendment and global carbon sequestration. U.S. Patent Application Publication No. US 2011/0172092 A1
11. Lee JW, Hawkins B, Day DM, Reicosky DC (2010) Sustainability: the capacity of smokeless biomass pyrolysis for energy production, global carbon capture and sequestration. Energ Environ Sci 3(11):1609–1812

Chapter 5
Characterization of Biochars Using Advanced Solid-State ^{13}C Nuclear Magnetic Resonance Spectroscopy

Jingdong Mao, Xiaoyan Cao, and Na Chen

Abstract In this chapter, we first briefly reviewed the knowledge of biochar chemical structures based on solid-state NMR. Then, the reason why the widely applied ^{13}C cross polarization/magic angle spinning (CP/MAS) technique is inappropriate for biochar characterization was explained. Afterwards, advanced solid-state NMR techniques for the characterization of biochars were introduced. ^{13}C direct polarization/magic angle spinning (DP/MAS) and DP/MAS with recoupled dipolar dephasing to quantify biochars are used to obtain quantitative aromaticity and nonprotonated aromatic fraction. The recoupled ^{1}H–^{13}C dipolar dephasing technique is applied to distinguish different aromatic carbons in biochars. Combined with the data from ^{1}H–^{13}C recoupled long-range dipolar dephasing, the information on the fraction of aromatic edge carbons can be used to obtain the structural models of aromatic cluster sizes. Finally, a case study on a slow-pyrolysis biochar produced from switchgrass was demonstrated.

1 Introduction

The conversion of biomass, such as switchgrass and corn stover, into renewable energy products has been widely investigated owing to the concerns over global warming and limited petroleum resources [4, 9]. This process can be achieved through the thermochemical route [5]. Thermochemical processing of biomass produces significant biochars. If wisely used, biochars can be beneficial resources but otherwise they could be wastes. Biochars have been used as soil conditioners, carbon sequestration agents, and adsorption agents [3, 12]. In addition, their

J. Mao (✉) • X. Cao • N. Chen
Department of Chemistry and Biochemistry, Old Dominion University,
Norfolk, VA 23529, USA
e-mail: JMao@odu.edu

J.W. Lee (ed.), *Advanced Biofuels and Bioproducts*, DOI 10.1007/978-1-4614-3348-4_5,

combustion can supply process heat [2]. In order to utilize biochars beneficially, the first step is to characterize them.

Various techniques have been employed to characterize biochars. Among them, solid-state NMR is regarded as one of the best choices because (1) it is nondestructive, (2) it can measure insoluble organic matter, and (3) it also provides comprehensive structural information [15]. However, solid-state NMR has been underutilized in the characterization of biochars and most seriously it has been applied inappropriately in many studies, leading to distorted structural information on chars. In this chapter, we first provide a short review about the chemical structure of biochars obtained from solid-state ^{13}C NMR. Next, the reason why the most-widely used ^{13}C cross polarization/magic angle spinning (CP/MAS) technique is inappropriate for biochar characterization is addressed. Then, the quantitative approach for char characterization using direct polarization (DP) techniques is introduced. Afterwards, the advanced solid-state NMR protocol for estimating aromatic cluster sizes of biochars is dealt with. To conclude, the characterization of biochars by advanced solid-state NMR techniques is demonstrated using a slow-pyrolysis biochar produced from switchgrass as an example. The major objective of this chapter is to clarify the misleading concepts regarding the characterization of biochars using solid-state NMR spectroscopy and to introduce advanced solid-state NMR techniques for biochar characterization.

2 Knowledge of Biochar Chemical Structure from Solid-State ^{13}C NMR

Various solid-state ^{13}C NMR techniques, such as CP/MAS and occasionally DP technique, have been employed to identify carbon functionality and aromaticity of biochars [1, 3, 7, 8, 10, 11, 13, 19, 23, 26]. In these studies, chemical structure of biochars to a greater extent depends upon the pyrolysis temperature, but is not much affected by heating rate and the nature of biomass [1, 13]. Biochars prepared at relatively low temperatures up to ~350°C retain spectral features of the original lignocellulosic composition of biomass [25]. For example, characteristic peaks of cellulose (*O*-alkyl carbons around 62, 72, 84 ppm, and di-*O*-alkyl carbons around 103 ppm), as well as those of lignin (methoxyl carbons ~57 ppm, aromatic carbons ~130 ppm, and aromatic C–O ~150 ppm) can still be observed in spectra of biochars within this temperature range (<350°C). For higher heat treatment temperature (HTT) biochars, a well-defined aromatic resonance evolves simultaneously with the decrease of the lignocellulosic resonances and signals of aliphatic, carboxyl, and carbonyl carbons. Lignin structures are more thermally stable than cellulose structures because characteristic peaks of lignin such as the phenolic shoulders around 150 ppm can survive even at temperatures about ~550°C [25]. For HTT about 600°C upwards, the general shapes of the ^{13}C NMR spectra of biochars are very alike, with a strong broad resonance line near 128 ppm in the aromatic region [1, 8, 22, 25].

Chemical transformation of lignocellulosic materials into graphitic structures with the temperatures between 800 and 1,000°C is well documented [1, 13, 25]. Aromatic cluster typical of chars is also reported to grow with increasing HTT [21].

3 Why Is ^{13}C Cross Polarization/Magic Angle Spinning Inappropriate for Biochar Characterization?

Solid-state ^{13}C NMR spectroscopy has been frequently employed to characterize organic matter. The most-commonly used technique is ^{13}C CP/MAS. In this technique, the magnetization from abundant ^{1}H is transferred to dilute ^{13}C by cross polarization and then ^{13}C magnetization is detected [20]. Its recycle delays depend on T_1^H (^{1}H spin–lattice relaxation time), rather than T_1^C (^{13}C spin–lattice relaxation time) [15]. Usually, T_1^H is much shorter than T_1^C. Therefore, this technique has the advantages of both enhancing sensitivity and shortening recycle delays. The combination of these two factors substantially reduces the measurement time. Despite its advantages, CP has inherent shortcomings which render it unreliable for biochar characterization, especially for quantitative characterization. For CP/MAS, CP efficiency is reduced for nonprotonated carbons, mobile components, or regions having short proton rotating-frame spin–lattice relaxation time ($T_{1\rho}^H$) [16]. Note that biochars usually contain significant nonprotonated fused-ring aromatic carbons. Fused-ring aromatic carbons are far away from protons, cannot cross polarize well with ^{1}H, and are thus difficult to detect by CP. Also, the biochars produced via pyrolysis contain significant radicals which shorten $T_{1\rho}^H$ [8]. These two problems cause significant signal loss, especially for fused-ring aromatics in biochars. Compared with quantitative DP, ^{13}C CP/MAS can only detect approximately 1/3 the aromaticity that ^{13}C DP/MAS can detect [3]. Solid-state ^{13}C CP/MAS with either regular CP or ramp CP cannot be used to quantify chars [15]. In extreme cases, ^{13}C CP/MAS may not even be able to provide qualitative structural information of chars.

4 Quantitative Structural Information Based on ^{13}C Direct Polarization/Magic Angle Spinning and DP/MAS with Recoupled Dipolar Dephasing

Realizing the drawbacks of CP, the char community starts to use DP to characterize chars [7]. In our protocol, we use ^{13}C DP/MAS and DP/MAS with recoupled dipolar dephasing to quantify biochars, especially to obtain quantitative aromaticity and nonprotonated aromatic fraction [17]. DP/MAS NMR is more robust to small missettings of spectrometer than is ^{13}C CP/MAS because no Hartmann-Hahn match of the radio-frequency field strengths is needed.

For ^{13}C DP/MAS spectra in the literature, there are usually two problems. The first is that they do not have a reliable technique to estimate the recycle delays required to obtain a fully relaxed spectrum. If recycle delays are not long enough and the signals of some components not fully relaxed before the next scan, then the DP/MAS spectra acquired would not be quantitative. However, if the recycle delays are set longer than necessary excessive measurement time would be required. The second problem is that their pulse sequences lack Hahn echo, which would lead to baseline distortion due to dead-time effects. To obtain reliable recycle delays before DP/MAS experiments, we use the cross polarization/spin–lattice relaxation time/total suppression of sidebands (CP/T_1-TOSS) technique to make sure that all carbon sites are relaxed to <5% within the recycle delays [16]. The detailed principle of this technique can be found elsewhere [16, 18]. Briefly, the *z*-period t_z in CP/T_1-TOSS is increased, typically from 1 ms through 5, 20, 40, 60, 100 s, and so on. These spectra are collected until the one with residual intensity <5% compared with the 1-ms CP/T_1-TOSS spectrum which is used as a reference spectrum. The z-period for the spectrum with the residual intensity less than 5% is the recycle delay which is used for the DP/MAS experiment. The advantage of the CP/T_1-TOSS experiment over inversion- or saturation-recovery experiments is that we know the fully relaxed value of the magnetization, which is zero. Therefore, with this approach we avoid the use of very long, unnecessary delay times. Moreover, in order to avoid spectral distortions, the "EXORCYCLE" phase cycling [18] is also employed for DP/MAS and DP/MAS with recoupled dipolar dephasing with Hahn echo. In addition, we use high-spinning speeds. Unlike CP/MAS, high spinning speeds can be combined with the DP/MAS without problems and thus spinning sidebands are small and do not overlap with the centerbands of other carbon signals.

Since biochars usually contain significant aromatics, especially nonprotonated aromatics, the characterization of nonprotonated aromatics is important for biochar study. We developed a technique called DP/MAS with recoupled dipolar dephasing for obtaining quantitative estimation of nonprotonated carbons and carbons of mobile groups [18]. Although it is very common to use routine 40-μs dipolar dephasing to identify nonprotonated carbons, high spinning speeds are required to obtain quantitative spectra at high fields. On the other hand, at high spinning frequencies, such as 14 kHz, the standard dipolar-dephasing pulse sequence simply with a gated-decoupling time such as 40 μs does not efficiently dephase the protonated carbon signals. This is because at the end of each completed rotation period, magic-angle spinning has at least partially refocused the C–H dipolar coupling [17]. In our method, by recoupling the C–H dipolar interaction using ^{13}C 180° pulse applied at the center of the undecoupled C–H dipolar evolution period, the failure of standard dipolar dephasing at high spinning speeds can be overcome [18]. The combination of DP/MAS with recoupled dipolar dephasing technique with DP/MAS at high spinning speeds allows for the acquisition of quantitative structural information on all carbons as well as nonprotonated carbons and carbons of mobile groups.

5 Selective Detection of Fused-Ring Aromatics by $^{1}H–^{13}C$ Recoupled Long-Range Dipolar Dephasing

Aromatics in biochars are in different chemical environments. For example, there are protonated aromatics, nonprotonated aromatics in the out-layers of aromatic clusters and bridgehead carbons. It is impossible to distinguish these different types of aromatics by using simple ^{13}C CP/MAS or DP/MAS techniques except that advanced solid-state NMR techniques are employed. Our recently developed advanced solid-state NMR technique, recoupled $^{1}H–^{13}C$ dipolar dephasing technique, can be employed to distinguish these aromatics [17]. It is based on long-range dipolar dephasing achieved by recoupling long-range C–H dipolar interactions using two ^{1}H 180° pulses per rotation period [17]. The recoupling fastens the dephasing of nonprotonated carbon signals by about three times compared to the standard dipolar dephasing without recoupling. Therefore, it provides much more efficient differential dephasing of different aromatic carbons. Moreover, this technique reduces the effects of spinning-speed dependent effective proton–proton dipolar couplings on the heteronuclear dephasing. The dephasing rates of individual aromatic rings are significantly faster than those of aromatic sites separated from the nearest protons by three or more bonds, such as those in fused-ring aromatics of biochars. After 0.9 ms of recoupled dipolar dephasing time, the signals of most individual aromatic rings are dephased while those of fused-ring aromatics remain at the 95% level [17]. In order to detect the fused-ring aromatic carbons efficiently which poorly cross polarize and prevent loss of the signals of interest, ^{13}C direct polarization is used. The combination of recoupled dipolar dephasing and direct polarization at 7-kHz MAS enables selective observation of signals from fused rings in biochars [3, 6, 14].

6 Aromatic Cluster Sizes Based on the Fraction of Aromatic Edge Carbons and $^{1}H–^{13}C$ Recoupled Long-Range Dipolar Dephasing

The fraction of aromatic bridgehead carbons (χ_{bridge}) is closely related to aromatic cluster sizes [3, 14]. If the fraction of carbons along the edges of aromatic rings is χ_{edge}, then

$$\chi_{bridge} = 1 - \chi_{edge} \tag{1}$$

Note that χ_{edge} decreases with increasing aromatic cluster sizes. For biochars with dominant aromatics, most of the aromatic edge carbons are aromatic C–H and aromatic C–O functional groups. The fraction of aromatic C–H, $\chi_{CH} = f_{aCH}/f_{ar}$, and that of aromatic C–O, $\chi_{C\text{-}O} = f_{aC\text{-}O} / f_{ar}$, can be determined based on the quantitative ^{13}C DP spectra using the techniques as shown in Sect. 4. Note that f_{aCH}, $f_{aC–O}$ and f_{ar} are the percentages of protonated aromatics, aromatic C–O and aromaticity,

respectively. The sum of the fractions of aromatic C–H and aromatic C–O gives the minimum aromatic edge fraction,

$$\chi_{\text{edge,min}} = \chi_{\text{CH}} + \chi_{\text{C-O}} \tag{2}$$

Correspondingly, the maximum bridgehead-carbon fraction would be $\chi_{\text{bridge,max}} = 1 - \chi_{\text{edge,min}}$.

In addition, alkyl C and C=O bonded to the aromatic rings can contribute to the edge carbon fraction. Similar to χ_{CH} and $\chi_{\text{C-O}}$, their fractions can be expressed as χ_{alkyl} and $\chi_{\text{C=O}}$, respectively. With them, we can determine a meaningful upper limit to the edge fraction of biochars,

$$\chi_{\text{edge,max}} = \chi_{\text{edge,min}} + \chi_{\text{alkyl}} + \chi_{\text{C=O}} \tag{3}$$

With $\chi_{\text{edge,max}}$, we can provide a lower limit to the number carbons in an aromatic cluster because along the lines of Solum et al. [24] it can be shown that

$$n_{\text{C,min}} \geq 6 / \chi^2_{\text{edge}} \geq 6 / \chi^2_{\text{edge,max}} \tag{4}$$

where $n_{\text{C,min}}$ is the minimum number of carbons in an aromatic cluster.

With the $n_{\text{C,min}}$, we can propose rough models of the aromatic cluster for a biochar. Moreover, using ^{1}H–^{13}C recoupled long-range dipolar dephasing technique, we can fine-tune the models. In order to achieve this, model compounds with known C–H distances or aromatic cluster sizes are included for calibration.

7 A Case Study on a Slow-Pyrolysis Biochar Produced from Switchgrass

A biochar produced from switchgrass via slow pyrolysis at 500°C [3] is used in this section as an example to demonstrate how we characterize biochars using advanced solid-state NMR techniques, mostly developed by Mao and Schmidt-Rohr. Figure 1 shows the spectra of ^{13}C DP/MAS, DP/MAS with recoupled dipolar dephasing, and CP/TOSS.

These spectra are dominated by aromatic signals around 128 ppm. The comparison of the spectra of DP/MAS and DP/MAS with recoupled dipolar dephasing indicates that most aromatics are nonprotonated (thin and thick lines of Fig. 1a). Only small alkyl signals, such as those from OCH, CCH_2C, and CCH_3 groups, are observed. In addition, small C=O resonances are observed. These alkyl signals are enhanced in the ^{13}C CP/TOSS spectrum due to overrepresentation of protonated carbons by CP (Fig. 1b). Based on the spectra of DP/MAS and DP/MAS with recoupled dipolar dephasing, the percentages of different functional groups are obtained and different parameters, such as aromaticity, $\chi_{\text{edge,max}}$, and n_{C} are derived. The aromaticity, χ_{CH}, $\chi_{\text{edge,min}}$, $\chi_{\text{edge,max}}$, and $n_{\text{C,min}}$, are 94%, 0.37, 0.44, 0.51, and >23 carbons, respectively, based on Sect. 6.

Figure 2 displays the curves of ^{1}H–^{13}C recoupled long-range dipolar dephasing of the biochar as well as those of carbons of model compounds, 3-methoxy benzamide, 1, 8-dihydroxy-3-methylanthraquinone, and lignin. The dephasing curves of model compounds provide the length-scale calibration approximately (Fig. 2).

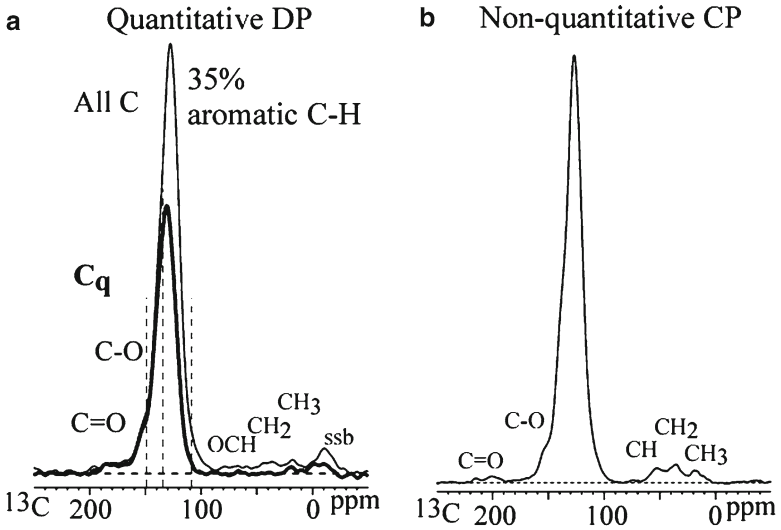

Fig. 1 (**a**) Quantitative ^{13}C DP/MAS spectrum (*thin line*) showing all carbons and the spectrum of ^{13}C DP/MAS with recoupled dipolar dephasing (*thick line*) selecting nonprotonated carbons and mobile CH_3. (**b**) Nonquantitative ^{13}C CP/TOSS spectrum. Note that its alkyl signals are enhanced compared with the DP/MAS spectrum. *ssb* spinning sidebands. The biochar was produced from switchgrass via slow pyrolysis at 500°C

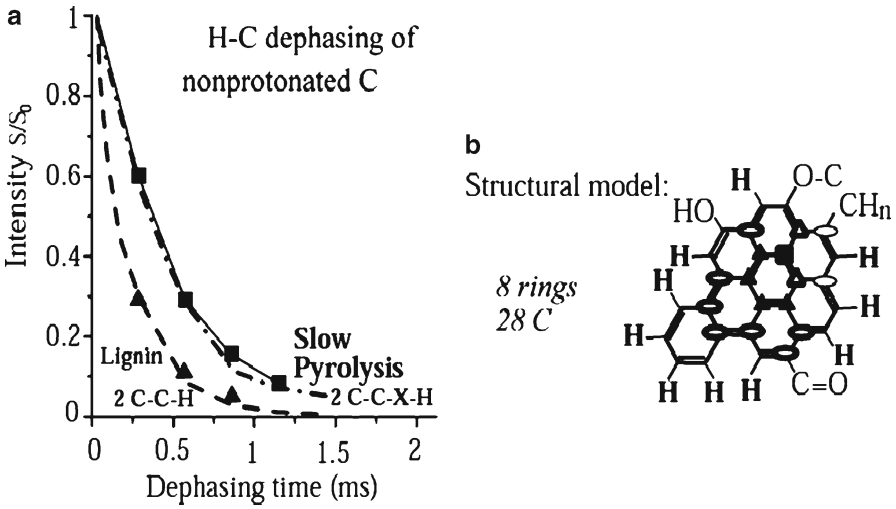

Fig. 2 (**a**) ^1H–^{13}C recoupled long-range dipolar dephasing curves. *Squares*: slow pyrolysis biochar. *Dash-dotted line*: carbons 11 and 13 of 1, 8-dihydroxy-3-methylanthraquinone, which are three bonds away from the two nearest protons. *Dashed line*: carbon 1 of 3-methoxy benzamide, which is two bonds away from the two nearest protons. *Triangles*: lignin. The dephasing rates of lignin and 3-methoxy benzamide are almost the same. (**b**) Structural model. Thin-line ellipse: Two bonds from multiple H. Thick-line ellipse: Two bonds from one H. Open triangle: Three bonds from multiple H. Filled triangle: Three bonds from one H. Filled square: Four bonds from one H, or more than four bonds from any H

The long-range dipolar dephasing curves indicate that the dephasing rate of the biochar almost coincides with the three-bond calibration curve of carbons 11 and 13 of 1, 8-dihydroxy-3-methylanthraquinone. This result indicates that the nonprotonated carbons in this biochar are at a three-bond distance from the nearest ^{1}H on average. Based on the dipolar-dephasing data, $n_{C,min}$ as well as the quantitative percentages of different functional groups obtained from DP, a typical average model of the aromatic cluster for this biochar is proposed, with 8 rings and 28 carbons (Fig. 2b).

Acknowledgments Profs. Klaus Schmidt-Rohr and Robert C. Brown and Ms. Catherine E. Brewer are acknowledged for kindly allowing us to use some of their biochar spectra and data.

References

1. Bardet M, Hediger S, Gerbaud G, Gambarelli S, Jacquot JF, Foray MF, Gadelle A (2007) Investigation with C-13 NMR, EPR and magnetic susceptibility measurements of char residues obtained by pyrolysis of biomass. Fuel 86:1966–1976
2. Boateng AA (2007) Characterization and thermal conversion of charcoal derived from fluidized-bed fast pyrolysis oil production of switchgrass. Ind Eng Chem Res 46:8857–8862
3. Brewer CE, Schmidt-Rohr K, Satrio JA, Brown RC (2009) Characterization of biochar from fast pyrolysis and gasification systems. Environ Prog Sustain Energ 28:386–396
4. Bridgwater T (2006) Biomass for energy. J Sci Food Agric 86:1755–1768
5. Cantrell KB, Ducey T, Ro KS, Hunt PG (2008) Livestock waste-to-bioenergy generation opportunities. Bioresour Technol 99:7941–7953
6. Cao XY, Ro KS, Chappell M, Li YA, Mao JD (2011) Chemical structures of swine-manure chars produced under different carbonization conditions investigated by advanced solid-state ^{13}C nuclear magnetic resonance (NMR) spectroscopy. Energy Fuel 25:388–397
7. Czimczik CI, Preston CM, Schmidt MWI, Werner RA, Schulze ED (2002) Effects of charring on mass, organic carbon, and stable carbon isotope composition of wood. Org Geochem 33:1207–1223
8. Freitas JCC, Bonagamba TJ, Emmerich FG (2001) Investigation of biomass- and polymer-based carbon materials using C-13 high-resolution solid-state NMR. Carbon 39:535–545
9. Hayes MHB (2006) Biochar and biofuels for a brighter future. Nature 443:144
10. Knicker H, Hilscher A, Gonzalez-Vila FJ, Almendros G (2008) A new conceptual model for the structural properties of char produced during vegetation fires. Org Geochem 39:935–939
11. Knicker H, Totsche KU, Almendros G, Gonzalez-Vila FJ (2005) Condensation degree of burnt peat and plant residues and the reliability of solid-state VACP MAS C-13 NMR spectra obtained from pyrogenic humic material. Org Geochem 36:1359–1377
12. Lehmann J, Gaunt J, Rondon M (2006) Bio-char sequestration in terrestrial ecosystems—a review. Mitig Adapt Strat Global Change 11:403–427
13. Link S, Arvelakis S, Spliethoff H, De Waard P, Samoson A (2008) Investigation of biomasses and chars obtained from pyrolysis of different biomasses with solid-state C-13 and Na-23 nuclear magnetic resonance spectroscopy. Energy Fuel 22:3523–3530
14. Mao JD, Fang XW, Lan YQ, Schimmelmann A, Mastalerz M, Xu L, Schmidt-Rohr K (2010) Chemical and nanometer-scale structure of kerogen and its change during thermal maturation investigated by advanced solid-state ^{13}C NMR spectroscopy. Geochim Cosmochim Acta 74:2110–2127
15. Mao JD, Hu WG, Ding GW, Schmidt-Rohr K, Davies G, Ghabbour EA, Xing BS (2002) Suitability of different C-13 solid-state NMR techniques in the characterization of humic acids. Int J Environ Anal Chem 82:183–196

16. Mao JD, Hu WG, Schmidt-Rohr K, Davies G, Ghabbour EA, Xing BS (2000) Quantitative characterization of humic substances by solid-state carbon-13 nuclear magnetic resonance. Soil Sci Soc Am J 64:873–884
17. Mao JD, Schmidt-Rohr K (2003) Recoupled long-range C-H dipolar dephasing in solid-state NMR, and its use for spectral selection of fused aromatic rings. J Magn Reson 162:217–227
18. Mao JD, Schmidt-Rohr K (2004) Accurate quantification of aromaticity and nonprotonated aromatic carbon fraction in natural organic matter by ^{13}C solid-state nuclear magnetic resonance. Environ Sci Technol 38:2680–2684
19. MarotoValer MM, Andresen JM, Rocha JD, Snape CE (1996) Quantitative solid-state C-13 NMR measurements on cokes, chars and coal tar pitch fractions. Fuel 75:1721–1726
20. Pines A, Gibby MG, Waugh JS (1973) Proton-enhanced NMR of dilute spins in solids. J Chem Phys 59:569–590
21. Preston CM, Schmidt MWI (2006) Black (pyrogenic) carbon: a synthesis of current knowledge and uncertainties with special consideration of boreal regions. Biogeosciences 3:397–420
22. Sharma RK, Hajaligol MR, Smith PAM, Wooten JB, Baliga V (2000) Characterization of char from pyrolysis of chlorogenic acid. Energy Fuel 14:1083–1093
23. Sharma RK, Wooten JB, Baliga VL, Martoglio-Smith PA, Hajaligol MR (2002) Characterization of char from the pyrolysis of tobacco. J Agric Food Chem 50:771–783
24. Solum MS, Pugmire RJ, Grant DM (1989) ^{13}C Solid-state NMR of Argonne premium coals. Energy Fuel 3:187–193
25. Solum MS, Pugmire RJ, Jagtoyen M, Derbyshire F (1995) Evolution of carbon structure in chemically activated wood. Carbon 33:1247–1254
26. Zhang XQ, Golding J, Burgar I (2002) Thermal decomposition chemistry of starch studied by C-13 high-resolution solid-state NMR spectroscopy. Polymer 43:5791–5796

Chapter 6
Biochar Fertilizer for Soil Amendment and Carbon Sequestration

James Weifu Lee, Bob Hawkins, Xiaonian Li, and Danny M. Day

Abstract Use of biochar fertilizer is potentially an attractive approach for soil amendment and carbon sequestration possibly at giga tons of carbon (GtC) scale. Cation exchange capacity (CEC) is an important parameter in retaining inorganic nutrients, such as K^+ and NH_4^+ in soil. This experimental study showed that the CEC value of biochar is related to the biomass pyrolysis temperature. Biochar materials made from the pelletized peanut hulls at pyrolysis temperature of about 400°C yield the best CEC value. As the pyrolysis temperature increases over 400°C, the CEC value decreases. The biochar produced from the 400°C pyrolysis possesses certain binding affinity for ammonium bicarbonate (NH_4HCO_3) probably because of the presence of more biochar surface functional groups. Addition of ammonium bicarbonate to biochar can help neutralize the pH of biochar material potentially beneficial for certain agricultural soil applications in relation to soil amendment and carbon sequestration.

J.W. Lee (✉)
Department of Chemistry and Biochemistry, Old Dominion University,
Physical Sciences Building 3100B, Norfolk, VA 23529, USA

Whiting School of Engineering, Johns Hopkins University,
118 Latrobe Hall, Baltimore, MD 21218, USA
e-mail: JLee349@jhu.edu; JWLee@odu.edu

B. Hawkins
BiocharConsulting, 375 Rumson Road, Athens, GA 30605, USA

X. Li
Zhejiang University of Technology, Hangzhou, China

D.M. Day
Eprida Power and Life Sciences, Inc., 6300 Powers Ferry Road, #307,
Atlanta, GA 30339, USA

J.W. Lee (ed.), *Advanced Biofuels and Bioproducts*, DOI 10.1007/978-1-4614-3348-4_6,

1 Introduction

The world currently faces a systematic problem of increased CO_2 emissions, decreased soil-carbon content, and global-climate change (global warming). The mean global atmospheric CO_2 concentration has increased from 280 ppm in the 1,700 s to 380 ppm in 2005 at a progressively faster rate [1] because of: (1) CO_2 emissions from fossil-fuel use; and (2) the CO_2 flux from land-use change, including land clearing such as "slash and burn," agriculture and intensive tillage. In certain areas, agriculture and intensive tillage have also caused a 30–50% decrease in soil organic carbon (SOC) since many soils were brought into cultivation more than 100 years ago [2]. To solve this massive global energy and environmental sustainability problem, it likely requires a comprehensive portfolio of R&D efforts with multiple energy technologies. Application of a modern smokeless biomass pyrolysis process for producing biofuels and biochar is possibly a significant approach for global carbon capture and sequestration [3]. This "carbon-negative" biomass-pyrolysis energy-production concept of applying biochar as a soil amendment and carbon sequestration agent was initiated in 2002 by two of us (Day and Lee) with a provisional US patent application followed by a PCT application [4]. Certain related studies, including biochar-related soil research, have also indicated the possibility of using biochar as a soil amendment for carbon sequestration [5–7]. According to our preliminary analysis, global use of biochar as soil amendment could potentially achieve carbon sequestration at giga tons of carbon (GtC) scale [8].

Globally, each year, there are about 6.6 Gt dry matter of biomass (3.3 GtC), such as crop stovers, that are appropriated but not used [9]. If this amount of biomass (3.3 Gt y^{-1}) is processed through controlled pyrolysis assuming 50% conversion of biomass C to stable biochar C and 33% of the biomass energy to crude biofuels (syngas and biooils), it could produce biochar (1.65 GtC y^{-1}) and crude biofuels (with heating value equivalent to that of 6,500 million barrels of crude oil). By storing 1.65 GtC y^{-1} of biochar (equivalent to 6 Gt of CO_2) into soil and/or underground reservoirs alone, it could offset the world's 8.67 GtC y^{-1} of fossil-fuel CO_2 emissions by 19%, which is quite significant. According to a recent life-cycle assessment [10], for each ton of dry waste biomass utilized through biomass pyrolysis with biochar returned to soil, it could provide a net sequestration of about 800–900 kg of CO_2 emissions (per ton of dry biomass). The life-cycle assessment also indicated that the biochar-producing biomass pyrolysis technology could be operated profitably if/when CO_2 emission reductions are valued at or above about \$60 ton^{-1} of CO_2 equivalent emissions. Therefore, the envisioned photosynthetic biomass production and biofuel/biochar-producing biomass-pyrolysis approach should be considered as an option to mitigate the problem of global greenhouse-gas emissions.

Putting biochar into soil can potentially improve soil fertility and reduce fertilizer runoff to benefit the soil and water environment in agricultural/forest watersheds. However, the biochar C itself is not a crop nutrient except its ash contents which can serve as mineral nutrients for crop growth. It is probably better to apply biochar along with certain fertilizers, such as NH_4HCO_3 and/or urea, to achieve maximal environmental and agricultural benefits [11]. One of the options is to produce a

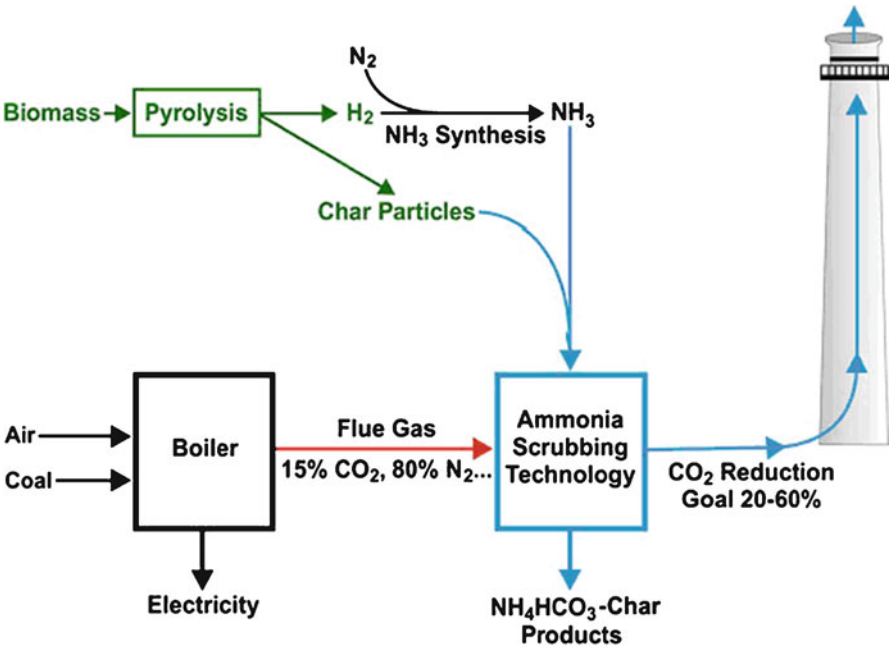

Fig. 1 This figure presents a conceptual design as an option to remove CO_2 emissions in industrial combustion facilities, such as a coal-fired power plant by flexible combinations of biomass pyrolysis and ammonia scrubbing. This CO_2-solidifying technology produces valuable soil amendment fertilizer products, such as NH_4HCO_3-char, that could be placed into soil and subsoil terrains through intelligent agricultural practice for soil amendment and carbon sequestration

biochar-NH_4HCO_3 (or biochar-urea) compound fertilizer that may make the biochar materials more suitable to stimulate plant growth and to maximally place the carbon of biochar and bicarbonate HCO_3^- into soils [3, 12]. As illustrated in Fig. 1, the ammonia-carbonation-based scrubbing technology process [13] can provide an option to integrate biomass pyrolysis with major industrial combustion facilities, such as a coal-fired power plant to solidify major flue-gas CO_2 emission and ppm levels of NO_x and SO_x emissions at the smokestacks into valuable fertilizers (mainly, NH_4HCO_3 with trace amount of other fertilizer species, such as NH_4NO_3 and $(NH_4)_2SO_4$) with biochar particles to produce a biochar-NH_4HCO_3 and/or biochar-urea fertilizer which could not only benefit agriculture, but also sequester carbon into soils for protecting the global environment [3, 14]. Using biochar samples produced by Eprida from peanut hulls, we performed certain experimental studies of the biochar materials with an ammonia carbonation process and cation exchange capacity (CEC) assays. In this paper, we report certain experimental studies of designer biochar production from peanut hulls and test the biochar materials with an ammonia carbonation process in relation to the possible application of biochar for soil amendment and carbon sequestration.

2 Experimental Materials and Methods

2.1 Biochar Materials Made with Temperature Variation

All of the charcoal samples were made in Omegalux LMF-3550 oven. A special box was constructed to allow preheated steam to flow through the charring material. The oven and steam flow settings for the charcoal production were: steam flow of 2.0 kg h^{-1}, with oven and steam temperature settings of 365, 385, 408, and 435°C. The material was removed from the oven when the temperature of the charcoal reached a maximum and stabilized for 5 min. The temperatures that were reached are: peanut hulls-371, 402, 426, 442°C. The batch system has been described in greater detail previously [15]. All of the char samples were crushed in a roller crusher and sieved to a size fraction of −850 +420 μm.

2.2 Cation Exchange Capacity Assay Protocol

CEC analysis was performed using the following method: The ground char sample was thoroughly mixed and 2 g was placed in a 250-mL Erlenmeyer flask. Hundred milliliters of 0.5 N HCl was added, the flask was covered with parafilm and shaken vigorously periodically for 2 h. Sample was filtered using a glass fiber filter in a Buchner funnel, washing with 100 mL portions of H_2O until wash shows no precipitate with $AgNO_3$. Filtrate was discarded. Moist char was immediately transferred to a clean 250-mL Erlenmeyer flask and a total of 100 mL 0.5 N $Ba(OAc)_2$ was added and a stopper placed on the flask. The mixture was shaken vigorously periodically for 1 h and was filtered, washing with three 100 mL portions H_2O. The char was discarded, and the filtrate was titrated with 0.0714 N NaOH using phenolphthalein to first pink. The following equation was used to calculate the CEC value:

$$\frac{\text{milliequivalent}}{100\,\text{g air} - \text{dried char}} = \frac{\text{mL} \times \text{normality NaOH} \times 100}{\text{(g) sample}} \tag{1}$$

2.3 Designer Biochar Material

Previous research has shown that a 400°C pyrolysis process produced a preferred biochar for agriculture and ammonia adsorption [3]. A 400°C biochar sample was produced by Day using pyrolysis of pelletized peanut hulls at 400°C. Specifically, the cross-draft reactor was brought up to 400°C empty with the exhaust from natural gas burner. Then, pelletized peanut hulls (biomass) were slowly fed in maintaining that internal reactor temperature. Once the biochar discharge sensor reached 400°C, the rotary discharge valve released biochar, the burner was switched off and the

Fig. 2 The NH_4HCO_3-char reactor experiment with the NH_3 scrubbing-CO_2-solidifying process in the gas-phase

system operated without any air or outside heat. This point coincides near the end of the exothermic zone for peanut shells. It also corresponds with the temperature range at which the resulting biochar had an increased fertilizer binding capacity as previously reported [3, 4]. The feed rate was controlled by the automated discharge of the biochar reaching 400°C and averaged 5–7 kg h^{-1}. The exothermic reaction allowed continuous feed to the pyrolysis reactor; however, the feed rate was 20% of what occurs when combustion of part of the pyrolysis vapors was used to augment the natural exothermic reaction.

2.4 Test of Biochar Material with Ammonia Carbonation

The designer biochar material made from the pelletized peanut hulls at 400°C was tested with a gas-phase ammonia carbonation process which is thermodynamically favored with the standard-free energy change (ΔG^0) of −18.05 kJ mol^{-1}:

$$NH_3(g) + CO_2(g) + H_2O(g) \rightarrow NH_4HCO_3(s) \quad (2)$$

In the experiments, about 500 g of the biochar material were packed into the reactor as illustrated in Fig. 2 to test whether the char material has binding affinity for the NH_4HCO_3 formed through the gas-phase ammonia-scrubbing CO_2-solidifying

process which is reported in ref. [13]. Briefly, a compressed gas containing 15 vol.% of CO_2 in N_2 (primary standard, supplied by Air Liquid) was taken as a synthetic flue gas. The synthetic flue gas was continuously fed into the reactor through a side port at the top of the reactor with a controlled constant flow rate at about 350 mL min^{-1} while the tail gas flowing out of the reactor through its bottom port. To mimic the moisture condition of a real-world flue gas, which commonly contains a nearly saturated amount of water vapor, the synthetic flue gas was humidified by bubbling it through a water tank kept at 40°C in an isothermal water bath (model RMS, Lauda) before it flowed into the reactor. The concentration of CO_2 in the tail gas that exited from the bottom of the reactor was monitored in-line with a digital gas analyzer (model 866, Honeywell) and recorded by DATAQ instruments. Prior to the detection of CO_2 concentration, the tail gas first went through a dilute aqueous sulfuric acid solution (1 N) for the adsorption of residual NH_3 and through an ice bath for the condensation of moisture. The compressed gas containing 15% (vol) of CO_2 in N_2 (primary standard, supplied by Air Liquid) and the pure N_2 (ultrahigh purity, supplied by Air Liquid) were used to calibrate the CO_2 detector prior to each experiment, using the same procedure as that used during the experiment. The NH_3 gas was generated by evaporation from anhydrous liquid NH_3 (purity ≥99.95%) that was purchased from Sigma-Aldrich. The flow rates of NH_3 gas and flue gas were controlled by calibrated mass flow controllers (MKS Instruments, Inc.). When the initial air in the reactor was removed by the constant flow of the humid flue gas for more than 15 min and when the concentration of CO_2 in the outlet gas reached a steady value, ammonia gas was then introduced through a central port located at the top of the glass tube reactor. Thus, all reactants were introduced from the top of the reactor. The ratio of NH_3 flow rate to the flue-gas flow rate was adjusted to about 0.12 where the steady-state CO_2 removal efficiency was about 44% for the biochar ammonia carbonation test.

3 Results and Discussions

3.1 Cation Exchange Capacity of Biochar Materials

The value of CEC was measured for the biochar materials made from the pelletized peanut hulls at pyrolysis temperature of 371, 402, 426, and 442°C. As shown in Fig. 3, the measurements demonstrated that the CEC value of the biochar materials is dependent on the pyrolysis temperature. Pyrolysis temperature of 402°C yielded the highest CEC value (18.2 meq/100 g) while the pyrolysis temperatures of 371, 426, and 442°C resulted in CEC values of 17.1, 16.1, and 13.9 meq/100 g, respectively. This experimental result indicated that it is important to control pyrolysis temperature for higher CEC value of biochar product. The optimal pyrolysis temperature for high-CEC biochar production is likely at around 400°C.

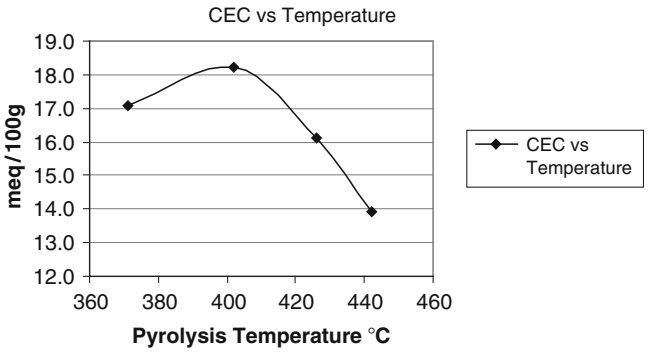

Fig. 3 Biochar cation exchange capacity (CEC) vs. pyrolysis temperature. Char samples were created at four temperatures in a range from 370 to 450°C and were analyzed for CEC. A peak value was obtained for the char sample created at 402°C with CEC values decreasing as pyrolysis temperature increases from this point

3.2 Biochar-NH_4HCO_3 Experimental Results

In this part of the study, we tested the compatibility between NH_4HCO_3 and the designer biochar material that was produced at 400°C from peanut hulls. Since the CO_2-solidifying-NH_4HCO_3 production process occurs in a gas phase, the char particles could potentially serve as nucleation site for the formation of solid NH_4HCO_3 crystals thus enhancing the CO_2-removal chemical engineering technology. The experimental objective was to explore the possibility of whether a compatible NH_4HCO_3-char fertilizer product can be created to enhance storage of carbons (both HCO_3^- and biochar) into soil and subsoil earth layers and also benefit the agricultural industry. The experimental result demonstrated that the biochar material indeed has certain binding affinity for the NH_4HCO_3 formed in the gas-phase process. In the experiments, when ammonia carbonation was initiated by introducing ammonia gas along with the moisturized synthetic flue gas into the reactor (with about 500 g of designed biochar material), the formation of ammonium salts (solid products) appeared immediately as a fog and white material that condensed on the biochar materials. As shown in Fig. 4, the char grains after treated with the ammonia-scrubbing CO_2-solidifying process became significantly whiter than the control biochar sample because of the deposition of NH_4HCO_3 onto the surfaces of the char grains by the process treatment.

This observation is consistent with the results of our pH measurements for the treated char, untreated char (control), and NH_4HCO_3-char mixture that was produced by mixing equal weight (50%/50% by weight) of NH_4HCO_3 and char. In the pH experiment, 1 g for each of these samples (the treated char, untreated char, and NH_4HCO_3-char mixture) was dissolved into 10 mL of distilled water. Then, pH values of the solutions were measured by a standard Beckman pH electrode system. As presented in Table 1, the pH measurement clearly demonstrated that the addition of NH_4HCO_3 can significantly neutralize the alkaline pH of the char material. The pH value of the untreated char material was 9.85 while that of the NH_4HCO_3-char

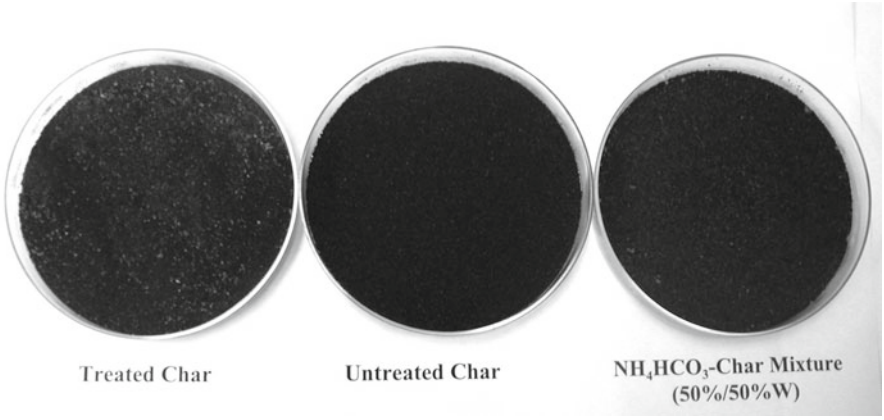

Fig. 4 Charcoal (char) material produced from pyrolysis of biomass peanut hull and treated with and without an ammonia-carbonation process

Table 1 Measurements of pH for the treated char, untreated char, and NH_4HCO_3-char mixture

Products	Char treated by NH_3-CO_2-solidifying process	Untreated char	NH_4HCO_3-char mixture (50%/50% by weight)
pH	8.76	9.85	7.89

mixture (50%/50% by weight) was 7.89. This is expected since the bicarbonate HCO_3^- of NH_4HCO_3 can act as a pH buffer in neutralizing certain alkaline ash components in the char material. The gas-phase ammonia-carbonation treatment (by the NH_3-CO_2-solidifying process) reduced the pH value of the biochar from 9.85 to 8.76. According to the pH change in the treated char, the NH_3 scrubbing-CO_2-solidifying process resulted in deposition of NH_4HCO_3 onto the char grains by roughly about 40% of the char weight.

These results demonstrated that the char material has certain binding affinity for NH_4HCO_3 and the pH value of the char material can be improved by the addition of NH_4HCO_3. The binding affinity for NH_4HCO_3 could be explained by the presence of biochar surface acids groups, such as carboxyl groups, that are known to form preferably at the biomass pyrolysis temperature of around 400°C [4]. The results also indicate that biochar could probably be used as an adsorbing filtration material along with the NH_3 scrubbing-CO_2-solidifying process to clean certain industrial flue gases and, at the same time, produce a valuable soil amendment and/or, perhaps, "organic slow-release" biochar fertilizer (such as biochar-NH_4HCO_3) that can potentially enhance sequestration of carbon into soil and subsoil earth layers, reduce NO_3^- run-off, and stimulate photosynthetic fixation of CO_2 from the atmosphere [12].

These experimental results may have practical implications for biochar soil applications. For examples, because of their alkaline ash contents, the pH of biochar material can sometimes be as high as about 10, which would be unfavorable for use in alkaline soils (pH above 8) such as those in the western part of the United States because the addition of an alkaline material could make the alkaline soil pH worse for plant growth. Since NH_4HCO_3 can act as a pH buffer, co-application of biochar and NH_4HCO_3 as a mixture or compound fertilizer is likely to improve biochar fertilizer pH. As shown in Table 1, mixing (50/50 by weight) with NH_4HCO_3 can neutralize the pH of biochar material from 9.85 to 7.89, which could make the biochar fertilizer pH more favorable to use in many soils, including (but not limited to) the alkaline soils. On the other hand, biochar can effectively adsorb ammonia (NH_3) and other nutrients to minimize fertilizer nutrient loss. This type of chemisorption properties is typical of biochar since the biomass pyrolysis thermochemical process involves the fracture of many chemical bonds initially present in the biomass feedstock. The product biochar carbon does not go through a fluid state during the pyrolysis; consequently many of these bonds are left "dangling" [16]. As described by Antal and Gronli [16], these dangling bonds are believed to give rise to some of the chemisorption properties of biochar. In addition, certain polar functional groups, such as hydroxyl (–OH) and carboxyl (–COOH) groups of the biochar materials, may give rise to the property of CEC, which is important also in helping retain nutrients, such as ammonium and potassium ions (NH_4^+ and K^+) in soil. Therefore, co-application of biochar and NH_4HCO_3 (or urea) can probably maximize the beneficial effects. Furthermore, as illustrated in Fig. 5, the bicarbonate HCO_3^- of NH_4HCO_3 (or urea) that could be used in this manner may stay in the alkaline soils, since its HCO_3^- could neutralize certain alkaline earth minerals, such as $[Ca(OH)]^+$ and/or Ca^{2+}, to form stable carbonated mineral products such as $CaCO_3$ that can serve as a permanent sequestration of the carbon in soil and/or subsoil earth layers. Therefore, co-use of NH_4HCO_3 and char materials together could allow continued formation of carbonated mineral products, such as $CaCO_3$ and/or $MgCO_3$, to sequester maximal amount of carbons into the soil and subsoil terrains while still maintaining good soil properties for plant growth. In addition, use of the carbon-based nitrogen fertilizer could also provide an option to help solve the environmental problem of nitrate (NO_3^-) run off from the current use of ammonium nitrate (NH_4NO_3) as a fertilizer in the United States. However, more research and development efforts are still needed to test this option.

Note, ammonium bicarbonate (NH_4HCO_3) has a quite limited stability; it can decompose at a temperature above a range of 36–60°C. For best result, therefore, a biochar-NH_4HCO_3 fertilizer should be applied immediately into/underneath soil or stored in a tightly sealed container (e.g., plastic bag) at temperatures below 27°C to minimize decomposition. If the stability of ammonium bicarbonate (NH_4HCO_3) is a problem, the alternative is to use biochar with urea which is much more stable. In addition, biochar material alone can also be used in soil application as well.

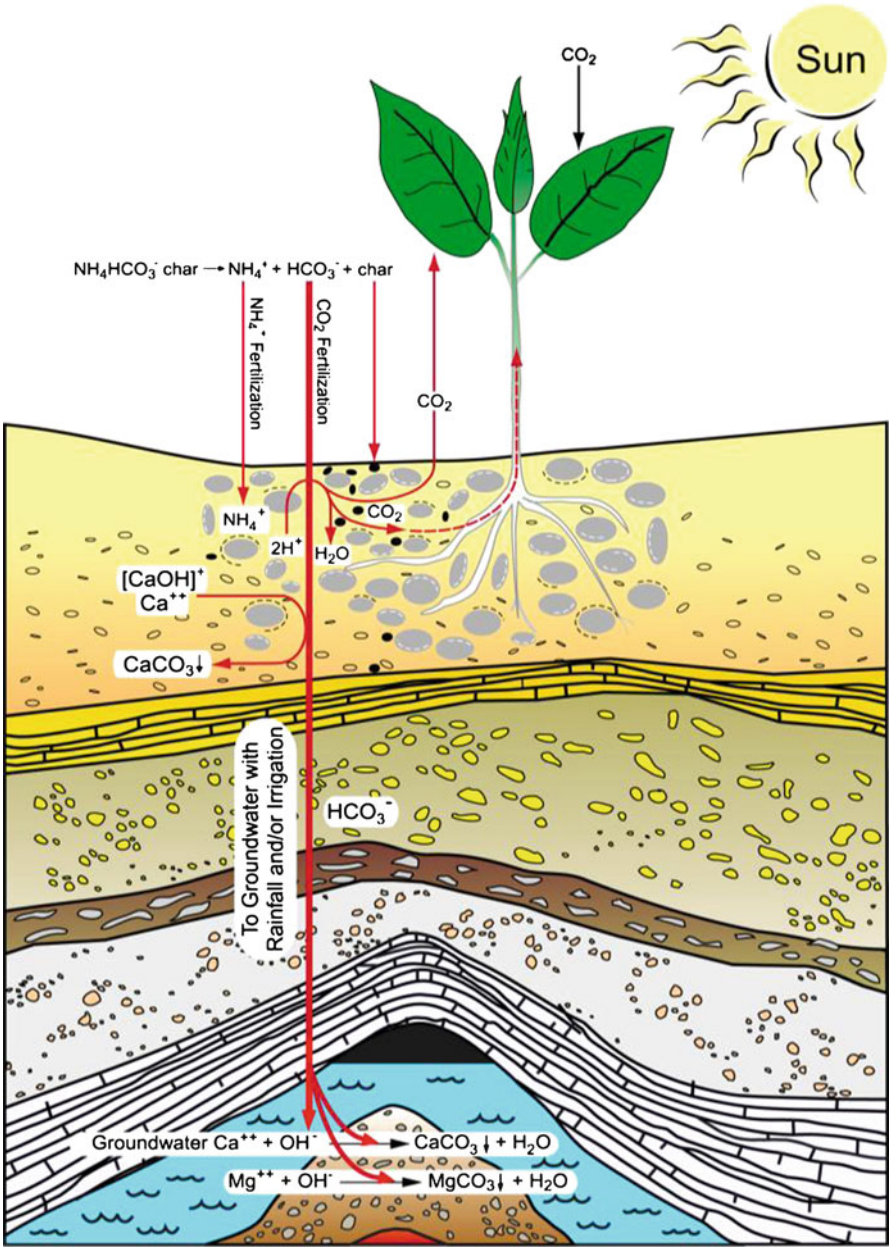

Fig. 5 Intelligent application of NH_4HCO_3-char fertilizer to enhance sequestration of carbon into soil/subsoil earth layers

4 Conclusions

The CEC value of biochar is related to the biomass pyrolysis temperature. Biochar materials made from peanut hulls at pyrolysis temperature of about 400°C yield the highest CEC value. As the pyrolysis temperature increases over 400°C, the CEC value decreases. The biochar materials appear to have certain binding affinity for ammonium bicarbonate (NH_4HCO_3) formed through a gas-phase ammonia carbonation reaction. The binding affinity for NH_4HCO_3 could be explained by the presence of biochar surface functional groups, such as carboxyl groups, that are known to form preferably at a pyrolysis temperature of around 400°C. Addition of ammonium bicarbonate to biochar can help neutralize biochar pH. Use of biochar fertilizer is potentially an attractive approach for soil amendment and carbon sequestration.

Acknowledgment The authors wish to thank Mac Post and Joe Katz for stimulating discussions. This research was supported in parts by Oak Ridge National Laboratory Director's Seed Money Project Funds and by the US Department of Energy (DOE) Office of Science Young Scientist Award and the US Presidential Early Career Award for Scientists and Engineers (to J.W. Lee). Oak Ridge National Laboratory is managed by UT-Battelle, LLC, for DOE under contract No. DE-AC05-00OR22725.

References

1. Raupach MR, Marland G, Ciais P, Quéré CL, Canadell JG, Klepper G, Field CB (2007) Global and regional drivers of accelerating CO_2 emissions. Proc Natl Acad Sci U S A 104(24): 10288–10293
2. Schlesinger WH (1985) Changes in soil carbon storage and associated properties with disturbance and recovery. In: Trabalha JR et al (eds) The changing carbon cycle: a global analysis. Springer, New York, NY, pp 194–220
3. Day D, Evans RJ, Lee JW, Reicosky D (2005) Economical CO_2, SOx, and NOx capture from fossil-fuel utilization with combined renewable hydrogen production and large-scale carbon sequestration. Energy 30:2558–2579
4. Day DM, Lee JW (2004) The production and use of a soil amendment made by the combined production of hydrogen, sequestered carbon and utilizing off gases containing carbon dioxide. PCT Int Appl, WO 2004037747 A2, 58
5. Gundale MJ, DeLuca TH (2007) Charcoal effects on soil solution chemistry and growth of Koeleria macrantha in the ponderosa pine/Douglas fir ecosystem. Biol Fertil Soils 43:303–311
6. Solomon D, Lehmann J, Thies J, Schafer T, Liang B, Kinyangi J, Neves E, Petersen J, Luizao F, Skjemstad J (2007) Molecular signature and sources of biochemical recalcitrance of organic C in Amazonian dark earths. Geochim Cosmochim Acta 71:2285–2298
7. Lehmann J, Gaunt J, Rondon M (2006) Bio-char sequestration in terrestrial ecosystems—a review. Mitig Adapt Strat Glob Chang 11:403–427
8. Lee JW, Hawkins B, Day DM, Reicosky DC (2010) Sustainability: the capacity of smokeless biomass pyrolysis for energy production, global carbon capture and sequestration. Energy Environ Sci 3(11):1609–1812
9. Krausmann F, Erb K, Gingrich S, Lauk C, Haberl H (2008) Global patterns of socioeconomic biomass flows in the year 2000: a comprehensive assessment of supply, consumption and constraints. Ecol Econ 65:471–487

10. Roberts K, Gloy BA, Joseph S, Scott NR, Lehmann J (2010) Life cycle assessment of biochar systems: estimating the energetic, economic, and climate change potential. Environ Sci Technol 44:827–833
11. Asai H, Samson BK, Stephan HM, Songyikhangsuthor K, Homma K, Kiyono Y, Inoue Y, Shiraiwa T, Horie T (2009) Biochar amendment techniques for upland rice production in Northern Laos 1. Soil physical properties, leaf SPAD and grain yield. Field Crop Res 111:81–84
12. Lee JW, Li R (2003) Integration of fossil energy systems with CO_2 sequestration through NH_4HCO_3 production. Energ Convers Manage 44(9):1535–1546
13. Li X, Hagaman E, Tsouris C, Lee JW (2003) Removal of carbon dioxide from flue gas by ammonia carbonation in the gas phase. Energy Fuel 17:69–74
14. Lee JW, Li R (2002) Method for reducing CO_2, CO, NOx, and SOx emissions. United States Patent No. 6,447,437 B1
15. Das KC, Singh K, Adolphson R, Hawkins B, Oglesby R, Lakly D, Day D (2009) Steam pyrolysis and catalytic steam reforming for hydrogen and biochar production. Appl Eng Agric 26(1):137–146
16. Antal MJ, Gronli M (2003) The art, science, and technology of charcoal production. Ind Eng Chem Res 42(8):1619–1640

Chapter 7
Selection and Use of Designer Biochars to Improve Characteristics of Southeastern USA Coastal Plain Degraded Soils

J.M. Novak and W.J. Busscher

Abstract The US Southeastern Coastal Plains have a long history of agricultural production. However, poor quality sandy soils hamper productivity. Soils have depleted organic carbon contents that lead to poor nutrient retention, reduced aggregation, and low plant-available soil water retention. Past soil management used reduced tillage to increase organic carbon but it deteriorated quickly in the hot, humid environment. Biochars can provide an alternative recalcitrant carbon source. Since biochar varies widely in characteristics, it must be designed to fit the needs of the soil—increased carbon, aggregation, nutrient retention, and plant-available water retention. Biochar design characteristics depend mainly on feedstock characteristics and method of pyrolysis. This review offers guidelines for designer biochar manufacture through feedstock selection and pyrolysis technique; it outlines potential usage to improve specific soil quality problems.

1 Introduction

The Southeastern Coastal Plains of the Carolinas have a long history of crop production by Paleo-Americans [63] and European settlers [15, 46, 103]. The region was initially settled by the Paleo-Americans [63], and they thrived by growing maize, beans, and squash and letting fields remain fallow after about 2 years of production. This rotation continued until the European settlers colonized the Carolinas in the seventeenth and eighteenth centuries [103]. With time, the European settlers shifted agriculture to more intensive corn, cotton, tobacco, rice, and timber production. Overuse of fields and poor land management accelerated depletion of

J.M. Novak (✉) • W.J. Busscher
Coastal Plains Soil, Water and Plant Research Center,
2611 W Lucas Street, Florence, SC 29501, USA
e-mail: jeff.novak@ars.usda.gov

J.W. Lee (ed.), *Advanced Biofuels and Bioproducts*, DOI 10.1007/978-1-4614-3348-4_7,

soil nutrients and enhanced erosion of topsoil [16]. Fields of depleted soils were quickly abandoned.

In addition to the physical and chemical soil problems, the coastal plain climate hindered agricultural productivity. For example, the South Carolina Coastal Plain has an annual rainfall of about 1,310 mm [86], which is sufficient for row crop production [89]. But, crop water stress is common because of poor temporal rainfall distribution [85] and low soil water storage [36]. Droughts can last several weeks and reduce yields.

USDA agencies such as the Natural Resource Conservation Service and the Agricultural Research Service, have developed soil and water conservation management practices for these soils that promote productivity. Non-inversion, deep tillage that physically disrupts a subsurface hard pan can promote deep crop root penetration while minimally disrupting the surface to reduce water runoff and erosion [1, 2]. Unfortunately, the beneficial effects of deep tillage are temporary; deep disruption must be redone annually [13, 19] and soil organic carbon (SOC) levels are concentrated at the surface or deteriorate in the hot, wet weather [77, 105].

Minimal tillage, where crop residues are left on the soil surface, can increase SOC levels in sandy soils [50, 69], a soil characteristic that is known to improve aggregation [34], water infiltration, and nutrient retention [102]. An ideal OC-enriched amendment for these soils would be one that is long-lasting and increases aggregation, fertility, and water retention. Recently, Laird [57] described how a long-lost technology could be adopted as a management strategy to revitalize soils. In South America, pre-Columbian Amazonian inhabitants improved their infertile soils by applying biochar [45, 61]. These inhabitants obtained biochar from trees cleared from the forest and organic wastes such as bones, carcasses, and other fire pits debris; they added biochar to soils using a “slash and char” process which increased soil productivity [45]. Carbon in the form of biochar is resistant to degradation [99], having remained in tropical Amazonian soils for centuries [63]. Following the biochar vision of Laird [57], applying biochar to sandy agricultural soils of the Southeastern Coastal Plain would be a similar management strategy aimed at overcoming soil physical and chemical deficiencies.

Biochars quality can be variable [21] and different biochars react differently in soils [62, 70]. Biochar properties should be known to be beneficial to a soil to avoid creating unwanted chemical or physical legacies. One biochar type will not resolve all issues in all soils because of differences in its quality, and in its interaction with soil particles, and microbes. Arguably, it may be more prudent to design a biochar with specific chemical and physical attributes that can target specific soil problems. A biochar designed for a specific purpose was first introduced by Day et al. [27] to produce a material that acted as a nutrient carrier while being able to resist leaching. Day and his team were able to sequester C, H, and N from coal gas emissions into a char-based product for use as an N fertilizer source. Novak et al. [70] also recognized that biochars could be designed with specific chemical and physical properties through feedstock selection, pyrolytic temperature, and residence time manipulation. The designer biochar concept was further refined through a cooperative research [71]. This novel concept caught the attention of the scientific community,

because shortly thereafter, others reported that biochar production can be managed to derive purposefully designed biochars that have properties tailored for specific end uses [6, 53, 98].

Biochar can be expensive to manufacturer with cost estimates of $220 per Mg using current technologies [64]. If biochar is applied to soils at a common rate of between 1 and 30 Mg ha^{-1} [9]; its cost per ha can range from $220 to $6,615. To be a feasible option under these conditions, biochar marketing will need to establish a profit balance of bio-oil/biochars/syngas production from the parent feedstocks [94]. Also, if C offsets come to fruition, biochar could be seen as an amendment that would benefit reductions in atmospheric CO_2 concentrations by increasing soil C sequestration. Additionally, N_2O is a potent greenhouse gas influencing global warming and a linkage has been established showing reduced N_2O emissions from soils treated with biochar [90, 96].

In this article, we offer guidelines to pyrolytically design biochar, evaluate relationships between feedstock selection and biochar quality, and match the correct biochars or their blends to targeted soil and greenhouse gas production problems. It is important to first, understand what soil problem needs to be modified, and second, select a feedstock and pyrolysis condition that develops a biochar specific for that targeted problem. Therefore, the objectives of this review are to (1) appraise the geomorphic, chemical, and physical characteristics of degraded southeastern sandy coastal plain soils, (2) describe past physical and chemical remediation strategies to revitalize these sandy soils, and (3) establish guidelines for manufacture and use of designer biochars and their blends that could improve soil deficiencies and reduce greenhouse gas emissions.

2 Description of Southeastern USA Coastal Plain Soils

2.1 Geomorphic Properties

The coastal plain is an expansive geomorphic region of the Southeastern USA that extends from southern New Jersey along the Atlantic coast through the coast of the Gulf of Mexico to South Texas. It comprises nearly 2/3 of the land area of South Carolina (Fig. 1); most of which is either in agriculture or forestry. The coastal plain was initially deposited during a series of sea level rises and recessions; it has been subject to depositional and erosional forces moving and relocating sediments from the Pliocene Epoch (1.8–5 million years ago, [91]) to today. Below Pliocene age sediments are geologic strata consisting of beds of multicolored sands, intermixed with gravel and clay beds laid down during the Tertiary Epoch from 5 to 38 million years ago [91].

Terraces and scarps commonly occur across the coastal plain that are reflective of glacioeustatic changes in ocean level, deposition of sediments, and river dissection during the last 5 million years [30]. The terraces are gently eastward-sloping on the surface, which are bounded by seaward-facing scarps [25]. These scarps are a

Fig. 1 View of the coastal plains of the Southeastern USA (*left*) and of South Carolina (*right*) from the fall line to the coast

few meters in height and demark a time when sea levels were higher. Some of the scarps are definitive on the landscape [32] and are used to divide the area into physiographic divisions consisting of (1) lower, (2) middle, and (3) upper coastal plain, based on topography, sediments, elevations above mean sea level, and soils [30]. Their elevations range from sea level to about 150 m.

2.2 *Pedogenic Activity Shapes Soil Morphology*

Because coastal sediments were deposited by sea level changes, fluvial activity, and by erosional processes over the past 35,000–5 million years [32], pedogenic activity has had millions of years to form sediments into soils. Stable coastal surfaces developed aged soils that include an eluvial (E) horizon, weathered clays [28], and a reddened argillic B horizon [29].

The upper coastal plain is highly dissected by streams, and is covered by extensively weathered well-drained soils [32]. The middle coastal plain is gently undulating with a swell and swale relief of 0.3–1.5 m [31]. Here, upland soils are well drained when located closer to drainage ways and depressions are poorly drained. Circular depressions are referred to as Carolina Bays [30].

The Norfolk and Bonneau soil series are examples of well-drained upland soils of the middle coastal plain (Fig. 2). They are classified as Paleudults and have well-developed E and clay-enriched argillic B horizons. Particle size and fertility analyses show that their topsoils are sandy and mildly acidic [72]. Their low pH is caused by leaching of sandy parent material and the predominance of alumino-hydroxy species on cation exchange sites [32]. The clay fraction also attests to the soil age; it can be composed primarily of kaolinite, gibbsite, and hydroxy-interlayer vermiculite with minor amounts of hydroxy (Fe and Al) interlayer chlorite [73, 88]. All of this leads to a soil with low cation exchange capacities (<2 to 4 $cmol_c\,kg^{-1}$, [55]).

Another characteristic of the Norfolk series is a subsurface hard layer (Fig. 3, left) that is caused by physical cementation and/or chemical precipitation of soluble Si between particles during wetting/drying cycles [22, 66]. This hard layer when dry

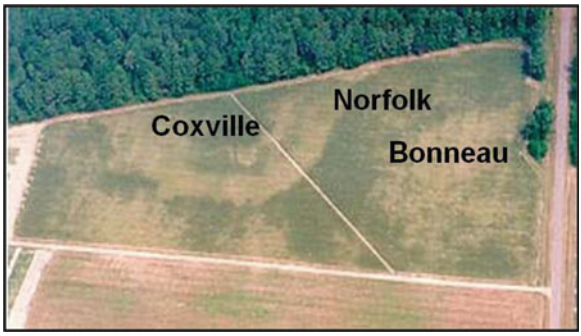

Fig. 2 Coxville (poorly drained), Norfolk (well-drained), and Bonneau (excessively well-drained) soil series in a Coastal Plain agricultural field (Darlington, SC)

Fig. 3 Poorly aggregated, massive structure of the E horizon (hard layer) of the Norfolk soil series (*left*). A deformed probe attempting to measure penetration resistance in the hard layer (*right*, photos courtesy of ARS Florence)

has penetration resistances that can deform the steel probe used to measure its strength (Fig. 3, right). In some cases, crop roots will grow along the top of the hard layer because high soil strength and lack of aggregation deters their penetration.

The Bonneau series also forms in upland areas. It has a thicker, hard E horizon and its argillic B horizon can have a lower boundary up to 102-cm deep. As shown in Fig. 2, the lack of vegetation on the Bonneau soil was due to crop moisture stress during a drought (2002). Crop growth was limited in this series because roots were unable to penetrate the hard layer to exploit water stored in the argillic B horizon.

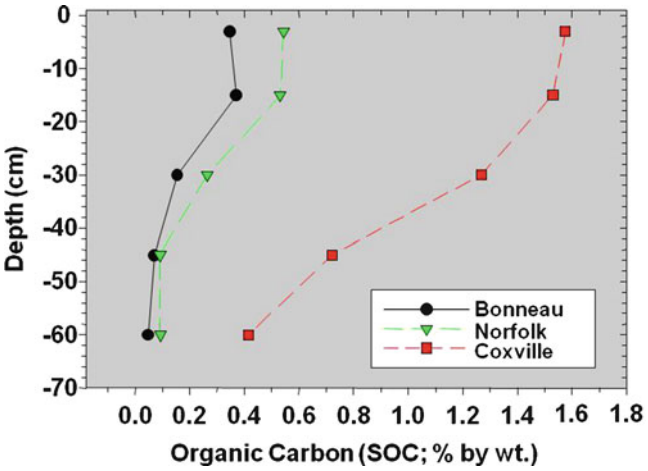

Fig. 4 Percentage by weight of soil organic carbon (SOC) in the profile of Bonneau, Norfolk, and Coxville soil series (profile data from field in Fig. 2)

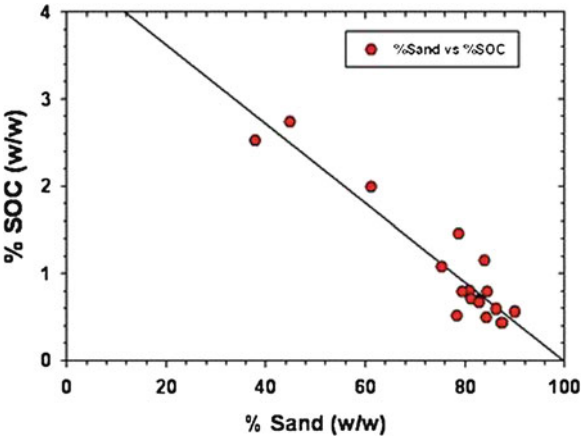

Fig. 5 Relationship between sand and SOC in topsoil (0–15-cm) of Norfolk, Bonneau, and Coxville soil series (samples collected from field shown in Fig. 2)

Deep coring into the Norfolk and Bonneau soil profiles shows that they have low SOC contents (Fig. 4). This can be explained by their high sand content (Fig. 5), and their lack of clay-size particles that are known to sorb SOC compounds and slow organic matter mineralization [101]. In contrast, the Coxville is a poorly drained Paleaquult, which forms in Carolina Bays (Fig. 2). Sediments from soils in upslope locations have eroded into the bay over millennia causing the Coxville to contain more clay. As shown in Fig. 4, the Coxville soil has more SOC in the profile than the Norfolk or Bonneau soil. Accumulation of SOC in the Coxville is also facilitated

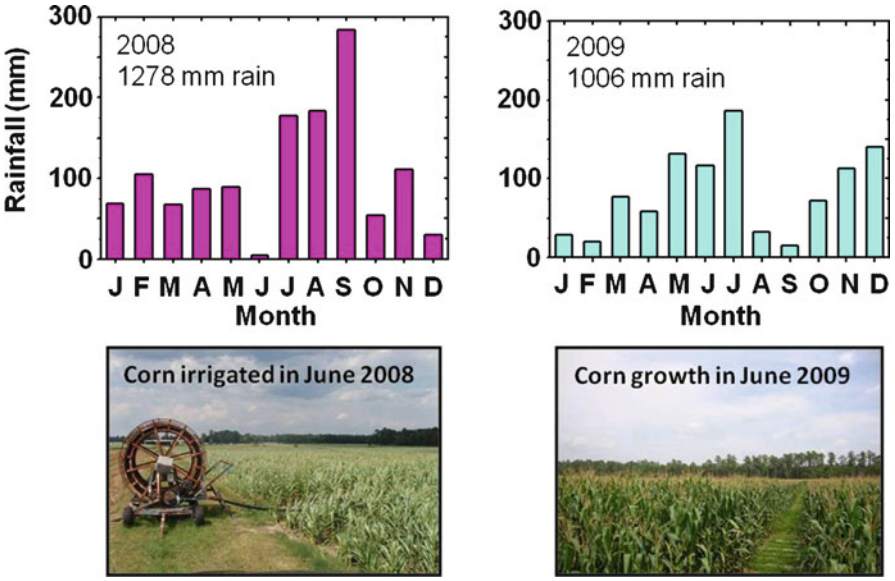

Fig. 6 Monthly rainfall totals during 2008 (*left*) and 2009 (*right*) recorded at the Clemson University, Pee Dee Research and Education Center, Florence, SC, USA and its influence on corn yields show the importance of water availability. Corn grows from mid April to early August. Its yields were 3.8–4.7 Mg ha^{-1} in 2008 and yields = 8.4–9.3 Mg ha^{-1} in 2009

by its poor internal drainage that slows oxidation [101]. The Coxville series has a greater ability to retain nutrients than the Norfolk and Bonneau because of its larger cation exchange capacity (5–15 $cmol_c kg^{-1}$, [55]).

2.3 Water Storage in Sandy Soils

Annual precipitation in the coastal plain region of South Carolina is high enough for crop production (1,310 mm, [86]). However, erratic rainfall with dry spells of a few days to a few weeks [16, 85] reduces production as seen in (Fig. 6) where less than 5 mm of rainfall was recorded in June 2008 in Darlington SC during the corn growing season (April to July). Low rainfall caused crop moisture stress to occur (Fig. 6, left), resulting in low corn yields (3.8–4.7 Mg ha^{-1}). In contrast, rainfall was sufficient during the 2009 corn growing season (Fig. 6, right) and yield was double the drought year (8.4–9.3 Mg ha^{-1}).

Low water storage [18, 79] and poorly aggregated, hard layers, that restricts root penetration to the top 25–30 cm of the soil profile [36] limit soil water holding capacity to ≈22.5 mm [37, 81]. During the hot summer, evapotranspiration rates of 16.8 mm day^{-1} for soybeans [82] will use this in less than 2 days. Unless water is replenished with rain or irrigation, crops will stress. In contrast, a finer-textured

SOC-enriched Coxville soil series can have between 29 and 51 mm of available H_2O per 300 mm of soil [79]. Under similar conditions, a soybean crop growing in the Coxville soil would have more time (1.7–3 days) before soil water is depleted.

2.4 Management Practices to Increase Soil Water Storage

Tillage management practices disrupt the subsurface hard layer to encourage deeper root growth and increase SOC levels to improve water storage. Physical disruption using deep tillage of the hard layer is expensive and requires specialized equipment [52]. Because hard layers re-cement [13, 19], deep tillage in the coastal plain is usually preformed annually [14]. In today's economy, annual deep tillage is expensive; therefore, less-expensive forms of minimum tillage or no-till are used to build-up SOC contents [8, 12, 50, 69]. Accumulation of SOC is beneficial because the effects have been shown to reduce soil strength [39].

Increases in SOC improve soil aggregation and pore space [8, 34, 93], which favor water infiltration and storage [102]. Minimum tillage systems favor SOC rebuilding, but in sandy coastal plain soils, the increase is depth-dependent [69, 72], and only a small portion (5%) of OC in crop residue is returned to the SOC pool [72]. Other minimal tillage studies reported that SOC increases are not long-lasting, but must be continually resupplied with fresh residue [77, 105].

Considering these problems, an ideal OC supplement should last longer, return more OC to the SOC pool, and increase aggregate formation and pore space. A promising soil amendment that can add recalcitrant OC while concomitantly improving soil chemical and physical issues is biochar [16, 57, 61].

3 Biochar Production and Properties

3.1 Biochar Production

Biochar is a byproduct of the biofuel industry [5, 58, 62]. It is produced by the pyrolysis of organic feedstocks at temperatures between 300 and 700°C in an oxygen-free or low oxygen noncombustible atmosphere. Different feedstocks are used to make biochars, including biomass energy crops, bioenergy residues, crop residues, manures, and kitchen wastes. During the pyrolytic process, these organic feedstocks thermally decompose, releasing volatile compounds, syngas and biochar. The volatile compounds can be recondensed and refined as bio-oil [11]. The biochar residual product has chemical and physical properties that depend on complex reactions during the pyrolysis process and are reported to vary with feedstock selection and pyrolysis conditions [38, 74].

Biochars can be made using various thermochemical processes systems such as slow/fast pyrolysis, flash pyrolysis, and gasification [58, 94]. Slow and fast pyrolysis

Table 1 Biochar percent ash (dry wt. basis), pH, and fertilizer ratios

				Fertilizer (100 kg^{-1} biochar)		
Feedstock	Pyrolysis (°C)	Ash (%)[a]	pH[a]	N	P	K
Peanut hull	400	8.2	7.9	3	0.3	2
	500	9.3	8.6	3	0.3	2
Pecan shell	350	2.4	5.9	0.3	0.03	0.2
	700	7.2	7.2	0.5	0.05	0.5
Poultry litter	350	35.9	8.7	5	3	6
	700	52.4	10.3	3	4	9
Switchgrass	250	2.6	5.4	0.4	0.1	0.5
	500	7.8	8	1	0.2	1
Hardwood	Fast	5.6	6.1	0.3	na	0.6
Pine chips[b]	465	5.6	6.1	0.3	0.08	0.4
Corn stover[b]	500	69.1	7.2	0.6	0.2	1.6

[a]From Novak et al. [74]
[b]Results courtesy of Drs. Don Reicosky and Kurt Spokas (USDA-ARS)

technologies are featured in this review. A more detailed explanation of gasification technologies for syngas production is available [58].

In the slow/fast pyrolysis systems, the feedstock (depending on the delivery feed scheme) can remain in the pyrolysis reactor anywhere from a few seconds to 24 h [94]. Pyrolysis reaction times vary among manufacturers because of differences in reactor temperature ramp settings, choices of dehydration (100–150°C) and carbonization temperatures (300–700°C), and cooling time. Under these conditions, biochar yields can range from 51 to 72% on an oven-dry C basis and between 29 and 57% on an air-dry mass basis [74]. More biochar is recovered at lower pyrolysis temperatures (around 350°C) because less volatile material is driven off as bio-oil. If maximizing bio-oil production is the goal, the manufacturer can adjust the slow pyrolysis process to operate at a higher temperature range (500–700°C). While more bio-oil is recovered, biochar mass yields will decline because of dehydration of hydroxyl groups and thermal degradation of ligno-cellulose structures [4, 5].

Biochars pyrolyzed at higher temperatures (500–700°C) tend to have greater ash contents, and hence, more alkaline pH values (Table 1). High temperature pyrolysis will concentrate the salts because of the loss of C-, O-, and H-containing compounds removed as volatiles [20, 43, 74]. Ash contents for several biochars pyrolyzed at the higher (400–700°C) temperatures regime ranged from 5.62 to 52.9% while at the lower temperature (<350°C) biochar ash contents ranged from 2.4 to 35.9% (Table 1). Biochar pyrolyzed from poultry litter had the highest ash content because of excretion of unassimilated nutrients [92] and from chemical additives to the litter to reduce N volatilization [74]. The high ash content also contributed to the poultry litter biochar having a calcareous pH (Table 1).

The elemental composition in several biochars is heterogeneous (Tables 1 and 2) because of differences in nutrient uptake by the raw feedstock [21] and by chemicals added to manure feedstocks prior to pyrolysis [74]. If the ash contains elements like

Table 2 Elemental composition of four biochars (μg g^{-1} on a dry-weight basis, unpublished data)[a]

Element	Hardwood	Cotton gin trash	Pine chips[b]	Corn stover[b]
Al	402	208	578	13,915
Ag	0	0	0.1	0.2
As	0.2	0.2	0.2	1.2
Ba	42	12	21	136
Ca	5,164	4,361	3,976	11,831
Cd	0.2	0	0	0
Cr	217	0.7	11	58
Cu	9.1	124	5.3	57
Fe	2,046	163	1,515	8,307
K	6,237	11,451	4,353	52,574
Mg	741	1,086	1,390	4,867
Mn	113	12	172	201
Na	480	384	805	8,525
Ni	8.5	4.3	0.6	18
Pb	2.4	0.4	2.6	31
Se	0.8	0.7	0.7	0.4
V	0.4	0.4	0.6	16
Zn	6.7	6.7	44	41

[a]Biochars digested using EPA method 3052 (HNO_3 + HF)
[b]Samples courtesy of Dr. Don Reicosky (USDA-ARS)

N, P, and K, then it could serve as a low grade fertilizer with a corresponding low N-P-K ratio (Table 1). These ratios were calculated based on the total contents of elements in the biochar, and does not necessarily reflect their plant availability status. Poultry litter and peanut hulls have a modest N-P-K fertilizer ratio while biochar made from pine chip and pecan shells had the lowest ratio (Table 1). Results from Table 2 show that the biochars pyrolyzed from different feedstocks can contain sizeable quantities of base cations such as Ca and Mg. While also being essential plant nutrients, the presence of Ca and Mg causes the biochar to act like a liming agent. As Novak et al. [73] reported pecan shell biochar had liming properties since it had an alkaline pH, and contained 3.6 and 0.7 g kg^{-1}, respectively, of Ca and Mg. Another important property of these four plant-based biochars (Table 2) is the low concentrations of heavy metals (i.e., Cd, Cr, Ni, Pb, and V). If these biochars are used as a soil amendment, low metal concentrations should ease environmental concerns.

In fast pyrolysis, the feedstock is placed in a retort and subjected to a very short burst (1–2 s in duration) of heat (400–600°C) usually under pressure [94]. These conditions also maximize bio-oil production (75%); however, lower biochar mass yields are recovered (≈12%, [94]). For comparative purposes, one biochar made from hardwood using the fast pyrolysis system was included in this review. Its ash content, pH value, and fertilizer ratio were fairly similar to characteristics of the low temperature (350°C) pecan shell biochar (Table 1).

There are considerable time advantages when using fast pyrolysis, including shorter residence, carbonization, and temperature squelching times. The choice of pyrolysis system (slow vs. fast) for biochar manufacturer will ultimately be decided by a balance between biochar, bio-oil, and syngas recovery [94].

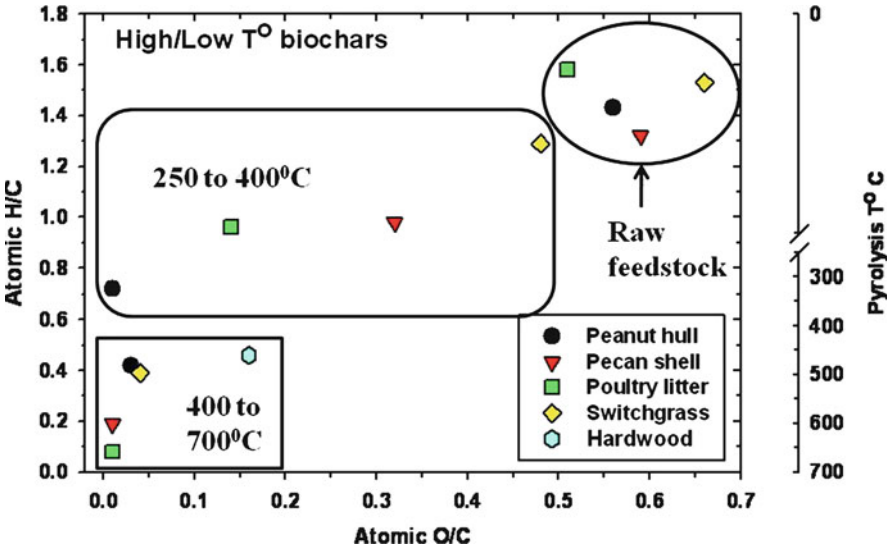

Fig. 7 Atomic ratio distribution shown in the Van Krevelen diagram for raw feedstocks and biochars pyrolyzed using two temperature ranges

3.2 Biochar Characterization

Pyrolysis systems cause many changes to the initial feedstock that inevitability is reflected in the biochars structural and elemental composition. These intensive thermal conditions during pyrolysis cause decomposition of organic structures from the raw feedstock through dehydrogenation, demethylation, and finally decarboxylation resulting in the release of a variety of organic compounds, including volatile C compounds, CH_4, and CO [7]. By assessing the elemental composition of the raw feedstock and the biochar, a determination of these released volatile compounds containing C, H, and O will result in major shifts in their atomic O/C and H/C ratios (Fig. 7).

The Van Krevelen diagram is a convenient way to show that the raw feedstocks are rich in H and O, and as the pyrolysis temperature increases, loss of volatile elements cause biochars to have decreasing O/C and H/C atomic ratios (Fig. 7). Consequently, manufacturers can quickly assess the degree of biochar production by examining for changes in the elemental concentrations of C, H, O, and N, and their associated ratios. For example, low H/C and O/C ratios indicate that the biochar is higher in aromatic structures [7, 48]. Biochars with O/C and H/C ratios in the 0.3–1.2 range indicate that it contains lignin and polysaccharide-like compounds [48]. Krull et al. [56] has listed atomic ratios, including the OC contents, in biochars processed from several feedstocks and pyrolysis temperatures.

Computation of a biochars atomic ratio requires that a sample be digested resulting in its loss for future experiments. Alternative, nondestructive methods for

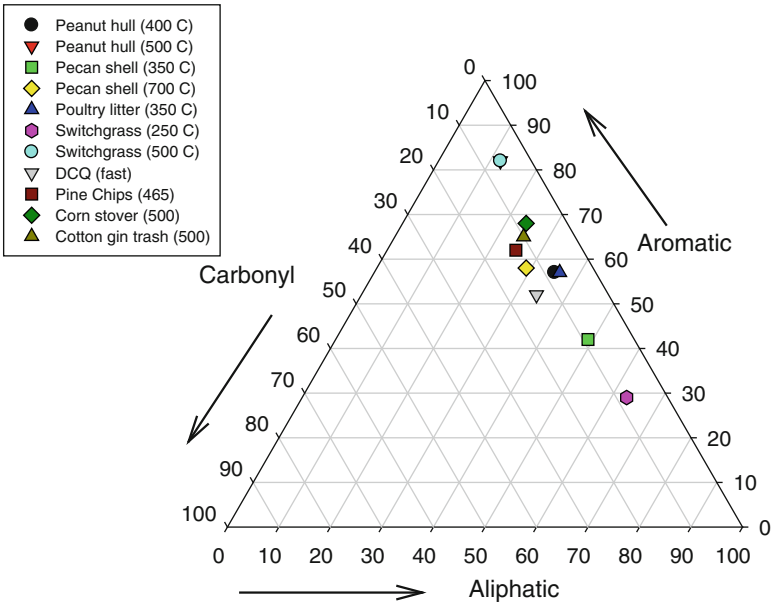

Fig. 8 Carbon distribution in biochars produced from various feedstocks using high (>400°C), low (<400°C) and fast pyrolysis (pine chip and corn stover results courtesy of Dr. Don Reicosky)

biochar characterization are available, such as solid-state ^{13}C nuclear magnetic resonance (NMR, [56]), and Fourier transformed infrared spectroscopy (FT-IR; [80, 84]). If ^{13}C NMR spectroscopy is used, each sample analyses may take several hours to 1 day to acquire the spectral pattern. As presented below, ^{13}C NMR spectroscopy is a more practical tool for examining progressive structural changes in biochars with increasing pyrolysis temperatures. Research has shown that plant-based feedstocks pyrolyzed between 350 and 400°C, cellulose and hemicellulose degradation occurs [7]. In the mid-range temperature of 400–500°C, additional structural modifications can occur through condensation of aromatic molecules in the basal sheets followed by loss of functional groups as a result of decarboxylation and demethylation reactions. At the higher pyrolysis temperature regime (500–700°C), biochars will be dominated by aromatic-C groups, with minor contributions of carbonyl-C, *O*-alkyl-C, and alkyl-C moieties [56, 74]. The dominance of C in aromatic groups in high temperature pyrolyzed biochar is evident when plotting the ^{13}C distribution in each biochars aliphatic, aromatic, and carbonyl region of the NMR spectral patterns (Fig. 8). Biochars pyrolyzed from switchgrass and peanut hull feedstocks at 500°C had the highest aromatic-C character (82%) among the 11 biochars evaluated. Lower temperature pyrolyzed biochars (250–350°C) have more C as aliphatic structures because their polysaccharide-like compounds have not been lost to thermal degradation [5].

As shown in Fig. 9 (top), the ^{13}C NMR spectra of cotton gin trash biochar (500°C) was dominated by a peak at 128 ppm due to resonance of aromatic C structures,

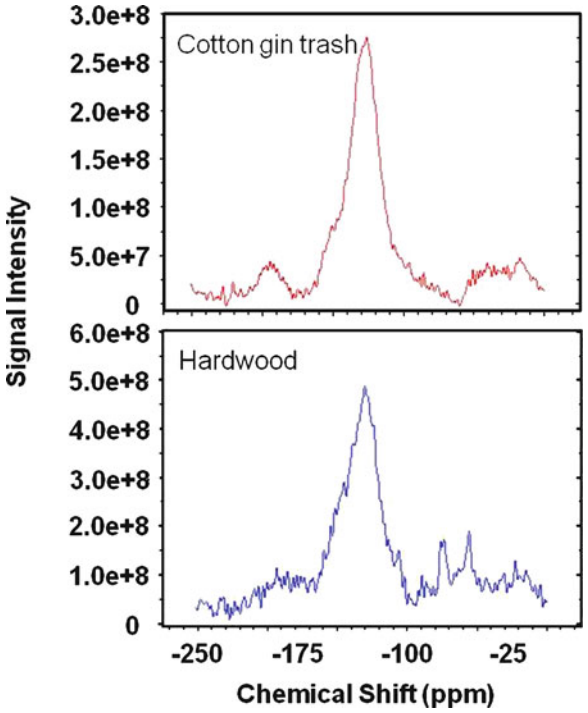

Fig. 9 ^{13}C NMR spectra of (*bottom*) hardwood biochar (fast pyrolysis) and (*top*) cotton gin trash (500°) biochar

while minor spectral peaks were recorded in the aliphatic-C (0–50 ppm), polysaccharide-C (60–110 ppm) and carboxylic-C (194 ppm) region. Integrating the area of the spectral region revealed that the cotton gin trash biochar contained 65% aromatic-C with only 12% occurring as polysaccharides. Most of the polysaccharide-like compounds in the cotton gin trash biochar were lost during pyrolysis at the higher temperature regime (500°C).

Biochar (Fig. 9, bottom), which has been produced from hardwoods using a fast pyrolysis system, had minor peaks at 56 and 75 ppm, respectively, which is indicative of methoxy and C–O groups in polysaccharides. Similar to gin trash biochar, the hardwood biochar was dominated by an aromatic-C peak (126 ppm) which accounted for 52% of the C distribution. A minor amount (20%) of the total C structures occurred in polysaccharide-like compounds.

Fourier transformed infrared spectroscopy can determine the presence of types of organic compounds in biochars [80, 84]. It is a robust system and uses the mid-infrared spectrum (4,000–500 cm^{-1}) to examine for sorption peaks that are diagnostic of rotational and vibrational movements of molecular structures and bonds within those structures [101]. On the one hand, there are issues with FT-IR analyses including broad peaks due to sorbed moisture [101] and sorption overlap that complicates ascribing the organic compound responsible for the sorption peaks [78]. On the other hand, very little sample is needed (few mg), it is nondestructive, and the results are more rapidly obtained when compared to ^{13}C NMR spectroscopy.

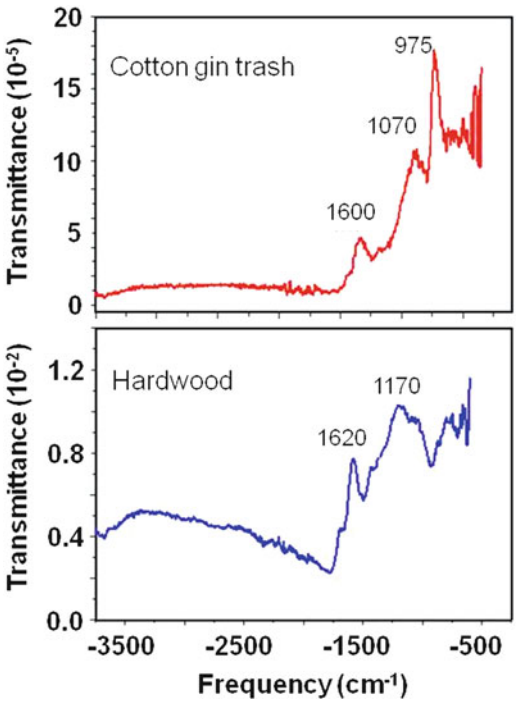

Fig. 10 FT-IR spectra of (*bottom*) hardwood biochar (fast pyrolysis) and (*top*) cotton gin trash biochar (500°C)

These properties make FT-IR an acceptable analytical tool for examination of biochar properties during manufacturer and for biochar mineralization studies. For example, FT-IR spectroscopy has been employed to determine structural and functional group changes during biochar mineralization in soils [23, 24, 75]. The FT-IR spectral analysis of biochar pyrolyzed from cotton gin trash (Fig. 10, top) and hardwood biochar (bottom) show broad peaks between 3,500 and 2,000 cm^{-1}, but also a few sharp peaks between 1,600 and 1,620, and 1,170–975 cm^{-1}. Surface hydroxyls and or sorbed water and C–H stretching are responsible for the broad beak between 3,500 and 2,000 cm^{-1}. Peaks at 1,620 and 1,600 cm^{-1} are ascribed to aromatic C=C and H-bonded C=O and peaks at 1,170, 1,070 and 975 cm^{-1} are indicative of C–O stretching of polysaccharides and OH deformation of COOH groups [101]. The aromatic peak in the FT-IR spectra of the hardwood biochar is more distinct than in the gin trash, which is consistent with ^{13}C NMR results.

4 Biochars Designed to Resolve Specific Soil Issues

Biochar pyrolyzed from organic feedstocks (i.e., woody wastes, crop residues, nutshells, manures, etc.) have the potential to increase long-term soil C sequestration, restore fertility, and promote aggregate formation in soils. Biochar application

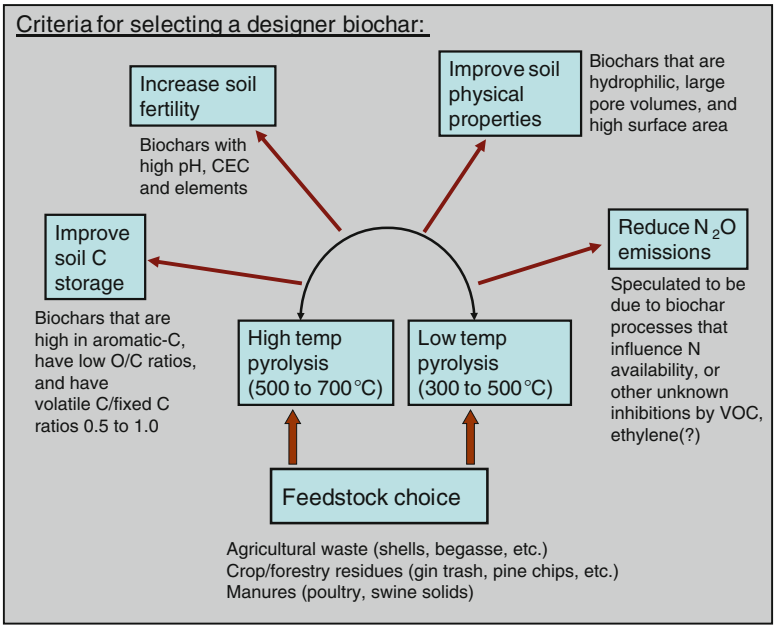

Fig. 11 Criteria for the manufacture of a designer biochar considering relationships between targeted soil properties, feedstock selection, and pyrolysis conditions

to soils unfortunately is not "a one-size fits all" principle, but biochars need to be crafted to target soil chemical and physical deficiencies. This is the creed of designing a biochar.

We can identify a targeted soil chemical and physical characteristics that could be improved, and explain how a designer biochar can be manufactured to possess properties that will ameliorate soil problems. In Fig. 11, we present a diagram that shows four problem areas of coastal plain soils described earlier, and then offers a pick of feedstock and pyrolysis temperature (high vs. low) to produce a biochar designed with specific properties to resolve the select soil problem. The next section discusses relationships between the designer biochar and definite soil problem.

4.1 Increasing Soil C Storage

Because of the coastal plain soils advanced age, the single most important soil quality issue to improve, arguably, is the low soil SOC contents (Fig. 4). While most of the OC from crop residue is lost within a few months [72]; the logical remedy would be to increase long-term SOC by applying a biochar that has recalcitrant properties (Fig. 11). Biochars suited to long-term C storage in soils have highly aromatic composition [45, 87] and black carbon with low O/C ratios (0.2–0.4, [68, 97]).

Table 3 Cumulative CO_2 evolved (mg)[a] from Norfolk E after mixing in 1% (w w^{-1}) crop/wood residue and pecan shell biochar (results submitted for publication)[b]

Norfolk E mixed with	Mean[c]
Control	0.77a
Corn stalk	1.75bc
Cotton hull	1.76b
Soybean	1.39b
Peanut hull	0.81a
Poultry litter	2.37c
Hardwood shavings	0.43a
Pecan shell biochar (700°C)	0.65a

[a]Measured with an Li-Cor 6250 CO_2 analyzer
[b]Sufficient raw crop/wood residues added to E horizon soil to obtain 1% (w w^{-1}) OC and each treatment ($n=3$) incubated for 67 day at 10% (w w^{-1}) soil moisture content
[c]Tested for significant differences using a 1-way ANOVA with means followed by a different letter being signficantly different

To design biochar with these properties, feedstocks should be pyrolyzed at high temperature (500–700°C) leading to biochar composed of poly-condensed aromatic structures [7, 48] and O/C ratio similar to charcoal (0.2–0.4, [49]). A good example of an appropriate feedstock choice is pecan shells, which after high temperature pyrolysis at 700°C, had 58% C in aromatic structures and an atomic O/C ratio of 0.02 [73]. After 67 days of laboratory incubation in a Norfolk E horizon, pecan shell biochar (700°C) had the lowest CO_2 evolved when compared to the control and several raw crop residues (Table 3). In fact, its CO_2 mass evolved was similar to soil treated with hardwood shavings. These are laboratory results that were obtained only after few months of biochar incubation in the sandy Norfolk soil. But, the relative difference in CO_2 evolution suggests that if pecan shells were pyrolyzed at a high temperature (700°C), they would serve as a suitable designer biochar to increase C sequestration in the sandy Norfolk soil. Other feedstocks (i.e., hardwoods, shells from other nut crops, etc.) may also be suitable, but should also have high aromaticity and atomic O/C ratios of <0.4.

Another characteristic for biochar stability in soils is its volatile matter/fixed carbon (VM/FC) ratio [3]. Biochar with VM/FC of 0.5–1.0 are speculated to be stable in soils [3]. As an acceptable index of biochars longevity in soil, the actual relationship between its VM/FC ratio with CO_2 evolution from soils/culture media needs further evaluation.

4.2 Improving Soil Fertility

Sandy soils in the coastal plain of South Carolina have inherently low soil fertility and a meager capacity to retain nutrients. Increased levels of SOC are regarded as an important determent to improve their fertility. Organic carbon compounds

Table 4 Mean fertility characteristics in a Norfolk Ap after 0 and 120 days laboratory incubation with 2% (w w^{-1}) peanut hull and hardwood biochars ($n=4$, unpublished data)[a]

Treatment	Pyrolysis (°C)	Incubation (day)	pH[b]	CEC ($mol_c kg^{-1}$)	Soil OC ($g\ kg^{-1}$)	Total *N* ($g\ kg^{-1}$)	Mehlich 1 extractable ($mg\ kg^{-1}$)			
							P	K	Ca	Mg
Control	–	0	5.6	2.2	2.78	0.35	28	37	131	24
		120	5.2a	1.8a	2.81a	0.22a	29a	14a	100a	14a
Peanut hull	400	0	7.3	2.7	18.80	0.77	47	319	173	46
		120	7.1b	2.4b	18.80	0.78b	39b	111b	174b	51b
	500	0	7.4	2.4	21.80	0.75	38	304	151	31
		120	7.4c	2.1ba	19.55	0.71b	33c	145c	159b	37c
Hardwood	Fast	0	6.1	2.6	18.42	0.35	28	85	187	28
		120	6.2d	2.3b	17.18	0.37c	22d	46d	154b	18d

[a]Treatments leached with di. H_2O four times during the 120 day incubation period
[b]Means of soil characteristics measured on day 120 of incubation within a column followed by a different letter are significantly different using a 1-Way ANOVA at a $P=0.05$ level of significance

returned as crop residues to sandy soils are temporal; a longer lasting solution is need. Therefore, it would be sensible to supplement sandy soils with biochar. This is not a new concept, but has been practiced by Amerindian populations for a long period of time [63]. In fact, it is arguably the starkest example of improving impoverished Amazonian soils. In this region, the inhabitants stock piled char-like material on red-colored, infertile soils to convert them into a dark earth colored soil called "terra preta do Indio" [45, 95, 100]. Today, large amounts of C supplied through biochar additions to the Terra Preta soils have lasted for thousands of years after they were deserted [61]. In fact, Glaser et al. [44] reported that as much as 250 Mg C ha^{-1} has been sequestered in the Terra Preta as compared to 100 Mg C ha^{-1} typically measured in surrounding untreated soils. The message is apparent that biochars applied to the Terra Preta soils improved their fertility while also supplying C in recalcitrant forms that have lasted for several thousand years.

Building on the fertility gains by applying biochars to Terra Preta soils, let us establish the Norfolk's Ap low fertility as the target issue to improve (Table 4). The next step would be selection of a feedstock and pyrolysis conditions (Fig. 11) that produces a biochar with properties chosen to compensate for these targeted (pH, SOC, N, P, etc.) problems. Among the biochar properties shown in Table 1, peanut hulls and poultry litter biochar contain greater N, P contents, and would act as a liming agent because of their alkaline pH. Biochars produced from the remainder of the feedstocks contain lesser amounts of nutrients or are not as alkaline. So, a logical choice would be to use peanut hull and poultry litter feedstock and the preference of pyrolysis temperature could be selected based on the desired biochars nutrient concentration or by its alkalinity. If more nutrients and a better liming agent are desired, then the biochars should be produced using a higher pyrolysis temperature (>500°C; Table 1).

The biochar application rates to this example Norfolk Ap, however, should be carefully chosen to avoid causing excessive alkaline or macronutrient imbalances.

Because this Norfolk Ap sample has a low buffer capacity, gross chemical changes occur with high biochar applications. For example, Novak et al. [74] reported that intensive application of poultry litter biochar (40 Mg ha^{-1}) to a Norfolk Ap resulted in high soil pH values (8–9.7) and excessively high Mehlich-1 extractable P concentrations (1,280–1,812 kg ha^{-1}). Under these conditions, the Norfolk Ap contained plant available P concentrations that were grossly in excess of soil plant P sufficiency levels [51]. These disproportionate P concentrations, if moved off-site, poses surface and ground water quality issues [17, 47]. Crops may also experience micronutrient deficiencies; micronutrients have low solubility at elevated soil pH levels [102].

Unwanted soil pH increases may be avoided by employing alternate feedstocks such as peanut hulls, pecan shells, hardwood, or pine chips because they contain modest N-P-K ratios and are not as alkaline (Table 1). It should be understandable that when applying biochar to soil, it is important to not create an additional problem while attempting to solve the target soil problem. The impact of biochars produced from these alternate feedstocks and under different pyrolysis conditions (high vs. low temperature) on the fertility of a Norfolk Ap was shown in Table 4. Both peanut hull (400 and 500°C) and hardwood biochars were added at 2% (w w^{-1}, 40–44 Mg ha^{-1}). The treatments were laboratory incubated for 4 months and were then leached monthly with water to simulate loss of nutrients due to rainfall and/or irrigation. All biochar treatments after 120 days of incubation significantly raised soil pH, SOC, and TN contents, CEC had mixed results, when compared to the control (Table 4). After 120 days of incubation, the CEC increases were not particularly large (<0.6 $cmol_c\ kg^{-1}$), but some of the increases were still significant. The Norfolk Ap fertility was increased because Mehlich 1 extractable P, K, Ca, and Mg were all significantly higher than the control (Table 4). Both peanut hull biochars caused the greatest increases in OC, TN, and K relative to the control. Both OC and Ca concentrations were increased after applying hardwood biochar; minimal improvement occurred in pH, TN, P, K, and Mg concentrations. These results imply that hardwood would be an appropriate feedstock for a biochar designed to improve SOC and Ca levels alone, without causing large upward shifts in soil pH. Unfortunately, hardwood did not improve other soil problems such as low N and P contents. If OC and N improvements were the target soil fertility issue, then peanut hull would be an appropriate feedstock and either pyrolysis temperature.

Water leaching of the treatments resulted in loss of K and some P, whereas mixed results were obtained for the other nutrients. Leaching of K is not unexpected in sandy soils; its monovalent charge causes it to be less attracted to cation exchange sites [102]. This Norfolk's Ap fertility status was improved by employing a biochar with appropriately designed characteristics. We avoided using an ill-suited biochar (poultry litter) in this situation because prior laboratory soil incubation showed that would cause a negative soil legacy (e.g., excessive nutrient concentrations, alkaline pH values, etc. [75]) potentially resulting in crop productivity declines. Poultry litter biochar has special chemical properties, such as high P and alkalinity, which may be useful as a fertilizer and lime source if their concentrations are diluted through blending with benign biochar (see Sect. 6).

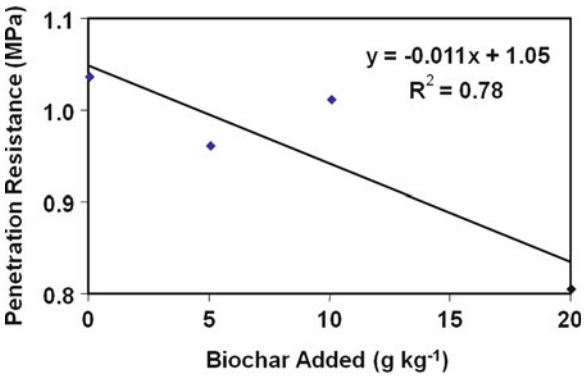

Fig. 12 Penetration resistance of a Norfolk Ap after 44 days of incubation with pecan shell biochar [15]

Biochars applications are not just limited to infertile soils, but the technology can be applied to fertile, mid-western soils as a supplement for increased C sequestration and to replace nutrients lost through plant uptake, erosion and leaching. Laird et al. [59] incubated a hardwood biochar produced by slow pyrolysis in an Iowa Mollisol (Typic Hapludoll) and reported significant increases in total N, OC and Mehlich 3 extractable P, K, Mg, and Ca concentrations. In a similar study, Laird et al. [60] reported that the same biochar reduced total N and dissolved P leaching from swine manure applied to this Mollisol. These results imply that hardwood biochar additions to a mid-western Mollisol can be an effective agricultural and environmental management option by improving fertility and minimizing nutrient leaching. The authors did not choose to investigate if other feedstocks and different pyrolysis temperatures could have resulted in biochars with designed characteristics to improve the biochars performance at modifying fertility and nutrient leaching.

4.3 Improving Soil Physical Issues

The Norfolk soil has several physical problems such as low water retention, and a poorly aggregated subsurface hard layer that challenges agricultural productivity. If these physical problems are targeted for improvement, then their upgrading would also require an assessment of bulk density and aggregate formation since these features significantly influence pore space available to store water and lessen root penetration resistance [102]. Designing a biochar to resolve these soil physical issues once more requires identifying a feedstock and pyrolysis conditions followed by an assessment of their performance. Biochars effects on bulk density, available water storage, and aggregate formation were evaluated in a similar manner as described in Table 4. Pecan shell biochar pyrolyzed at 700°C was further evaluated in the Norfolk Ap to assess its impacts on reducing penetration resistance (Fig. 12; [15]).

Table 5 Mean physical properties in a Norfolk Ap after 0 and 120 days laboratory incubation with 2% (w w^{-1}) peanut hull and DCQ (hardwood) biochars ($n=4$, data submitted for publication)[a]

Treatment	Pyrolysis (°C)	Incubation (day)	Bulk density (g cm^{-3})[b]	Available H_2O (mm/150 mm)	Aggregate wt.[c]	
					1.0-mm	0.5-mm
Control	–	0	1.37	–	–	–
		120	1.62a	8.82a	3.08a	18.94a
Peanut hull	400	0	1.49	–	–	–
		120	1.57a	21.64b	3.43b	20.33b
	500	0	1.57	–	–	–
		120	1.59a	17.78c	3.11a	19.92b
Hardwood	Fast	0	1.51	–	–	–
		120	1.57a	20.67b	3.46b	21.47c

[a]Treatments leached with di. H_2O four times during the 120 day incubation period
[b]Means of soil characteristics measured on day 120 of incubation within a column followed by a different letter are significantly different using a 1-Way ANOVA at a $P=0.05$ level of significance
[c]Percentage of total

The poor physical properties of the Norfolk Ap (control) are evident; it had the lowest available water, small amounts of 1.0 and 0.5 mm sized soil aggregates (Table 5), and the highest penetration resistance (Fig. 12). These physical properties were significantly improved after mixing in the four biochars relative to the control (Table 5 and Fig. 12). Closer examination of the significant differences in these measured properties will reveal the suitable feedstock and pyrolysis temperature for producing the designer biochar. Pecan shell biochar produced at 700°C was found to reduce soil strength in the Norfolk Ap, especially at the 40 Mg ha^{-1} application rate (Fig. 12; [15]). Mixed results, however, were obtained for pecan shell biochar to increase water retention [15]. Pecan shell biochar (700°C) is more suitable under these conditions with resolving soil penetration resistance. On the other hand, peanut hull biochar at the lower pyrolysis temperature (400°C) provided a greater increase in available water and in 1.0-mm aggregate formation. Lower soil water increases were obtained using the higher temperature (500°C) peanut hull biochar.

Biochar produced from hardwood under fast pyrolysis significantly improved two soil physical properties relative to the other treatments. Among these three feedstocks, the hardwood-based biochar appears to be a more appropriate feedstock selection for physical improvement. Hardwoods subject to fast pyrolysis may be the best feedstock for producing a designer biochar. If hardwood biochar is used to resolve soil physical issues, concomitant improvements of SOC and Ca concentrations are obtainable without elevating the Norfolk's pH.

4.4 Biochar and N_2O Dynamics

Greenhouse gas emissions as CO_2, CH_4, and N_2O as a result of fossil fuel usage and agricultural activity within the USA have increased 14% between 1990 and 2008 [40]. The agricultural sector was estimated by the US-EPA to contribute approximately 6%

of the total GHG emissions. Animal and crop production may account for as much as 70% of the annual global anthropogenic N_2O emitted [65]. Globally, N_2O is a significant contributor to the emission total (≈8%, [35]) and has a global warming potential of 298 times greater than CO_2 [41]. The large difference in N_2O radiative force with CO_2 causes it to have a larger destructive potential to the stratospheric ozone layer [26].

N_2O fluxes have been measured in agricultural field, but estimates of their overall contributions to the global GHG budget is difficult to estimate because fluxes have been linked to differences in soil N application, N form, soil pH, soil wetness, and tillage practices [33, 54, 76]. Nevertheless, the sizable hazard that N_2O poses for climate change relative to CO_2, suggests that it is important to have management strategies available to curtail N_2O production from agricultural soils. This will require both field and laboratory evaluations between feedstock, pyrolysis conditions, and biochar chemical properties on N_2O dynamics.

Both field and laboratory studies reported that biochar additions to soil can reduce N_2O emissions [42, 67, 83, 90, 96, 104]. In the field, biochar applications at 20 Mg ha^{-1} to soybean plots were found to cause a 50% curtailment in N_2O emissions [83]. While in the lab, N_2O production was suppressed by a variety of biochars produced from nut shell wastes and hardwoods [96] and from poultry litter and wood [90]. In fact, both studies employed biochars produced at different temperatures and reported difference in N_2O reduction. Neither study reported an over-arching biochar chemical/structural characteristic as responsible for reducing N_2O emissions.

Not all biochars will suppress N_2O emissions when added to soils, in fact, Spokas and Reicosky [96] reported that two out of 16 biochars stimulated N_2O production relative to the control. Similarly, Singh et al. [90] reported that a biochar produced from pyrolyzed poultry manure at 400°C stimulated N_2O production. Based on these reports, it is difficult to make suggestions (Fig. 11) to create a biochar tailored to effectively suppress N_2O production.

What we do know, however, is that biochars may suppress N_2O production if they have properties that influence N availability [90], decrease soil microbial activity [96], and improve soil physical properties that promotes aeration [58]. Whereas, others have reported soil N_2O production can be stimulated with biochar. These conflicting conclusions suggest that additional laboratory and field evaluations involving biochars produced from multi-feedstocks and under different pyrolysis conditions are needed.

5 Biochar Blends Create Hybrid Biochars

This review has shown that each biochar evaluated has a unique set of chemical and physical properties. While one biochar may be effective at resolving one soil problem, it may also have properties that are either benign or promote gross changes to another soil property. It would be beneficial, if a negative characteristic of a biochar could be turned into an advantage through blending. Blending of different biochars to produce a hybrid product with designed characteristics for a specific soil purpose

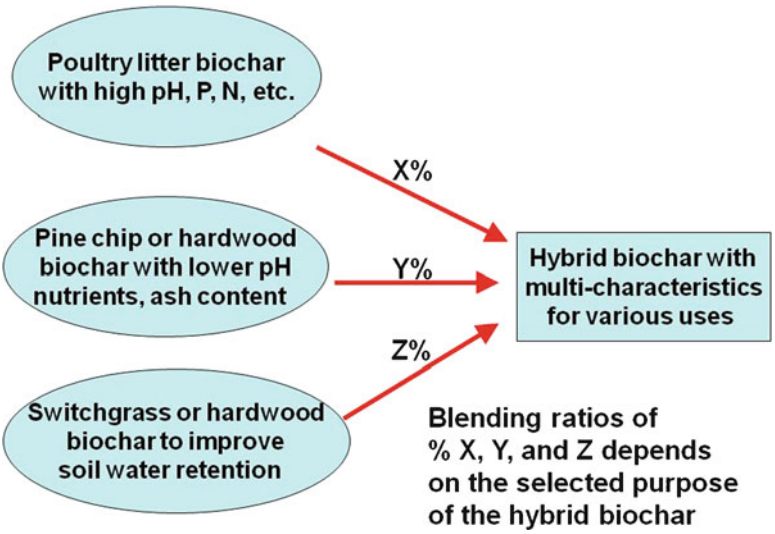

Fig. 13 Blending biochars creates a multifunctional hybrid biochar

is possible (Fig. 13). For instance, in acid environments, such as in mine reclamation, metals such as Al, Cu, Mn, Pb, and Zn are highly soluble [10]. These metals, in sufficient quantities, can pose a hazard to plants. A proper remediation strategy would be to reduce their solubility by raising the pH and/or by complexation with soil organic compounds. This may be achieved by applying a high temperature pyrolyzed biochar (>400°C) produced from peanut hulls, pecan shells, and switchgrass, which have alkaline pH values (Table 1). In fact, peanut hull biochar produced at both pyrolysis temperatures did raise the pH of a sandy soil (Table 2). Biochars made from other feedstocks (i.e., hardwoods, pine chips, poultry litter, etc.) may be unsuitable for application in mine spoil sites because of their inability to act as a liming agent or by potential increases in other nutrients solubility (i.e., P, Fe, etc.). The impact of biochars or blends on remediating mine reclamation sites is largely unknown, but could be a viable assignment for biochars found not to be suitable for agricultural soil improvement.

Poultry litter biochar, although it has some difficult characteristics, can still be used as a low-grade fertilizer (Table 1). It contained the highest N-P-K ratios, is extremely alkaline, and also contained high levels of Na [74]. Problems associated with these properties could be rebalanced or diminished by blending with other biochars (i.e., hardwood, pine chips, etc.) to produce a hybrid biochar (Fig. 13) that has more benign characteristics (Tables 1 and 3; lower N-P-K ratios, ash contents, pH, etc.) or added to improve another soil issue (i.e., low water holding capacity, etc.). The blending ratio of other biochars can be chosen depending upon the purpose of the hybrid biochar (Fig. 13). As an example, a hybrid biochar blend could consist of a mixture of hardwoods, pine chips, and poultry litter biochar; a blend designed to improve soil water storage while also delivering C, N, P and raising the pH as well.

Blending biochars for agricultural production or commercial purposes is beyond the concept stage. Commercial companies have internet sites advertising that their designer biochars made from blended materials that have their own unique properties. These companies have developed a biochar product that could be used in a number of different market sectors (greenhouse, nursery, golf courses, etc.) as a plant media, improvement in golf greens, or in site reclamation.

6 Conclusions

Biochars can be produced from diverse feedstocks and under a variety of pyrolysis conditions. Because resultant biochar properties vary, no one biochar will fit all soil improvement intentions. Each biochar has its own unique chemical and physical signature and when applied to soils may have a positive, negative, or a benign effect. To avoid creating unwanted long-lasting effects in soils, thus the concept of designer biochar was introduced and the utility of producing biochars tailored for specific soil problems was illustrated. If one biochar has unsatisfactory properties, then blends of biochars in unique proportions can be created to produce a hybrid biochar that has tailored characteristics to provide multiple benefits for specific soil problems. In this review, designer biochars were shown to have a positive effect by improving soil fertility and physical properties. In the future, biochars or their hybrid blends may also be formulated to reduce N_2O emissions.

Because of their costs, designer biochars may be regarded as a product for boutique markets; but, they would definitely improve production in agricultural fields if costs were reduced. Given the fact that biochars react in a different way in different soils, more research is needed to understand relationships between feedstock and pyrolysis conditions vs. biochar quality. Therefore, this review has suggested potential protocols and guidelines for the selection of feedstock's and pyrolysis conditions to produced biochars with tailored properties for selected soil problems.

Acknowledgments This publication is based on work supported by the US Department of Agriculture, Agriculture Research Service, under the ARS-GRACEnet project. Sincere gratitude is expressed to scientists, and support staff at the ARS-Florence location for their time and commitment on the myriad of biochar projects. Mention of specific product or vendor does not constitute a guarantee or warranty of the product by the U.S. Department of Agriculture or imply its approval of the exclusion of other products that may be suitable.

References

1. Adeoye KB, Mohamed-Saleem MA (1990) Comparison of effects of some tillage methods on soil physical properties and yield of maize and stylo in a degraded ferruginous soil. Soil Till Res 18:63–72
2. Akinci I, Cakir E et al (2004) The effect of subsoiling on soil resistance and cotton yields. Soil Till Res 77:203–210

3. Amonette JE, Hu Y et al (2009) Biochars are not created equal: a survey of their physical, structural, and chemical properties and implications for soil application. North American Biochar Conference, Boulder, CO. http://cees.colorado.edu/biochar_production.html. Accessed 2 Aug 2010
4. Amonette JE, Joseph S (2009) Characteristics of biochar: micro-chemical properties. In: Lehmann JL, Joseph S (eds) Biochar for environmental management. Earthscan, London
5. Antal MJ, Grønli M (2003) The art, science, and technology of charcoal production. Ind Eng Chem Res 42:1619–1640
6. Atkinson CJ, Fitzgerald JD et al (2010) Potential mechanism for achieving agricultural benefits from biochar application to temperate soils: a review. Plant Soil 337:1–18. doi:10.1007/s11104-010-0464-5
7. Baldock JA, Smernik RJ (2002) Chemical composition and bioavailability of thermally altered *Pinus renosa* (red pine) wood. Org Geochem 33:1093–1109
8. Beare MH, Hendrix PF et al (1994) Water-stable aggregates and organic matter fractions in conventional- and no-tillage soils. Soil Sci Soc Am J 58:777–786
9. Blackwell P, Riethmuller G et al (2009) Biochar application to soil. In: Lehmann JL, Joseph JS (eds) Biochar for environmental management. Earthscan, London
10. Bohn HL, McNeal BL et al (1979) Soil chemistry. Wiley, New York
11. Brown R (2009) Biochar production technology. In: Lehmann JL, Joseph JS (eds) Biochar for environmental management. Earthscan, London
12. Bruce RR, Langdale GW (1997) Soil carbon level dependence upon crop culture variables in a thermic-udic region. In: Paustian EA, Paul K et al (eds) Soil organic matter in temperate agroecosystems: long-term experiments in North America. CRC, Boca Raton
13. Busscher WJ, Lipiec J et al (2000) Improved root penetration of soil hard layers by selected genotype. Commun Soil Sci Plant Anal 31:3089–3101
14. Busscher WJ, Frederick JR (2001) Effect of penetration resistance and timing of rain on grain yield of narrow-row corn in a coastal plain loamy sand. Soil Till Res 63:15–24
15. Busscher WJ, Novak JM et al (2010) Influence of pecan biochar on physical properties of a Norfolk loamy sand. Soil Sci 175:10–14
16. Busscher WJ, Schomberg HH et al (2010) Soil and water conservation in the Southeastern United States: a look at conservation practices past, present and future. In: Zobeck TM, Schllinger WF (eds) Soil and water conservation in the United States. Soil Science Society of America Special Publication 60. SSSA, Madison
17. Cahoon LB, Mikucki JA et al (1999) Nitrogen and phosphorus imports to the Cape Fear and Neuse River Basins to support intensive livestock production. Environ Sci Technol 33:410–415
18. Campbell RB, Reicosky DC et al (1974) Physical properties and tillage of Paleudults in the southeastern Coastal Plain. J Soil Water Conserv 29:220–224
19. Carter MR, Holmstrom DA et al (1996) Persistence of deep loosening of naturally compacted subsoils in Nova Scotia. Can J Soil Sci 76:541–547
20. Chan KY, Van Zwieten L et al (2008) Using poultry litter biochars as soil amendments. Aust J Soil Sci 46:437–444
21. Chan KY, Xu Z (2009) Biochar: nutrient properties and their enhancements. In: Lehmann JL, Joseph S (eds) Biochar for environmental management. Earthscan, London
22. Chartres CJ, Kirby JM et al (1990) Poorly ordered silica and aluminosilicates as temporary cementing agents in hard-setting soils. Soil Sci Soc Am J 54:1060–1067
23. Cheng CH, Lehmann J et al (2006) Oxidation of black carbon by biotic and abiotic processes. Org Geochem 37:1477–1488
24. Cheng CH, Lehmann J et al (2008) Natural oxidation of black carbon in soils: changes in molecular form and surface charge along a climosequence. Geochim Cosmochim Acta 72:1598–1610
25. Cooke CW (1931) Seven coastal terraces in the southeastern states. Wash Acad Sci J 79:503–513

26. Crutzen PJ (1981) Atmospheric chemical processes of the oxides of nitrogen, including nitrous oxide. In: Delwiche CC (ed) Denitrification, nitrification and atmospheric nitrous oxide. Wiley, New York
27. Day D, Evans RJ et al (2005) Economical CO_2, SOx, and NOx capture from fossil-fuel utilization with combined renewable hydrogen production and large-scale carbon sequestration. Energy 30:2558–2579
28. Daniels RB, Gamble EE et al (1967) Relationship between A2 horizon characteristics and drainage in some fine loamy Ultisols. Soil Sci 104:364–369
29. Daniels RB, Gamble EE (1967) The edge effect in some Ultisols in the North Carolina coastal plain. Geoderma 1:117–124
30. Daniel RB, Buol SW et al (1999) Soil systems of North Carolina. North Carolina State University Technical Bulletin 314, Raleigh, NC
31. Daniels RB, Gamble EE et al (1971) Relationship between soil morphology and water-table levels on a dissected North Carolina Coastal Plain surface. Soil Sci Soc Am Proc 35:781–784
32. Daniels RB, Gamble EE et al (1978) Age of soil landscapes in the coastal plain of North Carolina. Soil Sci Soc Am J 42:98–104
33. Dendooven L, Duchateau L et al (1996) Denitrification as affected by the previous water regime of the soil. Soil Biol Biochem 28:239–245
34. Denef K, Zotarelli L et al (2007) Microaggregates associated carbon as a diagnostic fraction for management-induced changes in soil organic carbon in two Oxisols. Soil Biol Biochem 39:1165–1172
35. Denman KL, Brasseur G et al (2007) Coupling between changes in the climate system and biogeochemistry. In: Solomon S et al (eds) Climate change 2007: the physical science basis. Contribution of working groups I for the fourth assessment report of the Intergovernmental Panel on climate change. Cambridge Press, Cambridge
36. Doty CW, Campbell RB et al (1975) Crop response to chiseling and irrigation in soils with a compact A_2 horizon. Trans ASAE 18:668–672
37. Doty CW, Parsons JE (1979) Water requirements and water table variations for a controlled and reversible drainage system. Trans ASAE 22:532–539
38. Downie A, Crosky A et al (2009) Physical properties of biochar. In: Lehmann JL, Joseph S (eds) Biochar for environmental management. Earthscan, London
39. Ekwue EI, Stone RJ (1995) Organic matter effects on the strength properties of compacted agricultural soils. Trans ASAE 38:357–365
40. EPA (2010) Inventory of the U.S. greenhouse gas emissions and sinks: 1990-2008. U.S. EPA# 430-R-10-006. U.S. Environmental Protection Agency, Washington, DC. http://www.epa.gov/climatechange/emissions/usinventroyreport.html. Accessed 18 Aug 2010
41. Forester P, Ramaswamy V et al (2007) Changes in atmospheric constituents and in radiative forcing. In: Solomon S et al (eds) Climate change 2007: the physical science basis. Contribution of working groups I for the fourth assessment report of the Intergovernmental Panel on Climate Change. Cambridge Press, Cambridge
42. Fowles M (2007) Black carbon sequestration as an alternative to bioenergy. Biomass Bioenergy 31:426–432
43. Gaskin JW, Steiner C et al (2008) Effect of low-temperature pyrolysis conditions on biochar for agricultural use. Trans ASABE 51:2061–2069
44. Glaser B, Haumaier L et al (2001) The Terra Preta phenomenon—a model for sustainable agriculture in the humid tropics. Naturwissenschaften 88:37–41
45. Glaser BJ, Lehmann J et al (2002) Ameliorating physical and chemical properties of highly weathered soils in the tropics with charcoal-a review. Biol Fertil Soils 35:219–230
46. Gray LC (1933) History of agriculture in the southern United States to 1860. Carnegie Institution, Washington, DC
47. Haygarth PM, Hepworth L (1998) Forms of phosphorus transfer in hydrological pathways from soil under grazed grasslands. Eur J Soil Sci 49:65–72

48. Hammes K, Smernik RJ et al (2006) Synthesis and characterization of laboratory-charred grass straw (*Oryza sativa*) and chestnut wood (*Castanea sativa*) as reference material for black carbon quantification. Org Geochem 37:1629–1633
49. Hedges JI, Eglinton G et al (2000) The molecularly-uncharacterized component of nonliving organic matter in natural environments. Org Geochem 31:945–958
50. Hunt PG, Karlen DL et al (1996) Changes in carbon content of a Norfolk loamy sand after 14 yrs of conservation or conventional tillage. J Soil Water Conserv 51:255–258
51. Jones BJ Jr (2003) Agronomic handbook-management of crops, soils, and their fertility. CRC, Baca Raton
52. Karlen DL, Busscher WJ et al (1991) Drought condition energy requirement and subsoil effectiveness for selected deep tillage implements. Trans ASAE 34:1967–1972
53. Kinney TJ, Dean MR et al (2009) Engineering biochar hydrophobicity to mitigate risk of top-soil erosion. American Geophysical Union, Fall Meeting, Abstract #B41B-0301. http://absabs.harvard.edu/abs/2009AGUFM.B41B0301K. Accessed 18 July 2010
54. Kessavalou A, Mosier AR et al (1998) Fluxes of carbon dioxide, nitrous oxide, methane in grass sod and winter wheat-fallow tillage management. J Environ Qual 27:1094–1104
55. Kleiss HJ (1994) Relationship between geomorphic surfaces and low activity clay on the North Carolina coastal plain. Soil Sci 157:373–378
56. Krull ES, Baldock JA et al (2009) Characteristics of biochar: organo-chemical properties. In: Lehmann JL, Joseph JS (eds) Biochar for environmental management. Earthscan, London
57. Laird DA (2008) The charcoal vision: a win-win-win scenario for simultaneously producing bioenergy, permanently sequestering carbon, while improving soil and water quality. Agron J 100:178–181
58. Laird DA, Brown RC et al (2009) Review of the pyrolysis platform for coproducing bio-oil and biochar. Biofuels Bioprod Biorefin 3:547–562
59. Laird DA, Fleming P et al (2010) Impact of biochar amendments on the quality of a typical Midwestern agricultural soil. Geoderma. doi:10.1016/j.geoderma.2010.05.013
60. Laird DA, Fleming P et al (2010) Biochar impact on nutrient leaching from a Midwestern agricultural soil. Geoderma. doi:10.1016/j.geoderma.2010.05.012
61. Lehmann J, Gaunt J et al (2006) Bio-char sequestration in terrestrial ecosystems—a review. Mitigat Adapt Strateg Glob Change 11:403–427
62. Lehmann J, Joseph S (2009) Biochar for environmental management. Earthscan, London
63. Mann CC (2005) 1491: new revelations of the Americas before Columbus. Vintage and Anchor, New York
64. Miles T (2009) Converting wood and straw to biochar for agriculture. North American Biochar Conference, Boulder, CO, 9–12 August 2009. http://cees.colorado.edu/biochar_production.html. Accessed 18 July 2010
65. Mosier AR (2001) Exchange of gaseous nitrogen compounds between agricultural systems and the atmosphere. Plant Soil 228:17–27
66. Mullins CE (2000) Hardsetting soils. In: Summer ME (ed) Handbook of soil science. CRC, Boca Raton
67. Nerome M, Toyota K et al (2005) Supression of bacterial wilt of tomato by incorporation of municipal bio-waste charcoal in soil. Soil Microbiol 59:9–14
68. Nguyen BT, Lehmann J et al (2008) Long-term carbon dynamics in cultivated soils. Biogeochemistry 89:295–308
69. Novak JM, Bauer PJ et al (2007) Carbon dynamics under long-term conservation and disk tillage management in a Norfolk loamy sand. Soil Sci Soc Am J 71:453–456
70. Novak JM, Busscher WJ et al (2008a) Influence of pecan-derived biochar on chemical properties of a Norfolk loamy sand soil. American Society of Agronomy Annual Meeting, Houston, TX, 5–9 Oct 2008. http://www.biochar-international.org/. Accessed 18 July 2010
71. Novak JM, Busscher, WJ et al (2008b) Development of designer biochar to remediate degraded coastal plain soils. Abstract for a non-funded cooperative agreement project number 6657-12000-005-03. http://www.ars.usda.gov/research/projects/projects.htm?ACCN_NO=414939. Accessed 18 July 2010

72. Novak JM, Frederick JR et al (2009) Rebuilding organic carbon contents in coastal plain soils using conservation tillage systems. Soil Sci Soc Am J 73:622–629
73. Novak JM, Busscher WJ et al (2009) Impact of biochar amendment of fertility of a southeastern coastal plain soil. Soil Sci 174:105–112
74. Novak JM, Lima I et al (2009) Characterization of designer biochar produced at different temperatures and their effects on a loamy sand. Ann Environ Sci 3:195–206
75. Novak JM, Busscher WJ et al (2010) Short-term CO_2 mineralization after additions of biochar and switchgrass to a Typic Kandiudult. Geoderma 154:281–288
76. Parkin TB, Kasper TC (2006) Nitrous oxide emissions from corn-soybean systems in the Midwest. J Environ Qual 35:1496–1506
77. Parton WJ, Schimel D et al (1987) Analysis of factors controlling soil organic matter levels in Great Plains grasslands. Soil Sci Soc Am J 51:1173–1179
78. Pavia DL, Lampman GM et al (1979) Introduction to spectroscopy. Saunders College, Philadelphia
79. Peele TC, Beale OW et al (1970) The physical properties of some South Carolina soils. South Carolina Experiment Station Technical Bulletin No. 1037
80. Reeves JB, McCarty GM et al (2008) Mid-infrared diffuse reflectance spectroscopic examination of charred pine wood, nark, cellulose, and lignin: implications for the quantitative determination of charcoal in soils. Appl Spectrosc 62:182–189
81. Reicosky DC, Cassel DK et al (1977) Conservation tillage in the southeast. J Soil Water Conserv 32:13–19
82. Reicosky DC, Deaton DE (1979) Soybean water extraction, leaf water potential, and evapotranspiration during drought. Agron J 71:45–50
83. Rondon MA, Molina D et al (2006) Enhancing the productivity of crops and grasses while reducing greenhouse gas emissions through bio-char amendments to unfertile tropical soils. In: 18th World Congress of soil science, Philadelphia, PA, 9–15 July 2006
84. Rutherford DW, Wershaw RL et al (2004) Changes in composition and porosity during the thermal degradation of wood and wood components. U.S. Geological Survey Scientific Investigation Report 2004-5292
85. Sadler EJ, Camp CR (1986) Crop water use data available for the Southeastern USA. Trans ASAE 29:1070–1079
86. SCDNR (2010) Climate of South Carolina. South Carolina Department of Natural Resources. http://www.dnr.sc.gov/climate/SCD/Education/facts/climate_SC.pdf. Accessed 18 July 2010
87. Schmidt MW, Noack AG (2000) Black carbon in soils and sediments: analysis, distribution, implications, and current challenges. Global Biogeochem Cycles 14:777–793
88. Shaw JN, West LT et al (2004) Parent material influence on soil distribution and genesis in a Paleudult and Kandiudult complex, southeastern USA. Catena 57:157–174
89. Sheridan JM, Knisel WG et al (1979) Seasonal variation in rainfall and rainfall-deficiet periods in the Southern Coastal Plain and Flatwoods region of Georgia. Georgia Agricultural Experiment Stations Research Bulletin No 243
90. Singh BP, Hatton BJ et al (2010) Influence of biochars on nitrous oxide emission and nitrogen leaching from two contrasting soils. J Environ Qual. doi:10.2134/jeq2009.0138
91. Siple GE (1967) Geology and groundwater of the Savannah River Plant and vicinity South Carolina. U.S. Geological Survey Water Supply Paper 1841. USGS, Washington, DC
92. Sistani KR, Novak JM (2006) Trace metal accumulation, movement, and remediation in soils receiving animal manure. In: Prasad MBV et al (eds) Trace elements in the environment. Taylor and Francis, Boca Raton
93. Six J, Elliott ET et al (1999) Aggregate and soil organic matter dynamics under conventional and no-tillage systems. Soil Sci Soc Am J 63:1350–1358
94. Sohi S, Lopez-Capel E et al (2009) Biochar, climate change and soil: a review to guide future research. CSIRO Land and water Science Report 05/09. http://www.csiro.au/files/files/poei.pdf. Accessed 22 Aug 2010
95. Sombroek W, Ruvio ML et al (2003) Amazonian Dark Earths as carbon stores and sinks. In: Lehmann J et al (eds) Amazonian Dark Earths: origin, properties, management. Kluwer, Dordrecht

96. Spokas KA, Reicosky DC (2009) Impact of sixteen different biochars on soil greenhouse gas production. Ann Environ Sci 3:179–193
97. Spokas K (2010) Review of the stability of biochar in soils: predictability of O:C molar ratios. Carbon Manag 1:289–303. doi:10.4155/cmt.10.32
98. Steinbbeiss SG, Gleixner G et al (2009) Effect of biochar amendment on soil carbon balance and soil microbial activity. Soil Biol Biochem 41:1301–1310
99. Steiner C, Wenceslaus G et al (2007) Long term effects of manure, charcoal and mineral fertilizer on crop production and fertility on a highly weathered Central Amazonian upland soil. Plant Soil 291:275–290
100. Steiner C, Das KC et al (2008) Charcoal and smoke extract stimulate the soil microbial community in a highly weathered Xanthic Ferralsol. Pedobiologia 51:359–366
101. Stevenson FJ (1994) Humus chemistry: genesis, composition, reactions, 2nd edn. Wiley, New York
102. Thompson LM, Troeh FP (1978) Soils and soil fertility. McGraw-Hill, New York
103. Trimble SW (1974) Man-induced soil erosion on the Southern Piedmont: 1700-1970. Soil Conservation Society of America, Ankeny
104. Yanai Y, Toyota K et al (2007) Effects of charcoal addition on N_2O emissions from soil resulting from rewetting air-dried soil in short-term laboratory experiments. Soil Sci Plant Nutr 53:181–188
105. Wang Y, Admunson R et al (2000) Seasonal and altitudinal variation in decomposition and soil organic matter inferred from radiocarbon measurements of CO_2 flux. Global Biogeochem Cycles 14:199–211

Chapter 8
Biochar: A Coproduct to Bioenergy from Slow-Pyrolysis Technology

Adriana Downie and Lukas Van Zwieten

Abstract Well-engineered, slow-pyrolysis technology, optimized for the production of bioenergy and biochar from sustainable feedstocks, could deliver significant environmental and economic advantages to industry. Utilization of biochar products as a soil amendment could contribute to ongoing food security and agricultural productivity. Biochar production and sequestration can result in the net removal of greenhouse gases from the atmosphere, making the technology a potentially valuable tool for climate change mitigation. It is essential that the emerging industry is well regulated and that quality assurance and sustainability mechanisms are adopted. This will optimize the net benefit of the technology. Biochar products produced from different industries will vary greatly in characteristics. Equally, the drivers for different industries to adopt slow-pyrolysis technology will vary. Significant advantages provided by the technology across multiple industries may result in extensive adoption. The development of a biochar market is required, with the uncertainty in biochar price and market size, being a major contributor to lack of confidence in the business case for the technology. Markets for biochar as a product are diverse, ranging from broad acre agriculture to niche applications such as roof gardens, where its unique properties give it significant competitive advantages over alternatives.

1 Introduction

International interest in the adoption of modern slow-pyrolysis technology for the production of biochar products and bioenergy is growing. Solid, carbon-rich biochar can be a coproduct of pyrolysis and gasification technologies (Fig. 1), which have

A. Downie (✉)
Pacific Pyrolysis Pty Ltd, 56 Gindurra Road, Somersby, NSW 2250, Australia
e-mail: Adriana.downie@pacificpyrolysis.com

L. Van Zwieten
New South Wales Department of Primary Industries, Wollongbar, NSW 2477, Australia
e-mail: lukas.van.zwieten@dpi.nsw.gov.au

J.W. Lee (ed.), *Advanced Biofuels and Bioproducts*, DOI 10.1007/978-1-4614-3348-4_8,

Fig. 1 Biochar produced in a modern slow pyrolysis plant, operated by PacPyro, from greenwaste as a soil amendment and means to sequester carbon over the long term

traditionally had a focus on energy generation. Optimization of the technology for sustainable and economic biochar production, however, has recently garnered significant and escalating investment. This is due to a mounting body of scientific literature demonstrating its potential application as a valuable soil amendment, which not only enhances soil health and productivity but stores carbon [31]. Carbon storage in the terrestrial sink of agricultural soils via biochar could present a low-risk solution that sustainably reduces atmospheric loads of greenhouse gases [17].

When seeking to apply the technology to achieve atmospheric greenhouse gas stabilization and soil health for ongoing environmental sustainability, all aspects of the technology must be considered to ensure sustainability gains in one area are not undermined by consequences in another. This kind of thinking is driving the development of a new generation of pyrolysis technologies that deliver higher standards of process efficiency, reductions in emissions of pollutants, and improved public health and safety outcomes than is possible from traditional charcoal production technologies.

Another appeal of modern slow-pyrolysis technologies is that some have been engineered to process very low-grade waste organics [39]. That is, organic materials that have: high ash and moisture content; soil, stone, and other contamination; large particle size distributions; and few options for beneficial reuse. This enables modern slow-pyrolysis technologies to fit within the definition of a second-generation bioenergy solution, as it does not rely on food-based feedstocks or high-grade forestry products [26]. Significant sustainability and food security benefits can be achieved with the use of such technologies, as they do not compete for valuable resources, but provide resource recovery of waste materials [14]. Managing wastes, that by definition

are underutilized and may present an environmental risk, not only contributes to the sustainability credentials of pyrolysis technology, but also provides economic advantages. Low-grade feedstocks are typically low-cost and often have significant management costs, hence providing a revenue stream (or cost-saving) to a pyrolysis project providing an organic waste management service.

Along with revenue for waste services, slow-pyrolysis technology may generate revenue through the production of bioenergy, biochar, and environmental offsets. The technology can be applied at a scale that is large enough to get the economies-of-scale required to make a commercial business case, yet small enough that the distributed nature of organic feedstocks does not limit viability.

When slow-pyrolysis technology is utilized for bioenergy and biochar production the following benefits can be achieved:

- Generating renewable, distributed energy, improving energy security.
- Mitigating greenhouse gases and sequestering carbon.
- Recycling nutrients back to agricultural land while increasing soil carbon levels.
- Increasing the sustainability of agricultural production through enhancing soil health, hence improving food security.
- Improving land use outcomes through minimizing waste going to landfill.
- Ensuring environmental quality (air, water, and soil) and human health through strict environmental and operational standards.

2 Technology Overview

Pyrolysis technology relates to the heating of organic or fossil sources of solid carbon in a very low oxygen environment to temperatures over 400°C. The resulting thermal decomposition yields solid char, liquid bio-oils and tars, and syngas. The reaction conditions can be engineered to change the product ratios and properties [8, 15] as illustrated in Fig. 2. Pyrolysis technologies that optimize for bio-oil production facilitate fast heating rates, from ambient to highest heating temperature in seconds, and are therefore described as fast pyrolysis. Utilization of fast pyrolysis for biochar and bio-oil production has been the subject of a recent investigation [28]. The focus of this chapter, however, is on slow-pyrolysis technology, which via more steady heating rates, from ambient to highest heating temperature in minutes to hours, optimizes for the production of syngas and biochar. In modern systems designed for commercial biochar production, such as that operated by Pacific Pyrolysis Pty Ltd (see Fig. 3) bio-oil produced is cracked to syngas to circumvent the necessity to market or dispose of a bio-oil [16].

The utilization of slow pyrolysis for the production of charcoal is one of the oldest industries known to society [21]. Traditional systems vent all volatiles directly to the atmosphere and have very limited process controls. This results in environmentally damaging air pollution and risks to human health and safety [1, 9, 17, 37]. Modern slow-pyrolysis technology developers need to conform to the relevant regulatory and economic requirements. This means that high environmental standards need to be met and losses of potentially valuable products to the atmosphere eliminated.

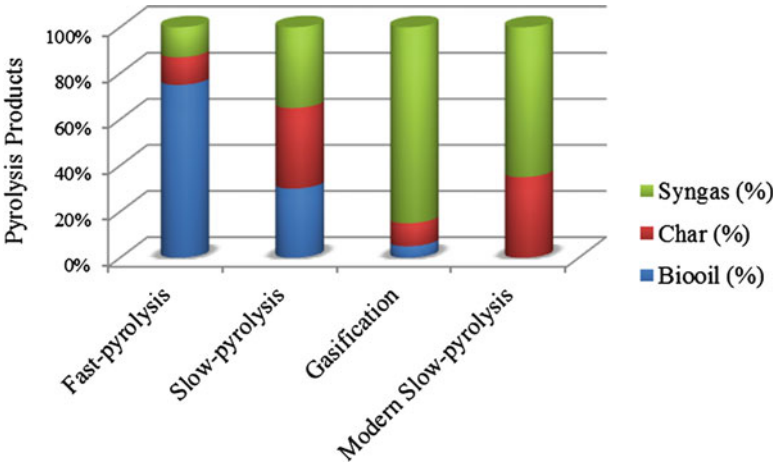

Fig. 2 Thermal conversion technology product splits. Fast and slow pyrolysis, gasification product data [8], modern slow-pyrolysis data [16]

Fig. 3 Pacific Pyrolysis Pty Ltd's slow-pyrolysis demonstration facility at Somersby, Australia. Production facility for Agrichar™ biochar and bioelectricity from syngas

Characteristics targeted by developers of modern slow-pyrolysis technologies for the economical and sustainable production of biochar include [8, 9, 28, 39]:

- Energy efficiency: continuous feed rather than batch processing, exothermic operation without air infiltration (i.e., pyrolysis conditions rather than gasification/combustion), waste heat recovery and recycling, utilization of insulation, lagging, and refractory.

- Reduced pollution: air emissions managed (i.e., no smoke, low NO_x burners, low organic pollutants such as dioxins, etc.).
- Improved biochar yields and quality: slow pyrolysis rather than gasification or fast pyrolysis (see Fig. 2), process control to ensure consistent product quality.
- Operability: decreased labor requirement (i.e., automated materials handling, continuous operation, etc.), steady-state operation resulting in control of product quality and quantity, high workplace health, and safety standards.
- Feedstock flexibility: allowing broader range of low-cost feedstocks to be processed.
- Scalability: sufficient size to reach the required economies-of-scale while small enough to not be limited by biomass availability.

Adequate precautions need to be taken to ensure that environmental standards are upheld. For example, technology should be designed to prevent the formation of toxic compounds such as PAHs and dioxins. There is extensive literature on the reaction conditions conducive to the formation of PAHs [3, 34, 43] and dioxins [24, 27, 29, 36], which can be referred to. It should be noted that these are usually in reference to more commonly employed thermal-conversion technologies such as gasifiers and incinerators; however, this knowledge can be adopted for pyrolysis reactor design.

3 Commercial Status of the Technology

Although charcoal production is one of the oldest industries the adoption of modern slow-pyrolysis technologies, optimized for biochar and bioenergy production, is in the early stages of commercialization [9, 28]. Adoption of the technology relies on building a convincing business case [10]. Although each application of the technology will have project-specific differences, the technology business case is built around the following framework.

3.1 Revenue Streams

The following revenue streams may be available to a biochar production business:

- Biochar sales.
- Energy sales such as electricity or thermal energy generated from liquid, solid, or gas products.
- Environmental offsets such as policy-driven fiscal incentives for greenhouse gas emissions abatement, renewable energy generation, waste reduction, etc.
- Organics waste management charges (perhaps offsetting landfill tipping fees).

Revenue streams may alternatively be cost-savings compared with business-as-usual operation. For example, energy generated may be used internally (embedded) by the industry operations and hence not generate a revenue stream from sales, but a cost-savings due to decreased retail energy requirements.

All revenue streams may not be available to all projects. For example, there may be no market for the energy, and/or the project may have to pay for feedstock making it a cost rather than a revenue stream. If however, one of the remaining revenue streams is very profitable, a reduction in the number of revenue streams may not necessarily result in an unviable project [10].

Some revenue streams are more economically certifiable than others in the project (and industry) development phase. That is, they represent a more reliable and lower risk source of income to the project. For example, at the time of writing there is no existing market for biochar demonstrated on a commercial scale. Therefore, the level of demand and market price for this new product is debatable (the value of biochar products is discussed further in Sect. 15). Energy, on the other hand, is a commoditized product with a long price and demand history. Energy sales are therefore considered a more economically certifiable or bankable form of revenue when developing a business case for a proposed biochar production facility.

3.2 Operating Costs

The following operating costs may be incurred by a biochar production business:

- Management, administration, monitoring, and reporting.
- Operations staff.
- Maintenance, service agreements, and sustaining capital.
- Debt servicing.
- Insurance.
- Transport of feedstocks and products.
- Consumables.
- Energy requirements (start-up, shut-down, and sustaining).

The magnitude of the project operating costs varies greatly depending on the location of the project and the regulatory regime it is subjected to. For example, in a developed country the cost of human resources is likely to be one of, if not, the most significant contributors to operating costs. However, in a developing country these resources come at a significantly lower cost. Likewise, in developing countries the level of administration, monitoring, and reporting required to meet government requirements could also be less and therefore represent a decreased operating cost.

3.3 Capital Costs

The following items are likely to contribute to the capital cost of establishing a modern slow-pyrolysis facility for biochar production:

- Site preparation and civil works such as buildings, roads, fences, etc.
- Feedstock harvesting and preprocessing equipment. This may include plant items such as; dewatering of sludges; grinders, shedders, or mills for size reduction; screens

or sieves for size selection; conveyors and/or screws for on-site transfer; pads, bays, buckets, and bins for storage; trucks and front end loaders for transport.
- Feedstock drying equipment (may be incorporated into the pyrolysis kiln design).
- Pyrolysis kiln.
- Biochar conditioning, blending, handling, and packaging.
- Syngas cleaning, cooling, and flaring equipment.
- Energy conversion technology. This may include a gas engine, turbine, boiler, etc. If electricity is produced, grid connection and metering is required. If bio-oil is produced, condensing, handling, and packaging equipment is required.
- Piping and instrumentation.
- Control systems.
- Emissions control.
- Ancillary services such as water, power, telephone, etc.
- Safety systems and controls.

Additional items typically added to the capital cost include:

- Project management.
- Procurement.
- Installation and commissioning.
- Technology license or development costs.
- Project structuring and contracting.
- Project development.
- Planning approvals and environmental consents.
- Financing.

The capacity factor of the project, or the number of hours the project is operating compared to periods of shut-down or derated operation, can also have a large impact on the business case. Capacity factors can be impacted by; technology-specific reliability and maintenance requirements, processing configuration (batch vs. continuous), integration with other industries (only producing feedstock or requiring energy for limited periods), or limitations imposed by planning and consents. For example, the project may run 24 h a day, 7 days a week, or 8 h a day, 5 days a week. If the quantity and value of the products produced per hour is the same, the greatly reduced production hours will result in a far greater burden per unit produced to payback the capital and fixed operating costs.

Uncertainty surrounding the business case is high due to the lack of any verified commercial biochar production business being in operation. Although the technology has been successfully demonstrated on a pilot-scale [16] (see Fig. 3), the technology faces the challenging hurdle faced by all new technologies and that is attracting the higher-risk investment required for the initial, commercial-scale demonstration projects. In typical commercialization pathways, this investment is made either by governments to enable the new industry or by an industry for which the opportunity presents an exceptional rate-of-return which warrants the risk to be taken on the new technology approach [20]. Once demonstrated, the rate-of-return required by projects utilizing the technology is expected to decrease in line with the decreased risk profile.

4 Opportunities for Industry

Adoption of slow-pyrolysis technology may eventually occur within stand-alone businesses whose core business is the production of biochar. It is likely however that the first projects will be driven by the advantages gained through integration with existing industry, which makes the technology more economically viable in the short-term. Case studies have been developed to explore how some major existing industries may utilize pyrolysis technology to overcome some of the challenges they face. Each industry examined in the case studies has a unique organics resource to manage. Resource recovery, energy security, greenhouse gas savings, and economic outcomes for each industry are discussed using a comparison between adoption of a slow-pyrolysis solution and business-as-usual.

4.1 Pulp and Paper

Worldwide, about 300 million metric tons of paper and paperboard are produced each year. About 2–4% (dry weight) of paper sludge is produced as a by-product of the paper making process [40]. The managed disposal of paper sludge is a significant challenge to the pulp and paper industry globally. The sludges produced by the paper industry can be divided into several categories: the waste paper sludge coming from the production of virgin wood fiber, called primary sludge; the waste paper sludge produced by removing inks from postconsumer fiber, called de-inking paper sludge; the activated sludge from the secondary systems, called secondary sludge; and combined waste paper and activated sludge, called combined sludge [7].

In the UK, paper mills produce a total of 250,000 dry tones of waste sludge per year [40]. This is most typically dewatered to about 30% dry matter and sent to a commercial landfill at considerable cost [40]. Slow-pyrolysis technology offers one of few options to traditional landfill, and presents significant advantages over alternatives such as land spreading, or incineration.

There are several advantages to be gained from producing biochar from paper sludge for land application, compared with using the sludge directly as has been proposed by some authors [4, 5, 40]. The sludge-derived biochar has improved physical characteristics, such as increased surface areas, and is more friable than the stodgy sludge. The carbon, carbonates, and nutrient contained in the sludges are concentrated in the biochar while the product itself is more readily transportable to markets due to being greatly reduced in volume and mass. Caution, however, should be exercised with flammability of the product. Testing against the Dangerous Goods, class 4, for combustible solids is recommended to ensure appropriate transporting controls are in place where needed.

Benefits of slow pyrolysis for the paper and pulp industry:

- Increased resource recovery of waste sludges.
- Decreased need for landfill.
- Value adding of paper sludge to marketable biochar product.
- Cheaper transport due to decreased mass and volume of product.
- Concentration of carbon and carbonates into biochar.
- Odor and pathogen elimination.
- Decreased greenhouse gases from landfill and direct land application.
- Stabilization of carbon for sequestration.

One of the challenges of processing sludges through thermochemical processes, such as pyrolysis, is the high moisture content which imposes a large energy burden to evaporate the water. This challenge can be overcome via blending the sludge with a higher calorific value and/or dryer organic material, such as waste wood and bark that are also commonly found at pulp mills. Alternatively, waste heat from existing boilers already in operation at the mill can be utilized to dry the material.

Biochar produced from paper sludge has been demonstrated to increase productivity in an acidic ferrosol, but had little influence in an alkaline calcarosol [53]. Further research is still required before the benefits across a wide range of soil types and crops are determined. This will allow cost-benefit analysis to be undertaken for farmers utilizing the product.

The high content of carbonates in the sludge material, due to the use of $CaCO_3$ as a whitening agent in the paper making process, means that their use on acidic soils for pH control is beneficial [7, 53]. Direct paper sludge application for acid-mine drainage treatment and in the removal of heavy metals in solution has been proposed [7]. These functions may be enhanced in the biochar derived from paper sludges due to their increased surface areas and adsorptive properties [18] compared with the unprocessed sludge.

The greatest uptake of paper sludge-derived biochar is to be expected when consumers have commercial quality and environmental assurances related to the product. Possible contaminants in the paper sludge should be assessed for each project application according to the processes used in production. Biochar qualities from each paper sludge source and pyrolysis process should also be reviewed to ensure all risks identified are managed [17]. Analysis of a primary sludge from an Italian mill suggest that the sludge does not represent a major threat for the environment in terms of heavy metal release [7]. If chlorine is used to whiten the paper, this could be a potential source of dioxins and furans [7], which should be monitored in sludge-derived products to be applied to the environment.

The net production of greenhouse gases of slow pyrolysis compared to business-as-usual management of paper sludges needs to be assessed on a case-by-case basis. However, the outcome is likely to be positively influenced by the improved resource

recovery of the sludge from landfill where a portion of the carbon would be released to the atmosphere as the potent greenhouse gas methane. The stabilization of the carbon into the biochar and the flow-on benefits of biochar application to soil, as discussed in Sect. 17, all contribute to a significantly enhanced greenhouse gas outcome compared to the standard practice for managing paper sludges. It is unlikely, due to paper sludges being very wet, that any energy will remain for export after energy is utilized for internal drying. If however, significant external energy sources from fossil fuels are required to allow the thermal conversion process to progress with this very wet feedstock, then any greenhouse gas advantages may be undermined. The energy efficiency of the specific slow-pyrolysis technology will need to be assessed through a complete life cycle assessment to ensure optimized environmental gains are realized in practice.

4.2 Municipal Organic Wastes

The United Nations *2008 Revision of World Population Prospects* estimates the world population, which stood at 6.8 billion in 2009, is projected to reach 9 billion in 2050 [50]. Most of the additional people expected by 2050 will be concentrated in developing countries, whose population is projected to rise from 5.6 billion in 2009 to 7.9 billion in 2050. This high growth in the rate of urbanization and development will drive significant increases in demand for energy production while generating ever-expanding volumes of centralized organic waste in urban centers. Organic wastes typically from urban centers are from parks and gardens, food waste, and wastewater solids from sewage treatment plants. The increasing dissociation of this organic waste resource from farming production areas significantly challenges the ongoing sustainability of rural crop production that relies on the effective cycling of carbon and nutrients [2]. Urban centers are also challenged with the lack of appropriate area for landfilling wastes, with the transporting of wet, bulky, and often odorous waste to landfills increasing in costs and social pressure (Fig. 4).

Slow-pyrolysis technology applied to municipal organic wastes may help in addressing these challenges experienced currently in urban centers that are expected to be exacerbated by the predicted growth in urban populations. The environmental and economic benefits of utilizing urban waste water sludges in thermal conversion processes has been demonstrated in the literature [12, 42]. Slow-pyrolysis processing of organic wastes could provide not only a renewable source of electricity, but it also fills in the missing link between soil carbon, nutrient cycling, and urban food consumption through the production of biochar. The nutrients and carbon contained in the organic wastes are concentrated into a greatly reduced mass and volume of biochar that is therefore more cost-effectively transported back to agricultural land.

The pyrolysis process effectively sterilizes the wastes so that biosecurity risk (human health, animal disease risk, plant pathogen, plant propagule, etc.) is greatly

Fig. 4 Processing of urban, source separated, green waste to reduce volume for landfilling

diminished. It should be noted, however, that there is potential for contamination in waste streams and therefore an evaluation, monitoring, and verification plan should be adopted to ensure the risk of applying contaminated biochar to land is mitigated [17].

Benefits for local governments of urban centers:

- Job creation.
- Renewable energy production.
- Increased resource recovery of waste organics.
- Decreased need for landfill.
- Value adding of wastes to marketable product.
- Decreased mass and volume of product—less to transport.
- Concentration of carbon and nutrients into biochar.
- Odor reduction.
- Improved biosecurity through pathogen destruction.
- Decreased greenhouse gases from landfill.
- Carbon offsets generated to contribute to achieving targets.
- Stabilization of carbon for sequestration.
- Enhanced energy security.
- Enhanced food security.

The production of biochar also presents some opportunities unique to urban uses. For example, the incorporation of gardens into the landscape of urban building development provides many environmental and social benefits. The concept of retrofitting existing roof areas with gardens, know as "green roofs," is becoming increasingly popular. One of the challenges of this practice is that existing roofs have load ratings that greatly limit the amount of heavy soil and water that they can support. Biochar has been demonstrated to have a low bulk density [18] and good water holding capacity [13] which potentially make it an ideal substrate for soil mixes which need to be light weight and retain moisture. Another advantage of biochar for this application is that it is recalcitrant and therefore breaks down slowly in the environment. This means that it will need to be replaced a lot less frequently than other low-bulk density substrates that are made from more labile carbon components. This becomes important when access to roof areas for bulk goods is difficult.

The use of slow-pyrolysis for producing thermal energy, in the form of high pressure hot water, from urban waste organics for district heating also presents a unique resource recovery opportunity. Local governments overseeing the delivery of both waste management and district heating services to the community are in position to implement such projects without the need for complicated counterparty agreements.

4.3 Intensive Agriculture

The intensification of agriculture is resulting in large stocks of high nutrient waste accumulating in localized areas [45]. Industries include; cattle feedlots, dairy cattle on hard-stands, piggeries, and poultry. This presents challenges of euthrophication, nutrient cycling, biosecurity, and disposal. Waste materials including; poultry litter (manure and bedding), deep litter piggery bedding, and mechanically managed beef feedlot manures could be utilized in a slow-pyrolysis process to produce energy and a high nutrient biochar. It should be noted that very wet wastes such as dairy slurry, manures washed out with water, are not likely to be suitable for pyrolysis technology as the energy required to drive off moisture in the thermal process would require significant external energy sources. These materials could, however, be utilized in biological conversion processes such as anaerobic digestion to enhance resource recovery.

In some regions where intensive agriculture is practiced, the drivers for improved management of livestock wastes are compelling due to:

- Nutrient saturation of surrounding land which prevents further land spreading.
- The bulky and wet nature of the material making it uneconomical to transport to broader markets.
- Regulatory requirements for biosecurity, where manures are not allowed to be transported and/or used on food crops due to public health risk.

- Expansion being limited by regulators due to lack of sustainable waste management.
- Social pressures to control and limit odors.

This risk is acutely managed in Europe where animal waste is routinely incinerated. However, in many regions there is no viable alternative in use other than land spreading, as landfill and incineration are expensive or have legislative barriers due to emissions and odor concerns. Slow-pyrolysis technology may offer the industry and regulators the opportunity to address this gap in the market and provide a viable means for mitigating public health risk while providing effective recovery of this valuable resource.

Benefits of slow-pyrolysis for intensive livestock production:

- Regional development and employment opportunities.
- Distributed energy security, which is essential to regional industries who experience frequent brown-outs through lack of capacity, which adversely effects productivity.
- Renewable energy production.
- Diversifying farm revenues.
- Ability to demonstrate waste management plans to regulators who may then allow continued operation or expansion.
- Resource recovery of carbon and nutrients.
- Decreased mass and volume of product—less to transport.
- Odor reduction.
- Improved biosecurity through pathogen destruction.
- Stabilization of carbon for sequestration.
- Enhanced food security.
- Offsetting of greenhouse gas emissions.

Operators in this sector in developed countries already invest in large capital items to optimize their processes. Slow-pyrolysis technology could be targeted at large beef feedlot operations or poultry producers, who manage enough waste to achieve the economies of scale required for a viable project. In many cases, these operations are vertically integrated in that they also grow the grain for the livestock and have meat processing and packing facilities. Hence, they have an internal requirement for the biochar and energy produced. Waste heat from the process could also contribute to space heating animal sheds in cooler climates, adsorption chillers in warmer climates, and for processing such as steam flaking of grain, which increases its digestibility for livestock.

The agricultural sector is a large greenhouse gas emitter, predominantly through livestock. The large emissions liability may be able to be offset partly through the integration of pyrolysis facilities into their operations. The greenhouse gas savings demonstrated from soils with biochar applied [47, 54] may be particularly relevant

to soils which have been saturated with nutrient via the historic application of high rates of animal manures.

5 Biochar Product Qualities and Marketing

Biochar characteristics are highly dependent on the feedstock and the processing conditions under which they were made [18]. Biochar quality control will be critical in establishing a valuable and reliable market for the product. Consumers are likely to be sensitive to the following biochar attributes:

- Homogeneity (consistent and repeatable).
- Visual appeal (packaging, contamination, color).
- Odors.
- Handling (convenient, low risk, economical).
- Availability (quantities and seasonality).
- Measurable productivity benefits; and of course.
- Price.

Standards for biochar products may be adopted to ensure that quality products are available on the market and that consumers are able to easily identify what they are purchasing [23].

As there are no commercial biochar production facilities established at the time of writing, the ability to marketing significant quantities of the product has not yet been tested. Despite the demand for biochar building on the back of increasing levels of research being published, along with media attention about its verified benefits, the lack of supply has meant that no market has been demonstrated at any significant scale. Therefore, the use of the product by consumers has been limited and hence their response to the products benefits and usability are unable to be gauged. If and when supply is established, according to standard market economics, the initial quantities of product are likely to attract a premium. Once the backlog of demand is exhausted, however, a more stable, commodity type market will be established.

The quantities and price points of the product required to satisfy this market are difficult to estimate. However, there is a large range of target markets where biochar could be applied:

- Potting mixes and home garden landscaping.
- Market gardens.
- Public parks and gardens.
- Playing fields.
- Turf industry.
- Horticulture and viticulture.
- Hydroponics.
- Cropping.
- Intensive pasture.

- Land remediation and mine site rehabilitation.
- Planted forestry.
- Urban landscaping.
- Green roofs.
- Industrial applications such as effluent clean-up.

Each of the potential markets identified has a different cost-benefit outcome from increased productivity. This will influence the price each primary producer or customer can afford to pay for the biochar product that provides the benefit. Therefore, it is likely that markets for biochar will be initially developed for high value uses. The exception may be where government incentives such as C offsets, may make biochar available for lower value applications, or where biochar production is subsidized by another revenue stream, such as electricity sales, and no high value applications for the biochar product exist in close vicinity to the production facility.

6 Biochar as a Soil Amendment

Biochar is attracting increasing scientific, political, and industry attention for its potential benefits as a soil amendment. Issues such as food security, declining soil fertility, climate change adaptation, and profitability, are all drivers for implementing new technologies or new farming systems. Application of biochar to soil has been shown to have effects ranging from very positive, through to neutral and even negative impacts for crop production. It is therefore essential that the mechanisms for action of biochar in soil be understood before it is applied.

The application of biochar to soil can influence a wide range of soil constraints, including low pH and high available Al [51], soil structure and nutrient availability [13], bioavailability of organic [56] and inorganic contaminants [25], cation exchange capacity (CEC) and nutrient retention [33, 46], and organic matter decline [32]. Biochars have a highly porous structure with surface areas sometimes exceeding 1,000 m^2/g [18]. Like activated charcoal, they adsorb organics, nutrients and gases, and are likely to provide habitats for bacteria, actinomycetes, and fungi [49]. Increases in water holding capacity following biochar application to soil have been well established [11, 41], and this may influence crop production, soil microbial populations, and population flux during wetting/drying cycles.

Soil constraints where biochar may provide benefits to productivity include:

- Low pH and high Al availability.
- Low CEC and nutrient holding capacity.
- Low water holding capacity, poor infiltration.
- Poor soil aeration, root development.
- Hard setting soils.
- Residual herbicide or heavy metal phytotoxicity.
- Presence of certain soil-borne diseases.

In some cases, biochar application to soil may influence nutrient availability and nutrient use efficiency [54]. The application of a low nutrient biochar derived from timber increased the retention of N in soil and uptake of N into crop biomass [48]. Lehmann et al. [30] showed that biochar reduced leaching of NH_4^+, maintaining it in the surface soil where it is available for plant uptake. Similarly, the application of charcoal derived from bamboo into a sludge composting system was shown to provide significant increases in N retention in the compost [25]. Increased fertility of soil resulting from biochar application is likely to increase crop vigor, and thus may enhance disease tolerance.

Biochar is also likely to influence a range of soil physical properties. For example, [11, 13] demonstrated significant declines in soil tensile strength following addition of biochar derived from green waste or pecan shells. These declines in soil tensile strength may allow for better crop root penetration (especially during dry periods), and will also reduce costs associated with soil preparation (such as tillage).

Biochar has been shown to increase biological N_2 fixation (BNF) of *Phaseolus vulgaris* [44], largely due to greater availability of plant micronutrients following biochar application. By increasing potential for BNF, and increasing N use efficiency, lower rates of synthetic N fertilizers may be acceptable for maintaining productivity. Synthetic N fertilizers have a significant C footprint, with over 4t CO_2 emission required per t N fertilizer produced [55].

Although there is a paucity of published data on the effects of biochar on soil-borne pathogens, evidence is mounting that control of certain pathogens may be possible. The addition of biochar (0.32, 1.60, and 3.20% (w/w)) to asparagus soils infested with *Fusarium* root rot pathogens increased asparagus plant weights and reduced Fusarium root rot disease [19]. Further, Matsubara et al. (2002) (cited in [49]) have shown that biochar inoculated with mycorrhizal fungi are effective in reducing Fusarium root rot disease in asparagus. A study of bacterial wilt suppression in tomatoes found that biochar derived from municipal organic waste reduced the incidence of disease in *Ralstonia solanacearum* infested soil [38]. The mechanism of disease suppression was attributed to the presence of calcium compounds, as well as improvements in the physical, chemical, and biological characteristics of the soil. Likewise, Ogawa [57] describes the use of biochars and biochar amended composts in reducing bacterial and fungal soil-borne diseases.

The economic value of biochar as an agricultural commodity is largely untested. Although the benefit of biochar in many systems has been described to increase crop yield, the cost-benefit ratio of applying the technology has not been completed. Van Zwieten et al. [52] discusses several mechanisms for valuing biochar as a commodity. Simply, it could be valued based on its nutrient or liming value, replacing commodities such as fertilizer or lime, alternatively, it could be valued according to benefits to productivity or projected productivity. A recent study [6] using biochar derived from *Eucalyptus* banded at a low rate of 1 ton/ha was shown to have a breakeven valuation of around Aus$170 per ton of biochar in broadacre wheat, assuming yield benefits for 12 years. In the cost-benefit outcome described by Van Zwieten et al. [52], biochar derived from poultry litter waste was valued at $300 per ton, based on the performance enhancement of three crops following the single

application of biochar. Clearly, the economic value of biochar will depend on its properties, but will also be driven by supply and demand, inherent value of the target enterprise, and demonstrated benefits.

7 Greenhouse Gas Outcomes

Slow-pyrolysis technology has the potential to deliver renewable energy, and biochar products while exhibiting a carbon negative greenhouse gas balance [22, 35]. The carbon sequestration achieved by the high carbon biochar product results in a net removal of carbon dioxide from the atmosphere. If organics are not used as fuel they decompose relatively quickly in the natural environment, releasing the carbon as CO_2 back to the atmosphere. Production of biochar from these organics removes this material from the short-term carbon cycle, into the long-term carbon cycle. Biochar is far more stable in the environment when compared to the original organics and prevents the release of the carbon in its structures (Fig. 5).

When compared to typical bioenergy GHG balances, where all of the carbon in the fuel source (biomass organics) is released through the energy cycle as greenhouse gases, in pyrolysis a portion of the carbon is stabilized as the biochar product. The coproduction of biochar along with renewable energy results in a significant net removal of GHGs from the atmosphere via this pathway. It should be noted, however, that not all biochar technologies are necessarily carbon negative as carbon

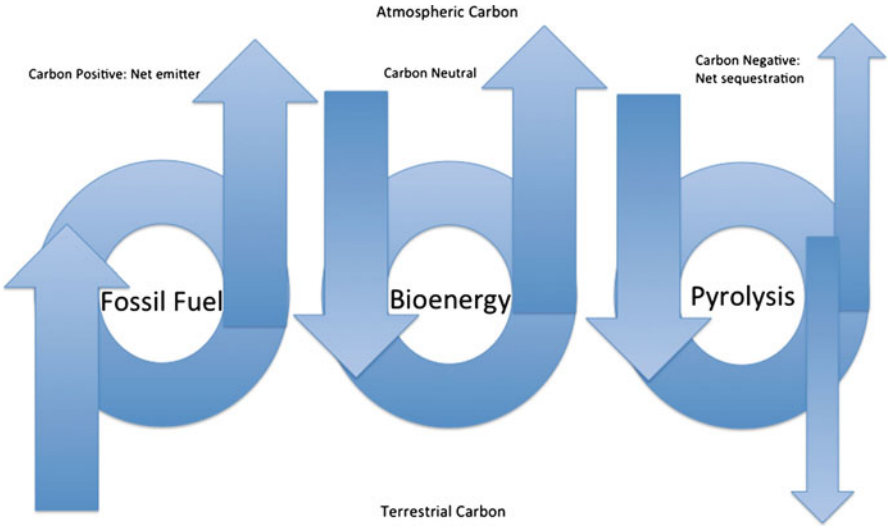

Fig. 5 Comparison of carbon balances: fossil fuel, bioenergy, and slow-pyrolysis for bioenergy and biochar

leakage and poor combustion systems can have a significant negative impact on the carbon lifecycle analysis [17]. It is essential that modeling, monitoring, and auditing of the system is carried out to verify carbon offsets generated.

Key pathways to GHG mitigation via production and use of biochar include:

- Renewable energy generation (displacing fossil fuel).
- Bio-sequestration (stabilizing organic carbon as biochar and storing it in terrestrial sinks).
- Stabilization of labile soil organic carbon onto biochar surfaces.
- Reduced agriculture emissions (from reduced; nitrous oxide from soil, fuel use, fertilizer use, and improved water use efficiency).
- Decreased emissions from waste biomass (including avoided methane generation from landfills and compost production).
- Increased agricultural productivity (increased biomass yields taking up more atmospheric carbon, less land area required for food production).

The sequestration of carbon via biochar and mitigation of GHGs are offset by various steps along the biochar production lifecycle. These aspects might include:

- Use of fossil fuels for harvesting, transporting, and processing.
- Fugitive emission from feedstock degradation being stored or preprocessed.
- Emissions from the processing plant, such as uncombusted syngas.
- Land use change, for example biomass requirements provide a market for more purpose-grown organics which may result in deforestation [14].

Technology considerations that should be optimized to ensure carbon negative balances are achieved:

- Energy efficiency of processes.
- Emissions control, including utilization of syngas.
- Limited distances for feedstock collection and product distribution.
- Alternate higher uses of organics is fully considered, e.g., waste organics are sourced over purpose-grown feedstocks.

The contribution biochar can make in maintaining soils for agricultural production during climate variability may prove a vital tool for adaptation.

8 Conclusions and Future Outlook

Well-engineered, slow-pyrolysis technology, optimized for the production of bioenergy and biochar from sustainable feedstocks, could deliver significant environmental and economical advantages to industry. The growing field of

scientific research on biochar by agronomists, soil and plant scientists, is leading to a rigourous body of knowledge on the effective use of biochar for agricultural productivity gains. This work will assist in justifying a market price for biochar products, which is needed to underpin the economic feasibility of the emerging industry. Several companies, such as Pacific Pyrolysis in Australia, are working towards commercializing new technology for the production of biochar along with bioenergy from low-grade organics. Establishing one or more commercial-scale production facilities dedicated to demonstrating the technical, environmental, and economic outcomes of the business will be an essential next step for the emerging industry.

References

1. Adam JC (2009) Improved and more environmentally friendly charcoal production system using a low-cost retort–kiln (eco-charcoal). Renew Energy 34:1923–1925
2. Asomani-Boateng R (2007) Closing the loop community-based organic solid waste recycling, urban gardening, and land use planning in Ghana, West Africa. J Plan Educ Res 27:132–145. doi:10.1177/0739456X07306392
3. Baek SO, Field RA, Goldstone ME, Kirk PW, Lester JN, Perry R (1991) Review of atmospheric polycyclic aromatic hydrocarbons: sources, fate and behavior. Water Air Soil Pollut 60:279–300
4. Bellamy KL, Chong C, Cline RA (1995) Paper sludge utilization in agriculture and container nursery culture. J Environ Qual 24:1074–1082
5. Beyer L, Frund R, Mueller K (1997) Short-term effects of a secondary paper mill sludge application on soil properties in a Psammentic Haplumbrept under cultivation. Sci Total Environ 197:127–137
6. Blackwell P, Krull E, Butler G, Herbert A, Solaiman Z (2010) Effect of banded biochar on dryland wheat production and fertiliser use in south-western Australia: an agronomic and economic perspective. Aust J Soil Res 48:531–545
7. Boni MR, D'Aprile L, De Casa G (2004) Environmental quality of primary paper sludge. J Hazard Mater 108:125–128
8. Bridgwater AV (2007) IEA Bioenergy Update 27: biomass pyrolysis. Biomass Bioenergy 31:1–5
9. Brown R (2009) Biochar Production Technology. In: Lehmann J, Joseph S (eds) Biochar for environmental management: science and technology. Earthscan, London, pp 127–139
10. Bryant D, Downie A (2007) Agrichar: building a commercial venture. International Agrichar Initiative, Terrigal, New South Wales, Australia, p. 18
11. Busscher W, Novak J, Evans D, Watts D, Niandou M, Ahmedna M (2010) Influence of pecan biochar on physical properties of a Norfolk loamy sand. Soil Sci 175:10
12. Cartmell E, Gostelow P, Riddell-Black D, Simms N, Oakey J, Morris J, Jeffrey P, Howsam P, Pollard SJ (2005) Biosolids a fuel or a waste? An integrated appraisal of five co-combustion scenarios with policy analysis. Environ Sci Technol 40:649–658. doi:10.1021/es052181g
13. Chan KY, Van Zwieten L, Meszaros I, Downie A, Joseph S (2007) Agronomic values of greenwaste biochar as a soil amendment. Aust J Soil Res 45:629–634
14. Cherubini F, Bird ND, Cowie A, Jungmeier G, Schlamadinger B, Woess-Gallasch S (2009) Energy- and greenhouse gas-based LCA of biofuel and bioenergy systems: key issues, ranges and recommendations. Resour Conserv Recy 53:434–447
15. Di Blasi C (2008) Modelling chemical and physical processes of wood and biomass pyrolysis. Prog Energ Combust 34:47–90
16. Downie A, Klatt P, Downie R, Munroe P (2007) Slow pyrolysis: Australian demonstration plant successful on multi-feedstocks. Bioenergy 2007 Conference, Jyväskylä, Finland

17. Downie A, Munroe P, Cowie A, Van Zwieten L, Lau DM (2012) Biochar as a geo-engineering climate solution: hazard identification and risk management. Crit Rev Env Sci Tec 42(3):225–250. doi:10.1080/10643389.2010.5079800
18. Downie A, Munroe P, Crosky A (2009) Characteristics of biochar—physical and structural properties. In: Lehmann J, Joseph S (eds) Biochar for environmental management: science and technology. Earthscan, London, pp 13–29
19. Elmer W, White JC, Pignatello JJ (2010) Impact of biochar addition to soil on the bioavailability of chemicals important in agriculture. Report. New Haven: University of Connecticut
20. Ernst & Young (2010) Navigating the valley of death Exploring mechanisms to finance emerging clean technologies in Australia. Report. Clean Energy Council, Southbank VIC, Australia
21. FAO (1983) Simple Technologies for Charcoal Making, FAO Forestry Paper 41. Food and Agriculture Organization of the United Nations, Rome
22. Gaunt J, Cowie A (2009) Biochar, Greenhouse Gas Accounting and Emissions Trading. In: Lehmann J, Joseph S (eds) Biochar for environmental management: science and technology. Earthscan, London
23. Glover M (2009) Taking biochar to market: some essential concepts for commercial success. In: Lehmann J, Joseph S (eds) Biochar for environmental management: science and technology. Earthscan, London, pp 375–392
24. Gullett BK, Bruce KR, Beach LO, Drago AM (1992) Mechanistic steps in the production of PCDD and PCDF during waste combustion. Chemosphere 25:1387–1392
25. Hua L, Wu WX, Liu YX, McBride M, Chen YX (2009) Reduction of nitrogen loss and Cu and Zn mobility during sludge composting with bamboo char-coal amendment. Environ Sci Pollut Res Int 16:1–9
26. IEA (2010) Sustainable Production of Second-Generation Biofuels - Potential and perspectives in major economies and developing countries. International Energy Agency, France
27. Kulkarni PS, Crespo JG, Afonso CAM (2008) Dioxins sources and current remediation technologies—a review. Environ Int 34:139–153
28. Laird DA, Brown RC, Amonette JE, Lehmann J (2009) Review of the pyrolysis platform for coproducing bio-oil and biochar. Biofuels Bioprod Bioref 3:547–562
29. Lavric ED, Konnov AA, De Ruyck J (2005) Surrogate compounds for dioxins in incineration. A review. Waste Manag 25:755–765
30. Lehmann J, da Silva JPJ, Steiner C, Nehls T, Zech W, Glaser B (2003) Nutrient availability and leaching in an archaeological Anthrosol and a Ferralsol of the Central Amazon basin: fertilizer, manure and charcoal amendments. Plant Soil 249:343–357
31. Lehmann J, Joseph S (2009) Biochar for environmental management: an introduction. In: Lehmann J, Joseph S (eds) Biochar for environmental management: science and technology. Earthscan, London
32. Lehmann J, Rondon M (2006) Bio-char soil management on highly weathered soils in the humid tropics. In: Uphoff N (ed) Biological approaches to sustainable soil systems. CRC, Boca Raton
33. Major J, Steiner C, Downie A, Lehmann J (2009) Biochar effects on nutrient leaching. In: Lehmann J, Joseph S (eds) Biochar for environmental management: science and technology. Earthscan, London, pp 271–282
34. Mastral A, Callean M (2000) A review on polycyclic aromatic hydrocarbon (PAH) emissions from energy generation. Environ Sci Technol 34:3051
35. Mathews JA (2007) Carbon-negative biofuels. Energy Policy 36:940–945
36. McKay G (2002) Dioxin characterisation, formation and minimisation during municipal solid waste (MSW) incineration: review. Chem Eng J 86:343–368
37. Namaalwa J, Sankhayan PL, Hofstad O (2007) A dynamic bio-economic model for analyzing deforestation and degradation: an application to woodlands in Uganda. Forest Policy Econ 9:479–495
38. Nerome M, Toyota K, Islam TMD, Nishijima T, Matsuoka T, Sato K, Yamaguchi Y (2005) Suppression of bacterial wilt of tomato by incorporation of municipal biowaste charcoal into soil. Soil Microorg 59:9–14

39. Pacific Pyrolysis Pty Ltd (2010) Pacific Pyrolysis slow pyrolysis technology
40. Phillips VR, Kirkpatrick N, Scotford IM, White RP, Burton RGO (1997) The use of paper-mill sludges on agricultural land. Bioresour Technol 60:73–80
41. Pietikainen J, Kiikkila O, Fritze H (2000) Charcoal as a habitat for microbes and its effect on the microbial community of the underlying humus. Oikos 89:231–242
42. Poulsen TG, Hansen JA (2003) Strategic environmental assessment of alternative sewage sludge management scenarios. Waste Manag Res 21:19. doi:10.1177/0734242X0302100103
43. Richter H, Howard JB (2000) Formation of polycyclic aromatic hydrocarbons and their growth to soot-a review of chemical reaction pathways. Progress in Energy and Combustion Science 26:565–608
44. Rondon M, Lehmann J, Ramírez J, Hurtado M (2007) Biological nitrogen fixation by common beans (*Phaseolus vulgaris* L.) increases with bio-char additions. Biol Fertil Soils 43:699–708
45. Sims JT, Maguire RO, Daniel H (2005) Manure Management. In: Hillel D (ed) Encyclopedia of soils in the environment. Elsevier, Oxford, pp 402–410
46. Singh B, Singh BP, Cowie AL (2010) Characterisation and evaluation of biochars for their application as a soil amendment. Aust J Soil Res 48:516–525. doi:doi:10.1071/SR10058
47. Singh BP, Hatton BJ, Singh B, Cowie AL, Kathuria A (2010) Influence of biochars on nitrous oxide emission and nitrogen leaching from two contrasting soils. J Environ Qual 1–12. doi:10.2134/jeq2009.0138
48. Steiner C, Glaser B, Teixeira WG, Lehmann J, Blum WEH, Zech W (2008) Nitrogen retention and plant uptake on a highly weathered central Amazonian Ferralsol amended with compost and charcoal. J Plant Nutr Soil Sci 171:893–899. doi:10.1002/jpln.200625199
49. Thies JE, Rillig MC (2009) Characteristics of biochar: biological properties. In: Lehmann J, Joseph S (eds) Biochar for environmental management. Earthscan, London, pp 85–105
50. UN (2009) World population prospects: the 2008 revision. Population Newsletter No. 87. United Nations
51. Van Zwieten L, Kimber S, Downie A, Morris S, Petty S, Rust J, Chan KY (2010) A glasshouse study on the interaction of low mineral ash biochar with nitrogen in a sandy soil. Aust J Soil Res 48:569–576. doi:doi:10.1071/SR10003
52. Van Zwieten L, Kimber S, Downie A, Orr L, Walker T, Sinclair K, Morris S, Joseph S, Petty S, Rust J, Chan KY (2010) Agro-economic valuation of biochar using field-derived data, International Biochar Conference, Rio de Janeiro, Brazil
53. Van Zwieten L, Kimber S, Morris S, Chan KY, Downie A, Rust J, Joseph S, Cowie A (2010) Effects of biochar from slow pyrolysis of papermill waste on agronomic performance and soil fertility. Plant Soil 327:235–246. doi:10.1007/s11104-009-0050-x
54. Van Zwieten L, Kimber S, Morris S, Downie A, Berger E, Rust J, Scheer C (2010) Influence of biochars on flux of N_2O and CO_2 from Ferrosol. Aust J Soil Res 48:555–568. doi:doi:10.1071/SR10004
55. Wood S, Cowie AL (2004) A review of greenhouse gas emissions factors for fertiliser production. IEA Bioenergy Task 38. www.ieabioenergy-task38.org/publications/GHG_Emissions_Fertlizer%20Production_July2004.pdf
56. Yu XY, Ying GG, Kookana RS (2009) Reduced plant uptake of pesticides with biochar additions to soil. Chemosphere 76:665–671
57. Ogawa M, Okimori Y (2010) Pioneering works in biochar research, Japan. Aust J Soil Res 48:489–500. Doi:10.1071/SR10006

Chapter 9
Catalytic Pyrolysis of Biomass

Stefan Czernik

Abstract Converting lignocellulosic biomass into biofuels compatible with the existing petroleum refinery infrastructure requires removal of oxygen from the carbohydrate and lignin-derived molecules. The necessary deoxygenation can be achieved through the rejection of water and carbon oxides which occurs at 400–600°C in the presence of catalysts. The yield of hydrocarbons could theoretically reach 35% of the biomass feedstock. So far, the highest yields achieved were in the range of 12–18%. The most promising deoxygenation catalysts belong to the group of medium-pore size zeolites such as ZSM-5. This chapter reviews the research in the field and provides numerous references to the original work in the area of catalytic pyrolysis of biomass. It also reports on some recent experimental results obtained at National Renewable Energy Laboratory.

1 Introduction

In recent years, high crude oil prices, national security concerns, and potential climate change consequences resulted in a significant increase of interest in biofuels. In addition to the commercial production of biodiesel and corn-based ethanol, research efforts intensified on developing processes for producing liquid fuels from lignocellulosic biomass. One of the emerging technologies is fast pyrolysis, a thermal decomposition of biomass carried out in the absence of oxygen with a very high heat transfer to the biomass particles. It produces high yields of a liquid product, called bio-oil, which contains up to 70% of the energy of the biomass feed [1]. However, certain bio-oil properties such as its low heating value, incomplete volatility, acidity, instability, and incompatibility with standard petroleum fuels significantly

S. Czernik (✉)
National Renewable Energy Laboratory,
1617 Cole Blvd, Golden, CO 80401, USA
e-mail: Stefan_Czernik@nrel.gov

J.W. Lee (ed.), *Advanced Biofuels and Bioproducts*, DOI 10.1007/978-1-4614-3348-4_9,

restrict its application [2]. The undesirable properties of pyrolysis oil result from the chemical composition of bio-oil that mostly consists of different classes of oxygenated organic compounds. The elimination of oxygen is thus necessary to transform bio-oil into a liquid fuel that would be broadly accepted and economically attractive. Two types of approaches that have been used to reject oxygen from organic molecules are hydrotreating and catalytic cracking [3]. The former uses hydrogen to remove oxygen in the form of water and resembles desulfurization/deoxygenation/denitrogenation processes widely used in petroleum refineries. The research on bio-oil hydrotreating was recently comprehensively reviewed [4]. The latter accomplishes the oxygen removal from bio-oil or directly from biomass in the form of water and carbon oxides. The following equation represents the best case scenario for deoxygenation of biomass pyrolysis vapors:

$$C_6H_8O_3 \rightarrow C_5H_6 + CO_2 + H_2O.$$

The yield of hydrocarbons could theoretically reach 50% based on pyrolysis vapor or 35% of the biomass feedstock. So far, the highest yields achieved were in the range of 12–18%. From different types of catalysts used to deoxygenate biomass-derived vapors and liquids the most effective appear to be shape-selective catalysts like zeolites. Such an approach offers several potential advantages over hydrotreating because it does not need hydrogen, occurs at atmospheric pressure, and can be close coupled with operating fast pyrolysis units.

1.1 Catalytic Conversion of Oxygenated Organic Compounds

Catalytic processing of oxygenated organic compounds accomplishes deoxygenation through simultaneous dehydration, decarboxylation, and decarbonylation reactions occurring in the presence of zeolite catalysts. In the late 1970s, synthetic zeolites such as ZSM-5 were successfully used to convert oxygenated organic compounds into hydrocarbons [5, 6]. ZSM-5 proved to be particularly effective for the conversion of methanol to gasoline range hydrocarbons [7], which led to the commercialization of the methanol-to-gasoline process by Mobil. This discovery also stimulated research focused on the production of hydrocarbons from biomass-derived pyrolysis oil and from biomass pyrolysis vapors. To enhance understanding of the reaction mechanisms and identify the most favorable process conditions research was conducted using model compounds representing different chemical classes of bio-oil components. Extensive research in this area has been performed in several centers, especially at Laval University [8, 9], University of Saskatchewan [10–13], University of Thessaloniki [14], University of The Basque Country [15, 16], University of Valencia [17], and at University of Massachusetts [18]. In general those studies showed that in the temperature range of 350–450°C oxygenated organic compounds in contact with zeolite catalysts undergo a suite of chemical reactions including dehydration, decarboxylation, cracking, aromatization, alkylation, condensation, and polymerization. The product was always a two-phase liquid (aqueous and organic) and gas, while coke deposits formed on the catalyst surface. The conversion and the product

composition varied depending on the class of compounds tested. Using a fixed bed of ZSM-5 catalyst, high conversions (>90%) were obtained for alcohols, aldehydes, ketones, acids, and esters while phenols and ethers remained mostly unchanged. Alcohols and ketones reacted to produce high yields of aromatic hydrocarbons while acids and esters were mostly converted to gas, water, and coke with low yield of hydrocarbons. For example, initially complete acetic acid conversion declined to 60% after 3 h on stream with the total hydrocarbon yield below 10%. The high production of coke resulting in a rapid catalyst deactivation was observed especially for the compounds having low (<1) effective hydrogen index defined in [19] as:

$$\left(\frac{\mathrm{H}}{\mathrm{C}}\right)_{\mathrm{eff}} = \left(\frac{\mathrm{H} - 2\mathrm{O}}{\mathrm{C}}\right),$$

where H, C, and O represent the number of moles of hydrogen, carbon, and oxygen in the feedstock. This coke is mostly produced by dehydration of oxygenated organic compounds containing high amount of oxygen; dehydration of low-oxygen-content compounds produces mostly hydrocarbons. Significant improvement in the production of hydrocarbons from low effective-hydrogen-index compounds such as acetic acid can be obtained by coprocessing with methanol, which has a hydrogen index equal 2 [19].

In parallel to model compound studies, zeolites were also applied for deoxygenation of biomass pyrolysis oils and its fractions [8, 10, 20]. The reported hydrocarbon yields were in the range of 12–15% but also high coke production and rapid catalyst deactivation were observed due to hydrogen deficiency (effective hydrogen index <0.3) of biomass pyrolysis oils.

1.2 Catalytic Conversion of Biomass to Hydrocarbons

Catalytic pyrolysis includes two common approaches. The first is a one-step process in which biomass pyrolysis is carried out in the presence of the catalyst, so that pyrolysis vapors and intermediates are in immediate contact with the catalyst. The second approach combines two consecutive steps: (a) fast pyrolysis and (b) catalytic cracking of the vapors carried out in separate reactors. In contrast to non-catalytic fast pyrolysis of biomass that produces mostly oxygenated compounds and only very small amount of hydrocarbons, the process carried out in the presence of a catalyst can dramatically change the product slate. The chromatograms in Fig. 1 show a dramatic difference in the product composition obtained from pyrolysis of oak wood performed at National Renewable Energy Laboratory (NREL) using a Pyroprobe-GC/MS system in the absence (upper) and in the presence of a ZSM-5 (Albemarle UPV-2) catalyst (lower). These results, though not obtained in a real reactor system, suggest that catalytic pyrolysis carried out in the optimized process conditions could produce almost completely deoxygenated liquid product from lignocellulosic biomass.

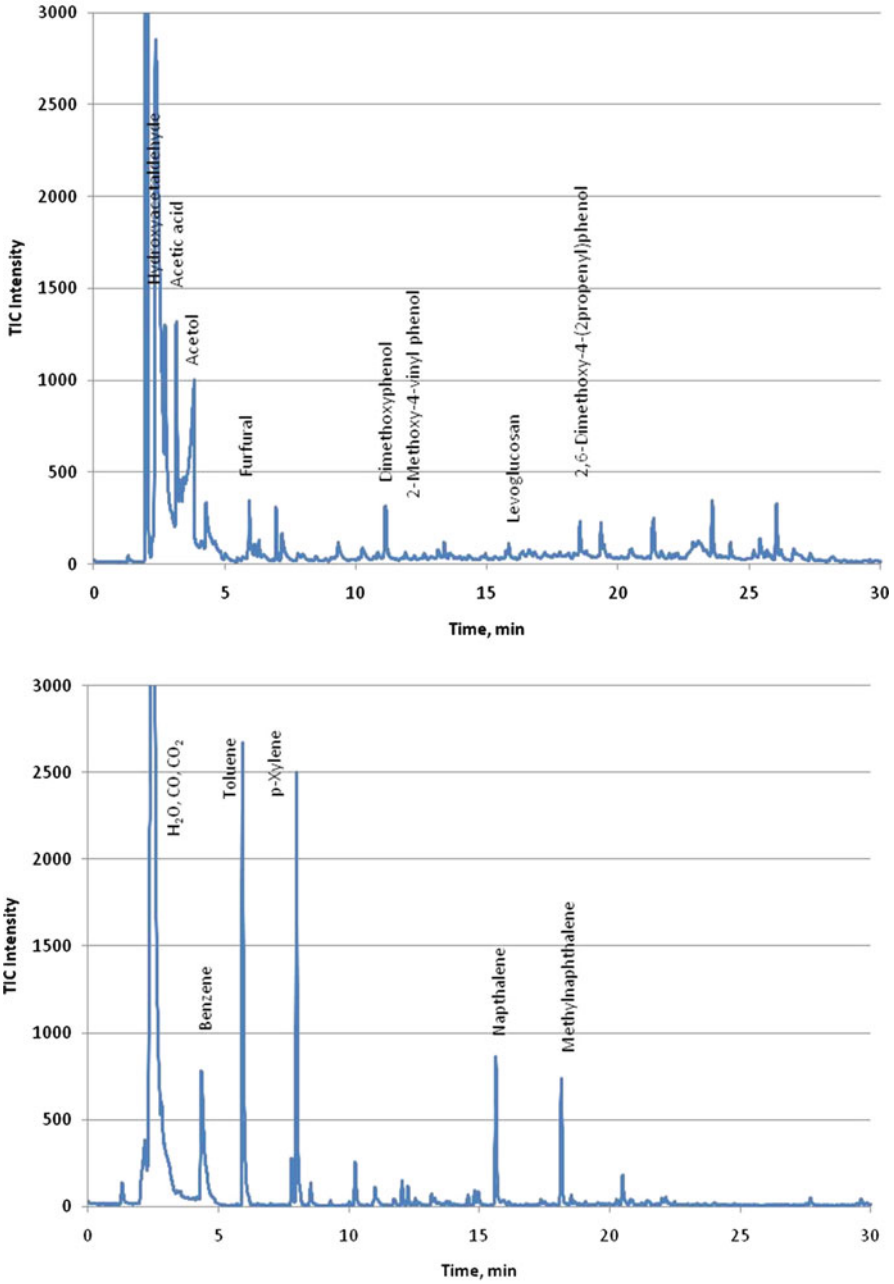

Fig. 1 Py-GC/MS of non-catalytic and catalytic (Albemarle UPV-2) pyrolysis of oak wood at 600°C

First attempts to catalytically deoxygenate biomass to produce hydrocarbons were reported in the 1980s [9, 19, 21]. That concept was further developed at the NREL [22, 23] with a demonstration of an integrated fast pyrolysis/catalytic cracking process in which vapors from the pyrolyzer were not condensed and collected as bio-oil but were directly fed to a catalytic reactor and converted to aromatic and olefin hydrocarbons. Using a pilot plant vortex reactor followed by a fixed-bed catalytic cracker (450°C, commercial Mobil MCSG-2 catalyst), they achieved 12.7% of total hydrocarbon yield based on wood feedstock. The technoeconomic evaluation of the process performed by the IEA Biomass Liquefaction Task based on this data estimated the production cost of gasoline at $0.97/gal (1992 $) for a biomass cost of $30/ton, which was not attractive at that time [24].

Extensive studies on catalytic pyrolysis of biomass in fluidized bed reactors were also carried out at several other research centers, especially at University of Leeds [25, 26], University of Thessaloniki [27], and Virginia Institute of Technology [28, 29]. In all of those studies aromatic hydrocarbons, including polycyclic (PAHs) and phenols constituted the majority of the organic liquid product.

Our previous research [30] focused on improving the process performance (increasing yield of hydrocarbons, decreasing coking) by modifying the catalyst composition. The presence of transition metals was expected to affect the mode of oxygen rejection by producing more carbon oxides and less water making that way more hydrogen available for incorporation into hydrocarbons. The performance measured as the total hydrocarbon yield was evaluated for 40 different catalysts using a micro-reactor/molecular-beam mass-spectrometer system. The highest yields of the desired hydrocarbon product from wood, 16 wt% including 3.5 wt% of toluene, were obtained at 600°C using NiZSM-5 though the yields produced by several other catalysts (gallium, cobalt, and iron-substituted ZSM-5 zeolites were within the experimental error estimated at ±3%. These yields are comparable to those obtained earlier in a similar system [31]). In this work we used a bench-scale system to collect and analyze the liquid product obtained from pyrolysis of wood in the presence of a promising commercial zeolite catalyst, UPV-2 from Albemarle.

2 Methods

The catalytic pyrolysis tests were performed using a 2-in. diameter fluidizing bed reactor system shown in Fig. 2. The Inconel 625 reactor supplied with a perforated distribution plate was placed inside a three-zone electric furnace. The reactor contained 250 g of a commercial ZSM-5 catalyst ground to a particle size of 200–350 μm. Either superheated steam or nitrogen (4 slm) at a pressure slightly above barometric was used as a fluidizing gas. The reactor was operated at the temperature of 500°C. Mixed wood of particle size less than 0.5 mm was pneumatically (3 slm nitrogen) fed to the reactor at a rate of 120 g/h controlled by a K-Tron feeder. The vapor/catalyst contact time was 0.7 s and the space velocity (WHSV) was 0.48 h^{-1}. The volatile product passed through a cyclone and hot-gas filter, which captured

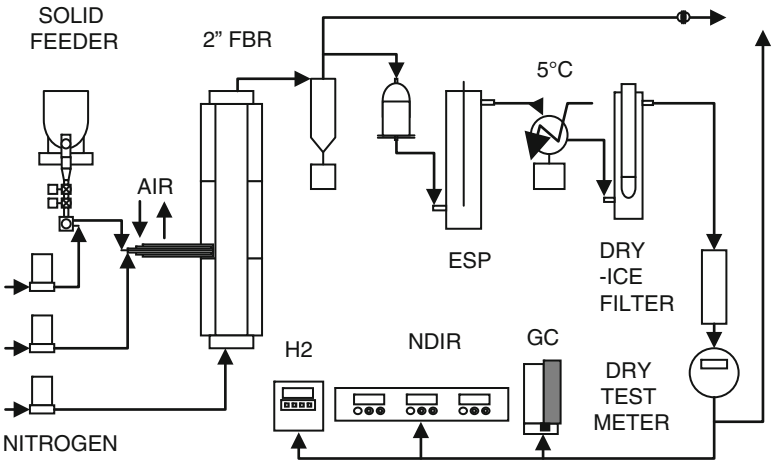

Fig. 2 Schematic of the 2-in. fluidized bed reactor system

fine catalyst particles and carbonaceous solids generated in the reactor, then (in most experiments) through an electrostatic precipitator (ESP) and two heat exchangers, which collected the liquid product.

The process gas flow rate was monitored by a mass flow meter and measured by a dry test meter. The concentrations of CO_2, CO, and methane in the product gas were monitored by a nondispersive infra-red analyzer (NDIR Model 300 from California Analytical Instruments). In addition, the gas was analyzed every 4 min by an online Varian micro gas chromatograph, which provided concentrations of hydrogen, carbon monoxide, carbon dioxide, methane, C_2–C_4 hydrocarbons, and nitrogen. The temperatures in the system, as well as the flows, were recorded and controlled by the OPTO data acquisition and control system.

3 Results and Discussion

During 5–6-h long experiments the product gas composition did not change significantly; CO and CO_2 were the major gas components with C_1–C_4 hydrocarbons accounting for approximately 20 vol% of the product gas. The product collected in the ESP that operated at the exit temperature of 80°C was a dark brown viscous liquid while that collected in the condensers was mostly water (90–95 wt%) with a thin layer of organics floating on the top. In every test significant amounts of carbon (coke and char) were produced which were collected in the reactor, the cyclone, and the filter. The carbon yields were determined by weight difference of the collected solids and of the initial catalysts. The yields of liquids corresponded to the weight of the fractions collected in the ESP and condensers, and the amount of gaseous product was calculated based on its volume and composition (excluding the carrier gas). Table 1 shows the results of two experiments carried out using the

Table 1 Product distribution from catalytic pyrolysis of mixed wood at 500°C using Albemarle UPV-2 catalyst

	Experiment 1		Experiment 2	
	g	%	g	%
Feed (mixed wood)	650		214	
Char/coke	99	15.2	50	23.4
Total liquid	262	40.3	78	36.4
Organic fraction	81	12.5	25	11.6
Aqueous fraction	181	27.8	53	24.8
Gas	180	27.7	54	25.2
C_1-C4 hydrocarbons	29	4.5	8	3.7
Total product	541	83.2	182	85.0

Albemarle catalyst. The first experiment was run for 6 h and the final ratio of catalyst to biomass was 0.38 and the second experiment was run from 2 h with a final catalyst to biomass ratio of 1.2.

Mass balance closures were in the range 83–85% with 15–17% not accounted for. These losses most likely comprised of noncondensed water and volatile organic compounds that were not analyzed by gas chromatography. The amounts of carbon solids (char and coke) were in the range of 15–23% of the weight of the feedstock while the yields of total liquid were 35–40%, and those of gas were 25–28%. Similar product distribution was reported by Zhang et al. [32], Aho et al. [33], and Agblevor et al. [28] in bubbling fluidized beds. However, Lappas et al. [27] achieved significantly higher yields of liquids using a fluidized catalytic cracking system (circulating fluidized bed) with ZSM-5 catalyst. The most likely reason for that was maintaining the catalyst activity by continuous regeneration.

The liquid product included three phases: a very thin top organic layer, the middle most abundant water-rich fraction, and the bottom dark brown organic fraction. The yield of the heavy organic fraction was about 12% based on the feedstock. The light liquid hydrocarbon phase was 3–5% of the total condensate. The analysis of the organic liquid from the first test showed the following elemental composition: C 67–68 wt%, H 6.2–6.6 wt%, O 25–26 wt%. The oxygen content of this liquid was significantly less than for crude bio-oil from a non-catalytic process that contains 45–50% oxygen (37–40% on water-free basis). The organic liquid from the second test was even much more deoxygenated and included 83% C, 7.3% H, and 9.6% O, which is the lowest known to us oxygen content from bench-scale catalytic pyrolysis reported in the literature ([27, 28, 32, 33], all report higher oxygen contents of 13.5–22%).

In both tests, the biomass carbon conversion to organic liquid was 20–22% with most of carbon converted to gas and char/coke. It seems that in our experiments the lignin part of the feedstock was partly depolymerized (M_w 330–350) while the carbohydrates were mostly converted to solids (char and coke), gas, and water. Agblevor et al. [29] had also concluded that the majority of the organic oil from catalytic pyrolysis in their experiments originated from lignin. The results showed that pyrolysis oil with highly reduced oxygen content can be produced by catalytic pyrolysis; however, the biomass carbon to liquid conversion was still low and more research is needed to improve the process performance.

References

1. Mohan D, Pittman CU, Steele PH (2006) Pyrolysis of wood/biomass for bio-oil: a critical review. Energy Fuel 20:848–889
2. Czernik S, Bridgwater AV (2004) Overview of applications of biomass fast pyrolysis oil. Energy Fuels 18:590–598
3. Bridgwater AV (1996) Production of high grade fuels and chemicals from catalytic pyrolysis of biomass. Catal Today 29:285–295
4. Elliott DC (2007) Historical developments in hydroprocessing bio-oils. Energy Fuel 21:792–1815
5. Chang CD, Silvestri AJ (1977) The conversion of methanol and other O-compounds to hydrocarbons over zeolites catalysts. J Catal 47:249–259
6. Weisz PB, Hagg WO, Rodewald PG (1979) Catalytic production of high grade fuel (gasoline) from biomass compounds by shape-selective catalysis. Science 206:57–58
7. Chang CD, Lang WH (1975) U.S. Patent 3 894 103
8. Chantal PD, Kaliaguin S, Grandmaison JL, Mahay A (1984) Production of hydrocarbons from aspen poplar pyrolytic oils over H-ZSM5. Appl Catal 10:317–332
9. Chantal PD, Kaliaguin S, Grandmaison JL (1985) Appl Catal 18:133
10. Sharma RK, Bakhshi NN (1993) Catalytic upgrading of pyrolysis oil. Energy Fuels 7:306–314
11. Adjaye JD, Bakhshi NN (1995) Catalytic conversion of a biomass-derived oil for fuels and chemicals I: model compound studies and reaction pathways. Biomass & Bioenergy 8:131–149
12. Adjaye JD, Bakhshi NN (1995) Production of hydrocarbons by catalytic upgrading of fast pyrolysis bio-oil, part I: conversion over various catalysts. Fuel Process Technol 45:161–184
13. Adjaye JD, Bakhshi NN (1995) Production of hydrocarbons by catalytic upgrading of fast pyrolysis bio-oil, part II: comparative catalyst performance and reaction pathways. Fuel Process Technol 45:185–204
14. Samolada MC, Papafotica A, Vasalos IA (2000) Catalyst evaluation for catalytic biomass pyrolysis. Energy Fuel 14:1161–1167
15. Gayubo AG, Aguayo AT, Atutxa A, Aguado R, Bilbao J (2004) Transformation of oxygenate components of biomass pyrolysis oil on HZSM-5 zeolite. I. Alcohols and phenols. Ind Eng Chem Res 43:2610–2618
16. Gayubo AG, Aguayo AT, Atutxa A, Aguado R, Olazar M, Bilbao J (2004) Transformation of oxygenate components of biomass pyrolysis oil on HZSM-5 zeolite. II. Aldehydes, ketones, and acids. Ind Eng Chem Res 43:2619–2626
17. Corma A, Huber G, Sauvanaud L, O'Connor P (2007) Processing biomass-derived oxygenates in the oil refinery: catalytic cracking (FCC) reaction pathways and role of catalyst. J Catal 247: 307–327
18. Carlson TR, Vispute TP, Huber G (2008) Green gasoline by catalytic fast pyrolysis of solid biomass-derived compounds. ChemSusChem 1:397–400
19. Chen NY, Walsh DE, Koenig LR (1988) Fluidized upgrading of wood pyrolysis liquids and related compounds. In: Soltes EJ, Milne TA (eds) Pyrolysis liquids from biomass. ACS, Washington, DC, pp 277–289
20. Renaud M, Grandmaison JL, Roy C, Kaliaguine S (1988) Low-pressure upgrading of vacuum-pyrolysis oils from wood. In: Soltes EJ, Milne TA (eds) Pyrolysis liquids from biomass. ACS, Washington, DC, pp 290–310
21. Frankiewicz TC (1981) Process for converting oxygenated hydrocarbons into hydrocarbons, U.S. Patent 4 308 411
22. Diebold JP, Chum HL, Evans RJ, Milne, TA, Reed TB, Scahill JW (1987). Low-pressure upgrading of primary pyrolysis oils from biomass and organic wastes. In: X, Klass DL (ed) Energy from biomass and wastes X. IGT, Chicago, pp. 801–830
23. Diebold J, Scahill J (1988) Biomass to gasoline: upgrading pyrolysis vapors to aromatic gasoline with zeolites catalysis at atmospheric pressure. In: Soltes EJ, Milne TA (eds) Pyrolysis liquids from biomass. ACS, Washington, DC, pp 264–276
24. Diebold JP, Beckman D, Bridgwater AV, Elliott DC, Solantausta Y (1994) IEA Technoeconomic analysis of the thermochemical conversion of biomass to gasoline by the NREL process. In:

Bridgwater AV (ed) Advances in thermochemical biomass conversion. Blackie, London, pp 1325–1342
25. Williams PT, Horne PA (1995) The influence of catalyst type on the composition of upgraded biomass pyrolysis oils. J Anal Appl Pyrol 31:39–61
26. Horne PA, Williams PT (1996) Upgrading of biomass-derived pyrolytic vapours over zeolite ZSM-5 catalyst: effect of catalyst dilution on product yields. Fuel 75:1043–1050
27. Lappas AA, Samolada MC, Iatridis DK, Voutetakis SS, Vasalos IA (2002) Biomass pyrolysis in a circulating fluid bed reactor for the production of fuels and chemicals. Fuel 81:2087–2095
28. Agblevor FA, Mante O, Abdoulmoumine N, McClung R (2010) Production of stable biomass pyrolysis oils using fractional catalytic pyrolysis. Energy Fuel 24:4087–4089
29. Agblevor FA, Beis S, Mante O, Abdoulmoumine N (2010) Fractional catalytic pyrolysis of hybrid poplar wood. Ind Eng Chem Res 49:3533–3538
30. French R, Czernik S (2010) Catalytic pyrolysis of biomass for biofuels production. Fuel Process Technol 91:25–32
31. Evans R, Milne T (1988) Molecular-beam, mass spectrometric studies of wood vapor and model compounds over an HSZM-5 catalyst. In: Soltes EJ, Milne TA (eds) Pyrolysis liquids from biomass. ACS, Washington, DC, pp 311–327
32. Zhang H, Xiao R, Huang H, Xiao G (2009) Comparison of non-catalytic and catalytic fast pyrolysis of corncob in a fluidized bed reactor. Biores Technol 100:1428–1434
33. Aho A, Kumar N, Eranen K, Salmi T, Hupa MM, Murzin DY (2008) Catalytic pyrolysis of woody biomass in a fluidized bed reactor: influence of the zeolite structure. Fuel 87:2493–2501

Chapter 10
Selective Fast Pyrolysis of Biomass to Produce Fuels and Chemicals

Xi-feng Zhu and Qiang Lu

Abstract Selective fast pyrolysis, differed from traditional fast pyrolysis which is usually aimed at the maximum bio-oil yield, is to selectively control or alter biomass pyrolytic pathways for obtaining specific products (high-grade liquid fuels or special chemicals). Fast pyrolysis of biomass can be regarded as the pyrolysis of its three major components, mainly including the following three pathways. The decomposition of lignin mainly produces various monomeric phenolic compounds as well as oligomers (pyrolytic lignins). The depolymerization of holocellulose (cellulose and hemicellulose) mainly generates anhydro-oligosaccharides, monomeric anhydrosugars (mainly levoglucosan), furans, and other products. The pyrolytic ring scission of holocellulose obtains various light products, such as hydroxyacetaldehyde and acetol. The pyrolytic pathways and the subsequent products are influenced by a number of factors, including the biomass type, feedstock properties, pyrolysis conditions (pyrolysis temperature, heating rate, vapor residence time, pressure, gaseous environment), catalysts, vapor filtration, and condensation. Therefore, selective fast pyrolysis can be achieved via proper control of these factors, such as biomass pretreatment or catalyst utilization. This chapter reviews the mechanisms and pathways of biomass pyrolysis, as well as the properties and applications of crude bio-oils. It also summarizes the recent advances in the selective fast pyrolysis of biomass, aiming at how to produce quality-improved liquid fuels, and specific chemicals such as levoglucosan, levoglucosenone, acetic acid, hydroxyacetaldehyde, furfural, 1-hydroxy-3,6-dioxabicyclo[3.2.1]octan-2-one, and phenolic compounds.

X.-f. Zhu (✉) • Q. Lu
Anhui Province Key Laboratory of Biomass Clean Energy,
University of Science and Technology of China, Hefei 230026, China
e-mail: xfzhu@ustc.edu.cn

J.W. Lee (ed.), *Advanced Biofuels and Bioproducts*, DOI 10.1007/978-1-4614-3348-4_10,

1 Introduction

With the increasing concern on fossil fuel storage and environmental problems, the utilization of renewable lignocellulosic biomass resources will play an increasing important role in the future. Biomass can be converted to a variety of fuels and chemicals by different technologies; one of them is fast pyrolysis which has received extensive interests in recent years [17, 58]. Fast pyrolysis of biomass is a thermal decomposition process that occurs in the absence of oxygen, with quick biomass decomposition and rapid vapor condensation, to convert biomass mainly into a liquid product (know as bio-oil) with the yield as high as 70–80 wt%. The essential principles to obtain high bio-oil yield include moderate pyrolysis temperature (around 500°C), very high heating rates (10^3–10^5°C/s), short vapor residence time (<2 s), and rapid quenching of pyrolysis vapors. A number of pyrolysis reactors have been developed for the bio-oil production, including bubbling fluidized bed, entrained bed, circulating fluidized bed, rotating cone, screw pyrolysis reactor, vacuum pyrolysis reactor, etc. In recent years, several research institutes (BTG, Dynamotive) have already established biomass fast pyrolysis demonstration plants, suggesting that the fast pyrolysis technique is near commercialization.

Crude bio-oils, also referred to as biomass pyrolysis liquids, pyrolysis oils, or bio-crude oils, are dark brown, free flowing liquids with an acrid or smoky odor. Chemically, bio-oils are complex mixtures of water and hundreds of organic compounds that belong to acids, aldehydes, ketones, alcohols, esters, anhydrosugars, furans, phenols, guaiacols, syringols, nitrogen compounds, as well as large molecular oligomers (holocellulose-derived anhydro-oligosaccharides and lignin-derived oligomers). There are many valuable compounds, and thus, bio-oils have the potential for useful chemicals recovery. However, most of the chemicals are in low contents, making their recovery not only technically difficult but also economically unattractive at present. Therefore, the commercialization of bio-oils for value-added chemicals requires the production of specific bio-oils with high contents of target products.

Selective fast pyrolysis, differed from conventional fast pyrolysis which is usually aimed at the maximum bio-oil yield, is to drive the pyrolysis of biomass towards the products of interest. Since the biomass pyrolytic pathways and the subsequent products are influenced by various factors, and thus, selective fast pyrolysis can be performed in different ways, mostly by catalyst utilization, to (1) maximize the yield of target products and (2) obtain target products with high purity. This manuscript is divided into two sections. The first section reviews the biomass fast pyrolysis reaction pathways and mechanisms, and the second section discusses the methods for the production of several value-added chemicals from selective fast pyrolysis of biomass.

2 Biomass Fast Pyrolysis Reaction Pathways and Mechanisms

2.1 Cellulose Fast Pyrolysis

Cellulose is the main component of lignocellulosic biomass and is predominantly located in the cell wall. It is a linear homopolysaccharide of β-D-glucopyranose units linked together by (1→4)-glycosidic bonds. Among the three major components of lignocellulosic biomass, the cellulose has received the most attention in its pyrolytic mechanism study.

Cellulose starts pyrolysis at as low as 150°C. At temperatures lower than 300°C, pyrolysis of cellulose mainly involves the reduction in degree of polymerization, the formation of free radicals, elimination of water, formation of carbonyl, carboxyl and hydroperoxide groups, and evolution of carbon monoxide and carbon dioxide, finally leaving a charred residue [31, 86]. The low temperature pyrolysis will produce very low yield of organic liquid products.

At temperatures above 300°C, the pyrolysis of cellulose involves many new reactions, mainly leading to a liquid product with the yield as high as 87 wt% [72]. Generally, cellulose is firstly decomposed to form activated cellulose [15]. Afterwards, two major parallel pathways will take place, the depolymerization and the fragmentation (ring scission), as shown in Fig. 1. The depolymerization process mainly forms anhydro-oligosaccharides, levoglucosan (LG) and other monomeric anhydrosugars, furans, cyclopentanones, pyrans, and other related derivatives. The ring scission process mainly obtains hydroxyacetaldehyde (HAA), acetol (HA), other linear carbonyls, linear alcohols, esters, and other products [46, 47, 71, 79]. In a recent study, Shen and Gu [87] proposed the detailed possible routes for the pyrolytic formation of several major products from cellulose, as shown in Fig. 2.

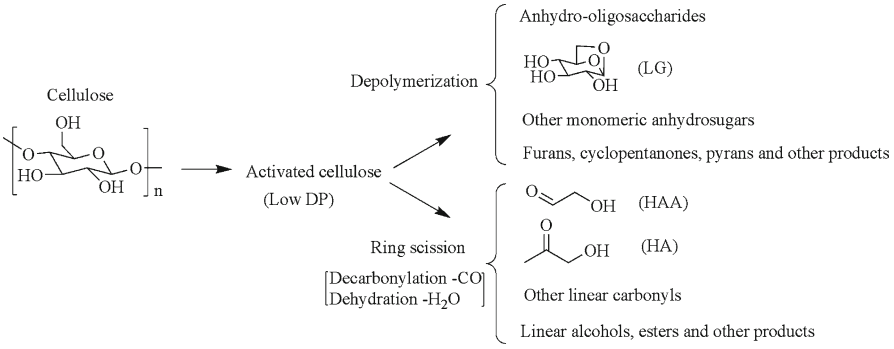

Fig. 1 The two parallel pyrolytic pathways during fast pyrolysis of cellulose at moderate temperatures

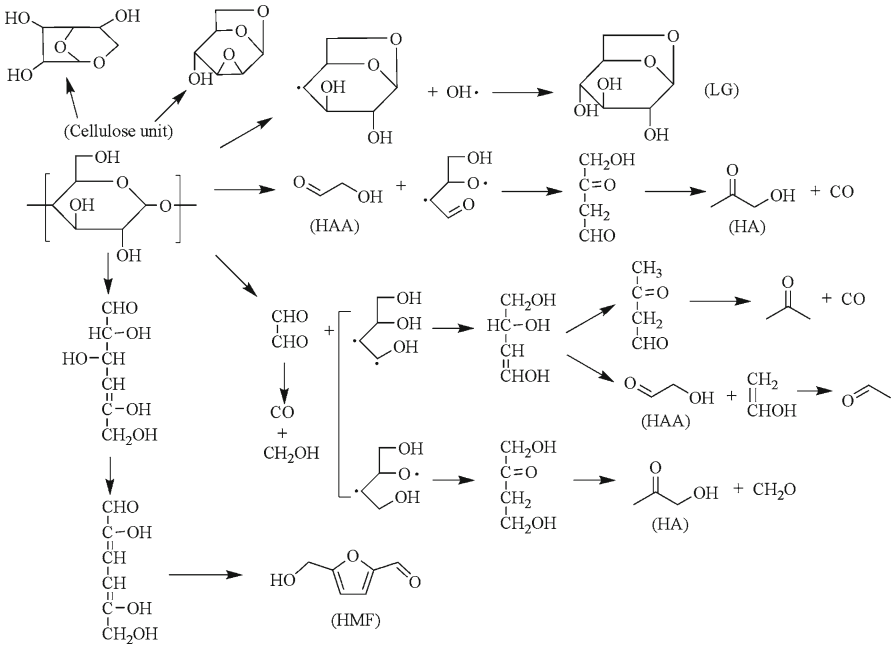

Fig. 2 The major pyrolytic pathways during cellulose fast pyrolysis (proposed by Shen and Gu [87])

2.2 *Hemicellulose Fast Pyrolysis*

Hemicelluloses are closely associated with cellulose in the cell wall as well as to lignin in the middle lamella. They are amorphous polysaccharides with building units belong either to hexoses (mainly D-glucose, D-mannose, and D-galactose) or to pentoses (mainly D-xylose and L-arabinose). The primary hemicellulose components are galactoglucomannans (glucomannans) and arabinoglucuronoxylan (xylan). Compared with cellulose, hemicelluloses have received less attention in their pyrolytic mechanism study.

Hemicelluloses are less thermally stable than cellulose, presumably due to the lack of crystallinity, and their pyrolysis is generally thought to be analogous to cellulose in the reaction mechanisms. Fast pyrolysis of glucomannans generates similar pyrolytic products as the cellulose, while the pyrolytic products from xylan differ more than those from cellulose [6]. Generally, xylan fast pyrolysis will obtain higher char yield than that from cellulose, and will not form a typical depolymerization product, like the LG from cellulose. A probable cause of this difference was explained by Ponder and Nichards [74]. During cellulose pyrolysis, the glucosyl cation from the scission of the common glucans can readily form a stable 1,6-anhydride with the free primary hydroxyl group at C-6, and finally yields the volatile LG. However, there is no feasible mechanism for intramolecular "stabilization" for the xylosyl cation

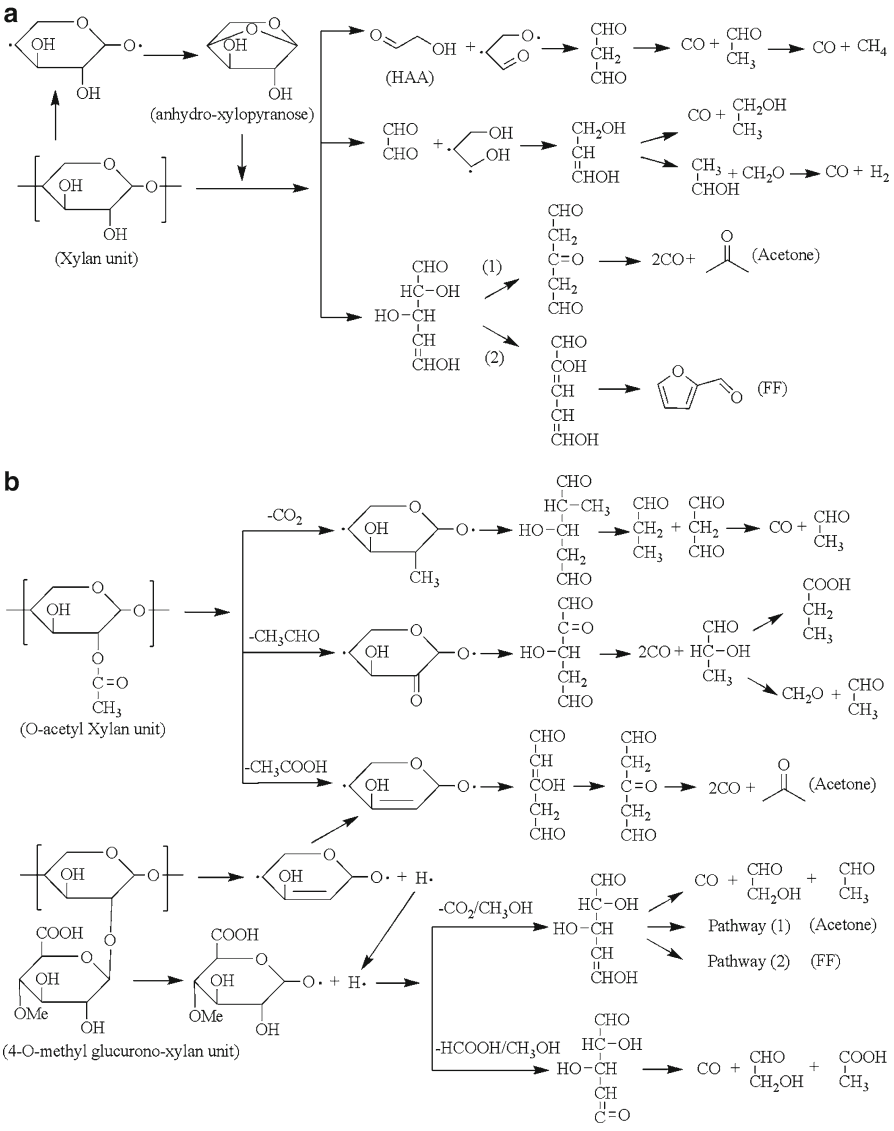

Fig. 3 The major pyrolytic pathways during xylan fast pyrolysis (proposed by Shen et al. [88]). (**a**) The main chain of *O*-acetyl-4-methylglucurono-xylan, (**b**) *O*-acetylxylan and 4-*O*-methyl-glucuronic acid unit

via anhydride formation, and hence, the xylosyl cation is more likely to enter the nonspecific dehydration pathways, resulting in the char formation rather volatiles.

In a recent study, Shen et al. [88] also proposed the detailed possible routes for the pyrolytic formation of several major products from main xylan chain, as well as the *O*-acetylxylan and 4-*O*-methylglucuronic acid unit, as shown in Fig. 3.

2.3 Lignin Fast Pyrolysis

Lignin is the amorphous material that surrounds cellulose fibers and cements them together. It is a complex, heterogeneous polymer formed by the polymerization of three phenyl propane monomers, i.e., guaiacyl (4-hydroxy-3-methoxyphenyl), syringyl (3,5-dimethoxy-4-hydroxyphenyl), and *p*-hydroxyphenyl units. Lignin is the most complicated, least understood, and most thermally stable component of biomass.

Primary pyrolysis of lignin begins with thermal softening at around 200°C, while most lignin pyrolysis occurs at higher temperatures, higher than the fast decomposition of cellulose. Fast pyrolysis of lignin will obtain higher char yield and lower liquid yield than holocellulose, and the liquid product can be classified into three groups, the large molecular oligomers (known as pyrolytic lignins), the monomeric phenolic compounds, as well as light compounds (such as methanol, HAA, acetic acid). The pyrolytic lignins are formed in much higher yield than the other two classes of products, usually account for 13.5–27.7 wt% of crude bio-oils on a water-free basis [37, 38, 65]. Several studies have been conducted to analyze them by various wet chemical and spectroscopic methods as well as pyrolysis-gas chromatography/mass spectrometry [12, 13, 38, 83, 84], and to find out that their average molecular weight is between 650 and 1,300 g/mol, and they are typically characterized by biphenyl, phenyl coumaran, diphenyl ethers, stilbene, and resinol structures.

2.4 Biomass Fast Pyrolysis

Biomass fast pyrolysis is the summation of its major components fast pyrolysis. In addition to the cellulose, hemicellulose, and lignin, biomass usually contains some extractives which would also decompose during fast pyrolysis, making the pyrolytic products more complex.

The biomass fast pyrolytic pathways and subsequent product distribution will be influenced by many factors, including biomass composition, feedstock property, pyrolysis temperature, heating rate, pressure, pyrolysis reactor configuration, and a combination of these variables. The detailed effects of these factors can be found in previous studies, and will not be shown here.

3 Chemicals Production from Selective Fast Pyrolysis of Biomass

3.1 Levoglucosan

LG (1,6-anhydro-β-D-glucopyranose) is the most important pyrolytic product of pure cellulose, formed through the depolymerization reaction. The chemistry of LG has long been known, and it can be used as a chiral synthon for the synthesis of

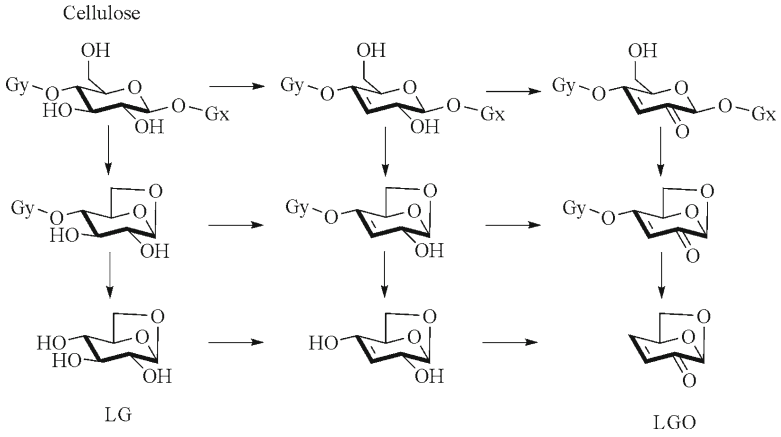

Fig. 4 The pyrolytic pathways for the formation of LGO from pyrolysis of cellulose

stereoregular polysaccharides possessing biological activities [11, 56]. Moreover, LG can also be hydrolyzed to glucose, providing a potentially rapid route to produce bio-ethanol [14].

Fast pyrolysis of pure cellulose can produce LG with the yield up to 40 wt%, but fast pyrolysis of raw biomass materials would produce much lower LG yield due to the presence of inorganic impurities. Even the minor amounts of alkaline cations would shift the pyrolytic pathways of cellulose, to promote the formation of ring-scission products (such as HAA, HA, etc.) and char on the expense of LG [61, 68]. Hence, it is necessary to use pure cellulose or demineralized biomass for the LG production. Furthermore, some studies pointed out that when small amounts of acids or acidic salts were added to demineralized biomass, the LG yield could be increased. For example, it was reported in an analytical pyrolysis study that, the LG content in the pyrolytic products was 5.3% from raw birch wood, 17.0% from decationized wood, 33.6% from wood impregnated with 1.0% phosphoric acid, and 27.3% from decationized wood adsorbed with iron ions [28].

The main difficulty in LG preparation is not the pyrolysis process, but its isolation from pyrolysis liquids. Due to its high boiling point (386°C), LG could not be simply recovered by distillation. Currently, several methods have been proposed or patented for the purification of LG [44, 57, 81].

3.2 Levoglucosenone

Levoglucosenone (LGO, 1,6-anhydro-3,4-dideoxy-β-D-pyranosen-2-one, or 6,8-dioxabicyclo[3.2.1]oct-2-en-4-one) is a sugar enone product of cellulose, formed from the combined depolymerization and dehydration reactions, with the possible pyrolytic pathways shown in Fig. 4 [66]. Its structure was firstly confirmed

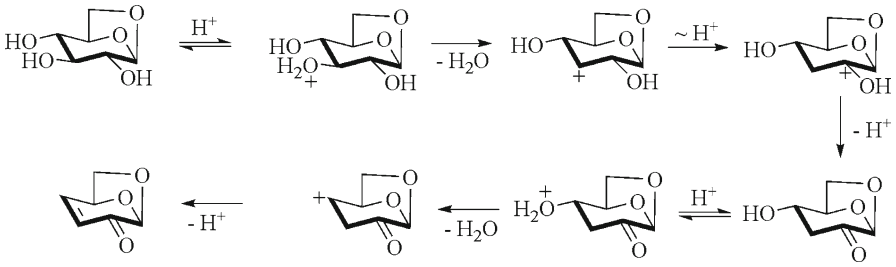

Fig. 5 The formation of LGO from acid-catalyzed decomposition of LG

in 1973 [41], and further confirmed and adopted by other researchers. LGO is an optically active organic compound in which all carbon atoms are different environments and which has easily modifiable functional groups. As a result, LGO can be used in the synthesis of various products (such as tetrodotoxin, thiosugar, ras activation inhibitors). The detailed applications of LGO can be found elsewhere [55].

LGO is formed in very low yield from fast pyrolysis of cellulose or biomass, but can be promoted by the addition of some acid catalysts in the pyrolytic process. A mechanism has been proposed for acid-catalyzed decomposition of LG to form the LGO, as shown in Fig. 5 [41].

Various acid catalysts exhibited the capability to promote the LGO formation, such as the $MgCl_2$ and $FeCl_3$ [45], $(NH_4)_2SO_4$ and $(NH_4)_2HPO_4$ [21, 69], CrO_3 and CrO_3+$CuSO_4$ [34], $ZnCl_2$ [22], M/MCM-41(M=Sn, Zr, Ti, Mg, etc.) [91]. However, almost all of these catalysts did not show high selectivity on the LGO, because they catalyzed the formation of several dehydrated products (LGO, LAC, DGP, FF, etc.), rather than LGO alone.

According to a series of studies performed by Dobele et al. [25–27], fast pyrolysis of cellulose/biomass impregnated with phosphoric acid could produce LGO with very high purity. The highest LGO yield reached 34 wt% from microcrystalline cellulose impregnated with 2% phosphoric acid, or 17.5 wt% from birch wood impregnated with 2.5% phosphoric acid. Other studies also confirmed the promising catalytic selectivity of the phosphoric acid on the LGO production [35, 64, 82]. Furthermore, Dobele et al. [28] reported that the pretreatment of cellulose/biomass with adsorption of $Fe_2(SO_4)_3$ provided another way to prepare LGO with high purity, but the selectivity of the $Fe_2(SO_4)_3$ on the LGO was a little lower than the phosphoric acid.

In a recent study, it was reported that fast pyrolysis of pure cellulose followed with catalytic cracking of the pyrolysis vapors with solid super acids (sulfated metal oxides, SO_4^{2-}/TiO_2, SO_4^{2-}/ZrO_2, SO_4^{2-}/SnO_2, etc.) allowed the production of LGO with the content reaching 40% (peak area% on the GC/MS ion chromatograms) in the pyrolytic products [49]. In fact, when the solid super acids were mechanically mixed with cellulose, fast pyrolysis of the mixture also produced LGO with high purity. Compared with the impregnation of catalysts (phosphoric acid or $Fe_2(SO_4)_3$) on the cellulose/biomass, the utilization of solid catalysts avoids the complex pretreatment process, and will offer a significant advantage on catalyst recycles.

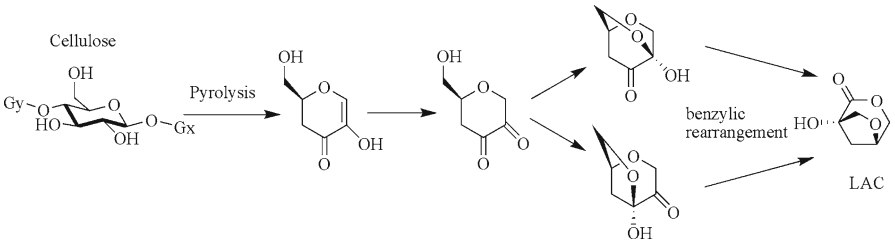

Fig. 6 The pyrolytic pathways for the formation of LAC from pyrolysis of cellulose

Compared with the LG, the LGO can be easily recovered from pyrolytic liquids by distillation, and a detailed purification method was proposed by Marshall [54].

3.2.1 1-Hydroxy-3,6-Dioxabicyclo[3.2.1]Octan-2-One

The 1-hydroxy-3,6-dioxabicyclo[3.2.1]octan-2-one (LAC) is another multifunctional C6-monomer formed from fast pyrolysis of cellulose. It was firstly identified by Furneaux et al. [36], who also proposed its possible pyrolytic formation pathways, as shown in Fig. 6. Compared with the LG and LGO, the LAC has received much less attention in either its production or application studies.

Similar to the LGO, the LAC is formed in very low yield during fast pyrolysis of cellulose, but can be promoted in the acid-catalyzed pyrolysis process. Most of the catalysts which could increase the LGO formation could also promote the LAC formation. Therefore, it is necessary to find out proper catalyst which has high selectivity on the LAC.

According to some previous studies, fast pyrolysis of cellulose mixed with nano-powder aluminum titanate at 350°C obtained the LGO and LAC as the major products, with the yields reaching 22 and 8.6 wt%, respectively. When the pyrolysis temperature was increased to 500°C, the LAC was formed as the only predominant product with high purity, but its yield was decreased to 6.2 wt% (the LGO yield was decreased to 0.77 wt%) [32, 33, 92]. As indicated above, the utilization of solid catalysts will provide a convenient way for the catalyst recycles. Further studies have also been conducted by them to use the LAC as a possible building block in the synthesis of fine chemicals.

3.3 Anhydro-Oligosaccharides

It is clearly demonstrated in previous studies that fast pyrolysis of cellulose will generate a range of anhydro-oligosaccharides, resulting from random cleavage of the polymer chain [48, 75, 78, 79]. Anhydro-oligosaccharides are potential for a number of possible uses, such as the preparation of glycoconjugates, the so-called anti-adhesive drugs, and so on.

Although fast pyrolysis is a known technique to produce anhydro-oligosaccharides from cellulose, very limited studies have been carried out to produce the oligomers as a target product. Piskorz et al. [73] initiated a flash pyrolysis study on this target product. Compared with conventional fast pyrolysis aiming at the maximum bio-oil yield, the production of anhydro-oligosaccharides required stricter reaction conditions: higher pyrolysis temperature (850–1,200°C) together with shorter residence time (35–75 ms). The short residence time was used to inhibit the conversion of large oligomers to monomer and dimer anhydrosaccharides. Anhydro-oligosaccharides in the range of G2–G7 were successfully produced with the yield up to near 20 wt%. These oligomers could be recovered as water soluble fraction from the reaction solid residues. Moreover, substantial amounts of larger oligomers (>G7) could also be produced but difficult to be identified.

Furthermore, if single anhydro-oligosaccharides can be produced and recovered, they should be more valuable than the mixed anhydro-oligosaccharides, but no reports are available in this research field at present.

3.4 Furfural

Furfural (FF) is a typical pyrolytic product formed from both of cellulose and hemicellulose. It is widely used as an organic solvent or an organic reagent for the production of medicines, resins, food additives, fuel additives, and other special chemicals. Currently, FF is industrially produced from agricultural raw materials rich in pentosan. By aqueous acid catalysis (e.g., sulfuric acid or phosphoric acid), the pentosan is firstly hydrolyzed to pentose which is then dehydrated to form FF [96].

Similar as the LGO and LAC, the formation of FF can be promoted in the acid-catalyzed pyrolysis of biomass [2, 29, 30, 50, 85, 89]. Zinc chloride ($ZnCl_2$) is one of the promising catalysts to produce FF. It was found that fast pyrolysis of cellulose impregnated with small amounts of $ZnCl_2$ (below 10 wt%) would generate several dehydrated products as the primary pyrolytic products, mainly the FF, LGO, LAC, and 1,4:3,6-dianhydro-α-D-glucopyranose (DGP). With the increasing of $ZnCl_2$ impregnation (at least 15 wt% or more), the $ZnCl_2$ catalysis would increase the FF formation, while decrease the anhydrosugars. Moreover, the secondary catalytic cracking of the primary pyrolysis vapors by $ZnCl_2$ could promote the conversion of LGO and other anhydrosugars to FF, leaving the FF as the only predominant product (Fig. 7). Compared with the cellulose, the $ZnCl_2$-catalzyed fast pyrolysis of xylan would obtain the FF as the only predominant product, and the FF yield would be higher than that from cellulose, indicating that biomass rich xylan would be suitable for the FF production.

In another study, microwave-assisted fast pyrolysis was applied to treat biomass mixed with various catalysts, and the results revealed that the $MgCl_2$ exhibited high selectivity on the FF production [93]. The highest FF content was more than 80% (peak area% on the GC/MS ion chromatograms) at the 8 g $MgCl_2$ mixed with 100 g biomass.

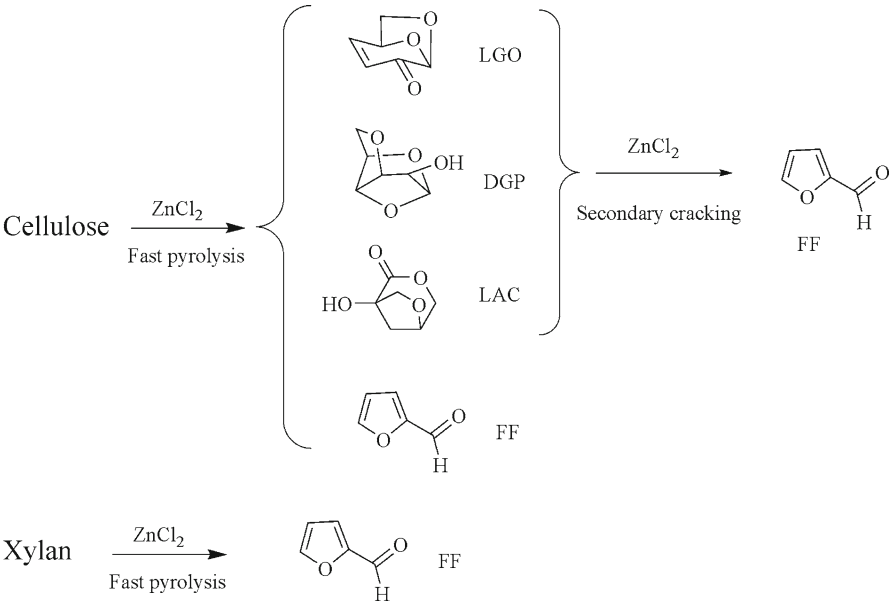

Fig. 7 The formation of FF during $ZnCl_2$-catalyzed fast pyrolysis of biomass

In addition, $ZnCl_2$ (or sometimes $MgCl_2$) is an effective chemical activation agent for the production of activated carbons from biomass. Hence, for the biomass pretreated by $ZnCl_2$ (or $MgCl_2$) impregnation, they can be firstly subjected to fast pyrolysis to produce FF. The solid residues which contained char and $ZnCl_2$ (or $MgCl_2$) could be further activated to produce activated carbons, so as to achieve the coproduction of FF and activated carbons.

3.5 Hydroxyacetaldehyde

HAA is formed as the most abundant linear carbonyl product from pyrolytic ring scission of holocellulose. It is the simplest aldehyde-alcohol or sugar, and can be used as an active meat-browning agent in food flavoring industry [39], or ingredient in cosmetic industry.

As been indicated above, during fast pyrolysis of biomass, the pyrolytic ring scission of holocellulose will be promoted by the small amounts of ash or alkaline cations [89], and hence, HAA can be formed with high yield in these conditions. Moreover, HAA could be further formed from the secondary cracking of the anhydrosugar products. As a result, HAA is usually the most abundant single organic compound in crude bio-oils produced from raw biomass materials.

Similar as the LG, the difficulty for the preparation of HAA mainly lies in its recovery from pyrolysis liquids, due to its high reactivity. An efficient purification method was patented by Stradal and Underwood [90].

3.6 Acetic Acid

During fast pyrolysis of biomass, acetic acid (AA) can be formed from different ways, with a large portion from deacetylation of hemicellulose, and a small portion from pyrolytic ring scission of holocellulose and side-chain cracking of lignin. The content of AA could be over 10 wt% in crude bio-oils produced from biomass rich in acetyl groups, and some preliminary studies have been reported for the recovery of AA [53]. AA is a common chemical, and is less valuable than other chemicals described above. According to its formation characteristics, selective fast pyrolysis of biomass to produce AA with high purity might be achieved in several different ways.

The deacetylation of hemicellulose occurs at relatively low temperature, lower than the fast decomposition of the major biomass components. Hence, AA can be produced from low temperature pyrolysis of biomass. It has already been confirmed that during carbonization or torrefaction of biomass at temperatures lower than 300°C, a liquid by-product rich in AA could be produced [76]. In fact, if biomass is subjected to fast pyrolysis at around 300°C for a short time period, part of the acetyl group would break down to form AA, while the other biomass components would not be greatly influenced. Therefore, a two-step process might be applied to treat biomass, with the first low-temperature fast pyrolysis to produce AA, followed with the moderate-temperature fast pyrolysis to produce bio-oil.

AA can also be prepared by catalytic pyrolysis of biomass. For example, Qi et al. [77] reported that catalytic pyrolysis of biomass using NaY catalyst produced abundant AA, with the content over 80% (peak area% on the GC/MS ion chromatograms) in the pyrolytic products.

In addition, during the production of FF through fast pyrolysis of biomass impregnated with $ZnCl_2$ (or $MgCl_2$), the catalysis of $ZnCl_2$ (or $MgCl_2$) inhibited most of the pyrolytic pathways, but not the AA formation. As a result, AA would be the second most important product in the catalytic organic products, and thus, it could be recovered as a by-product during preparation of FF.

3.7 Phenolic Compounds

The lignin-derived phenolic compounds (monomeric phenolic compounds and pyrolytic lignins) can be isolated from crude bio-oils by different methods [1, 7, 20], and they are known to be used as phenol replacement in production of phenol-formaldehyde resins [19, 40, 42, 80].

As indicated above, the monomeric phenolic compounds are usually formed in much lower yield than the pyrolytic lignins. Since the monomers are more reactive than the oligomers for resin production, and thus, it will be attractive to promote the production of monomeric phenolic compounds. According to some previous studies, fast pyrolysis of biomass impregnated with some alkaline compounds (NaOH, KOH) could increase the yield of monomeric phenolic compounds [23, 24, 63].

In another study, Pd/SBA-15 catalysts were employed to catalytic crack biomass fast pyrolysis vapors that contained a lot of pyrolytic lignins, and the results indicated that the Pd/SBA-15 catalysts were able to promote the conversion the pyrolytic lignins to monomeric phenolic compounds, and meanwhile to crack and decrease holocellulose-derived products. Hence, the content of the total monomeric phenolic compounds reached 55% (peak area% on the GC/MS ion chromatograms) in the catalytic pyrolytic products [51]. Some other catalysts were also confirmed to possess the catalytic capability to increase the yield of monomeric phenolic compounds or their content in the catalytic bio-oils [3, 8, 9, 62].

Furthermore, if single phenolic compounds could be produced and recovered, they should be much more valuable than the mixed phenolic compounds. According to a previous study done by Murwanashyaka et al. [59], the evolution of major monomeric phenolic compounds took place in the following order: methylguaiacol, ethylguaiacol, guaiacol, propenylsyringol, phenol, and catechol, which suggested that the production of specific phenolic compounds might be achieved by stepwise pyrolysis of biomass. Catalytic pyrolysis is another promising way. For example, during the catalytic cracking of biomass fast pyrolysis vapors with Pd/SBA-15 catalysts, the 4-ethyl-2-methoxy-phenol was increased greatly, with the content up to 10% (peak area% on the GC/MS ion chromatograms) in the pyrolytic products [51]. Some subsequent studies have also been reported for the recovery of pure single phenolic compounds [60].

3.8 Light Aromatic Hydrocarbons

Hydrocarbons are usually formed in very low yields during fast pyrolysis of biomass, but can be greatly increased by using proper cracking catalysts with deoxygenation capability [16]. Zeolite catalysts (such as HZSM-5, HY, etc.) are very effective to convert the highly oxygenated crude bio-oils or pyrolysis vapors to hydrocarbons which are dominated by several light aromatic hydrocarbons (benzene, toluene, xylene, and naphthalene) [43, 67, 70, 95, 97]. For example, in the studies performed by Adjaye et al. [4, 5], catalytic cracking of the crude bio-oil by HZSM-5 catalysts obtained a organic liquid product with up to 90 wt% of aromatic hydrocarbons, and the aromatic hydrocarbons contained abundant toluene (31.8 wt%) and xylene (33.1 wt%).

Other catalysts were also investigated for the production of light aromatic hydrocarbons. For example, Wang et al. [94] reported that catalytic pyrolysis of biomass using CoMo-S/Al_2O_3 catalyst produced the four light aromatic hydrocarbons (benzene, toluene, xylene, and naphthalene) with the yield reaching 6.3 wt% at 590°C.

3.9 Other Valuable Chemicals

In addition to the above chemicals, many other chemicals can be produced by selective fast pyrolysis of biomass. For example, Chen et al. [18] reported that fast pyrolysis

of biomass impregnated with Na_2CO_3 produced HA with high purity. Badri [10] revealed that catalytic pyrolysis of cotton with reactive dyes favored the formation of 5-hydroxymethyl-furfural (HMF) and 3-(hydroxymethyl)-furan. Lu et al. [51] found that fast pyrolysis of cellulose followed with catalytic cracking of the vapors by sulfated metal oxides could obtain high yields of furan and 5-methyl furfural. In another study, Lu et al. [52] confirmed that catalytic cracking of the biomass fast pyrolysis vapors using ZrO_2 and TiO_2 increased the formation of three light carbonyl products (acetaldehyde, acetone, and 2-butanone).

4 Conclusion

Most of the selective fast pyrolysis techniques are only in their early stage of development, and none of the techniques is commercially practical to produce specific chemicals in marketable quantities at present. Three aspects should be considered for the commercialization of the selective fast pyrolysis techniques, including (1) the technique to produce specific chemicals in high yield and purity, (2) the method to recover the target chemicals from pyrolysis liquids, and (3) the ready markets for the chemicals.

Among the above indicated chemicals, the LG, HAA, and AA can be produced without catalyst utilization, and thus, their large-scale production might be relatively easy to achieve through slight modification of the conventional fast pyrolysis technique. The production of other chemicals requires catalysts, which will add difficulty to their scale up. Various methods have been proposed for the chemicals recovery, and further studies should be conducted to reduce the purification cost. Finally, it is important to note that currently there are no existing markets for the LG, LGO, LAC, anhydro-oligosaccharides, and some other chemicals. Corresponding markets should be developed by manufacturers who would incorporate these chemicals into various products.

References

1. Achladas GE (1991) Analysis of biomass pyrolysis liquids—separation and characterization of phenols. J Chromatogr 542:263–275
2. Adam J, Blazso M, Meszaros E, Stocker M, Nilsen MH, Bouzga A, Hustad JE, Gronli M, Oye G (2005) Pyrolysis of biomass in the presence of Al-MCM-41 type catalysts. Fuel 84:1494–1502
3. Adam J, Antonakou E, Lappas A, Stocker M, Nilsen MH, Bouzga A, Hustad JE, Oye G (2006) In situ catalytic upgrading of biomass derived fast pyrolysis vapours in a fixed bed reactor using mesoporous materials. Micropor Mesopor Mat 96:93–101
4. Adjaye JD, Bakhshi NN (1995) Production of hydrocarbons by catalytic upgrading of a fast pyrolysis bio-oil. 1. Conversion over various catalysts. Fuel Process Technol 45:161–183
5. Adjaye JD, Katikaneni SPR, Bakhshi NN (1996) Catalytic conversion of a biofuel to hydrocarbons: effect of mixtures of HZSM-5 and silica-alumina catalysts on product distribution. Fuel Process Technol 48:115–143

6. Alen R, Kuoppala E, Oesch P (1996) Formation of the main degradation compound groups from wood and its components during pyrolysis. J Anal Appl Pyrol 36:137–148
7. Amen-Chen C, Pakdel H, Roy C (1997) Separation of phenols from Eucalyptus wood tar. Biomass Bioenergy 13:25–37
8. Antonakou E, Lappas A, Nilsen MH, Bouzga A, Stocker M (2006) Evaluation of various types of Al-MCM-41 materials as catalysts in biomass pyrolysis for the production of bio-fuels and chemicals. Fuel 85:2202–2212
9. Ates F, Isikdag MA (2009) Influence of temperature and alumina catalyst on pyrolysis of corncob. Fuel 88:1991–1997
10. Badri B (2008) The influence of reactive dyes on the pyrolysis of cotton. J Anal Appl Pyrol 81: 162–166
11. Bailliez V, Olesker A, Cleophax J (2004) Synthesis of polynitrogenated analogues of glucopyranoses from levoglucosan. Tetrahedron 60:1079–1085
12. Bayerbach R, Nguyen VD, Schurr U, Meier D (2006) Characterization of the water-insoluble fraction from fast pyrolysis liquids (pyrolytic lignin)—Part III. Molar mass characteristics by SEC, MALDI-TOF-MS, LDI-TOF-MS, and Py-FIMS. J Anal Appl Pyrol 77:95–101
13. Bayerbach R, Meier D (2009) Characterization of the water-insoluble fraction from fast pyrolysis liquids (pyrolytic lignin). Part IV: structure elucidation of oligomeric molecules. J Anal Appl Pyrol 85:98–107
14. Bennett NM, Helle SS, Duff SJB (2009) Extraction and hydrolysis of levoglucosan from pyrolysis oil. Bioresour Technol 100:6059–6063
15. Boutin O, Ferrer M, Lede J (1998) Radiant flash pyrolysis of cellulose—evidence for the formation of short life time intermediate liquid species. J Anal Appl Pyrol 47:13–31
16. Bridgwater A (1996) Production of high grade fuels and chemicals from catalytic pyrolysis of biomass. Catal Today 29:285–295
17. Bridgwater AV, Peacocke GVC (2000) Fast pyrolysis processes for biomass. Renew Sust Energy Rev 4:1–73
18. Chen MQ, Wang J, Zhang MX, Chen MG, Zhu XF, Min FF, Tan ZC (2008) Catalytic effects of eight inorganic additives on pyrolysis of pine wood sawdust by microwave heating. J Anal Appl Pyrol 82:145–150
19. Chum HL, Kreibich RE (1992) Process for preparing phenolic formaldehyde resole resin products derived from fractionated fast-pyrolysis oils. US 5091499
20. Deng L, Yan Z, Fu Y, Guo QX (2009) Green solvent for flash pyrolysis oil separation. Energ Fuel 23:3337–3338
21. Di Blasi C, Branca C, Galgano A (2007) Effects of diammonium phosphate on the yields and composition of products from wood pyrolysis. Ind Eng Chem Res 46:430–438
22. Di Blasi C, Branca C, Galgano A (2008) Products and global weight loss rates of wood decomposition catalyzed by zinc chloride. Energ Fuel 22:663–670
23. Di Blasi C, Galgano A, Branca C (2009) Effects of potassium hydroxide impregnation on wood pyrolysis. Energ Fuel 23:1045–1054
24. Di Blasi C, Galgano A, Branca C (2009) Influences of the chemical state of alkaline compounds and the nature of alkali metal on wood pyrolysis. Ind Eng Chem Res 48:3359–3369
25. Dobele G, Rossinskaja G, Telysheva G, Meier D, Faix O (1999) Cellulose dehydration and depolymerization reactions during pyrolysis in the presence of phosphoric acid. J Anal Appl Pyrol 49:307–317
26. Dobele G, Meier D, Faix O, Radtke S, Rossinskaja G, Telysheva G (2001) Volatile products of catalytic flash pyrolysis of celluloses. J Anal Appl Pyrol 58:453–463
27. Dobele G, Dizhbite T, Rossinskaja G, Telysheva G, Mier D, Radtke S, Faix O (2003) Pretreatment of biomass with phosphoric acid prior to fast pyrolysis—a promising method for obtaining 1,6-anhydrosaccharides in high yields. J Anal Appl Pyrol 68–9:197–211
28. Dobele G, Rossinskaja G, Diazbite T, Telysheva G, Meier D, Faix O (2005) Application of catalysts for obtaining 1,6-anhydrosaccharides from cellulose and wood by fast pyrolysis. J Anal Appl Pyrol 74:401–405

29. Encinar JM, Beltran FJ, Ramiro A, Gonzalez JF (1997) Catalyzed pyrolysis of grape and olive bagasse. Influence of catalyst type and chemical treatment. Ind Eng Chem Res 36:4176–4183
30. Encinar JM, Beltran FJ, Ramiro A (1998) Pyrolysis/gasification of agricultural residues by carbon dioxide in the presence of different additives: influence of variables. Fuel Process Technol 55:219–233
31. Evans RJ, Milne TA (1987) Molecular characterization of the pyrolysis of biomass. 1. Fundamentals. Energy Fuel 1:123–137
32. Fabbri D, Torri C, Baravelli V (2007) Effect of zeolites and nanopowder metal oxides on the distribution of chiral anhydrosugars evolved from pyrolysis of cellulose: an analytical study. J Anal Appl Pyrol 80:24–29
33. Fabbri D, Torri C, Mancini I (2007) Pyrolysis of cellulose catalysed by nanopowder metal oxides: production and characterisation of a chiral hydroxylactone and its role as building block. Green Chem 9:1374–1379
34. Fu QR, Argyropoulos DS, Tilotta DC, Lucia LA (2008) Understanding the pyrolysis of CCA-treated wood. Part I. Effect of metal ions. J Anal Appl Pyrol 81:60–64
35. Fu QR, Argyropoulos DS, Tilotta DC, Lucia LA (2008) Understanding the pyrolysis of CCA-treated wood. Part II. Effect of phosphoric acid. J Anal Appl Pyrol 82:140–144
36. Furneaux RH, Mason JM, Miller I (1988) A novel hydroxylactone from the Lewis acid catalyzed pyrolysis of cellulose. J Chem Soc Perkin Trans 1:49–51
37. Garcia-Perez M, Chaala A, Pakdel H, Kretschmer D, Roy C (2007) Characterization of bio-oils in chemical families. Biomass Bioenergy 31:222–242
38. Garcia-Perez M, Wang S, Shen J, Rhodes M, Lee WJ, Li CZ (2008) Effects of temperature on the formation of lignin-derived oligomers during the fast pyrolysis of Mallee woody biomass. Energ Fuel 22:2022–2032
39. Garham RG, Underwood GL (1993) Method of using fast pyrolysis liquids as liquid smoke. WO9105484
40. Giroux R, Freel B, Graham R (2001) Novel natural resin formulations. US6326461
41. Halpern Y, Riffer R, Broido A (1973) Levoglucosenone (1,6-Anhydro-3,4-dideoxy-Δ3-β-D-Pyranosen-2-one). A major product of the acid-catalyzed pyrolysis of cellulose and related carbohydrates. J Org Chem 38:204–209
42. Himmelblau A (1991) Method and apparatus for producing water-soluble resin and resin product made by that method. US5034498
43. Horne PA, Williams PT (1996) Upgrading of biomass-derived pyrolytic vapours over zeolite ZSM-5 catalyst: effect of catalyst dilution on product yields. Fuel 75:1043–1050
44. Howard J, Longley C, Morrison A, Fung D (1993) Process for isolating levoglucosan from pyrolysis liquids. CA2084906
45. Klampfl CW, Breuer G, Schwarzinger C, Koll B (2006) Investigations on the effect of metal ions on the products obtained from the pyrolysis of cellulose. Acta Chim Slov 53:437–443
46. Lanza R, Nogare DD, Canu P (2009) Gas phase chemistry in cellulose fast pyrolysis. Ind Eng Chem Res 48:1391–1399
47. Lin YC, Cho J, Tompsett GA, Westmoreland PR, Huber GW (2009) Kinetics and mechanism of cellulose pyrolysis. J Phys Chem C 113:20097–20107
48. Lomax JA, Commandeur JM, Arisz PW, Boon JJ (1991) Characterization of oligomers and sugar ring-cleavage products in the pyrolysate of cellulose. J Anal Appl Pyrol 19:65–79
49. Lu Q, Xiong WM, Li WZ, Guo QX, Zhu XF (2009) Catalytic pyrolysis of cellulose with sulfated metal oxides: a promising method for obtaining high yield of light furan compounds. Bioresour Technol 100:4871–4876
50. Lu Q, Li WZ, Zhang D, Zhu XF (2009) Analytical pyrolysis-gas chromatography/mass spectrometry (Py-GC/MS) of sawdust with Al/SBA-15 catalysts. J Anal Appl Pyrol 84:131–138
51. Lu Q, Tang Z, Zhang Y, Zhu XF (2010) Catalytic upgrading of biomass fast pyrolysis vapors with Pd/SBA-15 catalysts. Ind Eng Chem Res 49:2573–2580
52. Lu Q, Zhang Y, Tang Z, Li WZ, Zhu XF (2010) Catalytic upgrading of biomass fast pyrolysis vapors with titania and zirconia/titania based catalysts. Fuel 89(8):2096–2103. doi:10.1016/j.fuel.2010.02.030

53. Mahfud FH, van Geel FP, Venderbosch RH, Heeres HJ (2008) Acetic acid recovery from fast pyrolysis oil. An exploratory study on liquid-liquid reactive extraction using aliphatic tertiary amines. Sep Sci Technol 43:3056–3074
54. Marshall JA (2008) An improved preparation of levoglucosenone from cellulose. Iowa State University, Master thesis
55. Miftakhov MS, Valeev FA, Gaisina IN (1994) Levoglucosenone: the properties, reactions, and use in fine organic synthesis. Russ Chem Rev 63:869–882
56. Miftakhov MS, Ermolenko MS, Gaisina IN, Kuznetsov OM, Selezneva NK, Yusupova ZA, Muslukhov RR (2001) Chemistry of natural compounds, bioorganic, and biomolecular chemistry—synthesis of a C(9)-C(13) fragment of acutiphycin from levoglucosan. Russ Chem Bull 50:1101–1106
57. Moens L (1994) Isolation of levoglucosan from pyrolysis oil derived from cellulose. WO9405704
58. Mohan D, Pittman CU, Steele PH (2006) Pyrolysis of wood/biomass for bio-oil: a critical review. Energ Fuel 20:848–889
59. Murwanashyaka JN, Pakdel H, Roy C (2001) Step-wise and one-step vacuum pyrolysis of birch-derived biomass to monitor the evolution of phenols. J Anal Appl Pyrol 60:219–231
60. Murwanashyaka JN, Pakdel H, Roy C (2001) Separation of syringol from birch wood-derived vacuum pyrolysis oil. Sep Purif Technol 24:155–165
61. NikAzar M, Hajaligol MR, Sohrabi M, Dabir B (1997) Mineral matter effects in rapid pyrolysis of beech wood. Fuel Process Technol 51:7–17
62. Nilsen MH, Antonakou E, Bouzga A, Lappas A, Mathisen K, Stocker M (2007) Investigation of the effect of metal sites in Me-Al-MCM-41 (Me = Fe, Cu or Zn) on the catalytic behavior during the pyrolysis of wooden based biomass. Micropor Mesopor Mat 105:189–203
63. Nowakowski DJ, Jones JM, Brydson RMD, Ross AB (2007) Potassium catalysis in the pyrolysis behaviour of short rotation willow coppice. Fuel 86:2389–2402
64. Nowakowski DJ, Woodbridge CR, Jones JM (2008) Phosphorus catalysis in the pyrolysis behaviour of biomass. J Anal Appl Pyrol 83:197–204
65. Oasmaa A, Kuoppala E, Solantausta Y (2003) Fast pyrolysis of forestry residue. 2. Physicochemical composition of product liquid. Energy Fuel 17:433–443
66. Ohnishi A, Kato K, Takagi E (1975) Curie-point pyrolysis of cellulose. Polym J 7:431–437
67. Olazar M, Aguado R, Bilbao J, Barona A (2000) Pyrolysis of sawdust in a conical spouted-bed reactor with a HZSM-5 catalyst. AlChE J 46:1025–1033
68. Pan WP, Richards GN (1989) Influence of metal ions on volatile products of pyrolysis of wood. J Anal Appl Pyrol 16:117–126
69. Pappa A, Mikedi K, Tzamtzis N, Statheropoulos M (2006) TG-MS analysis for studying the effects of fire retardants on the pyrolysis of pine-needles and their components. J Therm Anal Calorim 84:655–661
70. Pattiya A, Titiloye JO, Bridgwater AV (2008) Fast pyrolysis of cassava rhizome in the presence of catalysts. J Anal Appl Pyrol 81:72–79
71. Piskorz J, Radlein D, Scott DS (1986) On the mechanism of the rapid pyrolysis of cellulose. J Anal Appl Pyrol 9:121–137
72. Piskorz J, Radlein D, Scott DS, Czernik S (1989) Pretreatment of wood and cellulose for production of sugars by fast pyrolysis. J Anal Appl Pyrol 16:127–142
73. Piskorz J, Majerski P, Radlein D, Vladars-Usas A, Scott DS (2000) Flash pyrolysis of cellulose for production of anhydro-oligomers. J Anal Appl Pyrol 56:145–166
74. Ponder GR, Richards GN (1991) Thermal synthesis and pyrolysis of a xylan. Carbohydr Res 218:143–155
75. Pouwels AD, Eijkel GB, Arisz PW, Boon JJ (1989) Evidence for oligomers in pyrolysates of microcrystalline cellulose. J Anal Appl Pyrol 15:71–84
76. Prins MJ, Ptasinski KJ, Janssen F (2006) Torrefaction of wood—Part 2. Analysis of products. J Anal Appl Pyrol 77:35–40
77. Qi WY, Hu CW, Li GY, Guo LH, Yang Y, Luo J, Miao X, Du Y (2006) Catalytic pyrolysis of several kinds of bamboos over zeolite NaY. Green Chem 8:183–190

78. Radlein D, Grinshpun A, Piskorz J, Scott DS (1987) On the presence of anhydro-oligosaccharides in the sirups from the fast pyrolysis of cellulose. J Anal Appl Pyrol 12:39–49
79. Radlein D, Piskorz J, Scott DS (1991) Fast pyrolysis of natural polysaccharides as a potential Industrial-process. J Anal Appl Pyrol 19:41–63
80. Roy C, Lu X, Pakdel H (2000) Process for the production of phenolic-rich pyrolysis oils for use in making phenol-formaldehyde resole resins. US6143856
81. Scott DS, Piskorz J, Radlein D, Majerski P (1996) Process for the production of anhydrosugars from lignin and cellulose containing biomass by pyrolysis. US5395455
82. Sarotti AM, Spanevello RA, Suarez AG (2007) An efficient microwave-assisted green transformation of cellulose into levoglucosenone. Advantages of the use of an experimental design approach. Green Chem 9:1137–1140
83. Scholze B, Meier D (2001) Characterization of the water-insoluble fraction from pyrolysis oil (pyrolytic lignin). Part I. PY-GC/MS, FTIR, and functional groups. J Anal Appl Pyrol 60:41–54
84. Scholze B, Hanser C, Meier D (2001) Characterization of the water-insoluble fraction from fast pyrolysis liquids (pyrolytic lignin). Part II. GPC, carbonyl groups, and C-13-NMR. J Anal Appl Pyrol 58:387–400
85. Shafizadeh F, Lai YZ (1972) Thermal degradation of 1,6-anhydro-β-D-glucopyranose. J Org Chem 37:278–284
86. Shafizadeh F (1982) Introduction to pyrolysis of biomass. J Anal Appl Pyrol 3:283–305
87. Shen DK, Gu S (2009) The mechanism for thermal decomposition of cellulose and its main products. Bioresour Technol 100:6496–6504
88. Shen DK, Gu S, Bridgwater AV (2010) Study on the pyrolytic behaviour of xylan-based hemicellulose using TG-FTIR and Py-GC-FTIR. J Anal Appl Pyrol 87:199–206
89. Shimada N, Kawamoto H, Saka S (2008) Different action of alkali/alkaline earth metal chlorides on cellulose pyrolysis. J Anal Appl Pyrol 81:80–87
90. Stradal JA, Underwood GL (1995) Process for producing hydroxyacetaldehyde. US5393542
91. Torri C, Lesci IG, Fabbri D (2009) Analytical study on the pyrolytic behaviour of cellulose in the presence of MCM-41 mesoporous materials. J Anal Appl Pyrol 85:192–196
92. Torri C, Lesci IG, Fabbri D (2009) Analytical study on the production of a hydroxylactone from catalytic pyrolysis of carbohydrates with nanopowder aluminium titanate. J Anal Appl Pyrol 84:25–30
93. Wan YQ, Chen P, Zhang B, Yang CY, Liu YH, Lin XY, Ruan R (2009) Microwave-assisted pyrolysis of biomass: Catalysts to improve product selectivity. J Anal Appl Pyrol 86:161–167
94. Wang C, Hao QL, Lu DQ, Ja QZ, Li GJ, Xu B (2008) Production of light aromatic hydrocarbons from biomass by catalytic pyrolysis. Chin J Catal 29:907–912
95. Williams PT, Nugranad N (2000) Comparison of products from the pyrolysis and catalytic pyrolysis of rice husks. Energy 25:493–513
96. Zeitsch KJ (2000) The chemistry and technology of furfural and its many by-products. Elsevier, Amsterdam
97. Zhang HY, Xiao R, Wang DH, Zhong ZP, Song M, Pan QW, He GY (2009) Catalytic fast pyrolysis of biomass in a fluidized bed with fresh and spent fluidized catalytic cracking (FCC) catalysts. Energy Fuels 23:6199–6206

Chapter 11
Sub- and Supercritical Water Technology for Biofuels

Sandeep Kumar

Abstract One of the major challenges in utilization of biomass is its high moisture content and variable composition. The conventional thermochemical conversion processes such as pyrolysis and gasification require dry biomass for production of biofuels. Sub- and supercritical water (critical point: 374°C, 22.1°MPa) technology, which can utilize wet biomass, capitalizes on the extraordinary solvent properties of water at elevated temperature for converting biomass to high energy density fuels and functional carbonaceous materials. Here, water acts as reactant as well as reaction medium in performing hydrolysis, depolymerization, dehydration, decarboxylation, and many other chemical reactions. One of the advantages is that the large parasitic energy losses that can consume much of the energy content of the biomass for moisture removal are avoided. In sub- and supercritical water-based processes, water is kept in liquid or supercritical phase by applying pressure greater than the vapor pressure of water. Thus, latent heat required for phase change of water from liquid to vapor phase (2.26 MJ/kg of water) is not needed. For a typical 250°C subcritical water process, the energy requirement to heat water from ambient condition to the reaction temperature is about 1 MJ/kg, equivalent to 6–8% of energy content of dry biomass.

1 Introduction

This chapter describes the application and current status of sub- and supercritical water (collectively called hydrothermal) technology for liquid fuels (bioethanol, biocrude), gaseous fuels (methane, hydrogen, synthesis gas), and solid fuels (biochar, other functional carbonaceous materials) production from biomass. Energy security, sustainability, and climate change concerns have led the world to look for

S. Kumar (✉)
Department of Civil and Environmental Engineering,
Old Dominion University, Norfolk, VA 23529, USA
e-mail: skumar@odu.edu

J.W. Lee (ed.), *Advanced Biofuels and Bioproducts*, DOI 10.1007/978-1-4614-3348-4_11, 147

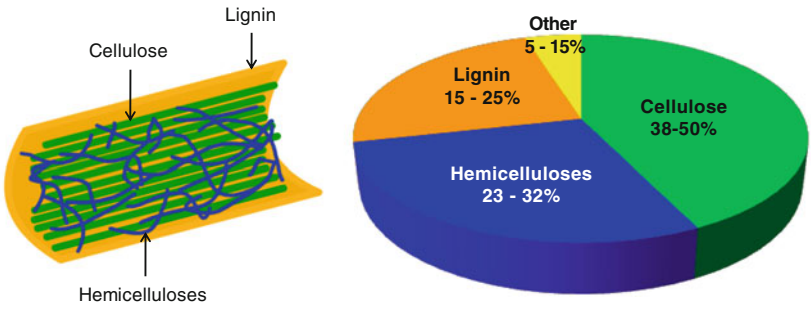

Fig. 1 Typical composition of lignocellulosic biomass

renewable and alternative energy resources. The large-scale substitution of petroleum-based fuels and products with renewable sources are needed to minimize the environmental issues [30]. Biomass is the world's fourth largest energy source, following coal, oil, and natural gas. Biomass is an attractive feedstock for fuel and biomaterials due to three main reasons. First, it is a carbon-neutral renewable resource that could be sustainably developed for the production of bioenergy and biomaterials. Second, it is environmentally benign, as it does not add to the green house gas emission, and possibly reduces NO_x and SO_x depending on the fossil fuels displaced. However, when combusted in traditional stoves, emission of polycyclic aromatic hydrocarbons, dioxins, furans, and heavy metals is an environmental health concern [89]. Third, it appears to have a significant economic potential given the fluctuating prices of the fossil fuels. Moreover, development of bio-based economy brings the opportunity for rural empowerment and also the energy security, since biomass resource is distributed all over the world.

In recent years, there is significant research interest on nonfood resources or so-called second-generation biofuels from lignocellulosic biomass. Lignocellulose is a generic term for describing the main constituents in most plants, namely cellulose, hemicellulose, and lignin (Fig. 1).

Lignocellulosic biomass, which is the non-starch-based fibrous part of plant material, is a renewable and abundantly available resource that can be considered as a potential feedstock for biofuels. The components of lignocelluloses form 3D polymeric composites to provide structure and rigidity to the plant. The composition of lignocellulosic materials varies with several factors such as type of plant, growth conditions, on the part of plant, and on the age of harvesting [28, 77, 87].

2 Structure and Composition of Lignocellulosic Biomass

Lignocelluloses are derived from wood, grass, agricultural residues, forestry waste, and municipal solid wastes. The major components of lignocellulosic material are cellulose, lignin, and hemicellulose, with others (extractives and ash) also present in

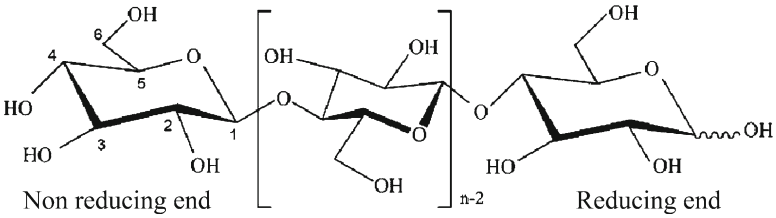

Fig. 2 Cellulose structure

small percentage. Cellulose and hemicelluloses are polymers based on different sugars, whereas lignin is an aromatic polymer mainly built of phenylpropanoid precursors. Composition of these polymers within single plant varies with age and stage of growth [90].

Cellulose: Discovered 150 years ago, cellulose is most abundant organic matter on the earth. It is the main structural constituent of plants and algal cell walls. Cellulose in wood is mixed with many polymers such as hemicelluloses and lignin. The fluffy fiber of cotton bolls is the purest naturally occurring form of cellulose. It is an unbranched chain and homopolymer of β-D-glucopyranose units linked together by (1→4)-glycosidic bonds with a repeating unit of $C_6H_{10}O_5$ strung together by β-glycosidic linkages (Fig. 2).

The β-linked glucose units in cellulose form long linear chains that associate to form nanometer-scale crystalline fibers called elemental fibrils that are highly stable and resistant to chemical attack because of the high degree of hydrogen bonding present between chains of native cellulose. Hemicellulose and lignin cover the cellulose microfibrils which are formed by assembly of elemental fibrils. Hydrogen bonding between cellulose chains makes the polymers more rigid, inhibiting the flexing of the molecules that must occur in the hydrolytic breaking of glycosidic linkages. Hydrolysis can reduce cellulose to a cellobiose repeating unit, $C_{12}H_{22}O_{11}$, and ultimately to glucose [70, 86, 99].

There are six known polymorphs of cellulose (I, II, III_I, III_{II}, IV_I, and IV_{II}) which can also interconvert. The interconversion of cellulose is shown in Fig. 3.

Cellulose I, also termed as native cellulose, has parallel arrangement of chains and is the only polymorph that occurs naturally. Cellulose II is converted through mercerization or solubilization–regeneration of native or other celluloses. Cellulose II is thermodynamically more stable structure with a low energy crystalline arrangement having an antiparallel arrangement of the strands (two cellulose chains lie antiparallel to one another) and some intersheet hydrogen bonding. Cellulose III_I and III_{II} can be obtained from Cellulose I and II, respectively, by treatment with liquid ammonia or some amines, whereas polymorphs IV_I and IV_{II} can be obtained from heating cellulose III_I and III_{II}, respectively, to 206°C in glycerol [70, 86, 98, 99]. Two decades ago, it was reported that native cellulose (cellulose I) exists as a mixture of two crystalline forms I_α and I_β, having triclinic and monoclinic unit cells, respectively [2]. Cellulose I_α is thermodynamically less stable, as shown by its conversion to cellulose I_β by annealing at 260°C. In both crystalline forms, cellobiose

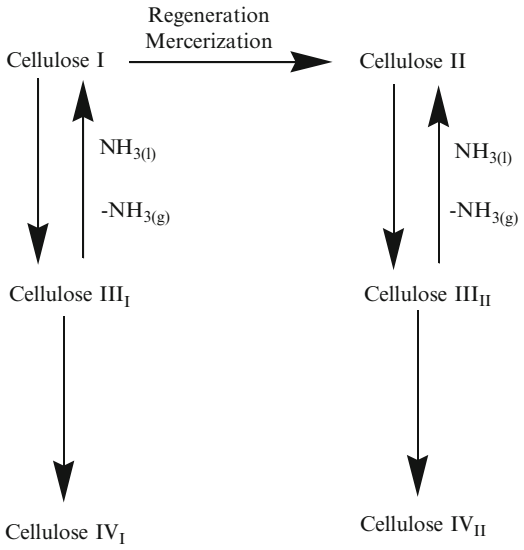

Fig. 3 Interconversion of polymorphs of cellulose [86]

is the repeating unit with a strong intra-chain H-bond from 3-OH to the preceding ring O5, whereas the interchain H-bonding and packing of the crystal are slightly different in the two forms [111].

The comparatively lower stability of I_α may provide the site of initial reaction in the microfibril. Cellulose molecules have reducing end groups, as chemical linkage between C1 carbon and the ring oxygen to form the pyranose ring. It is a hemiacetal group that allows the ring to open to form an aldehyde. The other end group is a secondary alcohol and commonly referred as the nonreducing end. The structural unit of cellulose has three hydroxyl groups, one primary and two secondary. These groups undergo chemical modifications (e.g., esterifications and etherifications) during the reactions. But the accessibility of the reactants is limited because of the high degree of crystallinity of the native cellulose [24].

Cellulases enzyme hydrolyze the β-1,4-glycosidic linkages of cellulose. They are divided in two classes and referred as endoglucanases (endo-1,4-β-glucanases, EGs) and cellobiohydrolases (exo-1,4-β-glucanases, CBHs). EGs hydrolyze preferably amorphous region of cellulose and releases new terminal ends. Whereas CBHs act on existing or EGs generated chain ends. Both enzymes can degrade amorphous cellulose, but only CBHs enzyme act efficiently on crystalline cellulose. Thus, CBHs and EGs work synergistically in cellulose hydrolysis and releases cellobiose molecules. β-glucosidases are required to further breakdown the cellobiose to two glucose molecules [90].

Hemicelluloses: Hemicelluloses are important carbohydrate fraction in plants made of mixed polysaccharides and stick to cellulose via hydrogen bonds, to create polysaccharide microfibrils. Together these give a strong rigidity to plant cell walls but the added lignin improves this strength greatly. The molecules are much smaller than the cellulose (degree of polymerization $\approx 10^2$) and are dominated by hydrogen bond from the 3-OH of one sugar to the ring oxygen of preceding sugar.

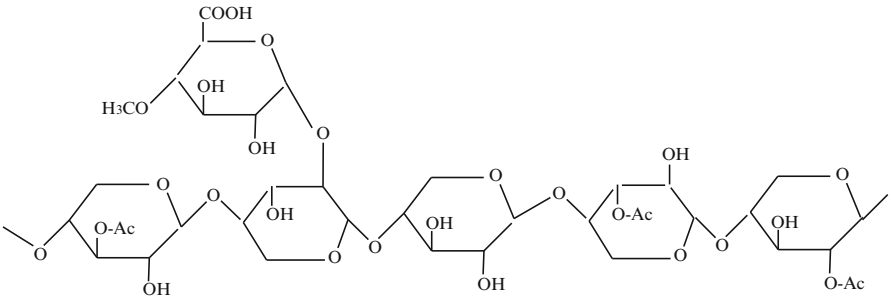

Fig. 4 A segment of hardwood xylan

Hemicelluloses are a class of polymers that contain mixed sugars. The monomeric form of mixed sugars can be six carbon sugars such as mannose, galactose, glucose, and 4-*O*-methyl-D-glucuronic acid and five carbon sugars such as xylose and arabinose depending upon the species. Unlike cellulose, hemicelluloses possess side chains (Fig. 4).

The side groups include acetic acid, pentoses (β-D-glucose, β-D-mannose, α-D-galactose), hexuronic acids (β-D-glucuronic acid, α-D-4-*O*-methylglucuronic acid, α-D-galacturonic acid), and deoxyhexoses (α-L-rhamnose α-L-fructose) and are responsible for the solubility of hemicelluloses in water and/or alkali. These side groups stop hemicelluloses molecules to aggregate and make them more susceptible to chemical degradation than cellulose. Within the plant, hemicelluloses are bound to cellulose and lignin component by covalent and noncovalent bonds in the cell wall and are thus fixed in the fiber structure [9, 97]. Xylans, mannans (glucomannans), and galactans are the major categories of hemicelluloses. The xylans have backbone of β-(1→4)-glycosidic linked xylose units and some of the xylose molecules have α-(1→2)-bonded 4-*O*-methylglucuronic acids. The xyloses also contain acetyl groups. In softwoods, xylose molecules are connected to arabinose side chains are connected to the xylose molecules by α-(1→3)-glycosidic bonds. Corncobs having a high xylan content are highly concentrated in xylans. Hardwoods have mannose and glucose units liked by β-(1→4)-glycosidic bonds. Acetyl and galactose groups are connected to glucose–mannose backbone structure in softwoods. A summary of hemicelluloses composition in hardwoods (deciduous trees) and in softwoods (coniferous trees) is given in Table 1.

Acetyl groups present in hardwood xylans and softwood galactoglucomannans are hydrolyzable by acid at elevated temperatures. The acetic acid released provides the acidity to the reaction media. The presence of uronic acid groups reduces the hydrolysis rate of glycocidic linkages appreciably [9]. Hemicelluloses are biodegraded to monomeric sugars and acetic acid. Xylan is the main carbohydrate found in hemicelluloses and degradation requires the cooperative action of a variety of hydrolytic enzymes. Endo-1,4-β-xylanase generates oligosaccharides from the cleavage of xylan and 1,4-β-xylosidase produces xylose from the xylan oligosaccharides. Hemicellulose biodegradation requires accessory enzymes such as xylan esterases, ferulic and *p*-coumeric esterases, α-l-arabinofuranosidases, and α-4-*O*-methyl glucuronidases to work synergistically on wood xylans and mannans [90, 114].

Table 1 Composition and degree of polymerization (DP) of hemicelluloses [9]

Hardwoods (deciduous trees)				Softwoods (coniferous trees)		
Hemicelluloses	Percentage	DP	Compounds	Percentage	DP	Compounds
Xylans	20–30	100–200	Xylose (Xyl), 4-*O*-methyl-glucuronic acid (Mga), Acetyl gr. (Ac)	5–10	70–130	Xylose (Xyl), 4-*O*-methyl-glucuronic acid (Mga), Acetyl gr. (Ac.)
Mannans	3–5	60–70	Mannose (Man), Glucose (Glu)	20–25	–	Mannose (Man), Glucose (Glu) Galactose (Gal), Acetyl group (Ac)
Galactans	0.5–2	–	Galactose (Gal), Arabinose (Ara), Rhamnose (Rha)	0.5–3	200–300	Galactose (Gal), Arabinose (Ara)

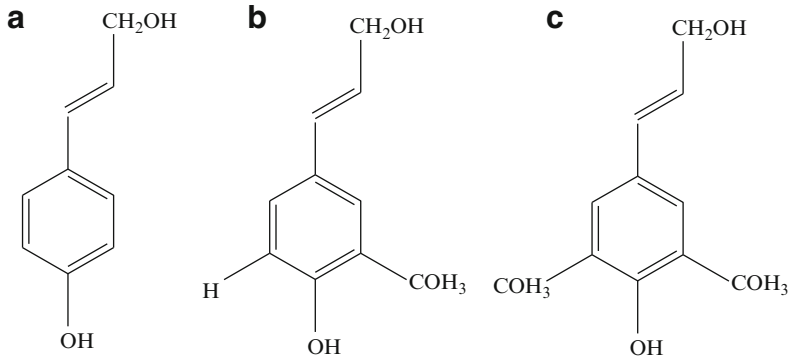

Fig. 5 Lignin monomers (**a**) *trans-p*-coumaryl alcohol, (**b**) coniferyl alcohol, and (**c**) sinapyl alcohol (redrawn from Bobleter) [9]

Lignin: Lignin is a complex aromatic polymer. It is synthesized by the generation of free radicals released during peroxidase-mediated dehydrogenation of three phenylpropionic alcohols: *trans-p*-coumaryl (*p*-hydroxyphenyl propanol), coniferyl alcohol (guaiacyl propanol), and sinapyl alcohol (syringyl propanol). The structures of these lignin monomers are shown in Fig. 5. The polymerization results in a heterogeneous structure whose basic units are linked by C–C and aryl-ether linkages, with aryl-glycerol β-aryl ether being the predominant structure. Lignin is an amorphous heteropolymer, nonwater soluble, and optically inactive [90].

The structural complexity of the lignin and its high molecular weight is the main reason why it is so hard to degrade by enzymes. Lignin content in wood or lignocellulosic varies based on the species type, growing conditions, part of the plant tested, and numerous other factors. Lignin mainly acts as adhesive or binder in wood that provides strength and structure to the cellular composites of the plant and protects against microorganism or chemical attack. It controls the fluid flow, acts as antioxidant by absorbing UV light, and stores energy. When lignin binds, it cross-links with the regular structure of the microfibrils made of cellulose and hemicelluloses [77, 112]. Isolated lignin shows maximum solubility in the solvents such as dioxane, acetone, methyl cellosolve (ethylene glycol monomethyl ether), tetrahydrofuran, dimethyl formaldehyde (DMF), and dimethyl sulfoxide (DMSO).

Carbon–carbon linkages are very resistant to chemical attack, and degradation of lignin is largely limited to the cleavages of ether units at α- and β-positions. Functional groups of lignin follow [3]:

– *Hydrolyzable ether linkages*: β-aryl, α-aryl, and α-alkyl ether linkages are the main hydrolyzable ether units in lignin. Lignin may also contain some α-ether linked l to carbohydrate, which is hydrolyzed at relatively lower rates.
– *Phenolic hydroxyl groups*: It plays an important role in promoting alkali-catalyzed cleavages of interunitary ether linkages, oxidative degradation of lignin, and in lignin modification reactions.
– *Aliphatic hydroxyl groups*: Two major aliphatic hydroxyl groups in lignin are located at the γ- and α-positions of the side chains. Aliphatic hydroxyl group at

α-position is a benzyl alcohol, which is very reactive and plays a dominant role in lignin reactions.
- *Uncondensed Units*: Units at position C2, C3, C5, and C6 are free or substituted by methyl groups are defined as uncondensed units. Hardwood lignin, which contains high syringical units, has high content of uncondensed units.
- *Unsaturated groups*: Lignin contains some unsaturated groups, mainly as coniferyl alcohol and coniferaldehyde end groups.
- *Ester group*: Grass lignins contain significant amount of *p*-coumeric acid and ferulic acid moieties, which are mainly esterified. These functional groups are liable to mild alkali treatment and mainly present at the α-position.
- *Methoxyl groups*: These groups are relatively resistant to both acidic and alkaline hydrolysis.
- *Accessibility*: Lignins have a very high tendency to form hydrogen bonds like hemicelluloses and cellulose.

Lignin empirical formulae are based on ratios of methoxy groups to phenylpropanoid groups (MeO:C_9). The general empirical formula for lignin monomers is $C_9H_{10}O_2$ $(OCH_3)_n$, where *n* is the ratio of MeO to C_9 groups. Where no experimental ratios have been found, they are estimated as follows: 0.94 for softwoods, 1.18 for grasses, 1.4 for hardwoods. These are averages of the lignin ratios found in the literature. Paper products, which are produced primarily from softwoods, are estimated to have a MeO: C_9 ratio of 0.94 (source: National Renewable Energy Laboratory, USA).

Extractives: Extractives are low to moderately high molecular weight compounds, which are soluble in water or organic solvents. They impart color, odor, and taste to the biomass. The composition of extractives varies widely based on the species and class of wood. Some of the important classes of extractives are terpenes, triglycerides, fatty acids, and phenolic compounds [8].

Ash: Ash contains metallic ions of sodium, potassium, calcium, and the corresponding ions of carbonate, phosphate, silicate, sulfate, chloride, etc.

3 Major Conversion Routes for Lignocellulosic Biomass to Biofuels

Lignocellulosic biomass consists of a variety of materials with distinctive physical and chemical characteristics. Typically it is categorized into either woody, herbaceous, or crop residues. Most of these biomass materials are already used, without preliminary conversion, as a fuel for heating purpose and also to produce steam for generating electricity. Direct combustion is best suited to biomass having low contents of moisture and ash. In fact, until the start of twentieth century, biomass and coal were the major sources of fuels and chemicals. The recent energy crisis, fluctuating oil prices, and political factors associated with the import of fossil fuels

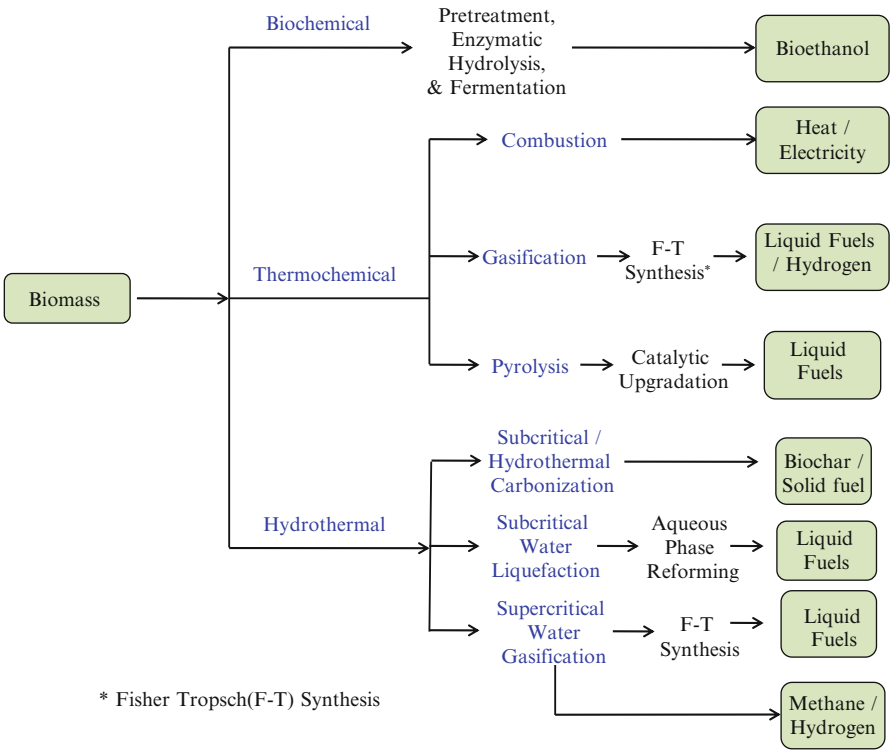

Fig. 6 Major pathways for the conversion of biomass to biofuels

have brought the focus again on the utilization of abundantly available biomass resources for producing easy-to-handle forms of energy such as gases, liquids, and charcoal [56, 134]. Biomass may be converted to energy by many different processes such as biochemical, thermochemical, and hydrothermal pathways depending on the raw characteristics of the material and the type of energy desired (Fig. 6).

Thermochemical processes depend on the relationship between heat and chemical action as a means of extracting and creating products and energy. Pyrolysis, gasification, and liquefaction which are conducted at a temperature of several hundred degrees Celsius are categorized in thermochemical processes. Pyrolysis is defined as the thermal degradation of biomass in the absence of oxygen to produce condensable vapors, gases, and charcoal; in some instances, a small amount of air may be admitted to promote this endothermic process. The products of pyrolysis can be gas, liquid, and/or solid. In flash pyrolysis, biomass is rapidly heated (e.g., at rates of 100–10,000°C/s) to 400–600°C, while limiting the vapor residence time to less than 2 s [4]. The oil production is maximized at the expense of char and gas. Pyrolysis processes typically use dry and finely ground biomass. Pyrolysis and direct liquefaction processes are sometimes confused with each other, and a simplified comparison of the two follows. Both are thermochemical processes in which feedstock organic compounds are converted into liquid products. In the case

of liquefaction, feedstock macromolecules are decomposed into fragments of light molecules in the presence of a suitable catalyst. At the same time, these fragments, which are unstable and reactive, repolymerize into oily compounds having appropriate molecular weights [19]. With pyrolysis, on the other hand, a catalyst is usually unnecessary, and the light decomposed fragments are converted to oily compounds through homogeneous reactions in the gas phase.

In gasification, oxygen-deficient thermal decomposition of organic matter primarily produces synthesis gas. Gasification can be thought of as a combination of pyrolysis and combustion. Gasification has a good potential for near-term commercial application due to the benefits over combustion including more flexibility in terms of energy applications, higher economical and thermodynamic efficiency at smaller scales, and potentially lower environmental impact when combined with gas cleaning and refining technologies. An efficient gasifier decomposes high molecular weight organic compounds released during pyrolysis into low molecular weight noncondensable compounds in a process referred to as tar cracking. Undesirable char that is produced during gasification participates in a series of endothermic reactions at temperatures above 800°C which converts carbon into a gaseous fuel. Typically gaseous products include: CO, H_2, and CH_4. Fisher–Tropsch synthesis can be used to convert the gaseous products into liquid fuels through the use of catalysts. Gasification and pyrolysis both requires feedstock that contains less than 10% moisture [49, 85].

Biochemical processes takes place at ambient to slightly higher temperature levels using a biological catalyst to bring out the desired chemical transformation. Bioethanol from lignocellulosic biomass is produced mainly via biochemical routes. The biomass is first pretreated by different pretreatment methods (discussed later) for the improving the accessibility of enzymes. After the pretreatment, biomass goes through the enzymatic hydrolysis for conversion of polysaccharides into monomeric sugars such as glucose, xylose, etc. Subsequently, sugars are fermented to ethanol by the use of different microorganisms using the process called simultaneous saccharification and co-fermentation (SSCF) [33].

4 Supercritical Fluid Technology

The unique physicochemical properties of dense supercritical fluids provide an attractive medium for chemical reactions and other processes. Fluids near critical points have solvent power comparable to that of liquids and are much more compressible than dilute gases. The transport properties of such fluids lie intermediate between gas- and liquid-like. Supercritical fluids are attracting much attention in various fields of science and technology. In the last decades, the number of applications has increased continuously in several areas such as:

- Supercritical water and carbon dioxide as alternative solvents
- Supercritical fluid extraction and purification
- Fine particle production by supercritical antisolvent (SAS) and rapid expansion of supercritical solutions (RESS)

– Supercritical fluid chromatography for analytical applications
– Supercritical steam cycle technology for power plants

Supercritical fluids can be advantageously exploited in environmentally benign separation and reaction processes, as well as for new kinds of materials processing. Although laboratory scale studies show excellent results, there are relatively few processes in industrial scale. The high pressure processes are generally expensive to design, build, operate, and maintain. Therefore, scaling up from laboratory to industrial scale of such processes can only be successful if clear benefits can be achieved in terms of high efficiency, conversion ratios, product quality, and cost advantages over the conventional processes [25, 104, 128].

4.1 Sub- and Supercritical Water

Water is an ecologically safe and abundantly available solvent in nature. Water has a relatively high critical point (374°C and 22.1 MPa) because of the strong interaction between the molecules due to strong hydrogen bond. Liquid water below the critical point is referred as subcritical water whereas water above the critical point is called supercritical water. Density and dielectric constant of the water medium play major role in solubilizing different compounds. Water at ambient conditions (25°C and 0.1 MPa) is good solvent for electrolytes because of its high dielectric constant 78.5), whereas most organic matters are poorly soluble under these conditions.

As water is heated, the H-bonding starts weakening, allowing dissociation of water into acidic hydronium ions (H_3O^+) and basic hydroxide ions (OH^-). Structure of water changes significantly near the critical point because of the breakage of infinite network of hydrogen bonds and water exists as separate clusters with a chain structure [52]. In fact, dielectric constant of water decreases considerably near the critical point, which causes a change in the dynamic viscosity and also increases self-diffusion coefficient of water [71].

Supercritical water has liquid-like density and gas-like transport properties, and behaves very differently than it does at room temperature. For example, it is highly nonpolar, permitting complete solubilization of most organic compounds and oxygen. The resulting single-phase mixture does not have many of the conventional transport limitations that are encountered in multiphase reactors. However, the polar species present, such as inorganic salts, are no longer soluble and start precipitating. The physicochemical properties of water, such as viscosity, ion product, density, and heat capacity, also change dramatically in the supercritical region with only a small change in the temperature or pressure, resulting in a substantial increase in the rates of chemical reactions. It is interesting to see (Fig. 7) that the dielectric behavior of 200°C water is similar to that of ambient methanol, 300°C water is similar to ambient acetone, 370°C water is similar to methylene chloride, and 50°C water is similar to ambient hexane.

In addition to the unusual dielectric behavior, transport properties of water are significantly different than the ambient water as presented in Table 2.

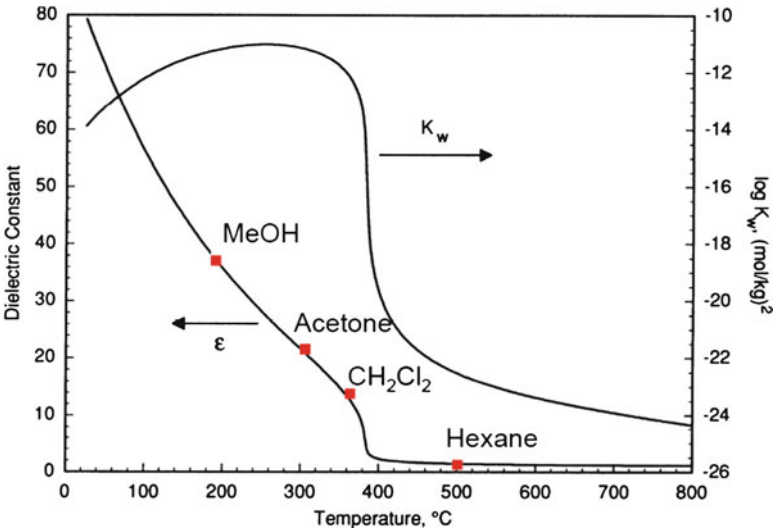

Fig. 7 Physical properties of water with temperature at 24 MPa [59]

Table 2 Comparison of ambient and supercritical water

	Ambient water	Supercritical water
Dielectric constant	78	<5
Solubility of organic compounds	Very low	Fully miscible
Solubility of oxygen	6 ppm	Fully miscible
Solubility of inorganic compounds	Very high	~0
Diffusivity ($cm^2\ s^{-1}$)	10^{-5}	10^{-3}
Viscosity ($gcm^{-1}\ s^{-1}$)	10^{-2}	10^{-4}
Density ($g\ cm^{-3}$)	1	0.2–0.9

5 Sub- and Supercritical Water Technology for Biofuels

The use of sub- and supercritical water media also known as hydrothermal media, which can be broadly defined as water-rich phase above 200°C, offers several advantages over the other biofuels production methods [94]. Some of the major benefits are

- Ability to wet biomass
- Can use mixed feedstock or waste biomass from other process residues
- High energy and separation efficiency (since water remains in liquid phase and the phase change is avoided)
- High throughputs
- Versatility of chemistry (solid, liquid, and gaseous fuels)
- Reduced mass transfer resistance
- Improved selectivity for the desired energy products (methane, hydrogen, liquid fuel) or biochemicals (sugars, furfural, organic acids, etc.)

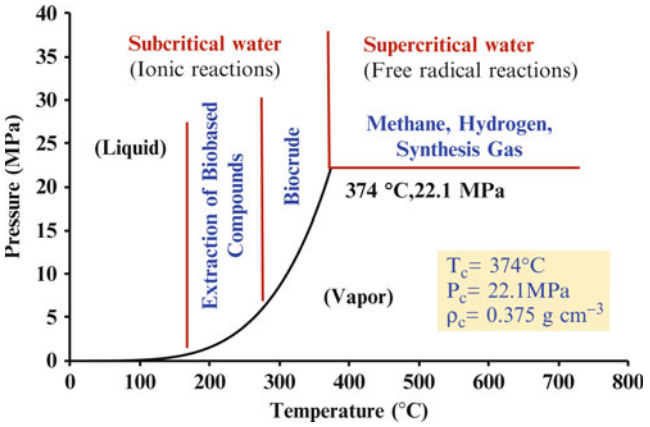

Fig. 8 Application referenced to pressure–temperature phase diagram of water

– No need to maintain specialized microbial cultures
– Products are completely sterilized with respect to any pathogens including biotoxins, bacteria, or viruses
– Processing of postfermentation residues

Since the process is conducted in liquid/water-rich phase, the energy required for phase change of water from liquid to vapor is avoided. This provides an opportunity to reduce the requirement of process heat compared to steam-based processes. As an example, we know that 2.869 MJ/kg of energy is required to convert ambient water from 25°C to steam at 250°C and 0.1 MPa whereas only 0.976 MJ/kg of energy is required to convert ambient water from 25°C to subcritical water at 250°C and 5 MPa. This energy need for heating water to subcritical condition (0.976 MJ/kg) is equivalent to 6–8% of energy contained in dry biomass. Generally, the higher heating value of dry biomass is in the range of 16–19 MJ/kg. This also means that the energy contained in the subcritical water is insufficient to vaporize the water on decompression. Further, it is possible to recover much of the heat from subcritical water. The technology can be applied to produce solid (biochar), liquid (bioethanol, biocrude/bio-oil), and gaseous (methane, hydrogen) fuels from biomass depending on the processing temperature and pressure as shown in Fig. 8.

The substantial changes in the physical and chemical properties of water in the vicinity of its critical point can be utilized advantageously for converting lignocellulosic biomass to desired biofuels [22, 94]. In fact, reactions in subcritical and supercritical water also provide a novel medium to conduct tunable reactions for the synthesis of specialty chemicals from biomass [76].

In the subcritical region, the ionization constant (K_w) of water increases with temperature and is about three orders of magnitude higher than that of ambient water (Fig. 7) and the dielectric constant (ε) of water drops from 80 to 20 [118].

A low dielectric constant allows subcritical water to dissolve organic compounds, while a high ionization constant allows subcritical water to provide an acidic

medium for the hydrolysis reactions. These ionic reactions can be dominant because of the liquid-like properties of subcritical water. Moreover, the physical properties of water, such as viscosity, density, dielectric constant, and ionic product, can be tuned by small changes in pressure and/or temperature in subcritical region [31, 79, 103]. In the supercritical region, density of water drops down to lower value. This means that ionic product of water is much lower and ionic reactions are inhibited because of the low relative dielectric constant of water. The lower density favors free-radical reactions, which may be favorable for gasification [61].

5.1 Reaction Pathways of Cellulose, Hemicelluloses, and Lignin in Hydrothermal Medium

Lignocellulosic biomass is a mixture of cellulose, hemicelluloses, and lignin which are held together by covalent bonding, various intermolecular bridges, and van der Waals forces forming a complex structure. Several studies have been conducted using model compounds such as cellulose, hemicelluloses, and lignin in sub- and supercritical water to establish the reaction pathways of these compounds in hydrothermal medium. The chemistry behind the reactions of the individual components of biomass under hydrothermal conditions is well understood. The generalized individual reaction pathways of the major components of biomass (cellulose, hemicelluloses, and lignin) are discussed in the following section.

5.2 Cellulose Reaction Pathways

Hydrothermal degradation of cellulose is a heterogeneous and pseudo-first-order reaction for which detailed chemistry and mechanism have been proposed earlier [9, 80, 81, 107]. Cellulose reaction in hydrothermal and catalyst free medium mainly proceeds via hydrolysis of glycosidic linkages. The long chain of cellulose starts breaking down in such condition to smaller molecular weight water soluble compounds (oligomers) and further to glucose (monomer). Glucose is water soluble and undergoes rapid degradation in hydrothermal medium at elevated temperature. The key products from the glucose decomposition are shown in Fig. 9. These products are formed mainly via dehydration, isomerization, reverse aldol condensation, and fragmentation reactions.

Hydrolysis of cellulose in supercritical water is very sensitive to residence time. A high residence time enhances the formation of organic acids such as acetic acid, formic acid, and lactic acid. Formation of acids makes the reaction medium more acidic, which is conducive for further degradation of hydrolysis products. Indeed after hydrolysis of cellulose in water at 320°C and 25 MPa for 9.9 s, more than half of the cellulose was converted to organic acids [100]. The solid cellulose-like

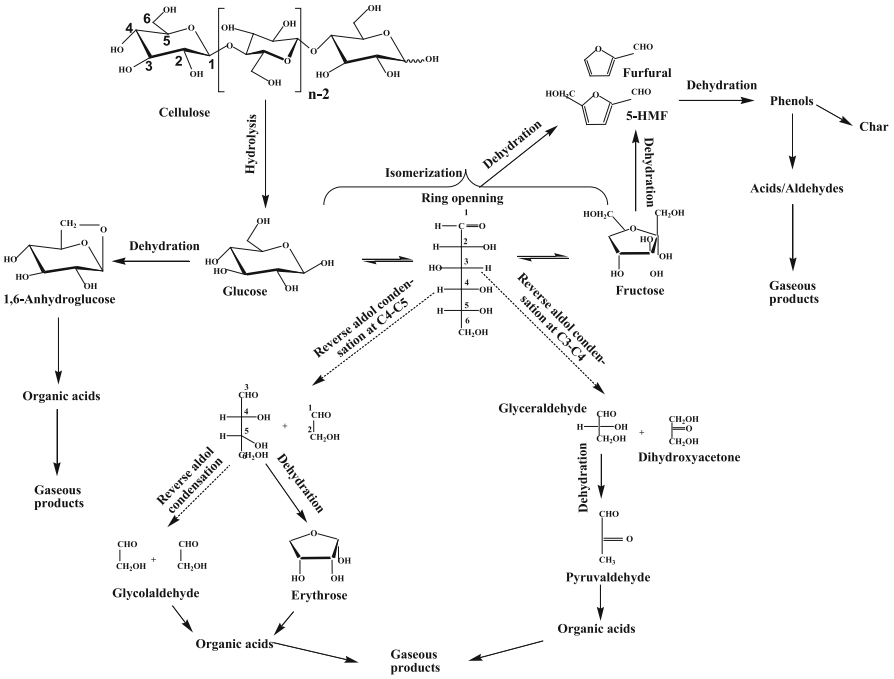

Fig. 9 Key reaction products from cellulose hydrolysis in catalyst free hydrothermal medium [50, 94, 101, 125]

residues have been inevitably observed because of the rapid change in the polarity of water in going from reaction condition to room temperature. These residues have been reported to have a lower viscosity-average degree of polymerization (DP_v) with no significant change in crystallinity as compared to untreated cellulose [63].

5.3 Hemicelluloses Reaction Pathways

Hemicelluloses are polysaccharides of five carbon sugars such as xylose or six carbon sugars other than glucose. They are usually branched and have much lower degree of polymerization. Branches in the chains do not allow the formation of tightly packed fibrils. Hemicelluloses are not crystalline and easily hydrolyzable to their respective monomers. In fact, about 95% of hemicelluloses were extracted as monomeric sugars using water at 34.5 MPa and 200–230°C in a span of just few minutes [80]. In hydrothermal medium, hemicelluloses are hydrolyzed to sugars, which subsequently degrade into furfural and other degradation compounds. Furfural (2-furaldehyde) is commercially produced from hemicelluloses-derived xylose [94].

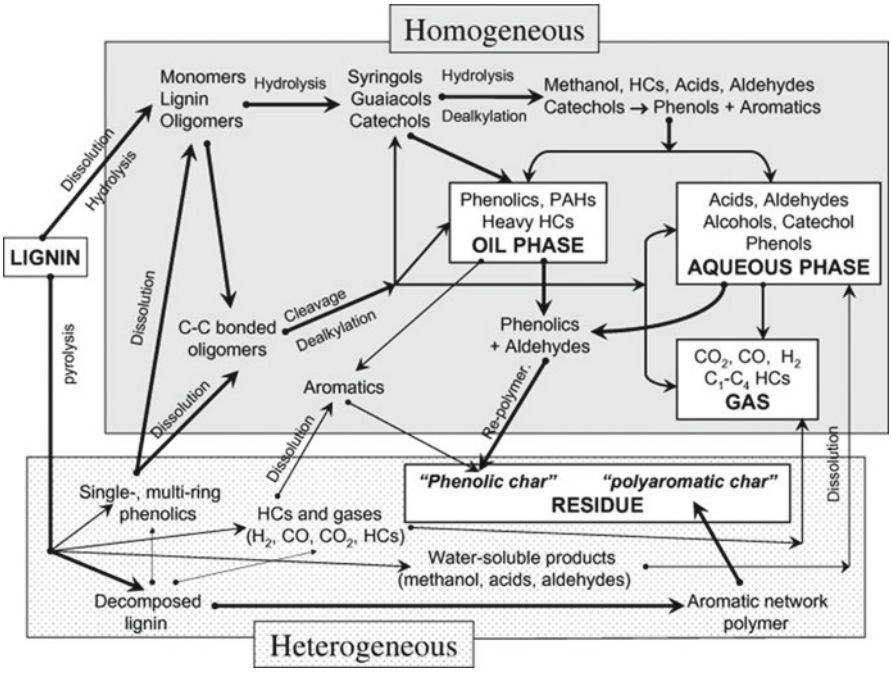

Fig. 10 Reaction pathway of lignin in supercritical water (reproduced from [29])

5.4 Lignin Reaction Pathways

Lignin is a complex and high molecular weight polymer of phenylpropane derivatives (*p*-coumaryl alcohol, coniferyl alcohol, and sinapyl alcohol). The density of hydrothermal medium is found to be a key parameter in lignin decomposition. In hydrothermal reaction medium, most of the hemicelluloses and part of the lignin are solubilized below 200°C. Lignin fragments have high chemical reactivity. Part of these fragments again cross-links and re-condenses to form high molecular weight water insoluble products [9]. Recently, Fang et al. have proposed the reaction pathway (Fig. 10) for lignin in supercritical water [29].

The reaction steps consist of four phases: oil phase, aqueous phase, gas phase, and a solid residue phase [6, 29]. Their study concluded that lignin can be completely dissolved and undergoes homogeneous hydrolysis and pyrolysis preventing further re-polymerization.

The following sections discuss about application of sub- and supercritical water/hydrothermal medium's properties for bioethanol, biocrude, biochar, and gaseous fuels production.

6 Subcritical Water/Hydrothermal Pretreatment of Biomass for Bioethanol Production

Lignocellulosic biomass has emerged as a potential renewable biomass resource for the bioethanol production [92, 117]. The concept is to hydrolyze the cellulose and hemicelluloses fraction of biomass (holocellulose) to recover C_5 and C_6 sugars and then ferment the sugars to bioethanol [93]. The recovered lignin in the process which has relatively higher heating value in the range of 24–26 MJ/kg is typically used for generating steam or providing the process heat. The biochemical pathways which can be realized at a very moderate process conditions using cellulase and accessory enzymes to convert holocelluloses to fermentable sugars are the most promising ones for large-scale bioethanol production. But the efficiency of this technology is limited due to the complex chemical structure of lignocellulose biomass and the inaccessibility of β-glycosidic linkages to cellulase enzymes because of the low surface area and small size of pores in multicomponent structure. Hence, pretreatment is nowadays viewed as a critical step in lignocellulose processing [66].

Pretreatment alters both the structural barrier (removal of lignin and hemicelluloses) and physical barrier (surface area, crystallinity, pore size distribution, degree of polymerization) which help in improving the accessibility of enzyme for hydrolysis [38, 67, 83]. It enhances the rate of production and the yield of monomeric sugars from biomass. Pretreatment is among the most costly step in the bioethanol conversion process as it may account for up to 40% of the processing cost. Moreover, it also affects the cost of upstream and downstream processes [69, 91, 130, 135]. Hence, an efficient, less energy intensive and cost-effective pretreatment method is a necessity for producing ethanol at an economically viable cost. Different pretreatment methods are broadly classified into physical, chemical, physicochemical, and biological processes. The conventional pretreatment, by using acids or alkalis, is associated with the serious economic and environmental constraints due to the heavy use of chemicals and chemical resistant materials [21, 43, 115].

Hydrothermal pretreatment employing subcritical water has attracted much attention because of its suitability as a nontoxic, environmentally benign and inexpensive media for chemical reactions [63, 76]. One of the most important benefits of using water instead of acid as pretreatment media is that there is no need of acid recovery process and related solid disposal and handling cost [21, 51]. Below the critical point, the ionization constant of water increases with temperature and is about three orders of magnitude higher than that of ambient water. Also, the dielectric constant of water decreases with temperature. A low dielectric constant allows liquid water to dissolve organic compounds, while a high ionization constant provides an acidic medium for the hydrolysis of biomass components via the cleavage of ether and ester bonds and favor the hydrolysis of hemicelluloses [31, 65, 79, 103]. The structural alterations due to the removal of hemicelluloses increase the accessibility and enzymatic hydrolysis of cellulose. Enzyme accessibility is increased as a result of the increase in mean pore size of the substrate which enhances the probability of the hydrolysis of glycosidic linkage [42].

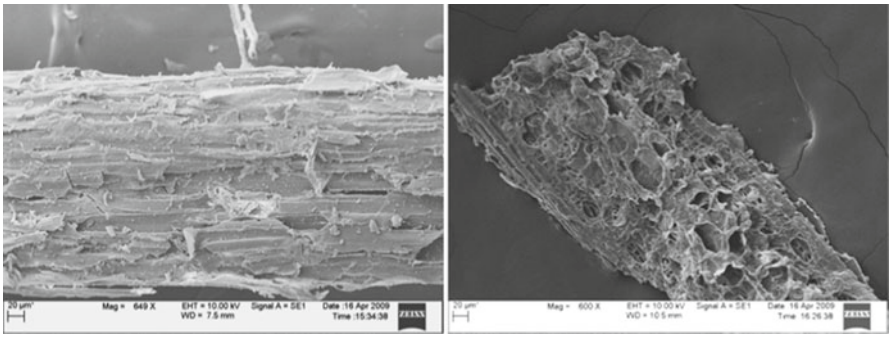

Fig. 11 SEM images of untreated and pretreated switchgrass at 150°C in the presence of 0.9 wt.% of K_2CO_3

Hydrothermal pretreatment is typically conducted in the range of 150–220°C. The temperature range, aiming for the fractionation of hemicelluloses, is decided based on the fact that at temperature below 100°C less/small extent of hydrolytic reaction is observed whereas cellulose hydrolysis and degradation become significant above 210°C [32, 41]. The severity factor (R_0) has been used by several researchers to measure the combined effect of temperature and residence time in hot water treatment of biomass processes [1, 88, 96]. The severity index is defined as

$$R_0 = t \times \exp\left\{\frac{T-100}{14.75}\right\}$$

where t is the residence time in minutes and T is temperature in °C.

Ether bonds of the hemicelluloses are most susceptible to breakage by the hydronium ions. Depending on the operational conditions, hemicelluloses are depolymerized to oligosaccharides and monomers, and the xylose recovery from biomass can be as high as 88–98%. For example, Suryawati et al. have reported 90% removal of hemicelluloses from Kanlow switchgrass at 200°C [116]. Acetic acid is also generated from the splitting of thermally labile acetyl groups of hemicelluloses. In further reactions, the hydronium ions generated from the autoionization of acetic acid also acts as catalyst and promotes the degradation of solubilized sugars. In fact, the formation of hydronium ions from acetic acid is much more than from water [32, 41].

The low pH (< 3) of the medium causes the precipitation of solubilized lignin and also catalyzes the degradation of hemicelluloses. To avoid the formation of inhibitors, the pH should be kept between 4 and 7 during the pretreatment. This pH range minimizes the formation of monosaccharides, and therefore the formations of degradation products that can further catalyze hydrolysis of the cellulosic material during pretreatment [10, 41, 58, 67, 82, 110, 128]. Maintaining the pH near neutral (5–7) helps in avoiding the formation of fermentation inhibitors during the pretreatment. The addition of small amount of K_2CO_3 increases the glucan digestibility even at low pretreatment temperatures (150–175°C) [66]. Figure 11 shows the SEM images

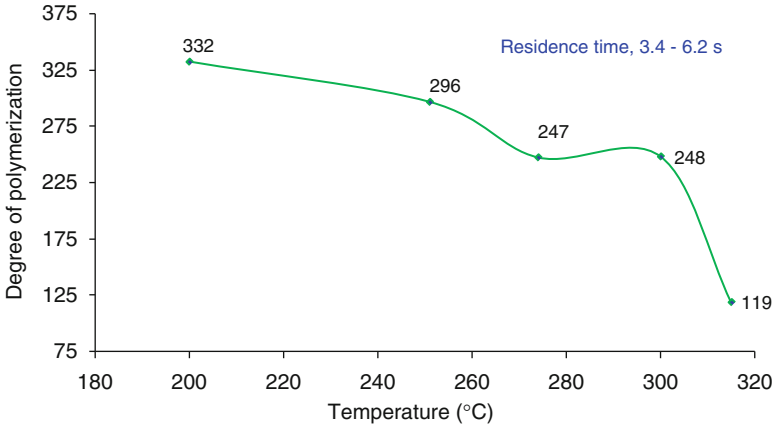

Fig. 12 Degree of polymerization (DP_v) vs. pretreatment temperature for microcrystalline cellulose(MCC) in subcritical water [63]

of untreated and hydrothermally pretreated switchgrass in a flow-through reactor where additional pores created after the pretreatment can be seen [62].

In general, the concentrations of solubilized products are lower in hydrothermal pretreatment compared to the steam pretreatment [9]. Since the hot compressed water is used instead of steam, the latent heat of evaporation is saved which makes it easier to apply for a continuous process [57]. Yang and Wyman have reported that flow-through process fractionated more hemicelluloses and lignin from corn stover as compared to batch system under the conditions of similar severity [132]. In a flow-through system, the product is continuously removed from the reactor which reduces the risk on condensation and precipitation of lignin components, making the biomass less digestible. The soluble lignin compounds are very reactive at the pretreatment temperature and if not removed rapidly part of these compounds recondense and precipitate on the biomass [68, 96].

In a subcritical water pretreatment study, the microcrystalline cellulose (MCC) pretreated at 315°C in a continuous flow reactor for about 4 s of residence time showed nearly threefold increase in the initial enzymatic reactivity as compared to the untreated MCC at 3.5 FPU/g of glucan enzyme loading [63]. The percentage crystallinity of MCC slightly increased after the subcritical water pretreatment and remained high (>81%) throughout the treatment range (200–315°C). Increase in percentage crystallinity is generally attributed to the hydrolysis and removal of the amorphous part of cellulose during pretreatment [63]. The DP_v of cellulose reduced with the pretreatment temperature and sharp decline was observed in cellulose samples pretreated at 315°C (Fig. 12). The DP_v of untreated MCC was 327. It decreased with temperature as expected, but reduced rapidly for treatment above 300°C.

7 Subcritical Water/Hydrothermal Liquefaction for Biocrude Production

Biocrude is defined as an aqueous carbohydrate solution (oxygenated hydrocarbon) produced from the liquefaction of biomass. Biocrude derived from the direct liquefaction of biomass can be converted to liquid fuel, hydrogen gas, or chemicals. Aqueous phase reforming processes have been successfully utilized for converting the biomass-derived, water-soluble carbohydrates to liquid alkanes and hydrogen [45, 46, 121]. Preliminary studies on the conversion of various biomass types into liquid fuels have indicated that hydrothermal liquefaction can be more attractive than pyrolysis or gasification. In these studies, typically 25% biomass slurry in water is treated at temperatures of 300–350°C and 12–18 MPa pressures for 5–20 min to yield a mixture of liquid, gas (mainly CO_2), and water. The liquid is a mixture with a wide molecular weight distribution and consists of various kinds of molecules. A large proportion of the oxygen is removed as carbon dioxide and the resulting biocrude contains only 10–13% oxygen, as compared to 40% in the dried biomass [35]. Hydrothermal upgrading (HTU) process was first developed by Shell, where biomass was subjected to subcritical water at 330°C to produce biocrude. Biocrude was further upgraded to liquid fuels via hydrodeoxygenation process [35]. In a conceptual process scheme, it was shown that each ton (dry basis) of biomass can produce 300 kg (or 95 gal) of liquid fuel.

Karagoez et al. investigated the distribution of products from hydrothermal liquefaction (280°C for 15 min) when wood (sawdust), nonwood biomass (rice husk), and model biomass components (e.g. lignin, cellulose) are used as feedstock. The produced bio-oil was characterized for their differences in the hydrocarbon compositions with respect to feedstock. Cellulose showed the highest conversion among the four samples investigated. Sawdust and rice husk had almost similar conversions. Liquid products were recovered with various solvents (ether, acetone, and ethyl acetate) and analyzed by GC–MS. The oil (ether extract) from the hydrothermal treatment of cellulose consisted of furan derivatives whereas lignin-derived oil contained phenolic compounds. The composition of oils (ether extract) from sawdust and rice husk contained both phenolic compounds and furans; however, phenolic compounds were dominant. Rice-husk-derived oil consists of more benzenediols than sawdust-derived oil. The volatility distribution of oxygenated hydrocarbons was carried out by C-NP gram and it showed that the majority of oxygenated hydrocarbons from sawdust, rice husk, and lignin were distributed at n-C_{11}, whereas they were distributed at n-C_8 and n-C_{10} in cellulose-derived oil. The gaseous products were carbon dioxide, carbon monoxide, methane in sawdust, rice husk, lignin, and cellulose [53, 54].

Liquefaction of biomass in subcritical water proceeds through a series of structural and chemical transformations involving [16]

- Solvolysis of biomass resulting in micellar-like structure
- Depolymerization of cellulose, hemicelluloses, and lignin
- Chemical and thermal decomposition of monomers to smaller molecules

Table 3 Some of the identified compounds in biocrude produced from switchgrass (>85% of confidence level) [65]

No.	GC retention time (min)	Compound	Area (%)	Quality (%)
1	9.0	Furfural	10.5	86
2	21.0	1,2-Benzenediol	3.8	94
3	21.6	2,3-Dihydrobenzofuran	2.6	86
4	21.9	2-Furancarboxaldehyde	30.2	94
5	24.3	2-Methoxy-4-vinylphenol	2.3	93
6	24.9	1,4-Benzenediol, 2-methyl-	2.1	96
7	25.3	Phenol, 2, 6-dimethoxy-	1.5	96
8	25.4	Benzaldehyde, 4-hydroxy-	1.4	95
9	26.5	Vanillin	3.0	97
10	29.7	Homovanillyl alcohol	1.0	87
11	32.6	Benzaldehyde, 4-hydroxy-3, 5-dimethoxy-	1.0	91

Demirbas has also reviewed the possible mechanism of liquefaction. Organic materials are converted to liquefied products through a series of physical and chemical changes such as solvolysis, depolymerization, dehydration, and decarboxylation. Solvolysis is a type of nucleophilic substitution where the nucleophile is a solvent molecule. This reaction results in micellar-like substructures of the feedstock. Depolymerization reactions lead to smaller molecules. Decarboxylation and dehydration lead to new molecules and the formation of carbon dioxide through splitting off of carboxyl groups [19].

Switchgrass was effectively liquefied to produce biocrude in subcritical water in a flow-through reactor. Biocrude composed of aqueous phase (water-soluble compound) and solid precipitates. The aqueous phase contained oligomers and monomers of five and six carbon sugars, degradation products (5-HMF and furfural), organic acids (lactic, formic, and acetic acid), 2-furancarboxaldehyde, and other phenolic products containing 5–9 carbon atoms. A small amount of potassium carbonate catalyzed the liquefaction and enhanced the decomposition of biomass to water-soluble products. The residual solid contained mainly lignin fractions. Based on the infrared spectroscopy and electron microscopy, it was confirmed that subcritical water treatment lead to a breakdown of lignocellulosic structure. Some of the identified compounds by GC–MS analysis (> 85% of confidence level) in biocrude from switchgrass liquefaction are given in Table 3.

Hydrolysis of cellulose in hydrothermal medium has been studied extensively. Several research studies have shown that subcritical and supercritical water can be used under a variety of conditions to rapidly (order of seconds) liquefy cellulose to sugar and its degradation products [18, 76, 102]. Hemicelluloses, an amorphous fraction of lignocellulosic have been successfully extracted up to 95% of its fraction as monomeric sugar and sugar products in hydrothermal medium in the range of 200–230°C in a very short reaction time [9, 80]. Low activation energy of lignin causes substantial degradation of lignin in hydrothermal medium at temperature

below 200°C. Reaction proceeds through the cleavage of aryl ether linkages, fragmentation, and dissolution [9]. Lignin depolymerization yields low molecular weight fragments having very reactive functional groups such as syringols, guaiacols, catechols, and phenols [29]. The density of water within the hydrothermal medium has been found to be a key parameter in deciding the product pathways [94].

The results of liquefaction studies on model compounds and the actual biomass in hydrothermal medium provides an opportunity for converting biomass to biocrude and other important chemicals. The hydrothermal medium (subcritical water) in the range of 250–350°C regions provides a favorable condition for conducting ionic reactions. In general, hydrothermal liquefaction conditions range from 250 to 380°C, 7–30 MPa with liquid water present, often in presence of alkaline catalyst [94]. Crystalline cellulose was successfully converted to monomers (mainly glucose) and oligomers by hydrolysis in subcritical water in a continuous flow reactor. More than 90% of the cellulose converts to water-soluble products above 330°C. The study showed that a high yield of hydrolysis products can be achieved at comparatively lower temperature (335°C) in subcritical water. For example, up to 66.8% of crystalline cellulose was converted to hydrolysis products at 335°C and 27.6 MPa in merely 4.7 s reaction time. With increase in the reaction time, the hydrolysis products degraded to glycoaldehyde, fructose, 1,3 dihydroxyacetone, anhydroglucose, 5-HMF, and furfural. Yield of glycoaldehyde, a retro-aldol condensation product of glucose, increased with a decrease in the density of supercritical water, and the yield of degradation products, 5-HMF and organic acids, increased with temperature and residence time. In supercritical water conditions, more than 80% of the cellulose converted into the degradation products (oxygenated hydrocarbons) and organic acids [64].

8 Hydrothermal Carbonization for Biochar Production

Biochar is the carbon rich, high energy density solid product resulting from the advanced thermal degradation of organic materials such as wood, manure, agricultural residues, etc. The less fibrous structure and high calorific value of biochar similar to that of coal makes it an excellent candidate for solid fuel. Table 4 compares some of the advantages of biochar as solid fuels over the raw biomass.

Biochar is resistant to decomposition upon land application and has a number of positive effects relating to soil fertility [10]. Pyrolysis and hydrothermal carbonization

Table 4 Comparison of biomass and biochar as solid fuel

Biomass	Biochar
High moisture retention	Low moisture retention and easily dried
Low heating value, so high transportation cost	High heating value, so less ($)/MJ cost during transportation
Perishable on storage	Not perishable and can be stored longer
Fibrous and so, difficult material handling	Friable, easier to compact and handle
Poor compatibility with coal for co-firing	Better compatibility with coal for co-firing

(HTC) are the two main processes for the production of biochar. Pyrolysis typically utilizes high quality dry biomass for biochar production where air pollution is primary concern during traditional pyrolysis operation due to the emission of volatile compounds. The HTC is an environment friendly and promising process that uses water as solvent. Besides being relatively simple process, HTC has a number of other practical advantages. The HTC process does not require dry biomass and also the final product can be easily filtered from the reaction solution. This way, complicated drying schemes and costly separation procedures are conceptually avoided.

The biomass feedstock typically contains 40–60% oxygen. Therefore, the removal of oxygen from biomass is the major objective for upgrading its energy density during biochar production. This objective can be accomplished by the removal of oxygen by dehydration, which removes oxygen in the form of water, and by decarboxylation, which removes oxygen in the form of carbon dioxide. Thermodynamically, water is fully oxidized compound and has no residual heating value. Therefore, water makes an ideal medium for conducting such reactions. Even in the excess of water, biomass undergoes dehydration reaction at elevated temperature and pressure [94]. Due to the increased ionization of water at elevated temperature, the biomass components undergo depolymerization mainly by hydrolysis reactions. The subcritical water in the temperature region of 180–250°C can effectively be utilized for the production of biochar from biomass [62]. The longer reaction time of the order of several hours is typically needed for the substantial removal of oxygen by dehydration and for the subsequent breakdown of the fibrous structure of biomass. The dehydration of biomass at lower temperature can be accelerated by the addition of small amount of acids.

In nature, coal is formed from plant material undergoing heat and pressure treatment over millions of years. The acceleration of coalification of biomass by a factor of 10^6–10^9 in hydrothermal medium under milder process conditions can be a considerable and technically attractive alternative for biochar production [120]. Essentially, all forms of biomass can be converted to biochar. Forest thinning, herbaceous grasses, crop residues, manure, and paper sludge are some of the potentially attractive feedstock. The enhanced transportation and solubilization properties of sub- and supercritical water (hydrothermal medium) play an important role in the transformation of biomass to high energy density fuels and functional materials [44]. Here, water acts as reactant as well as reaction medium which help in performing hydrolysis, depolymerization, dehydration, and decarboxylation reactions. The proton-catalyzed mechanism, direct nucleophilic attack mechanism, hydroxide-ion-catalyzed mechanism, and the radical mechanism play important roles in the conversion of biomass in hydrothermal medium [73, 95]. Under the umbrella of hydrothermal process, the conversion of a variety of biomass to chemicals, including organic monomer, biofuel, hydrogen, and biochar, has been studied widely. Through hydrothermal carbonization, a carbon-rich black solid as insoluble product is obtained from biomass in the range of 180–350°C [105, 120].

The earliest research focused on analyzing the changes in O/C and H/C atomic ratio to understand the chemical transformations taking place during HTC [7]. For example, Marta et al. studied the HTC of three different saccharides (glucose,

sucrose, and starch) at temperatures ranging from 170 to 240°C. The result showed that a carbon-rich solid product made up of uniform spherical micrometer-sized particles of diameter 0.4–6 mm range could be synthesized by modifying the reaction conditions. The formation of the carbon-rich solid through the HTC of saccharides was the consequence of dehydration, condensation, polymerization, and aromatization reactions. In a recent study, the same group of researchers used cellulose as starting material and successfully established that highly functionalized carbonaceous materials can be produced by HTC from cellulose in the range of 220–250°C [72]. The formation of this material follows essentially the path of a dehydration process, similar to that previously observed for the hydrothermal transformation of saccharides such as glucose, sucrose, or starch. In another recent study, Titirici et al. compared hydrothermal carbons synthesized from diverse monomeric sugars and their derivatives (5-hydroxymethyl-furfural-1-aldehyde (HMF) and furfural) under hydrothermal conditions at 180°C with respect to their chemical structures. The results showed that type of sugars has an effect on the structure of carbon-rich solids [119].

The traditional method for biochar production from biomass sources is slow pyrolysis, where dry biomass is used for the purpose in the range of 500–800°C. Antal Jr. and coworkers have developed another method for charcoal production which is named as flash carbonization. The process is conducted at elevated pressure by the ignition and control of a flash fire within a packed bed of biomass [122]. Considering the relatively high energy consumption needed in the pyrolysis process, HTC process which is typically conducted in subcritical water below 300°C might be an economical and efficient option for biochar production. The process is particularly important since it can utilize the wet biomass. Switchgrass was converted to biochar by HTC at 200–280°C. Compared with the reaction time and pressure, the temperature plays an important role in the conversion. With increase in temperature, biochar yield decreased but the heating value increased. The HHV of biochar produced at 280°C in just 1 h of HTC was comparable to the bituminous grade coal [62]. In October 2010, AVA-CO2, ZUG, Switzerland & KARLSRUHE launched the world's first industrial-size HTC plant. With an overall capacity of 14,400 L and an annual capacity to process 8,400 tons of biomass, the HTC reactor demonstrates an impressive way that the experts from AVA-CO2 have succeeded in constructing and operating a plant of industrial size.

9 Carbon-Rich Microspheres from Sugars in Subcritical Water

Carbon-rich microspheres can be formed by the HTC of sugar solution if treated for several minutes to hours at 180–200°C. Titirici et al. had studied the HTC of carbohydrate model compounds such as glucose and xylose. Their study reported the elemental carbon in the microsphere as 64 and 68% from glucose and xylose, respectively [119]. HTC of sugars is a potential alternative to produce uniform carbon-rich microspheres [120]. Kumar et al. studied the HTC of glucose solution to produce the carbon microspheres from soluble organic compounds (Fig. 13). The precipitated solids were globular with their diameter ranging from 0.2 to 2 μm and

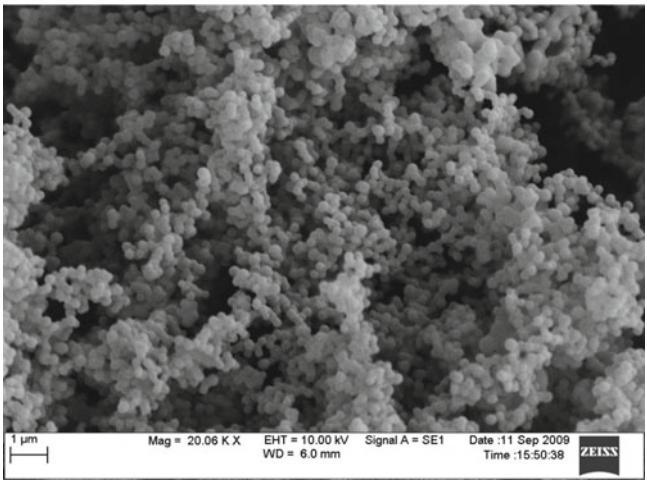

Fig. 13 SEM images of carbon microspheres produced via hydrothermal carbonization (HTC) from glucose solution at 200°C for 2 h [66]

having a higher heating value (HHV) of 24.8 MJ/kg which is comparable to lignin's HHV (24–26 MJ/kg) [62]. Glucose in hydrothermal medium at relatively low temperature (180–200°C) range and longer residence time (order of few hours) undergoes mainly dehydration and partial fragmentation (C–C bond breaking) reactions.

The intermediate compounds are mainly furan-like compounds, organic acids, and aldehydes [55]. Furan-like ring compounds may undergo polymerization via aldol condensation to form soluble polymers. Aromatization of soluble polymers takes place under the reaction condition and when the aromatic clusters in aqueous solution reach the critical supersaturation point, they precipitate as carbon-rich microspheres. The process can be a novel tool for recovering the water-soluble oxygenated hydrocarbons as high heating value carbon-rich microspheres. The yield of these microspheres depends on the sugar contents in liquid solution subjected to HTC. Majority of sugar compounds present in the liquid undergoes polycondensation and dehydration processes resulting in carbon-rich microspheres.

10 Supercritical Water/Hydrothermal Gasification

Gasification of biomass into fuel gases, such as synthesis gas or producer gas, is a promising route to produce renewable fuels, which is commonly accomplished via partial oxidation of the feedstock using sub-stoichiometric air or oxygen or by indirect heating with or without steam. Typically, gasification is performed using relatively dry feedstock with moisture < 10 wt.% at 700–1,000°C and near ambient pressures. The synthesis gas or "syngas" can be utilized to produce liquid fuels by Fischer–Tropsch synthesis. Supercritical water gasification is a novel method to process organic matter from biomass [26]. Relatively fast hydrolysis of biomass in supercritical

water leads to a rapid degradation of polymeric structure of biomass. The subsequent reactions also are rather fast, which leads to gas formation at relatively lower temperature compared to dry processes [60]. Above the critical point, the lower density of supercritical fluid favors free radical reactions and makes the reaction conditions conducive for the formation of methane and hydrogen gas [61]. There are two types of SCWG operations: (a) low temperature ranging from 350 to 600°C in the presence of metal catalysts, and (b) high temperature ranging from 500 to 750°C without catalyst or using nonmetallic catalysts [74]. For hydrogen formation from biomass, Watanabe et al. [126] used Zirconia (ZrO_2) to catalyze the reaction while Elliott et al. [27] and Byrd et al. [11] demonstrated the significant activity of Ru, Rh, and Ni as catalysts. Biomass is gasified to mainly methane and carbon dioxide in the presence of an added heterogeneous catalyst in near critical or supercritical water (350–400°C). At higher temperature in supercritical water, biomass is converted to hydrogen-rich gas without catalyst or with nonmetal catalysts [26]. As discussed earlier, part of lignin and hemicelluloses fraction of biomass undergo solvolysis within few minutes of the exposure to hydrothermal medium. The hydrothermolysis of remaining biomass fractions occurs at somewhat higher temperature. The initial products subsequently undergo a variety of isomerization, dehydration, fragmentation, and condensation reactions that ultimately form gas and tars [74]. There are numerous studies describing supercritical water gasification of cellulosic biomass for methane, hydrogen, or fuel gas production [75, 94]. The Pacific Northwest National Laboratory (PNNL) has extensively studied the catalytic hydrothermal gasification process for several feedstocks in the last 30 years. In a recent feedstock test project, lignin-rich biorefinery residues showed several levels of difficulty such as slow rate of conversion and plugging of feedlines, while algae feedstock were more reliably processed. The gasification was conducted using Ru/C gasification catalyst with a pelletized Raney nickel sulfur scrubbing bed.

The principal advantages of supercritical water for gasification are that process can utilize wet feedstock and can achieve high gasification efficiency at comparatively low temperature (400–700°C). The homogeneous reaction medium with a minimal mass transfer resistance favors decomposition of organic compounds into gases, decreasing formation of tar and char [12]. For example, the highly nonpolar nature of supercritical water permits complete solubilization of most organic compounds. The resulting single-phase mixture does not have many of the conventional transport limitations that are encountered in multiphase reactors. However, the polar species present, such as inorganic salts, are no longer soluble and start precipitating [64]. Due to the different reaction mechanisms, supercritical water exhibits some important inherent advantages over the conventional gasification such as:

- Energy intensive drying of biomass is avoided
- The homogeneous reaction medium
- Easier separation of gaseous products after the reaction
- Requires lower reaction temperature compared to the conventional gasification

Moreover, fuel gas is produced directly at high pressure, which means a smaller reactor volume and lower energy needed to pressurize the gas in a storage tank. The

nonvolatile inorganic constituents of the co-product residue are expected to remain in the aqueous solution. This makes the resulting fuel gas cleaner and less corrosive compared to the conventional dry processes. The presence of alkali salts catalyzes the gasification processes [64]. Due to insolubility of inorganic salts in supercritical water, the alkali salts precipitate out rapidly as fine particles and these in situ-generated particles provide extra surface area for heterogeneous catalysis [84]. The addition of alkali metal salts (e.g., $KHCO_3$, KOH, Na_2CO_3, K_2CO_3) also reduces coke formation and catalyzes the water-gas shift reaction [40]. For example, the addition of $KHCO_3$ leads to an increase in gas formation and a decrease in the amount of carbon monoxide [110]. For example, the use of K_2CO_3 in the reaction mixture during depolymerization of cellulose in subcritical water substantially enhanced gas formation [64]. SCW has been utilized to gasify coal. For example, Hui [48] obtained gas containing 70% hydrogen from gasification of a 24 wt.% coal-water-slurry with 2 wt.% sodium carboxymethyl cellulose and 1 wt.% K_2CO_3 at 580°C and 250 bar using a fluidized bed reactor.

11 Microalgae to Biofuels Using Sub- and Supercritical Water Technology

In general, conventional higher land plants are not very efficient in capturing solar energy. Even the fastest growing energy crops can convert solar energy to biomass at a yearly rate of no more than 1 W/m^2 [133]. However, the biomass productivity of microalgae, a photosynthetic microorganism, can be 50 times greater than switchgrass [20]. Microalgae grow in marine and freshwater environments. Due to their simple cellular structure and submergence in an aqueous environment where they are in vicinity of water, CO_2, and other nutrients, microalgae are generally more efficient in converting solar energy into biomass. Microalgae can be used to produce wide range of second-generation biofuels and bioactive compounds [47, 106]. They offer many potential advantages [14, 106, 133] over conventional biomass sources. Microalgae primarily comprise of varying proportion of proteins, carbohydrates, lipids, and ash. The percentages vary depending upon the species. Table 5 presents the general composition of different microalgae. What really makes algal biomass feasible for biofuels production is the fact that many forms of algae have

Table 5 General composition of different algae (% of dry matter) [5]

Alga	Protein	Carbohydrates	Lipids
Chlamydomonas rheinhardii	48	17	21
Chlorella vulgaris	51–58	12–17	14–22
Euglena gracilis	39–61	14–18	14–20
Porphyridium cruentum	28–39	40–57	9–14
Scenedesmus obliquus	50–56	10–17	12–14
Spirulina platensis	46–63	8–14	4–9

very high lipid contents. The biomass that is nonlipid provides a high-value co-product such as animal feed or fertilizer that offsets the cost of converting the algae to fuels. Growing algae also removes nitrogen and phosphorus from water and consumes atmospheric CO_2.

11.1 Major Challenges in the Conversion of Microalgae to Biofuels

Microalgae are considered as one of the most promising feedstock for biofuels. The biomass can be used for producing solid (biochar), liquid (biodiesel, liquid hydrocarbons, pyrolysis oil), and gaseous fuels (synthesis gas, methane, hydrogen). However, the attractive target is producing fungible fuels such as gasoline, diesel, and jet fuel ([37]; Rene H. [129]). Some of the major challenges in accomplishing the objective of cost-competitive biofuels production from microalgae are:

Dewatering: It is not uncommon to have less than one gram of algae per liter of water. Therefore, a cost-efficient harvesting and drying process is needed to produce a biomass suitable for oil recovery. Conversion processes that can process wet biomass are highly desirable for reducing the energy intensive dewatering cost.

High Nitrogen Content: Microalgae are rich in proteins (Table 5). The elemental composition (carbon, hydrogen, and oxygen) of microalgae is similar to other cellulosic biomass but differs in nitrogen contents. Apart from water, sunlight, and carbon dioxide, nitrogen and phosphorous are the primary nutrients which are required to grow microalgae. Based on the average elemental composition, microalgae can be represented by a general formula as $CH_{1.7}O_{0.4}N_{0.15}P_{0.0094}$. The nitrogen content varies between 4 and 8 wt.% of the dry biomass depending upon the physiological state and nutrient limitation condition of microalgae [37, 129]. Due to the high nitrogen content, NO_x emission and losses of nitrogen fertilizer are matter of great concern besides the high moisture content if whole microalgae are processed for biofuels [47].

The organically bound nitrogen converts to ammonia in reducing atmosphere and NO_x in combustion/oxidizing atmosphere during the biofuels conversion processes. In biogas production, high nitrogen contents lead to the ammonia toxicity during anaerobic digestion process. Also, high nitrogen contents are reported to inhibit the digestion of algal biomass. Similarly, presence of nitrogen in biomass will cause the formation of NO_x compounds during gasification process which is conducted in the limited supply of oxygen. NO_x is a greenhouse gas and heavily regulated environmental pollutant. Further, gas cleaning also adds to the cost, if synthesis gas is to be used for liquid fuels production via Fischer–Tropsch process. The nitrogen is mainly present as the protein in microalgae. Therefore, it is important to extract high value protein for the sustainable production of biofuels from microalgae. The major emphasis should be on the value addition to the nonfuels components and the recycle of nutrients as much as possible. The approach for producing biofuels from microalgae can be different compared to the conventional

cellulosic biomass processes. The high protein contents of microalgae make it a potential candidate for extracting protein [16] and the species which have the high lipid contents are best considered for biodiesel production via transesterification process [15, 23, 108].

Diverse Composition: More than 50,000 species of microalgae are reported to exist [78]. Algal biomass composition varies depending upon the species (Table 5). The challenge involves developing a process that can tolerate the complex compositions found with different species of algae. In order to make biofuels cost competitive, it is important to develop processes for the 100% utilization of algal biomass components.

11.2 Microalgae to Biofuels Conversion Processes

The most attractive target for fuel production from algae is the production of gasoline, diesel, and jet fuel [23, 36]. There are several competing pathways similar to lignocellulosic biomass for converting the biomass to liquid fuel, chemicals, and/or hydrogen.

The anaerobic digestion of microalgae is a process for production of biogas [34] which mainly contains CH_4 and CO_2 and is an environment friendly clean, cheap, and versatile gaseous fuel [39]. Vergara-Fernandez et al. reported that biogas production levels of 180.4 mL/g-d of biogas can be realized using a two-stage anaerobic digestion process with different strains of algae, with a methane concentration of 65% [124]. Unfortunately, biogas garners less importance than the common transportation fuels. The selling cost per unit energy is considerably lower than gasoline. Because the biogas produced is relatively low in value, the anaerobic process must be simple in design, have low operating cost, and produce gas at high rates.

Pyrolysis processes typically use dry and finely ground biomass. The oxygen content of bio-oils is usually 35–40 wt. %. The presence of oxygen is reason for substantially lower heating value of bio-oils compared to hydrocarbon fuels. Also of concern is the nitrogen content of algae, because this nitrogen tied up mostly as proteins is transformed to nitrogenous species such as pyridines. Removal of such oxygen is possible by decarboxylation, dehydration, and/or catalytic hydrotreating [123]. Therefore, bio-oils are required to be catalytically upgraded to make them fungible fuels. Considering the high moisture content of algae, pyrolysis that requires dried algae may not be an economical option and an inexpensive dewatering or extraction process will have to be developed [23]. In fact, very few studies have been reported on pyrolysis of algae for bio-oil. The bio-oil yield for the microalgae *Chlorella protothecoides* rose from 5.7 to 55.3% as the pyrolysis temperature rose from 250 to 500°C, and then gradually decreased to 51.8% and was obtained at 600°C [20]. The heating value of bio-oils from algae was in the range of 35 MJ/kg which is relatively higher than that from wood.

Gasification is another transformation pathway for production of liquid fuels from algae. Synthesis gas is produced through the thermal decomposition of organic

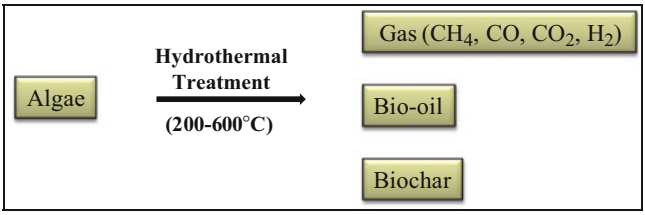

Fig. 14 Different fuels from microalgae using sub- and supercritical water technology

matter in oxygen-deficient conditions. The presence of sulfur and nitrogen in feedstock can be the cause of impurities in synthesis gas. Sulfur in microalgae is significantly low (< 0.1 wt.% dry basis) and hence may not be a matter of concern. However, high nitrogen contents of microalgae lead to the formation of NH_3, NO_x, and HCN gases. These impurities should be cleaned before synthesis gas is subjected to FT process for avoiding the catalyst deactivation. It is important to note that the tolerance limits for NH_3, NO_x, and HCN are reported to be 10 ppmv, 0.2 ppmv, and 10 ppb, respectively [113].

In view of challenges associated with utilizing wet biomass, principally the need for water and nitrogen removal, reactions in sub and supercritical water medium may be an attractive option for extracting valuable bioactive compounds and producing biofuels from microalgae. Figure 14 shows the possibility of producing different kind of biofuels using sub- and supercritical water technologies.

The reactions conditions can be tuned to conduct liquefaction, carbonization, or gasification in water medium based on the product requirement. Microalgae is nonfibrous compared to the lignocellulosic biomass and so feeding algae slurry at high pressure may be less challenging. In another recent study, it was reported that more than 80 wt.% of microalgae (*Chlorella vulgaris*) could be gasified in supercritical water. The studies were conducted in quartz capillaries under operating temperatures of 400–700°C and reaction times of 1–15 min in the presence of nickel-based catalysts. The dry gas composition from algae gasification in supercritical water was mainly comprised of CO_2, CO, CH_4, H_2, and some C_2–C_3 compounds [13].

12 Challenges of Hydrothermal Processing

Although in laboratory experiments excellent results have been achieved and the technology possesses many potential benefits over the conventional methods of processing biomass to biofuels or chemicals, there are certain issues, which need to be addressed.

– *Biomass feeding at high pressure*: As a "rule of thumb," the solid loading in excess of 15–20 wt.% is considered economical on commercial point of view.

Feeding slurries at high pressure is always challenging especially for the lab scale studies since low capacity slurry pumps are rarely available. Pumping slurry at large scale is less of a problem, where progressive cavity or similar pumps are commercially available.

- *Salt precipitation*: Plugging of reactors caused by the precipitation of inorganic salts above supercritical temperature and low density conditions. At room temperature, water is an excellent solvent for most salts. On the other hand, solubility of most salts is very low (typically 1–100 ppm) in supercritical water (low density) and precipitating salts may plug the reactors even at high flow velocities [59]. However, the problem may be used as an opportunity to produce a valuable fertilizer by-product of the process, if managed properly.
- *Corrosion*: The halogens, such as sulfur or phosphorous, present in the organic matter are converted to the respective acids, which may cause severe corrosion on the reactor wall under harsh reaction conditions. The corrosion problem can be reduced or avoided by selecting the right material of construction and or a slightly modified reactor concept.
- *Coking and deactivation of heterogeneous catalyst*: Some catalyst supports degrade or oxidize in hydrothermal conditions. Decline in catalyst activity is also observed with long period of exposure of catalyst during continuous process [94].

13 Energy Balance of Wet Processes

Most of the biomass feedstock such as forest residues, agricultural residues, food processing wastes, agricultural sludge, etc. contains moisture or large amounts of water. In conventional thermochemical processes, considerable amount of energy is required to evaporate water. In case of microalgae as feedstock, energy required for the dewatering process may account for more than 75% of the total energy consumption. Typical thermal dryers use significantly more energy per kilogram of evaporated water (3.3–3.9 MJ/kg). The drying steps lead to large parasitic energy losses that can consume much of the energy content of the biomass. In sub- and supercritical water processing, water is kept in liquid or supercritical phase by applying pressure greater than the vapor pressure of water at the reaction temperature. Thus, energy (latent heat of vaporization of water 2.26 MJ/kg) required for the phase change of water from liquid to vapor phase is avoided by carrying out the reactions under pressure. The specific energy requirements needed to affect the isobaric expansion from liquid-like to gas-like densities are typically lower than what is needed when boiling occurs under subcritical pressures at an intermediate temperature to form a two-phase mixture [94].

Xu et al. compared the energy balance for wet and dry process for converting microalgae to biofuels [131]. In their study, biodiesel, glycerol, pyrolysis oil, and producer gas were considered as products from conventional dry processes, whereas green diesel, hydrogen, producer gas, and CO_2 recycling were considered for the

wet/hydrothermal process products. The fossil energy ratio (FER) was selected as performance indicator which was defined as:

$$\mathrm{FER} = \frac{\mathrm{HHV}_{\mathrm{biofuel}}}{E_{\mathrm{input}}}$$

$\mathrm{HHV}_{\mathrm{biofuel}}$: Higher heating value of biofuel products.
E_{input}: Fossil energy input.

The FER for dry and wet process was reported as 1.50 and 1.37, respectively. The FER of 1 indicates that the same amount of fossil energy is consumed in the process of converting the fossil energy to a useable fuel. The analysis showed that the drying process in the dry route and the oil extraction process in the wet route consume a significant amount of energy. By coupling waste heat from a nearby power plant to the process, the energy balance can be improved and a potential FER up to 2.38 and 1.82 can be reached for the dry and wet route, respectively. Their study further concluded that the dry route may be more interesting on a short-term basis because of a higher FER, but for the long term, the wet route has more potential because of producing biofuels with a higher value. In the absence of existing commercial operations on wet processes, most of the cost is estimated based on the equipment used in supercritical water oxidation processes, as an example: one wet ton of organic waste with an organic content of 10°wt.% to below 300 US$ [59]. Being a high pressure system, major investment is attributed mainly to the equipment cost. The energy needed for pumping the feed at high pressure is significantly lower compared to the heat input required for heating the reactor at reaction temperature. In December 2010, Ignite Energy Resources, Australia declared that they have developed a supercritical Water (SCW) reactor technology for converting biomass and ancient coal into highly valuable oil and coal products.

References

1. Allen SG, Kam LC et al (1996) Fractionation of sugar cane with hot, compressed, liquid water. Ind Eng Chem Res 35(8):2709–2715
2. Atalla RH, Vanderhart DL (1984) Native cellulose: a composite of two distinct crystalline forms. Science 223(4633):283–285
3. Baeza J, Freer J (2001) Chemical characterization of wood and its components. In: Hon DNS, Shiraishi N (eds) Wood and cellulosic chemistry. Marcel Dekker, Inc, New York, pp 275–384
4. Balat M (2008) Mechanisms of thermochemical biomass conversion processes, part 1: reactions of pyrolysis. Energ Sourc, Part A 30:620–635
5. Becker EW (2007) Micro-algae as a source of protein. Biotechnol Adv 25:207–210
6. Behrendt F, Neubauer Y et al (2008) Direct liquefaction of biomass. Chem Eng Technol 31(5):667–677
7. Bergius F, Specht H (1913) Die Anwendung hoher Drucke bei chemischen Vorgängen und eine Nachbildung des Entstehungsprozesses der Steinkohle. Verlag Wilhelm Knapp, Halle an der Saale, p 58

8. Biermann CJ (1996) Handbook of pulping and paper making. Academic, San Diego
9. Bobleter O (1994) Hydrothermal degradation of polymers derived from plants. Prog Polym Sci 19:797–841
10. Bruun S, Luxhoi J (2008) Is biochar production really carbon-negative? Environ Sci Technol 42(5):1388
11. Byrd AJ, Pant KK et al (2007) Hydrogen production from Glucose using Ru/Al2O3 catalyst in supercritical water. Ind Eng Chem Res 46(11):3574–3579
12. Calzavara Y, Joussot-Dubien C et al (2005) Evaluation of biomass gasification in supercritical water process for hydrogen production. Energ Convers Manage 46:615–631
13. Chakinala AG, Brilman DWF et al (2010) Catalytic and non-catalytic supercritical water gasification of microalgae and glycerol. Ind Eng Chem Res 49(3):1113–1122
14. Chen P, Min M et al (2009) Review of the biological and engineering aspects of algae to fuels approach. Int J Agric Biol Eng 2(4):1–29
15. Chisti Y (2007) Biodiesel from microalgae. Biotechnol Adv 25(3):294–306
16. Chornet E, Overend RP (1985) Biomass liquefaction: an overview. In: Overend RP, Milne TA, Mudge LK (eds) Fundamentals of thermochemical biomass conversion. Elsevier Applied Science, New York, pp 967–1002
17. Chronakis IS (2000) Biosolar proteins from aquatic algae. In: Doxastakis G, Kiosseoglou V (eds) Developments in food science, vol 41. Elsevier, Amsterdam, pp 39–75
18. Deguchi S, Tsujii K et al (2008) Crystalline-to-amorphous transformation of cellulose in hot and compressed water and its implications for hydrothermal conversion. Green Chem 10:191–196
19. Demirbas A (2000) Mechanisms of liquefaction and pyrolysis reactions of biomass. Energ Convers Manage 41:633–646
20. Demirbaş A (2006) Oily products from mosses and algae via pyrolysis. Energ Sourc 28:933–940
21. Diaz MJ, Cara C et al (2010) Hydrothermal pre-treatment of rapeseed straw. Bioresour Technol 101(2010):2428–2435
22. Dinjus E, Kruse A (2004) Hot compressed water-a suitable and sustainable solvent and reaction medium? J Phys Condens Matter 16:S1161–S1169
23. DOE US (2010) National Algal Biofuels Technology Roadmap, U.S. Department of Energy, Office of Energy Efficiency and Renewable Energy, Biomass Program. Maryland
24. Dumitriu S (2004) Preparation and properties of cellulose bicomponent fibers. CRC Press, Boca Raton
25. Eckert CA, Knutson BL et al (1996) Supercritical fluids as solvents for chemical and materials processing. Nature 383(6598):313–318
26. Elliott DC (2008) Catalytic hydrothemal gasification of biomass. Biofuels Bioprod Bioref 2:254–265
27. Elliott DC, Sealock LJ et al (1993) Chemical processing in high-pressure aqueous environments. 2. Development of catalysts for gasification. Ind Eng Chem Res 32(8):1542–1548
28. Falkehag SI (1975) Synthesis of phenolic polymer. Appl Polym Symp 28:247–257
29. Fang Z, Sato T et al (2008) Reaction chemistry and phase behaviour of lignin in high-temperature and super critical water. Bioresour Technol 99:3424–3430
30. Farrell AE, Plevin RJ et al (2006) Ethanol can contribute to energy and environmental goals. Science 311:506–508
31. Franck EU (1987) Fluids at high pressures and temperatures. Pure Appl Chem 59(1):25–34
32. Garrote G, Dominguez H et al (1999) Hydrothermal processing of lignocellulosic materials. Holz als Roh- und Werkstoff 57(1999):191–202
33. Ghose TK, Roychoudhury PK, Ghosh P (1984) Simultaneous saccharification and fermentation (SSF) of lignocellulosics to ethanol under vacuum cycling and step feeding. Biotechnol Bioeng 26:377–381
34. Golueke CG, Oswald WJ et al (1957) Anaerobic digestion of algae. Appl Microbiol 5(1):47–55
35. Gourdiaan F, Peferoen D (1990) Liquid fuels from biomass via a hydrothermal process. Chem Eng Sci 45:2729–2734

36. Gouveia L, Oliveira AC (2009) Microalgae as a raw material for biofuels production. J Ind Microbiol Biotechnol 36:269–274
37. Greenwell HC, Laurens LML et al (2010) Placing microalgae on the biofuels priority list: a review of the technological challenges. J R Soc Interface 7(46):703–26
38. Gupta R, Lee YY (2008) Mechanism of cellulase reaction on pure cellulosic substrates. Biotechnol Bioeng 102(6):1570–1581
39. Gupta RB, Demirbas A (2010) Introduction. Gasoline, Diesel and Ethanol Biofuels from Grasses and Plants. Cambridge University Press, London, pp 1–24
40. Hao XH, Guo LJ et al (2003) Hydrogen production from glucose used as a model compound of biomass gasified in supercritical water. J Hydrogen Energy 28:55–64
41. Heitz M, Carrasco F et al (1986) Generalized correlations for aqueous liquefaction of lignocellulosics. Can J Chem Eng 64:647–650
42. Hendriks ATWM, Zeeman G (2009) Pretreatments to enhance the digestibility of lignocellulosic biomass. Bioresour Technol 100(1):10–18
43. Hsu T-A (1996) Pretreatment of biomass. In: Wyman CE (ed) Handbook on bioethanol: production and utilization. Taylor and Francis, Washington, DC
44. Hu B, Yu S-H et al (2008) Functional carboneceous materials from hydrothermal carbonization of biomass: an effective chemical process. Dalton Trans 40:5414–5423
45. Huber GW, Cheda JN et al (2005) Production of liquid alkanes by aqueous processing of biomass derived carbohydrates. Science 308:1446–1450
46. Huber GW, Iborra S et al (2006) Synthesis of transportation fuels from biomass: chemistry, catalysts, and engineering. Chem Rev 106:4044
47. Huesemann MH, Benemann JR (2009) Biofuels from microalgae: review of products, processes and potential, with special focus on *Dunaliella* sp. In: Ben-Amotz JEWPA, Subba Rao DV (eds) The Alga *Dunaliella*: biodiversity, Physiology, Genomics, and Biotechnology, vol 14. Science Publishers, New Hampshire, pp 445–474
48. Hui J, Youjun L et al (2010) Hydrogen production by coal gasification in supercritical water with a fluidised bed reactor. Int J Hydrogen Energy 35:7151–7160
49. Jong WD (2009) Sustainable hydrogen production by thermochemical biomass processing. In: Gupta RB (ed) Hydrogen fuel: production, transport and storage. CRC Press, Boca Raton, pp 185–225
50. Kabyemela BM, Adschiri R et al (1997) Rapid and selctive conversion of glucose to erythrose in supercritical water. Ind Eng Chem Res 36:5063–5067
51. Kadam KL, Chin CY et al (2009) Continuous biomass fractionation process for producing ethanol and low-molecular-weight lignin. Environ Prog Sustain Energy 28(1):89–99
52. Kalinichev AG, Churakov SV (1999) Size and topology of molecular clusters in supercritical water: a molecular dynamics simulation. Chem Phys Letters 302:411–417
53. Karagoez S, Bhaskar T et al (2005) Comparative studies of oil compositions produced from sawdust, rice husk, lignin and cellulose by hydrothermal treatment. Fuel 84(7–8):875–884
54. Karagoz S, Bhaskar T et al (2006) Hydrothermal upgrading of biomass: effect of K_2CO_3 concentration and biomass/water ratio on product distrubution. Bioresour Technol 97:90–98
55. Knez˘evic´ D, Swaai WPMV et al (2009) Hydrothermal conversion of biomass: I, glucose conversion in hot compressed water. Ind Eng Chem Res 48:4731–4743
56. Knill CJ, Kennedy JF (2005) Cellulosic biomass-derived products. In: Dumitriu S (ed) Polysaccharides: structural diversity and functional versatility. Marcel and Dekker, New York, pp 937–956
57. Kobayashi N, Okada N et al (2009) Characteristics of solid residues obtained from hot-compressed-water treatment of woody biomass. Ind Eng Chem Res 48:373–379
58. Kohlmann KL, Westgate PJ et al (1995) Enhanced enzyme activities on hydrated lignocellulosic substrates. In: Penner M, Saddler J (eds) American Chemical Society national meeting, vol 207, ACS symposium series No. 618. American Chemical Society, Washington, DC, pp 237–255
59. Kritzer P, Dinjus E (2001) An assessment of supercritical water oxidation (SCWO): existing problems, possible solutions and new reactor concepts. Chem Eng J 83:207–214

60. Kruse A (2009) Hydrothermal biomass gasification. J Supercrit Fluids 47(3):391–399
61. Kruse A, Gawlik A (2003) Biomass conversion in water at 330-410 C and 30-50 MPa: identification of key compounds for indicating different chemical reaction pathways. Ind Eng Chem Res 42:267–269
62. Kumar S (2010) Hydrothermal treatment for biofuels: lignocellulosic biomass to bioethanol, biocrude, and biochar. Ph.D. Dissertation, Department of Chemical Engineering. Auburn University, Auburn, p 258
63. Kumar S, Gupta R et al (2009) Cellulose pretreatment in subcritical water: effect of temperature on molecular structure and enzymatic reactivity. Bioresour Technol 101(2010): 1337–1347
64. Kumar S, Gupta RB (2008) Hydrolysis of microcrystalline cellulose in subcritical and supercritical water in a continuous flow reactor. Ind Eng Chem Res 47(23):9321–9329
65. Kumar S, Gupta RB (2009) Biocrude production from switchgrass using subcritical water. Energy Fuel 23(10):5151–5159
66. Kumar S, Kothari U et al (2011) Hydrothermal pretreatment of switchgrass and corn stover for production of ethanol and carbon microspheres. Biomass Bioenergy 35(2):956–968
67. Laxman RS, Lachke AH (2008) Bioethanol from lignocellulosic biomass, part 1: pretreatment of the substrates. In: Pandey A (ed) Handbook of plant-based biofuels. CRC Press, Boca Raton, pp 121–139
68. Liu C, Wyman CE (2003) The effect of flow rate of compressed hot water on xylan, lignin and total mass removal from corn stover. Ind Eng Chem Res 42:5409–5416
69. Lynd LR (1996) Overview and evaluation of fuel ethanol from cellulosic biomass: technology, economics, the environment, and policy. Ann Rev Energy Environ 21:403–465
70. Marchessault RH, Sarko A (1967) X-ray structure of polysaccharides. Adv Carbohydr Chem 22:421–482
71. Marcus Y (1999) On transport properties of hot liquid and supercritical water and their relationship to the hydrogen bonding. Fluid Phase Equilib 164:131–142
72. Marta S, Antonio BF (2009) The production of carbon materials by hydrothermal carbonization of cellulose. Carbon 47:2281–2289
73. Masaru W, Takafumi S et al (2004) Chemical reactions of C1 compounds in near-critical and supercritical water. Chem Rev 104:5803–5821
74. Matsumara Y, Minowa T et al (2005) Review—biomass gasification in near- and super-critical water: status and prospects. Biomass Bioenergy 29:269–2925
75. Matsumura Y, Minowa T et al (2005) Biomass gasification in near- and super-critical water: status and prospects. Biomass Bioenergy 29(4):269–292
76. Matsumura Y, Sasaki M et al (2006) Supercritical water treatment of biomass for energy and material recovery. Combust Sci Tech 178:509–536
77. Meister JJ (1996) Chemical modification of lignin. In: Hon DN-S (ed) Chemical modification of lignocellulosic materials. Marcel Dekker Inc., New York, pp 129–157
78. Mendes RL (2007) Supercritical Fluid Extraction of Active Compounds from Algae. In: Martinez JL (ed) Supercritical fluid extraction of nutraceuticals and bioactive compounds. CRC Press, Boca Raton, pp 189–213
79. Miyoshia H, Chena D et al (2004) A novel process utilizing subcritical water to recycle soda–lime–silicate glass. J Non-Cryst Solids 337(3):280–282
80. Mok WS, Antal MJ (1992) Uncatalyzed solvolysis of whole biomass hemicellulose by hot compressed liquid water. Ind Eng Chem Res 31:1157–1161
81. Mok WSL, Antal MJ, Varhegyi G (1992) Productive and parasitic pathways in dilute-acid-catalyzed hydrolysis of cellulose. Ind Eng Chem Res 31:94–100
82. Mosier N, Hendrickson R et al (2005) Optimization of pH controlled liquid hot water pretreatment of corn stover. Bioresour Technol 96:1986–1993
83. Mosier N, Wyman C et al (2005) Features of promising technologies for pretreatment of lignocellulosic biomass. Bioresour Technol 96(6):673–686
84. Muthukumaraa P, Gupta RB (2000) Sodium-carbonate assisted supercritical water oxidation of chlorinated waste. Ind Eng Chem Res 39:4555–4563

85. Ni M, Leung DYC et al (2006) An overview of hydrogen production from biomass. Fuel Process Tech 87:461–472
86. O'Sullivan AC (1997) Cellulose: the structure slowly unravels. Cellulose 4(3):173–207
87. Olsson L, Jorgensen H et al (2005) Bioethanol production from lignocellulosic material. In: Dumitriu S (ed) Polysachharides: structural diversity and functional versatility. Marcel Dekker, New York, pp 957–993
88. Overend RP, Chornet E (1987) Fractionation of lignocellulosics by steam-aqueous pretreatments. Philos Trans R Soc London A321:523–536
89. Pastircakova K (2004) Determination of trace metal concentrations in ashes from various biomass materials. Energy Educ Sci Technol 13:97–104
90. Pérez J, Muñoz-Dorado J et al (2002) Biodegradation and biological treatments of cellulose, hemicellulose and lignin: an overview. Int Microbiol 5:53–63
91. Pérez JA, Ballesteros I et al (2008) Optimizing Liquid Hot Water pretreatment conditions to enhance sugar recovery from wheat straw for fuel-ethanol production. Fuel 87:3640–3647
92. Perlack RD, Wright LL et al (2005) Biomass as a feedstock for a bioenergy and bioproducts industry:the technical feasibility of a billion-ton annual supply. A joint report sponsored by US Department of Energy and US Department of Agriculture, p 78
93. Petchpradab P, Yoshida T et al (2009) Hydrothermal pretreatment of rubber wood for the saccharification process. Ind Eng Chem Res 48(9):4587–4591
94. Peterson AA, Vogel F et al (2008) Thermochemical biofuel production in hydrothermal media:a review of sub- and supercritical water technologies. Energy Environ Sci 1:32–65
95. Phillip E (1999) Organic chemical reactions in supercritical water. Chem Rev 99:603–621
96. Rogalinski T, Ingram T et al (2008) Hydrolysis of lignocellulosic biomass in water under elevated temperatures and pressures. J Supercrit Fluids 47(1):54–63
97. Saha BC (2003) Hemicellulose bioconversion. J Ind Microbiol Biotechnol 30:279–291
98. Sarko A (1978) What is the crystalline structure of cellulose ? Tappi 61:59–61
99. Sarko A (1987) Cellulose—how much do we know about its structure? In: Kennedy JF (ed) Wood and cellulosics: industrial utilization, biotechnology, structure and properties. Ellis Horwood, Chichester, pp 55–70
100. Sasaki M, Fang Z et al (2000) Dissolution and hydrolysis of cellulose in subcritical and supercritical water. Ind Eng Chem Res 39:2883–2890
101. Sasaki M, Goto K et al (2002) Rapid and selective retro-aldol condensation of glucose to glycolaldehyde in supercritical water. Green Chem 4:285–287
102. Sasaki M, Kabyemela B et al (1998) Cellulose hydrolysis in subcritical and supercritical water. J Supercrit Fluids 1998(13):261–268
103. Savage PE (1999) Organic chemical reactions in supercritical water. Chem Rev 99:603–621
104. Savage PE, Gopalan S et al (1995) Reactions at supercritical conditions—applications and fundamentals. AIChE J 41(7):1723–1778
105. Savovaa D, Apakb E et al (2001) Biomass conversion to carbon adsorbents and gas. Biomass Bioenergy 21(2):133–142
106. Schenk PM, Thomas-Hall SR et al (2008) Second generation biofuels: high-efficiency microalgae for biodiesel production. Bioenergy Res 1:20–43
107. Schwald W, Bobleter O (1989) Hydrothermolysis of cellulose under static and dynamic conditions at high temperatures. J Carbohydr Chem 8(4):565–578
108. Sheehan J, Dunahay T, Benemann J, Roessler P (1998) A look back at the U.S. Department of Energy's Aquatic Species Program-Biodiesel from algae. U.S. Department of Energy's Office of Fuels Development
109. Sierra R, Smith A et al (2008) Producing fuels and chemicals from lignocellulosic biomass, vol 104, Chemical engineering progress. AIChE Publication, New York, pp S10–S18
110. Sinag A, Kruse A et al (2003) Key compounds of the hydropyrolysis of glucose in supercritical water in the presence of K2CO3. Ind Eng Chem Res 42:3516–3521
111. Sinnott ML (2007) Chapter 4: primary structure and conformation of oligosaccharides and polysaccharides. RSC publishing, Cambridge
112. Sjostrom E (1981) Wood chemistry: fundamentals and applications. Academic, New York

113. Spath PL, Dayton DC (2003) Preliminary screening-technical and economic assessment of synthesis gas to fuels and chemicals with emphasis on the potential for biomass-derived syngas. Fischer-Tropsch synthesis. National Renewable Energy Laboratory, Golden, pp 90–107
114. Sukumaran RK (2009) Bioethanol from lignocellulosic biomass: part II production of cellulases and hemicellulases. In: Pandey A (ed) Hand book of plant based biofuels. CRC Press, BocaRaton, pp 141–157
115. Sun Y, Cheng JJ (2002) Hydrolysis of lignocellulosic material for ethanol production: a review. Bioresour Technol 83:1–11
116. Suryawati L, Wilkins MR et al (2008) Simultaneous sacchrification and fermentation of Kanlow switchgrass pretreated by hydrothermolysis using Kluyveromyces marxianus IMB4. Biotechnol Bioeng 101(5):894–902
117. Taherzadeh MJ, Karimi K (2007) Enzyme based hydrolysis processes for ethanol from lignocellulosic materials: a review. BioResources 2(4):707–738
118. Tester JW, Holgate HR et al (1993) Supercritical water oxidation technology—process development and fundamental research. In: Tedder DW, Pohland FG (eds) Emerging technologies in hazardous waste management III. American Chemical Society, Washington, DC
119. Titirici M-M, Antonietti M et al (2008) Hydrothermal carbon from biomass: a comparision of the local structure from poly- to monosaccharides and pentoses/hexoses. Green Chem 10:1204–1212
120. Titirici M-M, Thomas A et al (2007) Back in the black: hydrothermal carbonization of plant material as an efficient chemical process to treat the CO_2 problem. New J Chem 31:787–789
121. Valenzuela MB, Jones CW et al (2006) Batch aqueous reforming of woody biomass. Energy Fuel 20:1744–1752
122. Varhegyi G, Szabo P et al (1998) TG, TG-MS, and FTIR characterization of high-yield biomass charcoals. Energy Fuel 12:969–974
123. Venderbosch R, Ardiyanti A et al (2010) Stabilization of biomass-derived pyrolysis oils. J Chem Technol Biotechnol 85(5):674–686
124. Vergara-Fernandez A, Vargas G et al (2008) Evaluation of marine algae as a source of biogas in a two-stage anaerobic reactor system. Biomass Bioenergy 32(4):338–344
125. Watanabe M, Aizawa Y et al (2005) Glucose reactions within the heating period and the effect of heating rate on the reactions in hot compressed water. Carbohydr Res 340:1931–1939
126. Watanabe M, Inomata H et al (2002) Catalytic hydrogen generation from biomass (glucose and cellulose) with ZrO2 in supercritical water. Biomass Bioenergy 22:405–410
127. Weil JR, Brewer M et al (1997) Continuous pH monitoring during pretreatment of yellow poplar wood sawdust by pressure cooking in water. Appl Biochem Biotechnol 68:21–40
128. Wellig B (2003) Transpiring wall reactor for supercritical water oxidation. Swiss Federal Institute of Technology, Zurich, Doctor of Technical Sciences, p 291
129. Wijffels RH, Barbosa J (2010) An outlook on microalgal biofuels. Science 329:796–799
130. Wyman CE, Dale BE et al (2005) Coordinated development of leading biomass pretreatment technologies. Bioresour Technol 96:1959–1966
131. Xu L, Brilman DWF et al (2011) Assessment of a dry and a wet route for the production of biofuels from microalgae: energy balance analysis. Bioresour Technol 102(8):5113–5122
132. Yang B, Wyman CE (2004) Effect of xylan and lignin removal by batch and flow through pretreatment on the enzymatic digestibility of corn stiver cellulose. Biotechnol Bioeng 86(1):88–95
133. Yanqun Li MH, Nan Wu, Lan CQ, Dubois-Calero N (2008) Biofuels from microalgae. Biotechnol Prog 24(4):815–820
134. Zhang B, Huang H-J et al (2008) Reaction kinetics of the hydrothermal treatment of lignin. Appl Biochem Biotechnol 147:119–131
135. Zhang Y-HP, Berson E et al (2009) Sessions 3 and 8: pretreatment and biomass recalcitrance: fundamentals and progress. Appl Biochem Biotechnol 153:80–83

Chapter 12
Biomass to Liquid Fuel via Fischer–Tropsch and Related Syntheses

Y.T. Shah

Abstract This chapter briefly reviews the state of art on the conversion of biomass to biofuels by gasification followed by the gas to liquid conversion of biosyngas via Fischer–Tropsch and related syntheses. An integrated process to produce heat, electricity, or fuel by gasification and Fischer–Tropsch synthesis is analyzed. The present state of gasification reactor technology is outlined. The strategies for syn-gas cleanup are delineated. The catalysis and processes for methanol, Fischer–Tropsch, and isosynthesis are briefly evaluated. Finally, various approaches to an integrated process design depending on the desired end results (heat, electricity, or fuel) and the associated economics for each approach are outlined and briefly discussed.

1 Introduction

The world energy demand is increasing at a faster rate than its supply. This is particularly true for the transportation fuel. The sources for total world energy supply at the present time are graphically illustrated in Fig. 1. It is clear from this graph that coal and renewable sources combine to provide as much energy as oil. Heat, electricity, and transportation fuel are the major forms of energy use. While heat and electricity are derived from all sources of energy, transportation fuel has been largely obtained from the oil and natural gas. Although the major world reserve of crudes, heavy oils, and natural gas reside in regions like Middle East, Canada, Venezuela, Russia, etc., the United States is the largest consumer of these forms of energy. In fact, because of the supply and demand discrepancies for the United States, more than 60% of oil consumed by the United States is imported from the foreign countries. Furthermore, the global supply of oil is decreasing, while the demand is increasing. One of the reasons

Y.T. Shah (✉)
Department of Engineering, Norfolk State University, Norfolk, VA 23504, USA
e-mail: ytshah@nsu.edu

J.W. Lee (ed.), *Advanced Biofuels and Bioproducts*, DOI 10.1007/978-1-4614-3348-4_12,

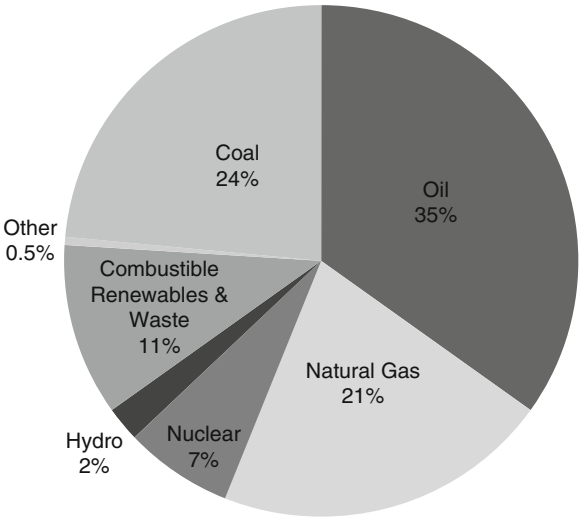

Fig. 1 Total world primary energy supply (after Olah et al. [3])

for this is the aggressive economic development and the resulting energy need by the countries such as China, India, Latin America, and Russia among others [1, 2].

It is imperative for the United States to be less dependent on foreign oil and develop alternate domestic sources to produce power for heat and electricity and synthetic oils. Besides crude oil and natural gas, the United States also uses considerable amount of coal, particularly for the power industries. The United States has the largest reserve of coal (which can last up to 200 years) [1, 2], which can also be a very good oil substitute for the production of transportation fuels. This can decrease the U.S. dependence on the foreign crude and heavy oil significantly. The technologies that have the most promise to convert coal to heat and electricity and/or liquid fuel include coal pyrolysis, combustion, and gasification. Gasification converts coal into producer gas with different amounts of methane, depending upon the gasification technology. The producer gas can either be used for heat and electricity or it can be converted into syngas (which largely contains CO and H_2) by reforming technology. The syngas can then be converted to a liquid fuel by means of Fischer–Tropsch (FT) synthesis. Both coal-based power production and CTL (coal-to-liquid) technology are commercially available. Unfortunately, they suffer from unacceptable production of green house gases (GHG) such as carbon dioxide and other harmful volatile organic compounds. While other toxic compounds can be removed from power generation and CTL plants, the sequestration of carbon dioxide still remains a major issue.

While for the past several decades the use of biomass for the source of heat, electricity, and transportation fuel has been extensively examined in Europe, Brazil, and several other countries, in recent years the use of biomass as a raw material for heat and electricity and transportation fuels is also becoming increasingly important in the United States. The energy available from renewable biomass sources in the United States has been estimated to be about 20% of the U.S. energy consumption [1, 2]. There are basically three classes of feedstocks derived from biomass that are appropriate for the production of renewable fuels for heat, electricity, and transportation

fuel: (1) starchy and edible feedstocks such as corn, beets, sugar cane, (2) triglyceride feedstocks such as soybeans, algae, jatropha, and about 350 other types of crop oils, and (3) lignocellulosic feedstocks. While, bioethanol and biodiesel derived from first two sources are commercialized and continue to be examined, it is the lignocellulosic biomass that is the most abundant class of biomass. While starch and triglycerides are only present in some crops, lignocellulose contributes structural integrity to plants and thus always present. In general, most energy crops and waste biomass, such as switch grass, miscanthus, agricultural residues, municipal wastes, animal wastes, waste from wood processing, waste from paper and pulp industries, etc., are lignocellulose that can be used for the generation of heat, electricity, and transportation fuel. The analysis carried out by EPA [4] shows that the use of biomass fuel sources results in the generation of significantly lower quantities of anthropogenic CO_2 emissions during power or fuel productions.

Biomass can be converted to biofuels in a number of different ways. For lignocellulosic biomass, thermochemical methods for the productions of biosyngas and bioliquids are very popular. These methods utilize gasification, reforming, pyrolysis, extraction, and liquefaction technologies to convert biomass into a variety of biogas and bioliquids. One method widely used is the gasification of biomass followed by reforming and gas cleaning to produce clean syngas. This syngas can be converted to a variety of bioliquids via well-known FT and related syntheses. This method is very versatile in that it can generate biofuels for heat, electricity, or transportation as well as for chemical feed stock. This brief chapter addresses three aspects of this method of biomass conversion: (a) basic chemistry and catalysis of FT and related processes for the conversion of biosyngas to bioliquids, (b) brief descriptions of various processes that currently exist for biomass to biosyngas and biosyngas to methanol and transportation fuels via FT and related syntheses, and (c) a brief assessment of an integrated process for the conversion of biomass to synthetic biodiesel fuel.

2 Fundamentals of Fischer–Tropsch and Related Chemistry and Catalysis

The general reactions for the hydrogenation of carbon monoxide are given as:

$$(2n+1)H_2 + nCO = C_nH_{2n+2} + nH_2O \tag{1}$$

$$(n+1)H_2 + 2nCO = C_nH_{2n+2} + nCO_2 \tag{2}$$

$$2nH_2 + nCO = C_nH_{2n} + nH_2O \tag{3}$$

$$nH_2 + 2nCO = C_nH_{2n} + nCO_2 \tag{4}$$

$$2nH_2 + nCO = C_nH_{2n+1}OH + (n-1)H_2O \tag{5}$$

$$(n+1)H_2 + (2n-1)CO = C_nH_{2n+1}OH + (n-1)CO_2 \tag{6}$$

Table 1 Influence of temperature and pressure on equilibrium conversion in a typical synthesis reaction: $20H_2 + 10CO = C_{10}H_{20} + 10H_2O$ (conversion = 80%) (after Anderson [5])

Temp. (°C)	Pressure atm abs
300	1
390	10
420	20
445	30
475	50

These reactions represent the formation of paraffins, monoolefins, and alcohols. The reactions generate water or carbon dioxide as by-products. As the concentration of carbon monoxide compared to that of hydrogen is increased, by-products change from water to carbon dioxide. However, the desired product can still be obtained during this change in the formation of the by-product.

Since the synthesis reactions lead to a smaller number of gaseous molecules, the equilibrium conversion at any given temperature increases with pressure. The influence of temperature and pressure on equilibrium conversion of reaction (3) is given in Table 1. As given in the table, for the formation of 1-decene (reaction (3)), an increase in pressure by 50 atm allows temperature to be increased by 175°C to obtain the same level of conversion.

Generally, the reactions forming carbon dioxide rather than water have larger equilibrium constants. The standard free energy per carbon atoms, $\Delta F^o/n$, for reactions producing methane is more negative than that of the reactions forming the higher hydrocarbons. In addition, the free energy of elemental carbon formation is more negative than that for the higher hydrocarbons; therefore, the production of higher hydrocarbons for liquid fuels must depend on the selectivity of the catalyst. The nature of the catalyst affects the Schultz-Flory chain growth distribution of FT products [6]. Also, as given in Table 2, different catalysts and promoters under various temperature and pressure conditions produce varying products from the reactions between carbon dioxide and hydrogen [8]. Three most commercialized reactions in Table 2 are methanol synthesis, FT synthesis, and isosynthesis. The last synthesis converts syngas into branched hydrocarbons. We will mainly focus our discussion on these three syntheses.

2.1 Methanol Synthesis

Methanol synthesis has been postulated to occur via two different types of reaction steps. One mechanistic view indicate methanol to be formed by direct reaction (7) between carbon monoxide and hydrogen as:

$$CO + 2H_2 = CH_3OH \tag{7}$$

Table 2 Products of reaction between carbon monoxide and hydrogen [7]

	Catalysts	Promoters	Temp. (°C)	Pressure (atm)	Product
Methane synthesis	Ru		250–500	1	Chiefly methane
	Ni	ThO_2, MgO	250–500	1	Chiefly methane
Fischer–Tropsch synthesis	Fe, Co, Ni	ThO_2, MgO, Al_2O_3, K_2O	150–350	1–30	Paraffinic and olefinic hydrocarbons up to waxes, plus small to large quantities of oxygenated products
	Ru		150–250	100–1,000	High molecular weight paraffinic hydrocarbons
Methanol synthesis	ZnO, Cu, Cr_2O_3, MnO		200–400	100–1,000	Methanol
Higher alcohol synthesis	Same as in C	Alkali	300–450	100–400	Methanol and higher alcohols
Isosynthesis	ThO_2, $ZnO + Al_2O_3$	K_2O	400–500	100–1,000	Saturated branched hydrocarbons
Oxosynthesis[a]	CO, Fe		100–200	100–200	Oxygenated organic compounds

[a]This reaction involves hydrogen, carbon monoxide, and olefins

Also,

$$CO_2 + H_2 = CO + H_2O \tag{8}$$

Thus, in this view, methanol is predominantly synthesized via direct hydrogenation of carbon monoxide (reaction (7)). The second reaction (8) is a reverse water gas shift (WGS) reaction. Experimental data containing 3–9% carbon dioxide in feed show a decrease in carbon dioxide concentration in the effluent stream indicating the presence of the second reaction. The first reaction (7) is exothermic, while the second reaction (8) is endothermic. In this mechanism, the presence of carbon dioxide in the feed is extremely important. Low carbon dioxide in the feed will result in lower methanol productivity. Typically, 2–4% of carbon dioxide is present in the syngas mixture for the vapor phase synthesis of methanol and the corresponding value for the liquid phase methanol synthesis is 4–8% [9, 10].

The second view implies that the principal chemical reactions that lead to the synthesis of methanol are [9–13]:

$$CO_2 + 3H_2 = CH_3OH + H_2O \tag{9}$$

$$CO + H_2O = CO_2 + H_2 \tag{10}$$

According to this view, the synthesis of methanol proceeds predominantly via direct hydrogenation of carbon dioxide and WGS reaction proceeds in the forward

Table 3 Commercial processes for methanol synthesis (after Lee et al. [14])

Process	Comments
The conventional ICI's 100 atm methanol process	$Cu/ZnO/Al_2O_3$ catalyst system; two parts: reforming and synthesis gas conversion
Haldor Topsoe A/S low pressure methanol process	Low capital cost; two stage reforming; suitable for smaller and larger plants (10,000 tons per day)
Kvaerner methanol process	Similar to Haldor Topsoe process; CO_2 can be used as supplementary feed; 2,000–3,000 mtpd typical size
Krupp Uhde's methanol process	Flexible feedstock, different steam reforming; at least 11 plants
Lurgi Ol-Gas-Chemie GMBH process	10,000 mtpd capacity; two stage reforming
Synetix LPM process	Large capacities; improved ICI's LPM
Liquid phase methanol process	Three stages developed by Chem Systems Inc.; slurry reactor; $Cu/ZnO/Al_2O_3$ catalyst at 230–260°C, 50–100 atm

direction. The WGS reaction produces carbon dioxide which in turn increases the productivity of the methanol production. A significant literature is available to justify each of these two mechanistic views for the methanol productions.

Numerous commercial processes for methanol synthesis are available. These processes have exploited both high and low pressure operations as well as both vapor phase and liquid phase operations. Some of the important commercial processes are outlined in Table 3. The details of these processes are given by Lee et al. [14].

2.2 FT Synthesis

The FT synthesis process can be made generally selective by proper choice of operating conditions and catalysts. Most of the studies over last several decades have been focused in this area. The status of the several FT processes through 1950 is given in Table 4. The yield of C_3^+ product per cubic meter of synthesis gas given in this table is very important because it directly relates to the purity of the synthesis gas. The cost of the production of purified synthesis gas can be as high as 70% of the total cost of the FT process [16]. Earlier work focused on Fe catalysts and the improvements in these catalysts that would increase their operability and selectivity and decrease the operating costs of FT process [16]. The efforts were made to prevent the reaction $2CO = CO_2 + C$ and improve the steady-state life of the catalyst. Significant developmental efforts were also made [17, 18] for a more active and mechanically stable catalyst to further reduce the yields of C_1 and C_2 [19]. The process improvement efforts were also focused on developing a catalyst which minimized the shift reaction.

It was suggested [8] that further selectivity in FT reactions can be attained by either poisoning acceptable catalysts with sulfur compounds or by selecting sulfides of less frequently used catalysts. Storch et al. [20] reported that the initial effect of small amounts of H_2S is the increase in nickel–manganese catalyst activity. This was also confirmed by Herrington and Woodward [21] for cobalt–thoria–kisselguhr

Table 4 Characteristics of various Fischer–Tropsch processes [15]

Catalyst	Temp. (°C)	Pressure (atm)	C_3^+, (g/m^3)	C_3^+,[a] (kg/m^3)	Gasoline[b]	Diesel[b]	H.O. + wax	Water-soluble chemicals[b]	Steel,[c] tons/(bbl day)	Motor octane number[d]	Cetane number
Granular catalyst, externally cooled, no gas recycle											
CO	175–200	1	140	8	56	33	11	[e]	2.7	50	100
CO	175–200	10	150	10	35	35	30	[e]	2.4	25	100
Fe	200–225	10	125	10	32	18	35	15	2.5	…	…
Granular catalyst, externally cooled, gas recycle											
CO	190–224	10	160	13	50	22	22	8	1.9	…	…
Fe	230	20	145	14	19	19	58	8	2.1	…	…
Fe	275	20	145	11	68	19	3	8	2.2	…	…
Powdered catalyst, oil slurry, gas recycle											
Fe	250–275	20	170	20	25	30	31	4	1.2	…	…
Granular catalyst, internally cooled, gas recycle											
Fe	240–280	20	170	58	58	10	24	8	0.7	74	78
Granular catalyst, hot-gas recycle											
Fe	300–320	20	140	32	70	17	1	12	0.7	75	50
Fluidized catalyst, gas recycle											
Fe	300–320	20	150	115	73	7	3	17	0.6	76	…

[a]Kilogram of total product, excluding water, carbon dioxide, methane, ethane, and ethylene per volume of reactor per unit time
[b]Weight percent of oil plus water-soluble product
[c]In converter and its accessories only
[d]Bauxite treated, but no T.F.L. added
[e]Very small, less than 1%

(100:18:100) catalysts. In their experiments, H_2S is mixed with the synthesis gas in small batches and no H_2S was eliminated in the off-gas during the course of sulfur poisoning experiments. The first addition of H_2S increased the yield of liquid hydrocarbons at constant temperature. As sulfur addition continued, there was a decrease in the yield of gaseous hydrocarbons. Total hydrocarbon yield increased with sulfur addition to the catalyst until 8 mg. of sulfur was added to each gram of catalyst. This work suggested the advantage of stopping sulfidization at low level (1–4 mg of sulfur/g of catalyst) to obtain the benefits of increased liquid hydrocarbons yield. The results also suggested that the catalyst might show the same behavior if presulfided to the same degree before introducing the synthesis gas. The patent of Storch et al. [22] showed that 69% of CO conversion can be obtained for a molybdenum disulfide catalyst alkalized with 2–3% KOH in a feed of $2H_2 + CO$ at 530°F and 13.6 atm. Products from this synthesis were low boiling with 30% of the product C_3^+ hydrocarbons and organic oxygenated compounds. Laynes [23] indicated that by allowing the sulfur content of the iron catalyst to build up to an optimum ratio and maintain at that level will minimize CO_2 formation during hydrogenation of CO to form hydrocarbons.

Over last several decades, a continuous effort to improve catalyst activity, selectivity, and stability has been carried out. Besides looking at different forms of iron catalysts, nickel, cobalt, and ruthenium catalysts have been extensively studied. Both cobalt and ruthenium catalysts with different types of promoters have been extensively examined by Exxon and other oil companies. Their studies indicate that while these catalysts give higher initial activity, they also tend to decay rapidly. Numerous patents on these catalysts have been reported by Exxon and other oil companies. In recent years, MOF (metal organic framework) have been tested to improve the selectivity of FT reactions. This work is being carried out at NETL in Pittsburgh and it is still at the development stage. More work in this area (perhaps using recent developments in nanotechnology) is needed.

2.3 Isosynthesis

Isosynthesis (for the production of branched hydrocarbons) is interesting because (a) under proper conditions it gives saturated branched-chain aliphatic hydrocarbons containing 4–8 carbon atoms, (b) compared to other types of synthesis, it is the only one that uses difficult reducible oxides as catalysts [24–27], and (c) it produces isobutane for high octane gasoline. The oxide catalysts that are used for this synthesis are thorium oxide, aluminum oxide, tungstic oxide, uranium oxide, and zinc oxide. The thoria and alumina catalysts can be prepared by precipitation from nitrate solutions by adding a hot sodium carbonate solution. The other oxide catalysts can be prepared by addition of alkali to their respective nitrate solutions except in the case of tungsten which can be precipitated from Na_2WO_4 solution by nitric acid addition.

The most effective catalysts for isosynthesis are the tetravalent oxides, thoria, ceria, and zirconia. Alumina and the other oxides are not as effective in producing

Table 5 Isosynthesis results over one-component catalysts (450°C, water gas conversion [28])

Catalyst	Water gas conversion			% Hydrocarbons	C no.	% *i*-C_4 in C_4 fraction
	30 atm	150 atm	300 atm			
Thoria[a]	19			2.1	2.1	
Thoria		46		5.1	2.6	88
Thoria			66	6.4	2.8	
Alumina[b]	54			11.0	1.4	
Alumina[b]		53		10.5	1.5	59
Alumina[a]			21	3.1	2.0	
W_2O_5	58			12.9	1.3	
ZrO_2[a]	9			1.0		
ZrO_2		31		3.5	2.1	82
ZrO_2			36	3.5	2.3	
UO_2[a]				3.7	1.4	
ZnO[a]	10			1.2	1.3	
ZnO			44	10.0	1.1	
CeO_2[a]	7			0.5	2.0	
CeO_2		10		1.0	2.4	81

[a]From nitrates
[b]From sodium aluminate (or tungstates)

isobutane. Other oxides such as chromia, lanthana, praseodymium oxide, magnesia, manganese oxide, titania, and berylia have been tested but they had lower activity. Of all the catalysts tested so far, thoria or promoted thoria has been the most promising catalysts. Unlike catalysts of iron group, thoria is not poisoned by sulfur compounds. In addition, an activity decline due to carbon deposition can be easily overcome by simply passing air over the catalyst to generate CO_2 at the synthesis temperature. Some typical results for one-component catalysts at various pressures are given in Table 5.

Thoria catalyzes the production of hydrocarbons with relatively high carbon number from synthesis gas. Furthermore, the so-called gasol hydrocarbons consisting of mainly C_3–C_4 also contain large amounts of isobutane. In contrast, the trivalent oxide alumina produced mainly methane and carbon with small amount of "gasol" and traces of isobutane. The most active divalent oxide, zinc oxide, produced no liquid hydrocarbons but mainly methane and alcohols. For thoria catalyst, the best temperature has been found to be between 375 and 475°C. Alcohol production dominated below 375°C and methane and LPG were the main products between pressure of 300 and 600 atm. Below 300 atm, gas conversion was small; above 600 atm, methane and dimethyl ether were obtained.

The effects of additions of various promoters on the performance of thoria catalysts have also been examined. Three promoters have been studied: (1) alkali to increase molecular weight of the product, (2) phosphoric acid to convert unsaturated hydrocarbons such as propane to *n*-butene to higher branched hydrocarbons particularly to dimers, and (3) zinc oxide and alumina to enhance the formation of alcohols and subsequently the dehydration of alcohols for the formation of branched hydrocarbons.

The alkali did not work well and the activity of thoria catalyst decreased with an increase in alkali content. The most effective promoter was alumina. For thoria–alumina catalyst, the literature data show [29] that the amount of isobutene increased with an addition of alumina; best results were obtained at 20% alumina on thorium oxide. Catalysts prepared by separate precipitation and mixing of the wet precipitates produced the highest *i*-C_4 (isobutane) yields. While "gasol" increased with an increase in temperature, C_5^+ and alcohols (not shown in the table) decreased with an increase in temperature. *i*-C_4 increased with an increase in temperature. In this study, thoria was precipitated from a nitrate solution with sodium carbonate while aluminum oxide was precipitated from a sodium aluminate solution using sulfuric acid. Finally, the best thoria–alumina–zinc oxide catalysts gave lower yields of isobutane and somewhat higher yield of C_5^+ hydrocarbons than thoria–alumina catalysts. Once again, just like for FT synthesis, most recent efforts on the catalyst development for isosynthesis are focused on improving product selectivity.

3 Processes for Syngas Productions and Syngas to Liquid Conversion

A process for converting fossil fuels such as crude oil, heavy oil, coal, shale oil, tar sand, bitumen, etc., or biomass to liquid fuels such as methanol, biogasoline, biodiesel, or biojet fuel, etc., generally contain five steps: pretreatment, gasification, gas cleaning and conditioning, FT process, and final product separation and possible upgrading. This section outlines some details of each of these steps with special attention to biomass feedstock.

3.1 Pretreatment

The first step is the pretreatment of fossil fuel or biomass. Here undesired impurities such as mineral matters, inorganic impurities (particularly in biomass), sulfur, etc., are removed and particle size of the feed stock is adjusted to satisfy the need of the subsequent gasification process. Pretreatment of coal requires removal of ash and sulfur along with adjustment of the particle size. The inorganic sulfur and ash are often removed by the floatation technique supported by the fine particle technology. Pretreatment step is particularly important for biomass. Unlike coal, biomass is a low density (both mass and energy) product and easily degradable in the natural environment. The storage and transportation of biomass are very problematic because of its low density and easy degradation. The reduction of biomass particle size to the desired level is also problematic because it requires high grinding energy. Biomass is generally wet and contains a large amount of water. The removal of this water is also important for high energy efficiency of the gasifier.

Numerous pretreatment processes for biomass have been examined. The advantages and disadvantages of these processes are outlined in Table 6.

Table 6 Summary of advantages and disadvantages of various biomass pretreatments [30]

Biomass pretreatment	Advantages	Disadvantages
Sizing (grinding, chipping, chunking, milling)	Adjusts the feedstock to the size requirement of the downstream use	Nonbrittle character of biomass creates problems for sizing Should be done before transportation but storage of sized materials increases dry matter losses and microbiological activities leading to GHG (CH_4, N_2O) emissions
Drying	Reduces dry matter losses, decomposition, self-ignition, and fungi developments during storage Increases potential energy input for steam generation	Natural drying is weather dependent; drying in dryers requires sizing
Bailing	Better for storage and transportation; higher density and lower moisture content	Cannot be used without sizing for gasification
Briquetting	Higher energy density, possibility for more efficient transport and storage Possibility for utilization of coal infrastructure for storage, milling, and feeding; rate of combustion comparable with coal Reduces spontaneous combustion	Easy moisture uptake leading to biological degradation and losses of structure Require special storage conditions Hydrophobic agents can be added to briquetting process, but these increase their costs significantly
Washing/leaching	Reduction of corrosion, slagging, fouling, sintering, and agglomeration of the bed washing is especially important in case of herbaceous feedstock Reduced wearing out of equipment, and system shut down risks	Increased moisture content of biomass Addition of dolomite or kaolin, which increases ash melting point, can also reduce negative effects of alkali compounds
Pelletizing	Higher energy density leads to better transportation, storage and grinding, and reduced health risks Possible utilization of coal infrastructure for feeding and milling (permits automatic handling and feeding)	Sensitive to mechanical damaging and can absorb moisture and swell, loose shape, and consistency Demanding with regard to storage conditions

(continued)

Table 6 (continued)

Biomass pretreatment	Advantages	Disadvantages
Torrefaction	Possibility for utilization of coal infrastructure for feeding and milling Improved hydrophobic nature—easy and safe storage, biological degradation almost impossible Improved grinding properties resulting in reduction of power consumption during sizing Increased uniformity and durability	No commercial process Torrefied biomass has low volumetric energy density
TOP process	Combines the advantages of torrefaction and pelletizing Better volumetric energy density leading to better storage and cheaper transportation Desired production capacity can be established with smaller equipment Easy utilization of coal infrastructure for feeding and milling	No commercial process Does not address the problems related to biomass chemical properties, i.e., corrosion, slagging, fouling, sintering, or agglomeration

For combustion and gasification, biomass particle size, water content, decay resistance, and inorganic impurities are important parameters. For these reasons, leaching and torrefaction are considered to be the two most important pretreatment steps. Leaching process will remove salts and other inorganic impurities from the biomass and can be easily carried out using hot water or steam. Torrefaction process makes biomass hydrophobic, easy to crush, and improve its resistance for decay. A typical comparison of grinding energy required for untreated and torrefied wood is illustrated in Fig. 2. This comparison clearly indicates the important role torrefaction can play in reducing the grinding energy of biomass. Torrefied biomass also has higher mass density and it is resistant to water and biological decay. These parameters help the transportation and storage of biomass. The positive features of torrified biomass for gasification are given in Table 7.

3.2 Gasification

For fossil fuel, the gasification technology is very mature and commercialized. Numerous gasifier technologies are available and they are well described in the literature [14]. Earlier commercial gasifiers tend to be low pressure gasifiers operating

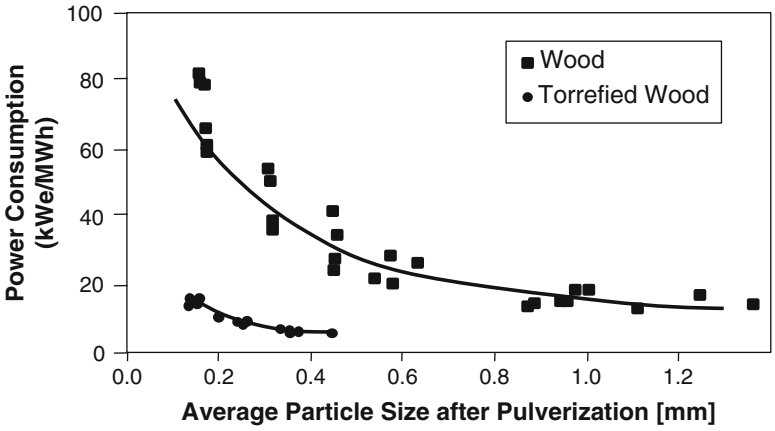

Fig. 2 Power consumption for size reduction: wood vs. torrefied wood [31–35]

Table 7 Positive features of torrefied biomass for gasification and other applications [32–35]

Torrefied product
Has lower moisture content and higher heating value
Is easy to store and transport
Is hydrophobic; does not gain humidity in storage and transportation
Is less susceptible to fungal attack
Is easy to burn, forms less smoke and ignites faster
Significantly conserves the chemical energy in biomass
Has heating value (11,000 Btu/lb) that compares well with coal (12,000 Btu/lb)
Generates electricity with a similar efficiency with that of coal (35% fuel to electricity) and considerably higher than that of untreated biomass (23% fuel to electricity)
Has grindability similar to that of coal
Requires grinding energy 7.5–15 times less than that for untreated biomass for the same particle size
Has mill capacity 2–6.5 times higher compared to untreated biomass
Possess better fluidization properties in the gasifiers
Is suitable for various applications in heating, fuel, steel, and new materials manufacturing industries

with a varying temperature to obtain producer gas with different levels of methane, carbon monoxide, hydrogen, carbon dioxide, and water with other small levels of hydrocarbons and impurities. High, medium, and low Btu gases produced by the gasifier depend on the level of methane in the producer gas. Generally, gasifier either uses air or oxygen. However, in recent years other gaseous carriers such as steam, hydrogen, and carbon dioxide have also been examined. The main purpose has been to improve energy efficiency, conversion, and an adjustment of the final composition of the producer gas. A notable effort on hydrogasification is being carried out at University of California at Riverside [36].

In recent years, high pressure gasifiers have also been tested and preferred. Some efforts have also been made to examine gasification under supercritical conditions.

- Entrained-flow dominates overall gasification market
- However - NO commercial-scale biomass/waste plants utilize entrained-flow gasifiers

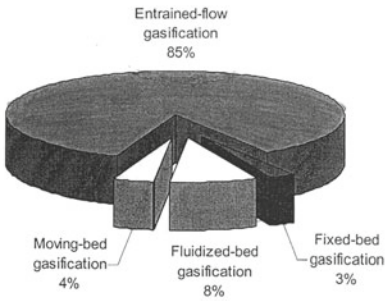

	Feed Class [count by plant]					
Technology Type	Biomass/ Waste	Coal	Gas	Petcoke	Petroleum	Grand Total
Entrained-flow gasification		41	22	9	60	132
Fixed-bed gasification	1	3				4
Fluidized-bed gasification	10	3				13
Moving-bed gasification	2	4				6
Grand Total	13	51	22	9	60	155

Fig. 3 Overview of commercial biomass gasification experience: 2004 world gasification survey [38, 39]

Both water and carbon dioxide have been used as supercritical media. These conditions, in general, reduce the required temperature for gasification and it also alters the composition of the producer gas (for example, with super critical water, more hydrogen and carbon dioxide are produced). A good review of gasification in supercritical water has been given by Guo et al. [37].

Numerous reactor technologies for the gasifier have also been tested. Earlier studies used fluidized bed (both homogeneous and turbulent), fixed bed, moving bed, and circulating fluidized bed (CFB) technologies. The CFB was popular because it allowed a better control of the residence time of feed stock within the gasifier. More recently, entrained bed gasifier (or even fast fluidized or transport bed) is used and this technology is recommended for new gasification processes. An overview of commercial gasification reactor technology that is being practiced is illustrated in Fig. 3 [38, 39]. It is clear from this figure that the entrained flow gasifier dominates the commercial market and it should be used for the future gasification of biomass. The entrained bed allows a small residence time with very little backmixing of solid particles. This type of reactor dynamics allows a better modeling and scale-up capability for such a reactor. The entrained bed reactor can also be circulating bed in order to maximize the residence time of the feedstock. Significant research on the design of gasifier internals has also been carried out to improve energy efficiency, reduce formation of harmful gaseous impurities, and reduce or better handle the slag formation within the reactor.

Most gasifiers are operated with dry feed, although GE has developed gasification technology for the slurry feed. Unlike for coal, dry feeding of biomass, particularly

Table 8 Product compositions and applications for various types of reforming reactions [42]

Reforming reaction	H_2/CO	Possible application
Dry reforming	1 or less	Polycarbonates, oxo-alcohol, formaldehyde, iron ore reduction
Partial oxidation	~2	Methanol, FT synthesis
Steam reforming and WGS reaction	>3	H_2 production, NH_3 synthesis

in the pressurized gasifier is a challenging problem. Several devices have been developed (e.g., Stamet) to effectively feed dry biomass in the gasifier. In general, coal gasification is operated at a higher temperature than biomass gasification. This is because biomass is more reactive and easy to thermally decompose. For FT application, a gasifier needs to produce syngas (carbon dioxide and hydrogen) as pure as possible. This is generally achieved by increasing the temperature of the gasifier (greater than 1,200°C). For biomass, a pressurized oxygen-blown entrained flow gasifier is preferred. This technology has been identified as an optimum technology for biosyngas production as it has the advantages of (a) high efficiency of biosyngas production [40], (b) fuel flexibility for all types of biomass, e.g., wood, straw and grassy materials, and coal with possibility to use coal as backup fuel, and (c) suitability for scales of several hundreds to a few thousand megawatt [41]. As discussed earlier, biomass requires significant pretreatment to allow stable feeding to the gasifier without excessive inert gas consumption. Torrefaction is one of the most promising routes, as it has efficiency up to 97% and torrefied biomass can be handled and fed to the gasifier with existing coal infrastructure. Entrained flow gasification for coal is a well established and commercial technology which can be readily adapted for biomass.

In order to get the right composition of syngas and removing methane from the exit gases, the gasifier is often followed by a reformer. The reformer adjusts the syngas composition that is most desirable for FT, methanol, or other syntheses. The typical H_2/CO ratios required for various end uses are described in Table 8. As shown, the nature of reforming process required depends on the end use of the syngas.

3.3 Gas Cleaning and Conditioning

The raw syngas from the gasifier needs significant cleaning and conditioning and treating before it is suitable for subsequent catalytic synthesis. A typical composition of the raw biosyngas from an air-blown CFB gasifier is given in Table 9. The syngas contains H_2/CO ratio of 0.9 and it makes up only 34 vol.% corresponding to 48.9% of chemical energy. The remainder of energy is mainly contained in CH_4, C_2H_4, and benzene (total of 44.4%). As mentioned before, this can be converted to CO and H_2 by appropriate reforming process. The major gas cleaning issue is the presence of 7 g/m^3 of tars in the gas. Tars are condensable organic compounds with boiling points

Table 9 Typical biosyngas composition for gasification of wood (15% moisture) at 850°C in an atmospheric air-blown CFB gasifier [43, 44]

Main components	Vol. %, dry	Impurities	mg/m^3
CO	18	NH_3, HCl, H_2S	2,480
H_2	16	All COS, CS_2, HCN, HBr	<25
CO_2	16	Dust, soot, ash	2,000
H_2O (relative to dry gas)	13		
N_2	42	*Tar classes*	
CH_4	5.5	Class 1 (unidentified)	330
Ethane, ethylene, acetylene	1.85	Class 2 (heteroatoms, phenols)	510
Benzene, toluene, xylene (BTX)	0.53	Class 3 (1 ring excl. BTX)	370
Sum of tars	0.12	Class 4 (2,3 rings, naphthalene)	7,550
Total	100	Class 5 (> or equal 4 ring)	650

between 80 and 350°C. When the temperature in the system decreases below 350°C, tars start condensing resulting in fouling and ultimately failing of the system. Typical inorganic biomass impurities are NH_3, HCl, and H_2S and in minor quantities COS, CS_2, HCN, and volatile metals. Also, 2 g/m^3 of solids are present in raw biosyngas.

A typical gas conditioning lineup comprises gas cooling, water gas shift (or other reforming), CO_2 removal, and impurities removal (e.g., H_2S, COS, HCN, volatile metals). Cooling can be achieved with a cooler or a water quench. While a cooler can utilize latent heat in the gas, for biomass there is an increased risk of fouling due to relative high alkaline and chloride concentrations compared with coal. In a gasifier using water quench, fouling problems are avoided. Except for gas cooling, there is a great deal of similarity in biosyngas conditioning and the treating of fossil fuel-based syngas. Thus, biosyngas can be cleaned using the available technologies for commercial coal to liquid operations. There are no biomass specific impurities that require a totally different gas cleaning approach [40].

In commercial FT operation, catalysts are replaced or regenerated after a certain operational period. The level of gas cleaning is a matter of economics between the cost of catalyst regeneration and the cost of cleaning up front. This economics may depend on the nature of FT synthesis and the catalyst. As a rule of thumb, a maximum value of 1 ppm V may be used for the sum of the nitrogen-containing (NH_3 + HCN) and sulfur-containing (H_2S + COS + CS_2) compounds. For the halides (HCl + HBr + HF) and alkaline metals, a lower level of 10 ppb V should be targeted. There are no limits regarding the poisoning of the catalysts by the tars. For FT synthesis, since gas is compressed to 25–60 atm pressure, the concentration of organic compounds must be below the dew point at FT pressure so as to avoid condensation of tars which can poison the catalyst and foul up the entire system. For thiophene and pyridine, the concentrations should be below ppmV level since they poison the catalysts. Solids should be removed completely as they foul the system and obstruct the operation of the fixed bed reactor. For H_2, CO, CO_2, CH_4, N_2, paraffins such as ethane and propane, and olefins such as ethylene and propene there are no standards. While hydrocarbons can be further reduced to CO and H_2 by reforming, their small concentrations do not affect the operation of the FT reactor. Often BTX (benzene, toluene, and xylene) are used as guidelines for gas cleaning.

3.4 FT Reactor

FT reactor can be either a fixed bed reactor or a slurry bed reactor. In earlier studies and commercialization, fixed bed reactor technology was extensively used. Since FT process is exothermic, a careful control of heat and mass transfer is very important for CO conversion and catalyst selectivity and stability. In the fixed bed reactor, special efforts have been made to design the reactor internals to remove the heat and control the reactor temperature. More recently, slurry bed reactor is preferred because it offers distinct advantages for the control of both mass and heat transfer problems that may affect the reactor performance. Slurry bed reactor also allows more flexibility in the use of the catalyst particle size. For coal and petroleum derived syngas, commercial FT reactors are being operated by Shell, Exxon, Sasol, Syntroleum among others all over the world. Shell GTL PEARL project in Qatar produces 70,000 bbld (barrels per day). Shell also has a smaller commercial plant in Bintulu, Malaysia which produces 14,700 bbld. Syntroleum operates FT process in Australia. Sasol-QP GTL ORYX-1 project in South Africa produces 34,000 Bbld. These and many other commercial technologies can be readily used for the FT process that uses biosyngas. The size of FT process will depend on the size of the gasifier for an integrated process. For example, a BTL (biomass to liquid) plant producing 2,100 Bbld will require a gasifier producing 250 MWth [38].

While existing commercial technology for GTL and CTL can be used for BTL, the scale of BTL plant is going to be important. Unlike, coal and natural gas, biomass is difficult to transport and store, and the cost of feed preparation of biomass can become an important factor in the scale of BTL process. This issue has been briefly discussed later in the economy of scale of BTL operation. Since FT process is oblivious to how syngas is produced (as long as its composition is not significantly varied), gasification technology is the key to the integration of GTL, CTL, or BTL process. In order to take advantage of the economy of scale, significant efforts are being made to examine CBTL (mixture of coal and biomass to liquid) process. As discussed later, this process offers some distinct advantages over CTL or BTL process.

3.5 Products Separations and Upgrading

The products from the FT reactor are generally separated as gas, liquid, and solid (which may include catalyst for a continuous slurry phase reactor). The off-gases can be recycled back to the gasifier or to FT reactor feed before or after a reforming stage. The catalysts from solids are separated and the remaining solids can also be recycled to the gasifier or a reformer. Portions of hot gas and solids can be used for process heat as well as for the generation of electricity through a downstream combustion process. The main liquid product is then upgraded to produce ASTM standard biodiesel, biogasoline, or biojet fuel using standard refining and hydroprocessing operations. As mentioned earlier, the nature of the liquid produced from FT reactor will depend on the nature of the catalyst, operating conditions, and H_2/CO ratio. The upgrading strategy will, therefore, depend on the nature of the liquid and the desired end-product.

4 An Integrated Process for Biomass to Biodiesel Oil Production via Fischer–Tropsch Synthesis

A schematic of typical integrated BTL process is shown in Fig. 4. Some modifications of this basic process are also being investigated. For example, researchers at University of California, Riverside are examining a process illustrated in Fig. 5. The key modification is the replacement of a conventional gasification by a hydrogasification reactor [36] to produce biosyngas from biomass. In general, various

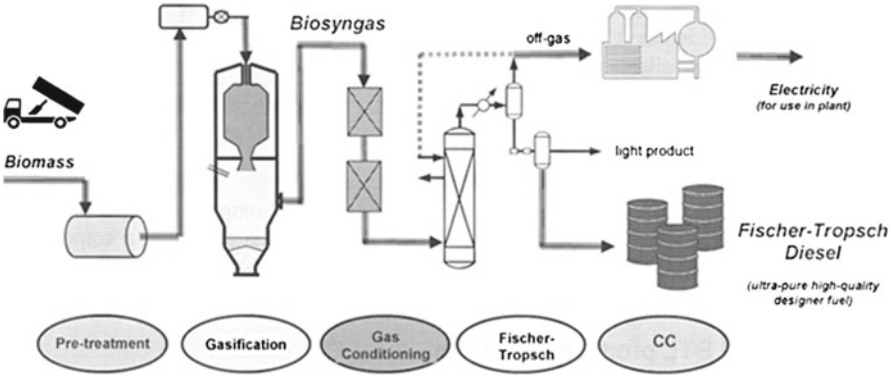

Fig. 4 Schematic lineup of the integrated BTL plant [38]

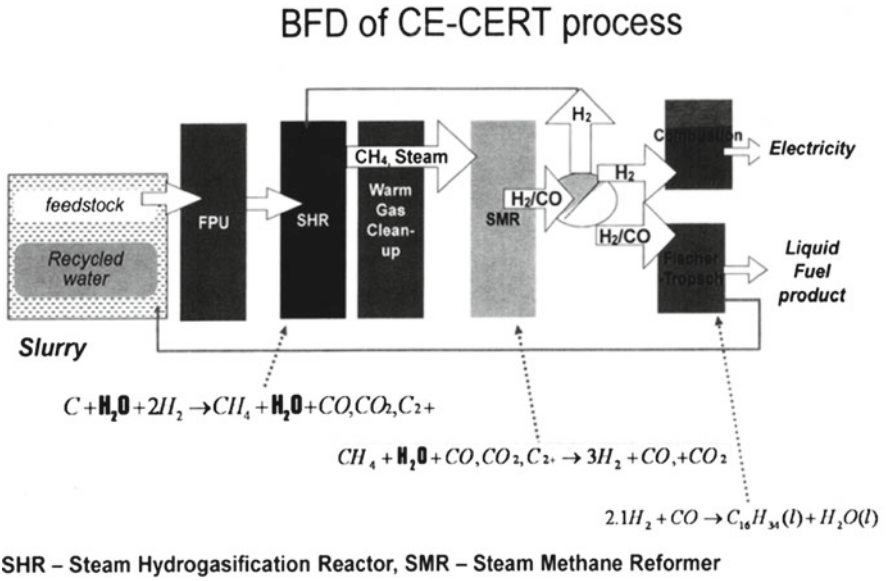

Fig. 5 A modified integrated BTL process [36]

modifications of an integrated BTL process are possible depending on the use of preferred technologies in basic five elements of an integrated BTL process.

Boerrigter et al. [43] point out that a design of an integrated BTL process depends on whether or not one takes a front-end approach or a back-end approach.

4.1 Front-End Approach

In the front-end approach, the scale of the plant is dependent upon the scale of the gasifier. The principal idea in this approach is that FT liquid, heat and electricity are the desired products. This is generally used for the gasifier of the size 1–100 MWth [45]. In this approach, the off-gases from FT reactor are used to generate heat and electricity in a combined cycle. The fundamental assumptions and other elements that justify this approach are:

1. The gasifier is small and air blown.
2. Once pass through FT reactor operation to avoid accumulations of inert like N_2 (present at 40 vol.% in biosyngas, CO_2, CH_4, and other gaseous C_1 to C_4 FT products).
3. No adjustment of H_2/CO ratio via WGS reaction and CO_2 removal thus reducing the cost of gas conditioning.
4. H_2 concentration is the limiting factor for the conversion of once-through FT synthesis. The unconverted H_2, CO and other hydrocarbons are used to generate heat and electricity. The conversion to liquid is, therefore, low. When the purpose of the tri-generation plant is to improve the production of FT liquid, a shift step is introduced as a part of the overall system. This step allows to maximize the total yield of $H_2 + CO$ in the FT synthesis.
5. The basic gas conditioning system will include the removal of tars and BTX by OLGA unit, the removal of inorganic impurities by wet gas cleaning technique, and the removal of H_2S and remaining trace impurities by ZnO and active carbon filters.

4.2 Back-End Approach

The objective of this approach is to convert feedstock into FT liquid as much as possible. The heat and particularly electricity generations are of secondary importance. This approach requires a large production capacity. Since FT process has a high fixed cost, the economy scale is important to produce FT liquid competitively with other biofuels such as bioethanol, biodiesel, as well as FT liquids derived from fossil fuels [46]. This means gasifiers of the size at least greater than 1,000 MWth are required. Fundamental assumptions and other elements of this approach are:

1. FT off-gas is recycled to the biomass gasifier to achieve maximum syngas conversion. Electricity is produced as a “by-product” from the relatively small recycle bleed stream.
2. The yield of syngas $H_2 + CO$ in the FT feed gas must be as high as possible.

3. Since significant energy remains in CH_4, C_2H_4, BTX, and tar, the process requires tar cracker and shift reactor or a reformer to convert all hydrocarbons into CO and H_2. The increase in feed H_2+CO and increase in their yields result in much higher production of FT liquids and wax and higher overall efficiency of 63.5%.
4. Both gasifier and tar cracker must be oxygen blown to reduce dilution of recycle stream by N_2 and other inert materials.
5. Unlike in the front-end approach, the part of gas conditioning system, CO_2 removal step is essential.

4.3 Economics of an Integrated BTL Process

Boerrigter [43] has studied the economics of BTL plant to produce green biodiesel from biomass using an integrated back-end approach to the plant design. His main conclusions are as follows:

1. Fixed cost for BTL plant is generally 60% higher than the one required for GTL plant of the same size. This is because the requirements of larger air separation unit, 50% more expensive gasifier because of the special solids handling, and the requirement of Rectisol unit for bulk gas cleaning.
2. BTL plants of 1,000–5,000 MWth (size of gasifiers) are optimal.
3. For production below 20,000 Bbld, fixed costs increase very rapidly.
4. The heart of BTL plant is a pressurized oxygen-blown slagging entrained flow gasifier. This technology is identified as an optimum technology for biosyngas production.
5. Torrefaction is the optimum biomass pretreatment technology for the entrained flow gasification.
6. Commercially available technologies can be used for the biosyngas cleaning and conditioning as well as for FT synthesis (both fixed bed and slurry bed).
7. Large-scale facilities are required to take advantage of economy of scale. The increase in transportation cost to provide large-scale facility is less important than decrease in fixed plant costs. For a large-scale process, the diesel generated from BTL plant is competitive with $60/bbl oil price.

5 Future Directions

While significant progress have been made (particularly in Europe) to commercialize BTL plants to generate green fuel, there are several drawbacks in the use of biomass alone as a feedstock for either generation of power or the production of synthetic oil. There is no consistent supply of biomass to operate a commercial sized power or fuel plant. For fuel production, the maximum advantage of the economy of scale requires 500,000 Bbl (barrels)/day of oil production. At the present time, the largest BTL (biomass-to-liquids) plant that may be built will most likely

Table 10 Advantages and disadvantages of use of coal and biomass mixture feed for gasification [50–55]

Advantages	Disadvantages
Economy of scale—smaller biomass plants alone are inefficient and risky	Expensive feed preparation
Lower costs associated with fossil fuel consumption	Complex feed systems for co-gasification
Less CO_2 discharge (see Fig. 2)	Two separate feed injectors, versus single feed injector, may affect the gasifier performance
More stable and reliable feed supply by the mixture	Negative impact of the slagging behavior of the combined ash in the gasifier
Provides more security, less risk	Additional complication to gas cleaning system
More positive public attitude towards use of fossil fuel, renewable fuel, and reliable multisource fuel supply	More tar and oil formation in raw syngas can be a problem depending on the gasification technology

produce 50,000 Bbl/day [47–49]. Also, as discussed earlier, biomass is difficult to store, feed, and transport and requires significant and costly pretreatment. One method that is presently being pursued is to obtain syngas by the gasification of coal and biomass mixture. Once the syngas (with appropriate methane content) from such a mixture is produced, it can be easily used either for power generation or producing a variety of transportation fuel by means of FT synthesis.

The advantages and disadvantages of the co-gasification of coal and biomass mixture are briefly presented in Table 10 [50–55]. As given in this table, co-gasification provides many advantages to the production of the syngas. Pure biomass gasification process is limited to small scale, has high capital (fixed) cost, has lower thermal efficiency, and carries shut down risk. All of these are alleviated by the use of coal. The mixture of coal and biomass provides a stable and reliable feed supply that generates less carbon dioxide. Coal can be considered as the "fly wheel" that allows a continuous plant operation when biomass feedstock is not easily available. Co-gasification reduces the cost associated with fossil fuel consumption although some types of biomass can add significant cost to the overall fuel production. These advantages provide more security and less risks for project financiers than the use of pure biomass and are likely to engender more positive public attitudes towards the use of coal for fuel generation.

Table 10 also presents some disadvantages of co-gasification process. As given in this table, feed preparation and complex feed systems can be expensive. Two separate feed injectors, versus a single feed injector, may affect the gasifier performance. The slagging behavior of combined ash of coal and biomass in the gasifier may have a negative impact [17, 50–55]. The gas cleaning system may have the additional complications due to a mixture of organic and inorganic impurities. Also, depending on the gasification technology, generation of more tar or oil in the product gas may be problematic [34, 36–43].

In summary, when coal and biomass are fed together as a mixture into a gasifier, the process of feeding should be uniform, consistent, and one that allows easy

fluidization in any types of gasifier. New short residence time gasifiers prefer dry feeding because it allows maximum flexibility in the allowable operating conditions of the gasifiers. The dry feeding also allows some flexibility in varying the nature of the coal–biomass mixture feedstock. Biomass also needs to be prepared such that it forms a homogenous mixture with coal. A successful CBTL process will truly open up new possibilities for fuel production that can use a wide variety of coal and biomass, our two sources of energy that can clearly replace our demands on oil.

References

1. IEA (2005) Clean Coal Center, Fuels for biomass co-firing, ISBN 92-9029-418-3
2. IEA (1999): World energy outlook, ISBN 92-64-17140-1, p 225
3. Olah GA, Geoppart A, Surya Prakash GK (2006) Beyond oil and gas: the methanol economy. Wiley-VCH Verlah Gmbh & Co, KGaA, Weinheim
4. EPA chart (2007) Greenhouse gas impacts of expanded and renewable and alternate fuels use, EPA420-F-07-035, April, 2007
5. Anderson RB (1956) Catalysis for FT reactions. In: "Catalysis" Emmett P (ed), vol 4., Rheinhold, New York, NY, p 1
6. NETL, personal communication (2009)
7. Storch HH, Golumbic N, Anderson RB (1951) The Fischer-Tropsch and related synthesis. Wiley, New York, NY
8. Van Herwijnen T, Van Doesburg H, Djong WA (1973) Kinetics of the methanation of CO and CO_2 on a nickel catalyst. J Catal 28:391
9. Cybulski A (1994) Liquid-phase methanol synthesis: catalysts, mechanism, kinetics, chemical equilibria, vapor-liquid equilibria, and modeling—a review. Catal Rev Sci Eng 36(4):557–615
10. Lee S (1990) Methanol synthesis technology. CRC Press, Boca Raton, FL
11. Klier K (1982) Methanol Synthesis. Adv Catal 31:243–313
12. Sawant A, Parameswaran V, Lee Sand Kulik CJ (1987) In-situ reduction of a methanol synthesis catalyst in a three phase slurry reactor. Fuel Sci and Tech Int 5(1):77–88
13. Chinchen GC, Mansfield K, Spenser MS (1990) Methanol synthesis; how does it work? CHEMTECH 29(11):692–699
14. Lee S (2006) Methanol synthesis from syngas. In: Lee S, Speight JG, Loyalka SK (eds) Hand book of alternate fuel technologies (chapter 9). CRC Press, Boca Raton, FL
15. Storch HH, Golumbic N, Anderson RB (1951) The Fischer-Tropsch and related synthesis. Wiley, New York, NY, p 437
16. Dalla Beta RA, Piken AG, Shelef M (1974) Heterogeneous methanation: initial rate of CO hydrogenarion on supported ruthenium and nickel. J Catal 35:54–60
17. Obernberger I, Thek G (2002) Physical characterization and chemical composition of Densifiedbiomass fuels with regard to their combustion behaviour. In: Proceedings of the first world conference on Pellets, Stockholm, Sweden
18. Boerrigter H, Van der Drift A. Van Ree R (2005) Biosyngas; markets, production technologies, and production concepts for biomass-based syngas. ECN-report, Petten, The Netherlands, ECN-CX-04-013 (2004); also ECN Biomass presentation at 1st International Biorefinery workshop, Washington, D.C. July 20–21 (2005)
19. Storch HH, Golumbic N, Anderson RB (1951) The Fischer-Tropsch and related synthesis. Wiley, New York, NY, p 439
20. Storch HH, Golumbic N, Anderson RB (1951) The Fischer-Tropsch and related synthesis. Wiley, New York, NY, p 314
21. Herrington EFG, Woodward LA (1939) H_2S effect on cobalt-thoria-kieselguhr catalyst for isosynthesis. Trans Faraday Soc 35:958–967

22. Storch HH, Golumbic N, Anderson RB (1951) The Fischer-Tropsch and related synthesis. Wiley, New York, NY, p 315
23. Laynes ET (to Hydrocarbon Research Inc.) (1948) U.S. Patent No. 2,445,426 (Aug 1948)
24. Pichler H Ziesecke HH (1950) The isosynthesis (transl by Brinkley R, Golumbic N) Bur Mines Bull, p 488
25. Pichler H, Ziesecke HH (1949) Isosynthesis by reduced oxide catalysts-part I. Berninst Chem 30:13–22
26. Pichler H, Ziesecke HH, Titzenthaler E (1949) Isosynthesis by reduced oxide catalysts-part II. Berninst Chem 30:333–347
27. Pichler H, Ziesecke HH, Traeger B (1950) Isosynthesis by reduced oxide catalysts-part III. Berninst Chem 31:361–374
28. Shah YT, Perrota A (1976) Catalysts for Fischer Tropsch and Isosynthesis. Ind Eng Prod Res Dev 15(2):123
29. Sastri MVC, Balaji Gupta R, Viswanathan B (1974) Interaction of hydrogen and carbon monoxide on cobalt catalysts, (Part II). J Catalysis 32:325
30. Shah YT, Gardner T. Biomass Torrefaction: Applications in Renewable Energy and Fuels. A chapter in Encyclopedia of Chemical Processing, Taylor and Francis Group, New York, NY (in Press).
31. van der Drift A, Boerrigter H, Coda B, Cieplik MK, Hemmes K (April, 2004) Entrained flow gasification of biomass: ash behavior, feeding issues, system analysis, Energy Research Center of the Netherland (ECN), Petten, The Netherlands, report C-04-039, p 58
32. Bergman PCA, Kiel JHA (2005) Torrefaction for biomass upgrading, published at 14 European biomass conference and exhibition, Paris, France, 17–21 Oct 2005; also report ECNRX-05-1 80,1-08
33. Bergman PCA, Boersma AR, Kiel JMA, Prins MJ, Ptasinski KJ, Janssen FJJG (2005) Torrefactionfor entrained flow gasification of biomass In: Van Swaaij WPM et al (ed) Proceedings of 2nd world biomass for energy industry and climate protection, Italy, 10–14 May 2004, p 679–682, also report ECN-C-05-026, ECN, Petten, The Netherlands
34. Bergman PCA (2005) ECN report ECN-c-05-073, Petten, The Netherlands, p 29
35. Bergman PCA, Boersma AR, Kiel JHA (2004) ECN-RX-04-029, p 78–82
36. Park CS, Hackett C, Norbeck JM (2005) Synthetic diesel fuel production from carbonaceous feed stocks. Presentation to ISAF XV, Int. symposia on alcohols and fuels, CERT, University of California, Riverside (Sept 2005)
37. Guo L, Cao C, Lu Y (2010) Supercritical water gasification of biomass and organic wastes. In: Momba M, Bux F (eds) Biomass (chapter 9) p 165; ISBN 978-953-307-113-8, pp 202 (Sept. 2010), Sciyo, Croatia downloaded from SCIYO.COM
38. Boerrigter H (2006) Economy of biomass to liquid (BTL) plants—an engineering assessment, ECN-C-o6-o19 (May 2006)
39. NETL Office of Systems, Analysis and Planning (2007) Co-conversion of coal and biomass into fuels with reduced carbon emissions, overview of Ongoing Scoping Study, Pittsburgh, PA (31 July 2007)
40. Boerrigter H, Calis HP, Slort DJ, Bodenstaff H, Kaandorp AJ, Uil H. den, Rabou LPLM, Gas cleaning for integrated biomass gasification (BG) and Fischer-Tropsch (FT) systems, Energy Research Center of the Netherland (ECN), Petten, The Netherlands, report C-04-056 (Nov 2004) p 59
41. Boerrigter H, Drift A van der (2004) Biosyngas: description of R&D trajectory necessary to reach large-scale implementation of renewable syngas from biomass, Energy Research Center of the Netherland (ECN), Petten, The Netherlands, report C-04-112 (Dec 2004) p 29
42. Shah YT, Gardner T (2011) Dry Reforming of Hydrocarbon Feedstocks. A paper submitted to Catalysis Review, Marcel Dekker, CRC Press, New York
43. Boerrigter H, Uil H den, Calis HP (2002) Green diesel from biomass via Fischer-Tropsch synthesis: new insights in gas cleaning and process design. In: Paper presented at pyrolysis and gasification of biomass and waste, Expert meeting, Strasbourg, France (30 Sept–1 Oct 2002)

44. Johansson TB Kelly H Reddy AKN Williams RH (1992) Renewables for fuels and electricity, UNCED (June, 1992)
45. Daey OC, Den Uil H, Boerrigter H (2000) Trigeneration from biomass and residues. In: Proceedings of progress in thermodynamical biomass conversion (PITBC), Tyrol, Austria (17–22 Sept 2000)
46. Callis HPA, Haan H, Boerrigter H, Van der Drift A, Peppink G, van den Broek R, Faaij A, Venderbosch RH (2002) Preliminary techno-economic analysis of large-scale synthesis gas manufacturing from imported biomass. In: Pyrolysis and gasification of biomass and waste, Expert Meeting, 30 Sept–1 Oct 2002, Strasbourg, France, pp 403–418. Also in SDE, Amsterdam, concept report (5 May 2002)
47. Bergman PCA, Boersma AR, Kiel JHA (Jul 2005) Torrefaction for entrained flow gasification of biomass, Energy Research Center of the Netherland (ECN), Petten, The Netherlands, report C-04-067
48. Gas-to-liquids news, vol V, No.6, p 11 (June 2002)
49. Natherlands Energy Research Center (ECN) (2002) ECN Biomass, Tar free producer gas. Poster presented on the Nederlandse Duurzame Energie Conferentie (NDEC), Rotterdam (27–28 Feb 2002)
50. Boerrigter H, Deurwaarder EP, Bergman PCA, Van Padsen SVB, Vann Ree Therman R (2004) Bio-refinery: high-efficient integrated production of renewable chemicals (transportation) fuels and products from biomass report ECN-RX-04-029, p 67–77
51. Boerrigter H, Van der Drift A (2005) Synthesis gas from biomass for fuels and chemicals, Paper for workshop organized by IEA Bioenergy Task 33 (biomass gasification) in conjunction with the SYNBIOS conference held in Stockholm, Sweden (May 2005)
52. Boerrigter H, Van der Drift A (2003) Liquid fuels from solid biomass: the ECN concept(s) for integrated FT-diesel production systems, Energy research Centre of the Netherlands (ECN), Petten, The Netherlands, report RX–03-060
53. Cavalov B, Peteves SD (2005) Status and perspectives of biomass-to liquid fuels in the European Union, European Commission, DC JRC. Institute for Energy, Petten, The Netherlands 92-894-9784-X, p 1141
54. Dacombe PJ, Jacobs JM, Kiel JHA (2003) Ash formation in entrained flow co-gasification of coal and biomass; ECN contribution to the ECSC project slag building behaviour during entrained bed coal gasification (SLABE), ECN, Petten, The Netherlands, ECN-CX-03-033
55. Livingston WR (2005) A review of the recent experience in Britain with the co-firing of biomass with coal in large pulvensed coal-fired boilers, Presented at lEA Exco Workshop on Biomass Co-firing, Mitsui Babcock, Renfrew, Scotland, Copenhagen

Chapter 13
Fischer–Tropsch Hydrocarbons Synthesis from a Simulated Biosyngas

N. Escalona, R. García, and P. Reyes

Abstract The gasification of biomass followed by a Fischer–Tropsch Synthesis (FTS) is a good alternative for synthesis of gasoline and/or diesel. However, this process may be considered as a high-cost technology, depending on crude oil and biomass raw material prices. The viability may be increased depending on the value of biomass, cost of transportation of biomass and the separation (conditioning) of gases produced in the gasification (elimination of CO_2, CH_4, N_2 and others). Nevertheless, this gas mixture "called biosyngas" may be used in the FTS without pre-conditioned for producing gasoline and/or diesel. The main focus of this chapter will be on the latest investigations in the FTS carried out in a microreactor from a simulated biosyngas (without conditioning), as an alternative to decrease the cost of this process. This chapter reports results of catalytic activity and characterization of Fe/SiO_2 and Co/SiO_2 catalysts and Cu, Re, Ru and Zn promoted Co/SiO_2 catalysts.

1 Introduction

Global warming has pushed the necessity to reduce the emissions of gases responsible for the Greenhouse effect, mainly CO_2. Public transportation produces approximately a 22% of the total CO_2, because of the use of fossil fuels. Nowadays there is great interest in the search of environmentally friendly fuels, in order to decrease the greenhouse gas emission. Biomass appears as an attractive alternative since it is a clean, renewable and sustainable energy resource. Different transformation routes have been used to convert biomass to liquid or gaseous fuels [1–5]. The first step of the overall process (biomass-to-liquid fuels, BTL) includes biomass gasification to yield a gas mixture mainly containing H_2, CO, CO_2 and CH_4, called biosyngas, which can then be

N. Escalona (✉) • R. García • P. Reyes
Universidad de Concepción, Facultad de Ciencias Químicas,
Casilla 160, Concepción, Chile
e-mail: nescalona@udec.cl

J.W. Lee (ed.), *Advanced Biofuels and Bioproducts*, DOI 10.1007/978-1-4614-3348-4_13,

adjusted to the desired H_2/CO ratio prior to being converted by the Fischer–Tropsch synthesis (FTS) [4, 5]. The FTS is the most important catalytic process in the synthesis of gasoline and/or diesel from syngas (H_2/CO) mixture [6]. The first commercial FTS plants operated with syngas mixtures produced from coal gasification, whereas the modern FTS units use CO/H_2 mixtures mainly obtained from the methane steam reforming, where the molar H_2/CO ratio is around of 2, which is much higher than the H_2/CO molar ratio close to 1 derived from biomass gasification [7, 8]. The metals used as catalysts in the FTS traditional are mainly Fe and Co promoted by K, Re, Cu or Zn [9, 10]. The hydrocarbons produced according to the FT synthesis using biosyngas mixtures are free of S and N, and in principle can be considered neutral in the CO_2 greenhouse effect. Significant efforts have been devoted to hydrocarbon synthesis using syngas mixtures produced according to the steam methane reforming technology [6–13]; however, the literature describing the production of hydrocarbons from biosyngas is quite limited [2, 14–19]. In this context, Tijmensen et al. [2] explore the technical and economic feasibility using an integrated biomass gasification and Fischer–Tropsch synthesis (BIG-FT). The results show that an integrated plant (BIG-FT) can only be profitable if the price of a barrel of oil exceeds US $50 per barrel, in agreement with Hamelinck et al. [5]. Additionally, the later author found that the cost of producing diesel from biomass by integrated gasification and FTS is 16 €/GJ. This value may decrease in the future to 9 €/GJ by further development and research in integrated technologies for the gasification and FTS. In these studies the biosyngas mixture used is pre-conditioned before being introduced to the FT reactor. In other words, the CO_2, CH_4, N_2 and other gases are removed from the mixture of feed. The cost of the gas removal processes has increased significantly. An alternative to lower the cost of production is to use biosyngas directly, without being pre-conditioned, in the FT synthesis. In this aspect, Jun et al. [14] studied the synthesis of liquid hydrocarbons over Fe/Cu/Al/K (100/6/16/4) catalysts using the biosyngas as feed. They found that this catalyst has a high fuel yield and selectivity to olefins. Recently, Co/SiO_2, CoM/SiO_2 (M = Cu, Re, Ru and Cu) and Fe/SiO_2 catalysts were studied in the SFT from simulated biosyngas feed [15, 16, 19]. These catalysts display a high CO conversion activity and the formation of hydrocarbon with Fe/SiO_2 and Co/SiO_2 catalysts was centred around of $C_{8–15}$ chain length, while the formation of hydrocarbon by Co/SiO_2 promoted was centred around of $C_{8–9}$ chain length. Therefore, the focus of this work is on the latest research in the FTS over Fe/SiO_2, Co/SiO_2 and Co/SiO_2-promoted using a model of biosyngas as feed.

2 Catalyst Preparation

2.1 Monometallic Systems

Metal-based catalysts containing metal-loading of 10–25 wt% in Fe and 10–30 wt% in Co were prepared by wet impregnation of commercial silica support (BASF D11-11, surface area (S_{BET}) = 136 $m^2\ g^{-1}$) with appropriate amounts of aqueous solution

Table 1 Cobalt and iron content (wt%), surface area (S_{BET}), total pore volume and cobalt particle size estimated from TEM of Fe/SiO_2 catalysts (taken from Refs. [16] and [19])

Catalysts	Metals (%)	Vp ($cm^3\ g^{-1}$)	S_{BET} ($m^2\ g^{-1}$)	TEM (nm)
Co (10)	10	0.26	123	37
Co (15)	15	0.22	119	38
Co (20)	20	0.20	113	41
Co (25)	25	0.20	100	47
Co (30)	30	0.20	104	52
Fe (10)	10	0.39	117	29
Fe (15)	15	0.38	86	32
Fe (20)	20	–	–	37
Fe (25)	25	0.37	78	40

of $Fe(NO_3)_2$ (Aldrich, p.a.) and $Co(NO_3)_2$ (Aldrich, p.a.), in a rotary evaporator, respectively. After impregnation, the samples were dried at 110°C for 12 h and then calcined at 450°C for 5 h. Prior to characterization and testing, the catalysts were activated in flowing hydrogen at 500°C for 12 h. The catalysts and the nomenclature used are listed in Table 1.

2.2 Bimetallic Systems

Co supported catalysts were prepared using SiO_2 (D11-11 $S_{BET} = 136\ m^2\ g^{-1}$) as a support. The support was impregnated with an aqueous solution of cobalt nitrate to get a catalyst containing 20 wt% of Co (expressed as metallic cobalt); whereas, bimetallic catalysts were prepared by co-impregnation of the support with aqueous solution of cobalt nitrate and the precursor of the second metal in appropriate amount to obtain 20 wt% of Co and 0.1 and 0.5 wt% of M (being M = Cu, Zn, Re or Ru). As precursor of the second metal, $Cu(NO_3)_2$, $Zn(NO_3)_2$, NH_4ReO_4 and $RuCl_{3*}xH_2O$ were used. The solids were dried overnight at 120°C and then calcined at 300°C (Co–Re and Co–Ru) or 500°C (Co–Cu and Co–Zn). The reduction was carried out in flowing hydrogen at 500°C, prior characterization or catalytic evaluation.

3 Catalyst Characterization

3.1 Characterization of Monometallic Systems

The S_{BET} and total pore volume (obtained at 0.95 of P/P^o) of calcined $Co(x)/SiO_2$ and $Fe(x)/SiO_2$ catalysts are shown in Table 1. As shown, the S_{BET} decreases slightly with the Co and Fe loading in both systems. This result suggests that Co and Fe species were highly dispersed into the pores of the silica substrate and that pore blockage was almost absent.

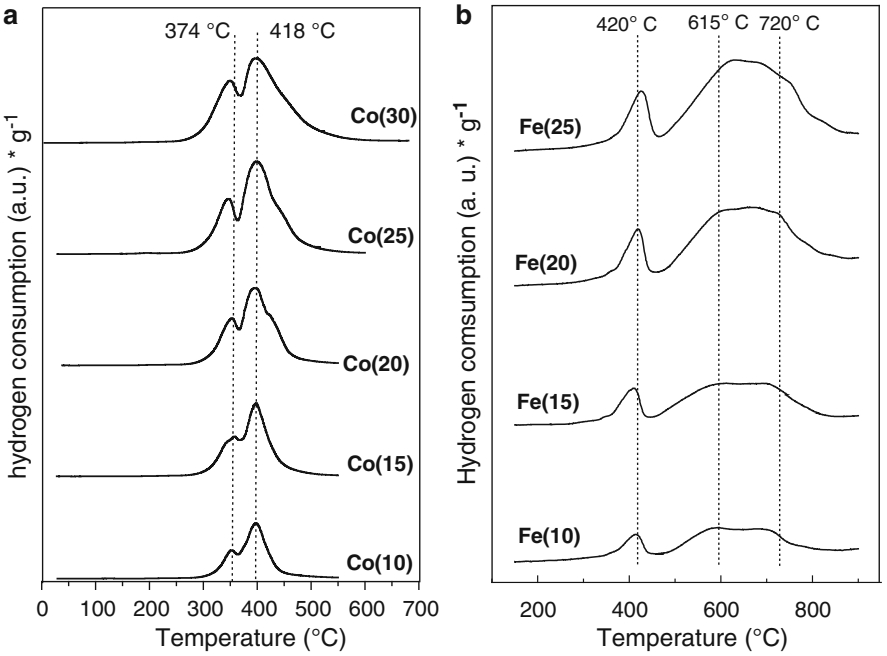

Fig. 1 Temperature programmed reduction profiles of (**a**) Co(x)/SiO_2 and (**b**) Fe(x)/SiO_2 catalysts (taken from Refs. [16] and [19])

In Table 1, the cobalt and iron particle average size estimated from TEM micrographs of Co(x)/SiO_2 and Fe(x)/SiO_2 catalysts are summarized. In general, both catalyst systems present a broadening in the metal particles size distribution upon increasing Co and Fe loading and the average particle was found to increase gradually with metals loading from 37 to 52 nm and from 29 to 40 nm for Co and Fe, respectively. Also, Table 1 shows that Fe catalysts display slightly lower metal particles size comparing to Co counterpart.

TPR profiles of the oxide precursors for both catalytic systems are given in Fig. 1 and show that the reduction process of the Co(x)/SiO_2 catalysts occurs in two distinct stages, while for the Fe(x)/SiO_2 catalysts occurs according to the three characteristic steps of the reduction of Fe_2O_3 species. For the Co(x)/SiO_2 catalysts the first peak centred at 350°C is ascribed to the transformation of Co_3O_4 to CoO, whereas the second stage centred to 406°C represents the reduction of CoO to Co [20, 21]. The relative intensity and width of the second reduction peak increases with Co-loading in a higher extent than the first peak, suggesting a higher reduction degree of CoO to metallic Co with an increase of the average diameter of Co_3O_4 particles, in agreement with results reported previously by Martinez et al. [22]. This is also in agreement with those results obtained by TEM. On the other hand, in Fig. 1b, the first peak centred at 420°C in the Fe(x)/SiO_2 catalysts is related to the transformation of Fe_2O_3 to Fe_3O_4, the second peak centred to 615°C represents the reduction of Fe_3O_4 to FeO and the third peak centred around 720°C corresponds to

Table 2 Relationship between the Co(Fe)/Si atomic surface ratio and the nominal surface density of Co and Fe for (a) $Co(x)/SiO_2$ catalysts and (b) $Fe(x)/SiO_2$ catalysts, respectively (taken from Refs. [16] and [19])

Catalysts	Si 2p (eV)	Co (Fe) $2p_{3/2}$ (eV)	Co(Fe)/Si (at/at)
Co(10)	103.5	778.0 (36)	0.020
		780.6 (64)	
Co(15)	103.4	778.0 (41)	0.033
		780.6 (59)	
Co(20)	103.5	778.0 (62)	0.043
		780.6 (38)	
Co(25)	103.4	778.0 (71)	0.063
		780.6 (29)	
Co(30)	103.4	778.0 (80)	0.092
		780.6 (20)	
Fe(10)	103.4	707.3 (12)	0.006
		710.5 (88)	
Fe(15)	103.4	707.3 (14)	0.009
		710.5 (88)	
Fe(20)	103.4	707.3 (20)	0.014
		710.5 (80)	
Fe(25)	103.4	707.3 (24)	0.029
		710.5 (76)	

the transformation of FeO to metallic Fe [23, 24]. The intensities of the three peaks gradually increase with the Fe loading. Figure 1b also shows that the position of the maximum reduction of three peaks does not change significantly as iron loading increases. This observation suggests that iron species are homogeneously dispersed on the surface of the silica carrier.

XPS results of reduced $Fe(x)/SiO_2$ and $Co(x)/SiO_2$ catalysts are summarized in Table 2. XP spectra showed that all catalysts in the Fe 2p and Co 2p region display the doublet corresponding to Fe $2p_{3/2}$–Fe $2p_{1/2}$ and Co $2p_{3/2}$–Co $2p_{1/2}$ for iron and cobalt species, respectively. Table 2 summarizes the most intense peaks of each doublet. Thus, the peak at 707.3 eV represents a signal due to metallic iron ($2p_{3/2}$) [25] and the peak at 710.5.3 eV is due to iron oxide ($2p_{3/2}$) [26]. Due to no satellite line is observed somewhere around 719.0 eV indicative of the presence of Fe^{3+} ions, it is inferred that the iron oxides responsible for the peak around 710.5 eV in the reduced catalysts comes from partially reduced iron oxides, such as Fe_3O_4 (magnetite) species. The relative intensities of the two Fe 2p components (peaks at 707.3 and 710.5 eV) are also included in Table 2 (in parentheses). It can be seen that the fraction of metallic iron determined on the surface region of these catalysts is much lower than the fraction of Fe oxides. In addition, the fraction of reduced iron to metallic state (peak at 707.3 eV) increases upon increasing the iron loading in the catalysts. This behaviour suggests that at low Fe content, the ionic Fe species strongly interact with the SiO_2 surface and therefore are difficult to reduce to the metal state under the experimental conditions of this work. On the contrary, in the catalysts with higher Fe loadings a higher proportion of tridimensional iron oxide structures are developed and therefore they can be easily reduced to zero valent

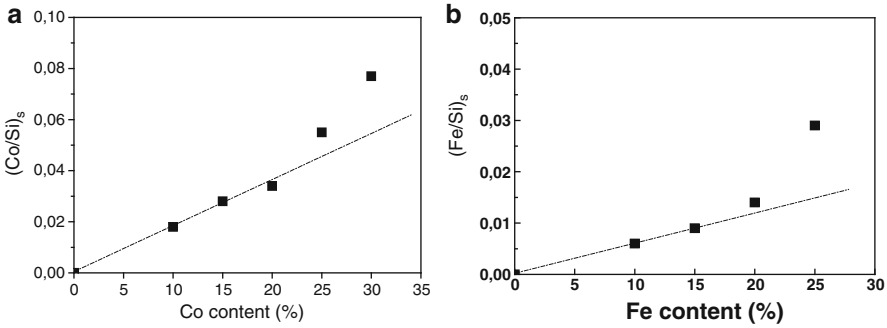

Fig. 2 Binding energies (eV) and atomic surface ratios of Co(Fe)/SiO_2 reduced catalysts (taken from Refs. [16] and [19])

oxidation state. On the other hand, the most intense $Co2p_{3/2}$ peak was fitted to two components: one at 778.0 eV belonging to metallic cobalt [27] and at 780.0 eV originated from cobalt oxide [28]. The relative intensities of the two Co 2p peaks were calculated and the values obtained are also showed in Table 2. It can be seen that the proportion of Co metallic phase increases gradually with Co-loading whereas the cobalt oxide phase follows an opposite trend. This behaviour suggests that at low Co content Co^{+2} interacts strongly with the SiO_2 support and is not completely reduced to metallic cobalt. Conversely, at higher Co-loading, cobalt is present in the form of larger particles which are easier to reduce.

In order to examine the extent of dispersion of the active phase over the silica surface, the Fe/Si and Co/Si atomic ratio were calculated (see Table 2). The variation of the Fe/Si and Co/Si atomic surface ratio as a function of metal-loading of the catalysts is shown in Fig. 2. Clearly, the Fe phase appears as rather large crystallites (around 32 nm) up to 15% of Fe. This trend is similar to that found with Co(x)/SiO_2 catalysts, where the activity increased almost linearly as Co-loading increases, reaching the maximum at about 20 wt% Co (around of 41 nm) and then levelled off. The observed deviation from linearity above 15% of Fe and 20% of Co suggests the formation of large segregated crystalline particles mainly on the external surface of the silica particles. The higher Fe/Si ratios were observed at higher Fe loading, especially for Fe(20)/SiO_2 and Fe(25)/SiO_2 catalysts. These results are likely due to the presence of a high density iron oxide particles and therefore keep less exposed the silica surface to incident photons. Similar behaviour was observed for Co(25)/SiO_2 and Co(30)/SiO_2 catalysts.

3.2 Characterization of Bimetallic Systems

Table 3 compiles the surface area and the metal particle size of Co promoted catalysts. It can be seen that the surface area is almost not affected by the addition of a promoter as expected. The metal dispersion is very low and TEM results

Table 3 Surface area (S_{BET}) and cobalt particle size estimated from TEM of Co–M (0.5)/SiO_2 catalysts (taken from Ref. [15])

Catalyst	S_{BET} ($m^2\ g^{-1}$)	TEM (nm)
Co/SiO_2	113	41
CoCu/SiO_2	106	34
CoRe/SiO_2	108	37
CoRu/SiO_2	104	34
CoZn/SiO_2	105	30

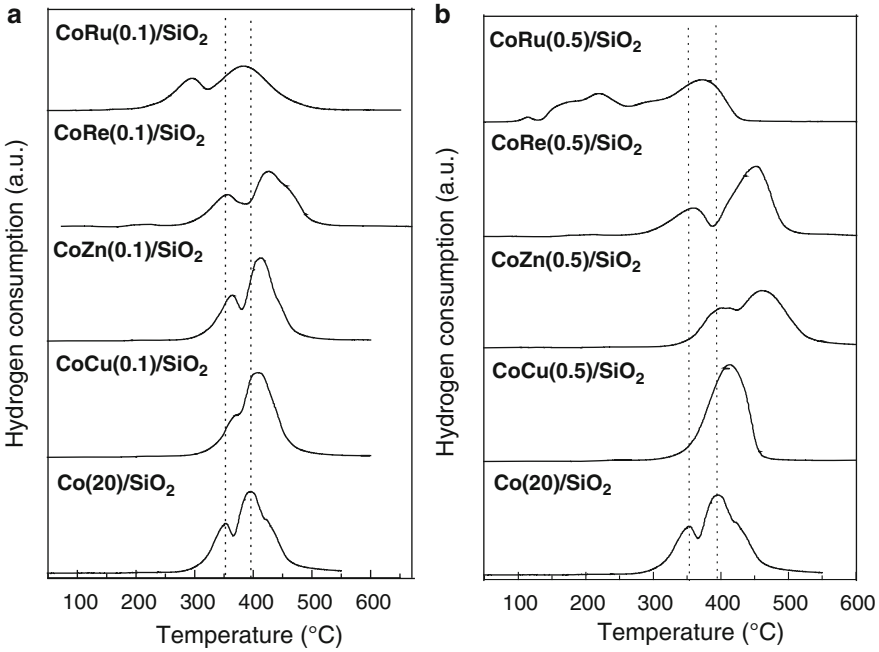

Fig. 3 Temperature programmed reduction profiles of Co–M/SiO_2 catalysts. (**a**) Series with 0.1 wt% of promoter. (**b**) Series with 0.5 wt% of promoter (taken from Ref. [15])

revealed that the promoter produces a decrease in the average metal particle size. However, this results is a consequence of a broadening in the metal particle size distribution, thus, the monometallic Co catalyst display a rather narrow distribution being most of the particles in the range 40 ± 5 nm, meanwhile in those promoted, a significant fraction of smaller particles close to 5 nm and also of larger sizes, higher than 100 nm appears.

TPR profiles of the studied samples are given in Fig. 3a, b. The profile of the samples promoted with Cu, Zn and Re with low promoter content displays a slight shift towards higher temperatures, whereas in that of Ru the shifts is to lower temperature.

Table 4 Binding energies of Si 2p, O 1s and Co 2p and Co/Si atomic surface ratios of reduced Co(20)M(x)/SiO_2 catalysts (M = Cu, Re, Ru, Zn) (taken from Ref. [15])

Catalyst	BE, eV Si 2p	BE, eV Co $2p_{3/2}$	$(Co/Si)_s$
Co/SiO_2	103.4	778.1 (62)	0.043
		780.5 (38)	
$CoCu(0.1)/SiO_2$	103.4	778.0 (82)	0.045
		780.4 (18)	
$CoRe(0.1)/SiO_2$	103.4	778.0 (87)	0.043
		780.4 (13)	
$CoRu(0.1)/SiO_2$	103.4	778.0 (88)	0.137
		780.4 (12)	
$CoZn(0.1)/SiO_2$	103.5	778.0 (65)	0.053
		780.1 (35)	
$CoCu(0.5)/SiO_2$	103.4	777.9 (80)	0.045
		780.5 (20)	
$CoRe(0.5)/SiO_2$	103.4	777.9 (90)	0.050
		780.3 (10)	
$CoRu(0.5)/SiO_2$	103.4	778.9 (90)	0.112
		780.3 (10)	
$CoZn(0.5)/SiO_2$	103.5	778.1 (67)	0.055
		780.3 (33)	

$(Co/Si)_b = 0.255$

This fact may be understood considering that the simultaneous presence of Cu (or Zn) and Co during calcinations, may lead to a mixed oxide (spinel type structures), which is more difficult to reduce than the simple oxides. The reduction of Fe oxides also takes place at higher temperatures than the Co oxides. Conversely, ruthenium oxide is reduced at lower temperature and by hydrogen spillover catalyses the reduction of cobalt oxides in bimetallic samples takes place at lower temperatures.

XPS results of reduced $Co(x)/SiO_2$ promoted catalysts are summarized in Table 4. XP spectra of Co $2p_{3/2}$ core level of the reduced samples showed the presence of Co° and Co^{2+} species and the extent of reduction is higher in the promoted samples, especially in those with Re and Ru due to the higher ability to dissociate hydrogen. Additionally, a slight enhancement in the Co/Si ratio in those samples promoted by Cu, Zn and Re account the higher dispersion of the bimetallic samples compared to the Co/SiO_2 catalyst. The increase in that ratio is much higher in those promoted with Ru, indicative of a higher dispersion degree, in line with TEM. As comparison, Co/Si atomic bulk ratio is 0.255 for the bimetallic catalysts. The observed changes may be understood on the basis of the precursors and support interaction. The cobalt nitrate solution has a pH of 5.6 being the pH values 5.6, 5.5 and 5.1 for Co–Re, Co–Zn and Co–Cu solutions, respectively. Upon the addition of the silica support the pH value drops to 4.2 ± 0.3 for these samples. On the other hand, in the Co–Ru system the pH of solution was 2.9 and decreases to 2.7 after silica addition. The isoelectric point of SiO_2 is 1–2 pH units. Therefore, differences in the interaction

between metal precursor and support should exist. Thus, even Co–Re, Co–Zn and Co–Cu systems exhibit similar features; Re is present in anionic form, whereas the others are cations, having different sites for anchorage on the support. The pH in these systems was almost the same, close to 4.2, and cobalt should be present as Co^{2+} and $CoOH^{+}$ species, whereas in the Co–Ru system, once the support was added the pH decreases to 2.73, Co being present at this pH essentially as Co^{2+}. After calcination and reduction treatments, the former species display a higher trend to form larger agglomerates than Co–Ru system.

4 Catalytic Activity

4.1 Activity of Monometallic Systems

Activity tests were carried out in a fixed bed stainless steel microreactor. The reaction conditions were: space velocity (GHSV) of 1,800 mL g^{-1} h^{-1}, pressure of 1 MPa and reaction temperature of 300°C. The feed was a synthetic representative mixture obtained from biomass gasification having $H_2/CO/CO_2/CH_4/N_2$ in the molar proportion 32/32/12/18/6, respectively [29]. Prior to the reaction, the catalysts were reduced in situ at 500°C during 12 h under hydrogen flow. The methodology of GC analysis was carried out according to previously reported works [15, 16, 18, 19].

The conversion of CO over $Co(x)/SiO_2$ and $Fe(x)/SiO_2$ catalysts as a function of metals loading at 300°C is shown in Fig. 4. The activity in both systems, expressed as percent of CO conversion, increases linearly with increasing of metals loading up to about 20% for $Co(x)/SiO_2$ catalysts and up to about 15% for $Fe(x)/SiO_2$ catalysts, and then slightly decreases. Similar behaviour has been reported by other authors; the maximum of CO conversion depends mainly on metal precursor salt, pretreatment conditions and type of support [30]. Such increase in performance for catalysts with metal-loadings up to 15 wt% for $Fe(x)/SiO_2$ catalysts and 20% wt%

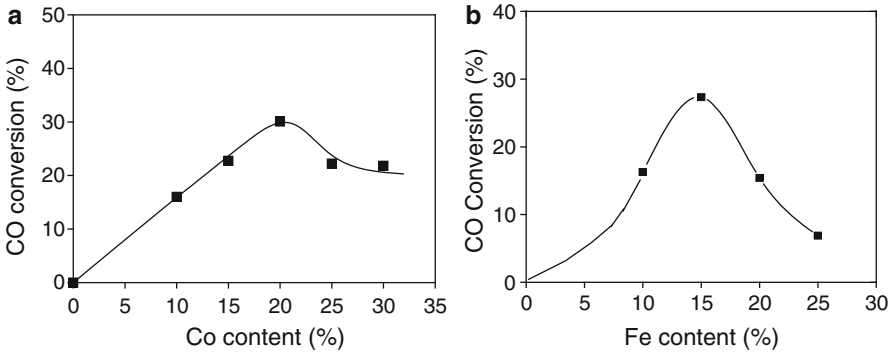

Fig. 4 CO conversion over (**a**) $Co(x)/SiO_2$ and (**b**) $Fe(x)/SiO_2$ catalysts as a function of metal-loading (taken from Refs. [16] and [19])

for $Co(x)/SiO_2$ catalysts are consistent with the observation that metal species are deposited relatively uniformly in both the external and internal surfaces of silica pores in the catalysts as it was revealed by the Fe(Co)/Si ratios derived from XPS analysis. However, a different picture emerges for higher metal-loadings. Above 15 wt% Fe-loading for $Fe(x)/SiO_2$ catalysts and 20 wt% for $Co(x)/SiO_2$ catalysts, some segregation of metal species towards the external surface of SiO_2 particles occurs; this phenomenon being more marked for the catalysts with the highest metal-loading in both catalytic systems. This result clearly shows that the activity drop is due to the loss of dispersion and the formation of the large metallic Co (or Fe) clusters.

The morphology of the Fe phase in these catalysts plays a major role on their performance. This is illustrated by comparing the highest CO conversion of the $Fe(15)/SiO_2$ catalyst, whose metal fraction in the reduced state is the lowest (14% metal by XPS), with the lowest CO conversion achieved on the $Fe(15)/SiO_2$ catalyst for which the fraction of metal area increased up to 24%. Therefore, the absence of direct correlation between the fraction of Fe metal and CO conversion indicates that other factors than metal dispersion must be considered to explain the catalytic performance. To explain this trend, it is suggested that the highest CO conversion achieved on the 15 wt% Fe catalyst is the result of two consecutive reactions (1) and (2):

$$\text{Production of HCs}: CO + H_2 \rightarrow [-CH_2-]_n + H_2O \quad (1)$$

$$\text{WGS reaction}: H_2O + CO \rightarrow CO_2 + H_2 \quad (2)$$

Thus, it is likely that the highly dispersed iron species within the pores of the substrate catalyse both the synthesis of hydrocarbons and WGS reactions with the subsequent increase in CO conversion. However, CO_2 selectivity data summarized in Table 6 indicates that CO_2 proportion decreases markedly upon increasing Fe-loading.

4.2 Activity of Bimetallic Systems

Table 5 compiles the conversion level and selectivity under steady state at 300°C and 10 atm for the studied catalysts. It can be seen that for low promoter content (0.1 wt%), the conversion of CO increases from approximately 26% for the Co/SiO_2 to values close to 32% for the promoted samples, except that promoted by Cu which exhibit a very low conversion level, close to 12%. In the series with 0.5 wt% of promoter the drop in the activity in the CoCu catalysts is even more drastic, reaching a conversion level of 8.3% and the CoZn catalyst also displays a decrease in the conversion compared with the monometallic Co/SiO_2 catalyst. Even though the cobalt particle size is smaller in the promoted samples, specially in which the promoter content is higher, and the reduction degree is higher, therefore, it should be expected for an enhancement in the catalytic activity, in those samples promoted with Zn and Cu, the opposite behaviour was observed. This may be

Table 5 Activity and selectivity results under steady state conditions in the Fischer–Tropsch reaction over Co–M/SiO_2 catalysts at 300°C and 10 bar (taken from Ref. [15])

Catalyst	Promoter (%)	Conversion CO (%)	Selectivity (C mol%)		
			CH_4	CO_2	C_{5+}
Co/SiO_2	0	25.8	93.5	0.4	6.1
$CoCu/SiO_2$	0.1	12.3	84.3	12.8	2.9
$CoRe/SiO_2$	0.1	29.7	80.3	3.3	16.4
$CoRu/SiO_2$	0.1	32.3	84.8	6.6	8.6
$CoZn/SiO_2$	0.1	28.9	86.2	9.3	4.5
$CoCu/SiO_2$	0.5	8.3	77.5	22.3	0.2
$CoRe/SiO_2$	0.5	32.2	82.1	8.3	9.6
$CoRu/SiO_2$	0.5	29.6	85.9	6.5	7.6
$CoZn/SiO_2$	0.5	22.6	85.4	7.1	7.5

interpreted as considering that in these samples the formation of spinel type oxides as a consequence of calcinations should be expected, thus reducing the extent of active sites. The presence of these mixed oxides species has already been reported for other systems. Other possibility for this behaviour is the blocking of the Co active sites by the copper itself. However, due to the small amount of promoter they were not detected by XPS.

5 Selectivity

5.1 Selectivity of Monometallic Systems

Table 6 shows the selectivity to CH_4, CO_2 and C_{5+} hydrocarbons for the $Co(x)/SiO_2$ and $Fe(x)/SiO_2$ catalysts as a function of metal-loading. In both catalytic systems a high selectivity to CH_4 was observed, similar to that observed for silica supported Co-promoted catalysts [16]. With regard to $Co(x)/SiO_2$ catalysts, the Co(20) catalyst displays the lowest CH_4 formation, whereas the other catalysts show a CH_4 formation close to 96%. The formation of CO_2 is constant and close to 0.5% in all the $Co(x)/SiO_2$ catalysts.

On the other hand, in $Fe(x)/SiO_2$ catalysts series the $Fe(10)/SiO_2$ catalyst displays the highest rate of formation of CO_2, which decreases with the increases of Fe content. In addition, the $Fe(x)/SiO_2$ catalysts show higher rate of formation of CO_2 compared to $Co(x)/SiO_2$ catalysts. This behaviour is expected because it is well known that Fe catalysts perform the WGS reaction [12]. The present and other CO_2 forming reactions cannot be discarded. For instance, a fraction of the CO_2 formed might well arise from recombination of the oxygen fragment coming from CO dissociation with other CO molecules as proposed by Krishnamoorthy et al. [11]. In this model, CO is adsorbed and dissociated on the catalyst surfaces origin; carbon

Table 6 Selectivity under steady state conditions in the Fischer–Tropsch reaction over $Co(x)/SiO_2$ catalysts at 300°C and 1 Mpa (taken from Refs. [16] and [19])

	Selectivity (C mol %)		
Catalyst	CH_4	CO_2	C_{5+}
Co (10)	96.5	0.5	3.0
Co (15)	96.4	0.4	3.2
Co (20)	93.5	0.4	6.1
Co (25)	95.4	0.5	4.1
Co (30)	96.4	0.4	3.1
Fe (10)	25.7	62.4	11.8
Fe (15)	20.5	31.6	47.8
Fe (20)	37.5	21.6	40.9
Fe (25)	75.0	19.0	5.9

and oxygen species adsorbed (C_a and O_a), whereas hydrogen does not play any role, as shown in the following reactions (3) and (4).

$$CO \rightarrow C_a + O_a \tag{3}$$

$$O_a + CO \rightarrow CO_2 \tag{4}$$

On the other hand, the $Co(x)/SiO_2$ catalysts display a low CO_2 formation being close to 0.5% in all the catalysts. Coke is also formed on the surface of $Co(x)/SiO_2$ catalysts and this can be explained by the disproportion reaction of carbon monoxide on the surface of Co crystallites according to the Boudouard reaction [31, 32]. Additionally, the CO_2 formation might also be explained by (3) and (4) similar to that of Fe/SiO_2 catalysts.

Table 6 also shows the highest formation rate of C_{5+} hydrocarbons on $Fe(15)/SiO_2$ catalyst. In general, $Fe(x)/SiO_2$ catalysts record values of selectivity of C_{5+} much larger than $Co(x)/SiO_2$ catalysts (around of 5%) [16]. This result suggests that $Fe(x)/SiO_2$ catalysts are more selective than $Co(x)/SiO_2$ ones for the production of liquid hydrocarbon from biosyngas. However, in the classic FT reactions where the H_2/CO ratio equals 2, $Co(x)/SiO_2$ catalysts are more active than $Fe(x)/SiO_2$ counterparts [6].

This different behaviour may result from the feed mixture employed. The feed mixture (biosyngas) employed here is H_2 deficient (H_2/CO ratio equal 1) and $Fe(x)/SiO_2$ catalysts may increase the formations of H_2 "in situ" via WGS reaction and therefore may improve the selectivity to C_{5+}.

Figure 5 shows the distribution of condensable products over $Fe(x)/SiO_2$ and $Co(x)/SiO_2$ catalysts as a function of metal-loading. Figure 5b shows that an increase in Fe-loading produces a shift in the distribution of condensable products. Thus, the C_9–C_{10} production of hydrocarbon chain increases with a decrease of Fe-loading. Similarly, the production of $C_{11–12}$ hydrocarbons increases with Fe-loading. This behaviour cannot be due to changes in the acidity of the catalysts upon increasing the reduction of Fe_2O_3 species with the raise of Fe content. Wan et al. [33] reported

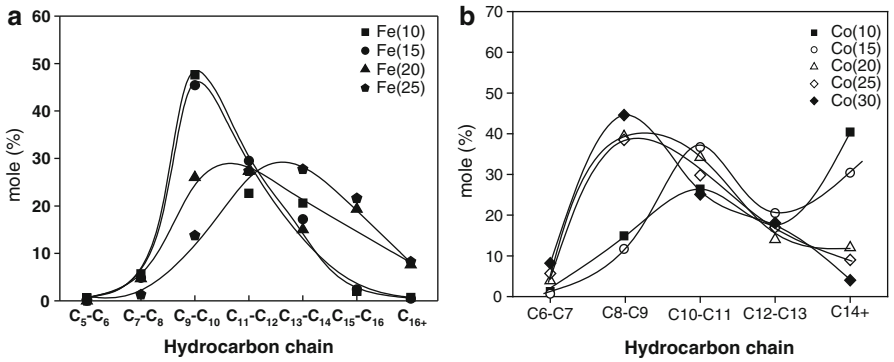

Fig. 5 Product distribution in the liquid extract produced in the Fischer–Tropsch reaction over (**a**) $Fe(x)/SiO_2$ catalysts and (**b**) $Co(x)/SiO_2$ catalysts (taken from Refs. [16] and [19])

that surface basicity suppresses the chemisorption of CO and facilitates the chemisorption of H_2, so it favours the production of low molecular weight products and enhances the hydrogenation capability. Therefore, the variation in the yield to hydrocarbon chain also may be related to metal particle size. The increases of Fe particle size could favour the formation of hydrocarbons centred in $C_{11–14}$ chain length. In general, this variation in the hydrocarbon selectivity on larger Fe particles can be attributed to the rate of secondary reactions such as olefin readsorption, as has been proposed earlier [34]. Bezemer et al. [35] and Girardon et al. [36] found that metal particles size has a strong impact on the cobalt selectivity, i.e. a decrease in cobalt particle size to 6–8 nm results in a higher selectivity to methane and higher yield to olefinic product. C_{5+} selectivity was also smaller with cobalt particles smaller than 6–8 nm. However, Khodakov [37] has shown that the catalytic properties of small cobalt particles in FT synthesis could be different from the larger ones. Therefore, the variation in the yield to hydrocarbon chain may be related to metal particle size. The increase of cobalt particle size favours the formation of hydrocarbons centred in C_8–C_9 chain length and decreases production of heavier hydrocarbons. This variation in the hydrocarbon selectivity on larger Co particles can be attributed to the rate of secondary reactions such as olefin readsorption, as has been proposed earlier [33].

5.2 Selectivity of Bimetallic Systems

Table 5 also shows the selectivity to CH_4, CO_2 and C_{5+} over bimetallic catalysts. High selectivity to CH_4 was observed for all catalysts, being even higher for the unpromoted Co catalyst. The condensable products, expressed as hydrocarbons with C length higher than C_5, are mainly obtained in those catalysts promoted by Ru and Re, with selectivity levels close to 10% or even higher in the CoRe (0.1) sample, as is shown in the Fig. 6.

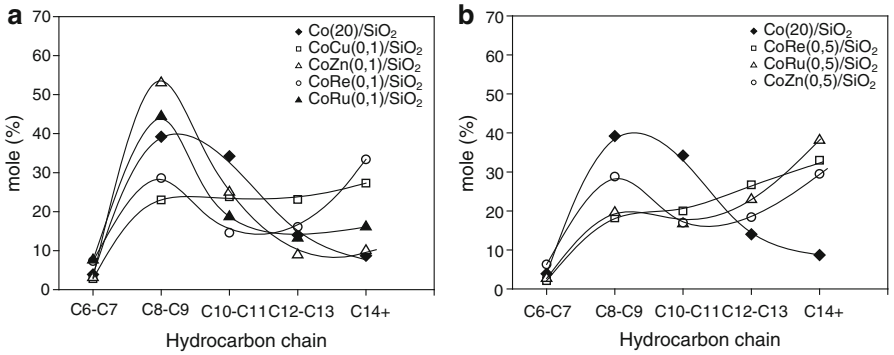

Fig. 6 Product distribution in the liquid extract produced in the Fisher–Tropsch reaction over Co–M/SiO_2 catalysts at 300°C and 10 bar. (**a**) Series with 0.1 wt% of promoter. (**b**) Series with 0.5 wt% of promoter (taken from Ref. [15])

The presence of the promoter produces a shift in the product distribution as can be seen in Fig. 6a, b. Thus, Co/SiO_2 catalyst showed a distribution with a higher proportion of C_8–C_{11}, whereas in those promoted Co catalysts the distribution is wider, increasing the proportion of larger hydrocarbons. This effect occurs in a higher extent as the promoter content increases.

This fact is attributed to a decrease in the metal particle size in agreement to that observed with Co(x)/SiO_2 catalysts. Moreover, the promoter, mainly Re and Ru, lead to a higher reduction degree of cobalt oxides and by hydrogen spillover contributes to keep in a reduced state the cobalt species, inhibiting the deactivation of the catalyst and it is also known that the presence of cobalt oxides (detected by XPS) promotes the formation of short chain hydrocarbons. It should be mentioned that the Co–Cu catalyst with 0.5 wt% of Cu did not produce liquid hydrocarbons, which may be attributed to the formation of highly dispersed $CuCo_2O_4$ spinels to the blocking of the Co active sites by the copper itself. On the other hand, Table 5 also gives the selectivity to CO_2 for the studied samples in which CoCu catalysts display the highest values (12.8–23.1%), being close to 6% for the other promoters. The formation of CO_2 may be explained for the equation proposed by Krishnamoorthy et al. [11].

6 Conclusions

The results reported in this chapter show that Fe/SiO_2 and Co/SiO_2 catalysts and Co/SiO_2 catalysts promoted by Cu, Re, Ru and Zn metal are active in the Fischer–Tropsch synthesis from a simulated biosyngas feed. The maximum conversion of CO is reached for metal-loading of 15 wt% for Fe/SiO_2 catalysts and 20 wt% for Co/SiO_2 catalysts, and then decreases at higher metal-loadings. The drop in activity is associated with the loss of active sites by formation of large metallic metal aggregates, mainly on the external surface of silica particles. In the Fe(x)/SiO_2

catalyst, the distribution of condensable products shifts to longer-chain hydrocarbons with the increase of iron content. This behaviour may be due to changes in the distribution of average particle size of Fe. Thus, $Fe(x)/SiO_2$ catalysts with a large average iron particle size, favours the formation of longer chain hydrocarbons. On the contrary, the selectivity to C_8–C_9 hydrocarbons increases, whereas the C_{14+} hydrocarbon follows an opposite trend upon increasing Co-loading in the $Co(x)/SiO_2$ catalyst. This different behaviour of selectivity may be due to changes in the reaction mechanism associated with the structure of the metallic phase. With regard to promoted Co/SiO_2 catalysts, the distribution of liquid hydrocarbons depends on the Co particles size and the reduction degree of cobalt species. Smaller metal particles and highly reduced cobalt contributes to the formation of hydrocarbons with higher chain lengths. The Co–Re and Co–Ru catalysts are those with higher activity and selectivity to higher hydrocarbons.

Acknowledgements The authors thank CONICYT for the financial support (FONDECYT 1070548 grant).

References

1. Demirbas A (2007) Progress and recent trends in biofuels. Prog Energy Combus Sci 33:1–18
2. Tijmensen MJA, Faaij APC, Hamelinck CN, van Hardeveld MRM (2002) Exploration of the possibilities for production of Fischer–Tropsch liquids and power via biomass gasification. Biomass Bioenergy 23:129–152
3. Huber GW, Iborra S, Corma A (2006) Synthesis of transportation fuels from biomass: chemistry, catalysts and engineering. Chem Rev 106:4044–4098
4. Prins MJ, Ptasinski KJ, Janssen FJJG (2004) Exergetic optimisation of a production process of Fischer–Tropsch fuels from biomass. Fuel Proc Technol 86:375–389
5. Hamelinck CN, Faaij APC, den Uil H, Boerrigter H (2004) Production of FT transportation fuels from biomass; technical options, process analysis and optimization, and development potential. Energy 29:1743–1771
6. Dry M (1981) In: Anderson JR, Boudart M (eds) Catalysis science and technology, vol I (Charter 4: The Fischer-Tropsch Synthesis). Springer, Berlin
7. Tomishige K, Asadullah M, Kunimori K (2004) Catalysis in the development of clean energy technologies. Catal Today 89:389–403
8. Chaudhari ST, Bej SK, Bakhshi NN, Dalai AK (2001) Steam gasification of biomass-derived char for the production of carbon monoxide-rich synthesis gas. Energy Fuel 15:736–742
9. Schulz H (1999) Short history and present trends of Fischer–Tropsch synthesis. Appl Catal A Gen 186:3–12
10. Dry ME (2002) The Fischer–Tropsch process: 1950–2000. Catal Today 71:227–241
11. Krishnamoorthy S, Li A, Iglesia E (2002) Pathways for CO_2 formation and conversion during Fischer–Tropsch synthesis on iron-based catalysts. Catal Lett 80:77–86
12. Davis BH (2009) Fischer–Tropsch synthesis: reaction mechanisms for iron catalysts. Catal Today 141:25–33
13. Dry ME (1996) Practical and theoretical aspects of the catalytic Fischer–Tropsch process. Appl Catal A Gen 138:319–344
14. Jun KW, Roh HS, Kim KS, Ryu JS, Lee KW (2004) Catalytic investigation for Fischer–Tropsch synthesis from bio-mass derived syngas. Appl Catal A Gen 259:221–226
15. Escalona N, Medina C, Garcia R, Reyes P (2009) Fischer–Tropsch reaction from a mixture similar to biosyngas. Influence of promoters on surface and catalytic properties of Co/SiO_2 catalysts. Catal Today 143:76–79

16. Medina C, García R, Reyes P, Fierro JLG, Escalona N (2010) Fischer–Tropsch synthesis from a simulated biosyngas feed over Co(x)/SiO_2 catalysts: effect of co-loading. Appl Catal A Gen 373: 71–75
17. Hamelinck CN, Faaij APC, den Uil H, Boerrigter H (2004) Production of FT transportation fuels from biomass; technical options, process analysis and optimisation, and development potential. Energy 29:1743–1771
18. Escalona N, Fuentealba S, Pecchi G (1999) Fischer–Tropsch synthesis over $LaFe_{1-x}Co_xO_3$ perovskites from a simulated biosyngas feed. Appl Catal A Gen 381:253–260
19. Ubilla P, García R, Fierro JLG, Escalona N (2010) Hydrocarbons synthesis from a simulated biosyngas feed over Fe/SiO_2 catalysts. J Chil Chem Soc 55:35–38
20. Saib AM, Claeys M, van Stenn E (2002) Silica supported cobalt Fischer–Tropsch catalysts: effect of pore diameter of support. Catal Today 71:395–402
21. Song D, Li J (2006) Effect of catalyst pore size on the catalytic performance of silica supported cobalt Fischer–Tropsch catalysts. J Mol Catal A Chem 247:206–212
22. Martinez A, Lopez C, Marquez F, Diaz IJ (2003) Fischer–Tropsch synthesis of hydrocarbons over mesoporous Co/SBA-15 catalysts: the influence of metal loading, cobalt precursor, and promoters. J Catal 220:486–499
23. Hayashi H, Zhe Chen L, Tago T, Kishida M, Wakabayashi K (2002) Catalytic properties of Fe/SiO_2 catalysts prepared using microemulsion for CO hydrogenation. Appl Catal A Gen 231:81–89
24. Bukur DB, Sivaraj C (2002) Supported iron catalysts for slurry phase Fischer–Tropsch synthesis. Appl Catal A Gen 231:201–214
25. Kuivila CS, Butt JB, Stair PC (1988) Characterization of surface species on iron synthesis catalysts by X-ray photoelectron spectroscopy. Appl Surf Sci 32:99–121
26. Tihay F, Pourroy G, Richard-Plouet M, Roger AC, Kiennemann A (2001) Effect of Fischer–Tropsch synthesis on the microstructure of Fe–Co-based metal/spinel composite materials. Appl Catal A Gen 206:29–42
27. Ernst B, Bensaddik A, Hilaire L, Chaumette P, Kiennemann A (1998) Study on a cobalt silica catalyst during reduction and Fischer–Tropsch reaction: in situ EXAFS compared to XPS and XRD. Catal Today 39:329–341
28. Zhou W, Chen J, Fang K, Sun Y (2006) The deactivation of Co/SiO_2 catalyst for Fischer–Tropsch synthesis at different ratios of H_2 to CO. Fuel Proc Technol 87:609616
29. Chaudhari ST, Bej SK, Bakhshi NN, Dalai AK (2001) Steam gasification of biomass-derived char for the production of carbon monoxide-rich synthesis gas. Energy Fuel 15:736–742
30. Khodakov AY, Griboval-Constant A, Bechara R, Zholobenko VL (2002) Pore size effects in Fischer–Tropsch synthesis over cobalt-supported mesoporous silicas. J Catal 206:230–241
31. Dalai AK, Davis BH (2008) Fischer–Tropsch synthesis: a review of water effects on the performances of unsupported and supported co catalysts. Appl Catal A Gen 348:1–15
32. de la Peña VA, Campos-Martin JM, Fierro JLG (2004) Strong enhancement of the Fischer–Tropsch synthesis on a Co/SiO_2 catalyst activate in syngas mixture. Catal Comm 5:635–638
33. Wan H, Wu B, Zhang C, Teng B, Tao Z, Yang Y, Zhu Y, Xiang H, Li Y (2006) Effect of Al_2O_3/SiO_2 ratio on iron-based catalysts for Fischer–Tropsch synthesis. Fuel 85:1371–1377
34. Borg Ø, Eri S, Blekkan EA, Storsæter S, Wigum H, Rytter E, Holmen A (2007) Fischer–Tropsch synthesis over γ-alumina-supported cobalt catalysts: effect of support variables. J Catal 248:89–100
35. Bezemer GL, Bitter JH, Kuipers HPCE, Oosterbeek H, Holewijn JE, Xu X, Kapteijn F, van Dillen AJ, de Jong KP (2006) Cobalt particle size effects in the Fischer–Tropsch reaction studied with carbon nanofiber supported catalysts. J Am Chem Soc 128:3956–3964
36. Girardon JS, Quinet E, Griboval-Constant A, Chernavskii PA, Gengembre L, Khodakov AY (2007) Cobalt dispersion, reducibility, and surface sites in promoted silica-supported Fischer–Tropsch catalysts. J Catal 248:143–157
37. Khodakov AY (2009) Fischer–Tropsch synthesis: relations between structure of cobalt catalysts and their catalytic performance. Catal Today 144:251–257

Chapter 14
To Synthesize Liquid Fuels on Precipitated Fe Catalyst with CO_2-Containing Syngas Gasified from Biomass

Wensheng Ning and Muneyoshi Yamada

Abstract Fischer–Tropsch (FT) synthesis is an effective method to produce liquid fuels from biomass. This chapter reports the study on precipitated Fe catalysts for conversion of CO_2-containing syngas to liquid fuels. The influences of promoter Zn, K, and Cu on CO_2 activation were analyzed by CO_2 temperature-programmed-desorption (CO_2-TPD). Cu has no strong effect to activate CO_2. K increases mainly CO_2 adsorption and is inferior to Zn in producing CO. The catalysts with high Zn/K ratio or low K content possess desorbed CO peak around 930 K in CO_2-TPD and decreased CO_2 selectivity resulted from CO_2 addition in FT synthesis. The Fe catalyst with high Zn/K ratio shows high C_2+ hydrocarbon selectivity for CO_2 hydrogenation, too. It indicates that the CO_2 contained in syngas is able to be activated by suitable promoter(s) for hydrocarbon synthesis at low temperature. The correlation between promoter composition and catalyst reactivity found for SiO_2-free Fe catalysts is effective for SiO_2-added Fe catalysts.

1 Introduction

The combustion-engine-based transportation system demands liquid fuels worldwide. Crude oil is currently the main source for liquid fuels; however, its reserve is limited. At the same time, the consumption of fuels generates significant pollutants that are damaging the environment. New technologies which can supply environmental-friendly fuels are required to overcome the above problems.

W. Ning (✉)
College of Chemical Engineering and Materials Science, Zhejiang University of Technology, Chaowang Road 18#, Hangzhou 310032, China
e-mail: wenshning@sohu.com

M. Yamada
Department of Applied Chemistry, Graduate School of Engineering, Tohoku University, Aoba 6-6-07, Aramaki, Aoba-ku, Sendai 980-8579, Japan

J.W. Lee (ed.), *Advanced Biofuels and Bioproducts*, DOI 10.1007/978-1-4614-3348-4_14,

1.1 Importance of Fischer–Tropsch Synthesis

Carbon-based energies are the main form used by human. Biomass was firstly used since the initial period of human appeared on earth. Wood (biomass) was the primary source for cooking, warmth, light, trains, and steamboats until 1885 [1]. During 1885–1950, coal became the most important fuel [1–3]. From 1955, the world entered oil age.

The supersession of one carbon-based source by another is mainly due to its energy content and feasibility to be transferred. For example, one-half ton of coal produces as much energy as two tons of wood and at half the cost [1]. Crude oil has high energy content, typically around 42 MJ/kg which is about one time higher than coal [4]. Furthermore, it is easy to be transferred via pipeline because it appears in liquid. Thus, crude oil is the perfect one among the known carbon-based energies.

However, the reserve of crude oil is limited. It is estimated that crude oil would be consumed in about 39 years according to the data of 1998 [3]. In the relatively near future, human will have to use natural gas and coal as energy source. Finally, the society will probably depend on biomass again because biomass is a regeneratable source. But it is not a simple reverse copy of energy history, biomass should be used efficiently, conveniently, and without impairment to environment [5, 6]. Besides the limited reserve, the detected crude oil distributes in narrow area. This puts risk on the energy security. The first oil embargo in 1973 triggered an energy crisis and indicated the importance of energy diversity. Since then, much effort is done to find alternative fuels. As a result, a lot of attention is paid to Fischer–Tropsch (FT) synthesis not only because it can produce plentiful liquid fuels from natural gas, coal, or biomass which are similar to those from petroleum, but also FT products are environmental-friendly [2, 7–10].

FT synthesis was first developed and practiced in Germany during 1930s and 1940s using cobalt catalysts. Subsequently, the process was commercialized on a large scale by Sasol (South African Coal, Oil and Gas Corporation) with promoted iron catalysts in South Africa [8, 11]. The two countries are rich of coal, so the FT synthesis was based on coal. From the end of the twentieth century, certain factors promoted the use of natural gas as raw materials for FT synthesis. One of them is to limit the emission of CO_2 by flaring of methane in the production of crude oil [8, 12, 13]. Nowadays, much effort is put on biomass to produce liquid fuels.

In general, FT process consists of two sequential operations [7]. One is syngas (mixture of CO and H_2) production from coal or natural gas and another is hydrocarbon synthesis from the syngas. During syngas preparation, the contained S, N is cleaned and the produced CO_2 is removed in order to obtain pure mixture of CO and H_2. The de-S and N treatment makes the FT product free of sulfur and nitrogen. The synthesized hydrocarbons have low aromatic content. The discharge of SO_X and NO_X is decreased in case of using FT products as fuels. It is also verified that low sulfur and aromatic contents leading to low yield of suspended particulate matter which is a pollutant to air [10].

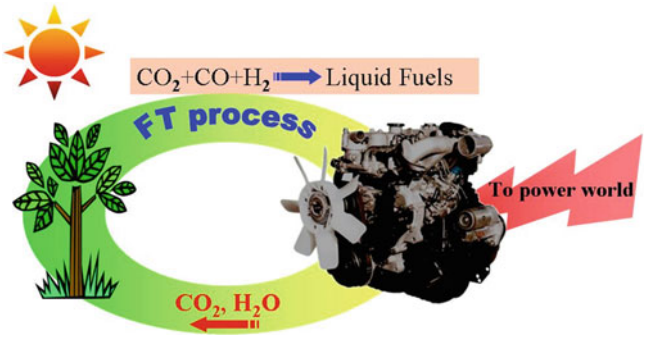

Fig. 1 Scheme of producing liquid fuels from biomass via gasification

1.2 Shortcoming of Current FT Technology

However, the current technology of FT synthesis should be improved further in view of environmental-friendly and economic profit.

One of the technical issues in the current FT process is the carbon efficiency. For example, only less than 80% carbon atoms can be converted from methane into hydrocarbons and the ratio is much lower for coal and biomass [2, 11, 14]. Other carbon atoms are discharged into atmosphere as CO_2 in the syngas production [15]. This operating model increases CO_2 emission which is responsible for green-house effect.

To use CO_2-containing syngas directly for FT synthesis is helpful to lessen CO_2 emission. By omitting de-CO_2 operation from FT process, some corresponding energy consumption is saved which would contribute to less CO_2 produced. It requires to develop catalysts active for CO_2-containing syngas.

By adopting the new FT synthesis with CO_2-containing syngas, a cycle with balanced carbon can be set up: (1) Hydrocarbons are synthesized from CO_2-containing syngas which is produced from biomass. (2) After the hydrocarbons are used up as fuels, the produced CO_2 is returned into biomass via photosynthesis. A schematic concept is shown in Fig. 1. Such cycling can contribute to a sustainable society.

1.3 Comparison of FT Catalysts

The metals Fe, Ni, Co, and Ru have the required FT activity for commercial application. Under practical operating conditions Ni produces too much CH_4, while the available supply of Ru is insufficient for large scale application. This leaves only Fe and Co as viable catalysts [11].

Fe and Co are commercial catalysts for FT synthesis with CO_2-free syngas. Riedel et al. [16] compared the performance of Fe and Co catalysts in the mixtures of CO, CO_2, and H_2. With increasing CO_2 and decreasing CO content in the feedgas,

the product composition shifts from a mixture of mainly higher hydrocarbons to almost exclusively methane for Co catalyst, while Fe-based catalyst synthesizes the same hydrocarbon products from CO_2/H_2 as from CO/H_2 syngas. Zhang et al. [17] also found that the CO_2 hydrogenation products contained about 70% or more methane for supported cobalt.

These distinctions are partly attributed to that Fe catalyst is active for WGS reaction, but Co catalyst has no such activity. On Fe catalyst, CO_2 can be hydrogenated into FT products by two steps as shown in (1) and (2): CO is converted from CO_2 by reverse WGS reaction, then produced CO is further hydrogenated to hydrocarbons [9, 11, 18]. In contrast, Co catalyst cannot convert CO_2 into CO.

$$CO_2 + H_2 \rightarrow CO + H_2O \tag{1}$$

$$CO + 2H_2 \rightarrow (CH_2) + H_2O \tag{2}$$

Another factor is the different prerequisites to achieve the kinetic regime of FT synthesis for Fe and Co catalysts. With Fe catalyst, the FT kinetic regime is generated through the formation of stable FT sites via carbiding, and their selectivity is invariant against changes of reactant concentrations [19]. On the contrary, the FT regime can exist only at a sufficiently high CO partial pressure for Co catalyst [20]. Therefore, Co is not fit to hydrogenate CO_2 in nature, while Fe is promiseful to FT synthesis from CO_2-containing syngas.

1.4 FT Synthesis with CO_2-Containing Syngas

In Part 1.2, it is suggested that to use CO_2-containing syngas directly for FT synthesis can solve the shortcoming of current FT technology. The studies of CO_2 hydrogenation and CO_2+CO hydrogenation on Fe catalysts are reviewed in the following.

In view of engineering, to use CO_2-containing syngas is easy to control temperature of synthesis reactor because of the lower exothermicity of the overall reaction of CO_2 as compared to CO [16]. Furthermore, a perceived disadvantage of using Fe-based catalysts for FT is that a large proportion of the CO in the syngas is converted to CO_2 rather than the desired hydrocarbons [21]. The addition of CO_2 to syngas can inhibit CO_2 formation from CO and may increase the ratio of CO to hydrocarbons rather than CO_2.

1.4.1 CO_2 Hydrogenation

It is well known that the hydrogenation of CO_2 proceeds via the CO intermediate [9, 11, 18, 22–26]. That is, during the hydrogenation of CO_2 over Fe catalysts, some CO_2 is firstly converted to CO through reverse WGS reaction and the formed CO is converted consecutively through FT reaction to hydrocarbons. In a previous study

of CO_2 hydrogenation [27], CO formation was found to be the essential step of producing C_2+ hydrocarbons with high conversion and selectivity. Pijolat et al. suggested that CO can be obtained in two different ways: by partial dissociation of CO_2 and by the reverse WGS reaction [28].

H_2 is adsorbed only on Fe [29, 30], but CO_2 adsorbed on both Fe and K [29–31]. Higher K content is beneficial for CO_2 conversion to FT product [16].

Iron carbides are responsible for the formation of olefins and long-chain hydrocarbons in CO_2 hydrogenation [32]. However, Ando et al. [18] found that the major surface phases of the Fe-Cu catalysts were FeO and/or $FeCO_3$ after CO_2 hydrogenation. Suo et al. [33] studied CO_2 hydrogenation on TiO_2-, ZrO_2-, and Al_2O_3-supported iron catalysts. The catalyst with the optimum ratio of iron cations vs. zero valent iron gave good catalytic activity and selectivity in the synthesis of C_2+ hydrocarbons from CO_2 and H_2.

The different views about the active phase in Fe catalysts for CO_2 hydrogenation indicate that much study is needed to make it clear.

1.4.2 Hydrogenation of CO_2 + CO

Jun et al. [9] reported the influence of H_2 content in feedgas on the conversion of CO and CO_2 to hydrocarbons. The reaction with H_2-deficient feed ($CO/CO_2 = 0.33$, $H_2/(2CO + 3CO_2) = 0.44$) showed that only CO was converted to hydrocarbons, while in H_2-enriched feed ($CO/CO_2 = 0.33$, $H_2/(2CO + 3CO_2) = 1$), CO_2 was converted to hydrocarbons as well as CO. The high concentration of H_2 was thought to promote the conversion of CO_2 to CO by reverse WGS reaction, followed by FT reaction in which CO was further hydrogenated to hydrocarbons.

Krishnamoorthy et al. [34] analyzed the ^{13}C content in CO, CO_2, hydrocarbons and oxygenates after $^{13}CO_2$ was added to $H_2/^{12}CO$ reactants (508 K, 0.8 MPa, $H_2/CO = 2$). No ^{13}C is detected in CO, suggesting that dilution of the CO reactant by ^{13}CO molecules formed from $^{13}CO_2$ via reverse WGS reaction is negligible at the reaction conditions. The hydrocarbon products have negligible ^{13}C content, indicating that CO_2 is much less reactive than CO towards chain initiation and growth. Similarly, the addition of $^{14}CO_2$ (1.4 mol%) to $H_2/^{12}CO$ (1:1) did not lead to detectable ^{14}C contents in CO and hydrocarbons on Fe catalysts (513 K, 0.1 MPa, $H_2/CO = 1$) [35]. However, Xu et al. [36] detected almost identical radioactivity per mole in hydrocarbons to that of the added $^{14}CO_2$ on a Fe-Si-K catalyst (543 K, 1.2 MPa, $H_2/CO/CO_2 = 60/10/30$), suggesting that each hydrocarbon molecule contained one ^{14}C from $^{14}CO_2$. The reaction temperature may decide the differences among the above studies.

Besides the studies on the possibility of CO_2 participating in FT synthesis [9, 34–37], it is reported that CO_2 added to syngas can affect selectivity of FT products such as C_5+ selectivity [34], olefin/paraffin ratio [16, 34]. Krishnamoorthy et al. found these phenomena resulted from conversion of CO_2 to CO via reverse WGS reaction with CO_2 addition to syngas [34], but the effects of CO_2 addition on the selectivity are much smaller at 508 K than at 543 K. Calculation [38] indicates that

a CO_2/CO ratio of 16/1 is required to avoid any CO_2 formation in the WGS reaction even under 543 K. The required ratio of CO_2/CO is 4.4 under the experimental conditions of 508 K and 2.14 MPa (H_2/CO = 2) [34]. These values also mean that CO_2 is not reactive to influence WGS reaction, too.

In the case of CO_2 cofed with CO, it can be converted to hydrocarbons at high temperature rather than low temperature. The factor is probably the thermodynamics of WGS reaction [39]. The extent of WGS reaction is thermodynamically favored at low temperatures. Correspondingly, reverse WGS reaction is evident at high temperature, and it promotes the CO_2 conversion to hydrocarbons.

At low temperature, to use the CO_2 contained in syngas relies mainly on the catalyst to activate CO_2. Therefore, our study was done at low temperature in order to develop Fe catalyst active for FT synthesis with CO_2-containing syngas.

2 Influences of Promoters on the Activation of CO_2 for Hydrocarbon Synthesis

The importance and benefit to develop precipitated Fe catalyst have been discussed in Part 1 which can use CO_2-containing syngas directly for hydrocarbon synthesis.

We have studied precipitated Fe catalyst since 2002 and reported some results [40–45]. It was found that promoter combination of Zn, K, and Cu can improve catalytic stability under CO_2-containing syngas [42].

In this part, the role of promoter Zn, K, and Cu on CO_2 activation is investigated by CO_2 temperature-programmed-desorption (TPD). A correlation is found between the characteristic of CO_2-TPD and CO_2 selectivity based on converted CO in FT synthesis. It indicates the possibility to convert CO_2 into hydrocarbons at low temperature. The possible is tested with CO_2 hydrogenation.

2.1 Experimental

The methods to prepare precipitated Fe catalyst and to test catalyst activity were given in previous works [40, 42]. The studied catalysts are expressed as Z*l*K*m*C*n*/Fe. *L*, *m*, and *n* are the nominal mass percent of promoter Zn, K, and Cu relative to Fe_2O_3, respectively.

The program for CO_2-TPD was to reduce 0.1 g catalyst in 95% CO/Ar at 573 K for 4 h and then purge it with He for 1 h at the same temperature. After the catalyst was cooled to 303 K in He atmosphere, it was exposed to 0.1 MPa CO_2 for 1 h. The CO_2-TPD was done with He as carrying gas and the catalyst was heated in 10 K min^{-1} to 1,073 K. Some of the exit gas was inducted into a differentially pumped atmospheric sampling system connected to a quadrupole mass spectrometer (LEDA-MASS Ltd.). The measurable partial pressure range is $10^{-5} \sim 10^{-11}$ Torr with Faraday detector.

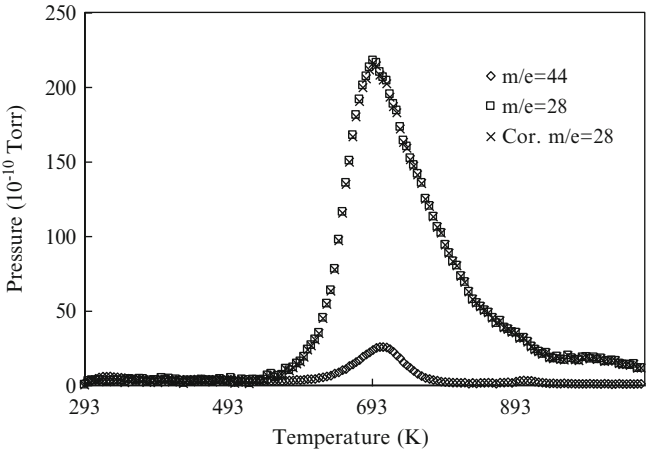

Fig. 2 TPD spectra of m/e = 44 and 28 species from CO-pretreated Fe catalyst after CO_2 adsorption for 1 h at 303 K

2.2 Results and Discussion

2.2.1 CO_2-TPD of Mono-Promoted Fe Catalysts

The species with mass-to-charge ratio (*m/e*) of 44 and 28 in the exited gas desorbed from catalyst were monitored during CO_2-TPD. Figure 2 is the result of unpromoted Fe catalyst. For the species of *m/e* = 44, there is a peak around 709 K. Due to the adopted experimental conditions that the catalyst was reduced by CO and contacted with CO_2 except for inert gas He and Ar, the species of *m/e* = 44 are assigned to CO_2. CO_2 can be cracked into fragment of *m/e* = 28 in the ionization region of mass spectrometer. According to the handbook of used mass spectrometer (LEDA-MASS Ltd.), the approximate intensity (Height) of the produced fragment is 8% relative to the peak of CO_2. The corrected curve of *m/e* = 28 is given in Fig. 2 after the distribution from CO_2 is deducted from the measured result of *m/e* = 28. The treatment produces only a very slight decrease of intensity. Importantly, the correction does not influence the position of peak. So, the detected signal of *m/e* = 28 is mainly from desorbed CO molecular. The CO results appeared in following figures are the corrected ones.

The detected CO may result from irreversibly adsorbed CO during CO reduction [46], the recombination of isolated carbon and oxygen in catalyst, and those evaluated from adsorbed CO_2. About the origin of dissociated carbon and oxygen, Bian et al. [47] assumed them from dissociatively adsorbed CO based on high-pressure syngas adsorption on H_2 or CO reduced Fe catalyst by diffuse reflectance FT-IR, whereas Li et al. [46] thought that the reaction of FeC_X with residual Fe oxides could produce CO_X ($CO + CO_2$) at higher temperatures. The reaction may happen by the help of lattice oxygen migration. Jiang et al. [48] studied syngas adsorption on

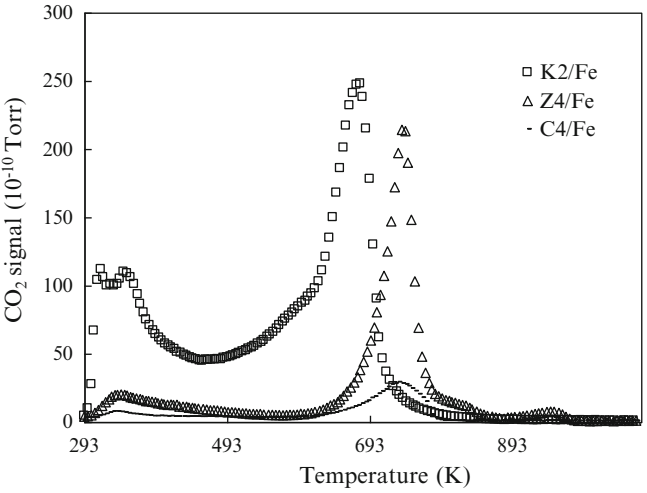

Fig. 3 Desorbed CO_2 from CO-pretreated K2/Fe, Z4/Fe, and C4/Fe catalysts after CO_2 adsorption for 1 h at 303 K

Fe and FeMn catalysts reduced by syngas. The results indicate the possibility of oxygen migrating from the lattice to the surface during heating in the absence of reducing gas. These works [46–48] also support that the carbon of FeC_X is active in TPD experiment. Adsorbed CO_2 may react with it and be converted into CO. Pijolat et al. [28] and Xu et al. [49] monitored CO_2-TPD of supported Fe catalysts. There was CO desorbed between 573 and 773 K, while CO_2 appeared below 593 K for Fe/Al_2O_3 [28]. On the contrary, CO and O_2 were detected with CO_2 simultaneously after CO_2 adsorption on K-Fe-Mn/Si-2 catalysts [49]. The difference of thermo-desorption spectra in these two studies may be related to the catalyst composition. Because the catalysts [28, 49] were reduced in H_2, there was no carbon in the catalysts except that from the adsorbed CO_2. Therefore, CO is formed exclusively from the CO_2 adsorbed on Fe catalyst.

Figure 3 shows the effect of promoter Zn, K, and Cu on desorbed CO_2. The result of C4/Fe is similar to that of unpromoted Fe catalyst in Fig. 2. Cu has no strong effect on CO_2 adsorption. However, Zn promotes the adsorption of CO_2 on catalyst in view of the desorbed CO_2 which is more than that from the unpromoted Fe catalyst. This is consistent with the work of Nam et al. [50]. They found that the amount of chemisorbed CO_2 on Fe-Zn catalyst was high. There is more CO_2 desorbed from K2/Fe than Z4/Fe. It may be due to the basicity of potassium which is attractive to CO_2 [16, 30, 49].

The detected CO with increased temperature is given in Fig. 4. Promoters K and Zn make the CO desorption complicated. Besides the twinborn peak with the desorbed CO_2 as the cases from unpromoted Fe and C4/Fe, there are other two peaks appeared at higher temperature for K2/Fe and Z4/Fe, respectively. On K2/Fe, around 775 K is a broad weak peak and a strong one happens at 1,050 K. The latter

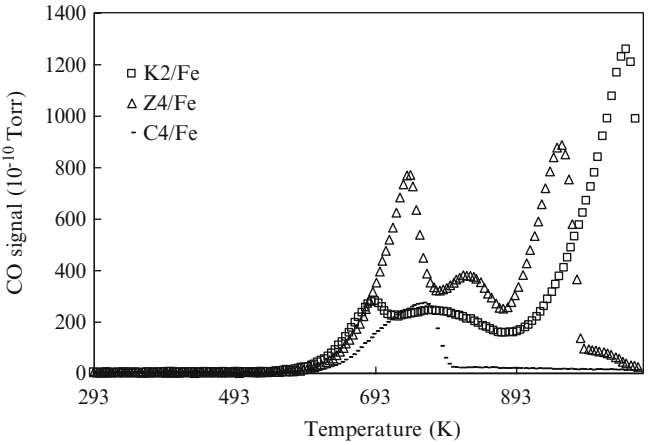

Fig. 4 Desorbed CO from CO-pretreated K2/Fe, Z4/Fe, and C4/Fe catalysts after CO_2 adsorption for 1 h at 303 K

may be attributed to the reaction of FeC_X with residual Fe oxides [46]. Z4/Fe has a clear medium peak and its third peak occurs at about 958 K which is lower than the corresponding one of K2/Fe.

It has been found that the reduction of Fe_2O_3 with CO occurs in two steps: facile reduction of Fe_2O_3 to Fe_3O_4, followed by slow reduction of Fe_3O_4 to iron carbide [46, 51]. After CO activation, Fe exists as Fe carbides and Fe_3O_4 [52, 53]. We investigated the reduction process of mono-promoted Fe catalysts with CO [54]. There are sharp peaks corresponding to CO consumption during C4/Fe reduction, while these peaks become extended with decreased intensity for catalyst K2/Fe and Z4/Fe. Therefore, the structure of reduced K2/Fe and Z4/Fe is more complicated than that of C4/Fe. The unhomogeneous structure of K2/Fe and Z4/Fe may be responsible for the CO desorbed at higher temperatures as shown in Fig. 4. CO adsorption on Fe catalysts had been studied by *in situ* diffuse reflectance FT-IR. The infrared spectra are changed evidently with Fe catalyst promoted by Mn or K [48, 55]. Detailed analysis on adsorbed bands discloses that Mn and K can influence the size of Fe^0 clusters formed in reduction.

2.2.2 Effect of Promoter Combination on CO_2-TPD

CO_2-TPD was used to study Fe catalysts promoted by different contents of Zn, K, and Cu. Figure 5 is the results of desorbed CO_2 from these catalysts. There is much CO_2 desorbed from the catalysts with 2 mass% K. However, the amount of CO_2 decreases evidently for the catalysts promoted by 1 mass% K. Potassium is a main factor to determine the adsorption of CO_2 on Fe catalyst [16, 30, 49]. For the catalysts with same content of K, Zn, and Cu show their influence. The amount of desorbed CO_2 decreases firstly when Zn and Cu contents increase from 2 to 4

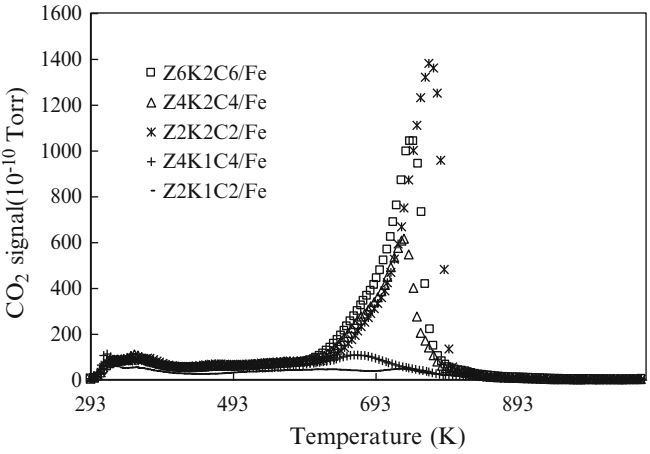

Fig. 5 Desorbed CO_2 from CO-pretreated Fe catalysts with different content of promoters after CO_2 adsorption for 1 h at 303 K

mass%, and then increase with the further raise of Zn and Cu content to 6 mass%. There is a slight increase for the 1 mass% K-promoted Fe catalysts after Zn and Cu contents are changed from 2 to 4 mass%.

Figure 6 illustrates the desorbed CO during CO_2-TPD. The peak around 763 K is related with the loading content of K which is similar to desorbed CO_2 from these catalysts. A sharp peak exists at this range for 2 mass% K-promoted catalysts, whereas it decreases greatly with the Fe catalysts promoted by 1 mass% K. On the contrary, 1 mass% K-added catalysts show the maximum of CO desorption around 930 K. In this temperature range, only Z6K2C6/Fe which belongs to the series of 2 mass% K-promoted catalysts has a clear desorption peak. The effect of K on desorption is displayed by the difference around 1,040 K, too. Much CO is desorbed from 2 mass% K-promoted catalysts, but catalysts Z4K1C4/Fe and Z2K1C2/Fe with low content of K do not emit CO in this temperature range.

Therefore, it can be concluded that K is the main component to control the adsorption and evolution of CO_2 based on the results revealed by TPD. Although Zn and Cu are inferior components relative to K, their action become larger in the case of higher ratio of Zn/K. Z6K2C6/Fe has a desorption peak at ~930 K contrasting with the flat pattern of Z4K2C4/Fe and decline of Z2K2C2/Fe in this range. Considering the results of mono-promoted Fe catalysts in Fig. 4, the CO peak around 930 K in Fig. 6 is related to the influence of Zn other than Cu on Fe catalyst structure.

2.2.3 CO_2 Selectivity of FT Reaction

The performances of Zn, K, and Cu-promoted Fe catalysts were studied under CO_2-free and CO_2-containing syngas, respectively. The CO_2 selectivity based on converted CO is given in Fig. 7. The catalysts can be divided into two categories.

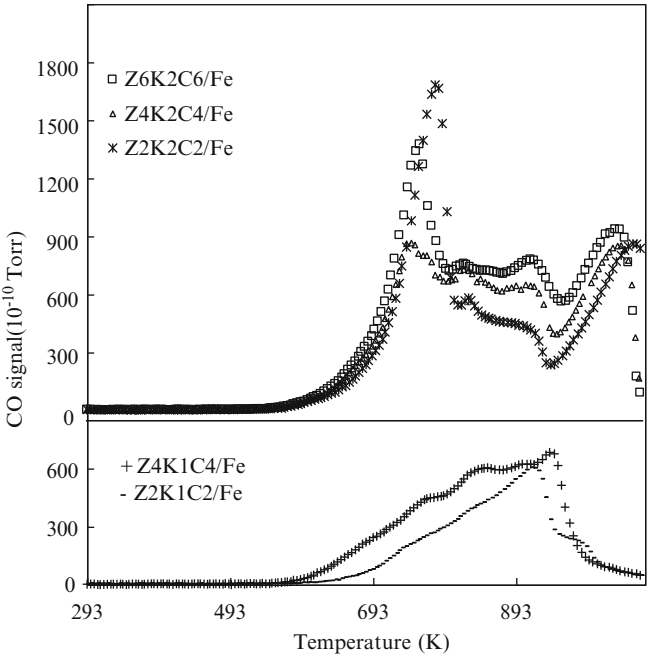

Fig. 6 Desorbed CO from CO-pretreated Fe catalysts with different content of promoters after CO_2 adsorption for 1 h at 303 K

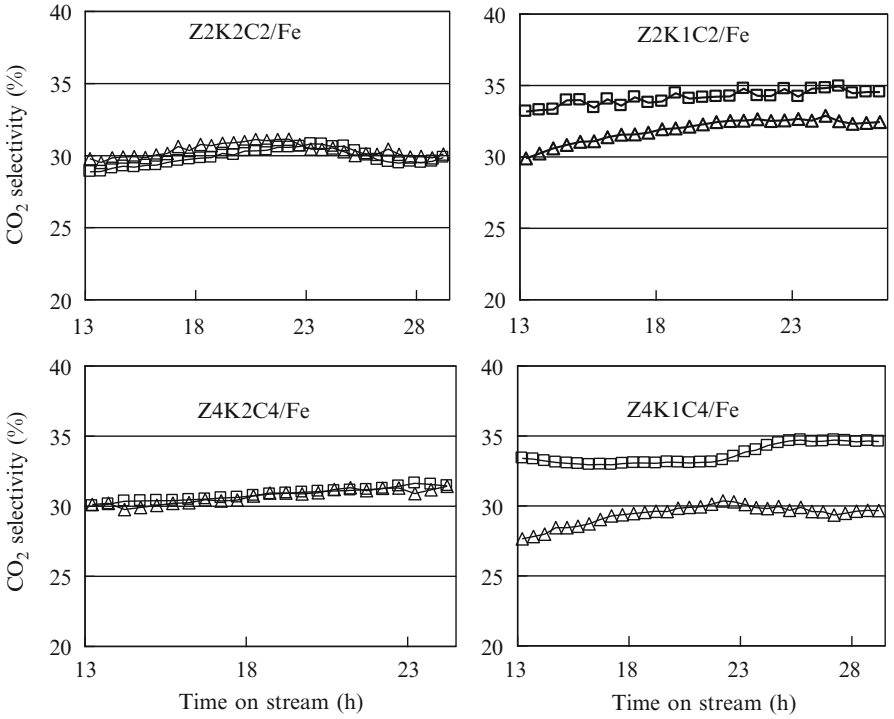

Fig. 7 Effect of promoter content on CO_2 selectivity on the catalysts pretreated by CO (T=503 K, P=1.6 MPa, *open square*: 33%CO/62%H_2/5%Ar, *open triangle*: 20%CO_2/25%CO/50%H_2/5%Ar)

For catalysts Z2K2C2/Fe and Z4K2C4/Fe, the CO_2 added into reactants does not influence the CO_2 selectivity, i.e., CO_2 is inert to react on these two catalysts. But the CO_2 selectivity decreases with the addition of CO_2 to reactants on catalysts Z2K1C2/Fe, Z4K1C4/Fe, and Z6K2C6/Fe (Not shown) which have lower K content or higher Zn/K ratio in them. The characteristic of CO_2 selectivity among these catalysts has a corresponding reflection in their CO_2-TPD. The catalyst showing CO desorption peak around 930 K (Fig. 6) is sensitive to the composition of reactants and added CO_2 brings forth decreased CO_2 selectivity during FT synthesis reaction.

It has been found that CO_2 is inert at low temperature [34, 37]. The result of Z2K2C2/Fe and Z4K2C4/Fe is consistent with this conclusion, but the result of Z6K2C6/Fe, Z4K1C4/Fe, and Z2K1C2/Fe suggests that higher Zn/K ratio or lower K content leads to the decrease of CO_2 selectivity. There are two possibilities for this phenomenon. The added CO_2 may inhibit CO_2 formation from WGS reaction or be converted into hydrocarbons itself. Both of the routes can result in decreased apparent CO_2 selectivity based on converted CO. Correspondingly, more CO is converted into hydrocarbons and the hydrocarbon selectivity can be increased. Although it cannot be discerned which route is in effect here, the results from Z6K2C6/Fe, Z4K1C4/Fe, and Z2K1C2/Fe show the possibility to use CO_2 contained in syngas for hydrocarbon synthesis at low temperature.

2.2.4 Activity and Selectivity of CO_2 Hydrogenation

The results of CO_2 selectivity shown in Fig. 7 only indicate that the Fe catalysts with high Zn/K ratio or low K content possess the possibility to use CO_2 contained in syngas for hydrocarbon synthesis at low temperature because the exact conversion from CO_2 to hydrocarbons cannot be decided in our experiments. Therefore, Z4K1C4/Fe and Z4K2C4/Fe were assessed under the reactants of CO_2 and H_2 in order to investigate the influence of Zn/K ratio on CO_2 hydrogenation [42].

Z4K1C4/Fe produces more C_2+ hydrocarbons than Z4K2C4/Fe, it indicates that the catalyst with higher Zn/K ratio is more active to hydrogenate CO_2 indirectly [9, 11, 18] or directly.

Furthermore, Z4K1C4/Fe shows similar activity and selectivity to those studied under 523 K [56], 538 K [30], or 623 K [33]. Based on the experimental results, we pointed out that it is possible to use CO_2 contained in syngas for hydrocarbon synthesis at low temperature by the help of suitable promoter(s) [42].

2.3 Conclusions

CO_2-TPD indicates that adsorbed CO_2 on promoted Fe catalysts can partly be converted into CO. Promoter K or Zn is able to increase the adsorption of CO_2 because more CO_2 and CO are desorbed from K2/Fe and Z4/Fe than that from unpromoted Fe catalyst. K mainly increases CO_2 adsorption and is inferior to Zn in producing CO.

Cu has no strong effect on CO_2-TPD. For the Fe catalysts copromoted by Zn, K, and Cu, the desorbed amount of CO_2 closely relies on the content of K although the content of Zn and Cu has effect on the amount of desorbed CO_2. The desorbed CO_2 from the tri-promoted catalysts with 2 mass% K is higher than the mono-promoted Fe catalyst by Zn or K, whereas the corresponding peak diminishes with the K content decreased to 1 mass%.

The combined promoters changes the CO desorption pattern evidently. The catalysts with high Zn/K ratio or low K content possess desorbed CO peak around 930 K. This peak reflects the possibility whether CO_2 added into syngas can influence CO_2 selectivity in FT synthesis. For the catalysts showing desorbed CO around 930 K, their CO_2 selectivity based on converted CO is decreased due to the added CO_2 in syngas.

The Fe catalyst with high Zn/K ratio shows high C_2+ hydrocarbon selectivity for CO_2 hydrogenation. It indicates that the CO_2 contained in syngas is able to be activated by suitable promoter(s) for hydrocarbon synthesis at low temperature.

3 Studies on Fe Catalysts with SiO_2 as Binder for CO_2 Hydrogenation

SiO_2 is one generally used structure promoter for precipitated Fe catalyst. It can not only increase the specific surface area of Fe catalyst, but also bind iron species to prevent its loss from catalyst particle during reaction. Several methods are used to introduce SiO_2 into precipitated Fe catalysts with potassium silicate, silica sol, and so on as silica source. Sasol impregnated washed precipitate with potassium waterglass solution [15]. Dlamini et al. added silica sol at different stages during catalyst preparation (before precipitation, after precipitation, after drying at 397 K, and after calcination at 723 K) [57]. This method was also used in the study of Yang et al. [58]. Some researchers introduced SiO_2 with hydrolyzed tetraethyl orthosilicate and added it to the iron(III) nitrate solution to give the desired level of silicon [59].

In this work, potassium silicate was selected as silica source and it was introduced before precipitation. The influences of Fe-Si interaction on precipitated Fe catalyst structure and activity had been partially reported [45]. Here, the influence of SiO_2 on precipitated Fe catalyst is reported in view of CO_2 hydrogenation.

3.1 Experimental

Catalysts were prepared in two methods. Method I was to precipitate a mixed solution of $Fe(NO_3)_3$ and potassium silicate with $(NH_4)_2CO_3$ solution. Method II was to precipitate $Fe(NO_3)_3$ solution with the mixed solution of $(NH_4)_2CO_3$ and potassium silicate. Then, the precipitate was washed with distilled water and centrifuged for

Table 1 Influence of promoter K on reactive performance of catalysts under $CO+H_2$ and CO_2+H_2

	$CO+H_2$			CO_2+H_2		
Catalyst	CO conversion (%)	CO_2 selectivity (%)	CH_4 selectivity (%)	CO_2 conversion (%)	CO selectivity (%)	CH_4 selectivity (%)
Z4K1C4/FS5-II	32.1	20.3	5.0	8.5	38.3	34.6
Z4K2C4/FS5-II	52.0	27.3	3.0	9.1	39.0	29.6

$T=503$ K, $P=1.6$ MPa, 6 Lh^{-1} $g\text{-}cat^{-1}$, $H_2/CO=2.0$ or $H_2/CO_2=2.0$

ten times. Promoters of Zn, K and Cu were usually impregnated onto the precipitate with $Zn(NO_3)_2$, KNO_3, and $Cu(NO_3)_2$ solution. After the precipitate was dried and calcined, it was shaped into desired particle size for activity test. The obtained catalysts are expressed as Z*l*K*m*C*n*/FS*r*-I or Z*l*K*m*C*n*/FS*r*-II according to the method to introduce SiO_2. In the above abbreviation of catalysts, Z, K, C, F, and S represent Zn, K, Cu, Fe, and SiO_2, respectively. *L*, *m*, *n, and r* are the nominal mass percent of corresponding materials relative to Fe_2O_3.

The activity of catalysts was tested in a stainless steel fixed bed reactor. A 1.0 g catalyst (80–150 μm) was mixed with 4.0 g quartz particles and filled into the reactor. After the catalysts were reduced in CO of 50 mL min^{-1} at 573 K for 6 h, it was cooled to room temperature. Then, the feedgas was changed into reactants of 1.6 MPa. The catalyst was heated to 503 K in about 3 h for activity evaluation. The detail parameters for activity testing are given with the experimental results.

3.2 Results and Discussion

3.2.1 Influence of SiO_2 on Catalytic Activity

Table 1 compared reactive performance of catalysts Z4K1C4/FS5-II and Z4K2C4/FS5-II under $CO+H_2$ and CO_2+H_2, respectively. In the case of CO hydrogenation, CO conversion and CO_2 selectivity are increased, but CH_4 selectivity is decreased with more K added into catalyst. These have been observed by other works [8, 34, 42, 60–62]. For CO_2 hydrogenation, catalysts Z4K1C4/FS5-II and Z4K2C4/FS5-II have similar CO_2 conversion and CO selectivity, but the latter possesses lower CH_4 selectivity than the former. Therefore, catalyst Z4K2C4/FS-II has higher selectivity to C_2+ hydrocarbons than Z4K1C4/FS-II. The relation between C_2+ hydrocarbons and K content is different to the result found in our previous work [42]. Furthermore, the two catalysts containing SiO_2 have higher CO selectivity and CH_4 selectivity than the catalysts without SiO_2. These changes are due to the addition of SiO_2 which decreases the amount of effective potassium [58, 63]. Promoter K is beneficial for carbon chain growth [11, 64]; however, this function is weakened by SiO_2. It is required to adjust the contents of promoter Zn, K and Cu with the introduction of SiO_2 to precipitated Fe catalyst.

Table 2 Reactive performance of Fe catalysts under $CO + H_2$

Catalyst	CO conversion (%)	CO_2 selectivity (%)	CH_4 selectivity (%)	H_2/CO (outlet)
Z6K4C8/FS10-I	92.7	37.7	2.3	10.1
Z4K2C8/FS10-I	83.7	33.4	2.5	4.2
Z8K3C6/FS10-I	66.4	29.4	2.4	2.4
Z6K2C2/FS15-I	65.3	21.0	2.9	1.9
Z4K4C2/FS10-II	90.2	37.7	1.7	7.6

$T = 508$ K, $P = 1.6$ MPa, 3 Lh^{-1} $g\text{-}cat^{-1}$, $H_2/CO = 1.5$

Table 3 Reactive performance of Fe catalysts under $CO_2 + H_2$

Catalyst	CO_2 conversion (%)	CO selectivity (%)	CH_4 selectivity (%)	Liquid hydrocarbon distribution (C mol%)		
				C_6–C_{10}	C_{11}–C_{15}	C_{16}+
Z6K4C8/FS10-I	7.9	55.1	14.3	95.7	3.1	1.2
Z8K3C6/FS10-I	6.2	53.1	31.9	97.5	2.5	0
Z6K2C2/FS15-I	9.1	30.1	29.3	89.9	8.1	2.0
Z6K4C8/FS15-II	9.1	31.3	25.4	83.1	10.9	6.0
Z6K4C8/FS15-II[a]	14.6	21.8	44.1	99.5	0.3	0.2

$T = 503$ K, $P = 1.6$ MPa, 6 Lh^{-1} $g\text{-}cat^{-1}$, $H_2/CO_2 = 2.0$
[a]$H_2/CO_2 = 5.0$

3.2.2 Reactive Performance of Fe Catalysts Under $CO + H_2$

We investigated the influences of introducing method of SiO_2 and its quantity on the reactive performance of Fe catalysts. Table 2 lists results of some catalysts. The contents of promoter Zn, K and Cu in catalyst were arranged by uniform design. CO conversion of these catalysts is distributed in a wide range. It reflects marked influence of promoter composition on catalyst performance. CH_4 selectivity is only influenced by promoter K content, and it decreases with increased K content. CO_2 selectivity is not completely relied on CO conversion. For example, Z8K3C6/FS10-I and Z6K2C2/FS15-I have similar CO conversion, but their CO_2 selectivity is different.

The molar ratio of H_2/CO in reactor outlet is given in Table 2 for the studied catalysts. All of them are higher than the H_2/CO ratio in reactor inlet. Such increase of H_2 content is resulted from WGS activity of Fe catalyst. It brings out H_2-rich tail gas after FT synthesis reaction.

In order to improve the converting efficiency of syngas in FT synthesis and produce profitable chemicals, some kinds of FT synthesis process have been projected [65]. It needs catalysts having corresponding performance to construct a desired process. The catalysts we studied are able to meet the requirement due to their performance distributed in wide range.

3.2.3 Reactive Performance of Fe Catalysts Under $CO_2 + H_2$

We also measured reactive performance of precipitated Fe catalysts for CO_2 hydrogenation and the results are shown in Table 3.

Comparing the results in Table 3 to Table 2, it can be found that the reactive performances of studied catalysts depend on reactant composition. For example, catalyst Z6K4C8/FS10-I is more active than Z6K2C2/FS15-I for CO hydrogenation, while the former is weaker than the latter to convert reactant in the case of CO_2 hydrogenation.

We had found that low K content is helpful to increase hydrocarbon yield and Fe catalyst with high Zn/K ratio shows high C_2+ hydrocarbon selectivity for CO_2 hydrogenation at lower reaction temperature [42]. The results of catalyst Z6K2C6/FS15-I in Table 3 still support the above conclusions after SiO_2 was introduced into precipitated Fe catalyst. Although the content of promoter K in it is the lowest among studied catalysts, more CO_2 is hydrogenated into hydrocarbons rather than terminated as CO. It supports that the CO_2 is able to be activated by suitable promoter(s) for hydrocarbon synthesis at lower temperature [42], too. The effect of H_2/CO_2 ratio on reactive performance of catalyst Z6K4C8/FS15-II is evident according to the results in Table 3. After the H_2/CO_2 ratio is increased to 5, more hydrocarbon is synthesized from CO_2, and most liquid products are in C_6–C_{10} range.

3.3 Conclusions

SiO_2 is used commonly as structure promoter for precipitated Fe catalyst in order to enhance its mechanical strength besides to increase its specific surface area. The influences of introducing method and the content of SiO_2 on the reactive performance of Fe catalyst were studied under $CO + H_2$ and $CO_2 + H_2$, respectively.

Although the amount of effective potassium is decreased by the introduced SiO_2, the correlation between promoter composition and catalyst reactivity found for SiO_2-free Fe catalysts is still in effect for SiO_2-added Fe catalysts. It is beneficial to improve precipitated Fe catalysts for FT synthesis with CO_2-containing syngas.

4 Perspectives

In order to develop precipitated Fe catalyst active to convert CO_2-containing syngas, we decompose the work into three steps. The first step is to develop Fe catalyst active to convert $CO + H_2$. The second one is to exploit Fe catalyst propitious for CO_2 hydrogenation or to activate CO_2 into CO. The third step is to set up guidance on how to couple the above two kinds of catalysts according to contents of CO_2 and CO in reactants in order to convert effectively CO_2-containing syngas into liquid fuels.

By now, the first step is nearly completed, and several Fe catalysts are found with high CO conversion during FT synthesis reaction. Much work is being done for the second aim. We have observed the relation between the pattern of CO_2-TPD and CO_2 hydrogenation activity for Fe catalysts promoted with Zn, K, and Cu. It helps us to find Fe catalysts active to hydrogenate CO_2 at low temperature. However, new

characteristic tool or method is needed to accelerate making up ideal Fe catalyst after SiO_2 is introduced into catalyst as support or binder. Based on the catalysts selected in the first two steps, it will be promise to complete the third step and realize acquiring liquid fuels efficiently from CO_2-containing syngas.

Acknowledgments This work is partially supported by the Science and Technology Department of Zhejiang Province (2009C21002), Zhejiang Provincial Natural Science Foundation of China (Y4100410) and National Ministry of Science and Technology of China (2009AA05Z435).

References

1. http://www.eia.doe.gov/kids/history/timelines/index.html
2. Dry ME (1999) Fischer-Tropsch reactions and the environment. Appl Catal A 189:185–190
3. Schobert HH, Song C (2002) Chemicals and materials from coal in the 21st century. Fuel 81:15–32
4. http://hypertextbook.com/facts/index-topics.shtml
5. Piel WJ (2001) Transportation fuels of the future? Fuel Proc Tech 71:167–179
6. Chum HL, Overend RP (2001) Biomass and renewable fuels. Fuel Proc Technol 71:187–195
7. Heinemann H (1981) A brief history of industrial catalysis. In: Anderson JR, Boudart M (eds) Catalysis, science and technology, vol 1. Springer, New York
8. Schulz H (1999) Short history and present trends of Fischer-Tropsch synthesis. Appl Catal A 186:3–12
9. Jun KW, Roh HS, Kim KS et al (2004) Catalytic investigation for Fischer-Tropsch synthesis from bio-mass derived syngas. Appl Catal A 259:221–226
10. Kahandawala MSP, Graham JL, Sidhu SS (2004) Particulate emission from combustion of diesel and Fischer-Tropsch fuels: a shock tube study. Energy Fuel 18:289–295
11. Dry ME (2002) The Fischer-Tropsch process: 1950–2000. Catal Today 71:227–241
12. Vosloo AC (2001) Fischer-Tropsch: a futuristic view. Fuel Proc Technol 71:149–155
13. Berg FR, Crajé MWJ, Kraan AM et al (2003) Reduction behaviour of Fe/ZrO_2 and $Fe/K/ZrO_2$ Fischer-Tropsch catalysts. Appl Catal A 242:403–416
14. Asadullah M, Miyazawa T, Ito S et al (2004) Gasification of different biomass in a dual-bed gasifier system combined with novel catalysts with high energy efficiency. Appl Catal A 267:95–102
15. Dry ME (1981) The Fischer-Tropsch synthesis. In: Anderson JR, Boudart M (eds) Catalysis, science and technology, vol 1. Springer, New York
16. Riedel T, Claeys M, Schulz H et al (1999) Comparative study of Fischer-Tropsch synthesis with H_2/CO and H_2/CO_2 syngas using Fe- and Co-based catalysts. Appl Catal A 186:201–213
17. Zhang Y, Jacobs G, Sparks DE et al (2002) CO and CO_2 hydrogenation study on supported cobalt Fischer-Tropsch synthesis catalysts. Catal Today 71:411–418
18. Ando H, Xu Q, Fujiwara M et al (1998) Hydrocarbon synthesis from CO_2 over Fe-Cu catalysts. Catal Today 45:229–234
19. Schulz H, Schaub G, Claeys M et al (1999) Transient initial kinetic regimes of Fischer-Tropsch synthesis. Appl Catal A 186:215–227
20. Schulz H, Steen E, Claeys M (1995) Specific inhibition as the kinetic principle of the Fischer-Tropsch synthesis. Topic Catal 2:223–234
21. Raje AP, Davis BH (1997) Fischer-Tropsch synthesis over iron-based catalysts in a slurry reactor. Reaction rates, selectivities and implications for improving hydrocarbon productivity. Catal Today 36:335–345
22. Nozaki F, Sodesawa T, Sathoh S et al (1987) Hydrogenation of carbon dioxide into light hydrocarbons at atmospheric pressure over Rh/Nb_2O_5 or Cu/SiO_2-Rh/Nb_2O_5 catalyst. J Catal 104:339–346

23. Thampi KR, Kiwi J, Gratzel M (1987) Methanation and photo-methanation of carbon dioxide at room temperature and atmospheric pressure. Nature 327:506–508
24. Barrault J, Alouche A (1990) Isotopic exchange measurements of the rate of interconversion of carbon-monoxide and carbon-dioxide over nickel supported on rare-earth-oxides. Appl Catal 58:255–267
25. Schild C, Wokaun A, Koeppel RA et al (1991) CO_2 hydrogenation over nickel/zirconia catalysts from amorphous precursors: on the mechanism of methane formation. J Phys Chem 95:6341–6346
26. Williams KJ, Boffa AB, Salmeron M et al (1991) The kinetics of CO_2 hydrogenation on a Rh foil promoted by titania overlayers. Catal Lett 9:415–426
27. Fujimoto K, Yokota K (1991) Effective hydrogenation of carbon-dioxide with 2-stage reaction system. Chem Lett 20:559–562
28. Pijolat M, Perrichon V, Primet M et al (1982) Hydrocondensation of carbon dioxide over an iron-alumina catalyst: a three-step model. J Mol Catal 17:367–380
29. Choi PH, Jun KW, Lee SJ et al (1996) Hydrogenation of carbon dioxide over alumina supported Fe-K catalysts. Catal Lett 40:115–118
30. Yan SR, Jun KW, Hong JS et al (2000) Promotion effect of Fe-Cu catalyst for the hydrogenation of CO_2 and application to slurry reactor. Appl Catal A 194–195:63–70
31. Dry ME, Shingles T, Boshoff LJ et al (1969) Heats of chemisorption on promoted iron surfaces and the role of alkali in Fischer-Tropsch synthesis. J Catal 15:190–199
32. Lee MD, Lee JF, Chang CS (1989) Hydrogenation of carbon-dioxide on unpromoted and potassium-promoted iron catalysts. Bull Chem Soc Jpn 62:2756–2758
33. Suo ZH, Kou Y, Niu JZ et al (1997) Characterization of TiO_2-, ZrO_2- and Al_2O_3-supported iron catalysts as used for CO_2 hydrogenation. Appl Catal A 148:301–313
34. Krishnamoorthy S, Li A, Iglesia E (2002) Pathways for CO_2 formation and conversion during Fischer-Tropsch synthesis on iron-based catalysts. Catal Lett 80:77–86
35. Hall WK, Kokes RJ, Emmett PJ (1957) Mechanism studies of the Fischer-Tropsch synthesis. The addition of radioactive methanol, carbon dioxide and gaseous formaldehyde. J Am Chem Soc 79:2983–2989
36. Xu L, Bao S, Houpt DJ et al (1997) Role of CO_2 in the initiation of chain growth and alcohol formation during the Fischer-Tropsch synthesis. Catal Today 36:347–355
37. Rostrup-Nielsen JR (2002) Syngas in perspective. Catal Today 71:243–247
38. Soled SL, Iglesia E, Miseo S et al (1995) Selective synthesis of α-olefins on Fe-Zn Fischer-Tropsch catalysts. Topic Catal 2:193–205
39. Smith JM, Ness HC (1975) Introduction to chemical engineering thermodynamics, 3rd edn. McGraw Hill, Tokyo
40. Ning W, Koizumi N, Chang H et al (2006) Phase transformation of unpromoted and promoted Fe catalysts and the formation of carbonaceous compounds during Fischer-Tropsch synthesis reaction. Appl Catal A 312:35–44
41. Ning W, Koizumi N, Yamada M (2007) Improvement of promoters on the Fischer-Tropsch activity of mechanically mixed Fe catalysts. Catal Commu 8:275–278
42. Ning W, Koizumi N, Yamada M (2009) Researching Fe catalyst suitable for CO_2-containing syngas for Fischer-Tropsch synthesis. Energy Fuel 23:4696–4700
43. Ning W, Chang H, Koizumi N et al (2006) Effects of K, Cu and Zn addition on the Fischer-Tropsch synthesis activity of the precipitated Fe catalyst in the absence and presence of CO_2 at low temperature. The 9th China-Japan Symposium on Coal and C1 Chemistry, Chengdu, China, October, pp 22–28
44. Ning W, Yang X, Lv D et al (2009) Consideration and practice to develop Fe catalysts for Fischer-Tropsch synthesis from coal-derived syngas. 13th Asian Chemical Congress, Shanghai, China, September, pp 13–16
45. Ning W, Wang X, Lin Q et al (2010) Study to control reactive performance of precipitated iron-based catalysts for Fischer-Tropsch synthesis. Chem Ind Eng Prog 29(suppl):378–379
46. Li S, Meitzner GD, Iglesia E (2001) Structure and site evolution of iron oxide catalyst precursors during the Fischer-Tropsch synthesis. J Phys Chem B 105:5743–5750

47. Bian G, Oonuki A, Koizumi N et al (2002) Studies with a precipitated iron Fischer-Tropsch catalyst reduced by H_2 or CO. J Mol Catal A 186:203–213
48. Jiang M, Koizumi N, Yamada M (2000) Adsorption properties of iron and iron-manganese catalysts investigated by in-situ diffuse reflectance FTIR spectroscopy. J Phys Chem B 104:7636–7643
49. Xu L, Wang Q, Liang D et al (1998) The promotions of MnO and K_2O to Fe/silicalite-2 catalyst for the production of light alkenes from CO_2 hydrogenation. Appl Catal A 173:19–25
50. Nam SS, Lee SJ, Kim H et al (1997) Catalytic conversion of carbon dioxide into hydrocarbons over zinc promoted iron catalysts. Energy Convers Manage 38:S397–S402
51. Bukur DB, Okabe K, Rosynek MP et al (1995) Activation studies with a precipitated iron catalyst for Fischer-Tropsch synthesis I. Characterization studies. J Catal 155:353–365
52. Shroff MD, Kalakkad DS, Coulter KE et al (1995) Activation of precipitated iron Fischer-Tropsch synthesis catalysts. J Catal 156:185–207
53. Sudsakorn K, Goodwin JG, Adeyiga AA (2003) Effect of activation method on Fe FTS catalysts: investigation at the site level using SSITKA. J Catal 213:204–210
54. Ning W (2005) Ph.D. Thesis. Tohoku University, Sendai, Japan
55. Jiang M, Koizumi N, Yamada M (2000) Characterization of potassium-promoted iron-manganese catalysts by in situ diffuse reflectance FTIR using NO, CO, and CO + H_2 as probes. Appl Catal A 204:49–58
56. Ando H, Matsumura Y, Souma Y (2000) A comparative study on hydrogenation of carbon dioxide and carbon monoxide over iron catalyst. J Mol Catal A 154:23–29
57. Dlamini H, Motjope T, Joorst G et al (2002) Changes in physico-chemical properties of iron-based Fischer-Tropsch catalyst induced by SiO_2 addition. Catal Lett 78:201–207
58. Yang Y, Xiang H-W, Tian L et al (2005) Structure and Fischer-Tropsch performance of iron-manganese catalyst incorporated with SiO_2. Appl Catal A 284:105–122
59. O'Brien RJ, Xu L, Spicer RL et al (1996) Activation study of precipitated iron Fischer-Tropsch catalysts. Energy Fuel 10:921–926
60. Anderson RB, Seligman B, Schultz JF et al (1952) Fischer-Tropsch synthesis. Some important variables of the synthesis on iron catalysts. Ind Eng Chem 44:391–397
61. Arakawa H, Bell AT (1983) Effects of potassium promotion on the activity and selectivity of iron Fischer-Tropsch catalysts. Ind Eng Chem Proc Des Dev 22:97–103
62. Bukur DB, Mukesh D, Patel SA (1990) Promoter effects on precipitated iron catalysts for Fischer-Tropsch synthesis. Ind Eng Chem Res 29:194–204
63. Bukur DB, Lang X, Mukesh D et al (1990) Binder/support effects on the activity and selectivity of iron catalysts in the Fischer-Tropsch synthesis. Ind Eng Chem Res 29:1588–1599
64. Dictor RA, Bell AT (1986) Fischer-Tropsch synthesis over reduced and unreduced iron oxide catalysts. J Catal 97:121–136
65. Raje A, Inga JR, Davis BH (1997) Fischer-Tropsch synthesis: process considerations based on performance of iron-based catalysts. Fuel 76:273–280

Part III
Cellulosic Biofuels

Chapter 15
Cellulosic Butanol Production from Agricultural Biomass and Residues: Recent Advances in Technology *

N. Qureshi, S. Liu, and T.C. Ezeji

Abstract This chapter details the recent advances made on bioconversion of lignocellulosic biomass to butanol, a superior biofuel that can be used in internal combustion engines or transportation industry. It should be noted that butanol producing cultures cannot tolerate or produce more than 20–30 g/L of acetone-butanol-ethanol (ABE) in batch reactors of which butanol is of the order of 13–18 g/L. This is due to toxicity of butanol to the culture. In order to overcome this challenge, two approaches have been applied: (1) developing more butanol tolerant strains using genetic engineering techniques and (2) employing process engineering approaches to simultaneously recover butanol from the fermentation broth thus not allowing butanol concentrations in the reactor to accumulate beyond culture's tolerance. By the application of the first approach, a number of butanol producing strains have been developed; however, none of these accumulated greater than 1,200 mg/L (1.2 g/L) butanol, while using the second approach total ABE up to 461 g/L has been produced. Attempts to improve the newly developed strains are continuing.

* Mention of trade names or commercial products in this article is solely for the purpose of providing scientific information and does not imply recommendation or endorsement by the United States Department of Agriculture. USDA is an equal opportunity provider and employer.

N. Qureshi (✉)
United States Department of Agriculture (USDA), Agricultural Research Service (ARS), National Center for Agricultural Utilization Research (NCAUR), Bioenergy Research Unit, Renewable Products Technology, 1815 N University Street, Peoria, IL 61604, USA
e-mail: Nasib.Qureshi@ars.usda.gov

S. Liu
United States Department of Agriculture (USDA), Agricultural Research Service (ARS), National Center for Agricultural Utilization Research (NCAUR), Renewable Products Technology, 1815 N University Street, Peoria, IL 61604, USA

T.C. Ezeji
Department of Animal Sciences and Ohio State Agricultural Research and Development Center (OARDC), The Ohio State University, 305 Gerlaugh Hall, 1680 Madison Avenue, Wooster, OH 44691, USA

J.W. Lee (ed.), *Advanced Biofuels and Bioproducts*, DOI 10.1007/978-1-4614-3348-4_15,

Lignocellulosic substrates have been used to produce butanol due to their abundant availability and economical prices usually in the range of $24–60/ton as opposed to corn prices which have been in the range of $153–218/ton during recent months. It should be noted that lignocellulosic substrates require separate hydrolysis prior to fermentation. In a more recent approach, hydrolysis and fermentation (and simultaneous recovery) have been integrated or combined to reduce the cost of butanol production from cellulosic substrates. Using such an approach, up to 192 g/L ABE was produced from 430 g/L cellulosic biomass/sugars. Additionally, this chapter provides details of process integration and simultaneous product recovery technologies for butanol production.

1 Introduction

Throughout the world, countries are promoting biofuel development with mandates and directives. The US, by using corn as the primary feedstock, produced 10.6 billion gallons of ethanol in 2009, and more than 12 billion gallons was produced in 2010 (Renewable fuels association 2010). Concomitantly there was a marked increase in the cost of corn, an important livestock feed component. The extent to which these two trends are associated is unknown and is subject to considerable debate. In any case, there is considerable interest in the production of biofuels using alternative substrates, such as lignocellulosic biomass. Butanol (also known as *n*-butanol), a superior biofuel than ethanol, can be produced by fermentation from lignocellulosic biomass and contains more energy on per gallon (or per lb) basis. In this fermentation, all three components (acetone, butanol, ethanol; ABE) are produced simultaneously with butanol being the major product.

Butanol, currently manufactured with petroleum feedstocks, is an important chemical with many applications in the production of solvents, plasticizers, butylamines, amino resins, butyl acetates, etc. [14]. In 2008, global consumption of butanol was estimated as 350 million gallons, according to the chemical giant BASF. Butanol has several advantages over ethanol as a fuel extender or fuel substitute. It has an energy content that is similar to gasoline, which means fewer gallons are required than ethanol to achieve the same energy output [42]. It has a lower vapor pressure than ethanol, which makes it safer to transport and use in combustion engines [14]. A car can also use butanol as a fuel with little or no modification to the engine [3]. In addition, the existing gasoline station and transport infrastructures can continue to be used for butanol transport without modification because butanol is less hygroscopic and less corrosive to the pipelines than ethanol. Currently, butanol is not used as a biofuel due to several challenges. These challenges include substrate cost, butanol toxicity/inhibition to the fermenting microorganisms, and the low butanol titer in the fermentation broth which results in high energy requirements for the recovery of butanol from this dilute stream. To solve the problem of butanol toxicity to the culture, a significant amount of research has been performed on the use of alternative fermentation and product recovery technologies for biobutanol production.

Technologies involving the use of immobilized and cell recycle continuous bioreactors, adsorption, gas stripping, separation using ionic liquids, liquid-liquid extraction, pervaporation, aqueous two phase separation, supercritical extraction, and perstraction have allowed the use of concentrated sugar solutions (up to 500 g/L) for butanol fermentation and the production of a highly concentrated butanol product stream [16, 20]. Typically, ABE fermentation by *Clostridium beijerinckii* proceeds in two phases. The first phase is called the acidogenic phase (acetic and butyric acid are produced) and is growth associated and the second is a solventogenic phase characterized by the uptake of acids and ABE production and which is relatively nongrowth associated [16, 20].

Scientific research including that published by the authors and others, demonstrates the ability of solventogenic *Clostridium* species to use pentose and hexose sugars, the major sugar components of lignocellulosic biomass, for growth and ABE production [15]. Lignocellulosic biomass represents the most abundant renewable energy resource on the planet. The "Billion Ton Study" published by the US Department of Energy (DOE) in 2005 indicated that there could be 1.3 billion dry tons of biomass available per year, enough to produce biofuels to meet more than one-third of the current demand for transportation fuels. Recent breakthroughs in the development of hybrid and electric cars could further reduce petroleum needs and increase this estimate to two-thirds. Collectively, while there is compelling evidence that solventogenic *Clostridium* species are the best natural butanol producing microorganisms with the capacity to use pentose and hexose sugars for butanol production, these microorganisms, including other fermenting microorganisms, use lignocellulosic biomass hydrolyzates poorly due to the presence of inhibitory compounds [15, 16, 18, 20].

Because of the recalcitrance of biomass, pretreatment is commonly used for the hydrolysis of the hemicellulose fraction and the disruption of the lignin sheath of biomass so that enzymatic hydrolysis of the cellulose fraction to glucose can be achieved with greater yield. Unfortunately, during pretreatment and hydrolysis, a complex mixture of microbial inhibitors is generated. Even biomass hydrolyzates produced from the most benign pretreatment and hydrolysis processes can contain some microbial inhibitors because some of the inhibitors are components of hemicellulose and lignin structures of biomass [19]. Consequently, removal of inhibitory compounds from hydrolyzates is typically necessary to facilitate efficient microbial growth and biofuel production. Considering the need of keeping low process costs, the removal of inhibitors from hydrolyzates prior to fermentation is not economically viable given the costs associated with additional processing steps and potential loss of fermentable sugars.

Development of inhibitor tolerant and hyperbutanol producing microbial strains that efficiently metabolize mixed sugars, and compatible advanced fermentation and recovery technologies will accelerate the development of a sustainable lignocellulosic biomass-to-biofuels industry. Many laboratories, including those of the authors, are currently involved in research directed toward strain development for efficient conversion of biomass to butanol and advanced fermentation and recovery techniques for butanol production. This chapter details the recent developments that have been made in this direction.

2 Butanol Producing Cultures

2.1 Traditional Strains

The naturally occurring butanol producing microbes are Gram-positive endospore-forming obligate anaerobes. They belong exclusively to the genus *Clostridium* which includes *C. acetobutylicum*, *C. aurantibutyricum, C. beijerinckii*, *C. cadaveris, C. pasteurianum, C. saccharoperbutylacetonicum, C. saccharobutylicum* (P262)*, C. sporogenes,* and *C. tetanomorphum* [30]. Among these producing strains, the highest butanol production trait was found in *C. acetobutylicum* and *C. beijerinckii* species. Extensive studies related to understanding the molecular mechanisms, developing butanol tolerant *Clostridial* strains were performed with *C. acetobutylicum* ATCC 824*, C. beijerinckii* NCIMB 8052, *C. beijerinckii* P260, and *C. beijerinckii* BA101 [6, 8, 26, 34, 68, 70, 73].

The physiological state of the cells is directly associated with ABE fermentation. Butyric and acetic acids are produced by *C. acetobutylicum* strains during the rapid anaerobic growth phase (acidogenesis phase), resulting in a decrease of the medium pH. Then the butyric and acetic acids are partially re-assimilated and converted into ABE (solventogenic phase) when the culture progresses into the stationary phase, consequently, the pH of the culture is stabilized or increased slightly [31].

The biochemical and molecular events that trigger the switch from acidogenesis to solventogenesis have begun to unfold with time. The decreases of acidogenic enzymes and increases of solventogenic enzymes were reported earlier [22, 29, 31]. The intracellular concentrations of coenzyme A (CoA) and derivatives were found playing regulatory roles [10, 46]. A recent study demonstrated increases of butyryl-phosphate (BuP) during the switch of solvent production and suggested a role of BuP in regulating the transition from acidogenesis to solventogenesis [75].

The completion of genome sequencing of both *C. acetobutylicum* ATCC 824 [44] and *C. beijerinckii* NCIMB 8052 [67] have facilitated microarray analyses to elucidate the molecular mechanism of the shift from acidogenesis to solventogenesis [2, 67]. A response regulator gene *spo0A* positively controls sporulation and promotes the expression of the solvent formation genes (*aad, ctfA, ctfB,* and *adc*) during stationary phase, thus enhancing solvent formation. Inactivation of *spo0A* in *C. acetobutylicum* led to the asporogenic strain SK01 with much reduced butanol production [25]. The overexpression of the *spo0A* in *C. acetobutylicum* ATCC 824 (pMSPOA) resulted in accelerated endospore formation but again decreased butanol production. The *spo0A* plays a regulatory role on sporulation vs. solvent gene expression. The overexpression apparently tips the balance in favor of accelerated sporulation at the expense of overall solvent production [25]. The expression of sporulation genes *spo0A* and *sigF* operon in *C. beijerinckii* NCIMB 8052 was induced during the acidogenic phase and increased significantly during the onset of solvent formation [67]. Interestingly, these genes were induced but the level of induction is two to eight-fold lower in the hyperbutanol-producing *C. beijerinckii* BA101 strain [67]. Based on the above-mentioned findings, the fine tuning of *spo0A* and *sigF* at transcriptional

and translational levels via pathway engineering will help to delay sporulation and to improve solvent production in *Clostridia*. However, it is challenging to perform genetic manipulations using the solvent producing *Clostridium* species. Major barriers include: (a) the strict anaerobic growth requirement, (b) the slow growth, and (c) the small number of genetic tools available to modify the *Clostridium* strains. Therefore, metabolic engineering of other fast-growing, nonspore-forming microbes should be explored for cost-effective butanol production.

2.2 Genetically Engineered Strains

The current fermentative production of butanol is not cost effective because of (1) a spore-forming life cycle, (2) butanol toxicity, (3) slow growth and instability of the producing strains and (4) production of other unwanted byproducts including butyrate, acetate, acetone, and ethanol [31]. In addition, no commercial microbes are available to ferment various lignocellulosic hydrolyzate mixtures into butanol. Thus, new microbes are needed for fermentative conversion of these hydrolyzates to butanol biofuel.

In the recent years, the fermentative production of butanol has been demonstrated in engineered strains of *Escherichia coli* [4, 30, 43] and *Saccharomyces cerevisiae* [71]. The entire butanol production pathway from *Clostridium* has been reconstructed and introduced into these model hosts. More recently, the pathway reconstruction strategy was applied to more robust and butanol tolerant species including *Pseudomonas putida*, *Bacillus subtilis* [43], *Lactobacillus brevis* [7], *Lactobacillus buchneri* [35], and *Corynebacterium glutamicum* [69]. Although the polycistronic expression of the butanol production pathway genes are achieved in these robust host cells, the butanol titers of these recombinant organisms are relatively low (Table 1) and has yet to exceed 19.50 g/L, a production level that can be achieved by *Clostridium* species [57].

Three of the highest butanol producing strains are the engineered *E. coli* strains JCL187, EB4.F, and BUT2, which can produce 552, 580, and 1,200 mg/L of butanol, respectively (Table 1). Although the *E. coli* BUT2 was reported as producing more butanol, the cells were first grown aerobically and later resuspended for anaerobic fermentation. Furthermore, these strains suffer from butanol toxicity (very sensitive to butanol) and can be killed by the accumulation of no more than 15 g/L butanol [32]. So far, no breakthrough improvement of butanol production strains from lignocellulosic biomass hydrolyzates has been reported and yet, more research is needed for strain development.

2.3 Potential of Gram-Positive Bacteria for Butanol Production

Gram-positive bacteria possess several desirable traits, including the ability to ferment multiple sugars simultaneously, to grow at lower pH values, and for some strains, to grow at a temperature range from 30 to 50°C [9]. The Gram-positive Lactic acid bacteria (LAB) are considered attractive biocatalysts for biomass to

Table 1 Genetically modified butanol producing strains

Culture	Max. tolerance (g/L)	Max. production (mg/L)	Substrate	Fermentation conditions and reference
Saccharomyces cerevisiae ESY7	Unknown	2.5	Glucose	Semianaerobic; Steen et al. [71]
Escherichia coli JCL 187	15	552	TB glucose or glycerol	Aerobically; Atsumi et al. [4]
E. coli JCL16, Kivd + ADH2 ilva + leuABCD	Unknown	44–237	Glucose and L-threonine	Nonfermentative pathway; Atsumi et al. [5]
E. coli BUT1	Unknown	320	Glucose	Resuspended cells for anaerobic fermentation; Inui et al. [30]
E. coli BUT2	Unknown	1,200	Glucose	
E. coli BL21 EB4.G	10	580	Glucose	Aerobically; Nielsen et al. [43]
Pseudomonas putida PS1.0	7.5	120	Glycerol	Aerobic, TB medium + 5 g/L glycerol; Nielsen et al. [43]
PS2.0	7.5	112	Glycerol	
Bacillus subtilis BK1.0	12.5	24	Glucose or glycerol	Anaerobic, TB medium + 5 g/L glucose or glycerol; Nielsen et al. [43]
Corynebacterium glutamicum pKS167	20	140	Glucose	Aerobic; Smith et al. [69]
Lactobacillus brevis pHYc-bcs	20–30	300	Glucose	Semiaerobically; Berezina et al. [7]
Lactobacillus brevis pHYc-thl-bcs	20–30	250	Glucose	Semiaerobically; Berezina et al. [7]
Lactobacillus buchneri pTRKH2692Thl	25–30	66	Glucose	Anaerobic; Liu et al. [35]
Lactococcus lactis pTRKH2692Thl	25–30	28	Glucose	Anaerobic; Liu et al. [35]

biofuels for several reasons. LAB have GRAS (Generally Recognized As Safe) status, lack cytochromes, and possess aero-tolerant or anaerobic and obligatory fermentative pathways. They ferment a variety of carbohydrates (both hexoses and pentoses) naturally for growth and fermentation [9]. LAB have relative small genomes [39] that range from 1.7 to 3.3 Mb. Genetic engineering tools are available in several model strains, and in fact, recombinant strains have been developed for production of B-vitamins, mannitol and sorbitol, lactic acid, bacteriocins, exopolysaccharides and oligosaccharides, and other chemicals [28]. In addition, LAB were isolated as source of spoilage in ABE production processes [76], and most LAB species are butanol tolerant ([32] and our unpublished data). Certain species, such as *L. brevis* and *L. buchneri,* are known to grow in the presence of inhibitors derived from plant materials such as wine polyphenolics or hop acids present in beer [36, 66], thus LAB and other nonspore-forming Gram-positive species should be further explored for biomass to butanol production by metabolic pathway reconstructions.

3 Production of Butanol from Agricultural Residues

Production of butanol is adversely affected by the high costs of traditional substrates such as glucose, corn, sugarcane molasses, and whey permeate. To reduce the cost of production, this biofuel could be produced from economically available renewable feedstocks such as corn stover, wheat, barley, and rice straws, corn fiber, switchgrass, alfalfa, reed canary grass, sugarcane bagasse, miscanthus, waste paper, distillers dry grains and solubles (DDGS), and soy molasses. Currently, costs of corn stover, grasses, and straws are in the range of $24–60/ton as opposed to corn which has ranged from $153–218/ton during recent months. It should be noted that while prices of these residue feedstocks are low, they are associated with additional process steps such as pretreatment, and hydrolysis prior to fermentation. Additionally, fermentation inhibitors are generated during the pretreatment process which either halt or slow down reaction rates or fermentation. This section describes production of butanol from wheat straw, barley straw, corn stover, switchgrass, corn fiber, and DDGS and challenges that are faced when handling these feedstocks for the production of this biofuel.

3.1 ABE Production from Wheat and Barley Straws, Corn Stover, Switchgrass, and Dried Distillers' Grains and Solubles

Wheat straw was found to be a novel substrate for the production of ABE in batch fermentation with total ABE production of 25 g/L. In this system, an ABE productivity of 0.60 g/L h was observed which is over 200% that obtained in a control glucose fermentation run ([57]; Table 2). It was speculated that dilute sulfuric acid pretreated and enzymatically hydrolyzed wheat straw (wheat straw hydrolyzate, WSH) contained fermentation stimulating components that enhanced both ABE production levels and productivity. A detailed discussion of fermentation stimulating components present in WSH has been given in Sect. 3.3.

Barley straw is another substrate that is economically available and appears to be similar to wheat straw. Initially, it was thought that the rate of fermentation of barley straw hydrolyzate (BSH) would be similar to that of WSH. However, it was observed that BSH is toxic to *C. beijerinckii* P260. In order to overcome this toxicity problem, a number of treatments were applied including diluting the hydrolyzate with water, mixing with WSH, and overliming. Although all three techniques were successful, overliming resulted in the highest production of ABE (26.64 g/L) suggesting that fermentation inhibitors were removed by overliming [61]. The control fermentation containing equivalent amount of glucose resulted in the production of 21.06 g/L ABE.

Corn stover, which is available in large quantities in the Midwestern region of the United States, can be converted to butanol after pretreatment with dilute sulfuric

Table 2 Production of butanol from various agricultural residues

Biomass	ABE before lime treatment (g/L)	ABE after lime treatment			Reference
		ABE (g/L)	Yield (–)	Productivity (g/L h)	
Control	21.06	[a]	[a]	[a]	Qureshi et al. [61]
WSH	25.00	[a]	[a]	[a]	Qureshi et al. [57]
BSH	7.09	26.64	0.43	0.39	Qureshi et al. [61]
CSH	[b]	26.27	0.44	0.31	Qureshi et al. [62]
CSH	25.70[c]	[a]	[a]	[a]	Parekh et al. [45]
CCH	20.50[d]	[d]	[d]	[d]	Marchal et al. [41]
SGH	1.48	[e]	[f]	[f]	Qureshi et al. [62]
DDGS	[b]	12.8	0.31	0.18	Ezeji and Blaschek [15]

[a] No treatment required as fermentation was good without treatment
[b] Resulted in no growth and no fermentation
[c] Cell recycle experiment (calculated values: yield 0.34, and productivity 1.07 g/L h). Culture used *Clostridium acetobutylicum* P262
[d] Detoxification not reported (perhaps it did not require)
[e] Poor cell growth and fermentation
[f] Not calculated due to poor growth and fermentation

acid and hydrolysis with enzymes. The reader is informed that untreated corn stover hydrolyzate (CSH) did not support cell growth and fermentation, suggesting that it was toxic to the culture. In order to relieve toxic effect, treatments similar to those used for BSH were applied followed by fermentation using *C. beijerinckii* P260. The lime treated hydrolyzate resulted in the production of 26.27 g/L ABE (Table 2) compared to 21.06 g/L using glucose as control [62]. Parekh et al. [45] also produced ABE from CSH employing *C. acetobutylicum* (renamed as *C. saccharobutylicum* P262). These investigators pretreated corn stover employing SO_2 followed by hydrolysis using enzymes. In their studies total ABE concentration of 25.70 g/L was achieved with a yield of 0.34 and a productivity of 1.07 g/L h. It is noteworthy to mention that their hydrolyzate was not toxic to the culture and required no additional treatment such as overliming prior to fermentation. It is likely that SO_2 pretreatment does not generate inhibitors that inhibit culture's viability and fermentative capacity. It is also possible that *Clostridium sacchrobutylicum* P262 is a more tolerant strain than *C. beijerinckii* P260. The reader is informed that productivity obtained in their system cannot be compared with that achieved in our CSH fermentations as these authors employed cell recycle fermentations that result in significantly improved productivity due to increased cell concentration in the reactor. Other authors that reported butanol production from CSH and corncob hydrolyzate (CCH) include Marchal et al. [41]. In these investigations corncobs were pretreated with steam expansion followed by enzymatic hydrolysis and fermentation in large reactor (48,000 L) which resulted in an ABE concentration of 20.50 g/L (Table 2).

Attempts have been made to produce butanol from switchgrass hydrolyzate (SGH). The switchgrass was pretreated and hydrolyzed in a similar manner as barley straw and corn stover and the hydrolyzate was subjected to butanol fermentation.

The untreated SGH did not result in the production of more than 1.48 g/L ABE [62]. When the SGH was diluted twofold with water, the culture produced 14.61 g/L ABE. In order to improve it further the SGH was mixed with WSH and fermented using *C. beijerinckii* P260. In this fermentation the culture produced 8.91 g/L ABE, while lime treated SGH resulted in poor cell growth (0.20 g/L) and no fermentation. It is likely that SGH still contained cell growth and fermentation inhibitors.

Studies were also performed to produce ABE from corn fiber hydrolyzate (CFH; [49]). It was found that untreated CFH was also toxic to the culture and it resulted in the production of 1.7 g/L ABE, while XAD-4 resin (trade name) treated CFH resulted in the production of 9.3 g/L ABE. This suggested that fermentation inhibitors were removed by the resin. Further investigations were performed on the production of ABE from corn fiber arabinoxylan and 9.60 g/L ABE was produced from this substrate in a batch system [51].

In an attempt to produce butanol from DDGS, Ezeji and Blaschek [15] pretreated this lignocellulosic substrate with dilute sulfuric acid, hot water, and ammonia fiber expansion (AFEX) followed by enzymatic hydrolysis. Upon hydrolysis 52.6, 48.8, and 41.4 g/L total sugars were obtained, respectively, from 150 g/L DDGS total solids. Fermentation of these hydrolyzates was then performed using a number of solventogenic cultures including *C. beijerinckii* P260. These cultures were not able to grow in the hydrolyzate due to the presence of toxic chemicals generated during dilute sulfuric acid pretreatment process, indicating that removal of toxic chemicals was essential prior to fermentation. Toxic chemicals were removed by overliming the hydrolyzate and the detoxified hydrolyzate supported cell growth and fermentation thus producing 12.8 g/L total ABE using *C. beijerinckii* P260. This system resulted in a productivity of 0.18 g/L h and an ABE yield of 0.31 [15].

3.2 Cellulosic Hydrolyzate Fermentation Inhibitors

As indicated above, conversion of cellulosic biomass to butanol requires pretreatment employing dilute sulfuric acid or dilute sodium hydroxide, or alkaline peroxide. During the pretreatment and neutralization process, inhibitors such as salts (sodium acetate, sodium chloride, and sodium sulfate), and chemicals including furfural, hydroxymethyl furfural (HMF), syringealdehyde, and acids (acetic, glucuronic, ferulic, and ρ-coumaric) are produced. Some of these chemicals are toxic to the culture. In a recent study it was observed that sodium sulfate [18], sodium chloride [59], glucuronic, ferulic, and ρ-coumaric acids, phenol, and syringealdehyde [18] were toxic to a butanol producing culture. Ferulic acid, at a concentration as low as 0.3 g/L, was a strong inhibitor to both cell growth and fermentation. On the contrary, syringealdehyde (0.3–1.0 g/L) was not so toxic to the cell growth; however, it resulted in complete arrest of ABE production [18]. As expected, phenol was found to be inhibitory to both cell growth and ABE production.

In order to produce ABE from agricultural residues successfully, inhibitors present in the hydrolyzates must be removed prior to fermentation. In recent studies, Qureshi

et al. [61, 62] attempted to produce butanol from untreated and treated BSH and CSH. ABE was successfully produced from the treated hydrolyzates, however, strong inhibition of cell growth was still observed. In case of BSH and CSH, 0.80 and 0.77 g/L cell mass was obtained as compared to 2.66 g/L in the control experiment in which glucose was used. It is likely that chemical inhibitors were removed from the hydrolyzates by overliming leaving behind salts that were generated during neutralization. In order to reduce or eliminate cell growth inhibition, it is recommended that salts also should be removed from the medium by electrodialysis [59] followed by fermentation. Possibly, removal of salts could improve both cell growth and productivity.

3.3 Hydrolyzate Fermentation Stimulators

In an interesting investigation, it was observed that some of the cellulosic hydrolyzate chemicals that are generated during the pretreatment or the neutralization process stimulate both cell growth and ABE production. These chemicals include sodium acetate, furfural, and HMF. In the presence of 8.9 g/L sodium acetate cell growth was slightly improved. In the control experiment 17.8 g/L ABE was produced while in the presence of 8.9 g/L acetate 20.3 g/L ABE was produced, showing an increase of 14%. An improvement in fermentation performance on supplementation of acetate has previously been documented [11, 24]. Inclusion of furfural and HMF (0.3–2.0 g/L) in the fermentation medium improved both cell concentration and ABE production [18]. It is suggested that acetate, furfural, and HMF are beneficial to this fermentation within a certain concentration range.

4 Product Separation Techniques

Butanol fermentation results in low butanol concentration in the fermentation broth due to toxicity of this product to the culture. A maximum concentration of butanol or ABE that can be produced in a batch process is limited to 20–30 g/L. This low concentration of ABE possesses the following problems: (1) low butanol/ABE productivity usually of the order of 0.30–0.50 g/L h; (2) use of dilute sugar solution as feed usually in the range of 50–60 g/L; and (3) energy inefficient recovery of the final product. Recovery of such a low amount of product (20–30 g/L) in combination with butanol's high boiling point (118°C; higher than water) requires a very high amount of energy for distillation thus making the process of butanol production uneconomic. Use of dilute sugar solution as feed for this fermentation requires more energy to prepare and sterilize it (feed) thus resulting in elevated capital and process costs.

In order to make butanol production economic from renewable biomass/residues, one or both of the following approaches should be considered: (1) developing a culture that can produce and tolerate high concentration of this product by application of

Table 3 Selected bioreactor systems employed for the production of butanol

Reactor type	Reactor life (h)	Productivity (g/L h)	ABE produced (g/L)	Sugar used (g/L)	Feed conc. (g/L)	Reference
Batch reactor	68	0.29	17.6	45.4	59.9	Ezeji et al. [17]
Fed-batch reactor[a]	201	0.98	232.8	500.1	500	Ezeji et al. [17]
Continuous reactor[a]	504	0.92	461.3	1125.0	250–500	Ezeji et al. [16, 20]
Immobilized cell reactor	597	15.8	7.9	20.4	61.8–62.5	Qureshi et al. [63]
Immobilized cell reactor[a]	–	16.2	8.1	55.3	55.3	Lienhardt et al. [33]
Immobilized cell reactor[b]	613	4.6	5.1	–	50–67	Huang et al. [27]
Cell recycle reactor[b]	193	4.5	16.0	45.5	45.5	Pierrot et al. [47]
Cell recycle reactor[b]	–	5.4	8.4	–	60.0	Afschar et al. [1]

[a] Integrated system with simultaneous product removal
[b] Some of the parameters are calculated values; — not reported

microbial genetics and/or (2) simultaneous removal of the toxic product from the fermentation broth using energy efficient alternative product recovery technique, an engineering approach. During the last 3 decades, progress in the first direction has been limited and no culture as yet has been developed that can tolerate or produce butanol (*n*-butanol) concentration in excess of 20 g/L, while approach number two has made significant strides in this direction. Simultaneous recovery of butanol from the fermentation broth has been beneficial for this process and following advancements have been made: (1) productivity in free cell fermentations has been improved by a factor of 2–3 (0.98 g/L h, [17]; and 15.8–16.2 g/L h in immobilized cell reactors, [33, 63]); (2) concentrated sugar solution up to 500 g/L have been used; and fermentations have been prolonged thus eliminating down time. Table 3 shows ABE productivity, type of reactor employed, reactor life, and concentration of sugar solution that has been used. Some of the techniques that have been employed for simultaneous product removal include adsorption [50, 74], N_2 gas stripping [13, 52], CO_2 & H_2 (fermentation gases) gas stripping [38, 55], pervaporation [23, 37, 56, 72], liquid-liquid extraction [53, 55, 64, 65], perstraction [54, 55], and reverse osmosis [21]. Details of these product separation techniques are published elsewhere [12, 37, 48].

5 Process Integration

The purpose of process integration is to combine more than one unit operations into a single unit to reduce both capital and operational cost. In butanol fermentation, early reports on process integration were published in the late 1980s and the early

1990s [13, 52] where butanol fermentation was integrated with product separation. In the case of butanol production by fermentation, following process integrations can occur depending upon the feedstock used:

1. Fermentation and recovery of butanol.
2. Hydrolysis of feedstock and fermentation to butanol.
3. Hydrolysis of feedstock, fermentation, and separation of butanol.

In the case of fermentation and recovery, feedstock does not require hydrolysis such as glucose or if it requires hydrolysis, the later can be performed by the butanol producing culture while fermentation occurs. An example of this is the production of butanol from whey permeate (a byproduct of cheese making industry) and simultaneous recovery by gas stripping. Whey permeate contains lactose (a disaccharide of glucose and galactose) which can be hydrolyzed by the culture into monomeric sugar units. Then both of these sugars can be converted to butanol. Butanol that is produced by the culture can be recovered simultaneously by one of the product recovery techniques mentioned in Sect. 4.

The second group is where a feedstock requires hydrolysis using exogenous enzymes. In this case, the butanol producing culture is not capable of hydrolyzing the substrate and hence either enzymes are added to the reactor or hydrolytic enzyme producing culture is propagated with the butanol producing culture. The conditions under which enzymes perform hydrolysis need to be close to the cultivation conditions of butanol producing culture. In this system, hydrolysis and fermentation are all combined. This group is called SSF (Simultaneous Saccharification and Fermentation). The third group is where hydrolysis, fermentation, and recovery are combined. In this case, enzymes or a hydrolytic enzyme producing culture hydrolyses the feedstock such as cellulosic biomass, the butanol producing culture performs fermentation, and application of product (butanol) recovery technique recovers the product simultaneously from the reactor. The third process can be abbreviated as SSFR (simultaneous saccharification, fermentation, and recovery).

5.1 Separate Hydrolysis, Fermentation, and Recovery

Although the cost of agricultural residues is much lower than the cost of other conventional substrates such as corn, the process of butanol production from residues requires additional process steps. One such step is the hydrolysis of residues to simple sugars prior to their conversion to butanol. Unless these residues are converted to simple sugars, they cannot be used by butanol producing cultures. The hydrolysis first requires pretreatment using dilute sulfuric acid or dilute alkali at 121°C or higher. This is done to make cellulosic fibers accessible to enzymes. For our studies dilute sulfuric acid was used in order to make the process simple [57]. Following pretreatment, the biomass was hydrolyzed with enzymes which were then fermented to butanol. Butanol or ABE was then recovered using the gas stripping technique [57]. It is suggested that any of the product recovery techniques described by

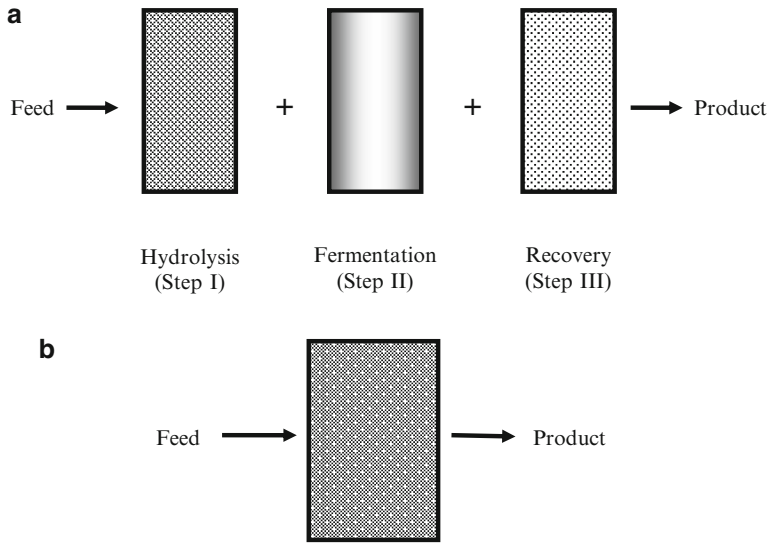

Fig. 1 A schematic diagram of production of butanol/ABE from lignocellulosic biomass employing *Clostridium beijerinckii* P260. (**a**) SHFR (separate hydrolysis fermentation and recovery process); (**b**) SSFR (simultaneous saccharification, fermentation, and recovery process; also known as an integrated process)

Maddox [37] or Qureshi [48] can be used for ABE removal. The overall process of production of butanol from cellulosic biomass by this process requires three separate steps (hydrolysis, fermentation, and recovery) and is called "Separate Hydrolysis, Fermentation, and Recovery (SHFR)." Figure 1a shows a schematic diagram of butanol production by this process.

5.2 Simultaneous Hydrolysis, Fermentation, and Recovery

The process described under this category aims at reducing the number of process steps (SSFR) as opposed to SHFR. In the SSFR process, after pretreatment of the cellulosic biomass, enzymes are added to the reactor and at the same time the reactor is inoculated with a butanol producing culture. Since optimum pH for hydrolytic enzymes and culture that produce butanol is the similar (5.0), these two unit operations can be performed simultaneously in the same reactor. It should be noted that enzymes perform more efficiently at 45°C while the optimum temperature for butanol producing culture is only 35°C. In spite of the different optimum temperatures for the enzymes and the culture, this process performs well. In order to make this

process more efficient, it is recommended that new hydrolytic enzymes be developed with 35°C as their optimum temperature. Since butanol is toxic to the microbial cells, the product should be removed simultaneously. Continuous removal of butanol from the fermentation broth would also prolong the reaction thus improving efficiency of the process further. A schematic diagram of the SSFR process is shown in Fig. 1b. The overall process benefits from this system as all three unit operations are performed in a single reactor. This system has been applied to butanol production from wheat straw [49, 58].

In a study, Marchal et al. [40] produced ABE in an integrated system where hydrolysis and fermentation were combined. These authors did not apply simultaneous product removal technique to remove ABE from the system/fermentation broth. In this system wheat straw was pretreated with alkali followed by washing the straw several times with tap water. Cellulase enzyme was prepared from *Trichoderma reesei* Cl-847 and added to the fermentation medium which was inoculated by *C. acetobutylicum* IFP 921. These investigations were performed in a 6 L bioreactor with 2 L medium containing 194 g (dry weight) of pretreated wheat straw, 12 g of dried corn steep liquor and 360 mL of undiluted enzyme preparation. Approximately 17.3 g/L ABE was produced from the wheat straw.

5.2.1 Batch Fermentation and Recovery

The studies on butanol production employing a SSFR process were performed using wheat straw as a substrate [60]. In this process wheat straw was pretreated with dilute sulfuric acid at 121°C for 1 h followed by cooling the mixture to 45°C and adjusting pH to 5.0 with concentrated NaOH solution. During these studies a number of experiments were performed with the following conclusions: (1) presence of sediments in the reactor does not inhibit fermentation; (2) agitation by gas stripping was necessary to improve mass transfer which helped wheat straw to hydrolyze to near completion and remove butanol simultaneously; and (3) hydrolysis of wheat straw to sugars using enzymes was slower than sugar utilization by the culture to produce butanol and often the culture was found deficient in sugar. This may have been due to different optimum temperatures for enzymes (45°C) and butanol fermentation (35°C). Although, SSFR in a batch reactor was successful, it had some problems that are listed below: (1) aseptic transfer of pretreated wheat straw to the bioreactor was difficult, introducing the possibility of contamination; (2) liquid sampling from the reactor was problematic due to the presence of significant amount of solids in the reactor; and (3) axial agitation of biomass and cell broth affects the culture negatively and hence agitation by gas stripping was considered as an option. While use of gas stripping was helpful, rate of butanol removal from the broth was low thus requiring a large amount of gas recycle. In a batch reactor where SSFR was applied a productivity of 0.31 g/L h was observed (when wheat straw was used) as compared to 0.30 g/L h when glucose was used as a substrate. In this integrated batch process 21.42 g/L total ABE was produced from 86 g/L wheat straw. This system resulted in an ABE yield of 0.37 (g ABE/g sugar released) based on 95% hydrolysis of wheat straw (Table 4).

Table 4 Production of butanol/ABE from wheat straw in simultaneous saccharification, fermentation, and recovery (SSFR) process

Process	Cellulosic sugars used (g/L)	Total ABE produced (g/L)	Productivity (g/L h)	Yield (–)	Reactor operation (h)	Reference
Batch SSFR	52.2	21.4	0.31	0.41	71	Qureshi et al. [60]
Fed-batch SSFR	430.0	192.0	0.36	0.44	533	Qureshi et al. [58]
Batch (no prod. recovery)	50.0	17.3	0.46[a]	0.35	38	Marchal et al. [40]

[a]Calculated value

5.2.2 Fed-Batch Fermentation and Recovery

Production of butanol in a fed-batch reactor is another system where hydrolysis, fermentation, and recovery can be combined (SSFR). Using such a system, butanol was produced from wheat straw [58]. The reactor was loaded with 86 g/L pretreated wheat straw, enzymes, and the butanol producing culture. The system was operated for 533 h at a pH 5.0 and temperature 35°C. During the initial period of 120 h, wheat straw was hydrolyzed completely by the added hydrolytic enzymes. In order to ascertain that the culture was not deficient in sugar, a mixture containing glucose, xylose, arabinose, galactose, and mannose was fed to the reactor to mimic their proportion in wheat straw. In a 1 L reaction mixture a total (including sugar present in WS) of 430 g sugar was used thus producing 192 g total ABE with a yield of 0.44 (Table 4). In this reactor, a productivity of 0.36 g/L h was achieved which is 20% higher than achieved (0.30 g/L h) in a control reactor. One of the major problems associated with this fermentation was that the culture had difficulty utilizing xylose in the later part of fermentation. In this system, gas stripping was used to agitate the treated biomass and recover ABE.

6 Economic Evaluation of Agricultural Residues to Butanol

In a recent economic study on production of butanol from WSH, it was identified that utility costs are one of the most significant factors that impact price of butanol. This was largely due to distillative recovery of butanol from fermentation broth. Wheat straw was treated using dilute sulfuric acid at 121°C and hydrolyzed using enzymes prior to fermentation to butanol. Fermentation was performed in batch reactors employing *C. beijerinckii* P260 followed by recovery by traditional distillation. It was estimated that distillative recovery of butanol would result in the production price of $1.37/kg ($4.26/gal) for a grass rooted/or green field plant while for an annexed plant this price would reduce to $1.07/kg ($3.33/gal). Recovery of butanol using a pervaporation membrane would further reduce this price to

$0.82/kg ($2.55/gal). This price is based on 2010 equipment purchase cost. In an interesting report, commercial production of acetone-butanol was achieved in Russia (then Soviet Union) from hemp waste, corncobs, and sunflower shells [76]. In addition to acetone-butanol, equal emphasis was placed on recovery of gases, vitamin B12, and methane production by digesting the effluent waste thus benefiting from all these coproducts which added to the profitability of the AB plant.

Acknowledgments N. Qureshi would like to thank Michael A. Cotta (United States Department of Agriculture, National Center for Agricultural Utilization Research, Bioenergy Research Unit, Peoria, IL) for reading this manuscript and providing valuable and constructive comments. Part of this work was supported by the hatch grant (Project No: OHO01222; Department of Animal Sciences, The Ohio State University) to T.C. Ezeji.

References

1. Afschar AS, Biebl H, Schaller K et al (1985) Production of acetone and butanol by *Clostridium acetobutylicum* in continuous culture with cell recycle. Appl Microbiol Biotechnol 22:394–398
2. Alsaker KV, Spitzer TR, Papoutsakis ET (2004) Transcriptional analysis of spo0A overexpression in *Clostridium acetobutylicum* and its effect on the cell's response to butanol stress. J Bacteriol 186:1959–1971
3. Antoni D, Zverlov VV, Schwarz WH (2007) Biofuels from microbes. Appl Microbiol Biotechnol 77:23–35
4. Atsumi S, Cann AF, Connor MR et al (2008) Metabolic engineering of *Escherichia coli* for 1-butanol production. Metab Eng 10:305–311
5. Atsumi S, Taizo Hanai T, Liao JC (2008) Non-fermentative pathways for synthesis of branched-chain higher alcohols as biofuels. Nature 451:86–90
6. Baer SH, Blaschek HP, Smith TL (1987) Effect of butanol challenge and temperature on lipid composition and membrane fluidity of butanol-tolerant *Clostridium acetobutylicum*. Appl Environ Microbiol 53:2854–2861
7. Berezina OV, Zakharova NV, Brandt A et al (2010) Reconstructing the clostridial n-butanol metabolic pathway in *Lactobacillus brevis*. Appl Microbiol Biotechnol 87:635–646
8. Borden JR, Papoutsakis ET (2007) Dynamics of genomic-library enrichment and identification of solvent tolerance genes for *Clostridium acetobutylicum*. Appl Environ Microbiol 73(9):3061–3068
9. Bothast RJ, Nichols NN, Dien BS (1999) Fermentations with new recombinant organisms. Biotechnol Prog 15(5):867–875
10. Boynton ZL, Bennett GN, Rudolph FB (1994) Intracellular concentrations of coenzyme A and its derivatives from *Clostridium acetobutylicum* ATCC 824 and their roles in enzyme regulation. Appl Environ Microbiol 60:39–44
11. Chen C-K, Blaschek HP (1999) Acetate enhances solvent production and prevents degeneration in *Clostridium beijerinckii* BA101. Appl Microbiol Biotechnol 52:170–173
12. Ennis BM, Gutierrez NA, Maddox IS (1986) The acetone-butanol-ethanol fermentation: a current assessment. Proc Biochem 21:131–147
13. Ennis BM, Marshall CT, Maddox IS et al (1986) Continuous product recovery by in-situ gas stripping/condensation during solvent production from whey permeate using *Clostridium acetobutylicum*. Biotechnol Lett 8:725–730
14. Ezeji TC, Blaschek HP (2007) Biofuel from butanol: advances in genetic and physiological manipulation of clostridia. BioWorld Eur 2:12–15
15. Ezeji TC, Blaschek HP (2008) Fermentation of dried distillers' grains and soluble (DDGS) hydrolysates to solvents and value-added products by solventogenic clostridia. Bioresour Technol 99:5232–5242

16. Ezeji TC, Milne C, Price ND et al (2010) Achievements and perspectives to overcome the poor solvent resistance in acetone and butanol-producing microorganisms. Appl Microbiol Biotechnol 85:1697–1712
17. Ezeji TC, Qureshi N, Blaschek HP (2004) Acetone butanol ethanol (ABE) production from concentrated substrate: reduction in substrate inhibition by fed-batch technique and product inhibition by gas stripping. Appl Microbiol Biotechnol 63:653–658
18. Ezeji TC, Qureshi N, Blaschek HP (2007) Butanol production from agricultural residues: impact of degradation products on *Clostridium beijerinckii* growth and butanol fermentation. Biotechnol Bioeng 97:1460–1469
19. Ezeji TC, Qureshi N, Blaschek HP (2007) Bioproduction of butanol from biomass: from genes to bioreactors. Curr Opin Biotechnol 18:220–227
20. Ezeji TC, Qureshi N, Blaschek HP (2012) Microbial production of a biofuel (acetone-butanol-ethanol) in a continuous bioreactor: Impact of bleed and simultaneous product recovery. Bioproc Biosyst Eng (In press)
21. Garcia A, Innotti EL, Fischer JL (1986) Butanol fermentation liquor production and separation by reverse osmosis. Biotechnol Bioeng 28:785–791
22. Gottschalk G, Gottwald M (1985) Internal pH of *Clostridium acetobutylicum* and its effect on the shift from acid to solvent formation. Arch Microbiol 143:42–46
23. Groot WJ, van der Lans RGJM, Luyben ChAM (1992) Technologies for butanol recovery integrated with fermentations. Proc Biochem 27:61–75
24. Gu Y, Hu S, Chen J et al (2009) Ammonium acetate enhances solvent production by *Clostridium acetobutylicum* EA 2018 using cassava as a fermentation medium. J Ind Microbiol Biotechnol 36:1225–1232
25. Harris LM, Welker NE, Papoutsakis ET (2002) Northern, morphological and fermentation analysis of *spo0A* inactivation and overexpression in *Clostridium acetobutylicum* ATCC 824. J Bacteriol 184:3586–3597
26. Hermann M, Fayolle F, Marchal R et al (1985) Isolation and characterization of butanol-resistant mutants of *Clostridium acetobutylicum*. Appl Environ Microbiol 50:1238–1243
27. Huang W-C, Ramey DE, Yang S-T (2004) Continuous production of butanol by *Clostridium acetobutylicum* immobilized in a fibrous bed reactor. Appl Biochem Biotechnol 113–116: 887–898
28. Hugenholtz J, Sybesma W, Groot MN et al (2002) Metabolic engineering of lactic acid bacteria for the production of nutraceuticals. Antonie Van Leeuwenhoek 82(1–4):217–235
29. Husemann MH, Papoutsakis ET (1989) Enzymes limiting butanol and acetone formation in continuous and batch cultures of *Clostridium acetobutylicum*. Appl Microbiol Biotechnol 31: 435–444
30. Inui M, Suda M, Kimura S et al (2008) Expression of *Clostridium acetobutylicum* butanol synthetic genes in *Escherichia coli*. Appl Microbiol Biotechnol 77:1305–1316
31. Jones DT, Woods DR (1986) Acetone-butanol fermentation revisited. Microbiol Rev 50:484–524
32. Knoshaug EP, Zhang M (2008) Butanol tolerance in a selection of microorganisms. Appl Biochem Biotechnol 153:13–20
33. Lienhardt J, Schripsema J, Qureshi N et al (2002) Butanol production by *Clostridium beijerinckii* BA101 in an immobilized cell biofilm reactor. Appl Biochem Biotechnol 98–100:591–598
34. Lin YL, Blaschek HP (1983) Butanol production by a butanol-tolerant strain of *Clostridium acetobutylicum* in extruded corn broth. Appl Environ Microbiol 45:966–973
35. Liu S, Bischoff KM, Qureshi N et al (2010) Functional expression of the thiolase gene *thl* from *Clostridium beijerinckii* P260 in *Lactococcus lactis* and *Lactobacillus buchneri*. N Biotechnol 27:283–288
36. Lonvaud-Funel A (1999) Lactic acid bacteria in the quality improvement and depreciation of wine. Antonie Van Leeuwenhoek 76(1–4):317–331
37. Maddox IS (1989) The acetone-butanol-ethanol fermentation: recent progress in technology. Biotechnol Genet Eng Rev 7:189–220
38. Maddox IS, Qureshi N, Roberts-Thomson K (1995) Production of acetone-butanol from concentrated substrates using *Clostridium acetobutylicum* in an integrated fermentation-product removal process. Proc Biochem 30:209–215

39. Makarova K, Slesareva A, Wolf Y et al (2006) Comparative genomics of the lactic acid bacteria. Proc Natl Acad Sci 103:15611–15616
40. Marchal R, Rebeller M, Vandecasteele JP (1984) Direct conversion of alkali-pretreated straw using simultaneous enzymatic hydrolysis and acetone-butanol fermentation. Biotechnol Lett 6:523–528
41. Marchal R, Ropars M, Pourquie J et al (1992) Large-scale enzymatic hydrolysis of agricultural lignocellulosic biomass. Part 2: conversion into acetone-butanol. Bioresour Technol 42:205–217
42. Ni Y, Sun Z (2009) Recent progress on industrial fermentative production of acetone-butanol-ethanol by *Clostridium acetobutylicum* in China. Appl Microbiol Biotechnol 83:415–423
43. Nielsen DR, Leonard E, Yoon SH et al (2009) Engineering alternative butanol production platforms in heterologous bacteria. Metab Eng 11:262–273
44. Nolling J, Breton G, Omelchenko MV et al (2001) Genome sequence and comparative analysis of the solvent-producing bacterium *Clostridium acetobutylicum*. J Bacteriol 183:4823–4838
45. Parekh SR, Parekh RS, Wayman M (1988) Ethanol and butanol production by fermentation of enzymatically saccharified SO_2-pretreated lignocellulosics. Enzyme Microb Technol 10: 660–668
46. Petersen DJ, Bennett GN (1991) Cloning of the *Clostridium acetobutylicum* ATCC 824 acetyl coenzyme A acetyltransferase (thiolase; EC 2.3.1.9) gene. Appl Environ Microbiol 57: 2735–2741
47. Pierrot P, Fick M, Engasser JM (1986) Continuous acetone-butanol fermentation with high productivity by cell ultrafiltration and recycling. Biotechnol Lett 8:253–256
48. Qureshi N (2009) Solvent production. In: Schaechter M (ed) Encyclopedia of microbiology. Elsevier Ltd, Oxford, UK pp 512–528
49. Qureshi N, Ezeji TC, Ebener J et al (2008) Butanol production by *Clostridium beijerinckii*. Part I: use of acid and enzyme hydrolyzed corn fiber. Bioresour Technol 99:5915–5922
50. Qureshi N, Hughes S, Maddox IS, Cotta MA (2005) Energy efficient recovery of butanol from fermentation broth by adsorption. Bioprocess Biosyst Eng 27:215–222
51. Qureshi N, Li X-L, Hughes S, Saha BC et al (2006) Butanol production from corn fiber xylan using *Clostridium acetobutylicum*. Biotechnol Prog 22:673–680
52. Qureshi N, Maddox IS (1991) Integration of continuous production and recovery of solvents from whey permeate: use of immobilized cells of *Clostridium acetobutylicum* in a fluidized bed reactor coupled with gas stripping. Bioproc Eng 6:63–69
53. Qureshi N, Maddox IS (1995) Continuous production of acetone butanol ethanol using immobilized cells of *Clostridium acetobutylicum* and integration with product removal by liquid-liquid extraction. J Ferm Bioeng 80:185–189
54. Qureshi N, Maddox IS (2005) Reduction in butanol inhibition by perstraction: utilization of concentrated lactose/whey permeate by *Clostridium acetobutylicum* to enhance butanol fermentation economics. Food Bioprod Proc C 83(C1):43–52
55. Qureshi N, Maddox IS, Friedl A (1992) Application of continuous substrate feeding to the ABE fermentation: relief of product inhibition using extraction, perstraction, stripping, and pervaporation. Biotechnol Prog 8:382–390
56. Qureshi N, Meagher MM, Hutkins RW (1999) Recovery of butanol from model solutions and fermentation broth using a silicalite/silicone membrane. J Membr Sci 158:115–125
57. Qureshi N, Saha BC, Cotta MA (2007) Butanol production from wheat straw hydrolysate using *Clostridium beijerinckii*. Bioprocess Biosyst Eng 30:419–427
58. Qureshi N, Saha BC, Cotta MA (2008) Butanol production from wheat straw by simultaneous saccharification and fermentation using *Clostridium beijerinckii*: part II—fed-batch fermentation. Biomass Bioenergy 32:176–183
59. Qureshi N, Saha BC, Hector RE et al (2008) Removal of fermentation inhibitors from alkaline peroxide pretreated and enzymatically hydrolyzed wheat straw: production of butanol from hydrolysate using *Clostridium beijerinckii* in batch reactors. Biomass Bioenergy 32: 1353–1358

60. Qureshi N, Saha BC, Hector RE et al (2008) Butanol production from wheat straw by simultaneous saccharification and fermentation using *Clostridium beijerinckii*: part I—batch fermentation. Biomass Bioenergy 32:168–175
61. Qureshi N, Saha BC, Dien B et al (2010) Production of butanol (a biofuel) from agricultural residues: part I—use of barley straw hydrolysate. Biomass Bioenergy 34:559–565
62. Qureshi N, Saha BC, Hector RE et al (2010) Production of butanol (a biofuel) from agricultural residues: part II—use of corn stover and switchgrass hydrolysate. Biomass Bioenergy 34: 566–571
63. Qureshi N, Schripsema J, Lienhardt J et al (2000) Continuous solvent production by *Clostridium beijerinckii* BA101 immobilized by adsorption onto brick. World J Microbiol Biotechnol 16: 377–382
64. Roffler SR, Blanch HW, Wilke CR (1987) In-situ recovery of butanol during fermentation: part I—batch extractive fermentation. Bioproc Eng 2:1–12
65. Roffler SR, Blanch HW, Wilke CR (1987) In-situ recovery of butanol during fermentation: part 2—fed-batch extractive fermentation. Bioproc Eng 2:181–190
66. Sakamoto K, Konings WN (2003) Beer spoilage bacteria and hop resistance. Int J Food Microbiol 89(2–3):105–124
67. Shi Z, Blaschek HP (2008) Transcriptional analysis of *Clostridium beijerinckii* NCIMB 8052 and the hyper-butanol-producing mutant BA101 during the shift from acidogenesis to solventogenesis. Appl Environ Microbiol 74:7709–7714
68. Sillers R, Al-Hinai MA, Papoutsakis ET (2009) Aldehyde-alcohol dehydrogenase and/or thiolase overexpression coupled with CoA transferase downregulation lead to higher alcohol titers and selectivity in *Clostridium acetobutylicum* fermentations. Biotechnol Bioeng 102: 38–49
69. Smith KM, Cho K-M, Liao JC (2010) Engineering *Corynebacterium glutamicum* for isobutanol production. Appl Microbiol Biotechnol 87:1045–1055
70. Soucaille P, Joliff G, Izard A et al (1987) Butanol tolerance and autobacteriocin production by *Clostridium acetobutylicum*. Curr Microbiol 14:295–299
71. Steen EJ, Chan R, Prasad N et al (2008) Metabolic engineering of *Saccharomyces cerevisiae* for the production of n-butanol. Microb Cell Fact 7:36
72. Thongsukmak A, Sirkar KK (2007) Pervaporative membranes highly selective for solvents present in fermentation broths. J Membr Sci 302:45–58
73. Tomas CA, Welker NE, Papoutsakis ET (2003) Overexpression of groESL in *Clostridium acetobutylicum* results in increased solvent production and tolerance, prolonged metabolism, and changes in the cell's transcriptional program. Appl Environ Microbiol 69:4951–4965
74. Yang X, Tsai G-J, Tsao GT (1994) Enhancement of *in situ* adsorption on the acetone-butanol fermentation by *Clostridium acetobutylicum*. Sep Technol 4:81–92
75. Zhao Y, Tomas CA, Rudolph FB et al (2005) Intracellular butyryl phosphate and acetyl phosphate concentrations in *Clostridium acetobutylicum* and their implications for solvent formation. Appl Environ Microbiol 71:530–537
76. Zverlov VV, Berezina O, Velikodvorskaya GA et al (2006) Bacterial acetone and butanol production by industrial fermentation in the Soviet Union: use of hydrolyzed agricultural waste for biorefinery. Appl Microbiol Biotechnol 71:587–597

Chapter 16
Consolidated Bioprocessing

Jeffrey G. Linger and Al Darzins

Abstract The production of ethanol and other biofuels through the biochemical conversion of lignocellulosic biomass represents a promising path towards sustainably achieving the immense global demand for liquid transportation fuels. While numerous cellulosic ethanol production process configurations exist, the one known as Consolidated Bioprocessing (CBP) stands alone in combining all biologically mediated events into the action of a single organism (i.e., production and secretion of saccharolytic enzymes, hydrolysis of cellulose and hemicellulose, and fermentation of six-carbon and five-carbon sugars into biofuels such as ethanol). We discuss here the major issues with developing CBP technologies including the promises and challenges, the two prominently pursued routes to achieve this technology and several of the most promising candidate organisms. CBP represents a low-risk, high-reward proposition and its pursuit by researchers is most certainly warranted as we look to the future.

1 Introduction

The biological conversion of lignocellulosic biomass (biomass) to fuels such as ethanol or butanol is broadly viewed as a very achievable means to producing large quantities of liquid transportation fuel from renewable resources in the shadow of a

J.G. Linger (✉)
National Bioenergy Center, National Renewable Energy Laboratory,
1617 Cole Blvd, Golden, CO 80401, USA
e-mail: Jeffrey.Linger@nrel.gov

A. Darzins
National Bioenergy Center, National Renewable Energy Laboratory,
1617 Cole Blvd, Golden, CO 80401, USA

DuPont Central Research and Development, 200 Powder Mill Road,
Wilmington, DE 19803, USA
e-mail: Al.Darzins@usa.dupont.com

J.W. Lee (ed.), *Advanced Biofuels and Bioproducts*, DOI 10.1007/978-1-4614-3348-4_16,

waning supply of fossil fuels and an ever-changing energy marketplace. The biochemical conversion of cellulosic biomass to ethanol, for example, represents a major untapped potential fuel source, with minimal environmental impacts [1]. The challenge has always been to make the ethanol production process financially competitive in the current fuel market [2, 3]. While the commercial conversion of starches and monomeric sugars to fuel is a relatively straightforward process, the utilization of biomass as a starting feedstock is rather complex owing in large part to the recalcitrance of biomass, and to the heterogeneity of the substrate. Biomass recalcitrance is a general term which refers to the resistance of plant cell walls to enzymatic deconstruction [2], while heterogeneity refers to the complex mixture of lignin, cellulose and hemicellulose consisting of numerous sugar polymers, and the various chemical side-chain modifications that exist in different amounts and whose ratios vary among biomass feedstocks. The particularly difficult nature of using lignocellulosic biomass as the feedstock for the biological production of ethanol has led to the development of numerous process configurations that can be used to break down biomass in distinct, yet nontrivial steps. These steps include chemical pretreatment, enzymatic deconstruction and depolymerization of cellulose and hemicellulose, fermentation of hexose sugars, and fermentation of the pentose sugars [4, 5]. The detailed discussion of biomass chemical pretreatment is beyond the scope of our focus, but we mention it here because it is an absolutely essential component of current process configurations and still represents a significant research effort within the field of biofuels production. While numerous process configurations exist that separate the different steps mentioned above, perhaps no other configuration has garnered as much attention or caught the imagination of researchers as much as the one known as "Consolidated Bioprocessing," also referred to as "CBP" [4, 6–12] (Fig. 1).

The concept of CBP refers to combining the four biologically mediated processing steps into the action of a single microorganism, or a consortium of microorganisms. As most CBP research has focused on single organisms, we limit our discussion to these candidates in this review. Essentially, an organism must produce and secrete multiple glycoside hydrolase enzymes to depolymerize the cellulose and hemicellulose within the pretreated biomass, uptake the newly released monomeric sugars, and metabolize both the five-carbon sugars and the six-carbon sugars to produce ethanol. While the concept is simple to describe, the intricacies of generating a viable CBP organism are extremely complex. In this review, we briefly discuss the promises and challenges of achieving commercially relevant CBP, the general strategies employed, and further discuss the advantages and disadvantages of candidate CBP organisms.

2 Rationale and Potential for Consolidated Bioprocessing

CBP puts the onus on a single microorganism to independently convert pretreated biomass directly to a biofuel such as ethanol. Not surprisingly, the ultimate driving factor behind the concept of developing consolidated processing technologies has

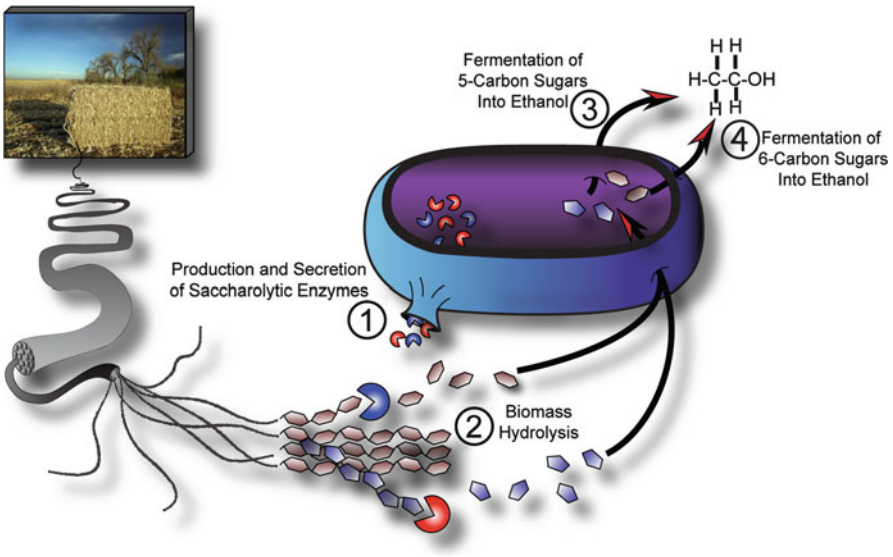

Fig. 1 Consolidated bioprocessing. The four biologically mediated steps to achieving consolidated bioprocessing are: (1) production and secretion of saccharolytic enzymes, (2) hydrolysis of cellulose and hemicellulose (biomass), (3) fermentation of five-carbon sugars into ethanol, (4) fermentation of six-carbon sugars into ethanol

always been cost reduction. The primary cost reduction comes from the fact that when the fermentation organism can produce and secrete the cellulolytic enzymes which are necessary to deconstruct biomass, it alleviates the need for a dedicated and separate enzyme production step. This would significantly reduce capital costs related to equipment used for enzyme production (if produced in-house), and would further decrease processing costs equal to the value of dedicated cellulase production (and delivery if produced externally). With this case laid out, the true value of pursuing a CBP technology is dependent upon the cost of generating enzymes separately. As the development of cellulase enzyme technologies progress and production costs continue to decrease so do the merits of pursuing CBP. However, while commercial enzyme costs have seemingly decreased over the last decade or so, they still represent a significant cost input into the conversion of biomass to ethanol. Accordingly, while perhaps not as attractive of a pursuit as it was a decade ago, the generation of a true CBP organism could still impart a substantial cost reduction to biofuels production. Emphasizing that point, it has recently been reported that the costs of pretreatment and the generation of cellulase enzymes remain the predominant financial barriers to realizing the full potential of cellulosic ethanol production [13, 14]. Furthermore, the development of more efficient microbial strain engineering techniques has made the task of creating a CBP organism less daunting than ever before, adding to the attraction of pursuing a CBP approach.

No one has yet identified a naturally existing microorganism that can produce and secrete sufficient cellulolytic activities, while simultaneously fermenting the

liberated sugars to a high titer of ethanol in the presence of toxic components found in lignocellulosic-derived hydrolysates. This is especially true given the trend of using higher percent solids loading, as a means of reducing water consumption during the process. As such, genetic engineering has played a key role in attempts to synthetically create such a commercially relevant organism. Two major strategies geared towards creating a CBP organism have generally been followed to date: The engineering of either a native cellulophile or a native ethanologen. These two strategies have also been previously referred to as the "native cellulolytic" and "recombinant cellulolytic" approaches, respectively [5].

3 Native Cellulophile Approach

At its foundation, this approach uses a microorganism that is very adept at utilizing cellulose as a growth substrate, and attempts to instill the ability in the organism to produce high yields and titers of ethanol in the presence of a biomass hydrolysate environment. This approach benefits from having the extremely complex process of deconstructing plant cell walls already programmed within the organism's metabolism. In this particular case, suites of cellulase enzymes do not need to be heterologously expressed thereby allowing metabolic engineering and strain adaptation approaches to focus solely on increasing ethanol production and on product and hydrolysate tolerance mechanisms, while reducing organic acid production. However, this is no trivial matter as most candidate cellulolytic organisms have only very minimal capabilities of producing ethanol anywhere near the yields and titers that would be required for a viable cellulosic ethanol production process. Further complicating the native cellulophile approach is that, generally speaking, the molecular biology tools for engineering candidate cellulolytic organisms have not been as well established relative to other commonly used model organisms. This makes the process of creating a robust fermentation organism from a cellulolytic candidate challenging to say the least. With that said, some progress has been made along this front and several cellulolytic candidate organisms have made it to the forefront as potential CBP host organisms including *Clostridium thermocellum*, *Clostridium phytofermentans*, *Clostridium cellulolyticum*, *Thermoanaerbacterium saccharolyticum*, and recently, *Trichoderma reesei*. We discuss the potential of several of these candidate microorganisms in further detail below.

3.1 Clostridium thermocellum

C. thermocellum is a thermophilic anaerobe with a naturally powerful cellulosome-based cellulolytic system that was first isolated in pure culture in 1954 [15]. Its prominence as a candidate CBP organism stems from its innate ability to deconstruct and ferment cellulose directly to ethanol, through a very efficient cellulose metabolism

at very high temperatures. Despite these positive attributes, native isolates can only generate very low levels of ethanol ranging from 0.08 to 0.29 g ethanol per g glucose equivalents [16–19] and cannot tolerate levels of the fermentation product exceeding 1.5% [20–23]. The phenotype of increased tolerance to ethanol has been successfully identified in some strains reportedly being able to tolerate ethanol concentrations approaching 7–8% in certain cases [23]. However, this was not in the presence of hydrolysate which has additional potent inhibitors present that can synergistically decrease tolerance to ethanol [24]. An additional detriment of *C. thermocellum* is that it lacks the native ability to ferment pentose sugars [7] which would leave the hemicellulose component of biomass unconverted in the process.

As with all current candidate CBP organisms, the creation of improved *C. thermocellum* strains requires the ability of the organism to be genetically manipulated, a capability that at one point remained quite elusive. Recently, however, researchers have developed methods to perform a variety of genetic manipulations [25–27], and very recently a group of researchers has developed the ability to perform targeted gene knockouts in *C. thermocellum* [26], which will be an essential tool for performing targeted metabolic engineering in this organism that was once seen as genetically rigid. While additional techniques will need to be established and further developed, this breakthrough makes this highly cellulolytic organism acquiescent towards genetic manipulations and more importantly shows that *C. thermocellum* will become a strong candidate organism for CBP. However, major hurdles still need to be overcome with the engineering of this organism including the incorporation of a pentose sugar fermentation pathway, and instilling the ability to produce and tolerate higher levels of ethanol while resisting the toxic environment of a cellulosic hydrolysate. It also seems quite likely that given this organism's ability to deconstruct native biomass, a less severe pretreatment configuration might be an option, thus reducing the toxicity of the hydrolysate. Nonetheless, *C. thermocellum* remains a prime candidate organism in the field of CBP owing predominately to its strong ability to deconstruct biomass.

3.2 Thermanaerobacterium saccharolyticum

While *T. saccharolyticum* cannot be considered as a strict CBP candidate since it is noncellulolytic, it does have important properties that give it some warranted attention potentially as a member of a CBP consortium. It is an anaerobic thermophilic bacterium but unlike *C. thermocellum*, *T. saccharolyticum* can ferment xylan and all other biomass-derived sugars making the engineering of this organism somewhat less complicated in that regard. Furthermore, high frequency gene transfer has been achieved in this organism [28, 29] increasing the capacity for strain engineering. Importantly, the catabolic pathways have been mapped out with key metabolic enzymes identified [30] providing the necessary knowledge base to address the relevant metabolic pathways. In fact, highly effective metabolic engineering has been performed on *T. saccharolyticum* allowing it to produce ethanol with a maximum

titer of 37 g/L, which while greatly lower than many ethanologens, is the highest reported for a thermophilic anaerobe [31]. While the use of this organism alone is unlikely to achieve the endpoints required for a robust CBP host, we feel that given its great promise as a biocatalyst for the conversion of hemicellulose, it is an organism worthy of future research endeavors.

3.3 Trichoderma reesei

Naturally occurring fungi such as *T. reesei* and *Aspergillus* species have the capability of secreting massive quantities of cellulases including endo-β glucanases, exo-β glucanases, and β glucosidases. The action of these three enzymes can work synergistically to solubilize lignocellulosic feedstocks yielding glucose that can be converted via fermentation to ethanol. Some arguments have recently been presented for developing *T. reesei* as a CBP host [78]. While research in this direction is still preliminary, we mention it here because it represents out-of-the-box thinking that will be required to drive CBP research forward. While *T. reesei* and other fungal species have been shown to harbor the metabolic pathways that are necessary to produce ethanol from sugars, the levels of ethanol produced by these microorganisms are nevertheless rather low compared to the more robust fermentation organisms such as *Zymomonas mobilis* and *Saccharomyces cerevisiae* [78]. Moreover, *T. reesei* is an obligate aerobe making ethanol production process more complicated through either strain engineering or process reconfiguration. Furthermore, its filamentous nature will make mixing within the fermentation tank challenging yet more essential than with a unicellular organism. Despite these formidable challenges, the raw cellulolytic power of *T. reesei* and the innate, if not overwhelming, ability to produce ethanol make it an intriguing CBP candidate. However, much more research will need to be done to determine the feasibility of using this organism as a CBP host.

4 Native Ethanologen Approach

The basic premise of the native ethanologen CBP approach is to start with a robust ethanologen, and engineer in it the ability to produce and secrete a suite of cellulolytic enzymes. This approach generally takes advantage of already having an excellent ethanol production system with ethanol tolerance mechanisms in place, and either natural or engineered abilities to utilize the major biomass-derived sugars including xylose and arabinose. With the metabolic foundation intact, the strain development effort can focus solely on producing large amounts of cellulases and directing them to the extracellular space. However, these related processes represent distinct challenges in and of themselves, and can indeed be quite complex. While most attempts at pursuing this route have expressed one to several separate cellulases, a native

cellulose-degrading organism will generally produce dozens of distinct enzymes in order to achieve this task. For example, *T. reesei* a cellulolytic fungi with the premiere cellulose-degrading enzyme, CBHI [32], expresses 10 cellulose-degrading and 16 hemicellulose-degrading enzymes [12]. Optimizing the functional expression of many enzymes can be complicated as it includes transcription, translation, peptide folding, and ensuring protein stability. Further complicating the case is that many enzymes, particularly of fungal origin, need post-translational modifications including glycosylation to achieve maximal activity or stability [33–35]. In addition, the enzymes must be targeted either directly or indirectly to be secreted extracellularly. Of course, the advantage that recombinant CBP organisms have over cellulolytic organisms in nature is that they are fed a partially deconstructed substrate due to thermochemical pretreatment, making the task of cellulose and hemicellulose depolymerization less daunting, and requiring fewer enzymes. At an absolute minimum, an endoglucanase, an exoglucanase (cellobiohydrolase) and a β-glucosidase will be required to fully depolymerize cellulose [36], and very likely additional accessory enzymes will be required, making the expression of sufficient enzymes a challenging task.

There are numerous ethanologens that have been considered as candidates for conversion to a CBP organism including *Escherichia coli* [7, 37, 38], *Klebsiella oxytoca* [7, 39–41], *Z. mobilis* [42–47], and several yeasts including *S. cerevisiae* [6, 9, 48–50]. Given their strong representation in the cellulosic biofuels research landscape, we will discuss *S. cerevisiae* and *Z. mobilis* in more detail below.

4.1 Saccharomyces cerevisiae

There are several species of yeast that have been explored as a base platform for developing a CBP organism including *Pichia stipitis* [51], *Candida shehatae* [52], *Pachysolen tannophilis* [53], and *S. cerevisiae* [9]. Each of these species has some very positive attributes. In fact, the former three microorganisms are naturally capable of fermenting both glucose and xylose to ethanol [54], and each produce some level of hemicellulolytic and/or cellulolytic enzymes. However, overall the ethanol production is generally low in these organisms making them less than ideal [55–57]. The fact, however, remains that *S. cerevisiae* is still the preeminent yeast candidate for CBP development, as excellently reviewed by van Zyl et al. [9]. The primary attributes of *S. cerevisiae* include its robust ability to produce ethanol, its extreme genetic malleability, its industrial affability, and the fact that it has been successfully engineered to ferment pentose sugars [58–61]. In general, the primary detriments to yeast include their tendency as a group to hyperglycosylate heterologously expressed enzymes that can negatively affect enzyme activity [62, 63], and the fact that secretion of heterologous proteins is subject to several bottlenecks that limit yield [64]. Additionally, when compared to organisms like *Z. mobilis*, yeast exhibits a relatively high formation of cellular mass thus lowering the potential ethanol yield [65]. However, the major hurdle to overcome with *S. cerevisiae* as is the case with all

ethanologen CBP candidates is achieving high level expression and secretion of saccharolytic enzymes.

There have been some major accomplishments in this respect including the ability to produce sufficient β-glucosidases to support rapid growth on cellobiose as the sole carbon source [66, 67]. This finding is important in that it suggests that cellobiose conversion will not be the limiting step in cellulose conversion and establishes research on heterologous endoglucanase and cellobiohydrolase expression as a higher priority.

The endoglucanases expressed in *S. cerevisiae* have been taken from diverse sources including *T. reesei*, *Aspergillus niger*, *Cellulomonas fimi*, *Thermoascus aurantiacus*, *Cryptococcus flavus*, *C. thermocellum*, *Bacillus subtilis*, and *Acidothermus cellulolyticus* among others [9]. Taken as a whole, these enzyme expression studies have been relatively successful; however, the overall level of extracellular endoglucanases remains low. The reported expression of high levels of these proteins must be carefully evaluated. For example, the expression of high levels of a significantly less active enzyme only puts a great metabolic burden on the cell. Importantly, van Zyl et al. [9] calculate based on the enzyme expression levels of *T. reesei* that a secreted endoglucanase needs to only comprise 0.3% of the total cellular protein in yeast to achieve sufficient extracellular endoglucanase levels. This should be within the acceptable limits of protein expression and secretion in *S. cerevisiae*. It seems that the major hurdle continues to be achieving high enough expression and secretion of β-exoglucanase activity.

Achieving sufficient extracellular production of cellobiohydrolase (CBH) activity seems to be the lynchpin to achieving a successful native ethanologen based approach to CBP, and this is true in the case of *S. cerevisiae* as well. The powerful cellobiohydrolase (CBHI) from *T. reesei* is the major cellulolytic enzyme produced, comprising an astounding 60% of total mass [68]. While numerous studies have attempted to express CBHI and other CBHs in *S. cerevisiae* none have been anywhere close to this amount, with the highest reported amount of secreted enzyme being 1.5% [9, 48, 69]. Importantly, however, researchers have demonstrated the direct hydrolysis and fermentation of amorphous cellulose using recombinant yeast providing an important step in the development of this organism [6]. It has been estimated that yeast-expressed CBH activity needs to be improved approximately 20–120 fold [69], but with improved strain development techniques, and a better understanding of recombinant protein expression and secretion in yeast, there is reason for guarded optimism along this front.

4.2 Zymomonas mobilis

One organism that lacks some of the potential problems encountered in *S. cerevisiae* and *C. thermocellum*, and is a strong candidate for CBP, is the gram-negative bacterium *Z. mobilis*. *Z. mobilis* was first identified as an organism causing cider sickness [70], and has since been studied for its outstanding ability to produce ethanol

to a high titer and yield [4, 42, 71–77]. Furthermore, *Z. mobilis* has a reduced cellular mass formation during fermentation, partially attributable to its sole use of the Entner-Doudoroff pathway [78] thus allowing *Z. mobilis* to approach the theoretical maximum ethanol yields during fermentation. As such, *Z. mobilis* has been used successfully in simultaneous saccharification and fermentation and simultaneous saccharification and cofermentation processes [79–81]. Additionally, while it can only natively ferment hexose sugars, it has been engineered to ferment the hemicellulosic pentose (C5) sugars, xylose [82], and arabinose [83].

A prerequisite to establishing *Z. mobilis* as a CBP organism is to achieve high levels of heterologous cellulase enzyme expression. While this is certainly no trivial task, definitive progress has been made along this front [44–46, 84–87]. Recently, our own research efforts focused on the expression and secretion of various cellulases in *Z. mobilis* demonstrating the ability of this microorganism to constitutively express high levels of cellulases (up to 5% of the total cellular protein). However, secretion of these enzymes was the major limiting factor to obtaining high levels of extracellular cellulases [47]. While we were able to detect approximately 25% of the total cellulolytic activity in the extracellular space, the fact remains that in the case of CBP, any enzyme that remains intracellular is not able to participate in biomass hydrolysis. While the secretion levels we achieved were significant and an important step towards the development of *Z. mobilis* into a CBP organism, there is certainly room for additional improvements. We anticipate that for *Z. mobilis* to be successfully developed into a CBP organism, methods to increase recombinant protein secretion will need to be greatly improved. We and others [42] have attempted to utilize *Z. mobilis* secretion signals belonging to either of the two major branches of the type II secretion apparatus (SecB-dependent [88] and the Twin Arginine Translocation pathway [89]), but feel that in order to secrete the large amounts of extracellular cellulases that will be required, the use of alternative strategies is going to be essential. This could be through enhancement of the type II pathways by coexpressing secretion machinery components, or through the use of alternative secretion systems including the type I secretion system that directly secretes from the cytoplasm to the extracellular space, bypassing a periplasmic intermediate step [90]. While significant hurdles still need to be overcome, including the expression of sufficient cellobiohydrolase activity, we feel that *Z. mobilis* remains one of the more promising ethanologens to be developed into a CBP organism.

5 Conclusions

While it is not entirely clear at this point as to which, if any, candidate microorganism will emerge as the preeminent CBP organism, ongoing research is still driving the field as a whole in a very positive direction. Definitive progress has been made towards developing CBP organisms over the last several years using both the native cellulophile, and native ethanologen-based approaches, and the potential of each strategy is higher than ever. Given the promising results along both fronts, and the

absence of any definitively prohibitive roadblocks, both directions are worthy of sustained future research efforts. Ultimately, the success of either strategies will likely hinge upon the sustained commitment to high-quality biofuels research and the use of genetic engineering techniques.

It is truly an exciting time in the field of biofuels with the pursuit of next generation technologies such as CBP in full swing. The inclusion of numerous candidate microorganisms being pursued in a number of different laboratories around the world can only help to strengthen the long-term prospects of this developing technology. It has been profoundly enlightening to partake in and witness the strategies employed by researchers to develop and ultimately deploy this technology. Modifying an organism in these drastic manners can be quite humbling when one understands the gap between normal biological activities and those required to achieve an economically and commercially feasible consolidated biofuels production process. However, over the last few decades substantial progress has been made along this pursuit. More importantly, while the ultimate goal of CBP research is to use a single microorganism or possibly a consortium to fully deconstruct and convert the released sugars to ethanol or alternative biofuels, this is not necessarily an all-or-none endeavor. For example, an ethanologen that could produce sufficient enzymes to saccharify half of the pretreated biomass with a CBP fermentation would require only half the amount of additional cellulase cocktails, thus halving the cost of enzyme loading. While this fall-back viewpoint can provide additional confidence going forward, we strongly feel that the achievement of true CBP is within reach and well worth the effort being put forth by researchers worldwide.

References

1. Lynd LR, Wyman CE, Gerngross TU (1999) Biocommodity engineering. Biotechnol Prog 15(5):777–793
2. Himmel ME (2007) Biomass recalcitrance: engineering plants and enzymes for biofuels production (vol 315, pg 804, 2007). Science 316(5827):982
3. Hill J, Nelson E, Tilman D et al (2006) Environmental, economic, and energetic costs and benefits of biodiesel and ethanol biofuels. Proc Natl Acad Sci USA 103(30):11206–11210
4. Lynd LR (1996) Overview and evaluation of fuel ethanol from cellulosic biomass: technology, economics, the environment, and policy. Annu Rev Energy Environ 21:403–465
5. Lynd LR, Weimer PJ, van Zyl WH et al (2002) Microbial cellulose utilization: fundamentals and biotechnology. Microbiol Mol Biol Rev 66(3):506–577
6. Den Haan R, Rose SH, Lynd LR et al (2007) Hydrolysis and fermentation of amorphous cellulose by recombinant *Saccharomyces cerevisiae*. Metab Eng 9(1):87–94
7. Lynd LR, van Zyl WH, McBride JE et al (2005) Consolidated bioprocessing of cellulosic biomass: an update. Curr Opin Biotechnol 16(5):577–583
8. Hong J, Wang Y, Kumagai H et al (2007) Construction of thermotolerant yeast expressing thermostable cellulase genes. J Biotechnol 130(2):114–123
9. van Zyl WH, Lynd LR, den Haan R et al (2007) Consolidated bioprocessing for bioethanol production using *Saccharomyces cerevisiae*. Adv Biochem Eng Biotechnol 108:205–235
10. Carere CR, Sparling R, Cicek N et al (2008) Third generation biofuels via direct cellulose fermentation. Int J Mol Sci 9(7):1342–1360

11. Lu YP, Zhang YHP, Lynd LR (2006) Enzyme-microbe synergy during cellulose hydrolysis by *Clostridium thermocellum*. Proc Natl Acad Sci USA 103(44):16165–16169
12. Xu Q, Singh A, Himmel ME (2009) Perspectives and new directions for the production of bioethanol using consolidated bioprocessing of lignocellulose. Curr Opin Biotechnol 20(3):364–371
13. Himmel ME, Ding SY, Johnson DK et al (2007) Biomass recalcitrance: engineering plants and enzymes for biofuels production. Science 315(5813):804–807
14. Foust TS, Ibsen KN, Dayton DC, Hess JR, Kenney KE (2008) The biorefinery, in biomass recalcitrance. In: Himmel ME (ed) Deconstructing the plant cell wall for bioenergy. Blackwell Publishing, London
15. McBee RH (1954) The characteristics of *Clostridium thermocellum*. J Bacteriol 67(4):505–506
16. Freier D, Mothershed CP, Wiegel J (1988) Characterization of *Clostridium-thermocellum* Jw20. Appl Environ Microbiol 54(1):204–211
17. Sai RM, Seenayya G (1989) Ethanol-production by *Clostridium-thermocellum* Ss8, a newly isolated thermophilic bacterium. Biotechnol Lett 11(8):589–592
18. Ram MS, Seenayya G (1991) Production of ethanol from straw and bamboo pulp by primary isolates of *Clostridium thermocellum*. World J Microbiol Biotechnol 7(3):372–378
19. Ram MS, Rao CV, Seenayya G (1991) Characteristics of *Clostridium thermocellum* strain Ss8—a broad saccharolytic thermophile. World J Microbiol Biotechnol 7(2):272–275
20. Herrero AA, Gomez RF, Snedecor B et al (1985) Growth-inhibition of *Clostridium thermocellum* by carboxylic-acids—a mechanism based on uncoupling by weak acids. Appl Microbiol Biotechnol 22(1):53–62
21. Tailliez P, Girard H, Longin R et al (1989) Cellulose fermentation by an asporogenous mutant and an ethanol-tolerant mutant of *Clostridium thermocellum*. Appl Environ Microbiol 55(1):203–206
22. Tailliez P, Girard H, Millet J et al (1989) Enhanced cellulose fermentation by an asporogenous and ethanol-tolerant mutant of *Clostridium thermocellum*. Appl Environ Microbiol 55(1):207–211
23. Rani KS, Seenayya G (1999) High ethanol tolerance of new isolates of *Clostridium thermocellum* strains SS21 and SS22. World J Microbiol Biotechnol 15(2):173–178
24. Pienkos PT, Zhang M (2009) Role of pretreatment and conditioning processes on toxicity of lignocellulosic biomass hydrolysates. Cellulose 16(4):743–762
25. Tyurin MV, Desai SG, Lynd LR (2004) Electrotransformation of *Clostridium thermocellum*. Appl Environ Microbiol 70(2):883–890
26. Tripathi SA, Olson DG, Argyros DA et al (2010) Development of *pyrF*-based genetic system for targeted gene deletion in *Clostridium thermocellum* and creation of a *pta* mutant. Appl Environ Microbiol 76(19):6591–6599
27. Zverlov VV, Klupp M, Krauss J et al (2008) Mutations in the scaffoldin gene, cipA, of *Clostridium thermocellum* with impaired cellulosome formation and cellulose hydrolysis: insertions of a new transposable element, IS1447, and implications for cellulase synergism on crystalline cellulose. J Bacteriol 190(12):4321–4327
28. Mai V, Lorenz WW, Wiegel J (1997) Transformation of *Thermoanaerobacterium sp*. strain JW/SL-YS485 with plasmid pIKM1 conferring kanamycin resistance. FEMS Microbiol Lett 148(2):163–167
29. Tyurin MV, Sullivan CR, Lynd LR (2005) Role of spontaneous current oscillations during high-efficiency electrotransformation of thermophilic anaerobes. Appl Environ Microbiol 71(12):8069–8076
30. Shaw AJ, Jenney FE, Adams MWW et al (2008) End-product pathways in the xylose fermenting bacterium, *Thermoanaerobacterium saccharolyticum*. Enzyme Microb Technol 42(6):453–458
31. Shaw AJ, Podkaminer KK, Desai SG et al (2008) Metabolic engineering of a thermophilic bacterium to produce ethanol at high yield. Proc Natl Acad Sci USA 105(37):13769–13774

32. Rabinovich ML, Melnik MS, Boloboba AV (2002) Microbial cellulases (review). Appl Biochem Microbiol 38(4):305–321
33. Harrison MJ, Nouwens AS, Jardine DR et al (1998) Modified glycosylation of cellobiohydrolase I from a high cellulase-producing mutant strain of *Trichoderma reesei*. Eur J Biochem 256(1):119–127
34. Srisodsuk M, Reinikainen T, Penttila M et al (1993) Role of the interdomain linker peptide of *Trichoderma-reesei* cellobiohydrolase-I in its interaction with crystalline cellulose. J Biol Chem 268(28):20756–20761
35. Knowles J, Lehtovaara P, Teeri T (1987) Cellulase families and their genes. Trends Biotechnol 5(9):255–261
36. Kumar R, Singh S, Singh OV (2008) Bioconversion of lignocellulosic biomass: biochemical and molecular perspectives. J Ind Microbiol Biotechnol 35(5):377–391
37. Ingram LO, Aldrich HC, Borges AC et al (1999) Enteric bacterial catalysts for fuel ethanol production. Biotechnol Prog 15(5):855–866
38. Tao H, Gonzalez R, Martinez A et al (2001) Engineering a homo-ethanol pathway in *Escherichia coli*: increased glycolytic flux and levels of expression of glycolytic genes during xylose fermentation. J Bacteriol 183(10):2979–2988
39. Zhou S, Davis FC, Ingram LO (2001) Gene integration and expression and extracellular secretion of *Erwinia chrysanthemi* endoglucanase CelY (celY) and CelZ (celZ) in ethanologenic *Klebsiella oxytoca* P2. Appl Environ Microbiol 67(1):6–14
40. Dien BS, Cotta MA, Jeffries TW (2003) Bacteria engineered for fuel ethanol production: current status. Appl Microbiol Biotechnol 63(3):258–266
41. Wood BE, Yomano LP, York SW et al (2005) Development of industrial-medium-required elimination of the 2,3-butanediol fermentation pathway to maintain ethanol yield in an ethanologenic strain of *Klebsiella oxytoca*. Biotechnol Prog 21(5):1366–1372
42. Yanase H, Nozaki K, Okamoto K (2005) Ethanol production from cellulosic materials by genetically engineered *Zymomonas mobilis*. Biotechnol Lett 27(4):259–263
43. Okamoto T, Yamano S, Ikeaga H et al (1994) Cloning of the *Acetobacter xylinum* cellulase gene and its expression in *Escherichia coli* and *Zymomonas mobilis*. Appl Microbiol Biotechnol 42(4):563–568
44. Brestic-Goachet N, Gunasekaran P, Cami B et al (1989) Transfer and expression of an *Erwinia chrysanthemi* cellulase gene in *Zymomonas mobilis*. J Gen Microbiol 135(4):893–902
45. Lejeune A, Eveleigh DE, Colson C (1988) Expression of an endoglucanase gene of *Pseudomonas fluorescens* var cellulosa in I. FEMS Microbiol Lett 49(3):363–366
46. Misawa N, Okamoto T, Nakamura K (1988) Expression of a cellulase gene in *Zymomonas mobilis*. J Biotechnol 7(3):167–178
47. Linger JG, Adney WS, Darzins A (2010) Heterologous expression and extracellular secretion of cellulolytic enzymes by *Zymomonas mobilis*. Appl Environ Microbiol 76(19):6360–6369
48. Penttila ME, Andre L, Lehtovaara P et al (1988) Efficient secretion of 2 fungal cellobiohydrolases by *Saccharomyces cerevisiae*. Gene 63(1):103–112
49. Van Rensburg P, Van Zyl WH, Pretorius IS (1998) Engineering yeast for efficient cellulose degradation. Yeast 14(1):67–76
50. van Rensburg P, van Zyl WH, Pretorius IS (1996) Co-expression of a *Phanerochaete chrysosporium* cellobiohydrolase gene and a *Butyrivibrio fibrisolvens* endo-beta-1,4-glucanase gene in *Saccharomyces cerevisiae*. Curr Genet 30(3):246–250
51. Agbogbo FK, Coward-Kelly G (2008) Cellulosic ethanol production using the naturally occurring xylose-fermenting yeast, *Pichia stipitis*. Biotechnol Lett 30(9):1515–1524
52. Prior BA, Kilian SG, Dupreez JC (1989) Fermentation of D-Xylose by the Yeasts *Candida shehatae* and *Pichia stipitis*—prospects and problems. Proc Biochem 24(1):21–32
53. Slininger PJ, Bolen PL, Kurtzman CP (1987) *Pachysolen tannophilus*—properties and process considerations for ethanol-production from D-xylose. Enzyme Microb Technol 9(1):5–15
54. Jeffries TW (2006) Engineering yeasts for xylose metabolism. Curr Opin Biotechnol 17(3):320–326

55. Agbogbo FK, Coward-Kelly G, Torry-Smith M et al (2006) Fermentation of glucose/xylose mixtures using *Pichia stipitis*. Proc Biochem 41(11):2333–2336
56. Delgenes JP, Moletta R, Navarro JM (1996) Effects of lignocellulose degradation products on ethanol fermentations of glucose and xylose by *Saccharomyces cerevisiae*, *Zymomonas mobilis*, *Pichia stipitis*, and *Candida shehatae*. Enzyme Microb Technol 19(3):220–225
57. Schneider H, Wang PY, Chan YK et al (1981) Conversion of D-xylose into ethanol by the yeast *Pachysolen tannophilus*. Biotechnol Lett 3(2):89–92
58. Wisselink HW, Toirkens MJ, Berriel MDF et al (2007) Engineering of *Saccharomyces cerevisiae* for efficient anaerobic alcoholic fermentation of L-arabinose. Appl Environ Microbiol 73(15):4881–4891
59. Becker J, Boles E (2003) A modified *Saccharomyces cerevisiae* strain that consumes L-arabinose and produces ethanol. Appl Environ Microbiol 69(7):4144–4150
60. Richard P, Verho R, Putkonen M et al (2003) Production of ethanol from L-arabinose by *Saccharomyces cerevisiae* containing a fungal L-arabinose pathway. FEMS Yeast Res 3(2):185–189
61. Karhumaa K, Wiedemann B, Hahn-Hagerdal B et al (2006) Co-utilization of L-arabinose and D-xylose by laboratory and industrial *Saccharomyces cerevisiae* strains. Microb Cell Fact 5:18
62. Ostergaard S, Olsson L, Nielsen J (2000) Metabolic engineering of *Saccharomyces cerevisiae*. Microbiol Mol Biol Rev 64(1):34–50
63. Vanarsdell JN, Kwok S, Schweickart VL et al (1987) Cloning, characterization, and expression in *Saccharomyces cerevisiae* of endoglucanase-I from *Trichoderma-reesei*. Biotechnology 5(1):60–64
64. Idiris A, Tohda H, Kumagai H et al (2010) Engineering of protein secretion in yeast: strategies and impact on protein production. Appl Microbiol Biotechnol 86(2):403–417
65. Karsch T, Stahl U, Esser K (1983) Ethanol production by *Zymomonas* and *Saccharomyces*, advantages and disadvantages. Eur J Appl Microbiol Biotechnol 18(6):387–391
66. van Rooyen R, Hahn-Hagerdal B, La Grange DC et al (2005) Construction of cellobiose-growing and fermenting *Saccharomyces cerevisiae* strains. J Biotechnol 120(3):284–295
67. McBride JE, Zietsman JJ, Van Zyl WH et al (2005) Utilization of cellobiose by recombinant beta-glucosidase-expressing strains of *Saccharomyces cerevisiae*: characterization and evaluation of the sufficiency of expression. Enzyme Microb Technol 37(1):93–101
68. Wood TM (1992) Fungal cellulases. Biochem Soc Trans 20(1):46–53
69. Den Haan R, Mcbride JE, La Grange DC et al (2007) Functional expression of cellobiohydrolases in *Saccharomyces cerevisiae* towards one-step conversion of cellulose to ethanol. Enzyme Microb Technol 40(5):1291–1299
70. Millis NF (1956) A study of the cider-sickness *bacillus*; a new variety of *Zymomonas anaerobia*. J Gen Microbiol 15(3):521–528
71. Rogers PL, Jeon YJ, Lee KJ et al (2007) *Zymomonas mobilis* for fuel ethanol and higher value products. Adv Biochem Eng Biotechnol 108:263–288
72. Lee KJ, Lefebvre M, Tribe DE et al (1980) High productivity ethanol fermentations with *Zymomonas mobilis* using continuous cell recycle. Biotechnol Lett 2(11):487–492
73. Lee KJ, Skotnicki ML, Tribe DE et al (1980) Kinetic-studies on a highly productive strain of *Zymomonas mobilis*. Biotechnol Lett 2(8):339–344
74. Rogers PL, Lee KJ, Tribe DE (1980) High productivity ethanol fermentations with *Zymomonas mobilis*. Proc Biochem 15(6):7–11
75. Lee KJ, Tribe DE, Rogers PL (1979) Ethanol-production by *Zymomonas mobilis* in continuous culture at high glucose concentrations. Biotechnol Lett 1(10):421–426
76. Rogers PL, Lee KJ, Tribe DE (1979) Kinetics of alcohol production by *Zymomonas mobilis* at high sugar concentrations. Biotechnol Lett 1(4):165–170
77. Skotnicki ML, Lee KJ, Tribe DE et al (1981) Comparison of ethanol-production by different *Zymomonas* strains. Appl Environ Microbiol 41(4):889–893
78. Swings J, Deley J (1977) Biology of *Zymomonas*. Bacteriol Rev 41(1):1–46

79. Spangler DJ, Emert GH (1986) Simultaneous saccharification fermentation with *Zymomonas mobilis*. Biotechnol Bioeng 28(1):115–118
80. Lee JH, Pagan RJ, Rogers PL (1983) Continuous simultaneous saccharification and fermentation of starch using *Zymomonas mobilis*. Biotechnol Bioeng 25(3):659–669
81. McMillan JD, Newman MM, Templeton DW et al (1999) Simultaneous saccharification and co-fermentation of dilute-acid pretreated yellow poplar hardwood to ethanol using xylose-fermenting *Zymomonas mobilis*. Appl Biochem Biotechnol 77–9:649–665
82. Metabolic Engineering of a Pentose Metabolism Pathway in Ethanologenic *Zymomonas mobilis* Min Zhang, Christina Eddy, Kristine Deanda, Mark Finkelstein, and Stephen Picataggio Science 13 January 1995: 267 (5195), 240-243. [DOI:10.1126/science.267.5195.240]
83. Deanda K, Zhang M, Eddy C et al (1996) Development of an arabinose-fermenting *Zymomonas mobilis* strain by metabolic pathway engineering. Appl Environ Microbiol 62(12):4465–4470
84. Carey VC, Walia SK, Ingram LO (1983) Expression of a lactose transposon (Tn951) in *Zymomonas mobilis*. Appl Environ Microbiol 46(5):1163–1168
85. Yanase H, Kurii J, Tonomura K (1986) Construction of a promoter-cloning vector in *Zymomonas mobilis*. Agric Biol Chem 50(11):2959–2961
86. Byun MOK, Kaper JB, Ingram LO (1986) Construction of a new vector for the expression of foreign genes in *Zymomonas mobilis*. J Ind Microbiol 1(1):9–15
87. Yoon P (1988) Pack, transfer of bacillus subtilis endo-β-1,4-glucanase gene into *Zymomonas anaerobia*. Biotechnol Lett 10(3):213–216
88. Sandkvist M (2001) Biology of type II secretion. Mol Microbiol 40(2):271–283
89. Lee PA, Tullman-Ercek D, Georgiou G (2006) The bacterial twin-arginine translocation pathway. Annu Rev Microbiol 60:373–395
90. Mergulhao FJ, Summers DK, Monteiro GA (2005) Recombinant protein secretion in *Escherichia coli*. Biotechnol Adv 23(3):177–202

Chapter 17
The Synthesis, Regulation and Modification of Lignocellulosic Biomass as a Resource for Biofuels and Bioproducts

Darby Harris, Carloalberto Petti, and Seth DeBolt

Abstract Most of the plant biomass is cell wall and therefore represents a renewable carbon source that could be exploited by humans for bioenergy and bioproducts. A thorough understanding of the type of cell wall being harvested and the molecules available will be crucial in developing the most efficient conversion processes. Herein, we review the structure, function, and biosynthesis of lignocellulosic biomass, paying particular attention to the most important bioresources present in the plant cell wall: cellulose, hemicellulose, and lignin. We also provide an update on key improvements being made to lignocellulosic biomass with respect to utilization as a second-generation biofuel and as a resource for bioproducts.

1 Terminology to Describe Cell Walls

Before we examine the details of cellulose, hemicellulose, and lignin biosynthesis we review some additional classification terms that describe the type of cell wall. Every plant cell forms a primary cell wall (PCW) early in the cell lifecycle that is continuously produced throughout the period of cell growth. The shape and morphogenesis of plant cells are defined by the capacity of the PCW to constrain cellular turgor pressure in a directed and controlled manner thereby permitting anisotropic expansion during cell growth. All PCWs contain cellulose and a hydrated matrix consisting of hemicelluloses and pectins, with some structural proteins. Two distinctive types of PCWs, either Type I or Type II, have traditionally been described within the angiosperms based on polysaccharide composition [24]. However, accumulating evidence from other plant species, for example, *Equisetum*, suggests that PCWs are

D. Harris • C. Petti • S. DeBolt (✉)
Department of Horticulture, N-318 Agricultural Science Center North,
University of Kentucky, Lexington, KY 40506, USA
e-mail: sdebo2@email.uky.edu

J.W. Lee (ed.), *Advanced Biofuels and Bioproducts*, DOI 10.1007/978-1-4614-3348-4_17,

best described as falling within a continuum rather than into specific classes. For the sake of general discussion on PCWs, the traditional classification can be maintained, although keeping in mind that some plant species may be found at either extremes of a particular range.

In general, Type I PCWs are present in dicots and liliaceous monocots while Type II PCWs can be found in the cereals and other grasses. The main defining feature used in describing the differences between the two wall types is the particular class of hemicelluloses (HCs) found within these walls. HCs, as discussed below, are heterogeneous in nature with multiple classes represented in different cell types, which is contrary to cellulose, a homogenous polymer present in roughly the same configuration in all cell walls. Type I walls contain mostly the xyloglucan form of HCs embedded in a pectinaceous gel cross-linked to structural proteins [24]. Type II walls contain much less pectin and fewer proteins and their HCs are primarily glucuronoarabinoxylans (GAXs) and mixed-linkage (1,3), (1,4)-β-D-glucans embedded in an acidic polysaccharide network of highly substituted GAXs [24]. In addition to PCWs, all plants deposit a thick secondary cell wall (SCW) around certain cell types after cell growth has ceased. The SCW primarily contains cellulose, HCs, and the polyphenolic compound lignin which provides added strength, protection, and hydrophobicity to plant tissues. The SCW is also the primary component of wood cells found in trees. In typical angiosperm trees such as *Populus* spp., the SCW consists of three layers (S1, S2, and S3), which are collectively composed of approximately 45% cellulose, 25% HCs, and 20–25% lignin [2]. In terms of cell type, over 50% of poplar wood is composed of xylem fibers which in turn contain most of their mass in the S2 layer of the SCW, thus making this the main area of focus in attempts to modify wood properties [113]. While most herbaceous plants lack woody tissue, the SCW is generally much thicker and more energy dense than the PCW in these species. Therefore, an important overall consideration for crops being used as feedstocks for bioenergy, such as grasses and fast growing woody crops, is that a majority of their cell wall polysaccharides and lignin will be bound up in the more recalcitrant SCW tissues.

2 Synthesis and Regulation of Key Cell Wall Biopolymers

2.1 Cellulose

As has been noted many times, the distinction given to cellulose as the most abundant carbohydrate found in plants also makes it the most abundant biopolymer in nature and an obvious target for bioconversion. In plant cells, cellulose exists in the form of paracrystalline microfibrils that are made up of multiple, unbranched, parallel glucan chains, which in turn are composed of (1,4) linked β-D-glucosyl residues that are alternatively rotated 180° along the polymer axis [80]. Plants synthesize cellulose at the plasma membrane by a symmetrical rosette of six globular protein complexes, collectively called the cellulose synthase complex (CSC) and totaling

25–30 nm in diameter [19]. Each lobe of the CSC rosette contains several structurally similar cellulose synthase (CESA) subunits [135]. CESAs are classified within family 2 of glycosyltransferases, which not only catalyze the addition of many glucose residues to a growing glucan chain (processive), but also invert each glucose residue to create β-linkages, thus making cellobiose the repeating unit [153]. CESAs polymerize β-1,4-glucan chains from the activated sugar donor UDP-glucose, which is supplied by either UDP-glucose pyrophosphorylase or sucrose synthase. Several reports have suggested that sucrose synthase provides most of the UDP-glucose to CESAs due to the existence of a membrane bound form of this enzyme that is often highly expressed in tissues actively producing cellulose [64] or by its effect on biomass production when over-expressed [36, 39]. However, it should be noted that there has not yet been any evidence to show direct physical association of sucrose synthase with the CSC and thus both sources of UDP-glucose are likely used. With regards to polymerization, although there is strong evidence to support the addition of glucosyl units to the nonreducing end of glucan chains, the molecular mechanism by which CESA create a β-1,4-glucan chain has not yet been elucidated [94, 96] (Fig. 1). Bioinformatic analyses have provided putative substrate binding and catalytic residues, however it is not clear whether glucan chains are synthesized by the addition of one or two glucosyl units [153]. The predicted CESA topology suggests the existence of eight transmembrane helices that anchor the protein in the plasma membrane. This even number of helices means that the N-terminal and C-terminal ends of the protein should reside on the same side of the plasma membrane. Current models have placed both termini on the cytoplasmic side of the membrane, which also allows for a cytoplasmic location for the putative substrate binding and catalytic sites. One of the hypothetical three-dimensional CESA structures suggests that the eight transmembrane helices form a pore in the plasma membrane through which the growing glucan chain passes to reach the cell wall [46]. Although there is still no reported crystal structure of a plant CESA, a clearer picture of how the glucan chain is transported to the cell wall is now emerging. The recent structure determination of subunit D in the CSC of *Gluconacetobacter xylinus* (AxCeSD) in complex with a short glucan (cellopentaose), suggested that glucan chains are indeed extruded through the PM via a distinct pore [85]. This study in a bacterial system bolsters the idea that the protein transmembrane helices define the membrane pore, and in the case of plant CESAs this would include the eight transmembrane helices, which would therefore facilitate glucan chain extrusion.

Current models of the CSC propose that each of the six protein complexes may synthesize six glucan chains, each glucan chain presumably synthesized by a single CESA protein, thus a total of 36 glucan chains are produced by a single rosette which then co-crystallize to form one microfibril [52, 54, 158] (Fig. 1). The length of individual glucan chains varies depending on the cell type and plant species examined, but in general can be from 1,000 to 8,000 (PCW) to as much as 16,000 (SCW) glucose molecules in length [185]. The formation of the crystalline structure of cellulose is highly dependent upon the hydrogen bonding of three hydroxyl groups that are present on each glucosyl residue [122, 123]. Most naturally occurring cellulose is referred to as cellulose I and maintains two coexisting phases, cellulose

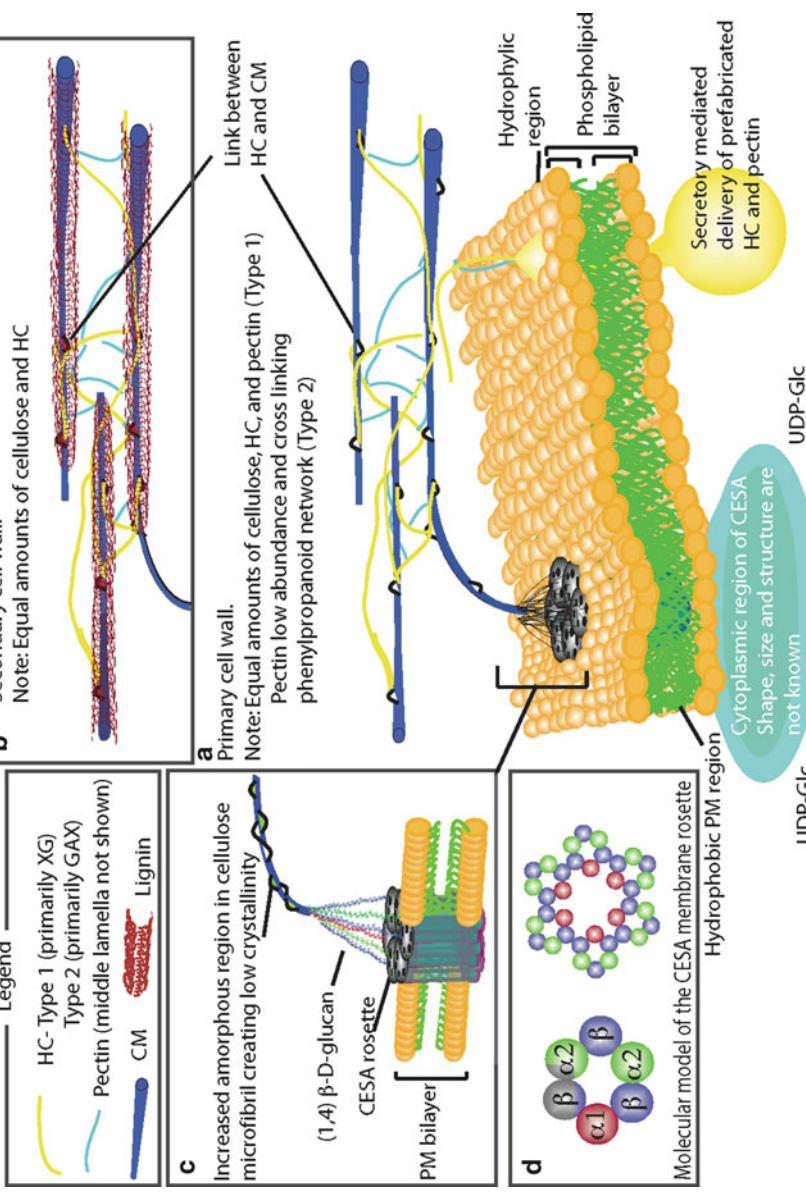
Legend
HC- Type 1 (primarily XG)
Type 2 (primarily GAX)
Pectin (middle lamella not shown)
CM
Lignin
b
Secondary cell wall.
Note: Equal amounts of cellulose and HC
a
Primary cell wall.
Note: Equal amounts of cellulose, HC, and pectin (Type 1)
Pectin low abundance and cross linking
phenylpropanoid network (Type 2)
Link between
HC and CM
c
Increased amorphous region in cellulose
microfibril creating low crystallinity
(1,4) β-D-glucan
CESA rosette
PM bilayer
d
Molecular model of the CESA membrane rosette
Hydrophobic PM region
Hydrophylic
region
Phospholipid
bilayer
Secretory mediated
delivery of prefabricated
HC and pectin
Cytoplasmic region of CESA
Shape, size and structure are
not known
UDP-Glc
UDP-Glc
UDP-Glc
UDP-Glc
UDP-Glc
UDP-Glc

Fig. 1 A model of the general structure of the plant cell wall matrix with emphasis on cellulose. (**a**) A simplified version of the primary cell wall (PCW) is shown as a network of cellulose microfibrils (CM) interlocked and coated by cross-linking hemicelluloses (HC) which are primarily xyloglucans (XG) in Type I walls and glucuronoarabinoxylans (GAX) in Type II walls. Together, CMs and HCs are embedded in a matrix of pectin (Type I) or acidic polysaccharides (Type II) with various levels of proteins (not shown) that aid in wall structure, assembly and degradation [189]. Cellulose is being synthesized at the plasma membrane (PM) by a rosette of six globular cellulose synthase (CESA) protein complexes [19, 81]. (**b**) The secondary cell wall (SCW) is produced by certain cell types as part of the maturation process after growth has ceased and consists primarily of CMs, HCs, and lignin. Lignification results in the coating of CMs with anhydrous lignin polymers that further strengthen the cell wall but also present a major barrier in the bioconversion process to biofuels by blocking access and causing adsorption of hydrolytic enzymes [118]. (**c**) Cellulose crystallinity is another important factor contributing to the recalcitrant nature of most lignocellulosic biomass to enzymatic degradation [118]. Genetic modification of various CESA proteins has been shown to reduce the crystallinity of the lignocellulosic biomass and enhance enzymatic degradation [76]. Here the glucan chains produced by the different CESA protein are color coordinated to match (**d**). (**d**) A molecular model of the CESA membrane rosette showing the molecular configuration of a single rosette subunit (*left*) and the complete CESA rosette (*right*). Each rosette subunit is identical, consisting of one molecule of α1, two molecules of α2 and three molecules of β type CESA proteins [52]. Only three possible types of protein–protein interactions are necessary (α1–β, α2–β, and β–β) for rosette assembly in the plasma membrane or for rosette–rosette interaction to constitute the array formation seen in the parenchyma cells of maize stem pith (not shown) [52]. Figure not to scale (reproduced from Harris and DeBolt [75])

Iα (triclinic unit cell) and cellulose Iβ (monoclinic unit cell). Terrestrial plants contain a higher proportion of cellulose Iβ that primarily composes the more crystalline inner chains of the microfibril core, while both forms of cellulose compose the chains in the surrounding paracrystalline sheath [143, 174]. The cellulose microfibril also contains intermittent regions of less ordered glucan chains that structurally create amorphous zones along the microfibril [127]. The mechanism by which amorphous zones form is unclear other than possibly by the random exclusion of portions of glucan chains during the assembly (crystallization) process. With regards to the mechanism by which glucan chains assemble, the sequence of amino acids that defines the pore in the bacterial subunit D appears crucial for creating the proper environment for glucan chain passage [85]. It has been speculated that an analogous pore structure, if present in plant CESA, may be responsible for correctly orienting the glucan chain to ensure proper hydrogen bonding to adjacent chains once it emerges from the CESA and into the cell wall environment [76]. If this idea is correct, mutations within the transmembrane helices of plant CESAs could affect the threading of the glucan chain through the membrane pore and could ultimately influence microfibril crystallization. Functionally, these amorphous zones along the microfibril are hypothesized to serve as attachment points for HCs that cross-link one microfibril to another and help strengthen the cell wall [82]. Importantly, both the degree of polymerization (glucan chain length) and degree of crystallization (inter- and intra-chain hydrogen bonding) are two intrinsic properties of cellulose that have some effect on its enzymatic hydrolysis [110]. In the model plant *Arabidopsis thaliana*, ten genes (*CESA1–10*) have been identified that code for the CESA proteins [153]. Biochemical and genetic evidence suggests that three *CESA* genes, *CESA4*, *-7*, and *-8* directly interact and are necessary for cellulose deposition during SCW formation [181, 186]. Similar evidence suggests that essential members of the PCW CSC include CESA1, -3, and a small family of CESA6-related proteins providing the third component that vary temporally and spatially [138]. Spatiotemporal regulation of *CESA* genes has recently been uncovered, with *CESA9* implicated in forming the SCW in epidermal testa cells of the *Arabidopsis* seed coat [172]. A similar set of *CESA* genes have been identified in the genomes of many higher plants including 10 genes in rice [178], 12 genes in maize [3, 84], 18 genes in poplar [53, 88], and 8 genes in barley [21] (see Table 1 for a complete list of mutations in *Arabidopsis CESA* genes).

Recently, CSI1 (cellulose synthase-interactive protein 1) was identified in *Arabidopsis* as the first protein, other than the CESA proteins, to interact with the CSC in higher plants [71]. However, a number of other proteins have been implicated in the overall process of cellulose synthesis by genetic approaches [59, 119, 159, 180, 195]. These include *korrigan* (*kor*) a membrane bound β-1,4-endoglucanase [121, 157, 217], *cobra* (*cob*) a glycosyl-phosphatidyl-inositol-anchored protein of unknown function [155, 161], *kobito/elongation defective 1* (*kob/eld1*) a novel plant-specific membrane protein of unknown function [17, 102, 129], and *ectopic lignin in pith* (*elp1*), a basic chitinase-like protein [203, 205]. In addition, research has shown that a reduction in expression of certain members of the receptor-like serine/threonine protein kinases (RLKs), specifically members of the wall-associated kinases (WAKs), leads to a loss of cell expansion and a dwarf phenotype [97, 190].

Table 1 Cellulose synthase (CESA) mutations in *Arabidopsis thaliana* and their source

Protein	Gene ID	Allele	Mutation	Phenotype	Cell wall	References
CESA1	At4g32410	*rsw1-1*	A549V	Root swelling, stunted growth (heat, temperature sensitive)	Primary	[4]
		rsw1-2	G631S	Lethality		[65]
		rsw1-10	T-DNA	Root swelling, stunted growth		[59]
		rsw1-20	D780N	Swollen root, abnormal dark morphology, reduced growth of hypocotyls and roots		[5]
		rsw1-45	E779K	Swollen root, abnormal dark morphology, reduced growth of hypocotyls and roots		[5]
		ags1-2	A903V	Semidominant resistance to quinoxyphen, mild growth phenotype		[73]
		cesa1	T-DNA	Gametophytic lethality, deformed and sterile pollen grains		[138]
CESA2	At4g39350	*atcesa2*	Ds	Microtubule orientation, abnormal cell expansion, cell wall defects in leaves	Primary	[34]
		cesa2	T-DNA	Short etiolated hypocotyl		[49, 138]
CESA3	At5g44030	*ixr1-1*	G998D	Semidominant resistance to isoxaben	Primary	[158]
		ixr1-2	T9421	Semidominant resistance to isoxaben, mild growth phenotype		[158]
		cev1	G617E	Stunted root growth, induction of defense responses		[57]
		eli1-1	S301F	Swollen root and hypocotyl, stunted growth, induction of defense response		[23]
		eli1-2	A522V	Swollen root and hypocotyl, stunted growth, induction of defense response		[23]
		rsw5	P1056S	Root swelling, stunted growth at permissive temperature		[192]
		than	P578S	Root swelling, stunted growth at permissive temperature, semidominant, lethality		[43]
		repp3	P578L	Shorten and swollen root, short etiolated hypocotyl in *PIN2::PIN1-HA;pin2* background		[60]
		cesa3	T-DNA	Gametophytic lethality, deformed and sterile pollen grains		[138]

(continued)

Table 1 (continued)

Protein	Gene ID	Allele	Mutation	Phenotype	Cell wall	References
CESA4	At5g44030	*irx5-1*	Ds	Irregular xylem vessels	Secondary	[181]
		irx5-2	W995Stop	Irregular xylem vessels		[181]
		irx5-3	Q263Stop	Irregular xylem vessels		[181]
CESA5	At5g64740	*cesa5*	T-DANA	Reduced mucilage deposition on seed coat	Primary	[73]
CESA6	At5g64740	*ixr2*	R1064W	Semidominant resistance to isoxaben	Primary	[50]
		prc1-1	Q720Stop	Swollen and stunted roots and dark-grown hypocotyls, many alleles		[59]
				Root hair phenotype		[166]
		cesa6	T-DNA	Subtle growth phenotypes		[138]
CESA7	At5g17420	*irx3*	W859Stop	Collapsed xylem, weak stem	Secondary	[183]
		fra5	P557T	Fragile fibers, weak stem, extremely thin fiber walls, semidominant		[206]
		mur10-1	W444Stop	Reduction in growth and dark-green coloration of aerial parts		[14]
		mur10-2	H734Y	Reduction in growth and dark-green coloration of aerial parts		[14]
CESA8	At4g18780	*irx1-1*	D683N	Weak stem, collapsed xylem vessels	Secondary	[182]
		irx1-2	S679L	Weak stem, collapsed xylem vessels		[182]
		fra6	R362K	Reduced fiber wall thickness		[206]
		lew2-1	W217Stop	Tolerant to osmotic stress, more severe than *irx1*		[30]
		lew2-2	L792F	Tolerant to osmotic stress, more severe than *irx1*		[30]
CESA9	At2g1770	*cesa9*	T-DNA	Depleted secondary cell wall in epidermal seed coat testa cells	Primary/ secondary	[172]

Adapted from Daras et al. [43]

An RLK in a separate family from the WAK proteins, but believed to act as a cell wall sensor, is THESEUS1, which has been show to attenuate, but not completely rescue, the shortened hypocotyl phenotype of the CESA6 null mutant *procuste* [78]. Additional regulation of CESA occurs through various members of the NAC-domain-containing and MYB transcription factors that have been shown to initiate the transition from PCW to SCW biogenesis by playing key roles in the SCW thickening of xylem fibers, vessels, and anther endothecium [95, 115, 116, 198, 210] (see Table 2 for a complete list of genes associated with cellulose biosynthesis in *Arabidopsis*). Finally, it has long been observed that the cortical microtubule array has a role in the guidance of CESA complex movement in the plasma membrane during cellulose deposition [47, 79]. Recent evidence using live-cell imaging has supported this fact [131] as well as suggesting a feedback mechanism between microtubules and CESA that goes both ways [45, 131, 146].

2.2 Hemicellulose

Plant cell walls also contain a heterogeneous group of polysaccharides termed the hemicelluloses (HCs) that make up 20–40% of total wall carbohydrates. Depending on the plant species, HCs may contain the pentose sugars β-D-xylose and α-L-arabinose; the hexoses β-D-mannose, β-D-glucose and β-D-galactose and/or the uronic acids α-D-glucuronic, α-D-4-*O*-methylgalacturonic and α-D-galacturonic acids. The assumed role of HCs in the cell wall is to interact with other polymers to ensure the proper physical properties of the wall. This interaction is most important with regards to the coating and tethering of cellulose microfibrils, which aids greatly in strengthening the cell wall. Of all the HCs identified, the synthesis of mannans is best understood and characterized [107]. However, the only mannans present in the vegetative tissue of plants at any significant amount are the galactoglucomannans (GGMs) found in the SCW of the softwood gymnosperms species such as conifer, with most mannans found as storage carbohydrates in the seeds of many plants [66]. The structure and synthesis of xyloglucans are perhaps the next most characterized HC, while present in the PCWs of most plants (as much as 25% in dicots), their minor presence in the SCW makes them less valuable as a source for bioenergy or biochemicals. It is the xylans that are the most abundant HCs, representing the major HC component of SCWs in the hardwoods and grasses (20–30% of total biomass) [160] (Fig. 1). Although the xylans are a diverse group of polysaccharides, one common feature is a backbone of (1,4) linked β-xylose residues [160]. The two subgroups of xylans most prominent within the cell walls of bioenergy feedstocks include the GAXs and the glucuronoxylans (GXs) [56]. The GAXs make up most of the HCs in the lignified tissues of grasses and cereals with disubstituted arabinofuranosyl residues on the xylopyranan backbone. The GXs represent the main HC component of the SCW in hardwoods and are linear polymers with substitution in position 2 by α-D-glucuronic acid (GA) and/or its *O*-4-methyl-derivative (MeGA). Therefore, because xylans are the major HC component of the SCW, their biosynthesis is detailed further.

Table 2 Additional mutations and genes in *Arabidopsis thaliana* implicated in cellulose biosynthesis

Protein	Gene ID	Allele	Mutation	Phenotype	Cell wall	References
CSI1	At2g22125	*Csi1*	T-DNA	Swollen root and dark-grown hypocotyl, reduced aerial organs, six alleles	Primary	[71]
CTL1	At1g05850	*elp1*	W181Stop	Swollen root and dark-grown hypocotyl, stunted growth, more root hairs	Primary	[205]
		pom1-1	T-DNA	Shorten swollen root under high sucrose conditions, many alleles		[77]
KOBITO	At3g08550	*kob1-1*	T-DNA	Swollen root and dark-grown hypocotyl, stunted growth, sterile	Primary	[129]
		kob1-2	G2795A[a]	Swollen root and dark-grown hypocotyl, stunted growth, sterile		[129]
		eld1-1	W426Stop	Shortened root and hypocotyl, severely stunted growth, sterile, lethality in soil		[102]
		eld1-2	T-DNA	Shortened root and hypocotyl, severely stunted growth, sterile, lethality in soil		[102]
		abi8	5 bp del	Shortened root, severely stunted growth, male sterile		[17]
KORRIGAN	At5g49720	*kor1-1*	T-DNA	Reduced growth of hypocotyl and root, mild growth phenotype	Primary	[121]
		kor1-2	T-DNA	Reduced growth of hypocotyl and root, strong growth phenotype		[217]
		irx2-1	P250L	Collapsed xylem	Secondary	[176]
		irx2-2	P553L	Collapsed xylem		[176]
		rsw2-1	G429R	Reduced growth of hypocotyl and root (heat, temperature sensitive)	Primary	[98]
		rsw2-3	S183N	Reduced growth of hypocotyl and root (heat, temperature sensitive)		[98]
		rsw2-4	G344R	Reduced growth of hypocotyl and root (heat, temperature sensitive)		[98]

COBRA	At5g60920	*cob-1*	G167R	Reduced hypocotyl, swollen root (sucrose sensitive), same in *cob-2*	Primary	[161]
		cob-3	W55R	Reduced hypocotyl, swollen root (sucrose sensitive)		[161]
		cob-4	T-DNA	Severely reduced hypocotyl, swollen root and aerial tissue (sucrose sensitive)		[155]
KINESIN-LIKE	At5g47820	*fra1*	84 bp del	Fragile fiber, stunted inflorescence stem, same in *fra1-2*, *fra1-3*	Primary/ secondary	[203]
		fra1-4	99 bp insert	Fragile fiber, stunted inflorescence stem		[203]
KATANIN1-p60	At1g80350	*fra2*	1 bp del	Fragile fiber, stunted inflorescence stem and aerial organs	Primary/ secondary	[20]
		bot1	EMS/T-DNA	Shorten hypocotyl, root, stem and aerial organs, many alleles		[8]
		erh3-1	H353Y	Short, swollen, hairy roots	Primary	[193]
		erh3-2	G274R	Severely short, swollen, hairy roots		[193]
		erh3-3	A406V	Short, swollen, hairy roots		[193]
		lue1	NS394	Decreased stem elongation in response to GA, impaired apical hook		[15]
THESEUS1	At5g54380	*the1-1*	G37D	Partially restores hypocotyl elongation in CESA6 null allele (*prc1-1*)	Primary	[78]
		the1-2	E150K	Partially restores hypocotyl elongation in CESA6 null allele (*prc1-1*)		[78]
		the1-3	T-DNA	Partially restores hypocotyl elongation in CESA6 null allele (*prc1-8*)		[78]
WAK2	At1g21270	*wak2*	cTAP[b]	Severely stunted inflorescence stem and aerial organs	Primary	[92]

[a]Nucleotide representing mutation at the splice acceptor site of the third intron resulting in a truncated protein
[b]Dominant negative allele created by the fusion of a tandem affinity tag (TAP[32]) on the C-terminus of WAK2

In general, plants synthesize HCs quite differently to that of cellulose, forming these polymers in the Golgi apparatus and then secreting them via Golgi vesicles across the plasma membrane and into the cell wall. The HC biosynthetic pathway is currently only partially resolved thereby the feasibility of altering their content in the cell walls is still limited. It still seems wide open how secretion is influenced by the cytoskeleton and localized membrane lipid environments. With respect to xylans biosynthesis, the pathway leading to UDP-xylose synthesis has been the object of numerous studies [10, 162]. UDP-xylose is formed from the decarboxylation of its immediate precursor, UDP-glucuronic acid [72], however there are two known pathways that lead to UDP-glucuronic acid synthesis. The pathway generally considered the most important is the conversion of UDP-glucose into UDP-glucuronic acid by UDP-glucose dehydrogenase, which accounts for approximately 50% of the UDP-glucuronic acid pool [139]. The second pathway, known as *myo*-inositol oxygenation, involves the conversion of *myo*-inositol into glucuronic acid, which is subsequently converted, through an intermediate step, into UDP-glucuronic acid. The intermediate step is catalyzed by a glucuronokinase which has been recently characterized and the *myo*-inositol pathway fully elucidated [139].

The structure of GXs suggests that various glycosyltransferases (GTs) are required for the genesis of the GX-backbone and backbone substitution. As many as 25 GTs were shown to be expressed during SCW synthesis in poplar and the FRAGILE FIBER8 (*FRA8*) implicated in normal xylem fiber development [207]. In addition, IRREGULAR XYLEM8 (*IRX8*) and IRREGULAR XYLEM9 (*IRX9*) are *Arabidopsis* homologs to three GTs from poplar expressed during SCW synthesis. A recent study showed that *IRX8* and *IRX9* are primarily expressed during fiber cell wall thickening and that they are targeted to the Golgi where GX biosynthesis occurs [137]. Single and double mutant analysis showed that the *irx8-irx9* double had a reduction of GX content in the inflorescence stems, *IRX9* is essential for the normal elongation of GX chains and that *FRA8* and *IRX8* are needed for the formation of the characteristic glycosyl sequence 1 (β-D-Xyl-(1-3)-α-L-Rha-(1-2)-α-D-GalA-(1-4)-D-Xyl-repeated four times) at the reducing end of GX as well as for a normal amount of GX chains [137]. The glycosyl sequence 1 was shown to be a primer for GX synthesis and the backbone is extended by adding xylose to the nonreducing end of the growing polysaccharide chain [137]. A mutation in the gene *PARVUS* leads to an almost complete disappearance of the glycosyl sequence 1 and it has been suggested that *PARVUS* is involved in the first transfer of the reducing xylose residue of the tetrameric sequence 1 to an unknown acceptor at the ER [101]. In another recent study, a close homolog of the *FRA8* gene, the *F8H* gene, was shown to have complete functional redundancy with *FRA8*, with no phenotypical alteration of the SCW thickening in the *F8H* knockout, while the *fra8*/*f8h* double mutant showed severe growth retardation and failure to bolt [100]. Two closely related genes, *IRX10* and *IRX10-L*, were recently characterized as being important for cell wall thickening and shown to have functional relevance in GX backbone elongation [197]. The single mutants showed no significant differences from the wild-type, however the double mutant was severely affected in size and cell wall thickening. The close relationship between these proteins suggested a partial

redundancy that was shown by complementation studies. However, depending on which was the mutant acting as pollen donor or pollen receptor, in the generation of the double mutant, rescue was not bidirectionally equivalent. *IRX10* was more efficient at rescuing thereby indicating greater functional importance than *IRX10-L* and demonstrating a lack of complete redundancy [197]. Further investigation of gene duplication in the GA pathway brought to evidence *IRX9-L* and *IRX14-L*, which acted as partially redundant to their similar counterpart *IRX9* and *IRX14* [196]. The only single mutant that showed stunted growth was *irx9*, whereas none of the *irx9-L1*, *irx9-L2* or *irx14* or *irx14-L* has a recognizable phenotype. On the contrary, gene-paired-double mutants showed a severe stunted phenotype and very little, if any, SCW formation [196]. Functional complementation studies showed that each pair of genes acted interchangeably and that they were all involved in xylan backbone elongation. However, when *irx9* was complemented by *IRX10* or *IRX14* and vice versa for each possible combination, rescue was not possible and the wild-type phenotype was not restored thereby clearly indicating that *IRX9*, *IRX10,* and *IRX14* are not interchangeable [196]. Despite the recent isolation of several mutants with reduced backbone, the mechanisms of GX synthesis and substitution are still unclear. Recently two Golgi-localized putative glycosyltransferases, GlucUronic acid substitution of Xylan (GUX)-1 and GUX2 that are required for the addition of both GA and MeGA branches to GX in *Arabidopsis* stem cell walls were identified [117]. The *gux1/gux2* double mutants showed loss of xylan glucuronyltransferase activity and lacked almost all-detectable xylan substitution, but showed no change in xylan backbone quantity, indicating backbone synthesis and substitution can be uncoupled. More importantly, although the weakened stems did not show collapsed xylem vessels thus allowing the plants to grow to normal size, the xylans from these plants were more readily extracted, were composed of a single monosaccharide, and required fewer enzymes for complete hydrolysis [117]. These results demonstrate the potential for manipulating and simplifying the structure of xylan to improve the properties of lignocellulose for bioenergy use.

The dissection of the arabinoxylan pathway was enhanced by a study showing the presence of arabinoxylan arabinosyltransferase activity in the microsomal and Golgi membranes isolated from wheat seedlings. The enzyme was further characterized but it was not possible to unequivocally correlate the transfer of arabinose to the arabinoxylan backbone [141]. Zeng et al. [201] showed the presence of glucuronyltransferase activity in wheat Golgi-enriched microsomes that is further increased by the presence of UDP-xylose in the reaction medium and results in the genesis of GAX chains thereby suggesting involvement in GAX biosynthesis. GAXs have been implicated in the formation of cross-linkages between ferulate residues in the cell wall of grasses that contributes to the intrinsic difficulty in the enzymatic accessibility of cellulose and HCs. The genes involved in feruloylation are still unknown, however Mitchell et al. [114] used a novel bioinformatic approach to propose a putative candidate gene family in rice which encompasses 12 members responsible for feruloylation of arabinoxylans [114]. Members of this family were down-regulated by a general multigene RNAi approach. Two constructs were designed, one to target subgroup I and II and the other to target III and IV, which led

to a general down-regulation of the transcript levels of diverse members of the gene family. A significant reduction of cell wall-ester-linked ferulic acid was observed for some of the most effectively down-regulated genes pointing these out as strong candidates involved in feruloylation [140].

2.3 Lignin

Lignin is a complex aromatic heteropolymer deposited within the SCWs of all vascular plants, and accounts for approximately 30% of the terrestrial organic carbon fixed annually in the biosphere, placing it second to cellulose as the most abundant biopolymer on earth [12]. Lignification aids the plant by providing added strength to xylem fibers that give support for upright growth, by waterproofing tracheary elements that make up the vascular system and by helping increase the resistance of plants to pathogen attack [12] (Fig. 1). Lignin content can vary with environmental factors, but in general comprises around 13–19% of the biomass in switchgrass (*Panicum virgatum*) [108, 173], 22–25% in *Miscanthus* (*Miscanthus* × *giganteus*) [18, 169], and around 20% in big bluestem (*Andropogon gerardii*) and eastern gamagrass (*Tripsacum dactyloides*) [173], all of which are C4 grass species that have potential as bioenergy feedstocks. In addition, lignin accounts for approximately 25–30% of the dry weight of potential hardwood bioenergy tree crops like poplar and can be even higher in softwood species [134]. The prominence of lignin in a majority of plant tissues has been recognized by reference to the nonstarch or nonsugar components of the plant body as simply "lignocellulosic" biomass. Traditional research attention was given to lignin with respect to chemical pulping and forage digestibility, but recently interest has intensified concerning conversion processes to biofuels and biochemicals. Much of the focus has centered on the fact that the cellulose microfibrils of the SCWs are embedded in a meshwork of HCs and lignin that create a barrier for cellulase enzymes and decrease saccharification efficiency. However, from a thermochemical conversion prospective, the association of lignin with cellulose is not a major issue and more important is the fact that lignin contains structural units that are more chemically reduced and energy dense than any of the cell wall carbohydrates and thus could serve as a source of hydrocarbon fuels and high-value chemicals, if means can be found to free those structural units from the polymer.

The ultimate source of lignin in the plant is the amino acid phenylalanine (Phe) which is derived from the shikimate biosynthesis pathway in the plastid [154]. Current evidence suggests that through the general phenylpropanoid and monolignol-specific pathways located on or near the cytosolic side of the ER membrane, Phe is deaminated to form cinnamic acid, followed by a series of ring hydroxylations, *O*-methylations and side-chain modifications culminating in the production of the *p*-hydroxycinnamyl alcohol monomers (monolignols) coniferyl and sinapyl alcohol, and to a lesser extent *p*-coumaryl alcohol [105]. Upon incorporation into the lignin polymer, these monomers are referred to as guaiacyl (G), syringyl (S), or *p*-hydroxyphenyl (H) units, respectively [149]. In general, angiosperm dicot lignins are

composed of G- and S-units, while gymnosperms, with a few notable exceptions, are composed almost entirely of G-units with minor amounts of H-units [188]. Most, if not all, of the enzymes required for monolignol biosynthesis are known and include: phenylalanine ammonia lyase (PAL), the three ER membrane bound cytochrome P450 monooxygenases cinnamate 4 hydoxylase (C4H), coumarate 3-hydroxylase (C3′H) and ferulate 5-hydroxylase (F5H), the two methyltransferases caffeoyl-CoA 3-*O*-methyltransferase (CCoAOMT) and caffeic acid/5-hydroxyferulic acid *O*-methyltransferase (COMT), the two oxidoreductases cinnamoyl-CoA reductase (CCR) and cinnamyl alcohol reductase (CAD) as well as two enzymes 4-coumarate-CoA ligase (4CL) and shikimate hydroxycinnamoyl transferase (HCT) that are involved in the generation of pathway intermediates [37, 38, 70, 93, 109, 144, 194].

Although it is uncertain how the newly synthesized monolignols are translocated to the apoplast (cell wall), once there most evidence suggests that the single electron oxidation of the monolignol phenol by wall-bound peroxidases and/or laccases followed by combinatorial radical coupling commences formal lignin polymerization [12]. Presumably, the coupling of two monolignols with one another initiates polymerization. Most likely due to the lack of steric hindrance, coupling between monolignols is favored at the central β carbon of their side chain, resulting in the most common β–β dimer, however β-*O*-4 and β-5 linked dimers can and do occur [188]. In order for polymerization to continue, the lignin dimer must be dehydrogenated once more to a phenolic radical before it can couple with the next monomer radical. Bond formation is again favored at the central β carbon of the monolignol side chain and depending on the bond configuration and the subunit composition of the dimer, the end-wise coupling process can produce either more β-*O*-4, when a monomer adds to S- and G-units (most common), or β-5 bonds that occur only when adding to G-units [13]. If only the three previously mentioned bonds contributed to lignin polymerization, then the lignin polymer would form a relatively straight linear chain. However, two oligolignol radicals with G-unit ends can also react to form 4-*O*-5 or 5-5 couplings that generate a branch-like quality to the polymer structure. In fact, lignin containing a high proportion of G-units is more highly cross-linked than lignin rich in S-units, which may contribute to the more rigid and hydrophobic character of G-unit lignin [13]. Therefore, the relative proportion of a given lignin monomer dictates the relative abundance of the inter-unit linkage present in the lignin polymer. Interestingly, the β-*O*-4 linkage is not only the most common linkage found in plants [62], but it is also the easiest of all the linkages to chemically cleave and increasing this linkage could potentially enhance the efficiency of conversion processes [75]. It should also be noted that an alternative hypothesis with regards to lignin polymerization suggests that lignin monomers are coupled with absolute structural control by proteins in the cell wall bearing arrays of dirigent sites, however there has been no genetic data yet produced to support this claim [188]. Additional evidence supporting the predominant radical coupling model of lignification has shown that all phenolic compounds, monolignols or otherwise, that enter into the region of the cell wall where oxidation and radical coupling occur have the potential to be radicalized and incorporated into the lignin polymer, suggesting a very flexible process not likely mediated by ligand-specific enzymes [188].

This phenomenon may also allow for a strategy of designing lignins for industrial applications, specifically by regulating the influx and species of monolignol or other phenolic compound into the cell wall [68]. And finally, regarding the global control of lignification, several transcription factors belonging to the MYB and NAC gene families, similar to those responsible for SCW biogenesis, have been shown to play a key role in regulating the expression of many of the genes in the monolignol biosynthesis pathway [204, 211].

3 Modification of Cell Wall Structure and Synthesis to Overcome Biomass Recalcitrance

A further understanding of the synthesis and regulation of the three major cell wall molecules (cellulose, hemicellulose, and lignin) will further clarify targets for genetic modification. However, the current understanding of plant cell wall biosynthesis is already allowing for intriguing results through approaches that use genetic modification combined with the latest conversion technologies. To begin, a great deal of research to date has focused on methods to improve the biochemical conversion efficiency of plant biomass with specific focus on how cellulose can be degraded by microbial enzymes into glucose for subsequent production of biofuels. The most mature conversion technology uses carbohydrate chemistry and fermentation technology for alcohol production. Other methods of processing the carbohydrates currently in development include fermentation by genetically altered microbes to various hydrocarbon products or the production of a targeted range of hydrocarbons for fuels and chemicals through the use of solid-phase catalysts under carefully controlled conditions [152]. Regardless of how the sugars are processed, the efficiency of the cellulose saccharification process is critical to making many of these types of bio-based production processes economically viable. Although there is still debate in the literature about the relative importance of all the factors that contribute to the recalcitrant nature of cellulose, the most studied aspects include the effect of coating by lignin and hemicelluloses, the degree of microfibril crystallinity and polymerization, and the accessible surface area of the microfibrils [118]. In spite of this debate, there is a general consensus that in order for cellulases to efficiently hydrolyze cellulosic substrates, the enzymes must first be able to access the individual glucan chains of the tightly packed and coated microfibril [110]. Traditionally, pretreatment of the lignocellulosic biomass has been employed to loosen the interactions of the microfibril with the other cell wall components, thus increasing access for the enzymes [118]. However, research centered on making genetic modifications in planta to produce cellulose that is more accessible to these enzymes and perhaps reduce or eliminate many pretreatment techniques has also developed.

A long-standing paradigm in forage quality and production states that as lignin content decrease, forage digestion rates for ruminant livestock increase, which in turn improves the ratio of food intake to weight gain [175]. This paradigm translates perfectly to the hydrolysis step of the biochemical conversion process with the net

result allowing for a decreased enzyme load while obtaining an increased breakdown rate of the biomass. The reason for this phenomenon not only concerns the increased access of the hydrolytic enzymes to the cellulose microfibrils due to the decreased lignin coat, but there is also a reduction in the nonproductive binding (adsorption) and inactivation of cellulases by the lignin component, thus resulting in less enzymes required to degrade the biomass [6]. Therefore, for the purpose of accessing the sugars within the wall, while much of the research in this area has traditionally focused on using pretreatment technology to eliminate lignin postharvest, reducing or modifying the lignin content in biomass is beginning to show great promise [37, 38, 145]. The genetic modification of the enzymes involved in lignin biosynthesis has gained a lot of momentum in recent years through the use of model plants to dissect the biosynthetic pathway [28, 120, 147, 148, 194]. Successful examples include the down-regulation of certain lignin biosynthetic pathways that has led to more digestible forage and better pulping efficiency for paper processing [126, 151]. Of particular interest for conversion technology was a study performed on transgenic alfalfa lines in which six lignin biosynthesis genes were independently down-regulated by antisense technology resulting in the identification of two transgenic lines (*HCT*, *C3′H*) that showed a significantly greater saccharification efficiency of their untreated biomass compared to that of the pretreated biomass controls [27]. This study lends further and more specific evidence to the suggestion that genetic reduction of lignin content can effectively overcome cell wall recalcitrance to saccharification using enzymatic hydrolysis and that these techniques could potentially preclude the need for acid pretreatment [27]. In addition, it has been recognized that many lignin mutants have a reduced growth phenotype, as was the case in this study, although remarkably, the 40% reduction in overall biomass of the *HCT* mutant was offset by a 166% increase in sugar production, thus reflecting a significant theoretical improvement in fermentable sugar production on a per plant basis [27].

A caveat with regards to lignin regulation states that partial elimination of lignin from tree crops like poplar has the potential to dramatically reduce their water use efficiency and hydraulic conductivity as well as increase xylem cavitation [38]. Therefore, developing a plant with less recalcitrant cell walls by significantly reducing lignin content may require either additional bioengineering or a completely alternative approach that attempts to modify or shift lignin to a more benign composition with respect to conversion processes, yet still allow normal plant development. Research into lignin "redesign" has shown that supplementation of coniferyl ferulate, a simple methoxylated analog of the natural conjugate coniferyl *p*-coumarate, into maize cell walls during the lignification process increased lignin extractability by up to twofold in aqueous NaOH pretreatment and increased cell wall hydrolysis and sugar release in pretreated and untreated cells [68]. In another study, the expression of a transgene encoding a high tyrosine-content peptide in the lignifying tissues of hybrid poplar resulted in a higher polysaccharide release after treatment of the biomass with hydrolytic enzymes [106]. Analysis is currently underway to determine if the tyrosine-rich peptides actually cross-linked with phenolic hydroxyl groups in the lignin to modify the lignocellulosic structure of the transgenic biomass. In a

related but different approach, this time targeting the UDP-xylose pathway, a monospecific UDP-glucose dehydrogenase, a dual-specific ADH-like UDP-glucose dehydrogenase and several UDP-glucuronate decarboxylases were cloned and expressed in xylogenic tobacco cells [10]. It was hypothesized that a lowering of xylan production in these cell lines, by the down-regulation of the UDP-glucuronate decarboxylase, might lead to alterations in lignin biosynthesis, a change in cellulose extractability and perhaps offers insights into how lignin is coupled to hemicelluloses in dicots [9]. Interestingly, despite the lower xylan content of the antisense lines, the lignin content and composition remained relatively unchanged, however the delignification properties were actually lower (lignin was harder to remove) and less cellulose was extracted than in control lines. Thus, it appears that the level of xylan relative to lignin may be an important factor in delignification properties and cellulose extractability, in this case reduced xylan may lead to a closer association between cellulose and lignin [9].

Regarding the potential for reducing cell wall recalcitrance through a reduction in cellulose crystallinity, one of the earliest discoveries was that of naturally occurring proteins that have the unique property of disrupting cellulose crystallinity. Upon analysis of various microbial carbohydrate-active enzymes, it was realized that many possess a contiguous sequence of amino acids termed a carbohydrate-binding module (CBM) that produces a discrete fold imparting carbohydrate-binding activity [165]. Further research showed that microbial enzymes possessing CBMs, such as cellulases and chitinases, are brought into close and prolonged contact with their recalcitrant substrates and have increased rates of substrate hydrolysis [165]. Interestingly, some CBMs expressed alone without the catalytic portion of the enzyme have displayed an ability to disrupt the corresponding substrate. This phenomenon was initially shown to disrupt the structure of cellulose microfibrils in vitro [51] and then later during heterologous expression in plant systems where the CBM was targeted to the cell wall [165]. Many of these heterologous expression studies with CBMs have noted that the reduction in cellulose crystallinity caused by the disruption effect of the CBM often coincides with an increase in cellulose biosynthesis and thus an overall increase in plant biomass. It has been postulated that this occurs through a physicomechanical mechanism by which the CBM molecule slides between the glucan chains as they are extruded from the CSC before they begin hydrogen bonding to adjacent chains, thus separating them in a wedge-like action which essentially uncouples the polymerization step from the crystallization step of cellulose biosynthesis [103].

In addition to CBMs from microbial sources, a group of pH-dependent wall-loosening plant proteins with close homology to CBMs, known as expansins, have been shown to be activated during the acid growth response of plant cells and to stimulate PCW enlargement by disrupting the noncovalent binding between wall polysaccharides [40]. Capitalizing on the ability of expansins to weaken networks of cellulose microfibrils [112], a recent study has shown that when added to a cellulase mixture, the protein swollenin (an expansin-like protein from *Trichoderma reesei* [156]) can enhance the degradation of crystalline cellulose into glucose providing an improvement for bioconversion technology [29]. Other plant proteins

of interest include the endo-β-1,4-glucanases (EGases), especially the relatively new subclass of the α-EGases that contain a functional and modular CBM conferring binding to crystalline cellulose [187]. The presence of a CBM in this plant EGase suggests that it may have a role in cellulose degradation which could include functions as diverse as cell wall disassembly during fruit softening and organ abscission, hydrolysis of polysaccharide chains at the cellulose microfibril periphery, or even cell wall assembly by regulating cellulose crystallinity during biosynthesis [187]. In addition, the binding of xyloglucans to cellulose microfibrils also suggests that these molecules may be involved in the *in muro* modification of cellulose. Xyloglucan *endo*-transglycosylases (XETs) are a group of enzymes able to carry out rearrangement of xyloglucans by cleavage and re-ligation that may occur in conjunction with other enzymes such as EGases. By using XETs specifically as the receptor anchor for chemical groups, chemical functionality and other modifications have been made to cellulose [212–214]. Taken together, the genetic manipulation of endogenous plant enzymes for the controlled growth and degradation of lignocellulosic biomass is an important avenue of research towards improving biomass processing of biofuel and biochemical feedstocks.

Another method that may hold promise for increasing the access of enzymes to cellulose and thus decreasing the need for pretreatment is that of increasing the more soluble amorphous zones within the cellulose microfibril [82]. In search of mutations that may cause an increase in enzymatic conversion efficiency, a recent study screened a majority of the available PCW mutants in *Arabidopsis* and found that a number of previously generated mutant plants yielded significantly more fermentable sugar than wild-type plants [76]. This study also measured the biomass crystallinity of these plants and discovered that two of the best enzymatic conversion mutants, *isoxaben resistance1-2* and *2-1* (*ixr1-2*, *ixr2-1*), had lower relative crystallinity index (RCI) values than wild-type plants. This evidence suggests that there may be fundamental changes in the orientation, size, or density of the cellulose crystallites composing the cellulose in these mutants, although further analysis of the cellulose is still needed to confirm this possibility [74, 76]. Regarding the nature of the *ixr1-2* and *ixr2-1* mutants, previous research has shown that these single point mutations reside in or near a transmembrane spanning domain in the C-terminus of CESA3 and CESA6, respectively [50, 158]. Speculating on the reasons for the increased saccharification efficiency and reduced RCI, perhaps these mutations alter the structure of the CESA protein, changing its orientation either within the plasma membrane or with respect to neighboring CESAs in the CSC. An unstable or improperly positioned CESA, even to a slight degree, could alter the path of the glucan chain during polymerization and effect its subsequent incorporation into the crystallizing microfibril either through poor proximity with the other glucan chains or through unstable hydrogen bonding angles. The overall effect could be an increase in the amorphous zones along the fibril length that might explain the increased saccharification and reduced RCI. An additional hypothesis for this data is that the altered cellulose array results in a proportional shift in the volume fraction of cellulose, hemicellulose and lignin in the cell wall that could result in an increased availability of cellulose to hydrolytic conversion. Whatever the case may be, it is

also interesting to note that the conversion process for these plants required less enzyme loading and less overall reaction time to that of wild-type, suggesting two areas of cost reduction for biofuel production [76].

In addition to the need for pretreatment of biomass to facilitate enzymatic breakdown of the recalcitrant cell walls, another costly step in the biochemical conversion process is the production of the hydrolytic enzymes (cellulases, xylanases, etc.) generally via microbial bioreactors. In fact, the combined costs of pretreatment and enzyme production can greatly reduce the ideal efficiency of biofuel production from lignocellulosic biomass, making the entire process two to threefold more expensive than production from maize grain starch [170]. To address the enzyme production question, it has been noted that plants are already used for the production of many industrial and pharmaceutical products, including enzymes and other proteins. Therefore, why not produce plant cell wall hydrolytic enzymes in the very bioenergy feedstock crops that they will be used to degrade? Research in this area has already shown that a biologically active heterologous thermostable endo-1,4-β-endoglucanase (E1) enzyme from *Acidothermus cellulolyticus* can be expressed in *Arabidopsis* [216], potato (*Solanum tuberosum* L.) [42], and tobacco (*Nicotiana* sp.) [215] plants. Initially, when combined with pretreatment processes such as ammonia fiber/freeze explosion (AFEX), approximately two-thirds of the activity of the heterologous E1 was lost [184]. However, further research has demonstrated that expressing the E1 enzyme in corn [11] and rice [128] followed by enzyme extraction from the dry transgenic biomass in a total soluble protein (TSP) preparation and then re-introduction to the biomass after AFEX pretreatment, led to successful conversion of some of the corn stover and rice straw into glucose [128, 150]. Continued research is focused on improving the heterologous expression process primarily by increasing the variety of hydrolytic enzymes that can be expressed as well as by increasing the levels of in planta enzyme production and the biological activity of these enzymes postextraction [170]. It is well known that in order to get near complete levels of cellulose and hemicellulose degradation from pretreated biomass, a number of cellulase (endoglucanase, exoglucanase, and β-glucosidase) and hemicellulase (endo-xylanases and exo-xylanases) enzymes must work synergistically to promote the solubilization and hydrolysis of these carbohydrates into their principle monosaccharide constituents [202]. Hence, attempts are currently being made to express all the required enzyme components for cell wall carbohydrate degradation, thus reducing the need for external supplementation. In addition to enzyme variety, the amount of enzyme produced is also critical. The *A. cellulolyticus* E1 enzyme has been produced in rice at amounts around 5% and in maize at 2% of plant TSP, however it has been estimated that levels need to be around 10% TSP to avoid the need for additional enzymes [170]. Strategies being used to increase the level of enzyme production include genetically engineering the chloroplast genome instead of the nuclear genome, better subcellular targeting of the enzymes after expression such as localization to the ER, apoplast or chloroplast, and the better matching of enzyme pH requirements with that of the subcellular compartment targeted for localization [170].

4 Modification of Cell Wall Structure and Synthesis to Increase Biomass Quantity and Energy Density

It is entirely possible that energy density may be the measure of the ideal energy plant rather than a less recalcitrant cell wall, in which case larger or more energy dense biomass crops will be preferred and traditional combustion or thermochemical-/catalytic-based conversions that can lead directly to liquid fuels will be used [152]. In fact, technology is already being developed to allow for industrial-scale conversion of biomass directly to liquid hydrocarbons via pyrolysis or gasification [124]. Determining all the factors that will comprise energy density in plants is still taking shape, however it is certain that engineering plant cells to grow larger and accumulate greater amounts of energy dense macromolecules will be an important goal. In addition, although there is still a great deal to learn at a fundamental level about the sensing and signaling mechanisms that alter carbon assimilation, carbon storage, and growth rate within the plant [168], research in this area has already uncovered useful modifications which increase plant biomass. These studies vary in approach, from the modification of plant growth regulators such as brassinosteriods in *Arabidopsis* [32] or gibberellins in poplar [58] to the gaining of a better understanding of the synchronization of the circadian clock and external light–dark cycles that can also result in improved plant growth [55]. Other studies have shown an increase in growth by the overexpression of heterologous enzymes in the cellulose biosynthesis pathway. Examples include yeast-derived invertases [22] and the *Arabidopsis* family A sucrose phosphate synthase [133], both expressed in transgenic tobacco. More specifically, the substrate ratios of cellulose biosynthesis have also been targeted, such as the overexpression of sucrose synthase (SuSy) and UDP-glucose pyrophosphorylase, targeted for their role as the only known suppliers of UDP-glucose to the CESA enzymes [36]. A good example has shown that the expression of cotton (*Gossypium hirsutum*) SuSy in hybrid poplar (*Populus alba* × *grandidentata*) affects carbon partitioning leading to an increase in cellulose production in the SCW without increasing plant growth, thus representing a good strategy to increase energy density in the plant [39]. Other studies such as the deregulation of ADP-glucose pyrophosphorylase, a key starch biosynthesis enzyme in rice [167] and the overexpression of purple acid phosphatase in tobacco [90] both show promising results for increasing plant biomass and cellulose synthesis, respectively. However, the authors of these last two studies have only speculated at the possible mechanism of action that produces the increases, thus reminding researchers of the difficulties inherent in elucidating the details of plant growth and regulation. For example, with regard to purple acid phosphatase, it was suggested that the enhanced activity of the CESAs was due to their activation by phosphorylation [90]. Indeed, several putative cytoplasmic phosphorylation sites have been identified in the CESAs of *Arabidopsis* using a phosphoproteomics approach [125]. Additional support for this hypothesis has shown that CESA7 is phosphorylated in vivo on two serine residues within the hyper-variable region of the protein, between the two putative catalytic domains and that this leads to its degradation via a proteosome-dependent pathway [179].

However, while there is increasing evidence to suggest phosphorylation/dephosphorylation as a mechanism for the regulation of the relative levels and activity of individual CESA proteins in a CSC, other mechanisms for CESA turnover, such as cysteine proteases [86] have also shown support. What these and other studies suggest is that there are many complex factors involved in the regulation of plant growth and cellulose biosynthesis and that perhaps a thorough understanding of what encompasses "normal" regulation is most important, followed by the continued identification of mutants with altered growth phenotypes and cellulose quality.

Recent discoveries that have added great insight into the molecular mechanisms involved in the biogenesis of the SCW include identification of several NAC domain transcription factors that all belong to one particular phylogenetic subgroup and are key transcriptional activators of SCW formation [164]. The NAC transcription factors identified to date include VND1-VND7 (*v*ascular-related *N*AC-*d*omain) that regulate differentiation of tracheary elements [95] and NST1 and NST3 (also known as SND1) (*N*AC *S*CW *t*hickening promoting factor) that promote secondary thickening in xylem fiber cells [115, 204, 210]. As this transcriptional network for regulation of the SCW has been further resolved, it has been shown that these NACs regulate a cascade of downstream transcription factors that in turn activate SCW biosynthetic genes [48]. Three members of the MYB transcription factor family, MYB26, MYB83, and MYB46, can also regulate secondary wall biosynthesis by either regulating the expression of NST1 and NST2 and thus control cell wall thickening in the anther endothecium or by serving as the direct target of NST3 and control cell wall thickening in fibers [111, 198, 208, 209]. Another potentially important study regarding these transcriptional switches showed that under appropriate growth conditions, hypocotyls of *Arabidopsis* had similar structure to the secondary xylem (wood) found in trees [26]. In the *nst1-1 nst3-1* double knockdown mutants of *Arabidopsis*, there was nearly complete suppression of SCW formation within secondary xylem fibers of the hypocotyls [115]. Interestingly, there are putative homologs of *NST1* and *NST3* in the poplar genome, therefore a common mechanism for the control of wood formation may exist in herbaceous and woody plants, and *NST*s along with other NACs could play an important role in SCW biosynthesis during wood formation. The further characterization of NAC genes could provide important tools for the genetic manipulation of fiber cells and thus modification of wood quality and production that could positively impact feedstocks for biofuels.

In response to gravity, many angiosperm trees significantly alter the normal development of the SCW on the upper surface of their branches and leaning trunks by forming tension wood (TW). The formation of TW results in wood cells with a SCW devoid of an S3 and most of an S2 layer and replaced by a gelatinous layer (G-layer) consisting of highly crystalline cellulose with a high degree of tensile strength due to the parallel orientation of the microfibrils [2]. The TW benefits the tree by exerting a tensile force that can pull a tree trunk vertical or hold a large branch horizontal thus keeping the leaves in an optimal position for gathering sunlight [16]. The potential interest in TW for bioconversion technology resides in the fact that the G-layer, present in both the xylem and the phloem fibers, is 98% crystalline cellulose and virtually devoid of lignin and hemicelluloses, thus

representing the purest form of cellulose occurring in woody tissues and increasing the overall cellulose content of the wood by about 10–20% [2, 87]. The process of TW formation can be experimentally induced and has therefore been a valuable model system to understanding the process of cellulose biosynthesis in trees. It has already been shown that orthologs to the CESA genes involved in SCW synthesis in *Arabidopsis* are upregulated during TW formation in aspen trees, including specific NAC genes [7]. In addition, a global analysis of the differential expression in transcripts and fluctuations in metabolites during TW formation in poplar identified many molecular players involved in the change in carbon flow into various cell wall components and mechanisms important for the formation of the G-layer [2]. A study of this type has provided a roadmap of sorts for the further functional analysis of genes involved in G-layer biosynthesis in TW and identification of areas for future genetic manipulation. An understanding of the molecular mechanism of highly crystalline cellulose production during TW generation in trees could provide a mechanism for the production of ectopic TW in trees and other plant species, resulting in an increase in overall cellulose content [67, 87].

As was mentioned previously, the expression and localization of CBMs to the plant cell wall can reduce cellulose crystallinity through the process of uncoupling cellulose polymerization with crystallization [165]. Interestingly, many of these same studies also report an increase in cellulose production with concomitant increases in plant biomass, presumably by the same uncoupling phenomenon [165]. Growth acceleration has also been shown for expansin-expressing transgenics of *Arabidopsis* [31], poplar [69], and rice [33]. In the same respect, the overexpression of EGases has been shown to cause enhanced plant growth, most likely due to their proposed role in PCW loosening. For example, poplar trees developed longer internodes and enhanced growth by the overexpression of the *Arabidopsis* EGase *cel1* [163]. Likewise, lignin down-regulation not only increases biomass digestibility, but it can also result in an increase in cellulose content [89, 104]. This phenomenon is most likely caused by a compensatory response by the plant to maintain the structural integrity of the cell wall and sustain directional growth. The combination of these two factors could be very beneficial for numerous different conversion processes to biofuels and platform chemicals, as the plant would have an increased concentration of more digestible cellulose. Research in this area has shown that transgenic poplar plants transformed with antisense constructs of the lignin biosynthesis gene *Pt4CL* result in trees with a 45% decrease in lignin and a 15% increase in cellulose content [89, 99]. As referred to earlier, directing the plant's energy and carbon storage into cellulose rather than lignin may result in compromising SCW strength, water conductivity and an increase in the susceptibility to pathogens [194]. Interestingly, classic plant-breeding programs to lower lignification, primarily for improvement in forage quality, have been pursued extensively for many plant species over a number of years, including various Bermuda grasses (*Cynodon dactylon*) [1], and the *brown midrib* class of cell wall mutants in maize (*bm*) and sorghum (*bmr*) [25]. Recently, a study showed that these maize and sorghum mutants not only show a clear reduction in lignin composition but also have improved fermentable sugar yields after enzymatic saccharification [189]. Equally important is

the fact that although initially most of the *brown midrib* mutants had compromised growth characteristics similar to those seen with some of the transgenic lignin mutants, these traits have been largely eliminated by conventional breeding methods [136]. Therefore, the genetic resources available from these and other plants [63, 171, 199] may provide a model to define cell wall and gene abnormalities that can be copied to accelerate the breeding program in bioenergy feedstocks.

The fact that lignin is the second most abundant biopolymer on earth after cellulose also makes it a potential target for direct conversion into biofuels. However, due to the nature of lignin biosynthesis, nonenzymatic conversion technologies will be needed to produce fuels and chemicals and currently there is a lack of selective and cost-efficient process available for lignin conversion. This fact has lead to the current use of the lignin residue produced from biorefining as a fuel that is burned to generate power, most often to run the biorefinery itself [44]. Yet there are many strategies, old and new, in development that could lead to the efficient extraction and depolymerization of lignin into its monomeric substituent groups, which in turn can be upgraded into hydrocarbons (reviewed in Zakzeski et al. [200]). Of these numerous methods, one of the newer more attractive strategies includes the use of thermolytic ionic liquids, which are essentially nonvolatile molten salts with a melting point less than 100°C [83], that recent studies have indicated are suitable as solvents for the dissolution of lignocellulosic materials [61, 91, 142]. The use of ionic liquids to dissolve lignocellulosic biomass may also pair quite well with the subsequent fermentation of the liberated carbohydrates into biofuels as the process can occur at near-ambient temperatures and pressures with the use of a very limited set of ionic liquid substructures. An alternative strategy to disassemble lignin also under development is Baeyer-Villiger oxidation, which involves the cleavage of carbon–carbon bonds adjacent to a carbonyl that can convert the aromatic rings in lignin to carboxylic acids and their lactones, thus taking advantage of the plethora of reactive sites present in lignin polymers [130]. The oxygenates that result from this oxidative deconstruction can then be deoxygenated via process like hydrodeoxygenation, to give hydrocarbons. Unfortunately, the high number of functional groups also means that a large number of reactions can take place at different sites in the polymer, producing small molecules, degraded polymer residues, and cross-linked polymers. In addition, the oxidation process can catalyze the hydrolysis of carbohydrates, especially the hemicellulose constituents, which can reduce yields for carbohydrate fermentation [177]. Therefore, research is focusing on improving oxidation methods that avoid cleaving the hemicelluloses as well as strategies to genetically alter lignin biosynthesis in plants to increase the more easily cleaved β-*O*-4 linkages. A third developing technology that shows strong potential is the thermal decomposition of lignocellulosic biomass via fast pyrolysis. This process results in the depolymerization and fragmentation of cellulose, hemicellulose, and lignin producing a dark brown, free-flowing liquid known as bio-oil [41]. Upon water addition to the bio-oil, fractionation of the liquid occurs, with the light oxygenates derived from the carbohydrates forming the water-soluble upper layer, and the lignin-derived oligomeric (aromatic) compounds settling in the lower water-insoluble layer [41]. The purity of the lignin-derived fraction can be further improved through the use of additional solvent fractionation methods [35]. Applications for the two

fractions include the production of calcium salts as environmentally friendly road deicers via the neutralization of carboxylic acids present in the water-soluble fraction and the replacement of phenol in phenol-formaldehyde resins using the water insoluble fraction. Although the lignin-derived aromatics are less reactive than phenol, 30–50% of the phenol can be replaced, producing high quality resins [41].

Acknowledgments This work was supported by the National Science Foundation (IOS: 0922947 and EFRI: 0937657).

References

1. Akin D (2007) Grass lignocellulose. Appl Biochem Biotechnol 137–140:3–15
2. Andersson-Gunneråas S, Mellerowicz EJ, Love J et al (2006) Biosynthesis of cellulose-enriched tension wood in *Populus*: global analysis of transcripts and metabolites identifies biochemical and developmental regulators in secondary wall biosynthesis. Plant J 45:144–165
3. Appenzeller L, Doblin M, Barreiro R et al (2004) Cellulose synthesis in maize: isolation and expression analysis of the cellulose synthase (*CesA*) gene family. Cellulose 11:287–299
4. Arioli T, Pend L, Betzner A et al (1998) Molecular analysis of cellulose biosynthesis in *Arabidopsis*. Science 279:717–720
5. Beeckman T, Przemeck GKH, Stamatiou G et al (2002) Genetic complexity of cellulose synthase A gene function in *Arabidopsis* embryogenesis. Plant Physiol 130:1883–1893
6. Berlin A, Gilkes N, Kurabi A et al (2005) Weak lignin-binding enzymes—a novel approach to improve activity of cellulases for hydrolysis of lignocellulosics. Appl Biochem Biotechnol 121:163–170
7. Bhandari S, Fujino T, Thammanagowda S et al (2006) Xylem-specific and tension stress-responsive coexpression of KORRIGAN endoglucanase and three secondary wall-associated cellulose synthase genes in aspen trees. Planta 224:828–837
8. Bichet A, Desnos T, Turner S et al (2001) *BOTERO1* is required for normal orientation of cortical microtubules and anisotropic cell expansion in *Arabidopsis*. Plant J 25:137–148
9. Bindschedler LV, Tuerck L, Maunders M et al (2007) Modification of hemicellulose content by antisense down-regulation of UDP-glucuronate decarboxylase in tobacco and its consequences for cellulose extractibility. Phytochemistry 68:2635–2648
10. Bindschedler LV, Wheatley E, Gay E et al (2005) Characterisation and expression of the pathway from UDP-glucose to UDP-xylose in differentiating tobacco tissue. Plant Mol Biol 57:285–301
11. Biswas GCG, Ransom C, Sticklen M (2006) Expression of biologically active *Acidothermus cellulolyticus* endoglucanase in transgenic maize plants. Plant Sci 171:617–623
12. Boerjan W, Ralph J, Baucher M (2003) Lignin biosynthesis. Annu Rev Plant Biol 54:519–546
13. Bonawitz ND, Chapple C (2010) The genetics of lignin biosynthesis: connecting genotype to phenotype. Annu Rev Genet 44:337–363
14. Bosca S, Barton CJ, Taylor NG et al (2006) Interactions between MUR10/CesA7-dependent secondary cellulose biosynthesis and primary cell wall structure. Plant Physiol 142: 1353–1363
15. Bouquin T, Mattsson O, Naested H et al (2003) The *Arabidopsis lue1* mutant defines a katanin p60 ortholog involved in hormonal control of microtubule orientation during cell growth. J Cell Sci 116:791–801
16. Bowling AJ, Vaughn KC (2008) Immunocytochemical characterization of tension wood: gelatinous fibers contain more than just cellulose. Am J Bot 95:655–663
17. Brocard-Gifford I, Lynch TJ, Garcia ME et al (2004) The *Arabidopsis thaliana* ABSCISIC ACID-INSENSITIVE8 locus encodes a novel protein mediating abscisic acid and sugar responses essential for growth. Plant Cell 16:406–421

18. Brosse N, Sannigrahi P, Ragauskas A (2009) Pretreatment of *Miscanthus* x *giganteus* using the ethanol organosolv process for ethanol production. Ind Eng Chem Res 48:8328–8334
19. Brown RM (1996) The biosynthesis of cellulose. J Macromol Sci A33:1345–1373
20. Burk DH, Liu B, Zhong R, Morrison WH et al (2001) A katanin-like protein regulates normal cell wall biosynthesis and cell elongation. Plant Cell 13:807–828
21. Burton RA, Shirley NJ, King BJ et al (2004) The *CesA* gene family of Barley. Quantitative analysis of transcripts reveals two groups of co-expressed genes. Plant Physiol 134: 224–236
22. Canam T, Park J-Y, Yu K et al (2006) Varied growth, biomass and cellulose content in tobacco expressing yeast-derived invertases. Planta 224:1315–1327
23. Caño-Delgado A, Penfield S, Smith C et al (2003) Reduced cellulose synthesis invokes lignification and defense responses in *Arabidopsis thaliana*. Plant J 34:351–362
24. Carpita NC, Gibeaut DM (1993) Structural models of primary-cell walls in flowering plants—consistency of molecular-structure with the physical-properties of the walls during growth. Plant J 3:1–30
25. Carpita NC, McCann MC (2008) Maize and sorghum: genetic resources for bioenergy grasses. Trends Plant Sci 13:415–420
26. Chaffey N, Cholewa E, Regan S et al (2002) Secondary xylem development in *Arabidopsis*: a model for wood formation. Physiol Plant 114:594–600
27. Chen F, Dixon RA (2007) Lignin modification improves fermentable sugar yields for biofuel production. Nat Biotechnol 25:759–761
28. Chen F, Srinivasa Reddy MS, Temple S et al (2006) Multi-site genetic modulation of monolignol biosynthesis suggests new routes for formation of syringyl lignin and wall-bound ferulic acid in alfalfa (*Medicago sativa* L.). Plant J 48:113–124
29. Chen X-A, Ishida N, Todaka N et al (2010) Promotion of efficient saccharification of crystalline cellulose by *Aspergillus fumigatus* Swo1. Appl Environ Microbiol 76:2556–2561
30. Chen Z, Hong X, Zhang H et al (2005) Disruption of the cellulose synthase gene, *AtCesA8/IRX1*, enhances drought and osmotic stress tolerance in *Arabidopsis*. Plant J 43:273–283
31. Cho H-T, Cosgrove DJ (2000) Altered expression of expansin modulates leaf growth and pedicel abscission in *Arabidopsis thaliana*. Proc Natl Acad Sci U S A 97:9783–9788
32. Choe S, Fujioka S, Noguchi T et al (2001) Overexpression of *DWARF4* in the brassinosteroid biosynthetic pathway results in increased vegetative growth and seed yield in *Arabidopsis*. Plant J 26:573–582
33. Choi D, Lee Y, Cho H-T et al (2003) Regulation of expansin gene expression affects growth and development in transgenic rice plants. Plant Cell 15:1386–1398
34. Chu Z, Chen H, Zhang Y et al (2007) Knockout of the *AtCESA2* gene affects microtubule orientation and causes abnormal cell expansion in *Arabidopsis*. Plant Physiol 143:213–224
35. Chum HL, Black SK (1990) Process for fractionating fast-pyrolysis oils, and products derived therefrom. Midwest Research Institute, Kansas City, MO
36. Coleman HD, Ellis DD, Gilbert M et al (2006) Up-regulation of sucrose synthase and UDP-glucose pyrophosphorylase impacts plant growth and metabolism. Plant Biotechnol J 4: 87–101
37. Coleman HD, Park JY, Nair R et al (2008) RNAi-mediated suppression of p-coumaroyl-CoA 3′-hydroxylase in hybrid poplar impacts lignin deposition and soluble secondary metabolism. Proc Natl Acad Sci U S A 105:4501–4506
38. Coleman HD, Samuels AL, Guy RD et al (2008) Perturbed lignification impacts tree growth in hybrid poplar—a function of sink strength, vascular integrity, and photosynthetic assimilation. Plant Physiol 148:1229–1237
39. Coleman HD, Yan J, Mansfield SD (2009) Sucrose synthase affects carbon partitioning to increase cellulose production and altered cell wall ultrastructure. Proc Natl Acad Sci U S A 106:13118–13123
40. Cosgrove DJ (2005) Growth of the plant cell wall. Nat Rev Mol Cell Biol 6:850–861
41. Czernik S, Bridgwater AV (2005) Application of biomass fast pyrolysis oil. In: Bridgwater AV (ed) Fast pyrolysis of biomass: a handbook, vol 3. CPL Press, Newbury, UK, pp 105–120

42. Dai Z, Hooker BS, Anderson DB et al (2000) Improved plant-based production of E1 endoglucanase using potato: expression optimization and tissue targeting. Mol Breed 6:277–285
43. Daras G, Rigas S, Penning B et al (2009) The *thanatos* mutation in *Arabidopsis thaliana* cellulose synthase 3 (*AtCesA3*) has a dominant-negative effect on cellulose synthesis and plant growth. New Phytol 184:114–126
44. DeBolt S, Campbell JE, Smith R Jr et al (2009) Life cycle assessment of native plants and marginal lands for bioenergy agriculture in Kentucky as a model for South-Eastern USA. Glob Chang Biol Bioenergy 1:308–316
45. DeBolt S, Gutierrez R, Ehrhardt DW et al (2007) Morlin, an inhibitor of cortical microtubule dynamics and cellulose synthase movement. Proc Natl Acad Sci U S A 104:5854–5859
46. Delmer DP (1999) Cellulose biosynthesis: exciting times for a difficult field of study. Annu Rev Plant Physiol Plant Mol Biol 50:245–276
47. Delmer DP, Amor Y (1995) Cellulose biosynthesis. Plant Cell 7:987–1000
48. Demura T, Ye Z-H (2010) Regulation of plant biomass production. Curr Opin Plant Biol 13:298–303
49. Desprez T, Juraniec M, Crowell EF et al (2007) Organization of cellulose synthase complexes involved in primary cell wall synthesis in *Arabidopsis thaliana*. Proc Natl Acad Sci U S A 104:15572–15577
50. Desprez T, Vernhettes S, Fagard M et al (2002) Resistance against herbicide isoxaben and cellulose deficiency caused by distinct mutations in same cellulose synthase isoform CESA6. Plant Physiol 128:482–490
51. Din N, Gilkes NR, Tekant B et al (1991) Non-hydrolytic disruption of cellulose fibres by the binding domain of a bacterial cellulase. Nat Biotechnol 9:1096–1099
52. Ding S-Y, Himmel ME (2006) The maize primary cell wall microfibril: a new model derived from direct visualization. J Agric Food Chem 54:597–606
53. Djerbi S, Lindskog M, Arvestad L et al (2005) The genome sequence of black cottonwood (*Populus trichocarpa*) reveals 18 conserved cellulose synthase (*CesA*) genes. Planta 221:739–746
54. Doblin MS, Kurek I, Jacob-Wilk D et al (2002) Cellulose biosynthesis in plants: from genes to rosettes. Plant Cell Physiol 43:1407–1420
55. Dodd AN, Salathia N, Hall A et al (2005) Plant circadian clocks increase photosynthesis, growth, survival, and competitive advantage. Science 309:630–633
56. Ebrigenova A (2006) Structural diversity and application potential of hemicelluloses. Macromol Symp 232:1–12
57. Ellis C, Karafyllidis I, Wasternack C et al (2002) The *Arabidopsis* mutant *cev1* links cell wall signaling to jasmonate and ethylene responses. Plant Cell 14:1557–1566
58. Eriksson ME, Israelsson M, Olsson O et al (2000) Increased gibberellin biosynthesis in transgenic trees promotes growth, biomass production and xylem fiber length. Nat Biotechnol 18:784–788
59. Fagard M, Desnos T, Desprez T et al (2000) *PROCUSTE1* encodes a cellulose synthase required for normal cell elongation specifically in roots and dark-grown hypocotyls of *Arabidopsis*. Plant Cell 12:2409–2424
60. Feraru E, Feraru MI, Kleine-Vehn J Jr et al (2011) PIN polarity maintenance by the cell wall in *Arabidopsis*. Curr Biol 21:338–343
61. Fort DA, Remsing RC, Swatloski RP et al (2007) Can ionic liquids dissolve wood? Processing and analysis of lignocellulosic materials with 1-n-butyl-3-methylimidazolium chloride. Green Chem 9:63–69
62. Freudenberg K, Chen CL, Harkin JM et al (1965) Observations on lignin. Chem Commun 224–225
63. Garvin DF, Gu Y-Q, Hasterok R et al (2008) Development of genetic and genomic research resources for *Brachypodium distachyon*, a new model system for grass crop research. Crop Sci 48:S69–S84
64. Geisler-Lee J, Geisler M, Coutinho PM et al (2006) Poplar carbohydrate-active enzymes. Gene identification and expression analyses. Plant Physiol 140:946–962

65. Gillmor CS, Poindexter P, Lorieau J et al (2002) α-Glucosidase I is required for cellulose biosynthesis and morphogenesis in *Arabidopsis*. J Cell Biol 156:1003–1013
66. Gírio FM, Fonseca C, Carvalherio F et al (2010) Hemicelluloses for fuel ethanol: a review. Bioresour Technol 101:4775–4800
67. Gomez LD, Steele-King CG, McQueen-Mason SJ (2008) Sustainable liquid biofuels from biomass: the writing's on the walls. New Phytol 178:473–485
68. Grabber JH, Hatfield RD, Lu F et al (2008) Coniferyl ferulate Incorporation into lignin enhances the alkaline delignification and enzymatic degradation of cell walls. Biomacromolecules 9:2510–2516
69. Gray-Mitsumune M, Blomqvist K, McQueen-Mason S et al (2008) Ectopic expression of a wood-abundant expansin PttEXPA1 promotes cell expansion in primary and secondary tissues in aspen. Plant Biotechnol J 6:62–72
70. Gross GG, Stöckigt J, Mansell RL et al (1973) Three novel enzymes involved in the reduction of ferulic acid to coniferyl alcohol in higher plants: ferulate: CoA ligase, feruloyl-CoA reductase and coniferyl alcohol oxidoreductase. FEBS Lett 31:283–286
71. Gu Y, Kaplinsky N, Bringmann M et al (2010) Identification of a cellulose synthase-associated protein required for cellulose biosynthesis. Proc Natl Acad Sci U S A 107: 12866–12871
72. Harper AD, Bar-Peled M (2002) Biosynthesis of UDP-xylose. Cloning and characterization of a novel *Arabidopsis* gene family, UXS, encoding soluble and putative membrane-bound UDP-glucuronic acid decarboxylase isoforms. Plant Physiol 130:2188–2198
73. Harris D, Corbin K, Wang T et al. (2012) Cellulose microfibril crystallinity is reduced by mutating the C-terminal transmembrane region residues of CESA1A-V903 and CESA3T-1942 of cellulose synthase. Proc Natl Acad Sci USA 109:4098–4103
74. Harris D, DeBolt S (2008) Relative crystallinity of plant biomass: studies on assembly, adaptation and acclimation. PLoS One 3:e2897
75. Harris D, DeBolt S (2010) Synthesis, regulation and utilization of lignocellulosic biomass. Plant Biotechnol J 8:244–262
76. Harris D, Stork J, DeBolt S (2009) Genetic modification in cellulose-synthase reduces crystallinity and improves biochemical conversion to fermentable sugar. Glob Chang Biol Bioenergy 1:51–61
77. Hauser M-T, Benfey PN (1993) Genetic regulation of root expansion in *Arabidopsis thaliana*. In: Pugdomenech P, Coruzzi G (eds) NATO-ASI plant molecular biology series. Springer, New York, pp 31–40
78. Hématy K, Sado PE, Van Tuinen A et al (2007) A receptor-like kinase mediates the response of *Arabidopsis* cells to the inhibition of cellulose synthesis. Curr Biol 17:922–931
79. Hepler PK, Newcomb EH (1964) Microtubules and fibrils in the cytoplasm of *coleus* cells undergoing secondary wall deposition. J Cell Biol 20:529–533
80. Hermans PH (1949) Physics and chemistry of cellulose fibres. Elsevier, Amsterdam
81. Herth W (1983) Arrays of plasma membrane "rosettes" in cellulose microfibril formation of Spirogyra. Planta 159:347–356
82. Himmel ME, Ding SY, Johnson DK et al (2007) Biomass recalcitrance: engineering plants and enzymes for biofuels production. Science 315:804–807
83. Holbrey JD, Seddon KR (1999) Ionic liquids. Clean Technol Environ Policy 1:223–236
84. Holland N, Holland D, Helentjaris T et al (2000) A comparative analysis of the plant cellulose synthase (*CesA*) gene family. Plant Physiol 123:1313–1324
85. Hu S-Q, Gao Y-G, Tajima K et al (2010) Structure of bacterial cellulose synthase subunit D octamer with four inner passageways. Proc Natl Acad Sci U S A 107:17957–17961
86. Jacob-Wilk D, Kurek I, Hogan P et al (2006) The cotton fiber zinc-binding domain of cellulose synthase A1 from *Gossypium hirsutum* displays rapid turnover in vitro and in vivo. Proc Natl Acad Sci U S A 103:12191–12196
87. Joshi C (2003) Xylem-specific and tension stress-responsive expression of cellulose synthase genes from aspen trees. Appl Biochem Biotechnol 105:17–25
88. Joshi CP, Bhandari S, Ranjan P et al (2004) Genomics of cellulose biosynthesis in poplars. New Phytol 164:53–61

89. Jouanin L, Goujon T, de Nadai V et al (2000) Lignification in transgenic poplars with extremely reduced caffeic acid O-methyltransferase activity. Plant Physiol 123:1363–1373
90. Kaida R, Satoh Y, Bulone V et al (2009) Activation of β-glucan synthases by wall-bound purple acid phosphatase in tobacco cells. Plant Physiol 150:1822–1830
91. Kilpeläinen I, Xie H, King A et al (2007) Dissolution of wood in ionic liquids. J Agric Food Chem 55:9142–9148
92. Kohorn BD, Johansen S, Shishido A et al (2009) Pectin activation of MAP kinase and gene expression is WAK2 dependent. Plant J 60:974–982
93. Koukol J, Conn EE (1961) The metabolism of aromatic compounds in higher plants. IV. Purification and properties of the phenylalanine deaminase of *Hordeum vulgare*. J Biol Chem 236:2692–2698
94. Koyama M, Helbert W, Imai T et al (1997) Parallel-up structure evidences the molecular directionality during biosynthesis of bacterial cellulose. Proc Natl Acad Sci U S A 94:9091–9095
95. Kubo M, Udagawa M, Nishikubo N et al (2005) Transcription switches for protoxylem and metaxylem vessel formation. Genes Dev 19:1855–1860
96. Lai-Kee-Him J, Chanzy H, Müller M et al (2002) In vitro versus in vivo cellulose microfibrils from plant primary wall synthases: structural differences. J Biol Chem 277:36931–36939
97. Lally D, Ingmire P, Tong H-Y et al (2001) Antisense expression of a cell wall-associated protein kinase, WAK4, inhibits cell elongation and alters morphology. Plant Cell 13:1317–1332
98. Lane D, Wiedemeier A, Peng L et al (2001) Temperature sensitive alleles of *RSW2* link the *KORRIGAN* endo-1,4-beta-glucanase to cellulose synthesis and cytokinesis in *Arabidopsis thaliana*. Plant Physiol 126:278–288
99. Lapierre C, Pollet B, Petit-Conil M et al (1999) Structural alterations of lignins in transgenic poplars with depressed cinnamyl alcohol dehydrogenase or caffeic acid O-methyltransferase activity have an opposite impact on the efficiency of industrial kraft pulping. Plant Physiol 119:153–163
100. Lee C, Teng Q, Huang W et al (2009) The F8H glycosyltransferase is a functional paralog of FRA8 involved in glucuronoxylan biosynthesis in *Arabidopsis*. Plant Cell Physiol 50:812–827
101. Lee C, Zhong R, Richardson EA et al (2007) The *PARVUS* gene is expressed in cells undergoing secondary wall thickening and is essential for glucuronoxylan biosynthesis. Plant Cell Physiol 48:1659–1672
102. Lertpiriyapong K, Sung ZR (2003) The elongation defective mutant of *Arabidopsis* is impaired in the gene encoding a serine-rich secreted protein. Plant Mol Biol 53:581–595
103. Levy I, Shani Z, Shoseyov O (2002) Modification of polysaccharides and plant cell wall by endo-1,4-β-glucanase and cellulose-binding domains. Biomol Eng 19:17–30
104. Li L, Zhou YH, Cheng XF et al (2003) Combinatorial modification of multiple lignin traits in trees through multigene cotransformation. Proc Natl Acad Sci U S A 100:4939–4944
105. Li X, Weng JK, Chapple C (2008) Improvement of biomass through lignin modification. Plant J 54:569–581
106. Liang H, Frost CJ, Wei X et al (2008) Improved sugar release from lignocellulosic material by introducing a tyrosine-rich cell wall peptide gene in poplar. Clean Soil Air Water 36:662–668
107. Liepman AH, Nairn CJ, Willats WGT et al (2007) Functional genomic analysis supports conservation of function among cellulose synthase-like a gene family members and suggests diverse roles of mannans in plants. Plant Physiol 143:1881–1893
108. Lynd LR, Wyman CE, Gerngross TU (1999) Biocommodity engineering. Biotechnol Prog 15:777–793
109. MacKay JJ, O'Malley DM, Presnell T et al (1997) Inheritance, gene expression, and lignin characterization in a mutant pine deficient in cinnamyl alcohol dehydrogenase. Proc Natl Acad Sci U S A 94:8255–8260
110. Mansfield SD, Mooney C, Saddler JN (1999) Substrate and enzyme characteristics that limit cellulose hydrolysis. Biotechnol Prog 15:804–816
111. McCarthy RL, Zhong R, Ye Z-H (2009) MYB83 is a direct target of SND1 and acts redundantly with MYB46 in the regulation of secondary cell wall biosynthesis in *Arabidopsis*. Plant Cell 50:1950–1964

112. McQueen-Mason S, Cosgrove DJ (1994) Disruption of hydrogen-bonding between plant-cell wall polymers by proteins that induce wall extension. Proc Natl Acad Sci U S A 91: 6574–6578
113. Mellerowicz EJ, Sundberg B (2008) Wood cell walls: biosynthesis, developmental dynamics and their implications for wood properties. Curr Opin Plant Biol 11:293–300
114. Mitchell RAC, Dupree P, Shewry PR (2007) A novel bioinformatics approach identifies candidate genes for the synthesis and feruloylation of arabinoxylan. Plant Physiol 144:43–53
115. Mitsuda N, Iwase A, Yamamoto H et al (2007) NAC transcription factors, NST1 and NST3, are key regulators of the formation of secondary walls in woody tissues of *Arabidopsis*. Plant Cell 19:270–280
116. Mitsuda N, Seki M, Shinozaki K et al (2005) The NAC transcription factors NST1 and NST2 of *Arabidopsis* regulate secondary wall thickenings and are required for anther dehiscence. Plant Cell 17:2993–3006
117. Mortimer J, Miles G, Brown D et al (2010) Absence of branches from xylan in *Arabidopsis gux* mutants reveals potential for simplification of lignocellulosic biomass. Proc Natl Acad Sci U S A 107:17409–17414
118. Mosier N, Wyman C, Dale B et al (2005) Features of promising technologies for pretreatment of lignocellulosic biomass. Bioresour Technol 96:673–686
119. Mouille G, Robin S, Lecomte M et al (2003) Classification and identification of *Arabidopsis* cell wall mutants using Fourier-transform infrared (FT-IR) microspectroscopy. Plant J 35:393–404
120. Nakashima J, Chen F, Jackson L et al (2008) Multi-site genetic modification of monolignol biosynthesis in alfalfa (*Medicago sativa*): effects on lignin composition in specific cell types. New Phytol 179:738–750
121. Nicol F, His I, Jauneau A et al (1998) A plasma membrane-bound putative endo-1,4-β-D-glucanase is required for normal wall assembly and cell elongation in *Arabidopsis*. EMBO J 17:5563–5576
122. Nishiyama Y, Langan P, Chanzy H (2002) Crystal structure and hydrogen-bonding system in cellulose 1β from synchrotron X-ray and neutron fiber diffraction. J Am Chem Soc 124:9074–9082
123. Nishiyama Y, Sugiyama J, Chanzy H et al (2003) Crystal structure and hydrogen bonding system in cellulose 1α from synchrotron X-ray and neutron fiber diffraction. J Am Chem Soc 125:14300–14306
124. National Science Foundation (2008) Breaking the chemical and engineering barriers to lignocellulosic biofuels: Next generation hydrocarbon biorefineries. In: Huber G (ed.) University of Massachusetts, Amherst, Washington, D.C.
125. Nühse TS, Stensballe A, Jensen ON et al (2004) Phosphoproteomics of the *Arabidopsis* plasma membrane and a new phosphorylation site database. Plant Cell 16:2394–2405
126. O'Connell A, Holt K, Piquemal J et al (2002) Improved paper pulp from plants with suppressed cinnamoyl-CoA reductase or cinnamyl alcohol dehydrogenase. Transgenic Res 11:495–503
127. O'Sullivan A (1997) Cellulose: the structure slowly unravels. Cellulose 4:173–207
128. Oraby H, Venkatesh B, Dale B et al (2007) Enhanced conversion of plant biomass into glucose using transgenic rice-produced endoglucanase for cellulosic ethanol. Transgenic Res 16:739–749
129. Pagant S, Bichet A, Sugimoto K et al (2002) KOBITO1 encodes a novel plasma membrane protein necessary for normal synthesis of cellulose during cell expansion in *Arabidopsis*. Plant Cell 14:2001–2013
130. Pan GX, Spencer L, Leary GJ (1999) Reactivity of ferulic acid and its derivatives toward hydrogen peroxide and peracetic acid. J Agric Food Chem 47:3325–3331
131. Paredez AR, Persson S, Ehrhardt DW et al (2008) Genetic evidence that cellulose synthase activity influences microtubule cortical array organization. Plant Physiol 147:1723–1734
132. Paredez AR, Somerville CR, Ehrhardt DW (2006) Visualization of cellulose synthase demonstrates functional association with microtubules. Science 312:1491–1495

133. Park J-Y, Canam T, Kang K-Y et al (2008) Over-expression of an *Arabidopsis* family A sucrose phosphate synthase (SPS) gene alters plant growth and fibre development. Transgenic Res 17:181–192
134. Pauly M, Keegstra K (2008) Cell-wall carbohydrates and their modification as a resource for biofuels. Plant J 54:559–568
135. Pear JR, Kawagoe Y, Schreckengost WE et al (1996) Higher plants contain homologs of the bacterial *celA* genes encoding the catalytic subunit of cellulose synthase. Proc Natl Acad Sci U S A 93:12637–12642
136. Pedersen JF, Vogel KP, Funnell DL (2005) Impact of reduced lignin on plant fitness. Crop Sci 45:812–819
137. Peña MJ, Zhong R, Zhou G-K et al (2007) *Arabidopsis irregular xylem8* and *irregular xylem9*: implications for the complexity of glucuronoxylan biosynthesis. Plant Cell 19:546–563
138. Persson S, Paredez A, Carroll A et al (2007) Genetic evidence for three unique components in primary cell-wall cellulose synthase complexes in *Arabidopsis*. Proc Natl Acad Sci U S A 104:15566–15571
139. Pieslinger AM, Hoepflinger MC, Tenhaken R (2010) Cloning of glucuronokinase from *Arabidopsis thaliana*, the last missing enzyme of the myo-inositol oxygenase pathway to nucleotide sugars. J Biol Chem 285:2902–2910
140. Piston F, Uauy C, Fu L et al (2010) Down-regulation of four putative arabinoxylan feruloyl transferase genes from family PF02458 reduces ester-linked ferulate content in rice cell walls. Planta 231:677–691
141. Porchia AC, Sørensen SO, Scheller HV (2002) Arabinoxylan biosynthesis in wheat. Characterization of arabinosyltransferase activity in golgi membranes. Plant Physiol 130:432–441
142. Pu Y, Jiang N, Ragauskas AJ (2007) Ionic liquid as a green solvent for lignin. J Wood Chem Technol 27:23–33
143. Qian X, Ding S-Y, Nimlos MR et al (2005) Atomic and electronic structures of molecular crystalline cellulose Iβ: a first-principles investigation. Macromolecules 38:10580–10589
144. Raes J, Rohde A, Christensen JH et al (2003) Genome-wide characterization of the lignification toolbox in *Arabidopsis*. Plant Physiol 133:1051–1071
145. Ragauskas AJ, Williams CK, Davison BH et al (2006) The path forward for biofuels and biomaterials. Science 311:484–489
146. Rajangam AS, Kumar M, Aspeborg H et al (2008) MAP20, a microtubule-associated protein in the secondary cell walls of hybrid aspen, is a target of the cellulose synthesis inhibitor 2,6-dichlorobenzonitrile. Plant Physiol 148:1283–1294
147. Ralph J, Akiyama T, Kim H et al (2006) Effects of coumarate 3-hydroxylase down-regulation on lignin structure. J Biol Chem 281:8843–8853
148. Ralph J, Kim H, Lu F et al (2008) Identification of the structure and origin of a thioacidolysis marker compound for ferulic acid incorporation into angiosperm lignins (and an indicator for cinnamoyl CoA reductase deficiency). Plant J 53:368–379
149. Ralph J, Lundquist K, Brunow G et al (2004) Lignins: natural polymers from oxidative coupling of 4-hydroxyphenylpropanoids. Phytochem Rev 3:29–60
150. Ransom C, Balan V, Biswas G et al (2007) Heterologous *Acidothermus cellulolyticus* 1,4-β-endoglucanase E1 produced within the corn biomass converts corn stover into glucose. Appl Biochem Biotechnol 137–140:207–219
151. Reddy MSS, Chen F, Shadle G et al (2005) Targeted down-regulation of cytochrome P450 enzymes for forage quality improvement in alfalfa (*Medicago sativa* L.). Proc Natl Acad Sci U S A 102:16573–16578
152. Regalbuto JR (2009) Cellulosic biofuels—got gasoline? Science 325:822–824
153. Richmond T (2000) Higher plant cellulose synthases. Genome Biol 1:30011–30016
154. Rippert P, Puyaubert J, Grisollet D et al (2009) Tyrosine and phenylalanine are synthesized within the plastids in *Arabidopsis*. Plant Physiol 149:1251–1260

155. Roudier F, Fernandez AG, Fujita M et al (2005) COBRA, an *Arabidopsis* extracellular glycosyl-phosphatidyl inositol-anchored protein, specifically controls highly anisotropic expansion through its involvement in cellulose microfibril orientation. Plant Cell 17:1749–1763
156. Saloheimo M, Paloheimo M, Hakola S et al (2002) Swollenin, a *Trichoderma reesei* protein with sequence similarity to the plant expansins, exhibits disruption activity on cellulosic materials. Eur J Biochem 269:4202–4211
157. Sato S, Kato T, Kakegawa K et al (2001) Role of the putative membrane-bound endo-1-4-beta-glucanase KORRIGAN in cell elongation and cellulose synthesis in *Arabidopsis thaliana*. Plant Cell Physiol 42:251–263
158. Scheible W-R, Eshed R, Richmond T et al (2001) Modifications of cellulose synthase confer resistance to isoxaben and thiazolidinone herbicides in *Arabidopsis Ixr1* mutants. Proc Natl Acad Sci U S A 98:10079–10084
159. Scheible W-R, Pauly M (2004) Glycosyltransferases and cell wall biosynthesis: novel players and insights. Curr Opin Plant Biol 7:285–295
160. Scheller HV, Ulvskov P (2010) Hemicelluloses. Annu Rev Plant Biol 61:263–289
161. Schindelman G, Morikami A, Jung J et al (2001) COBRA encodes a putative GPI-anchored protein, which is polarly localized and necessary for oriented cell expansion in *Arabidopsis*. Genes Dev 15:1115–1127
162. Seifert GJ (2004) Nucleotide sugar interconversions and cell wall biosynthesis: how to bring the inside to the outside. Curr Opin Plant Biol 7:277–284
163. Shani Z, Dekel M, Tsabary G et al (2004) Growth enhancement of transgenic poplar plants by overexpression of *Arabidopsis thaliana* endo-1,4-β-glucanase (cel1). Mol Breed 14:321–330
164. Shen H, Yin Y, Chen F et al (2009) A bioinformatic analysis of NAC genes for plant cell wall development in relation to lignocellulosic bioenergy production. BioEnergy Res 2:217–232
165. Shoseyov O, Shani Z, Levy I (2006) Carbohydrate binding modules: biochemical properties and novel applications. Microbiol Mol Biol Rev 70:283–295
166. Singh S, Fischer U, Singh M et al (2008) Insight into the early steps of root hair formation revealed by the *procuste1* cellulose synthase mutant of *Arabidopsis thaliana*. BMC Plant Biol 8:57
167. Smidansky E, Martin J, Hannah C et al (2003) Seed yield and plant biomass increases in rice are conferred by deregulation of endosperm ADP-glucose pyrophosphorylase. Planta 216:656–664
168. Smith AM, Stitt M (2007) Coordination of carbon supply and plant growth. Plant Cell Environ 30:1126–1149
169. Sørensen A, Teller PJ, Hilstrøm T et al (2008) Hydrolysis of *Miscanthus* for bioethanol production using dilute acid presoaking combined with wet explosion pre-treatment and enzymatic treatment. Bioresour Technol 99:6602–6607
170. Sticklen MB (2008) Plant genetic engineering for biofuel production: towards affordable cellulosic ethanol. Nat Rev Genet 9:433–443
171. Stokstad E (2006) GENOMICS: poplar tree sequence yields genome double take. Science 313:1556a
172. Stork J, Harris D, Griffiths J et al (2010) CELLULOSE SYNTHASE9 serves a nonredundant role in secondary cell wall synthesis in *Arabidopsis* epidermal testa cells. Plant Physiol 153:580–589
173. Stork J, Montross M, Smith R et al (2009) Regional examination shows potential for native feedstock options for cellulosic biofuel production. Glob Chang Biol Bioenergy 1:230–239
174. Sturcová A, His I, Apperley DC et al (2004) Structural details of crystalline cellulose from higher plants. Biomacromolecules 5:1333–1339
175. Sullivan JT (1955) Cellulose and lignin in forage grasses and their digestion coefficients. J Anim Sci 14:710–717
176. Szyjanowicz PMJ, McKinnon I, Taylor NG et al (2004) The *irregular xylem 2* mutant is an allele of *korrigan* that affects the secondary cell wall of *Arabidopsis thaliana*. Plant J 37:730–740

177. Tan H, Yang R, Sun W et al (2009) Peroxide-acetic acid pretreatment to remove bagasse lignin prior to enzymatic hydrolysis. Ind Eng Chem Res 49:1473–1479
178. Tanaka K, Murata K, Yamazaki M et al (2003) Three distinct rice cellulose synthase catalytic subunit genes required for cellulose synthesis in the secondary wall. Plant Physiol 133:73–83
179. Taylor NG (2007) Identification of cellulose synthase AtCesA7 (IRX3) in vivo phosphorylation sites—a potential role in regulating protein degradation. Plant Mol Biol 64:161–171
180. Taylor NG, Gardiner JC, Whiteman R et al (2004) Cellulose synthesis in the *Arabidopsis* secondary cell wall. Cellulose 11:329–338
181. Taylor NG, Howells RM, Huttly AK et al (2003) Interactions among three distinct CesA proteins essential for cellulose synthesis. Proc Natl Acad Sci U S A 100:1450–1455
182. Taylor NG, Laurie S, Turner SR (2000) Multiple cellulose synthase catalytic subunits are required for cellulose synthesis in *Arabidopsis*. Plant Cell 12:2529–2540
183. Taylor NG, Scheible WR, Cutler S (1999) The *irregular xylem3* locus of *Arabidopsis* encodes a cellulose synthase required for secondary cell wall synthesis. Plant Cell 11:769–779
184. Teymouri F, Alizadeh H, Laureano-Pérez L et al (2004) Effects of ammonia fiber explosion treatment on activity of endoglucanase from *Acidothermus cellulolyticus* in transgenic plant. Appl Biochem Biotechnol 116:1183–1191
185. Triplett B, Timpa J (1995) Characterization of cell-wall polymers from cotton ovule culture fiber cells by gel permeation chromatography. In Vitro Cell Dev Biol Plant 31:171–175
186. Turner SR, Somerville CR (1997) Collapsed xylem phenotype of *Arabidopsis* identifies mutants deficient in cellulose deposition in the secondary cell wall. Plant Cell 9:689–701
187. Urbanowicz BR, Catalá C, Irwin D et al (2007) A tomato endo-β-1,4-glucanase, SlCel9C1, represents a distinct subclass with a new family of carbohydrate binding modules (CBM49). J Biol Chem 282:12066–12074
188. Vanholme R, Demedts B, Morreel K et al (2010) Lignin biosynthesis and structure. Plant Physiol 153:895–905
189. Vergara CE, Carpita NC (2001) Beta-d-glycan synthases and the CesA gene family: lessons to be learned from the mixed-linkage (1 -> 3), (1 -> 4) beta-d-glucan synthase. Plant Mol Biol 47:145–160
190. Vermerris W, Saballos A, Ejeta G et al (2007) Molecular breeding to enhance ethanol production from corn and sorghum stover. Crop Sci 47:S142–S153
191. Wagner TA, Kohorn BD (2001) Wall-associated kinases are expressed throughout plant development and are required for cell expansion. Plant Cell 13:303–318
192. Wang J, Howles PA, Cork AH et al (2006) Chimeric proteins suggest that the catalytic and/or C-terminal domains give CesA1 and CesA3 access to their specific sites in the cellulose synthase of primary walls. Plant Physiol 142:685–695
193. Webb M, Jouannic S, Foreman J et al (2002) Cell specification in the *Arabidopsis* root epidermis requires the activity of *ECTOPIC ROOT HAIR 3*—a katanin-p60 protein. Development 129:123–131
194. Weng J-K, Li X, Stout J et al (2008) Independent origins of syringyl lignin in vascular plants. Proc Natl Acad Sci U S A 105:7887–7892
195. Williamson RE, Burn JE, Birch R et al (2001) Morphology of a cellulose-deficient mutant of *Arabidopsis thaliana*. Protoplasma 215:116–127
196. Wu A-M, Hörnblad E, Voxeur A et al (2010) Analysis of the *Arabidopsis IRX9*/*IRX9-L* and *IRX14*/*IRX14-L* pairs of glycosyltransferase genes reveals critical contributions to biosynthesis of the hemicellulose glucuronoxylan. Plant Physiol 153:542–554
197. Wu A-M, Rihouey C, Seveno M et al (2009) The *Arabidopsis* IRX10 and IRX10-LIKE glycosyltransferases are critical for glucuronoxylan biosynthesis during secondary cell wall formation. Plant J 57:718–731
198. Yang C, Xu Z, Song J et al (2007) *Arabidopsis* MYB26/MALE STERILE35 regulates secondary thickening in the endothecium and is essential for anther dehiscence. Plant Cell 19:534–548

199. Yu J, Hu S, Wang J et al (2002) A draft sequence of the rice genome (*Oryza sativa* L. ssp. indica). Science 296:79–92
200. Zakzeski J, Bruijnincx PCA, Jongerius AL et al (2010) The catalytic valorization of lignin for the production of renewable chemicals. Chem Rev 110:3552–3599
201. Zeng W, Chatterjee M, Faik A (2008) UDP-Xylose-stimulated glucuronyltransferase activity in wheat microsomal membranes: characterization and role in glucurono(arabino)xylan biosynthesis. Plant Physiol 147:78–91
202. Zhang YHP, Lynd LR (2004) Toward an aggregated understanding of enzymatic hydrolysis of cellulose: noncomplexed cellulase systems. Biotechnol Bioeng 88:797–824
203. Zhong R, Burk DH, Morrison WH III et al (2002) A kinesin-like protein is essential for oriented deposition of cellulose microfibrils and cell wall strength. Plant Cell 14:3101–3117
204. Zhong R, Demura T, Ye Z-H (2006) SND1, a NAC domain transcription factor, is a key regulator of secondary wall synthesis in fibers of *Arabidopsis*. Plant Cell 18:3158–3170
205. Zhong R, Kays SJ, Schroeder BP et al (2002) Mutation of a chitinase-like gene causes ectopic deposition of lignin, aberrant cell shapes, and overproduction of ethylene. Plant Cell 14:165–179
206. Zhong R, Morrison WH III, Freshour GD et al (2003) Expression of a mutant form of cellulose synthase AtCesA7 causes dominant negative effect on cellulose biosynthesis. Plant Physiol 132:786–795
207. Zhong R, Peña MJ, Zhou G-K et al (2005) *Arabidopsis Fragile Fiber8*, which encodes a putative glucuronyltransferase, is essential for normal secondary wall synthesis. Plant Cell 17:3390–3408
208. Zhong R, Richardson EA, Ye ZH (2007) The MYB46 transcription factor is a direct target of SND1 and regulates secondary wall biosynthesis in *Arabidopsis*. Plant Cell 19:2776–2792
209. Zhong R, Richardson EA, Ye ZH (2007) Two NAC domain transcription factors, SND1 and NST1, function redundantly in regulation of secondary wall synthesis in fibers of *Arabidopsis*. Planta 225:1603–1611
210. Zhong R, Ye Z-H (2007) Regulation of cell wall biosynthesis. Curr Opin Plant Biol 10:564–572
211. Zhou J, Lee C, Zhong R et al (2009) MYB58 and MYB63 are transcriptional activators of the lignin biosynthetic pathway during secondary cell wall formation in *Arabidopsis*. Plant Cell 21:248–266
212. Zhou Q, Baumann MJ, Piispanen PS et al (2006) Xyloglucan and xyloglucan endo-transglycosylases (XET): tools for ex vivo cellulose surface modification. Biocatal Biotransform 24:107–120
213. Zhou Q, Greffe L, Baumann MJ et al (2005) The use of xyloglucan as a molecular anchor for the elaboration of polymers from cellulose surfaces: a general route for the design of biocomposites. Macromolecules 38:3547–3549
214. Zhou Q, Rutland MW, Teeri TT et al (2007) Xyloglucan in cellulose modification. Cellulose 14:625–641
215. Ziegelhoffer T, Raasch JA, Austin-Phillips S (2001) Dramatic effects of truncation and sub-cellular targeting on the accumulation of recombinant microbial cellulase in tobacco. Mol Breed 8:147–158
216. Ziegler MT, Thomas SR, Danna KJ (2000) Accumulation of a thermostable endo-1,4-β-D-glucanase in the apoplast of *Arabidopsis thaliana* leaves. Mol Breed 6:37–46
217. Zuo J, Niu Q-W, Nishizawa N et al (2000) KORRIGAN, an *Arabidopsis* endo-1,4-β-glucanase, localizes to the cell plate by polarized targeting and is essential for cytokinesis. Plant Cell 12:1137–1152

Chapter 18
Genetic Modifications of Plant Cell Walls to Increase Biomass and Bioethanol Production

M. Abramson, O. Shoseyov, S. Hirsch, and Z. Shani

Abstract To date, most ethanolic fuel is generated from "first generation" crop feedstocks by conversion of soluble sugars and starch to bioethanol. However, these crops exploit land resources required for production of food. On the other hand, utilization of "second generation" lignocellulosic biofuels derived from the inedible parts of plants remains problematic as high energy inputs and harsh conditions are required to break down the composite cell walls into fermentable sugars. This chapter reviews and discusses genetic engineering approaches for the generation of plants modified to increase cellulose synthesis, enhance plant growth rates, cell wall porosity and solubility, as well as improve cell wall sugar yields following enzymatic hydrolysis. Strategies focusing on increased accessibility of cellulose-degrading enzymes to their substrates have been developed. These approaches reduce cell wall crystallinity or alter the hemicellulose–lignin complexes. A novel approach to cell wall modification involving the introduction of noncrystalline, soluble polysaccharides into cell walls is also presented. The use of such approaches may promote and accelerate the future use of lignocellulosic feedstocks for the bioethanol industry.

M. Abramson
The Robert H. Smith Institute of Plant Sciences and Genetics in Agriculture, and The Otto Warburg Minerva Center for Agricultural Biotechnology, Faculty of Agricultural, Food and Environmental Quality Sciences, The Hebrew University of Jerusalem, P.O. Box 12, Rehovot 76100, Israel

FuturaGene Ltd., 2 Pekeris Street, P.O. Box 199, Rehovot 76100, Israel

O. Shoseyov
The Robert H. Smith Institute of Plant Sciences and Genetics in Agriculture, and The Otto Warburg Minerva Center for Agricultural Biotechnology, Faculty of Agricultural, Food and Environmental Quality Sciences, The Hebrew University of Jerusalem, P.O. Box 12, Rehovot 76100, Israel

S. Hirsch • Z. Shani (✉)
FuturaGene Ltd., 2 Pekeris Street, P.O. Box 199, Rehovot 76100, Israel
e-mail: ziv@futuragene.com

J.W. Lee (ed.), *Advanced Biofuels and Bioproducts*, DOI 10.1007/978-1-4614-3348-4_18,

Abbreviations

CBD	Cellulose binding domain
CBM	Cellulose binding module
CDH	Cellobiose dehydrogenase
CesA	Cellulose synthase
FAE	Ferulic acid esterase
GX	Glucuronoxylan
HG	Homogalacturonan
PME	Pectin methylesterase
PMEi	Pectin methylesterase inhibitor
QTL	Quantitative trait locus
RGI	Rhamanogalacturonan I
SPS	Sucrose phosphate synthase
SuSy	Sucrose synthase
UGPase	UDP-glucose pyrophosphorylase

1 Introduction: The Increasing Importance of Lignocellulosic Biomass

Meeting the growing demands for energy supply while simultaneously promoting sustainable development is one of the greatest challenges facing humanity today. Many strategies and technologies have been proposed to offer alternative energy sources, but no ultimate solution has been developed thus far.

Paradoxically, prior to the development of the almost total dependency on fossil fuels, conversion of biomass to energy provided a means of heating, illumination, and cooking for centuries. The plant is a cheap, highly efficient energy generator as it converts light energy to simple sugars through photosynthesis and CO_2 fixation. Combustible and highly energetic polymers are then formed from these sugars, and generate a composite lignocellulosic secondary cell wall constituted of cellulose, hemicellulose, and lignin [102].

To date, most ethanol fuels have been generated from corn grain or sugarcane, often referred to as “first generation” biofuels. However, bioconversion of such feedstocks to biofuels exploits land sources necessary for food production, diverts essential crops from the human food chain and increases the cost of human and animal feed [36]. “Second generation” or biomass-derived biofuels are extracted from inedible plant tissues or from inedible plants and support sustainable development by processing the residual structural biomass after the food portions have been removed. Cellulosic ethanol can thus be formed from a variety of sources, including woody materials, agricultural residue and specially cultivated grasses. Ultimately, lignocellulosic-derived ethanol has the potential to provide for the vast majority of

global transportation fuel needs, while only slightly impacting food supplies, in a more cost-effective manner and with less net carbon dioxide emission than that from fossil fuel combustion [36, 108].

The plant cell wall is a composite material that provides structural integrity to plants as well as protection from pathogen invasion. The polyphenolic lignin portion, whose proportion and character can vary significantly among feedstock sources [30], sterically hinders access of enzymes and chemicals that degrade hemicellulose and cellulose. In addition to the degree of lignification, the cellulose crystallinity and its degree of polymerization [78] contribute to the recalcitrance of lignocellulosic feedstock to saccharifying chemicals or enzymes. These composite factors contribute to the result that decomposition of plant cell wall polysaccharides into fermentable sugars is more complicated than breaking down purified starch or sucrose to fermentable sugars. Conversion of lignocellulosic biomass to bioethanol requires cell wall breakdown in a pretreatment stage to degrade lignin and release polysaccharides before the conversion of such lignocellulosic biomass to bioethanol. The pretreatment requires toxic solvents and high energy inputs (e.g. high temperatures and pressure). These steps are then followed by saccharification of cellulose and hemicellulose to simple sugars via hydrolysis, and the free sugars are then fermented to ethanol. Thus, the leading technological barrier to effective employment of lignocellulosic biomass as a source of fermentable sugars lies in the economic breakdown of the polysaccharide wall [37].

Commercial realization of biofuel production requires an integrated solution combining appropriate biofuel crops, biomass modification techniques, and sophisticated process engineering. The application of recent advances in plant genetic engineering, carbohydrate chemistry, and increased knowledge of plant cell wall ultrastructure will together allow reengineering crop cell walls, which in turn facilitates lowering of biomass saccharification and conversion costs, while significantly increasing biofuel production yields. This review discusses the most recent plant cell wall modification and plant engineering technologies designed to improve sugar yields upon enzymatic hydrolysis and to reduce energy demands and cost of the bioethanol production.

2 The Structural Diversity of Plant Cell Walls

Plant cell walls are composed of several distinct chemical polymers arranged as a composite network. Their structural rigidity minimizes water loss and protects against various biotic and abiotic stresses. The plasticity of the plant cell wall allows cell elongation, plant growth and enables reorganization that accommodates environmental changes [18, 107, 120]. The construction and breakdown of the cell wall is complex, involving a large number of glycosyl synthases, hydrolytic and disruptive enzymes that act at different developmental stages in various cellular organelles. A thorough understanding of the synthesis and breakdown of the cell

wall will enable the development of techniques for effective manipulation of cell wall polymers for the production of biofuel. Recent reviews cover synthesis, composition, and remodeling of plant cell walls [18, 53, 105]; the fundamentals are outlined below.

The cell wall is generally divided into primary wall and secondary wall. Following cell division, the middle lamella and primary wall are formed. The primary wall determines the cell's shape and size and it basically consists of cellulose, hemicelluloses, pectin, structural proteins, and phenolic compounds. The amount and ratio between these components are highly depended on the primary wall type. While cellulose, or (1-4)-β-linked glucose, is the most abundant polysaccharide on earth, control of its biosynthesis is not completely understood. Cellulose synthesis occurs in the plasma membrane by hexagonal-shaped complexes termed rosettes, each containing 36 cellulose synthase modules (CesA) [3, 32]. A highly compact lattice of microfibrils is assembled and linked via hydrogen bonds that form crystalline cellulose. These microfibrils serve as a scaffold for the deposition of other wall components, such as hemicellulose and pectin [84, 119]. In contrast to cellulose, hemicellulose and pectin synthesis occurs in the Golgi bodies [94]. Hemicellulosic polysaccharides are complex and heterogeneous molecules which crosslink neighboring cellulose microfibrils. Cell walls of dicots or type I primary walls consist of equal amounts of xyloglucans and cellulose that are embedded in a rich pectin matrix and are further crosslinked with structural proteins. On the other hand, type II walls or cell walls of poaceae (grasses) and gymnosperms contain arabinoxylan instead of xyloglucan. Moreover, this kind of wall does not contain large amounts of pectin but contains phenolics that are crosslinked with arabinoxylan, thus strengthening the wall [18, 70, 90, 126].

Secondary wall deposition occurs in most plant cells and accounts for most of the cell wall mass. Secondary cell walls are composed of cellulose, hemicelluloses (mostly xylans), and lignin and include several layers that vary between species in the composition and ratio of components and in the arrangement of the cellulose microfibrils. The key differences between the secondary cell walls of distinct plant families lie in the quantity and nature of their hemicelluloses and Lignins. Lignins are the product of an oxidative combinatorial coupling of 4-hydroxyphenylpropanoids, principally involving the hydroxycinnamyl alcohols, coniferyl alcohol, sinapyl alcohol, and small amounts of *p*-coumaryl alcohol. These monolignols differ in their degree of aromatic methoxylation. Following coupling, the resulting units in the lignin polymer are the guaiacyl (G), syringyl (S), and *p*-hydroxyphenyl (H) units, respectively [100, 123, 124]. S lignin is unique to flowering plants while H and G lignins are fundamental to all vascular plants [131].

The hemicelluloses of poaceae and gymnosperms mainly comprises large amounts of glucuronoarabinoxylan (GAX) and galactoglucomannan in their secondary walls while woody angiosperms mostly contain glucuronoxylan (GX). GAX contains many arabinose residues which can be further esterified with ferulic acid. The hemicelluloses in the secondary wall are crosslinked with lignin and cellulose. The interactions of hemicelluloses with other components in the secondary cell wall is stronger than in the primary cell wall due to the presence of fewer side chains in

secondary wall hemicellulose [126]. In summary, cellulose crystallinity, degree of polymerization, hemicellulose species, and lignin content all influence cell wall resistance to enzymatic degradation and these constraints differ between different plant varieties.

3 Second-Generation Crops: Selection and Utilization

Extensive research has been performed to better understand the natural variability and chemical composition of potential biofuel feedstocks. Feedstocks for production of second-generation bioethanol include organic materials derived from herbaceous and woody energy crops, agricultural crop wastes and residues, wood wastes and residues, aquatic plants, and other waste materials, including some municipal wastes. The following section discusses the major lignocellulosic feedstock candidates for the bioethanol industry. To date, no feedstock has been branded as the "winner" source; each feedstock bears advantages alongside drawbacks. The authors are of the opinion that only integrated use of different feedstocks based on their geographic distribution can provide a sustainable solution. Figure 1 displays a lignocellulosic biomass to ethanol supply chain, from a dedicated feedstock grown in the field towards extracted polysaccharides that serve as the substrate for bioethanol production.

3.1 Straws and Stovers

Large portions of crop biomass is wasted during harvest, mostly in the form of straw that carries the grain [50]. This straw—from corn, barley, oat, rice, wheat, sorghum, and sugarcane are currently the major feedstocks used for second-generation biofuel production and yield nearly 1.5 billion tons of lignocellulosic biomass which can potentially provide up to 442 billion liters of bioethanol per year [67]. Seventeen years of research conducted by Gelfand et al. [45] potentially redefined the "food versus fuel" debate by concluding that growing grain for food and use of the residue stalks for biofuel is more energetically efficient than the use of grain for bioethanol. The cellulose, hemicelluloses, lignin, and ash content of some common straw feedstocks are presented in Table 1.

Relatively high percentages of lignin limit digestibility of residual biomass, while ash contains large amount of silica microparticles released at burning. Reduction of silica content in straw can enhance enzymatic digestibility, but may simultaneously reduce plant resistance to pathogens [50]. Thus, feedstock should be engineered to contain less silica while programming in alternative modes of disease resistance, such as genetic engineering or increased pesticide use.

Arabinoxylan is the major noncellulosic polysaccharide in cereals. It is composed of a xylose backbone with arabinose residues and contributes to the structural rigidity

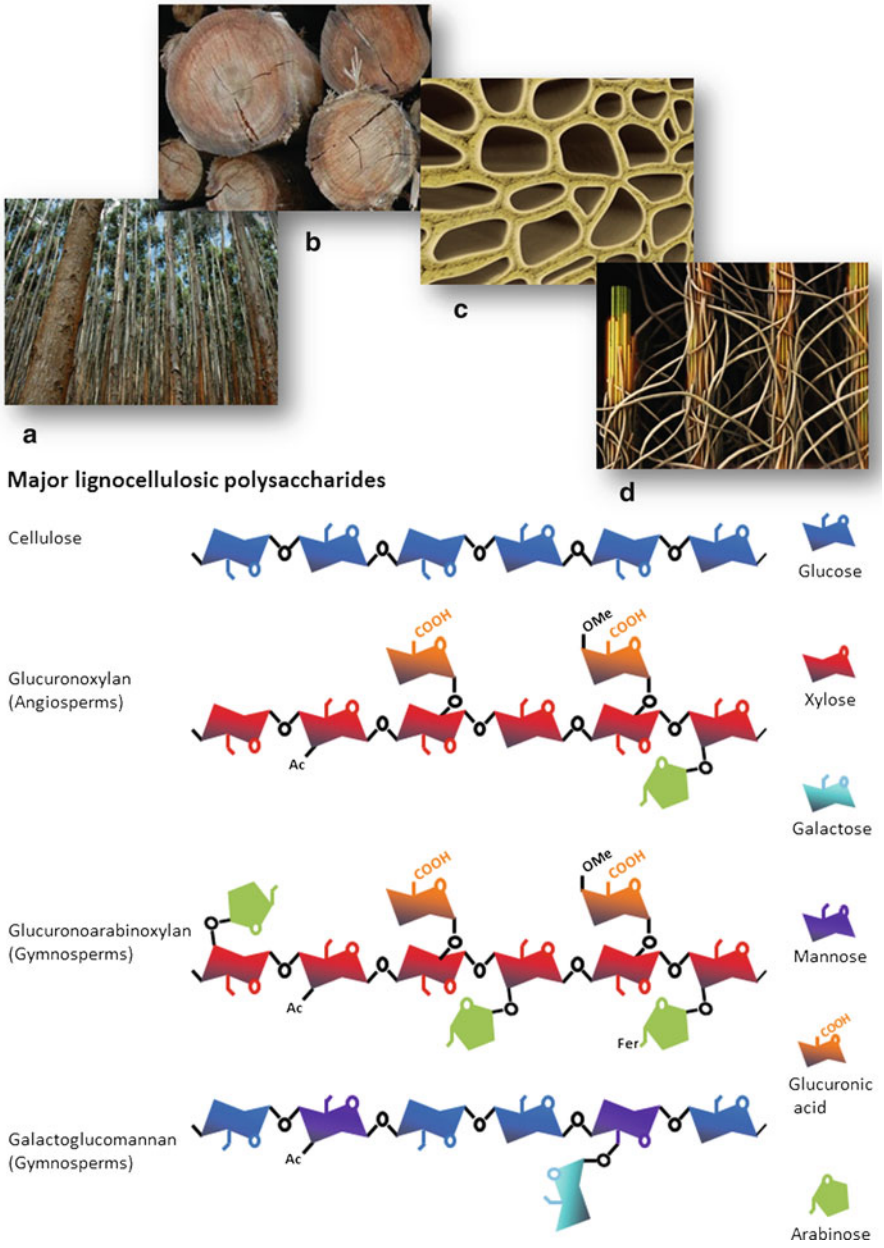

Fig. 1 From lignocellulosic feedstock to cell wall polysaccharides: dedicated forest (**a**), woody raw material prior to processing (**b**), cellular ultrastructure (**c**), and schematic organization of the polysaccharides inside the cell walls: cellulose—green and bright yellow strands; hemicelluloses—brown strands (**d**). Major lignocellulosic polysaccharides are represented *below the panel* pictures. "Fer" denotes esterification with ferulic acid

Table 1 Agricultural residues biomass chemical composition (% mass) [35]

	Cellulose (%)	Hemicellulose (%)	Total lignin (%)	Ash (%)
Corn stover	36	23	19	12
Sugarcane bagasse	39	23	24	5
Wheat straw	33	23	17	10

Table 2 Perennials biomass chemical composition (% mass) [35]

	Cellulose (%)	Hemicellulose (%)	Total lignin (%)	Ash (%)
Switchgrass	33	26	18	5
Miscanthus	42	27	13	3
Alfalfa	28	23	16	8
Tall fescue	25	19	13	11

of grass cell walls. Arabinoxylans can covalently bind ferulic acids and other phenolics [63], which in turn crosslink neighboring arabinoxylans and form ester bridges with lignin, hindering enzymatic degradation of polysaccharides.

3.2 Perennials and Forages: Switchgrass, Miscanthus, and Other Potential Crops

Forages and specially cultivated grasses are considered some of the prominent potential second-generation bioenergy crops and are the subject of intense research and discussion. The chief perennial feedstocks include switchgrass (*Panicum virgatum L.*), *Miscanthus giganteus* (*Miscanthus sinensis* × *Miscanthus sacchariflorus*), and alfalfa (*Medicago sativa* L.). Perennials require fewer agricultural resources and easily adapt to a range of environmental conditions when compared to first-generation grain crops [104]. The greatest advantages of switchgrass lies in its suitability to marginal and erosive lands and its responsiveness to nitrogen fertilization which can dramatically increase crop yields [83]. The cell wall composition of some of the perennial crops is presented in Table 2.

Miscanthus has the highest cellulose level when compared to other perennials and may result in higher ethanol yields, as ethanol production has been described to linearly increase with cellulose and hemicelluloses composition [62]. Furthermore, it has higher yields when compared to switchgrass [10, 57]. As with straws and stovers, perennials present the challenges of dealing with high lignin and ash content which lead to increased crop recalcitrance for saccharification. Conversion of switchgrass to fuel ethanol has been reported as less efficient than corn stover, wheat straw, and even wood residues [134]. Thus, the utilization of specially cultivated perennials may be advantageous only in marginal lands.

3.3 Woody Biomass Feedstocks

Apart from its significant economical value, wood can serve as a strategic option for improved energy security, particularly in countries with expansive forest areas. In some countries, bioethanol is already produced from wood in addition to fossil fuel. Several biorefineries utilize wood residue and waste to produce their own energy [25].

Sources of woody materials include residue left in natural forest, where 80–90% of such residues can be channeled to energy generation [39]. Specially cultivated short rotation energy forest plantations include several fast growing eucalyptus and poplar species. The world's total forest area has been estimated at four billion hectares in 2010, corresponding to 31% of the land area [40]. However, the availability of wood, and thus its potential as a biofuel, is unevenly distributed throughout the world. The Russian Federation, Brazil, Canada, the USA, and China are the five most forest-rich countries and account for more than half of the total forest area worldwide [40]. In the USA alone, forest lands can supply approximately 368 million dry tons of biomass annually. Forest-based biomass feedstock can be nearly doubled compared to the current supply by maximizing unexploited removals and residues [93]. A study correlating the chemical composition and ethanol production of five feedstock candidates demonstrated a higher ethanol production potential in aspen wood when compared to switchgrass, hybrid poplar and corn stover [62]. The authors concluded that ethanol production potential is highly correlated with cellulose and hemicelluloses composition.

The cell wall composition of common wood feedstocks is summarized in Table 3. The differences between the cell wall composition of hardwoods and softwoods lie mainly in the proportion and type of lignin and hemicelluloses. Softwoods possess a higher proportion of lignin, composed of only two monolignol building blocks as compared to the three found in hardwoods, rendering softwoods one of the most difficult feedstocks to hydrolyze [76]. Galactoglucomannans and arabinoglucuronoxylan are the major hemicellulosics of softwood. In contrast, hardwoods contain mostly glucuronoxylan and glucomannans. As in other feedstocks, wood recalcitrance to saccharification is highly influenced by the degree of lignin content. In addition, hemicellulosic branching and modification significantly influence wood resistance to cell wall degradation. Acetylation of glucuronoxylan in hardwoods or

Table 3 Wood biomass chemical composition (% mass) [35, 95]

	Cellulose (%)	Hemicellulose (%)	Total lignin (%)	Ash (%)
Hardwoods				
Aspen [62]	53	27	19	1
Hybrid poplar (DN-34) [35]	42	19	25	1
Eucalyptus urophylla [95]	53	19	24	0.4
Softwoods				
Norway spruce [95]	43	21	29	1
Douglas fir [95]	44	21	32	0.4

galactoglucomannans in softwood limits hemicellulose solubility. Uronic acids and arabinose linked to hemicelluloses can form bonds between neighboring hemicelluloses and ester bridges between hemicelluloses and lignin [97]. The completion of the sequencing of the eucalyptus and poplar genomes, including quantitative trait locus (QTL) mapping and the identification of specific genes will assist in breeding and generation of specialized eucalyptus and poplar hybrid clones with traits ideal for biofuel production [47, 106]. Nevertheless, many issues must be addressed before woody feedstocks can be used for large-scale liquid biofuel generation. The next section discusses cell wall modification by means of biotechnological tools in efforts to meet the need for higher sugar yields and biomass per unit of land and increased polysaccharide accessibility without jeopardizing essential crop traits.

4 Polysaccharide Modifications to Improve Lignocellulose Processability

4.1 Primary Wall Modification: Yield, Growth, and Porosity

The primary cell wall allows the plant to expand and elongate while maintaining mechanical strength and support. Elongation rates and cell size and shape are largely governed by primary wall plasticity and cell–cell adhesions. Thus, the primary wall has a direct impact on plant yield. Hence, growth zones are rich in modifying enzymes such as cellulases, xylanases, xyloglucanases and pectin modifying enzymes that allow cell expansion [81].

4.1.1 Cell Wall Modulation and Increased Plant Biomass via Overexpression of Glycoside Hydrolases

Plants synthesize an extensive family of glycoside hydrolases termed endoglucanases. Some are secreted to the extracellular matrix during growth and some form part of the cellulose synthase complex. Endoglucanases are naturally involved in the process of plant cell wall development and degradability. These enzymes are capable of hydrolyzing noncrystalline cellulose and xyloglucans, enabling xyloglucan–cellulose matrix remodeling and cell wall plasticity during growth and development via wall loosening [18, 113]. The *Arabidopsis* endo-(1-4)-β-glucanase protein (Cel1) accumulates in young, expanding tissues, playing a key role in cell elongation of rapidly growing tissues [109–112]. Heterologous overexpression of *cel1* in poplar trees or of poplar endoglocanase (*PaPopCel1*) in *Arabidopsis* resulted in longer internodes, increased cell elongation, and subsequent biomass accumulation [89, 111]. Mechanical analysis, studying leaf blade extension at constant load and breakage at changing load was conducted. An elongation vs. load curve demonstrated higher elongation rates in transgenic *Arabidopsis* leaf blades when compared to

wild type [89]. As highly crosslinked materials are more resistant to elongation under specific load, it is speculated that the cell wall of these transgenic plants contained less crosslinked material [89]. It is proposed that noncrystalline glucan chains intercalated with hemicelluloses are unraveled by endoglucanases, lowering the amount of tethered xyloglucans, ultimately increasing cell wall plasticity and allowing for continued cell wall deposition [56]. Similar results were obtained upon expression of *Aspergillus niger* xyloglucanase in poplar trees. Both stem length and cellulose content increased, but at the same time, the growth zone had reduced Young's elastic modulus [88]. Furthermore, when plants were placed horizontally, the basal regions of stems of these transgenic poplars failed to bend upward due to lower tensile strength in newly formed wood [6].

Overexpression of poplar endoglucanase *PaPopCel1* in the leguminous tropical tree *Paraserianthes falcataria*, resulted in increased biomass. Disturbance of the biological clock by altering the closing movements of the leaves was also detected [55]. Thus in summary, overexpression of endoglucanases can accelerate growth, but may also result in undesirable effects. Maximal benefits may be achieved by using specific promoters for targeting the gene product to specific organs or for restricting expression to specific developmental stages.

4.1.2 CBM Expression to Enhance Cell Wall Biosynthesis

Cellulose binding modules (CBMs) are noncatalytic modules that induce surface disruption of cellulose fibers [34] as they adsorb to accessible sites on cellulose substrates to form a complex held together by specific, noncovalent, thermodynamically preferred bonds [2, 75]. CBMs include bacterial and fungal cellulose binding domains (CBDs), expansins, and swolenins. All CBMs share highly similar structure and function [116]. Expansins are plant cell wall proteins involved in the extension and loosening of the plant cell wall, promoting plant growth and expansion [29]. Swollenins, originating from the cellulose-degrading fungus *Trichoderma reesei*, are CBMs that share sequence homology with expansin-like proteins and effectively disrupt cellulosic materials [21].

Plant growth and biomass can be increased by bacterial CBMs transgenically expressed in the cell wall [116], where the postulated mechanism is based on separation of cellulose-biosynthesis polymerization and crystallization steps [71]. This separation may result in more flexible cellulose microfibrils that consequently increase cellulose synthesis rates in the presence of CBMs. The first observations of enhanced elongation followed in vitro addition of low concentrations of exogenous bacterial CBM to peach pollen tubes and *Arabidopsis* seedlings [71, 117]. The cellulose generated in the presence of the CBM resembled the loose ribbon-like appearance of newly formed fibrils, as opposed to the well-arranged ribbons of control fibers formed in the absence of excess CBM [117]. Accelerated cell and plant growth has also been observed in transgenic tobacco, poplar, and potato plants expressing a cell wall-targeted *Clostridium cellulovorans* CBM [71, 103, 114, 115].

The xyloglucan–cellulose matrix of the primary wall must be loosened for cell expansion to occur [28]. Part of the expansion or fragmentation of cellulose microfibrils is due to expansin activity [30], often upregulated in growing tissues [23, 66, 127]. Expansins cause wall loosening in vitro [80] and are correlated with growth promotion in vivo [41]. Targeted expansin expression in transgenic *Arabidopsis* [22], rice [24], and poplar plants [49] resulted in enhanced growth rates. Most of the transgenic plants described above had fairly low expression levels of the nonnative bacterial CBMs or expansins. In contrast, high level expression of different CBMs resulted in retarded stem elongation and reduced mechanical properties in term of extensibility vs. constant load as well as collapsed stems [86, 101]. These results corroborate the first reported attempt to apply exogenous bacterial CBM to germinated *Arabidopsis* seedlings. At low concentrations, CBM enhanced root elongation, whereas higher concentrations inhibited the process in a dose-dependent manner [117].

The role of CBM expression in increased plant growth rates bears profound potential in yield enhancement challenges and can be utilized through genetic engineering with almost all biofuel feedstocks. Ectopic CBMs and/or glycoside hydrolase expression can change the carbon partitioning between source and sink tissues by creation of stronger sinks in cellulose synthesizing cells, leading to enhanced growth, biomass, and yield.

4.1.3 Pectic Polysaccharide Modification to Modulate Porosity and Solubility

Pectins are heterogeneous mixtures of polysaccharides that account for 10–20% of the primary walls of plants and play a major role in cell wall adhesion, porosity, structural integrity, and environmental response, especially in dicots. Homogalacturonan (HG), a polymer of D-galacturonic acid, and rhamnogalacturonan I (RGI), a branched heteropolymer containing a backbone of L-rhamnose and D-galacturonic acid with side chains of galactan, arabinan, and arabinogalactan, are the two most abundant pectic polysaccharides [17]. Cell wall porosity [8], plasticity [38], and cell–cell adhesion [132] are reported to be largely controlled by the composition and intermolecular bonds of the pectin matrix.

HG is synthesized and secreted in a highly methyl-esterified form and is de-esterified in the cell wall by pectin methylesterases (PMEs). PME-driven modification of pectin can increase cell wall rigidity by affecting the number of calcium bridges between pectin molecules [82]. PMEs are generally categorized as "linear (blockwise) de-methylesterifying" enzymes that promote calcium bridges or as "random (non-blockwise) de-methylesterifying" enzymes that induce pectinase activity [82]. Suppression of the "blockwise" PME gene in poplar stimulated fiber elongation and vessel elements [92]. In contrast, overexpression of the same PME gene in potato plants resulted in enhanced growth compared to control [96].

Methylesterification levels can also be modified by the use of PME inhibitors (PMEi). PMEi are proteins produced by plants that are capable of forming complexes

with plant PME and inhibit its activity in this manner [33]. Reduction of de-methyl-esterified HG levels in *Arabidopsis* plants expressing PMEi increased plant growth rate and efficiency of enzymatic saccharification, thus potentially minimizing the need for pretreatment for polysaccharide release [74].

The galactan, arabinan, and arabinogalactan side chains on RGI are proposed to regulate cell wall porosity by filling wall gaps [125]. Therefore, we suggest that reduction or modification of RGI side chains may result in a more porous cell wall structure, a process that could be achieved by targeted expression of the galactanases, arabinases, and α-L-arabinofuranosidase. Similarly, we postulate that de-acetylation of pectins may also lead to increased cell wall porosity and solubility as O-acetylation of pectin has often been associated with inhibition of enzymatic breakdown of polysaccharides and decreased polysaccharide solubility [91].

4.1.4 Manipulation of Sucrose Metabolism to Increase Cellulose Synthesis

Manipulation of the source-sink relationship provides us with an additional approach for growth enhancement, where increased sink potency can result in enhanced growth rates. Sucrose synthase (SuSy), sucrose phosphate synthase (SPS), invertase, UDP-glucose pyrophosphorylase (UGPase), and CesA complexes can each act as rate-limiting factors for carbon allocation towards cellulose synthesis [52].

UDP-glucose is the direct substrate for cellulose synthesis. SuSy catalyses the cleavage of sucrose to yield fructose and UDP-glucose which is then channeled to the CesA complex [32]. Increasing levels of UDP-glucose should increase cellulose synthesis rates and consequently stimulate photo-assimilation and biomass accumulation. The manipulation of enzymes that are involved in UDP-glucose metabolism for increased cellulose synthesis is described in the following examples. Invertase catalyses the cleavage of sucrose to glucose and fructose and enhances the UDP-glucose levels by elevating glucose levels inside the cell [52]. Furthermore, SPS recycles fructose to generate sucrose phosphate and acts in conjunction with sucrose phosphate phosphatase to provide a constant substrate for SuSy [52]. The resultant decreased cytoplasmic fructose concentrations also promote SuSy activity, by preventing product inhibition of SuSy [44]. Heterologous expression of invertase in tobacco plants resulted in a significant increase in biomass and more specifically of cellulose content [15]. Moreover, SPS overexpression led to enhanced plant growth, biomass accumulation, and fiber elongation in tobacco plants [87]. UGPase also increases UDP-glucose concentration. Transgenic tobacco plants simultaneously overexpressing *UGPase*, *SuSy*, and *SPS* demonstrated up to a 50% increase in growth rate compared to controls. [26].

4.2 *Secondary Wall Modification for Improved Processability and Enzyme Accessibility*

4.2.1 Genetic Manipulation of Cellulose Characteristics

One of the central aims of cell wall scientists today is to find a formula for manipulating cellulose polymer structure without impairing plant growth. It has been proposed that altering the degree of crystallization and polymerization in the cell wall can result in cellulose polymers more responsive to hydrolysis [60]. The highly organized crystalline domains of the cell walls are interrupted with less crystalline, "amorphous" regions. There is an inverse correlation between the degree of cellulose crystallinity and the initial rate of cellulose hydrolysis [64]. At least three CesA genes are required for assembly and function of a single cellulose synthase complex [119]. Genes, such as *CesA* and korrigan (*kor*), the membrane-localized β-1,4-glucanase, are directly involved in cellulose synthesis and modification [65, 85]. The *Arabidopsis* mutant *ixr1-2*, which bears a mutation within the conserved C-terminal transmembrane region of CesA3, has lower cellulose crystallinity. The cell walls of the transgenic plants had higher conversion rates to fermentable sugars than wild type, with only a slight decrease in growth rate [54]. It is suggested that the generation of the same amino acid change in CesA subunits (CesA4, 7 and 8) that modify the secondary cell wall may further increase the efficiency of biomass conversion in biofuel feedstocks [54].

Korrigan is part of the cellulose synthase complex and is a key membrane-bound endoglucanase required for cellulose biosynthesis [119]. Korrigan is believed to cleave stacking glucan chains of microfibrils at the beginning of their synthesis. In this way, it promotes accurate synthesis [122]. Overexpression of *Arabidopsis* korrigan (*AtKOR*) in hybrid poplar resulted in reduced crystallinity without any significant effect on cell wall composition and plant growth [77].

Cellulose crystalline structure can be further modified post-synthesis in the cell wall. For example, the extracellular fungal enzyme, cellobiose dehydrogenase (CDH) [136], enhances cellulose degradation in the presence of cellulase mixtures directly [7] by preventing recondensation of glycosidic bonds of cellulose chains nicked by endoglucanases [5], or indirectly by generating hydroxyl radicals in a Fenton type reaction [58]. CDH binding to cellulose is highly specific [59] and can lead to oxidation of highly crystalline as well as amorphous cellulose [16]. We hypothesized that the expression of CDH in plants cell walls can result in the disruption of the microcrystalline lattice through the modification of cellobiose to cellobiono-(1,5)-lactone via reduction of hydrogen bonds responsible for the highly crystalline structure of cellulose [1]. It is still unclear if and how plant fitness and growth are affected by reductions in cellulose crystallinity.

4.2.2 Modification of Hemicellulosic Polysaccharides

Increased cellulose accessibility and hydrolysis has been achieved by chemical removal of hemicelluloses [135]. Therefore, hemicelluloses can be viewed as contributors to the recalcitrance of lignocellulosic material to degradative processes. Hemicelluloses are crosslinked to lignin by three types of covalent linkages. The first type involves *p*-coumaric or ferulic acid, ether linked to lignin, and ester linked to hemicellulose sugars [43]. The second type relies on spontaneous ether linkage formation between OH-groups of saccharides and lignin alcohols [129]. The third type involves ester links between uronic acid residues of glucuronoxylans and hydroxyl groups of lignin alcohols [130]. Such crosslinks hinder cell wall degradation by solvents, enzymes and microbes and reduce plant digestibility. Hence, improved cell wall solubility and degradation can theoretically develop through cleavage of the links between lignin and hemicelluloses.

The first type of crosslinking is abundant among the hemicelluloses of grasses and related monocot cell walls and form lignin–carbohydrate complexes. The matrix properties of these complexes are further influenced by the character and number of hemicellulose side chains and by the nature of the crosslinking agents, such as arabinose or ferulic acid [126]. To date, only ferulic acid esterase (FAE) has been genetically introduced into plants cell walls in an attempt to enhance the accessibility of hydrolyzing enzymes to hemicellulose fibers by removing ferulic acid side chains and crosslinking bonds [12–14, 133]. Expression of a fungal FAE gene in transgenic ryegrass and tall fescue rendered the cell walls more accessible to endoxylanases with higher levels of fermentable sugars released upon cell wall hydrolysis [12–14].

Glucuronoxylans are the primary hemicellulosic component of hardwoods and account for ~20% of the woody cell wall [4]. Approximately 60–70% of the xylose residues in hardwood xylan are acetylated at the C2 and/or C3 positions [73]. O-acetylation of xyloglucan has often been considered an additional barrier to enzymatic hydrolysis of polysaccharides and decreased polysaccharide solubility [91]. Thus, the reduction in the degree of acetylation of cell wall polysaccharides may allow for enhanced rates of saccharification. The deacetylation of GX in vitro increases its water solubility [51]. In addition, acetylxylan esterases (AXEs) liberates acetic acid from partially acetylated 4-*O*-methyl glucuronoxylan [79] and may increase hemicellulose solubility and increase xylan degradation rates.

5 Alteration of Cell Wall Lignin Content and Composition

Lignin provides plants with mechanical support, resistance to a variety of pathogens and facilitates water transport. It is one of the greatest contributors to plant cell wall recalcitrance to enzymatic hydrolysis and is a major obstacle in pulp, paper, and bioethanol production processes. Various delignification and pretreatment techniques have been designed to remove lignin, solubilize several polysaccharides and increase cell wall surface area. The current methods require high energy inputs and

harsh conditions and are thus very costly and produce toxic by-products [118]. Lignin modification is generally considered as the most direct approach for cost reduction of pretreatment processes, but the potential knock-on effect on plant fitness must be carefully considered.

5.1 Modifications of the Lignin Biosynthetic Pathway

Extensive research efforts are currently being directed toward facilitating lignin removal from lignocellulose-rich materials. Central genes encoding lignin biosynthesis have been downregulated in attempts to reduce lignin content or to modify its composition and quality by adjusting guaiacyl:syringyl ratios. Lignin modification and gene silencing have been extensively studied and have been thoroughly reviewed by Baucher et al. [9] and Vanholme et al. [124].

Lignin biosynthesis is encoded by multigene families and involves many parallel signaling pathways for monolignol generation. Thus, due to such redundancy, downregulation of a single gene may or may not affect lignin structure and enhance digestibility without affecting growth [50]. Generally, there is an inverse correlation between enzymatic hydrolysis efficacy and lignin content, as has been demonstrated in transgenic alfalfa plants with downregulation of six genes along the lignin biosynthetic pathway [19, 20]. These plants yielded nearly twice as much cell wall sugar upon enzymatic hydrolysis following acidic pretreatment.

The principal differences between perennial alfalfas and woody trees include the absence of lodging in alfalfa, while lignin is an essential requirement for normal tree growth. Studies have demonstrated dwarfing and xylem collapse phenotypes upon gene silencing along the lignin biosythesis pathway in several woody species [27, 69, 128]. Downregulation of 4-coumarate: coenzyme A ligase (*Pt4CL1*) in poplar trees led to a 45% reduction in lignin content when grown under greenhouse conditions while normal cellulose content and cellular morphology were maintained in comparison to wild type [61]. When field tested, hybrid poplar trees, (*Populous tremula* × *alba*) with an identical gene downregulated, demonstrated reduced water conductivity and modulus of elasticity and increased wood tension [68]. These results are a reminder of the trade-off resulting from the removal of lignin and of the need to test transgenic trees under natural growth conditions.

Aside from lignin reduction, modifications of guaiacyl and syringyl ratios are thought to be involved in regulating cell wall digestibility where S-unit-enriched lignin polymers contain fewer crosslinked areas than guaiacyl unit-rich lignin [11], thereby facilitating cell wall degradation and sugar yield upon saccharification. Upregulation of ferulate 5-hydroxylase (F5H) produces S-rich lignins. F5H expression driven by a lignifying-specific cinnamate-4-hydroxylase (C4H) promoter yields lignin derived primarily from sinapyl alcohols [121]. The resulting lignin is relatively homogenous with a lower degree of polymerization. Cell walls of such S lignin-rich transgenic plants are more amenable to saccharification under acidic or basic pretreatment conditions than wild type plants [42].

Cautious application of similar engineering strategies toward the lignin metabolic pathways may hold promise for designing feedstock with lower recalcitrance and improved bioethanol production yields. However, lignin is also considered as a valuable by-product. Designing processes for enhanced lignin recovery from the pretreated liquors and increasing lignin content in feedstock are additional and contrasting new challenges in the overall economic balance of sustainable biofuel production.

5.2 The "Bio-Switch": Novel Lignin Modification by Exploiting Weak Spots

Novel strategies for silent lignin modification with minimal impacts on plant development have been initiated. For example, applications of temporally controlled chemical or biological switches can induce lignin loosening at predetermined times. Ralph et al. [99] have developed a chemical insertion of alternative nonnative monolignols to lignin using the combinatorial oxidative coupling mechanism of lignin biosynthesis. These designed lignins feature weak cleavable bonds termed "zips." The authors reported incorporation of ferulate-polysaccharides esters in grasses during the lignification process. The resultant grass cell walls were more easily hydrolyzed by enzymes following alkaline treatments than the wild type [99].

Ferulate-monolignol ester conjugates, such as coniferyl ferulate or sinapyl ferulate have not been identified in lignins, but are produced during lignan biosynthesis [46]. Plants successfully incorporated these new monolignols into lignin following the addition of the monolignols to the growing medium and these unique monolignols introduced easily cleavable ester "zips." Monolignol incorporation into corn cell walls increased saccharification efficiency over that of wild type and reduced the need for the pretreatment stage. Transgenic plants with ferulated monolignol-rich lignins [46, 98] may be produced in the future.

A novel method which increased cellulose accessibility without affecting lignin content or plant structural integrity was recently demonstrated by free radical coupling of tyrosine-rich peptides into lignin. The phenol–hydroxyl groups of the tyrosine-rich peptides serve as reactive sites for coupling with the lignin [72]. The resultant lignin has hot spots that are highly susceptible to protease cleavage, allowing enhanced enzymatic hydrolysis and ethanol yields. Liang et al. [72] transformed poplar trees (*Populus deltoides*×*nigra*) with a tyrosine-rich gene under the poplar phenylalanine ammonia-lyase (PAL2) secondary cell wall promoter. The transgenic plants had no changes in total lignin content or overall plant morphology when compared to wild type, but were more susceptible than wild type to protease digestion, and resulted in higher sugar release from the lignocellulose complexes [72].

6 The "Trojan Horse": Introduction of Soluble Polysaccharides into Plant Cell Walls

We proposed an additional novel cell wall remodeling approach by introducing algal and viral soluble polysaccharides to behave as "Trojan Horses" within the cell wall [1]. This new approach inserts novel polysaccharides into the plant cell wall, which may behave normally during plant growth, but allow enhanced solubility during processing. The "Trojan Horse" concept aims to reduce pretreatment input requirements by the intercalating soluble polymers into the cell wall, enabling channel formation, and permitting rapid solvent and enzyme penetration and cell wall disassembly during and after the pretreatment stage. Such polysaccharides can be formed via exogenous expression of one or more enzymes capable of exploiting natural plant building blocks for their synthesis. The polysaccharides can be designed to be secreted or produced during cell wall development and to intercalate between cellulose fibers or serve as soluble "hemicellulose-like" polymers, creating soluble "pockets." Polymers of the algae cell wall or bacterial exopolysaccharides can provide a rich source of soluble polysaccharides, such as alginate, carrageenan, acetan, hyaluronan, chitosan, and levan. Most of the metabolic and genetic pathways for the synthesis of these polysaccharides are complicated and only a few have been fully elucidated.

A very similar biological process occurs naturally in algae-virus host–pathogen interactions. The paramecium bursaria Chlorella virus (PBCV-1) encodes multiple enzymes involved in extracellular hyaluronan synthesis [31]. PBCV-1-infected chlorella algae produce hyaluronan within their cell walls. As a result, the cell walls of the virus-infected algae are more porous when compared to that of the uninfected algae [48]. We have introduced genes for hyaluronan synthase together with appropriate targeting sequences into tobacco plants. Preliminary results have demonstrated enhanced cellulose hydrolysis upon acidic pretreatment in transgenic tobacco when compared to wild type plants (Abramson et al., unpublished results). We postulate that expression of hyaluronan synthase in plants can result in a reduction or modification of pectin levels due to competition for UDP-glucuronic acid, a substrate for pectin synthesis. This may result in a change in the mechanical properties and ultrastructure of the cell wall. Thus, ideally, hyaluronan synthase expression should be placed under control of a specific developmental promoter. Finally, as in the case of other cell wall modifying genes, the consequences of expression of each gene must be calculated to minimize side effects detrimental to plant growth, fitness, and physical character.

7 Concluding Remarks

The secure supply of bio-energy will depend on the integration of various crop platforms as well as multiple technologies. These technologies will need to act upstream for plant modification and selection and downstream for processing to ensure the economic viability and environmental sustainability of future energy supplies.

Biotechnological tools can be utilized to develop and improve specific feedstocks as dedicated crops for biofuel production. Appropriate modification of plant cell walls by genetic engineering approaches could produce new plant varieties with significantly enhanced properties for the efficient exploitation of biomass for biofuel production. We believe that advanced technology solutions will require the manipulation of combinations of genes and metabolic pathways, acting on different feedstocks, each suited to specific geographic environments.

Furthermore, these developments which are essential for the biofuels industry will also be beneficial for the pulp and paper industry by minimizing the use of energy and chemicals during the paper making process and by increasing pulping efficiency.

Interdisciplinary research combining agronomy, plant molecular biology, genetics, microbiology, mechanical and chemical engineering will be essential to advance the breakthroughs required for the development of economical, applicable solutions. All of these new approaches will need to be carefully evaluated for their effect on overall plant fitness and development and environmental sustainability.

Acknowledgments We are grateful to Professor Jonathan Gressel for his critical review, comments, and corrections on earlier drafts of the manuscript.

References

1. Abramson M, Shoseyov O, Shani Z (2010) Plant cell wall reconstruction toward improved lignocellulosic production and processability. Plant Sci 178:61–72
2. Arantes V, Saddler JN (2010) Access to cellulose limits the efficiency of enzymatic hydrolysis: the role of amorphogenesis. Biotechnol Biofuels 3:4
3. Arioli T, Peng LC, Betzner AS, Burn J, Wittke W, Herth W, Camilleri C, Hofte H, Plazinski J, Birch R, Cork A, Glover J, Redmond J, Williamson RE (1998) Molecular analysis of cellulose biosynthesis in *Arabidopsis*. Science 279:717–720
4. Awano T, Takabe K, Fujita M (1998) Localization of glucuronoxylans in Japanese beech visualized by immunogold labelling. Protoplasma 202:213–222
5. Ayers AR, Ayers SB, Eriksson KE (1978) Cellobiose oxidase, purification and partial characterization of a hemoprotein from *Sporotrichum pulverulentum*. Eur J Biochem 90:171–181
6. Baba K, Park YW, Kaku T, Kaida R, Takeuchi M, Yoshida M, Hosoo Y, Ojio Y, Okuyama T, Taniguchi T, Ohmiya Y, Kondo T, Shani Z, Shoseyov O, Awano T, Serada S, Norioka N, Norioka S, Hayashi T (2009) Xyloglucan for generating tensile stress to bend tree stem. Mol Plant 2:893–903
7. Bao W, Renganathan V (1992) Cellobiose oxidase of *Phanerochaete chrysosporium* enhances crystalline cellulose degradation by cellulases. FEBS Lett 302:77–80

8. Baron-Epel O, Gharyal PK, Schindler M (1988) Pectins as mediators of wall porosity in soybean cells. Planta 175:389–395
9. Baucher M, Halpin C, Petit-Conil M, Boerjan W (2003) Lignin: genetic engineering and impact on pulping. Crit Rev Biochem Mol Biol 38:305–350
10. Boehmel C, Lewandowski I, Claupein W (2008) Comparing annual and perennial energy cropping systems with different management intensities. Agr Syst 96:224–236
11. Boerjan W, Ralph J, Baucher M (2003) Lignin biosynthesis. Annu Rev Plant Biol 54: 519–546
12. Buanafina MMD, Langdon T, Hauck B, Dalton S, Morris P (2008) Expression of a fungal ferulic acid esterase increases cell wall digestibility of tall fescue (*Festuca arundinacea*). Plant Biotechnol J 6:264–280
13. Buanafina MMD, Langdon T, Hauck B, Dalton S, Timms-Taravella E, Morris P (2010) Targeting expression of a fungal ferulic acid esterase to the apoplast, endoplasmic reticulum or golgi can disrupt feruloylation of the growing cell wall and increase the biodegradability of tall fescue (*Festuca arundinacea*). Plant Biotechnol J 8:316–331
14. Buanafina MMD, Langdon T, Hauck B, Dalton SJ, Morris P (2006) Manipulating the phenolic acid content and digestibility of Italian ryegrass (*Lolium multiflorum*) by vacuolar-targeted expression of a fungal ferulic acid esterase. Appl Biochem Biotechnol 130:416–426
15. Canam T, Park JY, Yu KY, Campbell MM, Ellis DD, Mansfield SD (2006) Varied growth, biomass and cellulose content in tobacco expressing yeast-derived invertases. Planta 224:1315–1327
16. Canevscini G, Borer P, Dreyer J (1991) Cellobiose dehydrogenases of *Sporotrichum Chrysosporium* thermophile. Eur J Biochem 198:43–52
17. Carpita N, McCann M (2000) The cell wall. In: Buchanan BB, Gruissem W, Jones RL (eds) Biochemistry and molecular biology of plants. American Society of Plant Physyologists, Rockville
18. Carpita NC, Gibeaut DM (1993) Structural models of primary cell walls in flowering plants: consistency of molecular structure with the physical properties of the walls during growth. Plant J 3:1–30
19. Chen F, Dixon RA (2007) Lignin modification improves fermentable sugar yields for biofuel production. Nat Biotechnol 25:759–761
20. Chen F, Srinivasa Reddy MS, Temple S, Jackson L, Shadle G, Dixon RA (2006) Multi-site genetic modulation of monolignol biosynthesis suggests new routes for formation of syringyl lignin and wall-bound ferulic acid in alfalfa (*Medicago sativa* L.). Plant J 48:113–124
21. Chen XA, Ishida N, Todaka N, Nakamura R, Maruyama J, Takahashi H, Kitamoto K (2010) Promotion of efficient saccharification of crystalline cellulose by *Aspergillus fumigatus* Swo1. Appl Environ Microbiol 76:2556–2561
22. Cho HT, Cosgrove DJ (2000) Altered expression of expansin modulates leaf growth and pedicel abscission in *Arabidopsis thaliana*. Proc Natl Acad Sci U S A 97:9783–9788
23. Cho HT, Cosgrove DJ (2002) Regulation of root hair initiation and expansin gene expression in *Arabidopsis*. Plant Cell 14:3237–3253
24. Choi D, Lee Y, Cho HT, Kende H (2003) Regulation of expansin gene expression affects growth and development in transgenic rice plants. Plant Cell 15:1386–1398
25. Clark J, Deswarte F (2008) The biorefinery concept–an integrated approach. In: Clark JH (ed) Introduction to chemicals from biomass. Renewable resources. Wiley, Padstow
26. Coleman HD, Beamish L, Reid A, Park JY, Mansfield SD (2010) Altered sucrose metabolism impacts plant biomass production and flower development. Transgenic Res 19:269–283
27. Coleman HD, Samuels AL, Guy RD, Mansfield SD (2008) Perturbed lignification impacts tree growth in hybrid poplar–a function of sink strength, vascular integrity, and photosynthetic assimilation. Plant Physiol 148:1229–1237
28. Cosgrove DJ (1993) Wall extensibility: its nature, measurement and relationship to plant cell growth. New Phytol 124:1–23
29. Cosgrove DJ (2000) Loosening of plant cell walls by expansins. Nature 407:321–326

30. Cosgrove DJ (2005) Growth of the plant cell wall. Nat Rev Mol Cell Biol 6:850–861
31. DeAngelis PL, Jing W, Graves MV, Burbank DE, VanEtten JL (1997) Hyaluronan synthase of chlorella virus PBCV-1. Science 278:1800–1803
32. Delmer DP (1999) Cellulose biosynthesis: exciting times for a difficult field of study. Annu Rev Plant Physiol Plant Mol Biol 50:245–276
33. Di Matteo A, Giovane A, Raiola A, Camardella L, Bonivento D, De Lorenzo G, Cervone F, Bellincampi D, Tsernoglou D (2005) Structural basis for the interaction between pectin methylesterase and a specific inhibitor protein. Plant Cell 17:849–858
34. Din N, Gilkes N, Tekant B, Miller R, Warren R, Kilburn D (1991) Non-hydrolytic disruption of cellulose fibres by the binding domain of a bacterial cellulase. Nat Biotechnol 9:1096–1099
35. DOE (2004) Biomass feedstock composition and property database. http://www.afdc.energy.gov/biomass/progs/search1.cgi. Accessed 15 Jun 2010
36. DOE (2005) GTL roadmap: systems biology for energy and environment. US department of energy. http://genomicsgtl.energy.gov/roadmap. Accessed 8 May 2010
37. DOE (2006) Breaking the biological barriers to cellulosic ethanol: a joint research agenda. U.S. Department of Energy. http://genomicsgtl.energy.gov/biofuels/b2bworkshop.shtml. Accessed 8 May 2010
38. Ezaki N, Kido N, Takahashi K, Katou K (2005) The role of wall Ca^{2+} in the regulation of wall extensibility during the acid-induced extension of soybean hypocotyl cell walls. Plant Cell Physiol 46:1831–1838
39. FAO (2008) Forests and energy. http://www.fao.org/docrep/010/i0139e/i0139e00.htm. Accessed 1 Aug 2010
40. FAO (2010) The global forest resources assessment. http://www.fao.org/forestry/fra/fra2010/en/. Accessed 1 Aug 2010
41. Fleming A, McQueen-Mason S, Mandel T, Kuhlemeier C (1997) Induction of leaf primordia by the cell wall protein expansin. Science 276:1415–1418
42. Franke R, McMichael CM, Meyer K, Shirley AM, Cusumano JC, Chapple C (2000) Modified lignin in tobacco and poplar plants over-expressing the *Arabidopsis* gene encoding ferulate 5-hydroxylase. Plant J 22:223–234
43. Fry SC (1986) Cross-linking of matrix polymers in the growing cell-walls of angiosperms. Annu Rev Plant Physiol 37:165–186
44. Gardner A, Davies HV, Burch LR (1992) Purification and properties of fructokinase from developing tubers of potato (*Solanum tuberosum* L.). Plant Physiol 100:178–183
45. Gelfand I, Snapp SS, Robertson GP (2010) Energy efficiency of conventional, organic, and alternative cropping systems for food and fuel at a site in the US Midwest. Environ Sci Technol 44:4006–4011
46. Grabber JH, Hatfield RD, Lu FC, Ralph J (2008) Coniferyl ferulate incorporation into lignin enhances the alkaline delignification and enzymatic degradation of cell walls. Biomacromolecules 9:2510–2516
47. Grattapaglia D, Kirst M (2008) Eucalyptus applied genomics: from gene sequences to breeding tools. New Phytol 179:911–929
48. Graves MV, Burbank DE, Roth R, Heuser J, DeAngelis PL, Van Etten JL (1999) Hyaluronan synthesis in virus PBCV-1-infected chlorella-like green algae. Virology 257:15–23
49. Gray-Mitsumune M, Blomquist K, McQueen-Mason S, Teeri TT, Sundberg B, Mellerowicz EJ (2008) Ectopic expression of a wood-abundant expansin *PttEXPA1* promotes cell expansion in primary and secondary tissues in aspen. Plant Biotechnol J 6:62–72
50. Gressel J (2008) Transgenics are imperative for biofuel crops. Plant Sci 174:246–263
51. Grondahl M, Teleman A, Gatenholm P (2003) Effect of acetylation on the material properties of glucuronoxylan from aspen wood. Carbohydr Polym 52:359–366
52. Haigler CH, Ivanova-Datcheva M, Hogan PS, Salnikov VV, Hwang S, Martin K, Delmer DP (2001) Carbon partitioning to cellulose synthesis. Plant Mol Biol 47:29–51
53. Harris D, DeBolt S (2010) Synthesis, regulation and utilization of lignocellulosic biomass. Plant Biotechnol J 8:244–262

54. Harris D, Stork J, Debolt S (2009) Genetic modification in cellulose-synthase reduces crystallinity and improves biochemical conversion to fermentable sugar. GCB Bioenergy 1:51–61
55. Hartati S, Sudarmonowati E, Park YW, Kaku T, Kaida R, Baba K, Hayashi T (2008) Overexpression of poplar cellulase accelerates growth and disturbs the closing movements of leaves in sengon. Plant Physiol 147:552–561
56. Hayashi T (1989) Xyloglucans in the primary-cell wall. Annu Rev Plant Physiol 40:139–168
57. Heaton E, Long S, Voigt T, Jones M, Clifton-Brown J (2004) *Miscanthus* for renewable energy generation: European Union experience and projections for Illinois. Mitig Adapt Strateg Glob change 9:433–451
58. Henriksson G, Johansson G, Pettersson G (2000) A critical review of cellobiose dehydrogenases. J Biotechnol 78:93–113
59. Henriksson G, Salumets A, Divne C, Pettersson G (1997) Studies of cellulose binding by cellobiose dehydrogenase and a comparison with cellobiohydrolase 1. Biochem J 324(pt 3):833–838
60. Himmel ME, Ding SY, Johnson DK, Adney WS, Nimlos MR, Brady JW, Foust TD (2007) Biomass recalcitrance: engineering plants and enzymes for biofuels production. Science 315:804–807
61. Hu WJ, Harding SA, Lung J, Popko JL, Ralph J, Stokke DD, Tsai CJ, Chiang VL (1999) Repression of lignin biosynthesis promotes cellulose accumulation and growth in transgenic trees. Nat Biotechnol 17:808–812
62. Huang HJ, Ramaswamy S, Al-Dajani W, Tschirner U, Cairncross RA (2009) Effect of biomass species and plant size on cellulosic ethanol: a comparative process and economic analysis. Biomass Bioenergy 33:234–246
63. Ishii T (1997) Structure and functions of feruloylated polysaccharides. Plant Sci 127:111–127
64. Jeoh T, Ishizawa CI, Davis MF, Himmel ME, Adney WS, Johnson DK (2007) Cellulase digestibility of pretreated biomass is limited by cellulose accessibility. Biotechnol Bioeng 98:112–122
65. Joshi CP, Mansfield SD (2007) The cellulose paradox—simple molecule, complex biosynthesis. Curr Opin Plant Biol 10:220–226
66. Jung J, O'Donoghue EM, Dijkwel PP, Brummell DA (2010) Expression of multiple expansin genes is associated with cell expansion in potato organs. Plant Sci 179:77–85
67. Kim S, Dale BE (2004) Global potential bioethanol production from wasted crops and crop residues. Biomass Bioenergy 26:361–375
68. Kitin P, Voelker S, Meinzer F, Beeckman H, Strauss S, Lachenbruch B (2010) Tyloses and phenolic deposits in xylem vessels impede water transport in low-lignin transgenic poplars: a study by cryo-fluorescence microscopy. Plant Physiol. doi:101104/pp 110156224
69. Leple JC, Dauwe R, Morreel K, Storme V, Lapierre C, Pollet B, Naumann A, Kang KY, Kim H, Ruel K, Lefebvre A, Joseleau JP, Grima-Pettenati J, De Rycke R, Andersson-Gunneras S, Erban A, Fehrle I, Petit-Conil M, Kopka J, Polle A, Messens E, Sundberg B, Mansfield SD, Ralph J, Pilate G, Boerjan W (2007) Downregulation of cinnamoyl-coenzyme A reductase in poplar: multiple-level phenotyping reveals effects on cell wall polymer metabolism and structure. Plant Cell 19:3669–3691
70. Lerouxel O, Cavalier DM, Liepman AH, Keegstra K (2006) Biosynthesis of plant cell wall polysaccharides—a complex process. Curr Opin Plant Biol 9:621–630
71. Levy I, Shani Z, Shoseyov O (2002) Modification of polysaccharides and plant cell wall by endo-1,4-beta-glucanase and cellulose-binding domains. Biomol Eng 19:17–30
72. Liang HY, Frost CJ, Wei XP, Brown NR, Carlson JE, Tien M (2008) Improved sugar release from lignocellulosic material by introducing a tyrosine-rich cell wall peptide gene in poplar. Clean Soil Air Water 36:662–668
73. Lindberg B, Rosell KG, Svensson S (1973) Positions of O-acetyl groups in birch xylan. Sven Papperstidn 76:30–32
74. Lionetti V, Francocci F, Ferrari S, Volpi C, Bellincampi D, Galletti R, D'Ovidio R, De Lorenzo G, Cervone F (2010) Engineering the cell wall by reducing de-methyl-esterified

homogalacturonan improves saccharification of plant tissues for bioconversion. Proc Natl Acad Sci U S A 107:616–621
75. Lynd LR, Weimer PJ, van Zyl WH, Pretorius IS (2002) Microbial cellulose utilization: fundamentals and biotechnology. Microbiol Mol Biol Rev 66:506–577
76. Mabee WE, Gregg DJ, Arato C, Berlin A, Bura R, Gilkes N, Mirochnik O, Pan XJ, Pye EK, Saddler JN (2006) Updates on softwood-to-ethanol process development. Appl Biochem Biotechnol 129:55–70
77. Maloney VJ, Mansfield SD (2010) Characterization and varied expression of a membrane-bound endo-beta-1,4-glucanase in hybrid poplar. Plant Biotechnol J 8:294–307
78. Mansfield SD, Mooney C, Saddler JN (1999) Substrate and enzyme characteristics that limit cellulose hydrolysis. Biotechnol Prog 15:804–816
79. Margolles-Clark E, Tenkanen M, Soderlund H, Penttila M (1996) Acetyl xylan esterase from *Trichoderma reesei* contains an active-site serine residue and a cellulose-binding domain. Eur J Biochem 237:553–560
80. McQueen-Mason S, Durachko D, Cosgrove D (1992) Two endogenous proteins that induce cell wall extension in plants. Plant Cell 4:1425–1433
81. Mellerowicz EJ, Sundberg B (2008) Wood cell walls: biosynthesis, developmental dynamics and their implications for wood properties. Curr Opin Plant Biol 11:293–300
82. Micheli F (2001) Pectin methylesterases: cell wall enzymes with important roles in plant physiology. Trends Plant Sci 6:414–419
83. Muir JP, Sanderson MA, Ocumpaugh WR, Jones RM, Reed RL (2001) Biomass production of 'Alamo' switchgrass in response to nitrogen, phosphorus, and row spacing. Agron J 93:896–901
84. Mutwil M, Debolt S, Persson S (2008) Cellulose synthesis: a complex complex. Curr Opin Plant Biol 11:252–257
85. Nicol F, His I, Jauneau A, Vernhettes S, Canut H, Hofte H (1998) A plasma membrane-bound putative endo-1,4-beta-D-glucanase is required for normal wall assembly and cell elongation in *Arabidopsis*. EMBO J 17:5563–5576
86. Obembe OO, Jacobsen E, Timmers J, Gilbert H, Blake AW, Knox JP, Visser RG, Vincken JP (2007) Promiscuous, non-catalytic, tandem carbohydrate-binding modules modulate the cell-wall structure and development of transgenic tobacco (*Nicotiana tabacum*) plants. J Plant Res 120:605–617
87. Park JY, Canam T, Kang KY, Ellis DD, Mansfield SD (2008) Over-expression of an *Arabidopsis* family A sucrose phosphate synthase (*SPS*) gene alters plant growth and fibre development. Transgenic Res 17:181–192
88. Park YW, Baba K, Furuta Y, Iida I, Sameshima K, Arai M, Hayashi T (2004) Enhancement of growth and cellulose accumulation by overexpression of xyloglucanase in poplar. FEBS Lett 564:183–187
89. Park YW, Tominaga R, Sugiyama J, Furuta Y, Tanimoto E, Samejima M, Sakai F, Hayashi T (2003) Enhancement of growth by expression of poplar cellulase in *Arabidopsis thaliana*. Plant J 33:1099–1106
90. Pauly M, Keegstra K (2008) Cell-wall carbohydrates and their modification as a resource for biofuels. Plant J 54:559–568
91. Pauly M, Scheller HV (2000) O-Acetylation of plant cell wall polysaccharides: identification and partial characterization of a rhamnogalacturonan O-acetyl-transferase from potato suspension-cultured cells. Planta 210:659–667
92. Pelloux J, Rusterucci C, Mellerowicz EJ (2007) New insights into pectin methylesterase structure and function. Trends Plant Sci 12:267–277
93. Perlack R, Wright L, Turhollow A, Graham R, Stokes B, Erbach D (2005) Biomass as feedstock for a bioenergy and bioproducts industry: the technical feasibility of a billion-ton annual supply. Oak Ridge National Laboratory, Oak Ridge

94. Perrin R, Wilkerson C, Keegstra K (2001) Golgi enzymes that synthesize plant cell wall polysaccharides: finding and evaluating candidates in the genomic era. Plant Mol Biol 47:115–130
95. Pettersen RC (1984) The chemical-composition of wood. In: Rowell RC (ed) The chemistry of solid wood. Advances in chemistry series. American chemical society, Washington, DC
96. Pilling J, Willmitzer L, Fisahn J (2000) Expression of a *Petunia inflata* pectin methyl esterase in *Solanum tuberosum* L. enhances stem elongation and modifies cation distribution. Planta 210:391–399
97. Ragauskas A, Nagy M, Kim D, Eckert C, Hallett J, Liotta C (2006) From wood to fuels: integrating biofuels and pulp production. Ind Biotechnol 2:55–65
98. Ralph J (2010) Hydroxycinnamates in lignification. Phytochem Rev 9:65–83
99. Ralph J, Grabber JH, Hatfield RD (1995) Lignin-ferulate cross-links in grasses—active incorporation of ferulate polysaccharide esters into ryegrass lignins. Carbohydr Res 275: 167–178
100. Ralph J, Lundquist K, Brunow G, Lu F, Kim H, Schatz P, Marita J, Hatfield R, Ralph S, Christensen J (2004) Lignins: natural polymers from oxidative coupling of 4-hydroxyphenyl-propanoids. Phytochem Rev 3:29–60
101. Rochange SF, Wenzel CL, McQueen-Mason SJ (2001) Impaired growth in transgenic plants over-expressing an expansin isoform. Plant Mol Biol 46:581–589
102. Rubin EM (2008) Genomics of cellulosic biofuels. Nature 454:841–845
103. Safra-Dassa L, Shani Z, Danin A, Roiz L, Shoseyov O, Wolf S (2006) Growth modulation of transgenic potato plants by heterologous expression of bacterial carbohydrate-binding module. Mol Breed 17:355–364
104. Sanderson MA, Adler PR (2008) Perennial forages as second generation bioenergy crops. Int J Mol Sci 9:768–788
105. Sandhu AP, Randhawa GS, Dhugga KS (2009) Plant cell wall matrix polysaccharide biosynthesis. Mol Plant 2:840–850
106. Sannigrahi P, Ragauskas AJ, Tuskan GA (2010) Poplar as a feedstock for biofuels: a review of compositional characteristics. Biofuel Bioprod Bioref 4:209–226
107. Sarkar P, Bosneaga E, Auer M (2009) Plant cell walls throughout evolution: towards a molecular understanding of their design principles. J Exp Bot 60:3615–3635
108. Schubert C (2006) Can biofuels finally take center stage? Nat Biotechnol 24:777–784
109. Shani Z, Dekel M, Jensen CS, Tzfira T, Goren R, Altman A, Shoseyov O (2000) *Arabidopsis thaliana* endo-1,4-beta-glucanase (*cel1*) promoter mediates *uidA* expression in elongating tissues of aspen (*Populus tremula*). J Plant Physiol 156:118–120
110. Shani Z, Dekel M, Roiz L, Horowitz M, Kolosovski N, Lapidot S, Alkan S, Koltai H, Tsabary G, Goren R, Shoseyov O (2006) Expression of endo-1,4-beta-glucanase (*cel1*) in *Arabidopsis thaliana* is associated with plant growth, xylem development and cell wall thickening. Plant Cell Rep 25:1067–1074
111. Shani Z, Dekel M, Tsabary G, Goren R, Shoseyov O (2004) Growth enhancement of transgenic poplar plants by overexpression of *Arabidopsis thaliana* endo-1,4-β-glucanase (*cel1*). Mol Breed 14:321–330
112. Shani Z, Dekel M, Tsabary G, Shoseyov O (1997) Cloning and characterization of elongation specific endo-1,4-beta-glucanase (*cel1*) from *Arabidopsis thaliana*. Plant Mol Biol 34:837–842
113. Shani Z, Shoseyov O (2006) Cell wall proteins as a tool for plant cell modification. In: Hayashi T (ed) The science and lore of the plant cell wall: biosynthesis, structure and function. Brown Walker Press, Boca Raton
114. Shani Z, Shpigel E, Roiz L, Goren R, Vinocur B, Tzfira T, Altman A, Shoseyov O (1999) Cellulose binding domain increases cellulose synthase activiry in *Acetobacter xylinum* and biomass of transgenic plants. In: Altman A, Ziv M, Izhar S (eds) Plant biotechnology and in vitro biology in the 21st century. Kluwer, Dordrecht
115. Shoseyov O, Levy I, Shani Z, Mansfield SD (2003) Modulation of wood fibers and paper by cellulose-binding domains. In: Mansfield D, Saddler JN (eds) Applications of enzymes to lignocellulosics. ACS symposium series, vol 855. American Chemical Society, Washington, DC

116. Shoseyov O, Shani Z, Levy I (2006) Carbohydrate binding modules: biochemical properties and novel applications. Microbiol Mol Biol Rev 70:283–295
117. Shpigel E, Roiz L, Goren R, Shoseyov O (1998) Bacterial cellulose-binding domain modulates in vitro elongation of different plant cells. Plant Physiol 117:1185–1194
118. Simmons BA, Loque D, Ralph J (2010) Advances in modifying lignin for enhanced biofuel production. Curr Opin Plant Biol 13:313–320
119. Somerville C (2006) Cellulose synthesis in higher plants. Annu Rev Cell Dev Biol 22:53–78
120. Somerville C, Bauer S, Brininstool G, Facette M, Hamann T, Milne J, Osborne E, Paredez A, Persson S, Raab T, Vorwerk S, Youngs H (2004) Toward a systems approach to understanding plant cell walls. Science 306:2206–2211
121. Stewart JJ, Akiyama T, Chapple C, Ralph J, Mansfield SD (2009) The effects on lignin structure of overexpression of ferulate 5-hydroxylase in hybrid poplar. Plant Physiol 150:621–635
122. Taylor NG (2008) Cellulose biosynthesis and deposition in higher plants. New Phytol 178:239–252
123. Van Parijs FR, Morreel K, Ralph J, Boerjan W, Merks RM (2010) Modeling lignin polymerization. I. simulation model of dehydrogenation polymers. Plant Physiol 153:1332–1344
124. Vanholme R, Morreel K, Ralph J, Boerjan W (2008) Lignin engineering. Curr Opin Plant Biol 11:278–285
125. Vincken J, Schols H, Oomen R, McCann M, Ulvskov P, Voragen A, Visser R (2003) If homogalacturonan were a side chain of rhamnogalacturonan I. Implications for cell wall architecture. Plant physiol 132:1781–1789
126. Vogel J (2008) Unique aspects of the grass cell wall. Curr Opin Plant Biol 11:301–307
127. Vogler H, Caderas D, Mandel T, Kuhlemeier C (2003) Domains of expansin gene expression define growth regions in the shoot apex of tomato. Plant Mol Biol 53:267–272
128. Wagner A, Donaldson L, Kim H, Phillips L, Flint H, Steward D, Torr K, Koch G, Schmitt U, Ralph J (2009) Suppression of 4-coumarate-CoA ligase in the coniferous gymnosperm *Pinus radiata*. Plant Physiol 149:370–383
129. Watanabe T, Koshijima T (1988) Evidence for an ester linkage between lignin and glucuronic acid in lignin-carbohydrate complexes by DDQ-oxidation. Agric Biol Chem 52:2953–2955
130. Watanabe T, Ohnishi J, Yamasaki Y, Kaizu S, Koshijima T (1989) Binding-site analysis of the ether linkages between lignin and hemicelluloses in lignin-carbohydrate complexes by DDQ-oxidation. Agric Biol Chem 53:2233–2252
131. Weng J, Chapple C (2010) The origin and evolution of lignin biosynthesis. New Phytol 187:273–285
132. Willats WG, Orfila C, Limberg G, Buchholt HC, van Alebeek GJ, Voragen AG, Marcus SE, Christensen TM, Mikkelsen JD, Murray BS, Knox JP (2001) Modulation of the degree and pattern of methyl-esterification of pectic homogalacturonan in plant cell walls. Implications for pectin methyl esterase action, matrix properties, and cell adhesion. J Biol Chem 276:19404–19413
133. Wong DWS (2006) Feruloyl esterase—a key enzyme in biomass degradation. Appl Biochem Biotechnol 133:87–112
134. Wyman CE, Spindler DD, Grohmann K (1992) Simultaneous saccharification and fermentation of several lignocellulosic feedstocks to fuel ethanol. Biomass Bioenergy 3:301–307
135. Yang B, Wyman CE (2004) Effect of xylan and lignin removal by batch and flowthrough pretreatment on the enzymatic digestibility of corn stover cellulose. Biotechnol Bioeng 86:88–95
136. Zamocky M, Ludwig R, Peterbauer C, Hallberg BM, Divne C, Nicholls P, Haltrich D (2006) Cellobiose dehydrogenase–a flavocytochrome from wood-degrading, phytopathogenic and saprotropic fungi. Curr Protein Pept Sci 7:255–280

Chapter 19
Natural and Designed Enzymes for Cellulose Degradation

Eva Cunha, Christine L. Hatem, and Doug Barrick

Abstract Biofuels hold significant promise as an environmentally friendly means to displace a significant amount of fossil fuel from the global liquid transportation fuel mix. Compared with current corn and sugarcane-based feedstocks, which are agriculturally intensive, lignocellulosic feedstocks are abundant, can be produced cheaply, and have a much smaller carbon footprint per unit energy output. However, conversion of cellulosic materials into simple sugars (an intermediate step in biofuel production) is a significant challenge, owing to the rigidity and high resistance of cellulose to degradation. Recent efforts to improve enzymatic breakdown of cellulose have taken advantage of expanding genome sequence databases, advances in structural biology of cellulose degradation enzymes (cellulases), biochemical studies of enzymatic breakdown of cellulose, and protein engineering studies. In this chapter, the structural features of cellulose and cellulose-degrading enzymes will be reviewed, along with methods used to determine cellulase activity. We will focus on models for synergistic effects among enzymes, strategies used by bacteria and fungi to increase reactivity through synergistic enhancement, and approaches by which synergistic enhancement can be engineered into artificial enzymes to be used for large-scale cellulose-based biofuels production.

1 Introduction

Global energy consumption and its impact on the environment represent the biggest challenge we face in the twenty-first century. Fossil fuel is becoming increasingly more difficult to find and extract, driving the cost of energy and negatively influencing international policy. Even if production can keep up with the increasing demands of

E. Cunha • C.L. Hatem • D. Barrick (✉)
T.C. Jenkins Department of Biophysics, Johns Hopkins University,
3400 North Charles Street, Baltimore, MD 21218, USA
e-mail: barrick@jhu.edu

J.W. Lee (ed.), *Advanced Biofuels and Bioproducts*, DOI 10.1007/978-1-4614-3348-4_19,

developing (and developed) nations, the environmental impact of both extraction and emission will worsen. Combustion of the reduced-carbon energy sources in fossil fuels produces greenhouse gasses (GHGs) and other pollutants. Both atmospheric CO_2 concentrations and global temperatures are increasing at a steady and alarming rate. Assuming the former is driving the latter, one widely accepted view states that to keep CO_2 levels below 750 ppm by 2050 (at three times the level of our pre-GHG-emitting economy, still considered by some to be quite dangerous), carbon-neutral renewables need to provide *twice our current global energy consumption* in a best-case scenario [33].

There are many alternative energy sources with the potential to displace significant amounts of CO_2 production from the global energy stream. Most of these involve energy from the sun, either directly or indirectly. Direct conversion using photovoltaic devices would produce electricity directly from sunlight. With the exception of manufacturing costs, the photovoltaic cycle is truly carbon-neutral. Photosynthesis in plants and algae provides a means to produce chemicals from sunlight, and in particular, reduced carbon that can be used for liquid transportation fuel. Production of reduced transportation fuel is carbon-negative, since CO_2 is removed from the atmosphere as a precursor. This CO_2 is then rereleased to the atmosphere when the fuel is burned, and when taken together with photosynthesis, can be run in a carbon-neutral way (indeed, prior to the industrial revolution, direct biomass combustion in the form of wood burning was the major mode of energy extraction for humans).

There are already significant amounts of transportation fuel produced by converting the reduced carbon in plants to ethanol. Currently, automobile fuel in the US includes 10% ethanol made from the starch and sugar in corn (maize) grain; in Brazil, significantly larger amounts of ethanol (derived from sucrose in sugarcane press juice) are used in automobile fuel, with many cars running on 100% ethanol.

The process by which ethanol is produced from corn grain and sugarcane can be separated conceptually into two steps. In the first step, termed saccharification, the simple six-carbon hexose units, glucose and fructose, are produced from starch by enzymatic or acid hydrolysis In the case of sucrose, the fermentative microorganisms themselves are generally able to carry out hydrolysis to glucose and fructose by means of their intrinsic enzymes, such as the invertase secreted by the yeast *Saccharomyces cerevisae*. These six-carbon sugars then serve as a feedstock for fermentation by microorganisms, much in the same way that beer or wine is produced. The problem with this approach is the high agricultural intensity and relatively low yield of sugar per unit biomass, as only a small part of the total plant material is utilized. This is especially true for corn produced in the US: high amounts of fertilizer and water are required, and most of the plant (the stalk, leaves, and root system) is not used in the process (the starch is concentrated in the corn kernels). Although estimates vary [41, 56], the net energy yield from corn-based ethanol is modest: about as much energy (currently from fossil fuel) is required to produce corn-based ethanol as is recovered from ethanol combustion, resulting in no net reduction in greenhouse gas emissions [9, 31].

If more of the reduced carbon produced by plants could be converted to fuel, thereby permitting less agriculturally intensive plants to be used as feedstock, we

could increase the net energy yield of bio-based ethanol (or other reduced-carbon fuels run off a saccharification stream). Most of the reduced carbon in plants is stored not as starch or simple oligosaccharides, but as lignocellulose. The primary role of lignocellulose is to provide structural rigidity to the plant cell walls. The major component of lignocellulose is cellulose, which generally comprises around 40–60% of the total dry mass, with hemicellulose and lignin also present in substantial amounts. Although all three components can be utilized for biofuel production by various routes, cellulose has the best potential as a feedstock for fermentative production of ethanol and other transportation fuels.

Cellulose is the most abundant biological polymer on earth, with 1.5×10^{12} tons synthesized per year [37]. A variety of rapidly growing plants have been identified that have favorable properties for producing lignocellulosic biomass agriculturally. For example, switchgrass is a perennial plant (it is planted once, and grows back every year), requires comparatively little water or nitrogen fertilizer, can be harvested and stored using conventional haying equipment, and attains a height of 10 ft in a single growing season. It has been estimated that if the lignocellulosic biomass from switchgrass could be recovered, the net energy yield for liquid fuel would be around 500% [64]. Moreover, there is a significant amount of waste cellulosic material (agricultural waste such as corn stover, the parts of the corn plant that are not corn kernels, and sugarcane bagasse, the stem and leaf material left after pressing; manure; waste from the timber and paper industries; municipal waste) that could be "recycled" into liquid fuel. A recent study by the USDA/Forest Service estimates that one billion tons of waste biomass is available in the US alone, which if converted to liquid fuel, could displace two billion barrels of crude oil per year, roughly one quarter of our total consumption (see http://www.eere.energy.gov/biomass/publications.html). Cellulose consists of simple chains of glucose, linked together by 1,4-glycosidic linkages (Fig. 1a), and thus, is very similar in covalent structure to starch.

Cellulose differs from starch in one simple but very important way: the configuration of the anomeric (C1) carbon in cellulose is β-, whereas in starch, it is α-. Whereas starch has a loose, open helical configuration, making it easily solubilized and readily accessible for enzymatic or physico-chemical breakdown, the structure of cellulose is very straight and regular, allowing adjacent cellulose chains to pack close together in parallel linear arrays into crystalline, insoluble fibers. Cellulose fibers are stabilized both by interchain hydrogen bonds and by close van der Waals contacts (Fig. 1b). These interactions make cellulose fibers very inaccessible both to enzymatic and physical degradation: cellulose remains crystalline at a temperature 300°C under 25 atm. of pressure [11].

Yet cellulosic biomass is not indestructible. On a global scale, the amount of lignocellulosic biomass is in a steady state, which means that its synthesis rate is matched by its rate of breakdown. In nature, this breakdown is facilitated almost entirely by microbes. Although plants do not use cellulose as a means to store carbon for future metabolic activity, bacteria and fungi do. These microbes have extensive arrays of genes encoding enzymes that specifically hydrolyze the 1,4-β-glycosidic linkages of cellulose, along with the linkages in hemicellulose and the covalent

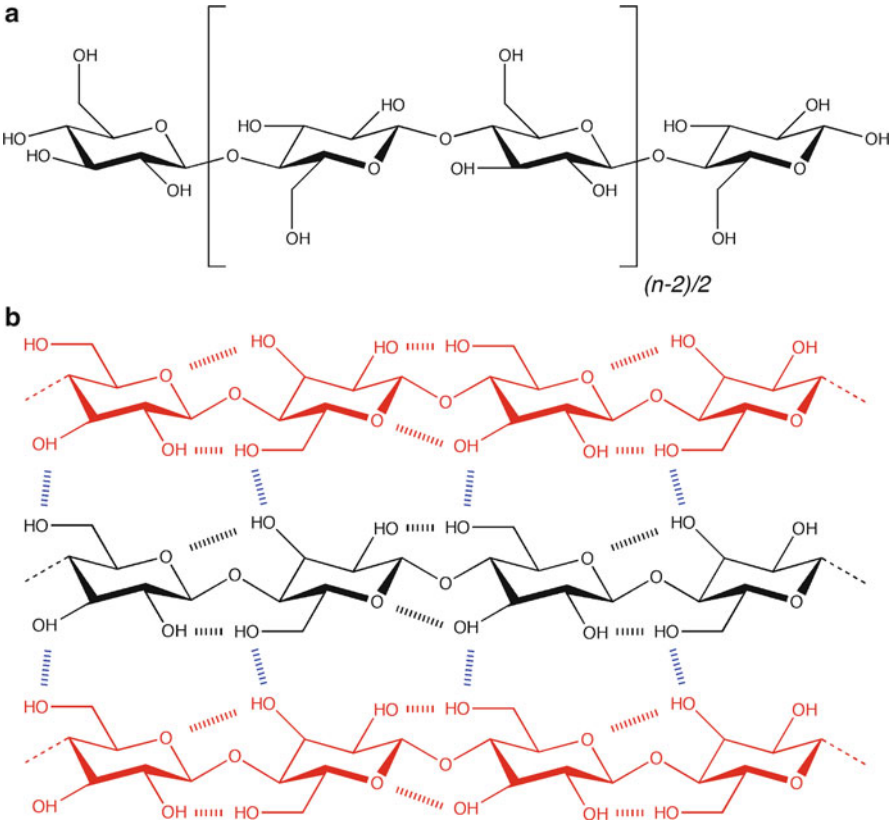

Fig. 1 The structure of cellulose. (**a**) Covalent structure of a cellulose chain (a polymer of 1,4′-β-D glucose) with *n* glucosyl residues. The repeating structural unit can be thought of as $[n-2]/2$ units of the disaccharide cellobiose (shown in *brackets*) with a terminal nonreducing sugar (*left*) and a terminal reducing sugar (*right*). (**b**) A model for the noncovalent structure of cellulose. Structural features of the Iα [53] form are represented. Strands are alternately colored *black* and *red*; intrastrand hydrogen bonds are represented using hashed bonds of the same color. Interstrand hydrogen bonds are represented using *blue* hashed bonds.

bonds of lignin [32]. These enzymes have been the subject of intense study, as they provide a potential means to saccharify lignocellulosic biomass on a large scale, much as α-amylases are used industrially in the saccharification of corn starch in ethanol production.

At present, the enzymes that degrade lignocellulose are the major roadblock to using cellulosic biomass as a cheap feedstock for biofuel production. One problem is that, compared with corn starch and cane sugar, lignocellulose is chemically diverse and highly heterogeneous, requiring a large variety of enzymes to be included in the saccharification process, as well as energy-intensive mechanical and chemical pretreatments to reduce its recalcitrance to enzymatic digestion. As described below, even without lignin and hemicellulose, pure cellulose can be highly

heterogeneous in its noncovalent architecture, and thus, in its reactivity. Nonetheless, substantial quantities of a variety of enzymes can now be produced (and are commercially available) to bring about nearly full conversion of the cellulose and hemicellulose portions of lignocellulose to sugars. The limiting factor is the cost of these enzymes. The cost problem is not likely to be solved by modifying current methods to make current enzymes more cheaply. Rather, progress is likely to be made by creating new enzymes that have higher activity against rigid cellulosic structures and that withstand the long incubation times and relatively harsh conditions needed for saccharification.[1]

This chapter explores on the enzymes used to degrade cellulosic biomass, as well as efforts to modify these enzymes to increase activity, and thus, decrease cost of biofuel production. We focus exclusively on cellulose and cellulose-degrading enzymes ("cellulases"). First we will describe the basic features of the enzymes that degrade cellulose, their sequence and structural features, and their higher order structure. Then we will give an overview of the types of cellulose used in laboratory assays, and the types of assays used to measure activity. We will then turn to studies that have sought to increase activity of cellulase, both at the level of individual catalytic domains, and by identifying and optimizing higher order "synergism" between catalytic domains, both in *trans* and in *cis*. Due to space limitations, only a representative set of results is discussed here. The reader is urged to see reviews by Zhang & Lynd [84], and a recent text devoted to biomass deconstruction [32], for additional information.

2 Catalytic Domains of Cellulases

Because of the importance of enzymes in industrial degradation and modification of cellulosic materials, a large number of cellulases have been identified and characterized. As with many areas of biochemical research, early studies involved isolation, purification, and characterization of activities of cellulose-degrading enzymes from natural sources (bacteria, fungi), with gene sequencing following these isolation procedures in a one-to-one pace. Results from these early studies set the stage to characterize a large number of cellulases, with different structures, sequences, and activities.

With the emergence of large-scale genome sequencing, and substantial application (supported by the US Department of Energy) to the genomes of biomass-degrading microbes, the number of putative cellulase sequences has grown much more quickly than biochemical characterization studies. Thus, there is a rich database of sequences

[1]Enzyme inactivation can result from a variety of irreversible processes, such as nonspecific adsorption to substrate, aggregation related to unfolding, and covalent chemical modification. These irreversible processes are favored by the relatively harsh conditions (high temperature and/or acidic or alkaline pH) used for pretreatments that increase digestibility.

that may have potentially useful activities. Thanks to the early (and ongoing) studies that connect biochemical activity to sequence and structure, many of these putative cellulase sequences can be grouped, based on primary sequence, into "families" and "clans" with similar folds and evolutionary origin. However, as will be discussed, this grouping is not sufficient to predict activity and substrate specificity. Here, different levels of classification will be discussed, along with their relative merits and/or shortcomings. Although we cannot yet predict function in full detail from primary sequence, structure, and/or taxonomy, the wealth of data and analysis in all three of these areas provides a good starting point.

2.1 Classification by Enzyme Classification (EC) Number

Before describing classification schemes, it is worth describing the different enzymatic activities of cellulases, as it is these properties one seeks to clearly define and delineate in a classification scheme. Indeed, one way to classify cellulases, provided function is known, is directly through the EC number, a classification scheme established and maintained by the International Union for Biochemistry and Molecular Biology (IUBMB; http://www.chem.qmul.ac.uk/iubmb/). EC classifications separate enzymes important for cellulose degradation into three groups. The two EC groups that hydrolyze the glycosidic bonds of cellulose are EC 3.2.1.4 and EC 3.2.1.91. From left to right, the 3 designates the hydrolase enzymes, the 2 further specifies glycosylase enzymes, and the 1 specifies glycosidase enzymes, that is, hydrolyzing O-glycosyl compounds. The 4 specifies endocellulolytic activity, that is, hydrolysis of *internal* (1→4)-β-D-glucosidic linkages in cellulose (Fig. 2a; EC 3.2.1.4 also includes hydrolases that act on lichenin and cereal β-D-glucans). The 91 specifies exocellulolytic activity, that is, hydrolysis of glycosidic bonds at the end of the cellulose chain (Fig. 2b), producing short chain cellooligosacharrides such as cellobiose (two glucose units connected by 1→4-β linkage).

The third group of enzymes important for cellulose hydrolysis are those of the group EC 3.2.1.21. These enzymes, termed β-glucosidases (and sometimes emulsins), hydrolyze the glycosidic bond of cellobiose, releasing β-D-glucose units (Fig. 2c). Thus, these enzymes are necessary to complete the transformation of cellulose to glucose. These enzymes also promote cellulose breakdown by increasing the activity of the exocellulases, which often show product inhibition by cellobiose.

Although the EC system provides a key distinction between the activities of cellulolytic enzymes, there are a few shortcomings of this classification. First, the boundaries between endocellulolytic (EC 3.2.1.4) and exocellulolytic (EC 3.2.1.91) activity are sometimes blurry, as some enzymes show both types of activity [71]. Second, the EC groupings include protein families with entirely different structures and, presumably, differing evolutionary origins [29]. Third, as is described in the following section, there are additional mechanistic differences among cellulases that are not resolved using just two categories.

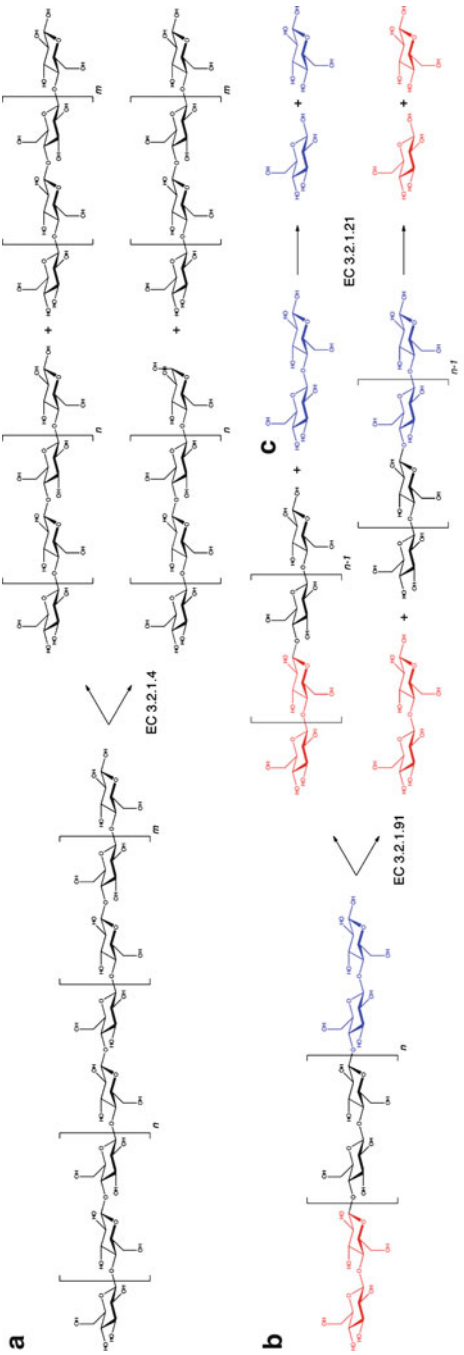

Fig. 2 Enzymatic breakdown of cellulose. (**a**) Reactions catalyzed by endocellulases (EC 3.2.1.4), both with retention (*upper*) and inversion (*lower*) at the anomeric carbon. The endocellulase reaction results in the formation of a new reducing and a new nonreducing end. (**b**) Reactions catalyzed by exocellulases (EC 3.2.1.91) on reducing (*top*) and nonreducing (*bottom*) ends. Both exocellulase reactions produce a new reducing and a new nonreducing end, and a cellobiose molecule. In nonreducing end reactivity, the new reducing end is on the soluble cellobiose product, whereas for reducing-end reactivity, the new reducing end is on the cellulose chain and likely remains part of the insoluble cellulose fiber. (**c**) Reactions catalyzed by β-glucosidases (EC 3.2.1.21). These enzymes (also called emulsins) indirectly accelerate exocellulase activity (**b**) by relieving product inhibition

2.2 Further Subdivision by Enzymatic Properties

The classification above resolves whether catalytic domains of cellulases hydrolyze glycosidic bonds at the end of cellulose chains (exocellulases) or in the middle (endocellulases). An important additional distinction among endocellulases is whether they are processive (binding to a cellulase chain and then hydrolyzing at multiple sites, perhaps in sequence on the chain) or nonprocessive (binding, hydrolyzing a single bond, and releasing). Comparison of multiple crystal structures of cellulases has revealed some of the basis of processivity, along with the basis for endo- vs. exocellulolytic activity (see [84] for a review). It should be emphasized that the type of processivity discussed above relates to individual catalytic domains, since the attachment of CBDs in *cis* is likely to significantly enhance processivity by tethering the enzyme to the substrate, as is the presence of multiple catalytic domains in a single polypeptide chain.

An important subdivision of the exocellulases is whether they attack the reducing end or nonreducing end of the cellulose chain [2]. In many cases, exocellulases produce the disaccharide cellobiose and are appropriately designated "cellobiohydrolases," although many exocellulases also produce longer oligosaccharides such as cellotriose and cellotetraose.

A final mechanistic subdivision that can be made is whether a cellulase cleaves the β-glucosidic bond with retention of chirality at the C1 position (producing the β-anomer) or with inversion (producing the α-anomer). For both mechanisms, cellulases use a pair of acidic (asp/glu) residues in a general acid/general base scheme. Other common features include water attack at the C1 position on the nonreducing side of the glycosidic bond to be cleaved and displacement of the O4-sugar. In the inverting mechanism, the water attacks C1 directly, with one of the acidic residues acting as a general base to abstract a proton from the attacking water, and the other acting as a general acid to protonate the O4 leaving group. In the retaining mechanism, the general base forms a covalent adduct (an ester linkage between the side-chain carboxyl and C1), displacing the O4, with protonation from the general acid. In a second step, water is activated by the general acid (now in its deprotonated conjugate base form), which attacks the C1 and displaces the C1-asp/glu linkage.

2.3 Classification Based on Sequence Features

For cellulases with well-characterized enzymatic properties, a classification scheme could be created that captures the reactivities described above. However, there are a large number of cellulase sequences that have been identified from DNA sequencing that have not been characterized biochemically. To include these new sequences in a classification scheme, and to represent the evolutionary relationships that connect them, a system has been developed [26] and refined [27, 28] that groups like sequences together. This information is available in a searchable database (CAZy, for carbohydrate-active enzyme database; http://www.cazy.org/) that includes

structural, functional, and phylogenetic information [7]. At the time of this writing, CAZy currently subdivides the glycohydrolase sequences (EC 3.2.1.x) into 122 distinct sequence families, designated GH1-GH122 (and 956 additional nonclassified sequences).

The GH families that are tagged with relevant EC numbers for cellulose degradation (EC 3.2.1.4, EC 3.2.1.21, and EC 3.2.1.91) are shown in Table 1. Although there are 21 families that contain one or more members from one of these three EC groups, the bulk of the cellulases are in GH families 5, 6, 7, 8, 9, 12, and 44, 45. GH families 5, 8, 9, 12, 44, and 45 are largely composed of endocellulases (at the exclusion of exocellulases), whereas GH families 6 and 7 include both endocellulases and exocellulases (Table 1); exocellulases in GH-6 act on the nonreducing end, whereas exocellulases in GH-7 act on the reducing end. There do not appear to be GH families composed exclusively of exocellulases. Nearly all β-glucosidases are in GH families 1 and 3.

2.4 *Structural Classification and "Clan" Designations*

On the whole, the sequenced-based groupings do a good job clustering enzymes with like structures and activities (Table 1). However, the presence of multiple activities within single GH families suggests that divergent evolution to new activities is not uncommon.[2] At the same time, structural comparisons show that a number of different GH families have the same fold ([58]; see Table 1, Fig. 3).

This is particularly true for $(\beta/\alpha)_8$-barrels (which can be decorated with additional domains, Fig. 3), $(\alpha/\alpha)_6$-barrels, and β-jelly rolls. It seems likely that the ubiquity of these folds reflect common, albeit more distant, evolutionary origins than are captured in the sequence families. To include structural similarity, a broader "clan" classification has been devised to group GH-families with the same fold ([29], also see [58]). Cellulases in different GH families with similar structures can be grouped into clans A, B, C, K, and M (Table 1). In addition, some GH families that have substantial numbers of characterized cellulases lack structural similarity to other GH families, and thus do not belong to a specific clan.

2.5 *Optimization of the Activity and Stability of Catalytic Domains*

One approach to increasing cellulase activity is to improve the activity of individual cellulase domains through site-directed mutagenesis. Several different parameters

[2] This is particularly notable given that most GH families in Table 1 include numerous enzymes with noncellulolytic activities.

Table 1 Cellulase families, enzymatic, and structural properties

GH family	# seq[a]	# char[b]	EC category[c] 3.2.1.4 (endo)	3.2.1.91 (exo)[e]	3.2.1.21 (β-glc)	R/I/U[d]	Fold	Clan	Formerly
1	2,599	215	0	0	122	R	$(\beta/\alpha)_8$	A	
3	2,763	165	0	0	97	R	$(\beta/\alpha)_8$-α/β-Fn3		
5	2,193	373	245	2	0	R	$(\beta/\alpha)_8$	A	A
6	267	53	18	38 (NR)	0	I	$(\beta/\alpha)_8$		B
7	579	69	25	43[f] (R)	0	R	β-jelly	B	C
8[g]	405	50	25	0	0	I	$(\alpha/\alpha)_6$	M	D
9	664	131	121	3	0	I	$(\alpha/\alpha)_6$		E
10[h]	1,019	205	5	0	0	R	$(\beta/\alpha)_8$	A	F
12	277	62	52	0	0	R	β-jelly	C	H
16[i]	1,614	156	1	0	0	R	β-jelly	B	
18[j]	3,513	372	2	0	0	R	$(\beta/\alpha)_8$	K	
19[k]	1,010	165	1	0	0	I	α[l]		
26[m]	323	40	3	0	0	R	$(\beta/\alpha)_8$	A	I
30	273	21	0	0	1	R	$(\beta/\alpha)_8$	A	
44	45	10	7	0	0	R	$(\beta/\alpha)_8$		J
45	158	42	42	0	0	I	β-barrel		K
48	129	16	5(P)	3 (R+NR)	0	I	$(\alpha/\alpha)_6$	M	L
51[n]	472	44	4	0	0	R	$(\beta/\alpha)_8+\beta^o$	A	
61[p]	152	3	2	0	0	U	β-sandwich		
74[q]	75	14	2	0	0	I	$(\beta_7$ propeller$)_2$		
116	139	3	0	0	1	R	U		

[a]The numbers in each EC column reflect the number of characterized enzymes in a given GH family with that particular activity

[b]The number of sequences in CAZy as of January 13, 2011

[c]The number of characterized enzymes in CAZy as of January 13, 2011

[d]Families with exocellulases are further characterized as acting at the reducing end (R), nonreducing end (NR), or both (R+NR)

[e]Retaining (R), inverting (I), or unknown (U) enzymatic mechanism

[f]Most GH-7 cellobiohydrolases are given generic EC 3.2.1 (glycosidase) numbers rather than EC 3.2.1.91

[g]Many characterized GH-8 enzymes are chitosanases (EC 3.2.1.132)

[h]Nearly all characterized GH-10 enzymes are endo-1,4-β-xylanases (EC 3.2.1.8)

[i]Nearly all characterized GH-16 enzymes are licheninases (EC 3.2.1.73) and β-agarases (EC 3.2.1.81)

[j]Nearly all characterized GH-18 enzymes are chitinases (EC 3.2.1.14)

[k]Nearly all characterized GH-19 enzymes are chitinases (EC 3.2.1.14)

[l]The structures of GH-19 chitinases are single-domain α-helical, although no GH-19 cellulases have been solved

[m]Nearly all characterized GH-26 enzymes are β-mannanases (EC 3.2.1.78)

[n]Nearly all characterized GH-51 enzymes are α-L-arabinofuranosidases (EC 3.2.1.55)
The three solved structures in the GH-51 family (all arabinofuranosidases) include an additional 12-strand β-jelly roll domain

[p]There is only weak evidence for β-endoglucanase activity in the GH-61 family, the structure of which more closely resembles a CBM

[q]Nearly all characterized GH-74 enzymes are xyloglucanases (EC 3.2.1.151)

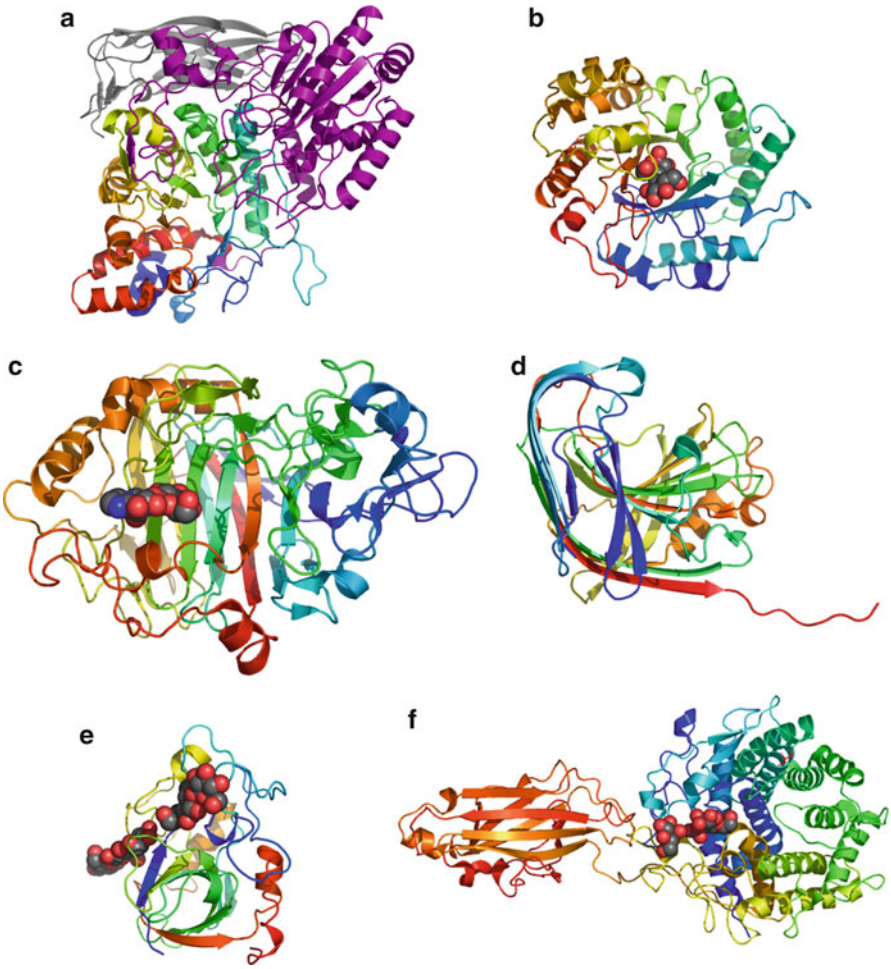

Fig. 3 Cellulase catalytic domain structures. Proteins are depicted as *ribbon diagrams*; colors are *blue* to *red* from N- to C-terminus. Substrates, substrate analogues, and products are rendered as CPK structures. (**a**) A β-glucosidase from the GH-3 family (2x42.pdb; Bgl3B from *Thermotoga neapolitana*), a $(\beta\alpha)_8$-barrel (*rainbow*) and accessory α/β and FnIII domains (*purple* and *gray*, respectively) [57]. (**b**) An endoglucanase from the GH-5 family (1edg.pdb; CelCCA from *Clostridium cellulolyticum*), a $(\beta\alpha)_8$ barrel. (**c**) An exocellulase from the GH-7 family (173w.pdb; Cel7D from *Phanerochaete chrysosporium*), a β-jellyroll [73]. (**d**) An endocellulase from the GH-12 family (3o7o.pdb; CelA from *Thermotoga maritima*), a β-jellyroll [17]. (**e**) An endocellulase of the GH-45 family (4eng.pdb; EGV from *Humicola insolens*), a β-barrel [10]. (**f**) An endocellulase from the GH-9 family (1k72.pdb; Cel9G from *C. cellulolyticum*), an $(\alpha/\alpha)_6$-barrel [44]. Images were generated using MacPyMOL [12]

can be optimized, including kinetic parameters (analogous to K_m and k_{cat}), specificity, processivity, susceptibility to product inhibition (and even substrate inhibition through nonproductive binding), thermostability, solvent/cosolvent compatibility, expression level, cellular localization, and relatedly, enzyme half-life. In the right

context, changes in any one of these parameters could lead to increased activity, and thus, decreased enzyme cost.

Strategies for mutagenesis include introduction of single-site substitution, guided either by structure or homology, random mutagenesis, loop deletion/insertion, and creation of chimeric catalytic domains by recombination of fragments from different genes. Changes in activity have been identified from simple biochemical isolation and characterization of single-site variants (reviewed in [65, 75]); alternatively, selection and directed evolution strategies have also been used to more rapidly explore sequence space (reviewed by Zhang et al. [81]).

One set of studies that illustrates the guided or rational (as opposed to random) mutagenesis approach involves a set of GH-12 homologues [63]. Mutations were identified from structure, sequence comparison, and homology modeling. In one approach, single-residue substitutions were identified as candidates to increase thermostability, based on the known stabilities of different homologues. A second approach involved making a multiple sequence alignment and changing the sequence towards the consensus. These approaches led to significant enhancement of thermostability of the less stable enzymes, in one case, increasing the T_m by around 7°C with a single alanine to valine substitution [63]. Although this approach is less likely to increase the stability of the most thermostable homologues, given the variation in activity among these enzymes, this approach provides a route to enhancing particular enzyme activities.

In a broader approach, modular structural elements from three CBII exocellulases (from the GH-6 family) were randomly recombined and were screened for expression and activity. This approach generated a large number of active, sequence-divergent recombinant enzymes. By correlating resistance to thermal inactivation with module identity, a second generation of highly thermotolerant enzymes were produced [23]. More recently, the same approach has been applied to CBH1 exocellulases from the GH-7 family [24].

3 Properties of Cellulosic Substrates

There are a large number of cellulosic substrates that are used in the laboratory to assay cellulase reactivity (Table 2). Cellulose is synthesized by plants, and some algae, bacteria, and fungi. In plants, cellulose microfibrils may be covered by hemicellulose polymers and lignin matrices [69]. Cellulose chains from plant fibers typically have a degree of polymerization (DP) of 300–10,000 glucosyl subunits [37]. Although direct assay of deconstruction of native lignocellulosic materials such as corn stover and sugarcane bagasse would be ideal for large-scale biofuel production, cellulase activity is more easily studied using simpler substrates that are enriched in the cellulosic fraction. Moreover, it is often preferable to perform cellulase assays with substrates that have been modified (either noncovalently or covalently) to enhance accessibility, uniformity, or solubility. The substrates listed in Table 2 are commercially available or can be prepared from commercial material by simple pretreatment steps.

Table 2 Cellulosic substrates used in laboratory assays of cellulase activity

	DP[a]	CR[b]	Assay[c]
Soluble substrates			
Carboxymethyl cellulose, CMC (–CH_2COOH)	400–3,200	0	End
Dyed CMC (e.g., Remazol Brilliant Blue-CMC)	400–3,200	0	End
Hydroxyethylcellulose, HEC $(CH_2CH_2OH)_n$	300–4,800	0	End
Dyed HEC (e.g., Ostazin brilliant red H3-HEC)	300–4,800	0	End
Cellodextrins	2–6	0	End, Exo, β-Gluc
Isotope-labeled cellodextrins	2–6	0	End, Exo, β-Gluc
4-Methylumbelliferyl oligosaccharides	2–6	0	End, Exo, β-Gluc
p-Nitrophenyl oligosaccharides	2–6	0	End, Exo, β-Gluc
Insoluble substrates			
Crystalline			
Whatman No. 1 filter paper	750–2,800[d]	53–90[e]	End, Exo
Avicel PH	<350	57–92[e]	End, Exo
Bacterial cellulose	2,000–8,000[f]	88[f]	End, Exo
Bacterial microcrystalline cellulose, BMCC	<10 to >1,000[g]	73–95[e]	End, Exo
Dyed Avicel (e.g., Remazol Brilliant Blue-Avicel)	<350	57–92[e]	End, Exo
Amorphous			
Phosphoric acid swollen cellulose, PASC	<350	0[d]–27[e]	End, Exo
Regenerated amorphous cellulase, RAC	<350	0[h]	End, Exo

End endocellulase; *Exo* exocellulase; *β-Gluc* β-glucosidase activity
[a]DP, degree of polymerization
[b]CR, crystallinity (percentage)
[c]Assay, type of activity most easily measured with a given substrate
[d]Data from Zhang et al. [81]
[e]Data from Park et al. [55]
[f]Data from Valjamae et al. [74]
[g]Data from Stalbrand et al. [67]
[h]Data from Zhang et al. [82]

3.1 Soluble Substrates

Although cellulose is insoluble in water because of its strong interchain interactions (Fig. 1b), single chains of cellulose can be solubilized by chemical modification of the hydroxyl groups, typically through reaction with alkyl chlorides to produce ether linkages. Carboxymethylcellulose (CMC), one of the most commonly used water-soluble substrates, results from reaction with chloroacetic acid. CMC has an overall negative charge at neutral pH, with charge density depending on the degree of substitution (DS). CMC preparations (as sodium salts) with a DS ranging from 0.7 to 1.2 substitutions per glucose unit are commercially available.

Because CMC is soluble, it is very easy to work with. However, in terms of informing on degradation of complex cellulosic substrates, it is probably least relevant.

Degradation of complex substrates requires interaction with the cellulose surface, and gaining access to individual chains that have strong surface interactions. CMC lacks these interfacial interactions. Moreover, since carboxymethylation is likely to impede substrate binding, only the subset of glycosidic bonds that lack modification are likely to be reactive.[3] Enebro et al. used liquid chromatography and mass spectrometry to determine the products of digestion of CMC by four different endocellulases. This study revealed differences among the four enzymes in tolerance to the number of substitutions in the binding region, the location of the substitution within the subunit, and the location of the substituted subunit relative to the cleavage site [13]. Assays with CMC show more reactivity with endocellulases than with exocellulases. This is likely a result of the decreased enzyme reactivity toward modified sites: endocellulases should be able to react with all internal sites with low modification, whereas exocellulases can only proceed from the end to the nearest site of high modification. One advantage of CMC as a stubstrate is that its strongly length-dependent viscosity provides a means to determine whether a cellulase has endolytic or exolytic properties.[4]

Another modified form of cellulose, hydroxyethylcellulose (HEC), has ether linkages between the hydroxyl groups and CH_2CH_2OH moieties. HEC is also soluble, although unlike CMC, it is uncharged; thus, a higher DS is needed to achieve water solubility than for CMC [42].

Water solubility is also achieved for very short unmodified cellulose oligosaccharides. These short chains, which are collectively referred to as "cellodextrins," range from two (cellobiose) to six (cellohexaose) glucosyl units. Cellodextrins are substrates for endoglucanases, exoglucanases, and β-glucosidases. Because of their small size, cellodextrins can be modified with greater chemical precision than long cellulose polymers. Substituted variants such as *p*-nitrophenyl oligosaccharides [77] and 4-methylumbelliferyl oligosaccharides [43] are used for spectroscopic assays of cellulase activity (see below). Isotopically labeled cellodextrins can be used to assay cellulase activity by mass spectrometry [2].

3.2 Insoluble Substrates

In general, cellulase activities measured using insoluble substrates are more likely to be relevant to large-scale biomass deconstruction than chemically modified, soluble chains. A variety of different insoluble substrates are used to measure cellulase activities. These substrates differ in their biological sources and pretreatment methods,

[3] Since modification is likely to be somewhat random, the odds of getting a block of i unmodified sugars in a row is nonzero, but it is likely to be quite small. Assuming each of the three hydroxyls per anhydroglucose are equally reactive and that their reaction does not influence reactivity of proximal hydroxyl groups, the probability is $(1-0.7/3)^3 i = 0.67^3 i$. For $i=3$, this is 0.09, and drops by a factor of 0.45 for every additional unmodified anhydroglucose.

[4] Endocellulase activity should strongly decrease the viscosity of CMC solutions by greatly decreasing chain length, whereas exocellulase activity should have little effect on viscosity.

and as a result, they have different structural and physical properties (Table 2). As a result, different substrates are more appropriate for different types of enzymes.

By pretreatment with acid (typically phosphoric acid), insoluble cellulose preparations can be obtained that have decreased crystallinity, and thus are typically more susceptible to enzymatic digestion than crystalline substrates [22]. Although published protocols differ in subtle but important ways, high concentrations of phosphoric acid can produce PASC (for phosphoric acid swollen cellulose, [78]). By prehydrating Avicel prior to acid treatment, Zhang et al. prepared an amorphous cellulose of even higher reactivity, which they term regenerated amorphous cellulose (RAC, [82]).

Cellulose substrates with high crystallinity include bacterial cellulose (BC), which has high DP values of 2,000–8,000, and a high 60–90% crystallinity index [37]. Microcrystalline cellulose, or "Avicel" PH, which is prepared by acid hydrolysis of wood pulp, has a lower DP value (150–300) [37], although it retains a high level of crystallinity. Because it has a high ratio of free ends to accessible β-glucosidic bonds due to its lower DP, Avicel is especially suited for the measurement of exoglucanase activity from a crystalline substrate [82]. Finally, Whatman No. 1 filter paper, manufactured from cotton linters, is highly heterogeneous and is often used for measuring total cellulase activity.

4 Cellulose Degradation Assays

Over the years, a large number of assays have been developed that report on cellulase activity. Most assays are quantitative, although many of these do not evaluate activity in real-time, but require postprocessing of digests at fixed time points, limiting the extent to which these assays allow kinetic data to be interpreted using mechanistic models (for example, models including Michaelis–Menten terms, processivity, prebinding, and diffusion). This type of treatment is further limited by the heterogeneity of various cellulosic substrates, and to time-dependent enzyme inactivation that is sometimes observed (especially with insoluble substrates). Other qualitative assays have been developed to screen for activity in live cells. Such screens have the potential to allow large numbers of engineered cellulases to be assayed quickly, without having to purify each protein. In this section, we briefly touch on different assays for activity, highlighting strengths, weaknesses, and when relevant, relative sensitivities to exocellulolytic vs. endocellulolytic activity. For a comprehensive description of different cellulase assays, see a review by Zhang, Himmel, and Mielenz [81].

4.1 Spectroscopic Assays

One of the most common approaches to measuring cellulase activity involves monitoring spectroscopic changes resulting from product formation or substrate

depletion. Some of these assays involve covalent attachment of a probe that changes its absorbance (or fluorescence) when released from cellulose. Other assays involve the addition of colorimetric reagents that react with product to produce an absorbance change. The easiest of these assays takes advantage of the reactivity of the reducing end of cellulose. The reducing end is in equilibrium with an aldehyde, which can reduce a chromogenic substrate. Each time a glycosidic bond is hydrolyzed, a new reducing end is produced, regardless of enzyme type (endo- vs. exocellulase vs. β-glucosidase).

Two methods to detect reducing end formation are the dinitrosalicylic acid (DNS) and the Nelson-Somogyi assays. In the DNS assay, oxidation of the reducing-end aldehyde to a carboxylic acid is coupled to the reduction of DNS to 3-amino-5-nitrosalicylic acid [45] [19]. Because this redox reaction requires elevated temperatures (typically 100°C) and high pH, the color must be developed as an end-point to the reaction, limiting the degree to which time-course of the reaction can be sampled. Another drawback in the DNS assays is a rather low sensitivity, due in part to the high absorbance of unreacted DNS. Sensitivity can also be adversely affected by buffer conditions and the presence of metals, and in some cases, the degree of cellulose polymerization [59].

In the Nelson-Somogyi assay, reducing sugar oxidation is coupled to a Cu^{2+} reduction to Cu^{1+}. In a subsequent step, Cu^{1+} is oxidized back to Cu^{2+} by an arsenomolybdate complex that becomes colored upon reduction [66]. Unlike the DNS method, the Nelson-Somogyi method depends neither on the substrate concentration nor on the degree of polymerization. However the Nelson-Somogyi assay is also sensitive to composition and to the nature of the substrate. The Nelson-Somogyi assay has higher sensitivity than the DNS assay, but is more cumbersome [6]. Both the DNS and Nelson-Somogyi assays can be performed on a variety of cellulosic substrates, including soluble substrates and insoluble amorphous and crystalline material. A number of additional colorimetric assays have been used to monitor cellulase activity [81].

Direct labeling methods to monitor cellulase activity include labeling of long-chain insoluble cellulose polymers with dyes such as azure [38] and fluorescein; hydrolysis is monitored by determining the amount of dye released into the soluble phase. By casting dyed cellulose films on the bottom of microtiter plates, this approach can be used to screen activity in a high-throughput format [25]. Short, water-soluble cellodextrins can also be labeled with spectroscopic probes (e.g., *p*-nitrophenyl [78]; 4-methylumbelliferyl [43]). These short-chain derivatives are useful for measuring β-glucosidase activity. β-glucosidase activity can also be assayed by monitoring the formation of free glucose, using coupled enzyme detection [83]; colorimetric assay kits are commercially available.

4.2 Viscometric Assays

Soluble cellulose chains (CMC and HEC) are long polymers, and thus in solution they act as strong viscogens. Upon endocellulase cleavage of these polymers into

shorter fragments, the viscosities of CMC and HEC solutions decrease as digestion progresses [14, 21]. Viscosity changes can easily be measured by using a vertical capillary tube (such as an Ostwald viscometer) to measure the time it takes for the solution level to fall a fixed distance into a reservoir. By repeating the measurement at different times, a time-resolved progress curve can be determined. Alternatively, viscosity can be measured with a rotating disc rheometer, which can be interfaced to a computer to give real-time measurements. Because exocellulases shorten cellulose chains by only two glucoside units per enzyme cycle, and because they are likely to be blocked after only a few steps by chemical modification, exocellulases produce very little change in viscosity. Thus, by comparing activity viscometrically and colorimetrically, exo- and endocellulolytic activity can be resolved [68].

4.3 Chromatographic Assays

Direct detection of low-molecular weight cellulose degradation products can be carried out by HPLC (high pressure liquid chromatography). Oligosaccharides of different length can be resolved and quantified by size exclusion chromatography [18]. Monosaccharides of different covalent structure (xylan, mannan, arabinose, etc.) can be resolved by ligand exchange chromatography, wherein the hydroxyl groups from the sugars interact specifically with resin-immobilized cations (Pb^{2+}, Ca^{2+}). Specificity is imparted by differences in the orientation of hydroxyl groups from sugar to sugar [36]. Although carbohydrates tend to have low extinction coefficients, they can readily be detected with an in-line refractometer, which provides high signal to noise. Spectrophotometric detection of labeled sugars has also been used, and depending on the site of labeling, can provide information relating to the specificity and mechanism of degradation. Thin layer chromatography (TLC) also allows cellulose degradation products (particularly, short oligosaccharides) to be resolved. Sugars can be detected by reacting reducing sugars with a colorimetric reagent directly on the TLC plate [20, 85].

4.4 Other Physical Assays

In addition to the assays above (colorimetry, viscometry, and chromatography), there are several other physical methods that have been used to quantify breakdown. While most of these methods have seen limited use, they have the advantage that they can directly monitor breakdown in real time. One particularly interesting approach is time-resolved isothermal batch calorimetry [51, 54]. Slurried cellulosic substrates are prepared, and enzymatic degradation is monitored by heat release as a function of time. In addition to following hydrolysis in real time, this method is well-suited for complex substrates (e.g., corn stover). Another real-time method for monitoring cellulose degradation is direct determination of mass-decrease from immobilized cellulose using a quartz crystal microbalance [35].

4.5 Plate Assays and Live-Cell Assays

In protein engineering applications, it is often desirable to use a screen that is qualitative, so that a small number of active enzymes (or enzyme combinations) can be resolved from a large background of inactive enzymes. Several methods can be used to screen colonies for cellulose degradation activity (reviewed in [60]). One of the most common plate screening methods uses celluloses with tightly bound dyes and fluorophores. Congo red dye interacts tightly with β-1,4-D-glucans including chemically modified carboxymethyl cellulose (CMC). Because CMC is large and does not diffuse in agar, CMC-bound dye will remain uniformly immobilized in the absence of cellulase activity. Cellulose hydrolysis releases the dye; subsequent diffusion results in a dye-free halo around colonies expressing active cellulase. The halo radius gives a semiquantitative indication of activity. In a similar approach, unlabelled soluble cellulose (e.g., CMC) can be included in the agar, and after incubation to allow for colony growth and cellulase activity, the remaining CMC is precipitated on the plate using ethanol, acetone, or cetylammonium bromide (CTAB). Precipitated CMC renders the plate opaque; colonies expressing active cellulase can be identified as having a clear halo [60].

Alternatively, cellulase activity can be selected for using agar plates in which the only source of carbon is cellulose. This approach requires both high purity cellulose (organic contaminants may provide an alternative carbon source) and a uniformly high DP (contaminating cellodextrins would also short-circuit the selection). This approach has also been used in liquid culture to select for yeast strains producing active cellulases on their surface. An advantage of this method is that saccharification products can be directly fermented by the yeast to produce ethanol, a process referred to as "consolidated bioprocessing" [18, 40, 72].

5 Synergy and Processivity as a Means for Efficient Cellulose Breakdown

Although many individual catalytic domains show measurable activity against cellulose, their activities are rather low. On their own, they would be poor catalysts for large-scale biofuel production. In nature, there are two ways that reactivity is enhanced. First, multiple different types of cellulases (endocellulases, exocellulases, β-glucosidases, as well as hemicellulases and lignases) are coordinately expressed, producing a synergistic enhancement of activity (Fig. 4; [76]).

Second, catalytic domains are attached (either covalently or noncovalently) to cellulose-binding modules (CBMs; see [5] for a review), which localizes enzyme activity to the cellulosic substrates, allowing for multiple rounds of hydrolysis (Fig. 5). In aerobic bacteria and fungi, this is achieved in *cis* by direct fusion of CBM-coding and catalytic domain-coding sequences in cellulase genes (Fig. 5b).

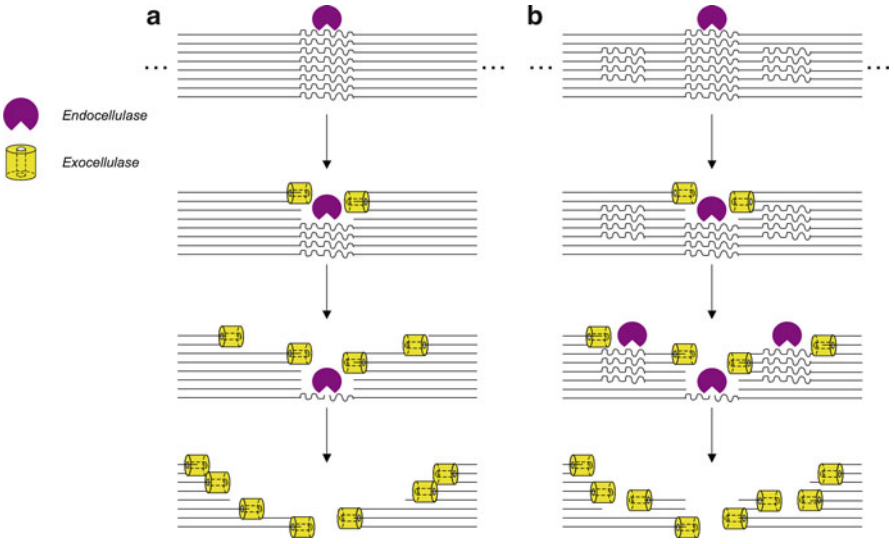

Fig. 4 Mechanistic models for synergy in *trans* between endocellulases (*purple circles*) and exocellulases (*yellow cylinders*). *Straight lines* represent crystalline domains of cellulase; *wavy lines* represent amorphous regions, where endocellulase accessibility and activity should be enhanced. Degradation of these amorphous regions by endocellulases produces new reducing and nonreducing ends that can be degraded by exocellulases (**a**), enhancing their reactivity. When exocellulase activity exposes internal amorphous regions (**b**), these regions can serve as additional sites for endocellulase degradation. Although not shown here, β-glucosidases can further enhance reactivity by relieving product inhibition of exocellulases, which in turn may further enhance endocellulase activity through the mechanism shown in (**b**). Likewise, lignases and hemicellulases can enhance the activity of cellulases by providing access to cellulose sites that would otherwise have been inaccessible (not shown)

In addition to enhancing activity by tethering to substrate surfaces, these accessory domains can directly enhance activity by providing structural integrity to the catalytic domain.

In anaerobic bacteria, particularly in the Clostridium genus, a strategy is used that incorporates both modes of enhancement. Although most catalytic domains in these bacteria are not covalently fused to CBMs, they are chained together noncovalently to molecular scaffolds at the cell surface, structures referred to as "cellulosomes" (Fig. 5c; [3, 39]). This is achieved by fusion of cellulases to domains called "dockerins." Dockerins bind tightly to domains called "cohesions," which are repeated in multiple copies in proteins called "scaffoldins." By attachment of multiple scaffoldins to the cell surface, a highly dendritic structure of different catalytic domains can be produced. Because scaffoldins often contain terminal CBMs, the cellulosome directly attaches the bacterium to the cellulosic substrate, ensuring a high local concentration of complementary catalytic domains at its surface.

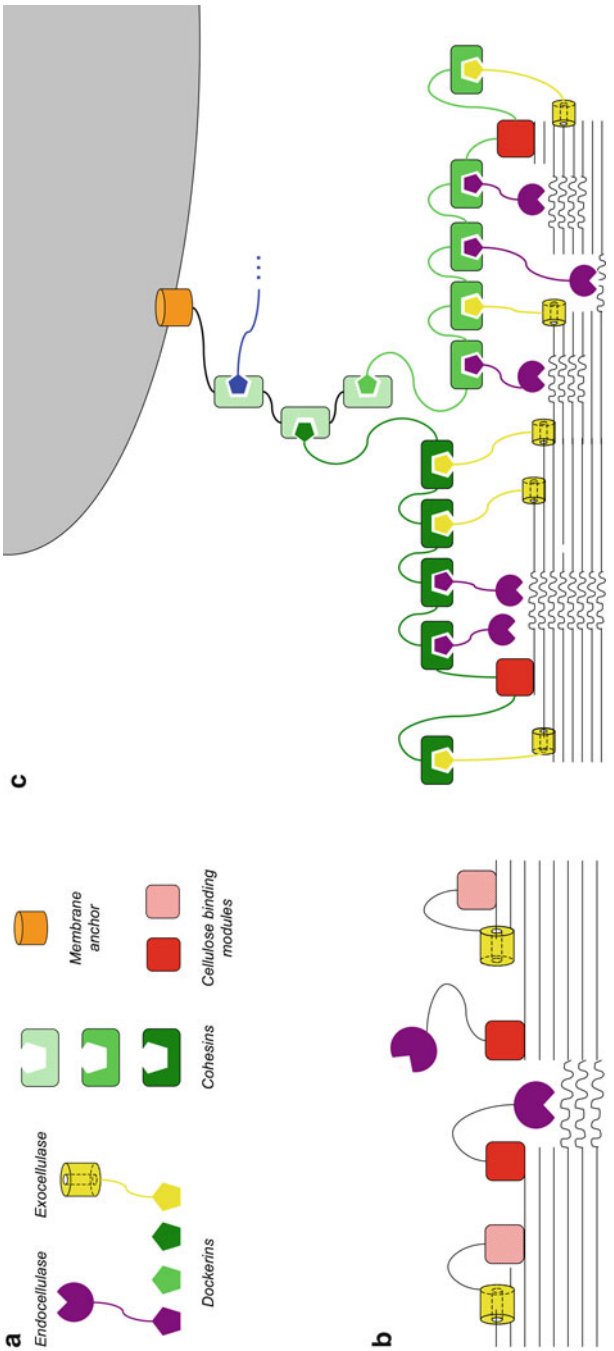

Fig. 5 Biological strategies for microbial enhancement of cellulose degradation. (**a**) Domains involved in cellulose degradation. Different colors represent different sequences. Cellulase catalytic domains are shown fused to dockerins, as in the cellulosomal strategy. (**b**) Noncellulosomal strategy, used by aerobic bacteria and fungi. Fusion of cellulase catalytic domains to cellulose-binding modules (CBMs) localizes enzymatic activity at the cellulose surface. (**c**) Cellulosomal strategy used by anaerobic bacteria. A primary scaffoldin carrying multiple cohesin domains is attached to the bacterial surface through an SLH membrane anchor. Secondary scaffoldins bind multiple cellulase catalytic domains that are fused to dockerin domains; dockerin–cohesin interactions are also used to attach these secondary scaffoldins to the primary scaffoldin. CBMs in the secondary scaffoldin anchor the cellulosome (and thus, indirectly, the bacterium) to the cell surface

5.1 Quantitative Definition of Synergy

The idea behind synergy is quite simple—a mix of enzymes is more active than the enzymes are on their own. In general, a synergy factor can be represented as the ratio of the activity of the mixture to that of the separate enzymes:

$$\mathrm{SF} = \frac{\alpha_{\mathrm{mix}}}{\sum_{i\,\mathrm{enzymes}} \alpha_i} \tag{1}$$

where α_{mix} is a representation of activity of the mix, and the denominator gives the sum from separate enzyme reactions. But the details of how this ratio is constructed (specifically, the form of α) can be somewhat tricky, especially when comparing synergy in *trans* with that in *cis*.

Enzyme activity is typically represented as the amount of product formed in a given interval of time, when a given amount (on a number scale, i.e., moles, picomoles, etc.) of enzyme is present. This type of "specific" activity (which will be referred to as $\overline{V}_i$, reflecting velocity) permits comparison of different enzymes without worrying about their concentrations. But when there are multiple enzymes together, what are the appropriate velocities? This is important for forming both the numerator and the denominator of (1). For the numerator, what enzyme concentration should be used? For the denominator, how should the activities be weighted? If there is very little of one enzyme, it should make a small contribution to product formation, even if it has a high specific activity. For the denominator of (1), the expected (nonsynergistic) total activity (moles of product produced per unit time) is the mole-weighted sum of the activity of each enzyme:

$$V_{\mathrm{total}} = \sum_{i\,\mathrm{enzymes}} n_i \times \overline{V}_i = \sum_{i\,\mathrm{enzymes}} V_i \tag{2}$$

where n_i is the number of moles of enzyme i present. In other words, the expected nonsynergistic value is the sum of the total activities of each separate enzyme (not adjusted for the amount of enzyme present). While this sum is useful for comparison to the actual activity of a mixture, it does not convey the same catalytic power as a specific activity. A quantity analogous to specific activity can be recovered by dividing the total velocity by the total number of moles of the i enzymes present:

$$\overline{V}_{\mathrm{total}} = \frac{\sum_{i\ enzymes} V_i}{\sum_{i\ enzymes} n_i} = \sum_{i\,\mathrm{enzymes}} \frac{n_i}{n_{\mathrm{total}}} \times \overline{V} = \sum_{i\,\mathrm{enzymes}} \chi_i \overline{V}_i \tag{3}$$

The right-most sum gives a total expected (nonsynergistic) activity of a mixture of enzymes in *trans* as the mole-fraction-weighted sum of specific activities. To calculate the numerator of (1), the total activity of the mix (V_{mix}, the amount product per unit time) should be divided by the total enzyme concentration (the sum of the moles of all enzymes). In this way, the synergy factor in *trans* becomes

$$\mathrm{SF}_{\mathrm{trans}} = \frac{V_{\mathrm{mix}} / n_{\mathrm{total}}}{\sum_{i\ enzymes} \chi_i \overline{V}_i} \tag{4}$$

A similar expression can be used when multiple catalytic domains are combined in *cis*, either through noncovalent attachment to a scaffold (Fig. 5c) or through covalent attachment in a single polypeptide chain. However, the total number of moles of enzyme (n_{total} in (5)) should count each catalytic domain separately, even though they are on the same molecules. For example, in 1 pmol of a chimeric enzyme with two catalytic domains, there are two $n_{total} = 2$ pmol total of catalytic domains. If the denominator is calculated as in (3), using mole-fraction-weighted specific activities of separate enzymes (in this case, the two mole fractions are 0.5), the resulting synergy factor

$$SF_{cis} = \frac{V_{cis} / n_{total}}{\sum_{i\ enzymes} \chi_i \bar{V}_i} \tag{5}$$

is influenced both by complementary activities that may result among the enzymes and by the effect of covalent attachment. The effects of covalent linkage can be isolated by comparing the specific activity in *cis* to that in *trans* (i.e., SF_{cis}/SF_{trans})

5.2 Examples of Synergy in Trans

As described above, noncovalent structural variation results in heterogeneity in cellulose reactivity, as does variation in reactivity at internal vs. terminal glycosidic bonds. The corresponding differences in reactivity towards different enzymes provide the potential for synergistic enhancements in reactivity among complementary enzymes (Figs. 4 and 5). The presence of hemicellulases further increases the potential for synergy.

Early studies on mixtures of cellulase components of fungi (typically catalytic domains fused with CBMs) demonstrated that some enzyme combinations lead to higher activities than the isolated components, although these synergistic effects often showed complex concentration dependences [4, 61, 79, 80]. These concentration dependences were often interpreted as a mixture of specific and nonspecific binding to insoluble cellulosic substrate, and also of physical formation of multienzyme complexes [79]. Although pairwise synergy in *trans* was established in these early studies, generalities and underlying principles were not.

A number of subsequent studies have confirmed synergy in *trans* between noncellulosomal cellulases and have suggested some general features. One very comprehensive study that demonstrated synergy in *trans* is from David Wilson's group at Cornell [34]. Purified noncellulosomal enzymes from the fungus *Hypocrea jecorina* (the teleomorph to anamorphic *Trichoderma reesei*) and the bacterium *Thermobifida fusca* (formerly named *Thermomonospora fusca*) were assayed separately and mixed in various combinations on a variety of cellulosic substrates. Although for several pairs (particularly endocellulases) the activities did not exceed that expected from a combination of isolated enzymes, other combinations (mostly

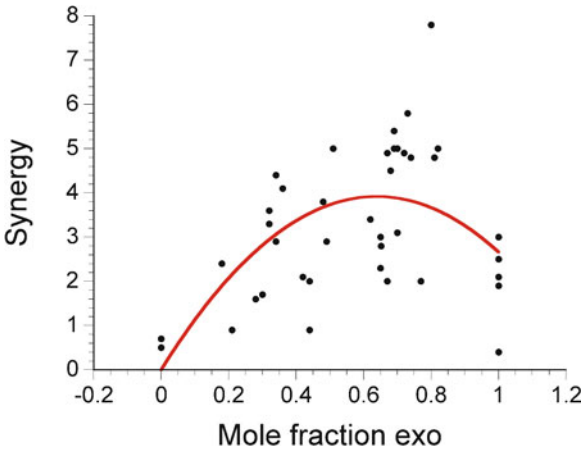

Fig. 6 Synergy in *trans* among a mixture of endocellulases and exocellulases against filter paper. Enzymes are from *Hypocrea jecorina* and *Thermobifida fusca* [34]. Synergy and the mole fraction of exocellulases (χ_{exo}) are as defined in the text ((4) and (6), respectively)

pairs and triples) showed substantial enhancement of activity (i.e., synergy). Synergistic mixtures include combinations of exocellulases and combinations of endocellulases and exocellulases, some of which produced a five- to sevenfold enhancement.

One way to evaluate the relationship between synergy and the endocellulase–exocellulase composition is to represent the mole fraction of exocellulases in a particular enzyme cocktail, i.e.,

$$\chi_{exo} = \frac{\sum [exo]_i}{\sum [exo]_i + \sum [end]_j} \tag{6}$$

Plotting synergistic enhancement vs. χ_{exo} for the data from Wilson's study ([34]; see Fig. 6) reflects the reactivity patterns described above.

Although there is considerable variation in synergy at a given value of χ_{exo}, a general trend can be seen in which activity is maximal around χ_{exo}=0.64, i.e., a 2:1 ratio of exocellulase to endocellulase.

A more recent optimization study of *trans* synergy among the cellulases of a related fungus, *Trichoderma veridi* (an anamorph of *Hypocrea rufa*), against steam-exploded corn stover revealed a similar level of synergy [86]. By using multiple regression techniques in which activities are represented with a combination of linear-, quadratic-, and cross-terms, an optimal χ_{exo} value of 0.64 was determined. Since these two studies used different enzymes, the exact agreement in χ_{exo} between the two studies is likely to be partly coincidental. Nonetheless, it is clear from both studies that synergy is optimized with a mixture of exocellulases and endocellulases, and suggestive that synergy can be maximized by biasing toward exocellulases. This bias has also been seen in earlier studies [52, 70]. However, one study has shown maximal synergy in enzyme mixes biased toward endocellulases [4].

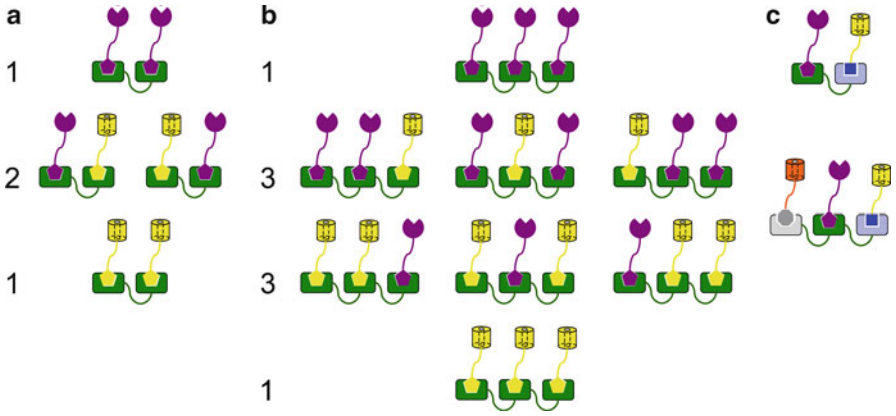

Fig. 7 Approaches to build designer cellulosomes using cellulosomal components. With nonspecific cohesin–dockerin interaction, a random distribution of homomeric and heteromeric species is expected. Even with two different enzymes, a distribution of products is expected (**a**), which increases in complexity with increasing valency (**b**). The distribution of products in (**a**) and (**b**) is given by the binomial distribution (*numbers*, *left*). If different cohesin–dockerin interactions with nonoverlapping specificities are used (**c**), cellulosomes can be designed with defined composition and architecture

5.3 Examples of Synergism in Cis

In addition to the synergistic enhancements seen by combining separate glycohydrolases in solution, synergistic enhancements have been seen when catalytic domains are tethered in a single complex. This enhancement can result from an increased local concentration of each of the enzymes in the complex. Effective concentration enhancements are well-known in physical organic and polymer chemistry and are likely to contribute substantially to cellulosome activity (Fig. 5). As described below, protein engineering efforts have attempted to recapitulate the multivalent architecture of the cellulosome.

Artificial cellulosomes. In the last decade, there have been several efforts to build miniaturized cellulosomes by protein engineering [1, 46–48, 62]. In these studies, the modular recognition domains of natural cellulosomes (cohesins, dockerins, and cellulose-binding modules) are used to make small, well-defined combiations of cellulases. This approach has the potential to leverage the large (and growing) number of cellulase (and hemicellulase) gene sequences available. One difficulty in preparing precisely defined minicellulosomes is that within a given species, the cohesin–dockerin interactions that bind glycohydrolase domains to scaffoldins are nonspecific. Thus, even with only two different cellulases, combination with a pair of tethered cohesin domains will produce a mix of products (Fig. 7). As more cellulases are included in the assembly, heterogeneity becomes even greater.

An elegant solution to this heterogeneity problem combines cohesins of different species of clostridia. By fusing two cohesins from different species (*Clostridium*

thermocellum and *Clostridium cellulolyticum*, which have orthogonal specificity for their species-cognate dockerins), Fierobe, Bayer, and coworkers have built miniature scaffoldins in which each cohesin interacts exclusively with a specific dockerin-containing cellulase [15]. The dockerin domains of different endocellulases from *C. cellulolyticum*, Cel5A and Cel48F, were replaced with homologous dockerin domains from *C. thermocellum*, and in combination with the wild-type *C. cellulolyticum* enzymes, mixtures could be specifically attached to hybrid scaffoldins containing a single CBM. These chimeras showed a synergistic enhancement of two- to threefold against Avicel, depending on which enzymes were combined [15]. By comparing to a hybrid scaffoldin lacking a CBM, the effects of enzyme proximity vs. substrate localization could be evaluated. Although deleting the CBM decreased activity somewhat, a modest (~1.5 fold) synergistic effect remained, suggesting proximity can enhance reactivity, even between endocellulase pairs.

A subsequent study with a larger repertoire of *C. cellulolyticum* endocellulases confirmed these results and showed that, in some cases, synergistic enhancement was as high as sevenfold [16]. As with the smaller set, enhancements resulted both from CBM interactions with substrate and from proximity of catalytic domains, although the relative contribution of these two factors depended on the identity of the catalytic domains. This study also showed that synergy is greatest on recalcitrant substrates with a high degree of crystallinity [16]. In some cases, synergy appears to be dependent on the domain structure of the engineered scaffoldin. For example, it appears that although having a single CBM increases cellulosome activity against insoluble substrates, having multiple CBMs appears to impede activity somewhat, perhaps by limiting the extent to which the enzyme complex can diffuse along the substrate [48].

One important strategy for increasing the reactivity of these minicellulosomes has been to use multivalent cohesin scaffolds to assemble catalytic domains from noncellulosomal sources. The activities of catalytic domains from noncellulosomal bacteria (and from *T. fusca*, in particular) tend to be greater than their cellulosomal counterparts. By fusing dockerin segments from cellulosomal bacteria to *T. fusca* catalytic domains, Wilson and coworkers built minicellulosomes that have significantly elevated reactivity [8].

Other templates. Several other noncellulosomal templates have been used to mimic the tethering effect of the cellulosome. Two studies in particular have used proteins with rotational symmetry to attach multiple cellulases to a single assembly. In one study, a homododecameric ring structure formed by the SP1 protein from the aspen tree was used to array cellulases via the cohesin–dockerin interaction [30]. By fusing the SP1 polypeptide to cohesin from *C. thermocellum*, and combining these ring structures with a second fusion of a cognate dockerin to the Cel5A endocellulase catalytic domain, high molecular weight complexes could be made that were active against CMC and showed a modest amount of synergy (1.5–2×, depending on linker length), compared to the dockerin-Cel5A fusion alone [30].

In a follow-up study, the same authors attached a dockerin-Cel6B exocellulase to the SP1-cohesin rings [50]. Although attachment of 12 Cel6B-dockerin fusions to the ring *decreased* activity, implying antisynergy in *cis*, the addition of

substoichiometric concentrations of a CBM-linked endocellulase (*T. fusca* Cel5A) in *trans* significantly increased activity against both PASC and filter paper. Though the mechanism(s) underlying this synergistic effect is unclear, the study is significant in that it demonstrates an in *cis* synergy (exocellulases attaching to the SP1 ring) that requires a *trans* component (addition of exocellulase-CBM). Though the authors conclude that the optimal exocellulase/endocellulase ratio is around 20:1, which is very different from the ~2:1 optimum described above, it may be that the critical parameter for this optimum is the number of freely diffusible particles with exocellulase activity. Assuming 12 exocellulases bound to each SP1 particle, the ratio of diffusible exocellulase complexes to endocellulase polypeptides is about 2:1 at this optimum.

In a second templating approach, cellulase domains were attached, via dockerin–cohesin interaction, to an 18 subunit archaeal type-II chaperonin, the rosettasome [49]. By circularly permuting the gene encoding the β-subunit of the rosettasome and fusing the new C-terminus to a cohesin module from *C. thermocellum*, the authors were able to assemble double-rings with nine subunits each, as assessed by electron microscopy. By adding mixtures of up to four different dockerin-containing cellulases from *C. thermocellum*, they were able to purify complexes that appear to be fully saturated with cellulases. These complexes, which the authors term "rosettazymes," show synergistic activity against Avicel in *cis*. This *cis* synergy is greater for mixtures of enzymes, especially those containing both exo- and endocellulolytic activity [49]. The authors point out that the high multivalency of the rosettazyme fusion permits very complex combinations of enzymes to be assembled, including complexes with 18 different enzymes. However, it should be kept in mind that without a high level of specificity to address each different enzyme to a unique site on the template, such complexes would be a very tiny fraction of the astronomical number of combinations of different enzymes that can be bound.

References

1. Arai T et al (2007) Synthesis of *Clostridium cellulovorans* minicellulosomes by intercellular complementation. Proc Natl Acad Sci U S A 104(5):1456–1460
2. Barr BK et al (1996) Identification of two functionally different classes of exocellulases. Biochemistry 35(2):586–592
3. Bayer EA et al (2004) The cellulosomes: multienzyme machines for degradation of plant cell wall polysaccharides. Annu Rev Microbiol 58:521–554
4. Beldman G et al (1988) Synergism in cellulose hydrolysis by endoglucanases and exoglucanases purified from *Trichoderma viride*. Biotechnol Bioeng 31(2):173–178
5. Boraston AB et al (2004) Carbohydrate-binding modules: fine-tuning polysaccharide recognition. Biochem J 382(pt 3):769–781
6. Breuil C, Saddler JN (1985) Comparison of the 3,5-dinitrosalicylic acid and Nelson-Somogyi methods of assaying for reducing sugars and determining cellulase activity. Enzyme Microb Technol 7(7):327–332
7. Cantarel BL et al (2009) The Carbohydrate-Active EnZymes database (CAZy): an expert resource for glycogenomics. Nucleic Acids Res 37(database issue):D233–D238

8. Caspi J et al (2008) Conversion of *Thermobifida fusca* free exoglucanases into cellulosomal components: comparative impact on cellulose-degrading activity. J Biotechnol 135(4):351–357
9. Charles D (2009) Biofuels. Corn-based ethanol flunks key test. Science 324(5927):587
10. Davies GJ et al (1996) Structure determination and refinement of the *Humicola insolens* endoglucanase V at 1.5 A resolution. Acta Crystallogr D Biol Crystallogr 52(pt 1):7–17
11. Deguchi S, Tsujii K, Horikoshi K (2006) Cooking cellulose in hot and compressed water. Chem Commun 31:3293–3295
12. DeLano WL (2003) MacPyMOL: PyMOL enhanced for Mac OS X. DeLano Scientific, Palo Alto
13. Enebro J et al (2009) Liquid chromatography combined with mass spectrometry for the investigation of endoglucanase selectivity on carboxymethyl cellulose. Carbohydr Res 344(16):2173–2181
14. Eriksson KE, Hollmark BH (1969) Kinetic studies of action of cellulase upon sodium carboxymethyl cellulose. Arch Biochem Biophys 133(2):233
15. Fierobe HP et al (2001) Design and production of active cellulosome chimeras. Selective incorporation of dockerin-containing enzymes into defined functional complexes. J Biol Chem 276(24):21257–21261
16. Fierobe HP et al (2002) Degradation of cellulose substrates by cellulosome chimeras. Substrate targeting versus proximity of enzyme components. J Biol Chem 277(51):49621–49630
17. Forse GJ et al (2011) Synthetic symmetrization in the crystallization and structure determination of CelA from *Thermotoga maritima*. Protein Sci 20(1):168–178
18. Fujita Y et al (2002) Direct and efficient production of ethanol from cellulosic material with a yeast strain displaying cellulolytic enzymes. Appl Environ Microbiol 68(10):5136–5141
19. Ghose TK (1987) Measurement of cellulase activities. Int Union Pure Appl Chem 59(2):257–268
20. Gilad R et al (2003) CelI, a noncellulosomal family 9 enzyme from *Clostridium thermocellum*, is a processive endoglucanase that degrades crystalline cellulose. J Bacteriol 185(2):391–398
21. Graça MAS, Bärlocher F, Gessner MO (2005) Methods to study litter decomposition: a practical guide. Springer, Dordrecht, p 329
22. Hall M et al (2010) Cellulose crystallinity–a key predictor of the enzymatic hydrolysis rate. FEBS J 277(6):1571–1582
23. Heinzelman P et al (2009) SCHEMA recombination of a fungal cellulase uncovers a single mutation that contributes markedly to stability. J Biol Chem 284(39):26229–26233
24. Heinzelman P et al (2010) Efficient screening of fungal cellobiohydrolase class I enzymes for thermostabilizing sequence blocks by SCHEMA structure-guided recombination. Protein Eng Des Sel 23(11):871–880
25. Helbert W et al (2003) Fluorescent cellulose microfibrils as substrate for the detection of cellulase activity. Biomacromolecules 4(3):481–487
26. Henrissat B (1991) A classification of glycosyl hydrolases based on amino acid sequence similarities. Biochem J 280(pt 2):309–316
27. Henrissat B, Bairoch A (1993) New families in the classification of glycosyl hydrolases based on amino acid sequence similarities. Biochem J 293(pt 3):781–788
28. Henrissat B, Bairoch A (1996) Updating the sequence-based classification of glycosyl hydrolases. Biochem J 316(pt 2):695–696
29. Henrissat B, Davies G (1997) Structural and sequence-based classification of glycoside hydrolases. Curr Opin Struct Biol 7(5):637–644
30. Heyman A et al (2007) Multiple display of catalytic modules on a protein scaffold: nano-fabrication of enzyme particles. J Biotechnol 131(4):433–439
31. Hill J et al (2009) Climate change and health costs of air emissions from biofuels and gasoline. Proc Natl Acad Sci U S A 106(6):2077–2082
32. Himmel ME (2008) Biomass recalcitrance: deconstructing the plant cell wall for bioenergy. Wiley-Blackwell, West Sussex
33. Hoffert MI et al (1998) Energy implications of future stabilization of atmospheric CO_2 content. Nature 395:881–884

34. Irwin DC et al (1993) Activity studies of eight purified cellulases: specificity, synergism, and binding domain effects. Biotechnol Bioeng 42(8):1002–1013
35. Josefsson P, Henriksson G, Wagberg L (2008) The physical action of cellulases revealed by a quartz crystal microbalance study using ultrathin cellulose films and pure cellulases. Biomacromolecules 9(1):249–254
36. Kaar WE et al (1991) The complete analysis of wood polysaccharides by HPLC. J Wood Chem Technol 11:447–463
37. Klemm D et al (2005) Cellulose: fascinating biopolymer and sustainable raw material. Angew Chem Int Ed Engl 44(22):3358–3393
38. Lai TE, Pullammanappallil PC, Clarke WP (2006) Quantification of cellulase activity using cellulose-azure. Talanta 69(1):68–72
39. Lamed R, Setter E, Bayer EA (1983) Characterization of a cellulose-binding, cellulase-containing complex in *Clostridium thermocellum*. J Bacteriol 156(2):828–836
40. Lilly M et al (2009) Heterologous expression of a *Clostridium minicellulosome* in *Saccharomyces cerevisiae*. FEMS Yeast Res 9(8):1236–1249
41. Liska AJ et al (2008) Improvements in life cycle energy efficiency and greenhouse gas emissions of corn-ethanol. J Ind Ecol 13(1):58–74
42. Majewicz TG, Podlas TJ (2000) Cellulose ethers. Kirk-Othmer encyclopedia of chemical technology. Wiley, New York
43. Malet C et al (1996) A specific chromophoric substrate for activity assays of 1,3-1,4-beta-D-glucan 4-glucanohydrolases. J Biotechnol 48(3):209–219
44. Mandelman D et al (2003) X-Ray crystal structure of the multidomain endoglucanase Cel9G from *Clostridium cellulolyticum* complexed with natural and synthetic cello-oligosaccharides. J Bacteriol 185(14):4127–4135
45. Miller GL (1959) Use of dinitrosalicylic acid reagent for determination of reducing sugar. Anal Chem 31(3):426–428
46. Mingardon F et al (2005) Heterologous production, assembly, and secretion of a minicellulosome by *Clostridium acetobutylicum* ATCC 824. Appl Environ Microbiol 71(3):1215–1222
47. Mingardon F et al (2007) Incorporation of fungal cellulases in bacterial minicellulosomes yields viable, synergistically acting cellulolytic complexes. Appl Environ Microbiol 73(12):3822–3832
48. Mingardon F et al (2007) Exploration of new geometries in cellulosome-like chimeras. Appl Environ Microbiol 73(22):7138–7149
49. Mitsuzawa S et al (2009) The rosettazyme: a synthetic cellulosome. J Biotechnol 143(2):139–144
50. Morais S et al (2010) Enhanced cellulose degradation by nano-complexed enzymes: synergism between a scaffold-linked exoglucanase and a free endoglucanase. J Biotechnol 147:205–211
51. Murphy L et al (2010) A calorimetric assay for enzymatic saccharification of biomass. Enzyme Microb Technol 46(2):141–146
52. Nidetzky B et al (1994) Cellulose hydrolysis by the cellulases from *Trichoderma reesei*: a new model for synergistic interaction. Biochem J 298(pt 3):705–710
53. Nishiyama Y et al (2003) Crystal structure and hydrogen bonding system in cellulose I(alpha) from synchrotron X-ray and neutron fiber diffraction. J Am Chem Soc 125(47):14300–14306
54. Olsen SN et al (2011) Kinetics of enzymatic high-solid hydrolysis of lignocellulosic biomass studied by calorimetry. Appl Biochem Biotechnol 163:626–635
55. Park S et al (2009) Measuring the crystallinity index of cellulose by solid state C-13 nuclear magnetic resonance. Cellulose 16(4):641–647
56. Plevin RJ (2009) Modeling corn ethanol and climate. a critical comparison of the BESS and GREET models. J Ind Ecol 13:495–507
57. Pozzo T et al (2010) Structural and functional analyses of beta-glucosidase 3B from *Thermotoga neapolitana*: a thermostable three-domain representative of glycoside hydrolase 3. J Mol Biol 397(3):724–739

58. Rabinovich ML, Melnick MS, Bolobova AV (2002) The structure and mechanism of action of cellulolytic enzymes. Biochemistry (Mosc) 67(8):850–871
59. Robyt JF, Whelan WJ (1972) Reducing value methods for maltodextrins. 1. Chain-length dependence of alkaline 3,5-dinitrosalicylate and chain-length independence of alkaline copper. Anal Biochem 45(2):510–516
60. Ruijssenaars HJ, Hartmans S (2001) Plate screening methods for the detection of polysaccharase-producing microorganisms. Appl Microbiol Biotechnol 55(2):143–149
61. Ryu DD, Kim C, Mandels M (1984) Competitive adsorption of cellulase components and its significance in a synergistic mechanism. Biotechnol Bioeng 26(5):488–496
62. Sabathe F, Soucaille P (2003) Characterization of the CipA scaffolding protein and in vivo production of a minicellulosome in *Clostridium acetobutylicum*. J Bacteriol 185(3):1092–1096
63. Sandgren M, Stahlberg J, Mitchinson C (2005) Structural and biochemical studies of GH family 12 cellulases: improved thermal stability, and ligand complexes. Prog Biophys Mol Biol 89(3):246–291
64. Schmer MR et al (2008) Net energy of cellulosic ethanol from switchgrass. Proc Natl Acad Sci U S A 105(2):464–469
65. Schulein M (2000) Protein engineering of cellulases. Biochim Biophys Acta 1543(2):239–252
66. Somogyi M (1952) Notes on sugar determination. J Biol Chem 195(1):19–23
67. Stalbrand H et al (1998) Analysis of molecular size distributions of cellulose molecules during hydrolysis of cellulose by recombinant *Cellulomonas fimi* beta-1,4-glucanases. Appl Environ Microbiol 64(7):2374–2379
68. Teeri TT (1997) Crystalline cellulose degradation: new insight into the function of cellobiohydrolases. Trends Biotechnol 15(5):160–167
69. Terashima N et al (2009) Nanostructural assembly of cellulose, hemicellulose, and lignin in the middle layer of secondary wall of ginkgo tracheid. J Wood Sci 55:409–416
70. Tomme P, Heriban V, Claeyssens M (1990) Adsorption of two cellobiohydrolases from *Trichoderma reesei* to Avicel: evidence for "exo-exo" synergism and possible "loose complex" formation. Biotechnol Lett 12:525–530
71. Tomme P et al (1996) Characterization of CenC, an enzyme from Cellulomonas fimi with both endo- and exoglucanase activities. J Bacteriol 178(14):4216–4223
72. Tsai SL, Goyal G, Chen W (2010) Surface display of a functional minicellulosome by intracellular complementation using a synthetic yeast consortium and its application to cellulose hydrolysis and ethanol production. Appl Environ Microbiol 76(22):7514–7520
73. Ubhayasekera W et al (2005) Structures of *Phanerochaete chrysosporium* Cel7D in complex with product and inhibitors. FEBS J 272(8):1952–1964
74. Valjamae P et al (1999) Acid hydrolysis of bacterial cellulose reveals different modes of synergistic action between cellobiohydrolase I and endoglucanase I. Eur J Biochem 266(2):327–334
75. Wilson DB (2004) Studies of *Thermobifida fusca* plant cell wall degrading enzymes. Chem Rec 4(2):72–82
76. Wilson DB (2008) Aerobic microbial cellulase systems. In: Himmel ME (ed) Biomass recalcitrance: deconstructing the plant cell wall for bioenergy. Blackwell, West Sussex, pp 374–392
77. Wood TM (1988) Methods for measuring cellulase activities. Methods Enzymol 160:87–112
78. Wood TM (1988) Preparation of crystalline, amorphous, and dyed cellulase substrates. Methods Enzymol 160:19–25
79. Wood TM, McCrae SI, Bhat KM (1989) The mechanism of fungal cellulase action. Synergism between enzyme components of Penicillium pinophilum cellulase in solubilizing hydrogen bond-ordered cellulose. Biochem J 260(1):37–43
80. Woodward J, Lima M, Lee NE (1988) The role of cellulase concentration in determining the degree of synergism in the hydrolysis of microcrystalline cellulose. Biochem J 255(3):895–899

81. Zhang Y-HP, Himmel ME, Mielenz JR (2006) Outlook for cellulase improvement: screening and selection strategies. Biotechnol Adv 24(5):452–481
82. Zhang YH et al (2006) A transition from cellulose swelling to cellulose dissolution by o-phosphoric acid: evidence from enzymatic hydrolysis and supramolecular structure. Biomacromolecules 7(2):644–648
83. Zhang YH, Lynd LR (2004) Kinetics and relative importance of phosphorolytic and hydrolytic cleavage of cellodextrins and cellobiose in cell extracts of *Clostridium thermocellum*. Appl Environ Microbiol 70(3):1563–1569
84. Zhang YH, Lynd LR (2004) Toward an aggregated understanding of enzymatic hydrolysis of cellulose: noncomplexed cellulase systems. Biotechnol Bioeng 88(7):797–824
85. Zhang YH, Lynd LR (2005) Cellulose utilization by *Clostridium thermocellum*: bioenergetics and hydrolysis product assimilation. Proc Natl Acad Sci U S A 102(20):7321–7325
86. Zhou J et al (2009) Optimization of cellulase mixture for efficient hydrolysis of steam-exploded corn stover by statistically designed experiments. Bioresour Technol 100(2):819–825

Part IV
Photobiological Production of Advanced Biofuels with Synthetic Biology

Chapter 20
Designer Transgenic Algae for Photobiological Production of Hydrogen from Water

James Weifu Lee

Abstract This chapter reports two inventions: designer proton-channel algae (US Patent No. 7,932,437 B2) and designer switchable photosystem-II algae (US Patent No. 7,642,405 B2), for more efficient and robust photobiological production of hydrogen (H_2) from water. Use of these inventions could eliminate the following six technical problems that severely limit the yield of algal H_2 production: (1) restriction of photosynthetic H_2 production by accumulation of a proton gradient, (2) competitive inhibition of photosynthetic H_2 production by CO_2, (3) requirement of bicarbonate binding at photosystem-II (PSII) for efficient photosynthetic activity, (4) competitive drainage of electrons by O_2 in algal H_2 production, (5) oxygen sensitivity of algal hydrogenase, and (6) the H_2–O_2 gas separation and safety issue. By eliminating these six technical problems that currently challenge those in the field, the designer algae approach could enhance photobiological production of hydrogen with a yield likely over ten times better than that of the wild-type.

1 Introduction

Photoautotrophic H_2-producing microorganisms, including microalgae such as *Chlamydomonas reinhardtii*, have the potential to be a clean energy resource. In the algal system, H_2 can be produced through hydrogenase-catalyzed reduction of protons by the electrons generated from photosynthetic oxidation of water using sunlight energy, as illustrated in Fig. 1. The net result is photoevolution of H_2 and

J.W. Lee (✉)
Department of Chemistry and Biochemistry, Old Dominion University,
Physical Sciences Building, Room 3100B, 4402 Elkhorn Avenue, Norfolk, VA 23529, USA

Johns Hopkins University, Whiting School of Engineering, 118 Latrobe Hall,
Baltimore, MD 21218, USA
e-mail: jwlee@ODU.edu; JLee349@JHU.edu

J.W. Lee (ed.), *Advanced Biofuels and Bioproducts*, DOI 10.1007/978-1-4614-3348-4_20,

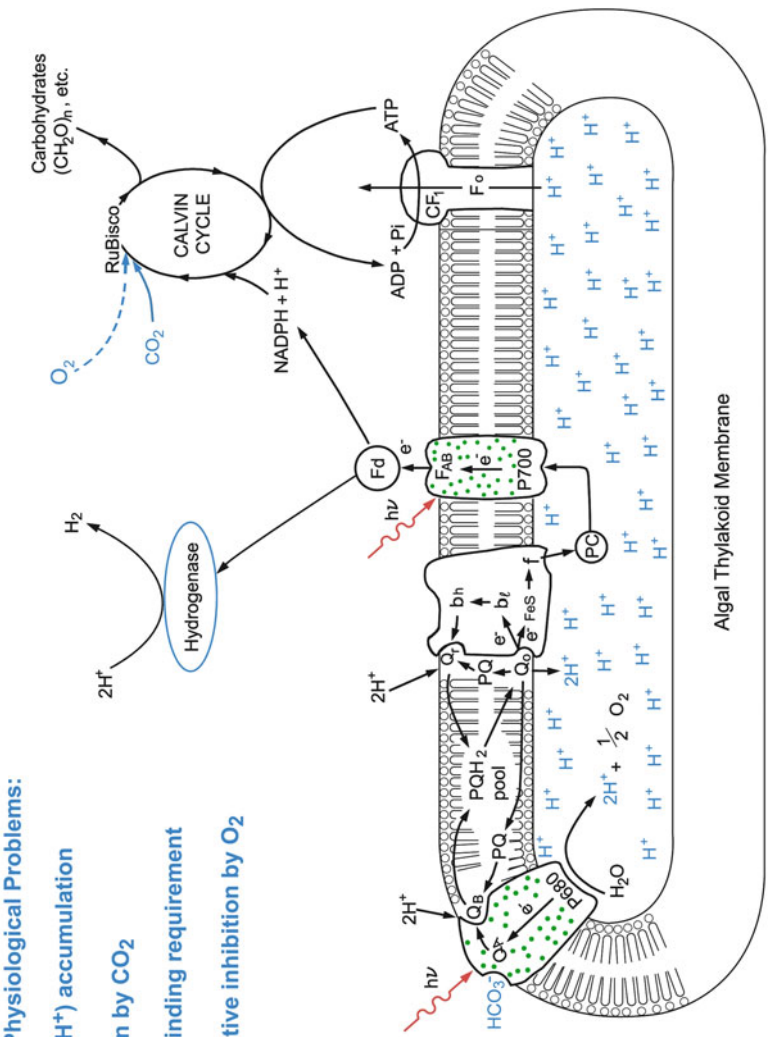

Fig. 1 Photosynthetic H_2 production pathway in wild-type algae such as *Chlamydomonas reinhardtii* has the four *trans*-thylakoidal proton gradient-related problems (shown in *blue*) that seriously limit the rate and the yield of H_2 production

O_2 from H_2O. Recently, there were a few interesting algal H_2 production research efforts as mentioned in some of the recent review articles [1, 2]. For example, sulfur-deprivation with *C. reinhardtii* was explored in trying to improve algal H_2 production [3, 4]. More recently, certain phylogenetic and molecular analyses were performed in H_2-producing green algae [5, 6]. However, so far, there was essentially no truly tangible fundamental improvement on the rate and the yield of algal photobiological H_2 production. Algal H_2 production remains impractical with very limited yield; and the solar-to-hydrogen energy conversion currently is still less than 0.1% [7], which clearly is not commercially viable.

According to a recent analysis, the most urgent and challenging technical barriers are the four *trans*-thylakoidal proton gradient-associated physiological problems [8] that seriously limit the rate and the yield of algal photobiological H_2 production: (1) accumulation of a proton gradient across the algal thylakoid membrane, (2) competition from carbon dioxide fixation, (3) requirement for bicarbonate binding at photosystem-II (PSII) for efficient photosynthetic activity, and (4) competitive drainage of electrons by molecular oxygen.

This chapter reports two inventions: designer proton-channel algae (US Patent No. 7,932,437 B2) and designer switchable photosystem-II algae (U.S. Patent Number: US 7,642,405 B2), which may enable efficient and robust photobiological production of hydrogen with an enhanced yield likely more than ten times better than that of the wild-type. The first invention (designer proton-channel algae [9]) uses a highly innovative "one stone killing four birds" approach to simultaneously eliminate all the four *trans*-thylakoidal proton gradient-associated physiological problems by genetic insertion of a polypeptide proton channel into algal thylakoid membrane using synthetic biology; whereas, the second invention [10] is on creating designer switchable photosystem-II algae for robust photobiological production of hydrogen from water splitting, which can eliminate all the following three molecular oxygen (O_2)-associated technical problems: (4) competitive drainage of electrons by molecular oxygen, (5) oxygen sensitivity of algal hydrogenase, and (6) the H_2–O_2 gas separation and safety issue.

The following describe the four *trans*-thylakoidal proton gradient-associated physiological problems that may be solved by the use of the designer proton-channel algae invention for enhanced photoautotrophic hydrogen production:

1. *Accumulation of a proton gradient across the algal thylakoid membrane*. For each hydrogen molecule (H_2) produced by photosynthesis, six protons are translocated across the algal thylakoid membrane (Fig. 1). Since the membrane has a limited permeability to protons, photosynthetic electron transport will result in accumulation of protons inside the lumen of the thylakoids, with no mechanism for dissipation. The resulting static back-proton gradient seriously impedes the electron transport, thus limiting the rate of H_2 production. This phenomenon can be explained by the difference between the Calvin-cycle CO_2-fixation process and the ferredoxin (Fd)/hydrogenase H_2 production pathway. In photosynthetic CO_2 fixation, this proton gradient across the thylakoid membrane is used by the

coupling factor CF_0CF_1 complex to drive the formation of ATP that is required by the Calvin cycle. However, the Fd/hydrogenase H_2 production pathway does not consume ATP. Consequently, under the conditions of H_2 photoevolution where the consumption of ATP by the Calvin cycle stops due to the absence of CO_2, the CF_0CF_1-mediated conduction of protons from the lumen to the stroma will quickly become limiting because of the accumulation of ATP and the shutdown of ATP synthase activity. As a result, photosynthetic H_2 production quickly results in an increased proton gradient across the thylakoid membrane that has no mechanism for dissipation. The static back-proton gradient seriously impedes the electron transport, thus limiting the rate of H_2 production, since electron transport from water through photosystem-II (PSII), plastoquinone (PQ), the cytochrome b/f (Cyt b/f) complex, plastocyanin (PC), and photosystem I (PSI) to the Fd/hydrogenase pathway is coupled with proton translocation across the thylakoid membrane, as illustrated in Fig. 1.

2. *Competition from carbon dioxide fixation*. Carbon dioxide (CO_2) fixation by the Calvin cycle can compete with the Fd/hydrogenase H_2 production pathway for photosynthetic electrons. This has been demonstrated in experimental studies [11]. Steady state H_2 photoevolution was inhibited to nearly zero by injecting 58 ppm of CO_2. Therefore, increasing the photosynthetic H_2 production would require a nearly CO_2-free environment. However, lowering the CO_2 concentration would countermand the following factor.
3. *Requirement for bicarbonate binding at PSII for efficient photosynthetic activity*. Experimental studies [12] have demonstrated that adding bicarbonate (HCO_3^-) to depleted samples can result in a six to sevenfold stimulation of PSII electron-transport activity. Because CO_2 and HCO_3^- are interchangeable in aqueous medium, removal of CO_2 can lead to depletion of HCO_3^-, and thereby reduce PSII electron-transport activity. This presents a dilemma when one tries to lower the CO_2 concentration in order to increase H_2 production.
4. *Competitive drainage of electrons by molecular oxygen*. In a previous study [13] performed by the author, a new molecular oxygen (O_2) sensitivity in algal H_2 production was discovered that is distinct from the O_2 sensitivity of hydrogenase per se and more significant. This is likely due to the background O_2, which apparently serves as a terminal electron acceptor through RuBisco's oxygenase activity at the Calvin cycle, in competition with the H_2-production pathway. Our experimental studies demonstrated that photosynthetic H_2 production can be inhibited by an O_2 concentration as low as about 500–1,000 ppm, while the algal hydrogenase is still active at an O_2 concentration as high as 5,000 ppm. This indicates that the drainage of electrons by O_2 in competition with the Fd/hydrogenase H_2 production pathway is a serious problem that must be solved in order for H_2 production to work efficiently.

2 Designer Proton-Channel Algae Concept

The Designer Proton-Channel Algae concept is disclosed in [8] to solve the four *trans*-thylakoidal proton gradient-associated problems identified above. Briefly, the envisioned proton-channel designer alga, which contains an inducible promoter (e.g., hydrogenase promoter)-controlled designer proton-channel gene, conceivably can perform autotrophic photosynthesis (Fig. 2a) just like a wild-type organism using ambient-air CO_2 as the carbon source and grow normally under aerobic conditions, such as in an open pond. When the algal culture is grown and ready for H_2 production, the designer proton-channel transgene will then be expressed simultaneously with the induction of the hydrogenase enzyme under anaerobic conditions because of the use of a hydrogenase promoter. The expression of the proton-channel gene will conceivably produce polypeptide proton channels in the algal thylakoid membrane (Fig. 2b). The following explains how the designer proton channel can solve the four problems to dramatically enhance photobiological H_2 production.

The basic idea is to insert an inducible, synthetically designed gene including a polypeptide proton-channel encoding sequence into the nuclear DNA of algae such as *C. reinhardtii.* When the designer gene is expressed, it will, conceivably, produce polypeptide proton channels in the algal thylakoid membrane that will allow protons to be conducted. This would, first of all, dissipate the proton gradient. Therefore, problem 1 (Proton accumulation in algal thylakoids) would be eliminated. Second, the designer proton channels would allow protons to pass through the membrane without making the ATP required by Calvin-cycle activity, causing the Calvin-cycle to shut down exactly as needed for photoautotrophic H_2 production. This would eliminate the competition for photosynthetic electrons with the H_2 production pathway caused by the Calvin-cycle CO_2 fixation (problem 2). Since photosynthetic H_2 production in the proton-channel-expressed designer alga would not require a CO_2-free environment, the requirement for bicarbonate (HCO_3^-) binding at PSII for efficient photosynthetic activity (problem 3) would no longer be an issue. The requirement could be satisfied in the designer alga by leaving some CO_2 in the medium to form the needed HCO_3^-. Finally, because the drainage of electrons by O_2 (problem 4) at the point of RuBisco, which also competes with the H_2-production pathway for photosynthetically generated electrons, is also *trans*-thylakoidal proton gradient-dependent, this problem would also be avoided by the dissipation of the proton gradient with the expression of the designer proton channel. That is, when the Calvin-cycle activity including RuBisco (and its oxygenase activity) is inactivated by lack of ATP formation owning to the action of the designer proton channel, O_2 would also no longer be able to act as a terminal electron acceptor there. Therefore, all four *trans*-thylakoidal proton gradient-associated physiological problems could be solved through the use of the conceived Designer Proton-Channel Algae approach. Theoretically, the maximum solar-to-hydrogen energy conversion efficiency allowed by this approach is estimated to be about 10%.

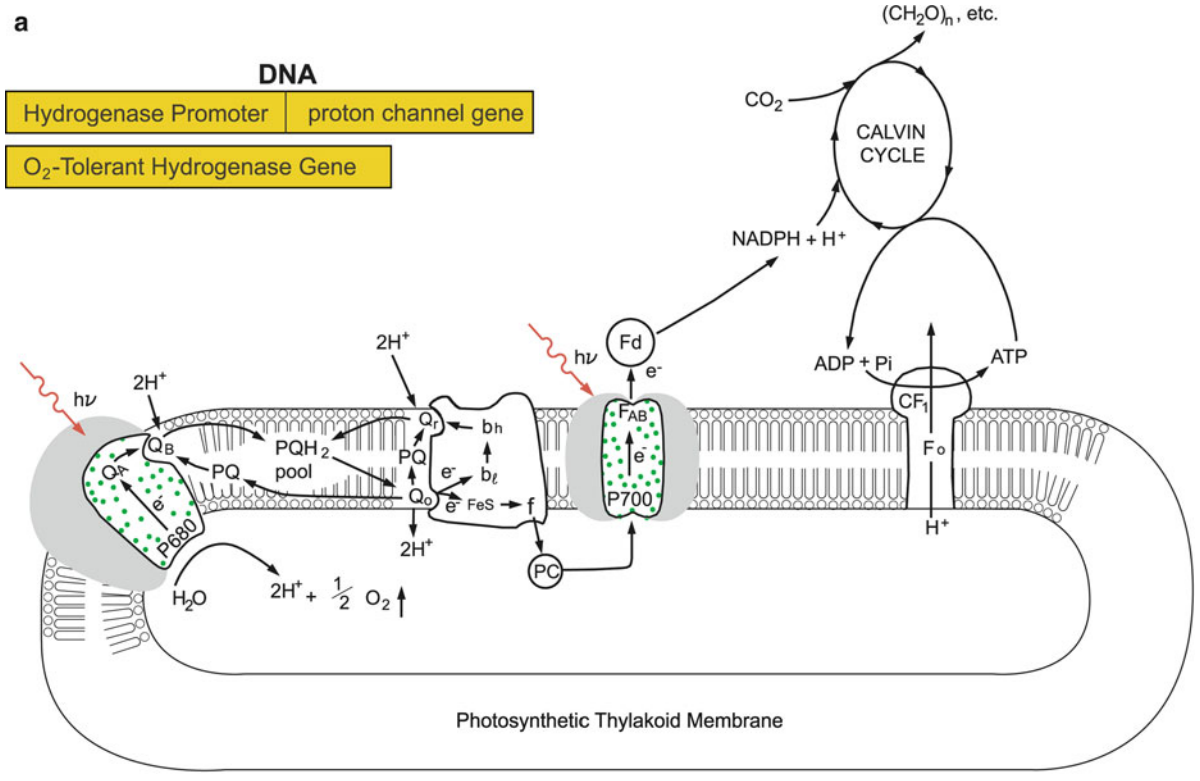

Fig. 2 (**a**) Concept of designer proton-channel alga performing photoautotrophic photosynthesis using CO_2 as the source of carbon and water as the source of electrons under normal aerobic conditions such as in an open pond. (**b**) Concept of designer proton-channel alga becoming an efficient "green machine" for enhanced photoautotrophic H_2 production from water splitting when the designer proton-channel gene is inducibly turned on under hydrogen-producing conditions, such as under anaerobic conditions

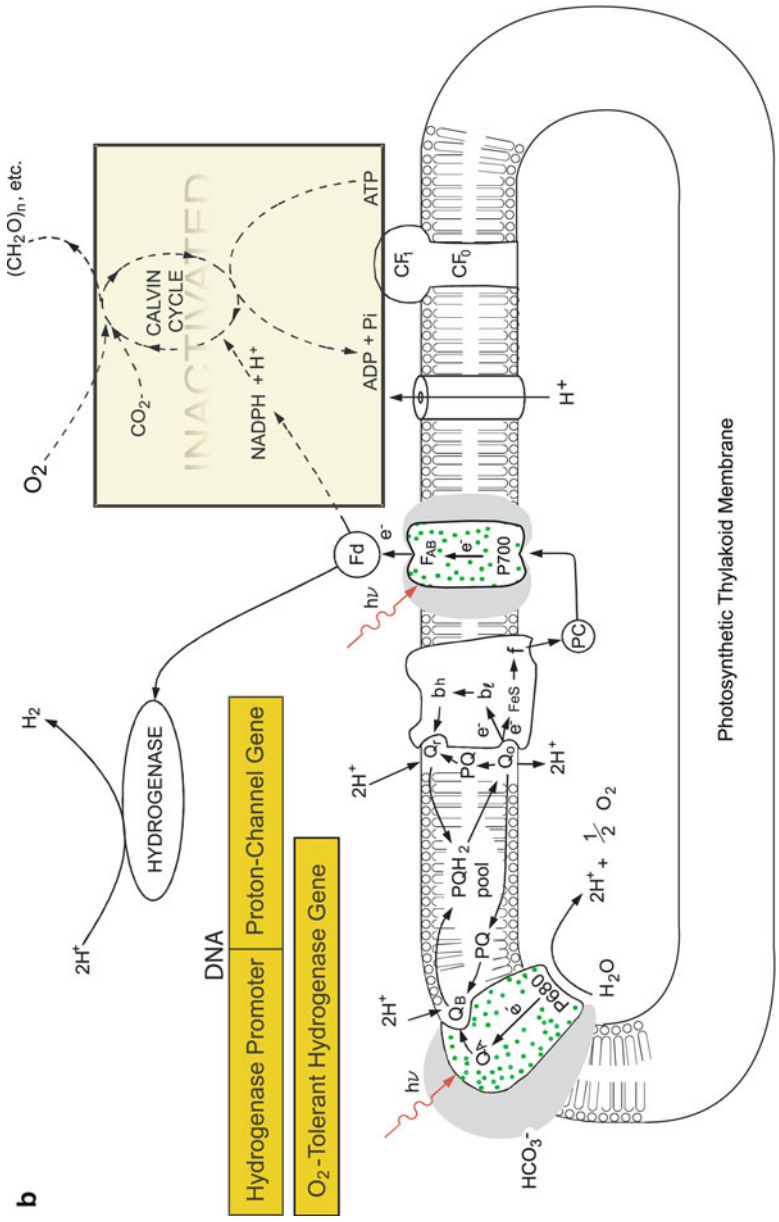

Fig. 2 (continued)

3 Preliminary Proof-of-Principle Scientific Experimental Demonstration

The Designer Proton-Channel Algae concept is supported by a number of independent studies [14–16] and by the author's own preliminary proof-of-principle study, making use of chemical proton uncouplers (such as carbonyl cyanide-*p*-trifluoro-methoxyphenylhydrazone (FCCP)) to simulate the proton-shuttling effect of a proton channel across the algal thylakoid membrane. They all indicated that the photobiological hydrogen production in *Chlamydomonas* is limited by the *trans*-thylakoidal proton gradient. For example, Fig. 3a presents a proof-of-principle assay result with *C. reinhardtii* under helium atmosphere. The data show that the addition of 5 μM FCCP at the steady state of photosynthetic hydrogen production led to a significant increase in the photoevolution of both H_2 and O_2.

According to the designer proton-channel algae concept, use of the proton-shuttling effect across the algal thylakoid membrane would show more dramatic enhancement of photosynthetic hydrogen production when there is a background level of molecular oxygen such as 1,000 ppm O_2 in a photobioreactor where the competitive drainage of electrons by molecular oxygen (problem 4) can take place. This predicted feature was also demonstrated in a proof-of-principal experiment using *C. reinhardtii* liquid culture under a helium atmosphere containing 1,000 ppm O_2 with addition of FCCP as well. As demonstrated by the experimental results in Fig. 3b, addition of 5 μM FCCP produced a dramatic reversal of O_2 inhibition on H_2 photoevolution under a helium atmosphere containing 1,000 ppm O_2. The rate of H_2 production rose to about 16 μmol H_2/mg Chl h. This FCCP-stimulated H_2 production is clearly photodependent. As soon as the actinic light was turned off, the H_2 production stopped. However, most of these chemical proton uncouplers—such as FCCP, carbonyl cyanide *m*-chlorophenylhydrazone (CCCP), and anilinothiophene—have undesirable side effects, including the acceleration of the deactivation of the water-splitting system Y (ADRY) effect [17], which can damage the photosynthetic activity in algal cells. As shown in Fig. 3b, the FCCP-enhanced photoevolution of H_2 can last for more than 4 h with some decay. This decay is due to the ADRY effect, in which FCCP gradually inhibits PSII activity by deactivation of the photosynthetic water-splitting complex in the S2 and S3 states. Furthermore, those chemical uncouplers (such as FCCP) are hazardous materials that are environmentally unacceptable for large-scale applications. Therefore, it is essential to use a designer polypeptide proton channel that does not have the ADRY effect to dramatically enhance H_2 production by eliminating the proton gradient-associated problems.

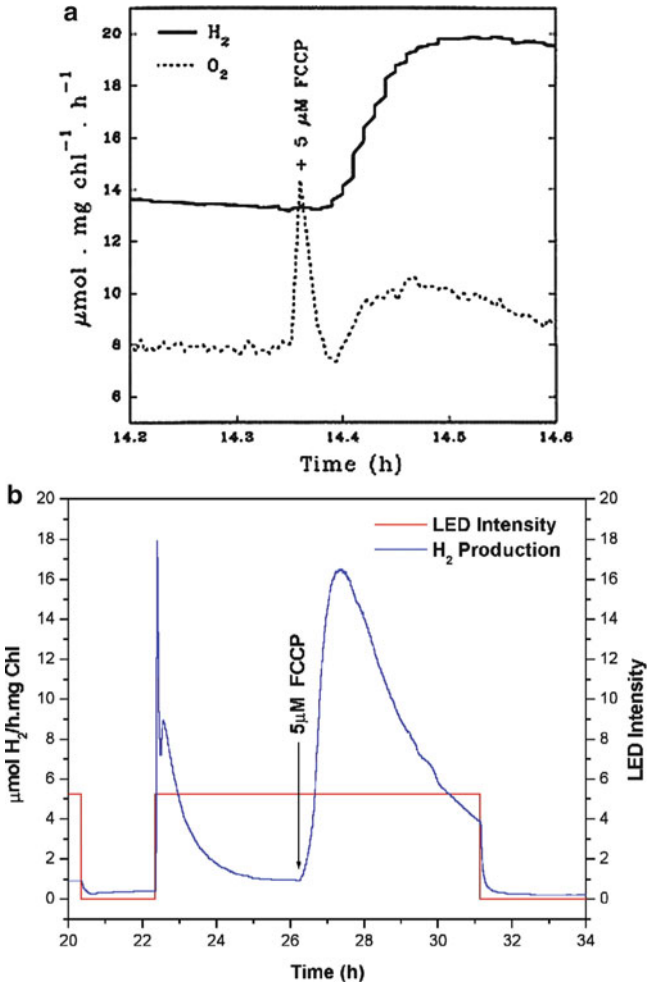

Fig. 3 (**a**) Photoevolution of H_2 and O_2 in *C. reinhardtii* under helium atmosphere in response to the addition of 5 μM FCCP. (**b**) Proof-of-principle experimental data that demonstrate significant stimulation of photosynthetic H_2 production in wild-type alga *C. reinhardtii* 137c following addition of the proton uncoupler FCCP in a background atmosphere of 1,000-ppm O_2 (reproduced from [13])

4 Application of Synthetic Biology Toward Creating the Envisioned Designer Algae

The envisioned transgenic designer algae comprise switchable transgenes wherein each transgene encodes for a proton-conductive channel in the algal photosynthetic thylakoid membrane for enhanced photobiological H_2 production. The programmable genetic insertion of proton channels into algal thylakoid membrane is achieved by transformation of a host alga with a DNA construct that contains a designer

polypeptide proton-channel gene linked with an externally inducible promoter such as a redox-condition-sensitive hydrogenase promoter serving as a genetic switch.

Examples of proton-conductive polypeptide or protein structures that can be used and/or modified for this application are the structures of melittin, gramicidin [18], CF_0 protein (the proton channel of chloroplast coupling factor CF_0CF_1), F_0 protein (the proton-channel structure of mitochondrial coupling factor F_0F_1), and their analogs including artificially designed polypeptide proton channels. That is, the molecular structure (and thus the DNA sequence) of a polypeptide proton channel can be designed according to these natural proton-channel structures and their analogs at a nanometer scale. Melittin is preferred for use in this application since in vitro assay has already demonstrated that melittin can work as a proton channel in thylakoid membrane [19].

As shown in Fig. 4a, the designer proton-channel transgene is a nucleic acid construct from 5′ to 3′ comprising typically: (a) a polymerase chain reaction forward (PCR FD) primer; (b) an externally inducible promoter; (c) a transit targeting sequence; (d) a designer proton-channel encoding sequence; (e) a transcription and translation terminator; and (f) a PCR reverse (RE) primer.

Another aspect is the innovative application of an externally inducible promoter such as a hydrogenase promoter. To function as intended, the designer proton-channel protein is inducibly expressed under hydrogen-producing conditions such as under anaerobic conditions. An algal hydrogenase promoter, such as the promoter of the hydrogenase gene (*Hyd1*) of *C. reinhardtii*, can be used as an effective genetic switch to control the expression of the proton channel gene to the exact time and conditions where it is needed for H_2 production. That is, the proton channels are synthesized only at the time when the hydrogenase is induced and ready for H_2 production under anaerobic conditions. Therefore, the hydrogenase promoter is employed as an inducible promoter for the DNA construct (Fig. 4a) to serve as a genetic switch to control the expression of the designer polypeptide proton-channel gene. The reason that the designer alga can perform autotrophic photosynthesis using CO_2 as the carbon source under aerobic condition is because the designer proton-channel gene is not expressed under aerobic conditions owning to the use of a hydrogenase promoter as a genetic switch, which can be turned on only under the anaerobic conditions when needed for photobiological H_2 production.

In addition to the hydrogenase promoter, other promoters can also be used to construct the desired genetic switch for designer proton-channel gene. *Chlamydomonas* cells contain several nuclear genes that are coordinately induced under anaerobic conditions. These include the hydrogenase structural gene itself (*Hyd1*), the *Cyc6* gene encoding the apoprotein of Cytochrome c_6, and the *Cpx1* gene encoding coprogen oxidase [20]. The regulatory regions for the latter two have been well characterized, and a region of ~100 bp proves sufficient to confer regulation by anaerobiosis in synthetic gene constructs. The promoter strengths of these three genes vary considerably; each may thus be selected to control the level of the designer proton-channel expression for enhanced photobiological production of H_2. There are a number of other regulated promoters that can also be used and/or modified to serve as the genetic switches. For example, the nitrate reductase (*Nia1*)

a

5' 3'

PCR FD Primer	Inducible Promoter	Targeting Sequence	Proton-Channel Sequence	Terminator	PCR RE Primer

Fig. 4 (**a**) The general design of the DNA construct for a designer proton-channel gene. (**b**) A photograph for the first set of designer proton channel genes that were synthesized in collaboration with Geneart

promoter which is induced by growth in nitrate medium and repressed in nitrate-deficient but ammonium-containing medium is used to control the expression of the designer genes according to the concentration levels of nitrate in a culture medium as well. Therefore, inducible promoters that can be used and/or modified in various embodiments to serve this purpose includes, but are not limited to, hydrogenase promoters, Cytochrome c_6 (*Cyc6*) promoter, *Nia1* promoter, *CabII-1* promoter, *Ca1* promoter, *Ca2* promoter, coprogen oxidase promoter, and/or their analogs and modified designer sequences.

Another aspect is the targeted insertion of designer proton channels into algal photosynthetic membrane or into both the photosynthetic membrane and other cellular membranes including the mitochondria and/or plasma membranes to suit for the specific applications. For example, in the case of green algae including *Chlamydomonas*, when recyclable growth of the designer algae culture is desired, it is best to insert the proton channels only into the algal thylakoid membrane, exactly where the action of proton channels is needed to enhance H_2 production. If expressed without a targeted insertion mechanism, the polypeptide proton channels might be inserted nonspecifically into other membrane systems including the mitochondria and plasma membranes in addition to the thylakoid membranes. Although an expression of the proton channel gene in such a nonspecific manner could still transform an algal cell into a more efficient and robust photosynthetic apparatus for H_2 production, other cellular functions such as the respiratory process would probably be disabled because of the potential effect of the proton channels that are nonspecifically inserted into other organelles such as the mitochondria. As a result, this type of algal cells with insertion of the proton channels into both the photosynthetic membrane and other cellular membranes, such as the mitochondrial membranes, can still be used for enhanced H_2 production, but the cells would probably no longer be able to grow or regenerate themselves after the expression of the designer proton channels is turned on. That is, when the expression of the designer proton channels is turned on in this type of nonregenerative proton-channel designer algae, the algal culture will become dedicated "green machine" materials for enhanced H_2 production and the cells will no longer be able to grow even if they are returned to aerobic condition because the other cellular functions such as the function of the mitochondria are impaired by the insertion of proton channels.

This nonregenerative feature provides a benefit: help ensure biosafety in using the genetically modified algae. This is because after the designer proton channels are inserted into both the photosynthetic membrane and the mitochondrial membranes, the designer algal cells become dedicated nonliving "green machine" materials for enhanced H_2 production, but without any potential risks of sexually passing any of their genes to any other cells. In various embodiments, the nonregenerative feature is achieved by use of two designer proton-channel genes: one with a mitochondrial-targeting sequence to insert proton channels into the algal mitochondrial membrane and one with a thylakoid-targeting sequence to insert proton channels into the algal thylakoid membrane. When the two designer proton-channel genes are both expressed, the designer cells immediately become dedicated nonliving "green machine" materials for enhanced H_2 production. Therefore, in one embodiment, it is a preferred practice to keep growing this type of nonregenerative proton-channel designer under aerobic conditions to continuously supply batches of grown designer algal cultures that are subsequently used for enhanced H_2 production expression of the proton channels into both the photosynthetic membrane and other cellular membranes such as the mitochondrial membranes under anaerobic conditions. After the nonregenerative proton-channel designer algal cultures are used for enhanced H_2 production under anaerobic conditions, they can be quite safely handled as nonliving biomass materials for disposal including possible use as a fertilizer or other biomass processes.

With a thylakoid-targeted mechanism that enables insertion of the polypeptide proton channels only into the thylakoid membrane so that all of the other cellular functions (including functions of the mitochondria, nucleus, and cell membranes) are kept intact, the result can be much better for certain applications. After the thylakoid-targeted insertion of proton channels, the cell will not only be able to produce H_2, but also to grow and regenerate itself when it is returned to aerobic conditions. Our daily experience with photoheterotrophically grown photosynthetic mutants of algae with acetate-containing culture media has demonstrated that this type of designer alga, which contains normal mitochondria, should be able to use the reducing power (NADH) from organic reserves (and/or some exogenous organic substrate such as acetate) to power the cell immediately after its return to aerobic conditions. Consequently, when the alga is returned to aerobic conditions after its use under anaerobic conditions for photoevolution of H_2 and O_2, the cell will stop making the polypeptide proton channels and start to restore its normal photoautotrophic capability by synthesizing new and functional thylakoids. Consequently, it is also possible to use this genetically transformed organism for repeated cycles of photoautotrophic growth under normal aerobic conditions and efficient production of H_2 and O_2 by photosynthetic water splitting under anaerobic conditions.

Targeted insertion of designer proton channel is accomplished through the use of a specific targeting DNA sequence that is located between the promoter and the designer proton-channel DNA as shown in the DNA construct (Fig. 4a). In various embodiments, there are a number of transit peptide sequences that can be selected and/or modified for use as the targeting sequence for the targeted insertion of the designer proton channels into algal photosynthetic membrane and, when desirable, other cellular membranes, such as mitochondrial membrane. The targeting sequences that can be used and/or modified for this purpose include (but are not limited to) the transit peptide sequences of: plastocyanin apoprotein (*Pcy1*), the LhcII apoproteins, OEE1 apoprotein (*PsbO*), OEE2 apoprotein (*PsbP*), OEE3 apoprotein (*PsbQ*), hydrogenase apoproteins (such as *Hyd1),* PSII-T apoprotein (*PsbT*), PSII-S apoprotein (*PsbS*), PSII-W apoprotein (*PsbW*), CF_0CF_1 subunit-γ apoprotein (*AtpC*), CF_0CF_1 subunit-δ apoprotein (*AtpD*), CF_0CF_1 subunit-II apoprotein (*AtpG*), photosystem I (PSI) apoproteins (such as, of genes *PsaD, PsaE, PsaF, PsaG, PasH*, and *PsaK*), Rubisco SSU apoproteins (such as *RbcS2*), α-tubulin (*TubA*), β-tubulin (*TubB2*), mitochondrial carbonic anhydrase apoproteins (*Ca1* and *Ca2*), and/or their analogs and modified designer sequences.

The following are examples of transit peptide sequences that could be chosen to guide the genetic insertion of the designer proton channels into algal thylakoid membrane: (1) The transit peptide from the plastocyanin gene targets the lumen of the thylakoids from which the biochemical properties of the designer proton-channel polypeptide may again generate insertion into the thylakoid membrane; (2) The *Hyd1* transit peptide confers importation of polypeptides into the stroma, from which the biochemical properties of the designer proton-channel protein may generate insertion into the thylakoid; (3) The transit peptides from the recently characterized Lhcb gene family members [21] lead the LhcII apoproteins directly to the thylakoid and may also do so for the designer proton-channel polypeptide in an

artificial construct; and (4) The transit peptide from the *Cyc6* gene targets the lumen of the thylakoids from which the biochemical properties of the designer proton-channel polypeptide may again generate insertion into the thylakoid.

As illustrated in Fig. 4a, the designer DNA construct also contains a terminator after the proton-channel encoding sequence and a pair of PCR [22] primers located each at the two ends of the DNA construct. The terminator DNA sequence, which is designed based on the sequences of natural gene terminators, is to ensure that the transcription and translation of the said designer proton-channel gene is properly terminated to produce an exact designer proton-channel protein as desired.

The two PCR primers are a PCR FD primer located at the beginning (the 3′ end) of the DNA construct and a PCR RE primer located at the other end as shown in Fig. 4a. This pair of PCR primers is designed to provide certain convenience when needed for relatively easy PCR amplification of the designer DNA construct, which is helpful not only during and after the designer DNA construct is synthesized in preparation for gene transformation, but also after the designer DNA construct is delivered into the genome of a host alga for verification of the designer proton-channel gene in the transformants. For example, after the transformation of the designer gene is accomplished in a *C. reinhardtii*-arg7 host cell using the techniques of electroporation and argininosuccinate lyase (*arg7*) complementation screening, the resulted transformants can be then analyzed by a PCR DNA assay of their nuclear DNA using this pair of PCR primers to verify whether the entire designer proton-channel gene (the DNA construct) is successfully incorporated into the genome of a given transformant. When the nuclear DNA PCR assay of a transformant can generate a PCR product that matches with the predicted DNA size and sequence according to the designer DNA construct, the successful incorporation of the designer proton-channel gene into the genome of the transformant is verified.

Using the molecular genetics arts described above, we designed and synthesized a number of designer proton-channel genes in collaboration with certain gene-synthesizing companies including Geneart USA. Figure 4b shows our first set of designer proton channel genes that were synthesized through collaboration with Geneart. The following presents some examples of the designer proton-channel genes (DNA constructs) that have synthesized and tested in genetic transformation experiments.

Figure 5a presents SEQ ID No. 1: example 1 of a detailed DNA construct of a designer proton-channel gene that includes a PCR FD primer (1–20), a 458-bp *HydA1* promoter (21–478), a Plastocyanin transit peptide DNA sequence (479–618), a Melittin DNA sequence (619–703), an *RbcS2* terminator (704–926), and a PCR RE primer (927–945). This DNA construct (example 1) has been delivered into the nuclear genome of a *C. reinhardtii*-arg7 host cell using the techniques of electroporation and *arg7* complementation screening to create the proton-channel designer alga. The 458-bp *HydA1* promoter (DNA sequence 21–478) is used as an example of an inducible promoter to control the expression of a Melittin proton channel (DNA sequence 619–703). The *RbcS2* terminator (DNA sequence 704–926) is employed to ensure that the transcription and translation of the proton-channel gene is properly terminated to produce the exact designer proton-channel protein

a

AGAAAATCTGGCACCACACCATAAGGGTCATAGAATCTAGCGTTATCCTTCCA
CGAGCGTGTGGCAGCCTGCTGGCGTGGACGAGCTGTCATGCGTTGTTCCGTTAT
GTGTCGTCAAACGCCTTCGAGCGCTGCCCGGAACAATGCGTACTAGTATAGGA
GCCATGAGGCAAGTGAACAGAAGCGGGCTGACTGGTCAAGGCGCACGATAGG
GCTGACGAGCGTGCTGACGGGGTGTACCGCCGAGTGTCCGCTGCATTCCCGCC
GGATTGGGAAATCGCGATGGTCGCGCATAGGCAAGCTCGCAAATGCTGTCAGC
TTATCTTACATGAACACACAAACACTCTCGCAGGCACTAGCCTCAAACCCTCGA
AACCTTTTTCCAACAGTTTACACCCCAATTCGGACGCCGCTCCAAGCTCGCTCC
GTTGCTCCTTCATCGCACCACCTATTATTTCTAATATCGTAGACGCGACAAG*ATG*
AAGGCTACTCTGCGTGCCCCCGCTTCCCGCGCCAGCGCTGTGCGCCCCGTCGCC
AGCCTGAAGGCCGCTGCTCAGCGCGTGGCCTCGGTCGCCGGTGTGTCGGTTGCC
TCTCTGGCCCTGACCCTGGCTGCCCACGCCATGGCCGGCATCGGCGCCGTGCTG
AAGGTCCTGACCACCGGCCTGCCCGCCCTGATCAGCTGGATCAAGCGCAAGCG
CCAGCAGTAAATGGAGGCGCTCGTTGATCTGAGCCTTGCCCCCTGACGAACGG
CGGTGGATGGAAGATACTGCTCTCAAGTGCTGAAGCGGTAGCTTAGCTCCCCGT
TTCGTGCTGATCAGTCTTTTTCAACACGTAAAAAGCGGAGGAGTTTTGCAATTT
TGTTGGTTGTAACGATCCTCCGTTGATTTTGGCCTCTTTCTCCATGGGCGGGCTG
GGCGTATTTGAAG**CGGTTCTCTCTTCTGCCGTT**

b

AGAAAATCTGGCACCACACCGAGCTGTCATGCGTTGTTCCGTTATGTGTCGTC
AAACGCCTTCGAGCGCTGCCCGGAACAATGCGTACTAGTATAGGAGCCATGAG
GCAAGTGAACAGAAGCGGGCTGACTGGTCAAGGCGCACGATAGGGCTGACGA
GCGTGCTGACGGGGTGTACCGCCGAGTGTCCGCTGCATTCCCGCCGGATTGGG
AAATCGCGATGGTCGCGCATAGGCAAGCTCGCAAATGCTGTCAGCTTATCTTAC
ATGAACACACAAACACTCTCGCAGGCACTAGCCTCAACTCGAGCAT*ATG*AAGG
CTACTCTGCGTGCCCCCGCTTCCCGCGCCAGCGCTGTGCGCCCCGTCGCCAGCC
TGAAGGCCGCTGCTCAGCGCGTGGCCTCGGTCGCCGGTGTGTCGGTTGCCTCTC
TGGCCCTGACCCTGGCTGCCCACGCCATGGCCGGCATCGGCGCCGTGCTGAAG
GTCCTGACCACCGGCCTGCCCGCCCTGATCAGCTGGATCAAGCGCAAGCGCCA
GCAGTAATCTAGATAAATGGAGGCGCTCGTTGATCTGAGCCTTGCCCCCTGACG
AACGGCGGTGGATGGAAGATACTGCTCTCAAGTGCTGAAGCGGTAGCTTAGCT
CCCCGTTTCGTGCTGATCAGTCTTTTTCAACACGTAAAAAGCGGAGGAGTTTTG
CAATTTTGTTGGTTGTAACGATCCTCCGTTGATTTTGGCCTCTTTCTCCATGGGC
GGGCTGGGCGTATTTGAAGC**GGTTCTCTCTTCTGCCGTT**

Fig. 5 (**a**) DNA sequence ID No. 1: A detailed DNA construct of a designer proton-channel gene (945 bp) that includes a polymerase chain reaction forward (PCR FD) primer (1–20), a 458-bp *HydA1* promoter (21–478), a Plastocyanin transit peptide DNA sequence (479–618), a Melittin DNA sequence (619–703), an *RbcS2* terminator (704–926), and a PCR reverse (RE) primer (927–945). (**b**) DNA sequence ID No. 2: A designer proton-channel gene sequence design (787 bp) that includes (from 5′ to 3′): a PCR FD primer (sequence 1–20), a 282-bp *HydA1* promoter (21–302), a Xho I NdeI site (303–311), a Plastocyanin transit peptide sequence (312–452), a Melittin proton channel (453–536), a XbaI site (537–545), a *RbcS2* terminator (546–768), and a PCR RE primer (769–787). (**c**) DNA sequence ID No. 3: A designer proton-channel gene sequence design (972 bp) that includes (from 5′ to 3′): a PCR FD primer (1–20), a 458-bp *HydA1* promoter (21–478), a *HydA1* transit peptide (479–646), a Melittin (647–730), an *RbcS2* terminator (731–953), and a PCR RE primer (954–972)

c

AGAAAATCTGGCACCACACCATAAGGGTCATAGAATCTAGCGTTATCCTTCCA
CGAGCGTGTGGCAGCCTGCTGGCGTGGACGAGCTGTCATGCGTTGTTCCGTTAT
GTGTCGTCAAACGCCTTCGAGCGCTGCCCGGAACAATGCGTACTAGTATAGGA
GCCATGAGGCAAGTGAACAGAAGCGGGCTGACTGGTCAAGGCGCACGATAGG
GCTGACGAGCGTGCTGACGGGGTGTACCGCCGAGTGTCCGCTGCATTCCCGCC
GGATTGGGAAATCGCGATGGTCGCGCATAGGCAAGCTCGCAAATGCTGTCAGC
TTATCTTACATGAACACACAAACACTCTCGCAGGCACTAGCCTCAAACCCTCGA
AACCTTTTTCCAACAGTTTACACCCCAATTCGGACGCCGCTCCAAGCTCGCTCC
GTTGCTCCTTCATCGCACCACCTATTATTTCTAATATCGTAGACGCGACAAGAT
GTCGGCGCTCGTGCTGAAGCCCTGCGCGGCCGTGTCTATTCGCGGCAGCTCCTG
CAGGGCGCGGCAGGTCGCCCCCCGCGCTCCGCTCGCAGCCAGCACCGTGCGTG
TAGCCCTTGCAACACTTGAGGCGCCCGCACGCCGCCTAGGCAACGTCGCTTGCG
CGGCTATGGCCGGCATCGGCGCCGTGCTGAAGGTCCTGACCACCGGCCTGCCC
GCCCTGATCAGCTGGATCAAGCGCAAGCGCCAGCAGTAAATGGAGGCGCTCGT
TGATCTGAGCCTTGCCCCCTGACGAACGGCGGTGGATGGAAGATACTGCTCTCA
AGTGCTGAAGCGGTAGCTTAGCTCCCCGTTTCGTGCTGATCAGTCTTTTTCAAC
ACGTAAAAAGCGGAGGAGTTTTGCAATTTTGTTGGTTGTAACGATCCTCCGTTG
ATTTTGGCCTCTTTCTCCATGGGCGGGCTGGGCGTATTTGAAGC**GGTTCTCTCT**
TCTGCCGTT

Fig. 5 (continued)

(Melittin) as desired. Because the *HydA1* promoter is a nuclear DNA that can control the expression only for nuclear genes, the synthetic proton-channel gene in this example is designed according to the codon usage of *Chlamydomonas* nuclear genome. Therefore, in this case, the designer proton-channel gene is transcribed in nucleus. Its mRNA is naturally translocated into cytosol, where the mRNA is translated to an apoprotein that consists of the Melittin protein (corresponding to DNA sequence 619–703) and the Plastocyanin transit peptide (corresponding to DNA sequence 479–618) linked together. The transit peptide of the apoprotein guides its transportation across the chloroplast membranes and into the thylakoids, where the transit peptide is cut off from the apoprotein and the resulting free melittin (polypeptide proton channel) insert itself into the thylakoid membrane from the lumen side. The action of the designer proton channel in the thylakoid membranes then provides the benefit of simultaneously eliminating the four proton gradient-related problems in relation to photobiological H_2 production. The two PCR primers (sequences 1–20 and 927–945) are selected from the sequence of a Human actin gene and can be paired with each other. Blasting the sequences against *Chlamydomonas* GenBank found no homologous sequences of them. Therefore, they can be used as appropriate PCR primers in DNA PCR assays for verification of the designer proton-channel gene in the transformed alga.

Figure 5b presents SEQ ID No. 2: example 2 of a designer proton-channel DNA construct that includes a PCR FD primer (sequence 1–20), a 282-bp *HydA1* promoter (21–302), a Xho I NdeI site (303–311), a Plastocyanin transit peptide sequence

(312–452), a Melittin proton channel (453–536), a XbaI site (537–545), a *RbcS2* terminator (546–768), and a PCR RE primer (769–787). This designer proton channel gene (example 2) is quite similar to example 1, SEQ ID No: 1, except that a shorter promoter sequence is used and restriction sites of Xho I NdeI and XbaI are added to make the key components such as the targeting sequence (312–452) and proton channel (453–536) as a modular unit that can be flexible replaced when necessary to save cost of gene synthesis and enhance work productivity. Note, the proton channel does not have to be a Melittin; a number of other proton-channel structures such as a gramicidin analog channel can also be used. This designer proton-channel gene (SEQ ID No: 2) has also been successfully delivered into the nuclear genome of a *C. reinhardtii*-arg7 host cell using the techniques of electroporation and *arg7* complementation screening to create the proton-channel designer alga.

Figure 5c presents SEQ ID No. 3: example 3 of a designer proton-channel DNA construct that includes a PCR FD primer (1–20), a 458-bp *HydA1* promoter (21–478), a *HydA1* transit peptide (479–646), a Melittin (647–730), an *RbcS2* terminator (731–953), and a PCR RE primer (954–972). This designer proton-channel gene (example 3) is also similar to example 1, with the exception that a *HydA1* transit peptide sequence (479–646) is used here so that the proton channel protein is synthesized in the cytosol, delivered into the chloroplast, and inserted into the thylakoid membrane from the stoma side. This designer proton-channel gene (SEQ ID No: 3) has also been successfully delivered into the nuclear genome of an algal host cell to create the proton-channel designer alga.

Using these designer proton channel genes in genetic transformation of *C. reinhardtii* host cells, many transformants have been generated (Fig. 6). Theoretically, these transformants are expected to contain the envisioned proton-channel designer alga that could provide significant impact (tenfold improvement) on technology development in the field of renewable photobiological H_2 production. Next, we need to screen/characterize these transformants to identify and optimize the desired proton-channel designer alga with iterative improvement through our progressive feedback approach of computer-assisted molecular design, designer gene expression, and experimental characterization/verification until the desired result for enhanced photobiological H_2 production is achieved.

5 Vision on How Designer Proton-Channel Algae May Be Used with a Photobioreactor for Hydrogen Production

The designer proton-channel alga could be used with bioreactor systems for efficient photobiological H_2 production (Fig. 7). As explained previously, the designer proton-channel algae, such as the one that contains a hydrogenase-promoter-controlled designer proton-channel gene, can grow normally under aerobic conditions (Fig. 3a) by autotrophic photosynthesis using air CO_2 in a manner similar to that of a wild-type organism. Therefore, to receive the maximal benefit by fully using the potential capabilities of the inducible proton-channel designer algae, it is a preferred practice

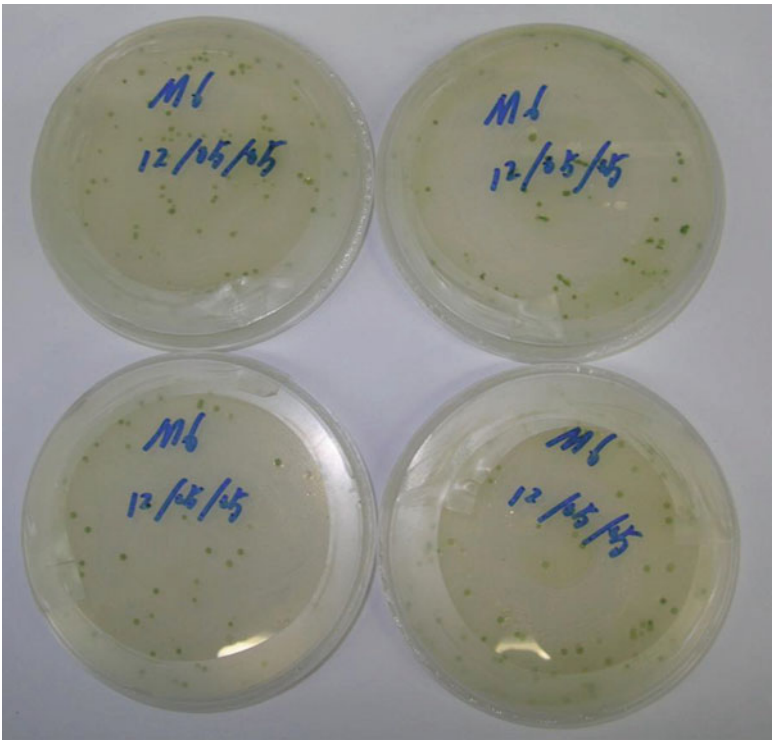

Fig. 6 We have successfully delivered the first set of synthetic genes (DNA) into our *Chlamydomonas* host cells by use of electroporation. Many colonies of designer proton-channel transformants have now successfully been obtained. Each of *green dots* shown in this photograph represents an algal colony grown from a single transformed cell that contains the designer proton-channel DNA construct

to grow the designer algae photoautotrophically using air CO_2 as the carbon source under the aerobic conditions in a minimal medium that contains the essential mineral (inorganic) nutrients. No organic substrate such as acetate is required to grow the designer algae under the normal conditions before the designer proton-channel gene is expressed.

Most of the algae grow rapidly in water through autotrophic photosynthesis using air CO_2 as long as there are sufficient mineral nutrients. The nutrient elements that are commonly required for algal growth are: N, P, and K at the concentrations of about 1–10 mM, and Mg, Ca, S, and Cl at the concentrations of about 0.5–1.0 mM plus some trace elements Mn, Fe, Cu, Zn, B, Co, Mo, etc. at micromolar concentration levels. All of the mineral nutrients are supplied in an aqueous minimal medium that is made with well-established recipes [23] of algal culture media using some water and relatively small amounts of inexpensive fertilizers and mineral salts, such as ammonium bicarbonate (NH_4HCO_3) (or ammonium nitrate, urea, ammonium

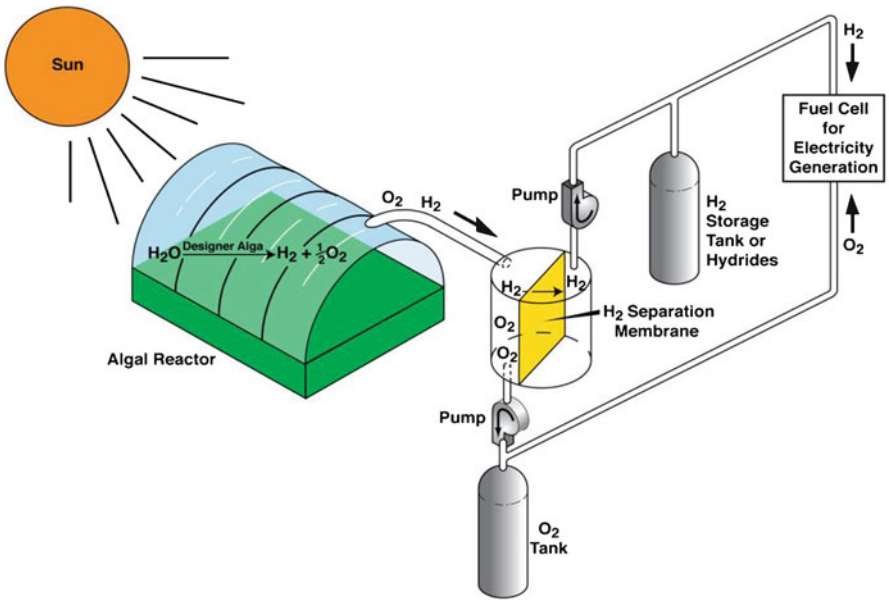

Fig. 7 The figure illustrates how the designer proton-channel algae may be used in an algal reactor and gas-separation-utilization system

chloride), potassium phosphates (K_2HPO_4 and KH_2PO_4), magnesium sulfate heptahydrate ($MgSO_4 \cdot 7H_2O$), calcium chloride ($CaCl_2$), zinc sulfate heptahydrate ($ZnSO_4 \cdot 7H_2O$), iron (II) sulfate heptahydrate ($FeSO_4 \cdot 7H_2O$), and boric acid (H_3BO_3), etc. That is, large amounts of designer algae cells (biocatalysts) can be inexpensively grown in a short period of time because, under aerobic conditions such as in an open pond, the designer algae photoautotrophically grow by themselves using air CO_2 as rapidly as their wild-type parental strains. This is a feature (benefit) that provides a cost-effective solution in generation of photoactive biocatalysts (the designer proton-channel algae) that are alternative to the silicone-photovoltaic-based technologies for renewable solar energy production.

When the algal culture is grown and ready for H_2 production, the grown algal culture is sealed or placed into certain specific conditions, such as anaerobic conditions that can be generated by removal of O_2 from the sealed algal reactor, to induce the expression of designer proton channels. When the designer proton-channel gene is expressed simultaneously with the induction of the hydrogenase enzyme under anaerobic conditions that can be achieved by removal of O_2 from the culture, the algal cells are essentially turned into efficient and robust "green machines" that are perfect for photoevolution of H_2 and O_2 by water splitting (Fig. 2b). Production of H_2 and O_2 by direct photosynthetic water splitting can, in principle, have high quantum yield. Theoretically, it requires only four photons to produce a H_2 molecule

and ½O_2 from water by this mechanism. The maximal theoretical sunlight-to-H_2 energy efficiency by the process of direct photosynthetic water splitting is about 10%, which is the highest possible among all the biological approaches. Application of the designer proton-channel algae maximally realizes the potential of this photosynthetic water-splitting process for H_2 production because all the four proton gradient-related physiological problems (illustrated in Fig. 1) that limit the rate of photobiological H_2 production from water are eliminated by use of the designer alga (Fig. 2a, b). Consequently, this approach has great potential when implemented properly with an algal H_2-production reactor and a gas-separation/utilization system (Fig. 7).

Figure 7 illustrates an algal reactor and gas-separation-utilization system for simultaneous photosynthetic production of H_2 and O_2 from water (H_2O) with effective harvesting and utilization of the gas products including (but not limited to) fuel-cell application for electricity generation. An algal reactor contains a quantity of the designer alga that is exposed to light, such as sunlight. The H_2 and O_2 produced in the algal reactor are pulled through a H_2 separation membrane by vacuum pumps. The O_2 on one side of the membrane is transferred to an O_2 storage tank and a fuel cell. The H_2 on the opposite side of the membrane is transferred to an H_2 storage tank and the fuel cell.

It is worthwhile to note that the removal of O_2 from algal culture can be achieved by a number of techniques, such as the use of a vacuum pump after the grown algal culture is sealed from atmospheric air O_2. Because the production of H_2 and O_2 by direct photosynthetic water occurs in the same bioreactor volume, an effective gas-products separation process, such as the nanometer membrane technology shown in Fig. 7 for effective separation of H_2 and O_2 from the gas mixture, is necessary. Furthermore, consideration must be taken for safe handling of the H_2 and O_2 mixture, which is potentially explosive in case that the concentration of gas mixture reaches the explosion limits. Innovative application of a vacuo-photosynthetic reactor and gas-separation system also helps address the safety issue by strictly maintaining the concentration of H_2 and O_2 well below the explosion limits by effectively removing the gas products from the bioreactor system. In addition, use of a fuel cell that effectively consumes H_2 and O_2 for electricity generation could also help to remove the gas products from the bioreactor and gas-separation system. Furthermore, use of certain hydrogen storage materials, such as metal hydrides that can effectively adsorb H_2, may also help to remove the H_2 gas product from the bioreactor and gas-separation system. Certain engineering technology, such as use of argon or hydrofluorocarbon gas as an inert retardant in the bioreactor and gas-separation system, also improves the safe handling of the H_2 and O_2 mixture.

More information on how to use the designer proton channel algae for hydrogen production can be found in PCT patent application WO 2007/134340 [24]. Furthermore, the next section of this chapter, which reports the technology of designer switchable photosystem-II algae, will provide another solution to the O_2 associated issues as well.

6 Designer Switchable-Photosystem-II Algae

According to the technology concept of designer switchable photosystem-II (PSII) algae, the designer transgenic algae comprise at least two transgenes for enhanced photobiological H_2 production. The first said transgene serves as a genetic switch that controls PSII oxygen evolution and the second one encodes for creation of free proton channels in algal photosynthetic membranes, such as thylakoid membrane. The switchable PSII designer algae, combined with the benefits of programmable creation of free proton channels in algal photosynthetic membranes, provides an effective new solution for efficient and robust photobiological H_2 production, by solving all the six major problems that currently challenge those in the field of photosynthetic H_2 production.

Accordingly, the switchable PSII designer alga is created by transformation of a host alga with at least one DNA construct as shown in Fig. 8a that contains a designer PSII suppressor gene linked with an externally inducible promoter such as a redox-condition-sensitive hydrogenase promoter serving as a genetic switch. According to this embodiment, the designer PSII suppressor is a PSII interfering RNA (iRNA) that can specifically suppress PSII oxygen evolution activity. The general design of the PSII suppressor gene is shown in its DNA construct, which comprises the following components: (a) a PCR FD primer; (b) an externally inducible promoter; (c) a PSII-iRNA sequence; (d) a transcription terminator; and (e) a PCR RE primer.

A second transgene, illustrated in Fig. 8b, that encodes an inducible CF_1-iRNA is added also into genome of the designer alga to create free CF_0 proton channels in

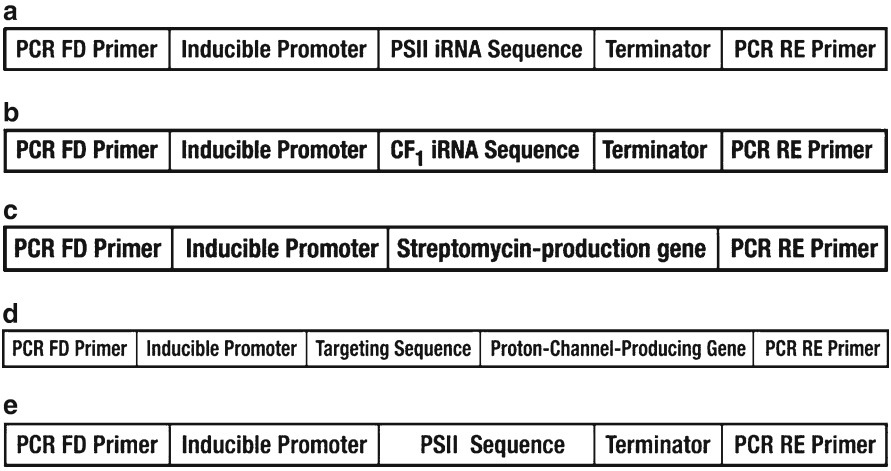

Fig. 8 (**a**) One embodiment of a DNA construct of a switchable photosystem II (PSII) suppressor gene. (**b**) Another embodiment of a DNA construct of a designer CF_1 suppressor gene. (**c**) Another embodiment of a DNA construct of a designer PSII inhibitor gene. (**d**) Another embodiment of a DNA construct of a designer proton-channel-producing gene. (**e**) Another embodiment of a DNA construct of a designer PSII-producing gene

algal photosynthetic membranes by suppressing the expression of CF_1 along with the suppression of PSII and the induction of the hydrogenase under certain specific conditions, such as the anaerobic conditions. The general design of the DNA construct for the CF_1 suppressor gene is shown in Fig. 8b, which includes the following components: (a) a PCR FD primer; (b) an externally inducible promoter; (c) a CF_1-iRNA sequence; (d) a transcription terminator; and (e) a PCR RE primer.

Hydrogenase promoter is an anaerobic inducible promoter that serves as a genetic switch to desirably control the expression of the designer transgenes (Fig. 8a–d). Therefore, the designer transgenes can be expressed only under certain specific conditions, such as the anaerobic conditions. Under aerobic conditions, the designer transgenes are normally not expressed, except for the designer PSII-producing gene illustrated in Fig. 8e. Consequently, as illustrated in Fig. 9a, the switchable PSII designer alga performs autotrophic photosynthesis using ambient-air CO_2 as the carbon source and grows normally, just like a wild-type organism under aerobic conditions, such as in an open pond. When the algal culture is grown and ready for H_2 production (when sufficient amounts of starch are accumulated through the normal oxygenic photosynthetic fixation of CO_2), the algal cells are placed under anaerobic conditions to express the designer transgenes simultaneously with the induction of the hydrogenase enzyme because of the use of the hydrogenase promoter.

As illustrated in Fig. 9b, the expression of the PSII inhibitor gene (as illustrated in Fig. 8a) will shut off PSII O_2 evolution so that the alga will produce H_2 by the metabolic (dark) and PSI-driven (light) H_2 production pathways without production of O_2. The source of electrons for the metabolic and PSI-driven H_2 production is organic reserves, such as starch (as illustrated in Fig. 9b) that are made in the previous cycle of oxygenic photosynthetic CO_2 fixation (Fig. 9a). Since the gas product in the embodiment illustrated in Fig. 9b is essentially pure H_2 and CO_2 without O_2, the problems of H_2 and O_2 mixture (including problems 1–3: drainage of electrons by O_2, poisoning of the hydrogenase enzyme by O_2, and the gas-separation and safety issues) are eliminated with the designer algae.

According to one embodiment, use of a proton channel in the algal photosynthetic thylakoid membrane also enhances this mode of PSI-driven H_2 production from organic reserves. As illustrated in Fig. 9b, operation of the PSI-driven H_2-production mechanism results in translocation of protons across the thylakoid membrane from the stroma into the lumen as the reducing power (NADH, NADPH, FADH) from degradation of organic reserves enters the PQ pool near the Q_r site of Cyt b/f complex and is then oxidized at the Q_o site. If a free proton-conducting channel is not present in the thylakoid membrane, protons could accumulate at the lumen (inside the thylakoids) and impede the electron transport for this PSI-driven H_2 production. Furthermore, the presence of a free proton-conducting channel in algal thylakoid membrane will ensure the inactivation of the Calvin-cycle activity that could compete with the Fd/hydrogenase H_2-production pathway for the electrons derived from the PSI-driven decomposition of the organic reserves. Therefore, it is a preferred practice to incorporate the benefits of a programmable thylakoid proton channel into the switchable PSII designer alga. This embodiment is achieved by delivery of a CF_1-suppresor transgene, as illustrated in Fig. 8b, also into the genome

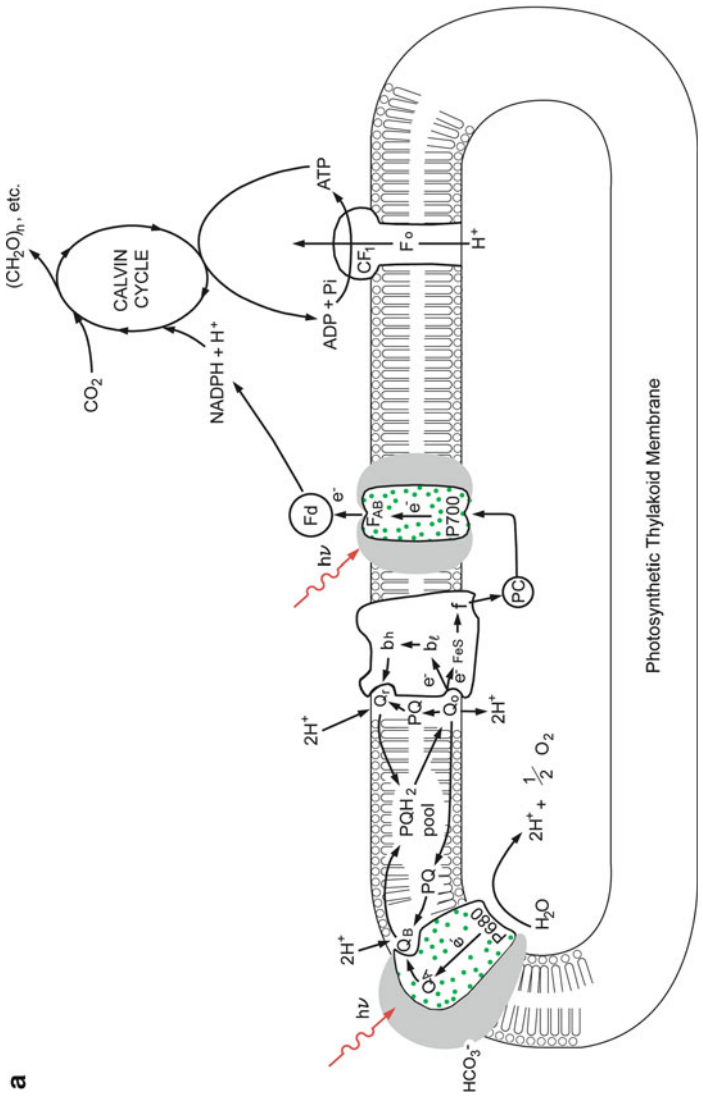

Fig. 9 (**a**) The switchable PSII designer alga capable of growing photoautotrophically and accumulating starch through oxygenic photosynthesis using ambient-air CO_2 under aerobic conditions such as in an aerobic reactor or open pond. (**b**) The photobiological H_2 production pathway in a switchable PSII designer alga when the designer PSII-iRNA (and/or PSII inhibitor such as streptomycin) gene and the designer CF_1-iRNA gene are expressed upon induction of the hydrogenase. (**c**) The photobiological H_2 production pathway in a switchable PSII designer alga when the designer PSII-suppressor (and/or inhibitor) gene and the designer proton-channel producing gene are expressed upon induction of the hydrogenase

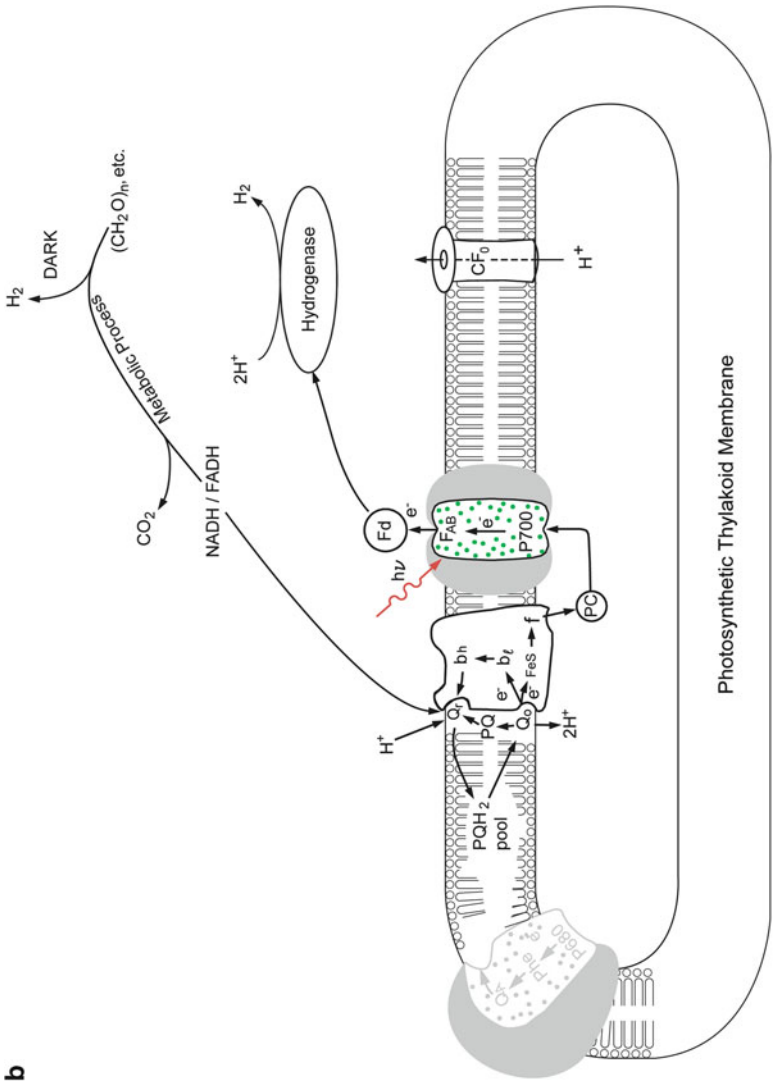

Fig. 9 (continued)

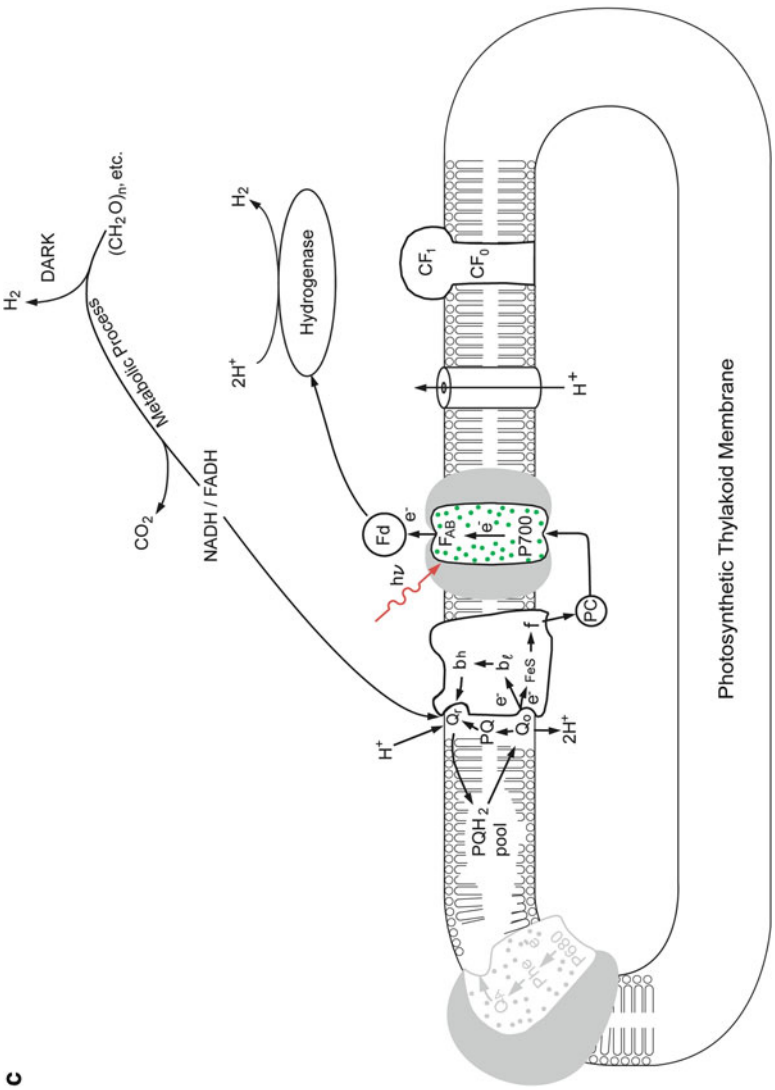

Fig. 9 (continued)

of the designer alga to create free CF_0 proton channels in algal photosynthetic membranes by inhibiting the expression of CF_1 with a CF_1-iRNA that the CF_1-suppresor transgene can produce under the anaerobic conditions upon the induction of the hydrogenase along with the suppression of PSII oxygen-evolving activity.

Therefore, the coexpression of the PSII suppressor, the CF_1 suppressor, and hydrogenase makes this alga a more efficient and robust system for production of H_2. This organism contains normal mitochondria, which can use the reducing power (NADH) from organic reserves (and/or exogenous substrates such as acetate) to power the cell immediately after its return to aerobic conditions. Therefore, when the algal cell is returned to aerobic conditions after its use under anaerobic conditions for production of H_2, the cell will stop generating nonfunctional PSII in thylakoid membranes and start to restore its normal photoautotrophic capability by synthesizing functional thylakoids. Consequently, it is possible to use this type of genetically transformed organism for repeated cycles of photoautotrophic culture growth (starch accumulation) under normal aerobic conditions (Fig. 9a) and efficient production of H_2 under anaerobic conditions (Fig. 9b).

One aspect is the innovative application of a genetic switch to control the expression of PSII activity for production of H_2 without the three O_2 problems (illustrated in Fig. 9a, b). This switchability is accomplished through application of an externally inducible promoter such as a hydrogenase promoter. To function as intended, the designer transgenes (Fig. 8a–d) must be inducibly expressed under anaerobic conditions. In one embodiment, an algal hydrogenase promoter, such as the promoter of the hydrogenase gene (*Hyd1*) of *C. reinhardtii*, is used as an effective genetic switch to control the expression of the designer genes to the exact time and conditions where they are needed for enhanced photobiological H_2 production as illustrated in Fig. 9b. That is, the designer transgenes will be expressed only at the time when the hydrogenase is induced and ready for H_2 production under anaerobic conditions. Therefore, the hydrogenase promoter can be employed as an inducible promoter for each of the DNA constructs to serve as a genetic switch to control the expression of the designer genes. The reason that the designer alga can perform autotrophic photosynthesis using CO_2 as the carbon source under aerobic condition (illustrated in Fig. 9a) is because the designer genes (illustrated in Fig. 8a–d) are not expressed under aerobic conditions owing to the use of a hydrogenase promoter, which can be turned on only under the anaerobic conditions when needed for photobiological H_2 production.

In addition to the hydrogenase promoter, there are other promoters that can also be used to construct the desired genetic switch for designer genes (Fig. 8a–d). For example, the *Nia1* promoter [25] which is induced by growth in nitrate medium and repressed in nitrate-deficient but ammonium-containing medium can be used to control the expression of certain designer genes, such as the designer PSII-producing gene illustrated in Fig. 8e, according to the concentration levels of nitrate in a culture medium as well. Therefore, inducible promoters that can be used and/or modified to serve for this purpose include, but are not limited to, hydrogenase promoters, *Cyc6* promoter, *Nia1* promoter, *CabII-1* promoter, *Ca1* promoter, *Ca2* promoter, coprogen oxidase promoter, and/or their analogs and modified designer sequences. Use of these externally inducible promoters can also create varieties of designer algae.

The PSII-iRNA DNA sequence (Fig. 8a) and the CF_1-iRNA DNA fragment (Fig. 8b) are artificially designed based on the principle of the emerging RNA interference technique. The RNA interference technique uses a piece of iRNA that can specifically bind with the mRNA of a particular gene, thus inhibiting (suppressing) the translation of the gene-specific mRNA to protein. Inactivation of PSII oxygen evolution activity is achieved by suppressing the expression of any key PSII components including its OEE1, D1, CP47, CP43, or D2 protein subunits. Therefore, the envisioned PSII iRNA further includes, but is not limited to, OEE1 iRNA, D1 iRNA, CP47 iRNA, CP43 iRNA, and/or D2 iRNA. For example, the OEE1 subunit [26] is a key component of the PSII oxygen-evolving complex (OEC) that is directly responsible for the oxygen evolution process. It is conceivable that deletion (suppression by an OEE1-specific iRNA) of the OEE1 subunit results in an OEE1-deficient PSII that is no longer able to evolve molecular oxygen by oxidation of water. The gene that encodes for the OEE1 subunit is *PsbO* (also known as *Psb1*), which is a nuclear DNA [27] that can be used with the hydrogenase promoter. Therefore, an anti-sense OEE1 DNA can be designed for generation of an anti-sense mRNA (iRNA) that can inhibit the synthesis of the OEE1 subunit by binding with the normal OEE1 mRNA. Unlike in the mammalian systems, where 21-nt probes are often used to target mRNA for inhibition, the iRNA in microbes (including the host organism *C. reinhardtii*) can be longer segments to be more gene-specific. It is a preferred practice to consider the following three criteria in designing the DNA sequence of the PSII suppressor (such as OEE1 iRNA): (a) the iRNA is a contiguous segment of the PSII subunit (e.g., OEE1) mRNA, typically with a length range of about 20–1,200 base pairs; (b) the iRNA is specific to the PSII subunit (e.g., OEE1), i.e., any significant portion of the iRNA does not have high sequence identity to part of an RNA of any other genes in the host organism such as *C. reinhardtii*; (c) the iRNA does not have significant self-complimentarity to form stable secondary structure that prevents hybridization with the mRNA of PSII subunit (e.g., OEE1). Because such a designed DNA fragment does not have any significant sequence similarity to other known genes, it (when transformed into the host alga) is able to produce an iRNA that specifically binds with normal mRNA of OEE1, thus selectively inhibiting the translation of the OEE1 mRNA into its protein. The CF_1-iRNA sequence is designed with similar principles. Therefore, the iRNA technique can be applied in conjunction with an inducible promoter, such as the hydrogenase promoter, as a genetic switch to create a desirable switchable PSII designer alga for improved photobiological H_2 production.

In the embodiments illustrated in Fig. 8a, b, each of the designer-suppressor DNA constructs also contains a terminator after the designer-suppressor encoding sequence. The terminator DNA sequence, which is designed based on the sequences of natural gene terminators, is to ensure that the transcription of said designer gene is properly terminated to produce an exact designer iRNA as desired.

In various embodiments, the host organisms for transformation of the designer genes (Fig. 8a–d) to create the transgenic designer photosynthetic organism are selected from the group that includes green algae, brown algae, red algae, blue-green algae, marine algae, freshwater algae, cold-tolerant algal strains, heat-tolerant

algal strains, H_2-consuming-activity-deleted algal strains, uptake hydrogenase-deleted algal strains, PSII-deficient algal strains, and combinations thereof. *C. reinhardtii* is a green alga that has had its genome sequenced. Therefore, it is a good model organism, although the technology is applicable to any of the algae mentioned above for enhanced photobiological H_2 production. Proper selection of host organisms for their genetic backgrounds and certain special features is also beneficial. For example, the switchable PSII designer alga created from a cold-tolerant host strain, such as *Chlamydomonas* cold strain CCMG1619 that has been characterized to produce H_2 as cold as 4°C, enables the use even in cold seasons or regions such as Canada. Meanwhile, the switchable PSII designer alga created from a thermophilic photosynthetic organism, such as *Synechococcus bigranulatus*, enables use into the hot seasons or areas such as Mexico and the Southwestern region of the United States including Nevada, California, Arizona, New Mexico, and Texas where the weather temperature can often be high. Furthermore, the switchable PSII designer alga created from a marine alga, such as *Platymonas subcordiformis*, enables using seawater, while the designer alga created from a freshwater alga, such as *C. reinhardtii*, uses freshwater.

Another feature is that various embodiments of the designer algae are devoid of any H_2-consuming activity that is not desirable for net H_2 production. That is, the switchable PSII designer algae will not consume any H_2 that it can produce. This feature, which further enhances the net efficiency for photobiological H_2 production, is incorporated by genetic inactivation or deletion of the H_2-consuming activity. The uptake hydrogenase activity is generally responsible for the H_2-consuming activity in algae. Therefore, this additional feature is incorporated by creating the designer algae from a host alga that has its uptake hydrogenase activity genetically deleted. Additional optional features of the designer algae include the benefits of reduced chlorophyll antenna size which has been demonstrated to provide higher photosynthetic productivity and O_2-tolerant hydrogenase like the [NiFe] hydrogenases of *Ralstonia eutropha*, which can function under aerobic conditions. In various embodiments, these optional features are incorporated into the designer algae also by use of an O_2-tolerant hydrogenase and/or chlorophyll antenna-deficient mutant (e.g., *C. reinhardtii* DS521) as a host organism for gene transformation with the designer DNA constructs (Fig. 8a–e).

There are a number of embodiments for constructing the switchable PSII designer algae by creating and/or using a genetically transmittable factor that can inducibly or programmably control PSII activity. That is, to create and/or use a factor that can be genetically encoded to programmably control PSII activity to solve the O_2-related problems in photobiological H_2 production. An additional example on how to create the switchable PSII designer algae is described as follows. This example utilizes a hydrogenase promoter-linked streptomycin-production gene (Fig. 8c) to also create a switchable PSII designer alga for production of H_2 without the three oxygen-related problems. It has been demonstrated that streptomycin is an inhibitor to the synthesis of a key PSII component, the D1 protein [28]. Without this D1 protein, PSII will no longer be able to perform photosynthetic water splitting to produce O_2. The gene for streptomycin biosynthesis has already been cloned [29, 30].

Therefore, it is now possible by application of synthetic biology techniques to use this streptomycin-production gene in conjunction with the hydrogenase promoter as a programmable switch to control PSII activity in photosynthetic organisms. Figure 8c presents a DNA construct that can be genetically transferred into a host alga to create a switchable PSII designer alga with a phenotype similar to that illustrated in Fig. 9a, b. That is, this designer alga containing the DNA construct can also grow and accumulate organic reserves (such as starch) by autotrophic photosynthesis using CO_2 under aerobic conditions, such as in an open pond (Fig. 9a). When the algal culture is grown and ready for H_2 production, the streptomycin-production gene is then expressed simultaneously with the induction of the hydrogenase enzyme under anaerobic conditions. The expression of the streptomycin-production gene inhibits the synthesis of the D1 protein, thus leading to gradual inactivation of PSII O_2 evolution and activation of H_2 production without O_2 production (Fig. 9b).

Another aspect is the combination of switchable PSII with programmable proton channel and additional features. In one embodiment, it is a preferred practice to apply the feature of the switchable PSII in combination with the benefits of creating a free proton channel in algal photosynthetic thylakoid membrane (Fig. 9b). Proton channels can be created not only by selectively suppressing the expression of CF_1 (Fig. 9b) using a designer CF_1-iRNA gene (Fig. 8b), but also, in another embodiment, by targeted genetic insertion of proton channels such as polypeptide (or protein) pores into algal photosynthetic thylakoid membrane (Fig. 9c) using a designer proton-channel gene (Fig. 8d). The detailed arts for targeted genetic insertion of proton channels into algal photosynthetic membrane have now been reported in the previous section of this chapter. The benefits of a proton channel created with a designer proton-channel producing gene (Fig. 8d) are similar to those created with a designer CF_1-iRNA gene while the features of the switchable PSII created with a designer PSII-iRNA gene are also similar to those created with a designer streptomycin (PSII inhibitor) producing gene. Therefore, these four types of designer genes (Fig. 8a–d) can be applied in various combinations to create the switchable PSII designer algae that also combine with the benefits of a free proton channel in algal photosynthetic thylakoid membranes under H_2-producing conditions as shown in Fig. 9b, c. This combination of benefits is also achieved by algal hybridization of a switchable PSII designer alga with another transformed alga that contains a designer proton-channel gene (Fig. 8b or d), in addition to transformation of a designer proton-channel gene using a switchable PSII designer alga as a host organism.

As mentioned previously, operation of the PSI-driven H_2-production mechanism results in translocation of protons across thylakoid membrane from the stroma into the lumen as the reducing power (NADH, NADPH, and FADH) from degradation of organic reserves enters the PQ pool near the Q_r site of Cyt b/f complex and is then oxidized at the Q_o site. If a free proton-conducting channel does not exist, protons could accumulate inside the thylakoids and impede the electron transport for this PSI-driven H_2 production. Use of a free proton-conducting channel eliminates the restriction of photosynthetic H_2 production by proton accumulation (problem 1). Furthermore, the presence of a free proton-conducting channel in algal thylakoid

membrane also ensures the needed inactivation of the Calvin-cycle activity (which is associated with problems 2–4) so that CO_2 and/or O_2 no longer act as a terminal electron acceptor through the Calvin-cycle activity to compete with the Fd/hydrogenase H_2-production pathway for the electrons derived from the PSI-driven decomposition of the organic reserves. Consequently, incorporation of a proton channel helps eliminate the four proton-gradient-related problems (1–4), while use of the switchable PSII solves the three O_2-related problems (4–6). Therefore, the combination of a switchable PSII with a proton channel in the switchable PSII designer alga (Fig. 9b, c) ensures to eliminate all the six technical problems that currently challenge those in the field of photobiological H_2 production.

7 Vision How Designer Switchable PSII Algae May Be Used with Photobioreactor for Hydrogen Production

The switchable PSII designer algae could be used with a photobioreactor and gas-product separation and utilization system, as illustrated in Fig. 10, for enhanced photobiological H_2 production. Figure 10 illustrates a system that includes an aerobic reactor connected to an anaerobic reactor. The aerobic reactor contains a quantity of algal culture in aerobic conditions. The anaerobic reactor contains a quantity of algal culture in anaerobic conditions. Both the aerobic reactor and the anaerobic reactor

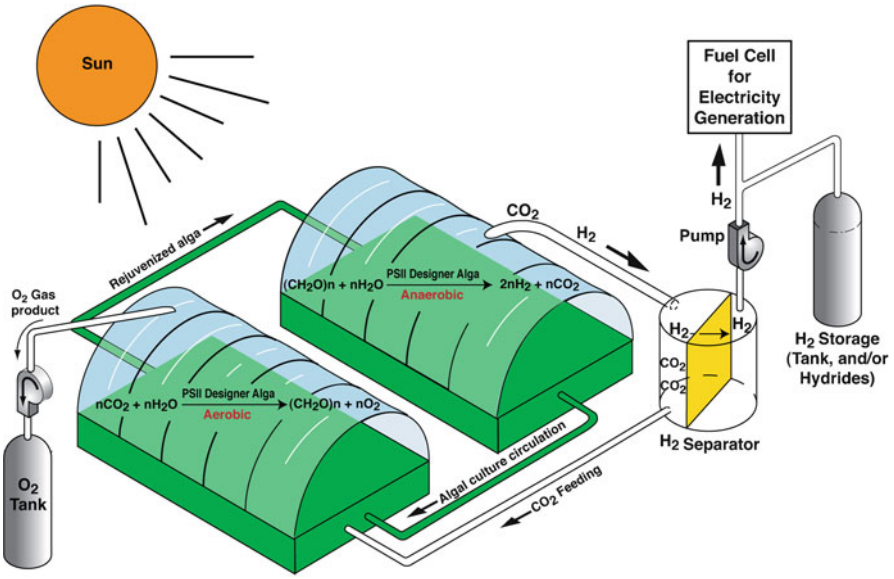

Fig. 10 A photobioreactor and gas-product separation and utilization system for photobiological hydrogen production using designer PSII algae

are exposed to light, such as sunlight. The CO_2 and H_2 produced in the anaerobic reactor are pulled through a H_2 separation membrane by a vacuum pump. The CO_2 on one side of the membrane is transferred to the aerobic reactor via line. The H_2 on the opposite side of the membrane is transferred to a H_2 storage tank and the fuel cell. The algal culture in the anaerobic reactor is transferred to the aerobic reactor when the algal culture is exhausted. The algal culture in the aerobic reactor is transferred to the anaerobic reactor when the algal culture is ready for H_2 production.

A single-organism (switchable PSII designer alga) two-stage H_2-production technology is illustrated in Fig. 10. In the illustrated single-organism-two-stage H_2-production system, organic reserves, such as starch, are accumulated through photoautotrophic algal culture growth by normal oxygenic photosynthesis using CO_2 and sunlight energy in an aerobic reactor where CO_2 and H_2O are converted into biomass materials such as starch $[(CH_2O)_n]$ by the normal autotrophic photosynthesis as illustrated in Fig. 9a:

$$nCO_2 + nH_2O \rightarrow (CH_2O)_n + nO_2 \quad (1)$$

When the algal culture is grown and significant amounts of organic reserves are accumulated in the designer algal cells, the culture is then placed under anaerobic conditions after flowing into an anaerobic reactor so that the inducible promoter (such as hydrogenase promoter)-linked designer gene (Fig. 8a or c) of PSII suppressor (inhibitor) (such as a PSII iRNA or streptomycin) will then be expressed, simultaneously upon the induction of the hydrogenase enzyme. As illustrated in Fig. 9b, the expression of the PSII inhibitor gene will shut off PSII O_2-evolution activity so that the alga will produce H_2 by the metabolic (dark) and PSI-driven (light) H_2 production pathways without production of O_2 with the following process reaction:

$$(CH_2O)_n + nH_2O \rightarrow 2nH_2 + nCO_2 \quad (2)$$

The source of electrons for the metabolic and PSI-driven H_2 production is organic reserves, such as starch (Fig. 9b) that are made in the previous cycle of oxygenic photosynthetic CO_2 fixation (Fig. 9a). Since the gas product in this case (Fig. 9b) is essentially pure H_2 and CO_2 without O_2 because of the inactivation of PSII O_2-evolution activity, a O_2-free condition in an algal bioreactor can now be easily maintained for H_2 production—all of the three O_2-related problems (including problems 4–6: drainage of electrons by O_2, poisoning of the hydrogenase enzyme by O_2, and the gas-separation and safety issues) are thus eliminated. This algal H_2-production system does not require an O_2-tolerant hydrogenase, neither does it require a H_2–O_2 gas-separation process. Consequently, the algal H_2-production process becomes more stable and efficient because both the drainage of electrons by O_2 and poisoning of the hydrogenase enzyme by O_2 do not occur with the designer algae.

In the anaerobic reactor, a designer proton-channel producing gene (Fig. 8d) and/or designer CF_1-suppressor gene (Fig. 8b) incorporated into the switchable PSII designer alga is expressed to create a free proton channel in algal photosynthetic thylakoid membrane along with the expression of the PSII suppressor gene upon induction of the hydrogenase. As shown in Fig. 9c and/or b, the expression of a free

proton channel in the algal photosynthetic thylakoid membrane greatly facilitates the needed flow of protons across the thylakoid membrane to further enhance the photobiological H_2-production process.

According to the process (2), the ratio of H_2 to CO_2 in the gas products should be about 2:1. That is, under an idealized condition, the gas products from the photobiological H_2-production process in the anaerobic reactor consists of about 67% H_2 and 33% CO_2. As shown in Fig. 10, the pure H_2 and CO_2 gas products from this photobiological H_2-production process in the anaerobic algal reactor are easily collected, separated, and stored/utilized with available engineering technologies including pipelines with a pump and nanometer membrane gas separation system (or a commercial pressure-swing gas-separation system) for separation of H_2 from CO_2.

It is worthwhile to note that the H_2 gas product from the photobiological H_2-production process is completely free of carbon monoxide (CO) because there is absolutely no mechanism (no CO-producing enzyme) for any CO generation in the algae. The H_2 gas product from this process is enzymatically pure, which is perfect for fuel-cell applications. Therefore, the H_2 gas product from this process can be immediately used by fuel-cell operations to generate electricity and/or collected into storage tanks/hydrides for cash sales. In the illustrated embodiment, the CO_2 gas product is fed into the algal culture medium for photosynthetic conversion back into biomass in the aerobic reactor. In various embodiments, the O_2 gas product from the aerobic algal reactor is collected in a tank or vented into the atmosphere.

The ideal net result of the single-organism (switchable PSII designer alga) two-stage H_2-production technology is the conversion of $2nH_2O$ to $2nH_2$ and nO_2 as a result of the summation of the two process (1 and 2). That is, the net result is the production of hydrogen and oxygen from water with no CO_2 emission. The maximal theoretical sunlight-to-H_2 energy conversion efficiency for this single-organism-two-stage H_2-production system is estimated to be about 5%.

Another feature is that the designer alga provides the capability for repeated cycles of photoautotrophic culture growth (starch accumulation) under normal aerobic conditions in an aerobic reactor (Fig. 9a) and efficient production of H_2 under anaerobic conditions in an anaerobic reactor (Fig. 9b). The switchable PSII designer alga contains normal mitochondria, which uses the reducing power (NADH) from organic reserves (and/or exogenous substrates, such as acetate) to power the cell immediately after its return to aerobic conditions. Therefore, when the algal cell is returned to aerobic conditions (aerobic reactor) after its use under anaerobic conditions (anaerobic reactor) for production of H_2, the cell will stop suppressing PSII activity in thylakoid membranes and start to restore its normal photoautotrophic capability by synthesizing functional thylakoids. Consequently, it is possible to use this type of genetically transformed organism for repeated cycles of photoautotrophic culture growth (starch accumulation) under normal aerobic conditions in an aerobic reaction (Fig. 9a) and efficient production of H_2 under anaerobic conditions in an anaerobic reactor (Fig. 9b). That is, this photobiological H_2-production technology can be operated continuously by circulating rejuvenated algal culture from the aerobic reactor into the anaerobic reactor while circulating the used algal culture from the anaerobic reactor (after its use for H_2 production) into the aerobic reactor

for rejuvenation by synthesizing functional thylakoids and accumulating organic reserves (starch) through photosynthetic CO_2 fixation.

There are additional ways that the switchable PSII designer algae can be used. For example, the used algal culture from the anaerobic reactor does not have to be circulated back to the aerobic reactor. Instead, the used algal culture is taken out to be used as fertilizers or biomass feed stocks for other processing because the photoautotrophic growth of the designer switchable PSII designer alga in an aerobic reactor continuously supplies algal cells to an anaerobic reactor for the photobiological H_2 production (Fig. 10). Another way is to use switchable PSII designer algae as biocatalysts to produce H_2 from organic substrates. This is done by adding organic substrates, such as acetate, organic acids, ethanol, methanol, propanol, butanol, acetone, carbohydrates, lipids, proteins, biomass materials, and combinations thereof, for quick photoheterotrophic growth in an aerobic reactor and for photobiological H_2 production in an anaerobic reactor.

Acknowledgments This work was conducted in part at Oak Ridge National Laboratory which is managed by UT-Battelle, LLC, for DOE under contract No. DE-AC05-00OR22725. The author wishes to thank his project team and friends including Drs. Marilyn Brown, Tim Armstrong, Elias Greenbaum, Barbara Evans, Dong Xu, and Prof. Laurie Mets for their wonderful support. The project work was supported in part by the U.S. DOE/EERE Photobiological Hydrogen Program.

References

1. Prince RC, Kheshgi HS (2005) The photobiological production of hydrogen: potential efficiency and effectiveness as a renewable fuel. Crit Rev Microbiol 31:19–31
2. Ghysels B, Franck F (2010) Hydrogen photo-evolution upon S deprivation stepwise: an illustration of microalgal photosynthetic and metabolic flexibility and a step stone for future biotechnological methods of renewable H_2 production. Photosynth Res 106:145–154
3. Melis A, Zhang L, Forestier M, Ghirardi ML, Seibert M (2000) Sustained photobiological hydrogen gas production upon reversible inactivation of oxygen evolution in the green alga *Chlamydomonas reinhardtii*. Plant Physiol 122:127–135
4. Ghirardi ML, Zhang L, Lee JW, Flynn T, Seibert M, Greenbaum E, Melis A (2000) Microalgae: a green source of renewable H_2. Trends Biotechnol 18:506–511
5. Nguyen AV, Thomas-Hall SR, Malnoë A, Timmins M, Mussgnug JH, Rupprecht J, Kruse O, Hankamer B, Schenk PM (2008) Transcriptome for photobiological hydrogen production induced by sulfur deprivation in the green alga *Chlamydomonas reinhardtii*. Eukaryot Cell 7(11):1965–1979
6. Timmins M, Thomas-Hall SR, Darling A, Zhang E, Hankamer B, Marx UC, Schenk PM (2009) Phylogenetic and molecular analysis of hydrogen-producing green algae. J Exp Bot 60(6):1691–1702
7. Berberoğlu H, Pilon L (2010) Maximizing the solar to H_2 energy conversion efficiency of outdoor photobioreactors using mixed cultures. Int J Hydrogen Energy 35(2):500–510
8. Lee JW (2007) Designer proton-channel transgenic algae for photobiological hydrogen production. PCT International Patent Application Publication Number: WO 2007/134340 A2
9. Lee JW (2011) Designer proton-channel transgenic algae for photobiological hydrogen production. US Patent 7,932,437 B2
10. Lee JW (2010) Switchable photosystem-II designer algae for photobiological hydrogen production. US Patent 7,642,405 B2

11. Cinco RM, MacInnis JM, Greenbaum E (1993) The role of carbon dioxide in light activated hydrogen production by *Chlamydomonas reinhardtii*. Photosynth Res 38:27–33
12. Eaton-Rye J, Govindjee R (1984) A study of the specific effect of bicarbonate on photosynthetic electron transport in the presence of methyl viologen. Photobiochem Photobiophys 8: 279–288
13. Lee JW, Greenbaum E (2003) A new oxygen sensitivity and its potential application in photosynthetic H_2 production. Appl Biochem Biotechnol 105–108:303–313
14. Cournac L, Mus F, Bernard L, Guedeney G, Vignais P, Peltier G (2002) Limiting steps of hydrogen production in *Chlamydomonas reinhardtii* and *Synechocystis PCC 6803* as analysed by light-induced gas exchange transients. Int J Hydrogen Energy 27:1229–1237
15. Guan Y, Zhang W, Deng M, Jin M, Yu X (2004) Significant enhancement of photobiological H_2 evolution by carbonylcyanide chlorophenylhydrazone (CCCP) in marine green alga *Platymonas subcordiformis*. Biotechnol Lett 26:1031–1035
16. Gaffron H, Rubin J (1942) Fermentative and photochemical production of hydrogen in algae. J Gen Physiol 26:219–240
17. Samuilov VD, Barsky EL, Kitashov AV (1995) ADRY agent-induced cyclic and non-cyclic electron transfer around photosystem II. In: Mathis P (ed) Photosynthesis: from light to biosphere, vol II. Kluwer Academic, Dordrecht, pp 267–270
18. Townsley LE, Tucker WA, Sham S, Hinton JF (2001) Structures of gramicidins A, B, and C incorporated into sodium dodecyl sulfate micelles. Biochemistry 40:11676
19. Doltchinkova V, Georgieva K, Traytcheva N, Slavov C, Mishev K (2004) Melittin-induced changes in thylakoid membranes: particle electrophoresis and light scattering study. Biophys Chem 109(204):387–397
20. Quinn JM, Barraco P, Ericksson M, Merchant S (2000) Coordinate copper- and oxygen responsive *Cyc6* and *Cpx1* expression in *Chlamydomonas* is mediated by the same element. J Biol Chem 275:6080–6089
21. Teramoto H, Ono T, Minigawa J (2001) Identification of Lhcb gene family encoding the light harvesting chlorophyll-a/b proteins of photosystem II in *Chlamydomonas reinhardtii*. Plant Cell Physiol 42(8):849–856
22. Sambrook J, Russell DW (2001) In vitro amplification of DNA by the polymerase chain reaction. In: Sambrook J, Russell DW (eds) Molecular cloning: a laboratory manual, vol 2, 3rd edn. Cold Spring Harbor Laboratory Press, Cold Spring Harbor, pp 8.1–8.113
23. Harris EH (2001) *Chlamydomonas* as a model organism. Annu Rev Plant Physiol Plant Mol Biol 52:363–406
24. Lee JW (2007) Designer proton-channel transgenic algae for photobiological hydrogen production. International Application Published Under the Patent Cooperation Treaty (PCT), WO 2007/134340 A2
25. Loppes R, Radoux M (2002) Two short regions of the promoter are essential for activation and repression of the nitrate reductase gene in *Chlamydomonas reinhardtii*. Mol Genet Genomics 268:42–48
26. Erickson JM (1998) Assembly of photosystem II. In: Rochaix J-D, Goldschmidt-Clermont M, Merchant S (eds) The molecular biology of chloroplast and mitochondria in *Chlamydomonas*. Kluwer Academic, Boston, pp 255–285
27. Ruffle SV, Sayre RT (1998) Functional analysis of photosystem II. In: Rochaix J-D, Goldschmidt-Clermont M, Merchant S (eds) The molecular biology of chloroplast and mitochondria in *Chlamydomonas*. Kluwer Academic, Boston, pp 287–322
28. Jiao DM, Ji BH (2001) Photoinhibition in indica and japonica subspecies of rice and their reciprocal F-1 hybrids. Aust J Plant Physiol 28:299–306
29. Kumada Y, Hurinouchi S, Uozumi T, Beppu T (1986) Cloning of a streptomycin-production gene directing synthesis of N-methyl-L-glucosamine. Gene 42:221–224
30. Aiba S, Onuki T, Kojima T, Nishida S, Imanaka T (1987) Cloning and expression of a DNA fragment containing regulator gene for streptomycin biosynthesis [patent written in Japanese]. Application No. JP 85-236475

Chapter 21
Designer Photosynthetic Organisms for Photobiological Production of Ethanol from Carbon Dioxide and Water

James Weifu Lee

Abstract This chapter describes an invention on photosynthetic ethanol production through application of synthetic biology. The designer plants, designer algae, and designer plant cells are created such that the endogenous photosynthesis regulation mechanism is tamed, and the reducing power (NADPH) and energy (ATP) acquired from the photosynthetic water splitting and proton gradient-coupled electron transport process are used for immediate synthesis of ethanol (CH_3CH_2OH) directly from carbon dioxide (CO_2) and water (H_2O). This photobiological ethanol-production method eliminates the problem of recalcitrant lignocellulosics by bypassing the bottleneck problem of the conventional biomass technology. The photosynthetic ethanol-production technology is expected to have a much higher solar-to-ethanol energy-conversion efficiency than the conventional technology. Furthermore, this approach enables the use of seawater for photobiological production of ethanol without requiring freshwater or agricultural soil, since the designer photosynthetic organisms can be created from certain marine algae that can use seawater.

1 Introduction

Ethanol (CH_3CH_2OH) can be used as a liquid fuel to run engines such as cars. A significant market for ethanol as a liquid fuel already exists in the current transportation and energy systems. In the United States, currently, ethanol is generated primarily from corn starch using a yeast-fermentation process. Therefore, the "cornstarch

J.W. Lee (✉)
Department of Chemistry & Biochemistry, Old Dominion University,
Physical Sciences Building, Room 3100B, 4402 Elkhorn Avenue, Norfolk, VA 23529, USA

Johns Hopkins University, Whiting School of Engineering, 118 Latrobe Hall,
Baltimore, MD 21218, USA
e-mail: jwlee@ODU.edu; JLee349@JHU.edu

J.W. Lee (ed.), *Advanced Biofuels and Bioproducts*, DOI 10.1007/978-1-4614-3348-4_21,

ethanol-production" process requires a number of energy-consuming steps including agricultural corn-crop cultivation, corn-grain harvesting, corn-grain starch processing, and starch-to-sugar-to-ethanol fermentation. Independent studies have recently shown that the net energy efficiency of the "cornstarch ethanol-production" process is actually negative in some cases. That is, the "cornstarch ethanol-production" process costs more energy than the energy value of its product ethanol. This is not surprising, understandably because the cornstarch that the current technology can use represents only a small fraction of the corn-crop biomass that includes the corn stalks, leaves, and roots. The cornstovers are commonly discarded in the agricultural fields where they slowly decompose back to CO_2, because they represent largely lignocellulosic biomass materials that the current biorefinery industry cannot efficiently use for ethanol production. There are research efforts in trying to make ethanol from lignocellulosic plant biomass materials—a concept called "cellulosic ethanol." However, plant biomass has evolved effective mechanisms for resisting assault on its cell-wall structural sugars from the microbial and animal kingdoms. This property underlies a natural recalcitrance, creating roadblocks to the cost-effective transformation of lignocellulosic biomass to fermentable sugars. Therefore, one of its problems known as the "lignocellulosic recalcitrance" represents a formidable technical barrier to the cost-effective conversion of plant biomass to fermentable sugars. That is, because of the recalcitrance problem, lignocellulosic biomasses (such as cornstover, switchgrass, and woody plant materials) could not be readily converted to fermentable sugars to make ethanol without certain pretreatment, which is often associated with high processing cost. Despite more than 25 years of R&D efforts in lignocellulosic biomass pretreatment and fermentative ethanol-production processing, the problem of recalcitrant lignocellulosics still remains as a formidable technical barrier that has not yet been eliminated so far. Furthermore, the steps of lignocellulosic biomass cultivation, harvesting, pretreatment processing, and cellulose-to-sugar-to-ethanol fermentation all cost energy. Therefore, any new technology that could bypass these bottleneck problems of the biomass technology would be useful.

Algae (such as *Chlamydomonas reinhardtii*, *Platymonas subcordiformis*, *Chlorella fusca*, *Dunaliella salina*, *Ankistrodesmus braunii*, and *Scenedesmus obliquus*), which can perform photosynthetic assimilation of CO_2 with O_2 evolution from water in a liquid culture medium with a maximal theoretical solar-to-biomass energy conversion of about 10%, have tremendous potential to be a clean and renewable energy resource. However, the wild-type oxygenic photosynthetic green plants, such as eukaryotic algae, do not possess the ability to produce ethanol directly from CO_2 and H_2O. As shown in Fig. 1, the wild-type photosynthesis uses the reducing power (NADPH) and energy (ATP) from the photosynthetic water splitting and proton gradient-coupled electron transport process through the algal thylakoid membrane system to reduce CO_2 into carbohydrates $(CH_2O)_n$ such as starch with a series of enzymes collectively called the "Calvin cycle" at the stroma region in an algal or green-plant chloroplast. The net result of the wild-type photosynthetic process is the conversion of CO_2 and H_2O into carbohydrates $(CH_2O)_n$ and O_2 using sunlight energy according to the following process reaction:

$$n\mathrm{CO_2} + n\mathrm{H_2O} \rightarrow (\mathrm{CH_2O})n + n\mathrm{O_2} \quad (1)$$

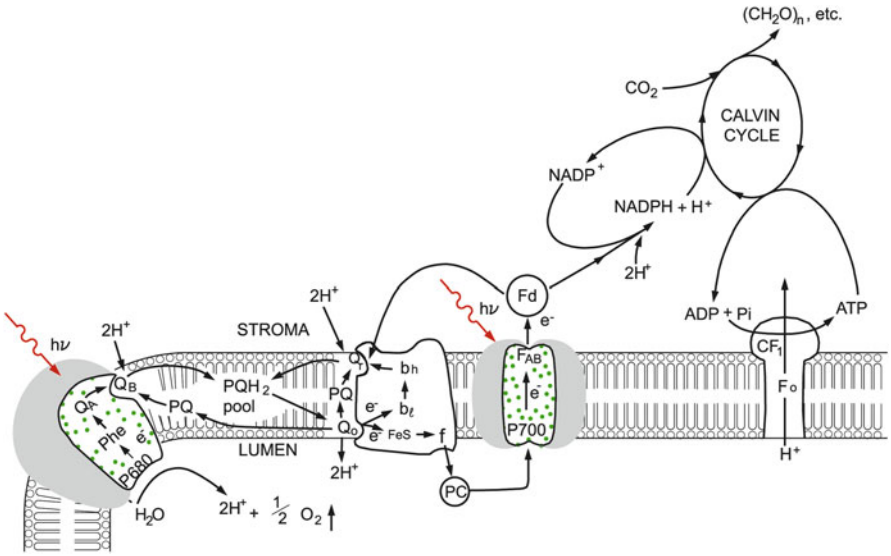

Fig. 1 Presents the oxygenic autotrophic photosynthetic pathway, which uses the reducing power (NADPH) and energy (ATP) from the photosynthetic water splitting and proton gradient-coupled electron transport process through the algal thylakoid membrane system to reduce CO_2 into carbohydrates $(CH_2O)n$ with a series of enzymes collectively called the "Calvin cycle" in the stroma region of an algal or green-plant chloroplast

The carbohydrates $(CH_2O)n$ are then further converted to all kinds of complicated cellular (biomass) materials including proteins, lipids, and cellulose and other cell-wall materials during cell metabolism and growth.

In certain algae such as *C. reinhardtii*, some of the organic reserves such as starch could be slowly metabolized to ethanol through a secondary fermentative metabolic pathway. The algal fermentative metabolic pathway is similar to the yeast-fermentation process, by which starch is breakdown to smaller sugars such as glucose that is, in turn, transformed into pyruvate by a glycolysis process. Pyruvate may then be converted to formate, acetate, and ethanol by a number of additional metabolic steps [1]. The efficiency of this secondary metabolic process is quite limited, probably because it could use only a small fraction of the limited organic reserve such as starch in an algal cell. The maximal concentration of ethanol that can be generated by the fermentative algal metabolic process is only about 1% or less, which is not high enough to become a viable technology for energy production. To be an economically viable technology, the ethanol concentration in a bioreactor medium is preferred to reach as high as about 3–5% before an ethanol-distillation process may be profitably applied. Therefore, a new ethanol-producing mechanism with a high solar-to-ethanol energy efficiency is needed.

This chapter reports an invention (U.S. Patent No. 7,973,214 B2) that can provide revolutionary designer organisms, which are capable of directly synthesizing ethanol from CO_2 and H_2O. The ethanol-production system provided by the present invention could bypass the bottleneck problems of the biomass technology mentioned above.

2 The Concept of Designer Photosynthetic Ethanol-Producing Organisms

The present invention [2] is directed to a revolutionary photosynthetic ethanol-production technology based on designer transgenic plants (e.g., algae) or plant cells. The designer plants and plant cells are created using genetic engineering techniques such that the endogenous photosynthesis regulation mechanism is tamed, and the reducing power (NADPH) and energy (ATP) acquired from the photosynthetic water splitting and proton gradient-coupled electron transport process can be used for immediate synthesis of ethanol (CH_3CH_2OH) directly from carbon dioxide (CO_2) and water (H_2O) according to the following process reaction:

$$2CO_2 + 3H_2O \rightarrow CH_3CH_2OH + 3O_2 \quad (2)$$

The ethanol-production methods of the present invention completely eliminate the problem of recalcitrant lignocellulosics by bypassing the bottleneck problem of the biomass technology. As shown in Fig. 2, the photosynthetic process in a designer organism effectively uses the reducing power (NADPH) and energy (ATP) from the photosynthetic water splitting and proton gradient-coupled electron transport process for immediate synthesis of ethanol (CH_3CH_2OH) directly from carbon dioxide (CO_2) and water (H_2O) without being drained into the other pathways for synthesis of the undesirable lignocellulosic materials that are very hard and often inefficient for the biorefinery industry to use. This approach is also different from the existing "cornstarch ethanol-production" process. In accordance with this invention, ethanol will be produced directly from carbon dioxide (CO_2) and water (H_2O) without having to go through many of the energy-consuming steps that the cornstarch ethanol-production process has to go through, including corn-crop cultivation, corn-grain harvesting, corn-grain cornstarch processing, and starch-to-sugar-to-ethanol fermentation. As a result, the photosynthetic ethanol-production technology of the present invention is expected to have a much (more than ten times) higher solar-to-ethanol energy-conversion efficiency than the current technology. Assuming a 10% solar energy-conversion efficiency for the proposed photosynthetic ethanol-production process, the maximal theoretical productivity (yield) could be about 88,700 kg of ethanol per acre per year, which could support about 70 cars (per year per acre). Therefore, this invention has the potential to bring a significant capability to the society in helping to ensure energy security. The present invention could also help protect the Earth's environment from the dangerous accumulation of CO_2 in the atmosphere, because the present methods convert CO_2 directly into clean ethanol energy.

A fundamental feature of the present methodology is utilizing a plant (e.g., an alga) or plant cells, introducing into the plant or plant cells nucleic acid molecules coding for a set of enzymes that can act on an intermediate product of the Calvin cycle and convert the intermediate product into ethanol as illustrated in Fig. 2, instead of making starch and other complicated cellular (biomass) materials as the end products by the wild-type photosynthetic pathway (Fig. 1). Accordingly, the

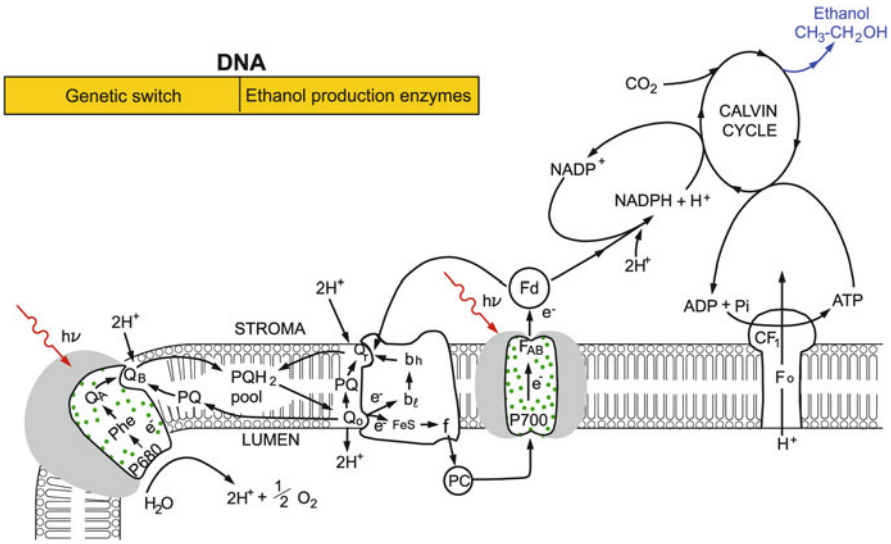

Fig. 2 A designer organism such as a designer alga becomes a "green machine" for production of ethanol directly from CO_2 and H_2O when the designer photosynthetic ethanol-producing pathway(s) is turned on

present invention provides, *inter alia*, methods for producing ethanol based on a designer plant (such as a designer alga), designer plant tissue, or designer plant cells, DNA constructs encoding genes of a designer ethanol-production pathway, as well as the designer algae, designer plants, designer plant tissues, and designer plant cells created. The various aspects of the present invention are described in further detail herein below.

2.1 Host Plant, Plant Tissue, and Plant Cell

According to the present invention, a designer organism or cell for the photosynthetic ethanol production of the invention can be created utilizing as host, any plant (including alga), plant tissue, or plant cells that have a photosynthetic capability, i.e., an active enzymatic pathway that captures light energy through photosynthesis, using this energy to convert inorganic substances into organic matter. Preferably, the host organism should have an adequate photosynthetic CO_2 fixation rate, for example, to support photosynthetic ethanol production from CO_2 and H_2O at least about 1,780 kg ethanol per acre per year, more preferably, 8,870 kg ethanol per acre per year, or even more preferably, 88,700 kg ethanol per acre per year.

In a preferred embodiment, an aquatic plant is utilized to create a designer plant. Aquatic plants, also called hydrophytic plants, are plants that live in or on aquatic environments, such as in water (including on or under the water surface) or permanently saturated soil. As used herein, aquatic plants include, for example, algae,

submersed aquatic herbs (*Hydrilla verticillata*, *Elodea densa*, *Hippuris vulgaris, Aponogeton boivinianus, Aponogeton rigidifolius, Aponogeton longiplumulosus, Didiplis diandra, Vesicularia dubyana, Hygrophilia augustifolia, Micranthemum umbrosum, Eichhornia azurea, Saururus cernuus, Cryptocoryne lingua, Hydrotriche hottoniiflora, Eustralis stellata, Vallisneria rubra, Hygrophila salicifolia, Cyperus helferi, Cryptocoryne petchii, Vallisneria americana, Vallisneria torta, Hydrotriche hottoniiflora, Crassula helmsii, Limnophila sessiliflora, Potamogeton perfoliatus, Rotala wallichii, Cryptocoryne becketii, Blyxa aubertii, Hygrophila difformmis*), duckweeds (*Spirodela polyrrhiza*, *Wolffia globosa, Lemna trisulca, Lemna gibba, Lemna minor, Landoltia punctata*), water cabbage (*Pistia stratiotes*), buttercups (*Ranunculus*), water caltrop (*Trapa natans* and *Trapa bicornis*), water lily (*Nymphaea lotus*, Nymphaeaceae and Nelumbonaceae), water hyacinth (*Eichhornia crassipes*), *Bolbitis heudelotii*, *Cabomba* sp., seagrasses (*Heteranthera zosterifolia*, Posidoniaceae, Zosteraceae, Hydrocharitaceae, and Cymodoceaceae). Ethanol produced from an aquatic plant can diffuse into water, permitting normal growth of the plants and more robust production of ethanol from the plants. Liquid cultures of aquatic plant tissues (including, but not limited to, multicellular algae) or cells (including, but not limited to, unicellular algae) are also highly preferred for use, since the ethanol molecules produced from a designer ethanol-production pathway can readily diffuse out of the cells or tissues into the liquid water medium, which can serve as a large pool to store the product ethanol that can be subsequently harvested by filtration and/or distillation techniques.

Although aquatic plants or cells are preferred host organisms for use in the methods of the present invention, tissue and cells of non-aquatic plants, which are photosynthetic and can be cultured in a liquid culture medium, can also be used to create designer tissue or cells for photosynthetic ethanol production. For example, the following tissue or cells of non-aquatic plants can also be selected for use as a host organism in this invention: the photoautotrophic shoot tissue culture of wood apple tree *Feronia limonia*, the chlorophyllous callus cultures of corn plant *Zea mays*, the green root cultures of Asteraceae and Solanaceae species, the tissue culture of sugarcane stalk parenchyma, the tissue culture of bryophyte *Physcomitrella patens*, the photosynthetic cell suspension cultures of soybean plant (*Glycine max*), the photoautotrophic and photomixotrophic culture of green Tobacco (*Nicotiana tabacum* L.) cells, the cell suspension culture of *Gisekia pharnaceoides* (a C_4 plant), the photosynthetic suspension cultured lines of *Amaranthus powellii* Wats., *Datura innoxia* Mill., *Gossypium hirsutum* L., and *Nicotiana tabacum*×*Nicotiana glutinosa* L. fusion hybrid.

By "liquid medium" is meant liquid water plus relatively small amounts of inorganic nutrients (e.g., N, P, K etc., commonly in their salt forms) for photoautotrophic cultures; and sometimes also including certain organic substrates (e.g., sucrose, glucose, or acetate) for photomixotrophic and/or photoheterotrophic cultures.

In an especially preferred embodiment, the plant utilized in the ethanol-production method of the present invention is an alga. The use of algae has several advantages. They can be grown in an open pond at large amounts and low costs. Harvest and purification of ethanol from the water phase is also easily accomplished by distillation or membrane separation.

Algae suitable for use in the present invention include both unicellular algae and multi-unicellular algae. Multicellular algae that can be selected for use in this invention include, but are not limited to, seaweeds such as *Ulva latissima* (sea lettuce), *Ascophyllum nodosum, Codium fragile, Fucus vesiculosus, Eucheuma denticulatum, Gracilaria gracilis, Hydrodictyon reticulatum, Laminaria japonica, Undaria pinntifida, Saccharina japonica, Porphyra yezoensis*, and *Porphyra tenera*. Suitable algae can also be chosen from the following divisions of algae: green algae (Chlorophyta), red algae (Rhodophyta), brown algae (Phaeophyta), and diatoms (Bacillariophyta). Suitable orders of green algae include Ulvales, Ulotrichales, Volvocales, Chlorellales, Schizogoniales, Oedogoniales, Zygnematales, Cladophorales, Siphonales, and Dasycladales. Suitable genera of Rhodophyta are Porphyra, Chondrus, Cyanidioschyzon, Porphyridium, Gracilaria, Kappaphycus, Gelidium, and Agardhiella. Suitable genera of Phaeophyta are Laminaria, Undaria, Macrocystis, Sargassum, and Dictyosiphon. A suitable genus of Cyanophyta is Phoridium. Suitable genera of Bacillariophyta are Cyclotella, Cylindrotheca, Navicula, Thalassiosira, and Phaeodactylum. Preferred species of algae for use in the present invention include *C. reinhardtii, P. subcordiformis, C. fusca, Chlorella sorokiniana, Chlorella vulgaris, "Chlorella" ellipsoidea, Chlorella* spp.*, D. salina, Dunaliella viridis, Dunaliella bardowil, Haematococcus pluvialis; Parachlorella kessleri, Betaphycus gelatinum, Chondrus crispus, Cyanidioschyzon merolae, Cyanidium caldarium*, *Galdieria sulphuraria, Gelidiella acerosa, Gracilaria changii*, *Kappaphycus alvarezii, Porphyra miniata, Ostreococcus tauri, P. yezoensis, Porphyridium* sp., *Palmaria palmata*, *Gracilaria* spp.*, Isochrysis galbana, Kappaphycus* spp.*, L. japonica, Laminaria* spp.*, Monostroma* spp.*, Nannochloropsis oculata*, *Porphyra* spp.*, Porphyridium* spp.*, Undaria pinnatifida, Ulva lactuca, Ulva* spp.*, Undaria* spp.*, Phaeodactylum Tricornutum, Navicula saprophila, Crypthecodinium cohnii, Cylindrotheca fusiformis, Cyclotella cryptica, Euglena gracilis, Amphidinium* sp., *Symbiodinium microadriaticum, Macrocystis pyrifera, A. braunii*, and *S. obliquus*.

Proper selection of host organisms for their genetic backgrounds and certain special features is also beneficial. For example, a photosynthetic-ethanol-producing designer alga created from cryophilic algae (psychrophiles) that can grow in snow and ice, and/or from cold-tolerant host strains such as *Chlamydomonas* cold strain CCMG1619, which has been characterized as capable of performing photosynthetic water splitting as cold as 4°C [3], permits ethanol production even in cold seasons or regions such as Canada. Meanwhile, a designer alga created from a thermophilic photosynthetic organism such as thermophilic algae *C. caldarium* and *G. sulphuraria* may permit the practice of this invention to be well extended into the hot seasons or areas such as Mexico and the Southwestern region of the United States including Nevada, California, Arizona, New Mexico and Texas, where the weather can often be hot. Furthermore, a photosynthetic-ethanol-producing designer alga created from a marine alga, such as *P. subcordiformis*, permits the practice of this invention using seawater, while the designer alga created from a freshwater alga such as *C. reinhardtii* can use freshwater. Additional optional features of a photosynthetic ethanol-producing designer alga include the benefits of reduced chlorophyll-antenna size, which has been demonstrated to provide higher photosynthetic productivity [4] and ethanol-tolerance

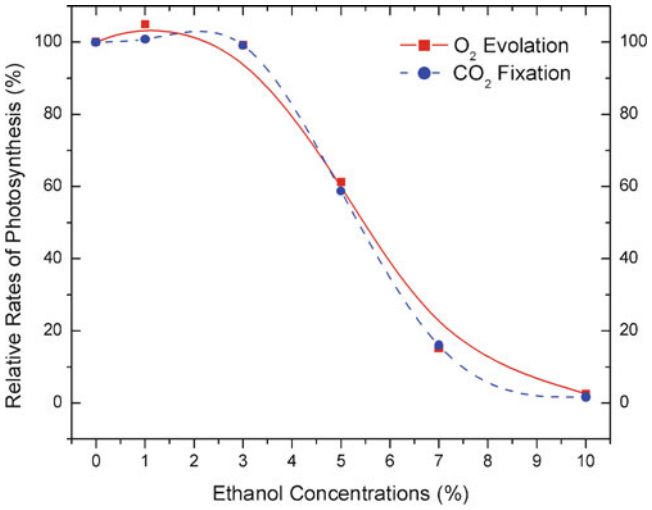

Fig. 3 Ethanol-tolerance assays demonstrated that green alga *Chlamydomonas reinhardtii* is capable of performing photosynthesis at an ethanol concentration as high as 3–5% in the culture medium under anaerobic conditions. The rates of photosynthesis were measured by both the light-dependent O_2 evolution and CO_2 fixation with various ethanol concentrations, and normalized to that (100% = 90 μmol/mg chl h) of the control culture (0% ethanol)

and allows for more robust and efficient photosynthetic production of ethanol from CO_2 and H_2O. For example, it has been demonstrated that *C. reinhardtii* can tolerate ethanol in the culture medium at a concentration up to about 3–5% (Fig. 3). These optional features can be incorporated into a designer alga, for example, by use of an ethanol-tolerant and/or chlorophyll antenna-deficient mutant (e.g., *C. reinhardtii* strain DS521) as a host organism, for genetic transformation with the designer ethanol-production-pathway genes. Therefore, in one of the various embodiments, a host alga is selected from the group consisting of green algae, red algae, brown algae, diatoms, marine algae, freshwater algae, unicellular algae, multicellular algae, seaweeds, cold-tolerant algal strains, heat-tolerant algal strains, ethanol-tolerant algal strains, and combinations thereof.

2.2 Creating a Designer Ethanol-Production Pathway in a Host

2.2.1 Selecting Appropriate Designer Enzymes

One of the key features in the present invention is the creation of a designer ethanol-production pathway to tame and work with the natural photosynthetic mechanisms to achieve the desirable synthesis of ethanol directly from CO_2 and H_2O. The natural photosynthetic mechanisms (illustrated in Fig. 1) include (1) the process of photosynthetic water splitting and proton gradient-coupled electron transport through the

thylakoid membrane of the chloroplast, which produces the reducing power (NADPH) and energy (ATP), and (2) the Calvin cycle, which reduces CO_2 by consumption of the reducing power (NADPH) and energy (ATP).

In accordance with the present invention, a series of enzymes are used to create a designer ethanol-production pathway that takes an intermediate product of the Calvin cycle and converts the intermediate product into ethanol. A "designer ethanol-production-pathway enzyme" is hereby defined as an enzyme that serves as a catalyst for at least one of the steps in a designer ethanol-production pathway. The intermediate products of the Calvin cycle are shown in Fig. 4a. According to the present invention, a number of intermediate products of the Calvin cycle can be utilized to create designer ethanol-production pathway(s); and the enzymes required for a designer ethanol-production pathway are selected depending on from which intermediate product of the Calvin cycle the designer ethanol-production pathway branches off.

In one example, a designer pathway is created that takes glyceraldehydes-3-phosphate and converts it into ethanol by using, for example, a set of enzymes consisting of glyceraldehyde-3-phosphate dehydrogenase, phosphoglycerate kinase, phosphoglycerate mutase, enolase, pyruvate kinase, pyruvate decarboxylase, and alcohol dehydrogenase, as shown in Fig. 4b. In this designer pathway, for conversion of one molecule of glyceraldehyde-3-phosphate to ethanol, an NADH molecule is generated from NAD^+ at the step from glyceraldehyde-3-phosphate to 1,3-diphosphoglycerate catalyzed by glyceraldehyde-3-phosphate dehydrogenase; meanwhile an NADH molecule is converted to NAD^+ at the terminal step catalyzed by alcohol dehydrogenase to reduce acetaldehyde to ethanol. Consequently, in this designer pathway (Fig. 4b), the number of NADH molecules consumed is balanced with the number of NADH molecules generated. Therefore, this designer ethanol-production pathway can operate continuously.

In another example, as shown in Fig. 4c, a designer pathway is created that takes the intermediate product, 3-phosphoglycerate, and converts it into ethanol by using, for example, a set of enzymes consisting of phosphoglycerate mutase, enolase, pyruvate kinase, pyruvate decarboxylase, and alcohol dehydrogenase. It can be seen that the last five enzymes of the designer pathway shown in Fig. 4b are identical with those utilized in the designer pathway shown in Fig. 4c. In other words, the designer enzymes depicted in Fig. 4b permit ethanol production from both the point of 3-phosphoglycerate and the point glyceraldehydes 3-phosphate in the Calvin cycle. These two pathways (Fig. 4b, c), however, have different characteristics. Unlike the glyceraldehyde-3-phosphate-branched ethanol-production pathway (Fig. 4b), the 3-phosphoglycerate-branched pathway which consists of the activities of only five enzymes as shown in Fig. 4c could not itself generate any NADH for use in the terminal step to reduce acetaldehyde to ethanol. That is, if (or when) an alcohol dehydrogenase that strictly uses only NADH but not NADPH is employed, it would require a supply of NADH for the 3-phosphoglycerate-branched pathway to operate. Consequently, in order for the 3-phosphoglycerate-branched ethanol-production pathway (Fig. 4c) to operate, it is important to use an alcohol dehydrogenase that can use NADPH which can be supplied by the photo-driven electron

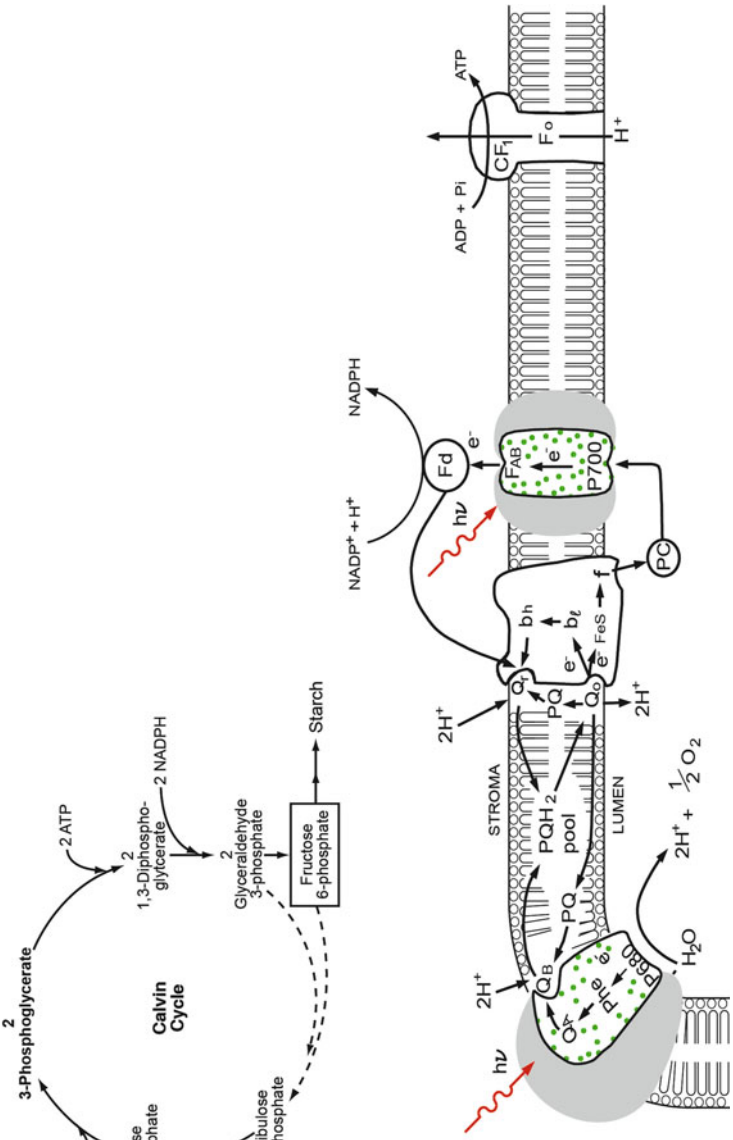

Fig. 4 (**a**) Depicts a designer alga using the normal Calvin cycle to perform photosynthesis for cell growth when the designer ethanol-production genes are switched off under normal aerobic conditions in the absence of an inducing factor.

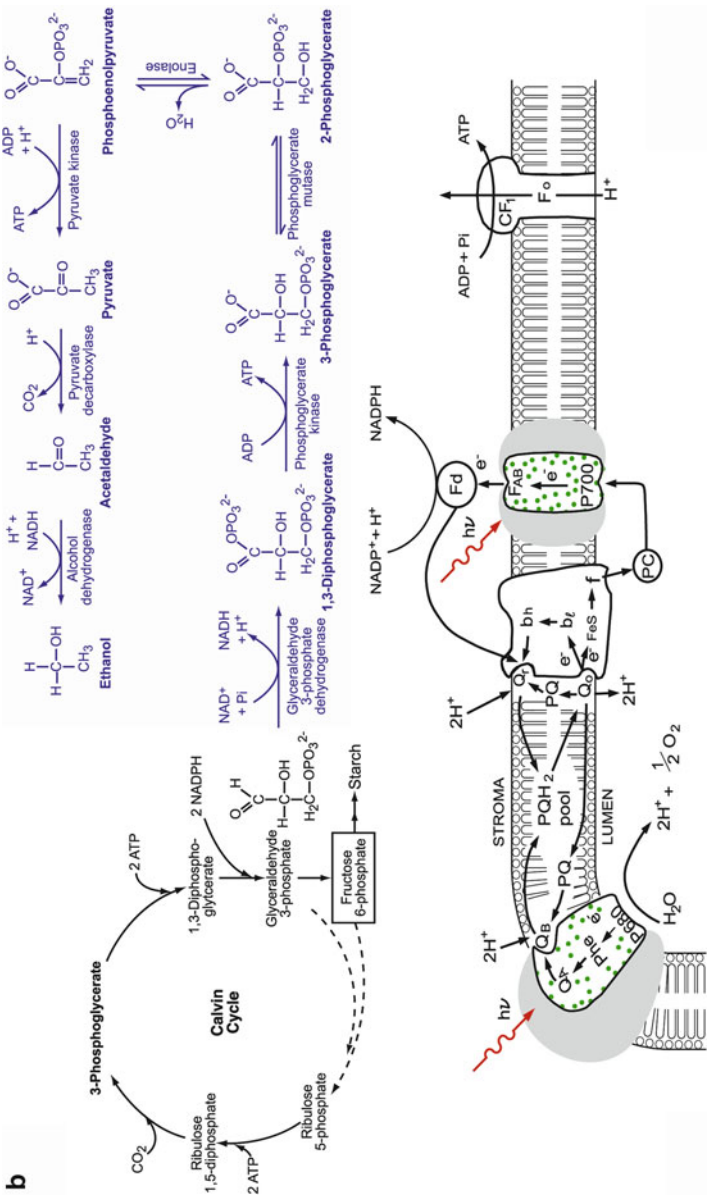

Fig. 4 (continued) (**b**) Illustrates an ethanol-production pathway (shown in *blue*) branched from the point of glyceraldehyde-3-phosphate at the Calvin cycle to produce ethanol directly from CO_2 and H_2O when the photosynthetic ethanol-producing pathway is turned on under certain specific inducing conditions such as under anaerobic conditions.

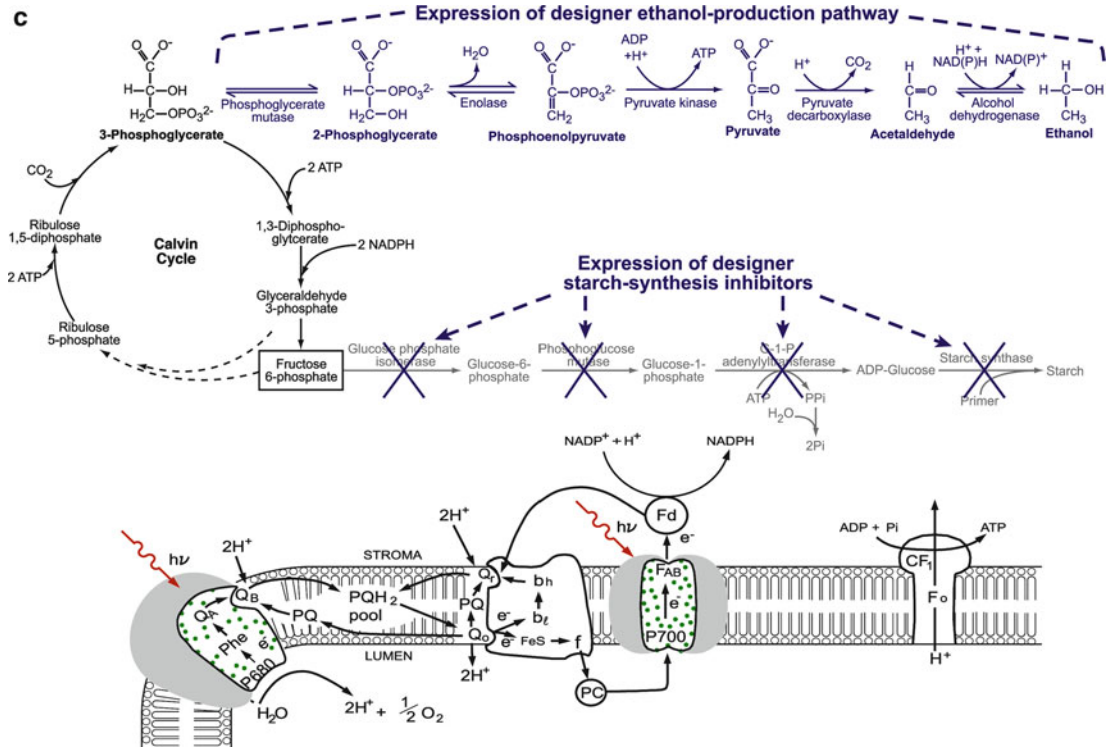

Fig. 4 (continued) (**c**) Illustrates an ethanol-production pathway (shown in *blue*) branched from the point of 3-phosphoglycerate at the Calvin cycle to produce ethanol directly from CO_2 and H_2O when the photosynthetic ethanol-producing pathway is turned on under certain specific inducing conditions such as under anaerobic conditions. It also illustrates the use of a starch-synthesis inhibitor gene(s) in combination with the designer ethanol-production pathway for further enhanced photosynthetic production of ethanol (CH_3CH_2OH) from carbon dioxide (CO_2) and water (H_2O) in the chloroplast of a designer organism such as a designer alga.

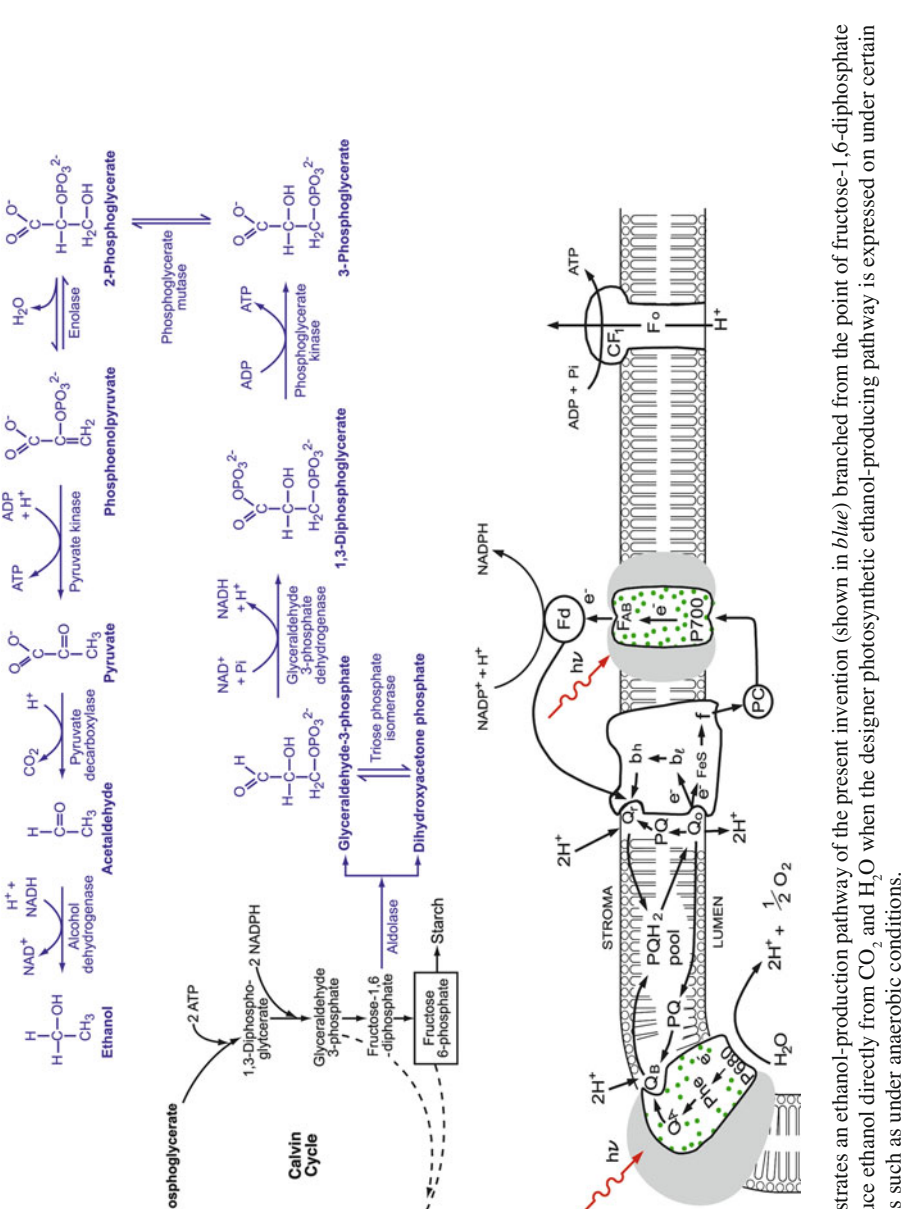

Fig. 4 (continued) (**d**) Illustrates an ethanol-production pathway of the present invention (shown in *blue*) branched from the point of fructose-1,6-diphosphate at the Calvin cycle to produce ethanol directly from CO_2 and H_2O when the designer photosynthetic ethanol-producing pathway is expressed on under certain specific inducing conditions such as under anaerobic conditions.

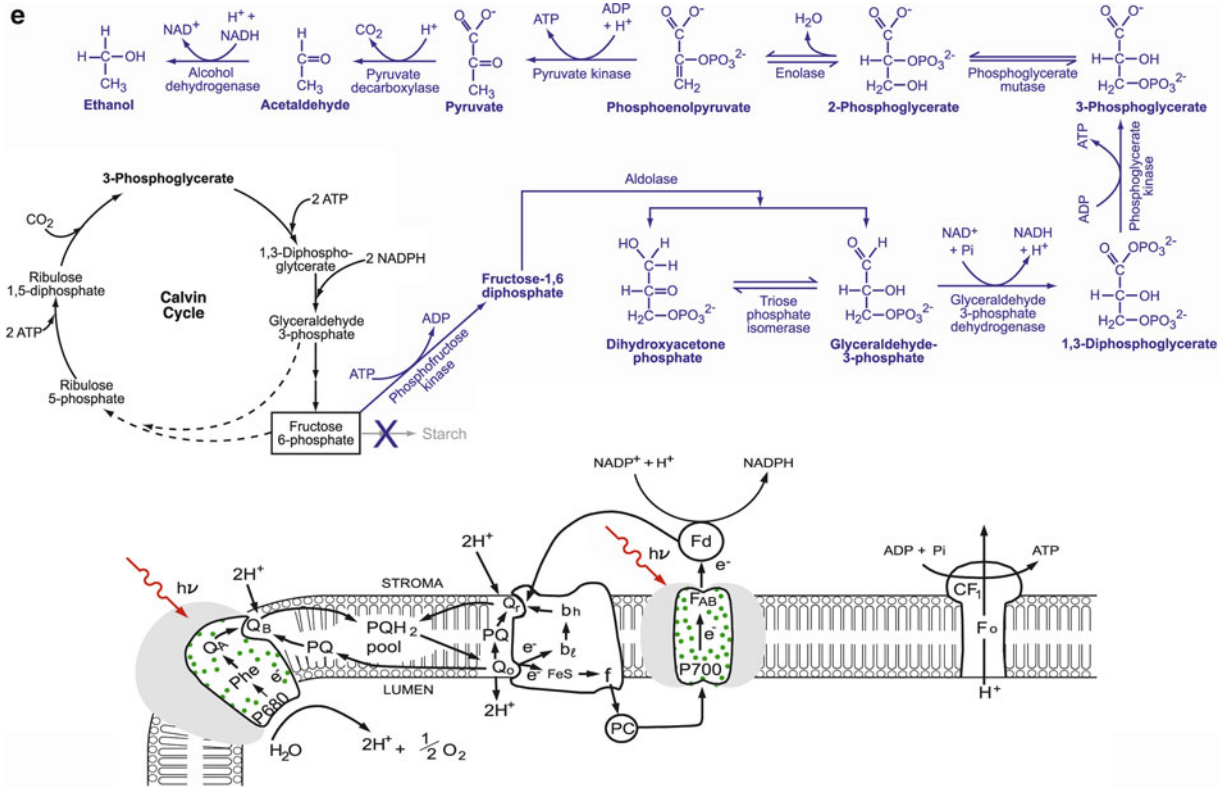

Fig. 4 (continued) (**e**) Illustrates an ethanol-production pathway of the present invention (shown in *blue*) branched from the point of fructose-6-phosphate at the Calvin cycle to produce ethanol directly from CO_2 and H_2O when the designer photosynthetic ethanol-producing pathway is expressed under certain inducing conditions such as under anaerobic conditions. It also illustrates the use of a starch-synthesis inhibitor gene(s) in combination of the designer ethanol-production pathway for further enhanced photosynthetic production of ethanol (CH_3CH_2OH) from carbon dioxide (CO_2) and water (H_2O)

transport process (Fig. 4c, bottom). Therefore, it is a preferred practice to use an alcohol dehydrogenase that can use NADPH or both NADPH and NADH (i.e., NAD(P)H) for this designer ethanol-production pathway (Fig. 4c). Alternatively, when an alcohol dehydrogenase that can use only NADH is employed, it is preferably here to use an additional embodiment that can confer an NADPH/NADH conversion mechanism (to supply NADH by converting NADPH to NADH, see more detail later in the text) in the designer organism's chloroplast to facilitate photosynthetic production of ethanol through the 3-phosphoglycerate-branched designer pathway.

In still another example, a designer pathway is created that takes fructose-1,6-diphosphate and converts it into ethanol by using, for example, a set of enzymes consisting of aldolase, triose phosphate isomerase, glyceraldehyde-3-phosphate dehydrogenase, phosphoglycerate kinase, phosphoglycerate mutase, enolase, pyruvate kinase, pyruvate decarboxylase, and alcohol dehydrogenase, as shown in Fig. 4d, with aldolase and triose phosphate isomerase being the only two additional enzymes relative to the designer pathway depicted in Fig. 4b. The addition of yet one more enzyme in the designer organism, phosphofructose kinase, permits the creation of another designer pathway which branches off from the point of fructose-6-phosphate for the production of ethanol (Fig. 4e). Like the glyceraldehyde-3-phosphate-branched ethanol-production pathway (Fig. 4b), both the fructose-1, 6-diphosphate-branched pathway (Fig. 4d) and the fructose-6-phosphate-branched pathway (Fig. 4e) can themselves generate NADH for use in their terminal step to reduce acetaldehyde to ethanol. In each of these designer ethanol-production pathways, the numbers of NADH molecules consumed are balanced with the numbers of NADH molecules generated. Therefore, these designer ethanol-production pathways can operate continuously.

Table 1 lists examples of the enzymes including those identified above for construction of the designer ethanol-production pathways. Throughout this specification, when reference is made to an enzyme, such as, for example, any of the enzymes listed in Table 1, it include their isozymes, functional analogs, designer modified enzymes, and combinations thereof. These enzymes can be selected for use in construction of the designer ethanol-production pathways. The "isozymes or functional analogs" refer to certain enzymes that have the same catalytic function but may or may not have exactly the same protein structures. For example, in *Saccharomyces bayanus*, there are four different genes (accession numbers: AY216992, AY216993, AY216994, and AY216995) encoding four alcohol dehydrogenases. These alcohol dehydrogenases essentially have the same function as an alcohol dehydrogenase, although there are some variations in their protein sequences. Therefore, the isozymes or functional analogs can also be selected and/or modified for use in construction of the designer ethanol-production pathway. The most essential feature of an enzyme is its active site that catalyzes the enzymatic reaction. Therefore, certain enzyme-protein fragment(s) or subunit(s) that contains such an active catalytic site may also be selected for use in this invention. For various reasons, some of the natural enzymes contain not only the essential catalytic structure but also other structure components that may or may not be desirable for a given application. With techniques

Table 1 Lists examples of enzymes for construction of designer ethanol-production pathways

Enzyme	Source (organism)	GenBank accession number, JGI protein ID or citation
Phosphoglycerate mutase (phosphoglyceromutase)	*Chlamydomonas reinhardtii* cytoplasm; *Aspergillus fumigatus; Coccidioides immitis; Leishmania braziliensis; Ajellomyces capsulatus; Monocercomonoides* sp.*; Aspergillus clavatus; Arabidopsis thaliana; Zea mays*	JGI Chlre2 protein ID 161689, GenBank: AF268078; XM_747847; XM_749597; XM_001248115; XM_001569263; XM_001539892; DQ665859; XM_001270940; NM_117020; M80912
Enolase	*C. reinhardtii* cytoplasm; *A. thaliana*; *Leishmania Mexicana; Lodderomyces elongisporus; Babesia bovis; Sclerotinia sclerotiorum; Pichia guilliermondii; Spirotrichonympha leidyi; Oryza sativa; T. pyriformis; Leuconostoc mesenteroides; Davidiella tassiana; Aspergillus oryzae; Schizosaccharomyces pombe; Brassica napus; Z. mays*	GenBank: X66412, P31683; AK222035;DQ221745; XM_001528071; XM_001611873; XM_001594215; XM_001483612; AB221057; EF122486, U09450; DQ845796; AB088633; U82438; D64113; U13799; AY307449; U17973
Pyruvate kinase	*C. reinhardtii* cytoplasm; *A. thaliana; Saccharomyces cerevisiae; B. bovis; S. sclerotiorum; Trichomonas vaginalis; P. guilliermondii; Pichia stipitis; L. elongisporus; C. immitis; T. pyriformis; Glycine max (soybean)*	JGI Chlre3 protein ID 138105; GenBank: AK229638; AY949876, AY949890, AY949888; XM_001612087; XM_001594710; XM_001329865; XM_001487289; XM_001384591; XM_001528210; XM_001240868; DQ845797; L08632
Pyruvate decarboxylase	*C. reinhardtii* cytoplasm; *P. stipitis; L. elongisporus; A. thaliana; Lycoris aurea; Chaetomium globosum; Citrus sinensis; Petunia x hybrida; Candida glabrata; Saccharomyces kluyveri; Z. mays; Rhizopus oryzae; Lotus corniculatus; Zymomonas mobilis; Lachancea kluyveri; O. sativa*	Chlre3 protein ID 127786, GenBank: E15259; XM_001387668; XM_001526215; NM_121744, NM_124878; DQ996286, DQ996285; XM_001219657; DQ001726; AY928611; AF545432; AY245517, AY245516, AY302469; AF370006; AF282846; AY227204; M15368; AF193853; U38199
Alcohol dehydrogenase	*C. reinhardtii* mitochondria; *Kluyveromyces lactis*; *Kluyveromyces marxianus; S. cerevisiae; Saccharomyces bayanus; P. stipitis*; *Entamoeba histolytica*; *T. vaginalis; L. braziliensis; Botryotinia fuckeliana; A. fumigatus; Dianthus caryophyllus; Saccharomyces pastorianus; L. kluyveri*	GenBank: AJ620190; XM_451932, X62766, X62767; X60224; Q04894, P25377; AY216992, AY216993, AY216994, AY216995; M88600, XM_001384263; D49910; XM_001315996; XM_001565062; XM_001559311; XM_726411; AY263389; AY217000, AY217001, AY217002, AY217003; AY216997, AY216998, AY216999, AY216996, AF218309

Glyceraldehyde-3-phosphate dehydrogenase	*Mesostigma viride* cytosol; *Triticum aestivum* cytosol; *C. reinhardtii* chloroplast; *B. fuckeliana; S. cerevisiae; Z. mobilis; Karenia brevis; A. capsulatus; P. stipitis; P. guilliermondii; K. marxianus, T. aestivum; A. thaliana*	GenBank: DQ873404; EF592180; L27668; XM_001549497; J01324; M18802; EU078558; XM_001539393; XM_001386423, XM_001386568; XM_001485596; DQ681075; EF592180; NM_101214
phosphoglycerate kinase	*C. reinhardtii* chloroplast; *Plasmodium vivax; B. bovis; B. fuckeliana; Monocercomonoides* sp.; *L. elongisporus; P. guilliermondii; A. thaliana; Helianthus annuus; O. sativa; Dictyostelium discoideum; Euglena gracilis; Chondrus crispus; Phaeodactylum tricornutum; Solanum tuberosum*	GenBank: U14912, AF244144; XM_001614707; XM_001610679; XM_001548271; DQ665858; XM_001523843; XM_001484377; NM_179576; DQ835564; EF122488; AF316577; AY647236; AY029776; AF108452; AF073473
Phosphofructose kinase	*C. reinhardtii; A. thaliana; A. capsulatus; Yarrowia lipolytica; P. stipitis; D. discoideum; Tetrahymena thermophila; Trypanosoma brucei; Plasmodium falciparum; Spinacia oleracea*	JGI Chlre2 protein ID 159495; GenBank: NM_001037043, NM_179694, NM_119066, NM_125551; XM_001537193; AY142710; XM_001382359, XM_001383014; XM_639070; XM_001017610; XM_838827; XM_001347929; DQ437575
Fructose-diphosphate aldolase	*C. reinhardtii* chloroplast*; Fragaria x ananassa* cytoplasm; *Homo sapiens; B. bovis; T. vaginalis; P. stipitis; A. thaliana*	GenBank: X69969; AF308587; NM_005165; XM_001609195; XM_001312327, XM_001312338; XM_001387466; NM_120057, NM_001036644
Triosephosphate isomerase	*A. thaliana; C. reinhardtii; S. sclerotiorum; Chlorella pyrenoidosa; P. guilliermondii; Euglena intermedia; Euglena longa; S. oleracea; Solanum chacoense; Hordeum vulgare; O. sativa*	GenBank: NM_127687, AF247559; AY742323; XM_001587391; AB240149; XM_001485684; DQ459379; AY742325; L36387; AY438596; U83414; EF575877
Glucose-1-phosphate adenylyltransferase	*A. thaliana; Z. mays; Chlamydia trachomatis*; *S. tuberosum (potato); Shigella flexneri; Lycopersicon esculentum*	GenBank: NM_127730, NM_124205, NM_121927, AY059862; EF694839, EF694838; AF087165; P55242; NP_709206; T07674
Starch synthase	*C. reinhardtii; Phaseolus vulgaris; O. sativa; A. thaliana; Colocasia esculenta; Amaranthus cruentus; Parachlorella kessleri; T. aestivum; Sorghum bicolor; Astragalus membranaceus; Perilla frutescens; Z. mays; Ipomoea batatas*	GenBank:AF026422, AF026421, DQ019314, AF433156; AB293998; D16202, AB115917, AY299404; AF121673, AK226881; NM_101044; AY225862, AY142712; DQ178026; AB232549; Y16340; AF168786; AF097922; AF210699; AF019297; AF068834

(continued)

Table 1 (continued)

Enzyme	Source (organism)	GenBank accession number, JGI protein ID or citation
Alpha-amylase	*H. vulgare* aleurone cells; *T. vaginalis; Phanerochaete chrysosporium; C. reinhardtii; A. thaliana*	GenBank: J04202; XM_001319100; EF143986; AY324649; NM_129551
Beta-amylase	*A. thaliana; H. vulgare; Musa acuminata*	GenBank: NM_113297; D21349; DQ166026
Starch phosphorylase	*Citrus hybrid cultivar* root; *S. tuberosum* chloroplast; *A. thaliana; T. aestivum; I. batatas*	GenBank: AY098895; P53535; NM_113857, NM_114564; AF275551; M64362
Phosphoglucomutase	*O. sativa* plastid; *A. capsulatus; P. stipitis; L. elongisporus; A. fumigatus; A. thaliana; Populus tomentosa; O. sativa; Z. mays*	GenBank: AC105932, AF455812; XM_001536436; XM_001383281; XM_001527445; XM_749345; NM_124561, NM_180508, AY128901; AY479974; AF455812; U89342, U89341
Glucosephosphate (glucose-6-phosphate) isomerase	*C. reinhardtii*; *S. cerevisiae; P. stipitis; A. capsulatus; S. oleracea* cytosol; *O. sativa* cytoplasm; *A. thaliana; Z. mays*	JGI Chlre3 protein ID 135202; GenBank: M21696; XM_001385873; XM_001537043; T09154; P42862; NM_123638, NM_118595; U17225
Hexokinase (glucokinase)	*A. capsulatus; P. stipitis; Pichia angusta; Thermosynechococcus elongates; B. bovis; S. chacoense; O. sativa; A. thaliana*	GenBank: XM_001541513; XM_001386652, AY278027; XM_001386035; NC_004113; XM_001608698; DQ177440; DQ116383; NM_112895
NADP(H) phosphatase	*Methanococcus jannaschii*	*The Journal Of Biological Chemistry* 280 (47): 39200–39207 (2005)
NAD kinase	*B. bovis; T. vaginalis*	GenBank: XM_001609395; XM_001324239

of bioinformatics-assisted molecular design, it is possible to select the essential catalytic structure(s) for use in construction of a designer DNA construct encoding a desirable designer enzyme. Therefore, in one of the various embodiments, a designer enzyme gene is created by artificial synthesis of a DNA construct according to bioinformatics-assisted molecular sequence design. With the computer-assisted synthetic biology approach, any DNA sequence (thus its protein structure) of a designer enzyme may be selectively modified to achieve more desirable results by design. Therefore, the terms "designer modified sequences" and "designer modified enzymes" are hereby defined as the DNA sequences and the enzyme proteins that are modified with bioinformatics-assisted molecular design. For example, when a DNA construct for a designer chloroplast-targeted enzyme is designed from the sequence of a mitochondrial enzyme, it is a preferred practice to modify some of the protein structures, for example, by selectively cutting out certain structure component(s) such as its mitochondrial transit-peptide sequence that is not suitable for the given application, and/or by adding certain peptide structures such as an exogenous chloroplast transit-peptide sequence (e.g., a 135-bp Rubisco small-subunit transit peptide (RbcS2)) that is needed to confer the ability in the chloroplast-targeted insertion of the designer protein. Therefore, one of the various embodiments flexibly employs the enzymes, their isozymes, functional analogs, designer modified enzymes, and/or the combinations thereof in construction of the designer ethanol-production pathway(s).

As shown in Table 1, many genes of the enzymes identified above have been cloned and/or sequenced from various organisms. Both genomic DNA and/or mRNA sequence data can be used in designing and synthesizing the designer DNA constructs for transformation of a host alga, plant, plant tissue or cells to create a designer organism for photobiological ethanol production (Fig. 5). However, because of possible variations often associated with various source organisms and cellular compartments with respect to a specific host organism and its chloroplast environment where the ethanol-production pathway(s) is designed to work with the Calvin cycle, certain molecular engineering artwork in DNA construct design including codon-usage optimization and sequence modification is often necessary for a designer DNA construct (Fig. 6) to work well. For example, if the source sequences are from cytosolic enzymes (sequences), a functional chloroplast-targeting sequence must be added to provide the capability for a designer unclear gene-encoded enzyme to insert into a host chloroplast to confer its function for a designer ethanol-production pathway. Furthermore, to provide the switchability for a designer ethanol-production pathway, it is also important to include a functional inducible promoter sequence such as the promoter of a hydrogenase (Hyd1) or nitrate reductase (Nia1) gene in certain designer DNA construct(s) as illustrated in Fig. 6a to control the expression of the designer gene(s). In addition, as mentioned before, certain functional derivatives or fragments of these enzymes (sequences), chloroplast-targeting transit peptide sequences, and inducible promoter sequences can also be selected for use in full, in part or in combinations thereof, to create the designer organisms according to various embodiments of this invention. The arts in creating and using the designer organisms are further described herein below.

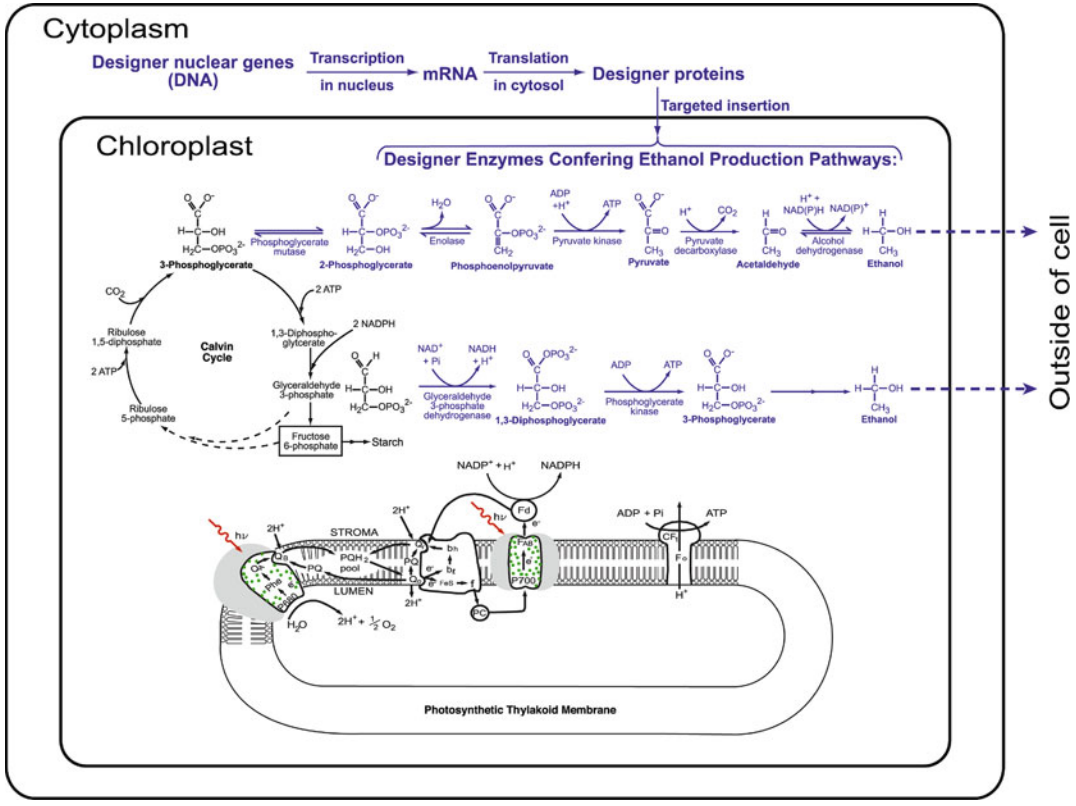

Fig. 5 Illustrates how the use of designer nuclear genes including their transcription in nucleus, translation in cytosol, and targeted insertion of designer proteins into chloroplast can form designer enzymes conferring the function of the designer ethanol-production pathway(s) for enhanced photosynthetic production of ethanol (CH_3CH_2OH) from carbon dioxide (CO_2) and water (H_2O) in the chloroplast of a designer organism such as a designer alga

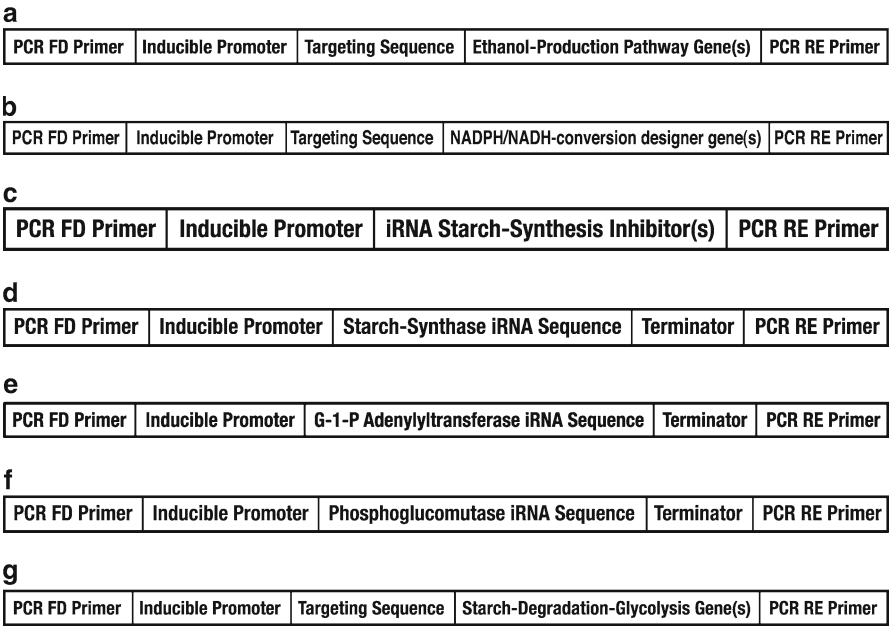

Fig. 6 (**a**) Presents a DNA construct for designer ethanol-production-pathway gene(s). (**b**) Presents a DNA construct for NADPH/NADH-conversion designer gene for NADPH/NADH inter-conversion. (**c**) Presents a DNA construct for a designer iRNA starch-synthesis inhibitor gene. (**d**) Presents a DNA construct for a designer starch-synthase iRNA gene. (**e**) Presents a DNA construct for a designer G-1-P adenylyltransferase iRNA gene. (**f**) Presents a DNA construct for a designer phosphoglucomutase iRNA gene. (**g**) Presents a DNA construct for a designer starch degradation–glycolysis gene(s)

2.2.2 Targeting the Designer Enzymes to the Stroma Region of Chloroplasts

Some of the designer enzymes discussed above, such as the alcohol dehydrogenase, pyruvate decarboxylase, phosphoglycerate mutase and enolase, are known to function in the glycolytic pathway in the cytoplasm, but chloroplasts generally do not possess these enzymes to function with the Calvin cycle. Therefore, nucleic acids encoding for these enzymes need to be genetically engineered such that the enzymes expressed are inserted into the chloroplasts to create a desirable designer organism of the present invention. Depending on the genetic background of a particular host organism, some of the designer enzymes discussed above may exist at some background levels in its native form in a wild-type chloroplast. For various reasons including often the lack of their controllability, however, some of the chloroplast background enzymes may or may not be sufficient to serve as a significant part of the designer ethanol-production pathway(s). Furthermore, a number of useful inducible promoters happen to function in the nuclear genome. For example, both the hydrogenase (Hyd1) promoter and the nitrate reductase (Nia1) promoter that can be used to control the expression of the designer ethanol-production pathways are located in the nuclear genome of *C. reinhardtii*, of which the genome has recently

been sequenced. Therefore, it is preferred to use nuclear-genome-encodable designer genes to confer a switchable ethanol-production pathway. Consequently, nucleic acids encoding for these enzymes also need to be genetically engineered with proper sequence modification such that the enzymes are controllably expressed and are inserted into the chloroplasts to create a designer ethanol-production pathway. Figure 5 illustrates how the use of designer nuclear genes including their transcription in nucleus, translation in cytosol, and targeted insertion of designer proteins into chloroplast, can form the designer enzymes conferring the function of the ethanol-production pathway(s) for photosynthetic production of ethanol (CH_3CH_2OH) from carbon dioxide (CO_2) and water (H_2O) in a designer organism.

Additionally, it is best to express the designer ethanol-producing-pathway enzymes only into chloroplasts (at the stroma region), exactly where the action of the enzymes is needed to enable photosynthetic production of ethanol. If expressed without a chloroplast-targeted insertion mechanism, the enzymes would just stay in the cytosol and not be able to directly interact with the Calvin cycle for ethanol production. Therefore, in addition to the obvious distinctive features in pathway designs and associated approaches, another significant distinction to the prior art is that the present invention innovatively employs a chloroplast-targeted mechanism for genetic insertion of many designer ethanol-production-pathway enzymes into chloroplast to directly interact with the Calvin cycle for photobiological ethanol production.

With a chloroplast stroma-targeted mechanism, the cells will not only be able to produce ethanol but also to grow and regenerate themselves when they are returned to conditions under which the designer pathway is turned off, such as under aerobic conditions when designer hydrogenase promoter-controlled ethanol-production-pathway genes are used. Designer algae, plants, or plant cells that contain normal mitochondria should be able to use the reducing power (NADH) from organic reserves (and/or some exogenous organic substrate such as acetate or sugar) to power the cells immediately after the return to aerobic conditions. Consequently, when the designer algae, plants, or plant cells are returned to aerobic conditions after use under anaerobic conditions for photosynthetic ethanol production, the cells will stop making the ethanol-producing enzymes and start to restore the normal photoautotrophic capability by synthesizing new and functional chloroplasts. Therefore, it is possible to use such genetically engineered designer alga/plant organisms for repeated cycles of photoautotrophic growth under normal aerobic conditions and efficient production of ethanol directly from CO_2 and H_2O under certain specific designer ethanol-producing conditions such as under anaerobic conditions.

The targeted insertion of designer ethanol-production enzymes can be accomplished through use of a DNA sequence that encodes for a stroma “signal” peptide. A stroma-protein signal (transit) peptide directs the transport and insertion of a newly synthesized protein into stroma. In accordance with one of the various embodiments, a specific targeting DNA sequence is preferably placed in-between the promoter and a designer ethanol-production-pathway enzyme sequence, as shown in a designer DNA construct (Fig. 6a). This targeting sequence encodes for a signal (transit) peptide that is synthesized as part of the apoprotein of an enzyme.

The transit peptide guides the insertion of an apoprotein of a designer ethanol-production-pathway enzyme into the chloroplast. After the apoprotein is inserted into the chloroplast, the transit peptide is cleaved off from the apoprotein, which then becomes an active enzyme.

A number of transit peptide sequences are suitable for use for the targeted insertion of the designer ethanol-production-pathway enzymes into chloroplast, including but not limited to the transit peptide sequences of: the hydrogenase apoproteins (such as HydA1 (Hyd1) and HydA2, GenBank accession number AJ308413, AF289201, AY090770), ferredoxin apoprotein (Frx1, accession numbers L10349, P07839), thioredoxin m apoprotein (Trx2, X62335), glutamine synthase apoprotein (Gs2, Q42689), LhcII apoproteins (AB051210, AB051208, AB051205), PSII-T apoprotein (PsbT), PSII-S apoprotein (PsbS), PSII-W apoprotein (PsbW), CF_0CF_1 subunit-γ apoprotein (AtpC), CF_0CF_1 subunit-Yδ apoprotein (AtpD, U41442), $CFoCF_1$ subunit-II apoprotein (AtpG), photosystem I (PSI) apoproteins (such as, of genes PsaD, PsaE, PsaF, PsaG, PsaH, and PsaK), and Rubisco SSU apoproteins (such as RbcS2, X04472). Throughout this specification, when reference is made to a transit peptide sequence, such as, for example, any of the transit peptide sequence described above, it includes their functional analogs, modified designer sequences, and combinations thereof. A "functional analog" or "modified designer sequence" in this context refers to a peptide sequence derived or modified (by, e.g., conservative substitution, moderate deletion or addition of amino acids, or modification of side chains of amino acids) based on a native transit peptide sequence, such as those identified above, that has the same function as the native transit peptide sequence, i.e., effecting targeted insertion of a desired enzyme.

In certain specific embodiments, the following transit peptide sequences are used to guide the insertion of the designer ethanol-production-pathway enzymes into the stroma region of the chloroplast: the Hyd1 transit peptide (having the amino acid sequence: msalvlkpca avsirgsscr arqvaprapl aastvrvala tleaparrlg nvacaa), the RbcS2 transit peptides (having the amino acid sequence: maaviakssv saavarpars svrp-maalkp avkaapvaap aqanq), ferredoxin transit peptide (having the amino acid sequence: mamamrs), the CF_0CF_1 subunit-δ transit peptide (having the amino acid sequence: mlaaksiagp rafkasavra apkagrrtvv vma), their analogs, functional derivatives, designer sequences, and combinations thereof.

2.2.3 Use of a Genetic Switch to Control the Expression of the Designer Ethanol-Producing Pathway

Another key feature of the invention is the application of a genetic switch to control the expression of the designer ethanol-producing pathway(s), as illustrated in Fig. 2. This switchability is accomplished through the use of an externally inducible promoter so that the designer transgenes are inducibly expressed under certain specific inducing conditions (Fig. 6a). Preferably, the promoter employed to control the expression of designer genes in a host is originated from the host itself or a closely related organism. The activities and inducibility of a promoter in a host cell can be

tested by placing the promoter in front of a reported gene, introducing this reporter construct into the host tissue or cells by any of the known DNA delivery techniques, and assessing the expression of the reporter gene.

In a preferred embodiment, the inducible promoter used to control the expression of designer genes is a promoter that is inducible by anaerobiosis, i.e., active under anaerobic conditions but inactive under aerobic conditions. A designer alga/plant organism can perform autotrophic photosynthesis using CO_2 as the carbon source under aerobic conditions (Fig. 4a), and when the designer organism culture is grown and ready for photosynthetic ethanol production, anaerobic conditions will be applied to turn on the promoter and the designer genes (Fig. 4b).

A number of promoters that become active under anaerobic conditions are suitable for use in the present invention. For example, the promoters of the hydrogenase genes (HydA1 (Hyd1) and HydA2, GenBank accession number: AJ308413, AF289201, AY090770) of *C. reinhardtii*, which is active under anaerobic conditions but inactive under aerobic conditions, can be used as an effective genetic switch to control the expression of the designer genes in a host alga, such as *C. reinhardtii*. In fact, *Chlamydomonas* cells contain several nuclear genes that are coordinately induced under anaerobic conditions. These include the hydrogenase structural gene itself (Hyd1), the Cyc6 gene encoding the apoprotein of Cytochrome C_6, and the Cpxl gene encoding coprogen oxidase. The regulatory regions for the latter two have been well characterized, and a region of about 100 bp proves sufficient to confer regulation by anaerobiosis in synthetic gene constructs [5]. Although the above inducible algal promoters may be suitable for use in other plant hosts, especially in plants closely related to algae, the promoters of the homologous genes from these other plants, including higher plants, can be obtained and employed to control the expression of designer genes in those plants.

In another embodiment, the inducible promoter used in the present invention is an algal nitrate reductase (Nia1) promoter, which is inducible by growth in a medium containing nitrate and repressed in a nitrate-deficient but ammonium-containing medium [6]. Therefore, the Nia1 (gene accession number AF203033) promoter can be selected for use to control the expression of the designer genes in an alga according to the concentration levels of nitrate in a culture medium. Additional inducible promoters that can also be selected for use in the present invention include, for example, the heat-shock protein promoter HSP70A [7] (accession number: DQ059999, AY456093, M98823), the promoter of CabII-1 gene (accession number M24072), the promoter of Ca1 gene (accession number P20507), and the promoter of Ca2 gene (accession number P24258). Throughout this specification, when reference is made to inducible promoter, such as, for example, any of the inducible promoters described above, it includes their analogs, functional derivatives, designer sequences, and combinations thereof. A "functional analog" or "modified designer sequence" in this context refers to a promoter sequence derived or modified (by, e.g., substitution, moderate deletion or addition or modification of nucleotides) based on a native promoter sequence, such as those identified hereinabove, that retains the function of the native promoter sequence.

2.2.4 DNA Constructs and Transformation into Plant Cells

DNA constructs are generated in order to introduce designer ethanol-production-pathway genes to a host alga, plant, plant tissue, or plant cells. That is, a nucleotide sequence encoding a designer ethanol-production-pathway enzyme is placed in a vector, in an operable linkage to a promoter, preferably an inducible promoter, and in an operable linkage to a nucleotide sequence coding for an appropriate chloroplast-targeting transit-peptide sequence. In a preferred embodiment, nucleic acid constructs are made to have the elements placed in the following 5′ (upstream) to 3′ (downstream) orientation: an externally inducible promoter, a transit targeting sequence, and a nucleic acid encoding a designer ethanol-production-pathway enzyme, and preferably an appropriate transcription termination sequence. One or more designer genes (DNA constructs) can be placed into one genetic vector. An example of such a construct is depicted in Fig. 6a. As shown in the embodiment illustrated in Fig. 6a, a designer ethanol-production-pathway transgene is a nucleic acid construct comprising: (a) a PCR forward primer; (b) an externally inducible promoter; (c) a transit targeting sequence; (d) a designer ethanol-production-pathway-enzyme-encoding sequence with an appropriate transcription termination sequence; and (e) a PCR reverse primer.

In accordance with various embodiments, any of the components (a) through (e) of this DNA construct are adjusted to suit for certain specific conditions. In practice, any of the components (a) through (e) of this DNA construct are applied in full or in part, and/or in any adjusted combination to achieve more desirable results. For example, when an algal hydrogenase promoter is used as an inducible promoter in the designer ethanol-production-pathway DNA construct, a transgenic designer alga that contains this DNA construct will be able to perform autotrophic photosynthesis (Fig. 4a) using ambient-air CO_2 as the carbon source and grows normally under aerobic conditions, such as in an open pond. When the algal culture is grown and ready for ethanol production, the designer transgene(s) can then be expressed by induction under anaerobic conditions because of the use of the hydrogenase promoter. The expression of the designer gene(s) produces a set of designer ethanol-production-pathway enzymes such as those illustrated in Fig. 4b to work with the Calvin cycle in the chloroplast for photobiological ethanol production.

The two PCR primers are a PCR forward primer (PCR FD primer) located at the beginning (the 5′ end) of the DNA construct and a PCR reverse primer (PCR RE primer) located at the other end (the 3′ end) as shown in Fig. 6a. This pair of PCR primers is designed to provide certain convenience when needed for relatively easy PCR amplification of the designer DNA construct, which is helpful not only during and after the designer DNA construct is synthesized in preparation for gene transformation, but also after the designer DNA construct is delivered into the genome of a host alga for verification of the designer gene in the transformants. For example, after the transformation of the designer gene is accomplished in a *C. reinhardtii*-arg7 host cell using the techniques of electroporation and argininosuccinate lyase (*arg7*) complementation screening, the resulted transformants can be then analyzed

by a PCR DNA assay of their nuclear DNA using this pair of PCR primers to verify whether the entire designer ethanol-production-pathway gene (the DNA construct) is successfully incorporated into the genome of a given transformant. When the nuclear DNA PCR assay of a transformant can generate a PCR product that matches with the predicted DNA size and sequence according to the designer DNA construct, the successful incorporation of the designer proton-channel gene into the genome of the transformant is verified.

Therefore, the various embodiments also teach the associated method to effectively create the designer transgenic algae, plants, or plant cells for photobiological ethanol production. This method, in one embodiment, includes the following steps: (a) Selecting an appropriate host alga, plant, plant tissue, or plant cells with respect to their genetic backgrounds and special features in relation to ethanol production; (b) Introducing the nucleic acid constructs of the designer proton-channel genes into the genome of said host alga, plant, plant tissue, or plant cells; (c) Verifying the incorporation of the designer genes in the transformed alga, plant, plant tissue, or plant cells with DNA PCR assays using the said PCR primers of the designer DNA construct; (d) Measuring and verifying the designer organism features such as the inducible expression of the designer ethanol-pathway genes for photosynthetic ethanol production from carbon dioxide and water by assays of mRNA, protein, and ethanol-production characteristics according to the specific designer features of the DNA construct(s) (Fig. 6a).

The above embodiment of the method for creating the designer transgenic organism for photobiological ethanol production can also be repeatedly applied for a plurality of operational cycles to achieve more desirable results. In various embodiments, any of the steps (a) through (d) of this method described above are adjusted to suit for certain specific conditions. In various embodiments, any of the steps (a) through (d) of the method are applied in full or in part, and/or in any adjusted combination. Examples of designer ethanol-production-pathway genes (DNA constructs) are shown in the sequence listings of the PCT International Patent Application Publication No. WO08039450.

The nucleic acid constructs may include additional appropriate sequences, for example, a selection marker gene, and an optional biomolecular tag sequence. Selectable markers that can be selected for use in the constructs include markers conferring resistances to kanamycin, hygromycin, spectinomycin, streptomycin, sulfonyl urea, among others, all of which have been cloned and are available to those skilled in the art. Alternatively, the selective marker is a nutrition marker gene that can complement a deficiency in the host organism. For example, the gene encoding argininosuccinate lyase (arg7) can be used as a selection marker gene in the designer construct, which permits identification of transformants when *C. reinhardtii* arg7- (minus) cells are used as host cells.

Nucleic acid constructs carrying designer genes can be delivered into a host alga, plant, or plant tissue or cells using the available gene-transformation techniques, such as electroporation, PEG-induced uptake, and ballistic delivery of DNA, and Agrobacterium-mediated transformation. For the purpose of delivering a designer construct into algal cells, the techniques of electroporation, glass bead, and biolistic

genegun can be selected for use as preferred methods; and an alga with single cells or simple thallus structure is preferred for use in transformation. Transformants can be identified and tested based on routine techniques.

2.3 Additional Host Modifications to Enhance Photosynthetic Ethanol Production

2.3.1 An NADPH/NADH Conversion Mechanism

According to the photosynthetic ethanol-production pathway illustrated in Figs. 4c and 7, to produce one molecule of ethanol from $2CO_2$ and $3H_2O$ is likely to require 8 ATP and 6 NADPH, both of which are generated by photosynthetic water splitting and photophosphorylation across the thylakoid membrane. In order for the 3-phosphoglycerate-branched ethanol-production pathway (Fig. 4c) to operate, it is a preferred practice to use an alcohol dehydrogenase that can use NADPH that is generated by the photo-driven electron transport process (Fig. 4c, bottom). The NADP(H)-dependent alcohol dehydrogenases (NCBI accession numbers: M88600, Q04894, and P25377) are examples of an alcohol dehydrogenase that can use NADPH. The *Kluyveromyces lactis* mitochondrial KlADH III enzyme (GenBank accession number: XM_451932) is an example of an alcohol dehydrogenase that is capable of accepting either NADP(H) or NAD(H). Such an alcohol dehydrogenase that can use both NADPH and NADH (i.e., NAD(P)H) can also be selected for use in this 3-phosphoglycerate-branched (Fig. 4c) and any of the other designer ethanol-production pathway(s) (Fig. 4b, d, e) as well. When an alcohol dehydrogenase that can only use NADH is employed, it may require an NADPH/NADH conversion mechanism in order for this 3-phosphoglycerate-branched ethanol-production pathway (Fig. 4c) to operate. However, depending on the genetic backgrounds of a host organism, a conversion mechanism between NADPH and NADH may exist in the host so that NADPH and NADH may be interchangeably used in the chloroplast. In addition, it is known that NADPH could be converted into NADH by a NADPH-phosphatase activity [8] and that NAD can be converted to NADP by a NAD kinase activity [9, 10]. Therefore, when enhanced NADPH/NADH conversion is desirable, the host may be genetically modified to enhance the NADPH phosphatase and NAD kinase activities. Thus, in one of the various embodiments, the photosynthetic ethanol-producing designer plant, designer alga or plant cell further contains additional designer transgenes (Fig. 6b) to inducibly express one or more enzymes to facilitate the NADPH/NADH inter-conversion, such as the NADPH phosphatase and NAD kinase (GenBank: XM_001609395, XM_001324239), in the stroma region of the algal chloroplast.

Another embodiment that can provide an NADPH/NADH conversion mechanism is by properly selecting an appropriate branching point at the Calvin cycle for a designer ethanol-production pathway to branch from. To confer this NADPH/NADH conversion mechanism by pathway design according to this embodiment, it

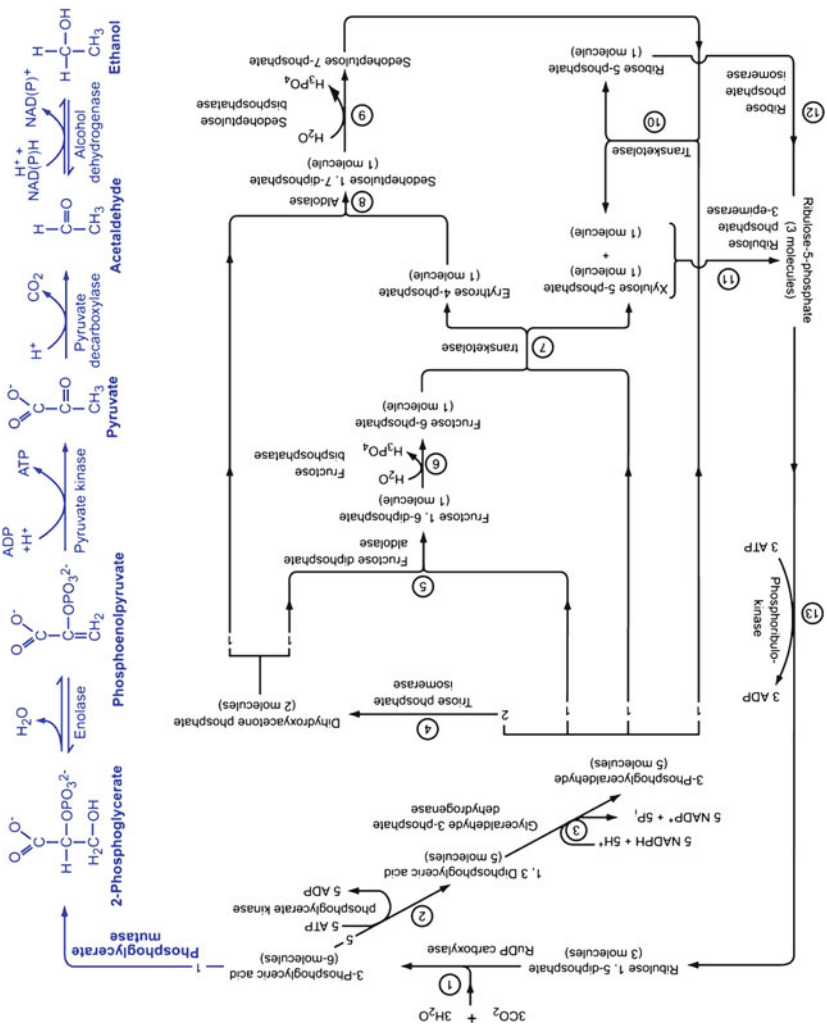

Fig. 7 Provides a more-detailed illustration showing how an ethanol-production pathway of the present invention (*blue*) may work with the Calvin cycle with material (C, H, O) balance for continuous production of ethanol from CO_2 and H_2O directly by photosynthesis

is a preferred practice to branch a designer ethanol-production pathway at or after the point of glyceraldehydes-3-phosphate of the Calvin cycle as shown in Fig. 4b, d, e. In these pathway designs, the NADPH/NADH conversion is achieved essentially by a two-step mechanism: (1) Use of the step with the Calvin-cycle's glyceraldehyde-3-phosphate dehydrogenase, which uses NADPH in reducing 1,3-diphosphoglycerate to glyceraldehydes-3-phosphate; and (2) use of the step with the designer pathway's NAD^+-dependent glyceraldehyde-3-phosphate dehydrogenase, which produces NADH in oxidizing glyceraldehyde-3-phosphate to 1,3-diphosphoglycerate. The net result of the two steps described above is the conversion of NADPH to NADH, which can supply the needed reducing power in the form of NADH for the designer ethanol-production pathway(s). For step (1), use of the Calvin-cycle's glyceraldehyde-3-phosphate dehydrogenase naturally in the host organism is usually sufficient. To confer this two-step NADPH/NADH conversion mechanism, it is important to use a NAD^+-dependent glyceraldehyde-3-phosphate dehydrogenase in the designer ethanol-production pathway(s). Therefore, in one of the various embodiments, it is a preferred practice to use a NAD^+-dependent glyceraldehyde-3-phosphate dehydrogenase, its isozymes, functional derivatives, analogs, designer modified enzymes and/or combinations thereof in the designer ethanol-production pathway(s) as illustrated in Fig. 4b, d, e.

2.3.2 iRNA Techniques to Further Tame Photosynthesis Regulation Mechanism

In another embodiment of the present invention, the host plant or cell is further modified to tame the Calvin cycle so that the host can directly produce liquid fuel ethanol instead of synthesizing starch, celluloses, and lignocelluloses that are often inefficient and hard for the biorefinery industry to use. According to the present invention, inactivation of starch-synthesis activity is achieved by suppressing the expression of any of the key enzymes, such as, starch synthase, glucose-1-phosphate (G-1-P) adenylyltransferase, phosphoglucomutase, and hexose-phosphate-isomerase of the starch-synthesis pathway which connects with the Calvin cycle (Fig. 4c).

Introduction of a genetically transmittable factor that can inhibit the starch-synthesis activity that is in competition with designer ethanol-production pathway(s) for the Calvin-cycle products can further enhance photosynthetic ethanol production. In a specific embodiment, a genetically encoded-able inhibitor (Fig. 6c) to the competitive starch-synthesis pathway is an interfering RNA (iRNA) molecule that specifically inhibits the synthesis of a starch-synthesis-pathway enzyme, for example, starch synthase, glucose-1-phosphate (G-1-P) adenylyltransferase, phosphoglucomutase, and/or hexose-phosphate-isomerase. Figure 6d–f depicts examples of a designer iRNA gene. The DNA sequences encoding starch-synthase iRNA, glucose-1-phosphate (G-1-P) adenylyltransferase iRNA, a phosphoglucomutase iRNA and/or a G-P-isomerase iRNA, respectively, can be designed and synthesized based on RNA interference techniques known to those skilled in the art [11]. Generally speaking, an interfering RNA (iRNA) molecule is anti-sense but complementary to

a normal mRNA of a particular protein (gene) so that such iRNA molecule can specifically bind with the normal mRNA of the particular gene, thus inhibiting (blocking) the translation of the gene-specific mRNA to protein [12, 13].

2.3.3 Designer Starch Degradation and Glycolysis Genes

In yet another embodiment of the present invention, the photobiological ethanol production is enhanced by incorporating an additional set of designer genes (Figs. 6g and 8a) that can facilitate starch degradation and glycolysis in combination with the designer ethanol-production gene(s) (Fig. 6a) in the chloroplast. Such additional designer genes for starch degradation include, for example, genes coding for amylase, starch phosphorylase, hexokinase, phosphoglucomutase, and glucose-phosphate-isomerase (G-P-isomerase). The designer glycolysis genes encode chloroplast-targeted glycolysis enzymes: glucosephosphate isomerase, phosphofructose kinase, aldolase, triose phosphate isomerase, glyceraldehyde-3-phosphate dehydrogenase, phosphoglycerate kinase, phosphoglycerate mutase, enolase, and pyruvate kinase. The designer starch degradation and glycolysis genes in combination with any of the ethanol-production pathways shown in Fig. 4b–e can form additional pathway(s) from starch to ethanol. Consequently, co-expression of the designer starch degradation and glycolysis genes with the ethanol-production-pathway genes can enhance photobiological production of ethanol as well. Therefore, this embodiment represents another approach to tame the Calvin cycle for enhanced photobiological production of ethanol. Figure 8a presents a full designer starch-to-ethanol-production pathway. In this case, some of the Calvin-cycle products flow through the starch-synthesis pathway followed by the starch-to-ethanol pathway (Fig. 8a). In this case, starch acts as a transient storage pool of the Calvin-cycle products before they can be converted to ethanol. This mechanism can be quite useful in maximizing the ethanol-production yield in certain cases. For example, at high sunlight intensity such as around noon, the rate of Calvin-cycle photosynthetic CO_2 fixation can be so high that may exceed the maximal rate capacity of an ethanol-production pathway(s); use of the starch-synthesis mechanism allows temporary storage of the excess photosynthetic products to be used later for ethanol production as well.

Similar to the benefits of using the Calvin-cycle-branched designer ethanol-production pathways (Fig. 4b–e), the use of the designer starch-to-ethanol pathway (Fig. 8a) can also help to convert the photosynthetic products to ethanol before the sugars could be converted into other complicated biomolecules such as lignocellulosic biomasses which cannot be readily used by the biorefinery industries. Therefore, appropriate use of the Calvin-cycle-branched designer ethanol-production pathway(s) (Fig. 4b–e) and/or the designer starch-to-ethanol pathway (Fig. 8a) may represent revolutionary *inter alia* technologies that can effectively bypass the bottleneck problems of the current biomass technology including the "lignocellulosic recalcitrance" problem. Figure 8b illustrates the use of a designer starch-to-ethanol pathway in combination with a Calvin-cycle-branched designer ethanol-production pathway for enhanced photobiological ethanol production.

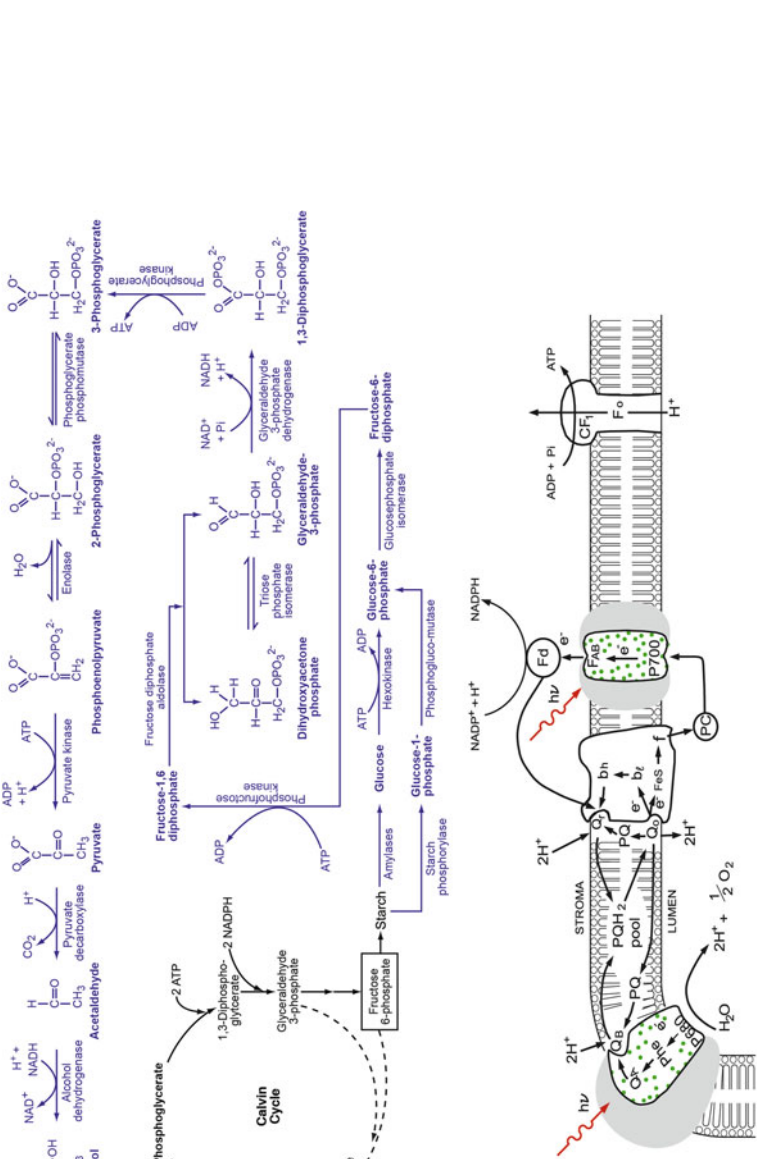

Fig. 8 (**a**) Illustrates an ethanol-production pathway (shown in *blue*) branched from the point of chloroplast starch to produce ethanol directly from CO_2 and H_2O when the designer photosynthetic ethanol-producing pathway is expressed on under certain specific inducing conditions such as under anaerobic conditions.

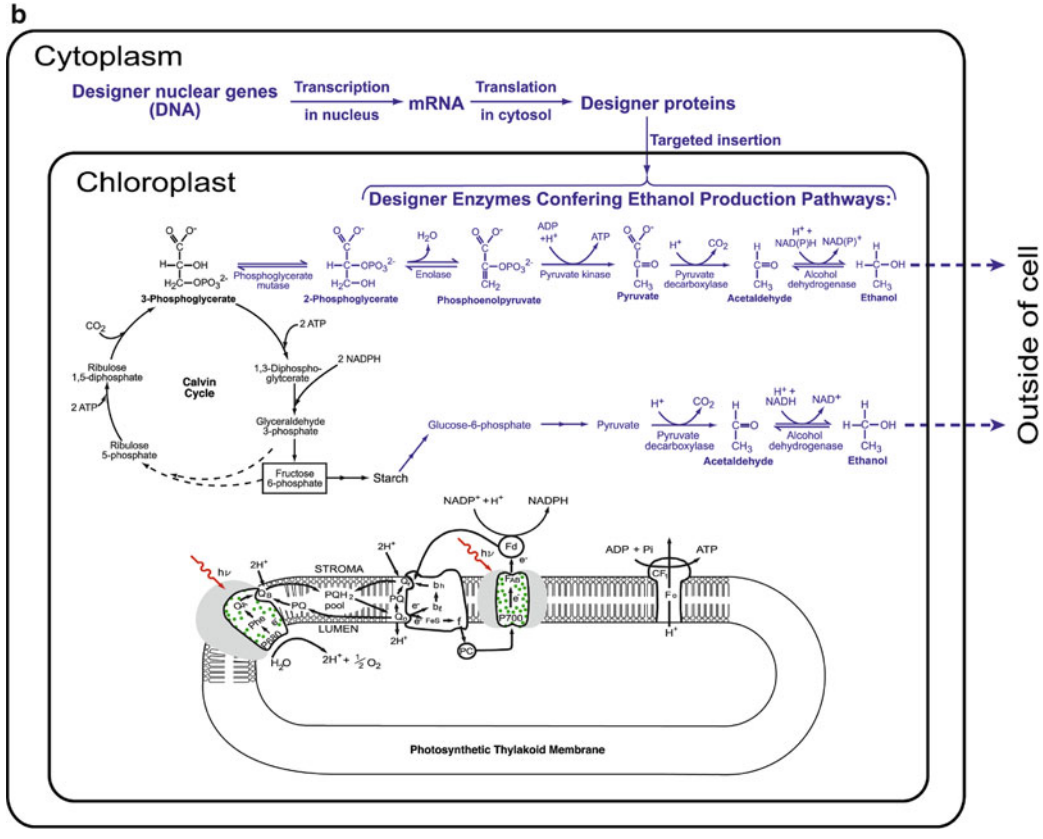

Fig. 8 (continued) (**b**) Illustrates photobiological production of ethanol (CH_3CH_2OH) from both the designer 3-phosphoglycerate-branched ethanol-production pathway and the designer starch-to-ethanol pathway in the chloroplast of a designer organism such as a designer alga when both of the designer pathways are expressed

Another feature is that a Calvin-cycle-branched designer ethanol-production pathway activity (Fig. 4b–e) can occur predominantly during the days when there is light because it uses an intermediate product of the Calvin cycle which requires supplies of reducing power (NADPH) and energy (ATP) generated by the photosynthetic water splitting and the light-driven proton-translocation-coupled electron transport process through the thylakoid membrane system. The designer starch-to-ethanol pathway (Fig. 8a), which can use the surplus sugar that has been stored as starch during photosynthesis, can operate not only during the days, but also at nights. Consequently, the use of a Calvin-cycle-branched designer ethanol-production pathway together with a designer starch-to-ethanol pathway as illustrated in Fig. 8b enables production of ethanol both during the days and at nights.

Because the expression for both the designer starch-to-ethanol pathway(s) and the Calvin-cycle-branched designer ethanol-production pathway(s) is controlled by the use of an inducible promoter such as an anaerobic hydrogenase promoter, this type of designer alga, plant or plant cells is also able to grow photoautotrophically under aerobic (normal) conditions. When the designer plant (e.g., designer alga) or plant cells are grown and ready for photobiological ethanol production, the cells are then placed under the specific inducing conditions such as under anaerobic conditions [or an ammonium-to-nitrate fertilizer use shift, if designer Nia1 promoter-controlled ethanol-production pathway(s) is used] for enhanced ethanol production, as shown in Fig. 8b.

3 Use of Photosynthetic Ethanol-Producing Designer Organisms with Photobioreactor-Ethanol-Harvesting (Distillation) Systems

The various embodiments further teach how the designer organisms may be used with a photobioreactor and an ethanol-separation-harvesting system for photosynthetic production of ethanol (CH_3CH_2OH) and O_2 directly from CO_2 and H_2O using sunlight (Figs. 9–11). There are a number of embodiments on how the designer organisms may be used for photobiological ethanol production. One of the preferred embodiments is to use the designer organisms for direct photosynthetic ethanol production from CO_2 and H_2O with a photobiological reactor and ethanol-harvesting (distillation) system (Fig. 9), which includes a specific operational process described as a series of the following steps: (a) Growing a designer transgenic organism photoautotrophically in minimal culture medium using air CO_2 as the carbon source under aerobic (normal) conditions before inducing the expression of the designer ethanol-production-pathway genes; (b) When the designer organism culture is grown and ready for ethanol production, sealing or placing the culture into a specific condition, such as an anaerobic condition that can be generated by removal of O_2 from the photobiological reactor, to induce the expression of designer ethanol-production genes; (c) When the designer ethanol-production-pathway enzymes are expressed and inserted into the stroma region of the designer organism's chloroplast,

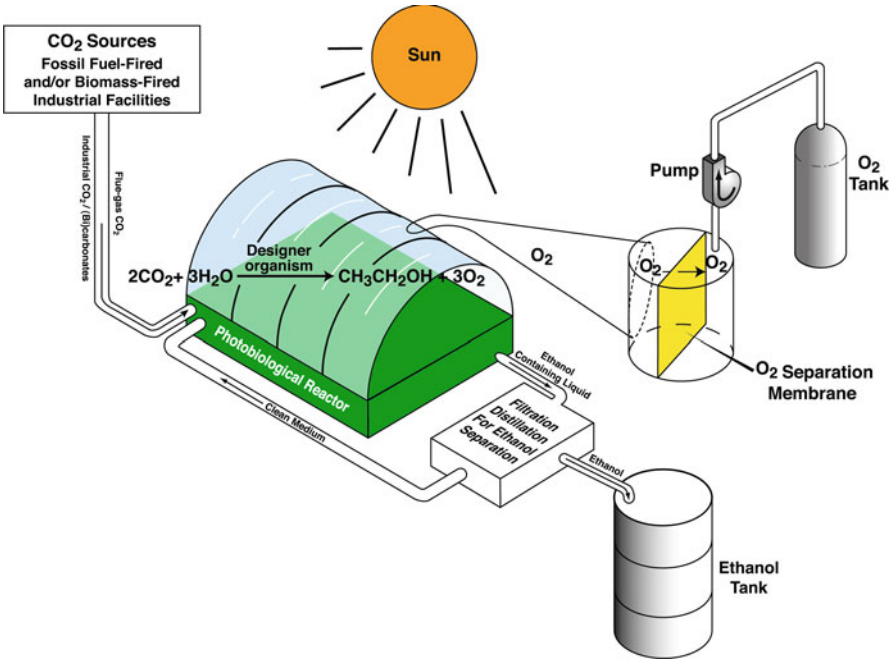

Fig. 9 Illustrates an operational process how the use of a designer organism such as designer alga may be coupled with industrial CO_2 sources through a pipeline, a photobioreactor (sealed), and ethanol-oxygen-harvesting system for photosynthetic production of ethanol and O_2 directly from CO_2 and H_2O using sunlight

supplying visible light energy such as sunlight for the designer-genes-expressed cells to work as the catalysts for photosynthetic ethanol production from CO_2 and H_2O; (d) Harvesting the ethanol product by any method known to those skilled in the art. For example, harvesting the ethanol product from the photobiological reactor by a combination of membrane filtration and ethanol-distillation techniques and flexibly collecting the O_2 gas product from the reactor.

The above process to use the designer organisms for photosynthetic CH_3CH_2OH and O_2 production from CO_2 and H_2O with a biological reactor and ethanol-harvesting (distillation) and gas product separation and collection system can be repeated for a plurality of operational cycles to achieve more desirable results. Any of the steps (a) through (d) of this process described above can also be adjusted in accordance of the invention to suit for certain specific conditions. In practice, any of the steps (a) through (d) of the process can be applied in full or in part, and/or in any adjusted combination as well for enhanced photobiological ethanol production in accordance of this invention.

The sources of CO_2 that can be used in this process include, but not limited to, industrial CO_2, (bi)carbonates, and atmospheric CO_2. For an example, flue-gas CO_2 from fossil fuel-fired and/or biomass-fired industrial facilities can be fed through a pipeline into a photobiological reactor in this process as illustrated in Fig. 9.

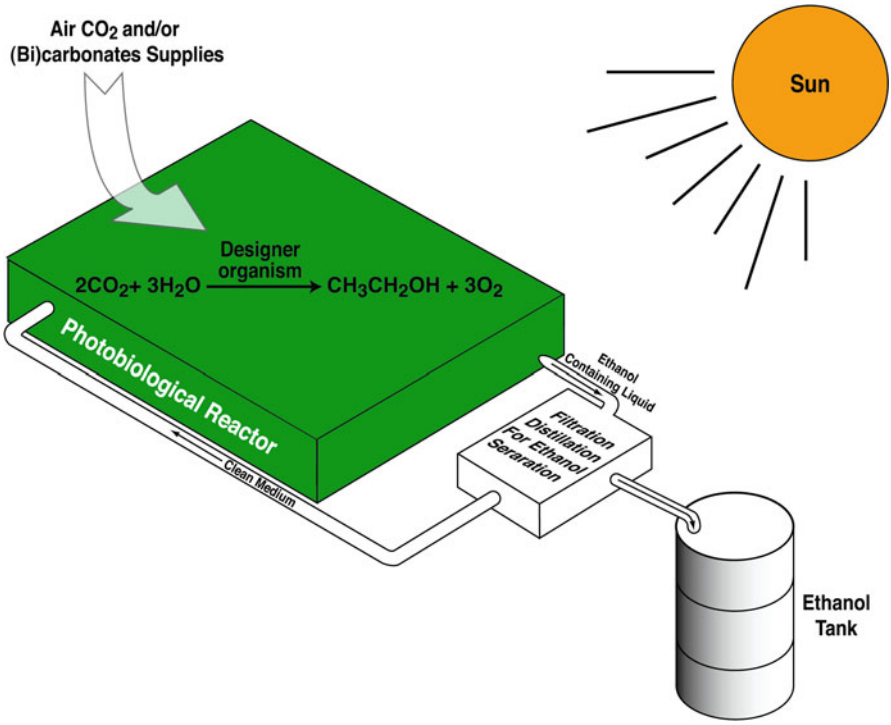

Fig. 10 Illustrates an operational process how a designer organism such as designer alga may be used through a photobioreactor and ethanol-separation/harvesting system with supplies of air CO_2 and/or (bi)carbonates for photosynthetic production of ethanol and O_2 directly from CO_2 and H_2O using sunlight

The industrial facilities that can generate CO_2 supplies for the designer photosynthetic ethanol-production process include (but not limited to): coal-fired power plants, iron and steelmaking industries, cement-manufacturing plants, petroleum refinery facilities, chemical fertilizer production factories, biomass-fired and/or fossil fuel-fired ethanol distillation/separation facilities, biomass-pyrolysis processes, smokestacks, fermentation bioreactors, biofuel-refinery facilities, and combinations thereof.

Alternatively, this designer photobiological ethanol-production process can also use the CO_2 in the environment and from the atmosphere (Figs. 10 and 11) as well. Gaseous CO_2, dissolved CO_2, bicarbonate, and carbonates can all be used by the designer-organism photobiological ethanol-production technology.

This embodiment is illustrated in more details here using designer algae as an example. As described above, designer algae of the present invention, such as the one that contains a set of designer HydA1 promoter-controlled designer ethanol-production-pathway genes, can grow normally under aerobic conditions by autotrophic photosynthesis using air CO_2 in a manner similar to that of a wild-type alga. The designer algae can grow also photoheterotrophically using an organic substrate as well.

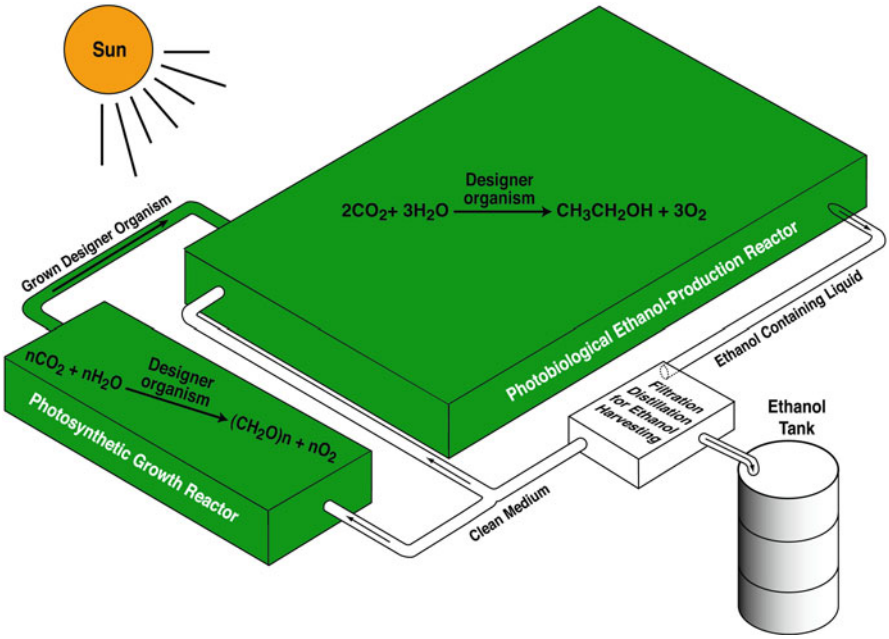

Fig. 11 Illustrates an operational process how a designer organism such as designer alga may be used with a photosynthetic culture-growth reactor, a photobiological ethanol-production reactor, and an ethanol-harvesting system for photosynthetic production of ethanol and O_2 directly from CO_2 and H_2O using sunlight

In a preferred embodiment, a designer alga is grown photoautotrophically using air CO_2 as the carbon source under the aerobic conditions as shown in Fig. 4a in a minimal medium that contains the essential mineral (inorganic) nutrients. No organic substrate such as acetate is required to grow a designer alga under the normal conditions before the designer photosynthetic ethanol-production genes are expressed. Most of the algae can grow rapidly in water through autotrophic photosynthesis using air CO_2 as long as there are sufficient mineral nutrients. The nutrient elements that are commonly required for algal growth are: N, P, and K at the concentrations of about 1–10 mM, and Mg, Ca, S, and Cl at the concentrations of about 0.5–1.0 mM, plus some trace elements Mn, Fe, Cu, Zn, B, Co, Mo among others at μM concentration levels. All of the mineral nutrients can be supplied in an aqueous minimal medium that can be made with well-established recipes of algal culture media using water and relatively small of inexpensive fertilizers and mineral salts such as ammonium bicarbonate (NH_4HCO_3) (or ammonium nitrate, urea, ammonium chloride), potassium phosphates (K_2HPO_4 and KH_2PO_4), magnesium sulfate heptahydrate ($MgSO_4 \cdot 7H_2O$), calcium chloride ($CaCl_2$), zinc sulfate heptahydrate ($ZnSO_4 \cdot 7H_2O$), iron (II) sulfate heptahydrate ($FeSO_4 \cdot 7H_2O$), and boric acid (H_3BO_3), among others. That is, large amounts of designer algae cells can be inexpensively grown in a short period of time because, under aerobic conditions such as in an open pond, the designer algae can photoautotrophically grow by themselves using air CO_2 as rapidly

as their wild-type parental strains. This is a significant feature (benefit) of the invention that could provide a cost-effective solution in generation of photoactive biocatalysts (the designer photosynthetic ethanol-producing algae) for renewable solar energy production.

When the algal culture is grown and ready for ethanol production, the grown algal culture is sealed or placed into certain specific conditions, such as anaerobic conditions that can be generated by removal of O_2 from the sealed photobiological reactor (Fig. 9), to induce the expression of designer photosynthetic ethanol-production-pathway genes. When the designer ethanol-production-pathway enzymes are expressed and inserted into the stroma region of algal chloroplast, visible light energy such as sunlight is supplied for the designer-genes-expressing algal cells to work as the catalysts for photosynthetic ethanol production from CO_2 and H_2O. When the designer genes are expressed, the algal cells can essentially become efficient and robust "green machines" that are perfect for photosynthetic production of ethanol (CH_3CH_2OH) and O_2 from CO_2 and H_2O. The ethanol product from the algal photobiological rector can be harvested by a combination of membrane filtration and ethanol-distillation techniques.

Photosynthetic production of CH_3CH_2OH and O_2 directly from CO_2 and H_2O in accordance with the present invention can, in principle, have high quantum yield. Theoretically, it requires only 24 photons to produce a CH_3CH_2OH and $3O_2$ from water and carbon dioxide by this mechanism. The maximal theoretical sunlight-to-ethanol energy efficiency by the process of direct photosynthetic ethanol production from CO_2 and H_2O is about 10%, which is the highest possible among all the biological approaches. Consequently, this approach has great potential when implemented properly with an algal reactor and ethanol-oxygen-harvesting system (Fig. 9).

The above process to use the designer algae for photosynthetic production of CH_3CH_2OH and O_2 from CO_2 and H_2O with an algal reactor and an ethanol-harvesting (distillation) and gas product separation and collection system (Fig. 9) can be repeated for a plurality of operational cycles to achieve more desirable results.

Another feature is that the designer switchable ethanol-production organism provides the capability for repeated cycles of photoautotrophic culture growth under normal aerobic conditions with a manner similar to that of a wild type (Fig. 1) and efficient photobiological production of ethanol (Fig. 2) when the designer ethanol-production pathway is switched on by an inducible promoter (such as hydrogenase promoter) at certain specific inducing conditions (such as under anaerobic conditions) in a bioreactor (Fig. 9). For example, the switchable designer alga with designer hydrogenase promoter-controlled ethanol-production genes contains normal mitochondria, which uses the reducing power (NADH) from organic reserves (and/or exogenous substrates, such as acetate) to power the cell immediately after its return to aerobic conditions. Therefore, when the algal cell is returned to aerobic conditions after its use under anaerobic conditions for production of ethanol, the cell will stop producing ethanol-production-pathway enzymes and start to restore its normal photoautotrophic capability by synthesizing normal functional chloroplast. Consequently, it is possible to use this type of genetically transformed organism for repeated cycles of photoautotrophic culture growth under normal aerobic conditions

(Fig. 1) and efficient production of ethanol under anaerobic conditions (Fig. 2) in an anaerobic reactor (Fig. 9). That is, this photobiological ethanol-production technology can be operated for a plurality of operational cycles by rejuvenating the used culture under aerobic conditions and recyclably using the rejuvenated algal culture under ethanol-producing conditions to achieve more desirable results. Optionally, this photobiological ethanol-production technology is operated continuously by circulating rejuvenated algal culture from an aerobic reactor into the anaerobic reactor while circulating the used algal culture from the anaerobic reactor (after its use for ethanol production) into the aerobic reactor for rejuvenation by synthesizing normal functional chloroplasts through photosynthetic CO_2 fixation and photoautotrophic growth.

Some of the designer organisms could grow photoautotrophically even with the ethanol-production pathway(s) switched on. Whether or how fast a designer organism could grow under the ethanol-producing conditions may depend on its genetic background and how much of the Calvin cycle products are still available for cell growth after use by the designer ethanol-production pathway(s). Designer organisms that can, under the ethanol-producing conditions, maintain essential cellular functions with an appropriate growth rate can also be used for continuous photobiological production of CH_3CH_2OH and O_2 from CO_2 and H_2O with a bioreactor and an ethanol-harvesting (distillation) system (Figs. 9 and 10).

There are additional ways that the switchable designer organisms can be used. For example, the used designer algal culture from a photobiological ethanol-production reactor does not have to be circulated back to a culture-growth reactor. Instead, the used algal culture is taken out to be used as fertilizers or biomass feed stocks for other processing because the photoautotrophic growth of the switchable designer alga in a culture-growth reactor (Fig. 11, left) is capable of continuously supplying algal cells to a photobiological ethanol-production reactor for the biofuel production (Fig. 11, right). This embodiment is, especially, helpful to using some of the designer organisms that can grow photoautotrophically only before but not after the ethanol-production pathway(s) is switched on. For example, as illustrated in Fig. 11, by keeping a continuously growing culture of a designer alga (that can grow photoautotrophically only before the ethanol-production pathway(s) is switched on) in a culture-growth reactor, it can provide continuous supplies of grown algal cells for use in a photobiological ethanol-production reactor. This approach makes it possible to use those designer organisms that can grow only before the ethanol-production pathway(s) is switched on for photobiological ethanol production as well.

Because of various reasons, some of the designer ethanol-production organisms could grow only photohetrotrophically or photomixotrophically but not photoautotrophically. Use of a culture-growth reactor as illustrated in Fig. 11 can also grow this type of designer ethanol-production organisms photohetrotrophically or photomixotrophically using organic substrates including, but not limited to, sucrose, glucose, acetate, ethanol, methanol, propanol, butanol, acetone, starch, hemicellulose, cellulose, lipids, proteins, organic acids, biomass materials, and combination thereof. The so-grown culture can also be supplied to a photobiological ethanol-production reactor for induction of the designer pathways for ethanol production as illustrated in Fig. 11. This modified embodiment on culture growth makes it possible to use those

designer organisms that can grow only photohetrotrophically, or photomixotrophically also for photobiological ethanol production as well.

For certain specific designer organisms with designer nitrate reductase (*Nia1*) promoter-controlled ethanol-production-pathway genes, the above photobiological reactor process may be further adjusted to achieve more beneficial results. For example, a designer alga that contains *Nia1* promoter-controlled ethanol-production-pathway genes can grow normally in a culture medium with ammonium (but no nitrate) by autotrophic photosynthesis using air CO_2 in a manner similar to that of a wild-type alga. This is because the expression of the ethanol-production-pathway genes in this designer organism will be turned on only in the presence of nitrate as desired owning to the use of nitrate reductase (*Nia1*) promoter in controlling the designer pathway expression. A significant feature of the designer organisms with *Nia1* promoter-controlled ethanol-production-pathway genes is that the expression of the designer ethanol-production pathways can be induced by manipulating the concentration levels of nitrate (NO_3^-) relative to that of ammonium (NH_4^+) in the culture medium without requiring any anaerobic conditions. That is, the expression of the designer ethanol-production pathway(s) can be induced under both aerobic and anaerobic conditions. This enables the designer photobiological ethanol-production process to operate even under aerobic conditions using atmospheric CO_2 (Fig. 10). Likewise, this type of designer organisms with *Nia1* promoter-controlled ethanol-production-pathway genes can grow photoautotrophically both under aerobic and anaerobic conditions as well. Therefore, as a further embodiment, the operational process of using designer organism with nitrate reductase (*Nia1*) promoter-controlled ethanol-production-pathway genes is adjusted to the following: (a) Growing a designer transgenic organism photoautotrophically in minimal culture medium in the presence of ammonium (NH_4^+) but no nitrate (NO_3^-) before inducing the expression of the designer ethanol-production-pathway genes; (b) When the designer organism culture is grown and ready for ethanol production, adding nitrate (NO_3^-) fertilizer into the culture medium to raise the concentration of nitrate (NO_3^-) relative to that of ammonium (NH_4^+) to induce the expression of designer ethanol-production-pathway genes; (c) When the designer ethanol-production-pathway enzymes are expressed and inserted into the stroma region of the designer organism's chloroplast, supplying visible light energy such as sunlight for the designer-genes-expressed cells to work as the catalysts for photosynthetic ethanol production from CO_2 and H_2O; (d) Harvesting the ethanol product from the photobiological reactor by a combination of membrane filtration and ethanol-distillation techniques.

Furthermore, the harvesting of ethanol product from photobiological liquid culture media can be achieved also through the use of another invention: greenhouse distillation that is disclosed in details in PCT International Patent Application Publication No. WO 2009/105714 A2. Briefly, when sunlight is used to drive photobiological ethanol production, it also generates waste heat in the liquid culture medium. Through combined use of a designer photosynthetic organism culture with a greenhouse distillation system, the waste solar heat associated with the photobiological ethanol-production process can be utilized in vaporizing the product ethanol (and water) for harvesting ethanol and producing freshwater by fractional greenhouse

distillation. Consequently, this approach can help improve the total process energy efficiency with minimal cost and high sunlight utilization efficiency [14].

In addition to ethanol production, it is also possible to use a designer organism or part of its designer ethanol-production pathway(s) to produce certain intermediate products including: acetaldehyde, pyruvate, phosphoenolpyruvate, 2-phosphoglycerate, 1,3-diphosphoglycerate, glyceraldehye-3-phosphate, dihydroxyacetone phosphate, fructose-1,6-diphosphate, fructose-6-phosphate, glucose-6-phosphate, and glucose-1-phosphate. Therefore, a further embodiment comprises an additional step of harvesting the intermediate products that can be produced also from an induced transgenic designer organism. The production of an intermediate product can be selectively enhanced by switching off a designer-enzyme activity that catalyzes its consumption in the designer pathways. The production of a said intermediate product can be enhanced also by using a designer organism with one or some of designer enzymes omitted from the designer ethanol-production pathways. For example, a designer organism with the alcohol dehydrogenase or pyruvate decarboxylase omitted from the designer pathway of Fig. 4b may be used to produce acetaldehyde or pyruvate, respectively.

Acknowledgments This work was supported in part by a Seed Money project at Oak Ridge National Laboratory (ORNL) which is managed by UT-Battelle, LLC, for DOE under contract no. DE-AC05-00OR22725. The author wishes to thank also the ORNL/Technology Transfer Office and the Laboratory for the nice support.

References

1. Gfeller R, Gibbs M (1984) Fermentative metabolism of *Chlamydomonas Reinhardtii*. Plant Physiol 75:212–218
2. Lee JW (2011) Designer organisms for photosynthetic production of ethanol from carbon dioxide and water. US Patent 7,973,214 B2
3. Lee JW, Blankinship SL, Greenbaum E (1995) Temperature effect on production of hydrogen and oxygen by *Chlamydomonas* cold strain CCMP1619 and wild type 137c. Appl Biochem Biotechnol 51(52):379–386
4. Lee JW, Mets L, Greenbaum E (2002) Improvement of photosynthetic efficiency at high light intensity through reduction of chlorophyll antenna size. Appl Biochem Biotechnol 98–100:37–48
5. Quinn JM, Barraco P, Ericksson M, Merchant S (2000) Coordinate copper- and oxygen-responsive Cyc6 and Cpx1 expression in Chlamydomonas is mediated by the same element. J Biol Chem 275:6080–6089
6. Loppes R, Radoux M (2002) Two short regions of the promoter are essential for activation and repression of the nitrate reductase gene in *Chlamydomonas reinhardtii*. Mol Genet Genomics 268:42–48
7. Schroda M, Blocker D, Beek C (2000) The HSP70A promoter as a tool for the improved expression of transgenes in *Chlamydomonas*. Plant J 21:121–131
8. Pattanayak D, Chatterjee S (1998) Nicotinamide adenine dinucleotide phosphate phosphatase facilitates dark reduction of nitrate: regulation by nitrate and ammonia. Biol Plant 41(1):75–84
9. Muto S, Miyachi S, Usuda H, Edwards G, Bassham J (1981) Light-induced conversion of nicotinamide adenine dinucleotide to nicotinamide adenine dinucleotide phosphate in higher plant leaves. Plant Physiol 68(2):324–328

10. Matsumura-Kadota H, Muto S, Miyachi S (1982) Light-induced conversion of NAD^+ to $NADP^+$ in Chlorella cells. Biochim Biophys Acta 679(2):300–307
11. Liszewski K (2003) Progress in RNA interference. Genet Eng News 23(11):1–59
12. Fire A, Xu S, Montgomery MK, Kostas SA, Driver SE, Mello CC (1998) Potent and specific genetic interference by double-stranded RNA in Caenorhabditis elegans. Nature 391(6669): 806–811
13. Dykxhoorn DM, Novina CD, Sharp PA (2003) Killing the messenger: short RNAs that silence gene expression. Nat Rev Mol Cell Biol 4(6):457–467
14. Lee JW (2009) Designer oxyphotobacteria and greenhouse distillation for photobiological ethanol production from carbon dioxide and water. PCT International Patent Application Publication Number: WO 2009/105714 A2

Chapter 22
Synthetic Biology for Photobiological Production of Butanol and Related Higher Alcohols from Carbon Dioxide and Water

James Weifu Lee

Abstract This chapter presents an invention on creating biosafety-guarded designer photosynthetic organisms for photobiological production of butanol and related higher alcohols. The designer photosynthetic organisms are created such that the endogenous photobiological regulation mechanism is tamed, and the reducing power (NADPH) and energy (ATP) acquired from the photosynthetic process are used for synthesis of butanol and/or related higher alcohols from carbon dioxide and water. This photobiological biofuels-production method eliminates the problem of recalcitrant lignocellulosics by bypassing it. This technology is expected to have a much higher solar-to-biofuels energy-conversion efficiency than the conventional biomass technology. Furthermore, this approach enables the use of seawater and/or groundwater for photobiological production of higher alcohols (such as 1-butanol and 2-methyl-1-butanol) without requiring freshwater or agricultural soil, since the designer photosynthetic organisms can be created from certain marine algae and/or cyanobacteria that can use seawater and/or certain groundwater.

1 Introduction

Butanol ($CH_3CH_2CH_2CH_2OH$) and/or related higher alcohols can be used as a liquid fuel to run engines such as cars. Butanol can replace gasoline and the energy contents of the two fuels are nearly the same (110,000 Btu per gallon for butanol; 115,000 Btu per gallon for gasoline). Butanol has many superior properties as an

J.W. Lee (✉)
Department of Chemistry and Biochemistry, Old Dominion University,
Physical Sciences Building, Room 3100B, 4402 Elkhorn Avenue, Norfolk, VA 23529, USA

Johns Hopkins University, Whiting School of Engineering, 118 Latrobe Hall,
Baltimore, MD 21218, USA
e-mail: jwlee@ODU.edu; JLee349@JHU.edu

J.W. Lee (ed.), *Advanced Biofuels and Bioproducts*, DOI 10.1007/978-1-4614-3348-4_22,

alternative fuel when compared to ethanol as well. These include: (1) butanol has higher energy content (110,000 Btu per gallon butanol) than ethanol (84,000 Btu per gallon ethanol); (2) butanol is six times less "evaporative" than ethanol and 13.5 times less evaporative than gasoline, making it safer to use as an oxygenate and thereby eliminating the need for very special blends during the summer and winter seasons; (3) butanol can be transported through the existing fuel infrastructure including the gasoline pipelines whereas ethanol must be shipped via rail, barge, or truck; and (4) butanol can be used as replacement for gasoline gallon for gallon, for example, 100% or any other percentage, whereas ethanol can only be used as an additive to gasoline up to about 85% (E-85) and then only after significant modification to the engine (while butanol can work as a 100% replacement fuel without having to modify the current car engine).

A significant potential market for butanol and/or related higher alcohols as a liquid fuel already exists in the current transportation and energy systems. Butanol is also used as an industrial solvent. In the United States, currently, butanol is manufactured primarily from petroleum. Historically (1900s–1950s), biobutanol was manufactured from corn and molasses in a fermentation process that also produced acetone and ethanol and was known as an ABE (acetone, butanol, ethanol) fermentation typically with certain butanol-producing bacteria such as *Clostridium acetobutylicum* and *Clostridium beijerinckii*. When the United States lost its low-cost sugar supply from Cuba around 1954, however, butanol production by fermentation declined mainly because the price of petroleum dropped below that of sugar. Recently, there is renewed R&D interest in producing butanol and/or ethanol from biomass such as corn starch using Clostridia- and/or yeast-fermentation process. However, similarly to the situation of "cornstarch ethanol production," the "cornstarch butanol production" process also requires a number of energy-consuming steps including agricultural corn-crop cultivation, corn-grain harvesting, corn-grain starch processing, and starch-to-sugar-to-butanol fermentation. The "cornstarch butanol production" process could also probably cost nearly as much energy as the energy value of its product butanol. This is not surprising, understandably because the cornstarch that the current technology can use represents only a small fraction of the corn crop biomass that includes the corn stalks, leaves, and roots. The cornstovers are commonly discarded in the agricultural fields where they slowly decompose back to CO_2, because they represent largely lignocellulosic biomass materials that the current biorefinery industry cannot efficiently use for ethanol or butanol production. There are research efforts in trying to make ethanol or butanol from lignocellulosic plant biomass materials—a concept called "cellulosic ethanol" or "cellulosic butanol." However, plant biomass has evolved effective mechanisms for resisting assault on its cell-wall structural sugars from the microbial and animal kingdoms. This property underlies a natural recalcitrance, creating roadblocks to the cost-effective transformation of lignocellulosic biomass to fermentable sugars. Therefore, one of its problems known as the "lignocellulosic recalcitrance" represents a formidable technical barrier to the cost-effective conversion of plant biomass to fermentable sugars. That is, because of the recalcitrance problem, lignocellulosic biomasses (such as cornstover, switchgrass, and woody plant materials) could not

be readily converted to fermentable sugars to make ethanol or butanol without certain pretreatment, which is often associated with high processing cost. Despite more than 25 years of R&D efforts in lignocellulosic biomass pretreatment and fermentative butanol-production processing, the problem of recalcitrant lignocellulosics still remains as a formidable technical barrier that has not yet been eliminated so far. Furthermore, the steps of lignocellulosic biomass cultivation, harvesting, pretreatment processing, and cellulose-to-sugar-to-butanol fermentation all cost energy. Therefore, any new technology that could bypass these bottleneck problems of the biomass technology would be useful.

Oxyphotobacteria (also known as blue-green algae including cyanobacteria and oxychlorobacteria) and algae (such as *Chlamydomonas reinhardtii*, *Platymonas subcordiformis*, *Chlorella fusca*, *Dunaliella salina*, *Ankistrodesmus braunii*, and *Scenedesmus obliquus*), which can perform photosynthetic assimilation of CO_2 with O_2 evolution from water in a liquid culture medium with a maximal theoretical solar-to-biomass energy conversion of about 10%, have tremendous potential to be a clean and renewable energy resource. However, the wild-type oxygenic photosynthetic organisms, such as green plants, blue-green algae, and eukaryotic algae, do not possess the ability to produce butanol directly from CO_2 and H_2O. The wild-type photosynthesis uses the reducing power (NADPH) and energy (ATP) from the photosynthetic water splitting and proton gradient-coupled electron transport process through the algal thylakoid membrane system to reduce CO_2 into carbohydrates $(CH_2O)_n$ such as starch with a series of enzymes collectively called the "Calvin cycle" at the stroma region in an algal or green-plant chloroplast. The net result of the wild-type photosynthetic process is the conversion of CO_2 and H_2O into carbohydrates $(CH_2O)_n$ and O_2 using sunlight energy according to the following process reaction:

$$nCO_2 + nH_2O \rightarrow (CH_2O)n + nO_2 \quad (1)$$

The carbohydrates $(CH_2O)n$ are then further converted to all kinds of complicated cellular (biomass) materials including proteins, lipids, and cellulose and other cell-wall materials during cell metabolism and growth.

In certain alga such as *C. reinhardtii*, some of the organic reserves such as starch could be slowly metabolized to ethanol (but not to butanol) through a secondary fermentative metabolic pathway. The algal fermentative metabolic pathway is similar to the yeast-fermentation process, by which starch is breakdown to smaller sugars such as glucose that is, in turn, transformed into pyruvate by a glycolysis process. Pyruvate may then be converted to formate, acetate, and ethanol by a number of additional metabolic steps [1]. The efficiency of this secondary metabolic process is quite limited, probably because it could use only a small fraction of the limited organic reserve such as starch in an algal cell. Furthermore, the native algal secondary metabolic process could not produce any butanol. As mentioned earlier, butanol (and/or related higher alcohols) has many superior physical properties to serve as a replacement for gasoline as a fuel. Therefore, a new photobiological butanol (and/or related higher alcohols)-producing mechanism with a high solar-to-biofuel energy efficiency is needed.

This chapter presents an invention on designer photosynthetic organisms, which are capable of directly synthesizing butanol and/or related higher alcohols from CO_2 and H_2O using sunlight. The photobiological butanol-production system provided by the present invention could bypass all the bottleneck problems of the biomass technology mentioned earlier. The photobiological butanol-production technology is expected to have a much higher solar-to-butanol energy-conversion efficiency than the current technology.

Furthermore, the designer alga approach enables the use of seawater and/or groundwater for photobiological production of biofuels without requiring freshwater or agricultural soil, since the biofuel-producing function can be placed through molecular genetics into certain marine algae and/or cyanobacteria that can use seawater and/or certain groundwater. They could be used also in a sealed photobioreactor that could be operated on a desert for production of butanol with highly efficient use of water since there will be little or no water loss by evaporation and/or transpiration that a common crop system would suffer. That is, this invention could provide a new generation of renewable energy (butanol and related higher alcohols) production technology without requiring arable land or freshwater resources, which may be strategically important to the sustainability for the world.

2 Designer Photosynthetic Organisms for Photobiological Production of Butanol and Related Higher Alcohols

The present invention [2, 3] is directed to a photobiological butanol and related high alcohols production technology based on designer photosynthetic organisms such as designer transgenic plants (e.g., algae and oxyphotobacteria) or plant cells. In this context throughout this specification, a "higher alcohol" or "related higher alcohol" refers to an alcohol that comprises at least four carbon atoms, which includes both straight and branched alcohols such as 1-butanol and 2-methyl-1-butanol. The Calvin-cycle-channeled and photosynthetic-NADPH-enhanced pathways are constructed with designer enzymes expressed through use of designer genes in host photosynthetic organisms such as algae and oxyphotobacteria (including cyanobacteria and oxychlorobacteria) organisms for photobiological production of butanol and related higher alcohols. The said butanol and related higher alcohols are selected from the group consisting of: 1-butanol, 2-methyl-1-butanol, isobutanol, 3-methyl-1-butanol, 1-hexanol, 1-octanol, 1-pentanol, 1-heptanol, 3-methyl-1-pentanol, 4-methyl-1-hexanol, 5-methyl-1-heptanol, 4-methyl-1-pentanol, 5-methyl-1-hexanol, and 6-methyl-1-heptanol. The designer plants and plant cells are created using genetic engineering techniques such that the endogenous photosynthesis regulation mechanism is tamed, and the reducing power (NADPH) and energy (ATP) acquired from the photosynthetic water splitting and proton gradient-coupled electron transport process can be used for immediate synthesis of higher alcohols, such as 1-butanol ($CH_3CH_2CH_2CH_2OH$) and 2-methyl-1-butanol ($CH_3CH_2CH(CH_3)$

CH_2OH), from carbon dioxide (CO_2) and water (H_2O) according to the following generalized process reaction (where *m*, *n*, *x,* and *y* are its molar coefficients) in accordance with the present invention:

$$m(CO_2) + n(H_2O) \rightarrow x(\text{higher alcohols}) + y(O_2) \quad (2)$$

The photobiological higher alcohols production methods of the present invention completely eliminate the problem of recalcitrant lignocellulosics by bypassing the bottleneck problem of the biomass technology. As shown in Fig. 1, for example, the photosynthetic process in a designer organism effectively uses the reducing power (NADPH) and energy (ATP) from the photosynthetic water splitting and proton gradient-coupled electron transport process for immediate synthesis of butanol ($CH_3CH_2CH_2CH_2OH$) directly from carbon dioxide (CO_2) and water (H_2O) without being drained into the other pathways for synthesis of the undesirable lignocellulosic materials that are very hard and often inefficient for the biorefinery industry to use. This approach is also different from the existing "cornstarch butanol production" process. In accordance with this invention, butanol can be produced directly from carbon dioxide (CO_2) and water (H_2O) without having to go through many of the energy consuming steps that the cornstarch butanol-production process has to go through, including corn crop cultivation, corn-grain harvesting, corn-grain cornstarch processing, and starch-to-sugar-to-butanol fermentation. As a result, the photosynthetic butanol-production technology of the present invention is expected to have a much (more than ten times) higher solar-to-butanol energy-conversion efficiency than the current technology. Assuming a 10% solar energy conversion efficiency for the envisioned photosynthetic butanol production process, the maximal theoretical productivity (yield) could be about 72,700 kg of butanol per acre per year, which could support about 70 cars (per year per acre). Therefore, this invention could bring a significant capability to the society in helping to ensure energy security. The present invention could also help protect the Earth's environment from the dangerous accumulation of CO_2 in the atmosphere, because the present methods convert CO_2 directly into clean advanced biofuels (e.g., butanol) energy.

A fundamental feature of the present methodology is utilizing a plant (e.g., an alga or oxyphotobacterium) or plant cells, introducing into the plant or plant cells nucleic acid molecules encoding for a set of enzymes that can act on an intermediate product of the Calvin cycle and convert the intermediate product into butanol as illustrated in Fig. 1, instead of making starch and other complicated cellular (biomass) materials as the end products by the wild-type photosynthetic pathways. Accordingly, the present invention provides, *inter alia*, methods for producing butanol and/or related higher alcohols based on a designer plant (such as a designer alga and a designer oxyphotobacterium), designer plant tissue, or designer plant cells, DNA constructs encoding genes of a designer butanol- and/or related higher alcohols-production pathway(s), as well as the designer algae, designer oxyphotobacteria (including designer cyanobacteria), designer plants, designer plant tissues, and designer plant cells created. The various aspects of the present invention are described in further detail hereinbelow.

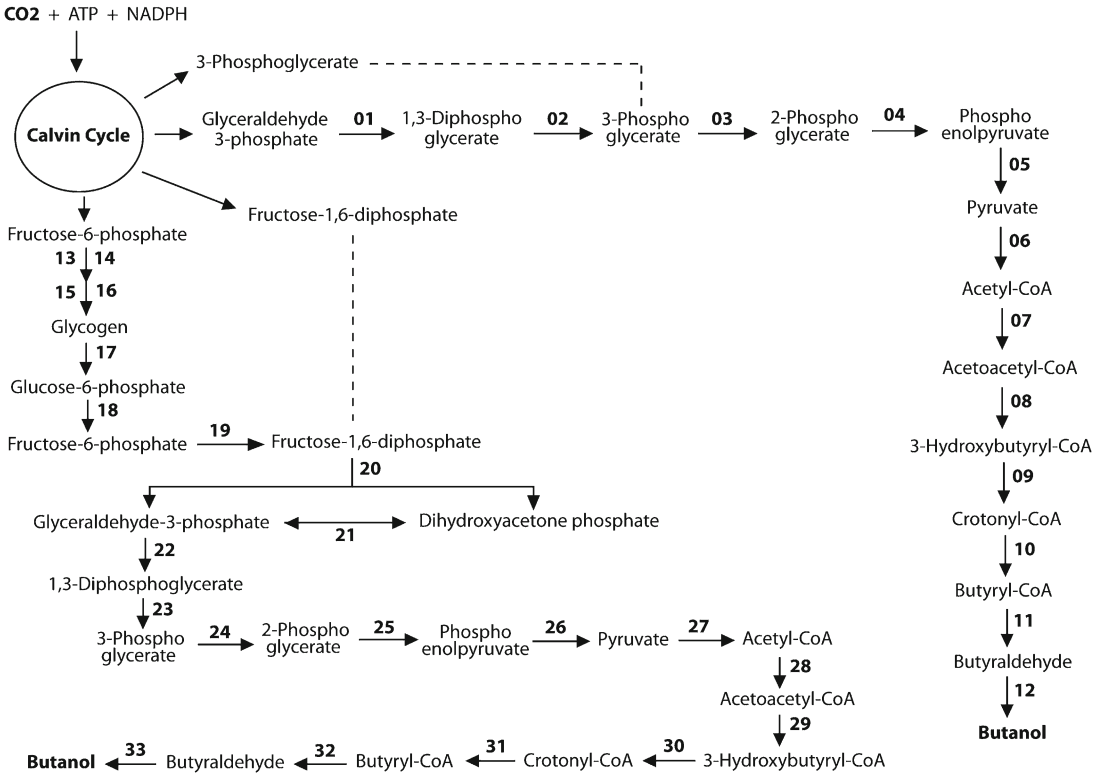

Fig. 1 Presents designer butanol-production pathways branched from the Calvin cycle using the reducing power (NADPH) and energy (ATP) from the photosynthetic water splitting and proton gradient-coupled electron transport process to reduce carbon dioxide (CO_2) into butanol $CH_3CH_2CH_2CH_2OH$ with a series of enzymatic reactions

2.1 Host Photosynthetic Organisms

According to the present invention, a designer organism or cell for the photosynthetic butanol and/or related higher alcohols production of the invention can be created utilizing as host, any plant (including alga and oxyphotobacterium), plant tissue, or plant cells that have a photosynthetic capability, i.e., an active photosynthetic apparatus and enzymatic pathway that captures light energy through photosynthesis, using this energy to convert inorganic substances into organic matter. Preferably, the host organism should have an adequate photosynthetic CO_2 fixation rate, for example, to support photosynthetic butanol (and/or related higher alcohols) production from CO_2 and H_2O at least about 1,450 kg butanol per acre per year, more preferably, 7,270 kg butanol per acre per year, or even more preferably, 72,700 kg butanol per acre per year.

In a preferred embodiment, an aquatic plant is utilized to create a designer plant. Aquatic plants, also called hydrophytic plants, are plants that live in or on aquatic environments, such as in water (including on or under the water surface) or permanently saturated soil. As used herein, aquatic plants include, for example, algae, blue-green algae (cyanobacteria and oxychlorobacteria), submersed aquatic herbs (*Hydrilla verticillata*, *Elodea densa*, *Hippuris vulgaris*, *Aponogeton boivinianus, Aponogeton rigidifolius*, *Aponogeton longiplumulosus*, *Didiplis diandra*, *Vesicularia dubyana*, *Hygrophilia augustifolia*, *Micranthemum umbrosum*, *Eichhornia azurea*, *Saururus cernuus*, *Cryptocoryne lingua*, *Hydrotriche hottoniiflora, Eustralis stellata*, *Vallisneria rubra*, *Hygrophila salicifolia*, *Cyperus helferi*, *Cryptocoryne petchii*, *Vallisneria americana*, *Vallisneria torta*, *H. hottoniiflora*, *Crassula helmsii*, *Limnophila sessiliflora*, *Potamogeton perfoliatus*, *Rotala wallichii*, *Cryptocoryne becketii*, *Blyxa aubertii*, *Hygrophila difformmis*), duckweeds (*Spirodela polyrrhiza*, *Wolffia globosa*, *Lemna trisulca*, *Lemna gibba*, *Lemna minor*, *Landoltia punctata*), water cabbage (*Pistia stratiotes*), buttercups (*Ranunculus*), water caltrop (*Trapa natans* and *Trapa bicornis*), water lily (*Nymphaea lotus*, *Nymphaeaceae* and *Nelumbonaceae*), water hyacinth (*Eichhornia crassipes*), *Bolbitis heudelotii*, *Cabomba* sp., seagrasses (*Heteranthera zosterifolia*, *Posidoniaceae*, *Zosteraceae*, *Hydrocharitaceae*, and *Cymodoceaceae*). Butanol (and/or related higher alcohols) produced from an aquatic plant can diffuse into water, permitting normal growth of the plants and more robust production of butanol from the plants. Liquid cultures of aquatic plant tissues (including, but not limited to, multicellular algae) or cells (including, but not limited to, unicellular algae) are also highly preferred for use, since the butanol (and/or related higher alcohols) molecules produced from a designer butanol (and/or related higher alcohols) production pathway(s) can readily diffuse out of the cells or tissues into the liquid water medium, which can serve as a large pool to store the product butanol (and/or related higher alcohols) that can be subsequently harvested by filtration and/or distillation/evaporation techniques.

Although aquatic plants or cells are preferred host organisms for use in the methods of the present invention, tissue and cells of nonaquatic plants, which are photosynthetic and can be cultured in a liquid culture medium, can also be used to create

designer tissue or cells for photosynthetic butanol (and/or related higher alcohols) production. For example, the following tissue or cells of nonaquatic plants can also be selected for use as a host organism in this invention: the photoautotrophic shoot tissue culture of wood apple tree *Feronia limonia*, the chlorophyllous callus-cultures of corn plant *Zea mays*, the green root cultures of Asteraceae and Solanaceae species, the tissue culture of sugarcane stalk parenchyma, the tissue culture of bryophyte *Physcomitrella patens*, the photosynthetic cell suspension cultures of soybean plant (*Glycine max*), the photoautotrophic and photomixotrophic culture of green Tobacco (*Nicofiana tabacum* L.) cells, the cell suspension culture of *Gisekia pharnaceoides* (a C_4 plant), the photosynthetic suspension cultured lines of *Amaranthus powellii* Wats., *Datura innoxia* Mill., *Gossypium hirsutum* L., and *N. tabacum* × *Nicotiana glutinosa* L. fusion hybrid.

By "liquid medium" is meant liquid water plus relatively small amounts of inorganic nutrients (e.g., N, P, K, etc., commonly in their salt forms) for photoautotrophic cultures; and sometimes also including certain organic substrates (e.g., sucrose, glucose, or acetate) for photomixotrophic and/or photoheterotrophic cultures.

In an especially preferred embodiment, the plant utilized in the butanol (and/or related higher alcohols) production method of the present invention is an alga or a blue-green alga. The use of algae and/or blue-green algae has several advantages. They can be grown in an open pond at large amounts and low costs. Harvest and purification of butanol (and/or related higher alcohols) from the water phase is also easily accomplished by distillation/evaporation or membrane separation.

Algae suitable for use in the present invention include both unicellular algae and multiunicellular algae. Multicellular algae that can be selected for use in this invention include, but are not limited to, seaweeds such as *Ulva latissima* (sea lettuce), *Ascophyllum nodosum*, *Codium fragile*, *Fucus vesiculosus*, *Eucheuma denticulatum*, *Gracilaria gracilis*, *Hydrodictyon reticulatum*, *Laminaria japonica*, *Undaria pinntifida*, *Saccharina japonica*, *Porphyra yezoensis*, and *Porphyra tenera*. Suitable algae can also be chosen from the following divisions of algae: green algae (Chlorophyta), red algae (Rhodophyta), brown algae (Phaeophyta), diatoms (Bacillariophyta), and blue-green algae (Oxyphotobacteria including Cyanophyta and Prochlorophytes). Suitable orders of green algae include Ulvales, Ulotrichales, Volvocales, Chlorellales, Schizogoniales, Oedogoniales, Zygnematales, Cladophorales, Siphonales, and Dasycladales. Suitable genera of Rhodophyta are Porphyra, Chondrus, Cyanidioschyzon, Porphyridium, Gracilaria, Kappaphycus, Gelidium, and Agardhiella. Suitable genera of Phaeophyta are Laminaria, Undaria, Macrocystis, Sargassum, and Dictyosiphon. Suitable genera of Cyanophyta (also known as Cyanobacteria) include (but not limited to) Phoridium, Synechocystis, Syncechococcus, Oscillatoria, and Anabaena. Suitable genera of Prochlorophytes (also known as oxychlorobacteria) include (but not limited to) Prochloron, Prochlorothrix, and Prochlorococcus. Suitable genera of Bacillariophyta are Cyclotella, Cylindrotheca, Navicula, Thalassiosira, and Phaeodactylum. Preferred species of algae for use in the present invention include: *C. reinhardtii*, *P. subcordiformis*, *C. fusca*, *Chlorella sorokiniana*, *Chlorella vulgaris*, "*Chlorella*" *ellipsoidea*, *Chlorella* spp., *D. salina*, *Dunaliella viridis*, *Dunaliella bardowil*, *Haematococcus*

pluvialis; *Parachlorella kessleri*, *Betaphycus gelatinum*, *Chondrus crispus*, *Cyanidioschyzon merolae*, *Cyanidium caldarium*, *Galdieria sulphuraria*, *Gelidiella acerosa*, *Gracilaria changii*, *Kappaphycus alvarezii*, *Porphyra miniata*, *Ostreococcus tauri*, *P. yezoensis*, *Porphyridium* sp., *Palmaria palmata*, *Gracilaria* spp., *Isochrysis galbana*, *Kappaphycus* spp., *L. japonica*, *Laminaria* spp., *Monostroma* spp., *Nannochloropsis oculata*, *Porphyra* spp., *Porphyridium* spp., *Undaria pinnatifida*, *Ulva lactuca*, *Ulva* spp., *Undaria* spp., *Phaeodactylum tricornutum*, *Navicula saprophila*, *Crypthecodinium cohnii*, *Cylindrotheca fusiformis*, *Cyclotella cryptica*, *Euglena gracilis*, *Amphidinium* sp., *Symbiodinium microadriaticum*, *Macrocystis pyrifera*, *A. braunii*, and *S. obliquus*.

Preferred species of blue-green algae (oxyphotobacteria including cyanobacteria and oxychlorobacteria) for use in the present invention include: *Thermosynechococcus elongatus* BP-1, *Nostoc* sp. PCC 7120, *Synechococcus elongatus* PCC 6301, *Syncechococcus* sp. strain PCC 7942, *Syncechococcus* sp. strain PCC 7002, *Syncechocystis* sp. strain PCC 6803, *Prochlorococcus marinus* MED4, *P. marinus* MIT 9313, *P. marinus* NATL1A, *Prochlorococcus* SS120, *Spirulina platensis (Arthrospira platensis)*, *Spirulina pacifica*, *Lyngbya majuscule*, *Anabaena* sp., *Synechocystis* sp., *Synechococcus elongates*, *Synechococcus (MC-A)*, *Trichodesmium* sp., *Richelia intracellularis*, *Synechococcus* WH7803, *Synechococcus* WH8102, *Nostoc punctiforme*, *Syncechococcus* sp. strain PCC 7943, *Synechocyitis* PCC 6714 phycocyanin-deficient mutant PD-1, *Cyanothece* strain 51142, *Cyanothece* sp. CCY0110, *Oscillatoria limosa*, *Lyngbya majuscula*, *Symploca muscorum*, *Gloeobacter violaceus*, *Prochloron didemni*, *Prochlorothrix hollandica*, *Synechococcus (MC-A)*, *Trichodesmium* sp., *R. intracellularis*, *P. marinus*, *Prochlorococcus* SS120, *Synechococcus* WH8102, *L. majuscula*, *S. muscorum*, *Synechococcus bigranulatus*, cryophilic *Oscillatoria* sp., *Phormidium* sp., *Nostoc* sp.*-1*, *Calothrix parietina*, thermophilic *S. bigranulatus*, *Synechococcus lividus*, thermophilic *Mastigocladus laminosus*, *Chlorogloeopsis fritschii* PCC 6912, *Synechococcus vulcanus*, *Synechococcus* sp. strain MA4, *Synechococcus* sp. strain MA19, and *T. elongatus*.

Proper selection of host photosynthetic organisms for their genetic backgrounds and certain special features is also beneficial. For example, a photosynthetic-butanol-producing designer alga created from cryophilic algae (psychrophiles) that can grow in snow and ice, and/or from cold-tolerant host strains such as *Chlamydomonas* cold strain CCMG1619, which has been characterized as capable of performing photosynthetic water splitting as cold as 4°C [4], permits photobiological butanol production even in cold seasons or regions such as Canada. Meanwhile, a designer alga created from a thermophilic/thermotolerant photosynthetic organism such as thermophilic algae *C. caldarium* and *G. sulphuraria* and/or thermophilic cyanobacteria (blue-green algae) such as *T. elongatus* BP-1 and *S. bigranulatus* may permit the practice of this invention to be well extended into the hot seasons or areas such as Mexico and the Southwestern region of the United States including Nevada, California, Arizona, New Mexico, and Texas, where the weather can often be hot. Furthermore, a photosynthetic-butanol-producing designer alga created from a marine alga, such as *P. subcordiformis*, permits the practice of this invention using seawater, while the designer alga created from a freshwater

alga such as *C. reinhardtii* can use freshwater. Additional optional features of a photosynthetic butanol (and/or related higher alcohols) producing designer alga include the benefits of reduced chlorophyll antenna size, which has been demonstrated to provide higher photosynthetic productivity [5] and butanol tolerance (and/or related higher alcohol tolerance) that allows for more robust and efficient photosynthetic production of butanol (and/or related higher alcohols) from CO_2 and H_2O. By use of a phycocyanin-deficient mutant of *Synechocystis* PCC 6714, it has been experimentally demonstrated that photoinhibition can be reduced also by reducing the content of light-harvesting pigments [6]. These optional features can be incorporated into a designer alga, for example, by use of a butanol-tolerant and/or chlorophyll antenna-deficient mutant (e.g., *C. reinhardtii* strain DS521) as a host organism, for genetic transformation with the designer butanol-production-pathway genes. Therefore, in one of the various embodiments, a host alga is selected from the group consisting of green algae, red algae, brown algae, blue-green algae (oxyphotobacteria including cyanobacteria and prochlorophytes), diatoms, marine algae, freshwater algae, unicellular algae, multicellular algae, seaweeds, cold-tolerant algal strains, heat-tolerant algal strains, light-harvesting-antenna-pigment-deficient mutants, butanol-tolerant algal strains, higher alcohols-tolerant algal strains, and combinations thereof.

2.2 Creating a Designer Butanol-Production Pathway in a Host

2.2.1 Selecting Appropriate Designer Enzymes

One of the key features in the present invention is the creation of a designer butanol-production pathway to tame and work with the natural photosynthetic mechanisms to achieve the desirable synthesis of butanol directly from CO_2 and H_2O. The natural photosynthetic mechanisms include (1) the process of photosynthetic water splitting and proton gradient-coupled electron transport through the thylakoid membrane, which produces the reducing power (NADPH) and energy (ATP), and (2) the Calvin cycle, which reduces CO_2 by consumption of the reducing power (NADPH) and energy (ATP).

In accordance with the present invention, a series of enzymes are used to create a designer butanol-production pathway that takes an intermediate product of the Calvin cycle and converts the intermediate product into butanol as illustrated in Fig. 1. A "designer butanol-production-pathway enzyme" is hereby defined as an enzyme that serves as a catalyst for at least one of the steps in a designer butanol-production pathway. According to the present invention, a number of intermediate products of the Calvin cycle can be utilized to create designer butanol-production pathway(s), and the enzymes required for a designer butanol-production pathway are selected depending upon from which intermediate product of the Calvin cycle the designer butanol-production pathway branches off from the Calvin cycle.

In one example, a designer pathway is created that takes glyceraldehyde-3-phosphate and converts it into butanol by using, for example, a set of enzymes consisting of, as shown with the numerical labels **01**-**12** in Fig. 1, glyceraldehyde-3-phosphate dehydrogenase **01**, phosphoglycerate kinase **02**, phosphoglycerate mutase **03**, enolase **04**, pyruvate kinase **05**, pyruvate-ferredoxin oxidoreductase **06**, thiolase **07**, 3-hydroxybutyryl-CoA dehydrogenase **08**, crotonase **09**, butyryl-CoA dehydrogenase **10**, butyraldehyde dehydrogenase **11**, and butanol dehydrogenase **12**. In this glyceraldehyde-3-phosphate-branched designer pathway, for conversion of two molecules of glyceraldehyde-3-phosphate to butanol, two NADH molecules are generated from NAD^+ at the step from glyceraldehyde-3-phosphate to 1,3-diphosphoglycerate catalyzed by glyceraldehyde-3-phosphate dehydrogenase **01**; meanwhile two molecules of NADH are converted to NAD^+: one at the step catalyzed by 3-hydroxybutyryl-CoA dehydrogenase **08** in reducing acetoacetyl-CoA to 3-hydroxybutyryl-CoA and another at the step catalyzed by butyryl-CoA dehydrogenase **10** in reducing crotonyl-CoA to butyryl-CoA. Consequently, in this glyceraldehyde-3-phosphate-branched designer pathway (**01**-**12**), the number of NADH molecules consumed is balanced with the number of NADH molecules generated. Furthermore, both the pathway step catalyzed by butyraldehyde dehydrogenase **11** (in reducing butyryl-CoA to butyraldehyde) and the terminal step catalyzed by butanol dehydrogenase **12** (in reducing butyraldehyde to butanol) can use NADPH, which can be regenerated by the photosynthetic water splitting and proton gradient-coupled electron transport process. Therefore, this glyceraldehyde-3-phosphate-branched designer butanol-production pathway can operate continuously.

In another example, a designer pathway is created that takes the intermediate product, 3-phosphoglycerate, and converts it into butanol by using, for example, a set of enzymes consisting of (as shown with the numerical labels **03**-**12** in Fig. 1) phosphoglycerate mutase **03**, enolase **04**, pyruvate kinase **05**, pyruvate-ferredoxin oxidoreductase **06**, thiolase **07**, 3-hydroxybutyryl-CoA dehydrogenase **08**, crotonase **09**, butyryl-CoA dehydrogenase **10**, butyraldehyde dehydrogenase **11**, and butanol dehydrogenase **12**. It is worthwhile to note that the last ten enzymes (**03**-**12**) of the glyceraldehyde-3-phosphate-branched designer butanol-producing pathway (**01**-**12**) are identical with those utilized in the 3-phosphoglycerate-branched designer pathway (**03**-**12**). In other words, the designer enzymes (**01**-**12**) of the glyceraldehyde-3-phosphate-branched pathway permit butanol production from both the point of 3-phosphoglycerate and the point glyceraldehyde-3-phosphate in the Calvin cycle. These two pathways, however, have different characteristics. Unlike the glyceraldehyde-3-phosphate-branched butanol-production pathway, the 3-phosphoglycerate-branched pathway which consists of the activities of only ten enzymes (**03**-**12**) could not itself generate any NADH that is required for use at two places: one at the step catalyzed by 3-hydroxybutyryl-CoA dehydrogenase **08** in reducing acetoacetyl-CoA to 3-hydroxybutyryl-CoA, and another at the step catalyzed by butyryl-CoA dehydrogenase **10** in reducing crotonyl-CoA to butyryl-CoA. That is, if (or when) a 3-hydroxybutyryl-CoA dehydrogenase and/or a butyryl-CoA dehydrogenase that can use strictly only NADH but not NADPH is employed, it would require a supply of NADH for the 3-phosphoglycerate-branched pathway (**03**-**12**) to operate.

Consequently, in order for the 3-phosphoglycerate-branched butanol-production pathway to operate, it is important to use a 3-hydroxybutyryl-CoA dehydrogenase **08** and a butyryl-CoA dehydrogenase **10** that can use NADPH which can be supplied by the photo-driven electron transport process. Therefore, it is a preferred practice to use a 3-hydroxybutyryl-CoA dehydrogenase and a butyryl-CoA dehydrogenase that can use NADPH or both NADPH and NADH (i.e., NAD(P)H) for this 3-phosphoglycerate-branched designer butanol-production pathway (**03**-**12** in Fig. 1). Alternatively, when a 3-hydroxybutyryl-CoA dehydrogenase and a butyryl-CoA dehydrogenase that can use only NADH are employed, it is preferably here to use an additional embodiment that can confer an NADPH/NADH conversion mechanism (to supply NADH by converting NADPH to NADH, see more detail later in the text) in the designer organism to facilitate photosynthetic production of butanol through the 3-phosphoglycerate-branched designer pathway.

In still another example, a designer pathway is created that takes fructose-1,6-diphosphate and converts it into butanol by using, as shown with the numerical labels **20**-**33** in Fig. 1, a set of enzymes consisting of aldolase **20**, triose phosphate isomerase **21**, glyceraldehyde-3-phosphate dehydrogenase **22**, phosphoglycerate kinase **23**, phosphoglycerate mutase **24**, enolase **25**, pyruvate kinase **26**, pyruvate-$NADP^+$ oxidoreductase (or pyruvate-ferredoxin oxidoreductase) **27**, thiolase **28**, 3-hydroxybutyryl-CoA dehydrogenase **29**, crotonase **30**, butyryl-CoA dehydrogenase **31**, butyraldehyde dehydrogenase **32**, and butanol dehydrogenase **33**, with aldolase **20** and triose phosphate isomerase **21** being the only two additional enzymes relative to the glyceraldehyde-3-phosphate-branched designer pathway. The use of a pyruvate-$NADP^+$ oxidoreductase **27** (instead of pyruvate-ferredoxin oxidoreductase) in catalyzing the conversion of a pyruvate molecule to acetyl-CoA enables production of an NADPH, which can be used in some other steps of the butanol-production pathway. The addition of yet one more enzyme in the designer organism, phosphofructose kinase **19**, permits the creation of another designer pathway which branches off from the point of fructose-6-phosphate of the Calvin cycle for the production of butanol. Like the glyceraldehyde-3-phosphate-branched butanol-production pathway, both the fructose-1,6-diphosphate-branched pathway (**20**-**33**) and the fructose-6-phosphate-branched pathway (**19**-**33**) can themselves generate NADH for use in the pathway at the step catalyzed by 3-hydroxybutyryl-CoA dehydrogenase **29** to reduce acetoacetyl-CoA to 3-hydroxybutyryl-CoA and at the step catalyzed by butyryl-CoA dehydrogenase **31** to reduce crotonyl-CoA to butyryl-CoA. In each of these designer butanol-production pathways, the numbers of NADH molecules consumed are balanced with the numbers of NADH molecules generated; and both the butyraldehyde dehydrogenase **32** (catalyzing the step in reducing butyryl-CoA to butyraldehyde) and the butanol dehydrogenase **33** (catalyzing the terminal step in reducing butyraldehyde to butanol) can all use NADPH, which can be regenerated by the photosynthetic water splitting and proton gradient-coupled electron transport process. Therefore, these designer butanol-production pathways can operate continuously.

Table 1 lists examples of the enzymes including those identified earlier for construction of the designer butanol-production pathways. Throughout this specification,

Table 1 Lists examples of enzymes for construction of designer Calvin-cycle-linked pathways for production of butanol and related higher alcohols

Enzyme/callout number	Source (organism)	GenBank accession number, JGI protein ID or citation
01 (also called as **22**): glyceraldehyde-3-phosphate dehydrogenase	*Mesostigma viride* cytosol; *Triticum aestivum* cytosol; *Chlamydomonas reinhardtii* chloroplast; *Botryotinia fuckeliana*; *Saccharomyces cerevisiae*; *Zymomonas mobilis*; *Karenia brevis*; *Ajellomyces capsulatus*; *Pichia stipitis*; *Pichia guilliermondii*; *Kluyveromyces marxianus*, *Triticum aestivum*; *Arabidopsis thaliana*; *Zea mays* cytosolic	GenBank: DQ873404; EF592180; L27668; XM_001549497; J01324; M18802; EU078558; XM_001539393; XM_001386423, XM_001386568; XM_001485596; DQ681075; EF592180; NM_101214; U45857, ZMU45856, U45855
02 (also as **23**): phosphoglycerate kinase	*Chlamydomonas reinhardtii* chloroplast; *Plasmodium vivax*; *Babesia bovis*; *Botryotinia fuckeliana*; *Monocercomonoides* sp.; *Lodderomyces elongisporus*; *Pichia guilliermondii*; *Arabidopsis thaliana*; *Helianthus annuus*; *Oryza sativa*; *Dictyostelium discoideum*; *Euglena gracilis*; *Chondrus crispus*; *Phaeodactylum tricornutum*; *Solanum tuberosum*	GenBank: U14912, AF244144; XM_001614707; XM_001610679; XM_001548271; DQ665858; XM_001523843; XM_001484377; NM_179576; DQ835564; EF122488; AF316577; AY647236; AY029776; AF108452; AF073473
03 (also as **24**): phosphoglycerate mutase (phosphoglycero-mutase)	*Oceanithermus profundus DSM 14977*; "*Nostoc azollae*" *0708*; *Thermotoga lettingae TMO*; *Syntrophothermus lipocalidus DSM 12680*; *Pelotomaculum thermopropionicum SI*; *Fervidobacterium nodosum Rt17-B1*; *Caldicellulosiruptor bescii DSM 6725*; *Fervidobacterium nodosum Rt17-B1*; *Thermotoga petrophila RKU-1*; *Deferribacter desulfuricans SSM1*; *Cyanobium* sp. *PCC 7001*; *Cyanothece* sp. *PCC 8802*; *Chlamydomonas reinhardtii* cytoplasm; *Aspergillus fumigatus*; *Coccidioides immitis*; *Leishmania braziliensis*; *Ajellomyces capsulatus*; *Monocercomonoides* sp.; *Aspergillus clavatus*; *Arabidopsis thaliana*; *Zea mays*	ADR35708; ADI65627, YP_003722750; YP_001470593, ABV33529; ADI02216, YP_003702781; YP_001212148; YP_001409891; YP_002573254, YP_002573195; ABS60234; ABQ47079, YP_001244998; YP_003496402, BAI80646; ZP_05046421; YP_003138980, YP_003138979; JGI Chlre2 protein ID 161689, GenBank: AF268078; XM_747847; XM_749597; XM_001248115; XM_001569263; XM_001539892; DQ665859; XM_001270940; NM_117020; M80912

(continued)

Table 1 (continued)

Enzyme/callout number	Source (organism)	GenBank accession number, JGI protein ID or citation
04 (also as **25**): enolase	*Syntrophothermus lipocalidus DSM 12680*; "*Nostoc azollae*" *0708*; *Thermotoga petrophila RKU-1*; *Spirochaeta thermophila DSM 6192*; *Cyanothece* sp. *PCC 7822*; *Hydrogenobacter thermophilus TK-6*; *Thermosynechococcus elongatus BP-1*; *Prochlorococcus marinus str. MIT 9301*; *Synechococcus* sp. *WH 5701*; *Trichodesmium erythraeum IMS101*; *Anabaena variabilis ATCC 29413*; *Nostoc* sp. *PCC 7120*; *Chlamydomonas reinhardtii* cytoplasm; *Arabidopsis thaliana*; *Leishmania mexicana*; *Lodderomyces elongisporus*; *Babesia bovis*; *Sclerotinia sclerotiorum*; *Pichia guilliermondii*; *Spirotrichonympha leidyi*; *Oryza sativa*; *Trimastix pyriformis*; *Leuconostoc mesenteroides*; *Davidiella tassiana*; *Aspergillus oryzae*; *Schizosaccharomyces pombe*; *Brassica napus*; *Zea mays*	ADI02602, YP_003703167; ADI63801; ABQ46079; YP_003875216, ADN02943; YP_003886899, ADN13624; YP_003432637, BAI69436; BAC08209; ABO16851; ZP_01083626; ABG51970; ABA23124; BAB75237; GenBank: X66412, P31683; AK222035;DQ221745; XM_001528071; XM_001611873; XM_001594215; XM_001483612; AB221057; EF122486, U09450; DQ845796; AB088633; U82438; D64113; U13799; AY307449; U17973
05 (also as **26**): pyruvate kinase	*Syntrophothermus lipocalidus DSM 12680*; *Cyanothece* sp. *PCC 8802*; *Thermotoga lettingae TMO*; *Caldicellulosiruptor bescii DSM 6725*; *Geobacillus kaustophilus HTA426*; *Thermosynechococcus elongatus BP-1*; *Thermosipho melanesiensis BI429*; *Thermotoga petrophila RKU-1*; *Caldicellulosiruptor saccharolyticus DSM 8903*; *Cyanothece* sp. *PCC 7425*; *Acaryochloris marina MBIC11017*; *Cyanothece* sp. *PCC 8801*; *Microcystis aeruginosa NIES-843*; *Cyanothece* sp. *PCC 7822*; *cyanobacterium UCYN-A*; *Arthrospira maxima CS-328*; *Synechococcus* sp. *PCC 7335*; *Chlamydomonas reinhardtii* cytoplasm; *Arabidopsis thaliana*; *Saccharomyces cerevisiae*; *Babesia bovis*; *Sclerotinia sclerotiorum*; *Trichomonas vaginalis*; *Pichia guilliermondii*; *Pichia stipitis*; *Lodderomyces elongisporus*; *Coccidioides immitis*; *Trimastix pyriformis*; *Glycine max (soybean)*	ADI02459, YP_003703024; YP_002372431; YP_001471580, ABV34516; YP_002573139; YP_148872; NP_681306, BAC08068; YP_001306168, ABR30783; YP_001244312, ABQ46736; ABP67416, YP_001180607; ACL43749, YP_002482578; YP_001514814; YP_003138017; YP_001655408; YP_003890281; YP_003422225; ZP_03273505; ZP_05035056; JGI Chlre3 protein ID 138105; GenBank: AK229638; AY949876, AY949890, AY949888; XM_001612087; XM_001594710; XM_001329865; XM_001487289; XM_001384591; XM_001528210; XM_001240868; DQ845797; L08632
06a (also as **27**): pyruvate-$NADP^+$ oxidoreductase	*Peranema trichophorum*; *Euglena gracilis*	GenBank: EF114757; AB021127, AJ278425

06b (also as **27**): pyruvate-ferredoxin oxidoreductase	*Mastigamoeba balamuthi*; *Desulfovibrio africanus*; *Entamoeba histolytica*; *Trichomonas vaginalis*; *Cryptosporidium parvum*; *Cryptosporidium baileyi*; *Giardia lamblia*; *Entamoeba histolytica*; *Hydrogenobacter thermophilus*; *Clostridium pasteurianum*	GenBank: AY101767; Y09702; U30149; XM_001582310, XM_001313670, XM_001321286, XM_001307087, XM_001311860, XM_001314776, XM_001307250; EF030517; EF030516; XM_764947; XM_651927; AB042412; Y17727
07 (also as **28**): thiolase	*Butyrivibrio fibrisolvens*; *butyrate-producing bacterium L2-50*; *Thermoanaerobacterium thermosaccharolyticum*	GenBank: AB190764; DQ987697; Z92974
08 (also as **29**): 3-hydroxybutyryl-CoA dehydrogenase	*Clostridium beijerinckii*; *Butyrivibrio fibrisolvens*; *Ajellomyces capsulatus*; *Aspergillus fumigatus*; *Aspergillus clavatus*; *Neosartorya fischeri*; *Butyrate-producing bacterium L2-50*; *Arabidopsis thaliana*; *Thermoanaerobacterium thermosaccharolyticum*	GenBank: AF494018; AB190764; XM_001537366; XM_741533; XM_001274776; XM_001262361; DQ987697; BT001208; Z92974
09 (also as **30**): crotonase	*Clostridium beijerinckii*; *Butyrivibrio fibrisolvens*; *Butyrate-producing bacterium L2-50*; *Thermoanaerobacterium thermosaccharolyticum*	GenBank: AF494018; AB190764; DQ987697; Z92974
10 (also as **31**): butyryl-CoA dehydrogenase	*Clostridium beijerinckii*; *Butyrivibrio fibrisolvens*; *Butyrate-producing bacterium L2-50*; *Thermoanaerobacterium thermosaccharolyticum*	GenBank: AF494018; AB190764; DQ987697; Z92974
11 (also as **32**): butyraldehyde dehydrogenase	*Clostridium saccharoperbutylacetonicum*	GenBank: AY251646
12a (also as **33**): NADH-dependent butanol dehydrogenase	*Geobacillus kaustophilus HTA426*; *Clostridium perfringens str. 13*; *Carboxydothermus hydrogenoformans*; *Pseudovibrio* sp. *JE062*; *Clostridium carboxidivorans P7*; *Bacillus pseudofirmus OF4*; *Oceanobacillus iheyensis HTE831*; *Slackia exigua ATCC 700122*; *Fusobacterium ulcerans ATCC 49185*; *Listeria monocytogenes FSL J1-175*; *Chlorobium chlorochromatii CaD3*; *Clostridium perfringens D str. JGS1721*; *Clostridium perfringens NCTC 8239*; *Clostridium perfringens CPE str. F4969*; *Clostridium perfringens B str. ATCC 3626*; *Clostridium botulinum NCTC 2916*; *Nostoc* sp. *PCC 7120*	YP_148778, BAD77210; NP_561774, BAB80564; AAG23613; ZP_05082669, EEA96294; ADO12118; ADC48983, YP_003425875; NP_693981, BAC15015; ZP_06159969, EEZ61452; ZP_05633940; ZP_05388801; ABB28961; ZP_02952811; ZP_02641897; ZP_02638128; ZP_02634798; EDT24774; ZP_02614964, ZP_02614746; NP_488606, BAB76265

(continued)

Table 1 (continued)

Enzyme/callout number	Source (organism)	GenBank accession number, JGI protein ID or citation
12b (also as **33**): NADPH-dependent butanol dehydrogenase	*Clostridium perfringens str. 13*; *Clostridium saccharobutylicum*; *Subdoligranulum variabile DSM 15176*; *Butyrivibrio crossotus DSM 2876*; *Oribacterium* sp. *oral taxon 078 str. F0262*; *Clostridium* sp. *M62/1*; *Clostridium hathewayi DSM 13479*; *Subdoligranulum variabile DSM 15176*; *Faecalibacterium prausnitzii A2-165*; *Blautia hansenii DSM 20583*; *Roseburia intestinalis L1-82*, *Bacillus cereus Rock3-28*; *Eubacterium rectale ATCC 33656*; *Clostridium* sp. *HGF2*; *Atopobium rimae ATCC 49626*; *Clostridium perfringens D str. JGS1721*; *Clostridium perfringens NCTC 8239*; *Clostridium butyricum 5521*; *Clostridium carboxidivorans P7*; *Clostridium botulinum E3 str. Alaska E43*; *Clostridium novyi NT*; *Clostridium botulinum B str. Eklund 17B*; *Thermococcus* sp. *AM4*; *Fusobacterium* sp. *D11*; *Anaerococcus vaginalis ATCC 51170*; *Clostridium perfringens CPE str. F4969*; *Clostridium perfringens B str. ATCC 3626*	NP_562172, BAB80962; AAA83520; EFB77036; EFF67629, ZP_05792927; ZP_06597730, EFE92592; EFE12215, ZP_06346636; EFC98086, ZP_06115415; ZP_05979561; ZP_05615704, EEU95840; ZP_05853889, EEX22072; ZP_04745071, EEU99657; ZP_04236939, EEL31374; YP_002938098, ACR75964; EFR36834; ZP_03568088; ZP_02952006; ZP_02642725; ZP_02950013, ZP_02950012; ZP_06856327; YP_001922606, YP_001922335, ACD52989; YP_878939; YP_001887401; EEB74113; EFD81183; ZP_05473100, EEU12061; EDT27639; EDT24389
13: starch synthase	*Chlamydomonas reinhardtii*; *Phaseolus vulgaris*; *Oryza sativa*; *Arabidopsis thaliana*; *Colocasia esculenta*; *Amaranthus cruentus*; *Parachlorella kessleri*; *Triticum aestivum*; *Sorghum bicolor*; *Astragalus membranaceus*; *Perilla frutescens*; *Zea mays*; *Ipomoea batatas*	GenBank:AF026422, AF026421, DQ019314, AF433156; AB293998; D16202, AB115917, AY299404; AF121673, AK226881; NM_101044; AY225862, AY142712; DQ178026; AB232549; Y16340; AF168786; AF097922; AF210699; AF019297; AF068834
14: glucose-1-phosphate adenylyltransferase	*Arabidopsis thaliana*; *Zea mays*; *Chlamydia trachomatis*; *Solanum tuberosum (potato)*; *Shigella flexneri*; *Lycopersicon esculentum*	GenBank: NM_127730, NM_124205, NM_121927, AY059862; EF694839, EF694838; AF087165; P55242; NP_709206; T07674
15: phosphoglucomutase	*Oryza sativa* plastid; *Ajellomyces capsulatus*; *Pichia stipitis*; *Lodderomyces elongisporus*; *Aspergillus fumigatus*; *Arabidopsis thaliana*; *Populus tomentosa*; *Oryza sativa*; *Zea mays*	GenBank: AC105932, AF455812; XM_001536436; XM_001383281; XM_001527445; XM_749345; NM_124561, NM_180508, AY128901; AY479974; AF455812; U89342, U89341
16: hexose-phosphate-isomerase	*Staphylococcus carnosus* subsp. *carnosus TM300*	YP_002633806, CAL27621

17: alpha-amylase; beta-amylase; starch phosphorylase	*Hordeum vulgare* aleurone cells; *Trichomonas vaginalis*; *Phanerochaete chrysosporium*; *Chlamydomonas reinhardtii*; *Arabidopsis thaliana*; *Dictyoglomus thermophilum* heat-stable amylase gene; *Arabidopsis thaliana*; *Hordeum vulgare*; *Musa acuminate*; *Citrus hybrid cultivar* root; *Solanum tuberosum* chloroplast; *Arabidopsis thaliana*; *Triticum aestivum*; *Ipomoea batatas*	GenBank: J04202; XM_001319100; EF143986; AY324649; NM_129551; X07896; GenBank: NM_113297; D21349; DQ166026; GenBank: AY098895; P53535; NM_113857, NM_114564; AF275551; M64362
18: glucose-phosphate (glucose-6-phosphate) isomerase	*Chlamydomonas reinhardtii*; *Saccharomyces cerevisiae*; *Pichia stipitis*; *Ajellomyces capsulatus*; *Spinacia oleracea* cytosol; *Oryza sativa* cytoplasm; *Arabidopsis thaliana*; *Zea mays*	JGI Chlre3 protein ID 135202; GenBank: M21696; XM_001385873; XM_001537043; T09154; P42862; NM_123638, NM_118595; U17225
19: phosphofructose kinase	*Chlamydomonas reinhardtii*; *Arabidopsis thaliana*; *Ajellomyces capsulatus*; *Yarrowia lipolytica*; *Pichia stipitis*; *Dictyostelium discoideum*; *Tetrahymena thermophila*; *Trypanosoma brucei*; *Plasmodium falciparum*; *Spinacia oleracea*	JGI Chlre2 protein ID 159495; GenBank: NM_001037043, NM_179694, NM_119066, NM_125551; XM_001537193; AY142710; XM_001382359, XM_001383014; XM_639070; XM_001017610; XM_838827; XM_001347929; DQ437575
20: fructose-diphosphate aldolase	*Chlamydomonas reinhardtii* chloroplast; *Fragaria x ananassa* cytoplasm; *Homo sapiens*; *Babesia bovis*; *Trichomonas vaginalis*; *Pichia stipitis*; *Arabidopsis thaliana*	GenBank: X69969; AF308587; NM_005165; XM_001609195; XM_001312327, XM_001312338; XM_001387466; NM_120057, NM_001036644
21: triose phosphate isomerase	*Arabidopsis thaliana*; *Chlamydomonas reinhardtii*; *Sclerotinia sclerotiorum*; *Chlorella pyrenoidosa*; *Pichia guilliermondii*; *Euglena intermedia*; *Euglena longa*; *Spinacia oleracea*; *Solanum chacoense*; *Hordeum vulgare*; *Oryza sativa*	GenBank: NM_127687, AF247559; AY742323; XM_001587391; AB240149; XM_001485684; DQ459379; AY742325; L36387; AY438596; U83414; EF575877

(continued)

Table 1 (continued)

Enzyme/callout number	Source (organism)	GenBank accession number, JGI protein ID or citation
34: NADPH-dependent glyceraldehyde-3-phosphate dehydrogenase	*Staphylococcus aureus 04-02981*; *Staphylococcus lugdunensis*; *Staphylococcus lugdunensis HKU09*; *Vibrio cholerae BX 330286*; *Vibrio* sp. *Ex25*; *Pseudomonas savastanoi pv.*; *Vibrio cholerae B33*; *Grimontia hollisae CIP 101886*; *Vibrio mimicus MB-451*, *Vibrio coralliilyticus ATCC BAA-450*; *Vibrio cholerae MJ-1236*; *Zea mays* cytosolic NADP dependent; *Apium graveolens*; *Vibrio cholerae B33*; *Vibrio cholerae TMA 21*; *Vibrio cholerae bv. albensis VL426*; *Vibrio orientalis CIP 102891*; *Vibrio cholerae MJ-1236*; *Vibrio cholerae CT 5369-93*; *Vibrio* sp. *RC586*; *Vibrio furnissii CIP 102972*; *Vibrio metschnikovii CIP 69.14*	ADC37857; ADC87332; YP_003471459; ZP_04395517; YP_003287699; ZP_07004478, EFI00105; ZP_04399616; ZP_06052988, EEY71738; ZP_06041160; ZP_05886203; YP_002876243; NP_001105589; AAF08296; EEO17521; EEO13209; EEO01829; ZP_05943395; ACQ62447; ZP_06049761; ZP_06079970; ZP_05878983; ZP_05883187
35: NAD-dependent glyceraldehyde-3-phosphate dehydrogenase	*Edwardsiella tarda FL6-60*; *Flavobacteriaceae bacterium 3519-10*; *Staphylococcus aureus 04-02981*; *Pseudomonas savastanoi pv. savastanoi NCPPB 3335*; *Vibrio cholerae MJ-1236*; *Streptococcus pyogenes NZ131*; *Helicobacter pylori 908*; *Streptococcus pyogenes NZ131*; *Staphylococcus lugdunensis HKU09*; *Vibrio* sp. *Ex25*; *Stenotrophomonas chelatiphaga*; *Pseudoxanthomonas dokdonensis*; *Stenotrophomonas maltophilia*; *Vibrio cholerae B33*; *Photobacterium damselae* subsp. *damselae CIP 102761*; *Vibrio* sp. *RC586*; *Grimontia hollisae CIP 101886*; *Vibrio furnissii CIP 102972*; *Acidithiobacillus caldus ATCC 51756*; *Nostoc* sp. *PCC 7120*; *Vibrio cholerae BX 330286*; *Vibrio cholerae TMA 21*; *Nostoc* sp. *PCC 7120*; *Pinus sylvestris*; *Cheilanthes yavapensis*; *Cheilanthes wootonii*; *Astrolepis laevis*	ADM41489; YP_003095198; ADC36961; ZP_07003925; ACQ61431, YP_002878104; YP_002285269; ADN80469; ACI60574; ADC88142; ACY51070; ADK67090; ADK67075; ADK67085, ACH90636; ZP_04401333; ZP_06155532; ZP_06080908; ZP_06052393; EEX42220; ZP_05292346; CAC41000; EEO22474; EEO13042; CAC41000; CAA04942; ACO58643, ACO58642; ACO58624, ACO58623; CBH41484, CBH41483

36: (R)-citramalate synthase (EC 2.3.1.182)	*Hydrogenobacter thermophilus TK-6*; *Geobacter bemidjiensis Bem*; *Geobacter sulfurreducens KN400*; *Methanobrevibacter ruminantium M1*; *Leptospira biflexa serovar Patoc strain "Patoc 1 (Paris)*;" *Leptospira biflexa serovar Monteralerio*; *Leptospira interrogans serovar Australis*; *Leptospira interrogans serovar Pomona*; *Leptospira interrogans serovar Autumnalis*; *Leptospira interrogans serovar Pyrogenes*; *Leptospira interrogans serovar Canicola*; *Leptospira interrogans serovar Lai*; *Acetohalobium arabaticum DSM 5501*; *Leadbetterella byssophila DSM 17132*; *Bacteroides xylanisolvens XB1A*; *Mucilaginibacter paludis DSM 18603*; *Prevotella ruminicola 23*; *Flavobacterium johnsoniae UW101*; *Victivallis vadensis ATCC BAA-548*; *Prevotella copri DSM 18205*; *Alistipes shahii WAL 8301*; *Methylobacter tundripaludum SV96*; *Methanosarcina mazei Go1*	YP_003433013, ADO45737, BAI69812; ACH38284; ADI84633; CP001719; ABK13757; ABK13756; ABK13755; ABK13753; ABK13754; ABK13752; ABK13751; ABK13750; ABK13749; ADL11763, YP_003998693; CBK66631; EFQ72644; ADE82919; ABQ04337; ZP_06244204, EFA99692; EFB36404, ZP_06251228; CBK64953; ZP_07654184; NP_632695
37: (R)-2-methylmalate dehydratase (large and small subunits) (EC 4.2.1.35)	*Eubacterium eligens ATCC 27750*; *Methanocaldococcus jannaschii*; *Sebaldella termitidis ATCC 33386*; *Eubacterium eligens ATCC 27750*	YP_002930810, YP_002930809; P81291; ACZ06998; ACR72362, ACR72361, ACR72363, YP_002930808
38: 3-isopropylmalate dehydratase (large + small subunits) (EC 4.2.1.33)	*Thermotoga petrophila RKU-1*; *Cyanothece* sp. *PCC 7822*; *Syntrophothermus lipocalidus DSM 12680*; *Caldicellulosiruptor saccharolyticus DSM 8903*; *Pelotomaculum thermopropionicum SI*, *Caldicellulosiruptor bescii DSM 6725*; *Caldicellulosiruptor saccharolyticus DSM 8903*; *E. coli*; *Spirochaeta thermophila DSM 6192*; *Pelotomaculum thermopropionicum SI*; *Hydrogenobacter thermophilus TK-6*; *Deferribacter desulfuricans SSM1*; *Anoxybacillus flavithermus WK1*; *Thermosynechococcus elongatus BP-1*; *Geobacillus kaustophilus HTA426*; *Synechocystis* sp. *PCC 6803*; *Chlamydomonas reinhardtii*	ABQ46641, ABQ46640; YP_003886427, YP_003889452; ADI02900, ADI02899, YP_003703465, ADI01294; ABP66933, ABP66934; YP_001211082, YP_001211083; YP_002573950, YP_002573949; YP_001180124, YP_001180125; leuC, ECK0074, JW0071; leuD, ECK0073, JW0070; YP_003875294, YP_003873373; YP_001213069, YP_001213068; YP_003433547, YP_003432351; YP_003495505, YP_003495504; ACJ32977, ACJ32978; BAC08461, BAC08786; BAD76941, BAD76940; BAA18738, BAA18298; XP_001702135, XP_001696402

(continued)

Table 1 (continued)

Enzyme/callout number	Source (organism)	GenBank accession number, JGI protein ID or citation
39: 3-isopropylmalate dehydrogenase (EC 1.1.1.85)	*Thermotoga petrophila RKU-1*; *Cyanothece* sp. *PCC 7822*; *Thermosynechococcus elongatus BP-1*; *Syntrophothermus lipocalidus DSM 12680*; *Caldicellulosiruptor bescii DSM 6725*; *Paludibacter propionicigenes WB4*; *Leadbetterella byssophila DSM 17132*; *Caldicellulosiruptor saccharolyticus DSM 8903*; *Thermus thermophilus*; *Pelotomaculum thermopropionicum SI*; *Geobacillus kaustophilus HTA426*; *Hydrogenobacter thermophilus TK-6*; *Spirochaeta thermophila DSM 6192*; *Deferribacter desulfuricans SSM1*; *Anoxybacillus flavithermus WK1*; *Volvox carteri f. nagariensis*; *Chlamydomonas reinhardtii*; *Ostreococcus tauri*	ABQ46392, YP_001243968; YP_003888480, ADN15205; BAC09152, NP_682390; ADI02898, YP_003703463; ADQ78220; YP_002573948; YP_003998692; ABP66935; AAA16706, YP_001180126; YP_001211084; YP_148510, BAD76942; YP_003433176; YP_003873639; YP_003495917; YP_002314961; XP_002955062, EFJ43816; XP_001701074, XP_001701073; XP_003083133
40: 2-isopropylmalate synthase (EC 2.3.3.13)	*Thermotoga petrophila RKU-1*; *Cyanothece* sp. *PCC 7822*; *Cyanothece* sp. *PCC 8802*; *Nostoc punctiforme PCC 73102*; *Pelotomaculum thermopropionicum SI*; *Hydrogenobacter thermophilus TK-6*; *E. coli*; *Caldicellulosiruptor saccharolyticus DSM 8903*; *Syntrophothermus lipocalidus DSM 12680*; *Geobacillus kaustophilus HTA426*; *Caldicellulosiruptor bescii DSM 6725*; *Anoxybacillus flavithermus WK1*; *Deferribacter desulfuricans SSM1*; *Thermosynechococcus elongatus BP-1*; *Spirochaeta thermophila DSM 6192*; *Thermotoga lettingae TMO*; *Volvox carteri f. nagariensis*; *Micromonas* sp. *RCC299*; *Micromonas pusilla CCMP1545*; *Chlamydomonas reinhardtii*	ABQ46395, YP_001243971; YP_003890122, ADN16847; ACU99797; ACC82459; YP_001211081; YP_003432474, BAI69273; NP_414616, AAC73185; ABP66753, YP_001179944; YP_003703466, ADI02901; YP_148511, BAD76943; YP_002572404; YP_002314960, ACJ32975; YP_003496874, BAI81118; NP_682187, BAC08949; ADN03009,YP_003875282; YP_001469896,ABV32832; XP_002945733, EFJ52728; ACO69978, XP_002508720; XP_003063010, EEH52949; XP_001696603, EDP08580

41: isopropylmalate isomerase large/small subunits (EC 4.2.1.33)	*Geobacillus kaustophilus HTA426*; *Anabaena variabilis ATCC 29413*; *Synechocystis* sp. *PCC 6803*; *Anoxybacillus flavithermus WK1*; *Thermosynechococcus elongatus BP-1*; *Spirochaeta thermophila DSM 6192*; *Salmonella enterica* subsp. *enterica serovar Typhimurium str. D23580*; *Staphylococcus aureus A5937*; *Francisella philomiragia* subsp. *philomiragia ATCC 25015*; *Neisseria lactamica*; *Francisella novicida U112*; *Staphylococcus aureus A5937*; *Staphylococcus aureus* subsp. *aureus 68–397*; *Fusobacterium* sp. *2_1_31*; *Francisella novicida GA99-3549*; *marine bacterium HP15*; *Bacillus licheniformis ATCC 14580*; *Rhodobacter sphaeroides 2.4.1*; *Bordetella petrii DSM 12804*; *Agrobacterium vitis S4*	YP_148509, YP_148508; YP_324467, YP_324466; NP_442926, NP_441618; YP_002314962, YP_002314963; NP_682024, NP_681699; YP_003873372; CBG23133, CBG23132; ZP_05702396; EET20545; AAA53236; ABK88972; EEV86047; ZP_05607839; EEO38992; EDN35429; ADP98363, ADP98362; YP_092517, YP_092516; YP_353947, YP_353945; YP_001631647, YP_001631646; YP_002551071, YP_002551071
42: 2-keto acid decarboxylase (EC 4.1.1.72, etc.)	*Lactococcus lactis*; *Lactococcus lactis* subsp. *lactis KF147*; *Lactococcus lactis* subsp. *Lactis*; *Kluyveromyces marxianus*; *Kluyveromyces lactis*; *Mycobacterium avium 104*; *Mycobacterium ulcerans Agy99*; *Mycobacterium bovis*; *Mycobacterium leprae*; *Proteus mirabilis HI4320*; *Staphylococcus aureus 04-02981*; *Acetobacter pasteurianus*; *Saccharomyces cerevisiae*; *Zymomonas mobilis* subsp. *mobilis CP4*; *Mycobacterium tuberculosis*; *Mycobacterium smegmatis str. MC2 155*; *Mycobacterium bovis BCG str. Pasteur 1173P2*	AAS49166; ADA65057, YP_003353820; CAG34226; AAA35267; CAA59953; A0QBE6; A0PL16; Q7U140; Q9CBD6; YP_002150004; ADC36400; AAM21208; CAA39398; AAA27696; O53865; A0R480; A1KGY5
43: alcohol dehydrogenase (NAD dependent) (EC 1.1.1.1)	*Thermoplasma volcanium GSS1*; *Gluconacetobacter hansenii ATCC 23769*; *Saccharomyces cerevisiae*; *Aeropyrum pernix K1*; *Rhodobacterales bacterium HTCC2083*; *Bradyrhizobium japonicum USDA 110*; *Syntrophothermus lipocalidus DSM 12680*; *Fervidobacterium nodosum Rt17-B1*; *Desulfotalea psychrophila LSv54*; *Acetobacter pasteurianus IFO 3283-03*; *Gluconobacter oxydans 621H*; *Aeromonas hydrophila* subsp. *hydrophila ATCC 7966*; *Acetobacter pasteurianus IFO 3283-01*; *Streptomyces hygroscopicus ATCC 53653*	BAB59540; ZP_06834544; CAA89136; NP_148480; ZP_05073895; NP_769420; ADI01021; YP_001411173; YP_065604; BAI03878; YP_192500; ABK38651; BAI00830; EFL29096

(continued)

Table 1 (continued)

Enzyme/callout number	Source (organism)	GenBank accession number, JGI protein ID or citation
44: alcohol dehydrogenase (NADPH dependent) (EC 1.1.1.2)	*Pelotomaculum thermopropionicum SI*; *Fusobacterium* sp. *7_1*; *Pichia pastoris GS115*; *Pichia pastoris GS115*; *Escherichia coli str. K-12 substr. MG1655*; *Clostridium hathewayi DSM 13479*; *Clostridium butyricum 5521*; *Fusobacterium ulcerans ATCC 49185*; *Fusobacterium* sp. *D11*; *Desulfovibrio desulfuricans* subsp. *desulfuricans str. G20*; *Clostridium novyi NT*; *Clostridium tetani E88*; *Aureobasidium pullulans*; *Scheffersomyces stipitis CBS 6054*, *Thermotoga lettingae TMO*; *Thermotoga petrophila RKU-1*; *Coprinopsis cinerea okayama7#130*; *Saccharomyces cerevisiae EC1118*; *Saccharomyces cerevisiae JAY291*	YP_001211038, BAF58669; ZP_04573952, EEO43462; XP_002494014, XP_002490014; CAY71835, XP_002492217, CAY67733; yqhD, NP_417484, AAC76047; EFC99049; ZP_02948287; ZP_05632371; ZP_05440863; YP_389756; YP_878957; NP_782735; ADG56699; ABN66271, XP_001384300; YP_001471424; YP_001244106; XP_001834460; CAY82157; EEU07174
45: phosphoenolpyruvate carboxylase (EC 4.1.1.31)	*Thermaerobacter subterraneus DSM 13965*; *Cyanothece* sp. *PCC 7822*; *Thermus* sp.; *Rhodothermus marinus*; *Thermosynechococcus elongatus BP-1*; *Leadbetterella byssophila DSM 17132*; *Riemerella anatipestifer DSM 15868*; *Mucilaginibacter paludis DSM 18603*; *Truepera radiovictrix DSM 17093*; *Ferrimonas balearica DSM 9799*; *Meiothermus silvanus DSM 9946*; *Nocardiopsis dassonvillei* subsp. *dassonvillei DSM 43111*; *E. coli*, *Meiothermus ruber DSM 1279*; *Olsenella uli DSM 7084*; *Ktedonobacter racemifer DSM 44963*; *Rhodopirellula baltica SH 1*; *Oceanithermus profundus DSM 14977*; *marine bacterium HP15*; *Marivirga tractuosa DSM 4126*; *Mucilaginibacter paludis DSM 18603*; *Streptomyces coelicolor A3(2)*; *Delftia acidovorans SPH-1*; *Actinobacillus pleuropneumoniae serovar 13 str. N273*; *Prochlorococcus marinus str. MIT 9301*; *Prochlorococcus marinus str. NATL1A*; *Prochlorococcus marinus str. MIT 9515*; *Clostridium cellulovorans 743B*; *Neisseria meningitidis Z2491*; *Deinococcus geothermalis DSM 11300*; *Micromonospora* sp. *L5*; *Chlorobium phaeobacteroides DSM 266*; *Arthrobacter* sp. *FB24*; *Rhodomicrobium vannielii ATCC 17100*; *Gordonia bronchialis DSM 43247*; *Thermus aquaticus Y51MC23*; *Burkholderia ambifaria IOP40-10*	EFR61439; YP_003887888; BAA07723; CAA67760; NP_682702, BAC09464; YP_003998059, ADQ17706; ADQ81501, YP_004045007; EFQ77722; YP_003706036; YP_003911597, ADN74523; YP_003685046; YP_003681843; ZP_07594313, ZP_07565817; ADD27759; YP_003801346, ADK68466; ZP_06967036, EFH90147; NP_866412, CAD78193; ADR36285; ADP96559; ADR23252; ZP_07746438; NP_627344; ABX34873; ZP_07544559; ABO18389; ABM76577; ABM72969; YP_003842669, ADL50905; CAM07667; ABF44963; ZP_06399624; ABL64615; YP_830113; YP_004010507; YP_003273502; ZP_03496338; ZP_02894226

46: aspartate aminotransferase (EC 2.6.1.1)	*Thermotoga lettingae TMO*; *Synechococcus elongatus PCC 6301*; *Synechococcus elongatus PCC 7942*; *Thermosipho melanesiensis BI429*; *Thermotoga petrophila RKU-1*; *Thermus thermophilus*; *Anoxybacillus flavithermus WK1*; *Bacillus* sp.; *E. coli*, *Pelotomaculum thermopropionicum SI*; *Phormidium lapideum*; *Fervidobacterium nodosum Rt17-B1*; *Geobacillus kaustophilus HTA426*; *Thermosynechococcus elongatus BP-1*; *Anoxybacillus flavithermus WK1*; *Geobacillus kaustophilus HTA426*; *Spirochaeta thermophila DSM 6192*; *Caldicellulosiruptor bescii DSM 6725*; *Caldicellulosiruptor saccharolyticus DSM 8903*; *Arabidopsis thaliana*; *Glycine max*; *Lupinus angustifolius*; *Chlamydomonas reinhardtii*; *Micromonas pusilla CCMP1545*	YP_001470126; YP_172275; YP_401562; YP_001306480; YP_001244588; BAA07487; YP_002315494; AAA22250; aspC: BAB34434; YP_001211971; BAB86290; YP_001410686, YP_001409589; YP_148025, YP_147632, YP_146225; NP_683147; ACJ34747; BAD77213, BAD76064; YP_003874653; YP_002572445; YP_001179582; AAA79371; AAA33942; CAA42430; XP_001696609; XP_003060871
47: aspartokinase (EC=2.7.2.4)	*Thermotoga lettingae TMO*; *Cyanothece* sp. *PCC 8802*; *Thermotoga petrophila RKU-1*; *Hydrogenobacter thermophilus TK-6*; *Anoxybacillus flavithermus WK1*; *Bacillus* sp.; *Spirochaeta thermophila DSM 6192*; *Anoxybacillus flavithermus WK1*; *Geobacillus kaustophilus HTA426*; *Syntrophothermus lipocalidus DSM 12680*; *E. coli*; *Thermosynechococcus elongatus BP-1*; *Fervidobacterium nodosum Rt17-B1*; *Spirochaeta thermophila DSM 6192*; *Pelotomaculum thermopropionicum SI*; *Caldicellulosiruptor saccharolyticus DSM 8903*; *Caldicellulosiruptor bescii DSM 6725*; *Thermosipho melanesiensis BI429*; *Thermotoga lettingae TMO*; *Arabidopsis thaliana*; *Chlamydomonas reinhardtii*	YP_001470361, ABV33297; YP_003136939; YP_001244864, YP_001243977; YP_003432105, BAI68904; ACJ35001; AAA22251; YP_003873788, ADN01515; ACJ34043, YP_002316986; BAD77480, YP_149048; ADI02230, YP_003702795; ZP_07594328, ZP_07565832; NP_682623, BAC09385; ABS59942, YP_001410786; YP_003873302, ADN01029; YP_001212149, YP_001211837; ABP66605; YP_002573821; YP_001307097, ABR31712; YP_001470985, ABV33921; CAA67376; XP_001698576, EDP08069, XP_001695256

(continued)

Table 1 (continued)

Enzyme/callout number	Source (organism)	GenBank accession number, JGI protein ID or citation
48: aspartate-semialdehyde dehydrogenase	*Thermotoga lettingae TMO*; *Trichodesmium erythraeum IMS101*; *Prochlorococcus marinus str. MIT 9303*; *Thermotoga petrophila RKU-1*; *Caldicellulosiruptor saccharolyticus DSM 8903*; *Syntrophothermus lipocalidus DSM 12680*; *E. coli*; *Fervidobacterium nodosum Rt17-B1*; *Caldicellulosiruptor bescii DSM 6725*; *Thermosipho melanesiensis BI429*; *Spirochaeta thermophila DSM 6192*; *Pelotomaculum thermopropionicum SI*; *Hydrogenobacter thermophilus TK-6*; *Anoxybacillus flavithermus WK1*; *Geobacillus kaustophilus HTA426*; *Deferribacter desulfuricans SSM1*; *Thermosynechococcus elongatus BP-1*; *Carboxydothermus hydrogenoformans*; *Chlamydomonas reinhardtii*; *Polytomella parva*; *Glycine max*; *Zea mays*; *Oryza sativa Indica Group*	YP_001470981, ABV33917; ABG50031; ABM76828; ABQ47283, YP_001244859; ABP67176, YP_001180367; ADI01804, YP_003702369; YP_001460230, YP_001464895; YP_001409594, ABS59937; YP_002573009; YP_001307092, ABR31707; YP_003875128, ADN02855; YP_001211836, BAF59467; YP_003432252, BAI69051; YP_002316029, ACJ34044; YP_147128, BAD75560; YP_003496635, BAI80879; NP_680860, BAC07622; AAG23574, AAG23573; XP_001695059, EDP02211; ABH11018; ACU30050; ACG41594; ABR26065
49: homoserine dehydrogenase	*Syntrophothermus lipocalidus DSM 12680*; *Cyanothece* sp. *PCC 7822*; *Caldicellulosiruptor bescii DSM 6725*; *Caldicellulosiruptor saccharolyticus DSM 8903*; *E. coli*; *Spirochaeta thermophila DSM 6192*; *Pelotomaculum thermopropionicum SI*; *Hydrogenobacter thermophilus TK-6*; *Anoxybacillus flavithermus WK1*; *Geobacillus kaustophilus HTA426*; *Deferribacter desulfuricans SSM1*; *Thermosynechococcus elongatus BP-1*; *Glycine max*; *Chlamydomonas reinhardtii*; *Micromonas* sp. *RCC299*	ADI02231, YP_003702796; YP_003887242; YP_002573819; ABP66607, YP_001179798; EFJ98002; YP_003873441, ADN01168; YP_001212151, BAF59782; YP_003431981, BAI68780; YP_002316756, ACJ34771; YP_148817, BAD77249; YP_003496401, BAI80645; NP_681068, BAC07830; ABG78600, AAZ98830; XP_001699712, EDP07408; ACO69662, XP_002508404
50: homoserine kinase (EC 2.7.1.39)	*Thermotoga petrophila RKU-1*; *Cyanothece* sp. *PCC 7822*; *Caldicellulosiruptor bescii DSM 6725*; *Caldicellulosiruptor saccharolyticus DSM 8903*; *E. coli*; *Anoxybacillus flavithermus WK1*; *Geobacillus kaustophilus HTA426*; *Thermosynechococcus elongatus BP-1*; *Pelotomaculum thermopropionicum SI*; *Hydrogenobacter thermophilus TK-6*; *Chlamydomonas reinhardtii*; *Prototheca wickerhamii*; *Arabidopsis thaliana*; *Glycine max*; *Zea mays*	YP_001243979, ABQ46403; YP_003886645; YP_002573820; ABP66606, YP_001179797; AP_000667, BAB96580; YP_002316754, ACJ34769; YP_148815, BAD77247; NP_682555, BAC09317; YP_001212150, BAF59781; YP_003433124, BAI69923; XP_001701899, EDP06874; ABC24954; NP_179318, AAD33097; ACU26535; ACG46592

51: threonine synthase (EC 4.2.99.2)	*Thermotoga petrophila RKU-1*; *Cyanothece* sp. *PCC 7425*; *Thermosipho melanesiensis BI429*; *Syntrophothermus lipocalidus DSM 12680*; *E. coli*; *Pelotomaculum thermopropionicum SI*; *Anoxybacillus flavithermus WK1*; *Caldicellulosiruptor bescii DSM 6725*; *Caldicellulosiruptor saccharolyticus DSM 8903*; *Hydrogenobacter thermophilus TK-6*; *Geobacillus kaustophilus HTA426*; *Thermosynechococcus elongatus BP-1*; *Spirochaeta thermophila DSM 6192*; *Deferribacter desulfuricans SSM1*; *Geobacillus kaustophilus HTA426*	YP_001243978, ABQ46402; YP_002485009; YP_001306558, ABR31173; ADI02519, YP_003703084; AP_000668, NP_414545; YP_001213220; YP_002316755, ACJ34770; YP_002572552; YP_001180015, ABP66824; YP_003433070, YP_003433019, BAI69869, BAI69818; YP_148816, YP_147614; NP_682017, NP_681772, BAC08534, BAC08779; YP_003873303, ADN01030; YP_003495358, BAI79602
52: threonine ammonia-lyase (EC 4.3.1.19)	*Geobacillus kaustophilus HTA426*; *Prochlorococcus marinus str. MIT 9202*; *Synechococcus* sp. *PCC 7335*; *Thermotoga petrophila RKU-1*; *Pelotomaculum thermopropionicum SI*; *Anoxybacillus flavithermus WK1*; *Deferribacter desulfuricans SSM1*; *E. coli*; *Neisseria lactamica ATCC 23970*; *Citrobacter youngae ATCC 29220*; *Neisseria polysaccharea ATCC 43768*; *Providencia rettgeri DSM 1131*; *Neisseria subflava NJ9703*; *Mannheimia haemolytica PHL213*; *Achromobacter piechaudii ATCC 43553*; *Neisseria meningitidis ATCC 13091*; *Synechococcus* sp. *CC9902*; *Synechococcus* sp. *PCC 7002*; *Synechococcus* sp. *WH 8109*; *Cyanobium* sp. *PCC 7001*; *Anabaena variabilis ATCC 29413*; *Microcoleus chthonoplastes PCC 7420*; *Chlamydomonas reinhardtii*	BAD76058, BAD75876, YP_147626, YP_147444; ZP_05137562; ZP_05035047; ABQ46585, YP_001244161; YP_001210652, BAF58283; YP_002315804, YP_002315746; YP_003497384, BAI81628; YP_001746093, ZP_07690697; EEZ76650, ZP_05986317; EFE07783, ZP_06571237; EFH23894, ZP_06863451; EFE52186, ZP_06127162; EFC51529, ZP_05985502; ZP_04978734; ZP_06687730, ZP_06684811; ZP_07369980, EFM04207; ABB26032; ACA99606; ZP_05790446, EEX07646; EDY39077, ZP_05045768; ABA20300; ZP_05029756; XP_001701816, EDP06791

(continued)

Table 1 (continued)

Enzyme/callout number	Source (organism)	GenBank accession number, JGI protein ID or citation
53: acetolactate synthase (EC 2.2.1.6)	*Caldicellulosiruptor saccharolyticus DSM 8903*; *Thermotoga petrophila RKU-1*; *Thermosynechococcus elongatus BP-1*; *Syntrophothermus lipocalidus DSM 12680*; *Pelotomaculum thermopropionicum SI*; *Geobacillus kaustophilus HTA426*; *Caldicellulosiruptor bescii DSM 6725*; *Hydrogenobacter thermophilus TK-6*; *Spirochaeta thermophila DSM 6192*; *Anoxybacillus flavithermus WK1*; *Deferribacter desulfuricans SSM1*; *Escherichia coli str. K-12 substr. W3110*; *Saccharomyces cerevisiae*, *Thermus aquaticus*; *Synechococcus* sp. *PCC 7002*; *Cyanothece* sp. *PCC 7424*; *Anabaena variabilis ATCC 29413*; *Nostoc* sp. *PCC 7120*; *Microcystis aeruginosa NIES-843*; *Synechocystis* sp. *PCC 6803*; *Synechococcus* sp. *JA-2-3B'a(2–13)*; *Synechococcus* sp. *JA-3-3Ab*; *Chlamydomonas reinhardtii*; *Volvox carteri*; *Bacillus subtilis* subsp. *subtilis str. 168*; *Bacillus licheniformis ATCC 14580*	ABP66750, ABP66751, YP_001179942, ABP66455, YP_001179941, YP_001179646; YP_001243976, YP_003345845, ADA66432, ADA66431, ABQ46399, YP_001243975, ABQ46400, YP_003345846; NP_682614, BAC09376, NP_681670, BAC08432, NP_682086; ADI02904, YP_003703469, ADI02903, YP_003703468; BAF58709, BAF58917, YP_001211286, YP_001211078; BAD76946, YP_148514, BAD76945, YP_148513; ACM59790, ACM59628, ACM59629, YP_002572563, YP_002572401, YP_002572402; YP_003432299, YP_003432300, BAI69099, BAI69098; YP_003874926, YP_003874927, ADN02654, ADN02653, ACJ33615, YP_002314957, ACJ32972, ACJ32973, YP_002314958; YP_003496879, BAI81123, YP_003496878, BAI81122; AP_004121, BAE77622, AP_004122, BAE77623, BAE77528, AP_004027, BAB96646, AP_000741; BAA12700; EDN64495,CAA89744, EDV09697; YP_001735999, ACB00744; YP_002376012; YP_324035; NP_487595, BAB75254; YP_001655615; NP_441297, BAA17984, CAA66718, NP_441304, NP_442206, BAA10276; YP_478353; YP_475372, ABD00213, ABD00270, YP_475476, YP_475533; AAC03784, AAB88292, XP_001700185, EDO98300, XP_001695168, EDP01876; AAC04854, AAB88296; CAB07802 (AlsS); AAU42663 (AlsS)

54: ketol-acid reductoisomerase (EC 1.1.1.86)	*Syntrophothermus lipocalidus DSM 12680*; *Caldicellulosiruptor saccharolyticus DSM 8903*; *E. coli*; *Thermotoga petrophila RKU-1*; *Calditerrivibrio nitroreducens DSM 19672*; *Spirochaeta thermophila DSM 6192*; *Pelotomaculum thermopropionicum SI*; *Cyanothece* sp. *PCC 7822*; *Hydrogenobacter thermophilus TK-6*; *Anoxybacillus flavithermus WK1*; *Caldicellulosiruptor bescii DSM 6725*; *Geobacillus kaustophilus HTA426*; *Deferribacter desulfuricans SSM1*; *Thermosynechococcus elongatus BP-1*; *Cyanothece* sp. *PCC 7425*; *Nostoc punctiforme PCC 73102*; *Trichodesmium erythraeum IMS101*; *Synechococcus* sp. *PCC 7335*; *Microcoleus chthonoplastes PCC 7420*; *Prochlorococcus marinus str. MIT 9301*; *Cyanobium* sp. *PCC 7001*; *Arthrospira* sp. *PCC 8005*; *Arabidopsis thaliana*; *Pisum sativum (pea)*; *Zea mays*; *Chlamydomonas reinhardtii*; *Polytomella parva*	ADI02902, YP_003703467; ABP66752, YP_001179943; AAA67577, YP_001460567; ABQ46398, YP_001243974; YP_004050904; YP_003874858, ADN02585; YP_001211079, BAF58710; YP_003885458; YP_003433279, BAI70078; YP_002314959, ACJ32974; YP_002572403; YP_148512, BAD76944; YP_003496877, BAI81121; NP_683044, BAC09806; YP_002482078; ACC82013; ABG53327; ZP_05036558; ZP_05026584; ABO18124; EDY39000; ZP_07166132; CAA48253, NP_001078309; CAA76854; ACG35752; XP_001702649, EDP06428; ABH11013
55: dihydroxy-acid dehydratase (EC 4.2.1.9)	*Thermotoga petrophila RKU-1*; *Cyanothece* sp. *PCC 7822*; *Marivirga tractuosa DSM 4126*; *Geobacillus kaustophilus HTA426*; *Syntrophothermus lipocalidus DSM 12680*; *Spirochaeta thermophila DSM 6192*; *Anoxybacillus flavithermus WK1*; *Caldicellulosiruptor bescii DSM 6725*; *Caldicellulosiruptor saccharolyticus DSM 8903*; *E. coli*; *Deferribacter desulfuricans SSM1*; *Thermosynechococcus elongatus BP-1*; *Hydrogenobacter thermophilus TK-6*; *Nostoc punctiforme PCC 73102*; "*Nostoc azollae*" *0708*; *Arthrospira maxima CS-328*; *Prochlorococcus marinus str. MIT 9301*; *Cyanobium* sp. *PCC 7001*; *Synechococcus* sp. *PCC 7335*; *Arthrospira platensis str. Paraca*; *Microcystis aeruginosa NIES-843*; *Chlamydomonas reinhardtii*; *Arabidopsis thaliana*; *Oryza sativa Indica Group*; *Glycine max*	YP_001243973, ABQ46397; YP_003887466; YP_004053736; YP_147899, BAD76331, YP_147822, BAD76254; ADI02905, YP_003703470; YP_003874669, ADN02396; YP_002315593; YP_002572562; YP_001179645, ABP66454; ADR29155, YP_001460564; YP_003496880, BAI81124; NP_681848, BAC08610; YP_003431766, BAI68565; ACC82168, ADN14191; ADI62939; EDZ97146; ABO17457; ZP_05044537, EDY37846; ZP_05037932; ZP_06383646; BAG02689; XP_001693179, EDP03205; BAB03011; ABR25557; ACU26534

(continued)

Table 1 (continued)

Enzyme/callout number	Source (organism)	GenBank accession number, JGI protein ID or citation
56: 2-methylbutyraldehyde reductase (EC 1.1.1.265)	*Schizosaccharomyces japonicus yFS275*; *Pichia pastoris GS115*; *Saccharomyces cerevisiae S288c*; *Aspergillus fumigatus Af293*; *Debaryomyces hansenii CBS767*; *Debaryomyces hansenii*; *Kluyveromyces lactis*; *Lachancea thermotolerans CBS 6340*; *Lachancea thermotolerans*; *Saccharomyces cerevisiae EC1118*; *Saccharomyces cerevisiae JAY291*	XP_002173231, EEB06938; XP_002490018, CAY67737, XM_002489973; DAA12209, NP_010656, NM_001180676; XP_752003; XP_002770138; CAR65507; CAH02579; XP_002554884; CAR24447, CAR23718; CAY78868; EEU08013
57: 3-methylbutanal reductase (EC 1.1.1.265)	*Saccharomyces cerevisiae S288c*; *Saccharomyces cerevisiae EC1118*; *Saccharomyces cerevisiae JAY291*	DAA10635, NM_001183405, NP_014490; CAY86141; EEU07090
07′: 3-ketothiolase (reversible)	*Geobacillus kaustophilus HTA426*; *Azohydromonas lata*; *Rhodoferax ferrireducens T118*; *Allochromatium vinosum*; *Dechloromonas aromatica RCB*; *Rhodobacter sphaeroides ATCC 17029*; *Rhodobacter sphaeroides ATCC 17025*; *Bacillus* sp. *256*; *Silicibacter lacuscaerulensis ITI-1157*; *Aspergillus fumigatus Af293*; *Rhizobium etli*; *Citreicella* sp. *SE45*; *Silicibacter* sp. *TrichCH4B*; *Azohydromonas lata*; *Chromobacterium violaceum*; *Dinoroseobacter shibae DFL 12*; *Alcaligenes* sp. *SH-69*; *Candida dubliniensis CD36*; *Pseudomonas* sp. *14-3*; *Aspergillus flavus NRRL3357*; *Aedes aegypti*; *Scheffersomyces stipitis CBS 6054*; *Cyanothece* sp. *PCC 7424*; *Cyanothece* sp. *PCC 7822*; *Microcystis aeruginosa NIES-843*	YP_147173, BAD75605; YP_523526; CAA01849, CAA01846; YP_286222; YP_001041914; YP_001166229; ABX11181; ZP_05785678; XP_752635; AAK21958; ZP_05784120, ZP_05781517; ZP_05742998; AAC83659, AAD10275; AAC69616; ABV95064; AAP41838; CAX43351, XP_002418052; CAK18903; XP_002375989; EAT37298, EAT37297, XP_001654752, XP_001654751; ABN68380, XP_001386409; YP_002375827, ACK68959; YP_003886602, ADN13327; BAG04828
08′: 3-hydroxyacyl-CoA dehydrogenase	*Syntrophothermus lipocalidus DSM 12680*; *Oceanithermus profundus DSM 14977*; *Anoxybacillus flavithermus WK1*; *Pelotomaculum thermopropionicum SI*; *Geobacillus kaustophilus HTA426*; *Deferribacter desulfuricans SSM1*; *Glomerella graminicola M1.001*; *Legionella pneumophila str. Corby*; *Aspergillus fumigatus Af293*; *Coprinopsis cinerea okayama7#130*; *Botryotinia fuckeliana B05.10*; *Coccidioides posadasii*; *E. coli*; *Chelativorans* sp. *BNC1*; *Nostoc punctiforme PCC 73102*; *Oscillatoria* sp. *PCC 6506*	YP_003702743, ADI02178, ADI01287, ADI01071; ADR36325; YP_002317076, YP_002315864; YP_001210823, BAF58454; YP_149248, YP_147889; YP_003497047, BAI81291; EFQ32520, EFQ35765; YP_001250712, ABQ55366; XP_748706, XP_748351; EAU80763; XP_001559519; ABH10642; YP_001462756; YP_675197; ACC81853, YP_001866796; ZP_07114022, CBN59220

09′: enoyl-CoA dehydratase	*Bordetella petrii*; *Bordetella petrii DSM 12804*; *Anoxybacillus flavithermus WK1*; *Geobacillus kaustophilus HTA426*; *Geobacillus kaustophilus*; *Syntrophothermus lipocalidus DSM 12680*; *Acinetobacter* sp. *SE19*; *Scheffersomyces stipitis CBS 6054*; *Laccaria bicolor S238N-H82*; *Alternaria alternate*; *Ajellomyces dermatitidis ER-3*; *Aspergillus fumigatus Af293*; *Cryptococcus neoformans var. neoformans JEC21*; *E. Coli*; *Aspergillus flavus NRRL3357*; *Laccaria bicolor S238N-H82*; *Neosartorya fischeri NRRL 181*; *Nostoc* sp. "*Peltigera membranacea cyanobiont*"	CAP41574; YP_001629844; YP_002315700, YP_002314932; YP_148541, YP_147845, BAD76199; BAD18341; ADI02939, ADI02740, ADI02007, ADI01364; AAG10018; ABN64617, XP_001382646; EDR09131, XP_001888157; BAH83503, EEQ91989; EAL93360, XP_755398; XP_572730; ADN73405, YP_001458194; XP_002377859; EDR01115; EAW18645; ADA69246
10′: 2-enoyl-CoA reductase	*Xanthomonas campestris pv. Campestris*; *Xanthomonas campestris pv. campestris str. B100*; *Xanthomonas campestris pv. musacearum NCPPB4381*; *Xanthomonas campestris pv. vasculorum NCPPB702*; *Aeromicrobium marinum DSM 15272*; *Rhodobacterales bacterium HTCC2083*; *Lysinibacillus fusiformis ZC1*; *Mycobacterium smegmatis str. MC2 155*; *Lysinibacillus sphaericus C3-41*; *Coprinopsis cinerea okayama7#130*; *Arthroderma gypseum CBS 118893*; *Paracoccidioides brasiliensis Pb01*; *Paracoccidioides brasiliensis Pb18*; *Ajellomyces capsulatus G186AR*; *Ostreococcus tauri*; *Jatropha curcas*	CAP53709; YP_001905744; ZP_06489037; ZP_06487845; ZP_07718056, EFQ82338; ZP_05074461, EDZ42121; ZP_07049092, EFI69525; YP_886510, ABK76225; YP_001699417, ACA41287; XP_002910885, EFI27391; EFR05506; XP_002796528, EEH39074; EEH43955; EEH03439; XP_003083795, CAL57762; ACS32302
11′: acyl-CoA reductase (EC 1.2.1.50)	*Clostridium cellulovorans 743B*; *Thermosphaera aggregans DSM 11486*; *Delftia acidovorans SPH-1*; *Comamonas testosteroni KF-1*; *Bifidobacterium longum* subsp. *infantis ATCC 15697*; *Clostridium papyrosolvens DSM 2782*; *Acidovorax avenae* subsp. *avenae ATCC 19860*; *Comamonas testosteroni KF-1*; *Aminomonas paucivorans DSM 12260*; *Herpetosiphon aurantiacus ATCC 23779*; *Clostridium beijerinckii NCIMB 8052*; *Geobacillus* sp. *G11MC16*; *Clostridium lentocellum DSM 5427*; *Leadbetterella byssophila DSM 17132*; *Actinosynnema mirum DSM 43827*; *Haliangium ochraceum DSM 14365*; *Photobacterium phosphoreum*; *Simmondsia chinensis*; *Hevea brasiliensis*; *Arabidopsis thaliana*	YP_003845606, ADL53842; YP_003649571, ADG90619; YP_001565543, ABX37158; ZP_03543536; YP_002321654, ACJ51276; ZP_05497968, EEU57047; ZP_06211782, EFA39209; EED67822; ZP_07740542, EFQ24431; ABX07240, YP_001547368; ABR34265, YP_001309221; ZP_03148237, EDY05596; ZP_06885967, EFG96716; YP_003997212, ADQ16859; YP_003101455, ACU37609; ACY16972, YP_003268865; AAT00788; AAD38039; AAR88762; ABE65991

(continued)

Table 1 (continued)

Enzyme/callout number	Source (organism)	GenBank accession number, JGI protein ID or citation
12′: hexanol dehydrogenase	*Mycobacterium chubuense NBB4*	ACZ56328
12″: octanol dehydrogenase (EC 1.1.1.73)	*Drosophila subobscura*	ABO61862, ABO65263, CAD43362, CAD43361, CAD54410, CAD43360, CAD43359, CAD43358, CAD43357, CAD43356
43′: short chain alcohol dehydrogenase	*Pyrococcus furiosus DSM 3638*; *Burkholderia vietnamiensis G4*; *Geobacillus thermoleovorans*; *Geobacillus kaustophilus HTA426*; *Anoxybacillus flavithermus WK1*; *Helicobacter pylori PeCan4*; *Mycobacterium chubuense NBB4*; *Mycobacterium avium* subsp. *avium ATCC 25291*; *Aspergillus oryzae*; *cyanobacterium UCYN-A*; *Anabaena circinalis AWQC131C*; *Cylindrospermopsis raciborskii T3*; *Helicobacter pylori Sat464*; *Helicobacter pylori Cuz20*; *Mycobacterium intracellulare ATCC 13950*; *Mycobacterium avium* subsp. *avium ATCC 25291*; *Gluconacetobacter hansenii ATCC 23769*; *Helicobacter pylori Shi470*; *Mycobacterium avium 104*; *Citrus sinensis*; *Gossypium hirsutum*; *Arabidopsis halleri*; *Paracoccidioides brasiliensis Pb01*; *Pyrenophora tritici-repentis Pt-1C-BFP*; *Ajellomyces capsulatus H143*; *Scheffersomyces stipitis CBS 6054*	AAC25556; ABO56626; BAA94092; YP_146837, BAD75269; YP_002314715, ACJ32730; YP_003927327, ADO07277; ACZ56328; ZP_05215778; BAE71320; YP_003421738, ADB95357; ABI75134; ABI75108; ADO05766; ADO04259; ZP_05228059, ZP_05228058; ZP_05215779; ZP_06834730, EFG83978; YP_001910563, ACD48533; YP_880627, ABK67217; ADH82118; ABD65462; ABZ02361, ABZ02360; XP_002792148, EEH34889; XP_001940779, EDU43498; EER38733; XP_001382930, ABN64901

when reference is made to an enzyme, such as, for example, any of the enzymes listed in Table 1, it includes their isozymes, functional analogs, and designer modified enzymes and combinations thereof. These enzymes can be selected for use in construction of the designer butanol-production pathways (such as those illustrated in Fig. 1). The "isozymes or functional analogs" refer to certain enzymes that have the same catalytic function but may or may not have exactly the same protein structures. The most essential feature of an enzyme is its active site that catalyzes the enzymatic reaction. Therefore, certain enzyme-protein fragment(s) or subunit(s) that contains such an active catalytic site may also be selected for use in this invention. For various reasons, some of the natural enzymes contain not only the essential catalytic structure but also other structure components that may or may not be desirable for a given application. With techniques of bioinformatics-assisted molecular designing, it is possible to select the essential catalytic structure(s) for use in construction of a designer DNA construct encoding a desirable designer enzyme. Therefore, in one of the various embodiments, a designer enzyme gene is created by artificial synthesis of a DNA construct according to bioinformatics-assisted molecular sequence design. With the computer-assisted synthetic biology approach, any DNA sequence (thus its protein structure) of a designer enzyme may be selectively modified to achieve more desirable results by design. Therefore, the terms "designer modified sequences" and "designer modified enzymes" are hereby defined as the DNA sequences and the enzyme proteins that are modified with bioinformatics-assisted molecular design. For example, when a DNA construct for a designer chloroplast-targeted enzyme is designed from the sequence of a mitochondrial enzyme, it is a preferred practice to modify some of the protein structures, for example, by selectively cutting out certain structure component(s) such as its mitochondrial transit-peptide sequence that is not suitable for the given application and/or by adding certain peptide structures such as an exogenous chloroplast transit-peptide sequence (e.g., a 135-bp Rubisco small-subunit transit peptide (RbcS2)) that is needed to confer the ability in the chloroplast-targeted insertion of the designer protein. Therefore, one of the various embodiments flexibly employs the enzymes, their isozymes, functional analogs, designer modified enzymes, and/or the combinations thereof in construction of the designer butanol-production pathway(s).

As shown in Table 1, many genes of the enzymes identified before have been cloned and/or sequenced from various organisms. Both genomic DNA and/or mRNA sequence data can be used in designing and synthesizing the designer DNA constructs for transformation of a host alga, oxyphotobacterium, plant, plant tissue or cells to create a designer organism for photobiological butanol production (Fig. 1). However, because of possible variations often associated with various source organisms and cellular compartments with respect to a specific host organism and its chloroplast/thylakoid environment where the butanol-production pathway(s) is designed to work with the Calvin cycle, certain molecular engineering art work in DNA construct design including codon-usage optimization and sequence modification is often necessary for a designer DNA construct (Fig. 2) to work well. For example, in creating a butanol-producing designer eukaryotic alga, if the source sequences are from cytosolic enzymes (sequences), a functional chloroplast-targeting sequence may be

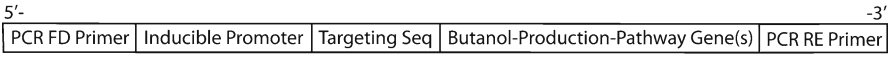

FIG. 2A

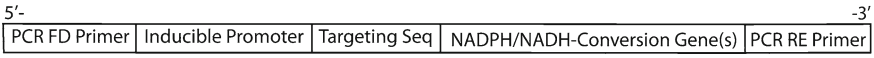

FIG. 2B

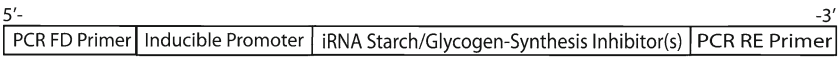

FIG. 2C

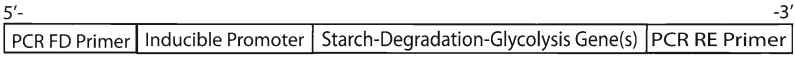

FIG. 2D

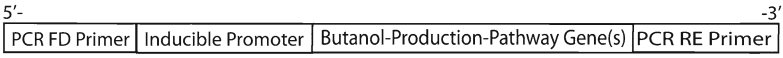

FIG. 2E

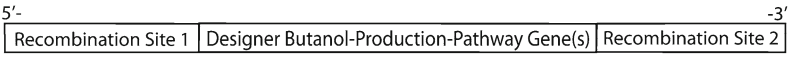

FIG. 2F

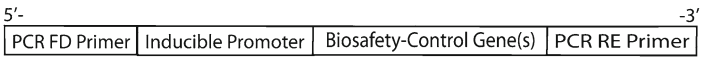

FIG. 2G

FIG. 2H

Fig. 2 (**a**) Presents a DNA construct for designer butanol-production-pathway gene(s). (**b**) Presents a DNA construct for NADPH/NADH-conversion designer gene for NADPH/NADH inter-conversion. (**c**) Presents a DNA construct for a designer iRNA starch/glycogen-synthesis inhibitor(s) gene. (**d**) Presents a DNA construct for a designer starch-degradation-glycolysis gene(s). (**e**) Presents a DNA construct of a designer butanol-production-pathway gene(s) for cytosolic expression. (**f**) Presents a DNA construct of a designer butanol-production-pathway gene(s) with two recombination sites for integrative genetic transformation in oxyphotobacteria. (**g**) Presents a DNA construct of a designer biosafety-control gene(s). (**h**) Presents a DNA construct of a designer proton-channel gene(s)

added to provide the capability for a designer unclear gene-encoded enzyme to insert into a host chloroplast to confer its function for a designer butanol-production pathway. Furthermore, to provide the switchability for a designer butanol-production pathway, it is also important to include a functional inducible promoter sequence such as the promoter of a hydrogenase (Hyd1) or nitrate reductase (Nia1) gene, or nitrite reductase (nirA) gene in certain designer DNA construct(s) as illustrated in Fig. 2a to control the expression of designer gene(s). In addition, as mentioned

before, certain functional derivatives or fragments of these enzymes (sequences), chloroplast-targeting transit peptide sequences, and inducible promoter sequences can also be selected for use in full, in part, or in combinations thereof to create the designer organisms according to various embodiments of this invention. The arts in creating and using the designer organisms are further described hereinbelow.

2.2.2 Targeting the Designer Enzymes to the Stroma Region of Chloroplasts

Some of the designer enzymes discussed earlier, such as pyruvate-ferredoxin oxidoreductase, thiolase, 3-hydroxybutyryl-CoA dehydrogenase, crotonase, butyryl-CoA dehydrogenase, butyraldehyde dehydrogenase, and butanol dehydrogenase, are known to function in certain special bacteria such as *Clostridium*; but wild-type plant chloroplasts generally do not possess these enzymes to function with the Calvin cycle. Therefore, in one of the various embodiments in creating a butanol-producing eukaryotic designer organism, designer nucleic acids encoding for these enzymes are expressed in the chloroplast(s) of a host cell. This can be accomplished by delivery of designer butanol-production-pathway gene(s) into the chloroplast genome of the eukaryotic host cell typically using a gene gun. In certain extent, the molecular genetics of chloroplasts are similar to that of cyanobacteria. After being delivered into the chloroplast, a designer DNA construct that contains a pair of proper recombination sites as illustrated in Fig. 2f can be incorporated into the chloroplast genome through a natural process of homologous DNA double recombination.

In another embodiment, nucleic acids encoding for these enzymes are genetically engineered such that the enzymes expressed are inserted into the chloroplasts to operate with the Calvin cycle there. Depending on the genetic background of a particular host organism, some of the designer enzymes discussed earlier such as phosphoglycerate mutase and enolase may exist at some background levels in its native form in a wild-type chloroplast. For various reasons including often the lack of their controllability, however, some of the chloroplast background enzymes may or may not be sufficient to serve as a significant part of the designer butanol-production pathway(s). Furthermore, a number of useful inducible promoters happen to function in the nuclear genome. For example, both the hydrogenase (Hyd1) promoter and the nitrate reductase (Nia1) promoter that can be used to control the expression of the designer butanol-production pathways are located in the nuclear genome of *C. reinhardtii*, of which the genome has recently been sequenced. Therefore, in one of the various embodiments, it is preferred to use nuclear-genome-encodable designer genes to confer a switchable butanol-production pathway. Consequently, nucleic acids encoding for these enzymes also need to be genetically engineered with proper sequence modification such that the enzymes are controllably expressed and are inserted into the chloroplasts to create a designer butanol-production pathway.

According to one of the various embodiments, it is best to express the designer butanol-producing-pathway enzymes only into chloroplasts (at the stroma region),

exactly where the action of the enzymes is needed to enable photosynthetic production of butanol. If expressed without a chloroplast-targeted insertion mechanism, the enzymes would just stay in the cytosol and not be able to directly interact with the Calvin cycle for butanol production. Therefore, in addition to the obvious distinctive features in pathway designs and associated approaches, another significant distinction is that one of the various embodiments innovatively employs a chloroplast-targeted mechanism for genetic insertion of many designer butanol-production-pathway enzymes into chloroplast to directly interact with the Calvin cycle for photobiological butanol production.

With a chloroplast stroma-targeted mechanism, the cells will not only be able to produce butanol but also to grow and regenerate themselves when they are returned to certain conditions under which the designer pathway is turned off, such as under aerobic conditions when designer hydrogenase promoter-controlled butanol-production-pathway genes are used. Designer algae, plants, or plant cells that contain normal mitochondria should be able to use the reducing power (NADH) from organic reserves (and/or some exogenous organic substrate such as acetate or sugar) to power the cells immediately after returning to aerobic conditions. Consequently, when the designer algae, plants, or plant cells are returned to aerobic conditions after use under anaerobic conditions for photosynthetic butanol production, the cells will stop making the butanol-producing-pathway enzymes and start to restore the normal photoautotrophic capability by synthesizing new and functional chloroplasts. Therefore, it is possible to use such genetically engineered designer alga/plant organisms for repeated cycles of photoautotrophic growth under normal aerobic conditions and efficient production of butanol directly from CO_2 and H_2O under certain specific designer butanol-producing conditions such as under anaerobic conditions and/or in the presence of nitrate when a Nia1 promoter-controlled butanol-production pathway is used.

The targeted insertion of designer butanol-production-pathway enzymes can be accomplished through use of a DNA sequence that encodes for a stroma "signal" peptide. A stroma-protein signal (transit) peptide directs the transport and insertion of a newly synthesized protein into stroma. In accordance with one of the various embodiments, a specific targeting DNA sequence is preferably placed in between the promoter and a designer butanol-production-pathway enzyme sequence, as shown in a designer DNA construct (Fig. 2a). This targeting sequence encodes for a signal (transit) peptide that is synthesized as part of the apoprotein of an enzyme in the cytosol. The transit peptide guides the insertion of an apoprotein of a designer butanol-production-pathway enzyme from cytosol into the chloroplast. After the apoprotein is inserted into the chloroplast, the transit peptide is cleaved off from the apoprotein, which then becomes an active enzyme.

A number of transit peptide sequences are suitable for use for the targeted insertion of the designer butanol-production-pathway enzymes into chloroplast, including but not limited to the transit peptide sequences of: the hydrogenase apoproteins (such as HydA1 (Hyd1) and HydA2, GenBank accession number AJ308413, AF289201, AY090770), ferredoxin apoprotein (Frx1, accession numbers L10349, P07839), thioredoxin m apoprotein (Trx2, X62335), glutamine synthase apoprotein

(Gs2, Q42689), LhcII apoproteins (AB051210, AB051208, AB051205), PSII-T apoprotein (PsbT), PSII-S apoprotein (PsbS), PSII-W apoprotein (PsbW), CF_0CF_1 subunit-γ apoprotein (AtpC), CF_0CF_1 subunit-δ apoprotein (AtpD, U41442), $CFoCF_1$ subunit-II apoprotein (AtpG), photosystem I (PSI) apoproteins (such as, of genes PsaD, PsaE, PsaF, PsaG, PsaH, and PsaK), Rubisco SSU apoproteins (such as RbcS2, X04472). Throughout this specification, when reference is made to a transit peptide sequence, such as, for example, any of the transit peptide sequence described earlier, it includes their functional analogs, modified designer sequences, and combinations thereof. A "functional analog" or "modified designer sequence" in this context refers to a peptide sequence derived or modified (by, e.g., conservative substitution, moderate deletion or addition of amino acids, or modification of side chains of amino acids) based on a native transit peptide sequence, such as those identified earlier, that has the same function as the native transit peptide sequence, i.e., effecting targeted insertion of a desired enzyme.

In certain specific embodiments, the following transit peptide sequences are used to guide the insertion of the designer butanol-production-pathway enzymes into the stroma region of the chloroplast: the Hyd1 transit peptide (having the amino acid sequence: msalvlkpca avsirgsscr arqvaprapl aastvrvala tleaparrlg nvacaa), the RbcS2 transit peptides (having the amino acid sequence: maaviakssv saavarpars svrpmaalkp avkaapvaap aqanq), ferredoxin transit peptide (having the amino acid sequence: mamamrs), the CF_0CF_1 subunit-δ transit peptide (having the amino acid sequence: mlaaksiagp rafkasavra apkagrrtvv vma), their analogs, functional derivatives, designer sequences, and combinations thereof.

2.2.3 Use of a Genetic Switch to Control the Expression of a Designer Butanol-Producing Pathway

Another key feature of the invention is the application of a genetic switch to control the expression of the designer butanol-producing pathway(s), as illustrated in Fig. 1. This switchability is accomplished through the use of an externally inducible promoter so that the designer transgenes are inducibly expressed under certain specific inducing conditions. Preferably, the promoter employed to control the expression of designer genes in a host is originated from the host itself or a closely related organism. The activities and inducibility of a promoter in a host cell can be tested by placing the promoter in front of a reporting gene, introducing this reporter construct into the host tissue or cells by any of the known DNA delivery techniques, and assessing the expression of the reporter gene.

In a preferred embodiment, the inducible promoter used to control the expression of designer genes is a promoter that is inducible by anaerobiosis, i.e., active under anaerobic conditions but inactive under aerobic conditions. A designer alga/plant organism can perform autotrophic photosynthesis using CO_2 as the carbon source under aerobic conditions, and when the designer organism culture is grown and ready for photosynthetic butanol production, anaerobic conditions will be applied to turn on the promoter and the designer genes that encode a designer butanol-production pathway(s).

A number of promoters that become active under anaerobic conditions are suitable for use in the present invention. For example, the promoters of the hydrogenase genes (HydA1 (Hyd1) and HydA2, GenBank accession number: AJ308413, AF289201, AY090770) of *C. reinhardtii*, which is active under anaerobic conditions but inactive under aerobic conditions, can be used as an effective genetic switch to control the expression of the designer genes in a host alga, such as *C. reinhardtii*. In fact, *Chlamydomonas* cells contain several nuclear genes that are coordinately induced under anaerobic conditions. These include the hydrogenase structural gene itself (Hyd1), the Cyc6 gene encoding the apoprotein of Cytochrome C_6, and the Cpxl gene encoding coprogen oxidase. The regulatory regions for the latter two have been well characterized, and a region of about 100 bp proves sufficient to confer regulation by anaerobiosis in synthetic gene constructs [7]. Although the above inducible algal promoters may be suitable for use in other plant hosts, especially in plants closely related to algae, the promoters of the homologous genes from these other plants, including higher plants, can be obtained and employed to control the expression of designer genes in those plants.

In another embodiment, the inducible promoter used in the present invention is an algal nitrate reductase (Nia1) promoter, which is inducible by growth in a medium containing nitrate and repressed in a nitrate-deficient but ammonium-containing medium [8]. Therefore, the Nia1 (gene accession number AF203033) promoter can be selected for use to control the expression of the designer genes in an alga according to the concentration levels of nitrate and ammonium in a culture medium. Additional inducible promoters that can also be selected for use in the present invention include, for example, the heat-shock protein promoter HSP70A [9] (accession number: DQ059999, AY456093, M98823), the promoter of CabII-1 gene (accession number M24072), the promoter of Ca1 gene (accession number P20507), and the promoter of Ca2 gene (accession number P24258).

In the case of blue-green algae (oxyphotobacteria including cyanobacteria and oxychlorobacteria), there are also a number of inducible promoters that can be selected for use in the present invention. For example, the promoters of the anaerobic-responsive bidirectional hydrogenase *hox* genes of *Nostoc* sp. PCC 7120 (GenBank: BA000019), *P. hollandica* (GenBank: U88400; *hoxUYH* operon promoter), *Synechocystis* sp. strain PCC 6803 (CyanoBase: sll1220 and sll1223), *S. elongatus* PCC 6301 (CyanoBase: syc1235_c), *A. platensis* (GenBank: ABC26906), *Cyanothece* sp. CCY0110 (GenBank: ZP_01727419), and *Synechococcus* sp. PCC 7002 (GenBank: AAN03566), which are active under anaerobic conditions but inactive under aerobic conditions [10], can be used as an effective genetic switch to control the expression of the designer genes in a host oxyphotobacterium, such as *Nostoc* sp. PCC 7120, *Synechocystis* sp. strain PCC 6803, *S. elongatus* PCC 6301, *Cyanothece* sp. CCY0110, *A. platensis*, or *Synechococcus* sp. PCC 7002.

In another embodiment in creating switchable butanol-production designer organisms such as switchable designer oxyphotobacteria, the inducible promoter selected for use is a nitrite reductase (*nirA*) promoter, which is inducible by growth in a medium containing nitrate and repressed in a nitrate deficient but ammonium-containing medium [11, 12]. Therefore, the *nirA* promoter sequences can be selected

for use to control the expression of the designer genes in a number of oxyphotobacteria according to the concentration levels of nitrate and ammonium in a culture medium. The *nirA* promoter sequences that can be selected and modified for use include (but not limited to) the *nirA* promoters of the following oxyphotobacteria: *S. elongatus* PCC 6301 (GenBank: AP008231, region 355890-255950), *Synechococcus* sp. (GenBank: X67680.1, D16303.1, D12723.1, and D00677), *Synechocystis* sp. PCC 6803 (GenBank: NP_442378, BA000022, AB001339, D63999-D64006, D90899-D90917), *Anabaena* sp. (GenBank: X99708.1), *Nostoc* sp. PCC 7120 (GenBank: BA000019.2 and AJ319648), *Plectonema boryanum* (GenBank: D31732.1), *S. elongatus* PCC 7942 (GenBank: P39661, CP000100.1), *T. elongatus* BP-1 (GenBank: BAC08901, NP_682139), *Phormidium laminosum* (GenBank: CAA79655, Q51879), *M. laminosus* (GenBank: ABD49353, ABD49351, ABD49349, ABD49347), *Anabaena variabilis* ATCC 29413 (GenBank: YP_325032), *P. marinus str*. MIT 9303 (GenBank: YP_001018981), *Synechococcus* sp. WH 8103 (GenBank: AAC17122), *Synechococcus* sp. WH 7805 (GenBank: ZP_01124915), and *Cyanothece* sp. CCY0110 (GenBank: ZP_01727861).

In yet another embodiment, an inducible promoter selected for use is the light- and heat-responsive chaperone gene *groE* promoter, which can be induced by heat and/or light [13]. A number of *groE* promoters such as the *groES* and *groEL* (chaperones) promoters are available for use as an inducible promoter in controlling the expression of the designer butanol-production-pathway enzymes. The *groE* promoter sequences that can be selected and modified for use in one of the various embodiments include (but not limited to) the *groES* and/or *groEL* promoters of the following oxyphotobacteria: *Synechocystis* sp. (GenBank: D12677.1), *Synechocystis* sp. PCC 6803 (GenBank: BA000022.2), *S. elongatus* PCC 6301 (GenBank: AP008231.1), *Synechococcus* sp. (GenBank: M58751.1), *S. elongatus* PCC 7942 (GenBank: CP000100.1), *Nostoc* sp. PCC 7120 (GenBank: BA000019.2), *A. variabilis* ATCC 29413 (GenBank: CP000117.1), *Anabaena* sp. L-31 (GenBank: AF324500); *T. elongatus* BP-1 (CyanoBase: tll0185, tll0186), *S. vulcanus* (GenBank: D78139), *Oscillatoria* sp. NKBG091600 (GenBank: AF054630), *P. marinus* MIT9313 (GenBank: BX572099), *P. marinus str*. MIT 9303 (GenBank: CP000554), *P. marinus str*. MIT 9211 (GenBank: ZP_01006613), *Synechococcus* sp. WH8102 (GenBank: BX569690), Synechococcus sp. CC9605 (GenBank: CP000110), *P. marinus* subsp. marinus str. CCMP1375 (GenBank: AE017126), and *P. marinus* MED4 (GenBank: BX548174).

Additional inducible promoters that can also be selected for use in the present invention include: for example, the metal (zinc)-inducible *smt* promoter of *Synechococcus* PCC 7942 [14]; the iron-responsive *idiA* promoter of *S. elongatus* PCC 7942 [15]; the redox-responsive cyanobacterial *crhR* promoter [16]; the heat-shock gene *hsp16.6* promoter of *Synechocystis* sp. PCC 6803 [17]; the small heat-shock protein (Hsp) promoter such as *S. vulcanus* gene *hspA* promoter [18]; the CO_2-responsive promoters of oxyphotobacterial carbonic-anhydrase genes (GenBank: EAZ90903, EAZ90685, ZP_01624337, EAW33650, ABB17341, AAT41924, CAO89711, ZP_00111671, YP_400464, AAC44830; and CyanoBase: all2929, PMT1568 slr0051, slr1347, and syc0167_c); the nitrate-reductase-gene

(*narB*) promoters (such as GenBank accession numbers: BAC08907, NP_682145, AAO25121; ABI46326, YP_732075, BAB72570, NP_484656); the green/red light-responsive promoters such as the light-regulated *cpcB2A2* promoter of *Fremyella diplosiphon* [19]; and the UV-light responsive promoters of cyanobacterial genes *lexA*, *recA,* and *ruvB* [20].

Furthermore, in one of the various embodiments, certain "semi-inducible" or constitutive promoters can also be selected for use in combination of an inducible promoter(s) for construction of a designer butanol-production pathway(s) as well. For example, the promoters of oxyphotobacterial Rubisco operon such as the *rbcL* genes (GenBank: X65960, ZP_01728542, Q3M674, BAF48766, NP_895035, 0907262A; CyanoBase: PMT1205, PMM0550, Pro0551, tll1506, SYNW1718, glr2156, alr1524, slr0009), which have certain light dependence but could be regarded almost as constitutive promoters, can also be selected for use in combination of an inducible promoter(s) such as the *nirA*, *hox*, and/or *groE* promoters for construction of the designer butanol-production pathway(s) as well.

Throughout this specification, when reference is made to inducible promoter, such as, for example, any of the inducible promoters described earlier, it includes their analogs, functional derivatives, designer sequences, and combinations thereof. A "functional analog" or "modified designer sequence" in this context refers to a promoter sequence derived or modified (by, e.g., substitution, moderate deletion or addition or modification of nucleotides) based on a native promoter sequence, such as those identified hereinabove, that retains the function of the native promoter sequence.

2.2.4 DNA Constructs and Transformation into Host Organisms

DNA constructs are generated in order to introduce designer butanol-production-pathway genes to a host alga, plant, plant tissue, or plant cells. That is, a nucleotide sequence encoding a designer butanol-production-pathway enzyme is placed in a vector, in an operable linkage to a promoter, preferably an inducible promoter, and in an operable linkage to a nucleotide sequence coding for an appropriate chloroplast-targeting transit-peptide sequence. In a preferred embodiment, nucleic acid constructs are made to have the elements placed in the following 5′ (upstream) to 3′ (downstream) orientation: an externally inducible promoter, a transit targeting sequence, and a nucleic acid encoding a designer butanol-production-pathway enzyme, and preferably an appropriate transcription termination sequence. One or more designer genes (DNA constructs) can be placed into one genetic vector. An example of such a construct is depicted in Fig. 2a. As shown in the embodiment illustrated in Fig. 2a, a designer butanol-production-pathway transgene is a nucleic acid construct comprising: (a) a PCR forward primer; (b) an externally inducible promoter; (c) a transit targeting sequence; (d) a designer butanol-production-pathway-enzyme-encoding sequence with an appropriate transcription termination sequence; and (e) a PCR reverse primer.

In accordance with various embodiments, any of the components (a)–(e) of this DNA construct are adjusted to suit for certain specific conditions. In practice, any of

the components (a)–(e) of this DNA construct are applied in full or in part, and/or in any adjusted combination to achieve more desirable results. For example, when an algal hydrogenase promoter is used as an inducible promoter in the designer butanol-production-pathway DNA construct, a transgenic designer alga that contains this DNA construct will be able to perform autotrophic photosynthesis using ambient air CO_2 as the carbon source and grows normally under aerobic conditions, such as in an open pond. When the algal culture is grown and ready for butanol production, the designer transgene(s) can then be expressed by induction under anaerobic conditions because of the use of the hydrogenase promoter. The expression of designer gene(s) produces a set of designer butanol-production-pathway enzymes to work with the Calvin cycle for photobiological butanol production (Fig. 1).

The two PCR primers are a PCR forward primer (PCR FD primer) located at the beginning (the 5′ end) of the DNA construct and a PCR reverse primer (PCR RE primer) located at the other end (the 3′ end) as shown in Fig. 2a. This pair of PCR primers is designed to provide certain convenience when needed for relatively easy PCR amplification of the designer DNA construct, which is helpful not only during and after the designer DNA construct is synthesized in preparation for gene transformation, but also after the designer DNA construct is delivered into the genome of a host alga for verification of the designer gene in the transformants. For example, after the transformation of the designer gene is accomplished in a *C. reinhardtii*-arg7 host cell using the techniques of electroporation and argininosuccinate lyase (*arg7*) complementation screening, the resulted transformants can be then analyzed by a PCR DNA assay of their nuclear DNA using this pair of PCR primers to verify whether the entire designer butanol-production-pathway gene (the DNA construct) is successfully incorporated into the genome of a given transformant. When the nuclear DNA PCR assay of a transformant can generate a PCR product that matches with the predicted DNA size and sequence according to the designer DNA construct, the successful incorporation of the designer gene(s) into the genome of the transformant is verified.

Therefore, the various embodiments also teach the associated method to effectively create the designer transgenic algae, plants, or plant cells for photobiological butanol production. This method, in one of embodiments, includes the following steps: (a) selecting an appropriate host alga, plant, plant tissue, or plant cells with respect to their genetic backgrounds and special features in relation to butanol production; (b) introducing the nucleic acid constructs of the designer genes into the genome of said host alga, plant, plant tissue, or plant cells; (c) verifying the incorporation of the designer genes in the transformed alga, plant, plant tissue, or plant cells with DNA PCR assays using the said PCR primers of the designer DNA construct; (d) measuring and verifying the designer organism features such as the inducible expression of the designer butanol-pathway genes for photosynthetic butanol production from carbon dioxide and water by assays of mRNA, protein, and butanol-production characteristics according to the specific designer features of the DNA construct(s) (Fig. 2a).

The above embodiment of the method for creating the designer transgenic organism for photobiological butanol production can also be repeatedly applied for a plurality of operational cycles to achieve more desirable results. In various embodiments, any of the steps (a)–(d) of this method described earlier are adjusted

to suit for certain specific conditions. In various embodiments, any of the steps (a)–(d) of the method are applied in full or in part, and/or in any adjusted combination. Many examples of designer butanol-production-pathway genes (DNA constructs) are shown in the sequence listings: SEQ ID NOS:1–57 of the PCT Patent Application Publication No. WO 09105733 and SEQ ID NOS:1–165 of the US Patent Application Publication No. 2011/0177571 A1.

The nucleic acid constructs, such as those presented in the examples earlier, may include additional appropriate sequences, for example, a selection marker gene, and an optional biomolecular tag sequence (such as the Lumio tag). Selectable markers that can be selected for use in the constructs include markers conferring resistances to kanamycin, hygromycin, spectinomycin, streptomycin, sulfonyl urea, gentamycin, chloramphenicol, among others, all of which have been cloned and are available to those skilled in the art. Alternatively, the selective marker is a nutrition marker gene that can complement a deficiency in the host organism. For example, the gene encoding argininosuccinate lyase (arg7) can be used as a selection marker gene in the designer construct, which permits identification of transformants when *C. reinhardtii* arg7- (minus) cells are used as host cells.

Nucleic acid constructs carrying designer genes can be delivered into a host alga, blue-green alga, plant, or plant tissue or cells using the available genetic transformation techniques, such as electroporation, PEG-induced uptake, and ballistic delivery of DNA, and Agrobacterium-mediated transformation. For the purpose of delivering a designer construct into algal cells, the techniques of electroporation, glass bead, and biolistic gene gun can be selected for use as preferred methods, and an alga with single cells or simple thallus structure is preferred for use in transformation. Transformants can be identified and tested based on routine techniques.

2.3 Additional Host Modifications to Enhance Photosynthetic Butanol Production

2.3.1 An NADPH/NADH Conversion Mechanism

According to the photosynthetic butanol production pathway(s), to produce one molecule of butanol from $4CO_2$ and $5H_2O$ is likely to require 14 ATP and 12 NADPH, both of which are generated by photosynthetic water splitting and photophosphorylation across the thylakoid membrane. In order for the 3-phosphoglycerate-branched butanol-production pathway (**03**-**12** in Fig. 1) to operate, it is a preferred practice to use a butanol-production-pathway enzyme(s) that can use NADPH that is generated by the photo-driven electron transport process. *Clostridium saccharoperbutylacetonicum* butanol dehydrogenase (GenBank accession number: AB257439) and butyraldehyde dehydrogenase (GenBank: AY251646) are examples of a butanol-production-pathway enzyme that is capable of accepting either NADP(H) or NAD(H). Such a butanol-production-pathway enzyme that can use both NADPH and NADH (i.e., NAD(P)H) can also be selected for use in this

3-phosphoglycerate branched and any of the other designer butanol-production pathway(s) (Fig. 1) as well. *C. beijerinckii* Butyryl-CoA dehydrogenase (GenBank: AF494018) and 3-hydroxybutyryl-CoA dehydrogenase (GenBank: AF494018) are examples of a butanol-production-pathway enzyme that can accept only NAD(H). When a butanol-production-pathway enzyme that can only use NADH is employed, it may require an NADPH/NADH conversion mechanism in order for this 3-phosphoglycerate-branched butanol-production pathway to operate well. However, depending on the genetic backgrounds of a host organism, a conversion mechanism between NADPH and NADH may exist in the host so that NADPH and NADH may be interchangeably used in the organism. In addition, it is known that NADPH could be converted into NADH by a NADPH-phosphatase activity [21] and that NAD can be converted to NADP by a NAD kinase activity [22, 23]. Therefore, when enhanced NADPH/NADH conversion is desirable, the host may be genetically modified to enhance the NADPH phosphatase and NAD kinase activities. Thus, in one of the various embodiments, the photosynthetic butanol-producing designer plant, designer alga, or plant cell further contains additional designer transgenes (Fig. 2b) to inducibly express one or more enzymes to facilitate the NADPH/NADH interconversion, such as the NADPH phosphatase and NAD kinase (GenBank: XM_001609395, XM_001324239), in the stroma region of the algal chloroplast.

Another embodiment that can provide an NADPH/NADH conversion mechanism is by properly selecting an appropriate branching point at the Calvin cycle for a designer butanol-production pathway to branch from. To confer this NADPH/NADH conversion mechanism by pathway design according to this embodiment, it is a preferred practice to branch a designer butanol-production pathway at or after the point of glyceraldehyde-3-phosphate of the Calvin cycle as shown in Fig. 1. In these pathway designs, the NADPH/NADH conversion is achieved essentially by a two-step mechanism: (1) use of the step with the Calvin cycle's glyceraldehyde-3-phosphate dehydrogenase, which uses NADPH in reducing 1,3-diphosphoglycerate to glyceraldehyde-3-phosphate; and (2) use of the step with the designer pathway's NAD^+-dependent glyceraldehyde-3-phosphate dehydrogenase **01**, which produces NADH in oxidizing glyceraldehyde-3-phosphate to 1,3-diphosphoglycerate. The net result of the two steps described earlier is the conversion of NADPH to NADH, which can supply the needed reducing power in the form of NADH for the designer butanol-production pathway(s). For step (1), use of the Calvin cycle's NADPH-dependent glyceraldehyde-3-phosphate dehydrogenase naturally in the host organism is usually sufficient. Consequently, introduction of a designer NAD^+-dependent glyceraldehyde-3-phosphate dehydrogenase **01** to work with the Calvin cycle's NADPH-dependent glyceraldehyde-3-phosphate dehydrogenase may confer the function of an NADPH/NADH conversion mechanism, which is needed for the 3-phosphoglycerate-branched butanol-production pathway (**03**-**12** in Fig. 1) to operate well. For this reason, the designer NAD^+-dependent glyceraldehyde-3-phosphate-dehydrogenase DNA construct (example 12, SEQ ID NO:12) is used also as an NADPH/NADH-conversion designer gene (Fig. 2b) to support the 3-phosphoglycerate-branched butanol-production pathway (**03**-**12** in Fig. 1) in one of the various embodiments. This also explains why it is important to use a NAD^+-dependent

glyceraldehyde-3-phosphate dehydrogenase **01** to confer this two-step NADPH/NADH conversion mechanism for the designer butanol-production pathway(s). Therefore, in one of the various embodiments, it is also a preferred practice to use a NAD^+-dependent glyceraldehyde-3-phosphate dehydrogenase, its isozymes, functional derivatives, analogs, designer modified enzymes, and/or combinations thereof in the designer butanol-production pathway(s) as illustrated in Fig. 1.

2.3.2 iRNA Techniques to Further Tame Photosynthesis Regulation Mechanism

In another embodiment of the present invention, the host plant or cell is further modified to tame the Calvin cycle so that the host can directly produce liquid fuel butanol instead of synthesizing starch (glycogen in the case of oxyphotobacteria), celluloses, and lignocelluloses that are often inefficient and hard for the biorefinery industry to use. According to the one of the various embodiments, inactivation of starch-synthesis activity is achieved by suppressing the expression of any of the key enzymes, such as starch synthase (glycogen synthase in the case of oxyphotobacteria) **13**, glucose-1-phosphate (G-1-P) adenylyltransferase **14**, phosphoglucomutase **15**, and hexose-phosphate-isomerase **16** of the starch-synthesis pathway which connects with the Calvin cycle (Fig. 1).

Introduction of a genetically transmittable factor that can inhibit the starch-synthesis activity that is in competition with designer butanol-production pathway(s) for the Calvin cycle products can further enhance photosynthetic butanol production. In a specific embodiment, a genetically encoded-able inhibitor (Fig. 2c) to the competitive starch-synthesis pathway is an interfering RNA (iRNA) molecule that specifically inhibits the synthesis of a starch-synthesis-pathway enzyme, for example, starch synthase **16**, glucose-1-phosphate (G-1-P) adenylyltransferase **15**, phosphoglucomutase **14**, and/or hexose-phosphate-isomerase **13** as shown with numerical labels **13**-**16** in Fig. 1. The DNA sequences encoding starch synthase iRNA, glucose-1-phosphate (G-1-P) adenylyltransferase iRNA, a phosphoglucomutase iRNA, and/or a G-P-isomerase iRNA, respectively, can be designed and synthesized based on RNA interference techniques known to those skilled in the art [24]. Generally speaking, an interfering RNA (iRNA) molecule is antisense but complementary to a normal mRNA of a particular protein (gene) so that such iRNA molecule can specifically bind with the normal mRNA of the particular gene, thus inhibiting (blocking) the translation of the gene-specific mRNA to protein [25, 26]. Examples of a designer starch-synthesis iRNA DNA construct (Fig. 2c) are shown in SEQ ID NO: 27 and 28 listed in the PCT Patent Application Publication No. WO 09105733.

2.3.3 Designer Starch Degradation and Glycolysis Genes

In yet another embodiment of the present invention, the photobiological butanol production is enhanced by incorporating an additional set of designer genes (Fig. 2d) that can facilitate starch/glycogen degradation and glycolysis in combination with

the designer butanol-production gene(s) (Fig. 2a). Such additional designer genes for starch degradation include, for example, genes coding for **17**: amylase, starch phosphorylase, hexokinase, phosphoglucomutase and for **18**: glucose-phosphate-isomerase (G-P-isomerase) as illustrated in Fig. 1. The designer glycolysis genes encode chloroplast-targeted glycolysis enzymes: glucosephosphate isomerase **18**, phosphofructose kinase **19**, aldolase **20**, triose phosphate isomerase **21**, glyceraldehyde-3-phosphate dehydrogenase **22**, phosphoglycerate kinase **23**, phosphoglycerate mutase **24**, enolase **25**, and pyruvate kinase **26**. The designer starch degradation and glycolysis genes in combination with any of the butanol-production pathways shown in Fig. 1 can form additional pathway(s) from starch/glycogen to butanol (**17**-**33**). Consequently, co-expression of the designer starch degradation and glycolysis genes with the butanol-production-pathway genes can enhance photobiological production of butanol as well. Therefore, this embodiment represents another approach to tame the Calvin cycle for enhanced photobiological production of butanol. In this case, some of the Calvin cycle products flow through the starch synthesis pathway (**13**-**16**) followed by the starch/glycogen-to-butanol pathway (**17**-**33**) as shown in Fig. 1. In this case, starch/glycogen acts as a transient storage pool of the Calvin cycle products before they can be converted to butanol. This mechanism can be quite useful in maximizing the butanol-production yield in certain cases. For example, at high sunlight intensity such as around noon, the rate of Calvin cycle photosynthetic CO_2 fixation can be so high that may exceed the maximal rate capacity of a butanol-production pathway(s); use of the starch-synthesis mechanism allows temporary storage of the excess photosynthetic products to be used later for butanol production as well.

Figure 1 also illustrates the use of a designer starch/glycogen-to-butanol pathway with designer enzymes (as labeled from **17** to **33**) in combination with a Calvin-cycle-branched designer butanol-production pathway(s) such as the glyceraldehyde-3-phosphate-branched butanol-production pathway **01**-**12** for enhanced photobiological butanol production. Similar to the benefits of using the Calvin-cycle-branched designer butanol-production pathways, the use of the designer starch/glycogen-to-butanol pathway (**17**-**33**) can also help to convert the photosynthetic products to butanol before the sugars could be converted into other complicated biomolecules such as lignocellulosic biomasses which cannot be readily used by the biorefinery industries. Therefore, appropriate use of the Calvin-cycle-branched designer butanol-production pathway(s) (such as **01**-**12**, **03**-**12**, and/or **20**-**33**) and/or the designer starch/glycogen-to-butanol pathway (**17**-**33**) may represent revolutionary *inter alia* technologies that can effectively bypass the bottleneck problems of the current biomass technology including the "lignocellulosic recalcitrance" problem.

Another feature is that a Calvin-cycle-branched designer butanol-production pathway activity (such as **01**-**12**, **03**-**12**, and/or **20**-**33**) can occur predominantly during the days when there is light because it uses an intermediate product of the Calvin cycle which requires supplies of reducing power (NADPH) and energy (ATP) generated by the photosynthetic water splitting and the light-driven proton-translocation-coupled electron transport process through the thylakoid membrane system. The designer starch/glycogen-to-butanol pathway (**17**-**33**) which can use the surplus sugar that has been stored as starch/glycogen during photosynthesis can operate not

only during the days, but also at nights. Consequently, the use of a Calvin-cycle-branched designer butanol-production pathway (such as **01**-**12**, **03**-**12**, and/or **20**-**33**) together with a designer starch/glycogen-to-butanol pathway(s) (**17**-**33**) as illustrated in Fig. 1 enables production of butanol both during the days and at nights.

Because the expression for both the designer starch/glycogen-to-butanol pathway(s) and the Calvin-cycle-branched designer butanol-production pathway(s) is controlled by the use of an inducible promoter such as an anaerobic hydrogenase promoter, this type of designer organisms is also able to grow photoautotrophically under aerobic (normal) conditions. When the designer photosynthetic organisms are grown and ready for photobiological butanol production, the cells are then placed under the specific inducing conditions such as under anaerobic conditions (or an ammonium-to-nitrate fertilizer use shift, if designer Nia1/nirA promoter-controlled butanol-production pathway(s) is used) for enhanced butanol production, as shown in Figs. 1 and 3. Examples of designer starch (glycogen)-degradation genes are shown in SEQ ID NO: 29–33 listed in the PCT Patent Application Publication No. WO 09105733.

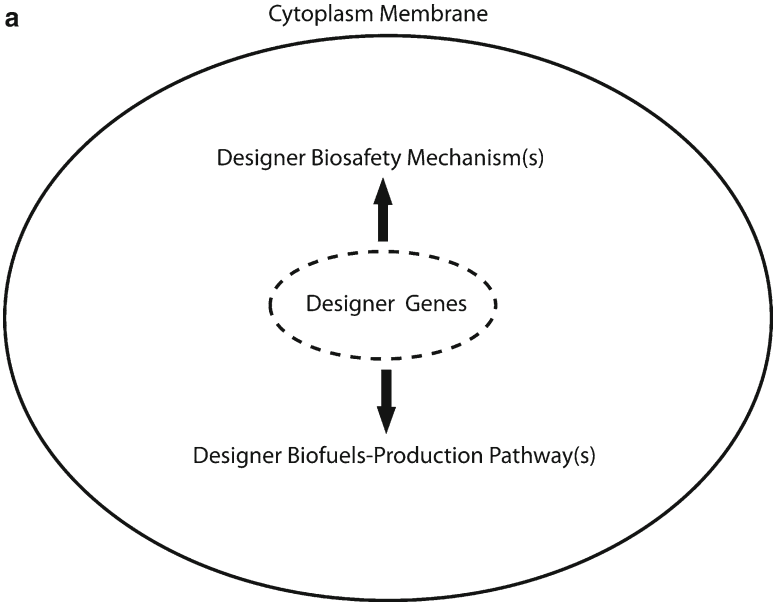

Fig. 3 (**a**) Illustrates a cell-division-controllable designer organism that contains two key functions: designer biosafety mechanism(s) and designer biofuel-production pathway(s). (**b**) Illustrates a cell-division-controllable designer organism for photobiological production of butanol ($CH_3CH_2CH_2CH_2OH$) from carbon dioxide (CO_2) and water (H_2O) with designer biosafety mechanism(s). (**c**) Illustrates a cell-division-controllable designer organism for biosafety-guarded photobiological production of other biofuels such as ethanol (CH_3CH_2OH) from carbon dioxide (CO_2) and water (H_2O)

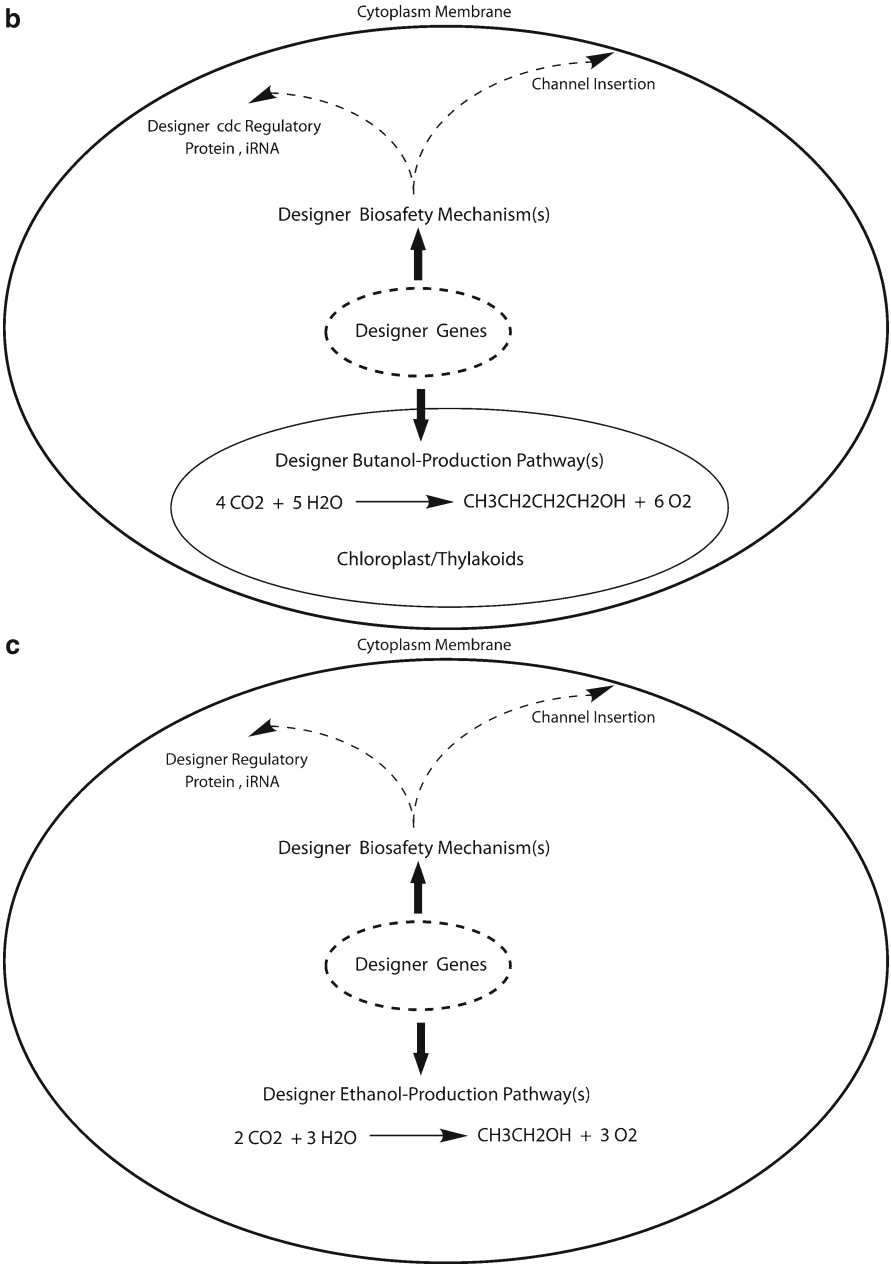

Fig. 3 (continued)

2.3.4 Distribution of Designer Butanol-Production Pathways Between Chloroplast and Cytoplasm

In yet another embodiment of the present invention, photobiological butanol productivity is enhanced by a selected distribution of the designer butanol-production pathway(s) between chloroplast and cytoplasm in a eukaryotic plant cell. That is, not all the designer butanol-production pathway(s) (Fig. 1) have to operate in the chloroplast; when needed, part of the designer butanol-production pathway(s) can operate in cytoplasm as well. For example, in one of the various embodiments, a significant part of the designer starch-to-butanol pathway activity from dihydroxyacetone phosphate to butanol (**21**-**33**) is designed to occur at the cytoplasm while the steps from starch to dihydroxyacetone phosphate (**17**-**20**) are in the chloroplast. In this example, the linkage between the chloroplast and cytoplasm parts of the designer pathway is accomplished by use of the triose phosphate-phosphate translocator, which facilitates translocation of dihydroxyacetone across the chloroplast membrane. By use of the triose phosphate-phosphate translocator, it also enables the glyceraldehyde-3-phospahte-branched designer butanol-production pathway to operate not only in chloroplast, but also in cytoplasm as well. The cytoplasm part of the designer butanol-production pathway can be constructed by use of designer butanol-production pathway genes (DNA constructs of Fig. 2a) with their chloroplast-targeting sequence omitted as shown in Fig. 2e.

2.3.5 Designer Oxyphotobacteria with Designer Butanol-Production Pathways in Cytoplasm

In prokaryotic photosynthetic organisms such as blue-green algae (oxyphotobacteria including cyanobacteria and oxychlorobacteria), which typically contain photosynthetic thylakoid membrane but no chloroplast structure, the Calvin cycle is located in the cytoplasm. In this special case, the entire designer butanol-production pathway(s) (Fig. 1) including (but not limited to) the glyceraldehyde-3-phosphate-branched butanol-production pathway (**01**-**12**), the 3-phosphpglycerate-branched butanol-production pathway (**03**-**12**), the fructose-1,6-diphosphate-branched pathway (**20**-**33**), the fructose-6-phosphate-branched pathway (**19**-**33**), and the starch (or glycogen)-to-butanol pathways (**17**-**33**) are adjusted in design to operate with the Calvin cycle in the cytoplasm of a blue-green alga. The construction of the cytoplasm designer butanol-production pathways can be accomplished by use of designer butanol-production pathway genes (DNA construct of Fig. 2a) with their chloroplast-targeting sequence all omitted. When the chloroplast-targeting sequence is omitted in the designer DNA construct(s) as illustrated in Fig. 2e, the designer gene(s) is transcribed and translated into designer enzymes in the cytoplasm whereby conferring the designer butanol-production pathway(s). The designer gene(s) can be incorporated into the chromosomal and/or plasmid DNA in host blue-green algae (oxyphotobacteria including cyanobacteria and oxychlorobacteria) by using the techniques of genetic transformation known to those skilled in the art. It is a preferred

practice to integrate the designer genes through an integrative transformation into the chromosomal DNA that can usually provide better genetic stability for the designer genes. In oxyphotobacteria such as cyanobacteria, integrative transformation can be achieved through a process of homologous DNA double recombination into the host's chromosomal DNA using a designer DNA construct as illustrated in Fig. 2f, which typically, from the 5′ upstream to the 3′ downstream, consists of: recombination site 1, a designer butanol-production-pathway gene(s), and recombination site 2. This type of DNA constructs (Fig. 2f) can be delivered into oxyphotobacteria (blue-green algae) with a number of available genetic transformation techniques including electroporation, natural transformation, and/or conjugation. The transgenic designer organisms created from blue-green algae are also called designer blue-green algae (designer oxyphotobacteria including designer cyanobacteria and designer oxychlorobacteria). Examples of designer oxyphotobacterial butanol-production-pathway genes are shown in SEQ ID NO: 34–45 listed in PCT Patent Application Publication No. WO 09105733. Recently, certain independent studies [27, 28] have also applied synthetic biology in certain model cyanobacteria such as *S. elongatus* PCC7942 for photobiological production of isobutanol and 1-butanol. According to another independent study [29] for this type of direct photosynthesis-to-biofuel process, the practical maximum solar-to-biofuel energy-conversion efficiency could be about 7.2% while the theoretical maximum solar-to-biofuel energy-conversion efficiency is calculated to be 12%.

2.4 Further Host Modifications to Help Ensure Biosafety

The present invention also provides biosafety-guarded photosynthetic biofuel (e.g., butanol and/or related higher alcohols) production methods based on cell-division-controllable designer transgenic plants (such as algae and oxyphotobacteria) or plant cells. For example, the cell-division-controllable designer photosynthetic organisms (Fig. 3) are created through the use of a designer biosafety-control gene(s) (Fig. 2g) in conjunction with the designer butanol-production-pathway gene(s) (Fig. 2a–f) such that their cell division and mating function can be controllably stopped to provide better biosafety features.

In one of the various embodiments, a fundamental feature is that a designer cell-division-controllable photosynthetic organism (such as an alga, plant cell, or oxyphotobacterium) contains two key functions (Fig. 3a): a designer biosafety mechanism(s) and a designer biofuel-production pathway(s). As shown in Fig. 3b, the designer biosafety feature(s) is conferred by a number of mechanisms including: (1) the inducible insertion of designer proton channels into cytoplasm membrane to permanently disable any cell division and mating capability, (2) the selective application of designer cell-division-cycle regulatory protein or interference RNA (iRNA) to permanently inhibit the cell division cycle and preferably keep the cell at the G_1 phase or G_0 state, and (3) the innovative use of a high-CO_2-requiring host photosynthetic organism for expression of the designer biofuel-production pathway(s).

Examples of the designer biofuel-production pathway(s) in a designer cell-division-controllable photosynthetic organism include the previously described designer butanol-production pathway(s), which work with the Calvin cycle to synthesize biofuel such as butanol directly from carbon dioxide (CO_2) and water (H_2O). The designer cell-division-control technology can help ensure biosafety in using the designer organisms for photosynthetic biofuel production. Accordingly, this embodiment provides, *inter alia*, biosafety-guarded methods for producing biofuel (e.g., butanol and/or related higher alcohols) based on a cell-division-controllable designer biofuel-producing alga, cyanobacterium, oxychlorobacterium, plant, or plant cells.

In one of the various embodiments, a cell-division-controllable designer butanol-producing eukaryotic alga or plant cell is created by introducing a designer proton-channel gene (Fig. 2h) into a host alga or plant cell (Fig. 3b). The expression of the designer proton-channel gene (Fig. 2h) is controlled by an inducible promoter such as the nitrate reductase (Nia1) promoter, which can also be used to control the expression of a designer biofuel-production-pathway gene(s). Therefore, before the expression of the designer gene(s) is induced, the designer organism can grow photoautotrophically using CO_2 as the carbon source and H_2O as the source of electrons just like wild-type organism. When the designer organism culture is grown and ready for photobiological production of biofuels, the cell culture is then placed under a specific inducing condition (such as by adding nitrate into the culture medium if the nitrate reductase (Nia1) promoter is used as an inducible promoter) to induce the expression of both the designer proton-channel gene and the designer biofuel-production-pathway gene(s). The expression of the proton-channel gene is designed to occur through its transcription in the nucleus and its translation in the cytosol. Because of the specific molecular design, the expressed proton channels are automatically inserted into the cytoplasm membrane, but leave the photosynthetic thylakoid membrane intact. The insertion of the designer proton channels into cytoplasm membrane collapses the proton gradient across the cytoplasm membrane so that the cell division and mating function are permanently disabled. However, the photosynthetic thylakoid membrane inside the chloroplast is kept intact (functional) so that the designer biofuel-production-pathway enzymes expressed into the stroma region can work with the Calvin cycle for photobiological production of biofuels from CO_2 and H_2O. That is, when both the designer proton-channel gene and the designer biofuel-production-pathway gene(s) are turned on, the designer organism becomes a nonreproducible cell for dedicated photosynthetic production of biofuels. Because the cell division and mating function are permanently disabled (killed) at this stage, the designer-organism culture is no longer a living matter except its catalytic function for photochemical conversion of CO_2 and H_2O into a biofuel. It will no longer be able to mate or exchange any genetic materials with any other cells, even if it somehow comes in contact with a wild-type cell as it would be the case of an accidental release into the environments.

According to one of the various embodiments, the nitrate reductase (Nia1) promoter or nitrite reductase (nirA) promoter is a preferred inducible promoter for use to control the expression of the designer genes. In the presence of ammonium (but not nitrate) in culture medium, for example, a designer organism with

Nia1-promoter-controlled designer proton-channel gene and biofuel-production-pathway gene(s) can grow photoauotrophically using CO_2 as the carbon source and H_2O as the source of electrons just like a wild-type organism. When the designer organism culture is grown and ready for photobiological production of biofuels, the expression of both the designer proton-channel gene and the designer biofuel-production-pathway gene(s) can then be induced by adding some nitrate fertilizer into the culture medium. Nitrate is widely present in soils and nearly all surface water on Earth. Therefore, even if a Nia1-promoter-controlled designer organism is accidentally released into the natural environment, it will soon die since the nitrate in the environment will trig the expression of a Nia1-promoter-controlled designer proton-channel gene which inserts proton channels into the cytoplasm membrane thereby killing the cell. That is, a designer photosynthetic organism with Nia1-promoter-controlled proton-channel gene is programmed to die as soon as it sees nitrate in the environment. This characteristic of cell-division-controllable designer organisms with Nia1-promoter-controlled proton-channel gene provides an added biosafety feature.

The art in constructing proton-channel gene (Fig. 2h) with a thylakoid-membrane-targeting sequence has recently been disclosed [30]. In the present invention of creating a cell-division-controllable designer organism, the thylakoid-membrane-targeting sequence must be omitted in the proton-channel gene design. For example, the essential components of a Nia1-promoter-controlled designer proton-channel gene can simply be a Nial promoter linked with a proton-channel-encoding sequence (without any thylakoid-membrane-targeting sequence) so that the proton channel will insert into the cytoplasm membrane but not into the photosynthetic thylakoid membrane.

According to one of the various embodiments, it is a preferred practice to use the same inducible promoter such as the Nial promoter to control the expression of both the designer proton-channel gene and the designer biofuel-production pathway genes. In this way, the designer biofuel-production pathway(s) can be inducibly expressed simultaneously with the expression of the designer proton-channel gene that terminates certain cellular functions including cell division and mating.

In one of the various embodiments, an inducible promoter that can be used in this designer biosafety embodiment is selected from the group consisting of the hydrogenase promoters (HydA1 (Hyd1) and HydA2, accession number: AJ308413, AF289201, AY090770), the Cyc6 gene promoter, the Cpxl gene promoter, the heat-shock protein promoter HSP70A, the CabII-1 gene (accession number M24072) promoter, the Ca1 gene (accession number P20507) promoter, the Ca2 gene (accession number P24258) promoter, the nitrate reductase (Nia1) promoter, the nitrite-reductase-gene (*nirA*) promoters, the bidirectional-hydrogenase-gene *hox* promoters, the light- and heat-responsive *groE* promoters, the Rubisco-operon *rbcL* promoters, the metal (zinc)-inducible *smt* promoter, the iron-responsive *idiA* promoter, the redox-responsive *crhR* promoter, the heat-shock-gene *hsp16.6* promoter, the small heat-shock protein (Hsp) promoter, the CO_2-responsive carbonic-anhydrase-gene promoters, the green/red light responsive *cpcB2A2* promoter, the UV-light responsive *lexA*, *recA,* and *ruvB* promoters, the nitrate-reductase-gene (*narB*) promoters, and combinations thereof.

In another embodiment, a cell-division-controllable designer photosynthetic organism is created by use of a carbonic anhydrase deficient mutant or a high-CO_2-requiring mutant as a host organism to create the designer biofuel-production organism. High-CO_2-requiring mutants that can be selected for use in this invention include (but not limited to): *C. reinhardtii* carbonic-anhydrase-deficient mutant-2-1C (CC-1219 cal mt-), *C. reinhardtii cia3* mutant [31], the high-CO_2-requiring mutant M3 of *Synechococcus* sp. Strain PCC 7942, or the carboxysome-deficient cells of *Synechocystis* sp. PCC 6803 [32] that lacks the CO_2-concentrating mechanism can grow photoautotrophically only under elevated CO_2 concentration level such as 0.2–3% CO_2.

Under atmospheric CO_2 concentration level (380 ppm), the carbonic anhydrase deficient or high-CO_2-requiring mutants commonly cannot survive. Therefore, the key concept here is that a high-CO_2-requiring designer biofuel-production organism that lacks the CO_2 concentrating mechanism will be grown and used for photobiological production of biofuels always under an elevated CO_2 concentration level (0.2–5% CO_2) in a sealed bioreactor with CO_2 feeding. Such a designer transgenic organism cannot survive when it is exposed to an atmospheric CO_2 concentration level (380 ppm = 0.038% CO_2) because its CO_2-concetrating mechanism (CCM) for effective photosynthetic CO_2 fixation has been impaired by the mutation. Even if such a designer organism is accidentally released into the natural environment, its cell will soon not be able to divide or mate, but die quickly of carbon starvation since it cannot effectively perform photosynthetic CO_2 fixation at the atmospheric CO_2 concentration (380 ppm). Therefore, use of such a high-CO_2-requiring mutant as a host organism for the genetic transformation of the designer biofuel-production-pathway gene(s) represents another way in creating the envisioned cell-division-controllable designer organisms for biosafety-guarded photobiological production of biofuels from CO_2 and H_2O. No designer proton-channel gene is required here.

In another embodiment, a cell-division-controllable designer organism (Fig. 3b) is created by use of a designer cell-division-cycle regulatory gene as a biosafety-control gene (Fig. 2g) that can control the expression of the cell-division-cycle (cdc) genes in the host organism so that it can inducibly turn off its reproductive functions such as permanently shutting off the cell division and mating capability upon specific induction of the designer gene.

Biologically, it is the expression of the natural cdc genes that controls the cell growth and cell division cycle in cyanobacteria, algae, and higher plant cells. The most basic function of the cell cycle is to duplicate accurately the vast amount of DNA in the chromosomes during the S phase (S for synthesis) and then segregate the copies precisely into two genetically identical daughter cells during the M phase (M for mitosis). Mitosis begins typically with chromosome condensation: the duplicated DNA strands, packaged into elongated chromosomes, condense into the much more compact chromosomes required for their segregation. The nuclear envelope then breaks down, and the replicated chromosomes, each consisting of a pair of sister chromatids, become attached to the microtubules of the mitotic spindle. As mitosis proceeds, the cell pauses briefly in a state called metaphase, when the chromosomes are aligned at the equator of the mitotic spindle, poised for segregation.

The sudden segregation of sister chromatids marks the beginning of anaphase during which the chromosomes move to opposite poles of the spindle, where they decondense and reform intact nuclei. The cell is then pinched into two by cytoplasmic division (cytokinesis) and the cell division is then complete. Note, most cells require much more time to grow and double their mass of proteins and organelles than they require to replicate their DNA (the S phase) and divide (the M phase). Therefore, there are two gap phases: a G_1 phase between M phase and S phase, and a G2 phase between S phase and mitosis. As a result, the eukaryotic cell cycle is traditionally divided into four sequential phases: G_1, S, G_2, and M. Physiologically, the two gap phases also provide time for the cell to monitor the internal and external environment to ensure that conditions are suitable and preparation are complete before the cell commits itself to the major upheavals of S phase and mitosis. The G_1 phase is especially important in this aspect. Its length can vary greatly depending on external conditions and extracellular signals from other cells. If extracellular conditions are unfavorable, for example, cells delay progress through G_1 and may even enter a specialized resting state known as G_0 (G zero), in which they remain for days, weeks, or even for years before resuming proliferation. Indeed, many cells remain permanently in G_0 state until they die.

In one of the various embodiments, a designer gene(s) that encodes a designer cdc-regulatory protein or a specific cdc-iRNA is used to inducibly inhibit the expression of certain cdc gene(s) to stop cell division and disable the mating capability when the designer gene(s) is trigged by a specific inducing condition. When the cell-division-controllable designer culture is grown and ready for photosynthetic production of biofuels, for example, it is a preferred practice to induce the expression of a specific designer cdc-iRNA gene(s) along with induction of the designer biofuel-production-pathway gene(s) so that the cells will permanently halt at the G_1 phase or G_0 state. In this way, the grown designer-organism cells become perfect catalysts for photosynthetic production of biofuels from CO_2 and H_2O while their functions of cell division and mating are permanently shut off at the G_1 phase or G_0 state to help ensure biosafety.

Use of the biosafety embodiments with various designer biofuel-production-pathways genes can create various biosafety-guarded photobiological biofuel producers (Fig. 3a–c). Note, SEQ ID NOS: 46 and 1–12 (listed in PCT Patent Application Publication No. WO 09105733) represent an example for a cell-division-controllable designer eukaryotic organism such as a cell-division-controllable designer alga (e.g., *Chlamydomonas*) that contains a designer Nial-promoter-controlled proton-channel gene (SEQ ID NO: 46) and a set of designer Nial-promoter-controlled butanol-production-pathway genes (SEQ ID NOS: 1–12). Because the designer proton-channel gene and the designer biofuel-production-pathway gene(s) are all controlled by the same Nial-promoter sequences, they can be simultaneously expressed upon induction by adding nitrate fertilizer into the culture medium to provide the biosafety-guarded photosynthetic biofuel-producing capability as illustrated in Fig. 3b. Use of the designer Nial-promoter-controlled butanol-production-pathway genes (SEQ ID NOS: 1–12) in a high CO_2-requiring host photosynthetic organism, such as *C. reinhardtii* carbonic-anhydrase-deficient mutant12-1C

(CC-1219 cal mt-) or *C. reinhardtii cia3* mutant, represents another example in creating a designer cell-division-controllable photosynthetic organism to help ensure biosafety.

This designer biosafety feature may be useful to the production of other biofuels such as biooils, biohydrogen, ethanol, hydrocarbons, and intermediate products as well. For example, this biosafety embodiment in combination with a set of designer ethanol-production-pathway genes can represent a cell-division-controllable ethanol producer (Fig. 3c).

2.5 More on Designer Calvin-Cycle-Channeled Production of Butanol and Related Higher Alcohols

The present invention further discloses designer Calvin-cycle-channeled and photosynthetic-NADPH (reduced nicotinamide adenine dinucleotide phosphate)-enhanced pathways, associated designer DNA constructs (designer genes), and designer transgenic photosynthetic organisms for photobiological production of butanol and related higher alcohols from carbon dioxide and water. In this context throughout this specification as mentioned before, a "higher alcohol" or "related higher alcohol" refers to an alcohol that comprises at least four carbon atoms, including both straight and branched higher alcohols such as 1-butanol and 2-methyl-1-butanol. The Calvin-cycle-channeled and photosynthetic-NADPH-enhanced pathways are constructed with designer enzymes expressed through use of designer genes in host photosynthetic organisms such as algae and oxyphotobacteria (including cyanobacteria and oxychlorobacteria) organisms for photobiological production of butanol and related higher alcohols. The said butanol and related higher alcohols are selected from the group consisting of: 1-butanol, 2-methyl-1-butanol, isobutanol, 3-methyl-1-butanol, 1-hexanol, 1-octanol, 1-pentanol, 1-heptanol, 3-methyl-1-pentanol, 4-methyl-1-hexanol, 5-methyl-1-heptanol, 4-methyl-1-pentanol, 5-methyl-1-hexanol, and 6-methyl-1-heptanol. The designer photosynthetic organisms such as designer transgenic algae and oxyphotobacteria (including cyanobacteria and oxychlorobacteria) comprise designer Calvin-cycle-channeled and photosynthetic NADPH-enhanced pathway gene(s) and biosafety-guarding technology for enhanced photobiological production of butanol and related higher alcohols from carbon dioxide and water.

Photosynthetic water splitting and its associated proton gradient-coupled electron transport process generates chemical energy intermediate in the form of adenosine triphosphate (ATP) and reducing power in the form of reduced nicotinamide adenine dinucleotide phosphate (NADPH). However, certain butanol-related metabolic pathway enzymes such as the NADH-dependent butanol dehydrogenase (GenBank accession numbers: YP_148778, NP_561774, AAG23613, ZP_05082669, ADO12118, ADC48983) can use only reduced nicotinamide adenine dinucleotide (NADH) but not NADPH. Therefore, to achieve a true coupling of a designer pathway with the Calvin cycle for photosynthetic production of butanol and related

higher alcohols, it is a preferred practice to use an effective NADPH/NADH conversion mechanism and/or NADPH-using enzyme(s) (such as NADPH-dependent enzymes) in construction of a compatible designer pathway(s) to couple with the photosynthesis/Calvin-cycle process in accordance with the present invention.

According to one of the various embodiments, a number of various designer Calvin-cycle-channeled pathways can be created by use of an NADPH/NADH conversion mechanism in combination with certain amino-acids-metabolic pathways for production of butanol and higher alcohols from carbon dioxide and water. The Calvin-cycle-channeled and photosynthetic-NADPH-enhanced pathways are constructed typically with designer enzymes that are selectively expressed through use of designer genes in a host photosynthetic organism such as a host alga or oxyphotobacterium for production of butanol and higher alcohols. A list of exemplary enzymes that can be selected for use in construction of the Calvin-cycle-channeled and photosynthetic-NADPH-enhanced pathways are presented in Table 1. As shown in Figs. 4–10, the net results of the designer Calvin-cycle-channeled and photosynthetic NADPH-enhanced pathways in working with the Calvin cycle are production of butanol and related higher alcohols from carbon dioxide (CO_2) and water (H_2O) using photosynthetically generated ATP (adenosine triphosphate) and NADPH (reduced nicotinamide adenine dinucleotide phosphate). A significant feature is the innovative utilization of an NADPH-dependent glyceraldehyde-3-phosphate dehydrogenase **34** and a nicotinamide adenine dinucleotide (NAD)-dependent glyceraldehyde-3-phosphate dehydrogenase **35** to serve as a NADPH/NADH conversion mechanism that can convert certain amount of photosynthetically generated NADPH to NADH which can then be used by NADH-requiring pathway enzymes such as an NADH-dependent alcohol dehydrogenase **43** (examples of its encoding gene with GenBank accession numbers are: BAB59540, CAA89136, NP_148480) for production of butanol and higher alcohols.

More specifically, an NADPH-dependent glyceraldehyde-3-phosphate dehydrogenase **34** (e.g., GenBank accession numbers: ADC37857, ADC87332, YP_003471459, ZP_04395517, YP_003287699, ZP_07004478, ZP_04399616) catalyzes the following reaction that uses NADPH in reducing 1,3-Diphosphoglycerate (1,3-DiPGA) to 3-Phosphoglyaldehyde (3-PGAld) and inorganic phosphate (Pi):

$$1,3\text{ - DiPGA} + \text{NADPH} + \text{H}^+ \rightarrow 3\text{ - PGAld} + \text{NADP}^+ + \text{Pi} \quad (3)$$

Meanwhile, an NAD-dependent glyceraldehyde-3-phosphate dehydrogenase **35** (e.g., GenBank: ADM41489, YP_003095198, ADC36961, ZP_07003925, ACQ61431, YP_002285269, ADN80469, ACI60574) catalyzes the oxidation of 3-PGAld by oxidized nicotinamide adenine dinucleotide (NAD^+) back to1,3-DiPGA:

$$3\text{ - PGAld} + \text{NAD}^+ + \text{Pi} \rightarrow 1,3\text{ - DiPGA} + \text{NADH} + \text{H}^+ \quad (4)$$

The net result of the enzymatic reactions (3) and (4) is the conversion of photosynthetically generated NADPH to NADH, which various NADH-requiring designer pathway enzymes such as NADH-dependent alcohol dehydrogenase **43** can use in

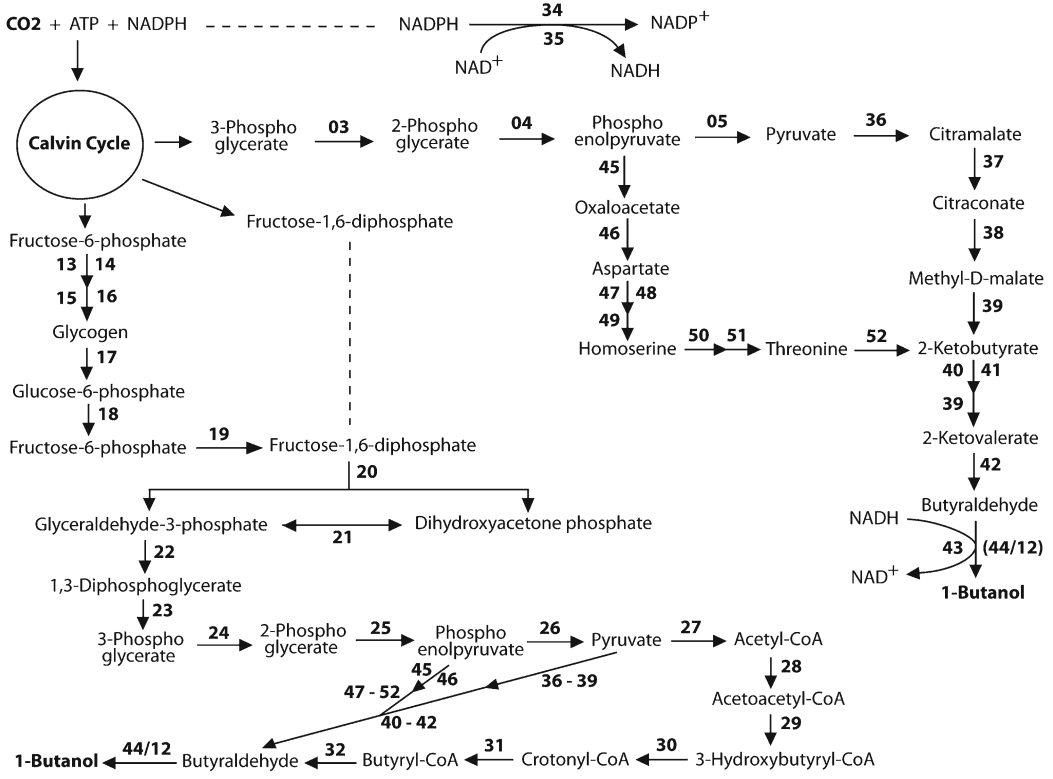

Fig. 4 Presents designer Calvin-cycle-channeled and photosynthetic NADPH-enhanced pathways using the reducing power (NADPH) and energy (ATP) from the photosynthetic water splitting and proton gradient-coupled electron transport process to reduce carbon dioxide (CO_2) into 1-butanol ($CH_3CH_2CH_2CH_2OH$) with a series of enzymatic reactions

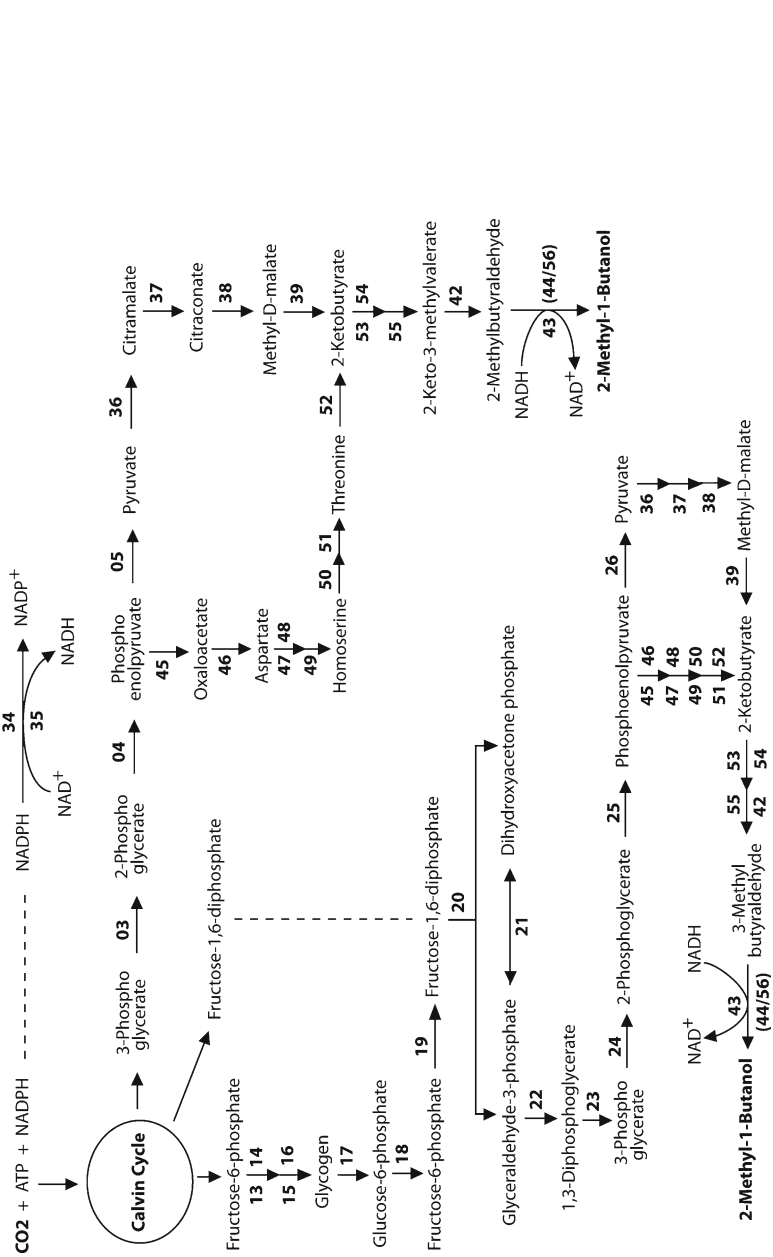

Fig. 5 Presents designer Calvin-cycle-channeled and photosynthetic NADPH-enhanced pathways using NADPH and ATP from the photosynthetic water splitting and proton gradient-coupled electron transport process to reduce carbon dioxide (CO_2) into 2-methyl-1-butanol ($CH_3CH_2CH(CH_3)CH_2OH$) with a series of enzymatic reactions

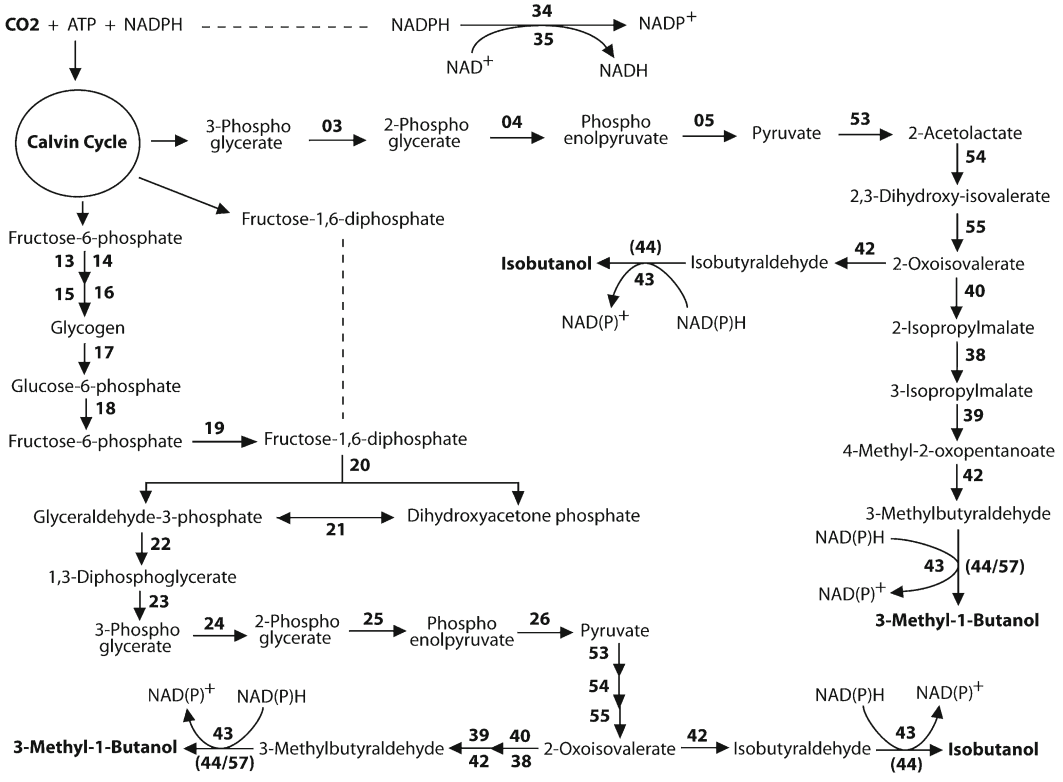

Fig. 6 Presents designer Calvin-cycle-channeled and photosynthetic NADPH-enhanced pathways using NADPH and ATP from the photosynthetic water splitting and proton gradient-coupled electron transport process to reduce carbon dioxide (CO_2) into isobutanol ($((CH_3)_2CHCH_2OH$) and 3-methyl-1-butanol ($CH_3CH(CH_3)CH_2CH_2OH$) with a series of enzymatic reactions

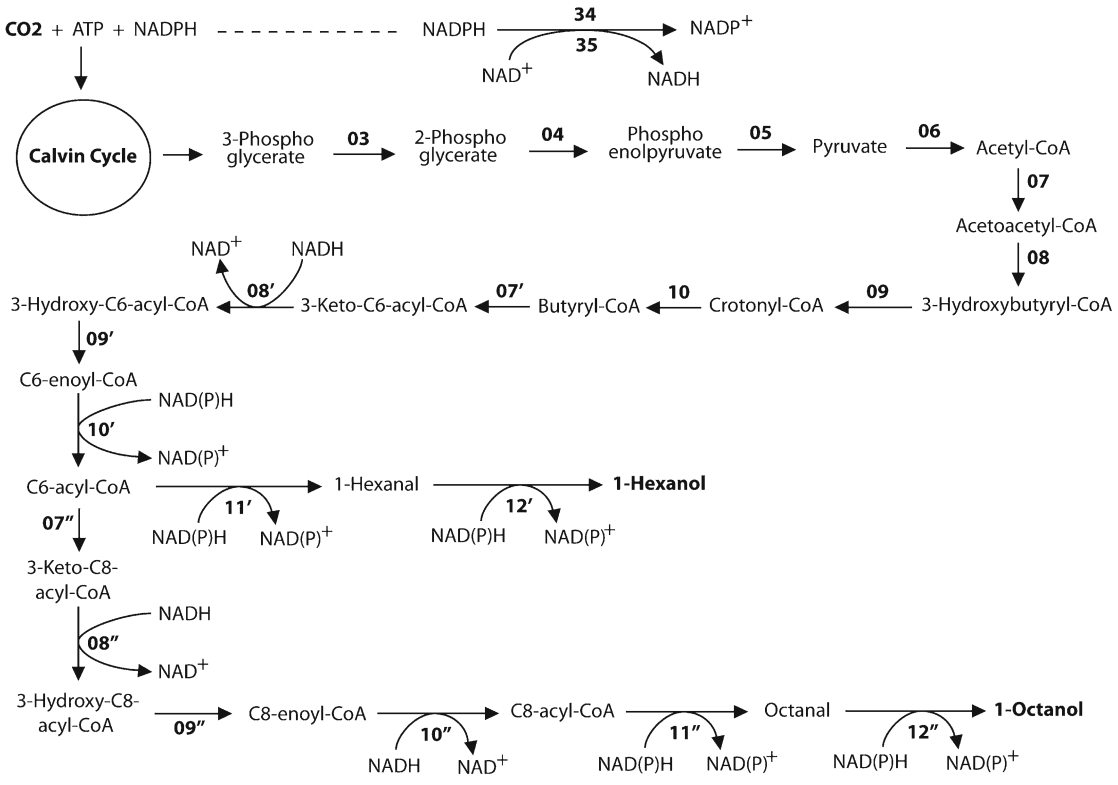

Fig. 7 Presents designer Calvin-cycle-channeled and photosynthetic NADPH-enhanced pathways using NADPH and ATP from the photosynthetic water splitting and proton gradient-coupled electron transport process to reduce carbon dioxide (CO_2) into 1-hexanol ($CH_3CH_2CH_2CH_2CH_2CH_2OH$) and 1-octanol ($CH_3CH_2CH_2CH_2CH_2CH_2CH_2CH_2OH$) with a series of enzymatic reactions

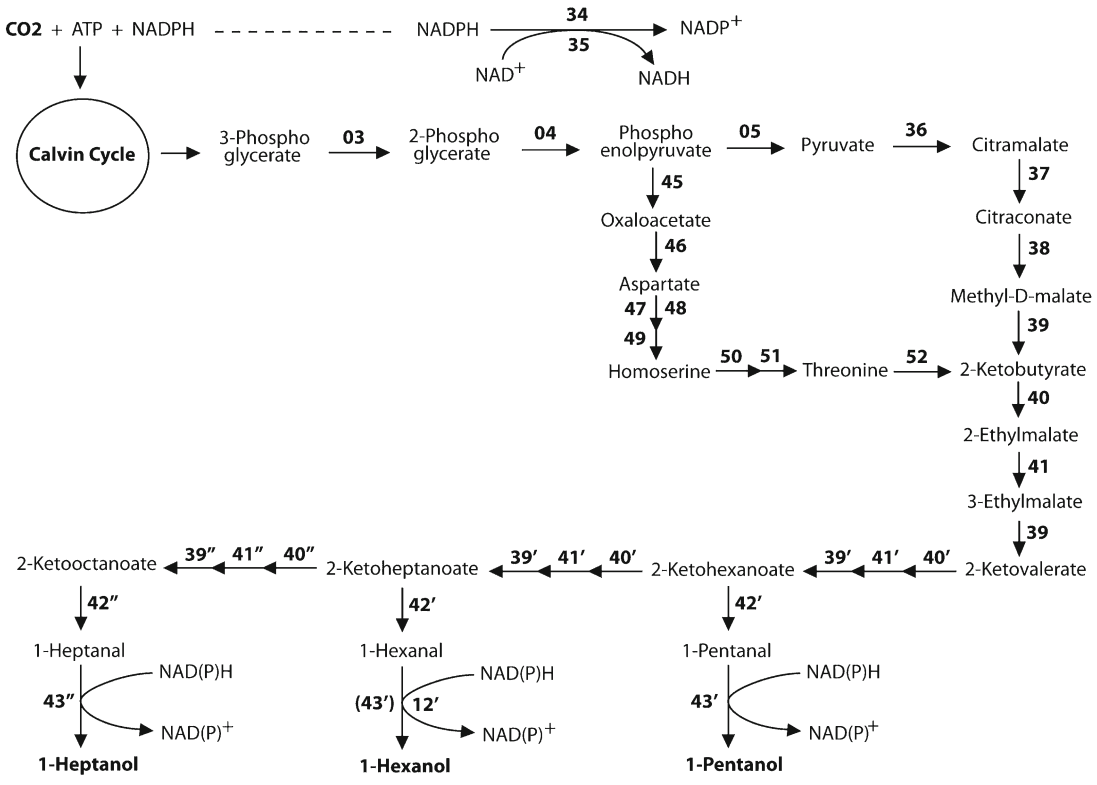

Fig. 8 Presents designer Calvin-cycle-channeled and photosynthetic NADPH-enhanced pathways using NADPH and ATP from the photosynthetic water splitting and proton gradient-coupled electron transport process to reduce carbon dioxide (CO_2) into 1-pentanol ($CH_3CH_2CH_2CH_2CH_2OH$), 1-hexanol ($CH_3CH_2CH_2CH_2CH_2CH_2OH$), and 1-heptanol ($CH_3CH_2CH_2CH_2CH_2CH_2CH_2OH$) with a series of enzymatic reactions

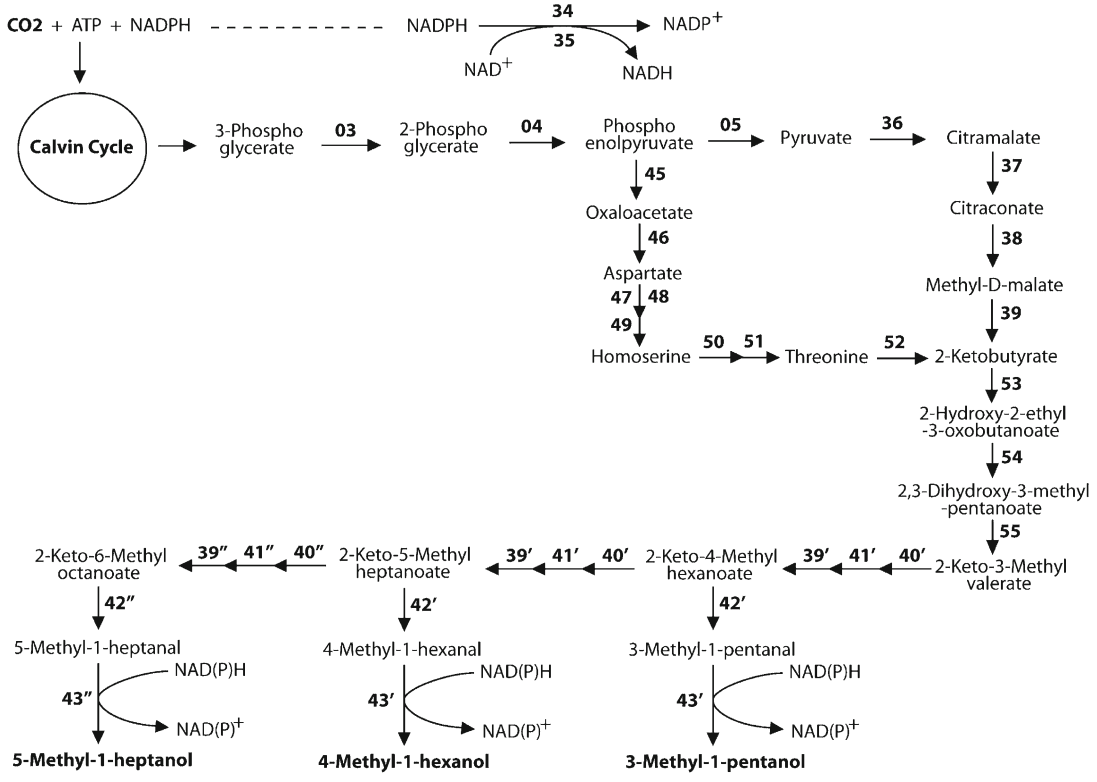

Fig. 9 Presents designer Calvin-cycle-channeled and photosynthetic NADPH-enhanced pathways using NADPH and ATP from the photosynthetic water splitting and proton gradient-coupled electron transport process to reduce carbon dioxide (CO_2) into 3-methyl-1-pentanol ($CH_3CH_2CH(CH_3)CH_2CH_2OH$), 4-methyl-1-hexanol ($CH_3CH_2CH(CH_3)CH_2CH_2CH_2OH$), and 5-methyl-1-heptanol ($CH_3CH_2CH(CH_3)CH_2CH_2CH_2CH_2OH$) with a series of enzymatic reactions

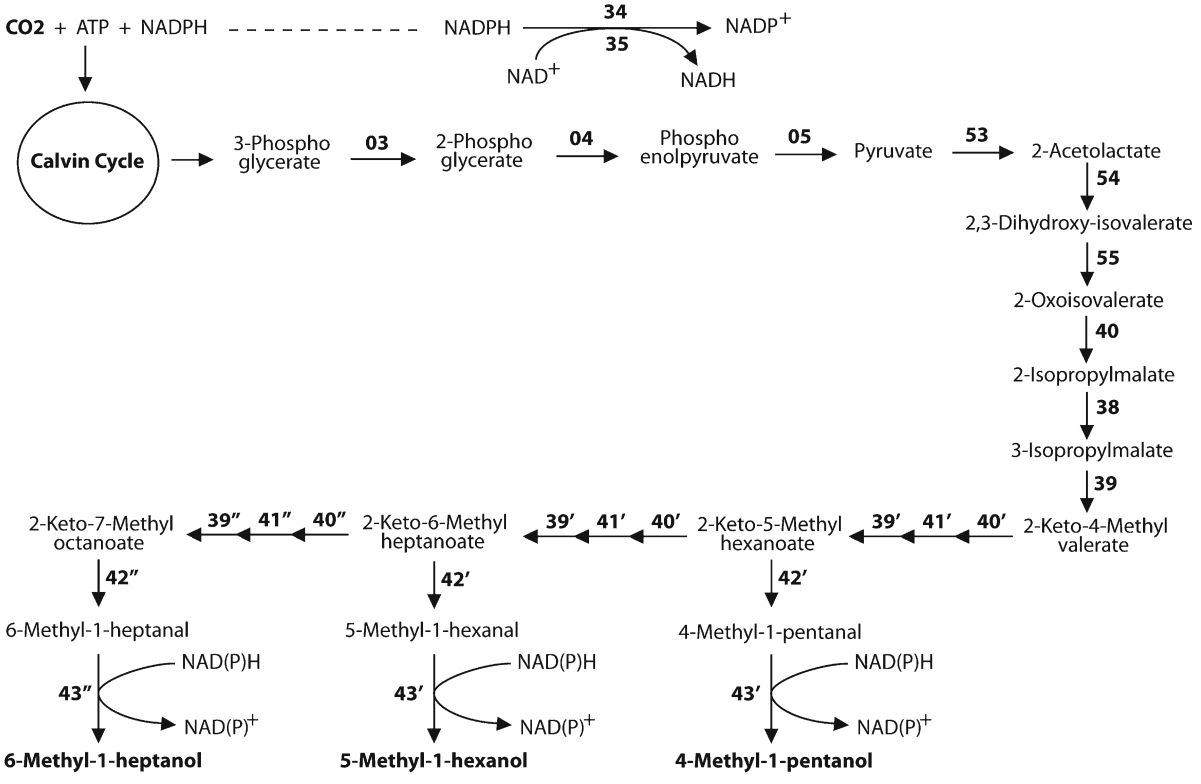

Fig. 10 Presents designer Calvin-cycle-channeled and photosynthetic NADPH-enhanced pathways using NADPH and ATP from the photosynthetic water splitting and proton gradient-coupled electron transport process to reduce carbon dioxide (CO_2) into 4-methyl-1-pentanol ($CH_3CH(CH_3)CH_2CH_2CH_2OH$), 5-methyl-1-hexanol ($CH_3CH(CH_3)CH_2CH_2CH_2CH_2OH$), and 6-methyl-1-heptanol ($CH_3CH(CH_3)CH_2CH_2CH_2CH_2CH_2OH$) with a series of enzymatic reactions

producing butanol and related higher alcohols. When there is too much NADH, this NADPH/NADH conversion system can run also reversely to balance the supply of NADH and NADPH. Therefore, it is a preferred practice to innovatively utilize this NADPH/NADH conversion system under control of a designer switchable promoter such as *nirA* (or Nial for eukaryotic system) promoter when/if needed to achieve robust production of butanol and related higher alcohols. Various designer Calvin-cycle-channeled pathways in combination of a NADPH/NADH conversion mechanism with certain amino-acids-metabolism-related pathways for photobiological production of butanol and related higher alcohols are further described hereinbelow.

2.6 Designer Calvin-Cycle-Channeled 1-Butanol Producing Pathways

According to one of the various embodiments, a designer Calvin-cycle-channeled pathway is created that takes the Calvin-cycle intermediate product, 3-phosphoglycerate, and converts it into 1-butanol by using, for example, a set of enzymes consisting of (as shown with the numerical labels **34**, **35**, **03**-**05**, **36**-**43** in Fig. 4): NADPH-dependent glyceraldehyde-3-phosphate dehydrogenase **34**, NAD-dependent glyceraldehyde-3-phosphate dehydrogenase **35**, phosphoglycerate mutase **03**, enolase **04**, pyruvate kinase **05**, citramalate synthase **36**, 2-methylmalate dehydratase **37**, 3-isopropylmalate dehydratase **38**, 3-isopropylmalate dehydrogenase **39**, 2-isopropylmalate synthase **40**, isopropylmalate isomerase **41**, 2-keto acid decarboxylase **42**, and alcohol dehydrogenase (NAD dependent) **43**. In this pathway design, as mentioned earlier, the NADPH-dependent glyceraldehyde-3-phosphate dehydrogenase **34** and NAD-dependent glyceraldehyde-3-phosphate dehydrogenase **35** serve as a NADPH/NADH conversion mechanism that can convert certain amount of photosynthetically generated NADPH to NADH which can be used by the NADH-requiring alcohol dehydrogenase **43** (examples of its encoding gene with the following GenBank accession numbers: BAB59540, CAA89136, NP_148480) for production of 1-butanol by reduction of butyraldehyde.

According to one of the various embodiments, it is a preferred practice to also use an NADPH-dependent alcohol dehydrogenase **44** that can use NADPH as the source of reductant so that it can help alleviate the requirement of NADH supply for enhanced photobiological production of butanol and other alcohols. As listed in Table 1, examples of NADPH-dependent alcohol dehydrogenase **44** include (but not limited to) the enzyme with any of the following GenBank accession numbers: YP_001211038, ZP_04573952, XP_002494014, CAY71835, NP_417484, EFC99049, and ZP_02948287.

Note, the 2-keto acid decarboxylase **42** (e.g., AAS49166, ADA65057, CAG34226, AAA35267, CAA59953, A0QBE6, A0PL16) and alcohol dehydrogenase **43** (and/or **44**) have quite broad substrate specificity. Consequently, their use can result in production of not only 1-butanol but also other alcohols such as propanol depending

on the genetic and metabolic background of the host photosynthetic organisms. This is because all 2-keto acids can be converted to alcohols by the 2-keto acid decarboxylase **42** and alcohol dehydrogenase **43** (and/or **44**) owning to their broad substrate specificity. Therefore, according to another embodiment, it is a preferred practice to use a substrate-specific enzyme such as butanol dehydrogenase **12** when/if production of 1-butanol is desirable. As listed in Table 1, examples of butanol dehydrogenase **12** are NADH-dependent butanol dehydrogenase (e.g., GenBank: YP_148778, NP_561774, AAG23613, ZP_05082669, ADO12118) and/or NAD(P)H-dependent butanol dehydrogenase (e.g., NP_562172, AAA83520, EFB77036, EFF67629, ZP_06597730, EFE12215, EFC98086, ZP_05979561).

In one of the various embodiments, another designer Calvin-cycle-channeled 1-butanol production pathway is created that takes the Calvin-cycle intermediate product, 3-phosphoglycerate, and converts it into 1-butanol by using, for example, a set of enzymes consisting of (as shown with the numerical labels **34**, **35**, **03**, **04**, **45**-**52**, and **40**-**43** (**44**/**12**) in Fig. 4): NADPH-dependent glyceraldehyde-3-phosphate dehydrogenase **34**, NAD-dependent glyceraldehyde-3-phosphate dehydrogenase **35**, phosphoglycerate mutase **03**, enolase **04**, phosphoenolpyruvate carboxylase **45**, aspartate aminotransferase **46**, aspartokinase **47**, aspartate-semialdehyde dehydrogenase **48**, homoserine dehydrogenase **49**, homoserine kinase **50**, threonine synthase **51**, threonine ammonia-lyase **52**, 2-isopropylmalate synthase **40**, isopropylmalate isomerase **41**, 3-isopropylmalate dehydrogenase **39**, 2-keto acid decarboxylase **42**, and NAD-dependent alcohol dehydrogenase **43** (and/or NADPH-dependent alcohol dehydrogenase **44**, or butanol dehydrogenase **12**).

According to another embodiment, the amino-acids-metabolism-related 1-butanol production pathways (numerical labels **03**-**05**, **36**-**43** and/or **03**, **04**, **45**-**52**, and **39**-**43** (**44**/**12**)) can operate in combination and/or in parallel with other photobiological butanol production pathways. For example, as shown also in Fig. 4, the Fructose-6-phosphate-branched 1-butanol production pathway (numerical labels **13**-**32** and **44**/**12**) can operate with the parts of amino-acids-metabolism-related pathways (numerical labels **36**-**42**, and/or **45**-**52** and **40**-**42**) with pyruvate and/or phosphoenolpyruvate as their joining points.

Examples of designer Calvin-cycle-channeled 1-butanol production pathway genes (DNA constructs) are shown in the DNA sequence listings (SEQ ID NOS: 58–81 of the US Patent Application Publication No. 2011/0177571 A1). The net results of the designer photosynthetic NADPH-enhanced pathways in working with the Calvin cycle (Fig. 4) are photobiological production of 1-butanol ($CH_3CH_2CH_2CH_2OH$) from carbon dioxide (CO_2) and water (H_2O) using photosynthetically generated ATP (adenosine triphosphate) and NADPH (reduced nicotinamide adenine dinucleotide phosphate) according to the following process reaction:

$$4CO_2 + 5H_2O \rightarrow CH_3CH_2CH_2CH_2OH + 6O_2 \quad (5)$$

2.7 Designer Calvin-Cycle-Channeled 2-Methyl-1-Butanol Producing Pathways

According to one of the various embodiments, a designer Calvin-cycle-channeled 2-Methyl-1-Butanol production pathway is created that takes the Calvin-cycle intermediate product, 3-phosphoglycerate, and converts it into 2-methyl-1-butanol by using, for example, a set of enzymes consisting of (as shown with the numerical labels **34**, **35**, **03**-**05**, **36**-**39**, **53**-**55**, **42**, **43**, or **44**/**56** in Fig. 5): NADPH-dependent glyceraldehyde-3-phosphate dehydrogenase **34**, NAD-dependent glyceraldehyde-3-phosphate dehydrogenase **35**, phosphoglycerate mutase **03**, enolase **04**, pyruvate kinase **05**, citramalate synthase **36**, 2-methylmalate dehydratase **37**, 3-isopropylmalate dehydratase **38**, 3-isopropylmalate dehydrogenase **39**, acetolactate synthase **53**, ketol-acid reductoisomerase **54**, dihydroxy-acid dehydratase **55**, 2-keto acid decarboxylase **42**, and NAD-dependent alcohol dehydrogenase **43** (or NADPH-dependent alcohol dehydrogenase **44**; more preferably, 2-methylbutyraldehyde reductase **56**).

In another embodiment, a designer Calvin-cycle-channeled 2-methyl-1-butanol production pathway is created that takes the intermediate product, 3-phosphoglycerate, and converts it into 2-methyl-1-butanol by using, for example, a set of enzymes consisting of (as shown with the numerical labels **34**, **35**, **03**, **04**, **45**-**55**, **42**, **43**, or **44**/**56** in Fig. 5): NADPH-dependent glyceraldehyde-3-phosphate dehydrogenase **34**, NAD-dependent glyceraldehyde-3-phosphate dehydrogenase **35**, phosphoglycerate mutase **03**, enolase **04**, phosphoenolpyruvate carboxylase **45**, aspartate aminotransferase **46**, aspartokinase **47**, aspartate-semialdehyde dehydrogenase **48**, homoserine dehydrogenase **49**, homoserine kinase **50**, threonine synthase **51**, threonine ammonia-lyase **52**, acetolactate synthase **53**, ketol-acid reductoisomerase **54**, dihydroxy-acid dehydratase **55**, 2-keto acid decarboxylase **42**, and NAD dependent alcohol dehydrogenase **43** (or NADPH dependent alcohol dehydrogenase **44**; more preferably, 2-methylbutyraldehyde reductase **56**).

These pathways (Fig. 5) are quite similar to those of Fig. 4, except that acetolactate synthase **53**, ketol-acid reductoisomerase **54**, dihydroxy-acid dehydratase **55**, and 2-methylbutyraldehyde reductase **56** are used to produce 2-Methyl-1-Butanol.

The net results of the designer photosynthetic NADPH-enhanced pathways in working with the Calvin cycle (Fig. 5) are production of 2-methyl-1-butanol ($CH_3CH_2CH(CH_3)CH_2OH$) from carbon dioxide (CO_2) and water (H_2O) using photosynthetically generated ATP and NADPH according to the following process reaction:

$$10CO_2 + 12H_2O \rightarrow 2CH_3CH_2CH(CH_3)CH_2OH + 15O_2 \quad (6)$$

2.8 Designer Calvin-Cycle-Channeled Pathways for Production of Isobutanol and 3-Methyl-1-Butanol

According to one of the various embodiments, a designer Calvin-cycle-channeled pathway is created that takes the Calvin-cycle intermediate product, 3-phosphoglycerate, and converts it into isobutanol by using, for example, a set of enzymes consisting of (as shown with numerical labels **34**, **35**, **03**-**05**, **53**-**55**, **42**, **43** (or **44**) in Fig. 6): NADPH-dependent glyceraldehyde-3-phosphate dehydrogenase **34**, NAD-dependent glyceraldehyde-3-phosphate dehydrogenase **35**, phosphoglycerate mutase **03**, enolase **04**, pyruvate kinase **05**, acetolactate synthase **53**, ketol-acid reductoisomerase **54**, dihydroxy-acid dehydratase **55**, 2-keto acid decarboxylase **42**, and NAD-dependent alcohol dehydrogenase **43** (or NADPH-dependent alcohol dehydrogenase **44**). The net result of this pathway in working with the Calvin cycle is photobiological production of isobutanol ($(CH_3)_2CHCH_2OH$) from carbon dioxide (CO_2) and water (H_2O) using photosynthetically generated ATP and NADPH according to the following process reaction:

$$4CO_2 + 5H_2O \rightarrow (CH_3)_2CHCH_2OH + 6O_2 \quad (7)$$

According to another embodiment, a designer Calvin-cycle-channeled pathway is created that takes the intermediate product, 3-phosphoglycerate, and converts it into 3-methyl-1-butanol by using, for example, a set of enzymes consisting of (as shown with the numerical labels **34**, **35**, **03**-**05**, **53**-**55**, **40**, **38**, **39**, **42**, **43** (or **44**/**57**) in Fig. 6): NADPH-dependent glyceraldehyde-3-phosphate dehydrogenase **34**, NAD-dependent glyceraldehyde-3-phosphate dehydrogenase **35**, phosphoglycerate mutase **03**, enolase **04**, pyruvate kinase **05**, acetolactate synthase **53**, ketol-acid reductoisomerase **54**, dihydroxy-acid dehydratase **55**, 2-isopropylmalate synthase **40**, 3-isopropylmalate dehydratase **38**, 3-isopropylmalate dehydrogenase **39**, 2-keto acid decarboxylase **42**, and NAD-dependent alcohol dehydrogenase **43** (or NADPH-dependent alcohol dehydrogenase **44**; or more preferably, 3-methylbutanal reductase **57**). The net result of this pathway in working with the Calvin cycle is photobiological production of 3-methyl-1-butanol ($CH_3CH(CH_3)CH_2CH_2OH$) from carbon dioxide (CO_2) and water (H_2O) using photosynthetically generated ATP and NADPH according to the following process reaction:

$$10CO_2 + 12H_2O \rightarrow 4CH_3CH(CH_3)CH_2CH_2OH + 15O_2 \quad (8)$$

These designer pathways (Fig. 6) share a number of designer pathway enzymes with those of Figs. 4 and 5, except that a 3-methylbutanal reductase **57** is preferably used for production of 3-methyl-1-butanol; they all have a common feature of using an NADPH-dependent glyceraldehyde-3-phosphate dehydrogenase **34** and an NAD-dependent glyceraldehyde-3-phosphate dehydrogenase **35** as an NADPH/NADH conversion mechanism to convert certain amount of photosynthetically generated NADPH to NADH which can be used by NADH-requiring pathway enzymes such as an NADH-requiring alcohol dehydrogenase **43**. The net results of the designer photosynthetic NADPH-enhanced pathways (Fig. 6) in working with the

Calvin cycle are also production of isobutanol ($(CH_3)_2CHCH_2OH$) and/or 3-methyl-1-butanol ($CH_3CH(CH_3)CH_2CH_2OH$) from carbon dioxide (CO_2) and water (H_2O) using photosynthetically generated ATP and NADPH.

2.9 Designer Calvin-Cycle-Channeled Pathways for Production of 1-Hexanol and 1-Octanol

According to one of the various embodiments, a designer Calvin-cycle-channeled pathway is created that takes the Calvin-cycle intermediate product, 3-phosphoglycerate, and converts it into 1-hexanol by using, for example, a set of enzymes consisting of (as shown with the numerical labels **34**, **35**, **03**-**10**, **07′**-**12′** in Fig. 7): NADPH-dependent glyceraldehyde-3-phosphate dehydrogenase **34**, NAD-dependent glyceraldehyde-3-phosphate dehydrogenase **35**, phosphoglycerate mutase **03**, enolase **04**, pyruvate kinase **05**, pyruvate-ferredoxin oxidoreductase **06**, thiolase **07**, 3-hydroxybutyryl-CoA dehydrogenase **08**, crotonase **09**, butyryl-CoA dehydrogenase **10**, designer 3-ketothiolase **07′**, designer 3-hydroxyacyl-CoA dehydrogenase **08′**, designer enoyl-CoA dehydratase **09′**, designer 2-enoyl-CoA reductase **10′**, designer acyl-CoA reductase **11′**, and hexanol dehydrogenase **12′**. The net result of this designer pathway in working with the Calvin cycle is photobiological production of 1-hexanol ($CH_3CH_2CH_2CH_2CH_2CH_2OH$) from carbon dioxide ($CO_2$) and water ($H_2O$) using photosynthetically generated ATP and NADPH according to the following process reaction:

$$6CO_2 + 7H_2O \rightarrow CH_3CH_2CH_2CH_2CH_2CH_2OH + 9O_2 \tag{9}$$

According to another embodiment, a designer Calvin-cycle-channeled pathway is created that takes the intermediate product, 3-phosphoglycerate, and converts it into 1-octanol by using, for example, a set of enzymes consisting of (as shown with the numerical labels **34**, **35**, **03**-**10**, **07′**-**10′**, and **07″**-**12″** in Fig. 7): NADPH-dependent glyceraldehyde-3-phosphate dehydrogenase **34**, NAD-dependent glyceraldehyde-3-phosphate dehydrogenase **35**, phosphoglycerate mutase **03**, enolase **04**, pyruvate kinase **05**, pyruvate-ferredoxin oxidoreductase **06**, thiolase **07**, 3-hydroxybutyryl-CoA dehydrogenase **08**, crotonase **09**, butyryl-CoA dehydrogenase **10**, designer 3-ketothiolase **07′**, designer 3-hydroxyacyl-CoA dehydrogenase **08′**, designer enoyl-CoA dehydratase **09′**, designer 2-enoyl-CoA reductase **10′**, designer 3-ketothiolase **07″**, designer 3-hydroxyacyl-CoA dehydrogenase **08″**, designer enoyl-CoA dehydratase **09″**, designer 2-enoyl-CoA reductase **10″**, designer acyl-CoA reductase **11″**, and octanol dehydrogenase **12″**.

These pathways represent a significant upgrade in the pathway designs with part of a previously disclosed 1-butanol production pathway (**03**-**10**). The key feature is the utilization of an NADPH-dependent glyceraldehyde-3-phosphate dehydrogenase **34** and an NAD-dependent glyceraldehyde-3-phosphate dehydrogenase **35** as a mechanism for NADPH/NADH conversion to drive an NADH-requiring designer

hydrocarbon chain elongation pathway (**07′-10′**) for 1-hexanol production (**07′-12′** as shown in Fig. 7). The net result of this pathway in working with the Calvin cycle is photobiological production of 1-octanol ($CH_3CH_2CH_2CH_2CH_2CH_2CH_2CH_2OH$) from carbon dioxide ($CO_2$) and water ($H_2O$) using photosynthetically generated ATP and NADPH according to the following process reaction:

$$8CO_2 + 9H_2O \rightarrow CH_3CH_2CH_2CH_2CH_2CH_2CH_2CH_2OH + 12O_2 \quad (10)$$

2.10 Designer Calvin-Cycle-Channeled Pathways for Production of 1-Pentanol, 1-Hexanol, and 1-Heptanol

According to one of the various embodiments, a designer Calvin-cycle-channeled pathway is created that takes the Calvin-cycle intermediate product, 3-phosphoglycerate, and converts it into 1-pentanol, 1-hexanol, and/or 1-heptanol by using, for example, a set of enzymes consisting of (as shown with the numerical labels **34**, **35**, **03**-**05**, **36**-**41**, **39**, **39′**-**43′**, **39′**-**43′**, **12′**, and **39″**-**43** in Fig. 8): NADPH-dependent glyceraldehyde-3-phosphate dehydrogenase **34**, NAD-dependent glyceraldehyde-3-phosphate dehydrogenase **35**, phosphoglycerate mutase **03**, enolase **04**, pyruvate kinase **05**, citramalate synthase **36**, 2-methylmalate dehydratase **37**, 3-isopropylmalate dehydratase **38**, 3-isopropylmalate dehydrogenase **39**, 2-isopropylmalate synthase **40**, isopropylmalate isomerase **41**, 3-isopropylmalate dehydrogenase **39**, designer isopropylmalate synthase **40′**, designer isopropylmalate isomerase **41′**, designer 3-isopropylmalate dehydrogenase **39′**, designer 2-keto acid decarboxylase **42′**, short-chain alcohol dehydrogenase **43′**, hexanol dehydrogenase **12′**, designer isopropylmalate synthase **40″**, designer isopropylmalate isomerase **41″**, designer 3-isopropylmalate dehydrogenase **39″**, designer 2-keto acid decarboxylase **42″**, and designer short-chain alcohol dehydrogenase **43″**. This designer pathway works with the Calvin cycle using photosynthetically generated ATP and NADPH for photobiological production of 1-pentanol ($CH_3CH_2CH_2CH_2CH_2OH$), 1-hexanol ($CH_3CH_2CH_2CH_2CH_2CH_2OH$), and/or 1-heptanol ($CH_3CH_2CH_2CH_2CH_2CH_2CH_2OH$) from carbon dioxide ($CO_2$) and water ($H_2O$) according to the following process reactions:

$$10CO_2 + 12H_2O \rightarrow 2CH_3CH_2CH_2CH_2CH_2OH + 15O_2 \quad (11)$$

$$6CO_2 + 7H_2O \rightarrow CH_3CH_2CH_2CH_2CH_2CH_2OH + 9O_2 \quad (12)$$

$$14CO_2 + 16H_2O \rightarrow 2CH_3CH_2CH_2CH_2CH_2CH_2CH_2OH + 21O_2 \quad (13)$$

According to another embodiment, a designer Calvin-cycle-channeled pathway is created that takes the intermediate product, 3-phosphoglycerate, and converts it into 1-pentanol, 1-hexanol, and/or 1-heptanol by using, for example, a set of enzymes consisting of (as shown with the numerical labels **34**, **35**, **03**, **04**, **45**-**52**, **40**, **41**, **39**, **39′**-**43′**, **39′**-**43′**, **12′**, and **39″**-**43″** in Fig. 8): NADPH-dependent glyceraldehyde-3-phosphate dehydrogenase **34**, NAD-dependent glyceraldehyde-3-phosphate

dehydrogenase **35**, phosphoglycerate mutase **03**, enolase **04**, phosphoenolpyruvate carboxylase **45**, aspartate aminotransferase **46**, aspartokinase **47**, aspartate-semialdehyde dehydrogenase **48**, homoserine dehydrogenase **49**, homoserine kinase **50**, threonine synthase **51**, threonine ammonia-lyase **52**, 2-isopropylmalate synthase **40**, isopropylmalate isomerase **41**, 3-isopropylmalate dehydrogenase **39**, designer isopropylmalate synthase **40′**, designer isopropylmalate isomerase **41′**, designer 3-isopropylmalate dehydrogenase **39′**, designer 2-keto acid decarboxylase **42′**, short-chain alcohol dehydrogenase **43′**, hexanol dehydrogenase **12′**, designer isopropylmalate synthase **40″**, designer isopropylmalate isomerase **41″**, designer 3-isopropylmalate dehydrogenase **39″**, designer 2-keto acid decarboxylase **42″**, and designer short-chain alcohol dehydrogenase **43″**.

These pathways (Fig. 8) share a common feature of using an NADPH-dependent glyceraldehyde-3-phosphate dehydrogenase **34** and an NAD-dependent glyceraldehyde-3-phosphate dehydrogenase **35** as a mechanism for NADPH/NADH conversion to drive production of 1-pentanol, 1-hexanol, and/or 1-heptanol through a designer Calvin-cycle-channeled pathway in combination with a designer hydrocarbon chain elongation pathway (**40′**, **41′**, **39′**). This embodiment also takes the advantage of the broad substrate specificity (promiscuity) of 2-isopropylmalate synthase **40**, isopropylmalate isomerase **41**, 3-isopropylmalate dehydrogenase **39**, 2-keto acid decarboxylase **42**, and short-chain alcohol dehydrogenase **43** so that they can be used also as: designer isopropylmalate synthase **40′**, designer isopropylmalate isomerase **41′**, designer 3-isopropylmalate dehydrogenase **39′**, designer 2-keto acid decarboxylase **42′**, and short-chain alcohol dehydrogenase **43′**; isopropylmalate synthase **40** , designer isopropylmalate isomerase **41″**, designer 3-isopropylmalate dehydrogenase **39″**, designer 2-keto acid decarboxylase **42″**, and designer short-chain alcohol dehydrogenase **43″**. In this case, proper selection of a short-chain alcohol dehydrogenase with certain promiscuity is also essential. To improve product specificity, it is a preferred practice to use substrate specific designer enzymes.

2.11 Designer Calvin-Cycle-Channeled Pathways for Production of 3-Methyl-1-Pentanol, 4-Methyl-1-Hexanol, and 5-Methyl-1-Heptanol

According to one of the various embodiments, a designer Calvin-cycle-channeled pathway is created that takes the Calvin-cycle intermediate product, 3-phosphoglycerate, and converts it into 3-methyl-1-pentanol, 4-methyl-1-hexanol, and/or 5-methyl-1-heptanol by using, for example, a set of enzymes consisting of (as shown with the numerical labels **34**, **35**, **03**-**05**, **36**-**39**, **53**-**55**, **39′**-**43′**, **39′**-**43′**, and **39″**-**43″** in Fig. 9): NADPH-dependent glyceraldehyde-3-phosphate dehydrogenase **34**, NAD-dependent glyceraldehyde-3-phosphate dehydrogenase **35**, phosphoglycerate mutase **03**, enolase **04**, pyruvate kinase **05**, citramalate synthase **36**, 2-methylmalate dehydratase **37**, 3-isopropylmalate dehydratase **38**, 3-isopropylmalate dehydrogenase **39**, acetolactate synthase **53**, ketol-acid reductoisomerase **54**, dihydroxy-acid

dehydratase **55**, designer isopropylmalate synthase **40′**, designer isopropylmalate isomerase **41′**, designer 3-isopropylmalate dehydrogenase **39′**, designer 2-keto acid decarboxylase **42′**, short-chain alcohol dehydrogenase **43′**, designer isopropylmalate synthase **40″**, designer isopropylmalate isomerase **41″**, designer 3-isopropylmalate dehydrogenase **39″**, designer 2-keto acid decarboxylase **42″**, and designer short-chain alcohol dehydrogenase **43″**.

According to another embodiment, a designer Calvin-cycle-channeled pathway is created that takes the intermediate product, 3-phosphoglycerate, and converts it into 3-methyl-1-pentanol, 4-methyl-1-hexanol, and/or 5-methyl-1-heptanol by using, for example, a set of enzymes consisting of (as shown with the numerical labels **34**, **35**, **03**, **04**, **45-55**, **39′-43′**, **39′-43′**, and **39″-43″** in Fig. 9): NADPH-dependent glyceraldehyde-3-phosphate dehydrogenase **34**, NAD-dependent glyceraldehyde-3-phosphate dehydrogenase **35**, phosphoglycerate mutase **03**, enolase **04**, phosphoenolpyruvate carboxylase **45**, aspartate aminotransferase **46**, aspartokinase **47**, aspartate-semialdehyde dehydrogenase **48**, homoserine dehydrogenase **49**, homoserine kinase **50**, threonine synthase **51**, threonine ammonia-lyase **52**, acetolactate synthase **53**, ketol-acid reductoisomerase **54**, dihydroxy-acid dehydratase **55**, designer isopropylmalate synthase **40′**, designer isopropylmalate isomerase **41′**, designer 3-isopropylmalate dehydrogenase **39′**, designer 2-keto acid decarboxylase **42′**, short-chain alcohol dehydrogenase **43′**, designer isopropylmalate synthase **40** , designer isopropylmalate isomerase **41″**, designer 3-isopropylmalate dehydrogenase **39″**, designer 2-keto acid decarboxylase **42″**, and designer short-chain alcohol dehydrogenase **43″**.

These pathways (Fig. 9) are similar to those of Fig. 8, except they use acetolactate synthase **53**, ketol-acid reductoisomerase **54**, dihydroxy-acid dehydratase **55** as part of the pathways for production of 3-methyl-1-pentanol, 4-methyl-1-hexanol, and/or 5-methyl-1-heptanol. They all share a common feature of using an NADPH-dependent glyceraldehyde-3-phosphate dehydrogenase **34** and an NAD-dependent glyceraldehyde-3-phosphate dehydrogenase **35** as a mechanism for NADPH/NADH conversion to drive production of 3-methyl-1-pentanol, 4-methyl-1-hexanol, and/or 5-methyl-1-heptanol through a designer Calvin-cycle-channeled pathway in combination with a hydrocarbon chain elongation pathway (**40′**, **41′**, **39′**). This embodiment also takes the advantage of the broad substrate specificity (promiscuity) of 2-isopropylmalate synthase **40**, isopropylmalate isomerase **41**, 3-isopropylmalate dehydrogenase **39**, 2-keto acid decarboxylase **42**, and short-chain alcohol dehydrogenase **43** so that they can also serve as: designer isopropylmalate synthase **40′**, designer isopropylmalate isomerase **41′**, designer 3-isopropylmalate dehydrogenase **39′**, designer 2-keto acid decarboxylase **42′**, and short-chain alcohol dehydrogenase **43′**; designer isopropylmalate synthase **40″**, designer isopropylmalate isomerase **41″**, designer 3-isopropylmalate dehydrogenase **39″**, designer 2-keto acid decarboxylase **42″**, and designer short-chain alcohol dehydrogenase **43″**.

The net results of the designer photosynthetic NADPH-enhanced pathways (Fig. 9) in working with the Calvin cycle are production of 3-methyl-1-pentanol ($CH_3CH_2CH(CH_3)CH_2CH_2OH$), 4-methyl-1-hexanol ($CH_3CH_2CH(CH_3)CH_2CH_2CH_2OH$), and 5-methyl-1-heptanol ($CH_3CH_2CH(CH_3)CH_2CH_2CH_2CH_2OH$) from

carbon dioxide (CO_2) and water (H_2O) using photosynthetically generated ATP and NADPH according to the following process reactions:

$$6CO_2 + 7H_2O \rightarrow CH_3CH_2CH(CH_3)CH_2CH_2OH + 9O_2 \quad (14)$$

$$14CO_2 + 16H_2O \rightarrow 2CH_3CH_2CH(CH_3)CH_2CH_2CH_2OH + 21O_2 \quad (15)$$

$$8CO_2 + 9H_2O \rightarrow CH_3CH_2CH(CH_3)CH_2CH_2CH_2CH_2OH + 12O_2 \quad (16)$$

2.12 *Designer Calvin-Cycle-Channeled Pathways for Production of 4-Methyl-1-Pentanol, 5-Methyl-1-Hexanol, and 6-Methyl-1-Heptanol*

According to one of the various embodiments, a designer Calvin-cycle-channeled pathway is created that takes the Calvin-cycle intermediate product, 3-phosphoglycerate, and converts it into 4-methyl-1-pentanol, 5-methyl-1-hexanol, and 6-methyl-1-heptanol by using, for example, a set of enzymes consisting of (as shown with the numerical labels **34**, **35**, **03**-**05**, **53**-**55**, **40**, **38**, **39**, **39′**-**43′**, **39′**-**43′**, and **39″**-**43″** in Fig. 10): NADPH-dependent glyceraldehyde-3-phosphate dehydrogenase **34**, NAD-dependent glyceraldehyde-3-phosphate dehydrogenase **35**, phosphoglycerate mutase **03**, enolase **04**, pyruvate kinase **05**, acetolactate synthase **53**, ketol-acid reductoisomerase **54**, dihydroxy-acid dehydratase **55**, isopropylmalate synthase **40**, dehydratase **38**, 3-isopropylmalate dehydrogenase **39**, designer isopropylmalate synthase **40′**, designer isopropylmalate isomerase **41′**, designer 3-isopropylmalate dehydrogenase **39′**, designer 2-keto acid decarboxylase **42′**, short-chain alcohol dehydrogenase **43′**, designer isopropylmalate synthase **40″**, designer isopropylmalate isomerase **41″**, designer 3-isopropylmalate dehydrogenase **39″**, designer 2-keto acid decarboxylase **42″**, and designer short-chain alcohol dehydrogenase **43″**.

This pathway (Fig. 10) is similar to those of Fig. 8, except that it does not use citramalate synthase **36** and 2-methylmalate dehydratase **37**, but uses acetolactate synthase **53**, ketol-acid reductoisomerase **54**, dihydroxy-acid dehydratase **55** as part of the pathways for production of 4-methyl-1-pentanol, 5-methyl-1-hexanol, and/or 6-methyl-1-heptanol. They all share a common feature of using an NADPH-dependent glyceraldehyde-3-phosphate dehydrogenase **34** and an NAD-dependent glyceraldehyde-3-phosphate dehydrogenase **35** as a mechanism for NADPH/NADH conversion to drive production of 3-methyl-1-butanol, 4-methyl-1-butanol, and 5-methyl-1-butanol through a Calvin-cycle-channeled pathway in combination with a designer hydrocarbon chain elongation pathway (**40′**, **41′**, **39′**). This embodiment also takes the advantage of the broad substrate specificity (promiscuity) of 2-isopropylmalate synthase **40**, isopropylmalate isomerase **41**, 3-isopropylmalate dehydrogenase **39**, 2-keto acid decarboxylase **42**, and short-chain alcohol dehydrogenase **43** so that they may also serve as: designer isopropylmalate synthase **40′**, designer isopropylmalate isomerase **41′**, designer 3-isopropylmalate dehydrogenase **39′**,

designer 2-keto acid decarboxylase **42′**, and short-chain alcohol dehydrogenase **43′**, designer isopropylmalate synthase **40″**, designer isopropylmalate isomerase **41″**, designer 3-isopropylmalate dehydrogenase **39″**, designer 2-keto acid decarboxylase **42″**, and designer short-chain alcohol dehydrogenase **43″**.

The net results of the designer photosynthetic NADPH-enhanced pathway in working with the Calvin cycle (Fig. 10) are production of 4-methyl-1-pentanol ($CH_3CH(CH_3)CH_2CH_2CH_2OH$), 5-methyl-1-hexanol ($CH_3CH(CH_3)CH_2CH_2CH_2CH_2OH$), and 6-methyl-1-heptanol ($CH_3CH(CH_3)CH_2CH_2CH_2CH_2CH_2OH$) from carbon dioxide ($CO_2$) and water ($H_2O$) using photosynthetically generated ATP and NADPH according to the following process reactions:

$$6CO_2 + 7H_2O \rightarrow CH_3CH(CH_3)CH_2CH_2CH_2OH + 9O_2 \quad (17)$$

$$14CO_2 + 16H_2O \rightarrow 2CH_3CH(CH_3)CH_2CH_2CH_2CH_2OH + 21O_2 \quad (18)$$

$$8CO_2 + 9H_2O \rightarrow CH_3CH(CH_3)CH_2CH_2CH_2CH_2CH_2OH + 12O_2 \quad (19)$$

3 Use of Designer Photosynthetic Organisms with Photobioreactor for Production and Harvesting of Butanol and Related Higher Alcohols

The designer photosynthetic organisms with designer Calvin-cycle channeled photosynthetic NADPH-enhanced pathways (Figs. 1 and 4–10) can be used with photobioreactors for production and harvesting of butanol and/or related higher alcohols. The said butanol and/or related higher alcohols are selected from the group consisting of: 1-butanol, 2-methyl-1-butanol, isobutanol, 3-methyl-1-butanol, 1-hexanol, 1-octanol, 1-pentanol, 1-heptanol, 3-methyl-1-pentanol, 4-methyl-1-hexanol, 5-methyl-1-heptanol, 4-methyl-1-pentanol, 5-methyl-1-hexanol, 6-methyl-1-heptanol, and combinations thereof.

The said designer photosynthetic organisms such as designer transgenic oxyphotobacteria and algae comprise designer Calvin-cycle-channeled and photosynthetic NADPH-enhanced pathway gene(s) and biosafety-guarding technology for enhanced photobiological production of butanol and related higher alcohols from carbon dioxide and water. According to one of the various embodiments, it is a preferred practice to grow designer photosynthetic organisms photoautotrophically using carbon dioxide (CO_2) and water (H_2O) as the sources of carbon and electrons with a culture medium containing inorganic nutrients. The nutrient elements that are commonly required for oxygenic photosynthetic organism growth are: N, P, and K at the concentrations of about 1–10 mM, and Mg, Ca, S, and Cl at the concentrations of about 0.5–1.0 mM, plus some trace elements Mn, Fe, Cu, Zn, B, Co, Mo among others at μM concentration levels. All of the mineral nutrients can be supplied in an aqueous minimal medium that can be made with well-established recipes of oxygenic photosynthetic organism (such as algal), culture media using water (freshwater

for the designer freshwater algae; seawater for the salt-tolerant designer marine algae), and relatively small of inexpensive fertilizers and mineral salts such as ammonium bicarbonate (NH_4HCO_3) (or ammonium nitrate, urea, ammonium chloride), potassium phosphates (K_2HPO_4 and KH_2PO_4), magnesium sulfate heptahydrate ($MgSO_4.7H_2O$), calcium chloride ($CaCl_2$), zinc sulfate heptahydrate ($ZnSO_4.7H_2O$), iron (II) sulfate heptahydrate ($FeSO_4.7\ H_2O$), and boric acid (H_3BO_3), among others. That is, large amounts of designer algae (or oxyphotobacteria) cells can be inexpensively grown in a short period of time because, under aerobic conditions such as in an open pond, the designer algae can photoautotrophically grow by themselves using air CO_2 as rapidly as their wild-type parental strains. This is a significant feature (benefit) of the invention that could provide a cost-effective solution in generation of photoactive biocatalysts (the designer photosynthetic biofuel-producing organisms such as designer algae or oxyphotobacteria) for renewable solar biofuel energy production.

According to one of the various embodiments, when designer photosynthetic organism culture is grown and ready for photobiological production of butanol and/or related higher alcohols, the designer photosynthetic organism cells are then induced to express the designer Calvin-cycle channeled photosynthetic NADPH-enhanced pathway(s) to photobiologically produce butanol and/or related higher alcohols from carbon dioxide and water. The method of induction is designer pathway gene(s) specific. For example, if/when a nirA promoter is used to control the designer Calvin-cycle channeled pathway gene(s) (such as those of SEQ ID NOS: 58–69, 72, and 73 listed in US Patent Application Publication No. 2011/0177571 A1) which represent a designer transgenic *Thermosynechococcus* that comprises the designer genes of a Calvin-cycle 3-phophoglycerate-branched photosynthetic NADPH-enhanced pathway (numerically labeled as **34**, **35**, **03**-**05**, **36**-**42**, and **12** in Fig. 4) for photobiological production of 1-butanol from carbon dioxide and water, the designer transgenic *Thermosynechococcus* is grown in a minimal liquid culture medium containing ammonium (but no nitrate) and other inorganic nutrients. When the designer transgenic *Thermosynechococcus* culture is grown and ready for photobiological production of biofuel 1-butanol, nitrate fertilizer will then be added into the culture medium to induce the expression of the designer nirA-controlled Calvin-cycle-channeled pathway to photobiologically produce 1-butanol from carbon dioxide and water in this example.

For the designer photosynthetic organism(s) with anaerobic promoter-controlled pathway(s) such as the designer transgenic *Nostoc* that contains designer *hox*-promoter-controlled Calvin-cycle 3-phophoglycerate-branched pathway genes of SEQ ID NOS: 104–109 (listed in US Patent Application Publication No. 2011/0177571 A1), anaerobic conditions can be used to induce the expression of the designer pathway gene(s) for photobiological production of 2-methyl-1-butanol from carbon dioxide and water (Fig. 5). That is, when the designer transgenic *Nostoc* culture is grown and ready for photobiological biofuel production, its cells will then be placed (or sealed) into certain anaerobic conditions to induce the expression of the designer *hox*-controlled pathway gene(s) to photobiologically produce 2-methyl-1-butanol from carbon dioxide and water.

For those designer photosynthetic organism(s) that contains a heat- and light-responsive promoter-controlled and nirA-promoter-controlled pathway(s) such as the designer transgenic *Prochlorococcus* that contains a set of designer *groE*-promoter-controlled and nirA-promoter-controlled Calvin-cycle 3-phophoglycerate-branched pathway genes of SEQ ID NOS: 110–118 (listed in US Patent Application Publication No. 2011/0177571 A1), light and heat are used in conjunction with nitrate addition to induce the expression of the designer pathway genes for photobiological production of isobutanol from carbon dioxide and water (Fig. 6).

According to another embodiment, use of designer marine algae or marine oxyphotobacteria enables the use of seawater and/or groundwater for photobiological production of biofuels without requiring freshwater or agricultural soil. For example, designer *P. marinus* that contains the designer genes of SEQ ID NOS: 110–117 and 119–122 (listed in US Patent Application Publication No. 2011/0177571 A1) can use seawater and/or certain groundwater for photoautotrophic growth and synthesis of 3-methyl-1-butanol from carbon dioxide and water with its *groE* promoter-controlled designer Calvin-cycle-channeled pathway (identified as **34** (native), **35**, **03**-**05**, **53**-**55**, **38**-**40**, **42**, and **57** in Fig. 6). The designer photosynthetic organisms can be used also in a sealed photobioreactor that is operated on a desert for production of isobutanol with highly efficient use of water since there will be little or no water loss by evaporation and/or transpiration that a common crop system would suffer. That is, this embodiment may represent a new generation of renewable energy (butanol and related higher alcohols) production technology without requiring arable land or freshwater resources.

According to another embodiment, use of nitrogen-fixing designer oxyphotobacteria enables photobiological production of biofuels without requiring nitrogen fertilizer. For example, the designer transgenic *Nostoc* that contains designer *hox*-promoter-controlled genes of SEQ ID NOS: 104–109 (listed in US Patent Application Publication No. 2011/0177571 A1) is capable of both fixing nitrogen (N_2) and photobiologically producing 2-methyl-1-butanol from carbon dioxide and water (Fig. 6). Therefore, use of the designer transgenic *Nostoc* enables photoautotrophic growth and 2-methyl-1-butanol synthesis from carbon dioxide and water without requiring nitrogen fertilizer.

Certain designer oxyphotobacteria are designed to perform multiple functions. For example, the designer transgenic *Cyanothece* that contains designer *nirA* promoter-controlled genes of SEQ ID NOS: 123–127 (listed in US Patent Application Publication No. 2011/0177571 A1) is capable of (1) using seawater, (2) N_2 fixing nitrogen, and photobiological producing 1-hexanol from carbon dioxide and water (Fig. 8). Use of this type of designer oxyphotobacteria enables photobiological production of advanced biofuels such as 1-hexanol using seawater and without requiring nitrogen fertilizer.

According to one of various embodiments, a method for photobiological production and harvesting of butanol and related higher alcohols comprises: (a) introducing a transgenic photosynthetic organism into a photobiological reactor system, the transgenic photosynthetic organism comprising transgenes coding for a set of enzymes configured to act on an intermediate product of a Calvin cycle and to convert the intermediate product into butanol and related higher alcohols; (b) using

reducing power and energy associated with the transgenic photosynthetic organism acquired from photosynthetic water splitting and proton gradient-coupled electron transport process in the photobioreactor to synthesize butanol and related higher alcohols from carbon dioxide and water; and (c) using a product separation process to harvest the synthesized butanol and/or related higher alcohols from the photobioreactor.

In summary, there are a number of embodiments on how the designer organisms may be used for photobiological butanol (and/or related higher alcohols) production. One of the preferred embodiments is to use the designer organisms for direct photosynthetic butanol production from CO_2 and H_2O with a photobiological reactor and butanol-harvesting (filtration and distillation/evaporation) system, which includes a specific operational process described as a series of the following steps: (a) growing a designer transgenic organism photoautotrophically in minimal culture medium using air CO_2 as the carbon source under aerobic (normal) conditions before inducing the expression of the designer butanol-production-pathway genes; (b) when the designer organism culture is grown and ready for butanol production, sealing or placing the culture into a specific condition to induce the expression of designer Calvin-cycle-channeled pathway genes; (c) when the designer pathway enzymes are expressed, supplying visible light energy such as sunlight for the designer-genes-expressed cells to work as the catalysts for photosynthetic production of butanol and/or related higher alcohols from CO_2 and H_2O; (d) harvesting the product butanol and/or related higher alcohols by any method known to those skilled in the art. For example, harvesting the butanol and/or related higher alcohols from the photobiological reactor can be achieved by a combination of membrane filtration and distillation/evaporation butanol-harvesting techniques.

The above process to use the designer organisms for photosynthetic production and harvesting of butanol and related higher alcohols can be repeated for a plurality of operational cycles to achieve more desirable results. Any of the steps (a)–(d) of this process described earlier can also be adjusted in accordance with the invention to suit for certain specific conditions. In practice, any of the steps (a)–(d) of the process can be applied in full or in part, and/or in any adjusted combination as well for enhanced photobiological production of butanol and higher alcohol in accordance with this invention.

In addition to butanol and/or related higher alcohols production, it is also possible to use a designer organism or part of its designer butanol (higher alcohols) production pathway(s) to produce certain intermediate products of the designer Calvin-cycle-channeled pathways (Figs. 1 and 4–10) including (but not limited to): butyraldehyde, butyryl-CoA, crotonyl-CoA, 3-hydroxybutyryl-CoA, acetoacetyl-CoA, acetyl-CoA, pyruvate, phosphoenolpyruvate, 2-phosphoglycerate, 1,3-diphosphoglycerate, glyceraldehye-3-phosphate, dihydroxyacetone phosphate, fructose-1,6-diphosphate, fructose-6-phosphate, glucose-6-phosphate, glucose, glucose-1-phosphate, citramalate, citraconate, methyl-D-malate, 2-ketobutyrate, 2-ketovalerate, oxaloacetate, aspartate, homoserine, threonine, 2-keto-3-methylvalerate, 2-methylbutyraldehyde, 3-methylbutyraldehyde, 4-methyl-2-oxopentanoate, 3-isopropylmalate, 2-isopropylmalate, 2-oxoisovalerate, 2,3-dihydroxy-isovalerate, 2-acetolactate, isobutyraldehyde, 3-keto-C6-acyl-CoA, 3-hydroxy-C6-acyl-CoA, C6-enoyl-CoA,

C6-acyl-CoA, 3-keto-C8-acyl-CoA, 3-hydroxy-C8-acyl-CoA, C8-enoyl-CoA, C8-acyl-CoA, octanal, 1-pentanol, 1-hexanal, 1-heptanal, 2-ketohexanoate, 2-ketoheptanoate, 2-ketooctanoate, 2-ethylmalate, 3-ethylmalate, 3-methyl-1-pentanal, 4-methyl-1-hexanal, 5-methyl-1-heptanal, 2-hydroxy-2-ethyl-3-oxobutanoate, 2,3-dihydroxy-3-methyl-pentanoate, 2-keto-4-methyl-hexanoate, 2-keto-5-methyl-heptnoate, 2-keto-6-methyl-octanoate, 4-methyl-1-pentanal, 5-methyl-1-hexanal, 6-methyl-1-heptanal, 2-keto-7-methyl-octanoate, 2-keto-6-methyl-heptanoate, and 2-keto-5-methyl-hexanoate.

According to one of various embodiments, therefore, a further embodiment comprises an additional step of harvesting the intermediate products that can be produced also from an induced transgenic designer organism. The production of an intermediate product can be selectively enhanced by switching off a designer-enzyme activity that catalyzes its consumption in the designer pathways. The production of a said intermediate product can be enhanced also by using a designer organism with one or some of designer enzymes omitted from the designer butanol-production pathways. For example, a designer organism with the butanol dehydrogenase or butyraldehyde dehydrogenase omitted from the designer pathway(s) of Fig. 1 may be used to produce butyraldehyde or butyryl-CoA, respectively. Therefore, the present invention has many applications for production of both advanced biofuels and/or bioproducts.

References

1. Gfeller R, Gibbs M (1984) Fermentative metabolism of *Chlamydomonas reinhardtii*. Plant Physiol 75:212–218
2. Lee JW (2009) Designer organisms for photobiological butanol production from carbon dioxide and water. PCT International Patent Application Publication Number WO 2009/105733 A2
3. Lee JW (2010) Designer Calvin-cycle-channeled production of butanol and related higher alcohols. US Patent Application Publication No. 2011/0177571 A1
4. Lee JW, Blankinship SL, Greenbaum E (1995) Temperature effect on production of hydrogen and oxygen by *Chlamydomonas* cold strain CCMP1619 and wild type 137c. Appl Biochem Biotechnol 51(52):379–386
5. Lee JW, Mets L, Greenbaum E (2002) Improvement of photosynthetic efficiency at high light intensity through reduction of chlorophyll antenna size. Appl Biochem Biotechnol 98–100: 37–48
6. Nakajima Y, Tsuzuki M, Ueda R (1999) Reduced photoinhibition of a phycocyanin-deficient mutant of *Synechocystis* PCC 6714. J Appl Phycol 10:447–452
7. Quinn JM, Barraco P, Ericksson M, Merchant S (2000) Coordinate copper- and oxygen-responsive Cyc6 and Cpx1 expression in *Chlamydomonas* is mediated by the same element. J Biol Chem 275:6080–6089
8. Loppes R, Radoux M (2002) Two short regions of the promoter are essential for activation and repression of the nitrate reductase gene in *Chlamydomonas reinhardtii*. Mol Genet Genomics 268:42–48
9. Schroda M, Blocker D, Beek CF (2000) The HSP70A promoter as a tool for the improved expression of transgenes in *Chlamydomonas*. Plant J 21:121–131
10. Sjoholm J, Oliveira P, Lindblad P (2007) Transcription and regulation of the bidirectional hydrogenase in the Cyanobacterium *Nostoc* sp. strain PCC 7120. Appl Environ Microbiol 73(17):5435–5446

11. Qi Q, Hao M, Ng WO, Slater SC, Baszis SR, Weiss JD, Valentin HE (2005) Application of the *Synechococcus nirA* promoter to establish an inducible expression system for engineering the *Synechocystis* tocopherol pathway. Appl Environ Microbiol 71(10):5678–5684
12. Maeda S, Kawaguchi Y, Ohe TA, Omata T (1998) *cis*-Acting sequences required for NtcB-dependent, nitrite-responsive positive regulation of the nitrate assimilation operon in the Cyanobacterium *Synechococcus* sp. strain PCC 7942. J Bacteriol 180(16):4080–4088
13. Kojima K, Nakamoto H (2007) A novel light- and heat-responsive regulation of the groE transcription in the absence of HrcA or CIRCE in cyanobacteria. FEBS Lett 581:1871–1880
14. Erbe JL, Adams AC, Taylor KB, Hall LM (1996) Cyanobacteria carrying an *smt-lux* transcriptional fusion as biosensors for the detection of heavy metal cations. J Ind Microbiol 17:80–83
15. Michel KP, Pistorius EK, Golden SS (2001) Unusual regulatory elements for iron deficiency induction of the *idiA* gene of *Synechococcus elongatus* PCC 7942. J Bacteriol 183(17): 5015–5024
16. Patterson-Fortin LM, Colvin KR, Owttrim GW (2006) A LexA-related protein regulates redox-sensitive expression of the cyanobacterial RNA helicase, *crhR*. Nucleic Acids Res 34(12):3446–3454
17. Fang F, Barnum SR (2004) Expression of the heat shock gene *hsp16.6* and promoter analysis in the Cyanobacterium, *Synechocystis* sp. PCC 6803. Curr Microbiol 49:192–198
18. Nakamoto H, Suzuki N, Roy SK (2000) Constitutive expression of a small heat-shock protein confers cellular thermotolerance and thermal protection to the photosynthetic apparatus in cyanobacteria. FEBS Lett 483:169–174
19. Casey ES, Grossman A (1994) In vivo and in vitro characterization of the light-regulated *cpcB2A2* promoter of *Fremyella diplosiphont*. J Bacteriol 176(20):6362–6374
20. Domain F, Houot L, Chauvat F, Cassier-Chauvat C (2004) Function and regulation of the cyanobacterial genes *lexA*, *recA* and *ruvB*: LexA is critical to the survival of cells facing inorganic carbon starvation. Mol Microbiol 53(1):65–80
21. Pattanayak D, Chatterjee SR (1998) Nicotinamide adenine dinucleotide phosphate phosphatase facilitates dark reduction of nitrate: regulation by nitrate and ammonia. Biol Plantarum 41(1):75–84
22. Muto S, Miyachi S, Usuda H, Edwards GE, Bassham JA (1981) Light-induced conversion of nicotinamide adenine dinucleotide to nicotinamide adenine dinucleotide phosphate in higher plant leaves. Plant Physiol 68(2):324–328
23. Matsumura-Kadota H, Muto S, Miyachi S (1982) Light-induced conversion of NAD^+ to $NADP^+$ in chlorella cells. Biochim Biophys Acta 679(2):300–307
24. Liszewski K (2003) Progress in RNA interference. Genet Eng News 23(11):1–59
25. Fire Xu, Montgomery K, Driver M (1998) Potent and specific genetic interference by double-stranded RNA in *Caenorhabditis elegans*. Nature 391(6669):806–811
26. Dykxhoorn DM, Novina CD, Sharp PA (2003) Killing the messenger: short RNAs that silence gene expression. Nat Rev Mol Cell Biol 4(6):457–467
27. Lan EI, Liao JC (2011) Metabolic engineeringofcyanobacteriafor1-butanolproduction from carbon dioxide. Metab Eng 13:353–363
28. Atsumi S, Higashide W, Liao JC (2009) Direct photosynthetic recycling of carbon dioxide to isobutyraldehyde. Nat Biotechnol 27(12):1177–1182
29. Robertson DE, Jacobson SA, Morgan F, Berry D, Church GM, Afeyan NB (2011) A new dawn for industrial photosynthesis. Photosynth Res 107:269–277
30. Lee JW (2007) Designer proton-channel transgenic algae for photobiological hydrogen production. PCT International Patent Application Publication Number: WO 2007/134340 A2
31. Hanson DT, Franklin LA, Samuelsson G, Badger MR (2003) The *Chlamydomonas reinhardtii* cia3 mutant lacking a thylakoid lumen-localized carbonic anhydrase is limited by CO_2 supply to Rubisco and not photosystem II function in vivo. Plant Physiol 132:2267–2275
32. Berry S, Fischer JH, Kruip J, Hauser M, Wildner GF (2005) Monitoring cytosolic pH of carboxysome-deficient cells of Synechocystis sp. PCC 6803 using fluorescence analysis. Plant Biol (Stuttg) 7:342–347

Part V
Lipids-Based Biodiesels

Chapter 23
Production of Biodiesel and Nontoxic *Jatropha* Seedcakes from *Jatropha curcas*

Novizar Nazir, Djumali Mangunwidjaja, and M.A. Yarmo

Abstract Different processes for transesterification of *Jatropha* biodiesel production are currently available. Among them are homogeneous catalysis, heterogeneous catalysis or enzyme catalysis alcohol treatment, supercritical alcohols, lipase-catalyzed in situ reactive extraction, and homogenous-catalyzed in situ transesterification. High cost of biodiesel production is the major impediment to its large-scale commercialization. Methods to reduce the production cost of biodiesel must be developed. One way to reduce production costs is to increase the added value of protein-rich *Jatropha* seedcakes, the by-product of oil extraction, through detoxification process. Development of integrated biodiesel production process and detoxification process results in two products, namely biodiesel and protein-rich seedcakes that can be used for animal feed. This chapter provides information concerning *Jatropha* potential, current development of biodiesel and nontoxic seedcakes production from *Jatropha curcas* and implication of biodiesel production on global warming, environmental impact, and energy efficiency.

N. Nazir (✉)
Faculty of Agricultural Technology, Andalas University, Padang, West Sumatra 25163, Indonesia
e-mail: nazir_novizar@yahoo.com

D. Mangunwidjaja
Department of Agroindustrial Technology, Bogor Agricultural University,
Bogor, West Java, Indonesia

M.A. Yarmo
School of Chemical Science and Food Technology,
Universiti Kebangsaan Malaysia, Bangi, Selangor, Malaysia

J.W. Lee (ed.), *Advanced Biofuels and Bioproducts*, DOI 10.1007/978-1-4614-3348-4_23,

1 Introduction

Biodiesel, an alternative diesel fuel, is made from renewable biological sources such as vegetable oils and animal fats. It is a clean combustion, biodegradable, nontoxic fuel and has low emission of carbon monoxide. These conditions give environmental benefits. Research found that the use of biodiesel has potential to reduce pollution levels and possible carcinogens ([12, 20, 22, 70, 92, 97]). In addition, practically biodiesel contains no sulfur and has good lubrication properties [38, 50, 70].

One source of vegetable oils which has good prospects to be developed as a raw material of biodiesel is *Jatropha curcas.* The oil which is produced from *Jatropha* has potential as an alternative fuel and not derived from food crops like corn, palm, soybean, etc. Thus, it is not competitive with food consumption.

The genus *Jatropha* belongs to the Euphorbiaceae family, consisting of about 170 species. Linnaeus [47] is the one who firstly gave the name *Jatropha* L. to the *Jatropha* in "Species Plantarum" and this is still acknowledged today. The genus name *Jatropha* is derived from the Greek word *jatr'os* (physician) and *troph'e* (food), which indicates its use as being edible or medicinally useful [35].

Jatropha was originated from tropical America, but now it grows well in many parts of tropic and subtropic regions in Africa and Asia. These small trees can grow to 20 ft high under favorable conditions in areas with low to high rainfall (200–1,500 mm/year). In low rainfall areas and in prolonged rainless periods, the plant let its leaves fall as a response to drought [64].

The fruit of *Jatropha* can be used for various purposes including fuel. The seeds *contain* viscous oil, which can be used as a diesel. In addition to being a source of oil, *Jatropha* also provides seedcake, by-product of oil extraction process, that serves as a highly nutritious and economic protein supplement in animal feed, if the toxins are removed [13]. The purpose of this review is to provide information concerning its potential and current development in the field of production of biodiesel and nontoxic seedcakes from *J. curcas* and the implication of biodiesel production on global warming, environmental impact, and energy efficiency.

2 Chemical and Physical Aspects of *Jatropha curcas*

2.1 Chemical Composition of Jatropha Kernel

The dry fruit husk of *Jatropha* represents around 35% of the fruit and host 1–4 seeds. Individual seeds of *Jatropha* have an average weight of 0.40 g to over 1 g. The seeds have hard, black outer shell containing a white kernel. The proportion of shell and kernel range from 350 to 400 g/kg and from 600 to 650 g/kg, respectively. The seeds contain about 300–350 g/kg oil which can be used directly as fuel or, in its transesterified form, as a substitute for diesel [54]. Figure 1 illustrates the whole plant of *J. curcas*, its parts, and its average proportion on dry weight basis starting with 1,000 kg of fruit.

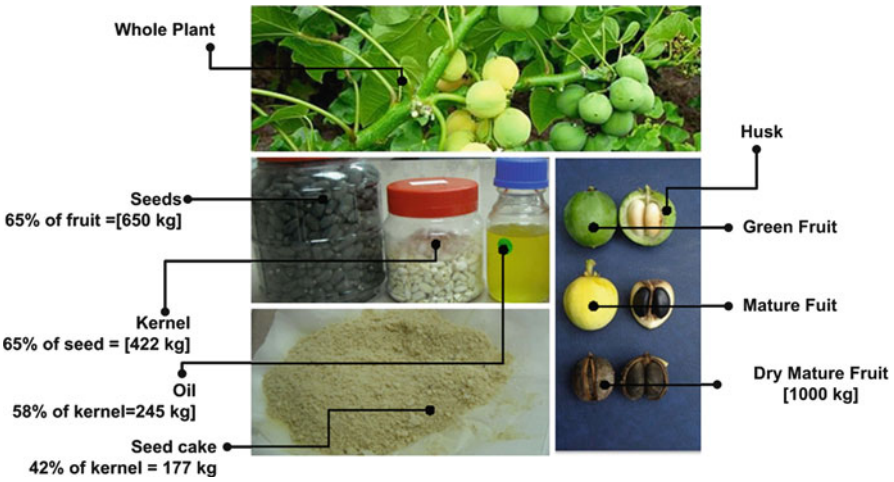

Fig. 1 Whole plant of *Jatropha curcas*, its parts, and the average proportion on dry weight basis starting with 1,000 kg of fruit

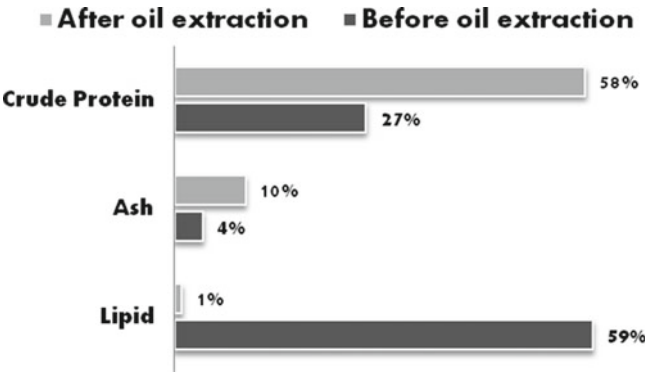

Fig. 2 Chemical composition of *Jatropha* kernel before oil extraction and after oil extraction

Assuming that 1 ha of land consisting of 2,500 *Jatropha* plants and each tree has 40 branches, and each branch has 3 bunches of fruit/year, and each cluster could produce 10–15 fruits/bunch (30–45 seeds), then the number of seeds that would be generated from area of 1 ha is 2,500 × 40 branch × 3 bunches × (10–15) fruits × 3 seed = 9,000,000 – 13,500,500 seeds. If 1 kg consists of 2,000 dry seeds, the production of *Jatropha* per hectare per year would be 4.5–6.75 tons of dry seeds/ha. Assuming that an average seed yield of 5 tons/ha (2 tons/acre) could be achieved, estimated theoretical yield of biodiesel is 750 kg/acre and its seedcake product is 500 kg/acre.

Kernel of *Jatropha* contains 27–32% of protein, 58–60% of oil, and 3.6–5.0% of ash content. After the oil extraction of kernel (fully defatted), *Jatropha* seedcake will have a protein content of 55–60%, lipid content of 0.6–1.5%, and ash content of 9.6–12.1% (Fig. 2), with high essential amino acid composition (Table 1)

Table 1 Amino acid composition (g/16 g nitrogen) of kernel meal from toxic, nontoxic genotypes, and protein concentrate obtained from *Jatropha* seedcake

Amino acid	Protein concentrate[a]	Toxic variety [55]	Nontoxic variety [55]	Soybean meal [55]
Essential amino acids				
Methionine	1.66	1.91	1.76	1.22
Cystine	1.34	2.24	1.58	1.70
Valine	5.18	5.19	5.30	4.59
Isoleucine	4.47	4.53	4.85	4.62
Leucine	7.08	6.94	7.50	7.72
Phenylalanine	5.42	4.34	4.89	4.84
Tyrosine	3.20	2.99	3.78	3.39
Histidine	3.51	3.30	3.08	2.50
Lysine	3.00	4.28	3.40	6.08
Arginine	14.16	11.80	12.90	7.13
Threonin	3.56	3.96	3.59	3.76
Tryptophan	1.21	1.31	ND	1.24
Nonessential amino acids				
Serine	5.23	4.80	4.82	5.67
Glutamic acid		14.68	15.91	16.90
Aspartic acid	12.50	9.49	9.92	11.30
Proline	5.45	4.96	3.80	4.86
Glycine	5.10	4.92	4.61	4.01
Alanine	5.47	5.21	4.94	4.23

ND not determined

[a]Proteins from the seed cakes were solubilized at pH 11 for 1 h at 60°C and the precipitation of these proteins was done by lowering the pH to 4 [54]

[53, 55, 56]. Composition of the essential amino acid of *Jatropha* (except lysine) confirms identical pattern with the existing amino acids in soybean [91].

2.2 *Fatty Acid Composition and Physicochemical Properties of Jatropha Oil*

Table 2 shows the fatty acid composition of *Jatropha* oil containing of 23.6% of saturated fatty acids mainly from palmitic, stearic, and myristic acid and 76.4% of unsaturated fatty acids which consist of mainly oleic, linoleic acid, and palmitoleic. The physicochemical properties of *Jatropha* oil which is extracted from the seeds of different origin viz., Malaysia, Indonesia, Thailand, Nigeria, Brazil, are given in Table 3.

The ability of fluid to pump and flow within an engine is determined by its viscosity. The desired viscosity of diesel fuel ranges from 1.9 to 4.1 cSt. Transesterification is one of the recognized and efficient methods to reduce the viscosity of the vegetable oil to make it suitable as a biodiesel [25].

Table 2 Fatty acids exist in *J. curcas* oil

			wt.%					
Generic name	Formula	Structure[a]	Foidl et al. [26][b]	Foidl et al. [26][c]	Gubitz et al. [29]	Haas and Mittelbach [31]	Azam et al. [11]	Average
Capric	$C_{10}H_{20}O_2$	C10:0	0.1	0.1				
Lauric	$C_{12}H_{24}O_2$	C12:0						
Miristic	$C_{14}H_{28}O_2$	C14:0	0.1	0.1	0–0.1		1.4	
Palmitic	$C_{16}H_{32}O_2$	C16:0	15.1	13.6	14.1–15.3	14.2	15.6	
Stearic	$C_{18}H_{36}O_2$	C18:0	7.1	7.4	3.7–9.8	6.9	9.7	
Arachidic	$C_{20}H_{40}O_2$	C20:0	0.2	0.3	0–0.3	–	0.4	
Behenic	$C_{22}H_{44}O_2$	C22:0	0.2	–	0–0.3	–	–	
Miristoleic	$C_{14}H_{20}O_2$	C14:1						
Palmitoleic	$C_{16}H_{30}O_2$	C16:1	0.9	0.8	0–1.3	1.4	–	
Oleic	$C_{18}H_{34}O_2$	C18:1	44.7	34.3	34.3–45.8	43.1	40.8	
Linoleic	$C_{18}H_{32}O_2$	C18:2	31.4	43.2	29.0–44.2	34.4	32.1	
Linolenic	$C_{18}H_{30}O_2$	C18:3	0.2	–	0–0.3	–		
Saturated			22.8	21.7	22.6	23.7	27.1	23.6
Unsaturated			77.2	78.3	77.4	76.3	78.9	76.4

[a]Number of carbon chain:number of double bond
[b]Variety of Caboverde
[c]Variety of Nicaragua

Table 3 Physicochemical properties of tropical *J. curcas* oil from different origin

Properties	Malaysia [73]	Indonesia [61]	Thailand [25]	Nigeria [8]	Brazil [21]
Density	0.90	0.90	0.90		0.92
Viscosity(cSt)	47.50	53.94	39.20		30.69
Iodine value	193.55	200.66	216.09	105.20	
Peroxide value	1.90				
Acid value	2.38	9.91		3.50	8.45
Free fatty acids (FFA) (%)	2.23			1.76	
Saponification value	197.8	183.2		198.85	

The iodine value is a measurement for the unsaturation level in fats and oils; a high iodine value is an indication of the presence of high unsaturation levels in the oils [43]. The high iodine value of *Jatropha* oil is due to the presence of high amounts of unsaturated fatty acids such as oleic and linoleic acid (Table 3).

The peroxide value determines the formation of hydro peroxides (primary oxidation products) [30]. This can be associated with the presence of higher amounts of polyunsaturated fatty acids such as linoleic acid (Table 3). The instability of any oil is directly related to the level of unsaturation.

Acid value ("acid number" or "acidity") is the mass of potassium hydroxide (KOH) in milligrams that is required to neutralize 1 g of chemical substance.

The acid value of edible oils or their corresponding esters indicates the quantity of free fatty acids (FFA) and mineral acids (negligible) present in the sample.

Fatty acids can be bound or attached to other molecules such as triglycerides or phospholipids. When they are not attached to other molecules, they are known as "free" fatty acids (FFA). FFA is detrimental to the biodiesel-making process. For biodiesel production purposes, FFA content of *Jatropha* oil indicates two types of *Jatropha* oil: low FFA oil (FFA<2.5%) and high FFA oil (FFA>2.5%) [61]. A high saponification value indicates that *Jatropha* oil possesses normal triglycerides and may be useful in the production of liquid soap and shampoo [30].

2.3 Jatropha Seeds and Its Toxicity

Even though the *Jatropha* seeds are rich in oil and crude protein, they are highly toxic and unsuitable for human or animal consumption. The toxic nature of oil and *Jatropha* seedcake has been demonstrated in several studies [1, 2, 5, 6, 46]. The toxic or irritant compounds found in *Jatropha* seedcake are phorbol ester (2.43 mg/g kernel in toxic varieties and 0.11 mg/g kernel of nontoxic varieties), lectin (102 mg/g kernel in toxic varieties and 51 mg/g kernel on nontoxic varieties), trypsin inhibitor activity (21.2 mg inhibitory/g meal in toxic varieties and inhibition of 26.5 mg/g meal in nontoxic varieties), phytate (9.7% in the *Jatropha* seedcake of toxic varieties and 8.9% in nontoxic varieties), and Saponin (equivalent to 2.3% diosgenin in *Jatropha* seedcake of toxic varieties and 3.4% in nontoxic varieties).

Curcin, a toxic protein isolated from the seeds, was found to inhibit protein synthesis in in vitro studies. The high concentration of phorbol esters in *Jatropha* seed has been identified as the main toxic agent of *Jatropha* which is responsible for the toxicity ([52, 4]. Several cases of poisoning *J. curcas* in humans after consumption of seeds by chance have been reported with symptoms of dizziness, vomiting, and diarrhea and in extreme conditions has been noted even cause death [13].

Lectin is also predicted to cause toxicity in *J. curcas* [16]. However, Aderibigbe et al. [3] and Aregheore et al. [9] show that the lectin is not the main toxic compounds in *Jatropha* seedcakes. Successful utilization of *Jatropha* seedcakes cannot be achieved without the removal of all of toxic and antinutritional compounds. Toxic-removal processes for seedcakes of low FFA *Jatropha* can be done directly by in situ transesterification [61] and through detoxification process using heat and chemical treatments for seedcakes of high FFA [9, 68].

3 *Jatropha* Oil as Feedstock of Biodiesel Production

The growing demand for lower-cost, nonfood, nonrainforest-based feedstock for biodiesel provides new opportunities and stimulate fresh investment in the production of lower-cost, alternative feedstock such as *Jatropha*. The governments in South Asia and Africa have identified between 20 and 50 million ha of suitable land

for *Jatropha* cultivation. Indonesia has identified nearly 23 million ha of *Jatropha* land potential. One hectare of *Jatropha* can produce between 1.5 and 2.5 tons of seed oil. *Jatropha* is now becoming one of the prime contenders for biodiesel feedstock supply in the near future [87]. This is due to the expansion of commercial-scale *Jatropha* production from India to Africa, Southeast Asia, and Latin America and to pilot programs and larger-scale ventures in China, Central Asia, South/Central America, and southern parts of the USA.

A variety of equipment is available to obtain oil from the seeds. The oil can be extracted mechanically using a press (ram, hydraulic, or screw) or chemically using organic solvents or water [12, 26, 65], three phase partitioning (TPP) extraction method [76], and supercritical extraction method [97].

The objective of oil preparation is to find an efficient and effective method in extracting oil from *Jatropha* seed. Technique of TPP with enzyme pretreatment and sonication constitutes an efficient procedure to obtain oil from *Jatropha* seed kernels. This technique can extract 97% oil within 2 h [77]. Extraction using ethyl acetate and methyl acetate is better than using hexane [83]. It was found that Gas-Assisted Mechanical Expression (GAME) process in *Jatropha* oil extraction is capable of reaching yields up to 30 wt.% higher than conventional expression under the same conditions [96].

3.1 Mechanical Press Extraction

In Indonesia, *Jatropha* oil is usually extracted by hydraulic press and screw press at 60°C heat treatment. The yield of *Jatropha* oil using hydraulic press method at maximum pressure of 20 tons is 47.2% and the oil extraction is done twice [84, 85].

In Tanzania presently, the *Jatropha* oil is obtained only mechanically with a ram press or a screw press, that is a small hand-press [89]. With the ram press method, the seeds are poured by giving a pressure on the seeds. About 5 kg of seed is needed to obtain 1 L of oil. The oil is extracted and then dripped into a container. The extraction rate of this press is quite low as the seedcake, which is left after the pressing, still contains part of the oil.

Larger expellers and screw presses which are run by an engine can also be used. The screw which turns continuously transports the seeds from one side of the press to the other while squeezing out the oil. The extraction rate of this press is higher because more oil is extracted from the seeds; the cake residue is also much dryer. The capacity of this screw is higher than that of the ram press. For example, the Sayari oil expeller, which is used in Tanzania, has a capacity of about 20 L/h (60 kg/h) and can extract 1 L of oil from 3 kg of seeds. The larger screw expellers, like Chinese expellers, can extract about 50 L/h (150 kg/h). After the oil is expelled, it is filtered by letting it stand for some times or pouring it through a cloth [89].

3.2 Aqueous and Solvent Extraction

Aqueous oil extraction (AOE) is a method in which *Jatropha* seeds are cracked and the shells are carefully removed. Shah et al. [78] used *Jatropha* kernels for oil extraction. The suspension was prepared with powdered (obtained by using a homogenizer) *Jatropha* kernels in distilled water, and then was incubated at desired temperature with constant shaking at 100 rpm for specified time period. The upper oil phase was collected after a centrifugation at 10,000 × *g* for 20 min. Enzyme-assisted AOE was performed similar to AOE. The difference is that the preparations, i.e., Protizymee, Cellulase, Pectinex Ultra SP-L, Promozyme, as well as mixture of all these enzymes, were added after the pH of the suspension was adjusted. The amounts of oil obtained were calculated as the percentage of total oil present in *Jatropha* kernels.

It is found that the use of ultrasonication as a pretreatment before aqueous oil extraction and aqueous enzymatic oil extraction is useful in the case of extraction of oil from the seeds of *J. curcas* L. [78]. The use of ultrasonication for a period of 10 min at pH 9.0 followed by AOE resulted in a yield of 67% of available oil. The maximum yield of 74% was obtained by ultrasonication for 5 min followed by aqueous enzymatic oil extraction using an alkaline protease at pH 9.0 (44 g oil/100 g *Jatropha* kernels was taken as 100% recovery). Use of ultrasonication can also reduce the process time from 18 to 6 h [78].

To obtain an optimized condition for an extraction using microwave is by using petroleum ether as the solvent, with the ratio of seed powder to solvent is at 1:3. It is done under a microwave power of 810 W for a total radiation time of 5 min [97]. The extraction rate was 31.49% with the oil product containing 5.22 mg/g of acid number and 8.78 meq/g of peroxide value. For the ultrasonic method, hexane was used as the solvent and the ratio of seed powder to solvent was 1:7; the soaking time applied is 18 h and the sonication is 0.5 h. The extraction rate was 37.37% containing 5.91 mg/g of acid number and 8.37 meq/g of peroxide value in the final oil product [97].

Alkyl acetates, especially methyl acetate and ethyl acetate, are important chemicals and suitable solvents for seed oil extraction which are assisted by Novozym 435 [83]. The results were compared to those obtained by extraction with *n*-hexane. Ground seeds were mixed with methyl acetate or ethyl acetate in screw-caped glass vials. And, 30% (w/w) of Novozym 435 based on theoretical oil content was added. The reactions were carried out at 50°C and 180 rpm for 6 h in a shaker which was fitted with a thermostat. After filtration, the ground seed mixture was mixed with another solvent and then extracted at the same condition for another 2 h. The two filtrates were pooled and centrifuged at 17,400 × *g* for 10 min; the supernatant was collected into a round bottom flask and the solvent was evaporated using a rotary evaporator. The oil content in g/100 g was 54.90% (*n*-Hexane), 55.92% (Methyl acetate), and 56.65% (Ethyl acetate) [83].

3.3 Three Phase Partitioning Extraction Method

TPP is a method which is carried out by cracking the *Jatropha* seeds and removing the shells; the kernels obtained are used for slurry preparation [76]. The slurry, with pH adjusted to the desired value with 0.1 N NaOH or 0.1 N HCl, was prepared by grinding the seed kernels in distilled water. Ammonium sulfate in an appropriate amount was added and vortexed gently; an appropriate amount of *tert*-butanol was added. Then, the slurry was incubated at 25°C for 1 h for the three phase formation. The three phases were then separated by centrifugation at 2,000 × *g* for 10 min. To obtain the oil, the upper organic layer was collected and evaporated on rotary evaporator (under reduced pressure at 50°C, for 5 min) [76].

Combining a recently developed technique of TPP with enzyme pretreatment and sonication may constitute an economical or efficient procedure for obtaining oil from *Jatropha* kernels [74]. This method only takes about 2 h. TPP has been evaluated for extraction of oil from *Jatropha* seeds. This process consisted of simultaneous addition of *t*-butanol (1:1, v/v) and 30% (w/v) ammonium sulfate to the slurry prepared from *Jatropha* seed kernels. Combination of sonication and enzyme treatment with a commercial preparation of fungal proteases at pH 9 resulted in 97% oil yield within 2 h [74].

3.4 Supercritical Carbondioxide Extraction Method

Supercritical Carbondioxide Extraction (SCE) is a process for the production of oil with high yields that do not use organic solvents. In this process, the oil is dissolved in CO_2 and extracted from the plant material [95]. SCE method developed by Yan et al. [96] resulted in the actual extraction rate 37.45%; the final oil product contained 0.79 mg/g of KOH and 3.63 meq/g of peroxide value. Here, seeds of *J. curcas* were collected and powdered. The extraction pressure was 43 MPa, temperature for the extraction was 45°C, the flow rate of CO_2 was 20 kg/h, and the extraction time was 80 min. Even though the cost of supercritical extraction methods was higher, the oil quality was the best and refining was not needed [96].

3.5 Gas-Assisted Mechanical Expression

GAME is another potential alternative process for the production of oil with high yields which do not use organic solvents. In this process, CO_2 is dissolved in the oil contained in the seeds before pressing the seeds [93]. It was found that at the same effective mechanical pressure (absolute mechanical pressure minus the actual CO_2-pressure), the liquid content was the same in both conventional and GAME press cakes. The liquid in the GAME press cake was saturated with CO_2 (typically

20–50 wt.%), reducing the oil content compared to the conventional cake by the same amount. The contribution of this effect increased with increasing solubility of the CO_2 in the oil. Furthermore, the dissolved CO_2 reduced the viscosity of oil by about an order of magnitude [93], which could increase oil extraction. Some additional oil was removed by entrainment in the gas flow during depressurization of the cake.

GAME has some advantages compared with conventional pressing. The first advantage of GAME is the increased yield at lower mechanical pressure. Compared with supercritical extraction, the amount of CO_2 that has to be recycled is reduced by two orders of magnitude from typically 1 kg of CO_2/kg of seeds [93] to 100 kg of CO_2/kg of seeds [69]. Therefore, the energy and equipment cost for the solvent recycle can be reduced. Compared with SCE, the second advantage of GAME is CO_2-pressure required is low, which is approximately 10 MPa. In contrast, for SCE extraction, pressures of 40–70 MPa are not unusual ([69]; Rosa et al. 2005). These two effects provide a significant reduction in the energy requirements for recycling and repressurising the CO_2. Additionally, some reports in literature suggest that the use of CO_2 at 7–20 MPa has a sterilizing effect on the substrates [80, 94]; this may be a beneficial side-effect of the GAME process.

The general applicability of the GAME process to enhance the oil recovery from oilseeds was shown by pressing experiments for sesame, linseed, rapeseed, *Jatropha,* and palm kernel by Willems et al. [95]. It was proved that GAME was capable of reaching yields that were up to 30 wt.% higher than conventional expression under the same conditions. Despite the lower yields for hulled seeds in conventional expression, GAME yields for hulled and dehulled seeds were very similar. The oil yields obtained for GAME increased with increasing effective mechanical pressure; the yields were the highest at a temperature of 100°C. These effects were similar to conventional expression. With CO_2-pressure up to 10 MPa, the oil yield increased significantly. However, increasing the CO_2-pressure above 10 MPa did not significantly increase the oil yield.

4 Production of Biodiesel

The method commonly used for production of biodiesel is the transesterification of vegetable oils with methanol, using alkali, acid, or enzyme catalyst. Transesterification, also called alcoholysis, is the reaction of triglycerides with alcohols to generate, for example, methyl or ethyl esters and glycerol as a by-product. Usually a catalyst is used to improve the reaction rate and yield. The reaction requires excess of alcohols to improve the efficiency of the transesterification process [54].

There are important variables that affect the yield of biodiesel from transesterification; they are: reaction temperature, molar ratio of alcohol and oil, catalyst, reaction time, presence of moisture and FFA, and mixing intensity [15, 77, 81]. The rate of reaction is strongly determined by the reaction temperature. However, given enough time will help the reaction proceed to near completion even

at room temperature. The reaction is commonly conducted close to the boiling point of alcohol at atmospheric pressure [77].

It is observed that the stoichiometry of the transesterification reaction needs 3 mol of alcohol/mol of triglyceride to yield 3 mol of fatty esters and 1 mol of glycerol. To shift the transesterification reaction to the right, it is necessary to use a large excess of alcohol or remove one of the products from the reaction mixture continuously. Wherever feasible, the second option is preferential because it can drive the reaction toward the completion. The reaction rate is at its highest if 100% excess methanol is used. In industrial processes, a molar ratio of 6:1 is normally used to obtain methyl ester yields higher than 98% by weight [77].

Catalysts are categorized as alkali, acid, enzymes, or heterogeneous catalyst. Among these, alkali catalysts such as sodium hydroxide, sodium methoxide, potassium hydroxide, and potassium methoxide are more effective [15]. It is found that alkali-catalyzed transesterification is much faster than acid-catalyzed reaction. However, acid-catalyzed transesterification reaction is more suitable if a vegetable oil has high FFA and water content. Most commercial transesterification reactions are conducted with alkaline catalysts. This is partly due to faster esterification and partly to alkaline catalysts which are less corrosive to industrial equipment than acidic catalysts. It is observed that sodium methoxide is more effective than sodium hydroxide. Sodium alkoxides are among the most efficient catalysts used for this purpose. However, due to its low cost, NaOH has been used widely in large-scale transesterification [15].

Different processes for transesterification of vegetable oils for the production of *J. curcas* biodiesel are currently available. Among them are homogenous catalysis treatment [14, 17, 26, 72, 83, 84, 88, 90], heterogeneous catalyst [34, 58] or enzyme catalysis alcohol treatment [55, 56, 73], supercritical alcohols treatments and subcritical methanol ([68, 86]) and Lipase-catalyzed in situ reactive extraction [82], and homogenous-catalyzed in situ transesterification [58].

4.1 Biodiesel Production Using Homogeneous Chemical Catalyst

Foidl et al. [26] reported a technical process for processing seed oil and production of methyl ester and ethyl ester from the oil of *Jatropha* seeds. The fuel properties were also determined. Production of biodiesel used two-step transesterification: alkali–alkali transesterification for methyl ester and alkali–acid transesterification for ethyl ester.

Chitra et al. [17] found that methyl ester yield of 98% was obtained using 20 wt.% methanol and 1.0% NaOH at 60°C. The maximum reaction time needed for a maximum ester yield was 90 min. Total biodiesel of 96% was obtained from experimental studies on large-scale production (reactor capacity of 75 kg). Esterification–transesterification reaction for *Jatropha* biodiesel was done by Sudradjat et al. [83, 84], but methyl ester yield was not reported.

Tiwari et al. [88] and Berchmans and Hirata [14] have developed a technique to produce biodiesel from *Jatropha* with high FFA contents (15% FFA). They selected two-stage transesterification processes to improve methyl ester yield. The first stage involved the acid pretreatment process to reduce the FFA level of crude *Jatropha* seed oil to less than 1%. The second was the alkali base-catalyzed transesterification process resulting in 90% methyl ester yield. Tiwari et al. [88] found that the optimum combination to reduce the FFA of *Jatropha* oil from 14% to less than 1% was 1.43% v/v H_2SO_4 acid catalyst, 0.28 v/v methanol-to-oil ratio, and 88-min reaction time at a reaction temperature of 60°C. This process produced yield of biodiesel of more than 99%.

Berchmans and Hirata [14] reduced the high FFA level of *Jatropha* oil to less than 1% by a two-step process. The first step was carried out with 0.60 w/w methanol-to-oil ratio in the presence of 1% w/w H_2SO_4 as an acid catalyst in 1 h reaction at 50°C. The second step was transesterified using 0.24 w/w methanol to oil and 1.4% w/w NaOH to oil as alkaline catalyst to produce biodiesel at 65°C. The final yield for methyl esters was achieved ca. 90% in 2 h.

4.2 Biodiesel Production Using Heterogeneous Solid Super Base Catalyst

An environmentally kind process was developed for the production of biodiesel from *Jatropha* oil using a heterogeneous solid super base catalyst and calcium oxide. The results revealed that under the optimum conditions of catalyst calcinations, temperature of 900°C, reaction temperature of 70°C, reaction time of 2.5 h, catalyst dosage of 1.5%, and methanol/oil molar ratio of 9:1, the oil conversion was 93% [34]. Nazir [58] found that the yield of JCO FAME could reach up to 94.35% using the following reaction conditions: 79.33 min reaction time, 10.41:1 methanol:oil molar ratio, and 0.99% of CaO catalyst at reaction temperature 65°C.

4.3 Biodiesel Production Using Heterogeneous Enzyme Catalyst

Interest in using lipases as enzymatic catalyst for the production of alkyl fatty acid esters continuously grows. Some people work on the triglyceride by converting them to methyl esters, while some work on fatty acids. One of the main obstacles to the biocatalytic production of biodiesel is high cost of the enzyme; enzyme recycling might be the solution to this problem.

It was found that *Pseudomonas fluorescens* lipase immobilized on kaolinite lost one third of its activity when it is used for the second time, but no further decrease was observed in successive applications. The initial decrease in activity was put down to enzyme desorption from the solid support that was not observed after repeated (ten times) use [36]. Repeated batch reactions revealed that *Rhizomucor miehei*

lipase had high stability, which retained about 70% of its initial conversion after 8 cycles (24 h each cycle). Meanwhile, under the same experimental conditions, *Thermomyces lanuginosa* retained only 35% of the initial conversion. This difference was credited to factors such as inactivation of the biocatalyst in the oil phase, the type of carrier which is used for the immobilization, or enzyme sensitivity to long-term methanol exposure [79].

It is observed that various substances can slow down lipase activity (methanol, glycerol, phospholipids); however, a number of ways have been proposed to overcome these problems [71]. Commonly, biocatalytic process does not produce soaps or other by-products. If the reaction completes, only esters and glycerol are produced. This makes purification steps much simpler and consequentially lowers plant costs. Once immobilized, lipases can be used many times or even in continuous processes. This resolves the major disadvantage related to high cost. In conclusion, if obtained by biocatalysis, biodiesel is an environmentally friendly fuel which will contribute to reducing negative impacts to the environment.

Modi et al. [56] used Propan-2-ol as an acyl acceptor for immobilized lipase-catalyzed preparation of biodiesel. The optimum conditions set for transesterification of crude *Jatropha* oil were 10% Novozym 435 (immobilized *Candida antarctica* lipase B) based on oil weight and alcohol to oil molar ratio of 4:1 at 50°C for 8 h. The maximum conversion reached using propan-2-ol was 92.8% from crude *Jatropha* oil. Reusability of the lipase was preserved over 12 repeated cycles with propan-2-ol as it reached to zero by the seventh cycle when methanol was utilized as an acyl acceptor, under standard reaction condition [55].

Modi et al. [55, 57] explored ethyl acetate as an acyl acceptor for immobilized lipase-catalyzed preparation of biodiesel from the crude oil of *J. curcas*. The optimum reaction conditions set for interesterification of the oils with ethyl acetate were 10% of Novozym 435 (immobilized *C. antarctica* lipase B) which is based on oil weight, ethylacetate to oil molar ratio of 11:1, and the reaction period of 12 h at 50°C. Under the above optimum conditions, the maximum result of ethyl esters was 91.3% of purity. Reusability of the lipase over repeated cycles in interesterification and ethanolysis was also examined under standard reaction conditions. The relative activity of lipase could be well preserved over 12 repeated cycles with ethyl acetate as it reached to zero by the sixth cycle when ethanol was used as an acyl acceptor.

Shah and Gupta [73] conducted a process of optimization of monoethyl esters of the long chain fatty acids (biodiesel) by alcoholysis of *Jatropha* oil using lipase. The process includes (a) screening of various commercial lipase preparations, (b) pH tuning, (c) immobilization, (d) varying water content in the reaction media, (e) varying amount of enzyme used, and (f) varying temperature of the reaction. The best yield 98% (w/w) was obtained by using *Pseudomonas cepacia* lipase which was immobilized on celite at 50°C in the presence of 4–5% (w/w) water in 8 h. The yield was not affected if analytical grade alcohol was replaced by commercial grade alcohol. This biocatalyst could be applied four times without loss of any activity.

In order to lower the cost of biodiesel fuel production from *Jatropha*, Tamalampudi et al. [85] used lipase producing whole cells of *Rhizopus oryzae* which was immobilized onto biomass support particles. The activity of *R. oryzae*

was compared to Novozym 435, the most effective lipase. Methanolysis of *Jatropha* oil progresses faster than other alcoholysis regardless of any lipase used. The maximum methyl ester content in the reaction mixture reached 80 wt.% after 60 h using *R. oryzae*, but 76% after 90 h using Novozym 435. Both lipases could be used for repeated batches. They also exhibited more than 90% of their initial activities after 5 cycles. Whole-cell immobilized *R. oryzae* is a promising biocatalyst for producing biodiesel from oil [85].

4.4 Biodiesel Production Using Supercritical Alcohols

The synthesis of biodiesel from *Jatropha* oil has been investigated in supercritical methanol and ethanol, without using any catalysts, from 200 to 400°C at 200 bar [68]. It is found that for the synthesis of biodiesel in supercritical alcohols with an optimum molar methanol oil ratio of 50:1, very high conversions (>80%) were obtained within 10 min and nearly complete conversions within 40 min. The conversion into ethyl esters is higher than that of methyl esters [68].

Tang et al. [86] studied transesterification of the crude *Jatropha* oil which was catalyzed by micro-NaOH (0.2 to 0.5 to 0.8 wt-‰) in supercritical methanol. When the catalyst content, reaction temperature, and molar ratio of methanol to oil were developed at 0.8 wt-‰ NaOH, 534 K, 7.0 MPa, and 24:1, respectively, the methyl ester yield reached 90.5% within 28 min.

4.5 Biodiesel Production Using Lipase-Catalyzed In Situ Reactive Extraction

According to Su et al. [82], extraction and lipase-catalyzed transesterification with methyl acetate and ethyl acetate can be done under the same conditions. They can be simply combined to a two-step-onepot in situ reactive extraction. First, the alkyl acetates were performed as the extraction solvent and afterwards as the transesterification agent. Then, by removing the catalyst, defatted plant material (by filtration), and the solvent (by evaporation), the methyl/ethyl esters were obtained.

The negative effects of glycerol and alcohol on lipase can be reduced by substituting short-chained alkyl acetates for short-chained alcohols as acyl acceptors for fatty acid esters production. Short-chained alkyl acetates are also appropriate solvents for seed oil extraction. Therefore, Su et al. [82] adopted methyl acetate and ethyl acetate as extraction solvents and transesterification reagents at the same time for in situ reactive extraction of *J. curcas* L seed. Fatty acid methyl esters and ethyl esters were respectively obtained with higher yields than those resulted in by conventional two-step extraction/transesterification. The improvement varied from 5.3 to 22%. The key parameters such as solvent/seed ratio and water content were

further examined to find their effects on the in situ reactive extraction. The highest *J. curcas* ethyl/ethyl esters could achieve 86.1 and 87.2%, respectively, under the optimized conditions [82].

This transesterification method reduces the risk of deactivation of enzyme by short-chained alcohol and glycerol because in the reaction short-chained alcohol is substituted with short-chained alkyl acetate and no glycerol is produced. Furthermore, such a route to fatty acid esters can decrease the expense associated with solvent extraction and oil cleanup. Due to its low cost production, in situ reactive extraction would be very promising for fatty acid esters production [82].

4.6 Biodiesel Production by In Situ Transesterification

In situ transesterification [32, 33, 39, 78], a biodiesel production method that utilizes the original agricultural products instead of purified oil as the source of triglycerides for direct transesterification, eliminates the costly hexane extraction process and works with virtually any lipid-bearing material. It could reduce the long production system associated with preextracted oil and maximize alkyl ester yield. The use of reagents and solvents is reduced, and the concern about waste disposal is avoided.

The experimental results showed that the amount of *J. curcas* seed oil dissolved in methanol was approximately 83% of the total oil and the conversion of this oil could achieve 98% under the following conditions: less than 2% moisture content in *J. curcas* seed flours, 0.3–0.335 mm particle size, 0.08 mol/L NaOH concentration in methanol, 171:1 methanol/oil molar ratio, 45.66°C reaction temperature, and 3.02 h reaction time. The use of alkaline methanol as extraction and reaction solvent, which would be useful for extraction oil and phorbol esters, would reduce the phorbol esters content in the *Jatropha* seedcake. The seedcakes after in situ transesterification is rich in protein and is a potential source of livestock feed [58].

5 Postreaction Processing of Biodiesel Production

Post reaction processing comprises ester/glycerol separation, ester washing, ester drying, alcohol recovery, and glycerol refining. These steps are very important in producing fuel-grade biodiesel and in decreasing biodiesel oil cost through alcohol recovery and glycerol refining.

For best economy and pollution prevention, alcohol must be fully recycled. Glycerol is an economically coproduct that should be fully refined [7]. As by-product, 1 mol of glycerol produces every 3 mol of methyl esters, which is equivalent to approximately 10 wt.% of the total product. Glycerol markets have reacted strongly to the increasing availability of glycerol. Although the global production of biodiesel is still limited, the market price of glycerol has dropped rapidly [37]. Therefore,

new uses for glycerol need to be developed and economical ways of the low-grade glycerol utilization should be further explored.

As *Jatropha* oil possesses a significant amount of fatty acids with double bonds, oxidative stability is of concern, especially when storing biodiesel over an extended period of time. The storage problem is worsening by storage conditions such as exposure to air and/or light, temperature above ambient, and the presence of extraneous materials (contaminants) with catalytic effect on oxidation [43]. The presence of air or oxygen will hydrolyze the oil to alcohol and acid. The presence of alcohol will lead to reduction in flash point and the presence of acid will increase the total acid number. All these conditions make methyl ester relatively unstable on storage and cause damage to engine parts [23]. That is why oxidation stability is an important criterion for biodiesel production.

The stability of biodiesel is very critical. Various strategies for the improvement of biodiesel fuel quality have been suggested. Biodiesel requires antioxidant to meet storage requirements and to ensure fuel quality at all points along the distribution chain. In order to meet EN 14112 specification, around 200 ppm concentration of antioxidant is required, except for palm biodiesel, which is much higher than those required for petroleum diesel. To minimize the dosage of antioxidant, appropriate blends of *Jatropha* and palm biodiesel are made. Antioxidant dosage could be reduced by 80–90% if palm oil biodiesel is blended with *Jatropha* biodiesel at around 20–40% concentration [72].

6 Nontoxic *Jatropha* Seedcake Production from *J. curcas*

Although *Jatropha* seeds are rich in oil and protein, they are very toxic and not good for human or animal consumption [40]. LD^{1}_{50} for phorbol ester consumption for male rat was 27.34 mg/kg body weight, and LD_5 and LD_{95} were 18.87 and 39.62 mg/kg body weight, respectively [44]. Utilization of *Jatropha* seedcakes cannot be achieved without the removal of antinutritional compounds [27]. Martinez-Herrera et al. [53] studied the nutritional quality and effects of various treatments (hydrothermal processing techniques, solvent extraction, solvent extraction plus $NaHCO_3$, and treatment with ionizing radiation) to disable antinutrient factor. Trypsin inhibitor can easily be removed using steam with a temperature of 121°C for 25 min. Phytate can be lowered slightly by irradiation at 10 kGy. The content of saponins can be reduced through extraction with ethanol and irradiation. Extraction with ethanol followed by 0.07% $NaHCO_3$ decreases phorbolester and lectin activity by 97.9% in seeds, while in vitro digestibility will increase between 78.6 and 80.6%. Heat treatment will increase in vitro digestibility to 86%.

[1] LD is lethal dose. The LD_{50} is the dose that kills half (50%) of the animals tested. The animals are usually rats or mice, although rabbits, guinea pigs, hamsters, and so on are sometimes used.

Jatropha seedcakes obtained from 4.0% NaOH treatment at a temperature of 121°C for 30 min followed either by washing two times with 92% methanol or four times with distilled water showed good results of detoxification. Phorbol ester content of seedcakes after detoxification with this treatment cannot be detected. However, the seedcakes which are only washed with water still have strong smell of NaOH. This has a negative revenue impact on the food intake. Washing with methanol looks promising for the detoxification of seedcakes as long as methanol used can be recycled [10]. Research by Chivandi et al. [18] demonstrated that *Jatropha* seedcakes detoxification using hexane and ethanol solvent treatment followed by hot steam 121°C for 30 min has not been able to eliminate the whole lectin and trypsin and still leaves phorbol ester residue (1.90 mg/g pulp). This figure is higher than the content of phorbol ester on nontoxic *Jatropha* (0.11 mg/g pulp).

Rakshit et al. [66] investigated the influence of heat and chemical detoxification of seedcakes and evaluated the growth and histology of rat. Research results indicated that the treatment of 2% NaOH or 2% $Ca(OH)_2$ followed by hot steam from the autoclave at a temperature of 131°C for 30 min and wash with water (1:5 w/v) reduce the phorbol ester content very significantly. However, the test diet on male rats showed the weight loss and the death of the rat on the day 9. According to Goel et al. [28], heat treatment followed by chemical extraction can eliminate phorbol ester and lower antinutrient and toxic substances in a meaningful way. *Jatropha* seedcakes treated in this way can be harmful to rats [48] and fish [28].

Makkar et al. [51] conducted a study to obtain the protein concentrate from the seedcakes. The highest protein concentrate was obtained when the seedcakes were first dissolved with NaOH so that the pH increased to 11 for 1 h and the temperature of 60°C, after which the protein was precipitated by lowering the pH to 4 using HCl. Concentrated protein produced by this treatment still contains phorbol ester from 0.86 to 1.48 mg/g and trypsin inhibitor which is estimated tenfold in the protein concentrate compared with that in seedcakes. Meanwhile, lectin and phytate also exist at a high level. These results indicate that the protein concentrates must be detoxified by removing the phorbol ester and disabling the lectin and trypsin inhibitors by heat treatment [51].

Nontoxic seedcakes can also be produced through in situ transesterification. The use of alkaline methanol as extraction and reaction solvent, which would be useful for extraction oil and phorbol esters, would reduce the phorbol esters content in the *Jatropha* seedcakes. The seedcakes, after in situ transesterification, are rich in protein and are potential sources for livestock feed. Experimental results showed that the amount of *Jatropha* seed oil dissolved in methanol was approximately 83% of the total oil. The conversion of this oil could achieve 98% under the following conditions: less than 2% moisture content in *Jatropha* seed flours, 0.3–0.335 mm particle size, 0.08 mol/L NaOH concentration in methanol, 171:1 methanol/oil mole ratio, 45.66°C reaction temperature, and 3.02 h reaction time [58].

7 Process Control of Integrated *Jatropha* Biodiesel Processing and Detoxification Process

There are three critical processes of production and three outputs that have to be considered; they are: (1) oil preparation, (2) transesterification reaction, and (3) post-reaction processing. In process control, we must ensure that both quantitative and qualitative product specification and economic performance meet health, safety, and environmental regulations. The tasks of control system are to ensure the stability of process, to minimize the influence of disturbance and perturbation, and to optimize the overall performance [19]. Figure 3 shows a schematic diagram of process control approach of integrated *Jatropha* biodiesel processing and detoxification process.

The following is a sequence of steps that could be employed to develop process control for a cost-effective and environmentally friendly *Jatropha* biodiesel production [60]:

1. Constructing a process flow diagram which identifies the major process operation.
2. Developing a strategy to improve the quality of *Jatropha* seed input. This strategy involves preharvest treatments and postharvest handling and technology.
3. Identifying the output characteristics that will be achieved.

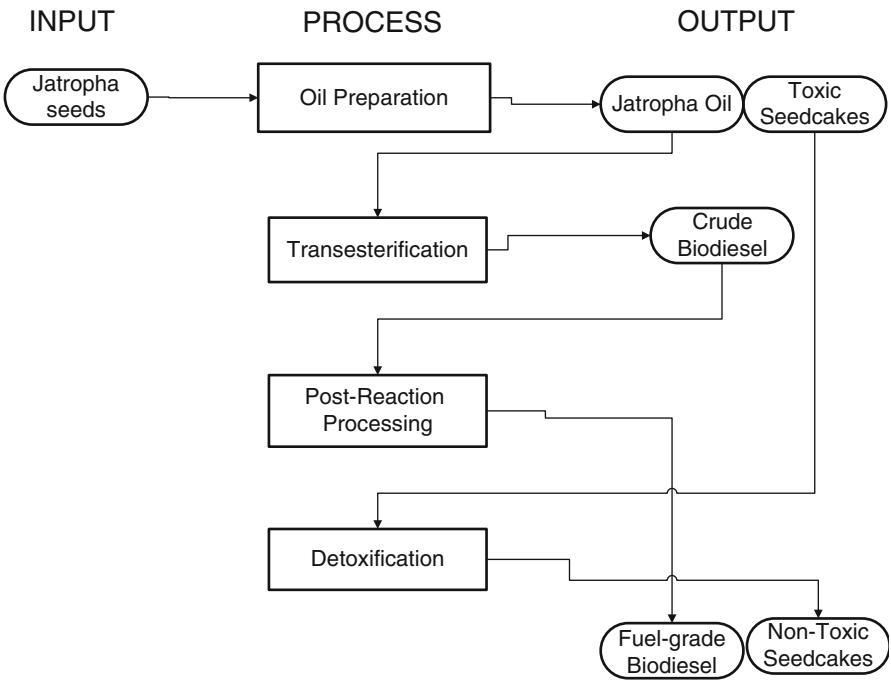

Fig. 3 Schematic diagram of the process control approach for integrated *Jatropha* biodiesel processing and detoxification process

4. Determining the principle process that will be applied for every output characteristics.
5. Identifying detection methods used to detect production problems and to prevent causes in the determined process.
6. Evaluating and analyzing cost feasibility of the process while always fulfilling health, safety, and environmental regulations.
7. Reviewing various possible actions for production system improvements.

8 Implication of Biodiesel Production on Global Warming, Environmental Impact Potential, and Energy

Since the cost and efficiency of the selected process will be tied up with the biodiesel production for a long time and affect the capital and operating costs and the environmental load of the product, selecting an appropriate process for the biodiesel production is a critical decision. Issues on capital and operating cost are relatively straightforward though issues on environmental load of the product are quite complicated [41]. One of the tools that can be employed to help answer the last issues is the life cycle assessment (LCA). The LCA is used to evaluate the environmental impact and other potential factors that a product (or service) has on the environment over the entire period of its life—from the extraction of the raw materials from which it is made, through the manufacturing, packaging, and marketing processes, and the use, reuse, and maintenance of the product, on to its eventual recycling or disposal as waste at the end of its useful life [41].

From the life cycle aspect, the growth of energy crops has raised concerns due to their high consumption of conventional fuels, fertilizers and pesticides for land preparation and biomass production, the materials and energy for oil extraction and biodiesel production, and the emissions and wastes which have been released to the environment. Figure 4 illustrates the system boundary for a LCA study of biodiesel production.

Nazir and Setyaningsih [59] developed a well-to-tank (WTT) life cycle inventory database of palm oil and *Jatropha* biodiesel and analyzed the environmental impacts of *Jatropha* and palm oil biodiesel by using the concept of life cycle thinking. The life cycle environmental impacts of *Jatropha* and palm oil biodiesel were compared and discussed. Table 4 shows the information related to materials and energy uses to produce 1 L biodiesel from *Jatropha* and palm oil.

8.1 Global Warming Potential of Biodiesel Production

The proportion of greenhouse gas (CHG) emissions from each material and energy used is shown in Fig. 5. The main contribution came from transesterification reaction for *J. curcas* and oil extraction for oil palm.

Biodiesel production from palm oil has bigger GHG emission than that from *Jatropha* oil.

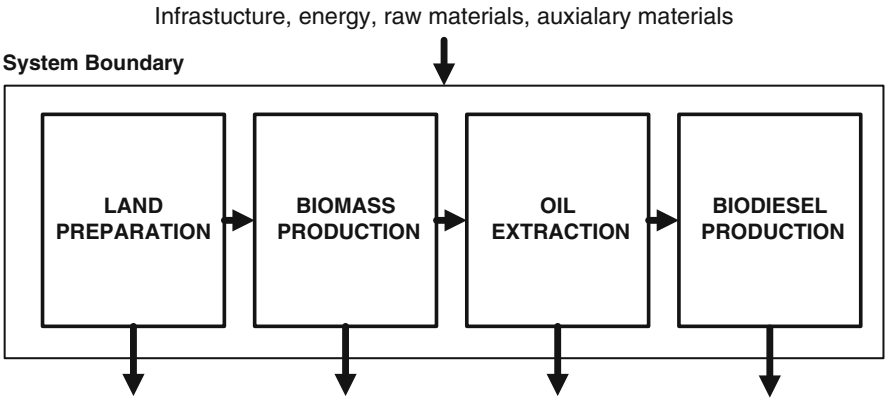

Fig. 4 The system boundary of *Jatropha* biodiesel production

Table 4 Materials and energy used in cultivation, oil extraction, and production of 1 L biodiesel from *J. curcas* oil and palm oil [59]

Input types	Input names	Unit	*J. curcas*	Oil palm
Cultivation				
Fertilizer	Urea	kg	0.135	0.265797
	KCl	kg	0.0675	0.399267
	DAP	kg	0.0336	0.072647
	Boron	kg	–	0.074327
Chemical	Herbicide	kg	0.0015	1.57232E−7
	Pesticide	kg	–	4.8224E−7
Fertilizing	Broadcaster	ha	3.59175E−6	0.000142
Plant protection	Field sprayer	ha	–	0.000142
Wood chopping	Mobile chopper	kg	–	4.53299
Transportation	Tractor/trailer	tkm	–	0.053299
	Lorry >16 ft	tkm	–	0.032132
	Freight	tkm	0.06708	0.111197
Land preparation	Diesel used	kg	0.0105	–
Provision	Stubble land	m^2	–	0.067579
Harvesting	Labor	MJ	0.007	0.004
Oil extraction				
Transportation	Tractor/trailer	tkm	–	0.00196
	Lorry >16 ft	tkm	–	0.37686
	Freight	tkm	0.002156	0.003267
	Electricity	MJ	0.0814	0.072
	Diesel	MJ	–	0.089
	Power and steam	MJ	–	4.967
Biodiesel production				
Chemical	Methanol	kg	0.14	0.09892
	Sulfuric acid	kg	0.0217	–
	NaOH	kg	0.00879	0.00998
Energy	Electricity	kWh	0.0852	0.036826
	Steam	kg	0.294	0.180

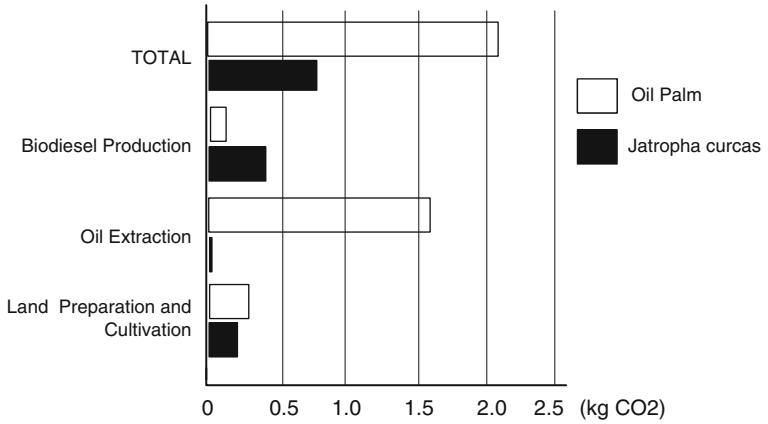

Fig. 5 Comparison of life cycle GHG emissions of biodiesel production from palm oil and *Jatropha* oil based on material and energy used in each steps of life cycle [59]

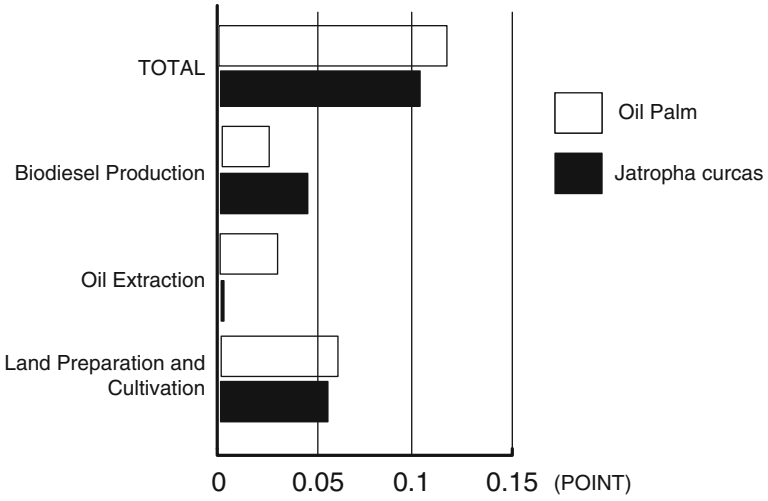

Fig. 6 Comparison of environmental impact of biodiesel production from palm oil and *Jatropha* oil based on material and energy used in each steps of life cycle [59]

8.2 Environmental Impact Potential of Biodiesel Production

Figure 6 shows the comparison of environmental impact of biodiesel production in each step of life cycle. Biodiesel production from palm oil has bigger total environmental impact than that of *Jatropha* oil. Cultivation contributes to the highest environmental impacts compared with other stages in the life cycle impact.

Table 5 The results of energy analysis biodiesel production

Fuel	Net energy value (NEV) (MJ/kg)	Net energy ratio (NER)	Net energy gain (%)	References
JCME	11.5	1.42	42.0	Prueksakorn and Gheewala [64]
POME	24.03	2.48	59.8	Papong et al. [63]

8.3 Net Energy Results of Life Cycle Impact Assessment

The life cycle energy analysis of *Jatropha* biodiesel production was conducted by evaluating direct energy input (such as electricity, diesel, gasoline, fuel oil, palm fiber, palm shell, etc.) and indirect energy input (energy accumulated in fertilizers, agrochemicals, and chemical production, excluding equipment and machinery used in the processes). The net energy value (NEV) and the net energy ratio (NER) can be estimated. The NEV is a measure of the energy gain or loss from the biodiesel used, which is defined as the energy content of the biodiesel minus the nonrenewable energy used in the life cycle of the biodiesel production [63]. The NER is a ratio of energy output to total energy input for the life cycle of the product [64].

Prueksakorn and Gheewala [64] calculated the energy consumption in every process in producing 1 kg of *Jatropha* biodiesel. The energy analysis results of the present situation of *Jatropha* biodiesel production compared to palm oil methyl ester is shown in Table 5. The results show that the selected biodiesel production process determines energy efficiency and environmental impacts.

9 Conclusions

High cost of biodiesel production is the major impediment to its large-scale commercialization. Methods to reduce the production cost of *Jatropha* biodiesel must be developed. One way to reduce production costs is to increase the added values of protein-rich *Jatropha* seedcakes, by-product of oil extraction, through detoxification process. The development of integrated biodiesel production process and the detoxification process results in two products, namely biodiesel and protein-rich seedcakes that can be used for animal feed. Assuming that an average seed yield on land of 5 tons/ha/year (2 tons/acre/year) could be achieved, the estimated theoretical maximum yield of biodiesel would be 750 kg/acre/year and seedcake products would be 500 kg/acre/year.

Since the cost and efficiency of the selected process will be closely correlated with the production for a long time and affect the capital and operating costs and the environmental load of the product, selecting an appropriate process for the biodiesel production is a critical decision. There are still many future potential improvement of biodiesel production of *J. curcas*. These include (1) development of better and

cheaper oil extraction and postreaction processing methods; (2) development of better and cheaper catalysts; (3) improvements in current technology for producing high-quality biodiesel with cheaper cost production; (4) development of technology to use methanol/ethanol in in situ extraction and transesterification; (5) development of technique to improve fuel stability of *Jatropha* biodiesel; (6) conversion of by-products, such as glycerol and seedcake to useful and value-added products, such as methanol and ethanol or glycerol *tert*-butyl ether (GTBE); and (7) development of integrated *Jatropha* biodiesel processing and detoxification process.

LCA has become an important decision-making tool for promoting alternative fuels because it can systematically analyze the fuel life cycle in terms of energy efficiency and environmental impacts. LCA analysis shows that the selected biodiesel production process determines energy efficiency and environmental impacts of *Jatropha* biodiesel production.

References

1. Adam SEI (1974) Toxic effects of *Jatropha curcas* in mice. Toxicology 2:67–76
2. Adam SEI, Magzoub M (1975) A toxicity of *Jatropha curcas* for goats. Toxicology 4: 347–354
3. Aderibigbe AO, Johnson C, Makkar HPS, Becker K, Foidl N (1997) Chemical composition and effect of heat on organic matter- and nitrogen-degradability and some antinutritional components of *Jatropha* meal. Anim Feed Sci Technol 67:223–243
4. Adolf W, Opferkuch HJ, Hecker E (1984) Irritant phorbol derivatives from four *Jatropha species*. Phytochemistry 23:129–132
5. Ahmed OMM, Adam SEI (1979) Toxicity of *Jatropha curcas* in sheep and goats. Res Vet Sci 27:89–96
6. Ahmed OMM, Adam SEI (1979) Effects of *Jatropha curcas* on calves. Vet Pathol 16:476–482
7. Akgun N, Iscan E (2008) Effects of process variables for biodiesel production by transesterification. Eur J Lipid Sci Technol 109:486–492
8. Akintayo ET (2004) Characteristic and composition of *Parkia biglobbossa* and *Jatropha curcas* oils and cakes. Bioresour Technol 92:307–310
9. Aregheore EM, Makkar HPS, Becker K (1998) Assessment of lectin activity in a toxic and a non-toxic variety of *Jatropha curcas* using latex agglutination and haemagglutination methods and inactivation of lectin by heat treatments. J Sci Food Agric 77:349–352
10. Aregheore EM, Makkar HPS, Becker K (2003) Detoxification of a toxic variety of *Jatropha curcas* using heat and chemical treatments, and preliminary nutritional evaluation with rats. South Pac J Nat Sci 21:50–56
11. Azam MM, Waris A, Nahar NM (2005) Prospect and potential of fatty acid methyl esters of some non-traditional seed oil for use as biodiesel in India. Biomass Bioenergy 29:293–302
12. Bajpay D, Tyagi VK (2006) Biodiesel: source, production, composition, properties and its benefit. J Oleo Sci 55:487–502
13. Becker K, Makkar HPS (2008) *Jatropha curcas*: a potential source for tomorrow's oil and biodiesel. Lipid Technol 20:104–107
14. Berchmans HJ, Hirata S (2008) Biodiesel production from *Jatropha curcas* L. seed oil with a high content of free fatty acids. Bioresour Technol 99:1716–1721
15. Caili G, Kusefoglu S (2008) Increased yields in biodiesel production from used cooking oils by two step process: comparison with one step process by using TGA. Fuel Process Technol 89:118–122

16. Cano-Asseleih LM, Plumbly RA, Hylands PJ (1989) Purification and partial characterization of the hemagglutination from seeds of *Jatropha curcas*. J Food Biochem 13:1–20
17. Chitra P, Venkatachalam P, Sampathrajan A (2005) Optimimisation of experimental condition for biodiesel production from alkali-catalysed transesterification of *Jatrupha curcas* oil. Energy Sustain Dev 9:13–18
18. Chivandi E, Mtimuni JP, Read JS, Makuza SM (2004) Effect of processing on phorbol ester concentration, total phenolics, trypsin, inhibitor activity and proximate composition of the Zimbabwean *Jatropha curcas* provenance: a potential livestock feed. Pak J Biol Sci 7: 1001–1005
19. Corriou JP (2004) Process control: theory and applications. Springer, London
20. Cvengros J, Cvengrosova Z (2004) Used frying oils and fats and their utilization in the production of methyl ester of higher fatty acid ester. Biomass Bioenergy 26:173–181
21. De Oliveira JS, Leite PM, de Souza LB, Mello VM, Silvab EC, Rubim JC, Meneghetti SMP, Suarez PAZ (2009) Characteristics and composition of *Jatropha gossypiifolia* and *Jatropha curcas* L. oils and application for biodiesel production. Biomass Bioenergy 33:449–453
22. Demirbaş A (2002) Biodiesel from vegetable oils via transesterification in supercritical methanol. Energy Conserv Manag 43:2349–2356
23. Dunn RO, Knothe G (2003) Oxidative stability of biodiesel in blends with jet fuel by analysis of oil stability index. J Am Oil Chem Soc 80:1047–1048
24. Emil A, Yaakob Z, Satheesh Kumar MN, Jahim JM, Salimon J (2010) Comparative evaluation of physicochemical properties of *Jatropha* seed oil from Malaysia, Indonesia and Thailand. J Am Oil Chem Soc. doi:10.1007/s11746-009-1537-6
25. Foidl N, Eder P (1997) Agro-industrial exploitation of *J. curcas*. In: Gubitz GM, Mittelbach M, Trabi M (eds) Biofuels and industrial products from *Jatropha curcas*. DBV, Graz, pp 88–91
26. Foidl N, Foidl G, Sanchez M, Mittelbach M, Hackel S (1995) *Jatropha curcas* L as a source for the production of biofuel in Nicaragua. Bioresour Technol 58:77–82
27. Gaur S (2009) Development and evaluation of effective process for the recovery of oil and detoxification of meal from *Jatropha curcas*. Thesis, Missouri University of Science and Technology, Missouri
28. Goel G, Makkar HPS, Francis G, Becker K (2007) Phorbol esters: structure, biological activity, and toxicity in animal. Int J Toxicol 26:279–288
29. Gubitz GM, Mittelbach M, Trabi M (1999) Exploitation of the tropical oil seed plant *Jatropha curcas* L. Bioresour Technol 67:73–82
30. Gunstone FD (2004) The chemistry of oils and fats: sources, composition, properties, and uses. Blackwell, London
31. Haas W, Mittelbach M (2000) Detoxification experiment with the seed oil from *Jatropha curcas* L. Ind Crops Prod 12:111–118
32. Harrington KJ, D'Arcy-Evans C (1985) Transesterification in situ of sunflower seed oil. Ind Eng Chem Prod Res Dev 62:314–318
33. Hass MJ, Scott KM, Marmer WN, Foglia TA (2004) *In situ* alkaline transesterification: an effective method for the production of fatty acid esters from vegetable oils. J Am Oil Chem Soc 81:83–89
34. Huaping Z, Zongbin WU, Yuanxiong C, Ping Z, Shijie D, Xiaohua L, Zongqiang M (2006) Preparation of biodiesel catalyzed by solid super base of calcium oxide and its refining process. Chin J Catal 27:391–396
35. Ingram J (1957) Notes on the cultivated Euphorbiaceae: 1. The flowers of the Euphorbiaceae; 2. *Cnidoscolus* and *Jatropha*. Baileya 5:107–117
36. Iso M, Chenb B, Eguchi M, Kudo T, Shrestha S (2001) Production of biodiesel fuel from triglycerides and alcohol using *immobilized lipase*. J Mol Catal B Enzym 16:53–58
37. Karinen RS, Krause AOI (2006) New biocomponents from glycerol. Appl Catal A Gen 306:128–133
38. Kazancev K, Makareviciene V, Paulauskas V, Janulis P (2006) Cold flow properties of fuel mixtures containing biodiesel derived from animal fatty waste. Eur J Lipid Sci Technol 108:753–758

39. Kildiran G, Ozgul-Yucel S, Turkay S (1996) In-situ alcoholysis of soybean oil. J Am Oil Chem Soc 73:225–228
40. King AJ, He W, Cuevas JA, Freudenberger M, Ramiaramanana D, Graham IA (2009) Potential of *Jatropha curcas* as a source of renewable oil and animal feed. J Exp Bot 60:2897–2905
41. Kiwjaroun C, Tubtimdee C, Piumsomboon P (2009) LCA studies comparing biodiesel synthesized by conventional and supercritical methanol methods. J Clean Prod 17:143–153
42. Knothe G (2003) Analyzing biodiesel: standards and other methods. J Am Oil Chem Soc 83:823–833
43. Leung DYC, Wu X, Leung MKH (2010) A review on biodiesel production using catalyzed transesterification. Appl Energy 87:1083–1095
44. Li CY, Devappa RK, Liu JX, Min Lu J, Makkar HPS, Becker K (2010) Toxicity of *Jatropha curcas* phorbol esters in mice. Food Chem Toxicol 48:620–625
45. Liberalino AA, Bambirra EA, Moraes-Santos T, Vieira EC (1988) *Jatropha curcas* L. seeds: chemical analysis and toxicity. Arq Biol Technol 31:539–550
46. Linnaeus C (1753) Species plantarum. In: *Jatropha*. Impensis Laurentii Salvii, Stockholm, pp 1006–1007
47. Lotero E, Liu Y, Lopez DE, Suwannakarn K, Bruce DA, Goodwin JG Jr (2004) Synthesis of biodiesel via acid catalysis. http://scienzechimiche.unipr.it/didattica/att/5dd4.5996.file.pdf. Accessed 12 Feb 2010
48. Makkar HPS, Becker K (1997) Study on nutritive potential and toxic constituents of different provenances of *Jatropha curcas*. J Agric Food Chem 45:3152–3157
49. Makkar HPS, Becker K, Sporer F, Wink M (1997) Studies on nutritive potential and toxic constituents of different provenances of *Jatropha curcas*. J Agric Food Chem 45:3152–3157
50. Makkar HPS, Aderibigbe AO, Becker K (1998) Comparative evaluation of non-toxic and toxic varieties of *Jatropha curcas* for chemical composition, digestibility, protein degradability and toxic factors. Food Chem 62:207–215
51. Makkar HPS, Francis G, Becker K (2008) Protein concentrate from *Jatropha curcas* screw-pressed seed cake and toxic and antinutritional factors in protein concentrate. J Sci Food Agric 88:1542–1548
52. Makkar H, Maes J, Greyt WD, Becker K (2009) Removal and degradation of phorbol esters during pre-treatment and transesterification of *Jatropha curcas* oil. J Am Oil Chem Soc 86:173–181
53. Martinez-Herrera J, Siddhuraju P, Francis G, Davila-Ortiz G, Becker K (2006) Chemical composition, toxic/anti-metabolic constituents, and effects of different treatments on their levels, in four provenances of *Jatropha curcas* L. from Mexico. Food Chem 96:80–89
54. Meher LC, Sagar VD, Naik SN (2006) Technical aspects of biodiesel production by transesterification—a review. J Renew Sustain Energy Rev 10:248–268
55. Modi MK, Reddy JRC, Rao BVSK, Prasad RBN (2006) Lipase-mediated conversion of vegetable oils into biodiesel using ethyl acetate as acyl acceptor. Biotechnol Lett 28: 1260–1264
56. Modi MK, Reddy JRC, Rao BVSK, Prasad RBN (2006) Lipase-mediated transformation of vegetable oils into biodiesel using propan-2-ol as acyl acceptor. Biotechnol Lett 28:637–640
57. Modi MK, Reddy JRC, Rao BVSK, Prasad RBN (2007) Lipase-mediated conversion of vegetable oils into biodiesel using ethyl acetate as acyl acceptor. Bioresour Technol 98:1260–1264
58. Nazir N (2010) Process development of biodiesel production from *Jatropha curcas* L. via in situ transesterification, heterogeneous catalysis and detoxification. PhD thesis, Institut Pertanian Bogor, Bogor
59. Nazir N, Setyaningsih D (2010) Life cycle assessment of biodiesel production from palm oil and *Jatropha* oil in Indonesia. Paper presented in Biomass-Asia 7th workshop, Jakarta, 29–30 Nov 2010
60. Nazir N, Ramli N, Mangunwidjaja D, Hambali E, Setyaningsih D, Yuliani S, Yarmo MA, Salimon J (2009) Extraction, transesterification and process control in biodiesel production from *Jatropha curcas:* review article. Eur J Lipid Sci Technol 111:1185–1200

61. Openshaw K (2000) A review of *Jatropha curcas*: an oil plant of unfulfilled promise. Biomass Bioenergy 19(1):1–15
62. Oyekunle JAO, Omode AA, Akinnifosi JO (2007) Physical properties of oils from some Nigerian non-convensional oilseeds. J Appl Sci 7:835–840
63. Papong S, Chom-In T, Noksa-nga S, Malakul P (2010) Life cycle energy efficiency and potentials of biodiesel production from palm oil in Thailand. Energy Policy 38:226–233
64. Prueksakorn K, Gheewala SH (2008) Full chain energy analysis of biodiesel from *Jatropha curcas* L. in Thailand. Environ Sci Technol 42:3388–3393
65. Rakshit KD, Bhagya S (2007) Effect of processing methods on the removal of toxic and antinutritional constituents of *Jatropha* meal: a potential protein source. J Food Sci Technol 3:88–95
66. Rakshit KD, Darukeshwara J, Rathina Raj K, Narasimhamurthy K, Saibaba P, Bhagya S (2008) Toxicity studies of detoxified *Jatropha* meal (*Jatropha curcas*) in rats. Food Chem Toxicol 46:3621–3625
67. Ramadhas AS, Jayaraj S, Mureleedharan C (2005) Biodiesel production from high FFA rubber seed oil. Fuel 84:335–340
68. Rathore V, Madras G (2007) Synthesis of biodiesel from edible and non-edible oils in supercritical alcohols and enzymatic synthesis in supercritical carbon dioxide. Fuel 8:2650–2659
69. Raventos M, Duarte S, Alarcon R (2002) Application and possibilities of supercritical CO_2 extraction in food processing industry: an overview. Food Sci Technol Int 8:269–284
70. Salimon J, Abdullah R (2008) Physicochemical properties of Malaysian *Jatropha* curcas seed oil. Sains Malays 37(4):379–382
71. Salis A, Monduzzi M, Solinas V (2007) Use of lipase for the production of biodiesel. In: Polaina J, MacCabe AP (eds) Industrial enzymes. Springer, Heidelberg, pp 317–339
72. Sarin R, Sharma M, Sinharay S, Malhotra RK (2007) *Jatropha* palm biodiesel blends: an optimum mix for Asia. Fuel 86:1365–1371
73. Shah S, Gupta MN (2007) Lipase catalyzed preparation of biodiesel from *Jatropha* oil in a solvent free system. Process Biochem 42:409–414
74. Shah S, Sharma A, Gupta MN (2004) Extraction of oil from *Jatropha curcas* L. seed kernels by enzyme assisted three phase partitioning. Ind Crops Prod 20:275–279
75. Shah S, Sharma A, Gupta MN (2005) Extraction of oil from *Jatropha curcas* L. seed kernels by combination of ultrasonication and aqueous enzymatic oil extraction. Bioresour Technol 96:121–123
76. Sharma A, Khare SK, Gupta MN (2002) Three phase partitioning for extraction of oil from soybean. Bioresour Technol 85:327–329
77. Sharma YC, Singh B, Upadhyay SN (2008) Advancements in development and characterization of biodiesel: a review. Fuel 87:2355–2373
78. Siler-Marinkovic S, Tomasevic A (1998) Transesterification of sunflower oil *in situ*. Fuel 77:1389–1391
79. Soumanou MM, Bornscheuer UT (2003) Lipase-catalyzed alcoholysis of vegetable oils. Eur J Lipid Sci Technol 105:656–660
80. Spilimbergo S, Bertucco A (2003) Non-thermal bacterial inactivation with dense CO_2. Biotechnol Bioeng 84:627–638
81. Srivastava A, Prasad R (2000) Triglycerides-based diesel fuel. Renew Sustain Energy Rev 4:111–133
82. Su EZ, Xu WQ, Gao KL, Zheng YZ, Wei DZ (2007) Lipase-catalyzed *in situ* reactive extraction of oilseeds with short-chained alkyl acetates for fatty acid esters production. J Mol Catal B Enzym 48:28–32
83. Sudradjat R, Hendra A, Iskandar W, Setyawan D (2005) Manufacture technology of biodiesel from jarak pagar plant seed oil. J Penel Hasil Hut 23:53–68
84. Sudradjat R, Jaya I, Setyawan D (2005) Estrans process optimization in biodiesel manufacturing from *Jatropha curcas* L. oil. J Penel Hasil Hut 23(4):239–257
85. Tamalampudi S, Talukder MRR, Hama S, Numata T, Kondo A, Fukuda H (2008) Enzymatic production of biodiesel from *Jatropha* oil: a comparative study of immobilized-whole cell and commercial lipases as a biocatalyst. Biochem Eng J 39:185–189

86. Tang Z, Wang L, Yang J (2007) Transesterification of the crude *Jatropha curcas* L. oil catalyzed by micro-NaOH in supercritical and subcritical. Eur J Lipid Sci Technol 109(6): 585–590
87. Thurmond W (2007) Feedstock trends: Jatropha. Biofuels International, September. http://www.emergingmarkets.com/biodiesel/pdf/BiofuelsInternational_FeedstockTrends_Jatropha_September07_WillThurmond.pdf. Accessed 12 Aug 2011
88. Tiwari AK, Kumar A, Raheman A (2007) Biodiesel production from *Jatropha* oil (*Jatropha curcas*) with high free fatty acids: an optimized process. Biomass Bioenergy 31:569–575
89. Van Eijck J, Romijn H (2008) Prospects for *Jatropha* biofuels in Tanzania: an analysis with strategic niche management. Energy Policy 36:311–325
90. Van Gerpen J (2005) Biodiesel processing and production. Fuel Process Technol 86:1097–1107
91. Vasconcelos IM et al (1997) Composition, toxic and antinutritional factors of newly developed cultivars of Brazilian soybean (*Glycine max*). J Sci Food Agric 75:419–426
92. Vasudevan P, Briggs M (2008) Biodiesel production—current state of the art and challenges: a review. J Ind Microbiol Biotechnol 35:421–430
93. Venter MJ, Willems P, Kuipers NJM, de Haan AB (2006) Gas assisted mechanical expression of cocoa butter from cocoa nibs and edible oils from oilseeds. J Supercrit Fluids 37:350–358
94. White A, Burns D, Christensen TW (2006) Effective terminal sterilization using supercritical carbon dioxide. J Biotechnol 123:504–515
95. Willems P, Kuipers NJM, de Haan AB (2008) Gas assisted mechanical expression of oilseeds: influence of process parameters on oil yield. J Supercrit Fluids 7:350–358
96. Yan ZH, Fang F, Long SJ, Zhu LC, Juan JL (2005) Technique of extracting oils from *Jatropha curcas*. Jiangsu J Agric Sci 21:69–70
97. Zhang Y, Dubé MA, McLean DD, Kates M (2003) Biodiesel production from waste cooking oil: 1. Process design and technological assessment. Bioresour Technol 89:1–16

Chapter 24
Biofuels from Microalgae: Towards Meeting Advanced Fuel Standards

Liam Brennan and Philip Owende

Abstract Continued reliance on fossil fuel reserves as the primary energy resource is increasingly becoming unsustainable, owing to the need for: minimal exposure to the associate price volatility, reduction of greenhouse gas emissions by energy conservation, and deployment of cleaner and locally produced energy feedstock (including recovery from waste). Based on current knowledge and technology projections, third-generation biofuels (low input-high yielding feedstock) specifically derived from microalgae are considered to be viable alternative energy resource. They are devoid of the major drawbacks associated with first-generation biofuels (mainly terrestrial crops, e.g. sugarcane, sugar beet, maize and rapeseed) and second-generation biofuels (derived from lignocellulosic energy crops and agricultural and forest biomass residues). This chapter focuses on technologies underpinning microalgae-to-biofuels production systems, and evaluates the scale-up and commercial potential of biofuel production, including benchmarking of fuel standards. It articulates the importance of integrating biofuels production with the production of high-value biomass fractions in a biorefinery concept. It also addresses sustainability of resource deployment through the synergistic coupling of microalgae propagation techniques with CO_2 sequestration and bioremediation of wastewater treatment potential for mitigation of environmental impacts associated with energy conversion and utilisation.

L. Brennan (✉)
School of Agriculture, Food Science and Veterinary Medicine,
Bioresources Research Centre, Charles Parsons Energy Research Programme,
University College Dublin, Belfield, Dublin 4, Ireland
e-mail: liam.brennan@ucd.ie

P. Owende
School of Agriculture, Food Science and Veterinary Medicine,
Bioresources Research Centre, Charles Parsons Energy Research Programme,
University College Dublin, Belfield, Dublin 4, Ireland

School of Informatics and Engineering, Institute of Technology Blanchardstown,
Blanchardstown Road North, Dublin 15, Ireland
e-mail: philip.owende@itb.ie

J.W. Lee (ed.), *Advanced Biofuels and Bioproducts*, DOI 10.1007/978-1-4614-3348-4_24,

1 Introduction

1.1 World Energy Outlook and Renewable Energy Deployment

The 2009 Copenhagen Climate Conference highlighted the growing importance of developing economic CO_2 neutral energy systems, and also recognised that the global temperature rise should be limited to less than 2°C to avoid severe climate change [105]. The global annual primary energy consumption in 2009 was estimated at 11,164 million tonnes of oil equivalent (mtoe), a reduction of 1.1% on the 2008 figures, which was attributed to the global economic recession [22]. Fossil fuels accounted for 88% of the primary energy consumption,[1] comprising of oil (35%), coal (29%) and natural gas (24%) as the major fuels, while nuclear energy and hydroelectricity account for 5 and 7% of total primary energy consumption, respectively [22]. It has been predicted that the global primary energy demand will increase by 40% for the period 2007–2030 [95, 103], mainly due to increases in demand from developing countries. Over the same period, it is also predicted that CO_2 emission reduction of 25–40% range will be required to maintain a 2°C limit in global temperature rise [105]. High dependence on fossil fuels is the largest contributor of greenhouse gas (GHG) emissions to the biosphere, with estimated global CO_2 emissions of 29 Gtonnes in 2006 [65]. It is therefore imperative to identify compatible mitigation strategies to minimise the excess CO_2 emissions as the associated climate change projections could have major consequences for nature as well as human systems [17, 96]. Consequently, renewable and carbon neutral fuels are essential to both environmental and economic sustainability; hence, biofuels will be key energy sources [152].

Biofuels refer to liquid, gas and solid fuels derived from biomass, the collective term for plant-derived matter (terrestrial and aquatic) other than that which has been fossilised. Biomass includes dedicated energy crops (viz. sugarcane, rapeseed, short-rotation woody crops, etc.), agricultural and forestry residues and agri-food waste. Classification includes first-, second- and third-generation biofuels. First-generation biofuels refer to those derived from sources like starch, sugar, animal fats and vegetable oil, usually extracted by conventional techniques of production (e.g. biodiesel, vegetable oil, biogas, bio-alcohols and syngas). Second-generation biofuels are derived from lignocellulosic biomass by thermochemical conversion processes such as gasification and Fischer–Tropsch process. The second-generation biofuels offer key advantages over the first-generation, including: possible use of a much wider range of raw material, especially waste, which may lower the cost of the feedstock significantly; the resulting fuels are of high-quality and clean-burning, with potentially a much lower well-to-wheels CO_2 profile; cultivation process (if any) could be less environmentally intensive than for ordinary agricultural crops

[1] Primary energy consumption comprises commercially traded fuels only, and excluding fuels such as wood, peat, animal waste, geothermal, wind and solar power generation.

(e.g. reduced or zero cultivation result in even lower GHG emissions from cultivation), and can be co-produced with electricity. Third-generation biofuels in this context refer to fuel extracts from micro- and macroalgae feedstock and from biomass crops that have been genetically modified in such a way that their structure or properties conform to the requirements of a particular bioconversion process. Technology frontiers for plant-based third-generation biofuels include the development of tree crops with weakened lignin content to ease conversion to fuels [101], and modified corn varieties with enzymes necessary to break down cellulose and hemi-cellulose into simple sugars in the leaves, allowing for more cost-effective, efficient production of ethanol from corn residue [200].

Through specific proven biochemical or thermochemical conversion processes (viz., esterification, anaerobic digestion, pyrolysis and thermochemical liquefaction), biomass can be converted to a range of biofuels such as ethanol, methane, hydrogen, biodiesel, and Fischer–Tropsch diesel [55]. Sustainable deployment of biofuels has therefore become a crucial strategy for limiting or reducing GHG emissions, enhancement of regional security of energy supply (including employment creation), and controlling price volatility in fossil fuel markets [23].

1.2 Principles of Clean Energy Production

Biofuels have been promoted as the future lead energy sources, with potential to significantly displace the current high dependence on fossil fuels [152]. The demand drivers in the transition from fossil fuels are seen as the: frequently unstable energy prices, need for security of supply, and accelerated climate change associated with fossil fuel usage [103]. For any significant impacts, the demand drivers and trends that support the biofuels industry must be fully integrated to develop a global market by concurrent:

1. Creation of awareness of environmental benefits of biofuels
2. The availability of new fuel vehicles
3. Development of financial markets for biofuels
4. Development of infrastructure that supports the new biofuels

To develop and sustain markets for biofuels, environmental benefits must be clear for consumers to support growth of the industry [2]. For example, available evidence suggests that consumers would be willing to pay a premium for transport fuels as long as the impact on GHG reduction is clear [130]. The world food demand, in most part, is inelastic [73], therefore, growing of biofuel feedstock instead of food will require new cropping areas for food production. Land-use changes, mainly through deforestation, affect the carbon balance in the atmosphere, which will have a major effect on the sustainability of biofuels [85] and damage consumer's image of biofuels as a clean source of energy. Also, the potential role of biofuels in rural development, especially in the creation of employment, must be clear.

Original equipment manufacturers (OEMs) are a critical driver for biofuels deployment as they are responsible for development of application technologies,

e.g. new fuel vehicles and ancillary equipment [57]. Faced with limited budgets for R&D, OEMs have focused on successive improvement of proven technologies of immediate commercial potential, e.g. flexi-fuel vehicles (FFV) for which blends of <10% ethanol are covered in warranties for new cars. Higher biofuel blends (e.g. E85) for FFV have been promoted differently between regulators in Europe and USA, therefore the market has not developed for OEMs to heavily invest resources in this technology area yet [2]. However, incentives for OEMs are required to secure innovations (e.g. more efficient biodiesel engines) that are capable of creating step-change to deployment of biofuels. For increased FFV deployment, clear benefit for consumers (viz., concessions in tax, insurance, etc.) are necessary to generate markets, hence, innovations in new technologies that will be capable of realizing the required step-change.

Biofuel-related financial markets are still immature and therefore present significant investment risk for fuel blenders/consumers [2, 211]. The infrastructure that facilitates regional operation and trade in biofuels is critical if an efficient market is to develop [2]. Currently, the key challenge is in integrating secure biofuels supply into the current fuel chains. For sustainability, such supply security could be achieved through the development of multiple feedstock scenarios capable of delivering fuel to specified standards.

Adaptability could be key to future success of biofuels as competiveness is weighed against a host of other energy carriers, apart from fossil fuels, e.g. electric cars. Therefore, judicious regulation in the quest for low carbon economies should support innovation and development in new technologies for delivery of cleaner fuels and to facilitate biofuel market penetration [56].

1.3 Principles of Clean Energy and Sustainable Energy Systems

Strategies for enhancing security of energy supply and mitigation of energy-related GHG emissions, include, *inter alia*, the need for: increased energy efficiency (i.e. decreasing energy use per unit of product, process or service); increased use of clean fossil energy (i.e. use of fossil fuels coupled with CO_2 sequestration and storage); and increased use of carbon neutral renewable energy, mainly biofuels [23, 196]. Conditions for technically and economically viable biofuel resources are that, they should be [100, 195]: cost-competitive against petroleum-based fuels, require low to no additional land use, enable air quality improvements (e.g. CO_2 sequestration), and require minimal water usage. Biofuels are technically carbon neutral, i.e. the release of CO_2 during conversion is equivalent to what is captured during growth of the parent material via the photosynthesis process [1]. However, they may not always be carbon neutral where energy from fossil fuels are used in the cultivation, harvesting, manufacture of fertiliser and herbicides, processing, and direct conversion to energy or specific energy carriers as depicted in the illustration in Fig.1 for biomass from willow short rotation coppice.

The deployment of first- and second-generation biofuels has generated a lot of controversy, mainly due to the negative impact on global food markets [144] and

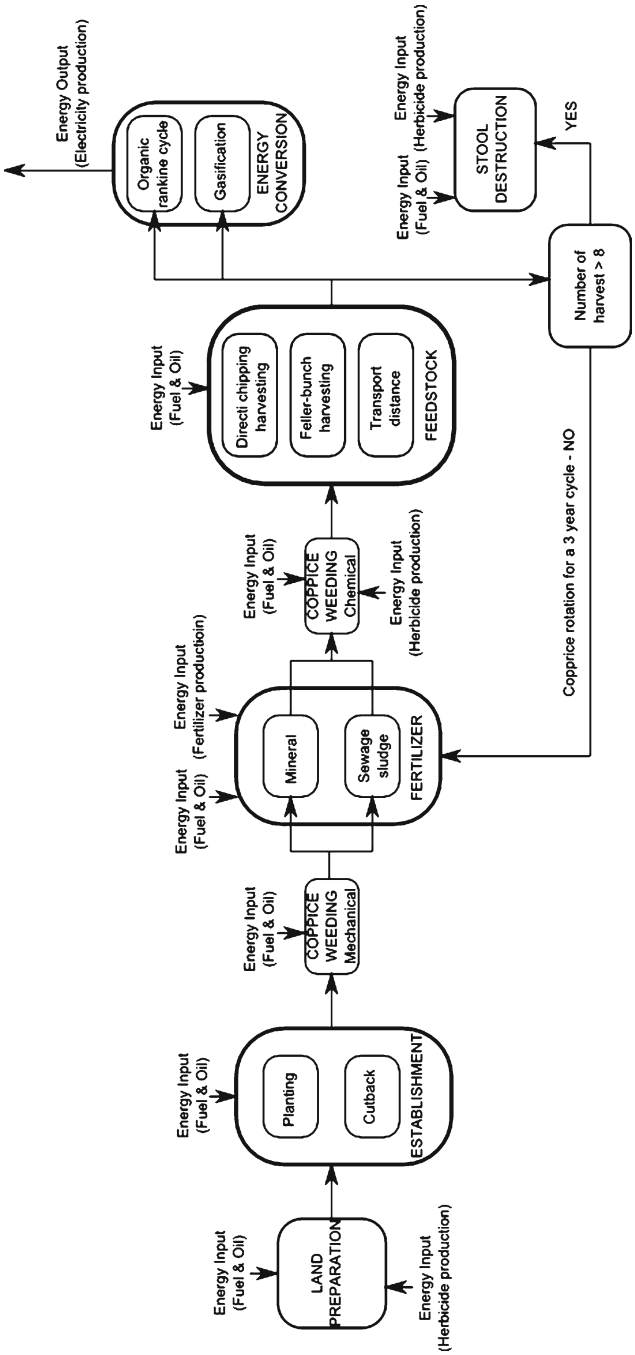

Fig. 1 System boundaries for willow short-rotation coppice production with energy inputs and outputs (Adapted from Goglio and Owende [79])

energy-intensive processes for conversion to fuels [226], respectively. Any effort towards increased production of biofuel-directed biomass must therefore consider the overall sustainability. Microalgae-derived biofuels are devoid of the major drawbacks associated with first- and second-generation biofuels. Their judicious exploitation could therefore make a significant contribution to meeting the primary energy demand, while simultaneously providing environmental benefits [218]

1.4 Microalgae-Derived Biofuels

Biofuels derived from microalgae are currently considered to be the most economical and technically viable route for producing biofuels to compete with petroleum-based fuels [40]. This is due to a number of intrinsic advantages they could have, when compared to biofuels extracted from terrestrial bioenergy crops. These include: (1) higher annual growth rates, e.g. rates of up to 37 tonnes ha^{-1} per annum have been recorded, primarily due to higher photosynthetic efficiencies when compared with terrestrial plants [221]; (2) higher lipid productivity (up to 75% dry weight for some algae species), with higher proportion of triacylglycerol (TAG) that is essential for efficient biodiesel production [185]; (3) microalgae production can effect biofixation of CO_2 (production utilises about 1.83 kg of CO_2 per kg of dry algal biomass yield) thus making a contribution to air quality improvement [38]; (4) capability of growing in wastewater, which offers the duel potential for integrating the treatment of organic effluent with biofuel production [28]; and (5) inherent yield of valuable co-products such as proteins and polyunsaturated fatty acids (PUFAs) may be used to enhance the economics of production systems [197]. Figure 2 summarises the distinct stages in the production and processing of microalgae to biofuel.

Despite the outlined advantages, there are still a number of significant obstacles to realisation of the full potential of microalgae-derived biofuels. They include: (1) energy-intensive downstream processes including pumping and dewatering of biomass, and conversion processes can result in negative energy balance [88]; (2) trade-off requirements in species selection and genetic enhancement for biofuel production vs. extraction of co-products [157]; and (3) need for techniques for enabling real-time control of pH, photoinhibition, evaporation and CO_2 diffusion losses in cultivation systems [213].

2 State-of-the-Art in Microalgae Biomass Production

2.1 Biology of Microalgae and Criteria for Biofuel-Directed Algae Strain Selection

Microalgae are thallophytes, i.e. primitive plants lacking roots, stems and leaves, have no sterile covering of cells around reproductive cells, and have chlorophyll *a* as the primary photosynthetic pigment [115]. Their structures are primarily for

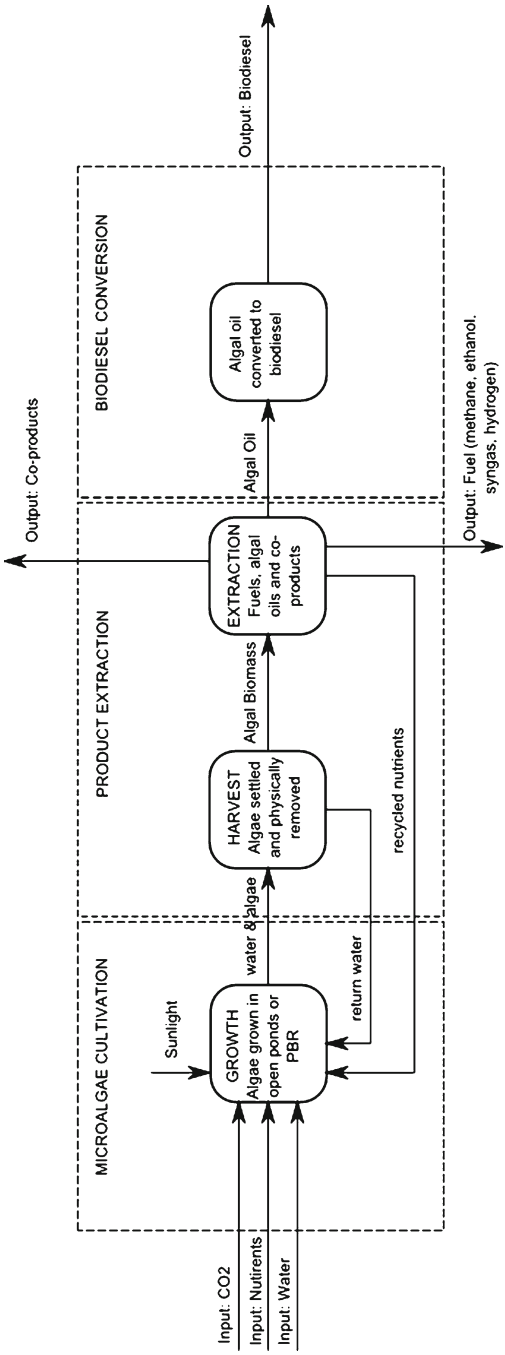

Fig. 2 Microalgae to biofuel process chain, including: cultivation, harvesting, algal oil extraction, and conversion of oils to biodiesel (Adapted from Gallagher and Brian [74])

energy conversion without any development beyond cells, a feature that allows them to rapidly adapt to prevailing environmental conditions [70]. It is estimated that more than 50,000 algal species exist in wide-ranging aquatic and terrestrial ecosystems [174]. For purposes of this chapter, definition of microalgae covers all unicellular and simple multi-cellular microorganisms, including both prokaryotic microalgae, i.e. cyanobacteria (Chloroxybacteria), and eukaryotic microalgae, i.e. green algae (Chlorophyta), red algae (Rhodophyta) and diatoms (Bacillariophyta).

Microalgae's main growth requirements are sunlight, carbon dioxide (CO_2) from the atmosphere and nutrients from the aquatic habitats. The inorganic nutrients required include nitrogen, phosphorus and silicon [202]. Artificial production systems attempt to replicate and enhance these requirements. For most production systems, sunlight is generally the primary limiting factor due to diurnal cycles coupled with seasonal variations, which limit the viability of commercial production in natural settings to areas with high solar radiation [165]. Under natural growth conditions, microalgae assimilate CO_2 from the air (ca. 360 ppmv CO_2) but they can also assimilate CO_2 from other sources such as discharge gases from industrial processes and soluble carbonates [218]. Most microalgae can tolerate and thrive at substantially higher levels of CO_2 (typically up to 150,000 ppmv) [17, 41, 62].

For biofuel-destined microalgae production, the major factors cited as determining economic viability include: inherent yield-determining factors (viz., strain selection, lipid productivity, photosynthetic efficiency), variations in production systems (viz. system type, artificial or natural lighting) and harvesting and conversion (viz. quality of product required, moisture content). The selection of appropriate strains and establishment of optimal growth conditions are important factors in the overall success of biofuel production [25, 162, 179, 191, 224]. The ideal strains for biofuel production should [23]: (1) have high lipid productivity; (2) be robust and able to survive the shear stresses encountered in photobioreactors (PBRs); (3) be able to dominate wild strains in open pond production systems; (4) have high CO_2 fixation capacity; (5) have limited nutrient requirements; (6) be tolerant to a wide range in temperatures resulting from the diurnal cycle and seasonal variations; (7) be able to produce valuable co-products; (8) have a fast productivity cycle; (9) have a high photosynthetic efficiency; and (10) display self-flocculation characteristics. Currently, there is no known algal strain capable of meeting all these requirements concurrently. However, Fig. 3 illustrates the key cell characteristics for biofuel production, encompassing requirements for energy-efficient downstream processing.

Table 1 summarises the characteristics of biofuel-directed microalgae species that have been investigated. It is shown that most of the species have naturally high lipid contents (ca. 2–75% dry weight). Increased concentration of lipids may be effected by optimising the growth-determining factors [91], such as nitrogen level [178, 222, 223, 227], light intensity [168, 222], temperature [168], salinity [168, 227], dissolved oxygen [106], and CO_2 concentration [41, 51]. However, it is noteworthy that increasing the concentration of lipids through manipulation of growth factors will not necessarily increase the overall lipid production, since biomass and lipid productivity are mutually exclusive [177, 191]. Production systems should aim to optimise triglycerides and free fatty acid (FFA) lipids which are more easily convertible to biofuel.

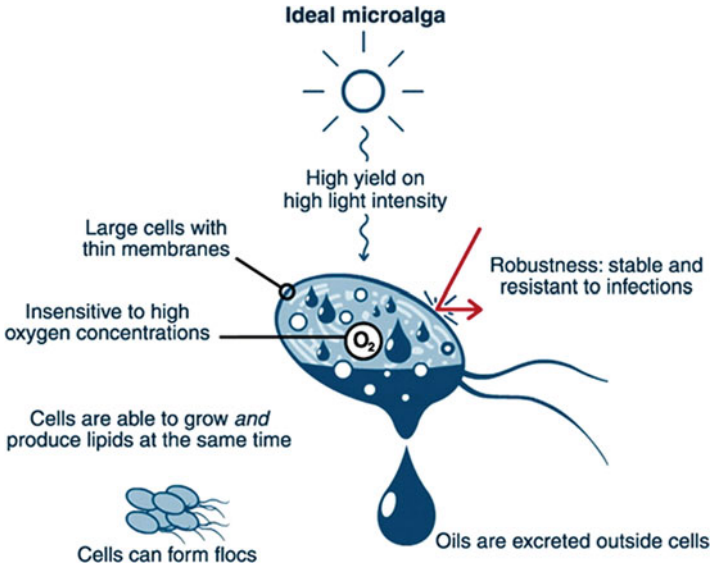

Fig. 3 The ideal photosynthetic cell factory for biofuels (Wijffels and Barbosa, 2010) (With permission from *Science* Journal/American Association for the Advancement of Science)

2.2 Optimisation of Algal Biomass Production

In phototrophic cultures, microalgae can be grown in two distinct production systems: open pond systems and enclosed PBRs. These production units control the environmental (viz. light, temperature, pH, salinity, nutrient qualitative and quantitative profiles, and dissolved oxygen), biological impact factors (viz. predation, viruses, competition and growth of epiphytes) and operational factors (viz. hydraulic residence time, harvesting rate, gas transfer rate, mixing equipment, shear rates and light exposure) that affect the growth of microalgae [106]. Full-scale operations of both open ponds and enclosed PBRs for biofuel-directed microalgae production are still mostly in demonstration phase, hence, their long-term operation performance will be required to counter the many uncertainties that prevail [162].

2.2.1 Open Pond Systems

Open pond systems can be categorised into natural waters (e.g. lakes, lagoons, ponds) and artificial ponds [20]. The raceway pond is the most commonly used artificial open pond system (Fig. 4) [97]. It typically consist of a closed loop, recirculation channel of between 0.2 and 0.5 m depth, usually constructed in concrete or compacted earth with a plastic lining [38]. In a continuous production cycle, algal broth and nutrients are introduced after the paddlewheel and circulated through channels to the harvest extraction point, generally located before the paddlewheel. The CO_2 requirement is obtained from air, but to enhance productivity and stabilise algae growth, submerged CO_2 aerators may be used [206].

Table 1 Characteristics of biofuel-directed microalgae species (Data sources: Becker [12], Balat and Balat [11], Griffiths and Harrison [82], Mata et al. [128])

Species	Phylum	Growth medium	Constituents (% dry weight)			P_{lipid} (mg L^{-1} day^{-1})	P_{volume} (g L^{-1} day^{-1})	P_{aerial} (g m^{-2} day^{-1})
			Lipids[a]	Proteins	Carbohydrates			
Anabaena cylindrica	Cyanobacteria	Freshwater	4–7	43–56	25–30	–	–	–
Ankistrodesmus sp.	Chlorophyta	Freshwater	24–31	–	–	–	–	11.5–17.4
Botryococcus braunii	Chlorophyta	Freshwater	25–75	–	–	–	0.02	3.0
Chaetoceros muelleri	Bacillariophyta	Marine	33.6	–	–	21.8	0.07	–
Chaetoceros calcitrans	Bacillariophyta	Marine	14.6–16.4	–	–	17.6	0.04	–
Chlamydomonas reinhardtii	Chlorophyta	Freshwater	21	48	17	–	–	–
Chlorella emersonii	Chlorophyta	Freshwater	25–63	–	–	10.3–50	0.036–0.041	0.91–0.97
Chlorella protothecoides	Chlorophyta	Freshwater	14.6–57.8	–	–	–	2–7.7	–
Chlorella pyrenoidosa	Chlorophyta	Freshwater	2	57	26	–	2.90–3.64	72.5
Chlorella sorokiniana	Chlorophyta	Freshwater	19–22	–	–	44.7	0.23–1.47	–
Chlorella vulgaris	Chlorophyta	Freshwater	11–22	51–58	12–17	11.2–40	0.02–0.2	0.57–0.95
Chlorococcum sp.	Chlorophyta	Freshwater	19.3	–	–	53.7	0.28	–
Crypthecodinium cohnii	Myzozoa	Marine	20–51.1	–	–	–	10	–
Dunaliella bioculata	Chlorophyta	Marine	8	49	4	–	–	–
Dunaliella primolecta	Chlorophyta	Marine	23.1	–	–	–	0.09	14
Dunaliella salina	Chlorophyta	Saline	6–25	57	32	116	0.22–0.34	1.6–3.5
Dunaliella tertiolecta	Chlorophyta	Marine	15–71	–	–	–	0.12	–
Euglena gracilis	Eustigmatophyta	Marine	14–20	39–61	14–18	–	7.7	–
Haematococcus pluvialis	Chlorophyta	Freshwater	25	–	–	–	0.05–0.06	10.2–36.4
Isochrysis galbana	Haptophyta	Marine	7–40	-	–	–	0.32–1.60	–

Nannochloris sp.	Chlorophyta	Marine	20–56	–	–	60.9–76.5	0.17–0.51	–
Nannochloropsis oculata	Eustigmatophyta	Marine	22.7—31	–	–	84–142	0.37–0.48	–
Nitzschia sp.	Bacillariophyta	Marine	16–47	–	–	–	–	8.8–21.6
Pavlova salina	Haptophyta	Marine	30.9	–	–	49.4	0.16	–
Pavlova lutheri	Haptophyta	Marine	35.5	–	–	40.2	0.14	–
Phaeodactylum tricornutum	Bacillariophyta	Marine	18–57	–	–	44.8	0.003–1.9	2.4–21
Porphyridium cruentum	Rhodophyta	Marine	9–18.8	28–39	40–57	34.8	0.36–1.50	25
Prymnesium parvum	Haptophyta	Marine	22–38	28–45	25–33	–	–	–
Scenedesmus dimorphus	Chlorophyta	Freshwater	16–40	8–18	21–52	–	–	–
Scenedesmus obliquus	Chlorophyta	Freshwater	11–55	50–56	10–17	–	0.004–0.74	–
Scenedesmus quadricauda	Chlorophyta	Freshwater	1.9–18.4	47	–	35.1	0.19	–
Skeletonema costatum	Bacillariophyta	Marine	13.5–51.3	–	–	17.4	0.08	–
Spirogyra sp.	Streptophyta	Freshwater	11–21	6–20	33–64	–	–	–
Spirulina maxima	Cyanobacteria	Saline	6–9	60–71	13–16	–	0.21–0.25	25
Spirulina platensis	Cyanobacteria	Saline	4–16.6	46–63	8–14	–	0.06–4.3	1.5–14.5
Tetraselmis maculata	Chlorophyta	Marine	3	52	15			
Tetraselmis suecica	Chlorophyta	Marine	8.5–23	–	–	27–36.4	0.12–0.32	19
Thalassiosira pseudonana	Bacillariophyta	Marine	20.6	–	–	17.4	0.08	–

[a]To date, there is no comprehensive data in literature that distinguish or isolate the triglyceride (TAG) and free fatty acid (FFA) content of microalgal lipids. However, available evidence indicates that certain species can achieve high percentage of TAG yield in relation to overall lipid content; such include *Nannochloropsis* sp. (95%), *Dunaliella parva* (95%) and *Phaeodactylum tricornutum* (70%). It is envisaged that continued research on biofuel-directed microalgae production will eventually make such demarcation possible for a range of viable species

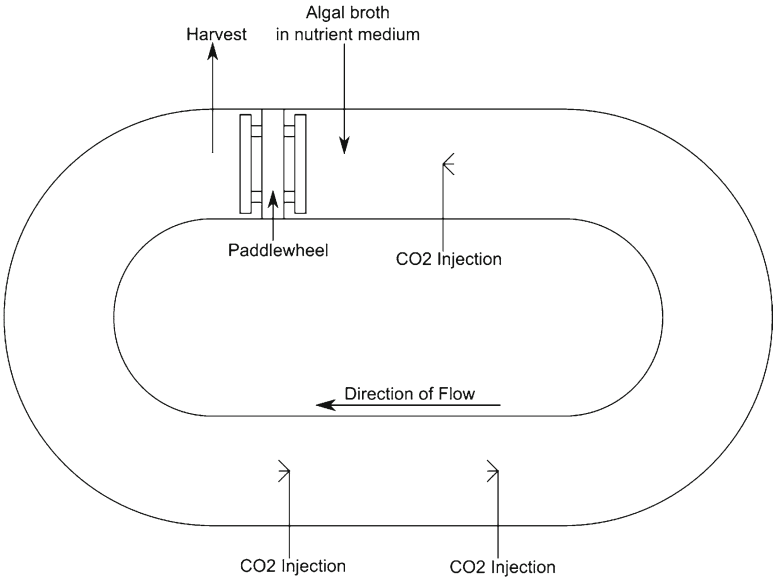

Fig. 4 Plan view of a raceway pond. Algae broth is introduced after the paddlewheel, and completes a cycle while being mechanically aerated with CO_2. It is harvested before the paddlewheel to start the cycle again (Adapted from Chisti [38])

Open pond systems are considered the cheapest to build and operate [128], have lower energy inputs [177], are more durable [128] and easier to maintain [213] when compared to enclosed PBRs. Therefore, open pond systems are perhaps more suitable for cultivating microalgae for biofuels [92]. However, open pond systems are more susceptible to contamination from invasive algae or bacteria, but monoculture production systems are still achievable for some highly selective species. For example, *Dunaliella salina* and *Spirulina* thrive under highly saline and high alkaline growth conditions, respectively [20]. They are also exposed to the prevailing environmental condition, which hinders the prospect of controlling temperature, evaporation and lighting [128]. Although they may occupy a large land area, they do not necessarily compete for land with existing agriculture crops, since they can be deployed on lands with marginal crop production potential [39]. Table 2 shows the typical yields in open pond production of selected algae species.

High algal biomass production rates are achievable with open pond systems, but the yields are lower compared to enclosed PBRs [38]. Currently, there are significant variations in the production rates reported in literature (Table 2), while the extrapolation of laboratory results has proved to be very poor bases for estimating the performance of full-scale production systems.

2.2.2 Enclosed Photobioreactors

Enclosed PBRs were developed to overcome the limitations of open pond production systems. The PBRs generally consist of an array of straight glass or plastic

Table 2 Biomass productivity for open pond systems (Adapted from Brennan and Owende [23])

Species	Cell density ($g\ L^{-1}$)	P_{aerial} ($g\ m^{-2}\ day^{-1}$)	P_{volume} ($g\ L^{-1}\ day^{-1}$)	PE (%)	Reference
Anabaena sp.	0.23	23.5	0.24	>2	[146]
Chlorella sp.	10	25	–	–	[189]
Chlorella sp.	40	23.5	–	6.48	[61]
Chlorella sp.	40	11.1	–	5.98	[61]
Chlorella sp.	40	32.2	–	5.42	[61]
Chlorella sp.	40	18.1	–	6.07	[61]
Haematococcus pluvialis	0.20	15.1	–	–	[93]
Not available	0.14	35	0.117	–	[38]
Various	–	19	–	–	[221]
Spirulina sp.	1.24	69.16	–	–	[145]
Spirulina platensis	0.47	14	0.05	–	[67, 97]
Spirulina platensis	–	–	0.18	–	[175]
Spirulina platensis	0.9	12.2	0.15	–	[167]
Spirulina platensis	1.6	19.4	0.32	–	[167]

(polypropylene acrylic or polyvinylchloride) tubes as shown in Figs. 5 and 6. Sunlight is captured by the tubular arrays of diameter ≤0.1 m and which may be aligned horizontally [142], vertically [181], inclined [214], or in a helix [220]. Algae cultures are recirculated in the arrays either with a mechanical pump or airlift system, the latter allowing CO_2 and O_2 to be exchanged between the liquid medium and aeration gas as well as providing a mechanism for mixing.

Enclosed PBRs offer better process control and therefore higher biomass productivity can be achieved when compared with open pond systems (Table 3). They permit the single species cultivation for prolonged periods due to reduced contamination risks, which also allows their use for production directed to pharmaceutical and cosmetics industry [213]. Vertically oriented PBRs minimise space requirements [164], and due to higher cell mass productivities attained, harvesting costs can also be reduced. Nevertheless, enclosed PBRs cost substantially more than open pond systems. Higher construction costs and more complex operational and maintenance procedures may potentially incur inferior net energy returns and cost-effectiveness [31,106]. Examples of large enclosed PBRs on record include the 25 m^3 plant at Mera Pharmaceuticals, Hawaii [155], and the 700 m^3 plant at the IGV in Klötze, Germany [164].

2.3 *Genetic Engineering of Microalgae*

Genetic engineering of microalgae can provide important and significant improvements for algal-biofuel production, by increasing the yields of TAGs to facilitate more efficient biodiesel conversion [187]. In the 1960s, the genome of *Anabaena* PCC7120 (Chloroxybacteria) was successfully cloned to produce a model organism for academic research [92]. However, for eukaryotic algae there is still a lack of understanding of the detailed molecular biological and regulation of lipid body

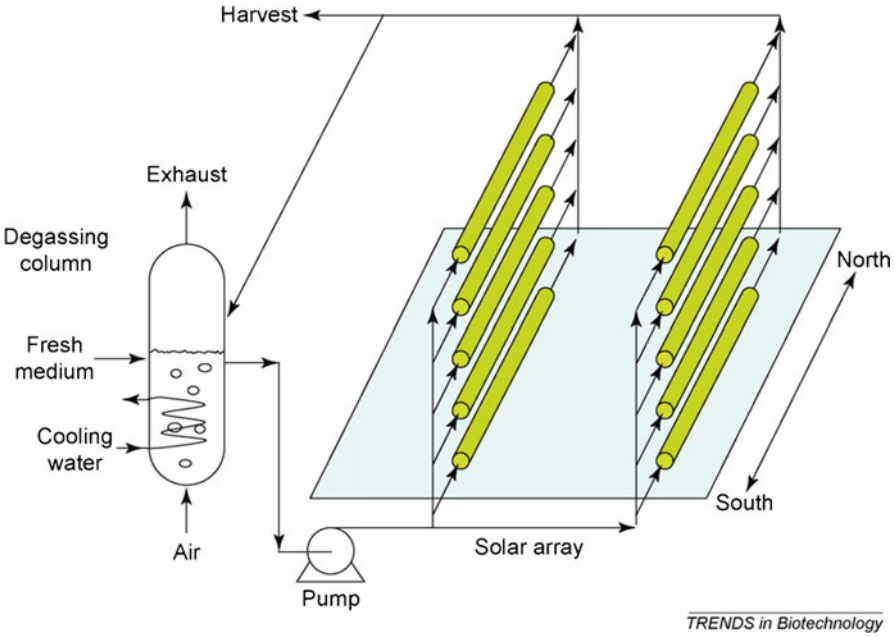

Fig. 5 Basic design of an enclosed horizontal tubular photobioreactor (Adapted from Chisti [39]). Two main sections, airlift system and solar receiver array. The degassing column allows for the transfer of O_2 out of the systems and transfer of CO_2 into the system as well as providing a means to harvest the biomass. The solar receiver provides a platform for growth enhancement by giving a high surface area to volume ratio (With permission from Elsevier Ltd.)

Fig. 6 A 400-litre vertical column photobioreactor in operation (Photo courtesy of Centre for Applied Energy Research, University of Kentucky, Lexington, KY, USA)

Table 3 Biomass productivity for enclosed photobioreactors (Adapted from Brennan and Owende [23])

Species	Reactor type	Volume (L)	X_{max} (g L^{-1})	P_{aerial} (g m^{-2} day^{-1})	P_{volume} (g L^{-1} day^{-1})	PE (%)	Reference
Chlorella sp.	Flat plate	400	–	22.8	3.8	5.6	[62]
Chlorella sp.	Flat plate	400	–	19.4	3.2	6.9	[62]
Chlorella sorokiniana	Inclined tubular	6	1.5	–	1.47	–	[214]
Chlorococcum sp.	Parabola	70	1.5	14.9	0.09	–	[182]
Chlorococcum sp.	Dome	130	1.5	11.0	0.1	–	[182]
Phaeodactylum tricornutum	Airlift tubular	200	–	20	1.2	–	[3]
P. tricornutum	Airlift tubular	200	–	32	1.9	2.3	[142]
P. tricornutum	Outdoor helical tubular	75	–	–	1.4	15	[84]
Porphyridium cruentum	Airlift tubular	200	3	–	1.5	–	[26]
H. pluvialis	Parallel tubular (AGM)	25,000	–	13	0.05	–	[155]
Haematococcus pluvialis	Bubble column	55	1.4	–	0.06	–	[76]
H. pluvialis	Airlift tubular	55	7	–	0.41	–	[76]
H. pluvialis	Flat plate	25,000	–	10.2	–	–	[93]
Nannochloropsis sp.	Flat plate	440	–	–	0.27	–	[32]
Spirulina platensis	Undular row tubular	11	6	47.7	2.7	–	[30]
S. platensis	Tubular	5.5	–	–	0.42	8.1	[45]
Spirulina sp.	Tubular	146	2.37	25.4	1.15	4.7	[29]
Tetraselmis sp.	Column	ca. 1,000	1.7	38.2	0.42	9.6	[36]

metabolism [187]. Therefore, genetic manipulation (transgenics) remains limited to a few selected algal laboratory models, i.e. *Chlamydomonas reinhardtii, Volvox carteri, Cyanidioschyzon merolae, Emiliania huxleyi*, and the diatoms *Phaeodactactylum tricornutum,* and *Thalassiosira pseudonana*. The expanding research interest in biofuel-directed microalgae has led to genetic engineered model organisms [13, 217] and general advances in algal transgenics. Additional genome sequencing for strains with suitable characteristics for biofuels and more universal genetic transformation tools that could enable further development of trangenetic based microalgae-derived biofuel production are considered to be necessary for further advancement [13]

The application of genetic engineering has progressed in several paths, with most recently, the direct manipulation of the microalgal lipid synthesis through gene expression and shunting of photosynthetic carbon partitioning to TAG synthesis [119]. The high expression of acetyl-coA carboxylase gene, which has a role in controlling the level of lipid accumulation, has lead to an improvement of lipid content in the engineered microalgae cells [92]. Another genetic engineering process for enhancing the lipid yields that has been tested is the shunting of pathways from starch production to lipid synthesis, by freeing precursor metabolites for desired biofuel products [187]. Both Li et al. [119] and Wang et al. [219] successfully induced inactivation of ADP-glucose pyrophosphorylase in a *C. reinhardtii* starchless mutant (*sta6*). Li et al. [119] reported a tenfold increase in lipid synthesis, while Wang et al. [219] reported a 30-fold increase in lipid synthesis, ultimately leading to a high concentration of TAG per cell. Therefore, future use of transgenics to improve TAG content of biofuel-directed microalgae is potentially an important bearing in the quest for economic production.

2.4 Commercial Production Scenarios and Strategies for Biofuel-Directed Microalgae

Five key strategies have been recognised to be key to cost reduction and acceleration of commercialisation of microalgae-derived biofuels (biodiesel, bio crude and drop-in fuels), including [208]: (1) Identification of algae species with high oil content and that will also grow quickly to produce fuels; (2) Using algal species with a high triglyceride (TAG) oil content; (3) Identification of low cost oil extraction and harvesting methods, which is still a significant economic challenge; (4) Since algal-biofuel production process is a complex composite of important sub-processes, reducing the number of steps is essential to providing easier, better and lower-cost systems; and (5) Fractionation marketing approach (biofuel and co-products) are critical to successful commercial production, e.g. potential co-production of green plastics, green detergents and cleaners, and biodegradable and non-toxic polymers secure premium price over traditional petroleum-based products.

Notable R&D investments have recently been committed to biofuel-directed microalgae production systems, in attempts to meet requirements in the outlined strategies, e.g. the commercial ventures by NASA and ExxonMobil. NASA in collaboration with Seambiotic Ltd, USA, is aiming to advance algae research by developing growth processes for microalgae, specifically for the production of

Table 4 Selection of algae production companies and their outlined strategies (Adapted from Singh and Sai Gu [194])

Company	Country	Cultivation method	Biofuel production pathway
Algenol Biofuels	USA	Enclosed system	Uses algae to produce and secrete ethanol from CO_2, water and sunlight
Aurora Biofuels	USA	Enclosed system	Uses genetically modified microalgae to produce biodiesel
LiveFuels Inc.	USA	Open pond	Plans to create "green crude" from microalgae to use in conventional refineries
FairEnergie GmbH	Germany	Enclosed system	Plans on using flue gas from a CHP plant to produce microalgae in conjunction with Subitec GmbH
E.ON Hanse AG	Germany	Enclosed system	Plans on using flue gas from a CHP plant to produce microalgae in conjunction with Subitec GmbH
OriginOil Inc.	USA	Open pond	Developing a "single-step extraction" method to reduce complex harvesting processes
PetroSun	USA	Open pond	Developing a "carbon neutral" process involving the pyrolysis of algal biomass
Sapphire Energy	USA	Enclosed system	Plans to create "green crude" from microalgae to use in conventional refineries
Seambiotic	Israel	Open pond	Utilising flue gas from coal burning power plants for algae cultivation
Solazyme Inc.	USA	Enclosed system	Algal fermentation production process to convert biomass directly into oil
Solena	USA	Enclosed system	Uses high-temperature plasma field to transform algal biomass into a synthetic gas
Solix Biofuels	USA	Enclosed system	Developing a scalable algae production system designed to enable the industrialisation of algae
Subitec GmbH	Germany	Enclosed system	4.13 m^3 Flat-panel-airlift photobioreactor production in conjunction with EnBW AG
Synthetic Genomics Inc.	USA	Enclosed and open pond systems	Genetically modifying microalgae to make a more efficient production process

aviation fuel [6]. ExxonMobil Corporation initiated a $600 million research programme in collaboration with Synthetic Genomics Inc. (SGI), aimed at creating superior strains of algae and developing more efficient production processes [6, 7].

In the EU, the public-funded Carbon Trust of UK plans to invest £26 million into algae research, and has initiated an £8 million Algal Biofuels Challenge (ABC) which aims to address the fundamental R&D requirements through collaborative research programmes involving 11 institutions. Research aims include [8]: (1) isolation and screening of algae strains, (2) maximising solar conversion efficiency, (3) achieving both high oil content and high productivity, (4) sustained algae cultivation in open ponds and (5) design and engineering of cost-effective production systems.

A €6 million UK and Irish joint project called BIOMARA aims to demonstrate the feasibility and viability of producing biofuels from marine biomass. BIOMARA deals with both macroalgae (seaweeds) and microalgae for expanded feedstock base, and will also evaluate environmental, social and economic impacts [9].

Private companies are also investing in biofuel-directed microalgae technology R&D through various different strategies (Table 4). Due to commercial sensitivity

and protection of intellectual property rights, very little information on technical and economic performance of these strategies is publicly available; therefore it was not possible to make an objective assessment of the performance as part of this chapter.

3 Integration of Algal Biomass Production with Environmental Impact Mitigation: Opportunities and Challenges

3.1 Bio-mitigation of CO_2 Emission

The rationale for enhancement of strategies for mitigation of CO_2 emissions related to energy production and utilisation has been outlined in a large body of environmental science research and the underpinning policy considerations pertaining to sustainable energy systems [83, 216]. Methods for CO_2 capture and storage include the use of physiochemical absorbents, injection into deep oceans and geological formations (e.g. saline aquifers and deep ocean basalt), and biological fixation [17]. However, it could be argued that biological fixation is the only economical and environmentally sustainable long-term strategy for CO_2 mitigation because the other strategies incur high cost and space requirements, and there are risks of CO_2 leakage over time [183]. It has also been argued that carbon capture and storage might be the easier technique for controlling GHG, than building energy conversion systems that do not emit them. Consequently, hypotheses for "artificial trees" that capture CO_2 much faster than terrestrial plants have been advanced [107].

Microalgae can be used for the biological capture and storage of CO_2 as they readily consume CO_2 during photosynthesis with a more efficient system than terrestrial energy crops [15, 218]. They can be used to capture CO_2 from three different sources, namely: the atmospheric CO_2, emission from power plants and industrial processes employing fossil fuels, and the CO_2 from soluble carbonate [218]. Capture of atmospheric CO_2 is the most basic carbon mitigation strategy that can be coupled to microalgae production systems. However, due to the relatively low concentration of atmospheric CO_2 (ca. 360 ppm), the potential biomass yield is limited, which makes it uneconomical [198]. The CO_2 emissions in the flue gases from power plants or industrial processes are of higher concentrations, usually 10–14% [207], and therefore offer better mitigation potential, with commensurate increase in algal biomass production. The process is practicable for both PBR and raceway pond microalgae production systems [17]. However, only a limited number of algae species are tolerant to the typical levels of SO_X and NO_X and the high temperatures of flue gases. A few species have the ability to assimilate CO_2 from soluble carbonates such as Na_2CO_3 and $NaHCO_3$ [218].

The selection of suitable microalgae strains has a significant effect on efficacy and cost-competitive of the CO_2 bio-mitigation process. Table 5 provides experimental data on ranges of known characteristics of selected species that have been

Table 5 CO_2 and biomass productivity for CO_2 mitigation species (Adapted from Brennan and Owende [23])

Microalgae	T (°C)	CO_2 (%)	P_{volume} (g L^{-1} day^{-1})	P_{CO_2} (g L^{-1} day^{-1})	Carbon utilisation efficiency (%)	Reference
Botryococcus braunii	25	10	0.027	–	–	[232]
B. braunii	25	Flue gas	0.077	–	–	[232]
Chlorella kessleri	30	18	0.087	–	–	[51]
Chlorella sp.	26	Air	0.682[a]	–	–	[42]
Chlorella sp.	26	2	1.445[a]	–	58	[42]
Chlorella sp.	26	5	0.899[a]	–	27	[42]
Chlorella sp.	26	10	0.106[a]	–	20	[42]
Chlorella sp.	26	15	0.099[a]	–	16	[42]
Chlorella vulgaris	25	10	0.105	–	–	[232]
C. vulgaris	25	Air	0.040	–	–	[188]
C. vulgaris	25	Air	0.024	–	–	[188]
C. vulgaris	27	15	–	0.624	–	[233]
Haematococcus pluvialis	20	16–34	0.076	0.143	–	[93]
Scenedesmus obliquus	–	Air	0.009	0.016	–	[80]
S. obliquus	–	Air	0.016	0.031	–	[80]
S. obliquus	30	18	0.14	0.260	–	[50]
Scenedesmus sp.	25	10	0.218	–	–	[232]
Scenedesmus sp.	25	Flue gas	0.203	–	–	[232]
Spirulina sp.	30	12	0.22	0.413	–	[50]

[a]Culture incubated for 4–8 days

Table 6 Summary results of microalgae performance in wastewater treatment with respect to nitrogen and phosphorus reduction

Species	Illumination period	Time (h)	Temperature (°C)	Elemental reduction (%)		Reference
				N	P	
Botryococcus braunii	24	–	25	27.3	–	[184]
Chlorella kessleri	24	72	–	18.8	–	[114]
C. kessleri	12/12	72	–	8.3	–	[114]
Phormidium bohneri	12/12	–	20	82	85	[63]
P. bohneri	–	90	–	98.3	–	[109]
Scenedesmus obliquus	24	188	25	100	97[a]	[127]
S. obliquus	–	–	–	21	73	[80]
S. obliquus	–	–	–	53	45	[80]
Spirulina sp.	–	–	–	93	72	[156]
Mixed species[b]	24	72	15	99.8	98.8	[37]
Mixed species[b]	24	72	25	99.7	99.1	[37]

[a]Max reduction percentage occurred after 94 h

[b]Fourteen strains were considered, including: *Botryococcus braunii, Chlorella protothecoides, Chlorella saccharophila var. saccharophila, Chlorella vulgaris, Cricosphaera carterae, Dunaliella tertiolecta, Nannochloris oculata, Spirulina platensis, Spirulina maxima, Tetraselmis suecica, Tetraselmis chuii, Phaeodactylum tricornutum, Pleurochrysis carterae*, and a consortium of wastewater isolates

studied. From the data, it can be seen that a wide range of species are capable of growing under enhanced CO_2 and flue gas conditions. The data for *Chlorella* sp. also show that carbon utilisation efficiency of the microalgae decreases with increase in CO_2 concentration in the flue gas. This would imply that, flue gas with higher CO_2 concentration may necessitate a recirculation through the algae production system to attain the same level of CO_2 extraction, or in order to meet a set level of residual CO_2 in the exhaust.

3.2 Bioremediation of Industrial Wastewaters

Wastewater sparged with CO_2 provides a conducive growth medium for microalgae, enabling faster production rates and reduced nutrient levels in treated wastewater (Table 6), decreased harvesting costs, and increased lipid production [123]. Therefore, coupling of the production of biofuel-directed microalgae with bioremediation of wastewaters is considered an important strategy for successful deployment [16, 123, 215].

Microalgae are efficient removers of chemical and organic contaminants, heavy metals, and pathogens from wastewater [150], which provide a pathway for combating eutrophication in conjunction with the production of microalgae as energy resource [228]. This characteristic enhances the sustainability potential of the production process, through potential savings on requirements for chemical remediation of wastewater [218], and minimises the need for freshwater for algae production [118, 195].

Microalgae have also exhibited significant potential for biological removal of hazardous or toxic compounds due to their negatively charged surfaces [106]. For example, they have demonstrated a strong absorption of polyvalent cations; an ion exchange capacity that is the basis for removal of heavy metals from wastewaters [149]. Another advantage is in the production of photosynthetic oxygen in wastewater, which reduces the need for external aeration. The oxygen is also required by bacteria for biodegradation of pollutants such as polycyclic aromatic hydrocarbons (PAHs), phenolics and organic solvents [149]. However, some of these pollutants are potent inhibitors of photosynthesis in microalgae because they can induce morphological changes in the cells that lead to physiological incompatibility [106].

4 State-of-the-Art in Microalgae Biomass Harvesting and the Extraction of Bioproducts

Figure 7 summarises the different stages of production and downstream processing of biofuel-directed microalgae. Each stage itemises the applicable techniques based on current knowledge.

4.1 Harvesting Techniques

The harvesting of microalgae biomass is a critical step in the production of biofuels from microalgae, because it determines the final quality of extracts, and energy inputs, and therefore overall sustainability, and it also prevents fouling of the production process [106,174]. Harvesting probably accounts for the highest component of the total cost of microalgae biomass production [59, 173]. This high cost is due to the low cell densities (typically in the 0.3–0.5 $g\,L^{-1}$ range) and the small size of the microalgal cells (typically <40 μm) [118], which results in low separation or dewatering efficiency and poor product quality under suboptimal growing conditions [49]. The selection of appropriate harvesting techniques is therefore critical

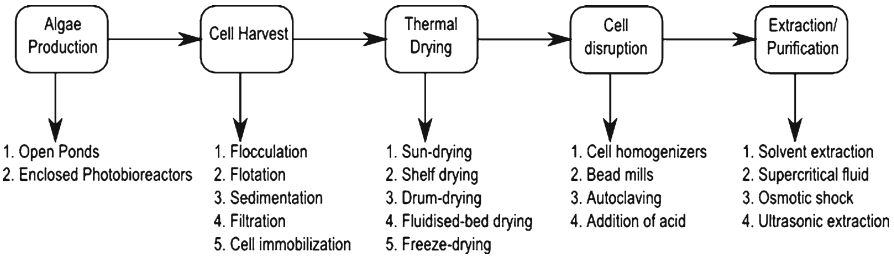

Fig. 7 Harvesting and processing pathways for microalgal-directed biofuels (Adapted from Schmid-Staiger [186])

to economic and environmentally sustainable harvesting [185]. For biofuel-directed production, harvesting process should not incur negative energy balance [187].

There is no universal harvesting method for microalgae, but typical processes used singly or in combinations include flocculation, flotation, filtration, sedimentation, filtration and cell immobilisation (Fig. 7). Factors such as strain, cell density, culture condition, growth media and value of target products determine both the cost of and ease of harvesting [106]. For example, the cyanobacterium *Spirulina's* long spiral shape (20–100 μm) naturally lends itself to cheaper and energy-efficient micro-screen harvesting method [14]. Overall, appropriate harvesting unit process should be able to: maximise the recovered biomass dry weight (varies with microalgae species, biomass concentration and cell sizes), minimise the cost of operation and maintenance (including energy consumption), and yield quality extracts [49].

Flocculation: Flocculation process aggregates the microalgal cells to increase the overall cluster sizes [128], and is generally used as a preparatory step for other harvesting methods [141]. It involves the addition of multivalent cations and cationic polymers to the culture medium to neutralise the negative charge that is carried on the surface of many microalgal cells [158]. Flocculation may also physically link one or more aggregates in a process referred to as bridging [141]. Since chemical flocculants are used, this process is unsuitable for food-grade products.

Flotation: Dissolved air flotation (DAF) process injects micro-air bubbles into the culture column, and as they rise to the surface, they trap microalgae cells [158,218]. Some microalgae production units such as the tubular PBRs promote flotation through high overflow rates which causes cells to move upwards [64,102]. Flotation has advantages in its moderate cost, low space requirement and rapid operation compared to other processes, but its technical viability has only been demonstrated in a few studies [33, 120]. The use of ozone produces more efficient solid–liquid separation compared to DAF [33]

Sedimentation: Gravity sedimentation is one of the most commonly used harvesting processes because of its capability to handle large volumes of culture, and suitability for low-value biomass [153]. However, it can only be applied to species with large cell size (>70 μm) like *Spirulina* [149]. Ultrasonic aggregation may be used as precursor to enhance sedimentation. The main advantages are that it is a non-fouling technique, therefore can be used for food-grade products, and it can also be operated continuously without inducing shear stress on the microalgal cells which causes cell destruction [21]. Centrifugal recovery (CR) sedimentation is only feasible for harvesting of high-value metabolites and extended shelf-life concentrates for aquaculture [86]. The process is rapid but energy-intensive, which makes it unsuited to harvesting biofuel-directed algae biomass, but it may be more economic in large-scale production systems [24].

Filtration: Conventional filtration processes with micro-strainers or rotating screen filters with backwash may be the most appropriate for harvesting of large cell algae (>70 μm) such as *Spirulina* [128], but they cannot be used for species of bacterial dimensions like *Scenedesmus, Nannochloropsis* and *Chlorella* [140]. Conventional

filtration is popular because of its mechanical simplicity, availability in large unit sizes, and filtration aids such as diatomaceous earth and cellulose can be used to improve efficiency [141]. Membrane filtration and ultra-filtration are possible alternatives to conventional filtration for the recovery of smaller microalgae cells (<30 μm) [161], albeit a more expensive process because of the need for membrane replacement and pumping [128]. It is also a more suitable process for fragile cells like *Dunaliella*, because it pre-disposes low trans-membrane pressure and low cross-flow velocity conditions [19]. It can also be used to remove protozoans and viruses from used algal culture medium, while retaining nutrients for recirculation [234].

Cell immobilisation: This process prevents cells from moving independently of its neighbours to all parts of the aqueous phase of the system [203]. It has been presented as an option for harvesting microalgae biomass in wastewater treatment systems, but more research is needed on the effects of immobilisation on algal cell physiology and biochemistry [125]. Assessment for large-scale applications is still limited [106].

Thermal drying: Drying is sometimes required after the harvesting steps to prevent fouling of the final biomass product. The most common drying methods include: sun-drying, and low-pressure shelf-drying [163], spray-drying [58], drum-drying [163], fluidised bed-drying [111] and freeze-drying [143]. Sun-drying is the most popular method due to the low cost, but disadvantages include long drying times, the requirement for large surface areas, and high material loss [163]. Spray-drying and freeze-drying are expensive processes commonly used for the high-value products and oils [58, 143].

4.2 Growth and Productivity Monitoring Systems

Timely harvesting and extraction in the algae culture growth cycle is a key element to maximising the yield of desired product in biofuel-directed production. A number of methods can be employed to monitor the growth and productivity of algae cultures, including: cell-count, biomass yield measurement, and measurement of quality and quantity of lipids. Such information is necessary during the course of production to support decisions on process control strategy that could enhance productivity (e.g. initiating nitrogen-limiting condition if required to boost lipid production).

Cell-count aims to estimate the size of the culture population and the rate of population increase [5]. The cell growth stages can be determined through periodic cell-counts for known volume of the culture medium. Cell-count can be done under a transmitted light microscope or epifluorescence microscope using a cell-counting chamber. The most commonly used counting chambers are: Sedgwick-Rafter counting slide, Palmer-Maloney slide and Haemocytometer.

Biomass measurement is important in determining the yield at the point of harvesting, and dry weight measurement is the most common technique. It involves filtering the culture material through a pre-dried and pre-weighted glass-fibre filter. The filter is then rinsed with distilled water, dried until moisture-free and reweighted [232].

Measurement of lipid quality and yield are key requirements of biofuel-directed microalgae production systems. The traditional lipid extraction from dried microalgae is usually performed by solvent extraction and gravimetric determination of yield [18]. However, the process is time consuming and only capable of providing results a considerable time after the sample is taken. Lately, real-time analytical methods have been used, including Fourier transform-infrared microspectroscopy (FT-IR) [52], epifluorescence with Nile Red staining [66] and multi-parameter flow cytometry with Nile Red [47]. The FT-IR handles whole-cell analysis, which involves the measurement of infrared absorption in relation to a range of molecular vibrational, modes to indentify and quantify specific macromolecules [151]. Nile Red, a lipid-soluble fluorescence probe, has some key advantages for microalgae biofuel-directed production. It is relatively photostable, and intensely fluorescent in organic solvents and hydrophobic environments. In conjunction with Nile Red staining, epifluorescence measurement can differentiate between neutral and polar lipids assuming appropriate choice of excitation and emission wavelengths.

Multi-parameter flow cytometry can be used for qualitative and quantitative assessment of biological and physical properties of cells [47]. It can be used to monitor cells, in situ, at near real time, for intrinsic light scatter and autofluorescence. For example, Fig. 8 shows the cytograms from flow cytometry analysis of *Nannochloropsis oculata* and *Isochrysis galbana*. The chlorophyll *a* (fluoresces at 673 nm when it is excited at 633 nm) is shown on the *y* axes and the secondary photosynthetic pigments (fucoxanthin in *I. galbana* and violaxanthin in *N. oculata*, they fluoresce at 530 nm when exited at 488 nm) on the *x*-axes. The cytograms show that the chlorophyll *a* is the dominant photosynthetic pigment (depicted by the higher relative fluorescence on the *y*-axis when compared to the *x*-axis of each cytogram) for both *N. oculata* and *I. galbana.* When used in conjunction with different dyes such as Nile Red staining, cell viability and lipid content may be evaluated. For biomass and lipids, the readings can be calibrated against quantitative techniques outlined above.

4.3 Extraction and Purification of Oils and Bioproducts

Extraction processes represent another major limitation to the processing of harvested biomass for biofuels, feed, or for higher-value products (viz. proteins, pigments and PUFAs). Extraction processes are highly specific and are generally dictated by the desired product and quality standard [128, 174]. Extraction of biofuels must consider the balance between the drying efficiency and cost-effectiveness in order to maximise energy output and the recovery of other valuable co-products to enhance cost-competitiveness [118, 187]. After harvesting, several approaches are available for extracting products from microalgal biomass, generally depending on the strength of the microalgal cell wall and product to be obtained (Fig. 7). They include mechanical action (e.g. high-pressure cell homogenisers, bead mills, ultrasounds, supercritical fluid and autoclave) or non-mechanical action (e.g. freezing, organic

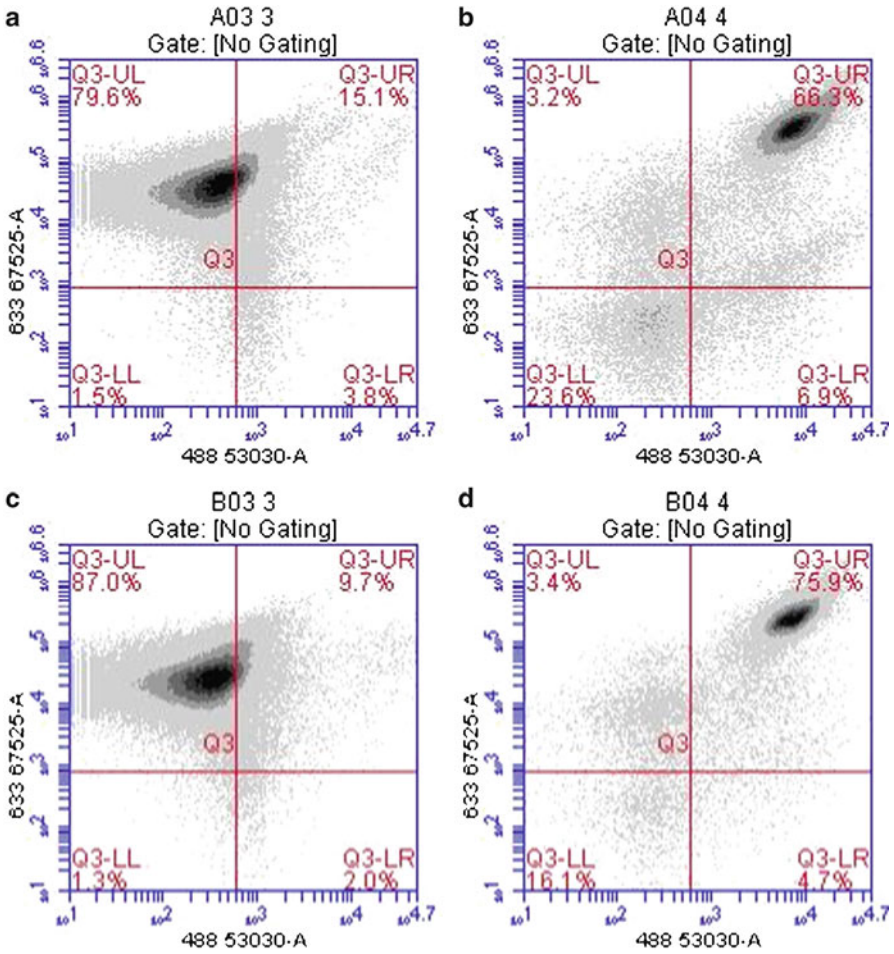

Fig. 8 Cell-intrinsic light scatter of *Nannochloropsis oculata* after 48 (**a**) and 120 h (**c**), and *Isochrysis galbana* after 48 (**b**) and 120 h (**d**). Each cytogram contains four quadrants (Q3-UL, Q3-UR, Q3-LR, Q3-LL) showing percentage values of cells present (Cytrograms courtesy of Flow Cytometry Core Facilities, UCD—Conway Institute of Biomolecular and Biomedical Research, University College Dublin)

solvents and osmotic shock) [128]. The respective assessments of these extractive methods are as follows:

1. The nature of cell walls strongly impacts on the extraction process by reducing cell biodegradability [193]. Cell disruption is often required for recovering intracellular products from microalgae. Most cell disruption methods have been adapted from applications on intracellular non-photosynthetic bioproducts [137], and have been used successfully on microalgal biomass [133]. The methods include the use of high-pressure cell homogenisers, bead mills, autoclaving, and addition of hydrochloric acid, sodium hydroxide, or alkaline lysis.

2. Solvent extraction is the most commonly used. Hexane solvent recovers >95% of the lipids [147]. Biomass is passed through an expeller or press and the pulp is mixed with hexane to extract the oils, and subsequently filtered out and the hexane/oil solution is separated by distillation [187]. For biofuel-directed extraction, it is desirable that the oil is extracted without significant contamination by other cellular components, such as DNA and chlorophyll [187].
3. Osmotic shock is the sudden reduction in osmotic pressure causing the cells to rupture and release cellular components. Microalgal species that lack cell walls (i.e. *Dunaliella* sp.) are suited to this process [187].
4. Ultrasonic extraction creates cavitation bubbles near cell walls and when these bubbles collapse, the shock waves developed cause the cell wall to rupture and release cellular components [187].
5. Supercritical fluid extraction generally uses CO_2 as an extraction solvent. It can achieve near 100% recovery of lipids under high pressure [147], but is a very energy-intensive and therefore may not be economical for biofuel extraction [187].

The outlined alternative production pathways for biofuel-directed microalgae are geared to addressing the economy of conversion to biofuels. However, there is special requirement for substantial conversion industry and research and development with regards to production systems, and energy efficiency and sustainability of the downstream harvesting and extraction processes. Ongoing research and development [212] suggests that the integration of production and downstream processing of biofuel-directed microalgae in a wider scheme of polyproduct systems, such as biorefineries, will be key to sustainable deployment of algae-derived biofuels.

5 Biorefinery Concept for Biofuel-Directed Microalgae

5.1 Conceptual Framework

Biorefining is the sustainable processing of biomass into a spectrum of marketable products and energy [94]. A biorefinery is a facility that integrates multiple biomass unit processes to produce energy, fuels, chemical products and biomaterials in a concept analogous to petroleum refineries depicted in Fig. 9 [201, 205]. The aim of a biorefinery is to deliver multiple products by depolymerising and deoxygenating the feedstock components, thereby maximising the value derived for the biomass feedstock [34]. It is based on the concept that: low-volume high-value outputs (proteins, carbohydrates, pigments, PUFAs, fertilisers and nutritional supplements) will increase the economic sustainability of the process; high-volume low-value outputs (biofuels, bulk chemicals and fertilisers) will meet specific standard and production targets, and there is an overall reduction of the unit's environmental footprint by reducing consumption of fossil fuel in the primary energy mix for

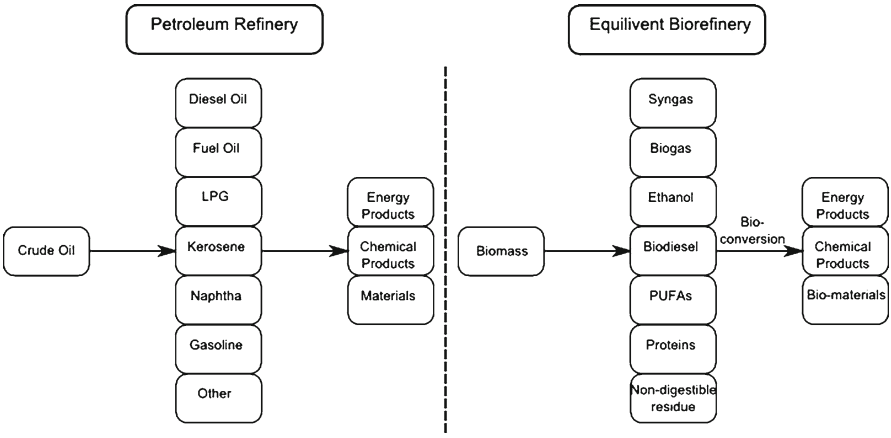

Fig. 9 Analogy of biorefinery concept for biomass with petroleum refinery

electricity generation [201]. Biorefineries are expected to run in a sustainable manner, and to a large extent, all energy requirements (heat and electricity) are generated internally from wastes and residues [34].

Biorefineries are based on four main technological processes, namely: thermochemical, biochemical, mechanical/physical and chemical processes [34]. The future of biorefineries is based on a feedstock-upgrading process where there is a limited number of processing pathways (e.g. thermochemical, biochemical, mechanical/physical and chemical processes), from which all the biofuels and high-value products will be derived [34]. Small- to medium-sized modular processing plants distributed in and around feedstock production areas minimise transportation costs [225].

Figure 10 shows a schematic biorefinery concept for biofuel-directed microalgae feedstock. It considers optimisation of biofuel processing (lipids), multiple product output (proteins, carbohydrates, pigments, PUFAs, fertilisers and nutritional supplements), material recycling and internal exchange, and the upgrade of individual process waste-streams to enhance material recovery and overall plant efficiency. The scenario considers the high-value co-products to biofuel production, if necessary, intended to subsidise it in the short term until markets have developed and costs stabilised. However, the co-product markets are small and easily saturated [199], which necessitates the identification of production threshold upon which all materials are directed to fuel production.

Co-location of an integrated biorefinery concept with CO_2-emitting industries facilitates the bio-mitigation of CO_2 emission which provides a complementary function that may be exploited to reduce cost and to enable sustainable utilisation of microalgae as a renewable energy resource [212]. This coupling will likely focus research efforts to overcome barriers to both carbon capture and production of biofuels and co-products. However, industrial CO_2 sources primarily view algae as a means of CO_2 capture as opposed to a method for producing biofuels and co-products, thus different goals between partners might be a major stumbling block in order for this type of co-location to be realised.

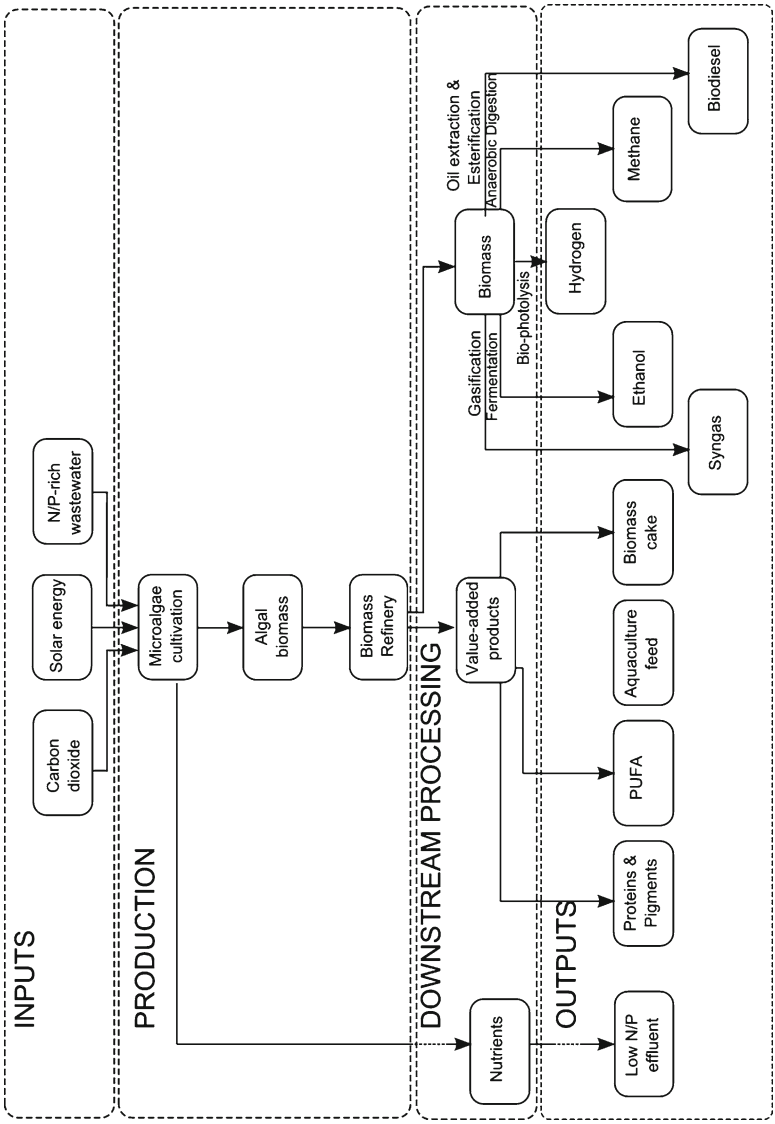

Fig. 10 Schematic of biorefinery concept utilising biofuel-directed microalgae feedstock

5.2 Algal Biomass-to-Liquid Fuel Pathways

5.2.1 Thermochemical Conversion

Thermochemical biomass conversion covers the thermal decomposition and chemical reformation of organic material in biomass to yield fuel and chemical products. Microalgae biomass can be converted into a fuel product by pyrolysis, thermochemical liquefaction and gasification [210].

Pyrolysis: Pyrolysis is the decomposition of biomass to bio-oil, syngas and charcoal at medium to high temperatures (350–750°C) under oxygen deficiency [81]. Microalgae biomass is suited to this process as their high lipid contents along with resolvable polysaccharides and proteins can be easily pyrolysed into bio-oils and syngas [92]. However, there are many technical challenges, notably, the high moisture content of the algal biomass and the bio-oil produced is generally high in nitrogen, and is acidic, unstable, viscous, and contains solids and dissolved water [35, 135]. Therefore, the derived bio-oils require further processing through hydrogenation and catalytic cracking to lower oxygen and remove alkalis [54].

Several studies have investigated the pyrolysis characteristics of microalgae biomass. Miao et al. [136] successfully carried out fast pyrolysis of *Chlorella prothothecoides* and *Microcystis aeruginosa* grown phototrophically. They recorded bio-oil yields of 18% (higher heating value (HHV) of 30 MJ kg^{-1}) and 24% (HHV of 29 MJ kg^{-1}), respectively. Miao et al. [136] recorded bio-oil yields of 57.9% (HHV of 41 MJ kg^{-1}) with heterotrophically grown *C. prothothecoides*, which was 3.4 times higher compared to phototrophic production. Demirbas [53] also obtained a bio-oil yield of 55.3% (HHV of 39.7 MJ kg^{-1}) at 502°C for *C. prothothecoides*. After extraction of bio-oil from *Nannochloropsis* sp. biomass, Pan et al. [159] pyrolysed the residual algal cake with and without a catalyst and recorded HHVs of 32.7 and 24.6 MJ kg^{-1}, respectively. Notably, the catalysed pyrolysis produced oil with a lower oxygen content and fewer harmful compounds.

Significant research gaps exist in current knowledge relating to the specifications of converting algal biomass into bio-oil. Optimal residence time, temperature, and the effect of different feedstock species and growing conditions on the pyrolysis process are all major areas that need further investigation.

Thermochemical liquefaction: Thermochemical liquefaction is a low-temperature (300–350°C), high-pressure process aided by a catalyst in the presence of hydrogen to produce bio-oil [81]. The process decomposes organic materials down to smaller higher-density molecules, by utilising the high activity of water at sub-critical conditions [160]. The ability of thermochemical liquefaction to take in wet microalgal biomass (thereby avoiding drying) and convert it to a bio-oil makes it more attractive for commercial exploitation [44, 60, 138]. However, the process reactors and fuel-feed systems for thermochemical liquefaction are more complex and expensive.

Several studies on thermochemical liquefaction of microalgae achieved positive outcomes. For example, maximum bio-oil yields of 64% (HHV of 45.9 MJ kg^{-1}) and

42% (HHV of 34.9 MJ kg^{-1}) were recorded for thermochemical liquefaction of *Botryococcus braunii* and *Dunaliella tertiolecta*, respectively [60, 138]. Thermochemical liquefaction is seen as a promising method for energy production due to its acceptance of high moisture content biomass. However, major research gaps exist in current knowledge with organic solid concentration, optimal residence time, temperature and catalytic conditions all major areas that require significant research.

Gasification: This process refers to the partial oxidation of biomass at high temperatures (800–1,000°C) to yield syngas, a mixture of predominantly CO, H_2 and CH_4 [44], which can be burnt directly or used as a fuel. Several studies have investigated the viability of energy production by gasification of microalgae biomass. For example, Hirano et al. [88] gasified *Spirulina* at temperatures ranging from 850 to 1,000°C and determined the gas composition required to attain a theoretical yield of methanol. The highest methanol yield of 0.64 g methanol per 1 g of algal biomass was achieved at 1,000°C. Tsukahara and Sawayama [210] concluded from their analysis that low-temperature gasification of microalgae to produce fuel and co-products is a viable pathway for bioenergy production and GHG mitigation.

5.2.2 Biochemical Conversion

Biochemical processes for the conversion of biomass into biofuels include anaerobic digestion, fermentation, and fuel production processes utilising algal metabolism such as photobiological hydrogen production.

Anaerobic digestion (AD): This is the bacterial conversion of organic material in the absence of oxygen over a temperature range of 30–65°C into biogas [34], which consists of primarily methane (CH_4) and carbon dioxide with trace amounts of hydrogen and sulphide. It is an appropriate conversion process for high moisture content biomass (80–90% moisture) and produces a gas with the energy content of about 20–40% of the lower heating value of the input feedstock.

This process is seen as most appropriate for the spent microalgae biomass and a necessary step to make microalgal biodiesel sustainable [193]. It is highly unlikely that microalgae will be grown specifically for conversion into biogas due to the high costs of production and cheaper alternative feedstocks being available (e.g. agriculture manure) [192]. Microalgae can contain a high proportion of proteins that result in low C/N ratios (ca. 10:1); therefore, increased ammonium production could degrade the anaerobic digestion process. The low C/N ratios may be corrected by appropriate co-digestion. For example [231], achieved a significant increase in methane production from 50/50 waste paper to microalgae biomass blend (1.17 mL L^{-1} per day) compared to anaerobic digestion of pure algae biomass (0.57 mL L^{-1} per day).

Fermentation: Process uses microorganism/or enzymes to convert organic materials which contain sugars, starch or cellulose into recoverable products (usually alcohols, e.g. ethanol or organic acids). Ethanol is currently the final product of choice for most fermentation processes. Some microalgae species such as *C. vulgaris*

are good feedstock for ethanol production due to their high starch content (ca. 37% dry weight) and the high conversion efficiencies (up to 65%) that have been recorded [89]. The evidence suggests that fermentation of microalgae biomass has potential as an energy conversion pathway, but the potential net energy and commercial returns should be addressed in the context of energy value of bio-ethanol compared with production of biodiesel [39].

Photobiological hydrogen production: Biological hydrogen production (Biohydrogen) is an appealing alternative to conventional liquid biofuel production as the naturally occurring molecule is a cleaner and more efficient energy carrier [44]. Microalgae species such as *C. reinhardtii*, *Chlorella fusca* and *Scenedesmus obliquus* possess the necessary genetic, metabolic and enzymatic characteristics to split water and photoproduce H_2 gas [78].

There are two fundamental approaches to photobiological H_2 production from water:

1. Direct production of H_2 during photosynthesis under anaerobic conditions. In this case, microalgae convert water molecules into hydrogen ions (H^+) and oxygen; the H^+ is subsequently converted by hydrogenase enzymes into H_2 [78, 105]. However, catalysis of hydrogenase is rapidly inhibited by the rising levels of photosynthetic oxygen, and hydrogen production is impeded [4, 28, 71, 131, 139]. Therefore, microalgae cultures for hydrogen production are operated under anaerobic condition.
2. Two-stage hydrogen production to overcome photosynthetic oxygen inhibition by separation of photosynthetic oxygen production and H_2 gas generation processes. In the first stage, microalgae are grown photosynthetically in normal conditions. In the second stage, microalgae production is operated under sulphur-limiting conditions thereby inducing anaerobic conditions and stimulating consistent hydrogen production [132]. This approach is limited over time (approximately after about 60 h of production) and theoretically produces less hydrogen when compared with direct production of H_2 [131]. The theoretical maximum yield of hydrogen by green algae two-stage production systems could be about 198 kg $H_2\,ha^{-1}$ per day [132].

5.3 *Clean Power Generation Strategies for Algae-Derived Biofuel: Process Life Cycle Analysis*

Life cycle analysis (LCA) is a systems approach that is aimed at evaluating the environmental impact of all processes that contribute to the entire life cycle of the product of interest, carried out in accordance with the ISO 14040 standard [187]. To objectively determine if microalgae biofuel production chains are environmentally sustainable it is deemed important to carry out a full LCA of the relevant process chains for rational boundary conditions. LCA can then be used to identify the "hotspots" in the process chains, i.e. where potential environmental burdens may be

dominant, and to identify downstream processes requiring technological improvement and innovation. Most LCAs incorporate impacts assessment such as GHG reduction potential and energy balance; additional impacts of processes such as the nitrogen cycle changes and recycling of spent biomass and nutrients (see biorefinery concept) provide more rational representation of the production process for algae-derived biofuels [106]. Currently, there are no validated life cycle inventories pertaining to microalgae-derived biofuel production process, e.g. water use and elemental and nutrient recycling, that could form bases for realistic scenarios [170].

The outlined limitations notwithstanding several LCA studies have been used to evaluate the potential environmental impacts of microalgae biofuel production systems. Liu and Ma [121] carried out an LCA of methanol production from microalgae and recorded a positive energy balance and reduction of environmental loading compared to equivalent fossil fuels. Campbell et al. [27] also recorded lower cost for producing algae-derived biodiesel with a substantial GHG reduction and a positive energy balance over petroleum diesel. However, they also noted that, for full-scale systems, the economic cost could exceed those for diesel due to inapplicable economies of scale, and the process being highly dependent upon the selection of algae species with high oil yields. For example, Lardon et al. [110] performed an LCA on biodiesel produced from *Chlorella vulgaris* grown in raceway ponds and recorded a negative energy balance (1.66 MJ of energy input to 1 MJ output).

Kadam [98] established the potential benefits to utilising recycled CO_2 towards microalgae production from LCA of algae co-firing scenario. He recorded lowered net fossil energy consumption, SO_x and NO_x, particulates, CO_2 and methane. Reijnders [173] has argued that, after considering the total fuel inputs during the biofuel life cycle (e.g. fossils fuel used for building the facilities and for operational activities such as supplying nutrients, mixing, harvesting and processing), microalgae-derived biodiesel is inferior to petroleum diesel. He illustrated that both ethanol from sugarcane (161–175 GJ ha^{-1} $year^{-1}$) and palm oil from oil palm (142–180 GJ ha^{-1} $year^{-1}$) returned higher net energy yield compared to methanol from microalgae (127 GJ ha^{-1} $year^{-1}$).

5.4 Fundamentals of Biofuel Standards and Benchmarking of Algal Biofuels

Although there are multiple conversion pathways for microalgae biomass conversion (see Sect. 5.2), biodiesel production through the extraction of algal bio-oil and subsequent esterification is as arguably the optimum route to biofuels with the current technologies [38, 92, 99, 104, 134, 185]. Esterification refers to the chemical reaction between TAG and alcohols to produce the mono-esters biodiesel [190]. Bio-oils from high lipid content microalgae (Table 1) are ideal for such conversion due to their high TAG contents [92]. Algae-derived biodiesel is a technically more attractive biofuel because, if sustainably produced, will incur zero net CO_2 emission, with only trace amounts of sulphur released in combustion [92], and contain

Table 7 Selected fuel properties for soybean biodiesel, algal biodiesel, diesel, EN14214 standard and ASTM D6751 standard (Adapted from [23,230])

Fuel property	Soybean biodiesel	Algal biodiesel	Diesel (EN590)	Biodiesel (EN14214)	Biodiesel (ASTM D6751)
HHV (MJ kg^{-1})	–	41	45.9	–	–
Kinematic viscosity (mm^2 s^{-1})	4.5	5.2	1.2–3.5	3.5–5.0	1.9–6.0
Density (kg L^{-1})	–	0.864	0.83–0.84	0.86–0.90	0.88
Carbon (wt%)	–	–	87	–	77
Hydrogen (wt%)	–	–	13	–	12
Oxygen (wt%)	–	–	0	–	11
Sulphur (wt%)	–	–	<0.05	<0.01	0.05
Flash point (K)	395	388	333–353	>374	373–443
Cloud point (K)	275	–	258–278	–	270–285
Pour point (K)	–	261	238–258	–	258–289
Cetane number	50	–	51	>51	48–60

no aromatic compounds or other harmful chemicals [124]. However, microalgae-derived bio-oils contain a high degree of PUFAs, which makes biodiesel products to be susceptible to oxidation in storage and therefore limits the potential utility [38].

Numerous research projects have been focused on improving the lipid content of microalgae species, to enhance the production process in order to make it more economically competitive [48, 112, 154, 219, 223, 229, 232]. The focus on improvement of the overall total lipid productivity may only achieve marginal economic gain, since algal lipids are composed of both neutral lipids (e.g. triglycerides, cholesterol) and polar lipids (e.g. phospholipids, galactolipids) that bear different desired qualities for biodiesel production. For Biodiesel Standard EN14214, the neutral lipids, i.e. FFAs and TAG content of the total lipid fraction, are the most suitable. Therefore, when TAG and FFA make up only a small percentage of the total lipid fraction [209], the oil is unsuitable for esterification, and additional processing (e.g. pyrolysis, thermochemical liquefaction) would be necessary before it can be used [104]. Microalgal biodiesel also tends to be unsuitable for long-term storage as the constituent esters hydrolyse back to the parent carboxylic acids. The reverse process results in polymerisation, thereby affecting the fuel quality, with potential negative impacts on engine service life [209].

Biodiesel fuels must meet stringent chemical, physical and quality requirements as specified in standards EN14214 and ASTM D6751 [68]; ASTM [10]. Table 7 benchmarks the performance characteristics of algal biodiesel against other common biodiesel fuels and petroleum diesel. Data on the properties of algal biodiesel are limited; therefore, it is still not possible to compare the full range of performance indicators against active diesel EN590 [69] and the biodiesel standards (EN14214 and ASTM D6751).

From available data, it can be seen that algal biodiesel compares favourably with both diesel and biodiesel standards. The HHV of algal biodiesel is lower when compared to diesel (EN590). The kinematic viscosity of algal biodiesel is within the standards but considerably higher than diesel (EN590). This indicates poor flow

properties of algal biodiesel for use in conventional diesel engines. The higher density of algal biodiesel enhances the fuels' energy density and potentially lower logistics/transportation associated with distribution. Recorded flash point is higher than diesel (EN590), which implies it is a safer fuel for handling and transportation, but could result in poor ignition in conventional diesel engines. The pour point is within the prescribed range in biodiesel standards, indicating the suitability for use in cold climates.

Biodiesel can be blended with diesel (EN590) for use by diesel engines. The most common biodiesel blends from terrestrial crops are B2 (2% biodiesel and 98% diesel (EN590)), B5 (5% biodiesel and 95% diesel (EN590)) and B20 (20% biodiesel and 80% diesel (EN590)) [11]. Such biodiesel blends will be more resistance to polymerisation improving its oxidative stability [204], which is a major limitation of microalgal biodiesel. Blending of microalgal biodiesel with diesel (EN590) could potentially enable it meet the required fuel standards and is the first step towards realising the potential of microalgae as a substitute for fossil fuel. Overall, the future potential of microalgae-derived biodiesel is ultimately dependent on the ability of production systems to meet active biodiesel standards. Therefore, research should aim to produce microalgae biomass with high proportion of TAG and FFA to minimise the cost of meeting these standards.

5.5 Other Algal Extracts with Commercial Value

Concurrent extraction of valuable co-products with biofuel production has significant potential since large-scale production of microalgae for biofuels will increase the availability of such products. The range of valuable products includes PUFAs, antioxidants, nutrition, fertiliser and other specialty applications (Table 8).

PUFAs: Microalgae are a primary source of PUFAs and supply whole food chains with these vital compounds because animals and higher plants lack the necessary enzymes to synthesise PUFAs. PUFAs are essential for human development and physiology [90], and minimise risks of cardiovascular disease [180]. Several microalgae species produce a range of PUFAs, e.g. docasahexanoic acid (DHA) is synthesised by *Crypthecodinium,* and *Schizochytrium*, eicosapentanoic acid (EPA) by *Nannochloropsis, Phaeodactylum,* and *Nitzschia*, γ-linolenic acid (GLA) by *Spirulina*, and arachidonic acid (AA) by *Porphyridium*. However, DHA is the only algal extract PUFA that is competitive against other primary sources [197].

Antioxidants: A number of algae-derived antioxidants are important in health food markets. The most common are β-carotene produced by *D. salina* [75] and astaxanthin produced by *Haematococcus pluvialis* [93].

Nutrition supplements: Microalgae-derived human health food supplement is currently limited to very few species, namely, *Spirulina*, *Dunaliella* and *Chlorella*. The limited number is due to strict food safety regulations, commercial factors, market demand and specific preparation requirements [166]. They are generally marketed

Table 8 Summary of co-products derived from microalgal biomass (Adapted from Hejazi and Wijffels [87], Lorenz and Cysewski [122], Pulz and Gross [166], Ratledge [169], Rosenberg et al. [179], Spolaore et al. [197], U.S. DOE [212])

Market	Product	Microalgae species	Potential applications/ industry
Polyunsaturated fatty acids	Docasahexanoic acid	*Crypthecodinium, Schizochytrium*	Nutritional food
	Eicosapentanoic acid	*Nannochloropsis, Phaeodactylum, Nitzschia, Pavlova*	
	γ-Linolenic acid	*Spirulina*	
	Arachidonic acid	*Porphyridium*	
Antioxidants	Astaxanthin	*Haematococcus pluvialis*	
	B-carotene	*Dunaliella salina*	Nutritional food, cosmetics
Fluorescent label	Phycoerythrin	*Spirulina*	Biomedical research, food colouring
	Phycocyanin	*Spirulina*	
Recombinant proteins	Cytokines-interleukin-6 (IL-6, IL-2, IL-12, IL-4)	–	Pharmaceuticals
	Interferon gamma and beta	–	
	Antivirals: Griffithsin, Cyanovirim, PmAV	–	
	Antibacterials: lysozyme, melittin, moricin, cecopin, techylepsin, defensin, magainin	–	
	Bioactive peptides: antifreeze protein	–	
	Anti-inflammatory peptides	–	
	Anticoagulating proteins	–	
	Neutralising antibodies, single chain antibodies against multiple viral and bacterial infections	–	
Nutrition	Aquaculture feed	*Isochrysis, Nannochloropsis, Tetraselmis*	Aquaculture
	Animal feed	Various	Agriculture
Polysaccharides	Agar	–	Nutritional food, thickening agent
	Alginates	–	
	Carrageenans	–	

as food supplement in tablet or powder form [197]. However, there is a concern that some cyanobacteria (e.g. *Spirulina*) contain the neurotoxin β-*N*-nethylamino-L-alanine (BMAA) which has been linked to Alzheimer's disease, Lou Gehrig's disease and amyptrophic lateral sclerosis-Parkinsonism dementia complex [46].

Specific microalgae species are also suitable for animal and aquaculture feed supplements. Such have beneficial aspects such as improved immune response and improved fertility in animals [166]. When used as feed for molluscs, shrimp and fish, some of the benefits include enhancement of immune systems, inducement of essential biological activities [148] and improvement of quality of culturing medium ("green-water" technique) [43].

Other specialty applications: There are many other special products and chemicals that can be derived from microalgae biomass. These applications represent a very small portion of the market but as further research is undertaken with expanded production of biofuel-directed microalgae, more products could become commercially viable. Current specialised applications include fluorescent labels and biomarkers [179], antivirals, antibacterials, bioactive peptides, anti-inflammatory peptides, anticoagulating proteins [201], and heavy isotope labels [179].

Fertiliser applications: Macroalgae biomass has been used as a plant fertiliser, to enhance soil structure and mineral composition [176, 212]. Used as soil additives, microalgal biomass enhances the soils' water-binding capacity and the mineral composition of the soil [106]. Biomass conversion technologies such as pyrolysis produce solid charcoal waste residue or *biochar* which has potential applications as a fertiliser and sequester for carbon [108, 116, 126, 129]. Incorporation of *biochar* into soil enhances the structure, increases soil fertility and productivity, neutralises acid soil [72] and is considered a long-term carbon sink that could reduce carbon emissions [113, 117]. Limited research suggests that *biochar* incorporation could lower soil emission of GHGs [77], but there are still uncertainties about the life cycle emissions of the *biochar* production [171, 172].

6 Conclusion

While the current research and technology development focus is on meeting advanced fuel standards, compelling evidence indicates that multiple product extraction is fundamental to successful commercial deployment of microalgae-derived biofuels. Process development in a biorefinery concept, that is designed to utilise the total value of algal biomass, combined with integrated applications of microalgae in carbon capture and bioremediation of wastewater treatment, with all based on viable system biology and scale-up feasibility (including logistics), will enhance the viability and future sustainability of microalgae as a biofuel resource.

Principal strategies for cost reduction and acceleration of commercialisation of the microalgae-derived biofuels include: identification of fast-growing algae species with high oil content, specifically, the FFAs and TAG; development of low-cost harvesting and algal-oil extraction and downstream processing into biofuels, and; concurrent extraction of useful co-products. Blending of algal biodiesel with conventional diesel is the first step towards successfully introducing microalgae-derived biodiesel into the market. Potential co-products such as green plastics, detergents and cleaners,

and biodegradable and non-toxic polymers could achieve the desired parity and eventually provide distinct resource advantage against petroleum-based products.

The technical viability of individual processes in the algal biomass-to-biofuel process chain hinges on the intrinsic properties of the selected microalgal strains to produce lipids, specifically, that with high proportion of TAG that is essential for efficient biodiesel production. Development of rapid in-situ biomass and lipid yield assessment techniques (e.g. infrared microspectroscopy and flow cytometry) will aid in identifying promising species, in-situ monitoring and maintaining optimal conditions for sustainable algal-biofuel production.

References

1. Abbasi T, Abbasi SA (2010) Biomass energy and the environmental impacts associated with its production and utilization. Renew Sustain Energy Rev 14(3):919–937
2. Accenture (2008) Biofuels' time of transition—achieving high performance in a world of increasing fuel diversity. Accenture, London
3. Acién Fernández FG, Fernandez Sevilla JM, Sanchez Perez JA, Molina Grima E, Chisti Y (2001) Airlift-driven external-loop tubular photobioreactors for outdoor production of microalgae: assessment of design and performance. Chem Eng Sci 56(8):2721–2732
4. Akkerman I, Janssen M, Rocha J, Wijffels RH (2002) Photobiological hydrogen production: photochemical efficiency and bioreactor design. Int J Hydrogen Energy 27(11):1195–1208
5. Anderson RA (2005) Algal culturing techniques. Elsevier, London
6. Anonymous (2009a) ExxonMobil and NASA to collaborate on algae. Focus on catalysts 12:3
7. Anonymous (2009). Synthetic genomics and ExxonMobil Research and Engineering Co agree to develop next generation biofuels using photosynthetic algae. Focus on catalysts 9:5
8. Anonymous (2009) UK takes on the world in global race to commercialise algae biofuels. http://www.carbontrust.co.uk/news/news/press-centre2010/2010/Pages/uk-takes-on-world-in-global-race.aspx. Accessed 8 Aug 2010
9. Anonymous (2010) BIOMARA. http://www.biomara.org/. Accessed 8 Aug 2010
10. International ASTM (2011) ASTM D6751–11 Standard specification for biodiesel fuel blend stock (B100) for middle distillate fuels. ASTM International, West Conshohocken, PA. doi: 10.1520/D6751-11, www.astm.org
11. Balat M, Balat H (2010) Progress in biodiesel processing. Appl Energy 87(6):1815–1835
12. Becker EW (1994) Microalgae: biotechnology and microbiology. Cambridge University Press, Cambridge
13. Beer LL, Boyd ES, Peters JW, Posewitz MC (2009) Engineering algae for biohydrogen and biofuel production. Curr Opin Biotechnol 20(3):264–271
14. Benemann JR, Oswald WJ (1996) Systems and economic analysis of microalgae ponds for conversion of CO_2 to biomass. US Department of Energy, Pittsburgh Energy Technology Centre
15. Benemann JR, Van Olst JC, Massingill MJ, Weissman JC, Brune DE (2003) The controlled eutrophication process: using microalgae for CO_2 utilization and agricultural fertilizer recycling. In: Gale J, Kaya Y (eds) Greenhouse gas control technologies—6th international conference. Pergamon, Oxford, pp 1433–1438
16. Benemann JR (1997) CO_2 mitigation with microalgae systems. Energy Convers Manage 38(suppl 1):475–479
17. Bilanovic D, Andargatchew A, Kroeger T, Shelef G (2009) Freshwater and marine microalgae sequestering of CO_2 at different C and N concentrations—response surface methodology analysis. Energy Convers Manage 50(2):262–267
18. Bligh E, Dyer WJ (1959) A rapid method of total lipid extraction and purification. Can J Biochem Physiol 37:911–917

19. Borowitzka MA (1997) Microalgae for aquaculture: opportunities and constraints. J Appl Phycol 9(5):393–401
20. Borowitzka MA (1999) Commercial production of microalgae: ponds, tanks, tubes and fermenters. J Biotechnol 70(1–3):313–321
21. Bosma R, van Spronsen WA, Tramper J, Wijffels RH (2003) Ultrasound, a new separation technique to harvest microalgae. J Appl Phycol 15(2):143–153
22. BP (2010) BP statistical review of world energy, June 2010
23. Brennan L, Owende P (2010) Biofuels from microalgae—a review of technologies for production, processing, and extractions of biofuels and co-products. Renew Sustain Energy Rev 14(2):557–577
24. Briggs M (2004) Widescale biodiesel production from algae. http://www.unh.edu/p2/biodiesel/article_alge.html. Accessed 19 April 2008
25. Bruton T, Lyons H, Lerat Y, Stanley M, Rasmussen MB (2009) A review of the potential of marine algae as a source of biofuel in Ireland. Sustainable Energy Ireland, Dublin
26. Camacho Rubio F, Acién Fernández FG, Sánchez Pérez JA, García Camacho F, Molina Grima E (1999) Prediction of dissolved oxygen and carbon dioxide concentration profiles in tubular photobioreactors for microalgal culture. Biotechnol Bioeng 62(1):71–86
27. Campbell PK, Beer T, Batten D (2009) Greenhouse gas sequestration by algae—energy and greenhouse gas life cycle studies. http://www.csiro.au/resources/Greenhouse-Sequestration-Algae.html. Accessed 19 July 2010
28. Cantrell KB, Ducey T, Ro KS, Hunt PG (2008) Livestock waste-to-bioenergy generation opportunities. Bioresour Technol 99(17):7941–7953
29. Carlozzi P (2000) Hydrodynamic aspects and *Arthrospira* growth in two outdoor tubular undulating row photobioreactors. Appl Microbiol Biotechnol 54(1):14–22
30. Carlozzi P (2003) Dilution of solar radiation through "culture" lamination in photobioreactor rows facing south-north: a way to improve the efficiency of light utilization by cyanobacteria (*Arthrospira platensis*). Biotechnol Bioeng 81(3):305–315
31. Carvalho AP, Meireles LA, Malcata FX (2006) Microalgal reactors: a review of enclosed system designs and performances. Biotechnol Prog 22(6):1490–1506
32. Cheng-Wu Z, Zmora O, Kopel R, Richmond A (2001) An industrial-size flat plate glass reactor for mass production of *Nannochloropsis* sp. (*Eustigmatophyceae*). Aquaculture 195(1–2):35–49
33. Cheng Ya-Ling, Juang Yu-Chuan, Liao Guan-Yu, Tsai P-W, Ho S-H, Yeh K-L, Chen C-Y et al (2010) Harvesting of *Scenedesmus obliquus* FSP-3 using dispersed ozone flotation. Bioresour Technol 102(1):82–87
34. Cherubini F (2010) The biorefinery concept: using biomass instead of oil for producing energy and chemicals. Energy Convers Manage 51(7):1412–1421
35. Chiaramonti D, Oasmaa A, Solantausta Y (2007) Power generation using fast pyrolysis liquids from biomass. Renew Sustain Energy Rev 11(6):1056–1086
36. Zittelli C, Graziella LR, Biondi N, Tredici MR (2006) Productivity and photosynthetic efficiency of outdoor cultures of *Tetraselmis suecica* in annular columns. Aquaculture 261(3):932–943
37. Chinnasamy S, Bhatnagar A, Hunt RW, Das KC (2010) Microalgae cultivation in a wastewater dominated by carpet mill effluents for biofuel applications. Bioresour Technol 101(9):3097–3105
38. Chisti Y (2007) Biodiesel from microalgae. Biotechnol Adv 25(3):294–306
39. Chisti Y (2008) Biodiesel from microalgae beats bioethanol. Trends Biotechnol 26(3):126–131
40. Chisti Y (2010) Fuel from microalgae. Biofuels 1(2):233–235
41. Chiu Sheng-Yi, Kao Chien-Ya, Tsai Ming-Ta, Ong S-C, Chen C-H, Lin C-S (2009) Lipid accumulation and CO_2 utilization of *Nannochloropsis oculata* in response to CO_2 aeration. Bioresour Technol 100(2):833–838
42. Chiu SY, Kao CY, Chen CH, Kuan TC, Ong SC, Lin CS (2008) Reduction of CO_2 by a high-density culture of *Chlorella* sp. in a semicontinuous photobioreactor. Bioresour Technol 99(9):3389–3396

43. Chuntapa B, Powtongsook S, Menasveta P (2003) Water quality control using *Spirulina platensis* in shrimp culture tanks. Aquaculture 220(1–4):355–366
44. Clark J, Deswarte F (2008) Introduction to chemicals from biomass, Wiley series in renewable resources. Wiley, New York
45. Converti A, Lodi A, Del Borghi A, Solisio C (2006) Cultivation of *Spirulina platensis* in a combined airlift-tubular reactor system. Biochem Eng J 32(1):13–18
46. Cox PA, Banack SA, Murch SJ, Rasmussen U, Tien G, Bidigare RR, Metcalf JS, Morrison LF, Codd GA, Bergman B (2005) Diverse taxa of cyanobacteria produce β-*N*-methylamino-L-alanine, a neurotoxic amino acid. Proc Natl Acad Sci U S A 102(14):5074–5078. doi:10.1073/pnas.0501526102
47. da Silva T, Santos C, Reis A (2009) Multi-parameter flow cytometry as a tool to monitor heterotrophic microalgal batch fermentations for oil production towards biodiesel. Biotechnol Bioprocess Eng 14(3):330–337
48. Damiani MC, Popovich CA, Constenla D, Leonardi PI (2010) Lipid analysis in *Haematococcus pluvialis* to assess its potential use as a biodiesel feedstock. Bioresour Technol 101(11): 3801–3807
49. Danquah MK, Gladman B, Moheimani N, Forde GM (2009) Microalgal growth characteristics and subsequent influence on dewatering efficiency. Chem Eng J 151(1–3):73–78
50. de Morais MG, Costa JA (2007) Biofixation of carbon dioxide by *Spirulina* sp. and *Scenedesmus obliquus* cultivated in a three-stage serial tubular photobioreactor. J Biotechnol 129(3):439–445
51. de Morais MG, Costa JA (2007) Isolation and selection of microalgae from coal fired thermoelectric power plant for biofixation of carbon dioxide. Energy Convers Manage 48(7): 2169–2173
52. Dean AP, Sigee DC, Estrada B, Pittman JK (2010) Using FTIR spectroscopy for rapid determination of lipid accumulation in response to nitrogen limitation in freshwater microalgae. Bioresour Technol 101(12):4499–4507
53. Demirbas A (2006) Oily products from mosses and algae via pyrolysis. Energy Sources 28(10):933–940
54. Demirbas A (2001) Biomass resource facilities and biomass conversion processing for fuels and chemicals. Energy Convers Manage 42(11):1357–1378
55. Demirbas A (2008) Comparison of transesterification methods for production of biodiesel from vegetable oils and fats. Energy Convers Manage 49(1):125–130
56. Demirbas A (2009) Political, economic and environmental impacts of biofuels: a review. Applied Energy 86(Suppl 1):S108–S117
57. Demirbas MF, Balat M (2006) Recent advances on the production and utilization trends of bio-fuels: a global perspective. Energy Convers Manage 47(15–16):2371–2381
58. Desmorieux H, Decaen N (2006) Convective drying of spirulina in thin layer. J Food Eng 66(4):497–503
59. Dismukes GC, Carrieri D, Bennette N, Ananyev GM, Posewitz MC (2008) Aquatic phototrophs: efficient alternatives to land-based crops for biofuels. Curr Opin Biotechnol 19(3):235–240
60. Dote Y, Sawayama S, Inoue S, Minowa T, Yokoyama Shin-ya (1994) Recovery of liquid fuel from hydrocarbon-rich microalgae by thermochemical liquefaction. Fuel 73(12):1855–1857
61. Doucha J, Lívanský K (2006) Productivity, CO_2/O_2 exchange and hydraulics in outdoor open high density microalgal (*Chlorella* sp.) photobioreactors operated in a Middle and Southern European climate. J Appl Phycol 18(6):811–826
62. Doucha J, Straka F, Lívanský K (2005) Utilization of flue gas for cultivation of microalgae (*Chlorella* sp.) in an outdoor open thin-layer photobioreactor. J Appl Phycol 17(5):403–412
63. Dumas A, Laliberté G, Lessard P, de la Noüe J (1998) Biotreatment of fish farm effluents using the cyanobacterium *Phormidium bohneri*. Aquacultural Engineering 17(1):57–68
64. Edzwald JK (1993) Algae, coagulants, and dissolved air flotation. Water Sci Technol 27:67–81
65. EIA (2006) International carbon dioxide emissions from the consumption of energy. http://www.eia.doe.gov/pub/international/iealf/tableh1co2.xls. Accessed 10 Feb 2009

66. Elsey D, Jameson D, Raleigh B, Cooney MJ (2007) Fluorescent measurement of microalgal neutral lipids. J Microbiol Methods 68(3):639–642
67. Eriksen N (2008) Production of phycocyanin—a pigment with applications in biology, biotechnology, foods and medicine. Appl Microbiol Biotechnol 80(1):1–14
68. European Commission for Standardization (2009) EN 14214:2008+A1:2009. In: Automotive fuels—fatty acid methyl esters (FAME) for diesel engines—requirements and test methods. CEN/TC 19—Gaseous and liquid fuels; lubricants and related products of petroleum, synthetic and biological origin, Brussels
69. European Commission for Standardization (2010) EN 590:2009+A1 (2010) In: Automotive fuels—diesel—requirements and test methods. CEN/TC 19—Gaseous and liquid fuels; lubricants and related products of petroleum, synthetic and biological origin, Brussels
70. Falkowski PG, Raven JA (1997) Aquatic photosynthesis. Blackwater Science, London
71. Fouchard S, Pruvost J, Degrenne B, Legrand J (2008) Investigation of H_2 production using the green microalga *Chlamydomonas reinhardtii* in a fully controlled photobioreactor fitted with on-line gas analysis. Int J Hydrogen Energy 33(13):3302–3310
72. Fowles M (2007) Black carbon sequestration as an alternative to bioenergy. Biomass Bioenergy 31(6):426–432
73. Fresco LO (2009) Challenges for food system adaptation today and tomorrow. Environ Sci Policy 12(4):378–385
74. Gallagher BJ (2010) The economics of producing biodiesel from algae. Renew Energy 36:158–162. doi:10.1016/j.renene.2010.06.016
75. García-González M, José Moreno J, Carlos Manzano F, Florencio J, Guerrero MG (2005) Production of *Dunaliella salina* biomass rich in 9-cis-β-carotene and lutein in a closed tubular photobioreactor. J Biotechnol 115(1):81–90
76. Garcia-Malea Lopez MC, Del Rio Sanchez E, Casas Lopez JL, Acién Fernández FG, Fernandez Sevilla JM, Rivas J, Guerrero MG, Molina Grima E (2006) Comparative analysis of the outdoor culture of *Haematococcus pluvialis* in tubular and bubble column photobioreactors. J Biotechnol 123(3):329–342
77. Gaunt JL, Lehmann J (2008) Energy balance and emissions associated with biochar sequestration and pyrolysis bioenergy production. Environ Sci Technol 42(11):4152–4158. doi:10.1021/es071361i
78. Ghirardi ML, Zhang L, Lee JW, Flynn T, Seibert M, Greenbaum E, Melis A (2000) Microalgae: a green source of renewable H_2. Trends Biotechnol 18(12):506–511
79. Goglio P, Owende PMO (2009) A screening LCA of short rotation coppice willow (*Salix* sp.) feedstock production system for small-scale electricity generation. Biosyst Eng 103(3):389–394
80. Gomez-Villa H, Voltolina D, Nieves M, Pina P (2005) Biomass production and nutrient budget in outdoor cultures of *Scenedesmus obliquus* (Chlorophyceae) in artificial wastewater, under the winter and summer conditions of Mazatlán, Sinaloa, Mexico. Vie et milieu 55(2):121–126
81. Goyal HB, Seal D, Saxena RC (2008) Bio-fuels from thermochemical conversion of renewable resources: a review. Renew Sustain Energy Rev 12(2):504–517
82. Griffiths M, Harrison S (2009) Lipid productivity as a key characteristic for choosing algal species for biodiesel production. J Appl Phycol 21(5):493–507
83. Gustavsson L, Madlener R (2003) CO_2 mitigation costs of large-scale bioenergy technologies in competitive electricity markets. Energy 28(14):1405–1425
84. Hall DO, Acién Fernández FG, Cañizares Guerrero E, Krishna Rao K, Molina Grima E (2003) Outdoor helical tubular photobioreactors for microalgal production: modeling of fluid-dynamics and mass transfer and assessment of biomass productivity. Biotechnol Bioeng 82(1):62–73
85. Havlík P, Schneider UA, Schmid E, Böttcher H, Fritz S, Skalský R, Aoki K et al (2011) Global land-use implications of first and second generation biofuel targets. Energy Policy 39:5690–5702
86. Heasman M, Diemar J, O'Connor W, Sushames T, Foulkes L (2000) Development of extended shelf-life microalgae concentrate diets harvested by centrifugation for bivalve molluscs—a summary. Aquacult Res 31(8–9):637–659

87. Hejazi MA, Wijffels RH (2004) Milking of microalgae. Trends Biotechnol 22(4):189–194
88. Hirano A, Hon-Nami K, Kunito S, Hada M, Ogushi Y (1998) Temperature effect on continuous gasification of microalgal biomass: theoretical yield of methanol production and its energy balance. Catalysis Today 45(1–4):399–404
89. Hirano A, Ueda R, Hirayama S, Ogushi Y (1997) CO_2 fixation and ethanol production with microalgal photosynthesis and intracellular anaerobic fermentation. Energy 22(2–3):137–142
90. Hu C, Li M, Li J, Zhu Q, Liu Z (2008) Variation of lipid and fatty acid compositions of the marine microalga *Pavlova viridis* (Prymnesiophyceae) under laboratory and outdoor culture conditions. World J Microbiol Biotechnol 24(7):1209–1214
91. Hu Q, Sommerfeld M, Jarvis E, Ghirardi M, Posewitz M, Seibert M, Darzins A (2008) Microalgal triacyglycerols as feedstocks for biofuel production. Plant J 54:621–639
92. Huang GuanHua, Chen F, Wei D, Zhang XueWu, Chen Gu (2010) Biodiesel production by microalgal biotechnology. Appl Energy 87(1):38–46
93. Huntley M, Redalje D (2007) CO_2 mitigation and renewable oil from photosynthetic microbes: a new appraisal. Mitig Adapt Strat Glob Chang 12(4):573–608
94. IEA (2007) IEA bioenergy task 42—countries report final. http://www.biorefinery.nl/fileadmin/biorefinery/docs/CountryReportsIEABioenergyTask42Final170809.pdf. Accessed 15 July 2010
95. IEA (2009) Global primary energy demand. http://www.iea.org. Accessed 8 July 2010
96. IPCC (2001) Climate change 2001: Impacts, adaptation, and vulnerability. In: A report of working group II of the intergovernmental panel on climatic change (IPCC), Cambridge
97. Jiménez C, Cossío BR, Labella D, Xavier Niell F (2003) The feasibility of industrial production of *Spirulina (Arthrospira)* in Southern Spain. Aquaculture 217(1–4):179–190
98. Kadam KL (2002) Environmental implications of power generation via coal-microalgae cofiring. Energy 27(10):905–922
99. Khan SA, Rashmi MZ, Hussain SP, Banerjee UC (2009) Prospects of biodiesel production from microalgae in India. Renew Sustain Energy Rev 13(9):2361–2372
100. Khosla V (2008) Where will biofuels and biomass feedstocks come from? http://www.khoslaventures.com/presentations/WhereWillBiomassComeFrom.doc
101. Kintisch E (2007) Clint chapple profile: how to make biofuels truly poplar. Science 315(5813):786. doi:10.1126/science.315.5813.786
102. Koopman B, Lincoln EP (1983) Autoflotation harvesting of algae from high-rate pond effluents. Agr Wastes 5(4):231–246
103. Kovacevic V, Wesseler J (2010) Cost-effectiveness analysis of algae energy production in the EU. Energy Policy 38(10):5749–5757
104. Krohn BJ, McNeff CV, Yan B, Nowlan D (2011) Production of algae-based biodiesel using the continuous catalytic Mcgyan® process. Bioresour Technol 102(1):94–100. doi:10.1016/j.biortech.2010.05.035
105. Kruse O, Hankamer B (2010) Microalgal hydrogen production. Curr Opin Biotechnol 21(3):238–243
106. Kumar A, Ergas S, Yuan X, Sahu A, Zhang Q, Jo Dewulf F, Malcata X, van Langenhove H (2010) Enhanced CO_2 fixation and biofuel production via microalgae: recent developments and future directions. Trends Biotechnol 28(7):371–380
107. Kunzig R (2010) Scrubbing the skies: pulling CO_2 back out of the air might be easier then building jets and cars that don't emit it. http://ngm.nationalgeographic.com/big-idea/13/carbon-capture. Accessed 26 Aug 2010
108. Lal R (2008) Black and buried carbons' impacts on soil quality and ecosystem services. Soil Till Res 99(1):1–3
109. Laliberté G, Lessard P, de la Noüe J, Sylvestre S (1997) Effect of phosphorus addition on nutrient removal from wastewater with the cyanobacterium *Phormidium bohneri*. Bioresour Technol 59(2–3):227–233
110. Lardon L, HeÌlias A, Sialve B, Steyer J-P, Bernard O (2009) Life-cycle assessment of biodiesel production from microalgae. Environ Sci Technol 43(17):6475–6481. doi:10.1021/es900705j

111. Leach G, Oliveira G, Morais R (1998) Spray-drying of *Dunaliella salina* to produce a β-carotene rich powder. J Ind Microbiol Biotechnol 20(2):82–85
112. Lee JY, Yoo C, Jun SY, Ahn CY, Oh HM (2010) Comparison of several methods for effective lipid extraction from microalgae. Bioresour Technol 101(Suppl 1):S75–S77
113. Lee JW, Hawkins B, Day DM, Reicosky DC (2010) Sustainability: the capacity of smokeless biomass pyrolysis for energy production, global carbon capture and sequestration. Energy Environ Sci 3(11):1695–1705
114. Lee K, Lee C-G (2001) Effect of light/dark cycles on wastewater treatments by microalgae. Biotechnol Bioprocess Eng 6(3):194–199
115. Lee RE (1980) Phycology. Cambridge University Press, New York
116. Lehmann J, Gaunt J, Rondon M (2006) Bio-char sequestration in terrestrial ecosystems. Mitig Adapt Strat Glob Chang 11:395–419
117. Lehmann J (2007) A handful of carbon. Nature 447(7141):143–144
118. Li Y, Horsman M, Nan Wu, Lan C, Dubois-Calero N (2008) Biofuels from microalgae. Biotechnol Prog 24(4):815–820
119. Li Y, Han D, Guongrong Hu, Dauvillee D, Sommerfeld M, Ball S, Qiang Hu (2010) *Chlamydomonas* starchless mutant defective in ADP-glucose pyrophosphorylase hyper-accumulates triacylglycerol. Metab Eng 12(4):387–391
120. Liu JC, Chen YM, Yi-Hsu Ju (1999) Separation of algal cells from water by column flotation. Sep Sci Technol 34(11):2259–2272
121. Liu J, Ma X (2009) The analysis on energy and environmental impacts of microalgae-based fuel methanol in China. Energy Policy 37(4):1479–1488
122. Lorenz RT, Cysewski GR (2000) Commercial potential for *Haematococcus* microalgae as a natural source of astaxanthin. Trends Biotechnol 18(4):160–167
123. Lundquist TJ (2008) Production of algae in conjunction with wastewater treatment. Paper presented at the NREL—AFOSR workshop on algal oil for jet fuel production, Arlington, VA, 20 Feb 2008
124. Ma F, Hanna MA (1999) Biodiesel production: a review. Bioresour Technol 70(1):1–15
125. Mallick N (2002) Biotechnological potential of immobilized algae for wastewater N, P and metal removal: a review. Biometals 15(4):377–390
126. Marris E (2006) Putting the carbon back: black is the new green. Nature 442(7103):624–626
127. Martínez ME, Sánchez S, Jiménez JM, El Yousfi F, Muñoz L (2000) Nitrogen and phosphorus removal from urban wastewater by the microalga *Scenedesmus obliquus*. Bioresour Technol 73(3):263–272
128. Mata TM, Martins AA, Caetano NS (2010) Microalgae for biodiesel production and other applications: a review. Renew Sustain Energy Rev 14(1):217–232
129. Mathews JA (2008) Carbon-negative biofuels. Energy Policy 36(3):940–945
130. McGuinness M, Keene R (2007) Consumers worldwide would switch to energy providers that help reduce greenhouse gas emissions, Accenture study finds. Accenture Newsroom. http://newsroom.accenture.com/article_display.cfm?article_id=4601. Accessed 27 July 2010
131. Melis A (2002) Green alga hydrogen production: progress, challenges and prospects. Int J Hydrogen Energy 27(11–12):1217–1228
132. Melis A, Happe T (2001) Hydrogen production. Green algae as a source of energy. Plant Physiol 127(3):740–748. doi:10.1104/pp. 010498
133. Mendes-Pinto MM, Raposo MFJ, Bowen J, Young AJ, Morais R (2001) Evaluation of different cell disruption processes on encysted cells of *Haematococcus pluvialis*: effects on astaxanthin recovery and implications for bio-availability. J Appl Phycol 13(1):19–24
134. Meng X, Yang J, Xin Xu, Zhang L, Nie Q, Xian M (2009) Biodiesel production from oleaginous microorganisms. Renew Energy 34(1):1–5
135. Miao X, Qingyu Wu (2004) High yield bio-oil production from fast pyrolysis by metabolic controlling of *Chlorella protothecoides*. J Biotechnol 110(1):85–93
136. Miao X, Qingyu Wu, Yang C (2004) Fast pyrolysis of microalgae to produce renewable fuels. J Anal Appl Pyrolysis 71(2):855–863

137. Middelberg APJ (1994) The release of intracellular bioproducts. In: Subramanian G (ed) Bioseparation and bioprocessing: a handbook. Wiley, Weinheim, pp 131–164
138. Minowa T, Yokoyama Shin-ya, Kishimoto M, Okakura T (1995) Oil production from algal cells of *Dunaliella tertiolecta* by direct thermochemical liquefaction. Fuel 74(12):1735–1738
139. Miura Y, Akano T, Fukatsu K, Miyasaka H, Mizoguchi T, Yagi K, Maeda I, Ikuta Y, Matsumoto H (1995) Hydrogen production by photosynthetic microorganisms. Energy Convers Manage 36(6–9):903–906
140. Mohn FH (1980) Experiences and strategies in the recovery of biomass in mass culture of microalgae. In: Shelef G, Soeder CJ (eds) Algal biomass. Elsevier, Amsterdam, pp 547–571
141. Molina Grima E, Belarbi EH, Acién Fernández FG, Robles Medina A, Chisti Y (2003) Recovery of microalgal biomass and metabolites: process options and economics. Biotechnol Adv 20(7–8):491–515
142. Molina Grima E, Fernandez J, Acién Fernández FG, Chisti Y (2001) Tubular photobioreactor design for algal cultures. J Biotechnol 92(2):113–131
143. Molina Grima E, Medina A, Giménez A, Sánchez Pérez J, Camacho F, García Sánchez J (1994) Comparison between extraction of lipids and fatty acids from microalgal biomass. J Am Oil Chem Soc 71(9):955–959
144. Moore A (2008) Biofuels are dead: long live biofuels(?)—Part one. New Biotechnol 25(1):6–12
145. Morais MG, Radmann EM, Andrade MR, Teixeira GG, Brusch LRF, Costa JAV (2009) Pilot scale semicontinuous production of *Spirulina* biomass in southern Brazil. Aquaculture 294(1–2):60–64
146. Moreno J, Vargas MA, Rodríguez H, Rivas J, Guerrero MG (2003) Outdoor cultivation of a nitrogen-fixing marine cyanobacterium, *Anabaena* sp. ATCC 33047. Biomol Eng 20(4–6):191–197
147. Muhs J, Viamajala S, Heydon B, Edwards M, Hu Q, Hobbs R, Allen M et al (2009) A summary of opportunities, challenges, and research needs—algae biofuels and carbon recycling. http://www.utah.gov/ustar/documents/63.pdf. Accessed 13 July 2010
148. Muller-Feuga A (2000) The role of microalgae in aquaculture: situation and trends. J Appl Phycol 12(3):527–534
149. Muñoz R, Guieysse B (2006) Algal-bacterial processes for the treatment of hazardous contaminants: a review. Water Res 40(15):2799–2815
150. Muñoz R, Köllner C, Guieysse B (2009) Biofilm photobioreactors for the treatment of industrial wastewaters. J Hazard Mater 161(1):29–34
151. Murdock JN, Wetzel DL (2009) FT-IR microspectroscopy enhances biological and ecological analysis of algae. Appl Spectrosc Rev 44:335–361
152. Nigam PS, Singh A (2011) Production of liquid biofuels from renewable resources. Progr Energy Combust Sci 37:52–68
153. Nurdogan Y, Oswald WJ (1996) Tube settling rate of high-rate pond algae. Water Sci Technol 33:229–241
154. Oh Sung Ho, Han JG, Kim Y, Ha Ji Hye, Kim SS, Jeong MH, Jeong HS et al (2009) Lipid production in *Porphyridium cruentum* grown under different culture conditions. J Biosci Bioeng 108(5):429–434
155. Olaizola M (2000) Commercial production of astaxanthin from *Haematococcus pluvialis* using 25,000-liter outdoor photobioreactors. J Appl Phycol 12(3):499–506
156. Olguín EJ, Galicia S, Mercado G, Pérez T (2003) Annual productivity of *Spirulina* (*Arthrospira*) and nutrient removal in a pig wastewater recycling process under tropical conditions. J Appl Phycol 15(2):249–257
157. Ono E, Cuello JL (2006) Feasibility assessment of microalgal carbon dioxide sequestration technology with photobioreactor and solar collector. Biosyst Eng 95(4):597–606
158. Packer M (2009) Algal capture of carbon dioxide; biomass generation as a tool for greenhouse gas mitigation with reference to New Zealand energy strategy and policy. Energy Policy 37(8):3428–3437

159. Pan P, Hu C, Yang W, Li Y, Dong L, Zhu L, Tong D, Qing R, Fan Y (2010) The direct pyrolysis and catalytic pyrolysis of *Nannochloropsis* sp. residue for renewable bio-oils. Bioresour Technol 101(12):4593–4599
160. Patil V, Tran K-Q, Giselrod HR (2008) Towards sustainable production of biofuels from microalgae. Int J Mol Sci 9(7):1188–1195
161. Petrusevski B, Bolier G, Van Breemen AN, Alaerts GJ (1995) Tangential flow filtration: a method to concentrate freshwater algae. Water Res 29(5):1419–1424
162. Pienkos PT, Darzins A (2009) The promise and challenges of microalgal-derived biofuels. Biofuels Bioprod Bioref 3(4):431–440
163. Prakash J, Pushparaj B, Carlozzi P, Torzillo G, Montaini E, Materassi R (1997) Microalgae drying by a simple solar device. Int J Solar Energy 18(4):303–311
164. Pulz O (2001) Photobioreactors: production systems for phototrophic microorganisms. Appl Environ Microbiol 57(3):287–293
165. Pulz O, Scheinbenbogan K (1998) Photobioreactors: design and performance with respect to light energy input. Adv Biochem Eng Biotechnol 59:123–152
166. Pulz O, Gross W (2004) Valuable products from biotechnology of microalgae. Appl Microbiol Biotechnol 65(6):635–648
167. Pushparaj B, Pelosi E, Tredici M, Pinzani E, Materassi R (1997) As integrated culture system for outdoor production of microalgae and cyanobacteria. J Appl Phycol 9(2):113–119
168. Qin J (2005) Bio-hydrocarbons from algae—impacts of temperature, light and salinity on algae growth. Rural Industries Research and Development Corporation, Barton, Australia
169. Ratledge C (2004) Fatty acid biosynthesis in microorganisms being used for single cell oil production. Biochimie 86(11):807–815
170. Regalbuto J (2010) An NSF perspective on next generation hydrocarbon biorefineries. Comp Chem Eng 34(9):1393–1396
171. Reijnders L (2009) Are forestation, bio-char and landfilled biomass adequate offsets for the climate effects of burning fossil fuels? Energy Policy 37(8):2839–2841
172. Reijnders L, Huijbregts MAJ (2008) Biogenic greenhouse gas emissions linked to the life cycles of biodiesel derived from European rapeseed and Brazilian soybeans. J Clean Prod 16(18):1943–1948
173. Reijnders L (2008) Do biofuels from microalgae beat biofuels from terrestrial plants? Trends Biotechnol 26(7):349–350
174. Richmond A, Cheng-Wu Z, Zarmi Y (2003) Efficient use of strong light for high photosynthetic productivity: interrelationships between the optical path, the optimal population density and cell-growth inhibition. Biomol Eng 20(4–6):229–236
175. Richmond A, Lichtenberg E, Stahl B, Vonshak A (1990) Quantitative assessment of the major limitations on productivity of *Spirulina platensis* in open raceways. J Appl Phycol 2(3):195–206
176. Riley H (2002) Effects of algal fibre and perlite on physical properties of various soils and on potato nutrition and quality on a gravelly loam soil in southern Norway. Acta Agric Scand B: Soil Plant Sci 52(2):86–95
177. Rodolfi L, Zittelli GC, Bassi N, Padovani G, Biondi N, Bonini G, Tredici MR (2008) Microalgae for oil: strain selection, induction of lipid synthesis and outdoor mass cultivation in a low-cost photobioreactor. Biotechnol Bioeng 102(1):100–112
178. Roessler PG (1990) Environmental control of glycerolipid metabolism in microalgae: commercial implications and future research directions. J Phycol 26:393–399
179. Rosenberg JN, Oyler GA, Wilkinson L, Betenbaugh MJ (2008) A green light for engineered algae: redirecting metabolism to fuel a biotechnology revolution. Curr Opin Biotechnol 19(5):430–436
180. Ruxton CHS, Reed SC, Simpson MJA, Millington KJ (2007) The health benefits of omega-3 polyunsaturated fatty acids: a review of the evidence. J Hum Nutr Diet 20(3):275–285
181. Sánchez Mirón A, Contreras Gomez A, Garca Camacho F, Molina Grima E, Chisti Y (1999) Comparative evaluation of compact photobioreactors for large-scale monoculture of microalgae. J Biotechnol 70(1–3):249–270

182. Sato T, Usui S, Tsuchiya Y, Kondo Y (2006) Invention of outdoor closed type photobioreactor for microalgae. Energy Convers Manage 47(6):791–799
183. Sawayama S, Minowa T, Yokoyama SY (1999) Possibility of renewable energy production and CO_2 mitigation by thermochemical liquefaction of microalgae. Biomass Bioenergy 17(1):33–39
184. Sawayama S, Inoue S, Dote Y, Yokoyama Shin-Ya (1995) CO_2 fixation and oil production through microalgae. Energy Convers Manage 36(6–9):729–731
185. Schenk P, Thomas-Hall S, Stephens E, Marx U, Mussgnug J, Posten C, Kruse O, Hankamer B (2008) Second generation biofuels: high-efficiency microalgae for biodiesel production. BioEnergy Res 1(1):20–43
186. Schmid-Staiger U (2009) Algae Biorefinery – Concepts. National German Workshop on Biorefineries, 15th September 2009, Worms, Germany.
187. Scott SA, Davey MP, Dennis JS, Horst I, Howe CJ, Lea-Smith DJ, Smith AG (2010) Biodiesel from algae: challenges and prospects. Curr Opin Biotechnol 21(3):277–286
188. Scragg AH, Illman AM, Carden A, Shales SW (2002) Growth of microalgae with increased calorific values in a tubular bioreactor. Biomass and Bioenergy 23(1):67–73
189. Setlik I, Veladimir S, Malek I (1970) Dual purpose open circulation units for large scale culture of algae in temperate zones. I. Basic design considerations and scheme of a pilot plant. Algol Stud (Trebon) 1(11)
190. Sharma YC, Singh B (2009) Development of biodiesel: current scenario. Renew Sustain Energy Rev 13(6–7):1646–1651
191. Sheehan J, Dunahay T, Benemann JR, Roessler P (1998) A look back a the U.S. Department of Energy's Aquatic Species Program—biodiesel from algae. U.S. Department of Energy
192. Shilton A, Guieysse B (2010) Sustainable sunlight to biogas is via marginal organics. Curr Opin Biotechnol 21(3):287–291
193. Sialve B, Bernet N, Bernard O (2009) Anaerobic digestion of microalgae as a necessary step to make microalgal biodiesel sustainable. Biotechnol Adv 27(4):409–416
194. Singh J, Gu S (2010) Commercialization potential of microalgae for biofuels production. Renew Sustain Energy Rev 14:2596–2610. doi:10.1016/j.rser.2010.06.014
195. Smith VH, Sturm BSM, deNoyelles FJ, Billings SA (2010) The ecology of algal biodiesel production. Trends Ecol Evol 25(5):301–309
196. Soest JP (2000) Climatic change: solutions in sight, Dutch perspective. Energy Policy Platform, Delft
197. Spolaore P, Joannis-Cassan C, Duran E, Isambert A (2006) Commercial applications of microalgae. J Biosci Bioeng 101(2):87–96
198. Stepan DJ, Shockey RE, Moe TA, Dorn R (2002) Carbon dioxide sequestering using microalgae systems. U.S. Department of Energy, Pittsburgh, PA
199. Stephens E, Ross IL, King Z, Mussgnug JH, Kruse O, Posten C, Borowitzka MA, Hankamer B (2010) An economic and technical evaluation of microalgal biofuels. Nat Biotechnol 28(2):126–128
200. Sticklen M (2006) Plant genetic engineering to improve biomass characteristics for biofuels. Curr Opin Biotechnol 17(3):315–319
201. Subhadra BG (2010) Sustainability of algal biofuel production using integrated renewable energy park (IREP) and algal biorefinery approach. Energy Policy 38(10):5892–5901
202. Suh IS, Lee CG (2003) Photobioreactor engineering: design and performance. Biotechnol Bioprocess Eng 8(6):313–321
203. Tampion J, Tampion MD (1987) Immobilized cells: principles and applications. Cambridge University Press, Cambridge
204. Tang H, Abunasser N, Wang A, Clark BR, Wadumesthrige K, Zeng S, Kim M et al (2008) Quality survey of biodiesel blends sold at retail stations. Fuel 87(13–14):2951–2955
205. Taylor G (2008) Biofuels and the biorefinery concept. Energy Policy 36(12):4406–4409
206. Terry KL, Raymond LP (1985) System design for the autotrophic production of microalgae. Enzyme Microbiol Technol 7(10):474–487
207. Thomsen L (2010) How 'green' are algae farms for biofuel production? Biofuels 1(4): 515–517

208. Thurmond W (2009) Five key strategies for algae biofuels commercialization. In: Algae 2020, Emerging Markets Online (EMO). Houston, TX.
209. Tran NH, Bartlett JR, Kannangara GSK, Milev AS, Volk H, Wilson MA (2010) Catalytic upgrading of biorefinery oil from micro-algae. Fuel 89(2):265–274
210. Tsukahara K, Sawayama S (2005) Liquid fuel production using microalgae. J Jpn Petrol Inst 48(5):251–259
211. Tyner WE, Taheripour F, Perkis D (2010) Comparison of fixed versus variable biofuels incentives. Energy Policy 38(10):5530–5540
212. U.S. DOE (2010) National algal biofuels technology roadmap. College Park, MD: U.S. Department of Energy, Office of Energy Efficiency and Renewable Energy, Biomass Program
213. Ugwu CU, Aoyagi H, Uchiyama H (2008) Photobioreactors for mass cultivation of algae. Bioresour Technol 99(10):4021–4028
214. Ugwu CU, Ogbonna J, Tanaka H (2002) Improvement of mass transfer characteristics and productivities of inclined tubular photobioreactors by installation of internal static mixers. Appl Microbiol Biotechnol 58(5):600–607
215. van Harmelen T, Oonk H (2006) Microalgae biofixation processes: applications and potential contributions to greenhouse gas mitigation options. International Network on Biofixation of CO_2 and Greenhouse Gas Abatement with Microalgae, Apeldoorn, The Netherlands
216. van Vuuren DP, de Vries HJM (2001) Mitigation scenarios in a world oriented at sustainable development: the role of technology, efficiency and timing. Climate Policy 1(2):189–210
217. Walker TL, Collet C, Purton S (2005) Algal transgenics in the genomic era. J Phycol 41(6):1077–1093
218. Wang B, Li Y, Nan Wu, Lan C (2008) CO_2 bio-mitigation using microalgae. Appl Microbiol Biotechnol 79(5):707–718
219. Wang Zi Teng, Ullrich N, Joo S, Waffenschmidt S, Goodenough U (2009) Algal lipid bodies: stress induction, purification, and biochemical characterization in wild-type and starchless *Chlamydomonas reinhardtii*. Eukaryot Cell 8(12):1856–1868. doi:10.1128/ec.00272-09
220. Watanabe Y, Saiki H (1997) Development of a photobioreactor incorporating *Chlorella* sp. for removal of CO_2 in stack gas. Energy Convers Manage 38(Suppl 1):S499–S503
221. Weissman JC, Tillett DM (1992) Design and operation of outdoor microalgae test facility. In: Brown LM, Sprague S (eds) Aquatic species report, NREL/MP-232-4174. National Renewable Energy Laboratory, pp. 32–57
222. Weldy CS, Huesemann M (2007) Lipid production by *Dunaliella salina* in batch culture: effects of nitrogen limitation and light intensity. US Dept Energy J Undergr Res 7(1):115–122
223. Widjaja A, Chien CC, Yi Hsu Ju (2009) Study of increasing lipid production from fresh water microalgae *Chlorella vulgaris*. J Taiwan Inst Chem Eng 40(1):13–20
224. Wijffels RH, Barbosa MJ (2010) An outlook on microalgal biofuels. Science 329(5993):796–799. doi:10.1126/science.1189003
225. Willems PA (2009) The biofuels landscape through the lens of industrial chemistry. Science 325(5941):707–708. doi:10.1126/science.1175502
226. Worrell E (2000) Energy use and energy intensity of the U.S. chemical industry. Lawrence Berkeley National Laboratory, Berkeley, CA
227. Wu WT, Hsieh CH (2008) Cultivation of microalgae for optimal oil production. J Biotechnol 136(Suppl 1):S521
228. Xin L, Hong-ying Hu, Ke G, Ying-xue S (2010) Effects of different nitrogen and phosphorus concentrations on the growth, nutrient uptake, and lipid accumulation of a freshwater microalga *Scenedesmus* sp. Bioresour Technol 101(14):5494–5500
229. Xiong W, Gao C, Yan D, Chao Wu, Qingyu Wu (2010) Double CO_2 fixation in photosynthesis-fermentation model enhances algal lipid synthesis for biodiesel production. Bioresour Technol 101(7):2287–2293
230. Xu H, Miao X, Qingyu Wu (2006) High quality biodiesel production from a microalga *Chlorella protothecoides* by heterotrophic growth in fermenters. J Biotechnol 126(4):499–507

231. Yen H-W, Brune DE (2007) Anaerobic co-digestion of algal sludge and waste paper to produce methane. Bioresour Technol 98(1):130–134
232. Yoo C, Jun So-Young, Lee J-Y, Ahn C-Y, Hee-Mock Oh (2010) Selection of microalgae for lipid production under high levels carbon dioxide. Bioresour Technol 101(1 Suppl 1): S71–S74
233. Yun Y-S, Lee SB, Park JM, Lee Choong-Il, Yang Ji-Won (1997) Carbon dioxide fixation by algal cultivation using wastewater nutrients. J Chem Technol Biotechnol 69(4):451–455
234. Zhang X, Qiang Hu, Sommerfeld M, Puruhito E, Chen Y (2010) Harvesting algal biomass for biofuels using ultrafiltration membranes. Bioresour Technol 101(14):5297–5304

Chapter 25
Bioprocess Engineering Aspects of Biodiesel and Bioethanol Production from Microalgae

Ronald Halim, Razif Harun, Paul A. Webley, and Michael K. Danquah

Abstract Rapid increase of atmospheric carbon dioxide together with depleted supplies of fossil fuel has led to an increased commercial interest in renewable fuels. Due to their high biomass productivity, rapid lipid accumulation and high carbohydrate storage capacity, microalgae are viewed as promising feedstocks for carbon-neutral biofuels. This chapter discusses process engineering steps for the production of biodiesel and bioethanol from microalgal biomass (harvesting, dewatering, pre-treatment, lipid extraction, lipid transmethylation, anaerobic fermentation). The suitability of microalgal lipid compositions for biodiesel conversion and the feasibility of using microalgae as raw materials for bioethanol production will also be evaluated. Specific to biodiesel production, the chapter provides an updated discussion on two of the most commonly used technologies for microalgal lipid extraction (organic solvent extraction and supercritical fluid extraction) and evaluates the effects of biomass pre-treatment on lipid extraction kinetics.

1 Introduction

As a response to climate change and rising fuel prices, the search for sustainable and renewable fuels is becoming increasingly important. Even though biomass-derived fuels, such as biodiesel and bioethanol, are believed to deliver positive environmental, social and economic outcomes compared to fossil fuels, they share similar problems, such as lack of availability and the requirement for a substantial arable land which competes with terrestrial food crops and heightens concern over food affordability [11, 18, 66].

R. Halim • R. Harun • P.A. Webley • M.K. Danquah (✉)
Bio Engineering Laboratory (BEL), Department of Chemical Engineering,
Monash University, Victoria 3800, Australia
e-mail: michael.danquah@eng.monash.edu.au; kobinadanquah@yahoo.com

J.W. Lee (ed.), *Advanced Biofuels and Bioproducts*, DOI 10.1007/978-1-4614-3348-4_25,

Table 1 Biochemical composition of various microalgal species. Figure is listed as wt.% of dry biomass. Adapted from Becker [5]

Strain	Protein	Carbohydrates	Lipids
Scenedesmus obliquus	50–56	10–17	12–14
Scenedesmus quadricauda	47	–	1.9
Scenedesmus dimorphus	8–18	21–52	16–40
Chlamydomonas rheinhardii	48	17	21
Chlorella vulgaris	51–58	12–17	14–22
Chlorella pyrenoidosa	57	26	2
Spirogyra sp.	6–20	33–64	11–21
Dunaliella bioculata	49	4	8
Dunaliella salina	57	32	6
Euglena gracilis	39–61	14–18	14–20
Prymnesium parvum	28–45	25–33	22–38
Tetraselmis maculate	52	15	3
Porphyridium cruentum	28–39	40–57	9–14
Spirulina platensis	46–63	8–14	4–9
Spirulina maxima	60–71	13–16	6–7
Synechoccus sp.	63	15	11
Anabaena cylindrical	43–56	25–30	4–7

Microalgae are currently considered to be one of the most promising alternative source for biofuels [56]. Microalgae can be grown in either saline water or freshwater with extremely high diversity of strains. Since they do not require arable land, they do not compete with food crops [64]. They also serve as an effective carbon sequestration platform due to their high CO_2 conversion efficiencies and offer higher areal productivity when compared to other biomass [57].

Due to its extensive use in the mariculture and the food supplement industry, microalgal biochemical composition has been thoroughly investigated [16, 20, 21, 28, 53]. Even though their exact biochemical constituents are known to substantially depend on classes and species, microalgae generally consists of 4–64 wt.% carbohydrates, 6–71 wt.% protein and 2–40 wt.% lipids on the basis of dry biomass [6, 51]. The biochemical composition of some microalgal strains are listed in Table 1 [5]. The high lipid and carbohydrate content of microalgal biomass facilitates its potential use as a biodiesel and bioethanol feedstock. The lipids are extracted out and converted to biodiesel, whilst the carbohydrates can be used in anaerobic yeast fermentation to produce bioethanol.

This chapter examines microalgae bioprocesses engineering for biodiesel and bioethanol production. It covers the downstream processes that are needed to produce biofuels from microalgae with an emphasis on the lipid extraction methods for biodiesel conversion, and the fermentation process for bioethanol production.

2 Suitability of Microalgal Biochemical Composition for Biodiesel Production

Lipids are broadly defined as any biological molecule which is soluble in an organic solvent and can be classified based on the polarity of their head groups [30]: (1) neutral lipids which comprise triacylglycerols (TG), diacylglycerols (DG), monoacylglycerols (MG), hydrocarbons (HC), sterols (ST), ketones (K), free fatty acids (FFA) and (2) polar lipids, which can be further sub-divided into phospholipids (PL) and glycolipids (GL). Neutral lipids are created by the cells to store energy, whilst polar lipids form integral parts of cell membranes. Fatty acids (FA) are carboxylic acid chains with unbranched alipathic tails. They are constituents of lipid molecules (both neutral and polar) and designated based on their two most important components; the total number of carbon atoms in the chain and the number of double bonds along the chain. Saturated fatty acids have no double bond, whilst unsaturated fatty acids consist of at least one double bond [61]. TG consists of three fatty acids ester-bonded to a glycerol backbone (Fig. 1). The composition and the fatty acid profile of microalgal lipids substantially varies with the species, its life cycle and its cultivation conditions (medium composition, temperature, illumination intensity, ratio of light and dark cycle, aeration rate) [61]. As shown by the lipid profiles of three microalgal species (*Nannochloropsis oculata*, *Pavlova lutheri*, *Isochrysis* sp.) in Fig. 2, microalgal cells harvested during stationary phase have higher TG contents and correspondingly lower polar lipid contents than the same species obtained during the logarithmic phase [20]. When deprived of aeration, some microalgal species have been shown to increase their lipid content from 10 wt.% to almost 20 wt.%. Due to these inter- and intra-specific variations, the suitability of microalgal lipids for biodiesel production cannot be generalized and will have to be examined on a case-by-case basis.

Microalgal lipids, obtained during the stationary phase (Fig. 2), comprise 51–57 wt.% polar lipid fractions and 43–49 wt.% neutral lipid fractions with TG serving as the most dominant neutral sub-class (20–41 wt.% of total lipid) [20]. Since acylglycerols (TG, DG and MG) are the only lipid fractions that can be transmethylated using current industrial-scale biodiesel transesterification [14, 31],

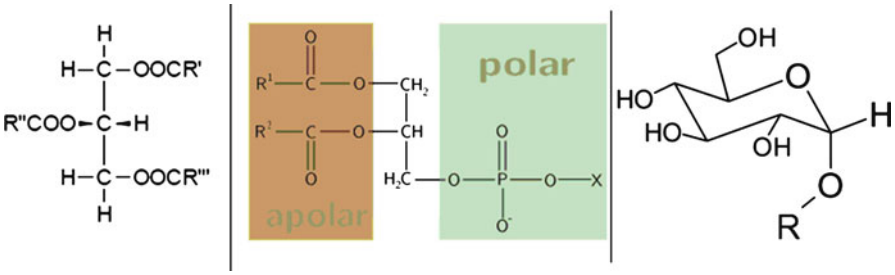

Fig. 1 Different lipid molecules: TG on the *left*, PL in the *middle*, and GL on the *right*. R in each molecule represents a fatty acid chain. Bipolarity of PL is illustrated

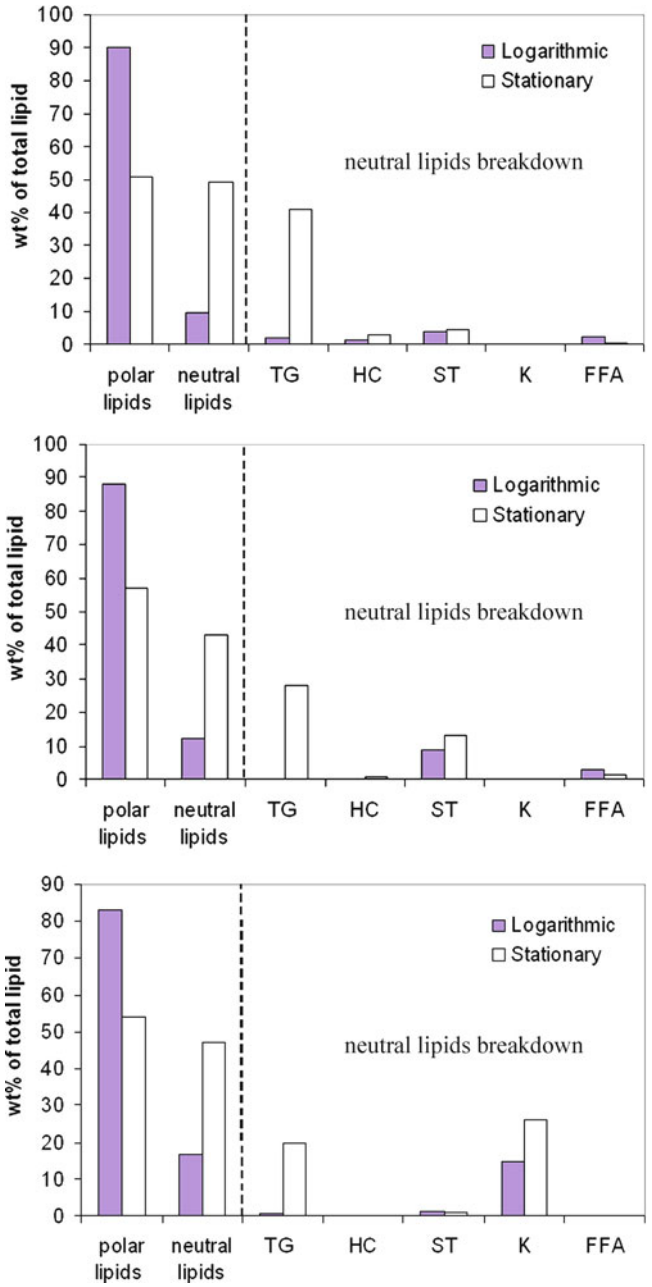

Fig. 2 Compositions of lipids extracted from three microalgal species during logarithmic and stationary phases. *Top*: *Nannochloropsis oculata*, *middle*: *Pavlova lutheri*, *bottom*: *Isochrysis* sp. For neutral lipids, *TG* triacylglycerols; *HC* hydrocarbons, *ST* sterols; *K* ketones; *FFA* free fatty acids. Modified from Dunstan et al. [20]

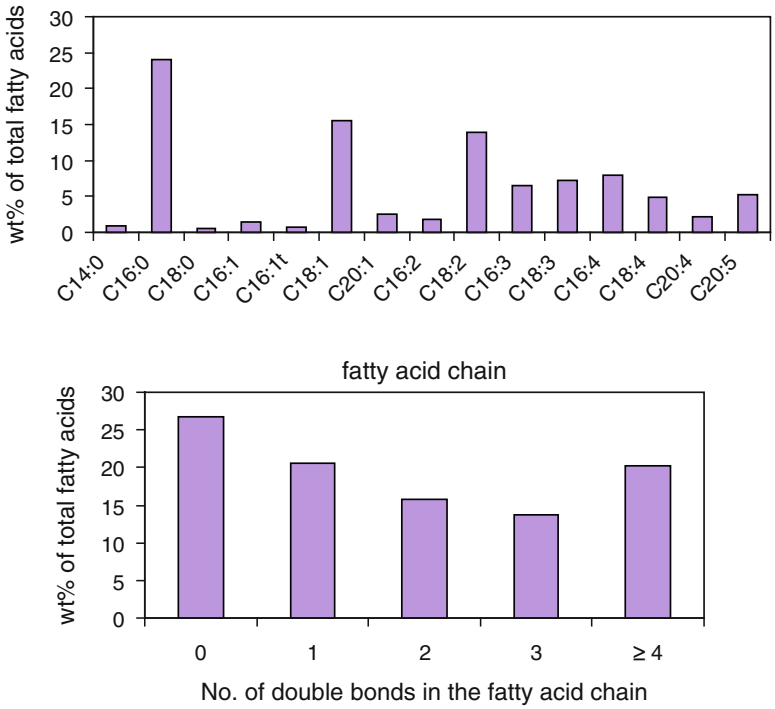

Fig. 3 Fatty acid composition of lipid extracted from species *Tetraselmis suecica* at the end of logarithmic phase (beginning of stationary phase): (*top*) in terms of fatty acid chain, (*bottom*) in terms of number of double bonds in the fatty acid chain. Modified from Volkman et al. [61]

stationary-phased microalgal lipids containing relatively high levels of polar lipid and non-acylglycerol neutral lipid impurities will need to be substantially purified before they can be converted to usable biodiesel. It has to be noted that logarithmic-phased microalgal lipids (Fig. 2) contain minimal TG contents and appear highly unattractive for biodiesel conversion [20].

Microalgal fatty acids range from 12 to 22 carbons in length and contain a mixture of saturated as well as unsaturated fatty acids. The number of double bonds in the fatty acid chains never exceeds 6 [39]. The fatty acid profile of lipid extracted from a common green microalgal species (*Tetraselmis suecica*) during the early stationary phase is examined for biodiesel production (Fig. 3) [61]. With C16:0, C18:1 and C18:2 being identified as the principal fatty acids, the microalgal lipid appears to have the fatty acid profile required to produce good-quality biodiesel. The relatively low proportion of saturated fatty acids (~25.5 wt.%) together with the trace amount of trans-conjugated unsaturated fatty acids (C16:1t being the only one at 0.8 wt.%) in the lipid is desirable. The crystal packing ability of these fatty acid classes produces biodiesel with detrimental cold flow properties (high cloud point and high pour point) [14, 31]. Additionally, the relatively modest amount of polyunsaturated

fatty acids (PUFA) with four or more double bonds (C16:4 being the highest at 7.9 wt.%) in the lipid is desirable as these acids are known to produce volatile biodiesel with low oxidation stability [31].

3 Suitability of Microalgal Biochemical Composition for Bioethanol Production

With roughly 61% of global bioethanol production, sugar crops such as sugar beet, sugar cane and molasses are the most widely used feedstocks for fermentation (Fig. 4). Corn comes second with roughly 20% of global production. However, production of bioethanol from these sources competes with the limited agricultural lands needed for food production [58]. Also both crops require more herbicides or nitrogen-based fertilizers than any other crop, thus have a high soil erosion potential [49]. High costs of pre-treatment, harvesting and transportation of these materials are some of the problems encountered with their utilization as raw materials for bioethanol production.

Lignocellulosic materials are alternative feedstocks that are being intensely explored for bioethanol production currently. The three major components of lignocellulose are cellulose, hemicellulose and lignin. Cellulose is a long-chain highly-uniform polymer of glucose monomers joined by β-linkages. Hemicellulose is another polysaccharide composed of many different sugar monomers, including xylose and mannose. Unlike cellulose, hemicellulose is not uniform in structure and tends to be more reactive. Both cellulose and hemicellulose can be fermented once their sugar monomers have been released through a process known as saccarification [52]. On the other hand, lignin is a polymer of phenylpropylene subunits and cannot be fermented. Lignin forms a crystalline protective structure around cellulose and

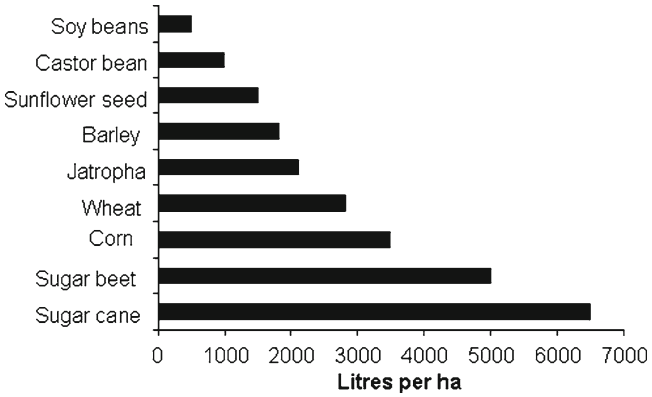

Fig. 4 Various feedstocks for ethanol production in 2006, modified from Global Fuel trends, www.earthtrends.com (accessed on 31/01/2010)

hemicellulose in the biomass and is very difficult to be biologically degraded. Such formation interferes with the saccarification, and hence fermentation, of cellulose and hemicellulose [36]. Therefore, lignocellulosic materials are more challenging to be used in fermentation. Moreover, the cost of ethanol production from these materials has been reported to be relatively higher compared to other feedstocks [58].

Microalgal biomass is currently being explored as a potential feedstock for bioethanol production. Microalgal cells contain carbohydrates that can be used as carbon sources for bioethanol production during fermentation, and this varies from strain to strain. Selection of the right strain is necessary in order to achieve the highest bioethanol yield. Table 1 shows the carbohydrates and protein contents of different microalgal strains. The production of bioethanol from microalgae provides many advantages: (1) Microalgal cells have a very short harvesting cycle (~1–10 days) compared to other feedstocks (harvest once or twice a year) [54], thus potentially providing enough supplies to meet bioethanol production demands in the future. (2) Compared with microalgal biodiesel, the process for producing microalgal bioethanol is more energy effective due to the utilization of simpler equipment or machinery to start up. (3) No delignification process is required since microalgae contain no lignin, thus reducing the production cost of bioethanol [13]. (4) The CO_2 by-product after the fermentation process can be recycled to the microalgal cultivation system, thus emitting minimal amount of carbon dioxide to the environment. (5) The leftover biomass (containing protein residue) after the fermentation process can be utilized as a fertilizer or an animal feed [27]. As such, the process of bioethanol production from microalgae is sustainable, environmentally friendly and cost efficient. The production of bioethanol from microalgae consists of four main stages: pre-treatment of microalgal biomass, hydrolysis, fermentation and product recovery. A more detailed outline of each stage is discussed in Sect. 6.

4 From Bioreactors to Biodiesel: Overview of Downstream Processes

Figure 5 shows the downstream processing steps required to produce biodiesel from microalgae, while Table 2 provides a list of different technologies currently available for each step. After the microalgal culture is harvested from the bioreactor, it is concentrated in the dewatering step to yield a wet paste. The microalgal pellets then undergo a pre-treatment step for preparation towards lipid extraction where lipids are extracted and separated from the cellular materials. The extracted lipids are then purified in the fractionation step before they are converted to biodiesel in the methylation step.

Large scale cultivation of microalgae is generally performed in either a raceway pond or a photobioreactor [11]. Even though there are numerous systems for microalgal cultivation, they can generally be classified into outdoor or indoor systems. In an outdoor system, the microalgae are grown in the open environment with variable culturing conditions, such as temperature and light intensity, and can

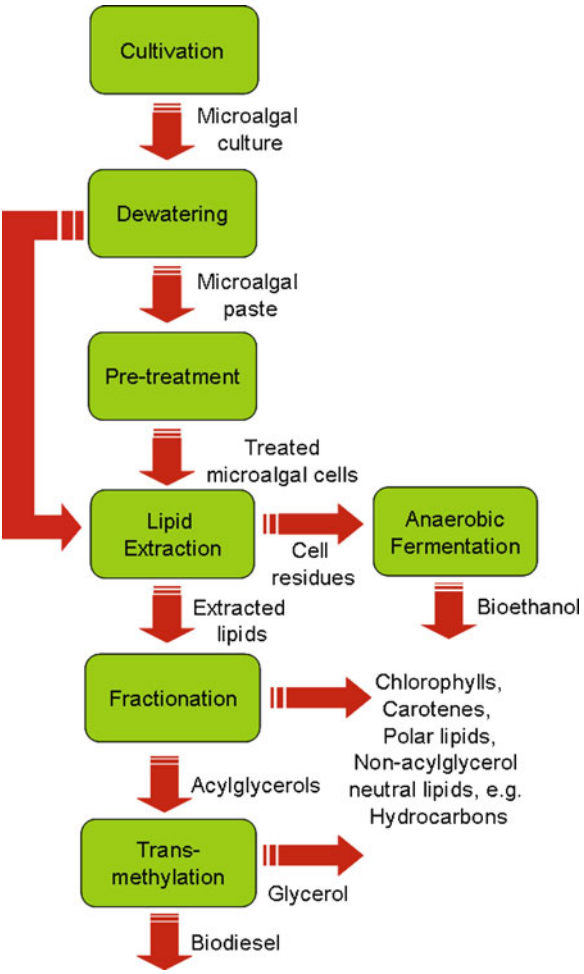

Fig. 5 Process flow diagram showing the upstream and downstream process steps needed to produce biodiesel and bioethanol from microalgae

potentially exhibit inconsistent growth rate and unpredictable biochemical evolution. On the other hand, the microalgae grown in an indoor system are placed in a greenhouse-type structure where cultivation conditions and biochemical evolution of the microalgal biomass can be tightly controlled. Even though the indoor system provides a more sound protection against local species invasion, it is not preferred due to its high operating cost. In either system, the culture must be aerated with CO_2 supply and replenished with growth medium consisting of essential elements such as nitrogen, phosphorous and iron [11].

Once the microalgal culture is harvested from its cultivation system, it exists as a very dilute aqueous suspension (between 0.1 and 1 wt.%). Since such large volumes of water are undesirable for downstream processing, the culture needs to be substantially concentrated [15, 45]. Different solid–liquid separation techniques, such as centrifugation, filtration, flocculation, are used to dewater the microalgal

Table 2 Different technologies available for each process step required to produce biodiesel from microalgae

Process step	Technologies
Cultivation	Raceway ponds
	Photobioreactors
Dewatering	Tangential flow filtration
	Pressure dewatering
	Flocculation
	Agglomeration
	Centrifugation
	Ultrasound separation
Pre-treatment: cell disruption	Ultrasonication
	Homogenization
	French pressing
	Bead beating
	Chemical lysis (acids and enzymes)
	Osmotic shock
Pre-treatment: drying	Oven drying
	Freeze drying
	Spray drying
Pre-treatment particulate size	Milling with specific sieve
Lipid extraction	Organic solvent extraction
	Supercritical fluid extraction
	Modified organic solvent extraction (soxhlet, ultrasound-assisted, microwave-assisted, accelerated)
Fractionation	Liquid chromatography
	Urea crystallization
Transmethylation	Acidic methylation
	Basic transmethylation

culture up to a solid concentration of 10 wt.% (Table 2). A cost-viable and energy-efficient concentrating technology is a current research endeavour.

After dewatering, the semi-wet microalgal paste undergoes pre-treatment steps before lipid extraction. Even though this pre-treatment step can be omitted, it is generally undertaken since the alteration of biomass conditions occurring in this step could lead to enhanced efficiency of subsequent lipid extraction [32, 33]. The treatment can be performed in multiple steps or as a single process. As one alternative, residual water which is known to prohibit effective lipid mass transfer during the extraction step is completely removed from the paste through simple drying. The desiccated cells can then be milled into powder before being extracted with eluting solvents. In a different scenario, the paste can be exposed to disruption methods which disintegrate cellular structures and force the release of intracellular lipids to the surrounding medium, thereby easing the lipid extraction process. Effects of cell pre-treatment on lipid extraction are further discussed in Sect. 5.3.

After pre-treatment, the microalgal biomass undergoes a lipid extraction step that results in the separation of lipids from the cellular matrix. The principles and

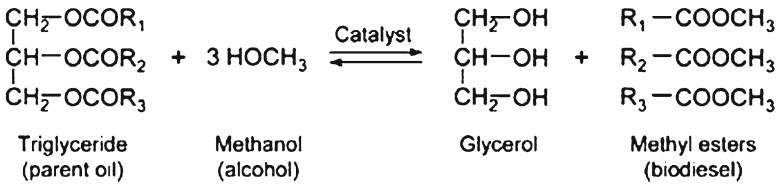

Fig. 6 Transesterification of acylglycerol (triacylglycerol is used as an example) with methanol and basic catalyst to produce biodiesel, extracted from Chisti [11]

processes involved in lipid extraction are discussed more thoroughly in Sect. 5. The isolated lipids are fractionated in order to remove unwanted non-lipid contaminants (such as carbohydrates, proteins and chlorophylls) and unusable lipid fractions (such as polar lipids and non-saponifiable neutral lipids) from the acylglycerols. Even though experimental methods, such as liquid chromatography and urea crystallizations, are available to perform this step on a bench scale [39], none of them is yet economically feasible to be retrofitted to a commercial scale.

In the transmethylation (also known as transesterification) step, the acylglycerols in the lipid extract are converted to fatty acid methyl ester (FAME) or biodiesel. Although a laboratory method to transmethylate polar lipids to biodiesel exists using toxic boron trifluoride or BF_3 [14, 61], the industrial applicability of this method has not been tested. The method described here employs an alkaline catalyst (either NaOH or KOH) specific to acylglycerols, and is used to industrially transmethylate plant and animal oils which consist mainly of TG. The lipids are reacted with methanol and the select alkaline catalyst in a specific ratio depending on the concentration of TG and the presence of free fatty acids. The final FAME conversion is a function of reaction temperature and duration. During the transmethylation, the alkaline catalyst cleaves the ester bonds holding the fatty acids to the glycerol backbone (Fig. 6) [11]. The liberated fatty acids are then reacted with methanol to form new molecules with lower viscosity (FAME). The by-products (glycerol, reformed catalyst and excess methanol) are separated from the desired FAME via gravity settling as well as repeated water washings [17, 19, 31].

In order for biodiesel from microalgae to be environmentally sustainable, the total CO_2 emitted in the downstream processes to produce usable biodiesel needs to be lower than or at least equal to the total CO_2 originally captured by the microalgae. Therefore, processes selected in each step should aim at minimizing energy consumption.

5 Lipid Extraction for Biodiesel Production

Depending on the degree of drying during the pre-treatment step, the state of the microalgal cells during lipid extraction can be either a wet paste (approximately 10–30 wt.% solid) or dried powder. During lipid extraction, lipid molecules are extracted out of the microalgal cells and separated from the cellular matrix.

The isolated lipids are often referred to as extracts or analytes. The selected lipid extraction method has to be lipid-specific in order to minimize the co-extraction of non-lipid contaminants (proteins, carbohydrates) and be able to exhibit some degree of selectivity towards biodiesel-convertible neutral lipid fractions (acylglycerols) in order to minimize the downstream removal of unusable lipid components (polar lipids and non-saponifiable neutral lipids) [39]. Additionally, the method should be efficient (both in terms of time and energy), non-reactive with the lipids, and relatively safe [30]. The practice of completely drying microalgal wet paste prior to lipid extraction is energetically prohibitive and needs to be avoided. As a consequence, the selected lipid extraction method needs to be effective when applied directly to microalgal wet paste. Two of the most commonly used microalgal lipid extraction technologies are reviewed: traditional organic solvent extraction and emerging supercritical fluid extraction.

5.1 Organic Solvent Extraction

5.1.1 Basic Principles

During lipid extraction, microalgal cells (either as a wet paste or dried biomass) are exposed to a non-polar organic solvent, such as hexane or chloroform, which interacts with the neutral lipid molecules and overcomes their weak hydrophobic interactions with other biomolecules. As a result, the neutral lipid molecules desorb from their cellular matrix and dissolve in the solvent [30, 39]. The remaining cell residue is then separated from the solvent via solid–liquid separation methods. The solvent is evaporated to yield dry lipid extract.

However, some neutral lipids are strongly linked via hydrogen or electrostatic bonds to other biomolecules, such as proteins and polar lipids, in the cell membrane. These bonds are too tough to be disrupted by the non-polar solvent alone and require the presence of a more reactive solvent for their destruction [30, 39]. A small amount of polar solvent (such as methanol or isopropanol) is thus added together with the non-polar solvent (such as hexane or chloroform) to facilitate the extraction of these membrane-associated neutral lipids. Unfortunately, the addition of a polar co-solvent also leads to the increased co-extraction of undesirable polar lipids.

When using a non-polar/polar solvent mixture (such as hexane/isopropanol or chloroform/methanol), both solvents are added to the microalgal cells (either as a wet paste or dried biomass) in the desired ratio at the same time. Upon removal of cell debris via solid–liquid separation, biphasic separation of the solvent mixture is induced by equivolume addition of the non-polar solvent (hexane for hexane/isopropanol mixture and chloroform for chloroform/methanol mixture) and water. Once the solvent mixture separates into two layers, the lipids (both neutral and polar fractions) will partition in the organic phase (a mixture of non-polar solvent and polar solvent), while the aqueous phase (a mixture of water and polar solvent) will contain co-extracted non-lipid contaminants (proteins and carbohydrates) [30, 39]. The organic phase is collected and the solvent is evaporated to obtain dry lipid extract.

5.1.2 Selection of Organic Solvents

In addition to satisfying the aforementioned criteria for the lipid extraction method, the selected organic solvents must be relatively cheap, relatively non-toxic, able to form two-phase with water for the removal of co-extracted non-lipids and volatile for recovery from the lipid extract [22, 39]. Furthermore, the solvent molecules must be sufficiently small so that permeation through the microalgal cell wall can be easily achieved.

Chloroform/methanol (2:1 v/v) is the most commonly used solvent mixture for laboratory-scale lipid extraction from any living tissue. The system uses residual endogenous water as a ternary component to enhance the extraction of polar lipids and does not require cells to be completely dried. Upon removal of the cell debris, the solvent mixture equilibrates with the dissolved lipids and separates into 2 phases upon addition of chloroform and water. The lower organic phase (chloroform with some methanol) contains most of the lipids while the upper aqueous phase (water with some methanol) contains most of the non-lipids [39]. Even though the extraction process using this solvent mixture is fast and quantitative, chloroform is a highly toxic solvent whose large-scale usage is environmentally unattractive. Since the method was originally developed by Folch et al. [23] for the isolation of total lipids from brain tissues, its effectiveness in extracting lipids from microalgal cells still needs further assessment.

Hexane/isopropanol (3:2 v/v) works in a similar fashion as the chloroform/methanol mixture. Upon biphasic separation, the upper organic phase (hexane with some isopropanol) contains most of the lipids while the lower aqueous phase (water with some isopropanol) contains most of the non-lipids. This solvent mixture is quickly replacing chloroform/methanol as a laboratory favourite due to its lower toxicity and its higher selectivity towards neutral lipids [26, 33, 46]. However, the hexane/isopropanol mixture has been reported to yield a lower lipid recovery than the chloroform/methanol mixture when applied to microalgal cells [33].

Even though alcohols, such as butanol and ethanol, are cheap and highly volatile, their use as pure lipid extraction solvents is limited due to their lower affinities towards neutral lipids. In a study conducted by Lee et al. [33], the performances of five different solvent mixtures during lipid extraction from bead-beaten *Botryococcus braunii* were evaluated (Fig. 7). Chloroform/methanol was found to be the best solvent mixture with a lipid yield of ~0.29 g/g dried microalgae, while all dichloroethane-based mixtures seemed rather ineffective.

5.1.3 Operating Parameters

Apart from cell pre-treatment and the selection of solvent mixtures, there are other variables which affect the performance of organic solvent lipid extraction. The temperature at which extraction is performed has been reported to influence lipid yield [22]. Even though increasing temperature from 30 to 60°C was initially observed to enhance lipid extraction rate from animal tissues, a rise beyond 70°C led to the

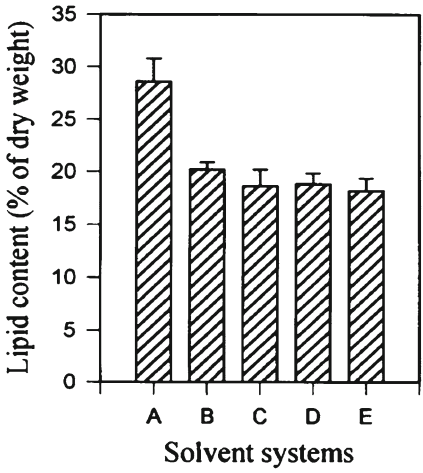

Fig. 7 Effect of solvent mixtures on lipid yield of organic solvent lipid extraction from microalgal species *Botryococcus braunii.* A: chloroform/methanol (2:1 v/v), B: hexane/isopropanol (3:2 v/v), C: dichloroethane/methanol (1:1 v/v), D: dichloroethane/ethanol (1:1 v/v), E: acetone/dichlomethane (1:1 v/v), extracted from Lee et al. [33]

degradation of thermo-labile components and adversely affected the lipid yield [23]. Other variables that influence organic solvent extraction include degree of agitation, solvent-to-biomass ratio, and the number of equilibrium establishments.

Even though organic solvent extraction has been in use for many decades for microalgal lipid recovery [48], the variables affecting its performance have not been thoroughly assessed and its application seems to have serious limitations. Not only does the process use large amounts of expensive and toxic solvents, organic solvent extraction requires energy-intensive evaporation for lipid recovery. Finally, the extent of lipid dissolution in a batch of organic solvent is thermodynamically limited by the lipid transfer equilibrium [62]. Once the solvent and the cellular matrix obtain their lipid partition equilibrium, no further extraction takes place.

5.1.4 Modifications to Organic Solvent Extraction

The organic solvent extraction described above is generally performed as a batch process. Even though lipid extraction in a batch mode is limited by the establishment of lipid partition equilibrium, a continuous organic solvent extraction which overcomes this limitation is not a viable option due to the high cost associated with supplying the increased solvent volume, even with an integrated solvent recovery system. As such, a system that is somehow able to continuously replenish cells with fresh solvent (hence avoiding equilibrium limitation) while simultaneously minimizing solvent consumption is desirable. The Soxhlet apparatus achieves this dual objective through its ingenious cycles of solvent evaporation and condensation [35, 62]. The apparatus has three compartments as shown in Fig. 8: the continuously heated solvent flask to store the extracting organic solvent, the Soxhlet extractor to hold the microalgal cells (existing as either a wet paste or dried biomass), and the continuously cooled condenser. The evaporated organic solvent from the heated

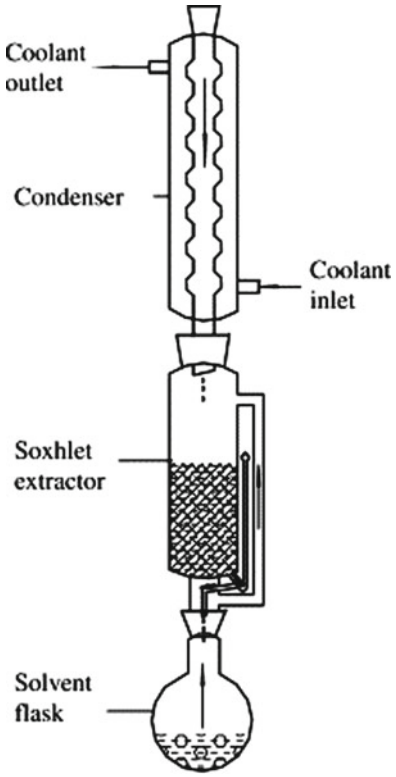

Fig. 8 The Soxhlet apparatus, extracted from Wang and Weller [62]

solvent flask enters the condenser. As the recondensing solvent is channelled into the Soxhlet extractor, it comes in contact with the microalgal cells to extract lipids. Once the rising solvent in the extractor reaches the overflow level, a syphon unloads the lipid-saturated solvent in the extractor back into the solvent flask. The solvent evaporates again while the extracted lipids remain in the solvent flask, and the cycle repeats. The operation continues until no more lipids are isolated in the Soxhlet extractor. Even though the semi-continuous Soxhlet apparatus solves the equilibrium limitation of a batch organic solvent extraction without any increase in solvent consumption, its high energy requirement for continuous distillation prevents its large-scale application [35, 62].

Three other modifications of organic solvent extraction have been reported: ultrasound-assisted, microwave-assisted and accelerated organic solvent extraction. Each of these modifications makes use of an auxiliary process to enhance lipid extraction by organic solvents [35, 62]. Ultrasound-assisted organic solvent extraction obtains higher extraction kinetics by using mechanical vibrations from sound waves not only to disrupt cellulosic cell walls but also to induce greater penetration of solvent molecules into the cellular structures. Microwave-assisted organic solvent extraction uses electromagnetic radiations within specific frequency to impart large amount of thermal energy into the cells, thereby disrupting their cellulosic cell walls and promoting lipid extraction. During accelerated organic solvent extraction, lipid extraction is

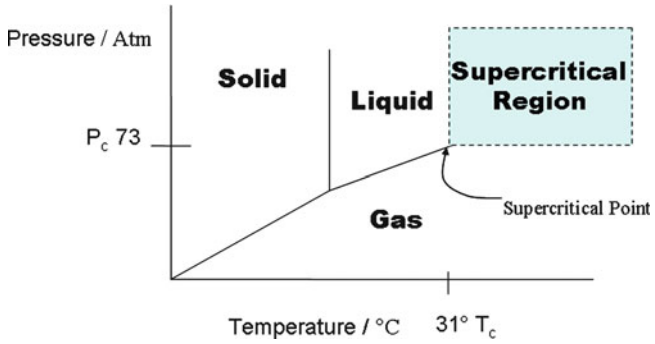

Fig. 9 Pressure (P)-temperature (T) phase diagram for carbon dioxide, showing the supercritical region

performed at elevated pressures and temperatures, but below critical conditions, in order to accelerate extraction kinetics. Even though all three of these modifications seem to show some promises, they have not been successfully transferred to the industrial scale due to their high energy requirements. Their effectiveness in extracting lipids from microalgal cells still needs further demonstration [35, 62].

5.2 Supercritical Fluid Extraction

Supercritical fluid extraction (SFE) is an emerging green technology that is a potential substitute to traditional organic solvent extraction.

5.2.1 Basic Principles

When the temperature and pressure of a fluid is raised over its critical values (T_c and P_c), the fluid is transformed to a supercritical state and exhibits properties similar to both a liquid and a gas (Fig. 9) [50, 59]. The intermediate properties of this state (Table 3) are found to significantly enhance the propensity of the fluid to extract lipids from living tissues. In comparison to organic solvent extraction, SFE is known to have the following advantages [40–42, 59]:

- Tunable selectivity
  The solvating power of a supercritical fluid is a function of its density which can be continuously adjusted by changing pressures and temperatures. Therefore, its selectivity can be tuned such that it interacts only with neutral lipids.
- More favourable mass transfer
  High diffusion coefficient (similar to a liquid) and low viscosity (similar to a gas) enable a supercritical fluid to penetrate through cellular matrices much more rapidly than an organic solvent, leading to a higher extraction rate and a shorter extraction time.

Table 3 Physical properties of a typical fluid in different states [59]

	Density (kg/m^3)	Viscosity (μPa s)	Diffusion coefficient (mm^2/s)
Gas	1	10	1–10
Supercritical fluid	100–1,000	50–100	0.01–0.1
Liquid	1,000	500–1,000	0.001

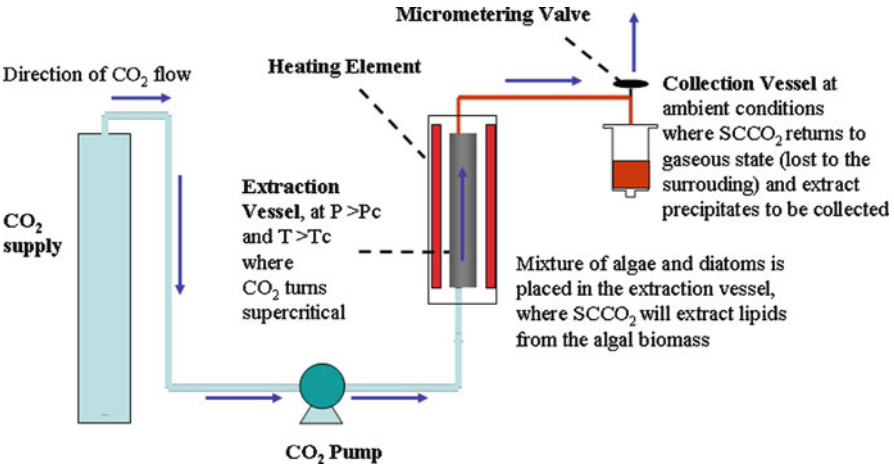

Fig. 10 Schematic diagram of a laboratory-scale $SCCO_2$ extraction system, modified from Applied Separations website [3]

- Production of solvent-free lipids
  Since the lipids obtained at the end of SFE are free from any solvent, no energy needs to be expended for solvent removal.

CO_2 is used as the primary solvent in most SFE applications for numerous reasons. Its moderate critical pressure (72 bar) enables a modest compression cost, while its low critical temperature (32°C) avoids possible degradation of thermally sensitive lipids. Its low toxicity, low flammability and lack of reactivity also facilitate for a safer SFE operation [37, 59]. In cases where microalgal cells are cultivated in synergy to a coal power station, the CO_2 for extraction can be conveniently supplied from the scrubbed flue gas of the station.

Figure 10 shows the schematics of a laboratory-scale supercritical carbon dioxide ($SCCO_2$) extraction system [3]. A mixture of microalgal cells (either as a wet paste or dried biomass) and packing materials (normally diatomaceous earth) in a specific ratio is packed into the extraction vessel equipped with a heating element. A feed pump delivers the CO_2 from its reservoir to the extraction vessel at a pressure greater than P_c. Once the vessel is heated ($T > T_c$), the compressed CO_2 is transformed to its supercritical state and performs lipid extraction on the microalgal cells. Lipid molecules are dissociated from the cellular structure and transferred into the eluting $SCCO_2$ in a diffusion-driven mechanism. The lipid-saturated $SCCO_2$ then leaves the extraction vessel and enters the collection vessel. The micrometering

valve at the entry to the vessel is opened to rapidly depressurize the incoming $SCCO_2$. Once completely decompressed, the $SCCO_2$ returns to its gaseous state and evaporates to the ambience, thereby forcing the extracted lipids to precipitate in the collection vessel. Even though $SCCO_2$ extraction can be operated as either a batch (static) or a continuous (dynamic) process, the dynamic operation is preferred as it generally leads to an improved yield [59]. Even though $SCCO_2$ process has been used to extract lipids from microalgal cells in a laboratory scale [1, 2, 7, 10, 28, 40–42, 53] its energy efficiency still needs to be assessed and is a subject of future research endeavour.

5.2.2 Operating Parameters

In addition to cell pre-treatment, as discussed in Sect. 5.3, the operating parameters that influence $SCCO_2$ lipid extraction include pressure, temperature, modifier addition, extraction time, fluid flow rate and packing density [50].

The solvent power and the selectivity of $SCCO_2$ are known to be direct functions of the fluid density [59]. Since pressure elevation at a constant temperature compresses the fluid to a higher density, it inevitably leads to an increase in the solvent power of the fluid. However, increasing pressure is often not desirable as it leads not only to a higher compression cost but also to a lower selectivity and to the co-extraction of unwanted cellular components. Since temperature increase at a given pressure leads to two simultaneous competing phenomena, its net effect on extraction kinetics is more difficult to predict. The decrease in fluid density reduces $SCCO_2$ solvent power while a concurrent increase in the lipid volatility enhances solute diffusion into the supercritical fluid [10, 59]. Table 4 compiles results from previous studies that investigated the effects of pressure change and temperature change on $SCCO_2$ lipid extraction from microalgae.

Due to its non-polar nature, $SCCO_2$ is unable to interact with either polar lipids or neutral lipids that form complexes with polar structures. Addition of a polar modifier, such as methanol, ethanol, toluene and methanol–water mixture, facilitates for total lipid extraction not only by enhancing the affinity of the fluid towards the aforementioned fractions but also by decreasing the fluid viscosity, thereby allowing the supercritical solvent to rapidly penetrate through the cellular matrices [50, 59]. In their study, Mendes et al. [42] showed that the addition of methanol significantly increases the extraction of γ-linolenic acid (from 0.05 wt.% of dry microalgae biomass to 0.44 wt.%) from the species *Spirulina maxima*. However, an increase in the extraction of polar lipids needs to be avoided as these fractions are not currently biodiesel convertible.

In a study conducted by Andrich et al. [1], the rate of lipid extraction from a *Nannochloropsis* sp. was found to decrease with extraction time (Fig. 11). Most of the available lipids (> 80%) were extracted within 5,000 s and continuing the extraction beyond 10,000 s did not seem to considerably increase the lipid yield. This asymptotic behaviour confirms the diffusion-driven characteristics of $SCCO_2$ extraction where the rate of lipid evolution is known to be directly proportional to the amount of unextracted lipids remaining in the cellular structures [1].

Table 4 Effects of pressure and temperature changes on $SCCO_2$ lipid extraction from algae

Study	Algae	Pressure or P (bar)	Temperature or T (°C)	Results
Sajilata et al. [53]	*Spirulina platensis*	316, 350, 400, 450, 484	40	Yield increased with *P* Maximum lipid yield = 8.63% of dry weight
Andrich et al. [1]	*Nannochloropsis* sp.	400, 550, 700	40, 55	At constant *T*, extraction rate increased with *P*. At constant *P*, extraction rate slightly increased with *T*. Overall yield was the same at any *T* and *P* Maximum lipid yield = 25.00% of dry weight
Mendes et al. [41]	*Spirulina maxima*	100, 250, 350	50, 60	At constant *T*, yield increased with *P* At constant *P*, yield slightly increased with *T* Maximum lipid yield = 3.10% of dry weight
Cheung [10]	*Hypnea charoides*	241, 310, 379	40, 50	At constant *T*, yield increased with *P* At low *P* (241 bar), yield decreased with *T*. At medium to high P (310 and 379 bar), yield increased with *T* Maximum lipid yield = 6.71% of dry weight
Mendes et al. [40]	*C. vulgaris*	200, 350	40, 55	At constant *T*, yield increased with *P*. At low *P* (200 bar), yield decreased with *T*. At high *P* (350 bar), yield increased with *T*. Maximum lipid yield = 13.00% of dry weight

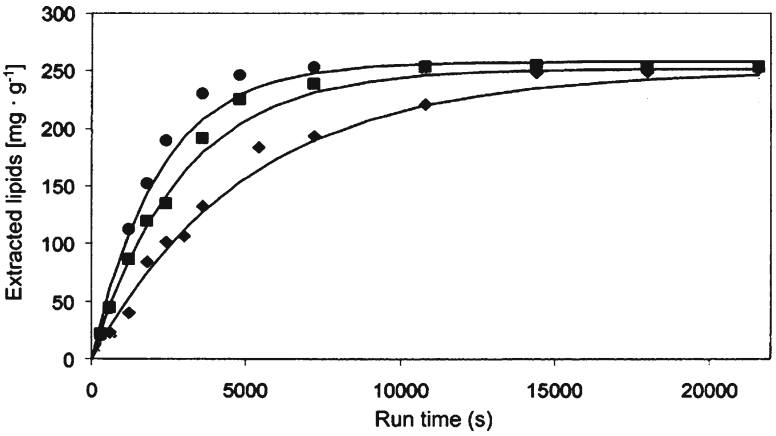

Fig. 11 Effect of pressure and extraction time on lipid yield of $SCCO_2$ lipid extraction from a *Nannochloropsis* sp. All extractions were performed at a constant temperature of 40°C: *filled circle* 70 MPa, *filled square* 55 MPa, *filled diamond* 40 MPa. Extracted from Andrich et al. [1]

The flow rate of $SCCO_2$ through the cellular matrix affects the lipid extraction kinetics. Even though increasing $SCCO_2$ flow rate facilitates for a more rapid diffusion of lipid molecules into the extracting fluid phase, higher flow rate often results in uneven fluid penetration within the matrix as well as elevated pressure requirement [50].

The manner in which cells are packed to form a fixed bed inside the extraction vessel plays a pivotal role in influencing extraction efficiency [50]. In the case of extraction from dried microalgal powder, packing density is a direct function of both microalgal powder particulate size and the amount of packing materials (normally diatomaceous earth) added per unit mass of powder. Although higher packing density increases the amount of total extractable lipids in the vessel, it often leads to fluid channelling effects, prevents the eluting solvent from performing homogenous extraction, and results in a lower overall lipid yield. Differences in packing density and packing uniformity have been found to be the reasons why some $SCCO_2$ extractions conducted under identical parameters achieve variable yields [50].

5.3 Effect of Cell Pre-treatment on Lipid Extraction

The effects of cellular pre-treatment on microalgal lipid extraction kinetics still need to be investigated. Using a combination of technologies shown in Table 2, the pre-treatment step can alter the following cellular conditions: degree of cell disruption, degree of intracellular water contents and, in the case of dried microalgal biomass, particulate size.

The efficiency of lipid extraction is known to increase with the degree of cell disruption. When intact cells are disintegrated during cell disruption process, some of the intracellular lipids are liberated from the cellular structures and released to the surrounding medium [12, 32, 43]. During the subsequent lipid extraction, the eluting solvent can directly interact with these free lipids without permeating into the cellular cytoplasm. As such, the extraction kinetics is enhanced due to decrease in mass transfer limitation and the process becomes completely dependent on the lipid solubility in the solvent. Lee et al. (1999) investigated the effects of prior cell disruption on chloroform/methanol (2/1 v/v) lipid extraction from the species *B. braunii*. Completely ruptured microalgal cells were found to yield almost twice the amount of lipids from intact cells. Also, among all the cell disruption technologies that were tested (sonication, homogenization, high pressure French press, bead beater and lyophilization), mechanical shearing with bead beater appears to be the most effective in rupturing the microalgal cells.

The degree by which the presence of intracellular water affects microalgal lipid extraction still requires investigation. Since water is assumed to act as a barrier that prohibits effective lipid mass transfer to the extracting solvent, microalgal cells are almost always completely dried before undergoing lipid extraction. However, other microorganisms (bacteria, yeasts and viruses) have been successfully extracted straightaway in their wet state (~90 wt.% water) using chloroform/methanol solvent mixture which requires the presence of residual water as a ternary component to

swell the cells, to enable better solvent access and to improve the extraction of polar lipids [30, 39]. For $SCCO_2$ extraction, the presence of intracellular water is known to result in freezing which causes flow impedance problems such as extraction vessel blockage and restrictor plugging [50, 55]. Among the different drying technologies available for microalgal biomass, freeze drying is preferred for its mild operating conditions. Thermal drying needs to be avoided as it leads to possible degradation of thermolabile analytes, results in evaporative loss of volatile analytes and yields cellular biomass with non-uniform particulate size as end-products. It should be noted that drying is different from dewatering. Dewatering removes extracellular water molecules by concentrating the dilute microalgal culture to a wet paste, whereas drying is the subsequent step that eliminates intracellular water molecules from the microalgal wet paste.

When extraction is performed on dried microalgal biomass, particulate size variation can significantly influence extraction kinetics. Decreasing microalgal particulate size generally benefits lipid extraction as it increases the surface area available for biomass-solvent contacts, and also improves solvent penetration into the matrix through shortening of diffusion pathways. However, exceedingly small particulate size often leads to fluid channelling effects in the extraction vessel and can reduce lipid yield as the extracted lipid molecules have a higher tendency to get re-adsorbed to the matrix surface [50].

5.4 Comparison Between Organic Solvent and $SCCO_2$ Extraction

Table 5 provides a preliminary comparison between organic solvent extraction and $SCCO_2$ extraction for lipid extraction from microalgae. A more thorough understanding of mass transfer mechanism and kinetic parameters involved in lipid extraction from microalgae is needed for an extensive comparison. Large use of toxic solvents and energy-intensive solvent-lipid separation represent the main disadvantages with commercial use of organic solvent extraction, while expensive fluid compression and high installation cost of an extraction pressure vessel remain the primary obstacles for large-scale $SCCO_2$ extraction [50]. The theoretical advantages of $SCCO_2$ extraction, such as tunable selectivity for specific lipid fractions and enhanced kinetics due to the fluid intermediate physicochemical properties, still need to be verified for microalgal lipid extraction.

6 Fermentation of Microalgal Biomass for Bioethanol Production

As mentioned in Sect. 3, the production of bioethanol from microalgae involves four main stages: (1) pre-treatment of the biomass to remove hemicellulose and to improve access to available cellulose, (2) hydrolysis of the cellulose (and potentially

Table 5 Comparison between organic solvent extraction and $SCCO_2$ extraction for microalgal lipid extraction

Criteria	Organic solvent extraction	$SCCO_2$ extraction
Lipid selectivity	Selectivity is not easily tuned. Costly post-extraction fractionation step may be needed	$SCCO_2$ tunable selectivity minimizes co-extraction of contaminants, hence reducing cost needed for downstream fractionation
Time	Solute transfer equilibrium limitation results in slow extraction rate and increases time needed for a complete extraction	Due to its intermediate liquid-gaseous properties, $SCCO_2$ extraction is much more rapid and can complete extraction within shorter period of time
Energy	It consumes little energy as extraction is conducted near ambient conditions. However, solvent needs to be removed in energy-intensive evaporation	It is highly energy-intensive as pressurization is needed in order to convert fluid to supercritical state
Installation and operating (non-energy and non-time related) cost	Expensive pure solvent is needed for extraction	Installation of large-scale pressure vessel needed for $SCCO_2$ extraction is extremely expensive. CO_2 derived from the flue gas of any power station has to be purified before it can be used for lipid extraction
Reaction to lipid	Solvent may react with lipid, especially during evaporation when it is removed from the lipids	$SCCO_2$ is non-reactive with lipids
Hazard and toxicity	Toxic solvent is used in a large volume	High-pressure hazard is possible though this should be easily avoided with good engineering design

the hemicelluloses) to form simple sugars, (3) fermentation of the simple sugars such as glucose (and potentially xylose) to form bioethanol, (4) product recovery where the bioethanol is purified for commercial applications. The overall process for bioethanol production is shown in Fig. 12.

6.1 Biomass Pre-treatment

Microalgal biomass requires pre-treatment before fermentation to enhance bioethanol production. Biomass pre-treatment process is a major contributing factor to bioethanol production cost. The carbohydrates of microalgae are stored inside the cell walls and between the intercellular matrices [60]. Thus, it is necessary to rupture the microalgal cell walls so that the entrapped carbohydrates can be released and, if

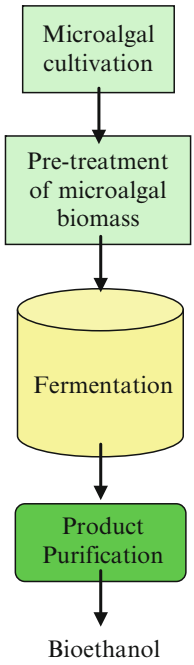

Fig. 12 Process flow diagram of bioethanol production from microalgae

necessary, broken down into simple sugars to be utilized in the fermentation process. Cell disruption methods can be classified as mechanical, chemical and biological [44, 47, 58]. Each of these methods is able to liberate the sugar molecules.

6.1.1 Physical Method

The physical methods include comminution (ball milling, hammer milling), irradiation (electron beam, microwave), steam exploration (high pressure steam) and hydrothermolysis (liquid hot water). These methods have been successfully used to pre-treat other biomass for bioethanol production [58]. Physical methods of biomass pre-treatment mostly result in decreasing biomass particle size and degree of depolymerisation of hemicellulose and cellulose, as well as in reducing cellulose crystallinity [29]. However, physical methods are energy intensive, and the rate of hydrolysis is slow.

6.1.2 Chemical Method

The chemicals involved in the pre-treatment of biomass can be divided into two types; acidic (sulphuric, hydrochloric, phosphoric) and alkaline (lime, sodium hydroxide ammonium sulfite). Nguyen et al. [47] reported that acid pre-treatment of

Chlamydomonas reinhardtii biomass yielded around 58% (w/w) of glucose and resulted in an ethanol yield of 29.2% (w/w) at the end of the fermentation process. Aside the promising results obtained for microalgae, the efficiency of this method has been widely verified for other feedstocks [4, 9]. The chemical methods are, by far, the most prevalent biomass pre-treatment method. This is due to the low cost of the process, and its effectiveness in hydrolysing the hemicelluloses and celluloses to sugars. They are often used in conjunction with an initial degree of physical pre-treatment to reduce the biomass particle size. Also, the chemical methods are preferred due to their low operating costs when compared to the energy-intensive physical methods [29]. Since microalgal biomass does not contain lignin, the method is efficient in converting complex carbohydrates to fermentable sugars. However, the utilization of hazardous chemicals in the process can cause severe corrosion to the fermentation vessel and the resulting irrecoverable salts may form part of the biomass, thus changing the fine and specific biomass structure and its biochemical composition.

6.1.3 Biological Method

This method involves the utilization of microorganisms such as fungi to reduce the cellulose and hemicellulose crystallinity of the biomass. It is an environmentally and energetically efficient process because the pre-treatment occurs under mild conditions (low temperature and pH around 6–7). However, the rate of hydrolysis using this method is too slow for industrial application, and some fermentable materials are consumed in the process. Whilst this method is unlikely to be used as a sole treatment of microalgal biomass, it could serve as the first step of a multi-step pre-treatment method [24].

6.2 Hydrolysis

Microalgal biomass can be pre-treated via hydrolysis using the cellulosic enzymes obtained from fungi, protozoa or bacteria. Widely used cellulosic enzymes are cellulase from *Thrichoderma reseei* and cellulase from *Aspergillus niger*. The cellulase enzyme consists of three main components [63]; (1) 1,4-β-D-glucan glucanohydrolases (endoglucanases); break down the cellulose crystallinity, (2) 1,4-β-D-glucan cellobiohydrolases and 1,4-β-D-glucan glucanohydrolases (exoglucanases); the exoglucanases hydrolyse the individual cellulose fibres into simple sugars and cellobiohydrolases attack the chain ends producing cellobiose, (3) β-D-glucoside glucohydrolases (β-glucosidases); release glucose monomers by hydrolysing the disaccharides and tetrasaccarides of cellulose and form glucose that is ready to be used in the fermentation process. Even though it is a common practice for biomass to be pre-treated prior to enzymatic hydrolysis, microalgal biomass can undergo the hydrolysis process directly without any pre-treatment due to its non-lignin composition. This makes production of bioethanol from microalgal biomass more economical.

Table 6 Microorganisms commonly used for industrial ethanol production

Organism	Natural sugar utilization pathways					Major products			
	Glu	Man	Gal	Xyl	Ara	EtOH	Other	O_2 needed	pH
Anaerobic bacteria	+	+	+	+	+	+	+	–	Neutral
Escherichia coli	+	+	+	+	+	–	+	–	Neutral
Zymomonas mobilis	+	–	–	–	–	+	–	–	Neutral
Saccharomyces cerevisiae	+	+	+	–	–	+	–	–	Acidic
Pichia stipitis	+	+	+	+	+	+	–	+	Acidic
Filamentous fungi	+	+	+	+	+	+	–	–	Acidic

6.3 Fermentation

Amongst the many microorganisms used for bioethanol production, *Saccharomyces* sp. remains the prime species. Currently, both alcoholic beverages and ethanol fuels are produced through fermentation performed by *Saccharomyces* sp. The species are resistant to high temperatures and provide a high ethanol tolerance level, allowing fermentation to continue at ethanol concentrations of 16–17% (v/v) [8]. Bacteria, particularly *Zymomonas mobilis* and *Escherichia coli*, have been successfully used to ferment biomass for bioethanol production [34]. However, bacteria are less robust than yeast and their growth requires a narrow pH range (6.0–8.0), thus less preferable to be used in the fermentation process. Table 6 shows some wild-type of microorganisms commonly used for industrial ethanol production. Most of the listed microorganisms fail to ferment xylose even though it is one of the sugars obtained from the hydrolysis process. In order to overcome the hurdle, genetically-modified microorganisms have been cultivated and tested to ferment xylose [25, 65]. To date, the successful use of genetically-modified strains for fermentation has been reported only at a laboratory scale.

The fermentation of simple sugars into bioethanol involves a glycolytic pathway which occurs in two major stages. The first stage is the conversion of the various sugar molecules to a common intermediate, glucose-6-phosphate. The second phase is the metabolism of each molecule of glucose-6-phosphate to yield two molecules of pyruvate [38]. The products from the glycolysis steps are further metabolized to complete the breakdown of glucose. Under anaerobic conditions, the pyruvate is further reduced to ethanol with a simultaneous release of CO_2 as a by-product.

6.4 Bioethanol Recovery

In order to obtain high-purity bioethanol, solids and other aqueous components associated with the bioethanol need to be removed by clarification and distillation respectively. This separation process, however, has not yet been demonstrated for

microalgal-bioethanol broth. The residual biomass produced after the separation process can theoretically be concentrated and converted to other products, such as animal feeds or fertilizers. The purity of bioethanol must satisfy international standards for fuel specifications, ASTM D5798—09B. The produced bioethanol can be either blended with gasoline to form E10 (10% bioethanol) and E85 (85% bioethanol) or used directly in vehicles as a substitute for gasoline. Each of the blends has its own specifications which vary from one country to another. The overall cost of bioethanol production from microalgae should be made low enough to compete with existing commercial fuels. Due to the lack of any existing pilot-scale production facility of bioethanol from microalgae, practical information on operating and production costs is not readily available.

Acknowledgement This work was supported by an Australian Research Council (ARC) Linkage grant between Bio-Fuel Pty Ltd (Victoria, Australia) and Monash University Department of Chemical Engineering (Victoria, Australia).

References

1. Andrich G, Nesti U, Venturi F, Zinnai A, Fiorentini R (2005) Supercritical fluid extraction of bioactive lipids from the microalgae *Nannochloropsis* sp. Eur J Lipid Sci Technol 107: 381–386
2. Andrich G, Zinnai A, Nesti U, Venturi F, Fiorentini R (2006) Supercritical fluid extraction of oil from microalga S*pirulina (Arthrospira) platensis*. Acta Aliment 35(2):195–203
3. Applied separations website (2009) http://www.appliedseparations.com/Supercritical/Lab_Inst/Analytical/SFE_2.asp. Accessed 30 June 2009
4. Ballesteros I, Ballesteros M, Manzanares P, Negro MJ, Oliva JM, Sailez F (2008) Dilute sulfuric acid pretreatment of cardoon for ethanol production. Biochem Eng J 42:84–91
5. Becker EW (1994) Microalgae: biotechnology and microbiology. In: Baddiley J, Carey NH, Higgins IJ, Potter WG (eds) Cambridge studies in biotechnology. Cambridge University Press, New York, p 178
6. Brown MR, Jeffrey SW, Volkman JK, Dunstan GA (1997) Nutritional properties of microalgae for mariculture. Aquaculture 151:315–331
7. Canela APRF, Rosa PTV, Marques MOM, Meireles MAA (2002) Supercritical fluid extraction of fatty acids and carotenoids from the microalgae *Spirulina maxima*. Ind Eng Chem Res 41:3012–3018
8. Casey GP, Ingledew WM (1986) Ethanol tolerance in yeasts. Crit rev microbiol 13:219–280
9. Chen M, Zhao J, Xia L (2009) Comparison of four different chemical pretreatments of corn stover for enhancing enzymatic digestibility. Biomass Bioenerg 33:1381–1385
10. Cheung P (1999) Temperature and pressure effects on supercritical carbon dioxide extraction of n-3 fatty acids from red seaweed. Food Chem 65:399–403
11. Chisti Y (2007) Research review paper: biodiesel from microalgae. Biotechnol Adv 25:294–306
12. Chisti Y, Moo-Young M (1986) Review: disruption of microbial cells for intracellular products. Enzyme Microb Technol 8:194–204
13. Choi S, Nguyen MT, Sim SJ (2010) Enzymatic pretreatment of *Chlamydomonas reinhardtii* biomass for ethanol production. Bioresour Technol 101:5330–5336
14. Christie WW (2007) Methylation of fatty acids—a beginner's guide. http://www.lipidlibrary.co.uk/topics/methests/index.htm. Accessed 5 Apr 2009

15. Danquah MK, Gladman B, Moheimani N, Forde GM (2009) Microalgal growth characteristics and subsequent influence on dewatering efficiency. Chem Eng J 151:73–78
16. De Angelis L, Rise P, Giavarini F, Galli C, Bolis CL, Colombo ML (2005) Marine macroalgae analyzed by mass spectrometry are rich sources of polyunsaturated fatty acids. J Mass Spectrom 40:1605–1608
17. Demirbas A (2008) Comparison of transesterification methods for production of biodiesel from vegetable oils and fats. Energ Convers Manage 49:125–130
18. Demirbas A (2009) Biofuels from agricultural biomass. Energ Source Part A, 31:1573–1582
19. Demirbas A, Karslioglu S (2007) Biodiesel production facilities from vegetable oils and animal fats. Energy Sources Part A 29:133–141
20. Dunstan GA, Volkman JK, Barrett SM, Garland CD (1993) Changes in the lipid composition and maximisation of the polyunsaturated fatty acid content of three microalgae grown in mass culture. J appl phycol 5:71–83
21. Dunstan GA, Volkman JK, Jeffrey SW, Barrett SM (1992) Biochemical composition of microalgae from the green algal classes Chlorophyceae and Prasinophyceae. 2. Lipid classes and fatty acids. J Exp Mar Biol Ecol 161:115–134
22. Fajardo AR, Cerdan LE, Medina AR, Fernandez FGA, Moreno PAG, Grima EM (2007) Lipid extraction from the microalga *Phaedactylum tricornutum*. Eur J Lipid Sci Tech 109:120–126
23. Folch J, Ascoli I, Lees M, Meath JA, Lebaron FN (1951) Preparation of lipide extracts from brain tissue. J Biol Chem 191(2):833–841
24. Galbe M, Zacchi G (2007) Pretreatment of lignocellulosic materials for efficient bioethanol production. Adv Biochem Eng Biotechnol 108:41–65
25. Garcia Sanchez R, Karhumaa K, Fonseca C (2010) Improved xylose and arabinose utilization by an industrial recombinant *Saccharomyces cerevisiae* strain using evolutionary engineering. Biotechnol Biofuels 3:13
26. Guckert JB, Cooksey KE, Jackson LL (1988) Lipid solvent systems are not equivalent for analysis of lipid classes in the microeukaryotic green alga, *Chlorella*. J Microbiol Methods 8:139–149
27. Harun R, Singh M, Forde GM (2010) Bioprocess engineering of microalgae to produce a variety of consumer products. Renew Sustain Energy Rev 14:1037–1047
28. Herrero M, Cifuentes A, Ibanez E (2006) Sub- and supercritical fluid extraction of functional ingredients from different natural sources: plants, food-by-products, algae and microalgae, a review. Food Chem 98:136–148
29. Hu G, Heitmann JA, Rojas OJ (2008) Feedstock pre-treatment strategies for ethanol from wood, bark and forest residues. Bioresour Technol 3:270–294
30. Kates M (1986) Definition and classification of lipids. In: Bordon RH, Knippenberg PH (eds) Techniques of lipidology: isolation, analysis, and identification of lipids. Elsevier, Amsterdam
31. Lang X, Dalai AK, Bakhshi NN, Reaney MJ, Hertz PB (2001) Preparation and characterization of bio-diesels from various bio-oils. Bioresour Technol 80:53–62
32. Lee JY, Yoo C, Jun SY, Ahn CY, Oh HM (2010) Comparison of several methods for effective lipid extraction from microalgae. Bioresour Technol 101:S75–S77
33. Lee SJ, Yoon BD, Oh HM (1998) Rapid method for the determination of lipid from the green algae *Botryococcus braunii*. Biotechnol Tech 7:553–556
34. Lin Y, Tanaka S (2006) Ethanol fermentation from biomass resources: current state and prospects. Appl Microbiol Biotechnol 69:627–642
35. Luque de Castro MD, Garcia-Ayuso LE (1998) Soxhlet extraction of solid materials: an outdated technique with a promising innovative future. Anal Chim Acta 369:1–10
36. Lynd LR (1996) Overview and evaluation of fuel ethanol from cellulosic biomass: technology, economics, the environment, and policy. Annu Rev Energ Environ 21:403–465
37. Macias-Sanchez MD, Mantell C, Rodriguez M, de la Ossa EM, Lubian LM, Montero O (2007) Supercritical fluid extraction of carotenoids and chlorophyll a from *Synechococcus* sp. J Supercrit Fluid 39:323–329
38. Madigan MT, Martinko JM, Parker J (2000) Nutrition and metabolism. In: Madigan MT, Martinko JM, Parker J (eds) Brock biology of microbiology. Prentice-Hall, New Jersey

39. Medina AR, Grima EM, Gimenez AG, Ibanez MJ (1998) Downstream processing of algal polyunsaturated fatty acids. Biotechnol Adv 16(3):517–580
40. Mendes RL, Coelho JP, Fernandes HL, Marrucho IJ, Cabral JM, Novais JM, Palavra AF (1995) Applications of supercritical CO_2 extraction to microalgae and plants. J Chem Technol Biotechnol 62:53–59
41. Mendes RL, Nobre BP, Cardoso MT, Pereira AP, Palavra AF (2003) Supercritical carbon dioxide extraction of compounds with pharmaceutical importance from microalgae. Inorg Chim Acta 357:328–334
42. Mendes RL, Reis AD, Palavra AF (2006) Supercritical CO_2 extraction of gamma-linolenic acid and other lipids from *Arthrospira* (*Spirulina*) *maxima*: comparison with organic solvent extraction. Food Chem 99:57–63
43. Mendes-Pinto MM, Raposo MFJ, Bowen J, Young AJ, Morais R (2001) Evaluation of different cell disruption processes on encysted cells of *Haematococcus pluvialis*: effects of astaxanthin recovery and implications for bio-availability. J appl phycol 13:19–24
44. Moen E (2008) Biological degradation of brown seaweeds. The potential of marine biomass for anaerobic biogas production. Scottish Association for Marine Science, Oban, Scotland
45. Molina Grima E, Belarbi E-H, Acien Fernandez FG, Robles Medina A, Chisti Y (2003) Recovery of microalgal biomass and metabolites: process options and economics. Biotechnol Adv 20:491–515
46. Nagle N, Lemke P (1990) Production of methyl ester fuel from microalgae. Appl Biochem Biotechnol 24:355–361
47. Nguyen MT, Choi SP, Lee J, Lee JH, Sim SJ (2009) Hydrothermal acid pretreatment of *Chlamydomonas reinhardtii* biomass for ethanol production. J Microbiol Biotechnol 19(2):161
48. Ota M, Kato Y, Watanabe H, Watanabe M, Sato Y, Smith R, Inomata H (2009) Fatty acid production from a highly CO_2 tolerant alga, *Chlorocuccum littorale*, in the presence of inorganic carbon and nitrate. Bioresour Technol 100:5237–5242
49. Pimentel D, Patzek TW (2008) Ethanol production: energy and economic issues related to U.S. and Brazilian sugarcane. In: Pimentel D (ed) Biofuels, solar, wind as renewable energy systems. Springer, Netherlands, pp 357–371
50. Pourmortazavi SM, Hajimirsadeghi SS (2007) Supercritical fluid extraction in plant essential and volatile oil analysis—review. J Chromatogr A 1163:2–24
51. Ramadan MF, Asker MHS, Ibrahim ZK (2008) Functional bioactive compounds and biological activities of *Spirulina platensis* lipids. Czech J Food Sci 26(3):211–222
52. Saha BC, Iten LB, Cotta MA, Wu YV (2005) Dilute acid pretreatment, enzymatic saccharification and fermentation of wheat straw to ethanol. Proc Biochem 40:3693–3700
53. Sajilata MG, Singhal RS, Kamat MY (2008) Supercritical CO_2 extraction of γ-linolenic acid (GLA) from *Spirulina platensis* ARM 740 using response surface methodology. J Food Eng 84:321–326
54. Schenk P, Thomas-Hall S, Stephens E (2008) Second generation biofuels: high efficiency microalgae for biodiesel production. BioEnerg Res 1:20–43
55. Schwartzberg HG (1997) Mass transfer in a countercurrent, supercritical extraction system for solutes in moist solids. Chem Eng Commun 157:1–22
56. Sheehan J, Dunahay T, Benemann J, Roessler P (1998) A look back at the US Department of Energy's Aquatic Species Program – biodiesel from algae. In: Close-Out Report by National Renewable Energy Laboratory, Golden, Colorado. Report no.: NREL/TP-580-24190. http://www.nrel.gov/docs/legosti/fy98/24190.pdf. Accessed 10 April 2009
57. Shenk P, Thomas-Hall S, Stephens E, Marx U, Mussgnug J, Posten C (2008) Second generation biofuels: high-efficiency microalgae for biodiesel production. BioEnerg Res 1(1):20–43
58. Sun Y, Cheng J (2002) Hydrolysis of lignocellulosic materials for ethanol production: a review. Bioresour Technol 83:1–11
59. Taylor LT (1996) Supercritical fluid extraction. Wiley, New York
60. Usov AI, Smirnova GP, Klochkova NG (2001) Polysaccharides of algae: 55 polysaccharide composition of several brown algae from Kamchatka Russian. J Bioorgan Chem 27:395–399
61. Volkman JK, Jeffrey SW, Nichols PD, Rogers GI, Garland CD (1989) Fatty acid and lipid composition of 10 species of microalgae used in mariculture. J Exp Mar Biol Ecol 128:219–240

62. Wang L, Weller CL (2006) Recent advances in extraction of nutraceuticals from plants. Trends Food Sci Tech 17:300–312
63. Wayman M (1969) Cellulases and their applications. American Chemical Society, Washington, DC
64. Widjaja A, Chien C-C, Ju Y-H (2009) Study of increasing lipid production from fresh water microalgae *Chlorella vulgaris*. J Taiwan Inst Chem Eng 40(1):13–20
65. Zhang X, Shen Y, Shi W (2010) Ethanolic cofermentation with glucose and xylose by the recombinant industrial strain *Saccharomyces cerevisiae* NAN-127 and the effect of furfural on xylitol production. Bioresour Technol 101:7104–7110
66. Zhu JY, Pan XJ (2010) Woody biomass pretreatment for cellulosic ethanol production: technology and energy consumption evaluation. Bioresour Technol 101(13):4992–5002

Chapter 26
Closed Bioreactors as Tools for Microalgae Production

Robert Dillschneider and Clemens Posten

Abstract A variety of high value products have so far been produced with algae and the transition to algae mass cultures for the energy market currently arouses the interest of research and industry. The key to efficient cultivation of microalgae is the optimization of photobioreactors that does not only allow for efficient light capture but also takes account of the specific physiological requirements of microalgae. Three fundamental reactor designs (bubble columns, flat plate reactors, and tubular reactors) are common and are discussed together with some elaborate derivatives in the following. Every concept excels with specific advantages in terms of light distribution, fluid dynamics, avoidance of gradients, and utilization of the intermittent light effect. However, the integration of all beneficial characteristics and simultaneously the compliance with energetic and economic constraints still imposes demanding challenges on engineering.

1 Products from Microalgae

A wide range of valuable substances have so far been produced with microalgae. Commercial applications partially aim at high value products, e.g., carotenoids or poly-unsaturated fatty acids (PFUAs) for the pharmaceutical and cosmetics industries. Microalgae biomass, rich in unsaturated fatty acids, is also a valuable source for food supplements and suitable for feed in aquacultures. Recent efforts explore the production of fine chemicals and energetic utilization of microalgae biomass and their products, e.g., biodiesel, ethanol, biogas, and hydrogen.

R. Dillschneider • C. Posten (✉)
Institute of Life Science Engineering, Division III: Bioprocess Engineering,
Fritz-Haber-Weg 2, 76131 Karlsruhe, Germany
e-mail: clemens.posten@kit.edu

J.W. Lee (ed.), *Advanced Biofuels and Bioproducts*, DOI 10.1007/978-1-4614-3348-4_26,

One of the most persuasive benefits for the energetic utilization of microalgae is their capability of efficiently converting incident solar radiation to biomass. In terms of efficiency phototrophic organisms and also entire cultivation systems can be evaluated by their photoconversion efficiency (PCE). This value represents the percentage of incident solar radiation which is ultimately stored as chemical energy of the biomass. In theory, microalgae can attain PCE values of 12.6% [51]. However, in practice a PCE value of only 5% is achievable [30]. The difference can be traced to physiological and physical causes. With regard to physiology, high oxygen concentrations induce respiration and therewith loss of biomass. Moreover, excess incident light energy is dissipated as fluorescence and heat. Physical causes comprise, amongst others, mutual shading of cells and reflectance of radiation at the surface of reactors. However, photobioreactor improvement aims at optimizing conditions, such as gas concentrations and illumination in order to minimize losses and to approach a generally assumed technical upper limit of 9% PCE [26, 30]. In temperate climates, PCE values for terrestrial plants are reported to be in the range of or even below 1% [6, 29].

For each individual application and valorization of products a certain price limit for the biomass is given and fundamentally influences the process design itself. Prices for pharmaceutical products are certainly higher than for biodiesel and therefore justify expensive processes. In this case, energy balances and process costs are not crucial for the overall profitability. In the aquaculture sector, production costs of dry microalgae biomass range from 50 to 150 US$/kg. Maximal values were even specified to reach 1,000 US$/kg [32]. Prices for biomass targeting the animal feed market need to decline to less than 10€ (circa 13 US$). Production cost for biomass targeting the energy market need to be even below these values [35].

Cultivation of microalgae for the energy market imposes challenging restraints for bioreactor design. Even though prices on the energy market are expected to continually increase in the next years and even decades, the continuing exploitation of fossil resources confines the upper price limit for alternative and sustainable energy sources. Gross margins earned with low-price products, such as hydrogen or biodiesel, are very small. Learning curve effects in microalgae cultivation and cost reduction of large scale implementation (economies of scale) are not only expected to reduce costs but are also necessary for price-competitive applications [5]. Moreover, an integrated utilization of products serving the energy market and the simultaneous valorization of side-products might be a promising approach to meet the challenge and increase the overall added value.

Nevertheless, price-competitive bioprocesses must be focused on and engineering must aim at providing low-cost bioreactors which attain high productivities. Moreover, a positive net energy balance is crucial for a competitive bioprocess and also fundamentally determines the ecologic benefit of the process. In order to meet both economic and energetic demands, development of novel photobioreactors requires the consideration and permanent assessment of the three indicators productivity, cost, and net energy gain.

1.1 Photobioreactors—General Considerations

The physiological requirements of microalgae determine the basic design of a photobioreactor. Phototrophic microorganisms capture sunlight or artificial light and transform light energy into chemical energy in the form of ATP and reduced NADPH which are essential for carbon fixation. A photobioreactor needs to supply cells with sufficient light and at the same time with enough carbon dioxide to build up carbon hydrates for anabolism and storage purpose. The generation of oxygen is stoichiometrically linked with carbon dioxide consumption. Accordingly, excess oxygen needs to be removed from the system. Furthermore, microalgae need inorganic nutrients and trace elements for growth. The stoichiometric demand of nitrogen and phosphorous, for example, can be deduced from the elemental composition of the microalgae.

In terms of hydrodynamics, a photobioreactor represents a three phase system with the liquid system providing the inorganic nutrients which are dissolved in the broth. The gaseous phase supplies carbon dioxide and excess oxygen is removed from the system via gas bubbles. Eventually, the solid phase consists of cells. A fourth interacting component is the superimposed light radiation field.

The major challenge, and the function of a bioreactor, is to provide favorable conditions which allow for high productivities and avoidance of inhibiting or limiting effects. However, considerable gradients of CO_2 and O_2 can affect growth. Light that impinges on the reactor surface (I_0) is absorbed and scattered and thus not all cells in the reactor receive light with the same intensity. Even local differences in concentrations of inorganic nutrients can occur (Fig. 1). No photobioreactor concept provides optimal mass transfer and light distribution in a manner that the occurrence of gradients is completely avoided.

Improvements of photobioreactor designs mainly focus on three key areas, namely light transfer, reaction (related to aeration), and hydrodynamics. It is not sufficient to address these aspects all separated from each other but there are significant interferences which mainly influence physiology, growth, and productivity in photobioreactors (Fig. 2). Yet in order to reduce complexity, experimental scale-down approaches try to separate interdependent influences to unravel underlying mechanisms influencing productivity [37].

These key aspects and their interdependency are further addressed in the following sections.

1.2 Light Distribution

Light impinges on the reactor surface, is absorbed by cells, scattered and reflected and thus light intensities necessarily decrease with increasing distance from the surface. Consequently, light cannot be provided with equal intensities for all cells

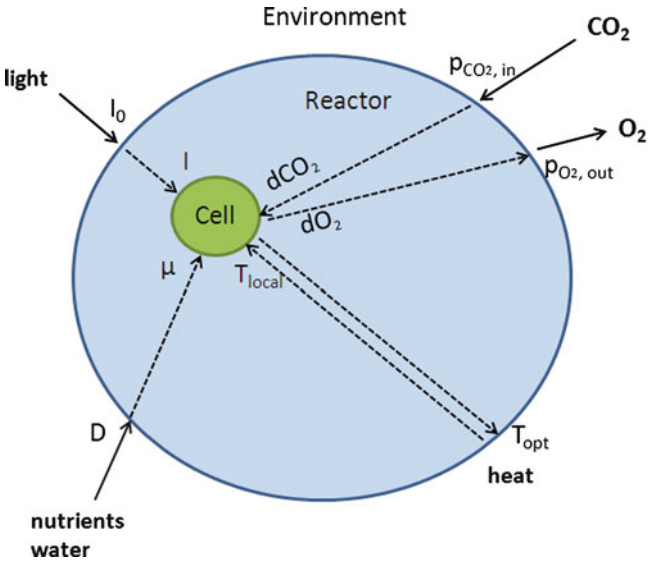

Fig. 1 Inhomogeneities affect behavior of single cells in a reactor. Light, CO_2 and nutrients are required for cell growth. O_2 and excess heat need to be removed from the reactor. Local differences in concentrations cause inhomogeneous conditions for growth. I_0 (I): incident (/local) light intensity; dCO_2 (/dO_2): dissolved CO_2 (/O_2); pCO_2, in (/pO_2, out): partial pressure of CO_2 (/O_2) entering (/leaving) the reactor; Topt (/Tlocal): optimal (/local) Temperature; D dilution rate, μ: specific growth rate

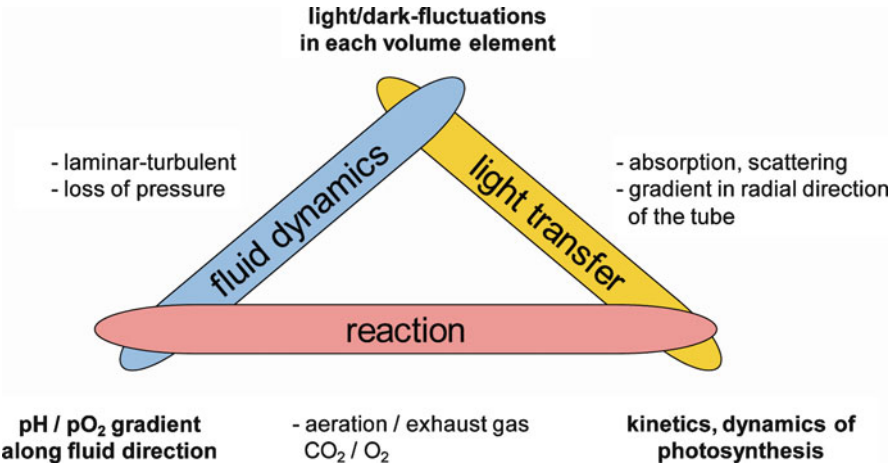

Fig. 2 Interdependency of biochemical reaction, light transfer, and fluid dynamics in a photobioprocess [37]

Table 1 Adjustment of reactor geometries to light utilization

Reactor type	Annular columns	Flat plate reactor	Tubular reactor	Plate reactor
Reactor volume (m^3)	0.12	0.25	7	6
Light path length (cm)	4.5	7	4	3
Illuminated surface area (m^2)	5.3	7.5	600	500
Aperture area (m^2)	1.47 (mutual shading) 1.23 (without shading)	–	110	100
Surface: aperture area ratio (−)	3.61 (mutual shading) 4.31 (without shading)	–	5.45	5.00
Surface: volume ratio (m)	44	30	86	83
Biomass concentration (DW) (g/L)	0.6–1.71	–	5–8	5–8
Productivity (DW) (g/L/day)	0.46	–	0.8–1.2	0.8–1.3
References	[9, 53]	[42]	[33]	[33]

within the reactor at the same time. Furthermore, the incident light intensity is subject to daily and seasonal changes, as well as weather influences. Even increasing cell concentrations strongly alter light distribution in the time course of a single cultivation due to absorption, scattering, and mutual shading.

All photobioreactor concepts apply the same common design principle of a limited light path length (Table 1). Light gradients in the reactor are inevitable. Nevertheless, a plate or tubular thickness that significantly exceeds the light path length, leads to an increased dark volume. This generally impairs the overall productivity because microalgae shift to respiratory metabolism when photosynthesis is stopped. The significance of respiratory losses can be deduced from respiratory maintenance metabolism during night hours. Respiration can cause a biomass loss of up to 25% of biomass produced during the day [11, 23].

Many attempts to simulate growth of algae cultures assume an exponential decline of light intensity with increasing distance from irradiated reactor surface [44]. High cell densities tremendously limit the light path length. Exemplary measurements show that at a cell concentration of 10 g/L (*Arthrospira platensis*), about 95% of incident light ($I_0 = 1{,}925$ µE/m^2/s) is absorbed or scattered along the first 2 mm of the light path [46].

However, high cell concentrations are desirable because downstream processing (DSP) usually requires high energy input, e.g., for centrifugation or spray drying. High cell concentrations increase efficiency of DSP by reducing energy input and cost per biomass yielded. Cell densities of about 5 g/L were reached with *Chlorella* in semicontinuous cultivation experiments in airlift-photobioreactors [12] and maximal dry weight concentrations of *Phaeodactylum tricornutum* cultures under outdoor conditions of around 7–8 g/L were attained in a Flat-Panel-Airlift reactor (Subitec, Germany) [35].

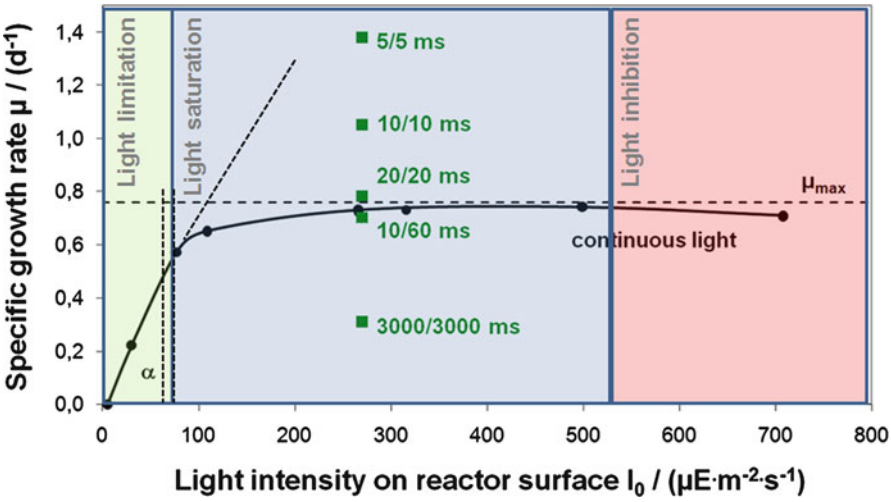

Fig. 3 Effect of light intensities on growth kinetics of *P purpureum* in turbidostat cultivation mode under homogenous light conditions (*filled circle* growth rates resulting from continuous illumination; *filled square* growth rates when cells are exposed to light/dark cycles)

Provided that the light path length exceeds the plate thickness in flat plate reactors, exponential growth of the culture can generally be achieved. Transmitted light is not necessarily "lost" but can be captured by other compartments of the facility, e.g., when parallel reactors are arranged in fence-like structures (Fig. 4). Otherwise, all photons will be absorbed thus leading to linear growth on condition that no substrates become limiting.

The tremendous implication on scale-up is that the rule of geometric similarity on different scales cannot be applied to photobioreactors. Instead, one dimension is more or less fixed. Scale-up is limited to the remaining dimensions.

The assumption that exposure of microalgae cultures to high irradiances necessarily increases productivity would be misleading.

A look at Fig. 3 reveals that growth rates show a linear increase with light intensities only in a very narrow range. As shown here for the model organism, *Porphyridium purpureum* cultures are light limited when light intensities impinging on the reactor surface range up to ca. 100 μE/m²/s. Higher intensities have almost no advantageous effect on growth kinetics since dark reactions in the CO_2 fixing Calvin–Benson cycle become kinetically limiting and therefore the availability of NADP+ and ADP for any further conversion of the H^+ gradient across the thylakoid membrane to NADPH and ATP is restricted. Excess light that is harvested by the algae is dissipated as heat or fluorescence by pigments [51]. Cells are said to be light saturated. Growth rates do not increase linearly when light intensities are raised but rather stay constant over a wide range. Such inefficient utilization of light will necessarily result in low PCE values.

Further increase in light intensities can even damage proteins involved in the photosynthetic apparatus and inhibit cell growth. This phenomenon is called

Fig. 4 Green wall panel in the Negev desert ([4])

light inhibition. It is characterized by reduced growth rates when light intensities are further increased [2].

The reaction of microalgae to various light intensities is affected by adaptation processes over the day cycle and also dependent on the specific strain. The latter should already be taken account of in screening programs for isolation of new strains.

An optimized operating point for photobioreactors lies in a range where light is limiting and saturation is avoided (as indicated by the vertical, dashed lines in Fig. 3). These conditions fundamentally determine photobioreactor geometry.

A high surface to aperture area (or ground area) is attributable to the fact that high midday summer light intensities need to be avoided and thus light is spread over a larger surface area. Otherwise, cultures would be exposed to the high light intensities that lead to saturation or even inhibition. This generally applied concept is referred to as "light dilution." Furthermore, limited light penetration depth confines reactor geometry in one dimension. Consequently, reactors are flat or consist of tubes with small diameters. Finally, a high surface to volume ratio is attributable to the other two demands on geometry.

The Green Wall Panel reactor is one example for light dilution in practice [45]. Vertical reactor compartments of flat panels in fence like arrangements collect light rays at large angles and therewith achieve a dilution effect (Fig. 4). In particular, high areal productivities and efficient light utilization can be obtained since the modules can be placed in relatively short distances (e.g., 1 m high modules, 0.9 m distance [36]) and even light-averted surfaces collect reflected and diffuse light [46].

Table 1 gives an overview of different reactor concepts and their corresponding surface to aperture area ratios.

Although individual reactor and scale-up concepts significantly vary, it becomes clear that all reactors provide high surface areas to collect the incident light (surface:volume ratios of 30–86 are shown) and small depths (3–7 cm) account for limited light path length. Moreover, all reactors dilute light that is collected from a certain area at least by a factor 3.6 (surface:aperture area ratios: 3.61–5.45) in order to avoid excess light intensities.

Midday light intensities of about 1,000 μE/m²/s are not uncommon in Europe in the summer season (2,000 μE/m²/s in equatorial regions) [10, 30]. Therewith, a surface to aperture area ratio of 10 or even more would be reasonable if the specific algal strain reacted similarly to high photon flux densities like *P. purpureum*, as depicted in Fig. 2.

Adjustments for every individual facility to the requirements and characteristics of the specific algae as well as the location, latitude, and climatic conditions need to be considered.

1.3 Fluid Dynamics

Appropriate mixing is the basis for sufficient mass transfer in bioprocesses and simultaneously prevents cell sedimentation. On the reactor scale, homogenous conditions in terms of equal supply with all nutrients and CO_2 is mainly determined by convection while on a cellular scale, mainly turbulent dispersion and diffusion influence mass transfer. Turbulences in the liquid phase reduce diffusion barriers around gas bubbles and therewith enhance not only carbon dioxide supply for photosynthetically active cells but also oxygen removal [23, 34]. Stoichiometric CO_2 demand of microalgae is strain-dependent and influenced by the physiological state as well as product formation (e.g., lipid accumulation) but can be considered to be in the range of 1.65 g/g biomass up to 3 g/g biomass for oil rich algae [26]. Low volumetric productivities of phototrophic cultures together with their related CO_2 demand imply that the intensity of mass transfer is generally less problematic than in heterotrophic bacterial cultures (up to two magnitudes smaller). Nevertheless, significant gradients along the way of gas bubbles through the reactor can occur. This is mainly caused by the fact that the light path length and therewith depth of a reactor is limited (see above). Consequently, scale-up is restricted to extension in the two other dimensions. Reactor geometries are not inherently comparable between different conceptual design approaches. The occurrence of CO_2 and O_2 gradients is particularly significant for reactors with long distances between several aeration and degassing points like in tubular reactors [39].

Therefore, hydrodynamics have to be carefully considered to make sure that high local oxygen concentrations, and thus a shift towards photorespiration, are avoided. For some species, oxygen concentrations higher than 120% air saturation can already cause inhibition. High oxygen concentrations can also cause [30] photooxidative damage when algae cultures are exposed to intense sunlight at the same time [10].

Similarly, a balanced distribution of CO_2 shall ensure that the local CO_2 partial pressure does not drop below 0.1–0.2 kPa in any region of the photobioreactor (Fig. 5) [54].

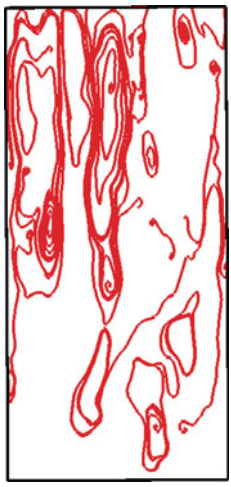

Fig. 5 CFD simulation of a plate bioreactor (height 1 m, width 0.5 m, thickness 0.1 m). The *red lines* indicate trajectories of volume elements, representing the axial dispersion

If partial pressure drops below that level growth kinetics can be limited [15, 49]. Gradients of CO_2 are also related to gradients of pH in the reactor since pH and CO_2 concentration are interconnected by the chemical equilibrium of carbon dioxide, hydrogen carbonate, and carbonate [39]. These coherences are shown in Fig. 2 by the intersection of the key areas, "hydrodynamics" and "reaction."

Mixing times of 100 s (at superficial gas velocities usually below 0.05 m/s) are not unusual for bubble column reactors. Upward liquid movement is induced by aeration; downward movement occurs close to the reactor wall. Axial dispersion coefficients are influenced by the superficial gas velocity and are typically in the range of 0.01–0.02 m^2/s. Radial dispersion coefficients, however, are one to two orders of magnitudes lower than axial dispersion coefficients, yet gain special importance in photobioreactors [8]. With regard to the superimposed light field and considering the fact that photosynthesis occurs especially close to the reactor wall, where enough light is available, an equalized gas distribution at the edge of the column is desirable. In addition, radial dispersion fundamentally determines the residence time of cells in dark and illuminated volume elements. Radial dispersion coefficients (especially in volume elements close to the edge of the reactor) can be increased with higher superficial gas velocities, yet shear stress imposed on the cells and high costs of increased auxiliary energy input considerably limit aeration rates.

The interdependency between "hydrodynamics" and "light distribution" (Fig. 2) is further addressed in the following section.

1.4 Intermittent Light Effect

In addition to the aforementioned efforts to ensure deep penetration of light into the culture, it must be constituted that the presence of dark volume elements in a photobioreactor does not necessarily decrease volumetric productivity of the system. On the contrary, the circulation of algal cells between sufficiently illuminated and

dark volume elements can increase the overall volumetric productivity in reactors at saturating light intensities. This phenomenon is referred to as intermittent (or "flashing") light effect [22]. As long as microalgae are located in illuminated areas, photons are captured and the photosynthetic apparatus generates ATP and NADPH (light reactions). Light reactions stop when cells are located in a dark volume element. Nevertheless, dark reactions, that are driven by ribulose bisphosphate carboxylase (Rubisco) and that are kinetically limiting for the overall CO_2 fixation process, can proceed. The overall productivity can eventually be increased in a reactor if light intensities exceed saturation levels and frequencies of circulation between dark and illuminated volume elements are beneficial for the algae cells.

Experiments with *Dunaliella* have shown that photosynthetic efficiency can be increased in comparison to continuous illumination for light/dark cycles of 5.32 Hz but efficiency is lower under slow cycles of 0.17 Hz [21]. Reasons for reduced efficiency when slow light/dark cycles are prevalent are not clear, yet. One possible reason might be interference with intracellular control loops on the epigenetic level [30]. Cycle frequencies of >1 Hz are recommended for *P. tricornutum* [24]. Optimal cycle frequencies are certainly strain-dependent and also strongly influenced by photon flux densities and spatial distribution of light in the liquid volume.

Usually, favorable light/dark cycle frequencies can be attained when prevalent flow regimes in reactors are turbulent so that sufficient radial mixing along the light path is guaranteed. However, this demand imposes two restrictions. Firstly, some algae species are sensitive to shear stress. Microeddies with dimensions comparable to cell size should be avoided. This restriction can be crucial for scale-up when specific light/dark cycles should be obtained but the high energy input required generates cell damaging flow regimes [25]. Secondly, high levels of auxiliary energy input are usually required to attain light/dark frequencies in a desirable order of magnitude. These energy inputs significantly exceed values necessary for sufficient mass transfer. Especially for energetic utilization of biomass the energy balance requires that energy input is minimal. Energy content of algae can range from 20 to 30 MJ/kg for oil rich algae [30]. Unfortunately, little information is available about the correlation between energy input and frequencies of light/dark cycles in different reactor geometries.

Computational flow dynamics (CFD) simulations can be implemented to estimate radial mixing velocities and therewith residence times in dark or illuminated volume elements. Biomass concentration, pigment composition, and light intensities at the surface of a reactor strongly influence the spatial light distribution and the associated ratio of dark and illuminated volume elements. Exemplary simulations for tubular reactors show that static helical mixers could increase light/dark cycle frequencies in a tubular reactor with a factor higher than 20 compared to plain tubes [27].

2 Closed Photobioreactor Designs

Closed photobioreactors enable axenic cultivation of microalgae, maximal control of culture parameters, e.g., pH and temperature, and prevent water loss due to evaporation, one major drawback of open pond cultivation systems [33].

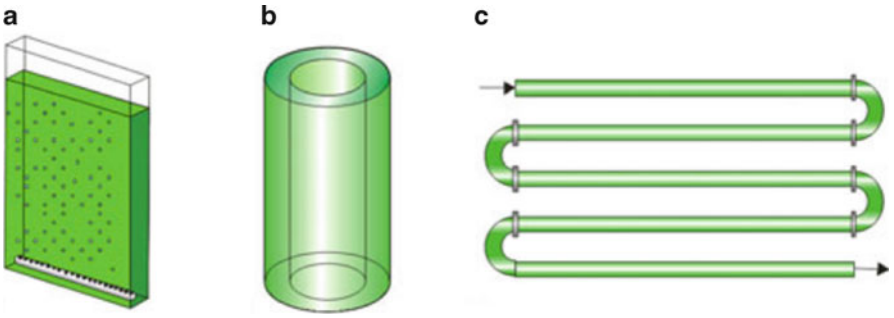

Fig. 6 Basic reactor geometries: (**a**) flat plate reactor; (**b**) bubble column (here represented by an annular column); (**c**) tubular reactor

Table 2 Power input (excluding light) of different reactors in outdoor experiments

Reactor type	Power input (W/m³)	Productivity (g/L/day)	References
Helical tube reactor (outdoor)	3,200	1.4	[18]
Tubular photobioreactor	300	0.3–0.7	[1]
Bubble column (outdoor)	109	0.4 (10 days average)	[41]
Flat panel airlift	100–200	Circa 0.76 (average)	[35]

Their solar light capturing surfaces consist of transparent materials with long shelf lives, e.g., poly(methyl methacrylate) (PMMA) [14, 41], borosilicate glass [28], or simply compartments of plastic film [31].

In general, three basic designs were developed on the basis of the aforementioned considerations. These are bubble columns, flat plate, and tubular reactors (Fig. 6). Mainly implementation of a short light path length and the principle of light dilution determine the fundamental geometries of these reactors.

With regard to economic considerations, investment costs should not exceed 50 US$/m² for biofuel production [30] and operating costs equally need to be minimized. The energy input is one important cost factor and likewise significantly influences the net energy gain. Table 2 gives an overview of power input of several reactors in outdoor experiments.

The main characteristics of three common reactor types are outlined in the following sections. Furthermore, some variants, adapted to the extended demands, such as low cost and high productivity, are shown.

2.1 Bubble Columns

Bubble columns generally consist of cylindrically shaped transparent vessels that are aerated by a gas distributor feeding gas bubbles with limited diameter and thus high gas/liquid exchange area into the system. Aeration does not only supply cultures

with carbon dioxide but also induces liquid movement and dispersion and thus contributes to a more equalized distribution of dissolved gasses and also prevents cells from settling. The superficial gas velocity (typical values between 0.01 and 0.05 m/s (e.g., [53, 9]) affects the radial dispersion coefficient and together with the diameter of gas bubbles determines the interfacial area for mass transfer. In an attempt to improve mass transfer and radial dispersion a system with two different gas distributors was tested. A first gas sparger provides bubbles with a smaller diameter mainly for carbon dioxide supply. The second gas distributor provides bubbles with a larger diameter that induce turbulences for improved radial mixing and increased radial dispersion coefficients. At the same time this system should diminish wall adhesion [16].

With regard to the geometrical structure of a bubble column photobioreactor there are several degrees of freedom. The ratio of length to diameter varies significantly. With regard to scale-up the diameter is limited by the light path length. The length of the column, in contrast, is limited by mass transfer and energetic considerations because a high hydrostatic pressure requires high power input for the aeration system [40]. A scale-up approach, in this case numbering-up, was demonstrated by the placement of several columns in specific distances and taking into consideration that column reactors mutually shade each other depending on the angle of incident light [9, 53].

A second cylinder can be installed in the center of the column to form an annular reactor [9]. Therewith, the dark liquid volume that does not contribute to the overall productivity is reduced. Simultaneously, the thickness of the column is adjusted to the short light path length and the scalability of the diameter is less restricted. Moreover, if the material chosen for the inner cylinder is transparent, this surface can additionally contribute to illumination of cultures. If energy input is not decisive for the economy of a process, additional light sources could be installed to illuminate cultures even from the inside of the annular reactor. However, this approach should not be taken into account for algae cultivation for the energy market.

The airlift principle can be applied to column reactors to improve axial transport. In this case, two interconnected compartments are separated in longitudinal direction. Aeration in just one compartment, the riser, induces and upward flow, while the liquid volume with a lower gas hold up flows down in the downcomer section [41].

Depending on the specific design of the reactor, illumination and dimension of riser and downcomer one should keep in mind that light/dark cycles can be induced. Especially unfavorable slow cycles should be avoided [30].

2.2 Flat Plate Reactors

The special design of flat plate photobioreactors with small distances between their translucent rectangular covers allows for cultivation with small layer thickness in response to the limited light path length (Figs. 4 and 6). Flat plate reactors can be compared with bubble columns with regard to aeration and mixing.

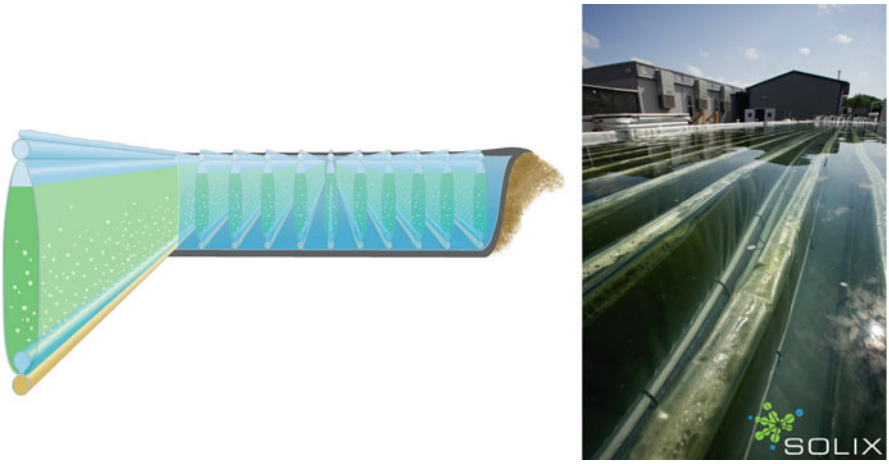

Fig. 7 Solix Biofuels' demonstration facility: schematic representation of the 3G reactor setup and photography of the production facility [43, 48]

Movement of gas bubbles through the reactor induces mixing mainly along the vertical axis. The main difference is given by the short thickness of flat plate reactors which generally amounts only a few centimeters (e.g., [42]). If biomass concentrations during operation, absorbance and incident light intensities can be reasonably estimated during the planning process, adjustment to the light path length can widely prevent the occurrence of dark volumes. The relatively simple geometry facilitates scale-up tremendously, e.g., when several reactor modules are placed in north–south oriented "fences" (Fig. 4).

Instead of using glass plates, in some applications plastic bags are fixed in a metallic frame (Green Wall Panel [45], see also Fig. 4). The replacement of glass by much cheaper, transparent, disposable plastic bags is particularly interesting for commercial application. In this case, the reaction vessel can be exchanged when fouling or contamination makes a further utilization unfavorable.

The company *Solix Biofuels* (Fort Collins, CO, USA), for example, cultivates algae in submerged flat plastic bags. In principle, the concept can be traced back to the basic design of flat plate reactors. The fundamental setup of the third generation reactor concept (3G) is depicted in Fig. 7. Major advantage of the submerged reaction compartments is the fact that additional temperature control is not necessary in the system because the surrounding water acts as temperature buffer. Moreover, construction costs for the reactor are reduced as there is no need for a special scaffold supporting the flat reaction compartments. The demonstration facility (southwestern Colorado) utilizes wastewater from coal-bed methane production. The innovative gas sparger system is integrated in the seam of the plastic bags and distributes CO_2 enriched gas of a nearby amine plant. Therewith, the concept aims at an integrated environmental-friendly biomass production connected with CO_2 capturing. According to the information given by the official website *Solix* produces 5,000–8,000 gallons of algal oil per acre, per year (circa 42–67 t/ha/a, assuming an

Fig. 8 Submerged flat panels in a *Proviron* photobioreactor [31]. *Left*: Floating reaction compartments in the inside of the reactor contain the algae suspension while the surrounding water serves mainly as temperature buffer and is equally important for the structure. *Right*: Exterior view at the reactor designed for outdoor applications

oil density of 900 kg/m^3) [43]. A fourth generation reactor is currently under development. Investigations on the replacement of the spargers by an integrated membrane aeration system are undertaken by the company [7, 47, 48].

Another commercially applied advancement of classic flat plate reactors was realized by *Proviron* (Hemiksem, Belgium) (Fig. 8). Their major focus was set on development of an efficient low-cost reactor suitable for large-scale outdoor applications. Their approach comprises the incorporation of flat growth compartments (less than 1 cm thick) within water-filled plastic bags without any rigid structure. The major part of the setup is represented by water-filled chambers that are separated from reaction compartments. Water diffuses the impinging solar radiation, which should result in an equalized light distribution within the water-filled chamber. At the same time, temperature is regulated without any additional energy input. Moreover, the water-filled chambers themselves constitute the scaffold of the reactor. In the future, the low auxiliary energy demand of 20 kW/ha should be further reduced with control strategies that aim at adaption of aeration to light. According to the company's outlook investment cost is expected to drop from currently 200,000€/ha to 100,000€/ha [31].

A straightforward approach to improve flat plate reactor productivity and enforce beneficial light/dark cycles was implemented in the flat-panel-airlift reactor [14], a concept that was further improved for large-scale outdoor applications by the company *Subitec* (Fig. 9). This reactor works according to the airlift principle. Compressed air is injected in the riser which induces an upward flow of liquid. Specific flow regimes are induced by the elaborate arrangement of interconnected chambers that are separated by baffles alternatively located at the front- and backside of the reactor. Therewith radial mixing is substantially improved and cells circulate between darker and more illuminated regions of the reactor. The specific design with indentations (acting as baffles) provides additional surfaces for light capturing and certainly contributes to light availability within the culture. After reaching the top of the flat plate reactor, the liquid volume descends in a downcomer with small diameter, so that the culture circulates repeatedly through the compartments.

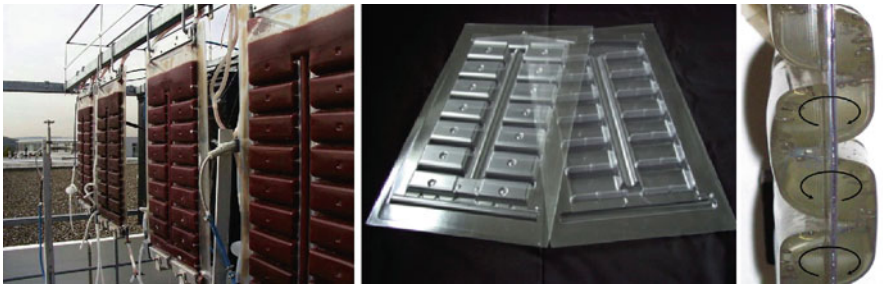

Fig. 9 Flat panel airlift reactor developed by *Subitec* (Stuttgart, Germany). *Left*: Outdoor cultivation with the flat panel airlift reactor. *Middle*: Forefront and backside of the reactor with characteristic slots and baffles. *Right*: Circular liquid flow through illuminated and dark zones is induced by the specific design with static mixers

According to information given by the company, the energy input ranges in between 100 and 200 W/m^3. Total energy consumed in the process referred to biomass produced is specified to be below 20 MJ/kg dry mass and thus below the average energy content of algae biomass (see above). Efforts are undertaken to further decrease this value [35].

To sum up, the flat-panel-airlift reactor concept integrates three beneficial characteristics: a short light path length, efficient mixing, and utilization of the intermittent light effect.

2.3 Tubular Reactors

The straight, looped or coiled transparent glass or plastic tubes of tubular reactors are usually arranged in horizontal or vertical arrays [18, 28]. Liquid flow is induced by pumping of the liquid volume or by airlift circulators [24].

Scale-up by increasing the tube diameter is limited with respect to light penetration depth into the culture. However, light is focused in radial direction to the center of the tube. This effect partially compensates for exponential decrease in light intensity due to absorption which is described by Lambert–Beer's law. Diameters in the range of 3–6 cm are common [18, 24]. The occurrence of dark volumes in the center of the reactor does not necessarily lower productivity. Induction of favorable light/dark cycles can be achieved by high liquid velocities or installation of static mixers and thus increase volumetric productivity [27]. Molina et al. suggested identical light/dark cycle frequencies on different scales as a suitable scale-up criterion for achieving similar productivities [24].

Since scale-up potential with regard to tube diameter is restricted, tube lengths are increased and modular units are multiplied, e.g., mounted on vertical scaffolds (Fig. 10).

Gas exchange is crucial for this type of reactor. Aeration and oxygen removal usually take place in specific gassing and degassing compartments, whereas gassing

Fig. 10 Tubular photobioreactor in Klötze, Germany (meanwhile belonging to the *Roquette group*)

at several points along a tubular track is a conceivable option. The flow regime within the tubes can be regarded as plug flow regime with minimal backward and forward mixing. Therefore, considerable spatial gradients of oxygen and CO_2 along tubular axis occur and gain importance with increasing lengths of tubes. Limited availability of carbon dioxide limits cell growth at some point. One should also keep in mind that pH gradients are concurrent with CO_2 gradients on account of the carbonic acid equilibrium [39]. Oxygen removal is another important aspect since oxygen supersaturation inhibits growth or even causes oxygen-induced cell damage [3]. Therefore, dimensions of the degassing section, length of tubes, liquid flow rates, and mass transfer must be reasonably adjusted in order to avoid detrimental oxygen concentrations and CO_2 limitation as well.

Tubular reactors can attain high productivities, e.g., 1.4 g/L/day in a helical reactor [18] or 1.9 g/L/day in an airlift-driven tubular reactor with flat arrangement of solar collecting tubes [25]. However, power supply for tubular reactors is usually much higher compared to the aforementioned alternative design concepts. Power supply in magnitudes ranging from 800 to 3,200 W/m³ [18, 42] is unfavorable for production of biodiesel and hydrogen. Therefore, tubular reactors should rather be used for cultivation of high value products, e.g., for the pharmaceutical market.

Most prominent commercial application of tubular photobioreactors is probably the biggest indoor tubular reactor, set up by the company *Bisantech* in Klötze, Germany (Fig. 10).

About 500 km of tubes with a total volume of circa 700 m³ are located in a greenhouse where tubes are arranged in vertically oriented scaffolds to attain maximum areal productivity.

The tubes are not all interconnected because gradients resulting from such an arrangement would necessarily lead to inhibiting accumulation of oxygen and simultaneously to carbon dioxide limitation. Before being recirculated through the tubular system, the culture suspension intermittently enters degassers. In the facility, temperature is actively regulated to adjust to optimal culture conditions [30]. The facility's output targets the nourishment market sector with production costs of circa 15€/kg [approximately 20 US$/kg] biomass. Productivities of 100 t/ha are attained under mixotrophic growth conditions (Prof. Steinberg, personal communication).

3 Concepts for Future Reactor Improvement

With regard to the aforementioned restrictions, an increase in PCE of more than a factor two cannot be expected. Process costs need to be drastically reduced by lower investment cost and lower demand for auxiliary energy to target a price range of less than 5 US$/kg biomass.

Aeration with membranes can be one major improvement for future reactor developments [13, 17]. The interfacial area for CO_2 input and O_2 removal from the culture in case of membrane gas exchange is defined by the surface area of the membrane itself and no longer by the surface of gas bubbles. This concept could drastically reduce the overall input of auxiliary energy since there is no longer the need to generate bubbles, and energy loss when bubbles fuse with the top headspace gas phase is avoided. However, gentle agitation will still be required for gas dispersion. A proof of concept is missing in photo-biotechnology but implementation of membrane systems are considered by *Solix Biofuels* [26, 47].

If beneficial light/dark cycles cannot be attained with low inputs of auxiliary energy, laminar flow patterns can be accepted if diffusion paths from gas membranes to all volume elements are small enough to supply all cells with CO_2 solely by diffusion. In this case, additional power input for dispersion could be spared and the overall energy balance tremendously improved. However, this approach requires large surface areas for membranes and a drastic reduction of diffusion path length and thus simultaneously light path length. Such a short light path length could, by contrast, allow for high cell concentrations which is favorable for DSP. This approach also lacks a proof of concept.

Future development will show if membrane gassing will be established on a large scale.

With regard to the current high demand of auxiliary energy for photobioreactors, reduction of the height of reactors could significantly contribute to increased energy efficiency. "Low ceiling" concepts aim at reducing the hydrostatic pressure and therewith the energy demand for aeration systems. Additional improvements in control engineering can certainly facilitate further energy saving in the future. Requirements of carbon dioxide and therewith removal of oxygen is dependent on cell concentration and on light availability in the culture. Therewith, carbon dioxide

supply and energy input for mixing should be adjusted to photosynthetic activity, photon flux-density respectively, and cell concentration. Proviron, for example, claims that the auxiliary energy input can be halved in the future by adapting aeration to light availability [31].

Infrared radiation is not photosynthetically convertible into chemical energy but contributes to heating of algae culture. Infrared reflecting materials or coatings could additionally improve the overall energy balance by reducing the energy required for cooling. Transparent materials with selective transmittance are available and were developed for the installation in buildings, cars, and greenhouses [19, 38, 50].

A different approach to the difficulty of light capturing and distribution aims at harvesting the light in a module that is spatially separated from the reactor itself. The Green Solar Collector [52] harvests light by moving lenses whose orientation is guided by a computer that calculates position and altitude of the sun in order to capture maximum amount of photons. The light is then focused and transported via plastic light guides where light is totally reflected. A change in refraction index releases the photons in the microalgae suspension. It is suggested that light redistributing plates are integrated in small distances from each other in airlift-photobioreactors. According to the authors biomass concentrations of up to 20 g/L could be maintained in such a setting with good light distribution and induction of beneficial high frequency light/dark cycles [20].

Spatially separated light harvesting and reactor modules can have beneficial advantages because parameters like temperature can be controlled more easily. Furthermore, influences of unfavorable weather conditions, such as hail, will be confined only to the light collector. That will positively influence maintenance costs.

Spatial separation of light harvest and cultivation differs from all other concepts presented here, but the basic principles of other reactor designs can also be retrieved here. In order to optimize light utilization and productivity, light path length is also limited in this reactor, as the reactor contains flat panel compartments with short light path lengths. Moreover, turbulent flow patterns, induced by aeration, ensure rapid circulation of microalgae between dark zones and illuminated volume elements in order to benefit from the intermittent light effect [20].

4 Conclusion

Many efforts in the field of photo-biotechnology have not brought out the “perfect” photobioreactor, yet. All basic concepts show specific advantages and disadvantages that finally lead to the development of more sophisticated reactors. These should be characterized by outstanding light utilization and mass transfer, yet be operated with minimum energy input. Moreover, diverse algae strains show different behavior in terms of light saturation, robustness towards shear stress, and other culture conditions. Therefore, benefits and drawbacks of different reactor concepts should be taken into account in terms of producing biomass or energy rich products

for the energy market. At the same time, adjustment of the particular system to the specific algae strain will be unavoidable. Nevertheless, high productivities and photoconversion efficiencies give rise to high expectations in this field of research.

References

1. Acién FG, Fernández JM, Magán JJ, Molina E (2012) Production cost of a real microalgae production plant and strategies to reduce it, Biotechnology Advances, ISSN 0734–9750, 10.1016/j.biotechadv.2012.02.055. http://www.sciencedirect.com/science/article/pii/S0734975012000420. Accessed 14 Feb 2012
2. Aro E-M, Virgin I, Andersson B (1993) Photoinhibition of Photosystem II. Inactivation, protein damage and turnover. Biochim Biophys Acta 1143(2):113–134
3. Babcock RW, Malda J, Radway JC (2002) Hydrodynamics and mass transfer in a tubular airlift photobioreactor. J Appl Phycol 14(3):169–184
4. Ben-Gurion University of the Negev—Microalgal Biotechnology Laboratory—facilities. http://bidr.bgu.ac.il/BIDR/research/algal/slide12.htm. Accessed 15 Aug 2010
5. Borowitzka M (1997) Microalgae for aquaculture: opportunities and constraints. J Appl Phycol 9(5):393–401
6. Boyer JS (1982) Plant productivity and environment. Science 218(4571):443–448
7. Buehner M, Young P, Willson B et al (2009) Microalgae growth modeling and control for a vertical flat panel photobioreactor. In: American control conference, vol 1–9. IEEE Press, Piscataway, NJ
8. Camacho Rubio F et al (2004) Mixing in bubble columns: a new approach for characterizing dispersion coefficients. Chem Eng Sci 59(20):4369–4376
9. Chini Zittelli G et al (2006) Productivity and photosynthetic efficiency of outdoor cultures of *Tetraselmis suecica* in annular columns. Aquaculture 261(3):932–943
10. Chisti Y (2008) Biodiesel from microalgae beats bioethanol. Trends Biotechnol 26(3):126–131
11. Chisti Y (2007) Biodiesel from microalgae. Biotechnol Adv 25(3):294–306
12. Chiu S et al (2009) The air-lift photobioreactors with flow patterning for high-density cultures of microalgae and carbon dioxide removal. Eng Life Sci 9(3):254–260
13. Cogne G, Cornet JF, Gros JB (2005) Design, operation, and modeling of a membrane photobioreactor to study the growth of the cyanobacterium *Arthrospira platensis* in space conditions. Biotechnol Prog 21(3):741–750
14. Degen J et al (2001) A novel airlift photobioreactor with baffles for improved light utilization through the flashing light effect. J Biotechnol 92(2):89–94
15. Doucha J, Straka F, Livansky K (2005) Utilization of flue gas for cultivation of microalgae (Chlorella sp.) in an outdoor open thin-layer photobioreactor. J Appl Phycol 17(5):403–412
16. Eriksen N, Poulsen B, Lønsmann Iversen J (1998) Dual sparging laboratory-scale photobioreactor for continuous production of microalgae. J Appl Phycol 10(4):377–382
17. Fan L-H et al (2008) Evaluation of a membrane-sparged helical tubular photobioreactor for carbon dioxide biofixation by *Chlorella vulgaris*. J Membr Sci 325(1):336–345
18. Hall DO et al (2003) Outdoor helical tubular photobioreactors for microalgal production: modeling of fluid-dynamics and mass transfer and assessment of biomass productivity. Biotechnol Bioeng 82(1):62–73
19. Holland L, Siddall G (1958) Heat-reflecting windows using gold and bismuth oxide films. Br J Appl Phys 9(9):359
20. Janssen M et al (2003) Enclosed outdoor photobioreactors: light regime, photosynthetic efficiency, scale-up, and future prospects. Biotechnol Bioeng 81(2):193–210
21. Janssen M et al (2001) Photosynthetic efficiency of *Dunaliella tertiolecta* under short light/dark cycles. Enzyme Microb Technol 29(4–5):298–305

22. Kok B (1956) Photosynthesis in flashing light. Biochim Biophys Acta 21(2):245–258
23. Kunjapur AM, Eldridge RB (2010) Photobioreactor design for commercial biofuel production from microalgae. Ind Eng Chem Res 49(8):3516–3526
24. Molina E et al (2000) Scale-up of tubular photobioreactors. J Appl Phycol 12(3):355–368
25. Molina E et al (2001) Tubular photobioreactor design for algal cultures. J Biotechnol 92(2):113–131
26. Morweiser M et al (2010) Developments and perspectives of photobioreactors for biofuel production. Appl Microbiol Biotechnol 87(4):1291–1301
27. Perner-Nochta I, Posten C (2007) Simulations of light intensity variation in photobioreactors. J Biotechnol 131(3):276–285
28. Perner-Nochta I, Lucumi A, Posten C (2007) Photoautotrophic cell and tissue culture in a tubular photobioreactor. Eng Life Sci 7(2):127–135
29. Posten C, Schaub G (2009) Microalgae and terrestrial biomass as source for fuels–a process view. J Biotechnol 142(1):64–69
30. Posten C (2009) Design principles of photo-bioreactors for cultivation of microalgae. Eng Life Sci 9(3):165–177
31. Proviron (2009) http://www.proviron.com/algae/GB/. Accessed 20 July 2010
32. Pulz O, Gross W (2004) Valuable products from biotechnology of microalgae. Appl Microbiol Biotechnol 65(6):635–648
33. Pulz O (2001) Photobioreactors: production systems for phototrophic microorganisms. Appl Microbiol Biotechnol 57(3):287–293
34. Richmond A (2004) Principles for attaining maximal microalgal productivity in photobioreactors: an overview. Hydrobiologia 512(1):33–37
35. Ripplinger P (2009) Industrial production of microalgal biomass with a Flat-Panel-Airlift-Bioreactor. Biotechnology Colloquium, Köthen
36. Rodolfi L et al (2009) Microalgae for oil: strain selection, induction of lipid synthesis and outdoor mass cultivation in a low-cost photobioreactor. Biotechnol Bioeng 102(1):100–112
37. Rosello Sastre R et al (2007) Scale-down of microalgae cultivations in tubular photo-bioreactors–a conceptual approach. J Biotechnol 132(2):127–133
38. Rosenberger S, Olbers G, Heinz D (2008) Infrared-reflective material comprising interference pigments having higher transmission in the visible region than in the NIR region. United States Patent 7410685
39. Rubio FC et al (1999) Prediction of dissolved oxygen and carbon dioxide concentration profiles in tubular photobioreactors for microalgal culture. Biotechnol Bioeng 62(1):71–86
40. Sánchez Mirón A et al (1999) Comparative evaluation of compact photobioreactors for large-scale monoculture of microalgae. J Biotechnol 70(1–3):249–270
41. Sánchez Mirón A et al (2002) Growth and biochemical characterization of microalgal biomass produced in bubble column and airlift photobioreactors: studies in fed-batch culture. Enzyme Microb Technol 31(7):1015–1023
42. Sierra E et al (2008) Characterization of a flat plate photobioreactor for the production of microalgae. Chem Eng J 138(1–3):136–147
43. Solix Biofuels (2010) http://www.solixbiofuels.com/. Accessed 20 July 2010
44. Sukenik A et al (1991) Optimizing algal biomass production in an outdoor pond: a simulation model. J Appl Phycol 3(3):191–201
45. Tredici MR, Rodolfi L (2004) Reactor for industrial culture of photosynthetic micro-organisms. Patent WO 2004/074423 A2 (to Universita `degli Studi di Firenze)
46. Tredici MR (2010) Photobiology of microalgae mass cultures: understanding the tools for the next green revolution. Biofuels 1:143–162
47. Willson B (2009) Low-cost photobioreactors for production of algae-biofuels. In: GTOBiofuels: science and innovation for sustainable development conference, San Francisco, CA
48. Willson B (2010) Got impact? Cross-disciplinary partnerships for large-scale global change. In: EWB-USA international conference

49. Yang Y, Gao K (2003) Effects of CO2 concentrations on the freshwater microalgae, *Chlamydomonas reinhardtii*, *Chlorella pyrenoidosa* and *Scenedesmus obliquus* (Chlorophyta). J Appl Phycol 15(5):379–389
50. Yatabe T, Nishihara T, Suzuki N (1987) Optical laminar structure. United States Patent 4639069
51. Zhu X-G, Long SP, Ort DR (2008) What is the maximum efficiency with which photosynthesis can convert solar energy into biomass? Curr Opin Biotechnol 19(2):153–159
52. Zijffers J-W et al (2008) Design process of an area-efficient photobioreactor. Marine Biotechnol 10(4):404–415
53. Zittelli GC, Rodolfi L, Tredici MR (2003) Mass cultivation of Nannochloropsis sp. in annular reactors. J Appl Phycol 15(2):107–114
54. Jacobi A, Ivanova D, Posten C (2010) Photobioreactors: Hydrodynamics and mass transfer in Computer Applications in Biotechnology (CAB). Leuven: IFAC. 162–167

Chapter 27
Alternative Methods for the Extraction of Hydrocarbons from *Botryococcus braunii*

Chiara Samorì and Cristian Torri

Abstract Lipid extraction is a critical step in the development of biofuels from microalgae. The use of toxic and polluting organic solvents should be reduced and the sustainability of the extraction procedures improved in order to develop an industrial extraction procedure. This could be done by reducing solvent amounts, avoiding use of harmful solvents, or eliminating the solvent at all. Here we describe two new processes to extract hydrocarbons from dried and water-suspended samples of the microalga *Botryococcus braunii*. The *first* one is a solvent-based procedure with switchable polarity solvents (SPS), a special class of green solvents easily convertible from a non-ionic form, with a high affinity towards non-polar compounds as *B. braunii* hydrocarbons, into an ionic salt after the addition of CO_2, useful to recover hydrocarbons. The two SPS chosen for the study, based on equimolar mixtures of 1,8-diazabicyclo-[5.4.0]-undec-7-ene (DBU) and an alcohol (DBU/octanol and DBU/ethanol), were tested for the extraction efficiency of lipids from freeze-dried *B. braunii* samples and compared with volatile organic solvents extraction. The DBU/octanol system was further evaluated for the extraction of hydrocarbons directly from algal culture samples. DBU/octanol exhibited the highest yields of extracted hydrocarbons from both freeze-dried and liquid algal samples (16 and 8.2%, respectively, against 7.8 and 5.6% with traditional organic solvents). The *second* procedure here proposed is the thermochemical conversion of algal biomass by using pyrolysis; this process allowed to obtain three valuable fractions, exploitable for energy purpose, fuel production, and soil carbon storage: a volatile fraction (37% on dry biomass weight), a solid fraction called biochar (38%) and, above all, a liquid fraction named bio-oil (25%), almost entirely composed by hydrocarbon-like material, thus directly usable as fuel.

C. Samorì (✉) • C. Torri
Interdepartmental Research Centre for Environmental Sciences (CIRSA),
University of Bologna, via S. Alberto 163, 48123 Ravenna, Italy
e-mail: chiara.samori3@unibo.it; cristian.torri@unibo.it

J.W. Lee (ed.), *Advanced Biofuels and Bioproducts*, DOI 10.1007/978-1-4614-3348-4_27,

1 Introduction

The need to replace fossil fuels with fuels derived from renewable biomass is currently focused on biodiesel from oleaginous plant seeds and ethanol from sugarcane/corn; however, this first-generation biofuels, primarily produced from food crops and mostly oil seeds, are limited in their ability to achieve targets for biofuel production, climate change mitigation, and economic growth; moreover, the recent dramatic increase of food stocks prices has become a worldwide emergency. Because of these environmental and social concerns, the attention is recently shifting towards the development of next-generation biofuels mainly produced from non-food feedstock [1], by converting for example the highly abundant and widespread non-edible lignocellulosic fraction of plants. A further exploitable source of biofuels relies on the aquatic environment, specifically on micro and macroalgae; lipids, which include acylglycerols and hydrocarbons, represent the most valuable fraction of microalgal biomass as their high energy content per mass unit is similar to conventional fuels. Several oleaginous microalgae (with lipid content exceeding 20% of their dry weight) have been exploited to this purpose [2], and the biodiesel obtained has been claimed to be more convenient than conventional biodiesel from plant seeds [3, 4]. Benefits rising from the utilization of aquatic over terrestrial biomass include: (1) higher sunlight use efficiency (about 5% vs. 1.5% [5]), (2) utilization of marginal areas (e.g. desert and coastal regions), (3) possible coupling with other activities (e.g. wastewater treatment, CO_2 sequestration) [6–9], (4) minor dependence on climatic conditions, (5) availability of a larger number of species, and (6) easier genetic manipulation to modify chemical composition (e.g. lipid content) [10]. However, the industrial development of fuels from microalgae is still hampered by higher overall costs with respect to both fossil fuel and first generation of biofuels counterparts: operating open ponds and bioreactors are expensive and the harvesting of algal biomass is energy costly [11]. For this reason, the net energy balance from microalgae cultivation is still debated [12, 13]. Moreover, besides the cost of growing and collecting microalgae, downstream processes are to be taken into account to evaluate the overall productivity. *Botryococcus braunii* is a freshwater colonial green microalga proposed as a future renewable source of fuels because it is capable of producing high levels of liquid hydrocarbons [14]. There are three main *B. braunii* races, each one synthesizing different types of olefinic hydrocarbons: the A, B, and L races. The A race (Fig. 1) accumulates linear olefins, odd numbered from C_{23} to C_{31}, chiefly C_{27}, C_{29}, and C_{31} dienes or trienes; some studies have revealed that oleic acid is the direct precursor of these specific olefins [15] and that decarboxylation of very long chain fatty acid derivatives, activated by a β-substituent, is the final step which leads to the formation of the terminal unsaturation [16]. The B race produces polyunsaturated triterpenes (botryococcenes), while the L race synthesizes one single tetraterpenoid hydrocarbon named lycopadiene [17, 18]. Both A and B races contain similar amounts of lipids (approximately 30% on a dry weight basis), but with a very different composition: in the A race hydrocarbons, non-polar lipids and polar lipids are, respectively, 25, 60, and 15% of the total lipids,

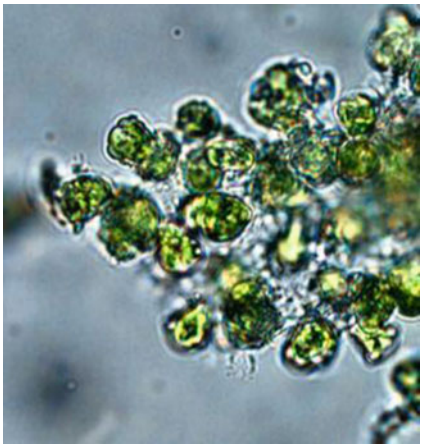

Fig. 1 *Botryococcus braunii*, A race

whereas in the B race the percentages are 71, 9, and 20%, clearly indicating that one quarter of the dried biomass of the B race is composed by hydrocarbons [19].

Specifically for *B. braunii,* the bulk of hydrocarbons is located in external cellular pools and it can be recovered from algal biomass by means of physical process, named cold press and typically used to extract more traditional food oils as olive oil, and by means of chemical process (extraction with solvents) or both [20]. The chemical process, mainly used for the extraction of industrial oils such as soybean and corn oils, is generally based on an extraction with *n*-hexane, to obtain vegetable oil in higher yields and with a faster and less expensive process [21]. However, the existing solvent approach is characterized by several problematic aspects, such as the high solvent/biomass ratio, solvent hazard (including solvent toxicity, volatility, and flammability) and large solvent losses (e.g. in the extraction process of soybean oil, *n*-hexane losses are 1 kg per tonne of beans processed [22]). Because of this general lack of "greenness" in the chemical extractive processes, in the last years different efforts have been made to reduce the use of toxic and polluting organic solvents and to improve the sustainability of the extraction procedures from aquatic and terrestrial biomass, for example by using supercritical fluids [23, 24].

Here we present two novel methods for the extraction of lipids from *B. braunii*, comparing the extraction efficiency of the new processes with those of traditional organic solvents. The *first method* [25] is a solvent-based process, more sustainable than the traditional solvent extraction because it involves the use of switchable polarity solvents (SPS) [26, 27], a "new" class of green solvents, considerable as reversible ionic liquids, with the unique and advantageous feature of having switching solubility behaviour, correlated with reversible polarity. This feature can be successfully exploited in practical applications as extraction procedures or chemical reactions, bypassing the cumbersome need to change solvent in each step of the process itself.

The *second method* is based on the thermochemical conversion of *B. braunii* biomass by using pyrolysis [28], in order to obtain, directly and in one step process, a liquid fraction rich in lipids, a gaseous fraction useful for energy purposes, and a soil-amending co-product called biochar [29].

2 *Botryococcus braunii* Characterization

Microalgae are in general characterized by a high content of three main groups of biomolecules, proteins, polysaccharides, and lipids, according to the species and to the environmental growth conditions. Figure 2 reports the chemical composition of *B. braunii* strain used in the present study [30, 31]; the protein concentration and the polysaccharides content were determined by using the Lowry procedure [32] and the Dubois method [33], respectively; the lipid content was determined by weight after a solvent extraction procedure (*n*-hexane and chloroform/methanol mixture) [34], the ashes were determined by 5 h calcination at 550°C, and the intracellular water amount of the samples was evaluated by Karl-Fischer titration.

Figure 2 shows that *B. braunii* is characterized by a high amount of lipids (29%) and carbohydrates (22%), and a minor but relevant amount of proteins (7%); this composition is typical of this alga in its late growth phase (stationary phase) when the accumulation of lipids becomes much more relevant than cellular duplication.

The amount of ashes (22%) is in line with the typical ash content of microalgae [35].

In addition to hydrocarbons, *B. braunii* also produces classic non-polar lipids as fatty acids, triacylglycerols, sterols, and polar lipids, as polyaldehydes, polyacetals, and non-polysaccharide biopolymers of very high molecular weight [36]. Thus, the oil extracted with *n*-hexane and chloroform/methanol mixture was initially analysed by GC-MS to qualitatively and quantitatively determine free fatty acid (after silylation), triacylglycerol (after transesterification), and hydrocarbon (Tables 1 and 2) contents; then it was fractionated on a chromatographic column, thus separating hydrocarbons, non-polar, and polar lipids (Fig. 3).

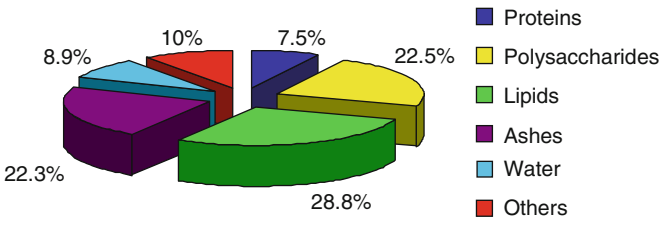

Fig. 2 Chemical composition of *B. braunii* A race after 50 days of growth

Table 1 Free fatty acid and bounded fatty acid yields on a dry weight basis in the lipid extract of *Botryococcus braunii*

Fatty acids	Free fatty acids yield (%)	Bounded fatty acids yield (%)
16:0	0.23±0.1	0.69±0.09
18:2	–	0.17±0.06
18:1	0.16±0.2	1.8±0.1
18:0	0.24±0.04	0.07±0.05
Total	0.64±0.3	2.7±0.3

Table 2 Hydrocarbon yields on a dry weight basis in the lipid extract of *B. braunii*

Hydrocarbons	Yield (%)
$C_{27}H_{52}$	0.65 ± 0.2
$C_{29}H_{56}$	2.8 ± 1
$C_{29}H_{54}$	0.57 ± 0.3
$C_{29}H_{54}$	1.4 ± 0.7
$C_{31}H_{60}$	2.5 ± 1
Total	7.8 ± 3

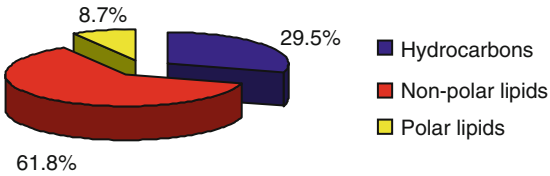

Fig. 3 Composition of *B. braunii* lipids

According to the literature [19], the lipid oil of the A strain of *B. braunii* is mainly composed by non-polar lipids (62%) and hydrocarbons (29%), whereas polar lipids represent only a minor part (9%) of the composition.

By comparing the total amount of hydrocarbons calculated by GC-MS (7.8% on dry weight basis) and the percentage of the first fraction of the lipid oil (8.4% on dry weight basis), it is clear that the first fraction is entirely composed of hydrocarbons. This correspondence is not true in the case of non-polar lipids; the amount of fatty acids calculated by GC-MS (3.3% on dry weight basis) is much lower than the percentage of the second fraction of the lipid oil (17.8% on dry weight basis), indicating that bounded fatty acids and free fatty acids represent only a very small fraction of all the non-polar lipids. As reported in the literature, the main part of the non-polar fraction is in fact composed by a class of high molecular weight ether lipids, not GC-MS detectable [37, 38]. These compounds are closely related to hydrocarbons, differently from what observed among the other vegetable ether lipids mainly based on glycerol (Fig. 4) [14]; the structures identified in the past years include alkadienyl-*O*-alkatrienyl ethers with an oxygen bridge between two C_{27} hydrocarbon chains [37], ether lipids with alkenylresorcinol linked by phenoxy bonds to one or two unsaturated hydrocarbon chains [39], or botryals, α-branched aldehydes originating from aldol condensation [38].

Thanks to their hydrocarbon nature, these non-polar ethers could be processed by cracking to obtain biofuels, analogously to hydrocarbons, increasing the exploitable fraction of *B. braunii* oil for energy and fuel purposes.

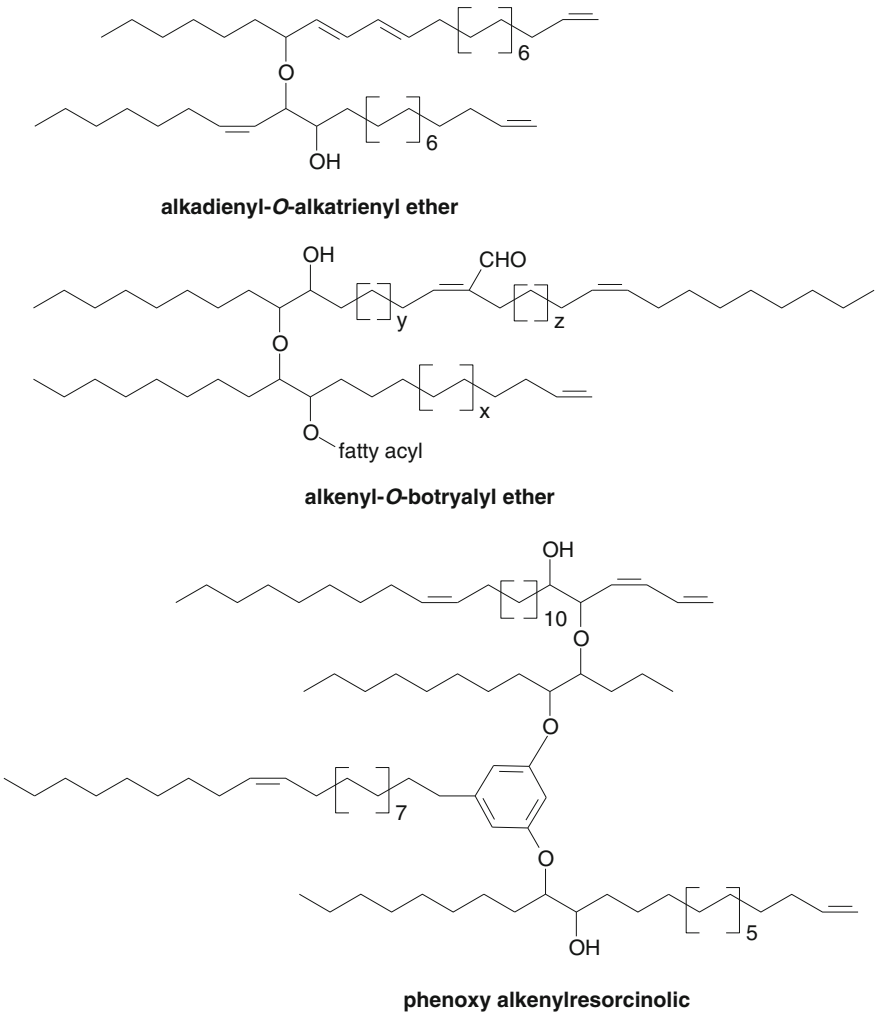

Fig. 4 Typical *B. braunii* high molecular weight non-polar lipids

3 Lipids Extraction Methods

3.1 Switchable Polarity Solvents SPS

The concept of "switchable compounds" and in particular of "switchable solvents" has been proposed for the first time by Jessop et al. few years ago [26]; this smart idea is based on the possibility to reversibly switch on and off some properties of a substance when a "trigger" is applied, from one version, with a specific set of properties, to another one, with very different properties. For solvents, such properties

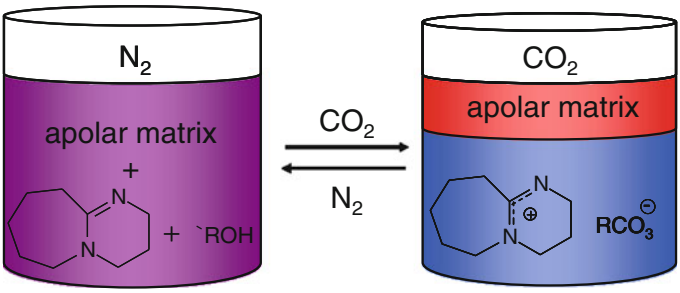

Fig. 5 SPS based on an equimolar mixture of DBU and an alcohol and its polarity switching after the addition of CO_2

can be polar/apolar, volatile/non-volatile, protic/aprotic. For the practical application of SPS, their switching solubility behaviour is a fundamental feature, correlated with their reversible polarity; an equimolar mixture of DBU (1,8-diazabicyclo-[5.4.0]-undec-7-ene) and an alcohol, for example, behaves as a slightly polar solvent, similar to chloroform, enabling to dissolve apolar compounds such as hydrocarbons, whereas the salt DBU alkylcarbonate, after CO_2 treatment, is a polar liquid, very similar to dimethylformamide and immiscible with hydrocarbons (Fig. 5) [26].

The major "greenness" of SPS respect to volatile organic solvents as *n*-hexane relies mainly on the possibility to develop safer, more economic and more sustainable processes. Chemical processes often involve many steps which can require many specific solvents; after each step, the solvent has to be removed and replaced with a new one, more suitable for the following step, increasing the economic costs and environmental impact of the process itself. Switchable solvents represent a valid answer to these cumbersome procedures, because their properties can be adjusted for the following step, enabling the same solvent to be used for several consecutive reactions or separation steps. Moreover, the recyclability of a SPS is based on the principle of adding and removing CO_2, and not on the recovery of the solvent by distillation; this means that the process of recycling is less expensive, less energy costly, and more environmentally friendly. Because of the peculiar recycle method, the solvents in the SPS formulation do not need to be volatile and this feature reduces the risks of fire and explosion, the release in the atmosphere, and the exposure for the operators.

Given the chemical nature of *B. braunii* lipid oil, the concept of "SPS" fits very well with the development of a new "greener" process of extraction [25]: the lipophilicity of the non-ionic form of SPS is suitable to extract apolar materials as algal hydrocarbons, whereas the ionic form of SPS, obtainable by a simple bubbling of CO_2, has a low affinity for these molecules, guaranteeing an easy recovery (Fig. 6).

The *first* important point in the development of the suitable SPS extraction process is the choice of the alcohol because it strictly influences the formation of the proper liquid carbonate anion. Previous works [40–42] have demonstrated that bicarbonate and methyl carbonate DBU salts have melting points lower than room temperature, whereas DBU salts with longer alkyl chains are liquids [43], therefore suitable for

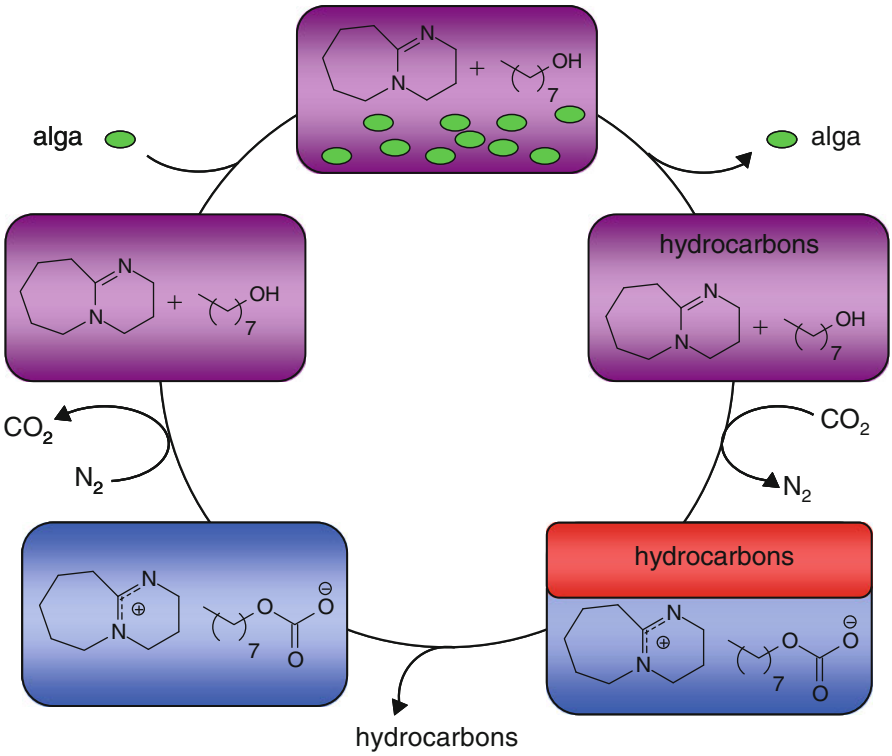

Fig. 6 Strategy for the extraction of hydrocarbons from freeze-dried samples of *B. braunii* by means of SPS exemplified for DBU/octanol

the extraction process. For this reason in our extraction process of *B. braunii,* DBU ethyl carbonate (melting points of 35°C) and DBU octyl carbonate (melting points of 30°C) were investigated as suitable candidate solvents (Table 3). In particular, the choice of an alcohol as octanol, hydrophobic and low volatile, should guarantee a good affinity with the apolar matrix which has to be extracted, and a scarce solubility in water, useful in the case of liquid samples.

The kinetics of the extraction process (Fig. 7) clearly shows that DBU/octanol and DBU/ethanol exhibit approximately the same behaviour, with similar hydrocarbons' amount extracted after 240 min (14 and 13% yields, respectively). Moreover, the hydrocarbons extraction with DBU/octanol is quite efficient from the beginning, with a yield of 9% after 20 min (65% of the yield at the end of the extraction time after 240 min).

A *second* important factor for the development of the extraction process with SPS is related to the chemical features of the process itself, and specifically to the eventuality that the presence of specific chemical compounds could prevent the switching of the system and the formation of the right DBU alkylcarbonate salt, affecting the separation process. Free fatty acids in the algal oil for example could

Table 3 Hydrocarbons and fatty acids extraction yields on dry weight basis with the SPS DBU/octanol and DBU/ethanol from freeze-dried samples of *B. braunii* [25]

Hydrocarbons	DBU/octanol extraction yield (%)	DBU/ethanol extraction yield (%)
$C_{27}H_{52}$	1.5±0.5	1.2±0.3
$C_{29}H_{56}$	5.6±2	4.8±1
$C_{29}H_{54}$	1.5±0.8	0.10±0.02
$C_{29}H_{54}$	3.1±0.3	2.8±0.1
$C_{31}H_{60}$	4.4±0.5	3.6±0.7
Total	16±2	12±2
Fatty acids		
16:0	0.17±0.01	0.11±0.08
18:2	–	0.10±0.04
18:1	0.39±0.03	0.34±0.2
18:0	0.11±0.08	0.04±0.02
Total	0.67±0.1	0.59±0.2

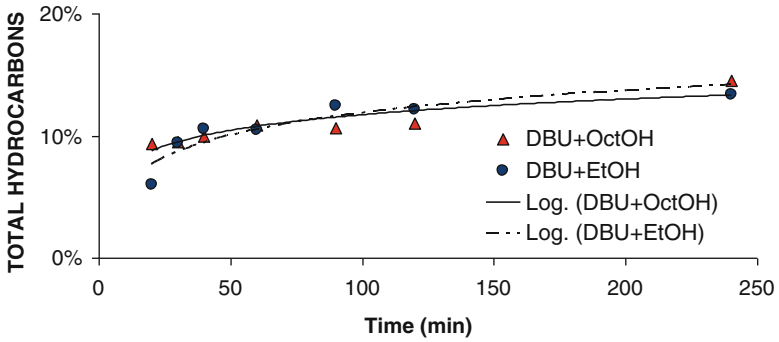

Fig. 7 Hydrocarbons extraction efficiency with time using the SPS DBU/octanol (*red triangle*) and DBU/ethanol (*blue circle*). *Dots* and *dashes curve*, and *continuous line* represent the logarithmic regression of DBU/octanol and DBU/ethanol data, respectively

form an ion pair with DBU, thus preventing the formation of a two-phases system when CO_2 is added and altering the stoichiometry of the SPS. In the case of *B. braunii,* the percentage of free fatty acids is 0.6–0.7% on a dry weight basis (Table 1), thus an irrelevant amount (about 0.18 mg) if compared with the amount of DBU used for the extraction (1 g) eventually able to react with free fatty acids. However, this eventuality could be a problem for the extraction of other kinds of oil with a high content of free fatty acids (as waste cooking oils [44]) and should be taken into account in the development of the extraction system.

A *third* relevant factor is the recyclability of the system, in terms of feasibility, contaminations of the algal oil, and losses. The efficiency of a non-ionic/ionic cycle with the SPS DBU/octanol in recovering pure hydrocarbons is about 81% of the total amount of hydrocarbons extracted, with 8.1% of hydrocarbons retained in the ionic SPS phase in the second half of the cycle, and about a 10% mechanical loss probably due to small samples size (in our work the extraction procedures were

accomplished on 30 mg of freeze-dried algal samples [25]). These results clearly indicate that the recovery of the hydrocarbons is very good, since the ionic form of SPS retains a rather small amount of the hydrocarbons in the extraction phase; moreover, this amount can be still reduced by scaling up the process and increasing the size of the samples.

The GC-MS evaluation of oil quality after the first cycle of extraction indicates that the oil still contains small amounts of octanol (0.3%) and DBU (0.4%), but bubbling extra CO_2 for 1 h at 40°C decreases the levels of contamination to undetectable values because of the precipitation of all the ionic liquid from the oil [25].

3.1.1 SPS for the Extraction of Liquid Algal Culture

Nowadays, algae industry is mainly focused on high value specialty products related to nutritional industry, sold from $10,000 to $100,000 per tonne; however, commodity products, as fuels, are usually sold for less than $1,000 per tonne. This means that, in order to obtain algae commodity products, the production costs of the current technologies have to be reduced of almost one order of magnitude. In particular, operating open ponds and processes as the harvest and the dewatering of algal biomass have a large impact on overall costs and energy balance. Thus, the development of a method in which algal metabolites, as hydrocarbons, can be directly extracted from the algal culture without energy costly steps can make the process more beneficial, economical, and sustainable.

The extraction of *B. braunii* hydrocarbons through a "liquid/liquid" method has been already accomplished by using *n*-hexane [45]; in our work, the SPS DBU/octanol was used analogously (Fig. 8), by exploiting the fact that octanol is a water-immiscible alcohol and that DBU, in spite of its water solubility, can be shifted into the organic phase through an adjustment of the pH to alkaline conditions (Fig. 9) [25].

Analogously to the obstacle represented by the presence of free fatty acids which could react with DBU hindering the switch of the non-ionic form of the SPS into the ionic one, also residual water in the system can be a problem. Spectroscopic data for the reaction between DBU and CO_2 in presence of water are in fact consistent with the formation of the salt DBU bicarbonate ($[DBUH^+][HCO_3^-]$) [40].

In our liquid/liquid extraction system after the adjusting of the pH of the aqueous phase with KOH, the water content in the upper organic phase (DBU/octanol) was 7% [25]. However, the residual water could be easily removed from DBU/octanol by bubbling N_2 in the system for 30 min at room temperature; after this time, the residual water was less than 0.1%, without any significant loss of the organic components (Fig. 10).

The extractions of *B. braunii* cultures were performed at room temperature, centrifuging the samples at different speeds and simulating a high (3,000 rpm) and a low energy (300 rpm) liquid/liquid extraction process from the growth medium (Table 4). Centrifuging was chosen as the best procedure to obtain a clearer separation (useful for small samples operation) of the aqueous and organic phases. This method allows to avoid vigorous stirring that should end up into an untreatable foaming, still maintaining a good extraction efficiency.

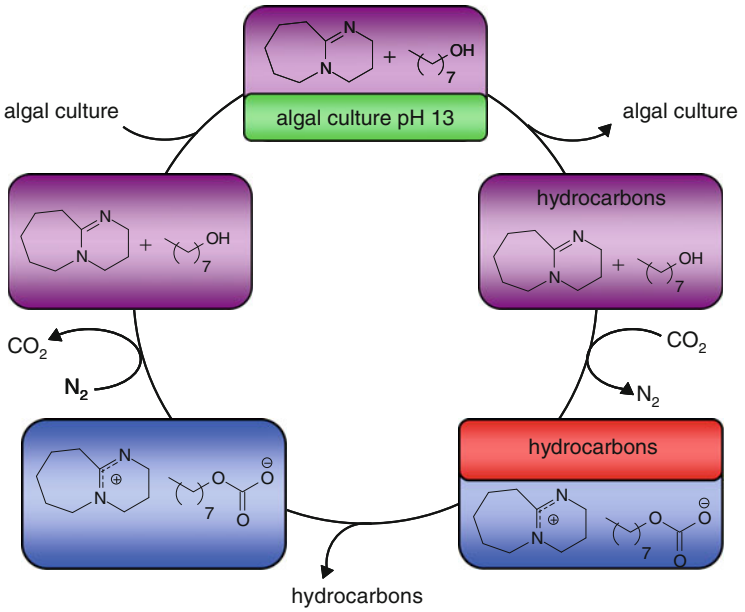

Fig. 8 Strategy for the extraction of hydrocarbons from *B. braunii* cultures by means of the switchable polarity solvent DBU/octanol

Fig. 9 Liquid/liquid extraction system of *B. braunii* culture with the SPS DBU/octanol

Although the extraction process is somewhat sluggish, the SPS DBU/octanol after 24 h at 300 rpm gives 8.2% hydrocarbon yield, almost an half of the yield achieved with DBU/octanol on freeze-dried samples (16%). Moreover, at higher rate (3,000 rpm) the extraction results faster, obtaining in 4 h approximately the same yields obtained at 300 rpm in 24 h. This can be explained by the fact that by raising the centrifuge rate, less dense algae (with higher hydrocarbon content) move quickly to the top of the water phase and release the hydrocarbons in the upper organic layer by contact.

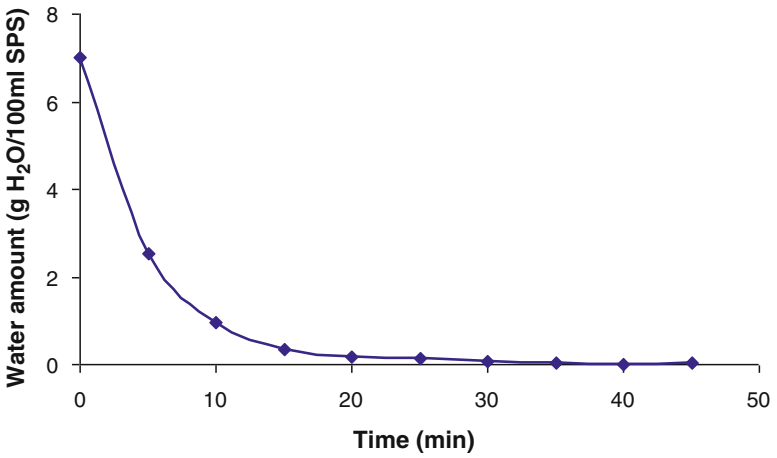

Fig. 10 Residual water removal from the SPS DBU/octanol after the extraction process of *B. braunii* cultures

Table 4 Hydrocarbon extraction efficiency with the SPS DBU/octanol on liquid culture samples

	Yield (%)		
	Extraction conditions		
Hydrocarbons	300 rpm, 2 h	300 rpm, 24 h	3,000 rpm, 4 h
$C_{27}H_{52}$	0.12 ± 0.05	0.60 ± 0.05	0.51 ± 0.3
$C_{29}H_{56}$	0.91 ± 0.3	2.9 ± 1	2.2 ± 0.1
$C_{29}H_{54}$	–	0.25 ± 0.1	0.25 ± 0.1
$C_{29}H_{54}$	0.72 ± 0.3	2.3 ± 0.9	2.0 ± 0.4
$C_{31}H_{60}$	0.75 ± 0.6	2.3 ± 0.8	2.3 ± 0.1
Total	2.5 ± 0.6	8.2 ± 1	7.0 ± 0.8

3.2 Pyrolysis

The thermochemical conversion of biomass through pyrolysis allows to convert dry biomass into a liquid, and to perform, at the same time, both the extraction of hydrocarbon-like material and the cracking of high molecular weight compounds (Fig. 11). The main advantages of this approach are: (1) avoiding the use of any solvent, thus increasing the "greenness" of the process and (2) producing useful co-products, like a combustible gas, usable as process energy source, and a biochar, suitable as soil-amending material as well as stable carbon sink. Thus, this strategy allows to exploit in different ways all the biomass constituents, the liquid bio-oil, and the residues (gas and biochar), increasing the net energy/CO_2 balance of a hypothetical algal cultivation (Fig. 12).

In the present work, *B. braunii* pellets were treated through a fixed bed pyrolysis at 500°C following the same experimental procedure described in the literature [46]. The yields of the three major pyrolysis fractions (bio-oil, biochar, and volatiles) and their composition are shown in Table 5.

Fig. 11 Bio-oil obtainable from the pyrolysis of *B. braunii*

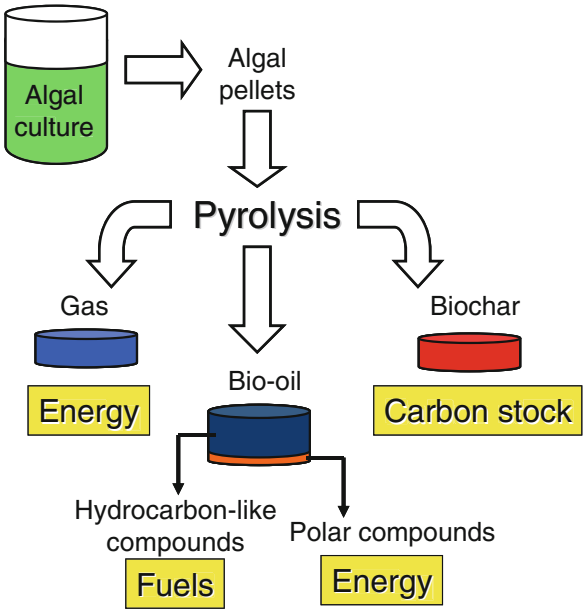

Fig. 12 Pyrolysis of *B. braunii* to obtain fuels, energy, and a stable carbon sink

Pyrolysis gas yield is 37%, corresponding to 28% yield after feedstock water subtraction.

Gas composition is evaluated by pyrolysis coupled with dynamic solid-phase micro-extraction (Py-SPME) followed by GC-MS analysis [47]. This technique is capable of giving information on the composition of gaseous and semi-volatile pyrolysis products, useful to obtain an overall picture of the most volatile compounds. The analysis reveals the presence of light hydrocarbons, aromatic hydrocarbons

Table 5 Yield on dry weight basis and percentage composition of pyrolysis fractions obtainable from *B. braunii*

Fractions	Yield (%)	Composition (%)	
Biochar	38 ± 2	Carbonaceus	48
		Ash	52
Bio-oil	25 ± 1	*n*-hexane-soluble	99
		n-hexane-insoluble	1
Volatiles	37 ± 1	Pyrolysis gas	76
		Feedstock water	23

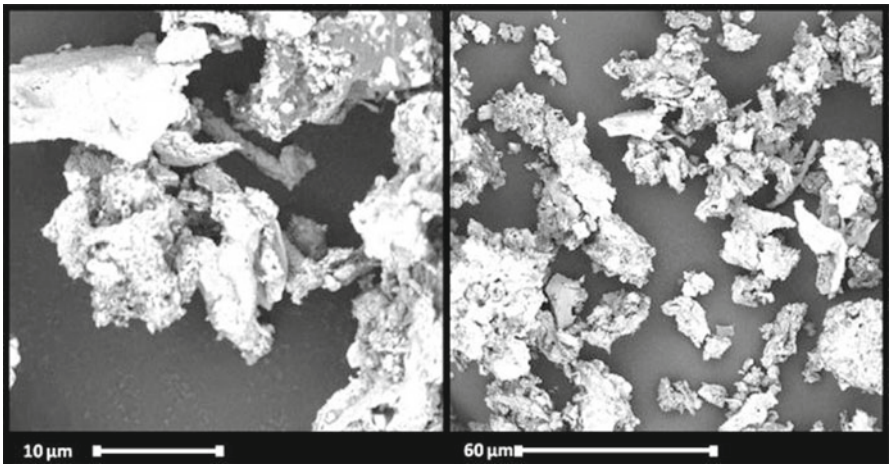

Fig. 13 SEM image of biochar obtained from fixed bed pyrolysis of *B. braunii* pellets

(mainly toluene), and some nitrogen-bearing aromatics (pyridine, indole) probably originated from pyrolysis of proteins.

Biochar yield is 38%, of which almost half of weight is composed by inorganic compounds; in fact, it retains almost all biomass ashes and for this reason biochar is not suitable as solid fuel, although usable as carbon stock. In order to evaluate the structural conformation of biochar, the material is visually characterized by scanning electronic microscopy (SEM) and the obtained pictures are shown in Fig. 13.

SEM image shows that biochar from 500°C pyrolysis is formed by a randomly aggregated sponge-like material. The dimension of particles is about 10–100 µm.

Bio-oil (25% on dry weight basis) is almost composed by a *n*-hexane soluble material; after hexane evaporation, this liquid fraction results in a black-reddish ash-free liquid (ashes less than 0.1%), relatively low viscous, of which only a very small part (1%) is insoluble in *n*-hexane. Moreover, the bio-oil is characterized by a negligible amount of water. This finding is quite surprising because the presence in the *B. braunii* feedstock of a significant amount of proteins (7%) and polysaccharides (20%), since the polar and oxygenated nature of these macromolecules, should give an expected larger amount of reaction water and of oil insoluble in *n*-hexane.

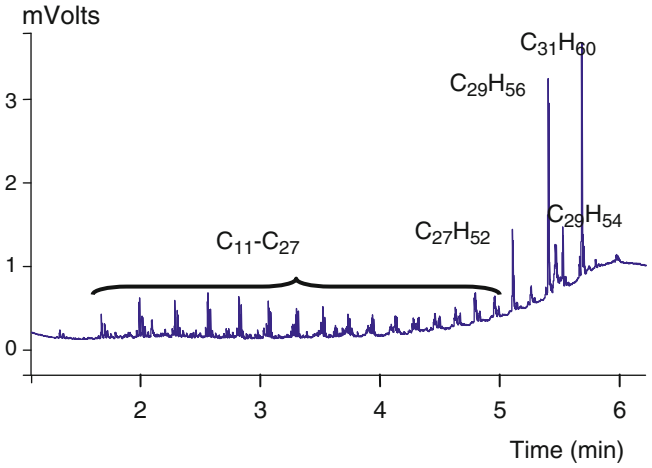

Fig. 14 GC-FID chromatogram of *B. braunii* pyrolysis oil

Reasonably, we can assume that the "vaporization" and hydrocarbon cracking processes are more effective than carbohydrate/proteins pyrolysis, and that the presence of non-lipid materials determines a low yield of pyrolysis products respect to hydrocarbon material. Nevertheless, if we consider the large carbohydrates content (20% of feedstock), usually able to produce a significant amount of organic tar (33% yield from cellulose using the same reactor [48]), such low amount of *n*-hexane-insoluble matter is noticeable. When a hydrocarbon-rich microalga as *B. braunii* is submitted to pyrolysis, proteins and polysaccharides form only a minor amount of bio-oil. From a practical point of view, this means that pyrolysis can be seen as a suitable "solvent-less extraction method" highly selective for hydrocarbons.

The chemical characterization by GC-FID and GC-MS of the *n*-hexane-soluble bio-oil reveals the presence of typical *B. braunii* linear dienes and trienes ($C_{27}H_{52}$, $C_{29}H_{56}$, $C_{29}H_{54}$ and $C_{31}H_{60}$) and, in addition, a series of random hydrocarbon fragments consisting in C_{11}–C_{27} alkanes and alkenes (Fig. 14). From a quantitative point of view, almost the whole amount of the pyrolysis oil (around 90%) consists of GC detectable compounds, indicating that heavy cross-linked hydrocarbon polymers are depolymerised to smaller fragments during the pyrolytic treatment.

In order to have information on the volatilization properties of this potential new fuel, thermogravimetric analysis (TGA) was also done (Fig. 15).

TGA of pyrolytic oil shows four weight loss steps characterized by different extent. First, weight loss, probably generated by a gradual volatilization of small random length C_{11}–C_{27} hydrocarbons, starts gradually from 50°C and becomes important at 200–300°C. Around 300°C, a sharp weight loss derivatives peak, probably deriving from the boiling of the olefin $C_{29}H_{56}$, is observed. In addition, two smaller weight losses are recorded at 380 and 450°C, probably related to $C_{31}H_{60}$ and residual high molecular weight matter in the oil. In general, TGA observation confirms the results obtained from GC analysis and gives an indication that

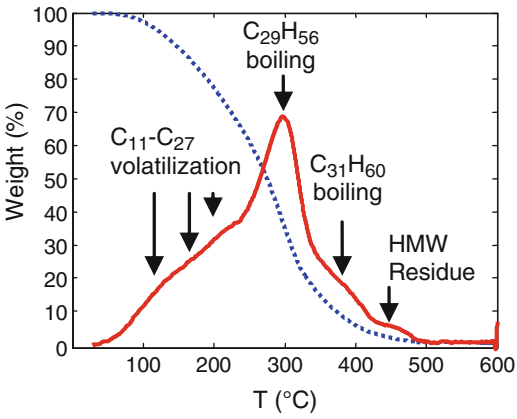

Fig. 15 TGA profile of *B. braunii* pyrolysis oil. *Dotted line*: percent weight change; *full line*: temperature derivate of weight change. *HMW* high molecular weight residue (e.g. ether lipids, or other long chain hydrocarbons)

n-hexane-soluble pyrolysis oil obtainable from *B. braunii* is lighter than *B. braunii* non-polar lipids and hydrocarbons from which it is produced (see Fig. 3). Moreover, whole *n*-hexane-soluble fraction boils out almost totally (>90% weight loss) before 400°C. This could be an indication that the liquid obtained could be directly used as fuel, without any further upgrading or modification.

4 Comparison of Different Lipids Extraction Methods

4.1 Solvent-Based Extraction Systems

The yields of linear olefins obtained through traditional organic solvents extraction (*n*-hexane, chloroform, and methanol) and SPS-based systems (DBU/octanol and DBU/ethanol) are compared in Fig. 16.

The SPS DBU/octanol is the best solvent in the extraction of freeze-dried samples (16 ± 2% total hydrocarbons yield on dry weight basis), followed by the SPS DBU/ethanol (12 ± 2% yield). The two SPS are both better than the extraction system based on traditional organic solvents that gives the lowest yields (7.8 ± 3%) after an extraction process performed at the same temperature and after the same time interval (60°C and 4 h).

Also, in the direct extraction of algal cultures, the SPS DBU/octanol affords better results than traditional organic solvents, under both the speed and time conditions we checked. It is important to underline that the SPS DBU/octanol gives an extractive yield of 8.2 ± 1% after 24 h at 300 rpm, which is slightly higher than that obtainable from freeze-dried sample with traditional organic solvents under reflux (7.8% yield). This is an indication that the extraction process can be improved from energetic, economic, and sustainability points of view, without the need of dewatering biomass, consuming energy to evaporate the solvent, and adopting special safety measures to reduce the risk for operators.

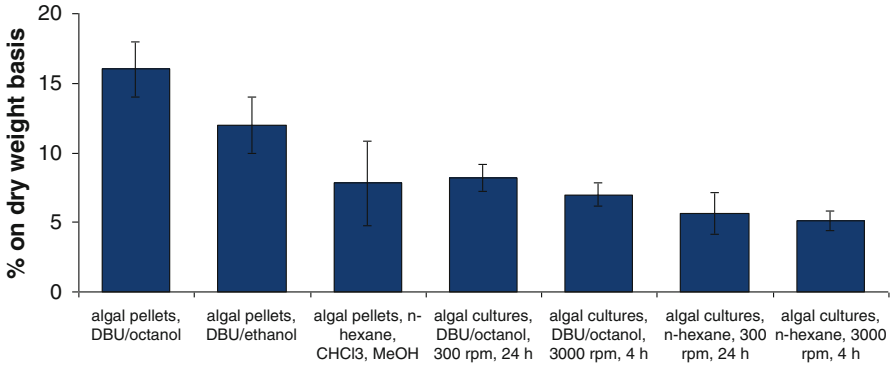

Fig. 16 Hydrocarbon extraction yields on a dry weight basis from freeze-dried samples and algal cultures obtained with different solvent systems

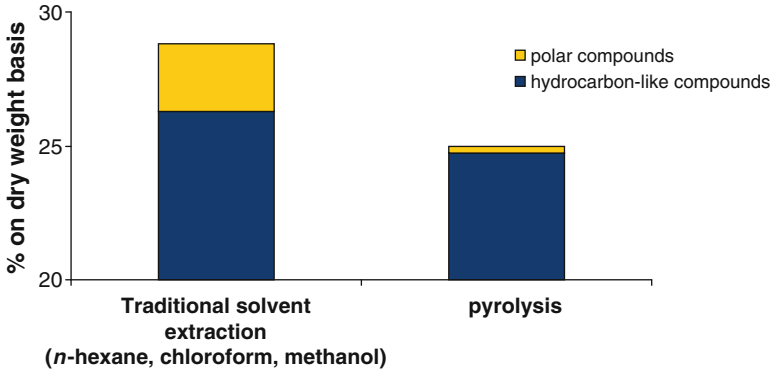

Fig. 17 Lipid oil yields on a dry weight basis obtained through traditional solvent extraction (*n*-hexane, chloroform, and methanol) and pyrolysis

4.2 Comparison Between Chemical and Thermochemical Extractions

Pyrolysis produces a hydrocarbon fuel composed by a minor amount of polar pyrolysis products. For this reason, from an operative point of view, pyrolysis could be considered as an "extraction process" for hydrocarbon-like substances and thus comparable with traditional solvent extraction.

Comparing traditional organic solvent extraction (with *n*-hexane, chloroform, and methanol) and thermochemical process, pyrolysis allows obtaining 90% of hydrocarbon-like materials of feedstock, as random length C_{11}–C_{31} alkanes and alkenes. As shown in Fig. 17, pyrolysis "extracts" selectively hydrocarbon-like material and produces very apolar oil that could be probably used directly as fuel, thanks to a similar composition with diesel fuel. On the other hand, traditional solvents extract more algal oil than pyrolysis, but this oil is heavier, due to presence of high molecular

weight ether lipids. Moreover, the oil extracted with traditional solvents is richer in polar lipids, detrimental for fuel quality and solubility in standard fuels.

One of the most important drawbacks of pyrolysis process is that biomass has to be dried (up to 50% of moisture) before pyrolysis, whereas, as shown above, solvent extraction can be applied directly on wet materials. Nevertheless, pyrolysis results in an interesting solvent-less technique if microalgae can be easily collected and pelletized, as in the case of colonial *B. braunii* culture.

5 Conclusions

Different methods for extracting biofuel from *B. braunii* were tested. Both SPS and solvent-less thermochemical extraction resulted effective for the purpose. This is mainly due to *B. braunii* intrinsic properties. In comparison with traditional organic solvents, SPS have the interesting feature of being effective also on aqueous samples, without dewatering biomass. On the other hand, pyrolysis, in spite of the need to operate with relatively dry samples, maximizes the output of the process due to the co-production of biochar, energy, and a higher quality fuel than that obtainable through solvent extraction.

Acknowledgements We acknowledge the Ministry MiUR and the University of Bologna (RFO program) for funding. We thank Prof. Rossella Pistocchi and co-workers for providing with *Botryococcus braunii* samples.

References

1. Williams PJL (2007) Biofuel: microalgae cut the social and ecological costs. Nature 450:478
2. Hu Q, Sommerfeld M, Jarvis E (2008) Microalgal triacylglycerols as feedstocks for biofuel production: perspectives and advances. Plant J 54(4):621–639
3. Chisti Y (2007) Biodiesel from microalgae. Biotechnol Adv 25(3):294–306
4. Chisti Y (2008) Biodiesel from microalgae beats bioethanol. Trends Biotechnol 26(3):126–131
5. Posten C, Schaub G (2009) Microalgae and terrestrial biomass as source for fuels-A process view. J Biotechnol 142(1):64–69
6. An JY, Sim SJ, Lee JS, Kim BW (2003) Hydrocarbon production from secondarily treated piggery wastewater by the green alga *Botryococcus braunii*. J Appl Phycol 15(2–3):185–191
7. Shen Y, Yuan W, Pei Z, Mao E (2008) Culture of microalga *Botryococcus* in livestock wastewater. T Asabe 51(4):1395–1400
8. Benemann JR (1997) CO_2 mitigation with microalgae systems. Energy Convers Manage 38:S475–S479
9. Wang B, Li YQ, Wu N, Lan CQ (2008) CO_2 bio-mitigation using microalgae. Appl Microbiol Biotechnol 79(5):707–718
10. Rosenberg JN, Oyler GA, Wilkinson L, Betenbaugh MJ (2008) A green light for engineered algae: redirecting metabolism to fuel a biotechnology revolution. Curr Opin Biotechnol 19(5):430–436
11. Molina Grima E, Belarbi EH, Acién Fernández FG, Robles Medina A, Chisti Y (2003) Recovery of microalgal biomass and metabolites: process options and economics. Biotechnol Adv 20:491–515

12. Chisti Y (2008) Response to Reijnders: do biofuels from microalgae beat biofuels from terrestrial plants? Trends Biotechnol 26(7):351–352
13. Reijnders L (2008) Do biofuels from microalgae beat biofuels from terrestrial plants? Trends Biotechnol 26(7):349–350
14. Metzger P, Largeau C (2005) *Botryococcus braunii*: a rich source for hydrocarbons and related ether lipids. Appl Microbiol Biotechnol 66(5):486–496
15. Templier J, Largeau C, Casadevall E (1987) Effect of various inhibitors on biosynthesis of non-isoprenoid hydrocarbons in *Botryococcus braunii*. Phytochemistry 26:377–383
16. ChanYong TP, Largeau C, Casadevall E (1986) Biosynthesis of non-isoprenoid hydrocarbons by the microalga *Botryococcus braunii*: evidence for an elongation decarboxylation mechanism; activation of decarboxylation. Nouv J Chim 10:701–707
17. Metzger P, Casadevall E, Pouet MJ, Pouet Y (1985) Structures of some botryococcenes: branched hydrocarbons from the b-race of the green alga *Botryococcus braunii*. Phytochemistry 24:2995–3002
18. Metzger P, Berkaloff C, Casadevall E, Coute A (1985) Alkadiene- and botryococcene-producing races of wild strains of *Botryococcus braunii*. Phytochemistry 24:2305–2312
19. Yamaguchi K, Nakano H, Murakami M, Konosu S, Nakayama O, Kanda M, Nakamura A, Iwamoto H (1987) Lipid composition of a green alga, *Botryococcus braunii*. Agric Biol Chem 51(2):493–498
20. Jae-Yon L, Chan Y, So-Young J, Chi-Yong A, Hee-Mock O (2010) Comparison of several methods for effective lipid extraction from microalgae. Biores Technol 101:S75–S77
21. Gouveia L, Oliveira AC (2009) Microalgae as a raw material for biofuels production. J Ind Microbiol Biotechnol 36(2):269–274
22. Erikson DR (1995) Practical handbook of soybean processing and utilisation. AOCS Press and United Soybean Board, St. Louis
23. Mendes RL, Nobre BP, Cardoso MT, Pereira AP, Palavra AF (2003) Supercritical carbon dioxide extraction of compounds with pharmaceutical importance from microalgae. Inorg Chim Acta 356:328–334
24. Mendes RL, Coelho JP, Fernandes HL (1995) Applications of supercritical CO_2 extraction to microalgae and plants. J Chem Technol Biotechnol 62:53–59
25. Samorì C, Torri C, Samorì G, Fabbri D, Galletti P, Guerrini F, Pistocchi R, Tagliavini E (2010) Extraction of hydrocarbons from microalga *Botryococcus braunii* with switchable solvents. Biores Technol 101:3274–3279
26. Jessop PG, Heldebrant DJ, Li X, Eckert CA, Liotta CL (2005) Reversible non polar-to-polar solvent. Nature 436:1102
27. Jessop PG, Phan L, Brown H, White J, Hodgson A (2009) Soybean oil extraction and separation using switchable or expanded solvents. Green Chem 11:53–59
28. Pan P, Hu C, Weinyan Y, Li Y, Dong L, Zhu L, Tong D, Qing R, Fan Y (2010) The direct pyrolysis and catalytic pyrolysis of nannochloropsis sp. Residue for renewable bio-oils. Biores Technol 101:4593–4599
29. Bird MI, Wurster CM, Paula Silva PH, Bass AM, de Nys R (2010) Algal biochar—production and properties. Biores Technol. doi:10.1016/j.biortech.2010.07.106
30. Samorì G (2008) Caratterizzazione chimico-biologica di *Botryococcus braunii* (Chlorophyceae) per la produzione di biocombustibili. Master degree Thesis, University of Bologna, Italy
31. Samorì C (2010) Use of solvents and environmental friendly materials for applications in Green Chemistry. Ph.D. Thesis, University of Bologna, Italy
32. Lowry OH, Rosebrough NJ, Farr AL, Randall RJ (1951) Protein measurement with the Folin-Phenol reagents. J Biol Chem 193:265–275
33. Dubois M, Gilles KA, Hamilton JK, Rebers PA, Smith F (1956) Colorimetric method for determination of sugars and related substances. Anal Chem 28:350–356
34. Largeau C, Casadevall E, Berkaloff C, Dhmelincourt P (1980) Sites of accumulation and composition of hydrocarbons in *Botryococcus braunii*. Phytochemistry 19:1043–1051
35. Zhu CJ, Lee YK (1997) Determination of biomass dry weight of marine microalgae. J Appl Phycol 9:189–194

36. Metzger P, Largeau C (2002) Natural polyacetals. In: Steinbüchel A (ed) Biopolymers, vol 9. Wiley-VCH, Weinheim, pp 113–127
37. Metzger P, Casadevall E (1991) Botryococcoid ethers, ether lipids from *Botryococcus braunii*. Phytochemistry 30:1439–1444
38. Metzger P, Casadevall E (1992) Ether lipids from *Botryococcus braunii* and their biosynthesis. Phytochemistry 31:2341–2349
39. Metzger P (1994) Phenolic ether lipids with an n-alkenylresorcinol moiety from a Bolivian strain of *Botryococcus braunii* (A race). Phytochemistry 36:195–212
40. Heldebrant DJ, Jessop PG, Thomas CA, Eckert CA, Liotta CL (2005) The reaction of 1,8-diazabicyclo-[5.4.0]-undec-7-ene (DBU) with carbon dioxide. J Org Chem 70:5335–5338
41. Munshi P, Main AD, Linehan J, Tai CC, Jessop PG (2002) Hydrogenation of carbon dioxide catalyzed by ruthenium trimethylphosphine complexes: the accelerating effect of certain alcohols and amines. J Am Chem Soc 124(27):7963–7971
42. Prez ER, Santos RHA, Gambardella MTP, de Macedo LGM, Rodrigues-Filho UP, Launay J, Franco DW (2004) Activation of carbon dioxide by bicyclic amidines. J Org Chem 69:8005–8011
43. Phan L, Chiu D, Heldebrant DJ, Huttenhower H, John E, Li X, Pollet P, Wang R, Eckert CA, Liotta CL, Jessop PG (2008) Switchable solvents consisting of amidine/alcohol or guanidine/alcohol mixtures. Ind Eng Chem Res 47(3):539–545
44. Canakci M, Van Gerpen J (2001) Biodiesel production from oils and fats with high free fatty acids. T Asae 44(6):1429–1436
45. Frenz J, Largeau C, Casadevall E (1989) Hydrocarbon recovery by extraction with a biocompatible solvent from free and immobilized cultures of *Botryococcus braunii*. Enzyme Microb Technol 11(11):717–724
46. Fabbri D, Torri C, Mancini I (2007) Pyrolysis of cellulose catalysed by nanopowder metal oxides: production and characterisation of a chiral hydroxylactone and its role as building block. Green Chem 9:1374–1379
47. Torri C, Fabbri D (2009) Application of off-line pyrolysis with dynamic solid-phase microextraction to the GC-MS analysis of biomass pyrolysis products. Microchem J 93:133–139
48. Torri C, Lesci IG, Fabbri D (2009) Analytical study on the pyrolytic behaviour of cellulose in the presence of MCM-41 mesoporous materials. J Anal Appl Pyrol 85:192–196

Chapter 28
Valorization of Waste Frying Oils and Animal Fats for Biodiesel Production

Teresa M. Mata, António A. Martins, and Nidia S. Caetano

Abstract The increased demand for biodiesel and the difficulties in obtaining enough quantities of raw materials for its production are stimulating the search for alternative feedstocks. Among the various possibilities, the utilization of residual fatty materials, in particular waste frying oils and animal fat residues from the meat and fish processing industries, are increasingly seen as viable options for biodiesel production. This work reviews the state of the art regarding the utilization of waste oils and animal fats as feedstocks for biodiesel production, which are characterized by the presence of high levels of impurities such as high acidity and moisture content. The relative advantages and disadvantages of the different routes for biodiesel production are presented and discussed in this chapter, focusing on their chemical and technological aspects. Also discussed are the questions related to the viability and potential economic advantages of using this type of feedstocks in biodiesel production for road transportation.

T.M. Mata (✉)
Laboratory for Process, Environmental and Energy Engineering (LEPAE), Faculty of Engineering, University of Porto (FEUP), R. Dr. Roberto Frias, s/n, 4200-465, Porto, Portugal
e-mail: tmata@fe.up.pt

A.A. Martins
Center for Transport Phenomena Studies (CEFT), Faculty of Engineering, University of Porto (FEUP), R. Dr. Roberto Frias, s/n, 4200-465, Porto, Portugal

N.S. Caetano
Laboratory for Process, Environmental and Energy Engineering (LEPAE), Faculty of Engineering, University of Porto (FEUP), R. Dr. Roberto Frias, s/n, 4200-465, Porto, Portugal

Department of Chemical Engineering, School of Engineering (ISEP), Polytechnic Institute of Porto (IPP), R. Dr. António Bernardino de Almeida, s/n, 4200-072, Porto, Portugal

J.W. Lee (ed.), *Advanced Biofuels and Bioproducts*, DOI 10.1007/978-1-4614-3348-4_28,

1 Introduction

As energy demands increase and the fossil fuel reserves are limited or are becoming harder and harder to explore, research is being directed towards the development of renewable fuels. This aspect is particularly relevant in the transportation sector, where the dependence on fossil fuels is even more evident and any possible alternative (e.g. fuel cells and hydrogen) is harder to develop and implement in practice. In the short term, especially in Europe, biodiesel (mono-alkyl esters of long-chain fatty acids) derived from renewable biological sources such as vegetable oils or animal fats are attracting a lot of attention. Among its main key features one can point out its renewability, biodegradability, improved viscosity, better quality of exhaust gases, and also the possibility of being used, as a petroleum diesel substitute or combined with diesel fuels, in conventional combustion ignition engines without significant modifications.

Biodiesel promises to supplement and even replace at a local/regional level fossil diesel while contributing to rural development and reducing the dependence on fossil fuels. However, under current production technology, its use in transportation even blended with diesel has some pros and cons. First, biodiesel production costs are higher than those of petroleum diesel, mainly due to its production from expensive edible vegetable oils that account for 88% of the total estimated cost for biodiesel production [90]. This is one of the major hurdles in biodiesel commercialization, making it difficult to compete in price with fossil diesel and requiring in many cases subsidies or fixed prices policies to be competitive with current fossil fuels or to fulfil specific national or international targets for the incorporation of bio-based fuels. Second, the continued development, market growth, and market share of biodiesel, with the corresponding need of raw materials for its production, has risks of their own and is causing more harm than good. For example, some of the most relevant feedstocks, such as soybean oil and palm oil, are placing additional pressure on food supplies during a period of great demand increase in developing countries and diverting valuable resources away from food production. Until new technologies and/or feedstocks unconnected with the human food supply chain are developed, the use of edible vegetable oils to produce biodiesel might further strain the already tight supplies of arable land and water all over the world, potentially pushing food prices up even further. Furthermore, biodiesel feedstocks are impacted by previous and current land use practices, and cultures are adapted to specific climate and soil conditions available in restricted regions of the world. Thus, moving a culture from one region of the world to another will surely influence the crop yield potential. For example, requiring the utilization of more fertilizers, having an impact on the local biodiversity as some of the species can be invasive and displace native species, or bringing pests with them, with potential direct consequences to local ecosystems. Also, a more intense agriculture normally increases the soil erosion due to carbon loss and nitrate and phosphorous loss [82].

To circumvent the problems referred above, new feedstocks are needed what is currently an extensive area of research. An example includes microalgae that have the ability to grow under harsher conditions, in areas unsuitable for agricultural

purposes, and with reduced needs for nutrients. This way, the competition with other crops for arable soil, in particular for human consumption, is greatly reduced. Also, microalgae are easy to cultivate and can grow at low cost with little attention, using water unsuitable for human consumption. However, very high energy requirement for drying the algal biomass is a barrier to its commercialization at present [66]. Another example is *Jatropha curcas L.*, currently at a very early stage of development for biodiesel production. Since the markets of the different products from this plant have not yet been properly explored or quantified, the optimum economic benefit of its production has not been achieved [57].

From the currently available alternative feedstocks for biodiesel production, some attention is being given to residual oil and fat, such as waste frying oils from restaurants or food industry, and animal fats resulting from the meat or fish processing industries, which otherwise need to be disposed off with care and represents an operational cost. Even though the residual oil or fat are of lesser quality than virgin vegetable oils and more difficult to process due to the presence of impurities or to their high acidity, they may be a good option for biodiesel production, allowing one to use a waste and treating it appropriately in the production of a product (biodiesel) with value that can be used internally by the company or sold out. Moreover, these fatty materials are available at a lower cost (in many cases even for free) and can be used as feedstock for biodiesel production. Araujo et al. [8] evaluated the biodiesel production from waste frying oil concluding that it can be economically feasible provided that logistics are well configured.

The most common animal fats that can be processed into biodiesel are beef tallow, pork lard, and poultry fat. Fish oils are also possible to be converted into biodiesel, although research in this area is not so advanced as for the animal fats. In most of these cases, the oil or fat are not readily available for use in biodiesel production, but need to be firstly extracted from the fatty residues. It is estimated that about 38% of the bovine, 20% of the pork, and 9% of the poultry are fatty material for rendering (e.g. bones, fat, head, other non edible materials, etc.) from which can be obtained about 12–15% of tallow, lard, or poultry fat that can be used for biodiesel production [25, 36].

The lipid content in fish varies a lot depending on the type of fish and by-product. For example, Gunasekera et al. [45] reported the lipid content of 17% in carp offal, 13% in carp roe, 57% in trout offal, 31% in fish frames, and 13% in "surimi" processing waste and fish meal. Oliveira and Bechtel [74] reported 11.5% of lipids in pink salmon heads and 4% in salmon viscera. Kotzamanis et al. [55] reported 12% of lipids in trout heads.

In the European Union, about one million tonnes of tallow is rendered each year [69]. The United States generates in average about 4 kg/person of yellow grease per year, and based on this statistic, Canada should produce about 120,000 tonne/year of waste fats of various origins [100]. Brazil generates about 1,382,472 tonne/year of beef tallow and 194,876 tonne/year of lard from slaughterhouses, which is normally used for producing meal and oil for animal feed [25]. The world fish capture and aquaculture production was in 2004 about 140 million tonnes of fish, from which about 25% was for non-food uses, in particular for the manufacture of fish oil and animal meal [34]. The amount of waste frying oil generated annually in several countries is also huge, accounting for more than 15 million tonnes, varying

according to the amount of edible oil consumed. For example, the United States generates around 10 million tonnes of waste frying oils, followed by China with 4.5 million tonnes and by the European Union with a potential amount ranging from 0.7 to 1.0 million tonnes [44]. However, the worldwide amount of waste oils generated should be much larger than that and it is expected to increase in the near future.

Some studies available in the open literature show some potential for these feedstocks. For example, Chua et al. [30] performed a LCA to study the environmental performance of biodiesel derived from waste frying oils in comparison with low sulphur diesel and concluded that biodiesel is superior in terms of global warming potential, life cycle energy efficiency, and fossil energy ratio. Godiganur et al. [41] tested biodiesel from fish oil in compression ignition engines, showing overall good combustion properties and environmental benefits. In particular, there are no major deviations in diesel engine's combustion and no significant changes in the engine performance. Moreover, there is a reduction of the main noxious emissions in comparison with fossil diesel, with the exception on the nitrogen oxide (NOx) emissions. Wyatt et al. [97] produced biodiesel from lard, beef tallow, and chicken fat by alkali-catalyzed transesterification. The biofuel obtained from these animal fats were tested and the NOx emissions determined and compared with soybean biodiesel as 20% volume blends (B20) in petroleum diesel. Results show that the three animal fat-based B20 fuels have lower NOx emission levels (3.2–6.2%) than the soy-based B20 fuel.

Animal fats and vegetable oils differ on their physical and chemical properties. While vegetable oils have a large amount of unsaturated fatty acids, animal fats have in their composition a large amount of saturated fatty acids [20]. Animal fats such as tallow or lard are solid at room temperature. An exception is the poultry fat which is liquid at room temperature and has in its composition a low percentage of saturated triglycerides, comparable to soybean oil. Fish oils contain a wide range of fatty acids, some of them with more than 18 atoms in their carbon chain and even some with an odd number of carbons [37]. Chiou et al. [28] analysed and compared the methyl esters derived from salmon oil extracted from fish processing by-products with methyl esters derived from corn oil, concluding that, although there are some differences in the fatty acid composition, salmon and corn oil methyl esters have similar physical properties.

The physical and chemical properties of waste frying oil and the corresponding fresh edible oil are almost identical, but differ from source to source depending on the oil source. Waste oils have normally higher moisture and free fatty acids (FFA) contents than fresh edible oil, particles of different composition, and also polymerized triglycerides are formed during frying due to the thermolytic, oxidative, and hydrolytic reactions that may occur [44]. Additionally, during frying, the oil is heated at temperatures of 160–200°C in the presence of air and light for a relatively long period of time, what contributes to increase its viscosity, specific heat, and darkens its colour.

For processing these fatty waste materials and to improve the quality of biodiesel produced, different solutions can be employed. For example, Guru et al. [46] studied biodiesel production from waste animal fats in a two-step catalytic process and adding organic-based nickel and magnesium compounds as additives in order to

achieve a reduction in the biodiesel pour point. Canoira et al. [22] evaluated biodiesel obtained from different mixtures of animal fat and soybean oil using a process simulation software (Aspen Plus™), concluding that a mix of 50% (v/v) of both raw materials is the most suitable to obtain a final product with a quality according to the standards and with the minimum costs. This is relevant to optimize the production processes and ensure that the costs of disposal should be higher than the costs of making biodiesel corrected by the potential economical gains, for example reducing the consumption of fossil fuels.

As most of the biodiesel feedstocks have similar characteristics, any improvement in the way how the pre-processing, reaction, and final processing are done, in particular related to the reaction time and final product quality, will have a profound impact in the production capacity and in the overall process. As two phases are formed and the diverse reactants are presented in different phases, the effects of mixing are significant to the process. The interfacial area between phases increases with high mixing intensity, facilitating the mass transfer between phases and naturally increasing the reaction rates [10]. Noureddini and Zhu [73] confirm these conclusions and have shown that, depending on the reaction stage, both the mass transport and the reaction kinetics are dominant aspects controlling the process performance.

In this work, the various steps for biodiesel production are described, depending on the characteristics of the waste oil or animal fat, having in mind the process improvement.

2 Biodiesel Production Processes

Processes for producing biodiesel from fatty waste materials should be similar to those from vegetable oils, the dominant feedstock according to the European point of view. Nevertheless, the special characteristics of these feedstocks, in particular their high content in FFA, moisture, and other contaminants, such as dirt and other chemicals that appear during processing and/or utilization of these fatty materials, requires that additional processing steps are employed, such as pre-treatment operations.

Currently, the process most widely used industrially for biodiesel production is the alkali-catalyzed transesterification of triglycerides, with low molecular weight alcohols and operated in batch mode. This process is more efficient and less corrosive than the acid-catalyzed transesterification, the reaction is faster, and requires lower amount of catalyst to carry out the reaction, presenting only problems in the glycerol separation. Also, the alkaline catalysts (NaOH, KOH, $NaOCH_3$, etc.) are the most commonly preferred and are cheaper than the ones employed in the acid-catalyzed process (H_2SO_4, HCl, etc.). However, the alkali-catalyzed process has several drawbacks, in particular it is very sensitive to the lipidic feedstock purity, mainly operating in batch mode and needing large reaction times to obtain a complete conversion of oil, and has complex biodiesel purification steps after the reaction. For waste fats, these factors have to be considered explicitly to ensure a proper conversion of the fats to biodiesel, meaning that in most cases pre-treatment steps

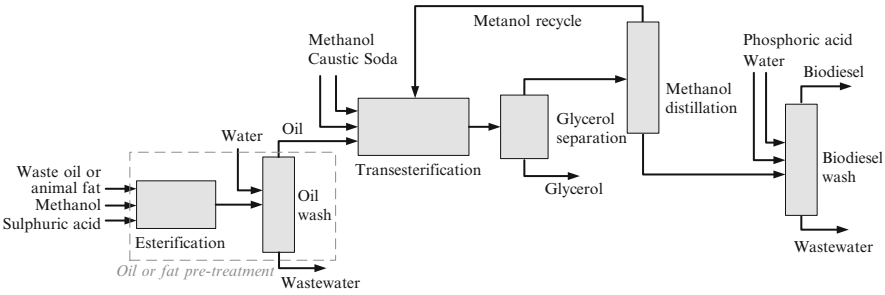

Fig. 1 Process flowsheet for biodiesel production from waste oil or animal fat with high acidity

are required. Figure 1 shows a simplified process flowsheet for biodiesel production from waste oil or animal fat with high acidity by alkali-catalyzed transesterification preceded by a pre-treatment by esterification.

2.1 Extraction of Oil or Fat from Fatty Waste Materials

Depending on the characteristics of the fatty waste materials, normally three main steps are performed:

- Extraction of the oil or fat from the fatty feedstock.
- Filtration and removal of contaminants.
- Neutralization or esterification of the FFA.

The extraction process is relevant in the meat and fish processing industry, as most types of fatty waste materials are normally associated with other materials, for example meat residues and bones or fish's heads and viscera. Thus, it is necessary to separate the oil or fat from the remaining materials. Depending on the fatty residues to separate, the process varies, involving for example heating or solvent extraction.

At the laboratory scale, the waste animal fats (e.g. tallow, lard, or poultry fat) collected from slaughterhouses or food processing companies can be melted and filtered in order to obtain the fat and remove gums, protein residues, and suspended particles [67]. For extracting the fish oil from the fish's residues, firstly fish's viscera and heads can be cooked thoroughly in boiling water. The supernatant oil is taken from the top of the boiling vessel and placed in a separatory funnel, where the oil is washed (with distilled water at about 60°C) and separated from the water and solid residues. The fish soapstock is squeezed and as a result the crude fish oil containing some solid impurities is separated from the cake of fish dregs. The resulting crude oil is centrifuged and placed in a separatory funnel where it is washed. Finally, the oil is vacuum-filtered to remove any remaining impurities.

Industrially, the bulk of the material to be rendered consists of the leftover parts of a slaughtered animal (fats, bones, and other parts). The first step in the rendering

process is the milling and grinding of a mixture of materials to generate a mass that is screw-conveyed to a batch digester where it remains for 4–5 h to be cooked with saturated vapour at about 110°C, until it loses about 70% of its moisture content. Then the digester is opened and its contents are discharged into a percolator tank, heated by steam, where the liquid fat separates from solids by percolation and sieving. After percolation, the fat is centrifuged and/or filtered and sent to a decanter tank for storage and eventual final separation from the aqueous phase present. The solid material removed from the fat in this operation is added to the solid material from percolation. The solid material is hot-pressed generating more fat that is added to the one percolated for purification. The pressed material is milled in a hammer mill, and then sent for screening to obtain the particle size of flour. The material retained in screening returns to the mill. Passing through the screening the meat/bone meal is bagged and stored for shipping and using in pet food [25].

The industrial process for extracting oil from fish by-products (e.g. heads, viscera, fish bones, and skin) operates in a continuous mode. Thus, after milling and grinding the fish, by-products are screw-conveyed to a continuous steam cooker with a residence time of about 15 min. After cooking, the coagulated mass is pre-strained in a strainer conveyor before entering a screw press that separates the press cake from the press liquor. The press cake is disintegrated in a tearing machine (a wet mill) and dried in an indirect steam dryer with internal rotating blades. The meal passes through a vibrating screen furnished with a magnet to remove extraneous matter-like pieces of wood and metal (e.g. fish hooks) before entering the hammer mill. The ground meal is automatically weighed out in bags that are closed and stored. The press liquor then passes through a buffer tank before separation into oil, "stick" water, and fine sludge in a centrifuge. The oil passes through a buffer tank before water and sludge impurities are removed (polishing) in the oil separator. After polishing, the oil often passes through an inspection tank before storage in the oil tank [35].

Another possibility for extracting lipids from fatty waste materials is by using an organic solvent, such as *n*-hexane. For example, Nebel and Mittelbach [72] tested nine solvents for extracting fat from meat and bone meal, obtaining about 15% fat with all solvents, but *n*-hexane was found to be the most suitable solvent to perform the extraction, because it is relatively cheap and has a low boiling point. The fat was then converted to methyl esters via a two-step process, whose quality was according to the European specification for biodiesel (EN 14214) except the cold-temperature behaviour and the oxidation stability. Oliveira and Bechtel [74] described a solvent extraction procedure using a 2:3 solution of isopropyl alcohol/hexane (99.9% purity) for extracting lipids from salmon's by-products including heads, viscera, frames, and skin.

2.2 Pre-treatment of Waste Oils and Fats

When dealing with high acidity feedstocks, in particular waste frying oils or animal fats from the meat or fish processing industry, one needs to perform a pre-treatment to guarantee that the transesterification reaction is performed in an efficient way and

that the quality of the biodiesel obtained follows all the applicable norms such as the EN 14214. Also, it is important to know their characteristics and the presence of contaminants that reduce the efficiency and effectiveness of the alkali-catalyzed transesterification.

For the removal of contaminants, of special concern is the presence of moisture that has a strong negative influence in the transesterification reaction. Water content of waste oils and animal fats may vary considerably depending on the origin. Rice et al. [81] reported a range of 1–5% (w/w) of water contents in waste frying oils. The presence of water inhibits the esterification and transesterification reactions, favours the hydrolysis of triglycerides and FFA, lowers the esters yield, and renders the ester and glycerol separation difficult [7, 18]. If the water concentration is greater than 0.5%, the ester conversion rate may drop below 90% [19]. Water also promotes soap formation in the presence of the alkali catalysts, increasing catalyst consumption and diminishing its efficiency. The water content in the feedstock should be lower than 0.06% (w/w) [64, 81]. Heating the waste frying oil or tallow over 100°C, to about 120°C, can boil off any excess water present in the feedstock. For other contaminants, other strategies should be employed in a case-by-case scenario.

The waste frying oils may have other impurities such as solid particles resulting from the food frying and sodium chloride that is added to the fried food. Depending on the feedstock characteristics, the separation of these solid particles may be accomplished by filtration, pressing, or centrifugation. The presence of chlorides may cause corrosion problems in the process equipment and piping system.

The acid value of oil is another important parameter to be determined, since it allows one to evaluate which is the most adequate method to produce biodiesel. For example, depending on the oil acidity, one- or two-step process can be used, where in a first step, the level of FFA is reduced to below 3% by acid-catalyzed esterification with methanol as reagent and sulphuric acid as catalyst and, in a second step, triglycerides in product from the first step are transesterified with methanol by using an alkaline catalyst to produce methyl esters and glycerol [94].

The FFA content of waste frying oil and animal fats vary widely. Waste oils typically contain 2–7% (w/w) of FFA [95], while animal fats may contain 15% FFA but can be as high as 40% [18, 93, 94]. In order to maximize the methyl esters yield, Freedman et al. [39] proposed to use vegetable oils with a FFA content lower than 0.5% (w/w) in order to not affect the yield of transesterification reaction. Rice et al. [81] reported that a reduction of FFA from 3.6 to 0.5% increased yields from 73 to 87%. Canakci and Van Gerpen [19] referred that a FFA level above 5% can lower the ester conversion rate below 90%. A study from the Sustainable Community Enterprises [85] concluded that due to its high acidity, salmon oil requires an esterification pre-treatment to be possible to perform the transesterification

In the presence of FFA and moisture, saponification reactions occur because the fatty acids react with the catalyst to produce soaps, decreasing the methyl esters yield, or even inhibiting the transesterification reaction. Even in small amounts, these contaminants can reduce the reaction rate by orders of magnitude [18]. Moreover, the formation of soap consumes catalyst and causes emulsions to be formed, which limits the mass transfer between phases, significantly reducing the

chemical reaction rate and the selectivity to biodiesel. This further complicates the separation of phases after the reaction completion and makes it difficult to recover and purify biodiesel [7].

The equations (1) and (2) represent, respectively, the saponification of FFA and esters.

$$\underset{\text{FFA}}{\text{R}-\text{COOH}} + \underset{\text{Metalic alkoxide}}{\text{NaOH}} \xrightarrow{\text{heat}} \underset{\text{Salt}}{\text{R}-\text{COONa}} + \underset{\text{Water}}{\text{H}_2\text{O}} \quad (1)$$

$$\underset{\text{Ester}}{\text{R}-\text{COOR}'} + \underset{\text{Metalic alkoxide}}{\text{NaOH}} \xrightarrow{\text{water}} \underset{\text{Salt}}{\text{R}-\text{COONa}} + \underset{\text{Alcohol}}{\text{OH}-\text{R}'} \quad (2)$$

Aryee et al. [9] used FTIR and titrimetric analytical methods for FFA determination in fish oils extracted from salmon skin, concluding that the FFA content of Atlantic salmon skin lipids increased linearly from 0.6 to 4.5% within the 120 days it was stored at 20°C, as a result of auto-oxidation. Wu and Bechtel [96] also found that the FFA level in salmon heads and viscera increases with the storage time and temperature. From a practical point of view, this results show that at least the fish oils should be used immediately after their extraction, limiting somehow the utilization at a local scale or when the logistical networks are efficient.

Refined vegetable oils normally do not need a pre-treatment in order to produce biodiesel. However, the waste frying oils and the animal fats with high acidity (more than 2.5% w/w of FFA) need a pre-treatment to reduce their FFA content. This is normally done by acid-catalyzed esterification, using H_2SO_4 as catalyst and methanol as reagent in the proportions of 2.25 g of methanol and 0.05 g of sulphuric acid per each gram of FFA in oil. From the several approaches proposed in literature such as esterification and distillation refining method [99], Bianchi et al. [14] concluded that esterification is the most attractive to lower the FFA content of waste animal fat to 0.5% (from a typical range of 10 to 25%) using a solid acid ion-exchange resin as catalyst.

During esterification, the FFA are converted to methyl esters, but the triglycerides remain essentially unconverted to esters for low methanol to oil molar ratios and short reactor residence times [7, 29, 51, 60]. The esterification reaction can be represented as follows

$$\underset{\text{FFA}}{\text{R}-\text{COOH}} + \underset{\text{methanol}}{\text{CH}_3\text{OH}} \xrightarrow{\text{acid catalyst}} \underset{\text{esters}}{\text{R}-\text{COOCH}_3} + \underset{\text{water}}{\text{H}_2\text{O}} \quad (3)$$

Since water is formed as a by-product during esterification, it needs to be removed or the reaction will be quenched prematurely. One possible approach is to remove water while the reaction occurs, for example, using a membrane reactor. Another approach is to perform the reaction in two rounds with the removal of methanol, sulphuric acid, and water phase in between, followed by the addition of more fresh reactant to perform a second-round reaction driving it closer to completion [19–21, 94]. Zhang et al. [100] suggested the addition of glycerine after the second-round reaction to remove all the water from the oil stream, having the advantage of removing the acid catalyst which may cause neutralization of the alkali-catalyst during the transesterification reaction.

2.3 Biodiesel Production Processes

2.3.1 Alkali-Catalyzed Process

The alkali-catalyzed transesterification of triglycerides (1) is the process normally used for low amounts of FFA present in triglycerides (less than 2.5% w/w) since this reaction is very sensitive to the oil or fat purity, requiring in many cases pre-treatment steps. The pre-treated oil can then be transesterified with an alkali-catalyst to convert triglycerides into methyl esters.

As shown in (4), transesterification is a multiple reaction including three reversible steps in series, where triglycerides are converted to diglycerides, then diglycerides are converted to monoglycerides, and monoglycerides are converted to fatty acid alkyl monoester (biodiesel) and glycerol (by-product). Although several alcohols can be used in this reaction, such as ethanol, methanol, or butanol to obtain respectively, methyl, ethyl, or butyl esters, it is methanol that is most commonly used due to its low cost by comparison with the other alcohols. An excess of alcohol needs to be used (normally an alcohol to oil molar ratio of 6:1) at a reaction temperature of about 60°C, if methanol is used, or 70°C for ethanol [39]. The amount of catalyst used in the mixture is in the range of 0.5–1.0% (w/w), a higher amount may have as consequences gel formation and difficulty in separating glycerol. Generally, the transesterification reaction is affected by operating conditions such as alcohol/oil molar ratio, kind of alcohol (e.g. methanol, ethanol, propanol, or butanol), type and amount of catalysts, reaction time and temperature, and purity of reactants.

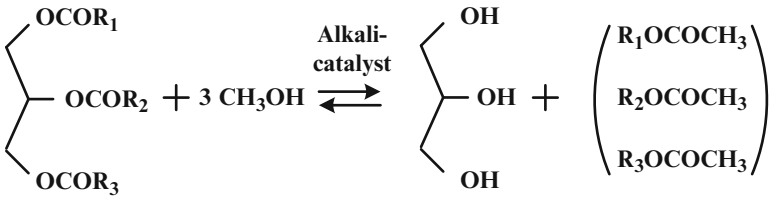

Triglycerides **Alcohol** **Glycerol** **Esters** (4)

After the chemicals are mixed for the transesterification, two essentially immiscible phases are formed: one non-polar containing triglycerides and esters, and the other polar containing glycerol and alcohol. As two immiscible phases are formed, the reactor vessels are intensely stirred to promote mass transfer [10]. Some emulsification also occurs due to saponification reaction since the alkalis catalyst is used [11]. For temperatures of 60 or 70°C, the conversion of the oil is complete in few hours [1].

Tashtoush et al. [91] performed experiments to determine the optimum conditions for converting animal fats into ethyl and methyl esters, concluding that absolute ethanol performs better than absolute methanol and that 50°C is the optimum temperature to perform the transesterification reaction, during 2 h maximum. Other authors have also devised different ways of using residual oils or fats with high FFA and moisture contents, for biodiesel production. For example, Alcantara et al. [3]

calculated the cetane index of waste frying oil and concluded that it is similar to that of fossil diesel fuel. Ma et al. [64] studied the effect of catalyst, FFA, and water in the transesterification of beef tallow, concluding that the presence of water has the most negative effect on the reaction conversion and should be kept beyond 0.06% (w/w), while FFA should be kept beyond 0.5% (w/w).

Piu [77] studied the production of biodiesel from waste animal fats, including the oil pre-treatment, biodiesel production, purification, and its final combustion in a diesel-powered generated for emissions determination, concluding that using 20/80 (v/v) of biodiesel/diesel blends has the better results in terms of NOx, CO, HC, and smoke emissions.

Alptekin and Canakci [5] studied the production of biodiesel from chicken fat extracted from chicken wastes (feathers, blood, offal, and trims) after the rendering process. These authors investigated the variables affecting the FFA level of chicken fats such as alcohol molar ratio, amount of acid catalyst, and reaction time by using a chicken fat with 13.45% FFA. The optimum esterification condition was found to be 20% (wt/wt) sulphuric acid and 40:1 of methanol:oil molar ratio, for a reaction time of 80 min at 60°C of temperature. For these conditions, the methyl ester yield was 87.4% after transesterification.

The alkali-catalyzed process suffers from some significant drawbacks, in particular the pronounced adverse effects of water, high acidity, and long reaction time in batch mode. Many options are being suggested and some are under development and even implementations to improve the process, in particular to be able to operate in continuous mode with reduced reaction time, and trying to reduce the operating costs, especially associated with the feedstocks consumption and with the biodiesel purification steps [11]. Some examples are listed bellow and some applications to waste fats are discussed in the next sub-sections

- Acid-catalyzed transesterification [56].
- Non-catalytic supercritical methanol or ethanol for the transesterification reaction [26, 58, 59, 65].
- Heterogeneous or Biological catalyzed process (inorganic chemical, enzymes, and living organisms) to avoid the need for the removal and recycling of the catalyst [16, 31, 54, 79].
- Transesterification with co-solvents to enhance the solubility of reactants, by diminishing the mixture polarity and increasing the reaction rate [15, 43].
- In situ transesterification [47].
- Microwave-assisted transesterification [61].
- Catalytic cracking [50].
- Ultrasonic reactors and cavitation reactors [32, 42].

2.3.2 Acid-Catalyzed Process

The usage of a strong acid instead of a strong base is better suited for high acidity feedstocks, a situation normally found in waste oils and fats, making it possible to

avoid the oil pre-treatment operation and providing high conversion rates with no soap formation [19, 49]. Nevertheless, it is seldom used due to its longer reaction times and higher temperatures required, when compared to the alkali-catalyzed process, and it is more corrosive to the process equipment [1, 19]. For example, Kulkarni and Dalai [56] report 88 and 95% conversion obtained, respectively, for 48 and 96 h reaction time.

Also, a higher methanol to oil molar ratio is needed to promote high equilibrium conversions of triglycerides to esters, which generally increases the production costs, due to an increase in the volume needed for the reactor and the separation of glycerol that becomes more difficult. Kulkarni and Dalai [56] report that 98% conversion is obtained for a methanol:oil molar ratio of 30:1 by comparison with a 87% conversion for a molar ratio of 6:1.

Among the several acid catalysts (e.g. sulphuric, sulfonic, phosphoric, or hydrochloric acid) that can be used, sulphuric acid is the most common. Zhang et al. [101] evaluated economically both the alkali-catalyzed and the acid-catalyzed process, concluding that though the first one, using virgin vegetable oil, has the lowest fixed capital cost, the second one, using waste frying oil, is more economically feasible overall.

Kulkarni and Dalai [56] present the effect of various parameters on the acid-catalyzed transesterification, showing that the FFA and moisture content of oils are the parameters that most affect the reaction conversion. For instance, with less than 0.5% water the conversion is above 90%, and for 3 or 5% of moisture the conversion is, respectively, 32 and 5%. The FFA effect is not so accentuated allowing one to obtain 90, 80, and 60% conversion for 5, 15, and 33% of FFA content, respectively.

Bhatti et al. [13] studied the effect of various parameters in the production of biodiesel from animal fats, concluding that the optimum conditions for 5 g of chicken and mutton tallow are, respectively, a temperature of 50 and 60°C, 1.25 and 2.5 g of H_2SO_4, and an oil:methanol molar ratio of 1:30 and 1:30, yielding $99.01 \pm 0.71\%$ and $93.21 \pm 5.07\%$ of methyl esters, after 24 h, in the presence of acid. Gas chromatographic analysis showed a total of 98.29 and 97.25% fatty acids in chicken and mutton fats, respectively.

2.3.3 Non-catalytic Supercritical Processes

Other interesting option for producing biodiesel from feedstocks with high concentration of impurities such as water and FFA is the transesterification of triglycerides with supercritical methanol, which is receiving a lot of attention [17, 58, 59]. This process is catalyst-free and it is able to obtain full conversion of the triglycerides in a matter of minutes [58], with the possibility of continuous operation mode [26].

The operation is also simpler, as the transesterification of triglycerides and methyl esterification of fatty acids occurs simultaneously without using any catalyst. Because no catalyst is used and has to be recovered, the downstream processing is much simpler, and soap-free glycerol can be obtained [89]. Other advantage this process presents is the insensitivity to the presence of impurities in the vegetable oil, such as water and FFA [59]. The presence of moisture is not only negligible, but it can also be advantageous in this process [6].

The reaction is carried out in supercritical methanol (or ethanol), in which feedstocks react with the alcohol under conditions of high pressure (above 100 atm) and high temperature (more than 276°C). At these conditions, the alcohol is in a supercritical gaseous state and the triglycerides are somewhat dissolved in a single phase. The reasons for this behaviour are not yet fully understood, but are certainly related to the high solubility of triglycerides in supercritical alcohol and solvent effects [65]. Also, some authors have observed a dependence on the type of alcohol and triglyceride used [4].

Notwithstanding its clear advantages over other processes, significant hurdles remain for the full scale implementation of supercritical production units. First of all, high temperatures and pressures are necessary to ensure that the alcohol is in supercritical state, requiring the utilization of special equipment designed to support these conditions. This will lead to high equipment and operational costs, making the process economics not so attractive when compared to other options. Also, the excess of methanol used in the reaction is much larger when compared to the conventional process; normally an alcohol/oil molar ratio of 42:1 is used, which needs to be recovered and recycled back to the reactor this way complicating the process design [58].

Alternatively, Cao et al. [23] proposed the supercritical methanol process, using propane as co-solvent, which decreases the reaction temperature and pressure, as well as the alcohol to oil molar ratio. This is because propane decreases the critical point of methanol allowing the supercritical reaction to be carried out under milder conditions than those of 424 atm and 350°C reported by Kusdiana and Saka [58]. In this case, the optimal reaction conditions are a temperature of 280°C, a pressure of 126 atm, an alcohol to oil molar ratio of 24:1, and propane to oil molar ratio of 0.05:1. At these conditions, 98% of oils are converted to biodiesel for a reaction time of 10 min. Kasteren and Nisworo [53] performed an economic analysis of this process, considering the industrial production of biodiesel from waste frying oil and concluded that it can compete with the existing alkali and acid-catalyzed processes.

2.3.4 Heterogeneous Catalyzed Process

A natural evolution in process development is the replacement of the homogeneous catalysis with a solid base catalyst, change that simplifies extensively the post-processing process. In particular, it makes it easier to operate in continuous mode, eases the catalyst separation and recycling after reaction, avoids the saponification problem, and yields a cleaner biodiesel product, a purer glycerol that can be more easily marketed.

Various types of heterogeneous catalysts are being considered and studied for biodiesel production, including titanium silicates, ion-exchange resins, and zeolite metal-supported catalysts, among others. Extensive reviews of the current status on the use of solid base catalysts can be found in Liu et al. [63] and Di Serio et al. [33]. Peng et al. [75] prepared, characterized, and studied a solid acid catalyst for its activity in the production of biodiesel from several feedstocks with a high FFA content, showing that heterogeneous catalysis is a worthy option to process those types of raw materials.

Heterogeneous catalysts such as zeolites and metals may also allow for the use of feedstocks with a high FFA content [16, 31, 54]. However, some scientific and technical barriers persist relatively to their application at industrial-scale. For instance, Albuquerque et al. [2] concluded that the catalyst activity strongly depends on the metal composition of the oxides used, and new materials with well-defined structures, high surface area, and adequate basic or acid properties have yet to be developed. Although many of the solid catalysts proposed in literature for biodiesel production have good catalytic performances, they require high temperatures and pressure to work properly. Also, it is necessary to address the questions of deactivation, reusability, and regeneration of the catalysts in practical conditions to assess their real potential for using in commercial applications. As heterogeneous catalyzed processes have advantages over homogeneous catalyzed and are easier to operate, more commercial applications will certainly be introduced in the near future with important impact on the biodiesel production.

2.3.5 Biological Catalyzed Process

Biological catalysts for biodiesel production, including both enzymes and living organisms, are considered to be one of the most promising alternatives for future use in biodiesel production [38, 79]. They can be implemented either in solution or supported (e.g. in biological films or in packed beds). An advantage of enzymes is that they do not require the utilization of nutrients. An advantage of living organisms is that they can be genetically engineered to improve their performance, resilience, and capacity to operate in harsher conditions.

Lipases obtained from different biological sources are examples of enzymes that can be used to perform the transesterification reaction and that have shown a good tolerance to the oil FFA content [95]. Kaieda et al. [52] show that different enzymes have different capacities and report that certain lipases can be used for biodiesel production even if the oil has high water and methanol contents.

Although extensive research has been devoted to this area, the use of bio-catalysts for biodiesel production is still at the laboratory stage [1, 79, 86, 87]. They can be more efficient, selective, require a lower reaction temperature, and produce less side products or wastes, when compared with other types of catalyzed processes, but the reaction rates are much lower than for the conventional process, normally taking several hours (8–12 h) for similar conversions.

Some of the main problems include the difficulty in determining:

- What are the best enzymes or microorganisms to perform the reaction, depending on the feedstocks characteristics and on the impurities that may exist?
- What are the optimum reaction conditions, in particular what are the optimal molar ratio of reactants, solvents to be used, temperature, and water content?
- How the enzymes will be used, if supported or in solution?
- How to recover and reuse the enzymes?
- How to avoid the enzymes' deactivation, or the living organisms' death?

Some studies can be found in literature addressing some of the problems listed above. For example, Shimada et al. [87] concluded that the best way to avoid the inhibition or deactivation of enzymes and maintain the enzyme activity for longer periods of time is their stepwise addition to the reaction mixture, in order to maintain the oil/methanol ratio at certain optimal levels. Although the addition of co-solvents appears in some cases to have a positive effect on the enzyme stability [1], there is still some work to be done in order to identify the most adequate solvents and how they influence the ongoing reaction.

2.3.6 Transesterification Reaction Using Co-solvents

The use of co-solvents such as dimethyl ether (DME), diethyl ether (DEE), methyl tert-butyl ether (MTBE) and tetra-hydro-furan (THF) has attracted much attention since they allow one to increase the reaction rate, under milder conditions, by diminishing the mixture polarity [15, 43].

For example, the use of co-solvents and high mixing intensity for the reaction reduces the need to use higher temperatures to enhance the solubility among reactants and the mass transfer between both phases [11]. Moreover, transesterification in supercritical methanol, employing propane and CO_2 as co-solvents, was also developed [23, 48, 84, 98]. Nevertheless, the selection of the appropriate co-solvent and the mixing intensity are critical factors contributing to the correct operation and performance of the reaction system.

Sabudak and Yildiz [83] studied biodiesel production from waste frying oils by applying three different processes: a one-step alkali-catalyzed transesterification, a two-step alkali-catalyzed transesterification, and a two-step acid-catalyzed transesterification followed by alkali-catalyzed transesterification. For each reaction, these authors added THF as a co-solvent concluding that the effect of THF on reaction yield is not significant, and instead of using the co-solvent, it is more economical to improve the mixing ability of the reactor.

2.3.7 In Situ Transesterification

In situ transesterification is another possibility that simplifies or even eliminates the need to perform the pre-processing of feedstocks, in particular the oil extraction and refining steps. The transesterification reaction is directly performed in the macerated oil seeds, such as soybeans flakes or animal fats containing the lipidic material [24, 40, 70, 88, 102].

Although the in situ transesterification was proposed some years ago, it has not yet been used extensively. Reasons for this may be the large molar ratios between oil and alcohol that are necessary to obtain full oil conversion and the dependence on the seeds characteristics and on its oil content [88]. This process may seem simple, but it is still not fully worked out for practical applications and it is not economically efficient.

Haas et al. [47] investigated biodiesel production by in situ transesterification using as feedstocks corn dried grains (a by-product of ethanol production) and meat and bone meal (a by-product of animal rendering). As a result, these authors achieved almost the maximum theoretical transesterification conversion (91.1%) at ambient pressure and 35°C of temperature. For a higher temperature of 55°C, no significant increase in the conversion was achieved. Partial drying of the corn grains contributed to reduce the methanol requirements to achieve a high degree of transesterification. For meat and bone meal, drying was not required to achieve a high degree (93.3%) of transesterification.

2.3.8 Microwave-Assisted Transesterification

Microwave-assisted transesterification is another possibility for biodiesel production from lipidic feedstocks with high acidity [61]. Refaat et al. [80] compared both microwave-assisted and the conventional process for producing biodiesel from high acidity feedstocks, concluding that reaction time is reduced by about 97% and separation time by about 94% using microwave irradiation.

Perin et al. [76] compared the acid-catalyzed and alkali-catalyzed transesterification assisted by microwave irradiation concluding that the best results are obtained under basic conditions, i.e. the reaction takes place in 5 min, and 95% conversion is obtained. Azcan and Danisman [12] have considered microwave heating to perform the transesterification of rapeseed oil, showing that increased yields and reduced reaction times are possible.

2.3.9 Catalytic Cracking

A variant of thermal cracking is the catalytic cracking, extensively used in the petrochemical industry to produce a significant percentage of the fossil-derived fuel currently used. This possibility has also been pursued for the production of biofuels from a wide variety of feedstocks, especially from low-value triglyceride-based biomass. The reaction takes place in fluid catalytic cracking (FCC) units where triglyceride molecules are transformed into water, CO_2, CO, and a mixture of hydrocarbons, some of the aromatic type [68]. The employment of a catalyst permits the utilization of milder conditions of temperature and pressure, with a better control of the final products [27, 92].

Hua et al. [50] studied the catalytic cracking transformation of vegetable oils and animal fats in the laboratory. The results show that they can be used as FCC feed singly or co-feeding with vacuum gas oil, which can give high yield (by mass) of liquefied petroleum gas (LPG), C2–C4 olefins, for example, 45% LPG, 47% C2–C4 olefins, and 77.6% total liquid yield produced with palm oil cracking. Co-feeding with vacuum gas oil gives a high yield of LPG (39.1%) and propylene (18.1%).

Different combinations of reactors and catalysts can be used, as for example pillared clays, alumina metal-supported catalysts, zeolites, among others. Also, the huge experience gathered in the petrochemical industry can be relevant in the development and implementation of cracking processes for biodiesel production.

2.4 Post-processing

After the transesterification reaction, the post-processing steps needed to purify biodiesel according to the existing regulations and norms are the same as those involved in the biodiesel production from currently edible vegetable oils. Although the final product composition in terms of esters may be different depending on the feedstocks used, their physical properties are similar and no significant differences are expected between the two variants.

After the reaction is finished, the mixture is allowed to separate into an upper layer of methyl esters and a lower layer of glycerol diluted with methanol. Glycerol is removed by allowing the two phases to form and settle. Then, any unreacted alcohol is air-stripped or vacuum-distilled away from the esters phase and recycled back to the reactor.

Depending on the process, water can be used to wash catalyst residues and sodium soaps from the methyl esters. Moreover, small amounts of concentrated phosphoric acid (H_3PO_4) can be added to the raw methyl esters to break down catalyst residues and sodium soaps. Predojevic [78] studied different purification steps of biodiesel obtained from waste frying oils, by a two-step alkali-catalyzed transesterification reaction, concluding that the best results are obtained when using silica gel and phosphoric acid treatments (with a yield of 92%) and the lowest yields (89%) are obtained using hot water. Also, Sabudak and Yildiz [83] applied three different purification methods to biodiesel produced from waste frying oils (water washing with distilled water, dry wash with addition of magnesol, and an ion-exchange resin) concluding that the most effective one is the ion-exchange resin.

The same situation occurs for the storage of biodiesel, where potential problems of decomposition may occur. For example, Lin and Lee [62] studied the oxidative stability of marine fish-oil biodiesel showing that the addition of antioxidant significantly retards the fuel deterioration over time, although it increases the kinematic viscosity and carbon residue at the beginning of the storage period. These authors also concluded that the operating temperature is a dominant factor in the deterioration of the fuel characteristics.

3 Economic and Environmental Considerations

As stated above, the conversion to biodiesel of waste oils and fats from the meat and fish processing industries represents an opportunity to valorize a residue and obtain a higher value product (biodiesel). In many situations, the adequate disposal of residual oils and fats represents an operational cost, as they cannot be burnt directly in a boiler without special equipment. Thus, from this point of view, there is an economic incentive to valorize those residues.

However, depending on the total quantity of residual oils and fats generated, different approaches have to be considered. If the total amount is small, as it is the case of the waste frying oils generated in restaurants, it will be easier to make the selective

collection of those materials to be processed in a centralized production facility. If a good logistic system is developed and properly implemented, and incentives are available for the residue producers, this is proved to be a good option [8], applicable even for the small- and medium-sized companies of the meat and fish processing industries. This situation may change if small and compact units for the production of small quantities of biodiesel from a wide variety of feedstocks become available, although the costs of energy and raw materials, and the hazards involved in the manipulation of dangerous chemicals may render this possibility impracticable.

However, if the quantity of residues generated is large, the option of having an in-house facility for the production of biodiesel may be viable from an economic point of view. In any case, the reduction in the consumption of fuel by the company, either by the utilization of biodiesel or by burning of the glycerol produced in the process, must be compared with the investment in equipment and operational costs due to the consumption of materials and energy necessary to produce biodiesel. With the increase in price of fossil fuels, this option is expected to become more and more attractive. It is also relevant for companies operating close by or even interconnected, that generate large quantities of residual fats, and that may be interested on a common processing plant to take care of all the fat residues generated in their activities.

From an environmental point of view, the valorization of residual oils and fats to biodiesel production makes sense. This corresponds to the reutilization of a waste material originated from a renewable source, thus reducing the consumption of non-renewable fossil fuels. Although at a first glance there is a reduction in greenhouse gas emissions, in particular of carbon dioxide [71], the actual reduction depends on how the residues are collected and transported to the production site. To minimize those emissions, the logistical network should be properly optimized, for example, by giving the residue generators special containers for storing the waste fats and defining the more adequate collection routes. Although for in-house biodiesel production facilities this problem does not occur, additional savings may be accomplished through an adequate process optimization and integration.

Moreover, with the advent of more stringent limits for greenhouse gas emissions and the development of trading schemes for carbon emissions, the production of biodiesel from residual oils and fats can be a good form to combine the environmental and the economical aspects to one's advantage. However, the current legislation and regulations still need to be improved or even created to be able to have a clear vision of the trade-offs involved on these decisions.

4 Conclusions

This article presents and discusses the main questions regarding the utilization of residual oils and fats for biodiesel production. Some key aspects are identified and strategies to deal with them are presented. Among them, the high content of FFA and moisture in waste frying oils and animal fats, as compared to fresh edible oils, makes the alkaline-catalyzed transesterification reaction to be less efficient for

biodiesel production. A pre-treatment method suitable to handle this type of feedstocks is presented. Also, more efficient and robust production processes are presented that are able to use feedstocks with the characteristics normally encountered in waste fats.

As the global demand for biodiesel increases and the pressure to be more environmental friendly, yet maintaining market competitiveness, increases, more and more waste residues will be seen as valuable raw materials. Besides helping companies to fulfil their goals, policy targets defined at governmental and regional levels may be easier to reach.

References

1. Akoh CC, Chang SW, Lee GC, Shaw JF (2007) Enzymatic approach to biodiesel production. J Agric Food Chem 55:8995–9005
2. Albuquerque MCG, Santamaría-González J, Mérida-Robles JM, Moreno-Tost R, Rodríguez-Castellón E, Jiménez-López A, Azevedo DCS, Cavalcante CL, Maireles-Torres P (2008) MgM (M=Al and Ca) oxides as basic catalysts in transesterification processes. Appl Catal Gen 347(2):162–168
3. Alcantara R, Amores J, Canoira L, Fidalgo E, Franco MJ, Navarro A (2000) Catalytic production of biodiesel from soy-bean oil, used frying oil and tallow. Biomass Bioenergy 18: 515–527
4. Alonzo DEL (2007) Heterogeneous catalysis and biodiesel forming reactions. PhD Thesis in Chemical Engineering, Graduate School of Clemson University
5. Alptekin E, Canakci M (2010) Optimization of pretreatment reaction for methyl ester production from chicken fat. Fuel 89:4035–4039
6. Al-Zuhair S (2007) Production of biodiesel: possibilities and challenges. Biofuels Bioprod Bior 1(1):57–66
7. Aranda DAG, Santos RTP, Tapanes NCO, Ramos ALD, Antunes OAC (2008) Acid-catalyzed homogeneous esterification reaction for biodiesel production from palm fatty acids. Catal Lett 122:20–25
8. Araujo VKWS, Hamacher S, Scavarda LF (2010) Economic assessment of biodiesel production from waste frying oils. Bioresour Technol 101:4415–4422
9. Aryee ANA, van de Voort FR, Simpson BK (2009) FTIR determination of free fatty acids in fish oils intended for biodiesel production. Process Biochem 44:401–405
10. Ataya F (2008) Mass transfer limitations in the transesterification of canola oil to fatty acid methyl ester. PhD Thesis in Chemical Engineering, University of Ottawa
11. Ataya F, Dube MA, Ternan M (2008) Transesterification of canola oil to fatty acid methyl ester (FAME) in a continuous flow liquid-liquid packed bed reactor. Energy Fuel 22:3551–3556
12. Azcan N, Danisman A (2008) Microwave assisted transesterification of rapeseed oil. Fuel 87:1781–1788
13. Bhatti HN, Hanif MA, Qasim M, Ata-ur-Rehman (2008) Biodiesel production from waste tallow. Fuel 87(13–14):2961–2966
14. Bianchi CL, Boffito DC, Pirola C, Ragaini V (2010) Low temperature de-acidification process of animal fat as a pre-step to biodiesel production. Catal Lett 134:179–183
15. Boocock DGB, Konar SK, Mao V, Sidi H (1996) Fast one-phase oil-rich processes for the preparation of vegetable oil methyl esters. Biomass Bioenergy 11(1):43–50
16. Brito A, Borges ME, Arvelo R, Garcia F, Diaz MC, Otero N (2007) Reuse of fried oil to obtain biodiesel: Zeolites Y as a catalyst. Int J Chem React Eng 5:Article A104

17. Bunyakiat K, Makmee S, Sawangkeaw R, Ngamprasertsith S (2006) Continuous production of biodiesel via transesterification from vegetable oils in supercritical methanol. Energy Fuel 20:812–817
18. Canakci M (2007) The potential of restaurant waste lipids as biodiesel feedstocks. Bioresour Technol 98(1):183–190
19. Canakci M, Van Gerpen J (1999) Biodiesel production via acid catalysis. Trans ASAE 42(5):1203–1210
20. Canakci M, Van Gerpen J (2001) Biodiesel production from oils and fats with high free fatty acids. Trans Am Soc Agric Eng 44(6):1429–1436
21. Canakci M, Van Gerpen J (2003) A pilot plant to produce biodiesel from high free fatty acid feedstocks. Trans Am Soc Agric Eng 46(4):945–954
22. Canoira L, Rodrıguez-Gamero M, Querol E, Alcantara R, Lapuerta M, Oliva F (2008) Biodiesel from low-grade animal fat: production process assessment and biodiesel properties characterization. Ind Eng Chem Res 47:7997–8004
23. Cao W, Han H, Zhang J (2005) Preparation of biodiesel from soybean oil using supercritical methanol and co-solvent. Fuel 84:347–351
24. Carrapiso AI, Timón ML, Petrón MJ, Tejeda JF, García C (2000) In situ transesterification of fatty acids from Iberian pig subcutaneous adipose tissue. Meat Sci 56:159–164
25. CETESB (2006) Graxarias—Processamento de materiais de matadouros e frigoríficos bovinos e suínos. Guia técnico ambiental de graxarias (Série P+L), Governo de São Paulo, 2006
26. Chen W, Wang C, Ying W, Wang W, Wu Y, Zhang J (2009) Continuous production of biodiesel via supercritical methanol transesterification in a tubular reactor. Part 1: thermophysical and transitive properties of supercritical methanol. Energy Fuel 23:526–532
27. Chew TL, Bhatia S (2009) Effect of catalyst additives on the production of biofuels from palm oil cracking in a transport riser reactor. Bioresour Technol 100:2540–2545
28. Chiou BS, El Mashad HM, Avena-Bustillos RJ, Dunn RO, Bechtel PJ, McHugh TH, Imam SH, Glenn GM, Orts WJ, Zhang R (2008) Biodiesel from waste salmon oil. Trans ASABE 51(3):797–802
29. Chongkhong S, Tongurai C, Chetpattananondh P (2009) Continuous esterification for biodiesel production from palm fatty acid distillate using economical process. Renew Energy 34(4):1059–1063
30. Chua CBH, Lee HM, Choong JS (2010) Low life cycle emissions and energy study of biodiesel derived from waste cooking oil and diesel in Singapore. Int J Life Cycle Ass 15:417–423
31. Chung K-H, Chang D-R, Park B-G (2008) Removal of free fatty acid in waste frying oil by esterification with methanol on zeolite catalysts. Bioresour Technol 99:7438–7443
32. Deshmane VG, Gogate PR, Pandit AB (2009) Ultrasound-assisted synthesis of biodiesel from palm fatty acid distillate. Ind Eng Chem Res 16(3):345–350
33. Di Serio M, Tesser R, Pengmei L, Santacesaria E (2008) Heterogeneous catalysts for biodiesel production. Energy Fuel 22:207–217
34. FAO (2007) Food and Agricultural Organization of the United Nations. The state of world fisheries and aquaculture 2006. FAO, Rome. ftp://ftp.fao.org/docrep/fao/009/a0699e/a0699e.pdf
35. FAO (2010) The production of fish meal and oil. Fisheries and Aquaculture Department of FAO Corporate Document Repository. http://www.fao.org/docrep/003/x6899e/x6899e04.html
36. Ferroli PCM, Neto MF, Filho NC, Castro JEE (2001) Fábricas de Subprodutos de Origem Animal: a Importância do Balanceamento das Cargas dos Digestores de Vísceras. Produção 10(2):5–20
37. Firestone D, Reina RJ (1986) Authenticity of vegetable oils. In: Hamilton RJ, Rossel JB (eds) Analysis of oils and fats. Elsevier Applied Science Publishers, New York
38. Fjerbaek L, Christensen KV, Norddahl B (2009) A review of the current state of biodiesel production using enzymatic transesterification. Biotechnol Bioeng 102(5):1298–1315
39. Freedman B, Pryde EH, Mounts TL (1984) Variables affecting the yields of fatty esters from transesterified vegetable oils. JAOCS 61:1638–1643
40. Georgogianni KG, Kontominas MG, Pomonis PJ, Avlonitis D, Gergis V (2008) Alkaline conventional and in situ transesterification of cottonseed oil for the production of biodiesel. Energy Fuel 22(3):2110–2115

41. Godiganur S, Murthy CS, Reddy RP (2010) Performance and emission characteristics of a Kirloskar HA394 diesel engine operated on fish oil methyl esters. Renew Energy 35:355–359
42. Gogate PR, Kabadi AM (2009) A review of applications of cavitation in biochemical engineering/biotechnology. Biochem Eng J 44:60–72
43. Guan G, Sakurai N, Kusakabe K (2009) Synthesis of biodiesel from sunflower oil at room temperature in the presence of various cosolvents. Chem Eng J 146:302–306
44. Gui MM, Lee KT, Bhatia S (2008) Feasibility of edible oil vs. non-edible oil vs. waste edible oil as biodiesel feedstock. Energy 33:1646–1653
45. Gunasekera RM, Turoczy NJ, De Silva SS, Gooley GJ (2002) An evaluation of the suitability of selected waste products in feeds for three fish species. J Aquat Food Prod Technol 11(1): 57–78
46. Guru M, Artukoglu BD, Keskin A, Koca A (2009) Biodiesel production from waste animal fat and improvement of its characteristics by synthesized nickel and magnesium additive. Energy Convers Manage 50:498–502
47. Haas MJ, Scott KM, Foglia TA, Marmer WN (2007) The general applicability of in situ transesterification for the production of fatty acid esters from a variety of feedstocks. JAOCS 84:963–970
48. Han H, Cao W, Zhang J (2005) Preparation of biodiesel from soybean oil using supercritical methanol and CO_2 as co-solvent. Process Biochem 40(9):3148–3151
49. Han M, Yi W, Wu Q, Liu Y, Hong Y, Wang D (2009) Preparation of biodiesel from waste oils catalyzed by a Brønsted acidic ionic liquid. Bioresour Technol 100:2308–2310
50. Hua T, Chunyi L, Chaohe Y, Honghong S (2008) Alternative processing technology for converting vegetable oils and animal fats to clean fuels and light olefins. Chin J Chem Eng 16(3):394–400
51. Issariyakul T, Kulkarni MG, Dalai AK, Bakhshi NN (2007) Production of biodiesel from waste fryer grease using mixed methanol/ethanol system. Fuel Process Technol 88(5):429–436
52. Kaieda M, Samukawa T, Kondo A, Fukuda H (2001) Effect of methanol and water contents on production of biodiesel, fuel from plant oil catalyzed by various lipases in a solvent-free system. J Biosci Bioeng 91(1):12–15
53. Kasteren JMN, Nisworo AP (2007) A process model to estimate the cost of industrial scale biodiesel production from waste cooking oil by supercritical transesterification. Resour Conserv Recy 50:442–458
54. Kiss A, Omota F, Dimian A, Rothenberg G (2006) The heterogeneous advantage: biodiesel by catalytic reactive distillation. Top Catal 40:141–150
55. Kotzamanis YP, Alexis MN, Andriopoulou A, Castritsi-Cathariou I, Fotis G (2001) Utilization of waste material resulting from trout processing in gilthead bream (*Sparus aurata* L.) diets. Aquacult Res 32:288–295
56. Kulkarni MG, Dalai AK (2006) Waste cooking oils—an economical source for biodiesel: a review. Ind Eng Chem Res 45:2901–2913
57. Kumar A, Sharma S (2008) An evaluation of multipurpose oil seed crop for industrial uses (*Jatropha curcas* L.): a review. Ind Crops Prod 28:1–10
58. Kusdiana D, Saka S (2001) Kinetics of transesterification in rapeseed oil to biodiesel fuels as treated in supercritical methanol. Fuel 80:693–698
59. Kusdiana D, Saka S (2004) Effects of water on biodiesel fuel production by supercritical methanol treatment. Bioresour Technol 91:289–295
60. Lepper H, Friesenhagen L (1986) Process for the production of fatty acid esters of short-chain aliphatic alcohols from fats and/or oils containing free fatty acids. US Patent 4608202
61. Lertsathapornsuk V, Pairintra R, Aryusuk K, Krisnangkura K (2008) Microwave assisted in continuous biodiesel production from waste frying palm oil and its performance in a 100 kW diesel generator. Fuel Process Technol 89:1330–1336
62. Lin C-Y, Lee J-C (2010) Oxidative stability of biodiesel produced from the crude fish oil from the waste parts of marine fish. J Food Agric Environ 8(2):992–995
63. Liu Y, Lotero E, Goodwin JG Jr, Lu C (2007) Transesterification of triacetin using solid Brønsted bases. J Catal 246:428–433

64. Ma F, Clements LD, Hanna MA (1998) The effects of catalyst, free fatty acids, and water on transesterification of beef tallow. Trans ASAE 41(5):1261–1264
65. Madras G, Kolluru C, Kumar R (2004) Synthesis of biodiesel in supercritical fluids. Fuel 83:2029–2033
66. Mata TM, Martins AA, Caetano NS (2010) Microalgae for biodiesel production and other applications: a review. Renew Sust Energy Rev 14:217–232
67. Mata TM, Cardoso N, Ornelas M, Neves S, Caetano NS (2010) Sustainable production of biodiesel from tallow, lard and poultry and its quality evaluation. In: Buratti SS (ed) Chemical engineering transactions, vol 19. AIDIC Servizi Srl, pp 13–18
68. Melero JA, Clavero MM, Calleja G, Miravalles AGR, Galindo T (2010) Production of biofuels via the catalytic cracking of mixtures of crude vegetable oils and nonedible animal fats with vacuum gas oil. Energy Fuel 24:707–717
69. Mittelbach M, Pelkmans L, Rice B (2000) Waste oils and fats as biodiesel feedstocks: an assessment of their potential in the EU, ALTENER Program, NTB-NETT Phase IV, Task 4 Final Report, Teagasc, Agriculture and Food Development Authority, Crops Research Centre, Oak Park, Carlow, Ireland
70. Mondala A, Liang K, Toghiani H, Hernandez R, French T (2009) Biodiesel production by in situ transesterification of municipal primary and secondary sludges. Bioresour Technol 100: 1203–1210
71. NBB (2010) Biodiesel—America's First Advanced Biofuel, National Biodiesel Board (NBB). http://www.biodiesel.org/tools/calculator/default.aspx?AspxAutoDetectCookieSupport=1
72. Nebel BA, Mittelbach M (2006) Biodiesel from extracted fat out of meat and bone meal. Eur J Lipid Sci Technol 108:398–403
73. Noureddini H, Zhu D (1997) Kinetics of transesterification of soybean oil. J Am Oil Chem Soc 74(11):1457–1463
74. Oliveira ACM, Bechtel PJ (2005) Lipid composition of Alaska pink salmon (*Oncorhynchus gorbuscha*) and Alaska walleye pollock (*Theragra chalcogramma*) byproducts. J Aquat Food Prod Technol 14(1):73–91
75. Peng B-X, Shu Q, Wang J-F, Wang G-R, Wang D-Z, Han M-H (2008) Biodiesel production from waste oil feedstocks by solid acid catalysis. Process Saf Environ Protect 86:441–447
76. Perin G, Álvaro G, Westphal E, Viana LH, Jacob RG, Lenardão EJ, D'Oca MGM (2008) Transesterification of castor oil assisted by microwave irradiation. Fuel 87:2838–2841
77. Piu KC (2001) Study on a biodiesel fuel produced from restaurant waste animal fats. Master Thesis, University of Hong Kong
78. Predojevic ZJ (2008) The production of biodiesel from waste frying oils: a comparison of different purification steps. Fuel 87:3522–3528
79. Ranganathan SV, Narasimhan SL, Muthukumar K (2008) An overview of enzymatic production of biodiesel. Bioresour Technol 99:3975–3981
80. Refaat AA, El Sheltawy ST, Sadek KU (2008) Optimum reaction time, performance and exhaust emissions of biodiesel produced by microwave irradiation. Int J Environ Sci Technol 5(3):315–322
81. Rice B, Frohlich A, Leonard R, Korbitz W (1997) Bio-diesel production based on waste cooking oil: promotion of the establishment of an industry in Ireland, Final Report, ALTENER CONTRACT No. XVII/4.1030/AL/77/95/IRL
82. Robertson GP, Dale VH, Doering OC, Hamburg SP, Melillo JM, Wander MM, Parton WJ, Adler PR, Barney JN, Cruse RM, Duke CS, Fearnside PM, Follett RF, Gibbs HK, Goldemberg J, Mladenoff DJ, Ojima D, Palmer MW, Sharpley A, Wallace L, Weathers KC, Wiens JA, Wilhelm WW (2008) Sustainable biofuels redux. Science 322(5898):49–50
83. Sabudak T, Yildiz M (2010) Biodiesel production from waste frying oils and its quality control. Waste Manag 30:799–803
84. Sawangkeaw R, Bunyakiat K, Ngamprasertsith S (2007) Effect of co-solvents on production of biodiesel via transesterification in supercritical methanol. Green Chem 9(6):679–685
85. SCE (2007) A feasibility study for fish oil biodiesel production. Final Report prepared by Sustainable community enterprises (SCE) for Clayoquot Biosphere Trust, Vancouver Island, BC, Canada, November

86. Shaw JF, Chang SW, Lin SC, Wu TT, Ju HY, Akoh CC, Chang RH, Shieh CJ (2008) Continuous enzymatic synthesis of biodiesel with Novozym 435. Energy Fuel 22:840–844
87. Shimada Y, Watanabe Y, Sugihara A, Tominaga Y (2002) Enzymatic alcoholysis for biodiesel fuel production and application of the reaction to oil processing. J Mol Catal B: Enzym 17:133–142
88. Siler-Marinkovic S, Tomasevic A (1998) Transesterification of sunflower oil in situ. Fuel 77(12):1389–1391
89. Soetaert W, Vandamme EJ (2009) Biofuels. Wiley, Chichester
90. Suwannakarn K (2008) Biodiesel production from high free fatty acid content feedstocks. PhD Thesis in Chemical Engineering, Clemson University
91. Tashtoush GM, Al-Widyan MY, Al-Jarrah MM (2004) Experimental study on evaluation and optimization of conversion of waste animal fat into biodiesel. Energy Convers Manage 45:2697–2711
92. Twaiq FAA, Mohamad AR, Bhatia S (2004) Performance of composite catalysts in palm oil cracking for the production of liquid fuels and chemicals. Fuel Process Technol 85:1283–1300
93. Van Gerpen J (2005) Biodiesel processing and production. Fuel Process Technol 86: 1097–1107
94. Van Gerpen JV, Shanks B, Pruszko R, Clements D, Knothe G (2004) Biodiesel Production Technology, National Renewable Energy Laboratory, NREL/SR-510-36244, Colorado, USA
95. Watanabe Y, Shimada Y, Sugihara A, Tominaga Y (2001) Enzymatic conversion of waste edible oil to biodiesel fuel in a fixed-bed bioreactor. J Am Oil Chem Soc 78(7):703–707
96. Wu TH, Bechtel PJ (2008) Salmon by-product storage and oil extraction. Food Chem 111(4):868–871
97. Wyatt VT, Hess MA, Dunn RO, Foglia TA, Haas MJ, Marmer WN (2005) Fuel properties and nitrogen oxide emission levels of biodiesel produced from animal fats. JAOCS 82(8):585–591
98. Yin J-Z, Xiao M, Song J-B (2008) Biodiesel from soybean oil in supercritical methanol with co-solvent. Energy Convers Manage 49:908–912
99. Yuan X, Liu J, Zeng G, Shi J, Tong J, Huang G (2008) Optimization of conversion of waste rapeseed oil with high FFA to biodiesel using response surface methodology. Renew Energy 33:1678–1684
100. Zhang Y, Dubé MA, McLean DD, Kates M (2003) Biodiesel production from waste cooking oil: 1. Process design and technological assessment. Bioresour Technol 89:1–16
101. Zhang Y, Dubé MA, McLean DD, Kates M (2003) Biodiesel production from waste cooking oil: 2. Economic assessment and sensitivity analysis. Bioresour Technol 90:229–240
102. Zheng S, Kate M, Dubé MA, McLean DD (2006) Acid-catalyzed production of biodiesel from waste frying oil. Biomass Bioenergy 30:267–272

Chapter 29
One-Step Conversion of Algal Biomass to Biodiesel with Formation of an Algal Char as Potential Fertilizer

E. Adair Johnson, Zhanfei Liu, Elodie Salmon, and Patrick G. Hatcher

Abstract We describe a new procedure for conversion of algal biomass into biodiesel using a single step process through the use of tetramethylammonium hydroxide (TMAH). The dried algae is placed in a laboratory-scale reactor with TMAH reagent (25% in methanol) under a blanket of flowing nitrogen gas and converted to a condensable gas-phase product (biodiesel) at temperatures ranging from 250 to 550°C. The condensed biodiesel is freed of methanol and analyzed by gas chromatography/mass spectrometry. Fatty acid methyl esters (FAME) are the main products of the reaction at all temperatures studied. Residues from the one-step conversion exhibit varying levels of transformation which may likely affect their end use.

1 Introduction

Because of increases in crude oil prices, limited resources of fossil fuels, and the growing concern of greenhouse gases, there has been a renewed interest in converting biomass, vegetable oils, and animal fats to biodiesel fuels [5, 9, 19]. There are many forms of biodiesel from biomass, but one form is commonly produced from vegetable, plant, and animal-based oils that are converted to fatty acid methyl esters (FAMEs) by a transesterification process [8, 22]. The traditional biological sources of biomass oils are soybean, sunflower, and rapeseed. A drawback to using these

E.A. Johnson • E. Salmon • P.G. Hatcher (✉)
Department of Chemistry and Biochemistry, Old Dominion University,
Norfolk, VA 23529, USA
e-mail: PHatcher@odu.edu

Z. Liu
Department of Chemistry and Biochemistry, Old Dominion University,
Norfolk, VA 23529, USA

Marine Science Institute, The University of Texas at Austin,
Port Aransas, TX 78373, USA

J.W. Lee (ed.), *Advanced Biofuels and Bioproducts*, DOI 10.1007/978-1-4614-3348-4_29,

biomass sources for producing biofuel is that they compete for land with agricultural crops used as food sources. Algae as a renewable biomass, however, eliminate many of the problems associated with traditional biomass sources.

The use of microalgae as a source of biodiesel is not a new concept and was a focus of the Department of Energy's "Aquatic Species Program" commenced in 1978 [28]. Although great progress was made, the program was discontinued in 1996 because of decreasing federal budgets and low petroleum costs [25]. With current higher petroleum costs and overall interest in biodiesel, the interest in algal-derived biofuel has increased significantly. Algae are an attractive form of biomass for biodiesel because they do not compete for land needed for food crops. They are an inexpensive and vast renewable resource, and some species are highly enriched with lipids [5]. The main advantage of microalgae is that they can exhibit doubling rates of once or twice a day, making them among the most efficient organisms at converting sunlight and atmospheric CO_2 into biomass. They can grow photosynthetically so that no carbon source other than CO_2 is required for growth. The combustion of any fuel from this biomass source will yield CO_2 previously fixed from existing atmospheric CO_2 so that the energy supply will be regarded as CO_2 neutral [27]. In comparison with other more traditional biomass fuel sources, algae have the potential to yield more energy per acre per unit time and appear to be the only source of biodiesel that has the potential to replace fossil diesel if used exclusively [5]. Weyer et al. [29] calculated the theoretical maximum for algal oil production to be on the order of 354,000 $L \cdot ha^{-1} \cdot year^{-1}$ of unrefined oil, with best cases examined ranging from 40,700 to 53,200 $L \cdot ha^{-1} \cdot year^{-1}$ of unrefined oil.

Finding an economical process to convert algae to biodiesel is one of the major challenges of producing algal biofuel on an industrial scale. The transesterification of oils to FAMEs through a base-catalyzed process is a common commercial technique known for about 100 years [4]. This chemical process converts the triglycerides from vegetable oils and animal fats into FAMEs via a multistep synthesis at temperatures less than 60°C [22]. There have been recent attempts to develop catalysts and processes to perform this conversion of the oil through a single-step process; however, we are unaware that anyone has demonstrated direct conversion to FAMEs by a one-step treatment of the biomass [4, 24, 30]. We report here a proposed method in which the conversion of algae to biodiesel involves only a one-step methylation/transesterification and simultaneous distillation of FAMEs at high temperature (e.g., 250°C) using the alkylation reagent Tetramethylammonium hydroxide (TMAH) and shown in (1) [7, 16, 17].

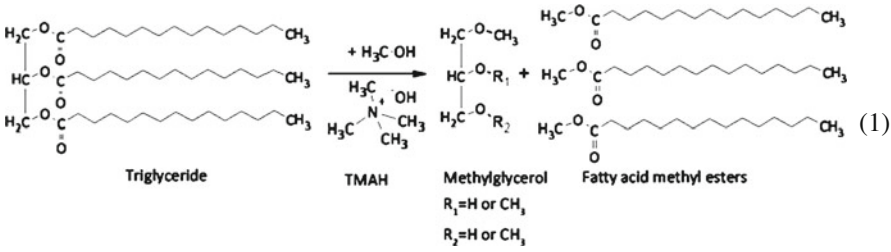

(1)

This reagent has previously been used for conversion of cooking oils to FAMEs at temperatures of less than 60°C as its strongly alkaline properties make it ideal for the conventional transesterification process [1, 4] in the presence of methanol.

The one-step thermal conversion of algae to biodiesel with TMAH was carried out in a reactor we consider only as a prototype for larger, more commercial units. Analysis of the collected liquid product was carried out using GC-MS to confirm the presence of FAMEs and other products. The unconverted residue was analyzed for use as a potential fertilizer by elemental analysis and solid-state ^{13}C nuclear magnetic resonance (NMR) to evaluate the extent of the transformation brought about by elevated temperatures in the reactor.

2 Methods

Sample Collection and Preparation: Both filtration and centrifugation were used to obtain highly concentrated samples of algae from various sources. Algae were collected from the effluent of the sewage treatment plant Virginia Initiative Plant (VIP), close to Old Dominion University (ODU), Norfolk, VA, from May, 2007 to February, 2008. The dominant algae at the VIP were *Centric diatoms* (10–30 μm), *Scenedesmus*/*Desmodesmus* spp., and *Chlorella* sp. Water from the wastewater facility with entrained algae was passed through a tangential flow ultrafiltration system (Millipore Pellicon) with 0.2 μm filter, and the retentate, as condensed algal concentrate, was collected. Total cell concentration and algae specification for each sample was examined under microscope [21]. To remove salts, the algal concentrate was centrifuged (6,500 RPM, 250 mL rotor, 30 min), and the supernatant was decanted and replaced with MilliQ water. This procedure was repeated twice. The final concentrate was freeze-dried before chemical treatment. Algae were also collected from the ODU Algae Farm located in Spring Grove, VA. This farm, established in 2008, is an open pond design in which mainly *Scenedesmus*/*Desmodesmus* spp. algae are being grown and harvested. Algae at the ODU algal farm were concentrated by use of a continuous flow centrifuge (Lavin Centrifuge Model 12–413 V). The concentrated algae, collected as a paste, were removed and lyophilized to dryness.

Conversion of Algae to Biodiesel in a Prototype Reactor: The TMAH method was adapted for the conversion of algae to biodiesel in a horizontal tube furnace reactor [16, 17, 26]. Approximately 1–2 g of algae sample was used in the prototype reactor (Fig. 1). Algae samples were placed in a 30-mL glass culture tube with 1–2 mL of a TMAH in methanol solution (25 wt%). The methanol was evaporated to dryness under N_2 and placed in the Thermo Scientific Lind-berg® Blue M reactor tube oven. The temperature was programmed to increase from 25°C to the desired temperature (250°C up to 550°C) over 15 min. The sample was held at final temperature for 45 min and the reactor was cooled to room temperature. An oxygen-free environment was created by using nitrogen gas flowing at a rate of approximately 100 mL/min. Gaseous vapors were collected and condensed in an ice bath. These condensed vapors were analyzed for FAME content by GC-MS.

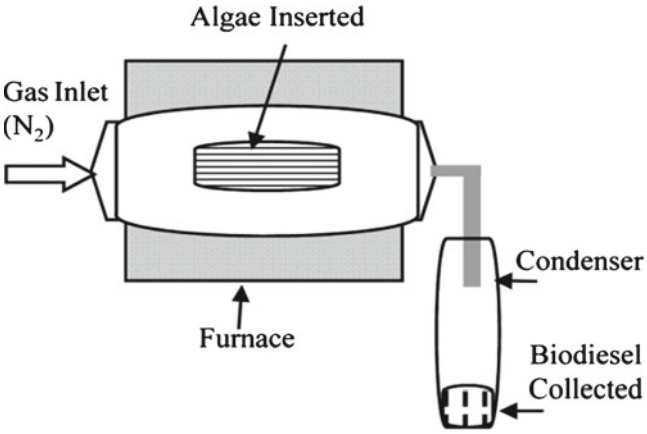

Fig. 1 Schematic diagram of the prototype reactor. Reactor is designed for use with TMAH in a batch mode

Identification by GC-MS: Samples were analyzed by an Agilent 6890 gas chromatograph interfaced to a Leco III mass spectrometer. The temperature was programmed from 50 to 300°C at a rate of 15°C/min. The mass spectrometer was repeatedly scanned in the low-resolution mode from 45 to 500 mass (u) at a rate of 20 spectra/s. Compounds were identified by their mass spectra. Most peaks were identified by comparison with the Wiley/NBS library and some were confirmed by comparison with standards. Quantitative measurements of the concentrations of individual peaks were made using an internal standard *n*-tetracosane as well as with external fatty acid methyl ester (FAME) standards. FAME standards were GLC-40, 50, and 90 standard mixtures (Supelco Analytical) containing fatty acid mixtures of $C_{16:0}$, $C_{18:0}$, $C_{20:0}$, and $C_{22:0}$; $C_{16:1}$, $C_{18:1}$, $C_{20:1}$, and $C_{22:1}$; and $C_{13:0}$, $C_{15:0}$, $C_{17:0}$, $C_{19:0}$, and $C_{21:0}$; respectively.

Elemental Carbon (C) and Nitrogen (N) Analysis of Algae Residue: The carbon (C) and nitrogen (N) contents of algae residues were determined by a Thermo Finnigan Flash 1112 Elemental Analyzer using a nicotinamide standard for calibration. Approximately 1–2 mg of each solid sample was placed in a 3.3×5-mm tin capsule for combustion. The method used for analysis was a furnace at 900°C, oven at 75°C, and carrier gas helium at 91 mL/min.

Solid-state ^{13}C NMR: The NMR cross-polarization magic angle spinning (CPMAS) ^{13}C experiments, with a recycle delay time of 1.0 s and 2,048 scans, were performed using a Bruker Avance II 400 spectrometer operating at 100 MHz for ^{13}C and 400 MHz for ^{1}H [18]. All the experiments were conducted using a 4-mm triple resonance probe. Dry algae and conversion residues were packed into a 5-mm Zirconia NMR rotor fitted with a Kel-F cap for analysis.

3 Results

The biodiesel in this study is produced by conversion of dry microalgae biomass from the VIP using a one-step thermochemolysis reaction into an open pyrolysis prototype reactor. The biomass may be used partially wet, but Hatcher and Liu recognized that drying increases the yield of FAMEs [15]. During this reaction, the transesterification occurs at a temperature sufficient to hydrolyze and alkylate triglycerides in the biomass [15]. This process is possible because the association of TMAH and methanol provides a single step high-temperature saponification and methylation of the ester functional groups of the triglycerides [11]. It is also likely that a transesterification occurs at lower temperatures (approximately 100°C) to produce the FAMEs, much like what is observed with alkali like sodium hydroxide [12] as long as there is residual methanol to act as a transesterification reagent. Using temperatures above 100°C and evaporating the methanol before insertion of the reaction mixture into the reactor created conditions that minimized the transesterification product at low temperatures. The produced FAMEs become volatile at reaction temperatures above 250°C and can be condensed at the exit of the reactor. To establish the optimum reaction temperature, multiple assays at temperatures ranging from 250 to 550°C were used. The volatile products trapped in an ice bath were collected and analyzed by GC-MS in order to identify and quantify the individual FAMEs and other products for each assayed reactor temperature.

The total ion chromatograms (TIC) for VIP algae assayed at 250 and 450°C are shown and peak identifications and their concentrations are reported (Fig. 2 and Table 1). Mostly linear saturated and unsaturated FAMEs are detected in the chromatogram. The dominant peaks are fatty acids, typical of biodiesel, containing $C_{14:0}$, $C_{16:0}$, $C_{16:1}$, and $C_{18:1}$ corresponding to peaks 1, 6, 5, and 9a, b in the table [8].

It is also worth noticing that both chromatograms of biodiesel produced at 250 and 450°C are very similar showing that the conversion of triglycerides to biodiesel using TMAH/MeOH reagent does not change its selectivity for FAMEs with respect to temperature. A similar pattern was observed at all assay temperatures. Minor amounts of other compounds are observed in the products.

All of the peaks correspond to FAMEs except peaks 4, 8, and 11 which are respectively ascribed to a C_{20} isoprenoid hydrocarbon, a lactone, and dodecanamide. The isoprenoid hydrocarbon probably is produced from chlorophyll and the dodecanamide from reaction of ammonia with triglycerides in the reaction chamber.

The yields of FAMEs are summed for each assay temperature along with an estimate of the standard deviation of the analysis for multiple assays at each temperature (Fig. 3). A yield of approximately 3% (±0.3%) is achieved at 250°C for the VIP algae. The highest yield of FAMEs, approximately 4% (±0.8 and 0.6%) of the dry biomass, is achieved at 350 and 450°C. At higher temperature, a slight decrease in yield of FAMEs is observed with a yield below 3% (±0.2%) at 550°C. Total lipid content obtained by Bligh-Dyer extraction was found to be on average 12% (±3.6%) from *Scenedesmus* spp., which is the dominant species from the VIP algae, and similar to reported values [3, 6, 31]. The lipid extract is determined by gravimetric

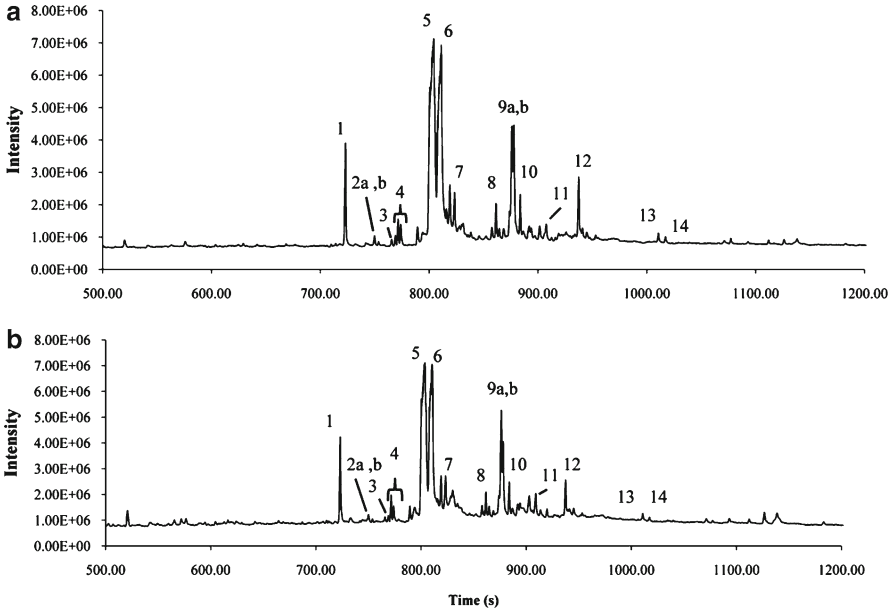

Fig. 2 Total ion chromatograph of Virginia initiative plant (VIP) algae run at (**a**) 250°C and (**b**) 450°C in a batch mode prototype reactor

Table 1 Major peaks identified from GC-MS TIC for VIP algae run in the reactor

ID	Compound name	
1	Methyl tetradecanoate	C14:0
2a	Iso-pentadecanoic acid, methyl ester	Iso-C15:0
2b	Anteiso-pentadecanoic acid, methyl ester	Anteiso-C15:0
3	Pentadecanoic acid, methyl ester	C15:0
4	Unsaturated C_{20} isoprenoid hydrocarbons	C20
5	11-hexadecenoic acid, methyl ester	C16:1
6	Hexadecanoic acid, methyl ester	C16:0
7	Hexadecadienoic acid, methyl ester	C16:2
8	Unidentified lactone product	
9a,b	Octadecenoic acid (Z)-, methyl ester	C18:1
10	Octadecanoic acid, methyl ester	C18:0
11	Dodecanamide	
12	5,8,11,14,17-eicosapentaenoic acid, methyl ester, (Z)-	C20:5
13	13-docosenoic acid, methyl ester	C22:1
14	Docosanoic acid, methyl ester	C22:0

yield and includes triglyceride lipids as well as other extractable organic and inorganic materials. The TMAH procedure only converts the triglycerides and free fatty acids to methyl esters, and we can determine that approximately 30–40% of the total extract is converted to FAMEs. Samples run at each temperature range show standard

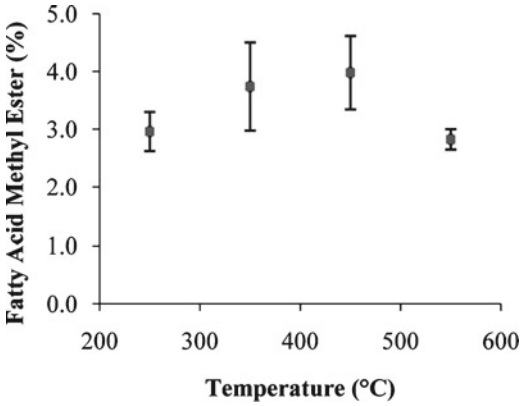

Fig. 3 Fatty acid methyl ester (FAME) yield in weight (%) from biofuel collected over a temperature range of 250–550°C. Yield is estimated from GC-MS data and fatty acid standards. Standard deviations are denoted by error bars (±0.3, 0.8, 0.6, and 0.2)

Table 2 Elemental composition of algae residues collected from Virginia initiative plant (VIP) algae run in the prototype reactor at different temperatures

Temperature	Average C%	Std dev. C	Average N%	Std dev. N	C/N ratio
No heating	44.92	2.85	6.18	1.14	7.27
250°C	46.67	1.76	5.83	0.8	8.01
350°C	41.35	1.61	4.81	0.56	8.60
450°C	35.56	1.38	3.78	0.66	9.41
550°C	36.63	1.43	4.31	0.31	8.50

Whole algae (no heating) were analyzed prior to heat treatment in a reactor. Std dev. is the standard deviation for replicates

deviation overlap of percent yield. Though a slightly higher yield is observed for algae run at 350 and 450°C, they are not significantly different from those run at the lower temperature of 250 and higher temperature of 550°C. The effect of temperature difference, however, is apparent in the algae residue after biodiesel collection.

The algal residue obtained following the thermochemolysis may potentially be useful as a fertilizer and even as an animal feed. Our initial goal was to examine its chemical composition for possible future evaluation as these end uses. Raw algae in coastal regions, such as seaweeds, have a long history of use as soil conditioners and fertilizers [14]. Seaweed composting, however, presents some problems such as high salinity and excessive sand content that can limit plant growth and development [10]. Using algal residue produced in our thermochemolysis reactor from freshwater algae would potentially eliminate these problems. The carbon and nitrogen content of algae and algal residues are collected at different temperatures (Table 2). The algal residue collected at 250°C had an average carbon of 46.67% and nitrogen of 5.83%. Both carbon and nitrogen values decreased slightly with increasing temperatures. The C/N ratios, however, were highest at a temperature of 450°C with a value of 9.41. Further testing is being conducted to verify the use of algae and algae residue as an organic fertilizer.

The solid-state CPMAS ^{13}C NMR spectra for whole algae and residue collected at various temperatures are displayed (Fig. 4). Whole algae samples collected both

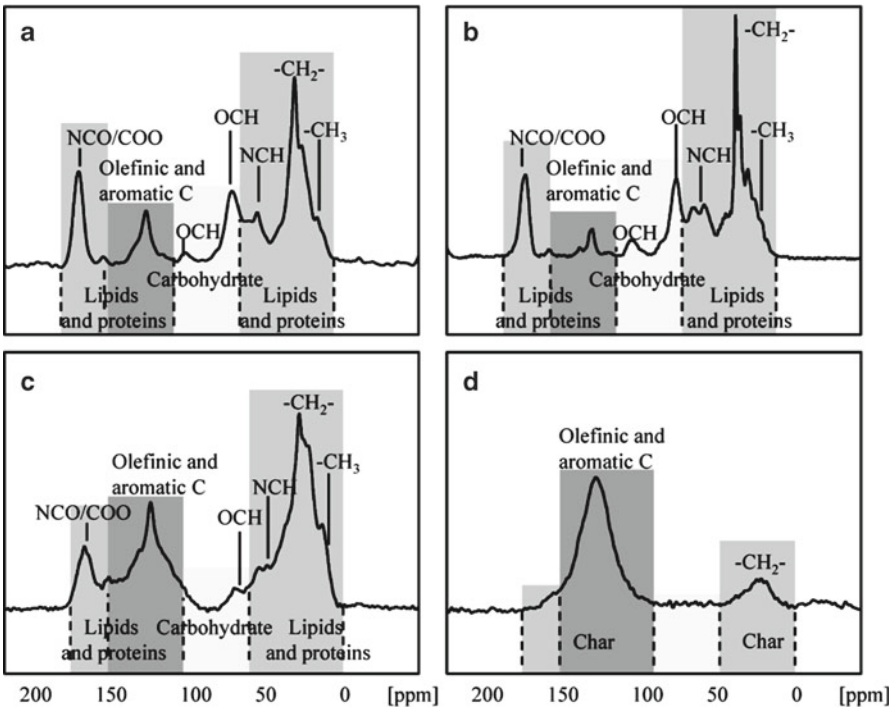

Fig. 4 ^{13}C solids NMR (**a**) whole algae VIP, (**b**) whole algae *Scenedesmus*/*Desmodesmus* spp. from algae farm Spring Grove, VA, (**c**) VIP algae residue from reactor at 250°C, (**d**) VIP algae residue from reactor at 450°C

from the VIP and the algal farm are shown. Dominant species in the VIP samples were microscopically identified as pennate diatoms and in the algae farm samples as *Scenedesmus*/*Desmodesmus* spp. The NMR spectra of the two algal collections are quite similar, being dominated by strong signals in the 0–60 ppm region, representing lipid-like aliphatic carbons and proteins. Carbohydrates, characterized by signals between 60 and 105 ppm, are subordinate components of the spectra indicating that they constitute a small fraction of the algal biomass. Peaks in the region for aromatic/olefinic carbons (105–160 ppm) are also subordinate, reflecting aromatic amino acids comprising proteinaceous components of the algae and olefinic structure contained in the lipids. The large peak at 175 ppm is assigned to amide and carboxyl groups, structural components of both lipids and proteins.

When the algal samples are treated with TMAH at different temperatures, some significant changes are observed in what remains as a residue. The spectrum shown has many of the same signals as the original algae, but contains significantly more olefinic/aromatic carbon (Fig. 4c). This is most likely an indicator that the 250°C heating has transformed the algae such that increased aromatization occurs. The transformation, however, is not overly drastic, suggesting that this residue probably has sufficiently preserved structures to be used as a fertilizer. It is well known that

heating materials containing carbohydrates and proteins (algae) together produces furanosic materials often referred to as melanoidins [2, 20].

The diminution of carbohydrates (60–105 ppm) and portions of the proteinaceous signals (NCH at 50 ppm) observed in this residue is consistent with the involvement of carbohydrates and proteins to form these aromatic substances. The presence of a peak at 160 ppm (assigned to the O-bearing aromatic carbons), along with a broad signal in the range between 105 and 150 ppm, is suggestive of furans, but also could be derived from heterocyclic N rings such as indoles or pyrroles. Usually, a signal at 160 ppm is assigned to phenolic substances that are commonly found in lignin. We know that lignin is not present within algae, so the emergence of this peak at 160 ppm can only be rationalized as that derived from furans or heterocyclic N. Heating to a temperature of 450°C causes drastic changes in the structure of the residue, which shows signals mainly like charred material. The high aromatic content and minor aliphatic content is suggestive of extensive polymerization into condensed aromatic moieties. We can speculate that the furans forming from carbohydrates might undergo cyclization and aromatization and eventual formation of dibenzofurans. The protein-derived heterocyclic N might probably undergo increased aromatization to structures similar to carbazoles. Interestingly, the C/N ratio for this material (9.41) coupled to the high aromatic content are suggestive of the fact that a significant amount of N-containing structures are embodied within aromatic units. Use of this material as a fertilizer where the N can be released via decomposition is unknown at this time.

4 Discussion

The results presented in this study indicate that in an oxygen-free environment at a temperature between 250 and 550°C, the methylating reagent TMAH directly converts algae biomass into the fatty acid methyl esters found in biodiesel. While algae, high in lipid content and rapid in growth, are an ideal biomass for biodiesel production, we suggest that this direct conversion process can be used with various forms of other types of biomass. For example, soybeans have been treated with TMAH/methanol and shown to give similar fatty acid methyl esters [15]. This process is also unique among biodiesel conversion technology in that the biomass introduced may be used wet, partially dried, or dried. Removing water from algal biomass is viewed as an important challenge to making conversion to biofuels feasible. The traditional transesterification process, in which sodium hydroxide is used to catalyze the reaction, requires the exclusion of water [12, 23]. There is also a requirement to remove free fatty acids in the transesterification process, mainly because the free fatty acids are converted to fatty acids salts which do not undergo transesterification. Grasset et al. have shown that the TMAH process can convert free fatty acids to their methyl esters [13]. Thus, we expect that removal of free fatty acids from algal oils would not be necessary. This, combined with the fact that complete water removal would be unnecessary, suggests that one could streamline any

commercial production of biodiesel using our proposed TMAH thermochemolysis methodology.

Although high temperatures of 450°C produce the highest yield of biodiesel, the ideal temperature for this TMAH process is 250°C or lower. Because the residual biomass char is not significantly altered, it is likely to be more useful as a fertilizer than would be a more highly charred product that one obtains at higher reaction temperatures. In addition, maintaining the reactor at a low temperature consumes less energy.

Acknowledgments We thank R.L. Cooper, T.A. Egerton, R.L. Hubbard, R. Mesfioui, and C.L. Wingreen for their help with sample collection and analysis. We thank all of those individuals from various departments at Old Dominion University (ODU) whose research has been invaluable towards this project, especially C. Burbage, A. Gordon, H. Marshall, and A. Stubbins. We also thank the College of Sciences Major Instrumentation Cluster (COSMIC), at ODU for the use of their NMR facility. This work is supported by the Virginia Coastal Energy Research Consortium (VCERC) and funded through the Commonwealth of Virginia.

References

1. Alcantara R, Amores J, Canoira L, Fidalgo E et al (2000) Catalytic production of biodiesel from soy-bean oil, used frying oil and tallow. Biomass Bioenergy 18:515–527
2. Allard B, Templer J, Largeau C (1998) An improved method for the isolation of artifact-free algaenans from microalgae. Org Geochem 28:543–548
3. Bligh EG, Dyer WJ (1959) A rapid method of total lipid extraction and purification. Can J Biochem Physiol 37:911–917
4. Cerce T, Peter S, Weidner E (2005) Biodiesel transesterification of biological oils with liquid catalysts: thermodynamic properties of oil-methanol-amine mixtures. Ind Eng Chem Res 44:9535–9541
5. Chisti Y (2007) Biodiesel from microalgae. Biotechnol Adv 25:294–306
6. Choi KJ, Nakhost Z, Barzana E et al (1987) Lipid content and fatty acid composition of green algae *Scenedesmus obliquus* grown in a constant cell density apparatus. Food Biotechnol 1:117–128
7. Clifford DJ, Carson DM, McKinney DE et al (1995) A new rapid technique for the characterization of lignin in vascular plants: thermochemolysis with tetramethylammonium hydroxide (TMAH). Org Geochem 23:169–175
8. Demirbas A (2009) Progress and recent trends in biodiesel fuels. Energy Convers Manage 50:14–34
9. Enweremadu CC, Mbarawa MM (2009) Technical aspects of production and analysis of biodiesel from used cooking oil: a review. Renew Sust Energy Rev 13:2205–2224
10. Eyras MC, Rostango CM, Defosse GE (1998) Biological evaluation of seaweed composting. Compost Sci Util 6:74–81
11. Fabbri D, Baravelli V, Chiavari G et al (2005) Dimethyl carbonate as a novel methylating reagent for fatty acids in analytical pyrolysis. J Chromatogr A 1065:257–264
12. Freedman B, Pryde EH, Mounts TL (1984) Variables affecting the yields of fatty esters from transesterified vegetable oils. J Am Oil Chem Soc 6:1638–1643
13. Grasset L, Guignard C, Ambles A (2002) Free and esterified aliphatic carboxylic acids in humin and humic acids from a peat sample as revealed by pyrolysis with tetramethylammonium hydroxide or tetraethylammonium acetate. Org Geochem 33:181–188

14. Haslam SFI, Hopkins DW (1996) Physical and biological effects of kelp (seaweed) added to soil. Appl Soil Ecol 3:257–261
15. Hatcher P, Liu Z (2009) Direct conversion of biomass to biodiesel fuel. U.S. Patent 0158638:1–6
16. Hatcher PG, Minard RD (1996) Comparison of dehydrogenase polymer (DHP) lignin with native lignin from gymnosperm wood by thermochemolysis using tetramethylammonium hydroxide (TMAH). Org Geochem 24:593–600
17. Hatcher PG, Nanny MA, Minard RD et al (1995) Comparison of two thermochemolytic methods for the analysis of lignin in decomposing gymnosperm wood: the CuO oxidation method and the method of thermochemolysis with tetramethylammonium hydroxide (TMAH). Org Geochem 23:881–888
18. Liu Z, Mao J, Peterson ML et al (2009) Characterization of sinking particles from the northwest Mediterranean Sea using advanced solid-state NMR. Geochim Cosmochim Acta 73:1014–1026
19. Ma F, Hanna MA (1999) Biodiesel production: a review. Bioresour Technol 70:1–15
20. Maillard LC (1912) Formation de matières humiques par action de polypeptides sur les sucres. Cr Acad Sci (Paris) 156:148–149
21. Marshall HG, Lacouture RV, Buchanan C et al (2006) Phytoplankton assemblages associated with water quality and salinity regions in Chesapeake Bay, USA. Estuar Coast Shelf Sci 69:10–18
22. McNeff CV, McNeff LC, Yan B et al (2008) A continuous catalytic system for biodiesel production. Appl Catal A Gen 343:39–48
23. Meher LC, Vidya Sagar D, Naik SN (2006) Technical aspects of biodiesel production by transesterification—a review. Renew Sust Energy Rev 10:248–268
24. Miao X, Wu Q, Yang CJ (2004) Fast pyrolysis of microalgae to produce renewable fuels. Anal Appl Pyrolysis 71:855–863
25. Pienkos PT, Darzins A (2009) The promise and challenges of microalgal-derived biofuels. Biofuel Bioprod Bioref 3:431–440
26. Pulchan KJ, Abrajano TA, Helleur RJ (1997) Characterization of tetramethylammonium hydroxide thermochemolysis products of near-shore marine sediments using gas chromatography/mass spectrometry and gas chromatography/combustion/isotope ratio mass spectrometry. J Anal Appl Pyrolysis 42:135–150
27. Scragg AH, Morrison J, Shales SW (2003) The use of a fuel containing *Chlorella vulgaris* in a diesel engine. Enzyme Microb Technol 33:884–889
28. Sheehan J, Dunahay T, Benemann J et al (1998) A look back at the U.S. Department of Energy's Aquatic Species Program: biodiesel from algae. National renewable energy laboratory (NREL) report. Golden, CO: NREL/TP-580-24190:1-328
29. Weyer KM, Bush DR, Darzins A et al (2010) Theoretical maximum algal oil production. Bioenergy Res 3:204–213
30. Yan S, Salley S, Ng KY (2009) Simultaneous transesterification and esterification of unrefined or waste oils over ZnO-La_2O_3 catalysts. Appl Catal A Gen 353:203–212
31. Yoo C, Jun S, Lee J et al (2010) Selection of microalgae for lipid production under high levels carbon dioxide. Bioresour Technol 101:S71–S74

Part VI
Life-Cycle Energy and Economics Analysis

Chapter 30
Process Economics and Greenhouse Gas Audit for Microalgal Biodiesel Production

Razif Harun, Mark Doyle, Rajprathab Gopiraj, Michael Davidson, Gareth M. Forde, and Michael K. Danquah

Abstract With the current global drive towards a low-emission economy, countries need to take a stance. For example, Australia, which is one of the world's largest polluters, has made a commitment that before 2020 its overall emissions would be reduced by 5–15% below the levels registered in the year 2000. To realise these targets, processes which capture carbon dioxide will prove critically important. One of such emerging processes is carbon dioxide capture for microalgae cultivation and subsequent downstream biomass processing for biodiesel production. This chapter will entail engineering scale-up, economic analysis and carbon audit to ascertain the viability of an industrial scale microalgal biodiesel production plant. This will involve the development of an industrial scale model to determine the feasibility of a real large-scale plant. Data from each process step (cultivation, dewatering, lipid extraction and biodiesel synthesis) will be presented individually and integrated into the overall process framework.

1 Introduction

Lack of sustainable energy resources currently threatens the survival of an increasingly globalised world economy. Due to the heavy dependence on limited fossil fuel resources, renewable alternatives which are able to compete with conventional energy options must soon be developed. Steady increases in the price of crude oil, for instance, are being observed, due to rising demands and the escalating scarcity of reserves. In addition, the increasing accumulation of CO_2 in the atmosphere and

R. Harun • M. Doyle • R. Gopiraj • M. Davidson • G.M. Forde • M.K. Danquah (✉)
Bioengineering Laboratory, Department of Chemical Engineering,
Monash University, 3800 Clayton, VIC, Australia
e-mail: michael.danquah@eng.monash.edu.au

J.W. Lee (ed.), *Advanced Biofuels and Bioproducts*, DOI 10.1007/978-1-4614-3348-4_30,

its impact on climate change have provided a significant driver for change. Amid growing concerns, global agreements to limit greenhouse gas (GHG) emissions, such as the Kyoto Protocol, have been formed. Directly resulting from such agreements, many developed countries have adopted the "cap-and-trade" carbon trading schemes in efforts to curb emissions. Thus projects which capture CO_2 to prevent release into the atmosphere will play a significant role in combating climate change.

Biofuels such as biodiesel and bioethanol are possible alternative fuels. Current biofuel production requires increasing amounts of arable land for biomass cultivation, which compete with terrestrial fuel crops, thus heightening concerns over food affordability. Microalgae offer a unique alternative as it does not compete for cultivation logistics with agricultural food crops. Microalgae could harbour a substantial amount of lipids for biodiesel production and carbohydrates for bioethanol production.

This chapter entails the engineering scale-up, economic analysis and carbon audit to ascertain the viability of an industrial scale microalgal biodiesel production plant. This will involve the creation of an industrial scale model that can be used to determine the feasibility of a large-scale plant. Four major stages are considered here: microalgal cultivation, dewatering, lipid extraction and transesterification (biodiesel production).

1.1 Design of Microalgal Processing Plant for Biodiesel Production

This section will explore the process engineering design for an industrial scale microalgal production plant for biodiesel production. The design will focus on four key process steps: biomass cultivation, dewatering, extraction and biodiesel production. Various unit operations for each process step are designed to compare their appropriateness, and recommendations are made to clearly define the unit operations that best optimise the process.

1.2 Cultivation Systems for Microalgae

Two most common cultivation systems for microalgae are open ponds and closed photobioreactors. Open ponds come in many different shapes and forms, each having certain advantages and drawbacks. The types of ponds that are currently used in research and industry include raceway ponds, shallow big ponds, circular ponds, tanks and closed ponds. The location of the pond is a critical factor in determining the type of pond, microalgal strain and intensity of available light for photosynthesis. Due to the lack of control associated with open systems, the pond efficiency is a function of the local climate [19]. They are limited by key growth parameters

including light intensity, temperature, pH and dissolved oxygen concentration. Contamination by predators is another issue involved with open ponds. Local climate and contamination can limit the cultivation system to unwanted algal strains which grow under severe conditions [13]. The cultivation system cost is a vital factor when comparing open and closed cultivation systems. It is well known that the cost involved with cultivation ponds are significantly less than that of closed systems. The construction, operating and maintenance costs of cultivation ponds are lower than photobioreactor options, the design of open ponds is technically less challenging, and they are more scalable [15]. Although cultivation ponds result in a relatively lower biomass concentration, the aforementioned features of the pond system make it a competitive cultivation option.

Tubular reactors are considered to be more appropriate for outdoor cultivation. The large illumination surface of the reactor which is created by translucent tubing is the main factor behind its outdoor suitability. The tubing can be arranged in various configurations and the appropriateness of the configuration depends on the specifications of the system. Common configurations include straight line and coiled tubing [35]. The geometry of the reactor is also important, as tubular reactors can be configured in a vertical, horizontal or inclined plane. Harun et al. [13] states that the major difference between the configurations is that the vertical design allows greater mass transfer and a decrease in energy usage, while the horizontal reactor is more scalable, but requires a large area of land. Tubular reactors make use of either airlift or air pump aeration for culture mixing. The airlift system is more preferred, especially for scale-up purposes. Previous studies have shown that the scale-up of a tubular photobioreactor can play havoc with the mass transfer of the culture [22]. Large build-up of dissolved oxygen may occur within the tubing during scale-up and this can inhibit cell growth. Figure 1 shows a schematic diagram for open ponds, horizontal tubular reactor (HTR) and external loop tubular reactor (ELR).

1.3 Design Considerations for Tubular Reactors

1.3.1 Airlift Pump

For the algae to grow optimally, the mass transfer characteristics of the photobioreactor must be optimised to suit the specific strain of algae. Mass transfer is achieved by pumping compressed air and carbon dioxide into the reactor, thus creating flow through the culture that is dispersed within the solar tubing [22]. It is preferred that the aeration and mixing of the cultures in tubular photobioreactors are carried out by an airlift pump [35]. The airlift pump must provide an adequate velocity to circulate the culture through the solar receiver so that the dissolved oxygen build up within the culture can be stripped by the degassing section before it accumulates. Airlift pumps are typically used in algal cultivation instead of standard mechanical pumps. Airlift pumps have been found to cause less damage to algal cells and are less expensive to instal than mechanical pumps [5].

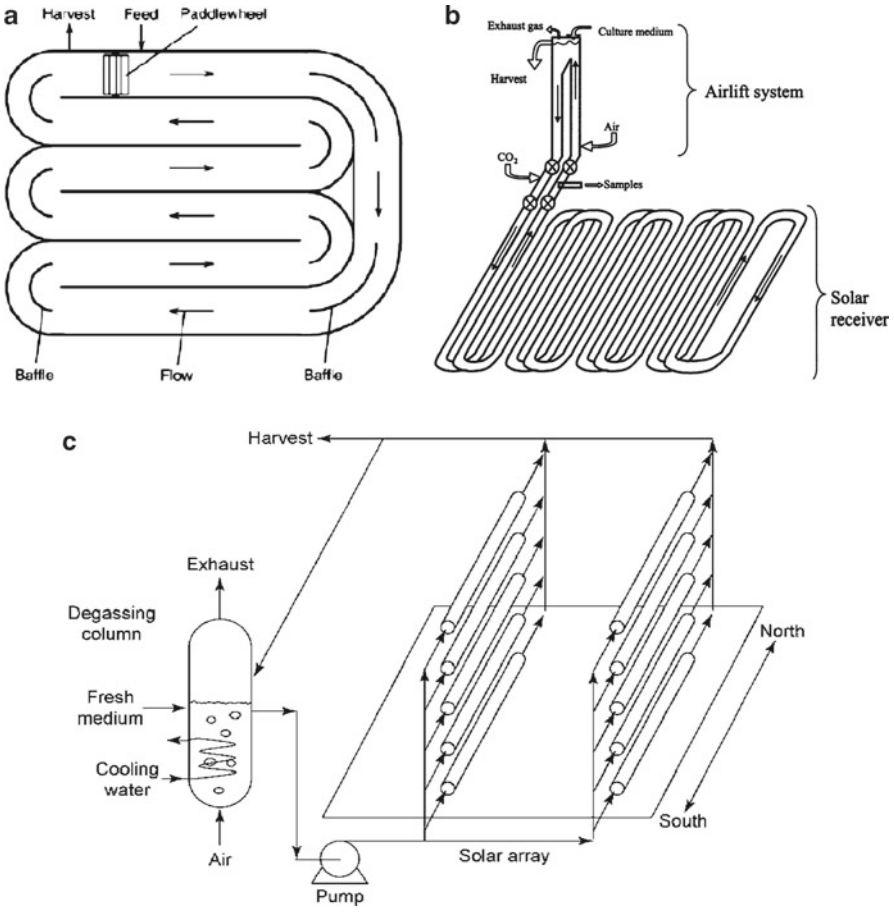

Fig. 1 Different configurations of microalgae cultivation system. (**a**) Raceway pond (RP) [5]. (**b**) External loop tubular reactor (ELR) [21]. (**c**) Horizontal tubular reactor (HTR) [5]

1.3.2 Degassing Column

The degassing section of the reactor plays an integral role in the success of the cultivation. The degasser is designed to remove accumulated dissolved oxygen and extricate gas bubbles from the culture. An excessive amount of bubbling within the tubing can hinder light absorption. Therefore, gas–liquid separators are employed [5]. It is required that the culture spends the least amount of time in the dark regions of the reactor. The degassing zone is considered to be optically deep in comparison with the solar receiver. It is a dark zone and hence it is unsuitable for growth. It is a necessity that the degassing section's volume is much lower than the volume of the solar receiver to allow the culture to spend longer periods in the section of the reactor that is optimal for biomass proliferation. The airlift pump controls the liquid

velocity in the solar tubing. The velocity required by the system will depend on the configuration of the tubing and gas holdup in the riser and downcomer regions within the airlift operation. Once the tubing geometrics are selected, the height of the airlift section and the appropriate areas for the downcomer and riser portions of the airlift can be determined.

1.3.3 Reactor Tubing

The solar receiver tubing must have a specified length so that photosynthetic growth can be optimised. It has been shown that the maximum tube length relies on three parameters: liquid velocity, dissolved oxygen concentration and the rate of oxygen production by photosynthesis. Generally, a tube run in a photobioreactor should not surpass 80 m. However, the maximum length of tubing is dependent on solar intensity, biomass concentration, liquid flow rate and initial oxygen concentration at the tubing entrance [22]. Molina Grima et al. [23] states that "other than "scale up" by multiplication of identical tubular modules, the only way to increase volume is by increasing length and/or diameter". Ten years on, the debate over scale-up is still prevalent, with no clear solution readily available. A possible solution to scale-up is to make use of current cultivation designs and employ several cultivation units to produce a significant amount of biomass. However, the process must produce enough biomass such that it will offset extensive equipment costs.

1.3.4 Solar Irradiance

To enhance biomass productivity, irradiance on the surface of the solar receiver tubes must be maximised. Solar irradiance is the power of electromagnetic radiation on the tubular surface which varies with location and weather conditions. The solar receiver tubes must be configured to maximise the irradiance on the surface tubes; thus the appropriate configuration should be chosen for the designated location.

The surface on which the tubes are located can be painted or covered with white sheeting to take advantage of the albedo effect. The albedo effect refers to improved irradiance by means of reflection [1]. In retrospect, the design of the photobioreactor is not as significant as the source of illumination. Generally, light is always the limiting factor with regard to algal cultures [7].

1.3.5 Dissolved Oxygen Accumulation

The cultivation process relies on photosynthesis. One of the major products from photosynthesis is oxygen; thus as the algae consumes carbon dioxide and photosynthesise, the culture experiences a significant increase in dissolved oxygen concentration. As mentioned above, excess dissolved oxygen within the culture can inhibit photosynthesis and cause photo-oxidative damage to cells. Molina Grima et al. [22]

found that the maximum dissolved oxygen concentration within the culture should not exceed the standard air saturation of the culture by more than 400%. This parameter constraint is one key issue involved with the scale-up of photobioreactors. Dissolved oxygen cannot be removed within the solar receiver, thus limiting the length of the tubular receiver.

1.3.6 Culture Velocity

The culture velocity within the solar receiver is very important, as the cells must be evenly distributed throughout the tubing to avoid extended periods within the dark zones located at the centre of the tubing. The maximum velocity obtained within the system is dependent on the size of micro-eddies in comparison to the algae cell dimension. Acién Fernández et al. [1] found that the maximum velocity in an external loop reactor (ELR) for *Phaeodactylum tricornutum* strain was 1 m/s. This velocity was obtained by a specific power input of 170 W/m^3. However, the actual velocity used in the ELR was 0.5 m/s due to issues associated with the mechanical properties of the solar receiver. The velocity must be high enough to ensure turbulence, thus preventing bio-sedimentation. However, the liquid velocity cannot be applied at gratuitous speeds, as this could potentially cause damage to the algal cells. Generally the liquid velocity must comply with two constraints: a turbulent Reynolds number and a micro eddy length that is significantly larger than the cell dimensions [1].

1.3.7 pH

The pH of the cultivation system increases as the algal cells photosynthesise. The consumption of carbon dioxide and the production of dissolved oxygen from photosynthesis can significantly alter the pH thereby impeding growth. The cultivation system requires a relatively neutral environment, usually maintained at pH ~8 [34]. To prevent variations in culture pH, appropriate control systems are incorporated to monitor the pH. Another technique to control variations in pH is to employ carbon dioxide injection points along the tube run. This prevents excessive culture pH and any carbon limitation that may occur [23]. However, this is not economically viable when considering large algal plants.

1.4 Cultivation System: Design Basis

The strain of microalgae considered for the design is *P. tricornutum*, which is a type of marine algae from the class *Bacillariophyceae* [31]. Figure 2 shows the proximate biochemical composition of *P. tricornutum*. The design basis for the cultivation system is 50,000 tonnes of dry biomass per year. The cultivation system will operate 330 days per year with the number of batches dependent on the type of cultivation

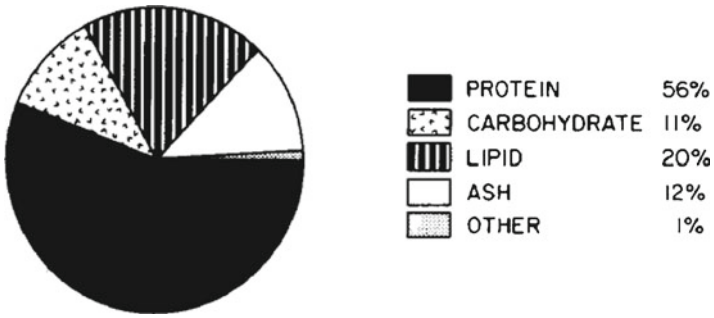

Fig. 2 Proximate composition of the marine algae *P. tricornutum* [33]

system employed, as well as the specific yields and productivities. Seawater is used as the major source of water due to the marine nature of the algal specie. The life span of the plant is fixed at 10 years. It is assumed that 80% of the biomass is removed from the cultivation system at the end of each batch. After 330 days of cultivation, the facility will shutdown for major maintenance. Dominant strains of algae and unwanted parasites can often enter the reactor and destroy the culture [5]; thus it is pivotal that the cultivation system is shutdown for scheduled maintenance periodically. The cultivation system will rely on carbon dioxide from a power station, and this will be the only source of carbon dioxide for photosynthesis. The carbon dioxide from the power station is assumed as a mixture with compressed air such that the mass fraction of carbon dioxide entering the cultivation system is 10%.

1.4.1 Cultivation System Sizing

The sizes of both photobioreactors (HTR and ELR) and the raceway pond are estimated based on the capacity to produce 50,000 tonnes of dry weight biomass annually. The volume and area of the horizontal photobioreactor were scaled up from the data presented by Chisti [6], the external loop bioreactor was scaled up from the design by Acién Fernández et al. [1], and the raceway pond was scaled up from the Outdoor Test Facility design in Roswell, NM [31]. Table 1 contains the annual production of biomass for each cultivation system and the biomass produced and harvested per batch.

1.5 Dewatering

Methods such as centrifugation, pressure filtration, vacuum filtration and tangential flow filtration (TFF) are used unaided to dewater microalgal biomass. This section explores the use of different dewatering methods either alone or as a preceding step to the aforementioned unit operations for microalgae dewatering.

Table 1 Annual microalgal biomass production design data for different cultivation systems

Variable	HTR	ELR	RP
Annual biomass production (tonnes)	50,000	50,000	50,000
Biomass required per BATCH (tonnes)	757.5	568.75	947.5
Biomass extracted per batch (tonnes)	606	455	758
Biomass concentration (kg/m^3)	4.525	3.8	0.585
Dilution rate (1/d)	0.25	0.33	0.2
Area required per cultivation unit (m^2)	947	12	1,050
Area per unit (m^2)	1,263	16	1,400
Total cultivation area (m^2)	5,284,365	8,980,263	8,098,291
Total area (m^2)	7,047,680	11,973,684	10,797,721
Total cultivation area (ha)	528	898	810
Total area (ha)	705	1,197	1,080
No. of units required	5,580	748,355	7,713
Total tubing length (m)	58,925,967	59,868,421	N/A
Cultivation areal productivity (kg/m^2 × d)	0.036	0.021	0.023
Total areal productivity (kg/m^2 × d)	0.027	0.016	0.018
Volumetric productivity (kg/m^3 × d)	1.131	1.267	0.117
Volume per cultivation unit (m^3)	30	0.2	210
Total volume (m^3)	167,403	149,671	1,619,658
Approximate annual CO_2 consumption (tonnes)	92,000	92,000	92,000
Energy dissipation (W/m^3)	60–170	60–170	
Energy dissipation (kWh/per unit)			3.24~

1.6 Flocculation

Flocculation is used to amass microalgae cells from the broth. Flocculation can be used as an initial dewatering step that will significantly enhance the ease of further processing. Microalgae carry a negative charge which prevents them from self aggregation within suspension. The surface charge on the algae can be countered by the addition of chemicals known as flocculants. These cationic moieties flocculate the algae without affecting the composition and toxicity of the product. Types of flocculants include $Al_2(SO_4)_3$ (aluminium sulphate), $FeCl_3$ (ferric chloride) and $Fe_2(SO_4)_3$ (ferric sulphate). These multivalent salts are commonly used and vary in effectiveness, which is directly related to the ionic charge of the flocculant.

The other types of flocculants used are polyelectrolytes, which are cationic polymers. Polymer flocculants have the advantage of physically linking cells together. The extent of aggregation by the polyelectrolyte depends on the specific properties of the polymer. Key polymer characteristics include charge, molecular weight and concentration. Increasing the molecular weight and charge on the polymers has been shown to increase their binding capabilities.

Lubian [18] showed that at a pH of approximately 4.5 and 6.5, the algal species *Rhodomonas baltica* achieved flocculation efficiencies of 68 and 77% at chitosan concentrations of 80 and 160 mg/L respectively. *Tetraselmis suecica* attained 42% efficiency at 80 mg dosage. When the pH of the cultures was pre-adjusted to 8, the algal species displayed efficiencies above 75%. At the moment, there is no reliable

correlation between algal taxonomic groups and the concentration of chitosan required for effective flocculation [14]. Lubian [18] observed that pH control is very critical to the performance of microalgal flocculation.

1.7 Centrifugation

Centrifugation is the preferred method for harvesting algal cells [2, 20, 21]. However, centrifugation can be extremely energy intensive, especially when considering large volumes. Centrifugation involves the application of centripetal acceleration to separate the algal culture into regions of greater and lesser densities. Once separated, the algae can be removed from the culture by simply decanting the supernatant spent medium. Filters can also be used during centrifugation to enhance the separation of the supernatant from the medium. Mohn [20] compared the appropriateness of different makes and brands of centrifuges for dewatering of microalgae. Key parameters included in the study consisted of the concentration factor produced, energy consumption, relative cost, operation mode and reliability.

1.8 Filtration

There are many different forms of filtration. These include dead-end filtration, microfiltration, pressure filtration, vacuum filtration and TFF. Filtration involves running the algal culture through filters with defined pore characteristics on which the algal cells accumulate, allowing the medium to pass through. The culture runs through the filters until the filter accumulates a thick algae paste [8]. It has been recognised that the use of filter presses under pressure or vacuum are effective methods to concentrate microalgal species that are considered to be large in hydrodynamic size such as *Spirulina plantensis*. The recovery of small dimensioned algae species such as *Dunaliella* and *Chlorella* with size similar to that of bacteria is difficult to perform with pressure or vacuum filtration methods. Recent studies show that TFF and pressure filtration can be considered as energy-efficient dewatering methods, as they consume optimum amounts of energy when considering the output and initial concentrations of the feedstock [8]. Simple filtration methods such as dead-end filtration are not effective dewatering methods on their own due to issues with back mixing. However, simple filters can be used in conjunction with centrifugation to create better separation [15].

1.9 Multiple Step Dewatering

Unit operations such as centrifugation and microfiltration may be preceded by flocculation to improve the efficiency of recovery [21]. Flocculants can improve dewatering characteristics during centrifugation and filtration because of their

binding capabilities. Flocculants can help to maintain cellular properties when the culture experiences high shear forces during processes such as centrifugation [3]. Multi-stage dewatering processes have the potential to significantly reduce the energy consumption involved with large-volume cultures. It is estimated that biomass recovery contributes up to 20–30% of the total biomass production cost [12]. Therefore, multi-stage dewatering processes have the potential to reduce the economics involved with biomass production.

1.10 Design of Algal Dewatering Systems

For design purposes, a basis of 50% weight by volume (w/v) of biomass is used as the minimum requirement from the dewatering stage. The design outlines the best dewatering configuration in terms of energy consumption and economics. It is assumed that the initial cultivation within the bioreactors will be staggered so that dewatering equipment costs can be reduced. The staggering of the cultivation is entirely dependent on the bioreactor configuration and the dilution rate employed.

1.10.1 Flocculation

The flocculation design is based on the use of chitosan, polyelectrolyte LT-25 with sodium hydroxide and polyelectrolyte LT-25 with ferric chloride as flocculants. The flocculant efficiency is dependent on dosage and the type of algal strain. Flocculation as a stand-alone option cannot achieve the 50% w/v basis required. However, its use as a preceding step to other unit operations could improve the dewatering process. Specific information on doses and efficiencies of different flocculants can be found in Table 2. From the design calculations, both chitosan and polyelectrolyte LT-25 with sodium hydroxide achieved the highest concentration factors and significantly reduced the culture volume. Table 3 shows data on the flocculation performances of the different flocculants investigated.

Table 2 Design specifications for flocculant dosages and efficiencies

Flocculation method	Efficiency	Efficiency (%)	Specific flocculants added	Amount of flocculant added
pH and polyelectrolyte	High	90	LT-25 and NaOH	0.5 mg/L and 1M diluted 1:2 (per 500L batch)
Ferric chloride and polyelectrolyte	High	80	LT-25 and $FeCl_3.6H_2O$	0.5 mg/L and 1M diluted 1:2 (per 500 L batch)
Chitosan	High	95	Chitosan	150 mg/L
Chitosan	High	90	Chitosan	400 mg/L
pH and polyelectrolyte	Low	30	LT-25 and NaOH	0.5 mg/L and 1M diluted 1:2 (per 500L batch)
Ferric chloride and polyelectrolyte	Low	30	LT-25 & $FeCl_3.6H_2O$	0.5 mg/L and 1M diluted 1:2 (per 500L batch)
Chitosan	Low	70	Chitosan	80 mg/L

Table 3 Data on culture volumes after flocculation for the different cultivation systems

	Reduction in culture volume (m^3)			Volume remaining (m^3)			New concentration (kg/m^3)			Concentration factor required		
Flocculant	HTR	ELR	RP	HTR	ELR	RP	HTR	ELR	RP	HTR	ELR	RP
pH & polyelectrolyte	120,530.2	107,763.1	1,166,153.8	13,392.2	11,973.7	129,572.6	36.2	30.4	4.7	13.8	16.4	106.8
Ferric chloride & polyelectrolyte	107137.9	95789.4	1.36581.2	26784.5	23947.4	259,145.3	18.1	15.2	2.3	27.6	32.9	213.7
Chitosan	127226.3	11,3750.0	1230940.2	6696.1	5986.8	64,786.3	72.4	60.8	9.4	6.9	8.2	53.4
Chitosan	120530.2	107,763.1	1,166,153.8	13,392.2	11,973.7	129,572.6	36.2	30.4	4.7	13.8	16.4	106.8
pH and polyelectrolyte	40,176.7	35,921.0	388,717.9	93745.7	83,815.8	907,008.5	5.2	4.3	0.7	96.7	115.1	747.9
Ferric chloride and polyelectrolyte	40,176.7	35921.0	388,717.9	93,745.7	83,815.8	907,008.5	5.2	4.3	0.7	96.7	115.1	747.9
Chitosan	93,745.7	83,815.8	907,008.5	40,176.7	35,921.0	388,717.9	12.1	10.1	1.6	41.4	49.3	320.5

1.10.2 Centrifugation

In the centrifugation method, the comparison data between Mohn [20] and the cultivation system design showed Westfalia self-cleaning disc-stack centrifuge and the Westfalia nozzle discharge centrifuge as centrifuges that meet the design basis requirements. Figure 3 shows energy consumption data from the centrifugation design for both HTR and ELR. Energy consumption associated with centrifugation of cultures from raceway ponds is found to be significantly higher than HTR and ELR.

1.10.3 Filtration

Danquah et al. [8] and Mohn [20] have presented data on the concentration factor and energy consumption of specific filtration units. These data, in conjunction with data from the cultivation section, enabled the determination of the most efficient filtration units, namely the Netzsch Chamber Filter, Dorr Olliver Vacuum Drum Filter, Dinglinger Suction Filter and Pellicon cassette TFF system. Figure 4 illustrates the energy consumptions of the different filtration systems investigated in this study. Although filtration methods appear to be an attractive dewatering option, they are associated with extensive running costs and hidden pre-concentration requirements.

1.10.4 Multi-Step Dewatering

Figure 5a, b compares the energy consumptions for different dewatering options with and without flocculation as a preceding step. It was found that a preceding flocculation step can decrease the energy consumption of the overall dewatering

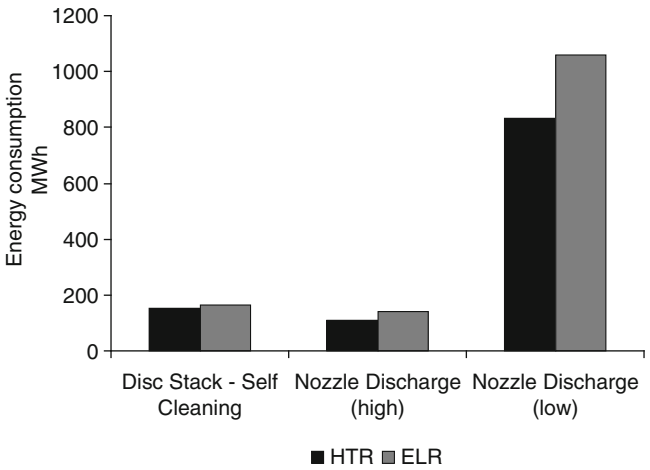

Fig. 3 Energy consumption for stand-alone dewatering by centrifugation

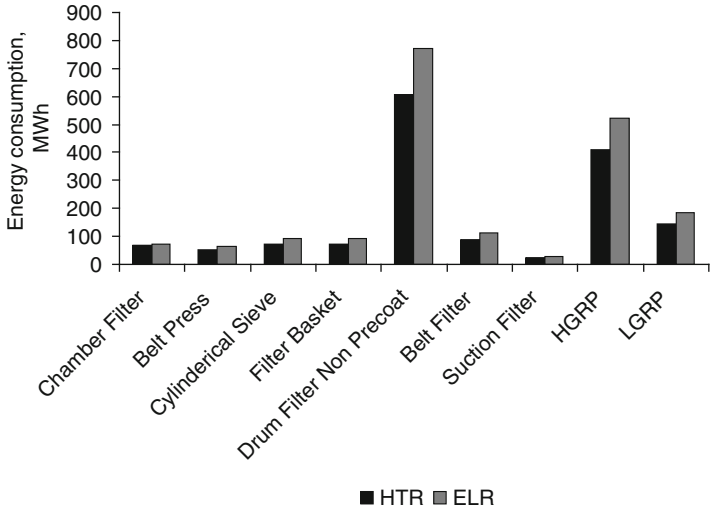

Fig. 4 Filtration energy consumption as a stand-alone dewatering option

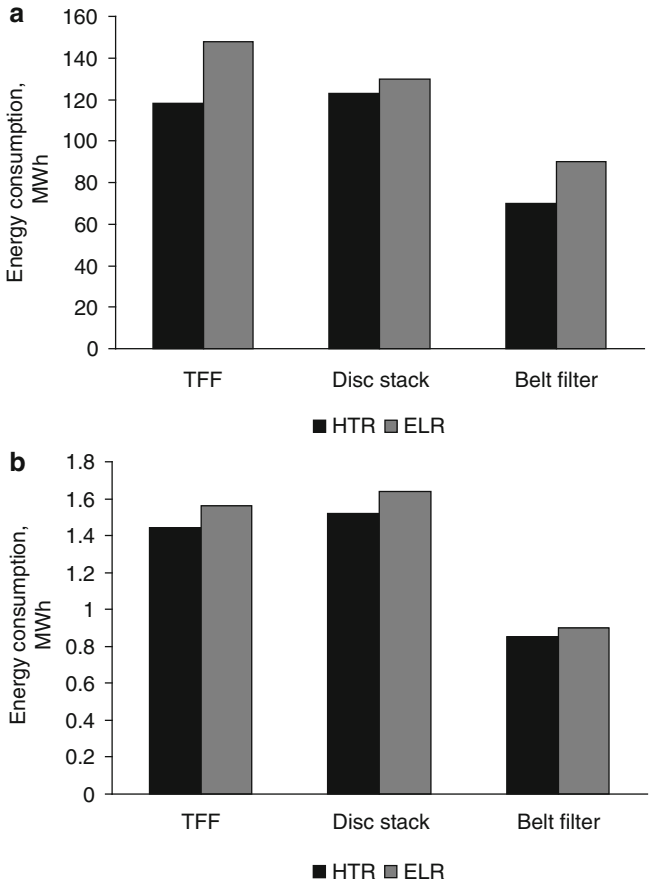

Fig. 5 Comparison of the energy consumption of dewatering units operating as a (**a**) stand-alone options and (**b**) options preceding flocculation

process by up to 98%. Flocculation is particularly critical when the culture volumes are extremely large. Heasman et al. [14] stated that a flocculation efficiency of 80% in a 24-h period is about the average standard requirement for a typical large-scale flocculation work. This study assumes no further processing requirement due to residual accumulation of flocculants, as shown by Lubian [18] that *P. tricornutum* achieved approximately 90% efficiency from diminutive flocculant dosages.

1.11 Lipid Extraction

Lipid extraction from microalgae can be performed in several ways. Some commonly used technologies include supercritical fluid extraction, oil press extraction, solvent extraction and ultrasound-assisted extraction. Oil press extraction involves the use of machinery to literally squeeze cells until they rupture to liberate intracellular lipid contents. The types of oil presses used for extraction include the ram press, screw press and expeller press. Solvent extraction, which is the most commonly used, involves the use of chemicals such as benzene, acetone and hexane. The interaction between the algal cells and the solvent causes cell wall rupture, thus causing equilibrial dissolution and liberation of intracellular lipids. Supercritical extraction makes use of fluid high pressures and temperatures (above the critical levels) to rupture the cells and liberate intracellular lipids. This method of extraction has proven to be time efficient but requires high operating cost [13]. The ultrasound technique makes use of cyclic sound pressure to rupture algal cells, and the resulting free intracellular lipid is harnessed using solvents. The advantages and disadvantages of each method are summarised in Table 4.

Table 4 Comparison of various extraction methods [13]

Extraction methods	Advantages	Limitations
Oil press	Easy to use, no solvent involved	Large amount of sample required, slow process
Solvent extraction	Solvent used are relatively inexpensive; reproducible	Most organic solvents are highly flammable and/or toxic; solvent recovery is expensive and energy intensive; large volume of solvent needed
Supercritical fluid extraction	Non-toxicity (absence of organic solvent in residue or extracts), "green solvent" used; non-flammable, and simple in operation	High capital cost; lack of necessary technology for successful continuous systems
Ultrasound	Reduced extraction time; reduced solvent consumption; greater penetration of solvent into cellular materials; improves the release of cell contents into the bulk medium	High power consumption; difficult to scale-up

1.12 Solvent Extraction

Molina Grima et al. [24] have shown that lipid extraction from *P. tricornutum* can be achieved on wet biomass. The study achieved 90% fatty acid yield on wet biomass in comparison to a 96% fatty acid yield from lyophilised biomass. The wet biomass was extracted at approximately 20% (w/v). The wet biomass leaving the dewatering stage from this study is at 50% (w/v). Therefore, the extraction method described by Molina Grima et al. [24] should provide enhanced interaction between the solvent and the cells. However, this extraction method involved three steps: (1) direct saponification of biomass oil, (2) extraction of unsaponifiable lipids and (3) extraction of purified free fatty acids (FFA) [24]; hence, it was compared to a similar method conducted by Ramirez Fajardo et al. [27], which was a two-step solvent extraction process. The two-step method involved lipid extraction using ethanol and lipid purification using a two-phase system of hexane and water. The crude lipid extraction involved a reaction between ethanol (96% v/v) and the biomass in an agitated tank for ~20 h. The crude lipid contains both saponifiable and unsaponifiable lipids. The saponifiable lipids include glycolipids and acylglycerols which are useful for biodiesel, whereas unsaponifiable lipids contain components such as amino acids and chlorophyll pigments which must be removed from the extract [27]. Water is added to the ethanol/crude-extract mixture to create a hydroalcoholic solution, and hexane is added to create a biphasic extraction system that separates the exploitable and unusable lipids thus purifying the extract. The majority of the saponifiable lipid will be found in the hexane phase, whereas the more polar components will remain in the hydroalcoholic phase [24]. It is assumed that hexane purification reaches 80% recovery after four continuous extractions.

1.13 Lipid Extraction Process Design

A basis of 90% total lipid recovery is assumed for design calculations. Using the proximal composition in Fig. 3, the annual yield of oil from *P. tricornutum* with 90% recovery is ~9,000 tonnes. However, this amount could reduce when the extract is purified and all unsaponifiable components are removed. The design is focussed on the use of solvent extraction on wet biomass with no cell lysis unit operation. Lee et al. [17] demonstrated that cell lysis before solvent extraction does not significantly affect lipid yield. This extraction method is employed due to its high lipid yields and minimal extraction steps. It also involves the use of low-solvent quantities. The total amount of saponifiable lipids extracted from *P. tricornutum* is approximately 6.4% of biomass (dry weight) [27]. Therefore, the daily yield of purified lipid from the extraction is approximately 7.78 tonnes. Figures 6 and 7 show the product yields from the crude lipid extraction and purification processes.

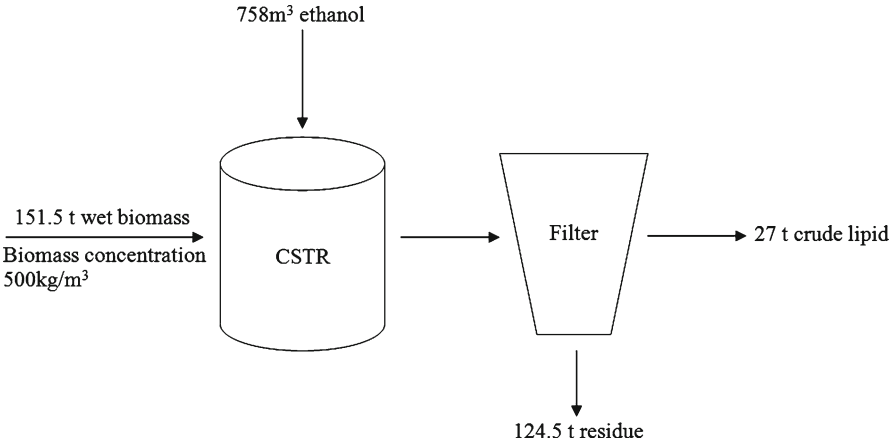

Fig. 6 Input and output flows from algal biomass lipid extraction

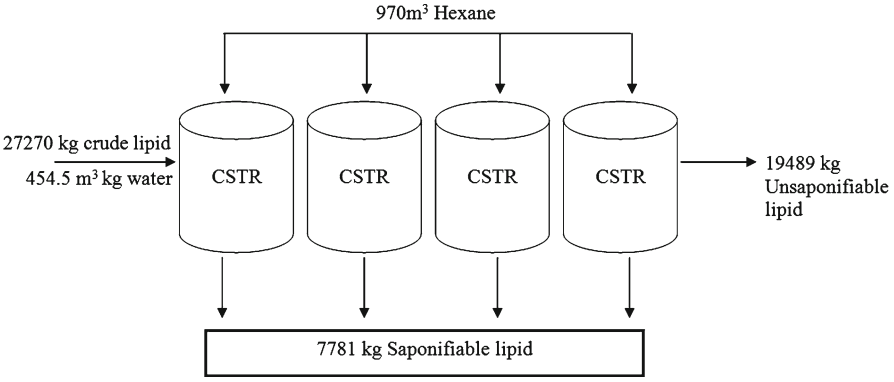

Fig. 7 Inputs and output flows from algal crude lipid purification

1.14 Biodiesel Production

Biodiesel is generally composed of several fatty acid esters including C12:0, C14:0, C16:0, C16:1, C18:0, C18:1, C18:2, C18:3, C20 and C22:1. After oil extraction and purification, the exploitable fatty acid chains from the lipid undergo transesterification to produce fatty acid methyl esters (FAME). The transesterification reaction involves the use of an acidic or alkali catalyst mixed with methanol [36]. The methanol group attaches itself to the fatty acid chains via the bond cleaving activity of the catalyst to produce FAME and glycerol. The methyl ester (biodiesel) produced from this reaction after glycerol separation is crude, hence must be washed, dried and decontaminated so that all water and particulates within the biodiesel are removed. The purified biodiesel must comply with the regulatory standards set by the Fuel Quality Standards Act 2000.

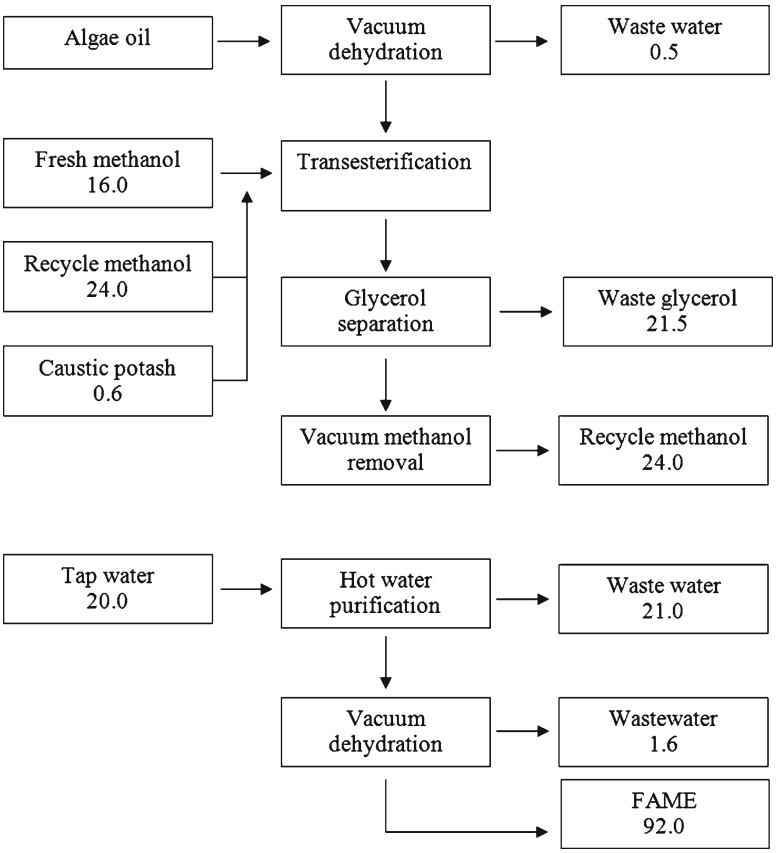

Fig. 8 Transesterification model modified from Sakai et al. [29]

1.15 Transesterification Process Design

This design study uses a potassium hydroxide (KOH) catalyst and methanol to synthesise FAME based on Sakai et al.'s [29] biodiesel production model, which states that 100 parts of oil and 40 parts of methanol with a KOH catalyst will produce 92 parts of FAME and 21.5 parts of crude glycerol. The study makes use of partially recycled methanol feedstock whose composition is 24 parts of recycled methanol and 16 parts of fresh methanol. Figure 8 shows the transesterification model. Applying this model to the oil yields from the solvent extraction gives a daily biodiesel production of ~7,158 kg/day and an annual production of ~2,360 tonnes. The yield of glycerol as a byproduct is ~1,673 kg/day.

1.16 Process Economics

Whilst the production of biodiesel from microalgae has been shown to be technically feasible, the viability of microalgal biodiesel as a practical alternative will be ultimately determined by its ability to become cost competitive with the current fuels.

1.17 The Economic Model

The economic analysis undertaken in this report puts the process technology into four major production stages: cultivation, dewatering, extraction and transesterification. The integration of these individual production stages was used to determine the total production cost of biodiesel from microalgae. To allow a greater comparability between the results of the analysis, the economic model applied a consistent approach to each production stage. This approach estimated the total production cost using a number of components, which included major equipment costs; individual fixed capital costs and fixed capital investment (FCI); annual costs; and running costs.

1.18 Major Equipment Costs

The first element necessary in estimating the total cost of each alternative unit operation technology was to determine the major equipment costs of each scaled-up production option. The primary source of costing information regarding standard process equipment such as pumps, tanks and compressors was provided in Peters et al. [26], whilst similar economic studies were employed to estimate the costing of more specialised equipments such as the raceway ponds [4], HTRs [10] and ELRs [21].

In the dewatering stage, the major equipment cost of centrifuge was based on information provided in Peters et al. [26], whilst the costs of the chamber, suction and vacuum filters were each estimated as a proportion of the centrifuge cost, using the ratios reported in Mohn [20]. In the esterification stage, costing for all equipment was scaled-up from a study completed by Sakai et al. [29]. All major equipment costs were scaled to current prices using appropriate indexing from the Chemical Engineering Plant Cost Index (CEPCI).

1.19 Individual Fixed Capital Costs and Fixed Capital Investment

Following the process recommended in Peters et al. [26], fixed costs including piping, electrical systems and contractor's fees were each estimated as a proportion of the total major equipment costs, using the factors adopted in the cost estimation of

a similar algae production facility by Molina Grima et al. [21]. This approach in estimating fixed costs as a proportion of the total major equipment costs is considered to typically yield results with accuracy within a ±10%. One major exception to this method was the estimation of land costs, which was examined in the cultivation stage of production. The system is assumed to be co-located with a power generation station. This location is selected to ensure adequate supply of free carbon dioxide, readily available in the form of flue gas. Taking this into consideration, the land cost of each system was modelled based on the cost of two large agricultural properties situated in the area; a 32 ha property in Moe South and a 36 ha property in Tyers (REA Group, 2009) in Australia. Based on the total reactor volume required and the area required for each reactor type (Table 1), the overall land requirement and cost for each system was estimated. The FCI was obtained by summing all fixed capital costs and the total major equipment costs.

1.20 Annual Costs

The annual costs represent a range of expenses incurred in the running of the plant from payroll charges to maintenance costs. The most significant of these costs is depreciation, which is calculated using the FCI based on 10-year plant life as recommended in Peters et al. [26]. All other annual costs were calculated using the methods specified in Molina Grima et al. [21] with the exception of labour, supervision, wastewater treatment, and goods and services tax. Labour was assumed to be constant, with 12 employees working during the day and 3 working at night, each charged at the standard labour hourly rate given in ENR (US $34.16). Supervision was also assumed to be constant, with two managers working during the day and one at night, charged at the skilled labour hourly rate again outlined in ENR (US $44.99). Wastewater treatment cost was also estimated based on the costing data reported by Molina Grima et al. [21]. Finally, goods and services taxes were charged at a rate of 10%, reflecting the tax codes applicable to Australia.

1.21 Running Costs

Electricity consumption and raw materials usage were the major running costs resulting from biomass production. Electricity consumption was of particular importance in this analysis as this contributes directly to carbon emissions. All carbon dioxide consumed by the system was assumed to be supplied free of charge through flue gas from the nearby power station. The analysis of electricity consumption centred on the pumping and mixing of fluids in each of the production stages, and the electricity consumed by the centrifuge or filtration equipment in dewatering the culture.

In the cultivation stage, the electricity consumed in pumping carbon dioxide and water throughout the system was estimated using electricity consumption data from

Sazdanoff [30]. Sazdanoff's consumption data were scaled-up volumetrically to meet the requirements outlined in Table 1. Also considered in the cultivation section was the electricity consumed in mixing the algal culture: by airlift pump in the reactor-style systems or paddle wheel in the raceway ponds. Electricity consumed by the airlift pumps and the paddle wheels was estimated using data from previous studies by Acién Fernández [1] and Sazdanoff [30], respectively. The only major raw material considered in the cultivation section was the cost of culture medium, where unit costs were based on Molina Grima et al. [21] and the quantity required was developed using information provided in Danquah et al. [8].

All pumping to the dewatering unit operation were assumed to be associated with the cultivation section, thus the only running costs involved in a single-stage dewatering process was the operation of the different dewatering systems. The energy consumption of the single-stage dewatering options was estimated primarily using data provided in Molina Grima et al. [21]. For the dual-stage process, other running costs such as the flocculant and the mixing of algal broth in the flocculation tanks were also considered. Chitosan was the preferred flocculant, with costs estimated at US $11/kg [9]. The electricity consumption in the mixing during flocculation was determined using the data provided in Sinnott [32].

A number of materials and solvents were required to extract saponifiable lipids from the dewatered biomass including ethanol, hexane and water. The quantities of the raw materials required were based on work by Ramirez Fajardo et al. [27], whereas costs were based on Molina Grima et al. [21].

1.22 Stage-Wise Economics Evaluation

1.22.1 Cultivation Economics

The economic model, as shown in Fig. 9, identified the raceway pond as the cheapest production system ($2.77/kg) followed by the HTR ($9.91/kg). The ELR was the most expensive option ($12.98). The greater complexity of the reactor-style systems was found to require a much greater level of FCI, $2.7 billion for the HTR system and $3.6 billion for the ELR system compared with only $0.73 billion for the raceway ponds. This FCI was represented in annual cost terms as the depreciation of the cultivation system, expressed in Fig. 9, by the black equipment cost portion of the graph. Figure 9 shows these higher equipment costs are the major contributors to the greater overall production cost. Furthermore, the magnitude of FCI required to build the reactor-style systems makes investment in these alternatives unlikely, at least on such a vast scale.

The running cost of each cultivation system is represented by the grey segment in Fig. 9 and is examined in greater detail in Fig. 10, which divides the costs into specific components. Notably, the major contributors to the annual running costs shown in Fig. 10 were found to vary greatly between the raceway pond and the reactor-style systems. Major contributors to the annual running costs of the raceway

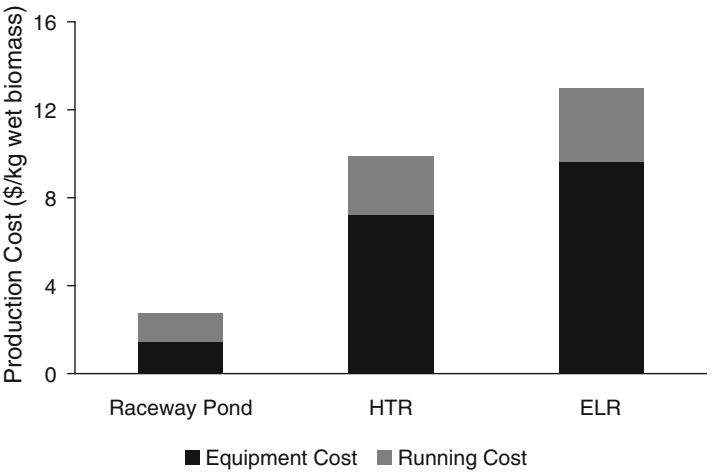

Fig. 9 Algae cultivation cost comparison for different cultivation systems

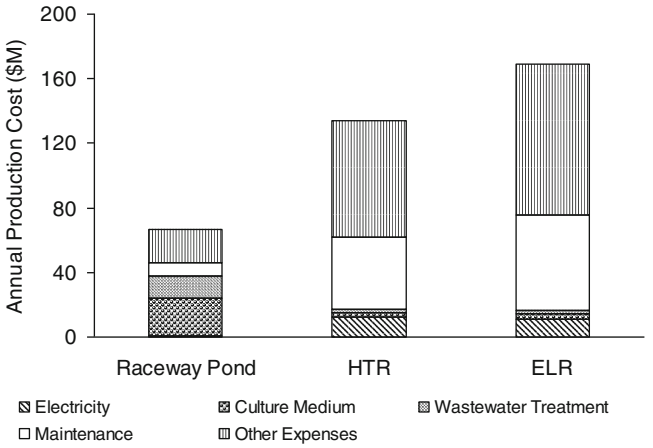

Fig. 10 Breakdown of annual running costs for different cultivation systems

pond were found to be the culture medium and the wastewater treatment, while in the reactor-style systems' electricity consumption and maintenance costs were the greatest contributors to running costs. The larger volume of fluid processed in the raceway pond system, due to its lower volumetric productivity, led to greater culture medium and wastewater treatment costs. In contrast, the larger maintenance costs of the HTR and ELR systems resulted from the greater complexity of the system operation.

The considerably larger electricity consumption of the reactor-style systems could be attributed to the use of an airlift pump to mix the culture, which used significantly larger amounts of energy to operate than the simple paddle wheel used

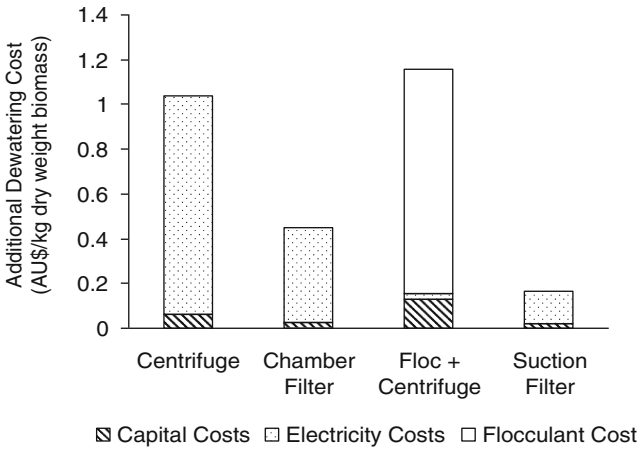

Fig. 11 Biomass dewatering costs for raceway pond (RP)

in the raceway pond system. Despite the lower production costs of the raceway pond system, it is necessary to account for the risk of additional costs resulting from contamination of the algal culture. This risk is a significant drawback in the use of raceway ponds for cultivation compared to the use of reactor-style systems. Contamination results from a lack of control and exposure to the external environment, and can lead to lower growth rates of biomass unsuitable for downstream.

1.22.2 Dewatering Economics

The major processes investigated as dewatering alternatives in this study include single-stage dewatering using centrifugation, chamber filtration, vacuum filtration, suction filtration and a dual-stage process using flocculation followed by centrifugation. In comparing the dewatering of different cultivation options, the raceway pond was approximately 15 times more expensive to dewater using a single-stage process than the reactor-style systems. This is primarily due to a combination of the significantly larger volume of the raceway pond and its much lower concentration of biomass, which requires the dewatering equipment to run for a greater length of time to process comparable amounts of dry biomass, leading to exorbitant energy costs. The costs of dewatering biomass from the raceway pond cultivation system using the four options investigated can be seen in Fig. 11. The capital costs necessary in the dewatering stage were found to be very low, whereas the contribution of running costs was found to be significantly larger. Of the alternatives shown in Fig. 11, the chamber and suction filtration options were found to be significantly cheaper than the single and dual-stage centrifuge systems, chiefly due to their lower electricity consumption.

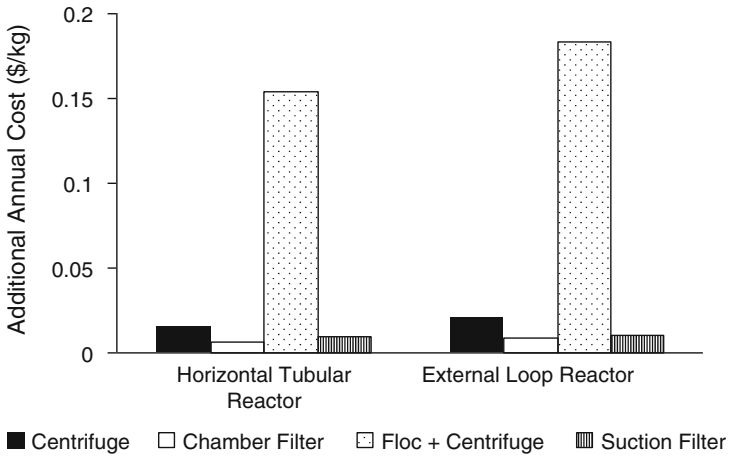

Fig. 12 Biomass dewatering cost for HTR and ELR

However, the large consumption of electricity demanded by single-stage centrifugal recovery has other major environmental and economic impacts, which makes the dual-stage dewatering process the preferred option. As previously noted, the costs in dewatering biomass from the reactor-style cultivation systems were considerably less than the cost in dewatering raceway pond culture. In Fig. 12 filtration again appeared to be the cheapest dewatering option; however, there were a number of aforementioned hidden costs associated with fouling which were not included in the model. Significantly, as shown by the dot shaded bar in Fig. 12, the higher capital costs relative to running costs made dual-stage dewatering uncompetitive at this smaller reactor volume and higher concentration of algae. Thus, due to its greater reliability and cost effectiveness, a single-stage centrifugal dewatering process would be the optimal production selection in the dewatering of reactor-style cultivation systems.

1.22.3 Extraction and Transesterification Economics

The cost of the extraction and transesterification stages was based on one biomass production process technology, with the results shown in Fig. 13. The extraction stage was found to be significantly more expensive than the transesterification stage. The major contributors to the extraction costs were the large fixed capital costs and the cost of large quantities of solvents, respectively. The main components of the fixed capital costs were the costs of large mixing tanks and the pumping capacity required in filling and emptying the tanks. The small cost incurred during transesterification resulted from the significantly reduced volume of materials that required processing, with only 7.8 tonnes of saponifiable lipid estimated to pass to

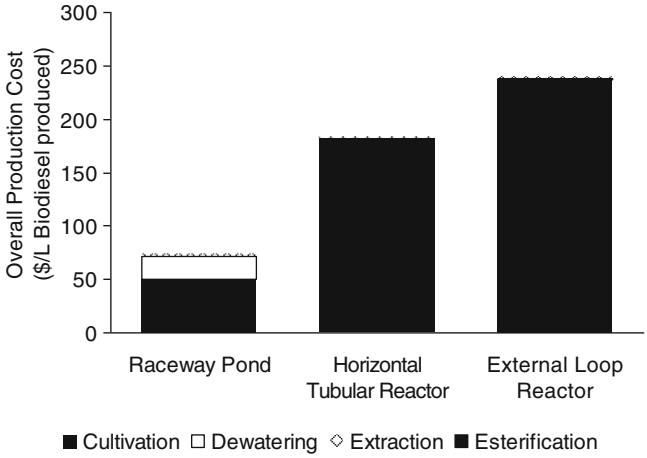

Fig. 13 Extraction and transesterification costs for algal lipids

the transesterification stage daily from the original 151 tonnes of biomass processed in the extraction stage. The electricity costs for both processes were minor, as shown in Fig. 13.

1.22.4 Overall Production Costs

Overall, considering the economic outcome, a raceway pond coupled with a dual-stage dewatering process would be the preferred method to produce biodiesel. Considering biodiesel as the only saleable product, production costs were estimated as approximately $74/L of biodiesel. The calculations are based on the assumptions that glycerol is allowed to be sold, residue from the process also sold as animal feed and carbon credits received as discussed in Sect. 7. However, including these in the model only reduced biodiesel production costs to $72.60/L. With petroleum-based diesel currently retailing at ~ $1.10/L, though this analysis incurred a −50% error, biodiesel from microalgae still remains far too expensive, as compared with traditional fuel.

1.23 Carbon and Energy Audit of Microalgal Biodiesel

Climate change is a significant issue in today's world. As accepted by the wider scientific, political and social communities, climate change is unequivocally—a greater than 90% chance—due to global warming caused by the activities of humans since the 1750s (IPCC 2007). Thus a project which absorbs CO_2, a major contributor

to global warming, would play a significant role in combating climate change. The importance of the microalgal biodiesel production is underlined by the ability of microalgae to absorb carbon dioxide. Carbon capturing occurs in the cultivation phase of the algae biomass, where CO_2 fixation occurs through the biological photosynthesis reaction. This CO_2 bio-sequestration has attracted attention due to the possibility of converting this harmful waste into a valuable product.

The carbon and energy audits are focused on Australia (but applicable elsewhere), and used as a basis for all the discussions in this section. To reach the CO_2 reduction targets, the Australian Federal Government has implemented two primary drivers: The National Greenhouse and Emission Reporting Act (NGER Act) which regulates and sets guidelines on how both Scope 1 (activity direct) and Scope 2 (activity dependent) emissions should be reported; and the Carbon Pollution Reduction Scheme (CPRS) which is the "cap-and-trade" scheme where emitters are required to purchase permits for their emissions.

Under CPRS, emitters who exceed certain limits are required to obtain permits for their Scope 1 emissions. For example, if Company A emits 10 tonnes of CO_2-e above a certain limit, the company is required to possess 10 permits (each permit is equivalent to 1 tonne of CO_2-e) (NGER Guidelines, 2008). The permit is either allocated to mitigate costs of the scheme to some key industries or auctioned to the highest bidder. There is a fixed amount of permits sold in line with the national emission cap, with an initial selling price of $25 per permit [37]. Companies would purchase permits if their internal costs of abatement are higher than the price of permits, and would directly reduce their emissions if their internal costs of abatement are lower than the price of permits. It is expected that permit prices might rise to between $35 and 50 per permit by 2020 [37]. The microalgal cultivation process which captures CO_2 will reduce the overall Scope 1 emissions of an industry and convert this harmful waste into valuable products. By undertaking a complete audit on the process, the exact capturing ability of the process will be ascertained and analysed.

1.24 Method of Carbon and Energy Audit

In ascertaining whether the microalgal biodiesel production process is carbon neutral or carbon negative (absorbs carbon dioxide) or carbon positive (releases carbon dioxide) a life cycle assessment (LCA) is carried out. The LCA is based on ISO 14,040 standards [11].

1.24.1 Life Cycle Assessment: Goal and Scope

The LCA is based on a solid understanding of the GHG neutrality of the process. The LCA will be conducted on the entire process, from the cultivation stage to the final processing stage (gate-to-gate assessment).

1.24.2 Life Cycle Assessment: System Boundary

The LCA system boundary is based on the physical boundary of the entire plant. Basically, a cordon is placed around the entire plant and an audit is performed on the inflow and outflow of GHGs and any energy input and output. However, as the process is developed stage-wise, the boundary is enclosed around the individual stages to simplify the audit. By including all possible factors which may affect the carbon neutrality of the process, the goal is to ensure the carbon audit is a true representation of the actual emissions from the process. Conducting such an extensive and in-depth audit allows an accurate analysis of whether such a process is feasible in reducing the GHG emissions.

1.24.3 Life Cycle Assessment: Inventory

Note that only Scope 1 and Scope 2 emissions are considered in this section. Scope 1 emissions refer to the release of GHG as a direct result of an activity or series of activities (including ancillary activities) that constitute the facility. Scope 2 emissions refer to emissions caused by the activity of the facility but in this case the emissions are not directly released from the facility [37]. Even though Scope 2 emissions are not direct emissions from within the system boundary, the activity within the system boundary causes these emissions to occur at another facility; hence, Scope 2 emissions are considered as well. An example of a Scope 2 emission is the emissions from electricity usage. Even though the use of electricity does not directly increase GHG emissions from within the system boundary, it creates GHG emissions at another facility which is the power station. As per the NGER Act, both Scope 1 and Scope 2 emission have to be reported; however, the financial liability of a corporation only rests with Scope 1 emissions as per CPRS. Scope 3 emissions (process unrelated emissions such as administrative and transportation emissions) are not be considered in this study, as there is insufficient information to undertake an accurate analysis. All GHGs and energy usage will be converted to tonnes of carbon dioxide equivalent (tonne CO_2-e) to enable ease of comparison. It is assumed that the plant is operating at normal conditions when the audit takes place, and all equipments utilise electricity from the grid, unless otherwise stated.

1.24.4 Life Cycle Assessment: Impact Analysis

By conducting the audit on the entire process, we wish to quantify the GHG capturing benefits achievable from this process. The quantified GHG emission saving can be used to calculate the economic benefits from the process and also its environmental impact.

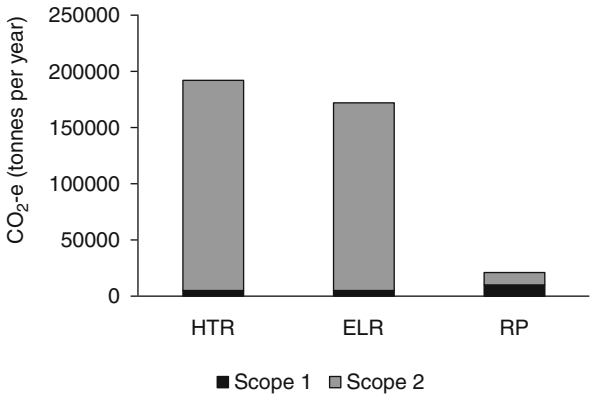

Fig. 14 Representation of the contributions of Scope 1 and Scope 2 emissions for each cultivation system

1.25 Audit and Discussion for Cultivation

The boundary for each system includes a flue gas pre-treatment phase which is common for all three cultivation options. The flue gas pre-treatment phase involves the pumping requirement to blend CO_2 with compressed air. The majority of emissions are Scope 2 electricity emissions, as shown in Fig. 14. The primary source of electricity in the chosen location is brown coal, and this is regarded as a high-emission intensive generator, thus the high emission factor of 1.22 CO_2-e/kWh is used (NGER, 2008).

As seen in Fig. 14, Scope 2 emissions for the HTR and ELR (primarily due to electricity consumption by the airlifts) are significantly higher than the Scope 2 emissions for the RP (due to the low electricity consumption by the paddle wheel). The Scope 2 emissions for the HTR and ELR are 186,691.52 tonnes CO_2-e/year and 166,916.41 tonnes CO_2-e/year, respectively; whilst for the RP the emissions are only 10,564.07 tonnes CO_2-e/year. Scope 1 emissions are due to the capturing efficiencies that exist in the cultivation system. For the HTR and ELP, the efficiency of absorption was set at 95% whilst for the RP the capturing efficiency was 90% [6]. Considering both emissions, it is clear that the RP is the best process option as it captures the highest amount of CO_2-e (71,213.70 tonnes CO_2-e/year). Note that in considering Scope 2 emissions, the audit considers emission produced in the generation of electricity—an emission from another independent facility. Thus RP is the most "truly" environmentally friendly option, as it considers all possible GHG emissions due to the process. However, under the CPRS requirements, only Scope 1 emissions are considered. If the CPRS requirements are considered then the HTR and ELR capture the largest amount of CO_2 gases: 87,157.89 tonnes CO_2-e/year. Thus if the algae cultivation process was part of an emission-intensive industry, the HTR and ELR would be the best option. However, it is important to consider economic factors such as the cost of electricity usage by the HTR and ELR systems.

1.26 Carbon Audit and Discussion for Dewatering

Two dewatering cases have been analysed in this section. The first study assumes that all cultivated biomass would either be produced solely by centrifugation or filtration and the second analysis considers a two-stage dewatering technique based on flocculation followed by centrifugation or filtration. The use of an initial flocculation step reduces the power usage in the subsequent centrifugation or filtration stage.

For a single-stage process, the calculations indicate that the dewatering of the RP culture is more energy intensive than that of the HTR or ELR. This trend is consistent across the majority of the centrifugation and filtration options. This is due to the significant volume of culture produced per batch in the RP system, and the greater degree of processing required in concentrating the RP culture as opposed to that of HTR or ELR. For the dewatering of the HTR and ELR cultures, the emissions produced are comparable for both centrifugation and filtration, as the total culture volume produced in these two cultivation options are about the same.

The second analysis was based on a two-step dewatering process: flocculation first step and a second step consisting of either centrifugation or filtration. A number of different flocculants were considered. The use of a two-step process significantly reduces the overall emissions compared with a one-step process as represented by the HTR cultivation system in Table 5. This trend is consistent for other types of cultivation systems. The percentage emission reduction from a one-step process to a two-step process is around 90%, which is a significant drop in emissions. The study clearly shows that the combination of chitosan 1 (95% efficiency of water removal) with a second-stage decanter bowl centrifugation has the greatest drop in emissions: 99.5% reduction for the HTR, 99.6% reduction for the ELR and 99.7% for the RP. The lowest net emission for the dewatering of the HTR culture was 1,690.73 tonnes CO_2-e/year which was for the dewatering process combination of chitosan 1 with a secondary vacuum–suction filtration method. The same combination of chitosan 1 and a suction filter produced the lowest emission of 2,686.37 tonnes CO_2-e/year for the dewatering of the ELR culture and 10,781.52 tonnes CO_2-e/year for the RP culture. Thus, the most desired dewatering combination per NGER regulations would be a first-stage chitosan 1 flocculation and a secondary stage suction filter. However, it is interesting to note that in terms of percentage reduction due to the addition of a flocculant, this combination has the lowest percentage reduction (only 9% for the HTR and 14.9% for the ELR culture). This is due to the low-energy consumption of the suction filter compared with its concentration factor. To concentrate a sample by 80 times, the energy input is only 0.1 kWh/m^3; thus even though the volume is reduced, the energy required to dewater the culture by a single or double stage process is insignificant.

NGER regulations consider both Scope 1 and 2 emissions, but there are no Scope 1 emissions associated with the dewatering stage. Thus with respect to CPRS requirements, the selection of dewatering options could only be reliant on economic and design considerations. The combinations which were studied in detail are the two flocculants of chitosan 2 and LT-25/NaOH with a secondary dewatering stage of either: centrifugation (disc stack or nozzle discharge) and filtration (chamber, suction, drum filtration or TFF). The data for the HTR, ELR and RP are given in Table 6. The results clearly indicate that chitosan 2 is the better option, as it creates

Table 5 The comparison of net emission reduction due to the implementation of a flocculation first step for the HTR cultivation system

Process Type	One step process	LT-25 and NaOH (high) (prestep)		LT-25 & $FeCl_3.6H_2O$ (high) (prestep)		Chitosan1 (high) (prestep)		Chitosan2 (high) (prestep)		LT-25 and NaOH (low) (prestep)		Chitosan (low) (prestep)	%
Centrifugation type	Tonne CO_2-e/year	Tonne CO_2-e/year	% Emis. Reduc.	Tonne CO_2-e/year	% Emission reduction	Tonne CO_2-e/year	% Emission reduction	Tonne CO_2-e/year	% Emission reduction	Tonne CO_2-e/year	% Emission reduction	Tonne CO_2-e/year	Emission reduction
Disc stack—self cleaning	12,411.87	1,840.06	85.17	2,305.51	81.42	1,723.70	86.11	1,840.06	85.17	9,287.18	25.17	3,081.25	75.17
Nozzle discharge (high)	8,936.55	1,796.62	79.90	2,131.74	76.15	1,712.84	80.83	1,796.62	79.90	7,158.55	19.90	2,690.28	69.90
Nozzle discharge (low)	67,024.09	2522.72	96.24	5036.12	92.49	1,894.36	97.17	2,522.72	96.24	42,737.17	36.24	9,225.12	86.24
Decanter bowl	1,083,217.64	15,225.13	98.59	5,5845.80	94.84	5,069.97	99.53	15,225.13	98.59	665,155.72	38.59	123,546.90	88.59
Pressure filtration													
Chamber filter	5,349.77	1,751.79	67.25	1,952.40	63.50	1,701.63	68.19	1,751.79	67.25	4,961.65	7.25	2,286.76	57.25
Belt press	4,137.29	1,736.63	58.02	1,891.78	54.27	1,697.84	58.96	1,736.63	58.02	4,219.00	−1.98	2,150.36	48.02
Cylindrical sieve	5,957.70	1,759.39	70.47	1,982.80	66.72	1,703.53	71.41	1,759.39	70.47	5,334.00	10.47	2,355.16	60.47
Filter basket	5,957.70	1,759.39	70.47	1,982.80	66.72	1,703.53	71.41	1,759.39	70.47	5,334.00	10.47	2,355.16	60.47
Vaccum filtration													
Drum filter non precoat	48,820.02	2,295.16	95.30	4,125.92	91.55	1,837.48	96.24	2,295.16	95.30	31,587.18	35.30	7,177.17	85.30
Belt filter	7,055.17	1,773.10	74.87	2,037.67	71.12	1,706.96	75.81	1,773.10	74.87	6,006.20	14.87	2,478.62	64.87
Suction filter	1,861.78	1,708.19	8.25	1,778.00	4.50	1,690.73	9.19	1,708.19	8.25	2,825.25	−51.75	1,894.36	−1.75
TFF filtration													
HGRP	3,3026.36	2,097.74	93.65	3,336.23	89.90	1,788.12	94.59	2,097.74	93.65	21,913.56	33.65	5,400.38	83.65
LGRP	11,791.28	1,832.31	84.46	2,274.48	80.71	1,721.76	85.40	1,832.31	84.46	8,907.07	24.46	3,011.43	74.46

Table 6 Emission results for HRT, ELR and RP for the selected flocculation and centrifugation/filtration processes

	One step process			Chitosan 2 (high) (prestep)			% Emission reduction			LT-25 and NaOH (prestep)			% Emission reduction		
Process type	HTR	ELR	RP	HTR	ELR	RP	HTR	ELR	RP	HTR	ELR	RP	HTR	ELR	RP
Centrifugation type	Tonne CO_2-e/year			Tonne CO_2-e/year						Tonne CO_2-e/year					
Disc stack—self cleaning	12411.87	17619.17	743104.68	1,840.06	2,898.35	19,722.00	85.17	83.55	97.35	9,287.18	13,469.85	465584.81	25.17	23.55	37.35
Nozzle discharge (high)	8936.55	15159.13	535035.37	1,796.62	2,836.69	1,7121.13	79.90	81.29	96.80	7,158.55	10,448.17	338142.35	19.90	31.08	36.8
Pressure filtration															
Chamber filter	5349.77	7594.22	320293.28	1,751.79	2,773.04	14,436.86	67.25	63.48	95.49	4,961.65	7,329.57	206612.83	7.25	3.48	35.49
Vaccum filtration															
Drum filter non precoat	48820.02	82813.77	2922878.42	2,295.16	3,544.39	46,969.17	95.30	95.72	98.39	31587.18	45,125.62	1800696.22	35.30	45.51	38.39
Suction filter	1861.78	3158.15	111465.70	1,708.19	2,711.15	11,826.51	8.25	14.15	89.39	2,825.25	4,296.87	78705.93	–51.7	–36.6	29.39
TFF filtration															
HGRP	33026.36	56022.87	1977304.63	2,097.74	3,264.14	35,149.50	93.65	94.17	98.22	21,913.56	31,393.52	1221532.28	33.65	43.96	38.22
LGRP	11791.28	2001.63	705949.45	1,832.31	2,887.34	1,9257.56	84.46	85.56	97.22	8,907.07	12,930.27	442827.23	24.46	35.35	37.27

the least amount of emissions. This is obviously due to the higher dewatering efficiency of chitosan 2: 90% compared with 30% for LT-25/NaOH. This reduces the energy requirements needed for the secondary centrifugation/filtration stage.

1.27 Carbon Audit and Discussion for Lipid Extraction

The extraction process involves the separation and purification of lipids from the dewatered biomass. The extraction technology investigated in this study is solvent extraction, involving lipid extraction as well as ethanol and lipid purification with a two-phase system of hexane and water. The only energy inputs for the extraction stage are the mixing and pumping requirements. Emissions from the mixing and pumping requirements are all Scope 2. The emissions due to mixing (1,127.28 tonnes of CO_2-e/year) are significantly larger than the emissions due to pumping (87.53 tonnes of CO_2-e/year). Mixing emissions account for 92.7% of the emission from the extraction phase due to large mixing and retention times during solvent extraction. The dewatered biomass volume and concentration are consistent for all three cultivation systems (HTR, ELR and RP), thus the emissions due to the extraction of lipids from biomass generated from any of the cultivation systems are the same. This is 1,214.81 tonnes of CO_2-e/year.

1.28 Carbon Audit and Discussion for Biodiesel Production

For biodiesel production, a transesterification process is used to convert the extracted and purified lipids into FAME. The process involves different unit operations. However, the emission sources can be categorised based on either steam or electricity usage. Both emissions are Scope 2. For the modelled facility, 1,834 MJ/year of steam and 470,716.3 kWh/year electricity are required. For this study, it was assumed that a natural gas boiler is used to produce the required steam and the emissions are calculated based on the amount of natural gas needed to produce the required energy. Net emissions from the production of biodiesel are 668.42 tonnes of CO_2-e/year. 85% of the emissions are due to power requirements in running the pumps and the remaining 15% is due to the production of steam. The extraction design chosen has a significant amount of pumping and filtration units, all of which are energy-intensive processes.

1.29 Process Recommendations

Based on economic and design considerations, the two-stage dewatering process of chitosan 2 and disc-stack centrifugation is recommended. The recommendation is based on an overall study of the process steps: cultivation, dewatering, extraction and biodiesel production. The net emission results for the complete process are

Table 7 The net results for scope 2 emissions for the total process based on two-step dewatering process

	HTR	ELR	RP
Process	Tonne CO_2-e/year		
Cultivation	186,691.52	166,916.41	10,564.07
Dewatering	1,840.06	2,898.35	19,722.00
Extraction	1,214.81	1,214.81	1,214.81
Processing	668.42	668.42	668.42
Total	190,414.80	171,697.99	32,169.29

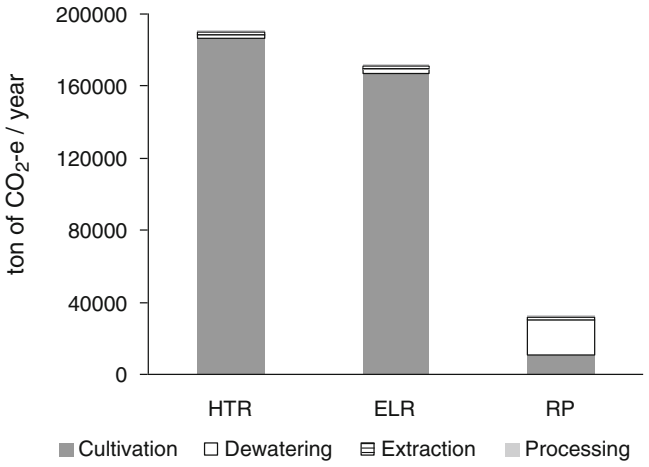

Fig. 15 Breakdown of scope 2 emissions for the different cultivation systems

shown in Table 7. The results from the Scope 2 emission audit indicate that the overall emissions from the HTR and ELR options are by a factor of 10 greater than that for the RP option. As seen in Fig. 15, the majority of the emissions for the HTR and ELR are due to emissions from the cultivation stage (98 and 97% of total emissions, respectively), whilst the emissions from the cultivation stage for the RP only amounts to 33% of total emissions. If the cultivation emissions were ignored, as seen in Fig. 16, the data indicate that to dewater, extract and produce biodiesel more emissions are produced for the RP, than for the ELR or the HTR. This is due to the emission rating to dewater large volumes of less concentrated algae culture from the RP.

The fundamental importance of this project is CO_2 biosequestration. By capturing CO_2, the process reduces the overall emissions which would otherwise be released into the atmosphere. This would reduce the number of permits the facility or an industry is required to obtain. The financial savings analysis shows that the HTR and ELR options save $2.18 million (87,000 permits) whilst the RP saves $2.04 million (82,000) per year. The higher permit saving for the HTR and ELR

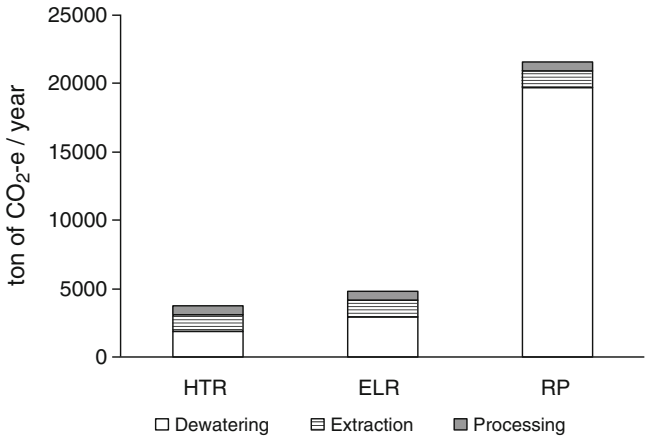

Fig. 16 Breakdown of scope 2 emissions for algae dewatering, extraction and transesterification

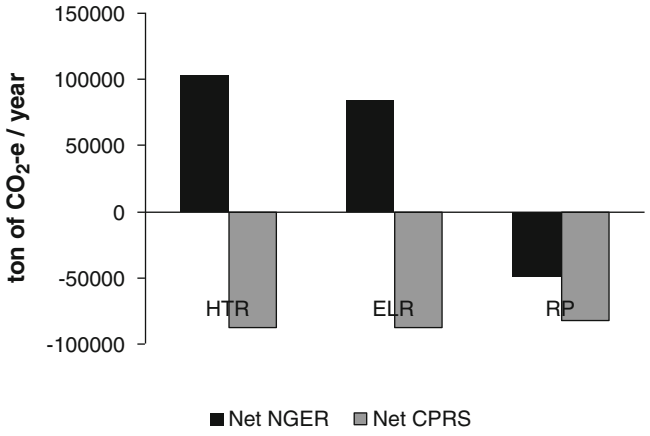

Fig. 17 The net emissions according to the CPRS and NGER requirements

options is due to the lower Scope 1 emissions resulting from their higher CO_2 capturing efficiencies. In terms of an overall outcome, the best option is RP cultivation followed by the two-stage dewatering process. As seen in Fig. 17, the HTR and ELR actually produce more emissions than the RP due to the high cultivation emission rating, whilst the RP has an overall negative emissions rating. As the use of HTR or ELR produces significantly more emissions than the RP, it has a greater negative environmental impact.

2 Conclusion

In terms of the design outcomes, the HTR and ELR appeared to be attractive options due to their ability to achieve high biomass concentrations during cultivation. However, the fixed capital cost involved with the HTR and ELR are up to 493% greater than that for the RP. The tubular reactors are difficult to scale-up due to issues of dark zones and dissolved oxygen build-up. Therefore, the number of units required proved to be significant. The results of the carbon audit indicated that the overall emissions from the HTR and the ELR were greater than that for the RP by a factor of 10. This was largely due to energy consumptions associated with the use of airlift pumps.

In dewatering, a two-stage process involving flocculation preceding centrifugation heavily reduced energy consumption with high reduction in emissions, compared with a single-stage process. The carbon study also indicated that dewatering using a two-stage process was more attractive as culture volume increased, even with a low-efficiency flocculant. In the extraction and transesterification stages only one design alternative was investigated, and on the basis of 50,000 tonnes biomass processing, the results were identical for the different cultivation system.

The overall findings from this study indicate that a RP cultivation stage, followed by a two-stage dewatering process is the optimum alternative. However, the economic study showed that this option is not feasible presently due to an excessively high cost of production of $74/L of biodiesel, which leads to an annual operating loss of $190 million. The carbon audit, however, indicates that the process is carbon neutral, capturing ~49,000 net tonnes of CO_2-e. In terms of environmental impact, the project is attractive. However, it would not be financially viable, as the value of carbon permits is only $2.0 million.

References

1. Acién Fernández F, Fernández Sevilla J, Sánchez Pérez J et al (2001) Airlift- driven external-loop tubular photobioreactors for outdoor production of microalgae: assessment of design and performance. Chem Eng Sci 56:2721–2732
2. Benemann J, Kopman B, Weissman D et al (1980) Development of microalgae harvesting and high-rate pond technologies in California. In: Shelef G, Soeder CJ (eds) Algae biomass. Elsevier, Amsterdam, pp 457–496
3. Bolto B (2006) Coagulation and flocculation with organic polyelectrolytes. Interface Sci Technol 10:63–88
4. Borowitzka M (1992) Algal biotechnology products and processes – matching science and economics. J Appl Phycol 4:267–279
5. Chisti Y (2008) Biodiesel from microalgae beats bioethanol. Trends Biotechnol 25:126–131
6. Chisti Y (2007) Biodiesel from microalgae. Biotechnol Adv 25:294–306
7. Chisti Y, Moo-Young M (2004) Bioreactors. In: Meyers RA (ed) Encyclopedia of physical science and technology, vol 2. Academic, San Diego, pp 247–271
8. Danquah M, Ang L, Uduman N et al (2009) Dewatering of microalgal culture for biodiesel production: exploring polymer flocculation and tangential flow filtration. J Chem Technol Biotechnol 84:1078–1083

9. Department of Planning (DOP) (2009) Model project on chitosan preparation. Department of Planning, Uttar Pradesh. http://planning.up.nic.in/innovations/inno3/fi/Chitosan.htm. Accessed 14 Apr 2009
10. Flickinger M, Drew S (1999) Encyclopedia of bioprocess technology fermentation, biocatalysis, and bioseparation. John Wiley and Sons, New York, NY
11. Gilliland M (1978) Energy analysis: a new public policy tool. Westview, Boulder, CO
12. Gudin C, Therpenier C (1986) Bioconversion of solar energy into organic chemicals by microalgae. Adv Biotechnol Processes 6:73–110
13. Harun R, Singh M, Forde GM et al (2010) Bioprocess engineering of microalgae to produce a variety of consumer products. Renew Sustain Energy Rev 14:1037–1047
14. Heasman M, Diemar J, O' Connor W et al (2000) Development of extended shelf-life microalgae concentrate diets harvested by centrifugation for bivalve molluscs – a summary. Aquacult Res 31:637–659
15. Hosikian A, Lim S, Halim R et al (2010) Chlorophyll extraction from microalgae: a review on the process engineering aspects. Int J Chem Eng. doi:10.1155/2010/391632
16. IPCC Fourth Assessment Report: Climate Change 2007. Metz B, Davidson OR, Bosch PR et al. Climate Change 2007: Mitigation of Climate Change Cambridge University Press, Cambridge, United Kingdom and New York, NY, USA.
17. Lee S, Yoon B, Oh H (1998) Rapid method for the determination of lipid from the green Alga *Botryococcus brauni*. Biotechnol Tech 12:553–556
18. Lubian L (1989) Concentrated cultured marine microalgae with chitosan. Aquacultur Eng 8:257–265
19. Masojidek J, Torzillo G (2008) Mass cultivation of fresh water microalgae. Encycl Ecol 3:2226–2235
20. Mohn F (1980) Experiences and strategies in the recovery of biomass from mass cultures of microalgae. In: Shelef G, Soeder CJ (eds) Algae biomass. Elsevier, Amsterdam, pp 547–571
21. Molina Grima E, Belarbi E, Acién Fernández F et al (2003) Recovery of microalgal biomass and metabolites: process options and economics. Biotechnol Adv 20:491–515
22. Molina Grima E, Fernández Sevilla J, Acién Fernández F et al (2001) Tubular photobioreactor design for algal cultures. J Biotechnol 92:113–131
23. Molina Grima E, Acién Fernández F, García Camacho F et al (1999) Photobioreactors: light regime, mass transfer and scaleup. J Biotechnol 70:231–247
24. Molina Grima E, Robles Medina A, Gimenez Gimenez A et al (1996) Gram scale purification of eicosapentaenoic acid (EPA, 20:5n-3) from wet *Phaeodactylum tricornutum* UTEX 640 biomass. J Appl Phycol 8:359–367
25. National Green house and Energy Reporting Guidelines (2008) Department of Climate Change Australia. http://www.climatechange.gov.au/government/initiatives/~/media/publications/greenhouse-report/nger-reporting-guidelines.ashx. Accessed 14 Apr 2009
26. Peters M, Timmerhaus K, West R (2003) Plant design and economics for chemical engineers, 5th edn. McGrath Hill, New York, NY
27. Ramirez Fajardo A, Esteban Cerdán L, Robles Medina A et al (2007) Lipid extraction from the microalga *Phaeodactylum tricornutum*. Eur J Lipid Sci Technol 109:120–126
28. REA Group. http://www.rea-group.com/irm/content/home.html. Accessed 14 Apr 2009.
29. Sakai T, Kawashima A, Koshikawa T (2009) Economic assessment of batch biodiesel production processes using homogeneous and heterogeneous alkali catalysts. Bioresour Technol 100:3268–3276
30. Sazdanoff N (2006) Modelling and simulation of the algae to biodiesel fuel cycle. Honors Thesis, Ohio State University, Columbus, OH. Accessed 9 April 2009
31. Sheehan J, Dunahay T, Benemann J et al (1998) A look back at the U.S. Department of Energy's Aquatic Species Program: biodiesel from algae. National Renewable Energy Laboratory, Report NREL/TP-580–24190
32. Sinnott R (2005) Chemical engineering design, vol 6, 4th edn. Butterworth-Heinemann, Oxford
33. Thomas W, Seibert D, Alden M et al (1984) Yields, photosynthetic efficiencies and proximate composition of dense marine microalgal cultures. I. Introduction and *Phaeodactylum tricornutum* experiments. Biomass 5:181–209

34. Tsukahara K, Sawayama S (2005) Liquid fuel production using microalgae. J Jpn Pet Inst 48:251–259
35. Ugwu W, Aoyagi H, Uchiyama H (2008) Photobioreactors for mass cultivation of algae. Bioresour Technol 99:4021–4028
36. Xu H, Miao X, Wu Q (2006) High quality biodiesel production from a microalga *Chlorella protothecoides* by heterotrophic growth in fermenters. J Biotechnol 126:499–507
37. White Paper—Department of Climate Change (2008) Carbon pollution reduction scheme: Australia's low pollution future. Department of Climate Change, Canberra

Chapter 31
Sustainability Considerations about Microalgae for Biodiesel Production

Teresa M. Mata, António A. Martins, Subhas K. Sikdar, Carlos A.V. Costa, and Nidia S. Caetano

Abstract This chapter describes how to perform a sustainability evaluation of microalgae biodiesel through its supply chain. A framework for selecting sustainability indicators that take into account all three dimensions of sustainability: economic, societal and environmental, is presented. Special attention is given to a useful definition of the boundary for the system and to the identification of the relevant impacts associated with the biodiesel supply chain stages. A set of sustainability indicators is proposed for quantitative sustainability assessment, based on the impacts deemed relevant for each supply chain stage. Some qualitative arguments

T.M. Mata (✉) • C.A.V. Costa
Laboratory for Process, Environmental and Energy Engineering (LEPAE),
Faculty of Engineering, University of Porto (FEUP), R. Dr. Roberto Frias, s/n,
4200-465 Porto, Portugal
e-mail: tmata@fe.up.pt

A.A. Martins
Center for Transport Phenomena Studies (CEFT), Faculty of Engineering,
University of Porto (FEUP), R. Dr. Roberto Frias, s/n, 4200-465 Porto, Portugal

S.K. Sikdar
National Risk Management Research Laboratory, Office of Research and Development,
U.S. Environmental Protection Agency, 26 West Martin Luther King Drive,
Cincinnati, OH 45268, USA

N.S. Caetano
Laboratory for Process, Environmental and Energy Engineering (LEPAE),
Faculty of Engineering, University of Porto (FEUP), R. Dr. Roberto Frias, s/n,
4200-465 Porto, Portugal

Department of Chemical Engineering, School of Engineering (ISEP),
Polytechnic Institute of Porto (IPP), R. Dr. António Bernardino de Almeida, s/n,
4200-072 Porto, Portugal

J.W. Lee (ed.), *Advanced Biofuels and Bioproducts*, DOI 10.1007/978-1-4614-3348-4_31,

are also presented to support the evaluation. Although microalgae appear to be superior in some respects to other currently used feedstocks, the development of large-scale microalgae production systems still needs further research.

1 Introduction

It is commonly accepted that our dependence on fossil fuel and the gradual rise of greenhouse gas (GHG) in the atmosphere are intimately coupled. Several strategies are being devised and currently implemented in the transportation sector of the economy to stem this GHG rise. Examples of Government and business strategies alike include the development of alternative fuels, more efficient engines or transportation means, transportation networks better fitted to the societal and economic needs of evolving human societies, among others. In the short term, biofuels, such as biodiesel or bioethanol, are seen as viable options to partially fulfill the objectives of reducing the environmental impacts, in particular of global warming.

Biodiesel has some important advantages over other currently sought potential solutions. It can be produced from a wide range of vegetable oils from agricultural crops (e.g. rapeseed, soy, sunflower, palm oil, hemp, among many others) or even residual materials, in particular animal fats from the meat or fish processing industries that are difficult to dispose of. The technology and know-how needed to produce it efficiently is already available, and setting up a production facility is relatively easy. The real challenge here is to have access to enough raw materials to meet the current demand, without compromising sustainable development. Although source-to-wheel assessments indicate that the use of biofuels in vehicles yields benefits in terms of GHG and other pollutant emissions (e.g. sulfur and nitrous oxides) when compared to petroleum-based fuels, their impact on the biodiversity loss and competition for arable land can be deleterious if general sustainability criteria are not met. Also, the precise amount of saved CO_2 emissions depends on the feedstocks used, the production processes, and on several other factors.

Thus, it is fundamental that the emerging biofuels sector is built on sound sustainability principles. In that regard, the European Commission recently put forward a broad set of sustainability criteria for biofuels in the Directive 2009/28/EC [3] for the promotion of renewable energy sources, which complement the targets already defined by the European Union concerning the utilization of biofuels. Some of the sustainability criteria in this new directive include that no raw material should be provided from undisturbed forests with important biodiversity, no land with carbon stock (wetlands or continuously forested areas) should be converted for biofuels production, the use of land for the production of biofuels must not be allowed to compete with the use of land for the production of food, a minimum of 35% GHG savings has to be attained, and also, societal considerations must be taken into account.

However, the increase in production and even the announced targets for biodiesel has raised some problems of its own. Nowadays, vegetable oils (edible or non-edible) and animal fats are the main feedstock for biodiesel production. As vegetable oils

are also used for human consumption, the competition for arable land and the expected increase in food prices have become significant concerns. Additionally, it increases the biodiesel production costs, hindering its usage, even if the environmental impact of biodiesel is smaller than that of fossil fuels. Production processes may not be most adequate and optimized for the available feedstocks. Also, to fulfill the EU target of 10% from domestic sources, the actual feedstocks supply and the domestic arable land available in Europe are not enough [17]. Moreover, extensive monoculture plantation, the conversion of high conservation-value forests, and other critical habitats for cultivation of biodiesel feedstocks are unacceptable. These habitats and associated biological diversity can be lost forever, due to the cutting of existing forests and the utilization of ecologically important areas [14]. Also of concern are jeopardizing food supplies of people living in developing countries that still strongly depend on agriculture.

Therefore, new feedstocks are needed to complement the existing ones. Examples include the utilization of agricultural crops not used for human consumption, such as lignocellulosic materials and microalgae, among others, with higher biomass productivity when compared with the currently used feedstocks [18]. All options have their specific advantages and drawbacks that have to be taken into account when selecting adequate feedstocks. As the majority of production processes associated with alternative feedstocks are still under development, decisions concerning their development and practical implementation should be made considering all three dimensions of sustainability: economic, societal and environmental.

Among the potential feedstocks, microalgae are increasingly seen as a viable option for the production of biodiesel and even other types of biofuels. This work attempts to evaluate the relative sustainability of microalgae biodiesel when compared with the currently used fuels, and to identify the key advantages and problems associated with their use for biodiesel production.

2 Sustainability Evaluation of Microalgae for Biodiesel Production

2.1 Framework for Defining Sustainability Indicators

The commonly understood three dimensions of sustainability as shown in Fig. 1 are largely interrelated, i.e. what is good for the environmental is also good for society, or what is good for the economy can be usually good for society, and so on.

As shown, sustainability exists at the intersection of the three domains representing the economy, environment, and society. We can state that a system becomes more sustainable when all three domains, as represented by the intersection of the three domains, show improvement as a result of a human intervention. This Venn diagram also facilitates identification of the dimensions of the metrics to be used to evaluate relative sustainability of a selected system. For instance, any indicator or

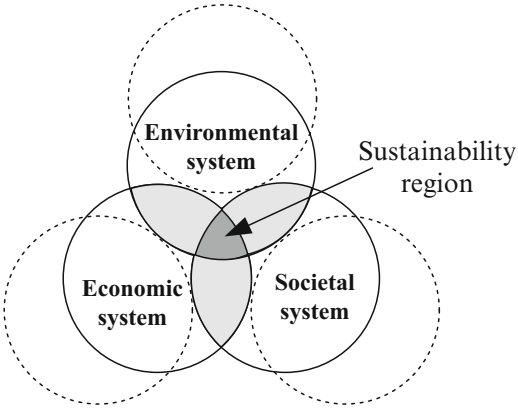

Fig. 1 Generally accepted model for sustainability

metric that represents all three dimensions, such as energy use, will be a 3D or 3D metric. Similarly other metrics could be 2D or 1D, depending on how many domains are represented.

When the task is to compare the relative sustainability of a system against alternatives, we need to consider the following actions in sequence: define the system, identify the metrics to be used and their dimensionality, prioritize them in terms of their significance, obtain values of those metrics for the competing alternatives, and compare them to arrive at a decision. A small set of indicators is ideally preferable because it simplifies analysis, and sometimes allows a decision by visual inspection of the values of the metrics. Though not always possible, it is advisable that the metrics are deemed to be necessary and sufficient, independent of each other, and are quantifiable.

In this work the framework previously used by Martins et al. [10] is applied for the sustainability evaluation of microalgae biofuels, taking into account the biofuel supply chain stages that include: microalgae cultivation and harvest, biomass processing, oil extraction and pre-treatment, biodiesel production and blending, distribution, and final use. In practice, one needs to first clearly define the system boundaries with identified supply chain. This process allows identification of the indicators to be used and the kinds of data to be collected for calculating their values. Then, all the relevant inputs and outputs (energy, water, materials, product, by-products, wastewater, gas emissions, solid wastes, etc.) should be identified and quantified, in order to be able to calculate the values of the selected metrics. Finally, when the values of the metrics for all possible alternatives are available, a decision on relative sustainability can be made either by inspection or by use of computational tools.

For deriving sustainability indicators and to evaluate microalgae biodiesel through its supply chain, the following sequential procedure (Fig. 2) can be applied:

1. System boundary definition, including inputs and outputs (energy and mass fluxes) through the supply chain.
2. Identification of the most relevant environmental, economic and societal impacts that ought to be considered and explicitly included in the indicators to be selected, as well as the data required for their calculation.

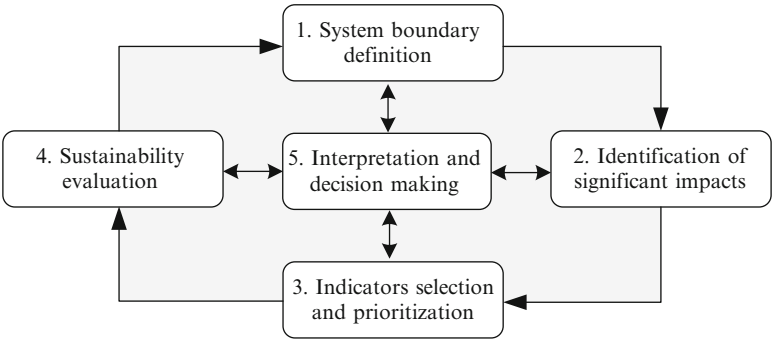

Fig. 2 Sequential procedure for defining sustainability indicators

3. Selection and prioritization of an adequate set of sustainability indicators based on technical input and data availability. All the relevant inputs and outputs should be identified and quantified, in order to be able to calculate the indicators values.
4. Calculation of the chosen indicator values for sustainability evaluation. The 3D, 2D and 1D metrics are calculated based on the inventory analysis of the process.
5. Interpretation and decision making. Decisions for improving the process are made based on the results of the indicators calculation and on the consideration of other issues, for example cost analysis.

2.2 System Boundary Definition for Microalgae Biodiesel Supply Chain

Microalgae are a class of microorganisms that number in thousands of species, which are present in a wide variety of ecosystems and live in a large variety of environment and environmental conditions. Under particular conditions, certain species produce large amounts of lipids and free fatty acids, compounds that are the basic raw materials for the production of biodiesel.

Other biofuels, such as bioethanol or higher alcohols, can also be obtained through the hydrolysis and fermentation of the algal biomass.

Alternatively, microalgal biomass can be gasified or pyrolysed to produce a range of other biofuels (biomass-to-liquid), hydrocarbons, biogas, and even biohydrogen. Another possibility is the production of high value chemicals, such as pigments, proteins, and nutraceuticals, simultaneously with the production of biofuels, thus diversifying the sources of income and improving the overall profitability.

In addition to the aforementioned advantages, the cultivation of microalgae opens new possibilities for its integration within existing or future processes, such as wastewater and flue gas treatments, removal and sequestration of GHG, in particular

carbon dioxide, with the potential for reducing additional environmental impacts. In fact, various studies demonstrated the potential use of microalgae for pollution control, and production of useful products, such as commodity chemicals, and energy cogeneration combustion [5, 12]. Thus microalgae can be environmentally sustainable, cost-effective and profitable for the production of biofuels and other bio-products. In a broader sense, microalgae can be seen as an important part of a biotechnology supply chain that can produce many of the basic chemicals necessary for the development.

In this study the system boundary (Fig. 3) is defined to include the supply chain stages of microalgae biodiesel [11], from algal cultivation and further processing to biodiesel production, assuming that no additional products are obtained from the process. Please note that a consumption step is absent as it is the same as for other biofuels. Therefore, the main differences will occur in the first stages of each fuel supply chain.

Although microalgae have similar oil content to other seed plants, there are significant variations in the overall biomass productivity, the resulting oil yield, and biodiesel productivity, with a clear advantage for microalgae. Also, the growth and harvest of microalgae needs much less land area than other feedstocks of agricultural origin, up to 49 or 132 times less when compared to rapeseed or soybean crops, respectively, for a 30% (w/w) oil content in algae biomass [11]. Also, they can reproduce themselves using photosynthesis to convert solar energy into chemical energy, completing an entire growing cycle every few days.

As different algae species have similar efficiencies concerning fuels production, the selection of the most adequate species should take into account their characteristics and other factors, such as the quantity of nutrients available, solar irradiation, as well as other environmental conditions [11]. From a practical point of view, microalgae are easy to cultivate, can grow with little or no attention, often using water unsuitable for human consumption, and it is easy to obtain the necessary nutrients [15]. They need not only nutrients (nitrogen and phosphorous), which are vital for the growth of algal biomass, but also adequate operating conditions (oxygen, carbon dioxide, pH, temperature, and light intensity). By manipulating these operating parameters one can easily control algal biomass growth and the composition of the algal populations even at a larger scale. De Pauw et al. [2] state that

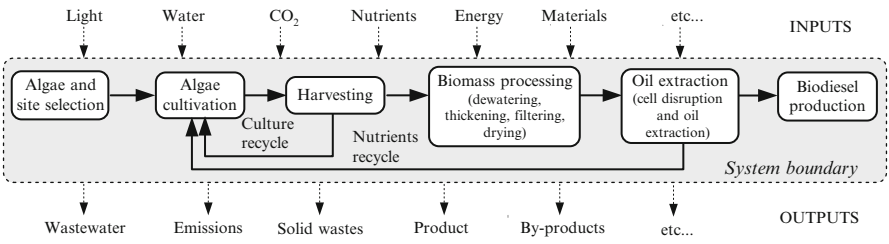

Fig. 3 System boundary including the supply chain stages of microalgae biodiesel

experience has repeatedly shown that properly managed algal cultures are quite resistant and that infections are often an indication of poor culture conditions.

Combined with their ability to grow under harsher conditions, and their reduced needs for nutrients, microalgae can be cultivated in areas unsuitable for agricultural purposes (on marginal or nonarable land), independently of the seasonal weather changes. This greatly reduces the competition for arable soil with other crops, in particular for human consumption, and can open up new economic opportunities for arid, drought, or salinity-affected regions [18]. Moreover, they are becoming an alternative oil source with favorable oil yields and much higher growth rates when compared to conventional biodiesel feedstocks.

Currently, much research effort is being focused on the algal production units, as in most cases it represents the key step that ultimately determines the economic viability of the process [11]. Microalgae cultivation units can be open or closed production systems, operated in multiple batch or continuous modes. These variations depend on the microalgae species selected, the expected environmental conditions, nutrients available, and the possibility to combine the microalgae growth with a pollution control strategy of other industry, for example, for the removal of CO_2 from flue gas emissions or the removal of nitrogen and phosphorus from a wastewater effluent. If closed cultivation systems with minimal evaporation are used, considerable savings in water consumption can also be achieved.

Some limitations on second generation biofuels from microalgal culture systems have been identified in the harvesting process (representing 20–30% of the total production cost) and in the supply of CO_2 for a high efficiency production [4]. A suitable harvesting method must be able to process large volumes of algal biomass and may involve one or more solid–liquid separation steps, such as sedimentation, centrifugation or filtration. Sometimes, an additional flocculation step is required, due to the need to remove large quantities of water. Drying and cell disruption for release of the metabolites of interest also represents a major economic limitation to the production of low cost commodities (foods, feeds, fuels) and also of higher value products (β-carotene, polysaccharides). Most common drying methods include spray-drying, drum-drying, freeze-drying and sun-drying, but the last one is not very effective because of the high water content of algal biomass. After drying, solvent extraction of lipids can be done directly from the lyophilized biomass using hexane or ethanol [11].

Even though, biodiesel feedstock's can vary significantly, the biodiesel production process currently used at industrial scale is the alkali-catalyzed transesterification process where triglycerides and an alcohol (usually methanol) react in the presence of an alkali catalyst (e.g. NaOH or KOH) to obtain fatty acid methyl esters (biodiesel) [11]. Also, depending on the oil acidity one or two process steps have to be performed, where in a first step, the level of free fatty acids is reduced to below 3% by acid-catalyzed esterification, using methanol as reagent and sulphuric acid as catalyst, for a portion of the methyl ester biodiesel and, in a second step, triglycerides in product from the first step are transesterified with methanol by using an alkaline catalyst to produce more of the same biodiesel and glycerol.

2.3 Indicators for the Sustainability Analysis of Microalgae Biodiesel

After defining the system boundary, all the relevant environmental, economic, and social impacts associated with the microalgae biodiesel supply chain stages have to be identified. These can be the following:

- Energy consumption
- Net GHG emissions
- Freshwater consumption
- Wastewater treatment
- Nutrients consumption (e.g. nitrates, phosphates, carbon source)
- Chemicals for oil extraction (e.g. n-hexane) and biodiesel production (e.g. CH_3OH, NaOH)
- Residual biomass management
- Land use
- Potential chemical risk
- Net cash flow generated
- Employment

Then, the relative significance or insignificance of these impacts are identified (for each supply chain stage) based on the authors current knowledge of the processes involved. For example, energy consumption is a significant impact in many supply chain stages, since it is needed for algae cultivation, harvesting, biomass processing, oil extraction, and biodiesel production, while land use is more significant for microalgae cultivation than in the remaining stages. Freshwater consumption is significant for the cultivation stage unless wastewater from another source, which can also be used as a source of nutrients, is used instead to cultivate microalgae.

After a careful analysis of the system under study, involving the identification of the impacts on the domains of sustainability that are significant for each supply chain stage, candidate indicators are selected for the sustainability analysis of microalgae biodiesel. The selected indicators have to fulfill the following conditions [10]:

- Form a coherent set of quantifiable variables consistent with the principles of sustainability
- Be representative of the physical system under study
- Be clear, simple, unambiguous, and not biased
- Be independent of each other and form a small set
- Be directly and easily calculated from system data

The dimensionality of metrics (3D, 2D or 1D) can then be determined [19, 20]. For example, “energy intensity” is a sustainability or 3D indicator, since it takes into account aspects of the three sustainability dimensions. The higher it is, the more negative the impact is for the environment, because of the waste generated in energy production. Yet, as it is positive for the economy, because it is essential for value creation and higher standards of living, it has both positive and negative societal

impacts, as future generations will be deprived of currently used sources of energy because of their depletion but lower emissions of pollutants will result from the consumption of biodiesel. Similarly, "land use intensity" contributes to soil degradation and biodiversity loss with a negative impact in the environment. It is positive for the economy, because of the value creation from crops produced. Yet, it may have a positive or a negative societal impact depending on how it contributes respectively to employment or land competition with other crops, in particular food crops. On the other hand "Contribution to Global Warming" also called as carbon footprint, can be seen as directly related to global warming and to the environmental effects of it. Also, it is expected that it will create an economic impact because of carbon trading or carbon taxes, if GHG control regulations are in place, this way being a 2D indicator.

After the candidate indicators have been selected, prioritization of the set of indicators follows, based on technical input and data availability. Only if the information exists it is possible to quantify the indicators and perform the sustainability analysis. The conclusions from the analysis will be more reliable if the data are of good quality.

The set of indicators that are of high priority for the sustainability evaluation of microalgae biodiesel are the following:

1. Life cycle energy efficiency (dimensionless), 3D
2. Fossil energy ratio (dimensionless), 1D
3. Land use intensity (m^2/MJ biodiesel/year), 3D
4. Contribution to global warming (kg CO_2-eq/MJ fuel), 2D

Table 1 synthesizes the sustainability indicators selected for evaluating the sustainability of microalgae systems for biodiesel production.

Similar metrics have been proposed by other authors in a biofuels or conventional fuels context. For example, Pradhan et al. [13] compared four biodiesel energy balances using two indicators: the net energy ratio and the renewability factor. Zhou et al. [22] proposed four indicators for a sustainability assessment of conventional fuels during their life cycles. Kim et al. [7] considered the land use change and GHG emissions associated with the production of biofuels.

The purpose of this article is to describe how to perform a sustainability analysis of microalgae biodiesel system comprising the entire supply chain, and also propose specific sustainability indicators. To the authors' knowledge, no full scale commercial plant for microalgae biodiesel exists at present. So, in the absence of commercially relevant data, the reliability of the values of the metrics used at present would be somewhat limited.

Although some suggestions can be found in literature [1, 6, 8, 9, 16, 21], there are no complete LCA studies with reliable data on biodiesel produced from microalgae. Also, the majority of the published studies analyzed hypothetical scenarios.

For example, Kadam [6] conducted an LCA to compare the environmental implications of electricity production via coal firing vs. coal/algae co-firing, using 50% of the flue gas from a 50 MW power station as the carbon source to grow microalgae. Results of this study show that when recycling CO_2 toward microalgae production it is possible to achieve an overall life cycle CO_2 saving of 36.7%.

Table 1 Indicators for the sustainability evaluation of microalgae biodiesel

Indicator	Definition
Life cycle energy efficiency (LCEE) (dimensionless)	It is the ratio of the total energy produced (energy output) to the total energy consumed (energy input) Lifecycle energy efficiency (LCEE) = energy output/energy input The energy content of by-products may be accounted for in the energy output if they are used for energy production in substitution of fossil fuel or electricity. LCEE also called net energy ratio (NER) measures the relative amount of energy that ends up in the final fuel products
Fossil energy ratio (FER) (dimensionless)	It is the ratio between the amount of energy that goes into the final fuel product (fuel energy output) and the amount of fossil energy input (non-renewable energy) required for the fuel production Fossil energy ratio (FER) = Fossil energy output/Fossil energy input FER is also called the renewability factor (RF) since it measures the degree to which a given fuel is or is not renewable. Larger the value of FER less fossil energy is used (assumed to be non-renewable) for the same energy output. A FER greater than one can be used to replace the energy used in producing it. Also, theoretically FER can be infinite if no fossil energy is needed for the fuel production meaning it is "completely" renewable
Land use intensity (m^2/MJ fuel/year)	It measures the area of land occupied per unit energy of product (e.g. the land needed for the biodiesel feedstocks cultivation, which affects biodiversity and life support functions)
Contribution to global warming (kg CO_2-eq/MJ fuel)	It measures the potential contribution of different GHG emissions (e.g. CO_2, CH_4, N_2O) to global warming (or greenhouse effect), expressed as equivalent CO_2 emission per unit energy of fuel product $$\text{Contribution to global warming} = \sum_i \text{GWP}_i \times E_i,$$ where E_i is the mass of greenhouse gas i emitted to the air and GWP_i is the Global Warming Potential of the substance i The total GHG emissions (E) through the fuel life cycle are calculated as [3] $$E = e_{ec} + e_l + e_p + e_{td} + e_u - e_{ccs} - e_{ccr} - e_{ee},$$ where e_{ec} are emissions from the extraction or cultivation of raw materials; e_l are annualized emissions from carbon stock changes caused by land use change; e_p are emissions from processing; e_{td} are emissions from transport and distribution; e_u are emissions from fuel usage; e_{ccs} are emission savings from carbon capture and sequestration; e_{ccr} are emission savings from carbon capture and replacement; and e_{ee} are emission savings from excess electricity from cogeneration

Lardon et al. [8] performed an LCA on the production of biodiesel from *Chlorella vulgaris*, showing that when this algae is grown in nitrogen-deprived conditions and the oil is extracted directly from the wet biomass without the need for drying, the biodiesel would have a GWP lower than fossil diesel but higher than biodiesel produced from rape seed oil or palm oil.

Lehr and Posten [9] estimated the energy needed for operating a photo-bioreactor compared to the possible chemical energy harvested. According to these authors the economical feasibility of biofuel production by algae cannot be obtained in the short term. The outstanding problems of cost and efficiency of microalgae cultivation for biodiesel need critical attention.

Rodolfi et al. [16] evaluated the biomass productivity, lipid content, and lipid productivity of 30 microalgal strains cultivated in 250 mL flasks. They suggested that in order for microalgae cultures to become an economic, renewable, and carbon-neutral source of transportation fuel, biofuels production needs to be combined with that of production of higher value co-products.

Clarens et al. [1] compared from a life cycle perspective, conventional crops (rapeseed, switch grass, and corn) with microalgae cultivation for biofuels production, concluding that microalgae have higher environmental impacts than these conventional crops in terms of energy use, GHG emissions, and water consumption regardless of cultivation location. These authors suggested that to reduce the impacts, flue gas could be used as a carbon source for producing algae near power plants and also wastewater treatment could be combined with algae cultivation as a source of nutrients.

Stephenson et al. [21] investigated the life cycle global warming potential (GWP) and the fossil energy requirements, for a hypothetical operation in which biodiesel is produced from the freshwater microalgae *C. vulgaris*. These authors concluded that for a more environmentally sustainable cultivation of these algae in open ponds instead if closed photo-bioreactors, it should be possible to achieve a lipids productivity target of 40 tons/ha/year. This way the GWP of microalgae would be about 80% lower than fossil diesel on a net energy content basis.

The utilization of microalgae, at least from a land use intensity point of view should be a viable option for substituting current feedstocks, as the former has much higher productivity when compared with existing feedstocks. However, the state of development at present precludes a more extensive utilization of microalgae for biodiesel production which could have a real impact in the fossil fuel market.

We can summarize the reasons for the delay of a more widespread usage of microalgae as a feedstock for biofuel production. First, there are still some hurdles to cross concerning their cultivation at large scale. Although some strains are already identified as promising for biofuel production, only a few of them have been attempted at an industrial scale. Critical information about the conditions in which microalgae give the highest yield of lipids or other components of interest is still lacking, especially the nutrient mix and sunlight necessary for inducing it [11]. Second, there are scaling problems when going from laboratory and pilot scale units to fully commercial plants. When growing microalgae in large open ponds, one has to ensure that all microorganisms receive an adequate amount of energy and nutrients, a difficult task when the cell concentration is very high. Third, other challenges are posed by the growth cycle of the microalgae, which should be better understood

in order to know when it is the best time for harvesting them, and that during the decline or death phase microalgae cultures are more susceptible to potential contaminations by other organisms that will compete for food and space.

Potential solutions for these problems include the selective growth of particularly resistant strains or even their genetic engineering in order to produce species better fitted for biofuels production. Fourth, the microalgae harvesting and processing steps, before the biodiesel production, are still under development. As described above, due to high water content of the algal biomass, some of the processes may require high quantities of energy, making the production of biodiesel from microalgae an energy intensive process, thus increasing its environmental impact [11].

Notwithstanding the possible difficulties, microalgae are seen as one of the most viable options in the medium to far future. Some of the reasons are directly related to their physiology. As simple organisms, they can grow very fast and produce lipids among other metabolites of interest, only requiring water with a given salinity and pH, sunlight, carbon dioxide and a source of nitrogen and other nutrients. This is clearly an advantage over agricultural feedstocks and even future cellulosic raw materials, which normally require pesticides, fertilizers, tillage, and other treatments for their production. Also, due to their diversity the probability of finding or engineering the most adequate microalgae strain is high and is easier to do than with the more complex plants.

3 Conclusions

In this work a set of sustainability indicators is proposed in order to assess the utilization of microalgae as a feedstock for biodiesel production from a supply chain point of view, the supply chain stages being cultivation of microalgae, harvesting, and further processing for biodiesel production. Microalgae can be a sustainable option as a feedstock for biofuels production, combining high productivity with high oil content. In particular, the land use intensity is clearly smaller when compared to other feedstocks, minimizing the questions directly linked with land use, and the loss of biodiversity. Also, microalgae have the potential to be used in the production of other chemicals of high added value or integrated in existing industrial processes for other beneficial purposes, such as carbon sequestration or wastewater treatment. However, more research is still needed to develop more economical industrial production systems and to fully explore the microalgae potentials.

References

1. Clarens AF, Resurreccion EP, White MA, Colosi LM (2010) Environmental life cycle comparison of algae to other bioenergy feedstocks. Environ Sci Technol 44:1813–1819
2. De Pauw N, Morales J, Persoone G (1984) Mass culture of microalgae in aquaculture systems: progress and constraints. Hydrobiologia 116(117):121–134

3. Directive 2009/28/EC of the European Parliament and of the Council on the promotion of the use of energy from renewable sources, 23 April 2009
4. Grima ME, Belarbi EH, Fernández FGA, Medina AR, Chisti Y (2003) Recovery of microalgal biomass and metabolites: process options and economics. Biotechnol Adv 20(7–8):491–515
5. Hodaifa G, Martínez ME, Sánchez S (2008) Use of industrial wastewater from olive-oil extraction for biomass production of *Scenedesmus obliquus*. Bioresour Technol 99(5):1111–1117
6. Kadam KL (2002) Environmental implications of power generation via coal microalgae co-firing. Energy 27:905–922
7. Kim H, Kim S, Dale BE (2009) Biofuels, land use change, and greenhouse gas emissions: some unexplored variables. Environ Sci Technol 43:961–967
8. Lardon L, Hélias A, Sialve B, Steyer JP, Bernard O (2009) Life-cycle assessment of biodiesel production from microalgae. Environ Sci Technol 43(17):6475–6481
9. Lehr F, Posten C (2009) Closed photo-bioreactors as tools for biofuel production. Curr Opin Biotechnol 20:280–285
10. Martins AA, Mata TM, Sikdar S, Costa C (2007) A framework for sustainability metrics. Ind Eng Chem Res 46(10):2962–2973
11. Mata TM, Martins AA, Caetano NS (2010) Microalgae for biodiesel production and other applications: a review. Renew Sustain Energy Rev 14:217–232
12. Murakami M, Yamada F, Nishide T, Muranaka T, Yamaguchi N, Takimoto Y (1998) The biological CO_2 fixation using *Chlorella* sp. with high capability in fixing CO_2. Stud Surf Sci Catal 114:315–320
13. Pradhan A, Shrestha DS, Van Gerpen J, Duffield J (2008) The energy balance of soybean oil biodiesel production: a review of past studies. Trans ASABE 51(1):185–194
14. RFA (2008) The Gallagher Review of the indirect effects of biofuels production. Renewable Fuel Agency (RFA)
15. Richmond A (2004) Handbook of microalgal culture: biotechnology and applied phycology. Blackwell, Oxford
16. Rodolfi L, Zittelli GC, Bassi N, Padovani G, Biondi N, Bonini G, Tredici MR (2009) Microalgae for oil: strain selection, induction of lipid synthesis and outdoor mass cultivation in a low-cost photobioreactor. Biotechnol Bioeng 102(1):100–112
17. Scarlat N, Dallemand JF, Pinilla FG (2008) Impact on agricultural land resources of biofuels production and use in the European Union. Conference and Exhibition on Bioenergy: Challenges and Opportunities, Guimarães, Portugal, April 6–9
18. Schenk PM, Thomas-Hall SR, Stephens E, Marx UC, Hruse O, Hankamer B (2008) Second generation biofuels: high-efficiency microalgae for biodiesel production. Bioenergy Res 1(1):20–43
19. Sikdar SK (2003) A journey towards sustainable development. A role for chemical engineers. Environ Progress 22(4):227–232
20. Sikdar SK (2003) Sustainable development and sustainability metrics. AIChE J 49(8): 1928–1932
21. Stephenson AL, Kazamia E, Dennis JS, Howe CJ, Scott SA, Smith AG (2010) Life-cycle assessment of potential algal biodiesel production in the United Kingdom: a comparison of raceways and air-lift tubular bioreactors. Energy Fuel 24(7):4062–4077
22. Zhou Z, Jiang H, Qin L (2007) Life cycle sustainability assessment of fuels. Fuel 86(1–2):256–263

Chapter 32
Life Cycle Assessment of Algae-to-Energy Systems

Andres Clarens and Lisa Colosi

Abstract Algae-derived bioenergy is being widely discussed as a promising alternative to bioenergy produced from terrestrial crops. Several life cycle assessment (LCA) studies have been published recently in an effort to anticipate the environmental impacts of large-scale algae-to-energy systems. LCA is a useful tool for understanding the environmental implications of technology, but it is very sensitive to modeling assumptions and techniques. In this chapter, the methodological issues surrounding LCA of algae-to-energy systems are reviewed in the context of several of the recent papers with a particular focus on system boundaries, cultivation techniques, metrics, coproduct allocation, and uncertainty. The issues raised here are useful in two regards: (1) they enable an understanding of the differences between the published studies and allow LCA practitioners and others to more directly interpret the results and (2) they serve as a good starting point for future analysis of algae-to-energy technologies.

1 Introduction

The promise of using algae as a bountiful and renewable source of bioenergy has been attracting increasing attention over the last few decades [26]. This is because algae have a number of characteristics that make them appealing relative to other bioenergy sources. They are generally fast growing and produce more biomass per area of land than most terrestrial crops [19]. Certain species generate high concentrations of lipids so they can be used to produce liquid fuels, such as biodiesel, using existing conversion technologies [18]. And since they are grown in water, they could

A. Clarens (✉) • L. Colosi
Civil and Environmental Engineering, University of Virginia,
Charlottesville, VA 22904, USA
e-mail: aclarens@virginia.edu

J.W. Lee (ed.), *Advanced Biofuels and Bioproducts*, DOI 10.1007/978-1-4614-3348-4_32,

also be cultivated in man-made ponds, which suggests their cultivation can be scaled up and operated in steady-state mode, greatly enhancing their potential for large-scale energy production. Over the past few years, interest in algae-to-energy technologies has surged for a variety of reasons. Among them is the idea that algae could be used to sequester CO_2 from fossil fuel burning sources, thereby reducing a major contributor to climate change [3]. Increasing petroleum prices, concerns about our dwindling fossil fuel reserves, and the perceived competition between food and fuel uses for crops that can be consumed as food have also contributed to interest in algae as a fuel source [23].

The heightened attention on algae-to-energy systems has resulted in a proliferation of academic and industrial publications describing these technologies. A number of these studies focus on quantifying the environmental impacts of algae-to-energy systems using life cycle assessment (LCA) techniques [8, 14, 24, 31]. LCA is a framework for assessing the environmental and energy implications of a process or product over its entire life cycle (LC), from resource extraction to final disposal. Over the past 10 years, LCA has emerged as a valuable tool for understanding the full environmental costs of complex engineering systems. It allows designers and engineers to avoid media shifting, whereby one environmental impact is avoided at the cost of some other, often hidden and worse, environmental burden [13]. LCA can also serve as a useful design tool that allows for a priori evaluation of different engineering decisions. By applying LCA in this way, it is possible that many traditional sources of pollution can be avoided upstream rather than remediated after they are generated. Even though LCA has been widely practiced for over a decade, only recently have the techniques been applied to algae-to-energy processes.

The algae-related LCA studies appearing in the academic literature to date offer multiple perspectives on how large-scale algae-to-energy systems might be deployed. These studies are largely speculative because there is a lack of empirical data for long-term operation of full-scale commercial algae cultivation systems. In general, the results of algae LCA studies published to date are difficult to compare because of key modeling differences. The differences originate from several stages of the analyses. To begin with, the *scope*, e.g., system boundaries and functional unit of the studies, is different. Second, the *data sources* used in the studies, the way in which the studies report their results (i.e., *metrics*), and the manner in which they allocate burdens to different processes (e.g., *coproducts*) also vary quite a bit. This variability is to be expected given that there are, as yet, no norms for the industry that would suggest the most reasonable set of assumptions. Finally, the unsatisfactory way in which the studies handle *uncertainty* speaks to the lack of data in this field. Table 1 highlights the array of different modeling assumptions that have been used in some of the LCA studies of algae-to-energy systems that have been published to date. It should be pointed out that each of these studies utilized a different functional unit and many use different modeling assumptions. Thus, it is no surprise that the results are difficult to compare.

In general, it cannot be said that one particular study is more or less “correct” than any of the others. LCA challenges exist even for processes and products that

Table 1 Select LC modeling assumptions for several studies appearing in the academic literature to date

Study	FU	Data sources	Coproducts	Uncertainty?
Stephenson et al. [31]	1 ton biodiesel	NREL US LCI	Digestion/electricity	No
Campbell et al. [5]	1-km diesel truck	Australian LCI	Digestion/electricity	No
Jorquera et al. [14]	1 ton dry solids	Literature review	None	No
Clarens et al. [8]	317 GJ	EcoInvent	None	Yes
Lardon et al. [17]	1 MJ fuel	EcoInvent	Glycerol	No

FU functional unit; *NETL US LCI* National Renewable Energy Laboratory of the United States Department of Energy Life Cycle Inventory Database [20]; *Australian LCI* Australian National Life Cycle Inventory Database; *EconInvent* Swiss National Life Cycle Inventory Database [34]

are well characterized and widely practiced. One widely cited, and related, example is the case of petroleum-based liquid fuels. Since the early 1990s, a substantial number of studies have been conducted describing the process of extracting the crude oil from the ground, transporting it, refining it, distributing and selling it, then burning it in cars and trucks [25]. Different studies resulted in very different estimates for the burdens of similar processes that are practiced in more or less the same manner around the world. To address these challenges, Argonne National Laboratory in the United States created the Greenhouse Gases and Regulated Emissions, and Energy Use in Transportation (GREET) model for estimating LC burdens associated with petroleum-based transportation fuels in 1996 [33]. By synthesizing the results from various published LC models, and normalizing the system boundaries and allocation assumptions among analyzed cases, the creators of GREET produced a meta-model that is more representative of petroleum fuel production than any one given analysis. This occurs because the meta-model effectively neutralizes (i.e., washes out) some assumptions that can make any one particular study either over- or underestimate the true impacts of a given process. Since the algae-to-energy industry is currently undergoing such rapid development, it seems timely to consider standardization of LC methodology to improve the accuracy of LCA for algae-derived fuels.

This chapter is written for two primary audiences. The first is the algae-to-energy researchers wishing to model LC impacts of specific products or processes. For these uses, the material presented here should serve as a useful primer into the language of LCA as it relates to algae-to-energy processes. The second audience is the broader scientific and journalistic community. This community has occasionally misinterpreted the results of several recent algae LCAs. The material presented here should help educate the science-literate reader who has no background in LCA so that they can better understand the implications and conclusions of algae LCA studies. It is expected that successful engagement of both audiences should improve the quality of future algae LCA studies and contribute to discourse about the merits of algae-to-energy technologies.

2 Goal and Scope Definition

A life cycle analyst's motives for carrying out an LCA can have important implications for the results of a study. These "zero order" assumptions are often rooted in the type of LCA being performed. LCAs fall broadly into one of two categories. *Attributional* LCAs are those in which all of the environmental impacts associated with a product or process are compiled and reported [1]. *Consequential* LCAs are those that evaluate the impacts of making a particular change to a process or product, or compare two technologies with related functions. Consequential LCAs are often more straightforward to perform because they permit for the canceling of unit processes or systems that are common between the technologies of interest. In the case of algae, most published LCA studies are attributional since there are few technological systems existing to which algae-to-energy can be compared. There is, however, an important role for consequential LCA as this field moves forward; since they can help identify and quantify what impacts might arise from evolving algae technologies. The decision to undertake an attributional or a consequential LCA is manifest most notably in decisions about the system boundaries and functional units of the study. System boundary decisions include all the elements associated with geographic areas, natural environments, time horizons, and others. The functional unit is the quantitative basis for the life cycle comparison and differs depending on the processes to be compared. Both are explored here.

2.1 System Boundaries

Most of the research on algae-to-energy systems carried out to date has been at the bench or demonstration scale [18]. This makes it difficult to say with much certainty what a full-scale algae-to-energy industrial facility would look like and herein lies one of the fundamental challenges of developing reliable LC estimates for algae production. Using best engineering judgment, it is possible to design hypothetical algae-to-energy facilities, but naturally, there is variability among these designs (Fig. 1). For example, one modeler might assume that algae should be cultivated in ponds, while another could assume photobioreactors [6]. Similarly, a belt filter press could be modeled as means to separate algae from the growth medium, whereas self-cleaning bowl centrifuges might be a viable alternative [24]. Both unit operations carry out the same dewatering function but with different requirements in terms of inlet and outlet concentration, demand for chemical flocculants used to accelerate the settling of the algae out of solution, and energy use profiles. Similarly, there are several technically viable options for extraction of oil from algae biomass, namely: sonication [28], bead mills [7], and enzymatic processes [11]. For conversion of algae biomass into biodiesel, one might choose decarboxylation of fatty acids [29] and digestion of non-fatty acid fraction [27] or the conventional transesterification route. Finally, the end-product of the algae-to-energy facility can

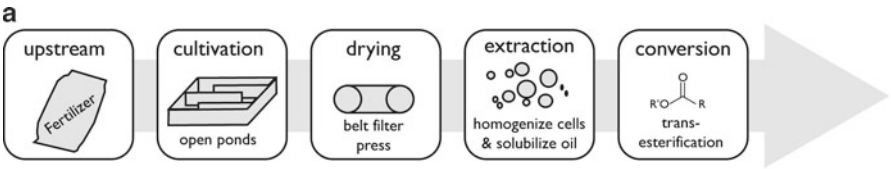

b

- flue gas reclamation [Kadam 2002] - wastewater reclamation [Brune 2009]	- closed photobioreactors [Chisti 2007] - air lift photobioreactor [Stephenson 2010]	- centrifuge [Clarens 2010] - solar drying [Sander 2010] - autoflocculation [Lardon 2009]	- sonication [Simon 1998] - bead mills [Chisti 1986] - enzymatic [Granhall 1972]	- combustion [Clarens 2010] - decarboxylation [Snare 2006] - digestion [Sialve 2009] - fermentation [Sander 2010]

Fig. 1 In selected system boundaries for an algae LCA study, one must typically select from (**a**) or capture all of (**b**) a large number of possible unit operations

also vary, because biodiesel is not the only energy carrier that can be produced from alga biomass [3]. It can be dried and combusted directly to generate electricity or it can be separated such that the carbohydrate fraction may be fermented to produce ethanol [24]. Naturally these two systems would have very different impacts.

As an example of the way in which systems boundaries selection can impact LCA results and conclusions, it's informative to consider two of the more thoroughly documented algae LCA studies that have been published to date: Clarens et al. [8] and Stephenson et al. [31]. Clarens et al. [8] used an energy-basis functional unit and only modeled cultivation-phase burdens for open pond systems. They did not account for the possibility that energy production from algae might also create valuable coproducts since they argue that it is still unclear whether there will be tenable markets for these coproducts. In contrast, Stephenson et al. [31] utilized a functional unit of 1 ton algae biodiesel to compare between open pond cultivation systems and photobioreactor cultivation systems. These authors included two types of valuable coproducts: electricity, as produced via combustion of natural gas generated during anaerobic digestion of residual (non-lipid) algae biomass, and glycerin. In light of these dramatically different sets of systems inputs, it's not surprising that each study reached different types of conclusions. Clarens et al. found algae-derived biomass energy to be generally more environmentally burdensome than corn, canola, or switchgrass alternatives. In contrast, Stephenson et al. found algae-derived biodiesel to be more environmentally beneficial than fossil-derived diesel.

Once an algae-to-energy process has been specified there is the additional uncertainty associated with setting system boundaries. LCA is typically intended to capture all of the environmental impacts of an engineered system. Naturally, in a highly interconnected technical world, system expansion results in models that become impossibly large and complex. For example, to produce carbon dioxide for use in industrial processes, it is necessary to model ammonia production since most of the carbon dioxide in this country comes from the steam reforming of hydrocarbons to produce hydrogen, most of which is used to produce ammonia via the Haber–Bosch process [21]. This in turn requires that we understand something about the way

natural gas is produced and transported in this country and the countless unit operations that allow us to purchase a canister of relatively pure carbon dioxide for the factory. To cope with this complexity, many LCA practitioners have set arbitrary boundaries around their processes of interest. For example, one study might state that any process contributing less that 5% of the total mass or energy or other impact to the final total is neglected. In this way the problem can be distilled down to something that is not computationally expensive and still yields good approximations of a process' impact.

Beyond system design and boundary setting, LCA analysts may chose to focus on specific pieces of a larger system to provide a desired level of resolution. For example, in their work, Clarens et al. considered only the cultivation of algae arguing that the uncertainties with that first step in the algae-to-energy life cycle should be addressed [8]. By focusing only on cultivation, the authors were able to explore the full implications of that important LC stage including crucial upstream impacts such as fertilizer production and carbon dioxide generation and delivery. In fact, a sensitivity analysis included in this chapter suggests that these two impacts are among the most important factors driving the overall life cycle burdens of algae production. Many of the other studies assume that the upstream impacts of delivering fertilizers and carbon dioxide should not be included. In Sander and Murthy, a cut off of 5% was assigned to LC contributions that would be neglected in the analysis [24] (Fig. 2). This represented the most rigorous treatment of boundaries from any of the studies published to date. However, this study also made certain assumptions, notably, that the effluent from a secondary wastewater treatment plant would contain enough nutrients to sustain a community of algae [4]. This assumption is not supported by stoichiometry or by the bench-scale research and as a result their estimates for algae life cycle impacts are most likely low.

2.2 Functional Unit

In all LC studies, a reference flow is needed to which all other modeling flows of the system will be related [13]. This flow must be a quantitative measure and for some industries, e.g., steel, the choice is usually obvious like X kg steel at the foundry. In other cases, including algae-to-energy systems, this decision can be more complicated. Recent studies have selected a wide variety of functional units (FU) including volume of biodiesel, dry mass of algae produced, kilometers of truck transport, and total energy embedded in the algae assuming the biomass is burned (see Table 2). All of these FUs are valid bases from which to evaluate algae LC, but this diversity in FUs does not make for straightforward comparison between studies. The lack of consensus on a standard FU reflects the lack of industry agreement on what the best products to make with the algae will be. Some of the assumptions about goal and scope setting carry over into the functional unit since a FU of liters of biodiesel will inherently exclude the value that could come from a by-product such as ethanol.

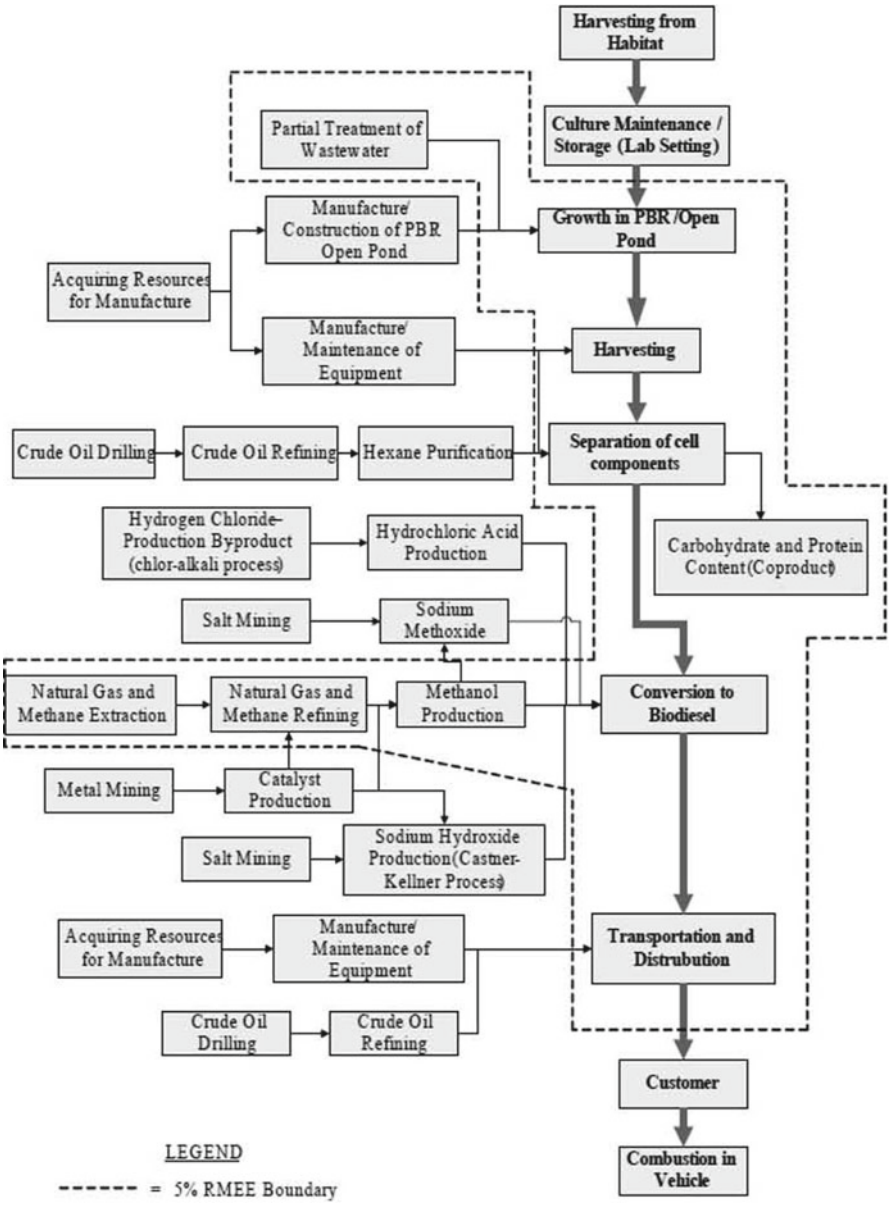

Fig. 2 Many studies assume that the upstream impacts of delivering fertilizers and carbon dioxide should not be included. A cut off of 5% was assigned to LC contributions that would be neglected in the analysis (from Sander and Murthy [24])

Table 2 Impact factors or metrics selected in several algae LCA studies

Study	Impacts
Stephenson et al. [31]	*GWP, energy use, water use*
Campbell et al. [5]	*GWP, energy use, land use*
Jorquera et al. [14]	*Energy use*
Clarens et al. [8]	*GWP, land use,* eutrophication, *water use, energy use*
Lardon et al. [17]	Abiotic depletion, acidification, eutrophication, *GWP*, ODP, human toxicity, marine toxicity, *land use*, ionizing radiation, and photochemical oxidation

Italicized metrics are common to multiple studies
GWP global warming potential; *ODP* ozone depleting potential

In LCA more broadly, FUs sometimes require that a performance constraint be applied in order to normalize between dissimilar systems. A carpet, for example, is quieter than a wood floor, even if the latter is more durable. Using a square meter of flooring as the functional unit may overlook performance characteristics (noise buffering and durability) that will ultimately impact the analysis [1]. In the case of algae, performance constraints are certainly limiting in a few important ways. When benchmarking algae to other terrestrial crops, it is useful to apply an FU that is commonly accepted by the biofuels industry. Though bushels of corn or liters of ethanol do not apply directly, analogs are possible. For example, algae might be compared in terms of dried biomass generated per unit area or liters of biodiesel produced per unit area per time. Energy content can be used as an FU, though it can overlook important differences between biomass. Algae may have a high heating value comparable to switchgrass though in practice, converting algae to usable fuel is quite a bit more straightforward.

3 Metrics

After the goal and scope of a study have been specified, a life cycle inventory (LCI) is typically carried out. The LCI is the accounting stage in which all the physical flows are reconciled with known emissions data to quantify the environmental burdens and resource requirements over the entire life cycle [1]. The outcome from this process is typically an exhaustive list of emissions factors; many more than can be reasonably expected or necessary in a report. Therefore, an important step in developing an LCA is the process of simplifying raw LCI data into specific metrics. Table 2 lists the impact metrics used in a few recent LCA papers of algae-to-energy systems. The differences in study endpoints contribute to the difficulties in comparing the results. The decision to include some metrics and exclude others can have important implications for the results and interpretation of the study. Most LCA guidebooks divide impact categories into three principle categories: resource use, ecological consequences, and human health [1]. Each category is discussed briefly here in the context of algae-to-energy systems.

3.1 Resource Use

Resource use is the most straightforward of the impact factor categories because the metrics involved are typically simple sums of flows from the environment. For example, total nonrenewable energy use, normalized by energy content, is a commonly encountered metric. Total land use is an important resource metric that has been hotly debated by the life cycle community because of the important upstream or indirect land use that is required to maintain the productivity of the agricultural region (e.g., land associated with production of fertilizer) or because of land could be used for alternative uses if not for agriculture (e.g., primary growth forest). Similarly, total water use is a resource that is relevant for most biofuel life cycle studies as shown in recent work [9]. An important distinction when it comes to water use is that of consumptive vs. nonconsumptive use. Most energy generation facilities use a large amount of water, primarily for cooling, so even though the amount of water needed for these systems is large, a comparatively small amount of the water is actually consumed [16].

Most models of biofuels systems include, at a minimum, total net energy use as a metric. This is an obvious and important metric because many biofuels such as ethanol consume a considerable amount of fossil fuels to generate a certain amount of ethanol. Recognizing that biofuels are not worth pursuing if there is no energetic gain, many studies have explored the net energy balance associated with alternative energy options. Algae-derived energy is no exception, and several studies report on the energy that is required to produce energy carriers from algae. Whether these estimates are net positive or net negative depends on the modeling assumptions selected in the study. In addition to energy use, there are at least two other impact factors that should be considered when evaluating algae-to-energy systems. The first is land use. Algae grow more efficiently than terrestrial crops, and so quantifying this parameter is important as a means to highlight one of algae's most pronounced advantages. Similarly, water use is an important parameter since large-scale algae cultivation is likely to require large volumes of water. How much, and how this relates to the water use of terrestrial crops is likely to be an important factor in water-limited growing regions. Including water as a key metric is important.

3.2 Ecological Consequences

A number of common metrics to describe ecological consequences are included in most LCAs. The most common example is global warming potential (GWP) which normalizes greenhouse gas emissions into one number with units of mass emissions in carbon dioxide equivalents. Since several chemicals typically contribute to specific ecological impacts, metrics are very useful for consolidating data. Other examples of common metrics in this class are ozone depleting potential, eutrophication potential, and acidification potential.

The most obvious ecological consequence to include in algae-to-energy studies is GWP since many algae-based energy systems are designed to produce intrinsically low carbon neutral fuels. Because of this desire to produce low carbon fuels, many algae projects have used "sequestration" to describe their activities. In reality, algae-to-energy systems are not a sequestration technology. Sequestration implies that there is long-term storage of CO_2 either as a solid carbonate mineral or in the subsurface under high pressure. In theory, algae could be grown and the biomass buried to sequester carbon, but it would be necessary to carefully control the conditions under which the carbon was buried such that the biomass was not simply digested by bacteria that could generate methane, effectively compounding the problem. What algae-to-energy systems can offer is a fuel that is closer to carbon neutral than conventional fossil fuels. That is, most of the carbon that will be emitted from the combustion of the fuel is not new carbon removed from the ground as in the case of coal or petroleum. This won't help mitigate the impacts of climate change by reducing atmospheric concentrations, but it will reduce the increase in this concentration by not contributing new carbon. How much carbon these processes can keep out of the atmosphere is a current topic of investigation. It is important for the industry to adapt norms with regard to the way it treats carbon dioxide for full transparency.

3.3 Human Health

Human health metrics are often overlooked in the analysis of alternative energy sources. Part of the reason for this is that, of the three classes of inputs surveyed here, these tend to have the highest embedded uncertainty. The exposure to hazardous substances varies significantly, and this can greatly impact the results of an analysis. Further, since limited toxicological data is available for many compounds, developing reliable causal relationships is a challenge. When impacts can be quantified in a life cycle context, they are often reported in terms of disability-adjusted life years.

Ignoring the contribution that human-health indicators may have on algae-to-energy life cycle studies could be an important oversight for several reasons. The most dangerous substances on the United States Environmental Protection Agency list of carcinogenic chemicals reveals that many are agricultural chemicals. If algae are deployed as an alternative to terrestrial agriculture, which is heavily reliant on harmful herbicides, fungicides, and pesticides, there could be a net advantage to adopting aquatic species for biomass generation. Of course, the algae cultivation sector is too young to know whether it will require significant flows of agricultural chemicals to cope with pests or other problems. Similarly, the water quality implications of large-scale algae cultivation could have mixed impacts. On the one hand, algae could remove contaminants from water sources, serving effectively like a large ecosystem-level "liver" for toxin removal. On the other hand, algae could excrete low levels of toxic chemicals as exemplified by coastal red tides. In short,

any large-scale production of algae is likely to have some human health consequence and even though it is difficult to predict how those will manifest at this early stage, it is not difficult to anticipate that better tools will be needed to understand these relationships as the technology matures and becomes deployed.

3.4 Metrics for Assessing Algae LC Impacts

Based on this discussion, there are at least four metrics that should be included in life cycle studies of algae-to-energy technologies:

- Net energy
- GWP
- Land use
- Water use

Net energy is important because efforts to use algae for fuel production are predicated on the assumption of a positive net energy balance. Similarly, GWP is important because of the expectation that algae-to-energy systems will be no more carbon intensive than conventional fossil fuels. In addition, land use and water use should be considered because of algae's high productivity relative to terrestrial crops and its unique requirements for water that set it apart from other sources of bioenergy.

4 Data Sources

A perennial problem with any LCA is identifying reliable and representative data sources. LCI data are available for many common raw materials (e.g., polyvinyl chloride) and manufacturing processes (e.g., extrusion), and, generally speaking, the more common a process, the better characterized it is from an LC perspective. Naturally, having multiple sources of data for a single process allows the user to evaluate the reliability of each source. In the production of algae, there are a large number of materials and processes that have been modeled from a life cycle standpoint that are quite useful. For example, reliable inventory data for a number of fertilizers, flocculants, and other industrial chemicals is readily available from a number of sources as highlighted in Table 3. Similarly, unit operations like pumping centrifugation can be easily modeled from first principles to derive energy use under conditions relevant to the specific process of interest [22].

As discussed earlier, current studies are somewhat limited by the fact that few full-scale algae-to-energy facilities are in operation. This makes it difficult to estimate the emissions from specific applications. For example, fugitive emissions from open ponds are expected to be nontrivial, and loss of this nutrient-rich medium could impact nearby receiving waters. Estimating this potential for eutrophication is highly speculative until actual ponds are in place from which data can be collected.

Table 3 Key data common to most algae-to-energy LC models and sources of data

	Purpose	Data sources
Unit operation		
Pumping (gas, liquid)	Move water and gases	Weidema [34]; Perry and Green [22]; Stephenson et al. [31]
Mixing (of medium)	Maintain suspension	
Dewatering	Separate algae and medium	
Homogenization	Cell lyses	
Separations (of oil)	Separate oil from biomass	
Transportation	Move products	
Material/Energy		
Electricity	Pumping, other unit ops.	NREL [20]; Weidema [34]
Natural Gas	Drying	
Fertilizer (N and P)	Cultivation	
Flocculent	Separations	

Similarly, there is little data to support assumptions about how often tubular photobioreactors would crack and require replacement, or the extent to which geotextiles are needed at the bottom of an open pond to prevent seepage of growth medium into the subsurface. Most of these estimates will be generally unreliable until some pilot plants are built in the coming years. In the meantime, analogous processes can sometimes be used to approximate the emissions associated with algae-related unit operations. For example, belt filter presses in wastewater treatment sludge handling can be used to approximate the impacts from an algae-to-energy unit operation, and as such, have been used by a number of authors [8, 31].

5 Allocation

Allocation refers to the broad category of assumptions that are needed to disaggregate highly interconnected industrial systems such that environmental impact can be assigned to specific processes. Since these decisions often introduce subjectivity into the analysis, the ISO (International Organization for Standards) standard for LCA effectively recommend that whenever possible, allocation decisions should be avoided [13]. Allocation questions arise often in LCA for processes that are multi-input (e.g., landfills), multi-output (e.g., oil refineries), or in which recycling occurs between processes (e.g., using coal fly ash from coal power production as a cement substitute) (Fig. 3). To study the LC of asphalt production, for example, it is possible to collect refinery-wide emissions estimates, but a question will remain about how to assign these impacts to asphalt as opposed to the other outputs from the plant such as gasoline, diesel, lubricants, and so on. The emissions can be allocated based on estimates of relative mass flow rates or the relative economic value of the outputs. Frequently, neither of these seems particularly satisfactory, because neither allocation rule has particular physical significance. What ISO recommends instead is to increase the level of detail of the model to tease out physical relationships between processes or products and specific environmental burdens. In the refinery

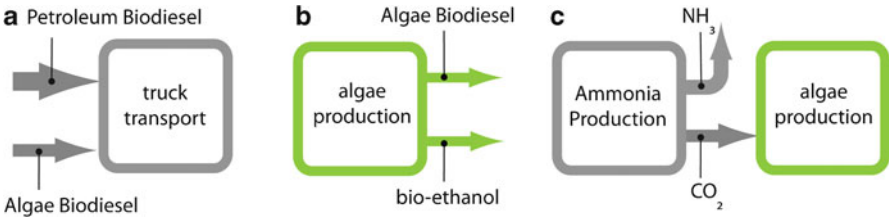

Fig. 3 Allocation decisions in algae-related LCA analysis can be broadly categorized into processes where (**a**) there are multiple inputs, (**b**) there are multiple outputs, or (**c**) there is recycling occurring between multiple sectors. In all cases decisions are required about how to divide life cycle burdens and these can have large effects on the final results

example, this would involve zooming in on the workings of the refinery to identify which specific unit operations are required for asphalt production and then only include those. The ISO standard acknowledges that allocation decisions are a major source of subjectivity in most LCAs.

In the life cycle modeling of algae-to-energy systems, there are several multi-input or multi-output processes that are likely to influence the environmental burden calculations. For example, when modeling the life cycle burdens of using an algae-derived fuel, it is likely that the fuel will be burned as a mixture with petroleum-based fuels. To account for the burdens assigned specifically to the algae content of the truck's fuel will require allocation. Similarly, coproducts from algae cultivation have been widely discussed since there are significant life cycle (and economic) credits to be had for producing high-value by-products along with an algae-derived energy source. At present, there is no consensus on how to allocate the burdens of coproducts in algae production, in large part because the chemistry of these by-products ranges greatly. A proposed algae-to-energy facility might ferment a portion of the non-lipid fraction of the cells to produce ethanol and assign itself credit for this production. But should this facility receive credits for avoiding the production of corn ethanol at some other location? Another plant might produce high-value pharmaceutical additives. Until normative assumptions are developed in the field it is imperative that researchers are transparent about their assumptions.

The delivery of large volumes of CO_2, a waste product from many industries, to algae cultivation facilities requires some allocation judgments, which can impact the results. Most industrial carbon dioxide in developed countries is a by-product of ammonia production. An ammonia plant can be modeled and the emissions quantified, but how much of the burden should be assigned to carbon dioxide vs. ammonia? An idealized plan produces about the same amount of both, but ammonia is the higher economic value product. Carbon dioxide is captured as a valuable by-product but without the ammonia, the plant would not exist. Some in the LC field argue that carbon dioxide should have burdens allocated to it using market price of the two commodities, even though this is an imperfect metric since prices change over time. Others suggest that the burdens should be allocated using a mass balance, but again here, this strategy neglects the fact that the facility exists to produce the more high-value product, ammonia.

6 Uncertainty

There are at least three types of uncertainty associated with most LC studies. The first has to do with modeling inputs. Although many LCA practitioners utilize a single average value for modeling inputs, all parameters generally exhibit a range of values in the real world and all measurements are subject to some unknown error. Key examples of algae modeling parameters that may have wide ranges of values or unknown measurement errors include algae yield; algae lipid content; conversion efficiency; and even life cycle impact factors (energy use, GWP, etc.) for material inputs such as electricity from the US grid, etc. The second type of uncertainty is associated with spatial and temporal differences in systems operation. These systematic differences in time and location can have important effects on LCA results; (e.g., it is reasonable to expect higher algae yields in sunnier parts of the country). The third and final type of uncertainty arises from extrapolation of bench-scale data to hypothetical full-scale systems. This type of uncertainty is largely unavoidable at present, in the absence of many full-scale algae-to-energy systems that have been in operation for any appreciable length of time.

Stochastic tools have become increasingly important for bounding uncertainty in LCA over the last few years (Fig. 4). Monte Carlo analysis is one of the common stochastic tools used by practitioners [30]. This method is useful for quantifying a range of probable output values from a series of input variables which have been assigned empirical or theoretical distributions. These distributions make it possible to encapsulate the three types of uncertainty referenced in the previous paragraph. Repeated sampling from the input distributions creates distributions of output values, which can be parameterized to give empirical estimates of mean or median. Empirical uncertainty for output parameters can also be quantified using standard deviations, standard errors, or percentiles [10]. Most life cycle software (e.g., SimaPro and GaBi) now include stochastic toolkits to perform Monte Carlo and related analyses. For LC practitioners using spreadsheet-based models, a number of commercial add-ins (e.g., Crystal Ball® and @Risk®) allow for flexible management of input and output distributions in models. It should be noted that few of the life

Fig. 4 Stochastic tools, such as Monte Carlo analysis, are receiving increasing attention from LC practitioners as means to systematically incorporate uncertainty into their analysis. Here, the process by which uncertainty in inputs is propagated through a spreadsheet model into empirical estimates of probabilistic output is demonstrated using screen shots from the CrystalBall Monte Carlo tool. (**a**) input distributions, (**b**) model, (**c**) stochastic outputs

cycle studies published to date have included uncertainty, largely because data availability is a limiting factor and the computational complexities are nontrivial. Moving forward, it will be necessary for algae life cycle models to address this uncertainty in a systematic fashion.

7 Interpretation

The final step in performing an LCA is interpretation of the results to highlight principal themes emerging from the study. In the process of conducting an LCA the analyst should develop a deep understand of the relationship between the model structure, assumptions, inputs, and the model outputs. The analyst should highlight the most important relationships for readers who lack the time or expertise to reproduce the analysis. The analyst is also tasked with developing broad conclusions from the analysis. Clearly, this process lends itself to subjective interpretation of results and must be handled carefully to ensure the results are as transparent and useful as possible.

One of the most common methods for minimizing subjectivity in data interpretation is to perform a sensitivity analysis in which the connection between modeling inputs and outputs is quantified. For example, Clarens et al., used a sensitivity analysis to report the top five input parameters driving energy use and greenhouse gas emissions during algae cultivation [8] (Fig. 5). The results, shown in Fig. 5, illustrate how the model outputs respond to a change of ±10% on the input parameters in turn. From these results it is clear that algae high heating value (i.e., lipid content), fertilizer production and application, and CO_2 production and application are driving the burdens.

An important element of data interpretation is understanding how errors in the model could propagate and impact final results. Errors can be introduced into the model in several ways, including inaccurate or poorly transcribed data sources, inaccurate relationships in the model, or unrealistic modeling assumptions. A common source of error in LCA models is double counting in which one emission is

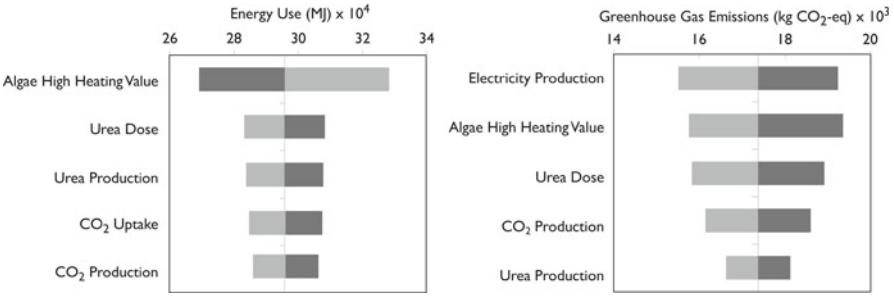

Fig. 5 In LCA sensitivity analysis allows for understanding both the sources of variability and for performing sensitivity analysis (adapted from Clarens et al. [8])

incorporated into multiple metrics. Some reactive nitrogen species, for example, can contribute to eutrophication of surface waters and global warming.

One of the most effective ways to interpret the results of an LCA and understand whether there are sources of error is to benchmark the results to related studies. In the case of algae, this step has been largely ignored, probably because there was little prior literature until recently. This does not mean that comparing data to analogous systems is not worthwhile. To illustrate this, Fig. 6 shows the energy use required to produce biodiesel from algae from four different studies (one paper has two cases). Following adjustment to a standardized functional unit of 1,000-L algae biodiesel (Fig. 6a), the values are compared to the results from conventional soy biodiesel, a thoroughly characterized process (dotted line) as reported by Hill et al. [12]. A preliminary comparison of the results (Fig. 6a) suggests that algae are either much better or much worse than conventional soy biodiesel. Based on this comparison alone, it would be difficult to say anything definitive about how favorable algae biodiesel may be relative to soy biodiesel.

Figure 6b summarizes the same results following adjustment of functional unit and system boundaries. As expected, these adjustments make the results of the four algae LCA papers more consistent. This increase in uniformity among studies can be quantified using coefficients of variation (CV), where CV is defined as the ratio or standard deviation to mean value. CV in Fig. 6a, reflecting only normalization of the functional unit, is 1.39. From Fig. 6b, we see that CV is dramatically reduced, to 0.46, following manual adjustment for system boundaries. This decrease emphasizes the substantial impact of systems boundaries selection, here standardization of upstream nutrient burdens and coproduct allocations, on the outcome of algae LCA studies. A third and final normalization can be carried out in which key model assumptions regarding algae attributes and separations/drying parameters are made uniform across all studies. These parameters have been identified by one or more authors as model inputs that are especially critical during LCA of energy production from algae. Results from this final step of the assimilation analysis are presented in Fig. 6c. This increase in uniformity among selected studies enables more meaningful comparison between algae biodiesel and an external benchmark, as shown visually in the figure. In Fig. 6c, the various estimates for algae biodiesel, derived independently, then normalized, are very close to the estimate for soy biodiesel.

During data interpretation, it is common to incorporate other elements that are exogenous to the LC model but which could inform analysis of the results. One common example of this is the incorporation of economic drivers into the model. Campbell et al., for example, performed a combined economic and environmental life cycle analysis of producing biodiesel from algae grown in near-shore salt-water ponds in Australia [5]. The results of this study suggest that, based on GHG emissions alone, algae perform favorably relative to conventional terrestrial crops. This study is noteworthy because it is the only one to consider growing the algae in salt water. Given the tremendous potential to grow salt water species on marginal, near coastal waters, this is an approach that has been experimentally proposed in several papers by Chisti but for which little life cycle modeling results exist [6].

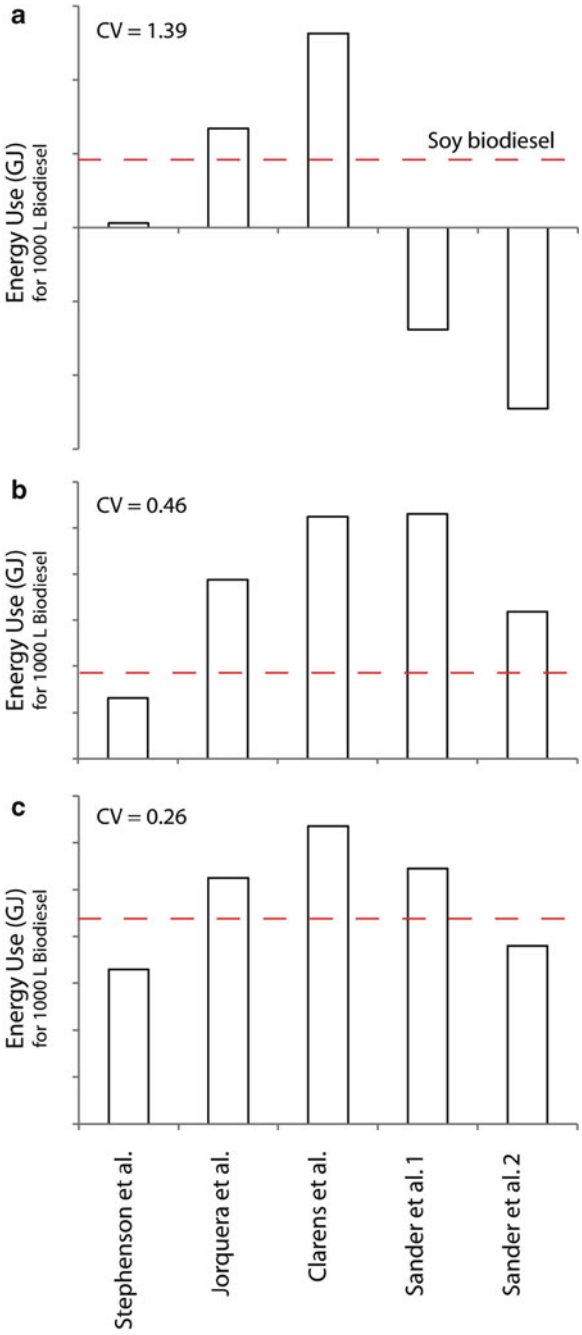

Fig. 6 A comparison of several recent LCA analyses of algae-to-energy systems depicts the energy use needed to produce biodiesel from algae cultivated in raceway open ponds following standardization of functional unit. (**a)** Depicts the raw data following adjustment of functional unit to 1,000 L biodiesel. (**b**) Depicts data from (**a**) following additional adjustment to system boundaries (i.e., upstream nutrient burdens and coproduct allocation). (**c**) Data from (**b**) following additional standardization of key drying assumptions. *Dotted line* represents energy use associated with production of one functional unit (1,000 L biodiesel) from soybeans [12]. *CV* coefficient of variation

8 Conclusions

This chapter surveyed some of the key challenges associated with utilizing LCA methodologies for studying algae-to-energy technology. These challenges have emerged over the last two years as a large number of systems-level life cycle studies of proposed algae-based energy technologies have appeared in the academic literature. Before 2009, only a few algae-to-energy LCAs had been published and even these were only nominally LCAs [15]. The assumptions about cultivation and drying that were used in these studies were not highly representative of previously published reports. The recent work better reflects the way that the industry expects algae-to-energy systems will be deployed in the field, but the results are difficult to compare directly because of the varied boundaries and assumption specified by the authors. This chapter has highlighted most of the normative judgments faced by LC practitioners and discussed each in the context of algae-to-energy systems in order to support future work in this area.

From the existing literature, several themes begin to emerge that will assist in designing future analyses. One of the most common is that recent LCAs echo many of the conclusions of the first-generation algae research conducted in the 1980s and 1990s. These studies suggested many of the system's-level implications of large-scale algae deployment [35]. Benneman's report to the United States Department of Energy concluded that open ponds would be the only economically viable way to grow algae for sequestering CO_2 from power plant flue gases [2]. Similarly, Votolina and others have suggested that algae-based wastewater treatment would be a technically competitive approach for conducting tertiary treatment of wastewater [32]. In both cases, these conclusions are well aligned with the results of more recent LCA studies, even though these early reports never use the term "LCA." A second important theme is that algae-to-energy systems have a long way to go technologically before they are viable from an environmental burden standpoint. In this regard, LCA is a powerful design tool because it allows for a focus of R&D on those processes that will have the most significant impact on reducing the burdens of the processes as a whole.

In light of the large amount of investment in the algae-to-energy field, it is likely that LC tools will continue to be used to understand and assess the impacts of these emerging technologies. In order for these studies to be more immediately comparable, it is important that the community develop nominal assumptions about how to handle algae systems. This chapter can serve as a first step toward developing these norms.

Acknowledgments The authors gratefully acknowledge funding for this study from a UVA Fund for Excellence in Science and Technology Grant.

References

1. Baumann H, Tillman A-M (2004) The Hitch Hiker's guide to LCA. An orientation in life cycle assessment methodology and application. Studentlitteratur, Lund
2. Benemann J, Oswald W (1996). Systems and economic analysis of microalgae ponds for conversion of CO_2 to biomass. Final report. US Department of Energy, Pittsburgh, p. 201
3. Brennan L, Owende P (2010) Biofuels from microalgae—a review of technologies for production, processing, and extractions of biofuels and co-products. Renew Sustain Energy Rev 14(2):557–577
4. Brune DE, Lundquist TJ et al (2009) Microalgal biomass for greenhouse gas reductions: potential for replacement of fossil fuels and animal feeds. J Environ Eng 135(11):1136–1144
5. Campbell PK, Beer T et al (2010) Life cycle assessment of biodiesel production from microalgae in ponds. Bioresour Technol 102(1):50–6
6. Chisti Y (2007) Biodiesel from microalgae. Biotechnol Adv 25(3):294–306
7. Chisti Y, Moo-Young M (1986) Disruption of microbial cells for intracellular products. Enzyme Microb Technol 8(4):194–204
8. Clarens AF, Resurreccion EP et al (2010) Environmental life cycle comparison of algae to other bioenergy feedstocks. Environ Sci Technol 44(5):1813–1819
9. Dominguez-Faus R, Powers SE et al (2009) The water footprint of biofuels: a drink or drive issue? Environ Sci Technol 43(9):3005–3010
10. Goedkoop M, Schryver AD et al (2007) Introduction to LCA with SimaPro 7. PRé Consultants, Amersfoort
11. Granhall U, Berg B (1972) Antimicrobial effects of Cellvibrio on blue-green algae. Arch Microbiol 84(3):234–242
12. Hill J, Nelson E et al (2006) Environmental, economic, and energetic costs and benefits of biodiesel and ethanol biofuels. Proc Natl Acad Sci U S A 103(30):11206–11210
13. ISO/TC207/SC5 (2006) ISO 14040: 2006 Environmental management—life cycle assessment—principles and framework. International Organization for Standardization, Geneva
14. Jorquera O, Kiperstok A et al (2010) Comparative energy life-cycle analyses of microalgal biomass production in open ponds and photobioreactors. Bioresour Technol 101(4):1406–1413
15. Kadam KL (2002) Environmental benefits on a life cycle basis of using bagasse-derived ethanol as a gasoline oxygenate in India. Energy Policy 30(5):371–384
16. King CW, Webber ME (2008) Water intensity of transportation. Environ Sci Technol 42(21):7866–7872
17. Lardon L, Hélias A et al (2009) Life-Cycle Assessment of Biodiesel Production from Microalgae. Environ Sci & Technol 43(17): 6475–6481
18. Miao X, Wu Q (2006) Biodiesel production from heterotrophic microalgal oil. Bioresour Technol 97(6):841–846
19. Molina Grima E, Belarbi EH et al (2003) Recovery of microalgal biomass and metabolites: process options and economics. Biotechnol Adv 20(7–8):491–515
20. NREL (2002) US LCI database project. Final phase I report. P. b. A. S. M. Institute. Franklin Associates, Sylvatica
21. Overcash M, Li Y et al (2007) A life cycle inventory of carbon dioxide as a solvent and additive for industry and in products. J Chem Technol Biotechnol 82(11):1023–1038
22. Perry RH, Green DW (2008) Perry's chemical engineers' handbook. McGraw-Hill, New York
23. Pienkos PT, Darzins A (2009) The promise and challenges of microalgal-derived biofuels. Biofuels Bioprod Bioref 3(4):431–440
24. Sander K, Murthy G (2010) Life cycle analysis of algae biodiesel. Int J Life Cycle Assess 15(7):704–714

25. Sheehan, J., V. Camobreco, et al. (2000). An overview of biodiesel and petroleum diesel life cycles. (Other information: PBD: 27 Apr 2000: Medium: ED; Size: vp) National Renewable Energy Laboratory (U.S.), Golden
26. Sheehan J, Dunahay T et al (1998) A look back at the U.S. Department of Energy Aquatic Species Program: biodiesel from algae. National Renewable Energy Laboratory, Golden, p 328
27. Sialve B, Bernet N et al (2009) Anaerobic digestion of microalgae as a necessary step to make microalgal biodiesel sustainable. Biotechnol Adv 27(4):409–416
28. Simon D, Helliwell S (1998) Extraction and quantification of chlorophyll a from freshwater green algae. Water Res 32(7):2220–2223
29. Snare M, Kubickova I et al (2006) Heterogeneous catalytic deoxygenation of stearic acid for production of biodiesel. Ind Eng Chem Res 45(16):5708–5715
30. Sonnemann GW, Schuhmacher M et al (2003) Uncertainty assessment by a Monte Carlo simulation in a life cycle inventory of electricity produced by a waste incinerator. J Clean Prod 11(3):279–292
31. Stephenson AL, Kazamia E et al (2010) Life-cycle assessment of potential algal biodiesel production in the United Kingdom: a comparison of raceways and air-lift tubular bioreactors. Energy Fuel 24(7):4062–4077
32. Votolina D, Cordero B et al (1998) Growth of *Scenedesmus* sp. in artificial wastewater. Bioresour Technol 68:265–268
33. Wang M (2010) The greenhouse gases, regulated emissions, and energy use in transportation (GREET) model D.o.E (DOE). UChicago Argonne, LLC, Chicago
34. Weidema, B. (2007). Ecoinvent Data v2.0. http://www.ecoinvent.org/. Accessed Apr 2008
35. Weissman JC, Tillett DM (1990) Design and operation of an outdoor microalgae test facility: large-scale system results. In: Brown LM, Sprague S (eds) Aquatic species project report. NREP, Golden

Part VII
High-Value Algal Products and Biomethane

Chapter 33
Cultivation of *Arthrospira (Spirulina) platensis* by Fed-Batch Process

João C.M. Carvalho, Raquel P. Bezerra, Marcelo C. Matsudo, and Sunao Sato

Abstract This chapter comments on fed-batch cultivation of *Arthrospira platensis* under different carbon and nitrogen sources, pH, temperature, light intensity, type of photobioreactor and typical parameters of the fed-batch process, such as feeding time, addition protocol and flow rate. Inexpensive nitrogen sources, such as urea, ammonium salts and nitrogen-rich wastewaters can be used for *A. platensis* cultivation, with results that can be comparable to those with classical nitrate sources. Closed photobioreactors are useful for preventing ammonia loss. The use of organic carbon sources needs to be carried out under aseptic conditions, and it is necessary to evaluate the best supplying conditions when using fed-batch process. The addition of CO_2 ensures the control of pH and, at the same time, supply of the carbon source into the culture medium. The fed-batch process can be useful for the production of *A. platensis* using CO_2 from industrial plants, particularly from industrial alcoholic fermentation.

1 Introduction

The cultivation of microalgae and cyanobacteria is an important current issue because of the possibility of supplying human needs related to food production and removal of atmospheric or industrial carbon dioxide. *Arthrospira* (*Spirulina*) *platensis*, *Dunaliella salina* and *Chlorella vulgaris* are among the most studied photosynthetic microorganisms, but several other cyanobacteria and microalgae have been investigated lately, mainly for biodiesel production.

J.C.M. Carvalho (✉) • R.P. Bezerra • M.C. Matsudo • S. Sato
Department of Biochemical and Pharmaceutical Technology, University of São Paulo, Av. Prof. Lineu Prestes 580, Bl. 16, São Paulo 05508-900, SP, Brazil
e-mail: jcmdcarv@usp.br

J.W. Lee (ed.), *Advanced Biofuels and Bioproducts*, DOI 10.1007/978-1-4614-3348-4_33,

The increasing demand for protein sources and other high biological value products, such as polyunsaturated fatty acids and pigments, associated with the need of the development of new technologies that contribute to the mitigation of environmental pollution indicates that the market for microorganisms such as *A. platensis* is going to increase in the coming years.

The previous uses of photosynthetic microorganisms as food are related to events in China 2,000 years ago, where *Nostoc* was used in periods of food shortage. Additionally, *Spirulina* sp. was consumed by the Aztecs in the Mexico Valley and by people living near Chad Lake in Central Africa [54]. They have been consumed by Africans, where French researchers first reported in 1940 the use of *Spirulina platensis* as food [54].

Currently, the correct scientific designation for *S. platensis* is *A. platensis* [95]. Despite this, in this chapter, it was maintained the denomination given by the authors of the cited works. The genus *Arthrospira* (family Cyanophyceae) encompasses the photosynthetic cyanobacteria with helically coiled trichomes along the entire length of the multicellular filaments and visible septa (Fig. 1). The last characteristic differentiates this genus from true *Spirulina* which has invisible septa [16].

Arthrospira (*Spirulina*) *platensis* is one of the most promising microorganisms, among microalgae and cyanobacteria, not only to be used as food but also for other industrial applications because of its composition.

It contains a great amount of polyunsaturated fatty acids and pigments such as phycocyanin and zeaxantine [24]. Palmitic, linoleic, γ-linolenic, and oleic acids are the predominant fatty acids in *S. platensis*. γ-Linolenic is only found in significant amounts in breast milk, some fruits, species of fungi and cyanobacteria [25].

S. platensis is also an interesting source of chlorophyll, since this microorganism synthesizes only chlorophyll *a*, which is more stable than chlorophyll *b*, very common in vegetables. Moreover the cell wall is composed of mucopolysaccharides and therefore easily digested [44], which is an advantage for the bioavailability of cell components.

This cyanobacterium shows low nucleic acid content in dry biomass (4–6%) in comparison with yeasts (8–12%) and other bacteria (20%) [3], so the daily intake of this biomass would not cause any damage to the human body [73].

Besides the high protein content in dry biomass, *S. platensis* shows a satisfactorily balanced amino acid content, possessing even methionine, which is absent in most microalgae [35]. About 20% of the cellular protein is represented by the main pigments in this microorganism, called phycobilins [82].

This biomass also contains important vitamins such as cyanocobalamin (B12), pyridoxine (B6), thiamin (B1), tocopherol (E), and phylloquinone or phytonadione (K) [12]. Moreover, recent studies indicate that some trace elements such as chromium III [57] and selenium [19] can be accumulated in *S. platensis* biomass depending on the cultivation conditions.

In fact, *Spirulina* spp. are noted in the literature as an alternative protein source, due to the high protein content in dry biomass (reaching as high as 70%), good digestibility, low nucleic acid content, and presence of vitamins, polyunsaturated fatty acids, immunomodulatory polysaccharides, pigments, and antioxidants [24].

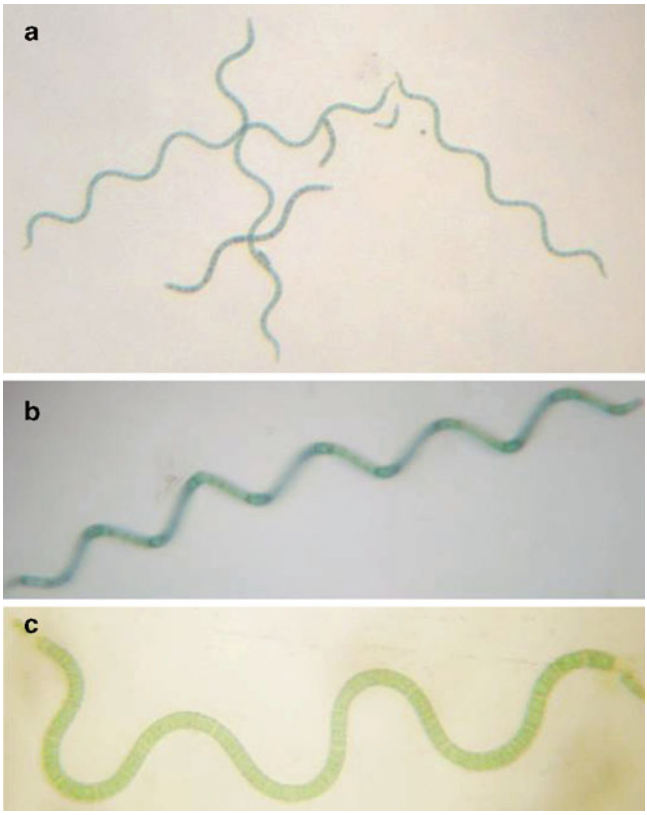

Fig. 1 Light microphotography of *Arthrospira platensis* (UTEX 1926). (**a**) Some trichomes (×100 magnification); (**b**) view of the helically coiled structure (×400 magnification); (**c**) view of a trichome with visible septa (×400 magnification)

S. platensis is mainly used as a food supplement. One of the applications is the use of this microorganism as a source of pigments for food industries [33, 69]. *S. platensis* was also shown to act as a prebiotic, improving the growth in vitro of lactic acid bacteria such as *Lactobacillus lactis*, *Lactobacillus delbrueckii* and *Lactobacillus bulgaricus* [73]. For application in animal feed, some researchers have studied the use of *S. platensis* in aquaculture, to feed shrimp larvae, for instance [46].

Another important aspect of this microorganism is the possibility of obtaining bioactive compounds [21]. Since the 1980s, several studies have evaluated the use of *S. platensis* as a dietary supplement for intestinal disorders [39], diabetes mellitus, hyperglycemia [74], hyperlipidemia [67, 85], anemia [17], and hypertension [102]. Moreover, it can act as an anti-inflammatory [101]. Recent studies also focused on the isolation of fatty acids, particularly the polyunsaturated ones, and pigments from photosynthetic microorganisms. Such characteristics indicate that this microorganism can be a source of molecules with potential use in pharmaceutical and cosmetic industries as well. Besides, *Arthrospira* (*Spirulina*) spp. have been

used for the removal of heavy metals from wastewater [27, 45], and it is important to emphasize its potential for CO_2 biofixation [114], including CO_2 from ethanol production plants [15, 40, 63].

In the large-scale production process, *S. platensis* can be easily cultivated due to the fact that it grows at high alkalinity and high salinity inorganic medium, with high content of carbonate and bicarbonate. These characteristics make it possible to inhibit or prevent contamination. Large-scale cultivation can thus be carried out in open ponds, which is very common in algae cultivation farms, where 5,000 m^2 ponds are employed [93], even though there are several studies about their cultivation in closed bioreactors. *A. platensis* biomass recovery is also facilitated due to its filamentous morphology.

Tacon and Jackson [104] list the following advantages for cultivation of *S. platensis*: they are able to use both organic and inorganic carbon sources; they exhibit a short generation time under optimum growth conditions; and they are easily cultivated in small areas. Cyanobacterial strains are carefully selected among collections around the world, which are periodically sub-cultured in the laboratory in order to maintain actively growing cells. Major criteria in the selection of strains are growth rate, biochemical composition, and resistance to environmental stress at each production site. It must be emphasized, however, that a strain that shows a good performance in the laboratory does not always display the same behavior in an outdoor open pond operation [93].

Even though microalgae and cyanobacteria have been used by humans for a long time, microalgal biotechnology has only begun in the middle of the last century. Currently, 5,000 tons of dry microalgal biomass is marketed per year, representing up to US$1.25B [99]. The production of photosynthetic microorganisms considerably increased in the world due to the possibility of using this kind of culture for oxygen production and as a source of protein for food in space travels [9].

At the end of the 1970s, Sosa Texcoco Co., in Mexico, was the first responsible for large-scale *Spirulina* production [23, 93]. Afterward, several countries such as Taiwan, India, USA and Japan also started producing this cyanobacterium in open ponds [93]. Among the different cyanobacterial species, *A. platensis* stands out due to its characteristics related to cell composition, cell growth and cell recovery.

2 Fed-Batch Process

Several kinds of processes for microorganism cultivation have been developed for different applications. These processes may be conveniently classified according to the chosen operation mode: batch, fed-batch, continuous, semi-continuous (repeated batch), and their variations. In a batch operation, neither substrate is added after the initial charge nor the product is removed until the end of the process. Some pharmaceutical products are produced by this process, but generally, batch operation is not commercially attractive [50], where its main application is in food and beverage production. Conventional batch process can lead to inhibitory concentrations of

substrate in reactors or even to formation of undesired products through direct metabolic pathways of the organism, decreasing the yield and/or productivity of the system.

The fed-batch process has been used in the cultivation of baker's yeast since 1920 [47]. However, Yoshida et al. [117] were the first to use the term "fed-batch process" in cataloging. Whereas the whole substrate is added at the beginning of cultivation in a batch process, in the fed-batch process one or more nutrients are added to the fermentor during cell growth, while cells and products remain in the fermentor until the end of operation [14].

The fed-batch process does not require any special piece of equipment in addition to equipment required for batch fermentation. It is only characterized by a little longer overall time cycle that is certainly acceptable by industrial practice where at present very effective procedures for sterilization and preventing contamination are commonly utilized [59].

The better operating procedure for this system is to start with small amounts of biomass and substrate, and to add more substrate when the greatest part of the initial substrate is already consumed by the microorganism [42]. The inlet substrate feed should be as concentrated as possible to minimize dilution and to avoid process limitation caused by the reactor size. According to Lee et al. [56], the feed control strategies are: simple indirect feed-back (single-loop) methods; nutrient feeding according to inferred substrate concentration or specific growth rate; and predetermined feeding strategies.

Two cases of fed-batch process can be considered: the production of a growth-associated product and the production of a non-growth-associated product. In the first case, it is desirable to extend the growth phase as much as possible, minimizing the changes in the fermentor as well as the specific growth rate, production of the product of interest, and avoiding the formation of by-products. For non-growth-associated products, the fed-batch process would be carried out in two phases: a growth phase in which cells grow up to the required concentration and then a production phase in which carbon source and other requirements for production are fed to the fermentor [59].

In the fed-batch cultivation, volume variation may happen depending on the substrate concentration added and the rate of evaporation in the system [14]. In the fixed volume fed-batch process, the limiting substrate is fed without diluting the culture. The culture volume can also be maintained practically constant by feeding the growth limiting substrate using a very concentrated solution. Alternatively, the substrate can be added by dialysis or, in a photosynthetic culture, radiation can be the growth limiting factor without affecting the culture volume [32]. Contrarily, the variable volume fed-batch process is one in which the volume changes throughout the cultivation time due to the diluted substrate feeding in the system.

Fed-batch culture has been widely employed for the production of various bioproducts including primary and secondary metabolites, proteins, and other biopolymers. It is used aiming to overcome different difficulties in cell cultivation. When a nutrient with high viscosity is used, this process usually reduces the viscosity of the medium, and toxic effects of components can also be limited by dilution [113].

The advantages of this process include: deviation of cell metabolism via the formation of the desired product; prevention of catabolite repression; prevention of formation of toxic substances in microbial metabolism; and control of the specific growth rate [116]; the main advantages are the possibilities of controlling both reaction rate and metabolic reactions by substrate feeding rate [36].

The fed-batch process has been also used to prevent or reduce substrate-associated growth inhibition by controlling nutrient supply. Since both overfeeding and underfeeding of nutrient is detrimental to cell growth and/or product formation, the development of a suitable feeding strategy is critical in fed-batch cultivation. Fed-batch fermentations can be the best option for some systems in which the nutrients or any other substrates are only sparingly soluble or are too toxic to add the whole requirement for a batch process at the start. This process is particularly important in *A. platensis* cultivation. In the next items, the factors that affect *A. platensis* growth are discussed, aiming to correlate them with the employment of the fed-batch process.

2.1 Light Intensity

Light intensity and duration of irradiation determine the growth rate and production yield, which is limited by the enzymatic mechanisms of the microorganism. This limit, referred to as light saturation point, is between 5 and 10 klux (60–120 μmol photons m^{-2} s^{-1}) according to Balloni et al. [4].

Vonshak et al. [110] showed that the light/dark cycle, to which cells in the ponds are exposed during the day, is an important factor that influences the growth rate and photosynthetic efficiency and it can be completed in seconds. The light regimes to which the cultures are submitted are considered to be an important factor in the productivity and yield of photosynthetic reactions [94, 105]. Several studies have been carried out focusing on the effect of different photosynthetic photon flux densities (PPFDs) incident on photobioreactors, but there are few reports focusing on the effects of the duration of the day and night cycles [66, 78].

The dark/light regime in the cells is influenced by the agitation, turbulence, and cell density in the ponds [82]. When light intensity is very low, cell growth is limited or there is no cell growth [4]. On the other hand, high light intensity results in increasing cell growth up to a light intensity at which it stops with increasing light intensity. The light intensity at which cell growth begins is known as the light limiting region, while the light intensity at which no further increase in growth takes place with increasing light intensity is known as the light saturation point. Further increase in light intensity neither increases the specific growth rate, nor hinders growth. The point at which increased light intensity decreases the specific growth rate is the point where photoinhibition begins [53]. A high-intensity light can induce photo-oxidative stress, resulting in photo-inhibition of photosynthesis, destruction of photosynthetic pigments and cell death [64].

Photo-inhibition is a reduction of the photosynthetic activities caused by the exposure to high PPFDs [119]. When the flux of photons absorbed by chloroplasts is too high, the concentration of high-energy electrons inside the cell is excessive, and they cannot be consumed through the Calvin cycle. These excessive electrons lead to the formation of H_2O_2, which can damage cell structures [20]. Even in densely populated outdoor cultures of *Spirulina* spp., photo-inhibition can be observed when light intensity is 60–70% of full sunlight [111].

Light intensity has a strong influence on cell growth, nitrogen-to-cell conversion factor and cell productivity, as well as biomass composition. According to Rangel-Yagui et al. [80], the best *S. platensis* growth carried out in 5-L open tanks was observed with 500 mg L^{-1} urea, added for 14 days by a exponentially feeding protocol, at a light intensity of 5,600 lux (67.2 μmol photons m^{-2} s^{-1}), whereas the highest concentration of chlorophyll in the biomass was observed at a light intensity of 1,400 lux (16.8 μmol photons m^{-2} s^{-1}). The best chlorophyll productivity was observed with 500 mg L^{-1} urea at a light intensity of 3,500 lux (42 μmol photons m^{-2} s^{-1}), providing the optimal balance between cell growth and biomass chlorophyll content. Under the best conditions for cell growth, maximum cell concentration using urea as a nitrogen source was higher than that obtained with the use of KNO_3, irrespective to the cultivation process (batch or fed-batch) used for cell growth with the latter nitrogen source. As expected, these findings highlight that the fed-batch process conducted properly is not hampered by light intensity. Using a different strategy, Danesi et al. [34] investigated the influence of light intensity reduction on *S. platensis* cultivation, using urea and KNO_3 as nitrogen sources applying fed-batch and batch processes, respectively, reducing the light intensity from 5 to 2 klux (60–24 μmol photons m^{-2} s^{-1}) on the 9th and the 13th day of cultivation. Increases of up to 29% in total chlorophyll production were observed for the cultivations with light intensity reduction, in comparison with the cultivations carried out at fixed light intensities. Irrespective of the time for light reduction, the use of urea as nitrogen source by fed-batch process led to higher cell growth, obtaining maximum cell concentration of about 1,800 mg L^{-1}.

Soletto et al. [96] showed that the photosynthetic efficiency of *S. platensis* in a bench-scale helical photobioreactor reached its maximum value (PE_{max} = 9.4%) at a PPFD of 125 μmol photons m^{-2} s^{-1}. The photo-inhibition threshold appeared to strongly depend on the CO_2 feeding rate: at high PPFD, an increase in the amount of fed CO_2 delayed the inhibitory effect on biomass growth, whereas at low PPFD, excessive CO_2 addition caused the photosynthetic microorganism to stop growing.

2.2 Temperature

Temperature is known to be a parameter of great importance for the growth of all the microorganisms, since it affects all metabolic activities as well as nutrient availability and uptake [109].

Vonshak [109] reported for *S. platensis* cultivation an optimum temperature ranging from 24 to 38°C, depending on the strain. However, satisfactory growth was shown starting at 20°C [81]. The usual optimal temperature for cultivation of *Spirulina* spp. is in the range 35–38°C [109]. However, it must be pointed out that this range of temperature is arbitrary. Many *Spirulina* strains will differ in their optimal growth temperature, as well as in their sensitivity to extreme ranges [109].

It was previously proposed [28, 98] that cell growth in different bioprocesses can be kinetically described assuming its direct dependence on the activity of one enzyme limiting the overall metabolism. Based on this supposition, the thermodynamics of the system was described resorting to the so-called thermodynamic approach, according to which the specific growth rate increases with temperature would be contrasted by a progressive activity decrease owing to "thermal inactivation" [87]. These authors, who worked with urea as a nitrogen source by a fed-batch process, demonstrated that the best growth temperature was 30°C, which is in accordance with previous results [48, 83]. Besides, Danesi et al. [33] performed *S. platensis* cultivation at 36.8°C, where there was decline in cell growth, thus suggesting possible thermal inactivation of this microorganism, as observed for other microorganisms [37, 90, 98]. Contrary to the use of nitrate as a nitrogen source [109], this cyanobacterium grew reasonably well even at lower temperature (23.3°C) when urea was used as a nitrogen source [87]. It could have happened due to the fact that urea hydrolysis to ammonia has less energy requirements than the reduction of nitrate to ammonia; therefore, the thermal situation at this temperature may be sufficient to sustain nitrogen metabolism. Moreover, when using nitrogen sources that lead to the presence of ammonia in the cultivation medium, the availability of the nitrogen source in the *A. platensis* cultivation depends on temperature. In fact, when urea is used as a nitrogen source, it can be hydrolyzed to ammonia by urease [93] and/or spontaneous hydrolysis in alkaline medium [33], releasing ammonia, which may be lost by off-gassing [86]. The temperature would then have a dual influence on the culture: besides the fact that higher temperatures can promote microorganism growth, it can also increase the off-gassing of ammonia to the environment and may lead to a nitrogen limitation in the culture medium. Such fact is particularly important when working with open ponds.

2.3 Nutrients

2.3.1 Carbon

Since *S. platensis* is composed of approximately 50% carbon [30], the use of carbon dioxide in the cyanobacterium cultivation may contribute significantly to reducing the cost of production and, at the same time, to reducing the emission of this greenhouse gas. Photosynthetic microorganisms can efficiently assimilate carbon dioxide from different sources, including the atmosphere, industrial exhaust gases, and soluble carbonate salts [112]. In fact, carbon dioxide taken up by photosynthetic

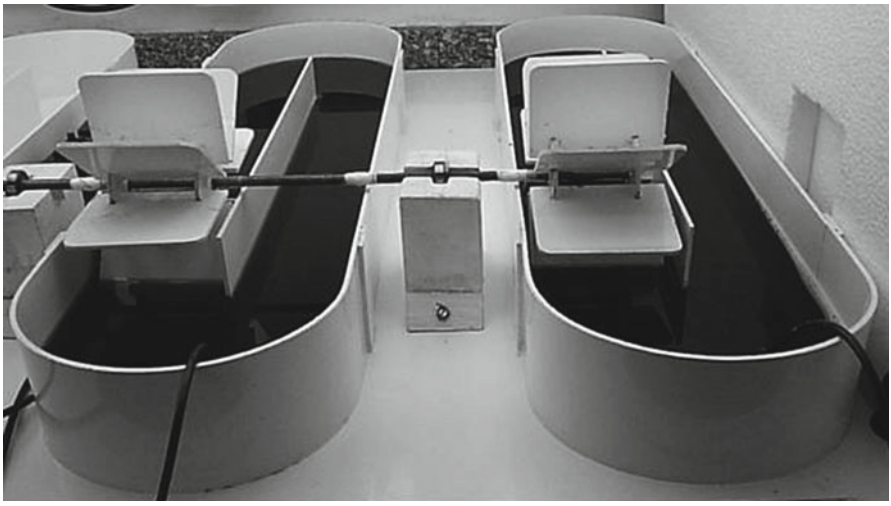

Fig. 2 Laboratory scale open tanks made of PVC sheets

microorganisms is among the most productive biological methods of treating industrial waste emissions, and the yield of biomass per acre is three- to fivefold greater than in typical crops [2, 55]. The most important trace gases, which intensify the greenhouse effect, are carbon dioxide (CO_2), methane (CH_4), nitrous oxide (N_2O), and ozone (O_3). Among all these emissions, carbon dioxide makes the greatest contribution to global warming. For this reason, most of the measures for mitigating climate change target the reduction of carbon dioxide emissions to the atmosphere [77]. In this sense, there are several studies that point out the use of carbon dioxide in the cultivation of *Arthrospira* (*Spirulina*) *platensis* [8, 15, 41, 63, 79, 96, 114].

Traditionally, *Arthrospira* spp. grow autotrophically in open tanks (Fig. 2) in the presence of high sodium carbonate and bicarbonate levels as carbon sources because they are relatively inexpensive and provide a high pH in the culture medium. Bicarbonate, the main carbon source, is actively transported into the cell, where the enzyme carbonic anhydrase, present intracellularly and/or in the periplasmic membrane, promotes the release of carbon dioxide. This is incorporated in the Calvin cycle to produce organic molecules such as carbohydrates, proteins, and lipids [52].

At low extracellular concentration of bicarbonate, cyanobacteria have the ability to accumulate bicarbonate intracellularly [30] and use carbon dioxide as a carbon source for its metabolism. In medium containing only carbonate, there is no increase in cell concentration and the pH remains almost unchanged, emphasizing the importance of bicarbonate in cyanobacterial metabolism [8].

Taking into account that cultivations in tubular photobioreactors (Fig. 3) lead to a high cell concentration, it is essential that CO_2 is added during cell growth to sustain it [63], thus justifying the fed-batch process for this carbon source. Soletto et al. [96] evaluated the performance of a bench-scale helical photobioreactor in fed-batch

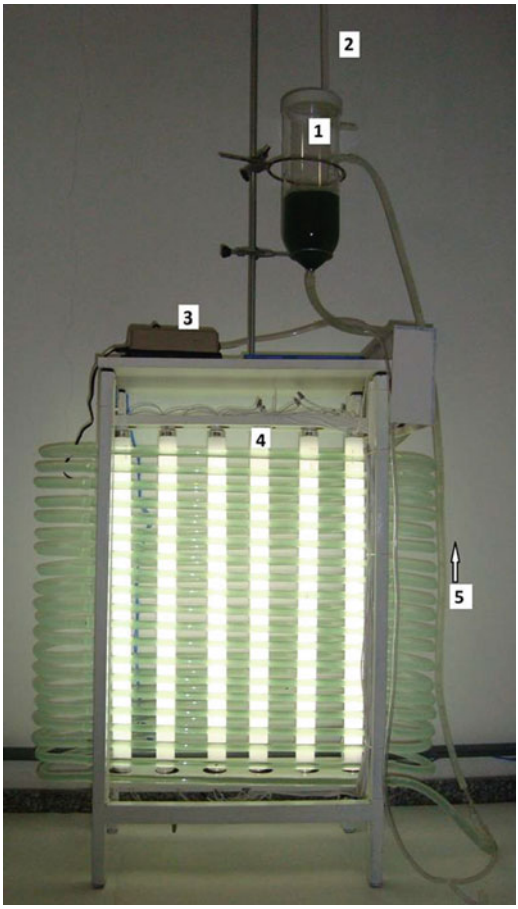

Fig. 3 Tubular photobioreactor. (1) Degasser; (2) condenser tube; (3) air pump; (4) 20 W fluorescent lamps; (5) airlift system

cultures of *S. platensis* under different conditions of light intensity and CO_2 feeding rate. The optimum feeding rate of carbon dioxide for the microalgal growth was correlated with the light intensity to which it was exposed. In general, the behavior of *S. platensis* was more influenced by the CO_2 feeding pattern at low PPFD. Irrespective of the light intensity studied, at a CO_2 feeding rate of 1.03 $g\,L^{-1}\,d^{-1}$, the excessive amount of CO_2 caused an inhibition of biomass growth due to excess carbon levels and likely due to pH reduction.

Matsudo et al. [63] studied the use of CO_2 released from alcoholic fermentation, without any prior treatment, for carbon source replacement and pH control, in the continuous cultivation of *A. platensis*, using urea as nitrogen source, in a bench scale tubular photobioreactor. Irrespective of the carbon source used in the cultivation of this cyanobacterium (pure CO_2 or from alcoholic fermentation), it was obtained similar behavior in cell growth. In both cases, the maximum cell concentration in steady state condition (X_s) occurred at dilution rate (D) of 0.2 d^{-1}, being

obtained $X_s = 2{,}446 \pm 75$ and $2{,}261 \pm 71$ mg L^{-1} in cultivations carried out using pure CO_2 and CO_2 from alcoholic fermentation, respectively. It was not observed any difference in the protein content of the dry biomass when these two kinds of carbon sources were used. The higher the D, the higher the protein contents of the dry biomass, which were as high as about 50% when the cultivations were carried with $D = 0.8$ d^{-1}. These results indicated that the possibility of using such cost-free carbon source and a cheap nitrogen source like urea may contribute to reduce the cost of culture medium. Besides, this work suggests that the biofixation of CO_2 released from alcoholic fermentation of sugar raw materials, which represents about 33% of the whole CO_2 involved in the use of ethanol as fuel, may help to mitigate the greenhouse effect.

Carvalho et al. [15] have proposed methods for the recovery and purification of CO_2 from alcoholic fermentation and/or burning of lignocellulosic materials and feed it into the cultivation of photosynthetic microorganisms. Application of the fed-batch process would be particularly important for the fixation of CO_2 from industrial plants. Such statement can be evidenced by the fact that the ethanol production in Brazil was as high as 27.5 billion liters in 2008/2009 [107], and it can be estimated that the release of CO_2 associated only with this fermentation process was about 20.8 billion kg. Moreover, considering that the all correspondent sugar cane bagasse was burned, an additional CO_2 production of about 83 billion kg would occur [108].

Regardless of the importance of the fed-batch process when using CO_2 as a carbon source, organic carbon sources are the most cited cases in which the fed-batch process is employed in the cultivation of photosynthetic microorganisms. Despite the increase in the risk of contamination, which requires running the process in closed reactors under aseptic conditions, the use of an organic carbon source can provide readily usable energy and make it possible to reach a high final biomass concentration. It can be done under dark (heterotrophic) or light (mixotrophic) conditions. Taking into account that the organic carbon source can lead to inhibition of the growth beyond a limit concentration [103] or even repress the formation of a desired metabolite, several fed-batch processes have been used to improve cell or metabolite production by different microalgae and cyanobacteria [20, 103] or even to remove organic pollutants from wastewater [58].

Márquez et al. [61] showed that *S. platensis* can grow heterotrophically in a medium containing glucose in aerobic and dark conditions but also mixotrophically under illuminated conditions. Chojnacka and Noworyta [20] also observed *Spirulina* sp. growth under heterotrophic conditions using glucose as carbon and energy sources. Chen et al. [19] showed that acetate may be used as a carbon source, in mixotrophic *S. platensis* cultivations, for the production of several photosynthetic pigments.

S. platensis can also use glycerol as the sole carbon source. Nevertheless, when this microorganism takes up glycerol for the first time, it forms aggregates of cells and a lag phase takes place. After the lag phase, however, it was possible to achieve a cell concentration higher than with cultivation using bicarbonate as the sole carbon source [68].

Three organic carbon sources differing in molecular complexity (glucose, acetate, and propionate) were tested by Lodi et al. [58] in a fed-batch mixotrophic process with minimum volume variation. To avoid carbon source accumulation in the medium, acetate and proprionate were added by pulse feeding equimolar amounts about 12 h after their complete depletion, namely acetate every 3.4 days and propionate every 4.0 days, whereas glucose was added once a day. The results of cultivations performed under continuous illumination show that glucose was metabolized for algal growth faster than acetate and proprionate. Besides, the values of nitrate and phosphate removals are near those observed with traditional biological treatment plants [29]. This suggests that mixotrophic metabolism of *S. platensis* could be exploited in a tertiary treatment system for simultaneous removals of mixtures of organic pollutants, nitrate, and phosphate [58].

The chlorophyll content in the biomass did not appreciably vary during the course of cultivations (2–5%), thereby indicating that most of the dry weight increase was the result of microbial growth. Besides, it was shown to be almost independent on the type of organic carbon source and about 17% lower than that determined by Danesi et al. [33] under autotrophic conditions, thus confirming the underutilization of the photosynthetic apparatus when cyanobacteria are grown with an organic carbon source [58].

Chen and Zhang [18] reported that *S. platensis* cell concentration in a fed-batch culture with intermittent glucose feeding with a peristaltic pump was 4.25-fold higher than in the mixotrophic batch culture and 5.1-fold higher than in the photoautotrophic batch culture. The biomass output rate of the fed-batch culture was 3.1-fold higher than in the mixotrophic batch culture and 3.8-fold that of the photoautotrophic culture. Additionally, these authors demonstrated that a mixotrophic fed-batch culture of *S. platensis* with glucose is suitable for the production of high-value products, particularly the light-induced pigments such as phycocyanin.

2.3.2 Nitrogen

Nitrogen is the second most abundant element, representing approximately 10% of the cell [30]. It is a key element for cell growth and reproduction, since it is an essential building block of nucleic acids and proteins.

Piorreck et al. [75] reported that higher nitrogen levels lead to an increase in biomass production. The high nitrogen concentration in cultures generates an upward trend in protein and chlorophyll levels in the cells. On the other hand, low nitrogen concentrations lead to a decrease in the level of these compounds, and also reduce the rate of cell division. There is also an increase in the percentage of total carbohydrates in the cells [89], and phycocyanin is degraded and used as a nitrogen source [11]. Less chlorophyll and carotenoids are produced under these conditions, providing color changes in the culture medium which tends to become yellow [26, 60, 89].

Numerous nitrogen-containing compounds can be used by different organisms as sources of nitrogen. These include, for instance, inorganic ions such as nitrate or

ammonium salts and simple organic compounds such as urea, amino acids, and some nitrogen-containing bases. Additionally, roughly half of the cyanobacteria are in principle capable of fixing N_2 [100], but in the genus *Spirulina*, only *Spirulina labyrinthyformis* is able to fix atmospheric nitrogen. It is a thermophilic species, isolated from hot springs, and has been reported to be capable of carrying out facultative anoxygenic photosynthesis at the expense of sulfides [23].

Studies in the literature have shown that the use of nitrate as a nitrogen source ensures high *A. platensis* concentrations, which justifies the wide use of the standard culture media of Zarrouk [118], Paoletti et al. [72] and Schlösser [92], which employ potassium nitrate or sodium nitrate.

When using nitrate as a nitrogen source, the microorganism needs to reduce it to nitrite, in a reaction catalyzed by the enzyme nitrate reductase, and then to ammonia, in a reaction catalyzed by the enzyme nitrite reductase [43] according to the needs of the cell. This reduction of nitrate to ammonia requires energy. In fact, comparison of the yield of growth on Gibbs energy obtained using either urea or KNO_3 in batch and fed-batch processes, respectively, pointed to the preference of *S. platensis* for the former nitrogen source, likely owing to more favorable bioenergetic conditions [88]. Such behavior was very evident at the end of cultivation, likely because photosynthesis efficiency decreased with increasing biomass concentration suggesting that biomass had used energy, under limited growth conditions, preferentially for maintenance rather than for growth [106], and consequently, it grows better with a nitrogen source that demands less energy. These facts point out that the fed-batch process carried out under optimal conditions does not hamper cell growth.

No negative effect of nitrate concentration during *A. platensis* cultivation has been reported. *S. platensis* cultivation using a fed-batch process with the addition of exponentially increasing mass flow of KNO_3 as the nitrogen source was studied by Rangel-Yagui et al. [80]. These authors reported that cell growth was similar to that obtained with the batch cultivations using nitrate as the nitrogen source. Although lower cell concentrations were not observed for the cultivations with fed-batch addition of KNO_3, there is no need for the use of this process as opposed to batch cultivation, since a batch process is easier to operate compared to a fed-batch process. It is worth mentioning that even nitrate nitrogen sources can be necessary to be added during the cell growth in cultivations with high final cell concentrations [41].

Alternative sources of nitrogen such as urea and ammonium salts can also be used to reduce production cost, replacing sodium or potassium nitrate, since urea and ammonium salts such as ammonium sulfate are widely used in agriculture.

Ammonia in alkaline medium is easily assimilated by the microorganism, since ammonia uptake involves simple diffusion followed by trapping through protonation, thanks to the membrane being permeable to ammonia but impermeable to ammonium ions [10].

As noted before, urea is hydrolyzed to ammonia in alkaline culture medium [33] and/or by urease action [93]. Since ammonia can be toxic to microalgae and cyanobacteria at high concentrations, the addition of urea in a fed-batch process makes this nitrogen source a promising substitute for nitrate salts in photosynthetic microorganism cultivations.

If ammonium salts and/or urea are added in large quantities at the beginning of cultivation, there is excessive formation of ammonia, leading to cell death. In fact, growth inhibition or even cell death can take place when using ammonium at relatively high concentrations because of the toxic effect of ammonia [1, 6]. Moreover, batch cultivations of *A. platensis* in 500-mL Erlenmeyer flasks using ammonium chloride as a nitrogen source resulted in nitrogen limitation below 1.6 mM nitrogen, whereas above 6.4 mM there was excess ammonia, inhibiting cell growth [13]. The use of low starting levels of ammonium chloride for batch *Spirulina* sp. production proved to hinder growth because of nitrogen limitation, with consequent decrease in biomass yield compared to the use of nitrate [30, 91]. Confirming these findings, Faintuch [38], studying different nitrogen sources in *Spirulina maxima* cultivation with a batch process, found that the use of alternative nitrogen sources instead of nitrate, such as ammonium chloride and urea, was limited to low concentrations of nutrient, resulting in low cell concentration.

Particularly in the use of ammoniacal nitrogen sources for *A. platensis* cultivation, the control of the nutrient flow can prevent inhibitory concentrations of ammonia in the culture medium [7, 13, 97]. The fed-batch addition of urea was shown to be an excellent protocol to ensure the optimum level of this compound in the growth medium, thereby allowing satisfactory *S. platensis* cultivation [33, 88, 106] and ammonium salts [7, 13, 41]. Despite the above inhibitory effect of ammonia, the fed-batch addition of ammonium salts or urea did in fact prevent any inhibitory effect, allowing such a cyanobacterium to reach a concentration comparable to that obtained with nitrate [13, 33, 41, 80].

A. platensis can grow with either nitrate or ammonium salts as the sole nitrogen source, but the simultaneous use of both is advantageous. The use of ammonium chloride alone as the nitrogen source in *A. platensis* cultures can lead to slightly lower cell concentration and biomass with reduced final contents of chlorophyll, lipids and proteins. On the other hand, the combination of potassium nitrate and ammonium chloride provides a way to deal with these issues. The presence of nitrate likely prevents a deficiency of nitrogen in cultures with ammonia, and the presence of ammonia reduces the amount of nitrate to be added, helping to reduce production costs. Moreover, the residual nitrate level in cultures with both nitrogen sources was much lower than that detected with one source alone, hence reducing the salinity, the environmental impact, and the disposal and/or the reutilization of effluent [84]. It would also be characterized as a fed-batch process with the use of two nitrogen sources, since one of them was fed during the microbial cultivation. These authors cultivated *A. platensis* in mini-tanks at 13 klux (156 μmol photons m^{-2} s^{-1}) using a mixture of potassium nitrate and ammonium chloride as nitrogen source. The addition of the total amount of potassium nitrate was made entirely at the beginning of the runs and ammonium chloride was added by daily pulse-feeding, using an exponentially increasing regime in order to avoid any inhibitory effect by ammonia or nitrogen deficiency. Higher maximum cell concentration was obtained in the cultivation with both nitrogen sources supplied in comparison to that obtained with cultivations carried out with ammonium chloride or potassium nitrate, separately. Ammonia lost by volatilization during the cultivation [13] leads to nitrate acting as

a reserve source of nitrogen when ammonia concentration in the culture medium is not sufficient, thus explaining the better results obtained with the two nitrogen sources combined.

Fed-batch process has also been employed to complement natural media. Costa et al. [31] supplemented the Mangueira Lagoon water with 1.125 mg L^{-1} of urea when *S. platensis* had reached the stationary phase (approximately 312 h), and this operation resulted in a 2.67-fold increase in the final biomass concentration.

Wastewater can also serve as nitrogen source. Olguín et al. [70] evaluated the annual productivity of *Spirulina* (*Arthrospira*) and its ability to remove nutrients in outdoor raceways treating anaerobic effluents from pig farm wastewater, diluted in a mixture of sea and fresh water, under tropical conditions. The average productivity of semi-continuous cultures during summer was 15.1 g m^{-2} d^{-1} with a pond depth of 0.20 m. Under the conditions studied, NH_4-N removal was in the range of 84–96% and *P* removal in the range of 72–87%, depending on the depth of the culture and the season. These findings show that the *Spirulina* can be used for ammonia removal from wastewater in processes in which the wastewater is fed periodically.

Aiming to remove nitrogen and phosphorus in shrimp cultivation, Chuntapa et al. [22] evaluated the simultaneous cultivation of *S. platensis* and this crustacean. In the absence of *S. platensis*, ammonium and nitrite concentrations ranged from 0.5 to 0.6 mg L^{-1}, while nitrate concentrations ranged from 16 to 18 mg L^{-1} by day 44. Considerable variability in nitrogen concentrations occurred when the *S. platensis* was not harvested from the ponds. Semi-continuous harvest of *S. platensis* reduced nitrate to 4 mg L^{-1}, while ammonium and nitrite ranged from 0.0 to 0.15 mg L^{-1}, respectively. Kamilya et al. [51] observed that the same microorganism could remove up to 92 and 48% of nitrogen and phosphorus, respectively, thus contributing to the reduction of eutrophication of fish farm effluent. Olguín [71] described a process using sea water together with pig farm wastewater for low-cost *S. platensis* production and an animal wastewater treatment as well.

2.4 pH

Standard culture medium for *Arthrospira* spp. cultivation is rich in bicarbonate and carbonate. This medium is alkaline due to the presence of these ions. At pH values below 6.4, carbon dioxide is the predominant form of carbon source. At pH values between 6.4 and 10.3, the predominant form is bicarbonate. Above pH 10.3, the predominant form is carbonate. Miller and Colman [65] reported that bicarbonate is the carbon form preferentially assimilated by cyanobacteria, which explains the decreasing of *Spirulina* biomass concentration in the pond at pH values above 10.2–10.4 [49].

Considering ammonia from ammonium salts or urea, in the chemical equilibrium established at pH 9.3, both ammonium ions and ammonia are present. At pH values below 7.0, the predominant form is ammonium ion and above pH 12.0, only the ammonia is present in culture medium.

Ammonia uptake by *S. platensis* is pH-dependent. In alkaline conditions, ammonia enters the cell by simple diffusion, driven by a pH gradient, and is intracellularly assimilated by the action of the enzyme glutamine synthetase [10].

It should also be mentioned that ammonia, depending on its concentration and pH of the medium, is toxic to most microorganisms [1], including *S. platensis* [6]. These authors found that at pH 7.0, *S. platensis* LB1475/a and *Anabaena* sp. were not affected by ammonia. However, at pH 10.0 with ammonia concentrations of 10 mM, only 50% of photosynthetic activity remained for the *S. platensis* LB1475/a, while for *Anabaena* sp. photosynthetic activity has ceased. Thus, since the use of ammonium salts or urea as nitrogen sources lead to a release of ammonia in the culture medium, it would be limited by process by which the cultivation is carried out.

Therefore, pH is a very important variable to be studied, since it may affect the form of the carbon reservoir, urea decomposition and how ammonia is presented in the culture medium (protonated or unprotonated). Sánchez-Luna et al. [87] studied the effect of pH on *A. platensis* cultivation using urea as nitrogen source and found that *A. platensis* grows well at pH 9.0–10.0, with an optimum pH of 9.5. This pH range is in agreement with Belay [5], who suggests maintaining the pH of the medium above 9.5 in outdoor cultivations aiming to avoid contamination by other microalgae.

2.5 Parameters of the Fed-Batch Process

Nutrient feeding during a fed-batch process can be done utilizing either constant or variable mass flow rate. Additionally, the addition regime can be either intermittent or continuous [14]. Pulse feeding is easier and less expensive because of the absence of pumping costs. On the other hand, it could lead to lower cell growth, productivity and nitrogen-to-cell conversion factor. During the continuous addition, a feed pump is always used for the continuous addition of substrate during cell growth. With intermittent addition, the substrate is added by pulses and the time between two pulses is another variable to be studied.

Danesi et al. [33] have evaluated the *S. platensis* growth using urea as a nitrogen source in a fed-batch process, and they tested different protocols for urea addition, namely:

1. Intermittent—exponentially increasing the amount added, every 24 h
2. Intermittent—exponentially increasing the amount added, every 48 h
3. Continuous—exponentially increasing the mass flow rate
4. Continuous—constant mass flow rate, using a controlled flow peristaltic pump

The addition of urea at intervals of 48 h led to the lowest maximum cell concentration, as a consequence of the lack of availability of the nitrogen to the microorganism between feeding times due to the lost of the nitrogen source in the ammonia form.

The best results, in terms of cell growth, show that the continuous form (protocol (iii)) is appropriate, bringing about better use of the nitrogen source and increasing

biomass growth. It was possible to achieve a gain of 37% in biomass and consequently larger total amounts of chlorophyll at a lower cost when compared with cultures grown with KNO_3. The fact that the water is being continually replaced (and not just once a day) in such experiment is also favorable, because it avoids the build up of high salinity conditions in the culture medium, that can hinder cellular growth. Nevertheless, comparing the results obtained at three temperatures studied (27, 30, and 33°C), the average maximum cell concentration was only 5.7% higher when urea fed continuously instead of intermittent addition every 24 h.

On the other hand, Sánchez-Luna et al. [86] compared the influence of the protocol of urea addition (pulse or continuous), under variable conditions of temperature and total feeding time, in order to select the best feeding regime for *S. platensis* fed-batch cultivation with constant flow rate. Urea was added to the culture by a fed-batch process at constant mass flow rate, following two different protocols: (a) intermittent addition every 24 h and (b) continuous feeding. Fed-batch cultivation of this cyanobacterium with constant urea feeding rate by pulse and continuous additions exhibited statistically coincident results. Because of the large solubility of this nitrogen source in water, it could be intermittently added avoiding the use of pumping equipments. Therefore, the addition of urea by daily pulse feeding at constant flow rates could be a useful protocol to be used in large-scale aquaculture facilities, implying lower costs for *A. platensis* biomass production.

An exponentially increasing feeding rate to supply urea is suitable for those cultures in which microbial growth can be inhibited by this nutrient or its derivatives. In fact, the highest nutrient supply takes place just at the end of the run, when biomass concentration achieves its maximum value. In this way, despite the inhibitory effect of ammonia coming from urea hydrolysis under alkaline conditions, the use of such a nitrogen source allowed *S. platensis* to reach a concentration comparable with that obtained with potassium nitrate in a batch run [33]. On the other hand, Sánchez-Luna et al. [87] observed that fed-batch autotrophic *A. platensis* cultivations, carried out at 6.0 klux (72 μmol photons m^{-2} s^{-1}) in 5.0-L open tanks at variable pH, temperature, and urea molar flow rate (K) resulted in a cell growth that followed a linear trend likely due to light limitation [13], thus justifying the use of constant mass flow rates. The use of urea as a nitrogen source prevented the inhibitory effect observed with ammonium chloride, and the growth curves did not exhibit any lag phase. The yield of biomass based on nitrogen progressively decreased with increasing urea molar flow rate. The statistical model pointed out pH = 9.5, T = 29°C, and K = 0.551 mM d^{-1} as the best conditions optimizing cell concentration and productivity, which do not differ much from the experimental observations.

Ammonium sulfate and urea have been tested as nitrogen sources for *S. platensis* cultivations, according to different batch and fed-batch protocols. The results showed that the use of urea in fed-batch culture led to better growth kinetics. Adoption of an appropriate slowly increasing urea feeding rate prevented the accumulation of ammonia in the medium as well as its well-known inhibition of biomass growth [97]. Preliminary batch cultivations were carried out to determine the actual nitrogen requirements of biomass as well as to establish the inhibition threshold of ammonia. Subsequent fed-batch runs, performed according to different feeding protocols,

allowed the selection of the best conditions for urea supply and demonstrated that growth kinetics may be comparable and even better than that obtained with the traditional nitrate-based culture media. Ammonia accumulation that usually inhibits biomass growth was in fact prevented following an appropriate pulse-feeding pattern. Although the highest productivity during the start-up was obtained with linearly increasing feeding rate, the use of a more slowly increasing pattern, aimed at minimizing ammonia accumulation, was shown to be the most suited for long-term cultivation. Therefore, the use of urea in a fed-batch process should be recognized as a possible way to decrease the costs of a large-scale plant for the production of this cyanobacterium.

In a recent study, Ferreira et al. [41] cultivating *A. platensis* in a tubular photobioreactor, which is useful in preventing ammonia loss by evaporation, observed that parabolic protocol for ammonium sulfate addition appeared to be the best one for biomass production comparable to those obtained using sodium nitrate as the conventional nitrogen source. Additionally, due to high cell growth observed in the cultivations, the demand for nitrogen was extremely high, reaching values around 12 mM per day. Taking into account that the inhibitory levels of ammonia is around 6 mM [13], in this case, considering the whole period of cultivation, the addition of 12 mM of ammonium sulfate per day in a single daily addition would probably lead to cell death. Thus, the daily addition was divided into eight times, which allowed a maximum cell concentration of approximately 14 $g\,L^{-1}$. In this work, a parabolic protocol for ammonium sulfate addition, in which the cells with 7% nitrogen was considered, led to biomass protein contents (35.6 ± 1.7%), comparable to that obtained in standard runs (35.5 ± 0.9%), thus demonstrating that the use of ammonium salts does not modify the cell composition.

Feeding time is a variable of great importance in the fed-batch process, where it is responsible for nutrient availability for the microorganisms. Concerning urea and ammonium salts for *A. platensis* cultivation, it is also very important to avoid any toxic effect of ammonia. A strict control of the feeding time in fed-batch culture in open ponds, at the same time, prevented the toxic effect exerted by excess ammonia or its loss by off-gassing [13]. As ammonia is the predominant nitrogenous species in the medium when ammonium chloride is used as a nitrogen source, an appropriate feeding time should be selected to maintain optimum ammonia levels throughout the whole cultivation. In fact, longer times limited growth because of the shortage of the nitrogen source, while shorter times affected the growth due to the occurrence of a displacement between nitrogen source supply and utilization [7].

Bezerra et al. [7] reported that a short feeding time results in the partial loss of ammonia when using NH_4Cl as nitrogen source and, consequently, growth limitation can occur. As evidenced by the increase in maximum cell concentration (X_m) from 1,111 to 1,633 mg L^{-1}, a longer feeding time favored *A. platensis* growth. In addition, the run with the longest time to achieve the stationary phase exhibited a lower value of X_m (1,561 mg L^{-1}), likely due to growth limitation by nitrogen beginning with the feeding step. This is in agreement with Carvalho et al. [13], who reported the existence of an optimum feeding time for cell production, below and above which biomass growth was affected by nitrogen source accumulation and consequent loss in the form of ammonia (feeding time of 12 days) or limitation

(feeding time of 20 days) in the medium. Both situations led to decreases in X_m and suggested some discrepancy between biological demand and availability of the nitrogen source.

The fed-batch cultivation can be carried out as a repeated fed-batch process, in which once the cultivation reaches a certain stage after which it is not effective anymore, a portion of the culture medium is removed from the bioreactor and replaced by fresh nutrient medium. It allows keeping part of the medium in the reactor at the end of cultivation, reusing the exponentially growing cells for subsequent runs, cheaply ensuring high starting cell levels, and avoiding long stopping of the process. Moreover, it is expected to increase cell productivity, ensuring high cell growth rate. These features could be usefully exploited to evaluate the possibility of using this process with urea as a nitrogen source in large-scale cultivations. This process is characterized by removing a constant fraction of volume of culture at fixed time intervals and can be maintained indefinitely, where the volume is replenished to its maximum value by adding medium culture with appropriate flow rate [76, 115]. This type of process was employed by Matsudo et al. [62] to evaluate if urea could be successfully employed when using repeated fed-batch cultivation of *A. platensis* in open ponds. This study showed that the repeated fed-batch process using urea as a nitrogen source was suited for long-term *A. platensis* cultivation, during which the maximum cell concentration, the nitrogen-to-cell conversion factor and the kinetic parameters remained stable when using an appropriate ratio of renewed to total volume and experimental protocols of urea addition. Moreover, it should be noted that the biomass protein content was not influenced by the experimental conditions. The maintenance of maximum cell concentration during three consecutive cycles and the absence of contamination probably take place due to the well-known ability of this microorganism to grow well in saline and alkaline inorganic environments.

In conclusion, the fed-batch process is a useful tool for supplying carbon and nitrogen in cultivations of *A. platensis* under different photobioreactor configurations. For each specific carbon and nitrogen source added, it is necessary to evaluate the experimental conditions that lead to both desired cell growth and composition. Besides classical factors that affect photosynthetic cell growth, such as carbon source, nitrogen source, other nutrients, pH, temperature, light intensity and salinity, the typical parameters of the fed-batch process, such as feeding time, addition protocol and flow rate, should be evaluated. The comments presented in this chapter demonstrate that the use of inexpensive nitrogen sources, such as urea, ammonium salts and nitrogen-rich wastewaters can be used for *A. platensis* cultivation, with results that can be comparable to those with classical nitrate sources. The results also show that closed photobioreactor is useful for preventing ammonia loss during *A. platensis* cultivation. The best form of supplying organic carbon needs to be evaluated, where different strategies are necessary for each organic carbon source employed. In cases of using organic carbon, the process needs to be carried out under aseptic conditions. Considering inorganic carbon sources, CO_2 has an important role in the growth of such cyanobacteria, where it needs to be added to the medium to maintain the carbon source level as well as pH. Finally, the fed-batch process was demonstrated to be useful for the production of *A. platensis* using CO_2 from industrial plants, particularly from industrial alcoholic fermentations.

References

1. Abeliovich A, Azov Y (1976) Toxicity of ammonia to algae in sewage oxidation ponds. Appl Environ Microbiol 31:801–806
2. Akimoto M, Ohara T, Ohtaguchi K, Koide K (1994) Carbon dioxide fixation and γ-linolenic acid production by the hot-spring alga *Cyanidium caldarium*. J Chem Eng 27:329–333
3. Araújo KGL, Facchinetti AD, Santos CP (2003) Influência da ingestão de biomassas de *Spirulina* (*Arthrospira sp*.) sobre o peso corporal e consumo de ração em ratos. Ciênc Tecnol Aliment 23:6–9
4. Balloni W, Tomaselli L, Giovannetti L, Margheri MC (1980) Biologia fondamentale del genere *Spirulina*. In: Materassi, R. (Ed.) Prospettive della coltura di *Spirulina* in Italia. CNR, Roma, pp. 49–82
5. Belay A (1997) Mass culture of *Spirulina* outdoors—the earthrise farms experience. In: Vonshak A (ed) *Spirulina platensis* (*Arthrospira*): physiology, cell-biology and biotechnology. Taylor & Francis, London, pp 131–158
6. Belkin S, Boussiba S (1991) High internal pH conveys ammonia resistance in *S. platensis*. Biores Technol 32:167–169
7. Bezerra RP, Matsudo MC, Converti A, Sato S, Carvalho JCM (2008) Influence of the ammonium chloride feeding time and the light intensity on the cultivation of *Spirulina* (*Arthrospira*) *platensis*. Biotechnol Bioeng 100:297–305
8. Binaghi L, Del Borghi A, Lodi A, Converti A, Del Borghi M (2003) Batch and fed-batch uptake of carbon dioxide by *Spirulina platensis*. Process Biochem 38:1341–1346
9. Borowitzka MA (1999) Commercial production of microalgae: ponds, tanks, tubes and fermenters. J Biotechnol 70:313–321
10. Boussiba S (1989) Ammonia uptake in the alkalophilic cyanobacterium *Spirulina platensis*. Plant Cell Physiol 30:303–308
11. Boussiba S, Richmond AE (1980) C-phycocyanin as a storage protein in the blue-green alga *Spirulina platensis*. Arch Microbiol 125:143–147
12. Branger B, Caudal JL, Delobel M, Ouoba H, Yameogo P, Ouedraogo D, Guerin D, Valea A, Cren L, Zombre C, Ancel P (2003) *Spirulina* as a food supplement in case of infant malnutrition in Burkina-Faso. Arch Pédiatr 10:424–431
13. Carvalho JCM, Francisco FR, Almeida KA, Sato S, Converti A (2004) Cultivation of *Arthrospira* (*Spirulina*) *platensis* by fed-batch addition of ammonium chloride at exponentially-increasing feeding rate. J Phycol 40:589–597
14. Carvalho JMC, Sato S (2001) Fermentação descontínua alimentada. In: Schmidell W, Lima U, Aquarone E, Borzani W (eds) Biotecnologia industrial, vol 2. Edgar Blücher, São Paulo, pp 205–218
15. Carvalho JCM, Sato S, Converti A, Bezerra RP, Matsudo MC, Vieira DCM, Ferreira LS, Rodrigues MS (1998) (applicants). Método de aproveitamento de dióxido de carbono e seu uso no cultivo de microrganismos fotossintetizantes. Brazil Patent Application No. 0805123-2, p 82 (published 22 Apr 2009)
16. Castenholz RW (1989) Subsection III, order *Oscillatoriales*. In: Stanley JT, Bryant MP, Pfenning N, Holt JG (eds) Bergey's manual of systematic bacteriology, vol 3. William and Wilkins, Baltimore, p 1771
17. Chamorro G, Salazar M, Araujo KG, Dos Santos CP, Cebalhos G, Castillo LF (2002) Update on the pharmacology of *Spirulina* (*Arthrospira*), an unconventional food. Arch Latinoam Nutr 52:232–240
18. Chen F, Zhang Y (1997) High cell density mixotrophic culture of Spirulina platensis on glucose for phycocyanin production using a fed-batch system. Enzyme Microb Technol 20:221–224
19. Chen T, Zhang W, Yang F, Bai Y, Wong Y (2006) Mixotrophic culture of high selenium-enriched *Spirulina platensis* on acetate and the enhanced production of photosynthetic pigments. Enzyme Microb Technol 39:103–107

20. Chojnacka K, Noworyta A (2004) Evaluation of *Spirulina* sp. growth in photoautotrophic, heterotrophic and mixotrophic cultures. Enzyme Microb Technol 34:461–465
21. Chronakis IS, Galatanu AN, Nylander T, Lindaman B (2000) The bevaviour of protein preparation from blue-green algae *Spirulina platensis* (strain Pacifica) at the air/water interface. Colloid Surf A 173:181–192
22. Chuntapa B, Powtongsook S, Menaaveta P (2003) Water quality control using *Spirulina platensis* in shrimp culture tanks. Aquaculture 220:355–366
23. Ciferi O, Tiboni O (1985) The biochemistry and industrial potential of *Spirulina*. Microbiology 39:503–526
24. Cohen Z (1997) The chemicals of *Spirulina*. In: Vonshak A (ed) Spirulina platensis (Arthrospira): physiology, cell-biology and biotechnology. Taylor & Francis, London, pp 175–204
25. Cohen ZV, Normann HA, Heimer Y (1993) Potential use of substituted pyridazinones for selecting polyunsaturated fatty acid overproducing cell lines of algae. Phytochemistry 33:259–264
26. Colla LM, Bertolin TE, Costa JAV (2004) Fatty acids profile of *Spirulina platensis* grown under different temperatures and nitrogen concentrations. Z Naturforsch 59c:55–59
27. Converti A, Lodi A, Del Borghi A, Solisio C (2006) Cultivation of *Spirulina platensis* in a combined airlift-tubular reactor system. Biochem Eng J 32:13–18
28. Converti A, Torre P, De Luca E, Perego P, Del Borghi M, Silva SS (2003) Continuous xylitol production from synthetic xylose solutions by *Candida guilliermondii*: influence of pH and temperature. Eng Life Sci 3:193–198
29. Converti A, Zilli M, Poloniecki RH, Del Borghi M, Ferraiolo G (1993) Influence of nutrient concentration in new operating criteria for biological removal of phosphorus from wastewaters. Water Res 27:791–798
30. Cornet JF, Dussap CG, Gros JB (1998) Kinetics and energetics of photosynthetic microorganisms in photobioreactors. Application to *Spirulina* growth. Adv Biochem Eng Biotechnol 59:155–194
31. Costa JAV, Colla LM, Duarte-Filho PF (2004) Improving *Spirulina platensis* biomass yield using a fed-batch process. Bioresour Technol 92:237–241
32. Crueger W, Crueger A (1982) Biotechnology. Sinauer Associates and Science Technology, Sunderland, p 368
33. Danesi EDG, Rangel-Yagui CO, Carvalho JCM, Sato S (2002) An investigation of effect of replacing nitrate by urea in the growth and production of chlorophyll by *Spirulina platensis*. Biomass Bioenerg 23:261–269
34. Danesi EDG, Rangel-Yagui CO, Carvalho JCM, Sato S (2004) Effect of reducing the light intensity in the growth and production of chlorophyll by *Spirulina platensis*. Biomass Bioenerg 26:329–335
35. Dillon JC, Phuc AP, Dubacq JP (1995) Nutritional value of the alga *Spirulina*. Plants Hum Nutr 77:32–46
36. Enfors SO, Häggström L (2000) Bioprocess technology fundamentals and applications. Royal Institute of Technology, Stockholm, p 356
37. Esener AA, Roels JA, Kossen NW (1981) The influence of temperature on the maximum specific growth rate of *Klebsiella pneumoniae*. Biotechnol Bioeng 23:1401–1405
38. Faintuch BL (1989) Análise comparativa da produção de biomassa a partir de três cianobactérias empregando distintas fontes nitrogenadas. Master dissertation, Faculty of Pharmaceutical Sciences, University of São Paulo, São Paulo
39. Farooq SM, Asokan D, Kalaiselvi P et al (2004) Prophylactic role of phycocyanin: a study of oxalate mediated renal cell injury. Chem Biol Interact 149:1–7
40. Ferraz CAM, Aquarone E, Florenzano G et al (1985) Utilização de subprodutos da indústria alcooleira na obtenção de biomassa de *Spirulina maxima.* Parte I—Emprego do anidrido carbônico. Rev Microbiol 16:179–187
41. Ferreira LS, Rodrigues MS, Converti A et al (2010) A new approach to ammonium sulphate feeding for fed-batch *Arthrospira* (*Spirulina*) *platensis* cultivation in tubular photobioreactor. Biotechnol Prog 26:1271–1277

42. Gregersen L, Jorgensen SB (1999) Supervision of fed-batch fermentation. Chem Eng J 75:69–76
43. Hattori A, Myers J (1966) Reduction of nitrate and nitrite by subcellular preparations of *Anabaena cylindrica*. I. Reduction of nitrite to ammonia. J Plant Physiol 41:1031
44. Henrikson R (1989) Earth food *Spirulina*. Ronore Enterprises Inc., Kenwood, p 180p
45. Hernández E, Olguín EJ (2002) Biosorption of heavy metals influenced by the chemical composition of *Spirulina* sp. (*Arthrospira*) biomass. Environ Technol 23:1369–1377
46. Jaime-Ceballos BJ, Hernández-Llamas A, Garcia-Galano T, Villarreal H (2006) Substitution of *Chaetoceros muelleri* by *Spirulina platensis* meal in diets for *Litopenaeus schmitti* larvae. Aquaculture 260:215–220
47. Jakobsen M, Cantor MD, Jespersen L (2002) Production of bread, cheese and meat. In: Osiewacz HD, Esser K, Bennett JW (eds) The Mycota, vol X, Industrial applications. Springer, Berlin, pp 3–22
48. Jensen S, Knutsen G (1993) Influence of light and temperature on photoinhibition of photosynthesis in *Spirulina platensis*. J Appl Phycol 5:495–504
49. Jiménez C, Cossío BR, Niell FX (2003) Relationship between physicochemical variables and productivity in open ponds for the production of *Spirulina*: a predictive model of algal yield. Aquaculture 221:331–345
50. Johnson A (1987) The control of fed-batch fermentation processes. A survey. Automatica 23:691–705
51. Kamilya D, Sarkar S, Maiti TK et al (2006) Growth and nutrient removal rates of *Spirulina platensis* and *Nostoc muscorum* in fish culture effluent: a laboratory-scale study. Aquacult Res 37:1594–1597
52. Kaplan A, Reinhold L (1999) CO_2 concentrating mechanisms in photosynthetic microorganisms. Annu Rev Plant Physiol Plant Mol Biol 50:539–570
53. Kommareddy A, Anderson G (2004) Study of light requirements of a photobioreactor. ASAE/CSAE Meeting Presentation. Winnipeg, MG, Canada. Paper No. MB04–111
54. Lacaz-Ruiz R (2003) Espirulina e Zootecnia. In: Lacaz-Ruiz R (ed) Espirulina—Estudos & Trabalhos. Roca, São Paulo, p 296
55. Law EA, Berning JL (1991) Photosynthetic efficiency optimization studies with macroalga *Gracilaria tikvihae*: implication for CO_2 emission control from power plants. Biores Technol 37:25–33
56. Lee J, Lee SY, Park S, Middelberg APJ (1999) Control of fed-batch fermentations. Biotechnol Adv 17:29–48
57. Li ZY, Guo SY, Li L (2006) Study on the process, thermodynamical isotherm and mechanism of Cr(III) uptake by *Spirulina platensis*. J Food Eng 75:129–136
58. Lodi A, Binaghi L, De Faveri D et al (2005) Fed-batch mixotrophic cultivation of *Arthrospira* (*Spirulina*) *platensis* (Cyanophyceae) with carbon source pulse feeding. Ann Microbiol 55:181–185
59. Longobardi GP (1994) Fed-batch versus batch fermentation. Bioprocess Eng 10:185–194
60. Lourenço SO (2006) Cultivo de Microalgas Marinhas—princípios e aplicações. RiMa, São Carlos
61. Márquez FJ, Sasaki K, Kakizono T et al (1993) Growth characteristics of *Spirulina platensis* in mixotrophic and heterotrophic conditions. J Ferment Bioeng 76:408–410
62. Matsudo MC, Bezerra RP, Sato S et al (2009) Repeated fed-batch cultivation of *Arthrospira* (*Spirulina*) *platensis* using urea as nitrogen source. Biochem Eng J 43:52–57
63. Matsudo MC, Bezerra RP, Sato S et al (2011) Use of CO_2 from alcoholic fermentation for continuous cultivation of *Arthrospira* (*Spirulina*) *platensis* in tubular photobioreactor using urea as nitrogen source. Biotechnol Prog 27:650–656
64. Merzlyak MN, Pogosyan SI, Lekhimena L et al (1996) Spectral characterization of photooxidation products formed in chlorophyll solution and upon photodamage to the Cyanobacterium *Anabaena variabilis*. Russ J Plant Physiol 43:186–195
65. Miller AG, Colman B (1980) Evidence for carbonate transport by the blue-green alga (cyanobacterium). Plant Physiol 65:397–402

66. Molina Grima E, Fernandéz FGA, Camacho FG et al (1999) Photobioreactors: light regime, mass transfer, and scale up. J Biotechnol 70:231–247
67. Nagaoka S, Shimizu K, Kaneko H et al (2005) A novel protein C-phycocyanin plays a crucial role in the hypocholesterolemic action of *Spirulina platensis* concentrate in rats. Nutr J 135:2425–2430
68. Narayan MS, Manoj GP, Vatchravelu K et al (2005) Utilization of glycerol as carbon source on the growth, pigment and lipid production in *Spirulina platensis*. Int J Food Sci Nutr 56:521–528
69. O'Callagan C (1996) Biotechnology in natural food colours: the role of bioprocessing. In: Hendry GA, Houghton JD (eds) Natural food colorants, 2nd edn. Blackie Academic Professional, London, pp 80–108
70. Olguín E, Galicia S, Mercado G et al (2003) Annual productivity of *Spirulina* (*Arthrospira*) and nutrient removal in a pig wastewater recycling process under tropical conditions. J Appl Phycol 15:249–257
71. Olguín EJ (2000) The cleaner production strategy applied to animal production. In: Hernádez E, Olguín EJ, Sánchez G (eds) Environmental biotechnology and cleaner bioprocesses. Taylor & Francis, London, pp 227–241
72. Paoletti C, Pushparaj B, Tomaselli L (1975) Ricerche sulla nutrizione minerale di *Spirulina platensis*. In: Congresso nazionale della società italiana di microbiologia, vol 17. Italian Society of Microbiology, Padua, pp 833–839
73. Parada JL, Caire GZ, Mulé MCZ et al (1998) Lactic acid bactéria growth promoters from *Spirulina platensis*. Int J Food Microbiol 45:225–228
74. Parikh P, Mani U, Iyer U (2001) Role of *Spirulina* in the control of glycemia and lipidemia in type 2 *diabetes mellitus*. J Med Food 4:193–199
75. Piorreck M, Hinnerk K, Pohl B, Pokl P (1984) Biomass production, total protein chlorophylls, lipids and fatty acids of freshwater green and blue green algae under different nitrogen regimes. Phytochemistry 23:207–216
76. Pirt J (1975) Principles of microbe and cell cultivation. Wiley, New York
77. Ploetz C (2009) Carbon capture and storage. In: Bullinger H-J (ed) and Behlau L (contributor) Technology guide principles—applications—trends. Springer, New York, 547p
78. Pulz O, Scheinbenbogen K (1998) Photobioreactors: design and performance with respect to light energy input. Adv Biochem Eng Biotechnol 59:123–152
79. Ramirez-Perez JC, Janes HW (2009) Carbon dioxide sequestration by *Spirulina platensis* in photo-bioreactors. Habitation 12:65–77
80. Rangel-Yagui CO, Danesi EDG, Carvalho JCM et al (2004) Chlorophyll production from *Spirulina platensis*: cultivation with urea addition by fed-batch process. Biores Technol 92:133–141
81. Richmond A (1983) Phototropic microalgae. In: Rahm HJ, Reed G (eds) Biotechnology, vol 3. Verlag Chemie, Weinheim, p 497
82. Richmond A (1988) *Spirulina*. In: Borowitzka MA, Borowitzka LJ (eds) Microalgal biotechnology. Cambridge University Press, Cambridge, pp 85–121
83. Richmond A, Qiang H (1997) Principles for efficient utilization of light for mass production of photoautotrophic microorganisms. Appl Biochem Biotechnol 63(65):649–658
84. Rodrigues MS, Ferreira LS, Converti A, Sato S, Carvalho JCM (2010) Fed-batch cultivation of *Arthrospira* (*Spirulina*) *platensis*: potassium nitrate and ammonium chloride as simultaneous nitrogen sources. Biores Technol 101:4491–4498
85. Samuels R, Mani UV, Iyer UM et al (2002) Hypocholesterolemic effect of *Spirulina* in patients with hyperlipidemic nephrotic syndrome. J Med Food 5:91–96
86. Sánchez-Luna LD, Converti A, Tonini GC et al (2004) Continuous and pulse feedings of urea as a nitrogen source in fed-batch cultivation of *Spirulina platensis*. Aquacult Eng 31: 237–245
87. Sánchez-Luna LD, Bezerra RP, Matsudo MC et al (2007) Influence of pH, temperature and urea molar flowrate on *Arthrospira platensis* fed-batch cultivation. A kinetic and thermodynamic approach. Biotechnol Bioeng 9:702–711

88. Sassano CEN, Carvalho JCM, Gioielli LA et al (2004) Kinetics and bioenergetics of *Spirulina platensis* cultivation by fed-batch addition of urea as nitrogen source. Appl Biochem Biotechnol 112:143–150
89. Sassano CEN, Gioielli LA, Ferreira LS et al (2010) Evaluation of the composition of continuously-cultivated *Arthrospira* (*Spirulina*) *platensis* using ammonium chloride as nitrogen source. Biomass Bioenerg 34:1732–1738
90. Saucedo-Castaneda G, Gutiérrez-Rojas M, Bacque G, Raimbault M et al (1990) Heat transfer simulation in solid substrate fermentation. Biotechnol Bioeng 35:802–808
91. Saxena PN, Ahmad MR, Shyam R (1983) Cultivation of *Spirulina* in sewage for poultry feed ammonia. Experientia 39:1077–1083
92. Schlösser UG (1982) Sammlung von Algenkulturen. Ber Deutsch Bot Ges 95:181–276
93. Shimamatsu H (2004) Mass production of *Spirulina*, an edible microalga. Hydrobiologia 512:39–44
94. Sicko-Goad L, Andresen NA (1991) Effect of growth and light/dark cycles on diatom lipid content and composition. J Phycol 27:710–718
95. Silva PC, Basson PW, Moe RL (1996) Catalogue of the Benthic marine algae of the Indian Ocean, vol 79. University of California Publications in Botany, Berkeley, p 1259
96. Soletto D, Binaghi L, Ferrari L et al (2008) Effects of carbon dioxide feeding rate and light intensity on the fed-batch pulse-feeding cultivation of *Spirulina platensis* in helical photobioreactor. Biochem Eng J 39:369–375
97. Soletto D, Binaghi L, Lodi A et al (2005) Batch and fed-batch cultivations of *Spirulina platensis* using ammonium sulphate and urea as nitrogen sources. Aquaculture 243:217–242
98. Solisio C, Lodi A, Converti A et al (2003) Influence of temperature on cadmium removal by *Sphaerotilus natans* by acidic solutions. Sep Sci Technol 38:3951–3966
99. Spolaore P, Joannis-Cassan C, Duran E et al (2006) Commercial applications of microalgae. J Biosci Bioeng 101:87–96
100. Stal LJ, Zehr JP (2008) Cyanobacterial nitrogen fixation in the ocean: diversity, regulation, and ecology. In: Herrero A, Flores H (eds) The *cyanobacteria*: molecular biology, genomics, and evolution. Caister Academic Press, Norfolk, UK, p 484
101. Subhashini J, Mahipal SV, Reddy MC et al (2004) Molecular mechanisms in C-phycocyanin induced apoptosis in human chronic myeloid leukemia cell line-K562. Biochem Pharmacol 68:453–462
102. Suetsuna K, Chen JR (2001) Identification of antihypertensive peptides from peptic digest of two microalgae, *Chlorella vulgaris* and *Spirulina platensis*. Marine Biotechnol 3:305–309
103. Swaaf ME, Sijtsma L, Pronk JT (2003) High-cell-density fed-batch cultivation of the docosahexaenoic acid producing marine alga *Crypthecodinium cohnii*. Biotechnol Bioeng 81:666–672
104. Tacon A, Jackson A (1985) Utilization of conventional and unconventional source in practical fish feeds.Nutrition and feeding in fish. Academic, London, pp 119–145
105. Toro JE (1989) The growth rate of two species of microalgae used in shellfish hatcheries cultured under two light regimes. Aquac Fish Manage 20:249–254
106. Torre P, Sassano CEN, Sato S et al (2003) Fed-batch addition of urea for *Spirulina platensis* cultivation. Thermodynamics and material and energy balances. Enzyme Microb Technol 33:698–707
107. UNICA—União da Indústria de Cana-de-açúcar. www.portalunica.com.br. Accessed 18 Dec 2010
108. Vasconcelos Y (2010) Projeto prevê o reaproveitamento de CO_2 para cultivo de microalgas e cianobactérias. Rev Pesq FAPESP 176:78–79
109. Vonshak A (1997) *Spirulina*: growth, physiology and biochemistry. In: Vonshak A (ed) *Spirulina platensis* (*Arthrospira*): physiology, cell-biology and biotechnology. Taylor and Francis, London, pp 43–65
110. Vonshak A, Boussiba S, Abeliovich A et al (1983) Production of *Spirulina* biomass: maintenance of monoalgal culture outdoors. Biotechnol Bioeng 25:341–349

111. Vonshak A, Richmond A (1988) Mass production of the blue-green alga *Spirulina*: an overview. Biomass 15:233–247
112. Wang B, Li Y, Wu N et al (2008) CO_2 bio-mitigation using microalgae. Appl Microbiol Biotechnol 79:707–718
113. Ward O (1989) Biotecnologia de la Fermentacion. Zaragoza. Editorial Acribia, 274p
114. Watanabe Y, Hall DO (1995) Photosynthetic CO_2 fixation technologies using a helical tubular bioreactor incorporating the filamentous cyanobacterium *Spirulina platensis*. Energ Convers Manage 36:721–724
115. Weigand WA (1981) Maximum cell productivity by repeated fed-batch culture for constant yield case. Biotechnol Bioeng 23:249–266
116. Yamane T, Shimizu S (1984) Fed-batch techniques in microbial processes. Adv Biochem Eng Biotechnol 30:148–194
117. Yoshida F, Yamane T, Nakamoto KI (1973) Fed-batch hydrocarbon fermentation with colloidal emulsion feed. Biotechnol Bioeng 15:257–270
118. Zarrouk C (1966) Contribution a l'etude d'une cyanophycee influence de divers facteurs physiques et chimiques sur la croissance e photosynthese de *Spirulina maxima*. Universite de Paris, Paris, France, pp 4–5
119. Zeng FMT, Vonshak A (1998) Adaptation of *Spirulina platensis* to salinity—stress. Comp Biochem Physiol A Mol Integr Physiol 120:113–118

Chapter 34
Bioprocess Development for Chlorophyll Extraction from Microalgae

Ronald Halim and Michael K. Danquah

Abstract Chlorophyll, a green pigment found abundantly in plants, algae, and cyanobacteria, plays a critical role in sustaining life on earth and has found many applications in pharmaceutical, food, as well as cosmetic industries. Because of their high intracellular chlorophyll accumulations (up to 10% of cell dry weight), green microalgae are recognized as promising alternative chlorophyll sources. Successful co-production of a high value product such as chlorophyll in a microalgal bio-refinery is desirable as it will alleviate the overall cost of producing microalgal biodiesel. This chapter evaluates the bioprocess engineering required to recover and to purify chlorophyll molecules from microalgae. The use of organic solvents and supercritical fluids to extract microalgal chlorophyll on a commercial scale is examined. The use of chromatographic techniques to purify the recovered chlorophylls is also reviewed. Finally, the chapter ends by presenting a case study which investigates the use of organic solvents (acetone and methanol) to extract chlorophyll from *Tetraselmis suecica* on a laboratory scale.

1 Introduction

Microalgae are microscopic unicellular organisms capable to convert solar energy to chemical energy via photosynthesis. They require carbon dioxide, light, water, and other nutrients which facilitate the photosynthetic process to grow and large-scale production of microalgal biomass normally uses open-ponds. Growing concern over the widespread exploitation of food crops for biodiesel production has

R. Halim • M.K. Danquah (✉)
Department of Chemical Engineering, Bio Engineering Laboratory (BEL),
Monash University, Melbourne, VIC 3800, Australia
e-mail: michael.danquah@eng.monash.edu.au; kobinadanquah@yahoo.com

J.W. Lee (ed.), *Advanced Biofuels and Bioproducts*, DOI 10.1007/978-1-4614-3348-4_34,

sparked an unprecedented level of commercial interests in exploring the use of microalgae as alternative biodiesel feedstocks. In addition to having high intracellular contents of biodiesel-convertible neutral lipids, microalgae contain numerous high-value bio-products that can also be harnessed such as different isomers of carotenoids, polysaccharides, polyunsaturated fatty acids, and phycobiliproteins [40]. These bio-products have extensive applications in food and pharmaceutical industries and their successful co-production from microalgae will significantly alleviate the high cost associated with microalgal biodiesel production. Unfortunately, lack of process understanding for the recovery and purification of these bio-products from the microalgal biomass has prevented the realization of their full potential applications.

Chlorophyll is one of the high-value bio-products that can be extracted from microalgae. As a pigment that selectively absorbs light in the red and blue regions, chlorophyll emits a green colour [24]. It is used as a natural food colouring agent and has antioxidant as well as antimutagenic properties [24]. The process of producing chlorophyll from microalgae begins with concentrating the highly dilute microalgal culture (biomass concentration = 0.1–1% w/v). The resulting paste is then dried to form powder before the cells are exposed to either an organic solvent or a supercritical fluid during chlorophyll extraction. These steps are explained more thoroughly in Sect. 4.

Chlorophyll is present abundantly in nature (plants, algae, and cyanobacteria) and plays a vital role in photosynthesis due to its "light harvesting" propensity. The specific functions that chlorophyll performs during photosynthesis can be viewed elsewhere [11, 20, 21]. Photosynthesis is a process which uses harvested light energy together with water and carbon dioxide to produce oxygen and carbohydrates; as such, it converts solar energy into chemical energy. The direct product from this chemical process, carbohydrate, is used as the primary building block for plants and eventually all living organisms [21]. The importance of photosynthesis for life on earth is further highlighted by plants forming the basis of all food chains. It is estimated that 1.2 billion tons of chlorophyll/year are produced globally by both terrestrial and aquatic organisms [21].

There are two types of chlorophyll, chlorophyll *a* and chlorophyll *b*. However, these bio-molecules are highly susceptible to oxidation and their exposure to weak acids, oxygen, or light rapidly results in the formation of numerous degradation products [11, 20, 24]. Figure 1 shows the structures making up chlorophyll molecules [21, 45, 51]. The skeleton of chlorophyll molecule is the porphyrin macrocycle (Fig. 1a), which comprises of four pyrrole rings. An attachment of a single isocyclic ring to one of the pyrrole rings gives rise to the phorbin structure (Fig. 1b). Each pyrrole ring contains four carbon atoms and one nitrogen atom. All of the nitrogen atoms face inward to create a central hole where an Mg^{2+} metal ion easily binds to form the chlorophyll structure (Fig. 1c). In chlorophyll *b*, the methyl group in ring II of chlorophyll *a* is replaced by a formyl group. This structural difference results in chlorophyll *a* being a blue/green pigment with maximum red absorbance at 660–665 nm and chlorophyll *b* being a green/yellow with maximum red absorbance at 642–652 nm [20]. Chlorophyll in plant cells is confined within chloroplasts

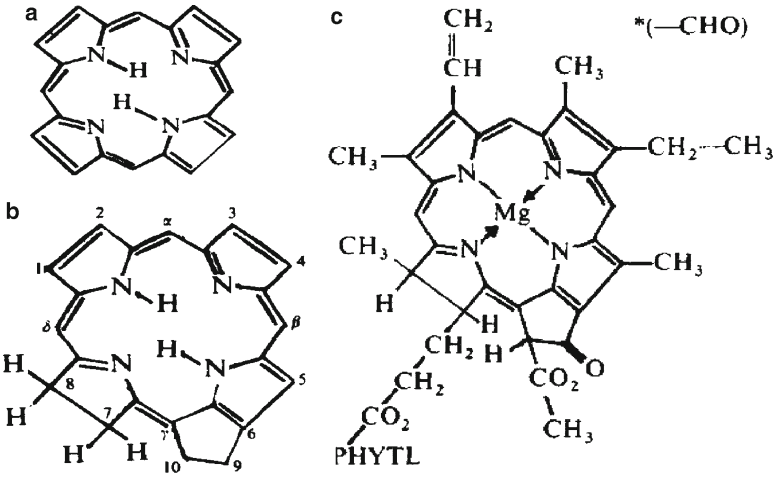

Fig. 1 Chemical structures of chlorophyll and its constituents, modified from Humphrey [20]. (**a**) Porphyrin macrocycle. (**b**) Phorbin. (**c**) Chlorophyll *a*, chlorophyll *b* is a variant with the methyl group in position 3 being replaced by a formyl group

where it is not only complexed with phospholipids, polypeptides, and tocopherols but also protected by a hydrophobic membrane [21].

When chlorophyll is removed from this original environment, its magnesium ion becomes unstable and may easily be displaced by a weak acid. This reaction leads to a series of reactions which eventually degrade the entire molecule. To increase stability, the magnesium ion in a free-standing chlorophyll molecule is often artificially substituted with a copper ion [21, 54].

2 Uses of Chlorophyll

2.1 Commercial Applications

Chlorophyll is often used as a natural colouring agent due to its green colour. Its use in the food industries is becoming increasingly popular due recent legislation shifts which mandated the use of natural colouring agents in preference to artificial agents [51]. There are, however, disadvantages associated with use of chlorophyll as a colouring agent. Not only is chlorophyll generally more expensive than artificial colourings, but also tends to be unstable under the different pH conditions of the foods to which it is added. To resolve this instability, the chlorophyll molecule must undergo a chemical modification which replaces its magnesium centre with a copper ion before it is mixed with the food materials. Since the modified chlorophyll cannot be metabolically absorbed and is eventually removed from the body as an excretion product, this complex is considered safe to replace the original

chlorophyll as a colouring agent in most developed countries. The concentration of free ionisable copper in the food must, however, be kept below 200 ppm under current regulations [20, 54].

2.2 Medical and Pharmaceutical Applications

Chlorophyll and its derivatives have found wide applications in the medical and pharmaceutical industries. Chlorophyll stimulates tissue growth through the facilitation of a rapid carbon dioxide and oxygen interchange between the tissue and the blood stream [8, 19, 50]. Because of this tissue-growth stimulating propensity, chlorophyll is able to prevent bacterial advancement in a wound and speeds up the wound-healing process [8, 50]. Some studies have found that chlorophyll can accelerate the rate of wound healing by more than 25%. Chlorophyll is used as a wound-healing accelerator in the treatment of ulcers and oral sepsis. Chronic ulcer is a significant health problem in society, with lengthy periods required for its treatment. The application of ointments containing chlorophyll derivatives on the ulcer was found not only to rapidly eliminate pain but also to improve the appearance of the affected tissues. The ulcer discharge and characteristic odour also decreased significantly after a few days of chlorophyll treatment [7]. The antibacterial property and deodorising nature of chlorophyll were found to be very helpful in the treatment of oral sepsis [15].

Chlorophyll and its derivatives have recently been identified as a powerful therapeutic for cancer chemoprevention due to their high displays of antioxidant and antimutagenic activities [12, 25]. Increasing consumption of fruits and vegetables that contains high levels of chlorophyll has been associated with reducing cancer risks.

3 Microalgae and Sustainability

Global warming can bring about extreme weather occurrences, rise in sea levels, extinction of species, retreat of glaciers, and many other calamities. The rise in global temperature is attributed to the high amount of carbon dioxide (CO_2) gases in the atmosphere [5, 13, 56]. CO_2 is emitted from the burning of fossil fuels for electricity, transport, and industrial processes [3]. The Kyoto Protocol in 1997 proposed a reduction of greenhouse gases by 5.2% based on the emissions in 1990.

Different CO_2 mitigation options have been considered to meet the proposed target [5]. The various strategies can be classified as either chemical-reaction-based approaches or biological mitigation. Chemical-reaction-based strategy captures CO_2 by reaction with other chemical compounds before the CO_2 is released into the atmosphere. The disadvantage of this method is that the chemical reactions can be very energy-intensive and costly. Furthermore, the wasted chemical compounds will need to be disposed of. On the other hand, biological mitigation seems more favourable as it not only captures CO_2 but also generates energy through photosynthesis [56].

Photosynthesis is carried out by all plants and any photosynthetic microorganism. Even though the use of plants to capture CO_2 is viable, it is inefficient due to their low photosynthetic rates. In contrast, owing to their structural and functional simplicities, microalgae are able to photosynthesize and hence capture CO_2 with an efficiency up to 10–50 times greater than that of higher-order plants [56]. Microalgae include both prokaryotic cyanobacteria and eukaryotic unicellular algal species [5]. In addition to CO_2 and sunlight, microalgae need nutrients, trace metals, and water to grow [2, 38, 46, 58]. In short, microalgal biomass is produced based on the following reaction:

$$CO_2 + H_2O + \text{nutrients} + \text{light energy} \rightarrow \text{biomass} + O_2$$

Unlike plants, microalgae can be grown with waste or brackish water as their high adaptability enables them to survive in a hostile environment contaminated with excess nitrogen, excess phosphorous, and heavy metals. In fact, microalgae can directly metabolize the excess nitrogen and phosphorous in waste water as nutrients for their cultivation. As such, microalgal cultivation does not interfere with use of fresh water, a limited resource in many parts of the world [2, 34, 38, 46, 58].

Among the 30,000 species of microalgae on Earth, many of them are known to contain a variety of high-value bio-products that can be commercially harnessed, such as biodiesel-convertible neutral lipids, different isomers of carotenoids, polysaccharides, polyunsaturated fatty acids, and phycobiliproteins [10]. In addition to being a CO_2 bio-sequester, commercial applications of microalgal biomass also include: (1) biodiesel through transesterification of its neutral lipids; (2) bio-ethanol through fermentation of its carbohydrates; (3) nutritional supplements for humans; (4) natural food colourants; (5) natural food source for many aquacultural species; (6) natural colourants in cosmetics; (7) bio-fertilizers through pyrolysis; (8) protein feed for farm animals [10, 14, 52]. Some of these applications require specific components of the biomass to be recovered while others utilize the entire cellular biomass.

4 Chlorophyll Production from Microalgae

Microalgae contain both chlorophyll *a* and chlorophyll *b*. Intracellular chlorophyll *a* content can vary from 0.0041 g/g dried microalgae (*Synechococcus* sp.) to 0.0185 g/g dried microalgae (*Nannochloropsis gaditana*) [53]. In green microalgae, the ratio of chlorophyll *a*/chlorophyll *b* ranges broadly from 0.64 to 5, in contrast to higher plants which have a narrower range from 1 to 1.4. The chlorophyll content and profile of a microalgal species continuously change depending on its life cycle and cultivation conditions (medium composition, nutrient availability, temperature, illumination intensity, ratio of light and dark cycle, aeration rate). Certain green microalgae, such as *Chlamydomonas*, *Chlorella*, and *Scenedesmus* sp., have mutants that can synthesize chlorophyll in the dark during heterotrophic growth [53].

Figure 2 shows the downstream processing steps required to produce chlorophyll from microalgae, while Table 1 provides a list of different technologies currently

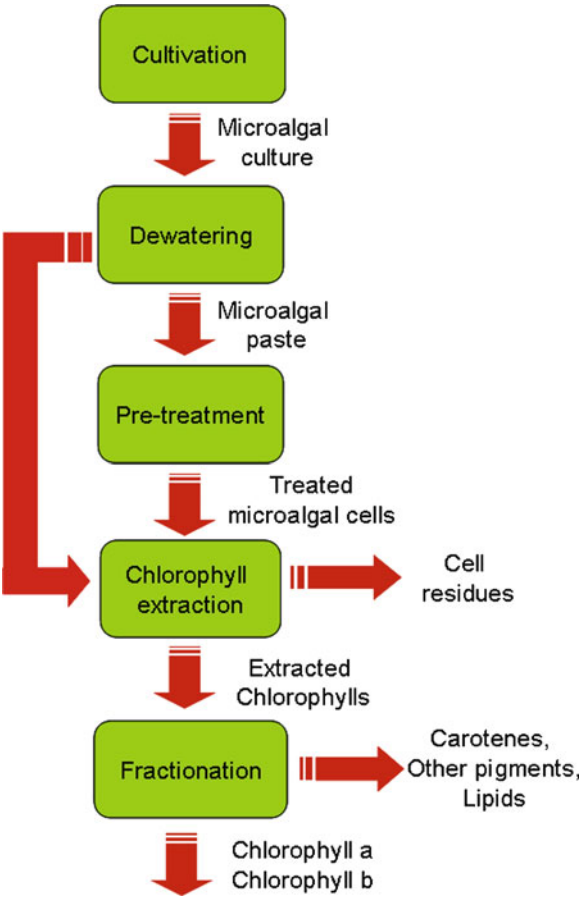

Fig. 2 Process flow diagram showing the downstream processing steps required to produce chlorophyll from microalgae

available for each step. After the microalgal culture is harvested from its cultivation system, it is concentrated in the dewatering step to yield a wet paste. Afterwards, the microalgal pellet undergoes a pre-treatment step for preparation towards chlorophyll extraction. The chlorophylls are then extracted from cellular materials before being purified in a fractionation step [24].

4.1 Cultivation System

There are two primary cultivation systems that are currently used to grow microalgae: (1) open-air system and (2) photobioreactors [4]. Table 2 compares the two cultivation systems in terms of important cultivation parameters. The selection of cultivation systems depends on several factors: the microalgal species, the availability of sunlight and water, the cost of land, the type of desired final product, and

Table 1 Different technologies available for each process step required for chlorophyll production from microalgae

Process step	Technologies
Cultivation	Raceway ponds
	Photobioreactors
Dewatering	Tangential flow filtration
	Pressure dewatering
	Flocculation
	Agglomeration
	Centrifugation
	Ultrasound separation
Pre-treatment: cell disruption	Ultrasonication
	Homogenization
	French pressing
	Bead beating
	Chemical lysis (acids and enzymes)
	Osmotic shock
Pre-treatment: drying	Oven drying
	Freeze drying
	Spray drying
Pre-treatment: powder size reduction	Milling with specific sieve
Chlorophyll extraction	Organic solvent extraction
	Supercritical fluid extraction
Fractionation	Paper chromatography
	Thin layer chromatography (TLC)
	High pressure liquid chromatography (HPLC)

Table 2 Comparison between microalgal cultivation systems [56]

Parameter	Raceway ponds	Tubular photobioreactors
Light efficiency	Fairly good	Excellent
Temperature control	None	Excellent
Gas transfer	Poor	Low–high
Oxygen production	Low	High
Accumulation	Low	Low–high
Hydrodynamic stress on algae	Difficult	Easy
Species control	None	Achievable
Sterility	Low	High
Cost to scale-up	Low	High
Volumetric productivity	High	Low

the supply of CO_2 [4, 53]. The amount of nutrients and certain metals (i.e., iron and magnesium) in the cultivation water is also important as it directly affects the growth rate and the CO_2 fixation efficiency of microalgal biomass. Research from an outdoor mass culture in New Mexico (US) shows that CO_2 fixation by microalgae increases with optimal nutrient level [58]. Susceptibility of the microalgal species to

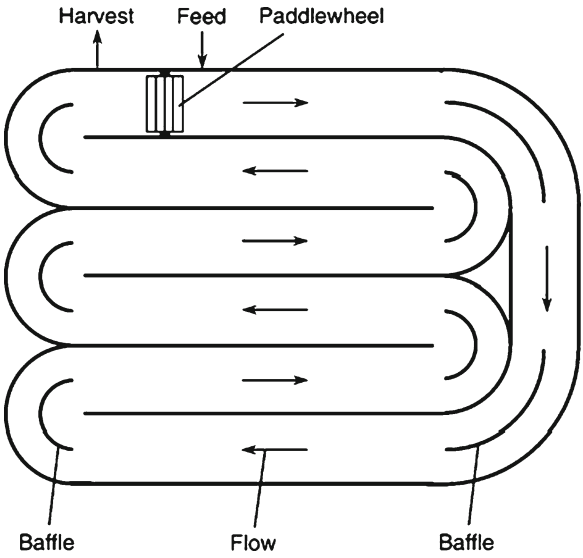

Fig. 3 Raceway pond for open-air microalgal cultivation, extracted from [9]

contamination by other microorganisms also needs to be considered when selecting cultivation systems. For example, *Tetraselmis*, *Skeletonem*, and *Isochrysis* are easily invaded by other local microorganisms and, as a result, are preferably cultivated in a closed photobioreactor system [4].

There are four different types of open-air systems: shallow big ponds, tanks, circular ponds, and raceway ponds [4]. Even though open-air systems are less complex to construct and cheaper to operate than photobioreactors, they suffer from numerous disadvantages, such as slower CO_2 diffusion, requirement for a large land area, substantial evaporative losses, poor light utilization, and difficulty in controlling cultivation conditions [55]. The depth of the open system also needs to be carefully calculated. The pond needs to be shallow enough for the penetrating sunlight to reach all the microalgal cells yet, at the same time, deep enough for sufficient mixing of the culture to occur. Maximum culture concentration that can be achieved in an open system varies between 0.1 and 0.5 g dried microalgae/L [4].

Among the open-air systems, the most common design is the raceway pond (Fig. 3) [56]. The raceway pond is made up of a closed loop recirculation channel with a paddle wheel that provides circulation and mixing. Baffles are also placed in the channel to guide the culture flow. To ensure uniform light penetration, the raceway pond is only 0.3 m in depth. The ponds are made from concrete or compacted earth that can be lined with plastic [9]. Companies, such as New Zealand's Aquaflow Bionomics and the US' Live Fuels Inc., have been using the raceway ponds to cultivate their microalgae.

Since photobioreactors have a "closed" design which allows users to tightly control cultivation conditions (temperature, degree of mixing, degree of illumination) as well as level of sterility, they are able to achieve significantly higher biomass productivity and CO_2 fixation rate for most microalgae than raceway ponds. There are

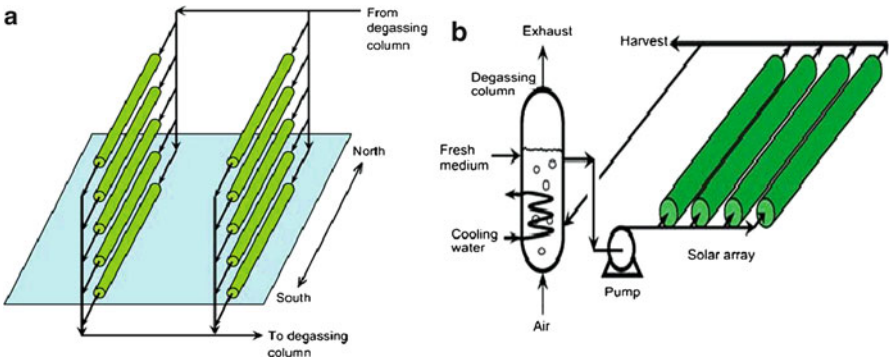

Fig. 4 Different configurations of tubular photobioreactors, extracted from [9]. (**a**) Parallel run horizontal tubes. (**b**) Fence-like tubular array

four different designs of photobioreactors: flat-plate, tubular, bubble-sparged vertical column, and airlift vertical column. Of these designs, tubular photobioreactors are the most popular [55]. Tubular photobioreactors are composed of an array of clear straight tubes made of thin glass or plastic (usually less than 0.1 m in diameter) to allow for maximum light penetration. The tubes are arranged either horizontally where they are placed parallel to each other flat on the ground or vertically where they are configured to form fence-like structures. Figure 4 shows the two different configurations of tubular photobioreactors [9].

Apart from the four primary designs, there are other types of photobioreactor systems that are currently used. The basics of the systems are the same with some modifications to maximize its efficiency. One such example is a 450-ft-long by 50-ft-wide photobioreactor made up of twin transparent plastic algal waterbeds patented by a company called A2BE Carbon Capture LLC. Another company, Green Shift Corporation based in New York, has produced a pilot-scale photobioreactor that is incorporated with an ethanol-producing facility to capture the CO_2 emitted from power plants [33].

4.2 Dewatering and Pre-treatment

Once the microalgal culture is harvested from its cultivation system, it exists as a dilute aqueous suspension (between 0.1 and 1 wt.%) and needs to be concentrated for downstream processing. Solid–liquid separation techniques (centrifugation, filtration, flocculation) are typically used to dewater the culture up to a solid concentration of 10 wt.% [9].

The dewatered microalgal paste then undergoes a pre-treatment step intended to enhance the efficiency of subsequent chlorophyll extraction. The pre-treatment can be performed in multiple steps or as a single process. As one alternative, the semi-wet paste is completely dried and the resulting biomass is milled into powder of

uniform size. Residual water in the paste needs to be removed as it is known to act as a barrier which impedes chlorophyll transfer from the microalgal cells into the extracting solvent. As another alternative, the paste can be exposed to disruption methods which destroy the microalgal cellular structures and force the release of intracellular chlorophylls to the surrounding medium. Exposing microalgal cells to mechanical cellular disruption methods (grinding, homogenization, and sonication) prior to solvent extraction has been found to increase final chlorophyll yield [28, 44, 49]. Simon and Helliwell [49] found that, without preliminary disruption, only a quarter of the available intracellular chlorophyll *a* can be extracted from microalgal cells.

4.3 Chlorophyll Extraction

4.3.1 Organic Solvent Extraction

Intracellular chlorophyll has traditionally been extracted from microalgal biomass using organic solvents [49]. The extraction process involves the organic solvent molecules penetrating through the cell membrane and dissolving the lipids as well as the lipoproteins of chloroplast membranes. Parameters which affect the yield of chlorophyll extraction by organic solvents include polarity of the organic solvents, storage conditions of the microalgal biomass, extraction duration, and number of extraction steps [44, 47]. Since chlorophyll is easily oxidized, extraction yield is also affected by the formation of degradation products. Chlorophyll starts degrading as soon as their molecules are exposed to excess light, atmospheric oxygen, high temperature, and acidic or basic pH condition [11].

Acetone, methanol, and ethanol are three of the most common solvents used to recover chlorophyll from microalgae. Table 3 summarizes key findings from previous studies on organic solvent extraction of microalgal chlorophyll. Jeffrey et al. [24], Simon and Helliwell [49], Sartory and Grobbelaar [44] found methanol and ethanol to be more efficient at extracting chlorophyll from microalgal biomass than acetone. Simon and Helliwell [49] conducted their sonication-assisted chlorophyll extractions in an ice bath and in the dark to prevent the formation of degradation products. They found that, with sonication, methanol recovered three times more chlorophyll than 90% acetone. Despite these findings, acetone remains the select primary solvent for chlorophyll extractions due to its known propensity to inhibit any chlorophyll degradation.

Macias-Sanchez et al. [28] recently used dimethyl formamide (DMF) to extract chlorophyll from microalgae and revealed the superiority of this solvent compared to the more traditional organic solvents, such as methanol, ethanol, and acetone. Extraction using DMF did not require prior cellular disruption as pigments were completely extracted after a few steps of soaking. Additionally, the chlorophyll remained stable for up to 20 days when stored in the dark at 5°C [32, 47]. The high toxicity associated with DMF, however, substantially decreased its appeal as an extraction solvent.

Table 3 Previous studies on organic solvent extraction of microalgal chlorophyll

Study	Algae species	Solvent	Cell disruption	Key results
Jeffrey et al. [24]	Phytoplankton	Methanol (90%), ethanol (90%), ethanol (100%), DMF	All	DMF is superior to all the other solvents used and cell lysis improves extraction in all cases
Macias-Sanchez et al. [28]	*Dunaliella Salina*	DMF, methanol	Ultrasound	DMF was found to be more efficient methanol
Sartory and Grobbelaar [44]	*Scenedesmus quadricauda, Selenastrum capricornutum, Microcystysis aeruginosa*	Ethanol (95%), methanol, acetone (90%)	Homogenisation, sonication, boiling	Methanol and 95% ethanol were superior to 90% acetone Boiling the algae in either methanol or 95% ethanol for 5 min and allowing extraction for 24 h resulted in the complete extraction of pigments without any formation of degradation products
Schumann et al. [47]	*Stichococcus, Chlorella*	Acetone, DMF	Grinding, ultrasound, bead beater	DMF was found to be the most efficient solvent Acetone extracted 56–100% of the amount of chlorophyll *a* extracted by DMF DMF does not require cell disruption Freeze drying before analysis aids extraction
Simon and Helliwell [49]	Freshwater algae, *Selenastrum obliquus*	Methanol and acetone	Probe sonication, bath sonication, tissue grinding, mortar, and pestle	Under sonication, methanol removed 3× more pigment than acetone. Under tissue grinding, methanol removed 20% more than acetone

Storage of the dried microalgal biomass at low temperatures (−18 or −20°C) was found to assist cell disruption and to promote chlorophyll extraction. In a study by Schumann et al. [47], freezing the biomass in liquid nitrogen followed by lyophilisation and then storage at −18°C was found to be the optimal storage procedure.

Sartory and Grobbelaar [44] found the efficiency of chlorophyll extraction from fresh water microalgae to be optimal when the extraction was carried out at the solvent's boiling point. It was shown that boiling the biomass for 3–5 min in methanol or acetone prior to 24-h extraction led to the complete recovery of chlorophyll *a* without the formation of any degradation products.

Such findings are contradictory to the general assumption that chlorophyll degraded upon slight temperature elevation.

The amount of chlorophyll extracted from a particular microalgal species was found to be highly dependent on its growth stage. Microalgae extracted in the stationary growth phase were shown to have significantly higher amount of chlorophyll *a* compared to the same species in the logarithmic phase [47].

4.3.2 Supercritical Fluid Extraction

Supercritical fluid extraction (SFE) represents an environmentally friendly alternative to organic solvent extraction. Even though it was first introduced in 1879 by Hannay and Hogarth, the extraction method did not gain much scientific attention until around 1960 [18, 39]. In addition to avoiding the use of toxic solvent, SFE has many apparent advantages over organic solvent extraction. It produces extracts of higher purity, requires less processing steps and can be operated at moderate temperatures to minimize extract degradation [39, 42]. Supercritical fluid generally has a high solvent power for non-polar components and a low affinity towards analytes with high molecular weights. The supercritical state is achieved when a substance is exposed to conditions exceeding its critical temperature (T_c) and pressure (P_c). In this state, the substance has a liquid-like density with a gas-like viscosity [6].

CO_2 is the most commonly used fluid for SFE as it is cheap, non-flammable, inert, and readily available. Figure 5 shows the phase diagram for CO_2 with its supercritical region. The critical temperature and pressure of CO_2 are 304.1 K and 7.38 MPa respectively. Supercritical carbon dioxide ($SCCO_2$) is often used in the extraction of thermolabile compounds as its low T_c enables complete extraction to occur without the application of excessive heating which may degrade analytes [29, 35]. $SCCO_2$ is a highly effective extractant due to its high diffusivity and its easily manipulated solvent strength. The solvent power of $SCCO_2$ towards a polar analyte can be improved by adding a polar modifier. The addition of methanol or water to $SCCO_2$ allowed for successful extraction of polar compounds [35], while ethanol addition was found to increase the yield of lipids from *Arthrospira maxima* [36]. $SCCO_2$ extraction has been applied in many fields including food industry, environmental science, and pharmaceuticals.

SFE can be classified as either an analytical or a preparative system. In the analytical system, SFE apparatus is directly combined with a chromatographic device.

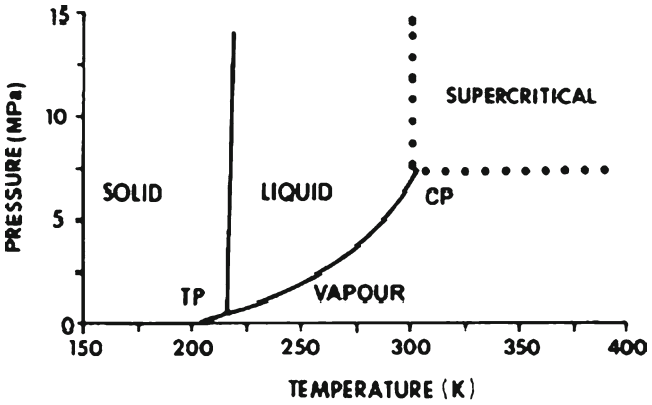

Fig. 5 *P–T* phase diagram for carbon dioxide [35]

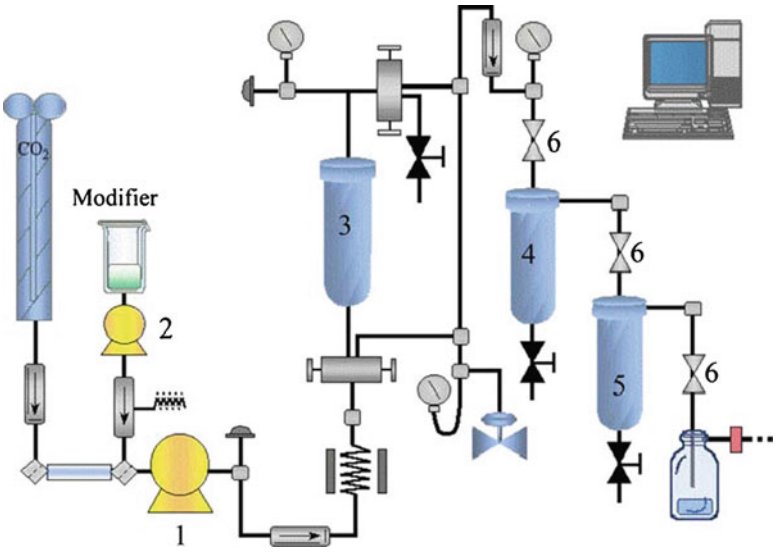

Fig. 6 Schematic diagram of supercritical fluid extraction (SFE) system, extracted from [17]. (1) CO_2 pump, (2) modifier pump, (3) extraction cell, (4) fractionation cell I, (5) fractionation cell II, (6) valve

Even though this system enables rapid analytes examination, it cannot be used as a production system as any extracted analytes are immediately consumed during the chromatographic analysis. On the other hand, the preparative system has been used to produce pilot-scale quantities of various analytes from microorganisms, including chlorophyll from microalgae. Figure 6 shows a pilot-scale preparative SFE system. It consists of a solvent (in this case CO_2) pump, a modifier pump, an extraction cell, valves, and two fractionation cells [17]. Detailed description of the SFE working

mechanism can be found elsewhere [17]. The microalgal biomass is placed in the extraction cell, while the supercritical fluid is depressurized in the fractionation cells equipped with temperature and pressure controllers. Upon depressurization, the supercritical fluid evaporates to the ambient as a gas, forcing analytes to precipitate in the fractionation cells. The dual-fractionation arrangement allows different analytes to be precipitated in each cell based on their differential solubilities in the evaporating supercritical fluid.

The use $SCCO_2$ process to extract chlorophyll *a* from microalgal species has been reported [30]. Optimum extraction conditions were found to be 60°C and 400 bar for *N. gaditana* and 60°C and 500 bar for *Synechococcus* sp. Chlorophyll *a* yields for the two microalgae at these optimum conditions were, respectively, 2.24 and 0.72 μg chlorophyll/mg dry weight microalgae. Even though these yields were not comparable to those of traditional methanol extraction (18.5 μg chlorophyll/mg dry weight microalgae for *N. gaditana* and 4.10 μg chlorophyll/mg dry weight microalgae for *Synechococcus* sp.), $SCCO_2$ extraction was found to be more selective and the extracted chlorophyll *a* appeared to contain less impurities. An extensive evaluation comparing the two extraction systems for isolating microalgal chlorophyll is, unfortunately, not yet possible due to limited knowledge on the supercritical process. The commercial feasibility of using $SCCO_2$ process to extract chlorophyll from microalgae is also a subject of further research.

4.4 Chlorophyll Fractionation and Purification on Chromatographic Adsorbents

Once recovered from microalgal biomass, the extracted chlorophyll mixture will have to be fractionated in order to separate out the different chlorophyll types and to remove unwanted components (neutral lipids, polar lipids, other pigments) that have been inevitably co-extracted. Chromatographic techniques are traditionally used to fractionate chlorophyll mixtures. The three types of chromatography that have been widely used are paper chromatography, thin layer chromatography (TLC), and high pressure liquid chromatography (HPLC) [1, 23, 31, 43].

Paper chromatography was used extensively during the early development of chromatographic techniques (1950s and 1960s). The method was able not only to separate chlorophyll into its fractions (*a*, *b*, and *c*) but also to effectively fractionate other pigments, such as pheophytins and carotenes [22]. However, the inception of TLC has resulted in the decline of paper chromatography usage. This later technique was preferred due to the ease in recovering pigment fractions from its adsorbent [31, 41]. Additionally, TLC requires less sample, is less laborious, and produces chromatograms with sharper resolutions [27, 41]. Organic adsorbents, such as sucrose and cellulose, were found to be the most effective stationary phases for use in two dimensional TLC. Even though the use of silica gel as a stationary phase was

effective in separating all plant pigments (except for some minor components), it was found to promote the formation of chlorophyll degradation products.

HPLC is superior to TLC because it requires even less sample for analysis, is faster and can be easily coupled with an automatic detection system [48, 57]. In addition to these, HPLC is more precise and has a higher degree of sensitivity. Reverse phase HPLC is preferred to normal phase as the latter does not separate polar compounds effectively. An additional drawback to normal phase HPLC is its lack of compatibility with aqueous samples. Several HPLC configurations have been employed, each being able to separate pigments to variable extent and different resolution [24]. There are different types of detectors that may be used to measure the concentrations of separated pigments as they exit the chromatographic column. The most commonly used detectors rely on fluorescence and absorbance analyses. Jeffrey et al. [24] found fluorescence detection to be more sensitive and more selective than absorbance detection especially when used to analyze chlorophylls amongst carotenoids. Table 4 summarizes previous studies on chromatographic fractionation of phytoplankton pigments. It is noted that the use of chromatographic techniques to purify recovered chlorophylls, albeit very effective on a laboratory scale, is not commercially applicable due to the high installation and operating costs associated with the techniques. Investigating a cost-viable, energy-efficient purification technology that can be retrofitted to industrial-scale chlorophyll production is a current research endeavour.

5 Case Study: Chlorophyll Extraction from *Tetraselmis suecica*

The work described here was carried out in the Department of Chemical Engineering, Monash University, in 2010 and has not been published elsewhere. The study describes the kinetics of chlorophyll extraction from *T. suecica* using acetone or methanol as an extractant. The three parameters investigated in order to optimize the extraction process were storage temperature of the biomass prior to chlorophyll extraction, level of intracellular water in the biomass during chlorophyll extraction, and average temperature during chlorophyll extraction.

5.1 Materials and Methods

5.1.1 Chemicals and Reagents

Chlorophyll *a* and chlorophyll *b* standards were purchased from Sigma-Aldrich Pty. Ltd (Australia). Organic solvents (100% acetone and 100% methanol) were analytical grade.

Table 4 Previous studies on HPLC fractionation of chlorophylls extracted from phytoplankton

Study	Mobile phase	Stationary phase	Key results
Jeffrey [23]	First dimension: 0.8% *n*-propanol in light petroleum (by volume) Second dimension: 20% chloroform in light petroleum (by volume)	Sucrose	In this two dimensional chromatography, there was complete separation of chlorophylls and carotenoids
Jeffrey et al. [24]	90:10 (v/v) methanol:acetone for 8 min at a flow rate 1 mL/min Pre-injection mix of sample 3:1 (v/v) sample: 0.5 M ammonium acetate	3 μm C18 Pecosphere	This simple isocratic protocol was able to separate only chlorophyll *a* from other pigments and compounds
Jeffrey et al. [24]	Solvent A is 80:20 (v/v) methanol:0.5 M ammonium acetate Solvent B is 90:10 methanol: acetone Elution order: 0–3 min: solvent A; 3–17 min: solvent B. flow rates: 1 mL/min Pre-injection mix of sample 3:1 (v/v) sample: 0.5 M ammonium acetate	3 μm C18 Pecosphere	This step-isocratic protocol was found to successfully separate the three chlorophylls (*a*, *b*, and *c*) and ten other derivative products
Jeffrey et al. [24]	Solvent A is 80:20 (v/v) methanol:0.5 M ammonium acetate Solvent B is 90:10 (v/v) acetonitrile:water Solvent C is ethyl acetate Elution order: 0–4 min: linear gradient from 100% A to 100% B 4–18 min: linear gradient to 20% B and 80% C 18–21 min: linear gradient to 100% B 21–24 min: 1inear gradient to 100% A 24–29 min: isocratic flow of 100% A	3 μm C18 Pecosphere	This ternary gradient protocol was found to separate over 50 pigments. The resolution of this protocol is higher than that of Wright and Shearer [57]. Additionally no ion pairing reagent is required, as in Mantoura and Llewellyn [32]
Lynn Co and Schanderl [27]	Three different solvent systems were experimented **Solvent system 1** (modified Bauer solvents): First dimension is benzene: petroleum ether: acetone (10:2.5:2 v/v/v). Second dimension is benzene: petroleum ether: acetone: methanol (10:2.5:1:0.25 v/v/v) **Solvent system 2:** First dimension is benzene: petroleum ether: acetone: methanol (10:2.5:1:0.25 v/v/v). Second dimension is petroleum ether: acetone: *n*-propanol (8:2:0.5 v/v/v) **Solvent system 3:** First dimension is benzene: petroleum ether: acetone (10:2.5:2 v/v/v). Second dimension is petroleum ether: acetone: *n*-propanol (8:2:0.5 v/v/v)	Silica Gel	Two dimensional chromatography was carried out on silica gel. Eight major pigments as well as eight to ten minor derivatives were successfully separated with these solvent systems

Madgwick [31]	30 mL of 1:1 (v/v) diethyl ether: petroleum spirit	Glucose	One dimensional ascending thin layer chromatography was used Spectrophotometric analysis was found to overestimate chlorophyll *c* by up to 22% and to underestimate chlorophyll *b* by 10–20%. Chlorophyll *a* was, however, correctly quantified
Mantoura and Llewellyn [32]	Solvent P (ion pairing reagent) is made of 1.5 g tetrabutyl ammonium acetate and 7.7 g of ammonium acetate dissolved in 100 mL of water. Primary eluant is solvent P: water: methanol (10:10:80 v/v/v). Secondary eluant is 20:80 (v/v) acetone:methanol 0–10 min: linear gradient from primary eluant to secondary eluant 10–22 min: isocratic flow of secondary eluant	Four different columns: C3 Zorbax, C8 Zorbax, C18 Zorbax, Shandon Hypersil ODS	High resolution separation of chlorophylls and all major pigments were achieved. The method obtained a high recovery (over 90%) of pigments
Riley and Wilson [41]	Petroleum ether: ethyl acetate: diethyl amine (58:30:12 v/v/v)	Silica gel	All plant pigments were separated except for some minor components
Sartory [43]	Solvent A is 97% methanol. Solvent B is 97% acetone Elution order: 0–15 min: 100% solvent A. 15–20 min: linear gradient to 77% solvent A: 23% solvent B. Then isocratic flow of 77% solvent A: 23% solvent B. Flow rate: 1 mL/min	Sep-Pak C18 Bondapak	HPLC was found to be a rapid, sensitive, and selective method that successfully separated chlorophylls and its derivatives to high resolutions. Recovery of total pigments by HPLC is greater than 96% Spectrophotometric analysis overestimated chlorophyll *a* and underestimated chlorophyll *b*
Wright and Shearer [57]	Linear gradient from 90% acetonitrile to ethyl acetate for 20 min at a flow rate of 2 mL/min	C18 octadecyl silica	Carotenes, chlorophylls, xanthophylls and their degradation products were successfully separated with high resolutions

5.1.2 Strain and Cultivation

T. suecica was cultivated in outdoor bag bioreactors using a modified F medium [16]. Each bioreactor contained up to120 L of culture and was aerated with compressed air. Temperature and illumination depended on day-to-day weather conditions. Microalgal cultures from multiple bioreactors were harvested at the same time (with a concentration of ~0.5 g/L), concentrated via industrial centrifugation, and then mixed together to create a homogeneous culture from which all the biomass needed for the study was obtained.

5.1.3 Dewatering

The homogeneous culture was further dewatered in a laboratory centrifuge (Heraeus Multifuge 3S-R, Kendro, Germany) at 4,500 rpm for 10 min. The supernatant was discarded and the resulting microalgal paste was rinsed with deionised water to remove residual salts. The paste was then stored in the dark at either 4 or −20°C until further use.

5.1.4 Extraction Pre-treatment

In experiments where extraction was carried out on dried microalgae, microalgal paste (stored at either 4 or −20°C) was dried at 65°C in an oven (Model UNE 500 PA, Memmert GmbH+Co., Germany) for 16 h. A pestle and mortar was used to grind the dried biomass into powder. In experiments where extraction was carried out on the wet paste, the microalgal paste obtained from centrifugation (stored at 4°C) was used directly. The solid concentration of the paste (22.4 wt.%) was determined by drying a portion of the paste and comparing its pre-dried mass to that of the corresponding dried biomass.

5.1.5 Chlorophyll Extraction

For acetone extraction, 100 mL of 100% acetone was added to either 1 g of microalgal powder or 4.47 g of microalgal paste (equivalent to 1 g of microalgal powder). For methanol extraction, 100 mL of 100% methanol was added to 1 g of microalgal powder. The conical flask where solvent extraction was carried out was wrapped in aluminium foil to avoid photo-degradation of the chlorophyll molecules and sealed with a stopper to prevent solvent from evaporating. The extraction mixture was agitated moderately on a hot plate magnetic stirrer for 8 h.

Acetone extraction was conducted at three separate temperatures, 10, 20 (ambient), and 40°C, while methanol extraction occurred only at ambient. For 10°C extraction, the conical flask was immersed in a beaker filled with ice and the entire setup was placed on a stirrer. The temperature inside the flask was monitored every hour and an appropriate amount of ice was added or removed in order to sustain the desired

Table 5 Wavelength maximas, A_{max}, and specific absorbance coefficents, α, of chlorophyll *a* and chlorophyll *b* in different solvent mixtures

	90% Acetone 10% Water	90% Methanol 10% Water
A_{max} (*a*) (nm)	664	665
A_{max} (*b*) (nm)	647	652
$\alpha_{(a)\ max\ a}$ (mL/mg/cm)	109.18	60.64
$\alpha_{(a)\ max\ b}$ (mL/mg/cm)	30.11	27.40
$\alpha_{(b)\ max\ a}$ (mL/mg/cm)	12.87	38.39
$\alpha_{(b)\ max\ b}$ (mL/mg/cm)	70.78	67.90

$\alpha_{(a)\ max\ a}$ is the specific abosorbance coefficient of chlorophyll *a* at the maxima of chlorophyll *a*; $\alpha_{(a)\ max\ b}$ is the specific absorbance coefficient of chlorophyll *a* at the maxima of chlorophyll *b*; $\alpha_{(b)\ max\ a}$ is the specific abosorbance coefficient of chlorophyll *b* at the maxima of chlorophyll *a*; $\alpha_{(b)\ max\ b}$ is the specific absorbance coefficient of chlorophyll *b* at the maxima of chlorophyll *b*

temperature. The 40°C experiment was conducted by adjusting the heating element of the hot plate magnetic stirrer every hour to sustain the desired temperature.

For each extraction, a small amount of the solvent (0.5 mL) was sampled every hour with a pipette to enable chlorophyll quantification. The acetone extract sample was diluted 24× with a mixture of 90 vol.% acetone and 10 vol.% water to ensure that its spectrophotometric absorbance reading was within the linear range of the 90% acetone chlorophyll (both *a* and *b*) calibration curves. Similarly, the methanol extract sample was diluted 24 times with a mixture of 90 vol.% methanol and 10 vol.% water. The introduction of water to the extract was intended to prevent potential pigment degradation. Each extraction was repeated in triplicates.

5.1.6 Spectrophotometric Determination

Chlorophyll content (*a* and *b*) was determined spectrophotometrically at the maximum absorption wavelengths for each chlorophyll. DR 5000 UV–vis spectrophotometer from Hach, USA, was used for all analyses. The wavelength maxima, A_{max}, for chlorophyll *a* and chlorophyll *b* are, respectively, 664 and 647 nm in 90% acetone and 665 and 652 nm in 90% methanol. One milligram of either chlorophyll *a* or chlorophyll *b* standard was dissolved in either a mixture of acetone (45 mL) and water (5 mL) or a mixture of methanol (45 mL) and water (5 mL) to form stock solutions. All of the stock solutions were then diluted with their respective solvent mixtures (either 90% acetone or 90% methanol) to form standard solutions with five different concentrations (0.004, 0.008, 0.0012, 0.0016, and 0.02 mg/mL). Calibration curves of each chlorophyll type in a particular solvent mixture were created by plotting the absorbance of its standard solutions (at the maxima of both chlorophyll *a* and chlorophyll *b*) against concentration. In accordance to Lambert–Beer law, specific absorbance coefficient, α (in mL/mg/cm), is the gradient of the linear portion of the calibration curve [26]. Table 5 summarizes the wavelength maximas,

A_{max}, and the specific absorbance coefficents, α, of chlorophyll *a* and chlorophyll *b* in 90% acetone and 90% methanol. Concentrations of chlorophyll *a* and chlorophyll *b* in a pigment extract containing both chlorophylls can be simultaneously determined using an extension of Lambert–Beer law which takes into account the contribution of chlorophyll *b* absorbance to the absorbance of chlorophyll *a* at chlorophyll *a* maxima and vice versa. Principles of this extended theorem and the derivation of its formulae can viewed elsewhere [26]. Based on the α values obtained in Table 5, concentration of chlorophyll *a*, C_a (mg/mL), and concentration of chlrorophyll *b*, C_b (mg/mL), in the diluted extract sample are calculated as follows:

For extracts in 90% acetone and 10% water,

$$C_a = 0.00964\mathrm{A}_{664} - 0.00175\mathrm{A}_{647} \tag{1}$$

$$C_b = 0.01487\mathrm{A}_{647} - 0.00410\mathrm{A}_{664} \tag{2}$$

where A_{664} and A_{647} are the absorbances of the diluted extract sample at 664 and 647 nm respectively.

For extracts in 90% methanol and 10% water,

$$C_\mathrm{a} = 0.02215\mathrm{A}_{665} - 0.01252\mathrm{A}_{652} \tag{3}$$

$$C_\mathrm{b} = 0.01978\mathrm{A}_{652} - 0.00894\mathrm{A}_{665} \tag{4}$$

Where A_{665} and A_{652} are the absorbances of the diluted extract sample at 665 and 652 nm respectively.

The concentrations of chlorophyll in the original extract sample were obtained by multiplying the concentrations of chlorophyll in the diluted extract sample with a dilution factor of 24. Chlorophyll *a* yield (g chlorophyll *a*/g dried microalgae) was the product of concentration of chlorophyll *a* in the original extract sample and volume of acetone or methanol used in extraction (100 mL). Chlorophyll *b* yield was calculated in a similar manner, while chlorophyll yield was the sum of chlorophyll *a* and chlorophyll *b* yields.

5.2 Results and Discussions

Figure 7 illustrates typical extraction curves obtained in all experiments using either acetone or methanol as an extracting solvent. Even though the specific chlorophyll yields were different between the various extractions, the trends in which the yield evolved throughout experimental duration were similar from one extraction to another. From the two curves presented, it can be observed that chlorophyll yield increased most rapidly in the beginning and that the rate of extraction decreased with experimental time. For extraction using methanol, the majority of extraction (more than 80%) was achieved within the first 2 h and extending the extraction time

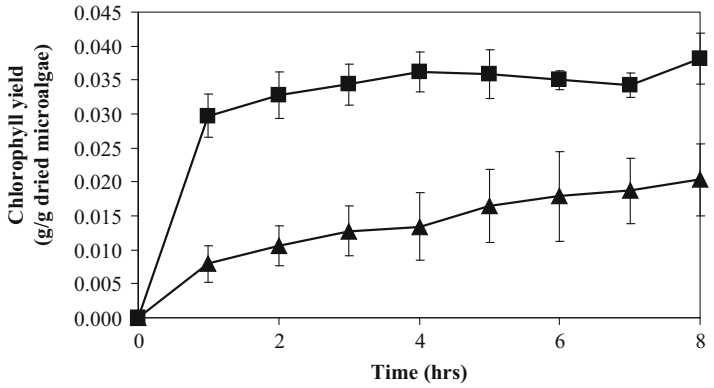

Fig. 7 Effect of extracting solvent on chlorophyll yield. *Filled square* experiment no. 4, extracting solvent: methanol, storage temperature of the biomass prior to the extraction: 4°C, biomass condition during the extraction: powder, extraction temperature: ambient. *Filled triangle* experiment no. 2, extracting solvent: acetone, storage temperature of the biomass prior to the extraction: 4°C, biomass condition during the extraction: powder, extraction temperature: ambient

beyond this point hardly affected the final chlorophyll yield. This asymptotic behaviour advocates for the diffusion-driven nature of chlorophyll extraction, where extraction rate is directly proportional to the amount of unextracted intracellular chlorophyll [37].

Table 6 shows the final chlorophyll yields for the various extractions in the study. The final chlorophyll yields (between 0.020 and 0.045 g/g microalgae) are slightly higher than the typical amount expected from the species (~0.020 g/g dried microalgae) [53]. It is noted that chlorophyll contents of a particular microalgal species are highly dependent on the culture conditions adopted and are not always comparable from one study to another. The highest chlorophyll yield (0.045 g/g dried microalgae) in the study was obtained when extraction was performed using acetone at ambient temperature directly on wet microalgal paste that had previously been stored at 4°C (exp no. 3).

The ratio of chlorophyll *a* : chlorophyll *b* in the extract remained similar for most extractions (between 2.0 and 2.5) with the exception of experiment no. 3 where extraction was performed directly from wet paste (ratio of chlorophyll $a{:}b = 1.3$). All of the chlorophyll ratios reported in Table 6 fall within the normal range of green algae (between 0.64 and 5) [53] and verify chlorophyll *a* as the principal chlorophyll in this microalgal biomass. The decrease in chlorophyll ratio during wet extraction can be explained by the difference in polarity between chlorophyll *a* and chlorophyll *b*. The presence of a formyl group (−CHO) instead of a methyl group ($-CH_3$) in ring II position of its cyclic molecule makes chlorophyll *b* slightly more polar than chlorophyll *a*. During extraction from wet paste, the water molecules in the paste dissolved in the acetone and increased the solvent's polarity. As such, the

Table 6 Final yields of chlorophyll (after 8 h of extraction) under different experimental parameters

Exp No.	Storage temperature of the biomass prior to the extraction (°C)	Biomass condition during the extraction	Extracting solvent	Extraction temperature (°C)	Final chlorophyll *a* yield (g/g dried microalgae)	Final chlorophyll *b* yield (g/g dried microalgae)	Final chlorophyll *a* yield : final chlorophyll *b* yield	Final chlorophyll yield (g/g dried microalgae)
1	−20	Powder	Acetone	Ambient	0.018 ± 0.006	0.007 ± 0.003	2.5	0.026 ± 0.008
2	4	Powder	Acetone	Ambient	0.014 ± 0.003	0.006 ± 0.002	2.2	0.020 ± 0.005
3	4	Paste	Acetone	Ambient	0.025 ± 0.005	0.020 ± 0.005	1.3	0.045 ± 0.010
4	4	Powder	Methanol	Ambient	0.025 ± 0.003	0.013 ± 0.001	2.0	0.038 ± 0.004
5	4	Powder	Acetone	10	0.015 ± 0.005	0.007 ± 0.002	2.1	0.022 ± 0.007
6	4	Powder	Acetone	40	0.028 ± 0.003	0.013 ± 0.002	2.1	0.041 ± 0.005

Yields are represented as: average of three replicates ± maximum error. Final chlorophyll yield = final chlorophyll *a* yield + final chlorophyll *b* yield. Amount of water in powder = 0 wt.%, amount of water in paste = 77.6 wt.%

solvent was able to interact more favourably towards chlorophyll *b*, resulting in its increased co-extraction and the decreased chlorophyll ratio.

A decrease in the storage temperature of microalgal paste prior to chlorophyll extraction (exp no. 2 compared to exp no. 1) was observed to increase final chlorophyll extraction yields (both *a* and *b*). The combination of freezing and thawing actions which occurred only when paste was stored at −20°C was expected to rupture a portion of the microalgal cell membranes. The partial cell disruption would then liberate intracellular chlorophyll molecules directly into the extracting solvent, thereby enabling more rapid solvent-analyte interaction and producing the increased final chlorophyll yield.

Acetone extraction from wet microalgal paste produced more than twice the final chlorophyll yield of the same extraction from dried microalgal powder (exp no. 3 compared to exp no. 2). Several potential reasons can be attributed to this significant yield discrepancy. The prior exposure of the powder to thermal drying (65°C for 16 h) oxidized some the more susceptible chlorophyll molecules and depleted the biomass of chlorophyll contents. On the other hand, the presence of water in the paste allowed the biomass to form a homogeneous mixture with the extracting solvent and increased chlorophyll extraction through enhanced solvent-analyte interaction. As previously discussed, the water in the paste also acted as a co-solvent and increased the selective extraction of chlorophyll *b*.

Figure 7 shows extraction with methanol to be significantly more efficient than extraction with acetone. Methanol extraction (exp no. 4) produced almost twice the chlorophyll yield of an equivalent acetone extraction (exp no. 2). Despite a similar finding from previous studies [24, 49], acetone is still the preferred solvent for majority of chlorophyll extraction works due to its known propensity to reduce the co-extraction of chlorophyllase enzyme responsible for chlorophyll degradation [11, 24]. The continuous decrease in chlorophyll yield of methanol extraction after 4 h of operating time (Fig. 7) indicates the onset of chlorophyll degradation in that solvent. In the future, the co-extracted chlorophyllase enzyme should be inactivated by spiking the methanol with a small quantity of metal carbonate (sodium, calcium, and magnesium) throughout the extraction [11].

From experiment 5, 2, and 6, chlorophyll yield is observed to increase with extraction temperature. Operating the extraction at 40°C rather than at ambient temperature (approximately 20°C) increased chlorophyll yield by more than 100%. Increasing the temperature of chlorophyll extraction results in two simultaneous competing effects. Rapid thermal degradation depletes the overall chlorophyll content of the biomass and can potentially reduce extraction yield, while the increase of chlorophyll solubility in the extracting solvent enhances mass transfer and can potentially improve extraction yield. In our case, the temperature rise seemed to lead to an increase in chlorophyll solubility that more than offset the decrease in chlorophyll content due to thermal degradation and resulted in a higher final chlorophyll yield. A previous study by Sartory and Grobbelaar [44] found that chlorophyll extraction from microalgal biomass reached its optimum efficiency when the extraction was carried out at an elevated temperature near the boiling point of the extracting solvent.

References

1. Abaychi JK, Riley JP (1979) The determination of phytoplankton pigments by high-performance liquid chromatography. Anal Chim Acta 107:1–11
2. Becker EW (1994) Microalgae: biotechnology and microbiology. Cambridge University Press, Cambridge, New York
3. Benemann JR (1997) CO2 mitigation with microalgae systems. Energ Convers Manage 38(suppl 1):S475–S479
4. Borowitzka MA (1990) Commercial production of microalgae: ponds, tanks, tubes and fermenters. J Biotechnol 70(1–3):313–321
5. Brennan L, Owende P (2010) Biofuels from microalgae—a review of technologies for production, processing, and extractions of biofuels and co-products. Renew Sustain Energy Rev 14(2):557–577
6. Brunner G (2005) Supercritical fluids: technology and application to food processing. J Food Eng 67(1–2):21–33
7. Cady JB, Morgan WS (1948) Treatment of chronic ulcers with chlorophyll: review of a series of fifty cases. Am J Surg 75(4):562–569
8. Carpenter EB (1949) Clinical experiences with chlorophyll preparations: with particular reference to chronic osteomyelitis and chronic ulcers. Am J Surg 77(2):167–171
9. Chisti Y (2007) Biodiesel from microalgae. Biotechnol Adv 25(3):294–306
10. Cohen Z (ed) (1999) Chemicals from microalgae. Taylor & Francis, London
11. Cubas C, Gloria Lobo M, González M (2008) Optimization of the extraction of chlorophylls in green beans (*Phaseolus vulgaris* L.) by N,N-dimethylformamide using response surface methodology. J Food Comp Anal 21(2):125–133
12. Ferruzzi MG, Blakeslee J (2007) Digestion, absorption, and cancer preventative activity of dietary chlorophyll derivatives. Nutr Res 27(1):1–12
13. Florides GA, Christodoulides P (2009) Global warming and carbon dioxide through sciences. Environ Int 35(2):390–401
14. Ghirardi ML, Zhang L, Lee JW, Flynn T, Seibert M, Greenbaum E, Melis A (2000) Microalgae: a green source of renewable H2. Trends Biotechnol 18(12):506–511
15. Goldberg SL (1943) The use of water soluble chlorophyll in oral sepsis: an experimental study of 300 cases. Am J Surg 62(1):117–123
16. Halim R, Gladman B, Danquah MK, Webley PA (2011) Oil extraction from microalgae for biodiesel production. Bioresour Technol 102:178–185
17. Herrero M, Cifuentes A, Ibanez E (2006) Sub- and supercritical fluid extraction of functional ingredients from different natural sources: plants, food-by-products, algae and microalgae—a review. Food Chem 98(1):136–148
18. Herrero M, Mendiola JA, Cifuentes A, Ibáñez E (2010) Supercritical fluid extraction: recent advances and applications. J Chromatogr A 1217(16):2495–2511
19. Horwitz B (1951) Role of chlorophyll in proctology. Am J Surg 81(1):81–84
20. Humphrey AM (1980) Chlorophyll. Food Chem 5(1):57–67
21. Humphrey AM (2004) Chlorophyll as a color and functional ingredient. J Food Sci 69(5):422–425
22. Jeffrey SW (1961) Paper-chromatographic separation of chlorophylls and carotenoids from marine algae. Biochem J 80(2):336–342
23. Jeffrey SW (1968) Quantitative thin-layer chromatography of chlorophylls and carotenoids from marine algae. Biochim Biophys Acta 162(2):271
24. Jeffrey SW, Mantoura RFC, Wright SW (eds) (1997) Phytoplankton pigments in oceanography: guidelines to modern methods. UNESCO, Paris
25. Lanfer-Marquez UM, Barros RMC, Sinnecker P (2005) Antioxidant activity of chlorophylls and their derivatives. Food Res Int 38(8–9):885–891
26. Lichtenthaler HK, Buschmann C (2001) Chlorophylls and carotenoids: measurement and characterization by UV–VIS spectroscopy. In: Wrolstad RE, Acree TE, Decker EA, Penner

MH, Reid DS, Schwartz SJ, Shoemaker CF, Smith DM, Sporns P (eds) Current protocols in food analytical chemistry. Wiley, New York
27. Lynn Co DYC, Schanderl SH (1967) Separation of chlorophylls and related plant pigments by two-dimensional thin-layer chromatography. J Chromatogr A 26:442–448
28. Macias-Sanchez MD, Mantell C, Rodriguez M, de la Ossa EM, Lubian LM, Montero O (2009) Comparison of supercritical fluid and ultrasound-assisted extraction of carotenoids and chlorophyll a from *Dunaliella salina*. Talanta 77(3):948–952
29. Macías-Sánchez MD, Mantell C, Rodríguez M, Martínez de la Ossa E, Lubián LM, Montero O (2005) Supercritical fluid extraction of carotenoids and chlorophyll a from *Nannochloropsis gaditana*. J Food Eng 66(2):245–251
30. Macías-Sánchez MD, Mantell C, Rodríguez M, Martínez de la Ossa E, Lubián LM, Montero O (2007) Supercritical fluid extraction of carotenoids and chlorophyll a from *Synechococcus* sp. J Supercrit Fluids 39(3):323–329
31. Madgwick JC (1966) Chromatographic determination of chlorophylls in algal cultures and phytoplankton. Deep Sea Res Oceanogr Abstr 13(3):459–466
32. Mantoura RFC, Llewellyn CA (1983) The rapid-determination of algal chlorophyll and carotenoid-pigments and their breakdown products in natural-waters by reverse-phase high-performance liquid chromatography. Anal Chim Acta 151(2):297–314
33. Marsh G (2009) Small wonders: biomass from algae. Renew Energ Focus 9(7):74–76, 78
34. Masojídek J, Torzillo G (2008) Mass cultivation of freshwater microalgae. In: Sven Erik J, Brian F (eds) Encyclopedia of ecology. Academic Press, Oxford, pp 2226–2235
35. Mendes RL, Nobre BP, Cardoso MT, Pereira AP, Palavra AF (2003) Supercritical carbon dioxide extraction of compounds with pharmaceutical importance from microalgae. Inorg Chim Acta 356:328–334
36. Mendes RL, Reis AD, Palavra AF (2006) Supercritical CO_2 extraction of [gamma]-linolenic acid and other lipids from *Arthrospira* (*Spirulina*) *maxima*: comparison with organic solvent extraction. Food Chem 99(1):57–63
37. Ozkal SG, Salgin U, Yener ME (2005) Supercritical carbon dioxide extraction of hazelnut oil. J Food Eng 69:217–223
38. Packer M (2009) Algal capture of carbon dioxide; biomass generation as a tool for greenhouse gas mitigation with reference to New Zealand energy strategy and policy. Energy Policy 37(9):3428–3437
39. Ramsey E, Sun Q, Zhang Z, Zhang C, Gou W (2009) Mini-review: green sustainable processes using supercritical fluid carbon dioxide. J Environ Sci 21(6):720–726
40. Rasmussen RS, Morrissey MT (2007) Marine biotechnology for production of food ingredients. In: Steve LT (ed) Advances in food and nutrition research. Academic, Oxford, pp 237–92
41. Riley JP, Wilson TRS (1965) The use of thin-layer chromatography for the separation and identification of phytoplankton pigments. J Mar Biol Assoc UK 45:583–591
42. Sahena F, Zaidul ISM, Jinap S, Karim AA, Abbas KA, Norulaini NAN, Omar AKM (2009) Application of supercritical CO2 in lipid extraction—a review. J Food Eng 95(2):240–253
43. Sartory DP (1985) The determination of algal chlorophyllous pigments by high-performance liquid chromatography and spectrophotometry. Water Res 19(5):605–610
44. Sartory DP, Grobbelaar JU (1984) Extraction of chlorophyll *a* from freshwater phytoplankton for spectrophotometric analysis. Hydrobiologia 114(3):177–187
45. Scheer H (2004) Chlorophylls and carotenoids. In: William JL, Lane MD (eds.) Encyclopedia of biological chemistry. Elsevier, New York, pp 430–437
46. Schenk P, Thomas-Hall S, Stephens E, Marx U, Mussgnug J, Posten C, Kruse O, Hankamer B (2008) Second generation biofuels: high-efficiency microalgae for biodiesel production. Bioenergy Res 1(1):20–43
47. Schumann R, Haubner N, Klausch S, Karsten U (2005) Chlorophyll extraction methods for the quantification of green microalgae colonizing building facades. Int Biodeter Biodegr 55(3): 213–222
48. Shoaf WT (1978) Rapid method for the separation of chlorophylls a and b by high-pressure liquid chromatography. J Chromatogr A 152(1):247–249

49. Simon D, Helliwell S (1998) Extraction and quantification of chlorophyll a from freshwater green algae. Water Res 32(7):2220–2223
50. Smith LW, Livingston AE (1945) Wound healing: an experimental study of water soluble chlorophyll derivatives in conjunction with various antibacterial agents. Am J Surg 67(1):30–39
51. Spears K (1988) Developments in food colourings: the natural alternatives. Trends Biotechnol 6(11):283–288
52. Spolaore P, Joannis-Cassan C, Duran E, Isambert A (2006) Commercial applications of microalgae. J Biosci Bioeng 101(2):87–96
53. Thompson GA Jr (1996) Review: lipids and membrane function in green algae. Biochim Biophys Acta 1302:17–45
54. Timberlake CF, Henry BS (1986) Plant pigments as natural food colours. Endeavour 10(1):31–36
55. Ugwu CU, Aoyagi H, Uchiyama H (2008) Photobioreactors for mass cultivation of algae. Bioresour Technol 99(10):4021–4028
56. Wang B, Li Y, Wu N, Lan CQ (2008) CO2 bio-mitigation using microalgae. Appl Microbiol Biotechnol 79(5):707–718
57. Wright SW, Shearer JD (1984) Rapid extraction and high-performance liquid chromatography of chlorophylls and carotenoids from marine-phytoplankton. J Chromatogr 294:281–295
58. Zeiler KG, Heacox DA, Toon ST, Kadam KL, Brown LM (1995) The use of microalgae for assimilation and utilization of carbon dioxide from fossil fuel-fired power plant flue gas. Energ Convers Manage 36(6–9):707–712

Chapter 35
Screening for Bioactive Compounds from Algae

Miguel Herrero, Jose A. Mendiola, Merichel Plaza, and Elena Ibañez

Abstract At present, functional foods are seen as a good alternative to maintain or even improve human health, mainly for the well-known correlation between diet and health. This fact has brought about a great interest for seeking new bioactive products of natural origin to be used as functional ingredients, being, nowadays, one of the main areas of research in Food Science and Technology. Among the different sources that can be used to extract bioactives, algae have become one of the most promising. Algae have an enormous biodiversity and can be seen as natural factories for producing bioactive compounds since either by growing techniques or by genetic engineering approaches, they can improve their natural content of certain valuable compounds. In this book chapter, a revision about the different types of bioactives that have been described in algae is presented including compounds, such as lipids, carotenoids, proteins, phenolics, vitamins, polysaccharides, etc. Also, the modern green techniques used to achieve the selective extraction of such bioactives are presented and the methods for fast screening of bioactivity described.

1 Bioactive Compounds and Functional Foods

The important economic, cultural, and scientific development of our society has strongly contributed to changes in life-style and food habits. For instance, highly caloric and unbalanced diets are commonly consumed in developing countries; this fact, together with a decrease in physical activity has raised the incidence of cardiovascular diseases, diabetes, obesity, etc. [41]. If we also consider the increasing life expectancies, it is easy to realize that different solutions should be found to reduce the expected health costs in a near future.

M. Herrero • J.A. Mendiola • M. Plaza • E. Ibañez (✉)
Institute of Food Science Research, CIAL (CSIC-UAM),
Nicolás Cabrera 9, Campus Cantoblanco, 28049 Madrid, Spain
e-mail: elena@ifi.csic.es

J.W. Lee (ed.), *Advanced Biofuels and Bioproducts*, DOI 10.1007/978-1-4614-3348-4_35,

One of the possible solutions are the so called functional foods. The concept of functional food as a mean to protect consumer's health was developed at the beginning of the 1980s in Japan, based on several scientific studies demonstrating the correlation between diet and a lower incidence of chronic diseases [3]. In 1993, the Ministry of Health and Welfare established a policy for "Foods for Specified Health Uses" (FOSHU) by which health claims of some selected functional foods were legally permitted and regulated [4]. In Europe, in the second half of the 1990s, a working group coordinated by the European Section of the International Life Science Institute (ILSI) and supported by the European Commission, was created to promote the action FUFOSE (Functional Food Science in Europe, IV Framework Program) to encourage the scientific study on functional foods. A definition of functional food as "the food that besides its nutritious effects, has a demonstrated benefit for one or more functions of the human organism, improving the state of health or well-being or reducing the risk of disease" [26] was established. In this definition, it is necessary to emphasize some new aspects: (a) the functional effect is different from the nutritious one; (b) the functional effect must be demonstrated satisfactorily; and (c) the benefit can consist in an improvement of a physiological function or in a reduction of risk of developing a pathological process. Besides, the functional foods need to be effective at the normal consumed doses and should have a presentation typical of a food product. At present, functional foods are regulated in the European Union by the guideline approved in December 2006 (Regulation (CE) 1924/2006 of the European Parliament and of the Council, December 20, 2006: nutrition and health claims made on foods). In this directive, the nutritional allegations and/or healthy properties of the new products are regulated, including their presentation, labeling, and promotion.

Considering this background, it is easy to understand the interest that functional foods have raised not only for consumers, but also for the food industry. Thus, we can consider that a new, enormous market for the food industry has been opened; as Sloan in 1999 already suggested: "foods for the not-so-healthy" [180].

But, how it is possible to convert a traditional food into a functional food? Again, there is not a single answer since many approaches can be used in order to improve the beneficial action of a certain food, ranging from more or less sophisticated biotechnological processes to several other processes to remove or increase the content of a specific compound. Many times, a functional food is obtained through the addition of a component or a series of ingredients that either are not present in the analogous conventional food or are present at lower concentrations. These ingredients are called functional ingredients and are mainly micronutrients, such as ω3 fatty acids, linoleic acids, phytosterols, soluble fiber (inulin and fructooligosaccharides, called prebiotics), probiotics (microorganisms able to improve the activity in the intestinal tract and the immune system), carotenoids, polyphenols, vitamins, etc., able to exert a specific healthy action into the organism [45, 179].

Algae can be found in nearly any aquatic and terrestrial habitat, showing a huge biodiversity and various morphologies ranging from phytoplankton species to large kelp [129]. Algae are photosynthetic organisms that possess reproductive simple structures; the number of algal species remains unknown although has been estimated

at between one and ten million [112] and, as mentioned, can exist from unicellular microscopic organisms (microalgae) to multicellular of great size (macroalgae). For instance, microalgae use light energy and carbon dioxide with higher photosynthetic efficiency than plants for the production of biomass [7, 113] and have been suggested as a source of biofuel production, to purify wastewater [123, 134], to extract high added value foods and pharmaceutical products, or as food for aquaculture [182].

In fact, algae are organisms that live in complex habitats sometimes submitted to extreme conditions (changes of salinity, temperature, nutrients, UV–Vis irradiation), thus, they have to adapt rapidly to the new environmental conditions to survive, producing a great variety of secondary (biologically active) metabolites, which cannot be found in other organisms [18]. Moreover, most of them are easy to cultivate, they grow rapidly (for many of the species) and there exists the possibility of controlling the production of some bioactive compounds either by manipulating the cultivation conditions or by using more sophisticated genetic engineering approaches. Therefore, algae and microalgae can be considered as genuine natural reactors being, in some cases, a good alternative to chemical synthesis for certain compounds. Therefore, considering the enormous biodiversity of algae and the recent developments in genetic engineering, investigations related to the search of new biologically active compounds from algae can be seen as an almost unlimited field, being this group of organisms one of the most promising sources for new products. In this sense, previous reports have suggested both, micro- and macroalgae as a very interesting natural source of new compounds with biological activity that could be used as functional ingredients [141, 142].

Moreover, another important aspect to be considered is the development of appropriate, fast, cost-effective, and environmental-friendly extraction procedures able to isolate the compounds of interest from these natural sources. In this chapter, green extraction techniques, such as supercritical fluid extraction (SFE) and pressurized liquid extraction (PLE) together with ultrasound-assisted extraction (UAE) and microwave-assisted extraction (MAE) are presented, and applications to algae bioactive's extraction are discussed. A revision about the different types of bioactives that have been described in algae is presented, including compounds such as lipids, carotenoids, proteins, phenolics, vitamins, polysaccharides, etc. In this chapter, a short description of methods for fast screening of bioactivity (mainly antioxidant activity) is included, considering chemical and biological methods. Finally, future research trends and research needs for the attainment of bioactives from algae are critically commented.

2 Green Extraction Techniques for Bioactive Compounds

Today, there is a wide range of classical or conventional extraction techniques that have been traditionally employed for the extraction of interesting compounds from natural matrices, such as algae. In this group, techniques such as Soxhlet, liquid–liquid

extraction (LLE), solid–liquid extraction (SLE), and other techniques based on the use of organic solvents are included. Although these techniques are routinely used, they have several well-known drawbacks; they are time consuming, laborious, they lack of automation and therefore are more prone to present low reproducibility, have low selectivity and/or provide low extraction yields. These shortcomings can be partially or completely overcome by using the newly developed advanced extraction techniques. This new kind of extraction techniques are characterized by being faster, more selective towards the compounds to be extracted, and also very important nowadays, these techniques are more environmentally friendly. In fact, by using the considered advanced extraction techniques, the use of toxic solvents is highly limited. In the next sections, the most important advanced extraction techniques that have been employed to extract bioactive compounds from algae are briefly described and commented.

2.1 Supercritical Fluid Extraction

SFE is based on the use of solvents at temperatures and pressures above their critical points. This technique has been already employed to extract a wide variety of interesting compounds from very different food-related materials [108], and algae are no exception [54]. One of the most valuable characteristics of SFE is the highly reduced (often to zero) employment of toxic organic solvents. In this sense, carbon dioxide is the most used supercritical solvent employed to extract bioactives from natural samples. In fact, CO_2 has a series of interesting properties for bioactives extraction; is cheap, its critical conditions are easily attainable (30.9°C and 73.8 bar), is an environmentally friendly solvent that, besides, is considered generally recognized as safe (GRAS) for its use in the food industry. When submitted to supercritical conditions, CO_2 presents a high diffusivity whereas its solvent strength and density can be highly modified by tuning the temperature and pressure applied. Another important characteristic of this technique, when using supercritical CO_2, is the possibility of attaining solvent-free extracts. Once the extraction procedure is finished, the depressurization of the system allows the gasification of the CO_2, remaining in the collector the compounds that were extracted from the matrix and solubilized in the CO_2 at high pressures. These properties are responsible for the great use of supercritical CO_2 for extraction of bioactive compounds.

Nevertheless, in spite of the potential of this technique, its usefulness will be related to the type of compounds to be extracted from the algae. Considering the low polarity of supercritical CO_2, SFE will be more suitable for the extraction of compounds with low polarity. In this regard, SFE using CO_2 has proven useful for the extraction of fatty acids [159], carotenoids from *Dunaliella salina* [66] and other microalgae [97], pigments from *Chlorella vulgaris* [82], or even interesting volatile compounds from the brown alga *Dictyopteris membranacea* [31], among other interesting applications. Supercritical CO_2 has also the advantage of obtaining a

quite "clean" extract when compared to other conventional extraction techniques. In fact, the selectivity obtained through the use of supercritical CO_2 will also allow the attainment of more purified extracts reducing to a great extent the amount of interfering compounds extracted from the complex algae matrix. However, if the extraction of more polar compounds is aimed, other strategies have to be devised. The main alternative in this case is the use of a given percentage of a modifier together with the supercritical fluid. This modifier (entrainer or cosolvent) typically is a polar organic solvent. When added to the supercritical fluid, this modifier will produce a change on the properties of the extracting mixture, allowing the collection of more polar compounds, increasing the polarity of the solvent used for the extraction and also the range of applications for SFE.

Several parameters are involved in the extraction of bioactives from algae by SFE. Among them, it is necessary to precisely control the effect of the extraction temperature, pressure, addition and, in that case, proportion and type of modifier, amount of sample to be extracted as well as its particle size and use of dispersing agents. The first parameters are more related to the solubility of the interesting compounds in the supercritical fluid, since changes on the extraction temperature and pressure will have a strong influence on the solvent properties, such as density. The type and proportion of modifier are also key factors in determining the solubility of the compound of interest in the supercritical fluid; in this sense, the most commonly employed organic solvent to extract bioactives from algae is ethanol in a range of 5–10% [127, 136]. Other modifiers, such as methanol [85] or acetone [82], have been also employed in some SFE algae applications, although the latter was shown to be less effective for pigments extraction from algae than ethanol [82]. Vegetable oils, notably olive oil, also demonstrated to be effective when added to supercritical CO_2 as modifiers or cosolvents in a proportion of 10%, for the extraction of the carotenoid astaxanthin from *Haematococcus pluvialis* [88]. In fact, in this application, the addition of 10% olive oil provided comparable results to those obtained using ethanol as cosolvent [88]. In contrast, the rest of parameters are more related to the efficiency of the extraction procedure. It is well known that the influence of the physical state of the sample on the outcome of the extraction, as well as its particle size. The crushing degree was a very significant factor in the extraction of carotenoids from *H. pluvialis* microalga [127]. It was demonstrated how an increase in the crushing procedure produced an enhancement in the carotenoid extraction yield. This effect could respond to an increase of the mass transfer rates as a consequence of the lower particle size as well as to the increase of carotenoids in the medium as a result of the disruption of cells in the heavier crushing procedure [127].

Although supercritical solvents have a diffusivity in the matrix higher than liquids, a decrease in the sample particle size generally produces an increase in the extraction yield obtained, mainly due to the increment in the contact surface between sample and solvent, thus increasing the mass transfer. Nevertheless, in some applications the use of dispersing agents (e.g., diatomaceous earth) as well as the employment of Hydromatrix in order to absorb the liquid portion from the sample can be useful.

2.2 Pressurized Liquid Extraction

PLE is another technique that, nowadays, is regarded as an advanced extraction technique, due to the advantages that presents over other traditional extraction mechanism. PLE is based on the use of high temperatures and pressures so that the solvent is maintained in the liquid state during the whole extraction procedure. As a result of the application of these particular conditions, faster extraction processes are obtained in which generally the extraction yield is significantly higher than that obtained using traditional extraction techniques, besides, using lower amounts of organic solvents. Moreover, most of the instruments used for PLE are automated, allowing the development of less labor intensive methods and improving reproducibility.

The principles governing this kind of extraction and providing the above mentioned characteristics are: (a) the mass transfer rate is improved as a result of the increment on the solubility of the compounds as a consequence of the increase of the extraction temperature; (b) under the PLE experimental conditions, the surface tension of the solvent is reduced, allowing a better penetration of the solvent into the sample matrix, increasing likewise the mass transfer; (c) the effect of the pressure theoretically could help to matrix disruption, increasing again the mass transfer rate.

Method development in PLE is by far easier than in SFE, since less parameters influencing the extraction should be considered. Once the solvent has been selected according to the nature of the compounds to be extracted, only two parameters are of significant importance: extraction time and extraction temperature. Although the extraction pressure could help to disrupt the matrix enhancing the mass transfer of the analytes contained on it, as it has been already mentioned, in practice, several reports have shown that the influence of this parameter is not significant once the pressure is high enough to maintain the solvent in the liquid state. The extraction temperature has to be optimized always keeping in mind the possible thermal degradation effects that might occur over the interesting extracted compounds. Although generally an increase in the temperature produces the subsequent increase in the extraction yield, for bioactive compounds, too high temperatures might lead to the degradation of these compounds. Therefore, this value should be carefully maximized just to the level in which the interesting compounds start to get degraded. On the other hand, the extraction time has to be minimum enough to have an adequate mass transfer. Longer extraction times would result on slower extraction procedures and could also favor the thermal degradation, once the solvent solution is saturated with analytes from the food matrix. Therefore, quite simple experimental designs, such as full factorial designs with two factors and three levels can be useful to optimize the bioactives PLE extraction conditions.

Compared to SFE, the possibility of choosing among a high number of solvents causes PLE to be more versatile in terms of polarity of the bioactive compounds to be extracted and thus, the solvent will be selected depending on their nature. However, this technique is considered by far less selective than SFE. Therefore, it is

important to keep in mind, that even if the extraction of the bioactives is attained, it would be possible to find other interfering compounds in the obtained extract. To avoid this problem, other steps can be included. For instance, an extraction step using hexane/acetone as solvent was performed before the PLE of phenolic compounds from several algae species using 80% methanol in water at 130°C for 20 min (two 10 min cycles) [132]. Ethanol has been selected to extract antioxidants from different species, such as *Synechocystis* sp. and *Himanthalia elongata* [143] or antimicrobial compounds from *H. pluvialis* [165]. Generally, the best extraction conditions in these applications were obtained at mild temperatures, around 100°C.

Moreover, PLE can be applied using a wide variety of extraction solvents, although GRAS extraction solvents, like ethanol, are most commonly used. When the extraction solvent is water, this technique is commonly called subcritical water extraction (SWE). The principles of extraction are the same, but in this case, another parameter has critical importance, the dielectric constant of water. This property of water is greatly modified with the increasing temperature when water is maintained in the liquid state. In fact, the value of dielectric constant of water (ε) can vary from 80 at room temperature to values around 25 when is submitted to temperatures of ca. 250°C. This value is similar to the one presented by some organic solvents at room temperature, such as ethanol or methanol, and thus, the use of SWE could be an alternative to the use of this type of solvents in some applications. This technique has been already used to explore the possibility of obtaining antioxidants from different microalgae species [52, 55]. However, the wide development of novel applications for the extraction of bioactives from algae by using SWE has not been fully explored so far.

2.3 Others

Ultrasound-assisted extraction (UAE) is also widely considered as an advanced extraction technique. This technique uses high-frequency sounds, usually higher than 16 kHz and a limited amount of solvent in order to produce an effective extraction of the compounds of interest in the solvent employed, increasing their mass transfer and solubility, by disrupting the food matrix being extracted. As in PLE, the selection of the suitable solvent for extraction by UAE will be made depending on the compounds of interest. For instance, a mixture of dichloromethane/methanol (2:1) was employed to extract lipids from microalgae using UAE [140]. For more polar compounds, such as chlorophylls, methanol was demonstrated as a more effective solvent [175]. This technique has the advantage of providing faster extraction processes compared to conventional techniques. UAE was compared to other solvent-based extraction of pigments and fatty acids from several algae samples. It was demonstrated that UAE was simple, allowed extraction of interesting compounds and did not produce alteration or breakdown products [197]. However, when this technique was directly compared to SFE for the extraction of carotenoids from *D. salina*, it was shown that SFE was more effective for the extraction of these low

polarity compounds, above all in terms of selectivity [98]. At certain conditions, in which a complex sample is being extracted containing the interesting compounds as well as other polar compounds, SFE was demonstrated to be more selective than UAE [98]. UAE has been also employed to extract polysaccharides derived from *Chlorella pyrenoidosa* [171].

When sonicating the samples for a given period of time, an increase in the temperature of the sample can be observed as a result of the vibration of the molecules. For this reason, considering that most of bioactives are thermally labile compounds, it is common to proceed in a temperature controlled environment. For instance, pigments and fatty acids were obtained from algae at −4°C using 35 kHz and 80 W for 90 min [197]. The use of temperatures below 4–5°C allows a better preservation of the extracted compounds, that otherwise, could be degraded.

The last advanced extraction technique also used for bioactives extraction from algae is MAE. In MAE, the sample is heated by using microwaves, at typical powers of 700 W for a short time. Compared to traditional extraction techniques, the use of microwaves allows the decreasing of extraction times significantly limiting also the amount of solvent needed. Again, the temperature will be an important parameter to be controlled. Once selected the extraction solvent for the extraction of bioactives from algae, the microwaves power as well as the extraction time has to be defined. Experimental designs can be useful in determining the best extraction conditions. For instance, response surface methodology was employed to optimize the MAE of astaxanthin from *H. pluvialis* [203]. By using this statistical approach, the microwave power (141 W), extraction time (83 s), solvent volume (9.8 mL), and number of extracting cycles (4 cycles) were optimized. At present, MAE has not been extensively applied to extraction of bioactives from algae, although given its success in the extraction of plant materials, it can be easily inferred the great possibilities for its application to algae samples.

3 Fast Screening for Bioactivity

In general terms, the bioactivity of algal and microalgal extracts can be tested using two big groups of techniques: chemical and biological methods. Since no universal method to test bioactivity exists, marine extracts are commonly evaluated by using several methods.

As will be seen in Sect. 4, most of the bioactive compounds that can be found in algae and microalgae have been described to possess antioxidant activity; thus, most of the chemical methods that will be explained in this section are directed to measure different parameters related to the antioxidant activity.

On the other hand, marine compounds have been associated with a high number of bioactivities (mainly pharmacological activities) that can be tested by biological or biochemical methods. In this sense, several reviews covering both general and specific subject areas of marine pharmacology have been published. This kind of review articles has been grouped by Mayer et al. [105] as: (a) general marine pharmacology;

(b) antimicrobial marine pharmacology; (c) cardiovascular pharmacology; (d) antituberculosis, antimalarial, and antifungal marine pharmacology; (e) antiviral marine pharmacology; (f) anti-inflammatory marine pharmacology; (g) nervous system marine pharmacology; and (h) miscellaneous molecular targets.

3.1 Chemical Methods

3.1.1 Antioxidant Activity

Interest in natural antioxidants for both health and improved food stabilization has intensified dramatically since the last decade of the twentieth century. Health applications have been stimulated by observations that free radicals and oxidation are involved in many physiological functions and cause pathological conditions. Natural antioxidants offer food, pharmaceutical, nutraceutical, and cosmetic manufacturers a "green" label, minimal regulatory interference with use, and the possibility of multiple actions that improve and extend food and pharmaceutical stabilization [168]. Determining antioxidant capacity has become a very active research topic, and a plethora of antioxidant assay methods are currently in use. Despite of it, there are no standard methods due to the sheer volume of claims and the frequent contradictory results of "antioxidant activities" of several products.

Reactive oxygen species which include superoxide anion ($O_2^{-\bullet}$, a free radical), the hydroxyl radical ($^{\bullet}OH$) and hydrogen peroxide (H_2O_2) are produced by ultraviolet light, ionizing radiation, chemical reaction, and metabolic processes. These reactive species may contribute to cytotoxicity and metabolic changes, such as chromosome aberrations, protein oxidation, muscle injury, and morphologic and central nervous system changes in animals and humans [34]. Effective antioxidants must be able to react with all these radicals in addition to lipids, so, consideration of multiple radical reactivity, in antioxidant testing, is critical.

In general terms, three big groups can be distinguished: chain reaction methods, direct competition methods, and indirect methods [154].

1. Among the *chain reaction methods* two approaches have been used: measuring the lipid peroxidation reactions or the kinetics of substrate oxidation.

   There are two modes of lipid peroxidation that may be used for testing. The first one is autoxidation, in which the process is progressing spontaneously, with self-acceleration due to accumulation of lipid hydroperoxide (LOOH). The kinetics of autoxidation is highly sensitive to admixtures of transition metals and to the initial concentration of LOOH. As a result, the repeatability of experiments based on the autoxidation is still a problem. The second, much more promising approach, is based on the use of the kinetic model of the controlled chain reaction. This mode offers to obtain reliable, easily interpretable, and repeatable data. This approach has been applied, among others, to test natural water-soluble antioxidants, microheterogeneous systems, micelles, liposomes, lipoproteins (basically low-density lipoprotein [LDL]), biological membranes, and blood plasma [154].

When choosing a substrate of oxidation, preference should be given to individual compounds. Among individual lipids, methyl linoleate, and linoleic acid seem to be the most convenient. These compounds are relatively cheap and their oxidation is quite representative of the most essential features of biologically relevant lipid peroxidation. The main disadvantage, when using them in biological materials, is that the extract must be free of the elected compound, as it is impossible to provide the identity of substrate. Besides, biologically originated substrates usually contain endogenous chain-breaking antioxidants (vitamin E, etc.), which can intervene in the testing procedure.

2. The *direct competition methods* are kinetic models, where natural antioxidants compete for the peroxyl radical with a reference-free radical scavenger:

   - β-Carotene bleaching: competitive bleaching β-carotene during the autoxidation of linoleic acid in aqueous emulsion monitored as decay of absorbance in the visible region. The addition of an antioxidant results in retarding β-carotene decay [114].
   - Free-radical induced decay of fluorescence of R-phycoerythrin: The intensity of fluorescence of phycoerythrin decreases with time under the flux of the peroxyl radical formed at the thermolysis of APPH (2,2′-azobis-2-methyl-propanimidamide) in aqueous buffer. In the presence of a tested sample containing chain-breaking antioxidants, the decay of PE fluorescence is retarded [147].
   - Crocin bleaching test: Crocin (strongly absorbent in the visible range) undergoes bleaching under attack of the peroxyl radical. The addition of a sample containing chain-breaking antioxidants results in the decrease in the rate of crocin decay [12].
   - Potassium iodide test: KI reacts with the AAPH-derived peroxyl radical with the formation of molecular iodine. The latter is determined using an automatic potentiometric titrator with sodium thiosulfate. In the presence of antioxidant-containing samples, the rate of iodine release decreases [154].

3. When the *indirect approach method* is applied, the ability of an antioxidant to scavenge some free radicals is tested, which is not associated to the real oxidative degradation, or effects of transient metals. For instance, some stable colored free radicals are popular due to their intensive absorbance in the visible region [154]. There are two ways for presenting results, as equivalents of a known antioxidant compound (i.e., Trolox Equivalent Antioxidant Capacity, TEAC) or as the concentration needed to reduce concentration of free radicals by 50% (EC_{50}).

   - DPPH$^{\bullet}$ test: It is based on the capability of stable-free radical 2,2-diphenyl-1-picrylhydrazyl (DPPH$^{\bullet}$) to react with H-donors. As DPPH$^{\bullet}$ shows a very intensive absorption in the visible region (514–518 nm), it can be easily determined by the UV–Vis spectroscopy [13]. This method has been applied online with TLC [65] and HPLC [5] to determine antioxidant activity in different algae extracts.
   - ABTS test: The decay of the radical cation $ABTS^{+\bullet}$ (2,2′-azinobis(3-ethylbenzothiaziline-6-sulfonate) radical cation) produced by the oxidation of $ABTS^{+\bullet}$

caused by the addition of an antioxidant-containing sample is measured. $ABTS^{+\bullet}$ has a strong absorption in the range of 600–750 nm and can be easily determined spectrophotometrically. In the absence of antioxidants, $ABTS^{+\bullet}$ is rather stable, but it reacts energetically with an H-atom donor, such as phenolics, being converted into a noncolored form of ABTS [115].

- Ferric reducing antioxidant power (FRAP): The FRAP assay is based on the ability of antioxidants to reduce Fe^{3+} to Fe^{2+} [154]; if the reaction is coupled to the presence of some colored Fe^{2+} chelating compound like 2,4,6-trypyridyl-*s*-triazine, it can be measured spectrophotometrically.
- Cyclic voltammetry: The general principle of this method is as follows: the electrochemical oxidation of a certain compound on an inert carbon glassy electrode is accompanied by the appearance of the current at a certain potential; while the potential at which a cyclic voltammetry peak appears is determined by the redox properties of the tested compound, the value of the current is proportional to the quantity of this compound, in the presence of an antioxidant compound the signal will be lower [155].

3.2 Biological Methods

3.2.1 Antihelmintic, Antifungal, and Antibacterial Activity

In terms of antibacterial and antifungal activity, several compounds have been described in extracts from algal origin. Compounds like phenols, indoles, peptides, steroidal glycosides, terpenes, fatty acid, and so on. Basically, the method consists on letting the organism grow in the presence of the extract or compound. For example, Mendiola et al. [109] used a broth microdilution method to test the minimum inhibitory concentration (MIC) of *Spirulina* extracts on the growing of several bacteria and fungi. Tests were done in microwell plates, prepared by dispensing into each well culture broth plus inocula and 30 μL of the different extract dilutions. After incubation, the MIC of each extract was determined by visual inspection of the well bottoms, since bacterial growth was indicated by the presence of a white "pellet" on the well bottom. The lowest concentration of the extract that inhibited growth of the microorganism, as detected as lack of the white "pellet," was designated the MIC. The minimum bactericidal and fungicidal concentration was determined by making subcultures from the clear wells which did not show any growth.

Among antihelmintic compounds derived from algae, sesquiterpenes, like β-bisabolene, are the most actives. The most common method to measure its activity is to grow the helminths (worms, i.e., *Nocardia brasiliensis*) in the presence of the alga extract. For example, Davyt et al. [22] used tissue-culture 24-well plates. They prepared dilutions in DMSO for each compound, in order to obtain the desired concentration after the addition of 10 μL into each well. The percentage of dead worms was determined on day 5 and corrected by controls and compared with synthetic drugs.

3.2.2 Anticoagulant Activity

Polysaccharides, especially sulfated polysaccharides, are the main anticoagulant compounds isolated from algae and microalgae. Its activity is commonly measured providing the compound in vivo and measuring in vitro how coagulant factors are varied. For example, Drozd et al. [27] administered fucoidans (5 or 10 mg/kg) into the jugular vein of male Wistar rats, collected the blood and measure the inhibition of Xa factor (anti-Xa- or aHa-activity) and thrombin (anti-IIa or aIIa-activity). Specific activity was calculated in U/mg by comparison of optical density of the test and standard solutions during hydrolysis of chromogenic substrates.

3.2.3 Antiviral Activity

The antiviral family is one of the widest families of bioactive compounds isolated from marine sources, or at least one of the most studied. In this group, there are compounds like polysaccharides, terpenoids, proteins, sulfated flavones, and fatty acids. When measuring the antiviral activity, the general trend is to treat well-known mammal cells with the extract and then monitor the viral infection with the microscope. Huheihel et al. [63] used green monkey kidney cells (vero cells) treated with polysaccharides extracted from *Porphyridium* sp., the cell culture was treated with herpes simplex viruses. Each day, the cultures were examined for evidence of the cytopathic effect, defined as areas of complete destruction of cells or of morphologically modified cells and expressed as the percentage of damaged cells in the inspected fields.

But similar test can be done in vivo, Huheihel et al. [63] applying locally (eyes and mouth) *Porphyridium* extracts in rabbits and rats; later, the animals were exposed to the virus. Inflammatory effects, illness, and weight changes were recorded over a period of 4 weeks posttreatment.

3.2.4 Anti-inflammatory Activity

Inflammatory processes are related with several cardiovascular diseases and oxidative stress, therefore its study is of high interest. Among anti-inflammatory compounds from algal sources astaxanthine, terpenes, sterols, indols, and shikimate-derivatives have been described [105]. There is a huge amount of enzymes and secondary metabolites involved in inflammatory processes, but the general trend is to measure the expression of some of those metabolites and/or enzymes when cells involved in the inflammatory response are "activated." Leukocytes are among the most studied models; leukocyte migration has been shown to be one of the first steps in the initiation of an inflammatory/immune response and is essential for accumulation of active immune cells at sites of inflammation. The chemotaxis assay used to analyze the test material is designed to assess the ability of a test material to inhibit the migration of polymorphonuclear leukocytes (PMNs) toward a known chemotactic agent.

For example, polysaccharides from red microalga primarily inhibited the migration of PMNs toward a standard chemoattractant molecule and also partially blocked adhesion of PMNs to endothelial cells [101].

3.2.5 Toxicological Tests

It is well known that despite the bioactive (beneficial) compounds, several toxic compounds can be accumulated in algae and microalgae. Compounds like alkaloids, domoic acid, azaspiracid, brevetoxin, okadaic acid, pectenotoxin, or microcystins have been described.

Therefore, sometimes it is required to perform some toxicological tests mainly based in the mouse bioassay. Article 5 of a European Commission Decision dated 15 March 2002, laying down rules related to maximum permitted levels of certain biotoxins and methods of analysis for marine bivalve molluscs and other seafood states: "When the results of the analyses performed demonstrate discrepancies between the different methods, the mouse bioassay should be considered as the reference method." The basic procedure involves i.p. injection of an extract of the sample containing the toxin and observing the symptoms. A deeper review on toxicological analysis can be read in the book edited by Gilbert and Şenyuva "Bioactive compounds in Foods" [42].

4 Bioactive Compounds from Algae and Microalgae

Algae are important sources of various bioactive compounds with different physiological effects (toxic or curative) on human health. Many of them possess antioxidant, antimicrobial, and antiviral activities that are important for the protection of algal cells against stress conditions. The discovery of new analytical methods and techniques is important for the study of metabolites in algae and similar organisms with respect to their applications in pharmacology and the food industry [132].

4.1 Carotenoids

Carotenoids are prominent for their distribution, structural diversity, and various functions. More than 600 different naturally occurring carotenoids are now known, not including *cis* and *trans* isomers, all derived from the same basic C_{40} isoprenoid skeleton by modifications, such as cyclization, substitution, elimination, addition, and rearrangement. The different carotenoids have been isolated and characterized from natural sources as plants [43, 187], algae [142, 143], bacteria [183, 191], yeast [119], and fungi [70].

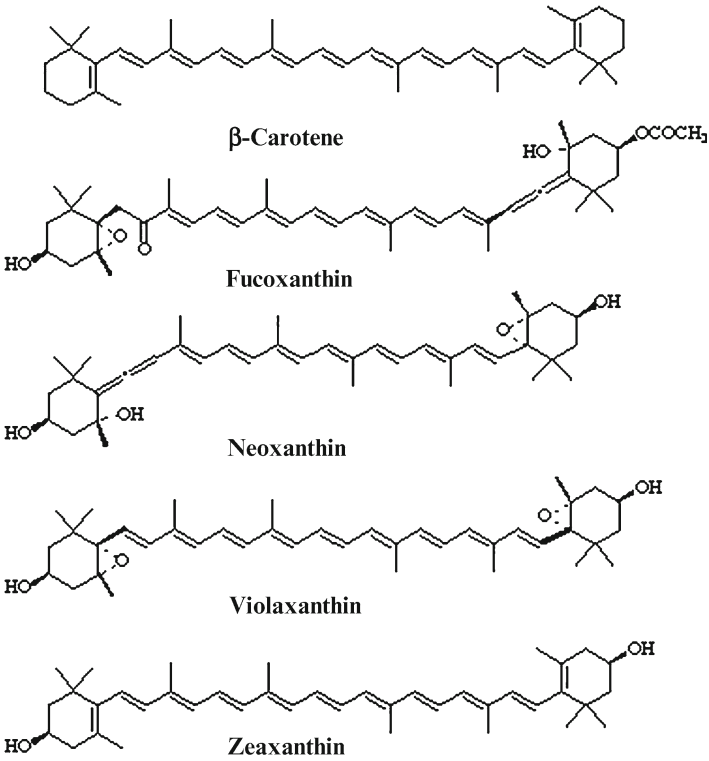

Fig. 1 Structures of the principal carotenoids in algae

Carotenoids play a key role in oxygenic photosynthesis, as accessory pigments for harvesting light or as structural molecules that stabilize protein folding in the photosynthetic apparatus. Carotenoids are powerful antioxidants. The beneficial effects of carotenoids have been well documented from the numerous clinical and epidemiological studies in various populations. Due to its high antioxidant activity, carotenoids have been proposed as cancer prevention agents [173], potential life extenders [88], and inhibitors of ulcer [74], heart attack, and coronary artery disease [151, 194].

All photosynthetic eukaryotes are able to synthesize lycopene, a C_{40} polyene, which is the precursor of two different carotenoid synthesis pathways, the β,ε-carotene and the β,β-carotene pathways [169]. Xanthophylls are oxidation products of carotenes; diversification of xanthophylls increases by the inclusion of allene or acetylene groups. Allenic and acetylenic carotenoids are highly represented in algae, and at least 30 different carotenoids have been identified in this group [169]. The distribution of carotenoids having different molecular structures or the presence of specific biosynthesis pathways can be an index for algae classification. For example, the major carotenoids that occur in seaweeds (Fig. 1) include β-carotene, lutein, violax-

anthin, neoxanthin, and zeaxanthin in green algae (Chlorophytes); α- and β-carotene, lutein, and zeaxanthin in red seaweeds (Rhodophytes) and β-carotene, violaxanthin, and fucoxanthin in brown algae (Phaeophytes).

Carotenoid composition of algae can present great variations mainly related to environmental factors, such as water temperature, salinity, light, and nutrients available. Most of the environmental parameters vary according to season, and the changes in ecological conditions can stimulate or inhibit the biosynthesis of several nutrients, such as carotenoids. For example, *D. salina* is a green microalga, well known for being one of the main natural sources of β-carotene. Under particular conditions, this microalga is able to produce β-carotene up to 14% of its dry weight. Moreover, the particular growing conditions able to maximize the production of β-carotene at industrial scale have been investigated [48–50, 84, 198, 118, 206]. Because β-carotene may play important roles in preventing degenerative diseases due to its associated antioxidant activity, different procedures have been studied, not only for the production of this compound but also for its extraction and isolation [66, 97, 106, 118]. The most widely employed technique has probably been SFE. The low polarity characteristics of the supercritical CO_2 make this solvent appropriate for the β-carotene extraction from this microalga [66, 97, 106, 118].

Other example is the green microalgae *H. pluvialis* that produces chlorophylls a and b and primary carotenoids, namely, β-carotene, lutein, violaxanthin, neoxanthin, and zeaxanthin, while it has the ability to accumulate, under stress conditions, large quantities of astaxanthin, up to 2–3% on a dry weight basis [150]. Using this carotenogenesis process, it undergoes different changes in cell physiology and morphology, giving as a result large red palmelloid cells [76, 204]. Astaxanthin is present in lipid globules outside the chloroplast, its functions in the cell include protection against light-related damage by reducing the amount of light available to the light-harvesting pigmented protein complexes. These pigments possess powerful biological activities, including antioxidant capacity [19], ulcer prevention [74] as well as immunomodulation and cancer prevention [130]. In fact, the extraction of astaxanthin has been thoroughly investigated. Different methods have been tested, including neat supercritical CO_2 [189] or supercritical CO_2 with different cosolvents [127], PLE [25, 67], MAE [203], direct extraction with vegetable oils [76] or solvents [75], or even treating cells with various solvents and organic acids at 70°C before acetone extraction, with the aim to facilitate the astaxanthin extraction from the thick cell wall without affecting the original astaxanthin esters profile [166].

Fucoxanthin is the most characteristic pigment of brown algae, and is also one of the most abundant carotenoids in nature [61], accounting for more than 10% of estimated total natural production of carotenoids [103]. Fucoxanthin is an oxygenated carotenoid that is very effective in inhibiting cell growth and inducing apoptosis in human cancer cells [60, 87]; it also has anti-inflammatory [172], antioxidant [158], antiobesity [99], and antidiabetic [100] properties.

4.2 Lipidic Fraction

The content and composition of algal lipids vary with species, geographical location, season, temperature, salinity, light intensity, or combination of these factors. In general, algae contain up to 1–3% of dry weight of lipids, being glycolipids the major lipid class in all algae, followed by neutral and phospholipids.

The major polar lipids that can be found in microalgae are monogalactosyl diacylglycerols (MGDGs), digalactosyl diacylglycerols (DGDGs), and phosphatidylglycerol (PG) [2]. Although these compounds, primarily MGDGs and DGDGs, have been known for more than 40 years, their importance has been recently raised by the description of their different, mainly anti-inflammatory, functional activities [15]. For example, glycol analogs of ceramides and of PG with antithrombotic and anti-inflammatory activities have been reported in cyanobacteria [2]. MGDGs and DGDGs contain a galactose linked to the sn-3 position of the glycerol backbone. These polar lipids are found in the thylakoid membrane of the cells. For instance, several polar lipids have been identified in *Spirulina platensis*, such as, four MGDGs, three PGs and two sulfoquinovosyl diacylglycerol [57], in *Croococcidiopsis* sp. [2], in *Sargassum thunbergii* [81], and *Phormidium tenue* [124] among others.

On the other hand, most of the alga's lipid content is made of polyunsaturated fatty acids (PUFAs) which accumulation also relies on environmental factors. For example, it is known that algae accumulate PUFAs when there is decrease in the environmental temperature [80]. In this sense, it has been described that tropical species contain less lipid (<1%) than cold water species (1.6%) [125].

PUFAs are essential nutrients for humans, and must be obtained from food. ω-3 and ω-6 long chain PUFAs are structural and functional components of cell membranes. The ω-3 to ω-6 ratio is closely matched, a factor that has been found to be important in balanced diet [176]. Likewise, these fatty acids are precursors of eicosanoids, which exert hormonal and immunological activity. This means ω-3 and ω-6 should be consumed in a balanced proportion, with the ideal ratio ω-6:ω-3 ranging from 3:1 to 5:1 [184].

The properties of the long-chain ω-3 fatty acids eicosapentaenoic acid (EPA) (ω-3 $C_{20:5}$) and docosahexaenoic acid (DHA) (ω-3 $C_{22:6}$) have been followed with considerable interest in the last few years. In particular, the vascular protective effects of long-chain ω-3 fatty acids are well documented [17, 170, 207]. Green algae show interesting levels of alpha linolenic acid (ω-3 $C_{18:3}$). The red and brown algae are particularly rich in fatty acids with 20 carbon atoms: EPA and arachidonic acid (ω-6 $C_{20:4}$).

S. platensis is a microalga belonging to the group of cyanobacteria (or blue-green algae) and is a natural source of DHA, which can account for up to 9.1% of the total fatty acids content [199].

Table 1 [133, 161] presents the typical composition of different fatty acids in algae. As can be seen, in all algae studied except *Undaria pinnatifida* and *Ulva lactuca* the single most abundant fatty acid was palmitic acid (which in *Phorphyra* sp. accounted for 63.19% of all fatty acids) while in *U. pinnatifida* the palmitic acid

Table 1 Fatty acids profile of different algae according to Sánchez-Machado et al. [161] and Ortiz et al. [133]

	Chlorophytes	Phaeophytes			Rhodophytes	
Fatty acids	*Ulva lactuca*	*Himanthalia elongata*	*Undaria pinnatifida*	*Laminaria ochroleuca*	*Palmaria* sp.	*Porphyra* sp.
$C_{14:0}$	1.14±0.22	5.85±0.35	3.17±0.31	4.97±0.20	13.76±0.61	0.53±0.21
$C_{16:0}$	14.00±1.12	32.53±1.61	16.51±1.35	28.51±1.87	45.44±1.84	63.19±1.93
$C_{16:1}$ ω7	1.87±0.21	2.79±0.25	3.70±0.88	5.62±0.71	5.26±0.63	6.22±0.70
$C_{16:3}$ ω4	–	4.38±1.33	2.31±1.94	0.87±0.10	1.20±0.16	1.56±0.51
$C_{18:0}$	8.39±0.12	0.68±0.15	0.69±0.08	0.34±0.14	1.28±0.12	1.23±0.10
$C_{18:1}$ ω9	27.43±1.91	19.96±2.01	6.79±0.90	13.62±1.24	3.13±0.47	6.70±1.16
$C_{18:1}$ ω7	–	–	–	–	2.08±0.68	1.29±0.68
$C_{18:2}$ ω6	8.31±1.21	4.39±0.34	6.23±0.32	6.79±0.61	0.69±013	1.17±013
$C_{18:3}$ ω3	4.38±0.31	8.79±0.71	11.97±1.75	5.15±0.71	0.59±0.26	0.23±0.16
$C_{18:4}$ ω3	0.41±0.01	3.53±0.56	22.60±2.48	10.77±1.85	0.74±0.47	0.24±0.35
$C_{20:1}$ ω9	4.21±0.50	–	–	–	0.20±0.10	4.70±0.26
$C_{20:4}$ ω6	0.34±0.01	10.69±1.30	15.87±1.68	14.20±0.66	1.45±0.31	6.80±1.18
$C_{20:4}$ ω3	–	0.88±1.80	0.70±0.14	0.54±0.90	0.14±0.03	0.07±0.02
$C_{20:5}$ ω3	1.01±0.01	5.50±1.78	9.43±0.69	8.62±0.56	24.05±2.59	6.03±0.95
Saturated fatty acid	23.53±1.46	30.06±2.11	20.39±1.73	33.82±2.21	60.48±2.58	64.95±2.24
Monounsaturated	33.51±2.62	22.75±2.26	10.50±1.78	19.23±1.99	10.67±1.55	18.91±2.81
PUFAs	14.45±1.55	38.16±7.84	69.11±9.01	46.94±4.58	28.86±3.94	16.10±3.31
PUFAs ω6	8.65±1.22	15.08±1.64	22.10±2.00	20.99±1.27	2.14±0.45	7.97±1.31
PUFAs ω3	5.80±0.33	18.70±4.84	44.70±5.05	25.08±3.21	25.52±3.34	7.20±1.48
Ratio ω6/ω3	1.49	0.81	0.49	0.83	0.13	1.21

content (16.51%) was only exceeded by that of octadecatetraenoic acid (ω-3 $C_{18:4}$) (22.6%), and in *U. lactuca* the $C_{16:0}$ content (14.0%) was only exceeded by that of oleic acid (ω-9 $C_{18:1}$) (27.43%). However, all the seaweeds also contained the essential fatty acids linoleic acid (ω-6 $C_{18:2}$) and linolenic acid and the icosanoid precursors, arachidonic acid and EPA. Furthermore, the ω-6:ω-3 ratio, which the WHO currently recommends should be no higher than 10 in the diet as a whole, was at most 1.49 so that these algae may be used for reduction of ω-6:ω-3 ratio. Saturated fatty acid contents were higher in the red algae (*Palmaria* sp. and *Porphyra* sp.) than in the brown and green algae, and vice versa for relative total unsaturated fatty acid contents. Whereas in the red algae, C_{20} PUFAs were as a class 8–12 times more abundant than C_{18} PUFAs, in green algae the opposite occur while in brown algae these two classes of fatty acids were more or less equally abundant. Relative essential fatty acid contents were higher in brown and green algae than in red algae.

Several researchers have reported the fatty acid composition of total lipids of different species of *Sargassum*. Heiba et al. [47] studied the fatty acids present in four different *Sargassum* species in the Phaeophyta class that contained heptadecanoic acid ($C_{17:0}$), eicosanoic acid ($C_{20:0}$), eicosatrienoic acid (ω-3 $C_{20:3}$), and DHA. On the other hand, Khotimchenko [80], working with seven *Sargassum* species from different parts of the world, determined similar fatty acid compositions in all of them. The site of collection only seemed to affect palmitic acid ($C_{16:0}$) and C_{20} PUFA contents and was connected mainly with water temperature.

Aquatic plants possess conjugated fatty acids (CFA) with carbon chain length varying from 16 to 22, as natural constituents in their lipids; both trienes and tetraenes occur in aquatic plant lipids. There is not much information available on the literature, only a few reports on the occurrence of these conjugated polyenes in *Tydemania expeditionis*, *Hydrolithon reinboldii* [69], *Ptilota* [205], *Acanthophora* [8], and *Anadyomene stellata* [6] have been published. Various enzymes in aquatic plants are thought to be responsible for the formation of conjugated trienes/tetraenes endogenously. The enzymes responsible for the formation of CFA can be grouped into three main categories of conjugases, oxidases, and isomerases. Hideki and Yuto [58] studied the selective cytotoxicity of eight species of marine algae extracts to several human leukemic cell lines. It has been reported recently that conjugated PUFA, such as conjugated EPA, conjugated AA, and conjugated DHA, prepared by alkali isomerization had profound cytotoxic effects against human cancer cell lines [102].

Besides fatty acids, unsaponifiable fraction of algae contain carotenoids (see Sect. 4.1), tocopherols (see Sect. 4.5), and sterols. The distribution of major sterol composition in macroalgae has been used for chemotaxonomic classification. Recent biological studies have demonstrated that sterols and sterol derivatives possess biological activities. Currently, phytosterols (C_{28} and C_{29} sterols) are playing a key role in nutraceutic and pharmaceutical industries because they are precursors of some bioactive molecules (e.g., ergosterol is a precursor of vitamin D_2, also used for the production of cortisone and hormone flavone and has some therapeutic applications to treat hypercholesterolemia). Phytosterols have also been shown to lower total and LDL cholesterol levels in human by inhibiting cholesterol absorption from

the intestine [37]. High serum concentrations of total or LDL cholesterol are major risk factors for coronary heart disease, a major cause for morbidity and mortality in developed countries. In addition to their cholesterol lowering properties, phytosterols possess anti-inflammatory and anti-atherogenicity activity and may possess anticancer and antioxidative activities [37].

From a chemotaxonomic point of view, literature data show that major sterols in red algae are C_{27} compounds and cholesterol occur in substantial amount. It is generally the primary sterol. Desmosterol and 22E-dehydrocholesterol are present in high concentrations and may even be the major sterols in any red algae.

Sterol content in green algae is similar to higher plants, and also contains large amounts of cholesterol. But in green algae, the dominant sterol seems to vary within the order and within the family.

In brown algae, the dominant sterol is fucosterol and cholesterol is present only in small amounts.

Fucosterol content in *H. elongata* and *U. pinnatifida* was 1,706 μg/g of dry weight and 1,136 μg/g of dry weight, respectively, as demonstrated by Sánchez-Machado et al. [162]. Mean desmosterol content in the red algae ranged from 187 μg/g for *Palmaria* sp. to 337 μg/g for *Porphyra* sp. Cholesterol, in general, was present at very low quantities, except in *Porphyra* sp. that can contain up to 8.6% of the total content of sterols as cholesterol [162].

Sterol content determined in red alga *Chondrus crispus* showed that the main sterol was cholesterol (>94%), containing smaller amounts of 7-dehydrocholesterol and stigmasterol and minimum amounts of campesterol, sitosterol, and 22-dehydrocholesterol [188].

According to the investigation carried out by Kapetanovic et al. [77], the sterol fractions of the green alga *Codium dichotomum* and the brown alga *Fucus virsoides* contained practically one sterol each, comprising more than 90% of the total sterols (cholesterol in the former and fucosterol in the latter). The main sterols in the green alga *U. lactuca* were cholesterol and isofucosterol, while in the brown algae *Cystoseira adriatica*, the principal sterols were cholesterol and stigmast-5-en-3 beta-ol, while the characteristic sterol of the brown algae, fucosterol, was found only in low concentration [77]. However, fucosterol was the major sterol present in *Cystoseira abies-marina* (96.9%), containing low concentration of 24-methylenecholesterol (1.1%), brassicasterol (1.2%), and cholesterol (0.7%) [120].

4.3 Proteins

The protein content in algae can be as high as 47% of the dry weight [35], but these levels vary according to the season and the species. The protein content of brown algae is generally low (5–15% of the dry weight), whereas higher protein contents are recorded for green and red algae (10–30% of the dry weight). Except for brown algae *U. pinnatifida* which has a protein level between 11 and 24% (dry weight) [35]. Higher protein level were recorded for red algae, such as *Porphyra tenera*

Table 2 Amino acid profile of different algae according to Dawczynski et al. [23] (g/16 g N)

Amino acids	*Porphyra* sp.	*Undaria pinnatifida*	*Laminaria* sp.	*Hizikia fusiforme*
Essential amino acids				
Histidine	2.6±0.4	2.5±0.3	2.2±0.4	2.6±0.4
Isoleucine	3.1±0.5	4.1±0.3	2.7±0.9	4.0±0.4
Leucine	5.5±0.9	7.4±0.6	4.9±1.7	6.7±0.6
Lysine	4.9±0.9	5.6±0.4	3.9±1.4	3.1±0.3
Methionine	1.8±0.7	1.7±0.5	0.9±0.2	1.6±0.1
Phenyl alanine	3.3±0.4	4.7±0.3	3.2±1.0	4.6±0.4
Tyrosine	3.4±2.1	2.9±0.5	1.7±0.5	2.8±0.4
Threonine	5.3±0.8	4.4±0.6	3.5±0.6	4.1±0.5
Tryptophan	0.7±0.1	0.7±0.1	0.5±0.5	0.4±0.0
Arginine	5.9±0.4	5.2±0.2	3.3±1.1	4.5±0.3
Cysteine	1.2±0.2	0.9±0.2	1.2±0.3	0.9±0.1
Valine	5.2±1.0	5.2±0.5	3.8±1.0	4.9±0.5
Nonessential amino acids				
Asparagine/aspartate	8.5±1.0	8.7±1.1	12.5±2.8	9.1±1.0
Glutamine/glutamate	10.2±2.6	14.5±3.2	23.8±7.5	18.7±2.4
Serine	4.0±0.5	4.0±0.4	3.3±0.6	3.7±0.3
Glycine	5.1±1.3	5.1±0.7	4.0±1.1	4.8±0.5
Alanine	6.2±2.2	4.7±0.6	5.7±2.8	4.3±0.4
Proline	3.5±1.0	3.6±1.6	3.1±1.1	3.8±0.4
Taurine	4.3±2.1	0.1±0.1	0.3±0.2	0.6±0.2

(33–47% of dry mass) [35] or *Palmaria palmata* (8–35 of dry mass) [121]. These levels are comparable to those found in soybean.

There are studies about the variation of protein content of marine algae as a function of the seasonal period [1, 39]. Higher protein levels were observed during the end of the winter period and spring whereas lower amounts were recorded during summer.

The in vivo digestibility of algal protein is not well documented, and available studies about their assimilation by humans have not provided conclusive results. However, several researchers have described a high rate of alga protein degradation in vitro by proteolytic enzymes. For instance, the relative digestibility of alkali-soluble proteins from *P. tenera* is higher than 70% [38]. On the other hand, some compounds limiting the digestibility of alga proteins, such as phenolic compounds or polysaccharides, have been described. Studies performed on brown algae show the strong inhibitory action of soluble fiber on in vitro pepsin activity and their negative effects on protein digestibility [59].

Typical amino acid composition of different species of algae is outlined in Table 2 according to Dawczynski et al. [23]. The quality of food protein depends on its essential amino acids. These algae present high concentration of arginine, valine, leucine, lysine, threonine, isoleucine, glycine, and alanine, although the predominant amino acids are glutamine and asparagine. Glutamine and asparagine exhibit interesting properties in flavor development, and glutamine is the main responsible in the taste sensation of "Umami."

The concentration of essential amino acids, such as, threonine, valine, isoleucine, leucine, phenyl alanine, lysine, and methionine, are higher in *U. pinnatifida* than in *Laminaria* sp. *U. pinnatifida* has higher concentrations of Lysine that has *Hizikia fusiforme* and *Laminaria* sp. has higher concentrations of Cysteine than has *U. pinnatifida.* Interestingly, taurine is not a typical component of traditional European food and taurine content represents a nutrient feature which is characteristic of red algae, such as *Phorphyra* sp. Taurine is detected at low concentrations in brown algae varieties.

In general, algae possess proteins that have a high nutritional value since they contained all the essential amino acids in significant amounts (see Table 2).

The organoleptic characteristic of algae are principally due to their free amino acid profile [126], which in turn depends on environmental factors in its culture grounds [44]. Generally, the free amino acid fraction of algae is mainly composed of alanine, aminobutyric acid, taurine, ornithine, citrulline, and hydroxyproline [89].

Other proteins present only in red and blue-green algae are phycobiliproteins (phycocyanin in blue-green algae, phycoerythrin in red algae), a group of protein involved in photosynthesis. Purified phycobiliproteins can have several uses, such as cosmetics, colorants in food, and fluorescent labels, in different analytical techniques [33, 138]. These proteins are characterized by having a tetrapyrrolic pigment, called phycobilin, covalently attached to their structure. Important medical and pharmacological properties, such as hepatoprotective, anti-inflammatory, and antioxidant properties [9, 10, 156], have been described and are thought to be basically related to the presence of phycobilin. Besides, phycobiliproteins might have an important role in different photodynamic therapies of various cancerous tumors and leukemia treatment [157]. Different works have been aimed to the selective extraction and analysis of the phycobiliproteins from algae, such as Herrero et al. [53] and Simó et al. [174], that identified the two subunits of each protein, namely allophycocyanin-α, allophycocyanin-β, c-phycocyanin-α, and c-phycocyanin-β, from *S. platensis*. In the red microalga *Porphyridium* spp., the red-colored pigment phycoerythrin [62, 195] has been described.

4.4 Polysaccharides and Dietary Fibers

Algae contain large amounts of polysaccharides, notably cell wall structural polysaccharides that are extruded by the hydrocolloid industry: alginate from brown algae, carrageenans, and agar from red algae. Edible algae contain 33–50% total fibers, which is higher than the levels found in higher plants. Other minor polysaccharides are found in the cell wall: fucoidans (from brown algae), xylans (from certain red and green algae), ulvans (from green algae), and cellulose (which occur in all genera, but at lower levels than found in higher plants). Algae also contain storage polysaccharides, notably laminarin (β-1,3 glucan) in brown algae and floridean starch (amylopectin-like glucan) in red algae [16]. Most of these polysaccharides are not digested by humans and can be regarded as dietary fibers.

Table 3 Dietary fiber contents of sea vegetables, seaweed by-products, and land plants (according to Mabeau and Fleurence [95])

	Fiber (% dry weight)		
Source	Soluble	Insoluble	Total
Phaeophytes			
Undaria pinnatifida	30.0	5.3	35.3
Hizikia fusiforme	32.9	16.3	49.2
Himanthalia elongate	25.7	7.0	32.7
Laminaria digitala	32.6	4.7	37.3
Chlorophytes			
Ulva lactuca	21.3	16.8	38.1
Enteromorpha spp.	17.2	16.2	33.4
Rhodophytes			
Porphyra tenera	17.9	6.8	34.7
Kappaphycus	41.5	29.2	70.7
High plants			
Apple	5.9	8.3	14.2
Cabbage	16.8	17.5	34.3

Water soluble and water insoluble fibers have different physiological effects associated. Insoluble fiber primarily promotes the movement of material through the digestive system, thereby improving laxation. Therefore, insoluble fiber can increase feelings of satiety [178]. The majority of insoluble fiber is fermented in the large intestine, supporting the growth of intestinal microflora, including probiotic species. Soluble fiber can help to lower blood cholesterol and regulate blood glucose levels [190]. The insoluble fibers include cellulose, hemicellulose, and lignin; the soluble fibers include the oligosaccharides, pectins, β-glucans, and galactomanan gums.

Table 3 shows, for comparison, the dietary fiber content in some sea vegetables, seaweed by-products and plants [95]. As can be seen, algae contain slightly more fiber than cabbage, although the amounts consumed in the diet would be lower. The red alga *Kappaphycus* shows the highest levels of total fiber (70.7% dry weight).

Algae contain sulfated polysaccharides which possesses important functional properties. For instance, fucoidans (soluble fiber), polysaccharides containing substantial percentages of L-fucose and sulfate ester groups, are constituents of brown algae. For the past decade, fucoidans isolated from different brown algae have been extensively studied due to their varied biological activities, including anticoagulant and antithrombotic, antiviral, antitumoral and immunomodulatory, anti-inflammatory, blood lipids reducing, antioxidant and anticomplementary properties, activity against hepatopathy, uropathy, and renalpathy, gastric protective effects, and therapeutic potential in surgery [94]. Compared to other sulfated polysaccharides, fucoidans are widely available from various kinds of cheap sources, so more and more fucoidans have been investigated in recent years as natural sources of drugs or functional ingredients. Fucoidans had been isolated of different brown algae, such as, *U. pinnatifida*

[92], *Laminaria angustata* [83], *Sargassum stenophyllum* [29], *H. fusiforme* [93], *Adenocytis utricularis* [146], and *Cystoseira canariensis* [149].

Red algae contain water soluble sulfated polysaccharide galactan, agar, and carrageenans. One of the most studied marine-sulfated homopolysaccharides class, together with fucoidans, are the sulfated galactans. In general, the sulfated galactans are polymers of α-L- and α-D- or β-D-galactopyranosyl units. Unrelated to their natural biological roles as components of the biological wall, the sulfated galactans show important and potent pharmacological actions. These include antiviral, antitumoral, immunomodulation, antiangiogenic, anti-inflammatory, anticoagulant, and antithrombotic properties [144]. Their beneficial effects on the cardiovascular system are the most studied and exploited clinical actions, especially due to the serious need for new antithrombotic drugs as a consequence of the continuously increasing incidence of thromboembolic diseases [145]. Sulfated galactans have been identified in several red algae, among others, *Grateloupia elliptica*, *Sinkoraena lancifolia*, *Halymenia dilatata*, *Grateloupia lanceolata*, *Lomentaria catenata*, *Martensia denticulata*, *Schizymenia dubyi*, and *C. crispus* [91].

Agar extracted from species, such as *Gracilaria* and *Gelidium*, is composed of a mixture of the sulfated galactans D-galactose and 3,6-anhydro-α-L-lactose. The term agarose and agaropectin represent an oversimplification of the agar structure.

Carrageenan is a generic name for a group of linear-sulfated galactans, obtained by extraction from numerous species of marine red algae. These carbohydrates consist of a linear structure of alternating disaccharide repeat units containing 3-linked β-D-galactopyranose and 5-linked α-D-galactopyranose.

Porphyrans, the sulfated polysaccharides making up the hot-water soluble portion of the cell wall, are the main components of *Porphyra*. Structurally, they have a linear backbone of alternating 3-linked β-D-galactosyl units and 4-linked α-L-galactosyl 6-sulfate or 3,6-anhydro-α-L-galactosyl units. In a former study, the content of ester sulfate in porphyran extracted from *Porphyra haitanensis* was measured ranging from 16 to 19% and showing generic antioxidant activity [202]. Several investigations of the structure and function of porphyrans isolated from different species have been undertaken [122, 201]. Although the chemical components and structures show great variation, porphyrans have also been shown to have immunoregulatory and antitumor activities [128, 135].

On the other hand, green algae, such as those of the genera *Ulva* and *Enteromorpha*, contain sulfated heteropolysaccharides in their mucilaginous matrix [72]. Sulfated polysaccharides extracted from the green algae belonging to Ulvales (*Ulva* and *Enteromorpha*) are ulvan. Ulvan is a heteropolysaccharide, mainly composed of rhamnose, xylose, glucose, glucuronic acid, iduronic acid, and sulfate, with smaller amounts of mannose, arabinose, and galactose. The mainly repeating disaccharide units are (β-D-Glcp A-(1→4)-α-L-Rhap 3S) and (α-L-ldop A-(1→4)-α-L-Rhap 3S) [139]. Most of the recent work on Ulvales cell wall polysaccharides focused on ulvan as it display several physicochemical and biological features of potential interest for food, pharmaceutical, agricultural, and chemical applications. Ulvans have been shown to have antioxidant [148], antitumor [104], and antihyperlipidemic [139] activities.

4.5 Vitamins

As marine algae can carry on photosynthesis, they are able to synthesize all vitamins that high plants produce. The vitamin profile of algae can vary according to algal species, season, alga growth stage, and environmental parameters. The edible algae (especially of *Porphyra* spp.) contain large amounts of water-soluble vitamin C and B complex, and the fat-soluble vitamin A and E [71]. Algae are a good source of pro-vitamin A (see Sect. 4.1).

Algae provide a worthwhile source of vitamin C. The levels of vitamin C average 500–3,000 mg/kg of dry matter for the green and brown algae, which are comparable to concentration in parsley, blackcurrant, and peppers; whereas the red algae contain vitamin C levels of around 100–800 mg/kg [16]. Vitamin C is of interest for many reasons: it strengthens the immune defense system, activates the intestinal absorption of iron, controls the formation of conjunctive tissue and the protidic matrix of bony tissue, and also acts in trapping free radicals and regenerating vitamin E [16].

Brown algae contain higher levels of vitamin E (23–412 mg/kg of dry matter) than green and red algae (8 mg/kg of dry matter). *H. elongata* presents high levels of α-tocopherol as demonstrated by Sánchez-Machado et al. [160]; for example, the content of α-tocopherol in *H. elongata* dehydrated (33 μg/g dry weight) was considerably higher than *H. elongata* canned (12.0 μg/g dry weight), which clearly indicates the important effect of the processing on this compound. The highest levels of vitamin E in brown algae are observed in Fucaceae (e.g., *Ascophyllum* and *Fucus* sp.), which contain between 200 and 600 mg of tocopherols/kg of dry matter [96]. The red microalga *Porphyridium cruentum* also presents high levels of tocopherols as demonstrated by Durmaz et al. [30]; for example, the contents of α- and γ-tocopherols were 55.2 and 51.3 μg/g dry weight, respectively. These tocopherols (vitamin E) are lipid-soluble antioxidants that are considered essential nutrients because of their ability to protect membrane lipids from oxidative damage [193]. Vitamin E has effect in the prevention of many diseases, such as atherosclerosis, heart disease, and also neurodegenerative diseases, such as multiple sclerosis [68, 73], thus also making it a very interesting functional compound. Generally, brown algae contain α-, β-, and γ-tocopherols, while green and red algae contain only α-tocopherol [16]. Mendiola et al. studied the possible use of SFE to obtain fractions enriched with vitamin E from *S. platensis* [110].

Algae are also an important source of B vitamins; for instance, algae contain vitamin B_{12}, which is particularly recommended in the treatment of the effects of aging, of chronic fatigue syndrome and anemia. Algae are also one of the few vegetables sources of vitamin B_{12}. *U. lactuca* can provide this vitamin, in excess of the recommended dietary allowances for Ireland fixed at 1.4 μg/day, with 5 μg in 8 g of dry foodstuff [36]. *Spirulina* is the richest source of B_{12} and the daily ingestion of 1 g of *Spirulina* would be enough to meet its daily requirement [196]. This may provide an alternate source of vitamin B_{12} for vegetarians or vegans.

On a dry matter basis, thiamine (vitamin B_1) content ranges from 0.14 μg/g in dried *H. elongata* to 2.02 μg/g in dried *Porphyra*, and riboflavin (vitamin B_2)

content varies between 0.31 μg/g in canned *H. elongata* to 6.15 μg/g in dried *Porphyra* [163]. The amount of folate (as folic acid or vitamin B_9) in the algae studied by Rodríguez-Bernaldo de Quirós et al. [153] (*H. elongata*, *Laminaria ochroleuca*, *Palmaria* spp., *U. pinnatifida*, and *Porphyra* spp.) ranged from 61.4 to 161.6 μg/100 g of dry matter.

In conclusion, the algae have an original vitamin profile, which might complement the vitamin profiles of land vegetables.

4.6 Phenolic Compounds

Phenols are an important group of natural products with antioxidant and other biological activities. These compounds play an important role in algal cell defense against abiotic and biotic stress. Several authors have recently published results regarding the total phenol content and antioxidant activity of algae [40]. Cinnamic acid esters (*n*-butyl 3,5-dimethoxy-4-hydroxycinnamate and isopropyl 3,5-dimethoxy-4-hydroxycinnamate) and methyl 3,4,5-trihydroxybenzoate were studied using 1H and 13C NMR in brown algae *Spatoglossum variabile* [46]. Some of the first polyphenols found in algae (*Fucus* and *Ascophyllum* spp.) were phlorotannins. They are formed from the oligomeric structures of phloroglucinol (1,3,5-trihydroxybenzene) [137]. Also, some flavanone glycosides have been found even in fresh water algae [86].

The main bioactivity associated to phenolic compounds is antioxidant activity, which is also the main bioactivity of algal and microalgal phenolics [89]. Duan et al. [28] have demonstrated that antioxidant potency of crude extract from red algae (*Polysiphoma urceoiata*) correlated well with the total phenolic content. Strong correlation also existed between the polyphenol content and DPPH radical scavenging activity of a seaweed (*H. fusiformis*) extract [177]. Using electron spin resonance spectrometry and comet assay, Heo et al. [51] found that phenolic content in seaweeds could raise up to 1,352 μg/g on dry weight basis. The content and profile of phenolic substances in marine algae vary with the species. In marine brown algae, a group of polymers called phlorotannins comprises the major phenolic compounds [20], such as fucols, phlorethols, fucophlorethols, fuhalols, and halogenated and sulfited phlorotannins. Takamatsu et al. [186] showed that bromophenols isolated from several red marine algae exhibited antioxidant activities. These findings suggest that phlorotannins, the natural antioxidant compounds found in edible brown algae, can protect food products against oxidative degradation as well as prevent and/or treat free radical-related diseases [89].

Some algal phenolic compounds have been associated with anti-inflammatory activity, such as rutin, hesperidin, morin, caffeic acid, catechol, catechin, and epigallocatechin gallate, whose have been identified in *Porphyra* genus. Kazłowska et al. [79] have studied recently the phenolic compounds in *Porphyra dentata*, they identified catechol, rutin, and hesperidin in crude extract using HPLC-DAD. They demonstrated that the crude extract and the phenolic compounds inhibited the

production of nitric oxide in LPS-stimulated RAW 264.7 cells. Their results indicate that catechol and rutin, but not hesperidin, are primary bioactive phenolic compounds in the crude extract to suppress NO production in LPS-stimulated macrophages via NF-κB-dependent iNOS gene transcription. Data also explained the anti-inflammatory use and possible mechanism of *P. dentata* in iNOS-implicated diseases.

4.7 Bioactive Volatiles

In another chapter of the present book, volatile compounds from algae and microalgae are studied as an energy production source. Biogeneous hydrocarbons of the marine system, alkenes (mono, di, and cyclic) were originated from algae. One characteristic of crude oils that distinguishes them from biogeneous hydrocarbons is their content in cyclo alkenes and aromatic compounds [32]. But hydrocarbons are not the only volatile compounds that can be found in algae and microalgae. In fact, there is a huge number of secondary metabolites with proved antimicrobial and therapeutic activities while some of these volatile compounds have been also related to climate modifications.

When attacked by herbivores, land plants can produce a variety of volatile compounds that attract carnivorous mutualists. Plants and carnivores can benefit from this symbiotic relationship, because the induced defensive interaction increases foraging success of the carnivores, while reducing the grazing pressure exerted by the herbivores on the plants. Steinke et al. [185] reviewed whether aquatic plant use volatile chemical cues in analogous tritrophic interactions.

In general, naturally produced volatile and semivolatile compounds play an essential role in the survival of organisms for chemical defense and food gathering, but high amounts of volatile compounds could produce tremendous environmental actions. Marine algae produce several classes of biogenic gases, such as nonmethane hydrocarbons, organohalogens, ammonia and methylamines, and dimethylsulfide. These gases can transfer to the air, affect atmospheric chemistry, and are climatically important. Grazing increases dimethylsulfide and ammonia concentrations, and it is possible that other environmentally relevant volatiles are also produced during this process.

Other compounds produced by seaweeds with high importance for environment are halogenated hydrocarbons. Stratospheric ozone depletion and volatile-halogenated compounds are strongly connected with each other since the discovery that a massive loss of ozone in the polar stratosphere is catalyzed by halogen radicals derived from chlorocarbons and chlorofluorocarbons. Furthermore, so far unknown natural sources of volatile organohalogens may also contribute to a further destruction of the ozone layer. Marine macroalgae species from the polar regions were investigated [90] for their importance as natural sources of volatile halogenated compounds released into the biosphere. Several different halogenated C_1 to C_4 hydrocarbons were identified and their release rates determined. Although, at present,

marine macroalgae are apparently not the major source on a global scale, they may become more important in the future due to the influence of changing abiotic factors, such as photon fluence rate, nutrient concentration, temperature, and salinity on the formation of volatile organohalogens.

The release of volatile compounds with defensive functions has been studied in many algae, for example the brown alga *Dictyota menstrualis* [21]. Although the amphipod *Ashinaga longimana* preferentially consumes the alga *D. menstrualis*, its feeding rates can be reduced significantly by high concentrations of diterpenoid dictyols (dictyol E, pachydictyol A, and dictyodial) produced by the alga. The pattern of variation in the chemical defenses of some seaweed species suggests herbivore-induced increases of chemical defenses may be responsible for intraspecific variation in chemical defenses. For example, seaweeds from areas of coral reefs where herbivory is intense often produce more potent and higher concentrations of chemical defenses than plants from habitats where herbivory is less intense. Their findings suggested that seaweeds are not passive participants in seaweed-herbivore interactions, but can actively alter their susceptibility to herbivores in ecological time. Induced responses to herbivory help explain both spatial (i.e., within-thallus, within-site, and among-site) and temporal variation in the chemical defenses of the algae.

As seen above, macroalgae produce volatiles with defensive functions against herbivores, but microalgae also produce defensive volatile compounds. In this sense, it is common in many microalgae to share the ecological niche with bacteria and other microorganism. Therefore, the defensive compounds secreted by microalgae possess antibacterial, antifungal or antiprotozoal activity. The nature of these compounds is highly varied. Microalgae have been screened for potential antimicrobial activity, which have been attributed to different compounds belonging to a range of chemical classes, including indoles, terpenes, acetogenins, phenols, fatty acids, and volatile-halogenated hydrocarbons [105]. For example, pressurized ethanol and supercritical CO_2 extracts of microalgae *D. salina* were studied for their antibacterial activity against *Escherichia coli* and *S. aureus* and for their antifungal activity against *Candida albicans* and *Aspergillus niger* [56, 111]. In the broth microdilution assay, a high antimicrobial activity against *C. albicans*, *E. coli*, and *S. aureus* was observed but not against *A. niger*. In this work, a GC-MS analysis was performed to associate the antimicrobial activity found, it was concluded that antimicrobial activity of *D. salina* extracts could be linked to the presence of terpenic (β-cyclocitral and α and β-ionone) and indolic (methyl-1H-indole derivative) compounds, Fig. 2.

Terpenoids from algae have also been associated with antiviral activity, for example the above mentioned *D. menstrualis* produces a terpenoid able to inhibit HIV-1 reverse transcriptase as demonstrated by Souza et al. [181]; or terpenoid derived from plastoquinone that produces *Sargassum* sp., which acts in the lipid oxidation chain and inhibit cytomegalovirus growing [64].

Short chain fatty acids from microalgae are also volatile compounds associated with antibacterial activity. Santoyo et al. [165] tested, using the broth microdilution assay, extracts obtained from the red hematocysts without flagella (red phase) of

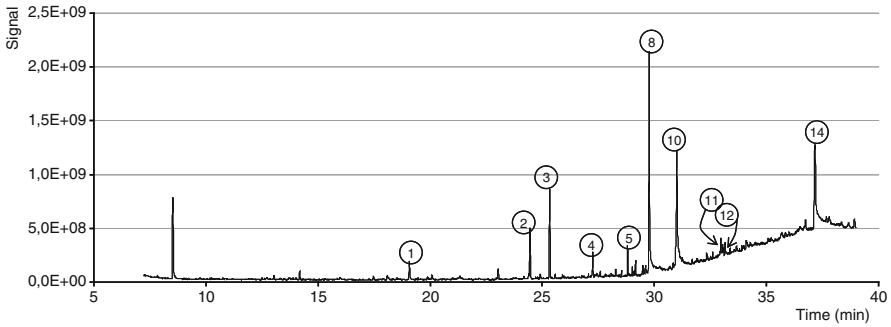

Fig. 2 GC-MS chromatogram of the volatile fraction of *Dunaliella salina* extract [111]. (1) 3,3-Dimethyl-2,7-octanedione; (2) β-ionone; (3) 5,6,7,7a-tetrahydro-4,4,7a-trimethyl-2(4H)-benzofuranone; (4) 4-oxo-β-ionone; (5) neophytadiene; (6) nerolidol; (7) 9-hexadecanoic ethyl ester; (8) hexadecanoic acid; (9) phytol; (10) 9,12,15-octadecatrienoic acid methyl ester; (11) 1H-indole derivative; (12) hexadecanoic acid monoglyceride; (13) neophytadiene derivative; (14) vitamin E. Reprinted with permission from the *Journal of Food Protection.* Copyright held by the International Association for Food Protection, Des Moines, IA, USA

H. pluvialis microalga. In this work, it was concluded that the presence of short chain fatty acid (butanoic, hexanoic) highly inhibited the growing of gram positive and negative bacteria.

4.8 Other Bioactive Compounds

Seaweeds are known to be high in mineral content. More than 30% of the dry weight of marine algae is ash which contains various kinds of minerals, as they are bathed in the rich seawater. Some of the minerals are necessary for our health while some are toxic in varying degrees. Most of the macroalgae have high Ca, Mg, P, K, Na, and Fe contents [116], as can be seen in Table 4.

In comparison with higher plants, their outstanding feature is their high iodine content [89]. Seaweeds are the best natural sources of biomolecular dietary I. Some seaweeds contain 1,000 times as much iodine as found in a marine fish like cod. Seaweeds provide di-iodotyrosin (I_2T) which is precursor to essential thyroid hormones thyroxine (T4) and triiodothyronine (T3) [14].

The mineral content in general is highly dependant on the environmental growing conditions (season, temperature, physiological state, geographic variations…). For example, in a recent study of *Porphyra* and *Laminaria* from France, Spain, Korea, and Japan [152] it was found, by using ICP-MS, that seaweeds from Korea and Japan tended to display the highest concentrations of Pb and Cd. In contrast, Spanish and French samples showed the highest levels of some microelements essential to human nutrition. Moreover, *Porphyra* presented

Table 4 Mineral content of some edible seaweeds [116]

Seaweed	Na[a]	K[a]	Mg[a]	Ca[a]	P[a]	Fe[b]	Zn[b]	Cu[b]	Mn[b]	Cr[b]	B[b]
Chlorella	10.4	11.0	3.53	2.30	19.2	1,185	24.7	6.21	77.8	1.38	27.5
Spirulina	10.1	14.9	4.76	2.96	12.6	1,480	59.2	7.26	240	1.08	33.0
Arame	12.0	14.5	6.55	6.79	0.78	63.4	27.2	4.30	3.94	0.77	37.0
Hijiki	16.2	54.5	6.85	6.49	1.02	56.4	16.2	2.02	6.20	0.55	117
Kombu	27.1	90.9	6.72	5.74	4.76	73.8	18.2	1.64	4.67	0.71	89.5
Kombu-Kelp	21.2	48.7	5.61	4.52	2.35	76.4	19.3	1.95	3.90	0.43	87.5
Wakame	62.6	64.8	12.0	4.94	6.04	70.9	22.5	3.41	6.94	0.40	69.0
Wakame-instant	74.9	1.49	9.43	5.31	3.52	304	50.7	3.07	11.4	0.93	33.0
Dulse	22.8	105	3.46	2.08	4.97	717	37.0	4.60	27.5	0.98	52.0
Korzický čaj	20.8	20.4	11.4	52.8	0.60	283	16.4	4.70	20.0	8.01	107
Nori	8.55	26.0	40.6	5.72	2.02	1,833	19.4	15.8	360	4.90	69.5

[a]Results expressed in mg/kg dry weight
[b]Results expressed in μg/kg dry weight

higher concentrations of most elements (Cd, Co, Cr, Mo, Ni, Pb, Sb, Se, and V), except for As, than *Laminaria*.

However, the linkage of certain minerals with anionic polysaccharides (alginate, agar, or carrageenan) might limit the absorption and extraction of these minerals. In such cases, mineral availability is a function of the type of linkage between the polysaccharide and the mineral. For instance, the weakness of the linkages between polysaccharides and iodine allows rapid release of this element. In contrast, the strong affinity of divalent cations (particularly Ca^{2+}) for carboxylic polysaccharides (alginates) probably limits the availability of associated minerals. From a nutritional standpoint, this high affinity might be compensated by the high mineral contents of seaweeds [95].

Other compounds with proven bioactivity are those related with photosynthesis, mainly pigments such as chlorophylls, carotenoids or proteins like opsins. Among them chlorophylls are the most wide spread compounds. Chlorophylls and their intermediate metabolites have proved its contribution to antioxidant and antimicrobial activities. For example, in supercritical CO_2 extracts of *S. platensis*, chlorophyll-*a*, pheophytin-a, pheophytin-a O-allomer, and pyropheophytin-a were detected by LC-MS/MS among the contributors to antioxidant activity measured by DPPH radical scavenging method [107]. On the other hand, phytol was detected by GC-MS among the bactericidal compounds present in *D. salina* extracts [111], as can be observed in Fig. 2, being all of them secondary metabolites of chlorophylls.

Certain alkaloids have been isolated from seaweeds. Among the many chemical classes present in plant species, alkaloids stand out as one of major importance in the development of new drugs, because they possess a wide variety of chemical structures and have been identified as responsible for many of the pharmacological properties of medicinal plants. Caulerpin, a bisindole alkaloid, was isolated from the green alga *Caulerpa racemosa* in 2009 [24]. This alkaloid showed low toxicity and a variety of important biological activities already described in the literature,

among which it is important to mention the antitumor, growth regulator and the plant root growth stimulant properties. De Souza et al. isolated caulerpin from lipoid extract of *C. racemosa* and its structure was identified by spectroscopic methods, including IR and NMR techniques and demonstrated in vivo and in vitro its anti-nociceptive and anti-inflammatory activities [24].

Microalgae have been also studied in the search of alkaloids, in this sense most of this research has been conducted to identify toxins [78]. The non-sulfated alkaloid toxins of freshwater cyanobacteria (anatoxins and saxitoxin) are all neurotoxins. The sulfated polysaccharides, C-toxins and gonyautoxins are also neurotoxins, but the sulfated alkaloid cylindrospermopsin blocks protein synthesis with a major impact on liver cells. Some marine cyanobacteria also contain alkaloids (lyngbyatoxins, aplysiatoxins) which are dermatoxins (skin irritants), but have also been associated with gastroenteritis and more general symptoms such as fever [78]. Several freshwater bloom forming cyanobacterial genera, including Anabaena, Aphanizomenon, Oscillatoria, and Cylindrospermum, produce the neurotoxin, anatoxin-a, an alkaloid with a high toxicity to animals [117].

5 Conclusions and Future Outlooks

In this book chapter, we presented some of the bioactive compounds that can be obtained from algae (macro- and microalgae) with potential use as functional food ingredients. The description did not attempt to be exhaustive since, considering the huge biodiversity of algae and the strong influence of growing conditions on bioactive formation, the list of compounds and combination could be countless. On the other hand, we try to give an overview of the enormous possibilities of algae as natural reactors able to synthesize a myriad of compounds of different polarities and with different physiological effects on human health. Many of these compounds can be major components, such as proteins, lipids, and carbohydrates and other minor components (metabolites) generated to protect algal cells against stress conditions. Most of them are useful for the food industry as macronutrients (fiber, proteins, etc.) while others have an enormous future as functional ingredients to prevent or even improve the health status of a human being.

In this chapter, we also presented new technologies to extract valuable compounds from algae, these processes have in common their "green" label, the possibility of improving the efficiency through process optimization, the removal of toxic solvents, the improved cost efficiency and the enhancement of selectivity and isolation steps. Several examples are described in the text demonstrating the usefulness and the advantages of such processes compared to conventional extraction ones. But, this step cannot be considered isolated but integrated in a more holistic concept of what should be a sustainable process considering algae as raw materials.

In this sense, we can think about algae (mainly microalgae) as (1) a sustainable source of mass and energy, since their processing meets the requirements for energy efficiency (transformation, growing biomass [164]; (2) a supply of clean energy for

the future if overproduction of oil is obtained that can be lately used for large-scale biodiesel production [112, 192]; (3) an efficient CO_2 sequestrant for greenhouse gas emissions control (Kyoto Protocol) [167, 200]; and (4) a valuable source of bioactives [11, 131].

If we are able to think about a whole process involving the optimization of all these steps: efficient production of biomass using CO_2 formed by combustion of fossil fuels in thermoelectric power plants, extraction of valuable bioactives using environmentally friendly processes to obtain high added value products that, on the other hand, leave intact residues, and process of oily fraction of biomass to produce biofuels, we will be able to work toward a sustainable, efficient, and economically viable process with many important positive implications for the economy, the environment and the human health. But, to reach this goal, it is mandatory to work with multidisciplinary teams involving scientists with expertise from phycology, molecular biology, agronomy, chemical engineering, food science and technology, environmental chemistry, economics, and so on.

Other nondirect benefits from this sustainable process are: the recovery of lands unsuitable for agricultural purposes, since the requirements for algae are less demanding, the advancement of genetic engineering basic studies, since more knowledge is needed to select and manipulate the most convenient strains and genes to overproduce the substances of interest, and a more efficient use of energy and sunlight. Working on sustainable processes is one of the best ways of investing in our future and in our planet's future.

References

1. Abdel-Fattah AF, Sary HH (1987) Selective isolation of glycoprotein materials from the green seaweed *Ulva lactuca*. J Biochem 20:61–65
2. Antonopoulou S, Karantonis HC, Nomikos T, Oikonomou A, Fragopoulou E, Pantazidou A (2005) Bioactive polar lipids from *Croococcidiopsis* sp. (Cyanobacteria). Comp Biochem Physiol B Biochem Mol Biol 142:269–282
3. Arai S (1996) Studies of functional foods in Japan—state of the art. Biosci Biotechnol Biochem 60:9–15
4. Arai S (2000) Functional food science in Japan: state of the art. BioFactor 12:13–16
5. Bandoniene D, Mukovic M (2002) On-line HPLC-DPPH method for evaluation of radical scavenging phenols extracted from apples (*Malus domestica* L). J Agric Food Chem 50:2482–2487
6. Bemis DL, Jacobs RS, Bailcv TG (1996) Production of arachidonic acid metabolites in chloroplasts isolated from the green alga, *Anadyomene stellata*. FASEB J 10:A150
7. Benemann JR (1997) CO_2 mitigation with microalgae systems. Energy Convers Mgmt 38:475–479
8. Bhaskar N, Kinami T, Miyashita K, Park SB, Endo Y, Fujimoto K (2004) Occurrence of conjugated polyenoic fatty acids in seaweeds from the Indian Ocean. Z Naturforsch C 59:310–314
9. Bhat BV, Gaikwad NW, Madyastha KM (1998) Hepatoprotective effect of C-phycocyanin protection for carbon tetrachloride and R-(+)-pulegone-mediated hepatotoxicity in rats. Biochem Biophys Res Commun 249:428–431

10. Bhat BV, Madyastha KM (2000) C-Phycocyanin: a potent peroxyl radical scavenger in vivo and in vitro. Biochem Biophys Res Commun 275:20–25
11. Borowitzka MA (1995) Microalgae as sources of pharmaceuticals and other biologically active compounds. J Appl Phycol 7:3–15
12. Bors W, Michel C, Saran M (1984) Inhibition of bleaching of the carotenoid crocin. Biochim Biophys Acta 796:312–319
13. Brand-Williams W, Cuvelier ME, Berset C (1995) Use of a free radical method to evaluate antioxidant activity. Lebensm Wiss Technol 28:25–30
14. Bravarmand LE, Utigar RD (1991) The thyroid A fundamental and clinical text. Lippincott Publications, Philadelphia
15. Bruno A, Rossi C, Marcolongo G, Di Lena A, Venzo A, Berrie CH, Corda D (2005) Selective in vivo anti-inflammatory action of the galactolipid monogalactosyldiacylglycerol. Eur J Pharmacol 524:159–168
16. Burtin P (2003) Nutritional value of seaweeds. Electron J Environ Agric Food Chem 2:498–503
17. Calzolari I, Fumagalli S, Marchionni N, Di Bari M (2009) Polyunsaturated fatty acids and cardiovascular disease. Curr Pharm Des 15:4149–4156
18. Carlucci MJ, Scolaro LA, Damonte EB (1999) Inhibitory action of natural carrageenans on Herpes simplex virus infection of mouse astrocytes. Chemotherapy 45(6):429–436
19. Cerón MC, García-Malea MC, Rivas J, Acien FG, Fernandez JM, Del Río E, Guerrero MG, Molina E (2007) Antioxidant activity of *Haematococcus pluviales* cells grown in continuous culture as a function of their carotenoid and fatty acid content. Appl Microbiol Biotechnol 74:1112–1119
20. Chkikvishvili ID, Ramazanov ZM (2000) Phenolic substances of brown algae and their antioxidant activity. Appl Biochem Microbiol 36:289–291
21. Cronin G, Hay ME (1996) Induction of seaweed chemical defenses by amphipod grazing. Ecology 77:2287–2301
22. Davyt D, Fernandez R, Suescun L, Mombru AW, Saldaña J, Dominguez L, Fujii L, Manta E (2006) Bisabolanes from the red alga *Laurencia scoparia*. J Nat Prod 69:1113–1116
23. Dawczynski C, Schubert R, Jahreis G (2007) Amino acids, fatty acids, and dietary fibre in edible seaweed products. Food Chem 103:891–899
24. De Souza ÉT, De Lira DP, De Queiroz AC, Da Silva DJC, De Aquino AB, Campessato Mella EA, Lorenzo VP, Alexandre-Moreira MS (2009) The antinociceptive and anti-inflammatory activities of caulerpin, a bisindole alkaloid isolated from seaweeds of the genus *Caulerpa*. Mar Drugs 7:689–704
25. Denery JR, Dragull K, Tang CS, Li QX (2004) Pressurized fluid extraction of carotenoids from *Haematococcus pluvialis* and *Dunaliella salina* and kavalactones from *Piper methysticum*. Anal Chim Acta 501:175–181
26. Diplock AT, Aggett PJ, Ashwell M, Bornet F, Fern EB, Roberfroid MB (1999) Scientific concepts of functional foods in Europe: consensus document. Br J Nutr 81:S1–S27
27. Drozd NN, Tolstenkov AS, Makarov VA, Kuznetsova TA, Besednova NN, Shevchenko NM, Zvyagintseva TN (2006) Pharmacodynamic parameters of anticoagulants based on sulfated polysaccharides from marine algae. Bull Exp Biol Med 142:591–593
28. Duan XJ, Zhang WW, Li XM, Wang BG (2006) Evaluation of antioxidant property of extract and fractions obtained from a red alga, *Polysiphonia urceolata*. Food Chem 95:37–43
29. Duarate M, Cardoso M, Noseda M (2001) Structural studies on fucoidans from the brown seaweed *Sargassum stenophyllum*. Carbohydr Res 333:281–293
30. Durmaz Y, Monteiro M, Bandarra N, Gökpinar S, Isik O (2007) The effect of low temperature on fatty composition and tocopherols of the red microalgae, *Porphyridium cruentum*. J Appl Phycol 19:223–227
31. El Hattab M, Culioli G, Piovetti L, Chitour SE, Valls RJ (2007) Comparison of various extraction methods for identification and determination of volatile metabolites from the brown alga *Dictyopteris membranacea*. J Chromatogr A 1143:1–7
32. Erakin S, Güven KC (2008) The volatile petroleum hydrocarbons in marine algae around Turkish coasts. Acta Pharm Sci 50:167–182

33. Eriksen NT (2008) Production of phycocyanin—a pigment with applications in biology, biotechnology, foods and medicine. Appl Microbiol Biotechnol 80:1–14
34. Fang YZ, Yang S, Wu GY (2002) Free radicals, antioxidants, and nutrition. Nutrition 18:872–879
35. Fleurence J (1999) Seaweed proteins: biochemical, nutritional aspects and potential uses. Trends Food Sci Technol 10:25–28
36. Food Safety Authority of Ireland (1999) Recommended dietary allowances for Ireland. Food Safety Authority of Ireland, Dublin
37. Francavilla M, Trotta P, Luque R (2010) Phytosterols from *Dunaliella tertiolecta* and *Duanliella salina*: a potentially novel industrial application. Bioresour Technol 101:4144–4150
38. Fujiwara-Arasaki T, Mino N, Kuroda M (1984) The protein value in human nutrition of edible marine algae in Japan. Hydrobiologia 116(117):513–516
39. Galland-Irmouli AV, Fleurence J, Lamghari R, Luçon M, Rouxel C, Barbaroux O, Bronowicki JP, Vuillaume C, Guéant JL (1999) Nutritional value of proteins from edible seaweed *Palmaria palmata* (dulse). J Nutr Biochem 10:353–359
40. Ganesan P, Kumar CS, Bhaskar N (2008) Antioxidant properties of methanol extract and its solvent fractions obtained from selected Indian red seaweeds. Bioresour Technol 99:2717–2723
41. Geslain-Lanéelle C (2006) Summary report: EFSA Conference on Nutrition and Health Claims, 8-10 November 2006, Bologna, Italy ISBN: 978-92-9199-063-4
42. Gilbert J, Şenyuva HZ (2008) Bioactive compounds in foods. Blackwell Publishing Ltd., Oxford, UK. ISBN 978-1-4051-5875-6
43. González-Molina E, Domínguez-Perles R, Moreno DA, García-Viguera C (2010) Natural bioactive compounds of Cutrus limon for food and health. J Pharm Biomed Anal 51(2):327–345
44. Harada K, Osumi Y, Fukuda N, Amano H, Noda H (1990) Changes of amino acid composition of Nori *Porphyra* spp during storage. Nippon Suisan Gakk 56:606–612
45. Hasler CM (2002) Functional foods: benefits, concerns and challenges—a position paper from the American Council on Science and Health. J Nutr 132:3772–3781
46. Hayat S, Atta-ur-Rahman CMI, Khan KM, Abbaskhan A (2002) Two new cinnamic acid esters from marine brown alga *Spatoglossum variabile*. Chem Pharm Bull 50:1297–1299
47. Heiba H, Al-Easa HS, Rizk AFM (1997) Fatty acid composition of twelve algae from the coastal zones of Qatar. Plant Foods Hum Nutr 51:27–34
48. Hejazi MA, Andrysiewicx E, Tramper J, Wijffels RH (2003) Effect of mixing rate on beta-carotene production and extraction by *Dunaliella salina* in two-phase bioreactors. Biotechnol Bioeng 84:591–596
49. Hejazi MA, Kleinegris D, Wijffels RH (2004) Mechanism of extraction of β-carotene from microalga *Dunaliella salina* in two phase bioreactors. Biotechnol Bioeng 88:593–600
50. Hejazi MA, Holwerda E, Wijffels RH (2004) Milking microalga *Dunaliella salina* for bgr-carotene production in two-phase bioreactors. Biotechnol Bioeng 85:475–481
51. Heo SJ, Park PJ, Park EJ, Kim SK, Jon YJ (2005) Antioxidant activity of enzymatic extracts from a brown seaweed *Ecklonia cava* by electron spin resonance spectrometry and comet assay. Eur Food Res Technol 221:41–47
52. Herrero M, Ibáñez E, Señorans FJ, Cifuentes AJ (2004) Pressurized liquid extracts from *Spirulina platensis* microalga: determination of their antioxidant activity and preliminary analysis by micellar electrokinetic chromatography. J Chromatogr A 1047:195–203
53. Herrero M, Simó C, Ibáñez E, Cifuentes A (2005) Capillary electrophoresis-mass spectrometry of *Spirulina platensis* proteins obtained by pressurized liquid extraction. Electrophoresis 26:4215–4224
54. Herrero M, Cifuentes A, Ibáñez E (2006) Sub- and supercritical fluid extraction of functional ingredients from different natural sources: plants, food-by-products, algae and microalgae: a review. Food Chem 98:136–148
55. Herrero M, Jaime L, Martín-Álvarez PJ, Cifuentes A, Ibáñez E (2006) Optimization of the extraction of antioxidants from *Dunaliella salina* microalga by pressurized liquids. J Agric Food Chem 54:5597–5603
56. Herrero M, Ibáñez E, Cifuentes A, Reglero G, Santoyo S (2006) *Dunaliella salina* microalga pressurized liquid extracts as potential antimicrobials. J Food Prot 69:2471–2477

57. Herrero M, Vicente MJ, Cifuentes A, Ibáñez E (2007) Characterization by high-performance liquid chromatography/electrospray ionization quadrupole time-of-flight mass spectrometry of the lipid fraction of *Spirulina platensis* pressurized ethanol extract. Rapid Commun Mass Spectrom 21:1729–1738
58. Hideki H, Yuto K (1997) Selective cytotoxicity of marine algae extracts to several human leukemic cell lines. Cytotechnology 25:213–219
59. Horie Y, Sugase K, Horie K (1995) Physiological differences of soluble and insoluble dietary fibre fractions of brown algae and mushrooms in pepsin activity in vitro and protein digestibility. Asian Pacific J Clin Nutr 4:251–255
60. Hosokawa M, Wanezaki S, Miyauchi K, Kurihara H, Kohno H, Kawabata J, Odashima S, Takahashi K (1999) Apoptosis inducing effect of fucoxanthin on human leukemia cell HL-60. Food Sci Technol Res 5:243–246
61. Hosokawa M, Kudo M, Maeda H, Kohno H, Tanaka T, Myashita K (2004) Fucoxanthin induces apoptosis and enhances the antiproliferative effect of the PPAR ligand, troglitazone, on colon cancer cells. Biochim Biophys Acta 1675:113–119
62. Huang J, Wang J, Chen BL, Wang MZ, Liang SZ (2006) Isolation and purification of phycoerythrin from *Porphyridium cruentum* and its spectrum characteristics. J Plant Resour Environ 15:20–24
63. Huheihel M, Ishanu V, Tal J, Arad SM (2002) Activity of *Porphyridium* sp. polysaccharide against herpes simplex viruses in vitro and in vivo. J Biochem Biophys Methods 50:189–200
64. Iwashima M, Mori J, Ting X, Matsunaga T, Hayashi K, Shinoda D, Saito H, Sankawa U, Hayashi T (2005) Antioxidant and antiviral activities of plastoquinones from the brown alga *Sargassum micracanthum*, and a new chromene derivative converted from the plastoquinones. Biol Pharm Bull 28:374–377
65. Jaime L, Mendiola JA, Herrero M et al (2005) Separation and characterization of antioxidants from *Spirulina platensis* microalga combining pressurized liquid extraction, TLC, and HPLC-DAD. J Sep Sci 28:2111–2119
66. Jaime L, Mendiola JA, Ibañez E, Martín-Álvarez PJ, Cifuentes A, Reglero G, Señorans FJ (2007) Beta-carotene isomer composition of *Dunaliella salina* microalga sub- and supercritical carbon dioxide extracts. Antioxidant activity measurement. J Agric Food Chem 55:10585–10590
67. Jaime L, Rodríguez-Meizoso I, Cifuentes A, Santoyo S, Suarez S, Ibáñez E, Señorans F (2010) Pressurized liquids as an alternative process to antioxidant compounds extraction from *Haematococcus pluvialis* microalgae. LWT Food Sci Technol 43:105–112
68. Jialal I, Traber M, Devaraj S (2001) Is there a vitamin E paradox? Curr Opin Lipidol 12:49–53
69. Jiang RA, Hay ME, Fairchild CR, Prudhomme J, Le Roch K, Aalbersberg W, Kubanek J (2008) Antineoplastic unsaturated fatty acids from Fijian macroalgae. Phytochemistry 69:2495–2500
70. Jim JM, Lee J, Lee YW (2010) Characterization of carotenoids biosynthetic genes in the ascomycete *Gibberella zeae*. FEMS Microbiol Lett 302(2):197–202
71. Jiménez-Escrig A, Goñi I (1999) Evaluación nutricional y efectos fisiológucos de macroalgas marinas comestibles. Arch Latinoam Nutr 49:114–120
72. Jiménez-Escrig A, Sánchez-Muniz FJ (2000) Dietary fibre from edible seaweeds: chemical structure physicochemical properties and effects on cholesterol metabolism. Nutr Res 20:585–598
73. Johnson S (2000) The possible role of gradual accumulation of copper, cadmium, lead and iron and gradual depletion of zinc, magnesium, selenium, vitamins B2, B6, D and E and essential fatty acids in multiple sclerosis. Med Hypotheses 55:239–241
74. Kamath BS, Srikanta BM, Dharmesh SM, Sarada R, Ravishankar GA (2008) Ulcer preventive and antioxidative properties of astaxanthin from *Haematococcus pluvialis*. Eur J Pharmacol 590:387–395
75. Kang CD, Sim SJ (2007) Selective extraction of free astaxanthin from *Haematococcus* culture using a tandem organic solvent system. Biotechnol Prog 23:866–871
76. Kang CD, Sim SJ (2008) Direct extraction of astaxanthin from *Haematococcus* culture using vegetable oils. Biotechnol Lett 30:441–444

77. Kapetanovic R, Sladic D, Popov S, Zlatovic M, Kljajic Z, Gasic MJ (2005) Sterol composition of the Adriatic sea algae *Ulva lactuca*, *Codium dichotonium*, *Cystoseira adriatica* and *Fucus virsoides*. J Serb Chem Soc 70:1395–1400
78. Katircioğlu H, Akin BS, Atici T (2004) Microalgal toxin(s): characteristics and importance. Afr J Biotechnol 3:667–674
79. Kazłowska K, Hsu T, Hou CC, Yang WC, Tsai GJ (2010) Anti-inflammatory properties of phenolic compounds and crude extract from *Porphyra dentate*. J Ethnopharmacol 128:123–130
80. Khotimchenko SV (1991) Fatty acid composition of seven *Sargassum* species. Phytochemistry 30:2639–2641
81. Kim YH, Kim EH, Lee C, Kim MH, Rho JR (2007) Two new monogalactosyl diacylglycerols from brown alga *Sargassum thunbergii*. Lipids 42:395–399
82. Kitada K, Machmudah S, Sasaki M, Goto M, Nakashima Y, Kumamoto S, Hasegawa T (2009) Supercritical CO_2 extraction of pigment components with pharmaceutical importance from *Chlorella vulgaris*. J Chem Technol Biotechnol 84:657–661
83. Kitamura K, Matsuo M, Yasui T (1991) Fucoidan from brown seaweed *Laminaria angusta* var longissima. Agric Biol Chem 55:615–616
84. Kleinegris D, Wijffels RH (2004) Mechanism of extraction of b-carotene from microalga *Dunaliellea salina* in two-phase bioreactors. Biotechnol Bioeng 88:593–600
85. Klejdus B, Kopecky J, Benesova L, Vacek J (2009) Solid-phase/supercritical-fluid extraction for liquid chromatography of phenolic compounds in freshwater microalgae and selected cyanobacterial species. J Chromatogr A 1216:763–771
86. Konishi T, Yamazoe K, Kanzato M, Konoshima T, Fujiwara Y (2003) Three diterpenoids (excoecarins V1-V3) and a flavanone glycoside from the fresh stem of *Excoecaria agallocha*. Chem Pharm Bull 51:1142–1146
87. Kotate-Nara E, Kushiro M, Zhang H, Sagawara T, Miyashita K, Nagao A (2001) Carotenoids affect proliferation of human prostate cancer cells. J Nutr 131:3303–3306
88. Krichnavaruk S, Shotipruk A, Goto M, Pavasant P (2008) Supercritical carbon dioxide extraction of astaxanthin from *Haematococcus pluvialis* with vegetable oils as co-solvent. Bioresour Technol 99:5556–5560
89. Kumar CS, Ganesan P, Suresh PV, Bhaskar N (2008) Seaweeds as a source of nutritionally beneficial compounds—a review. J Food Sci Technol 45:1–13
90. Laturnus F (2001) Marine macroalgae in polar regions as natural sources for volatile organohalogens. Environ Sci Pollut Res Int 8:103–108
91. Lee SH, Athukorala Y (2008) Simple separation of anticoagulant sulfates galactan from marine red algae. J Appl Phycol 20:1053–1059
92. Lee JB, Hayashi K, Hashimoto M, Nakano T, Hayashi T (2004) Novel antiviral fucoidan from sporophyll of *Undaria pinnatifida* (Mekabu). Chem Pharm Bull 52:1091–1094
93. Li B, Xin JW, Sun JL, Xu SY (2006) Structural investigation of a fucoidan containing a fucose-free core from the brown seaweed *Hizikia fusiforme*. Carbohydr Res 341:1135–1146
94. Li B, Lu F, Wei X, Zhao R (2008) Fucoidan: structure and bioactivity. Molecules 13:1671–1695
95. Mabeau S, Fleurence J (1993) Seaweed in food products: biochemical and nutritional aspects. Trends Food Sci Technol 4:103–107
96. MacArtain P, Gill CIR, Brooks M, Campbell R, Rowland IR (2007) Nutritional value of edible seaweeds. Nutr Rev 65:535–543
97. Macias-Sanchez MD, Serrano CM, Rodriguez MR, Martinez de la Ossa E (2009) Kinetics of the supercritical fluid extraction of carotenoids from microalgae with CO_2 and ethanol as cosolvent. Chem Eng J 150:104–113
98. Macias-Sanchez MD, Mantell C, Rodriguez M, Martinez de la Ossa E, Lubian LM, Montero O (2009) Comparison of supercritical fluid and ultrasound-assisted extraction of carotenoids and chlorophyll a from *Dunaliella salina*. Talanta 77:948–952
99. Maeda H, Hosokawa M, Sashima T, Funayama K, Miyashita K (2005) Fucoxanthin from edible seaweed, *Undaria pinnatifida*, shows antiobesity effect through UCP1 expression in white adipose tissues. Biochem Biophys Res Commun 332:392–397

100. Maeda H, Hosokawa M, Sashima T, Miyashita K (2007) Dietary combination of fucoxanthin and fish oil attenuates the weight gain of white adipose tissue and decreases blood glucose in obese/diabetic KK-A^y mice. J Agric Food Chem 55:7701–7706
101. Matsui MS, Muizzuddin N, Arad S, Marenus K (2003) Sulfated polysaccharides from red microalgae have antiinflammatory properties in vitro and in vivo. Appl Biochem Biotechnol 104:13–22
102. Matsumoto N, Endo Y, Fujimoto K, Koike S, Matsumoto W (2001) The inhibitory effect of conjugated and polyunsaturated fatty acids on the growth of human cancer cell lines. Tohoku J Agric Res 52:1–12
103. Matsuno T (2001) Aquatic animal carotenoids. Fish Sci 67:771–783
104. Mayer AMS, Lehmann VKS (2001) Marine pharmacology in 1999: antitumor and cytotoxic compounds. Anticancer Res 21:2489–2500
105. Mayer AMS, Rodríguez AD, Berlinck RGS, Hamann MT (2009) Marine pharmacology in 2005–6: marine compounds with antihelmintic, antibacterial, anticoagulant, antifungal, anti-inflammatory, antimalarial, antiprotozoal, antituberculosis, and antiviral activities, affecting the cardiovascular, immune and nervous systems, and other miscellaneous mechanisms of action. Biochim Biophys Acta 1790:283–308
106. Mendes RL, Nobre BP, Carodoso MT, Pereira AP, Palavra AF (2003) Supercritical carbon dioxide extraction of compounds with pharmaceutical importance from microalgae. Inorg Chim Acta 356:328–334
107. Mendiola JA, Marín FR, Hernández SF, Arredondo BO, Señoráns FJ, Ibañez E, Reglero G (2005) Characterization via liquid chromatography coupled to diode array detector and tandem mass spectrometry of supercritical fluid antioxidant extracts of *Spirulina platensis* microalga. J Sep Sci 28:1031–1038
108. Mendiola JA, Herrero M, Cifuentes A, Ibáñez E (2007) Use of compressed fluids for sample preparation: food applications. J Chromatogr A 1152:234–246
109. Mendiola JA, Jaime L, Santoyo S, Reglero G, Cifuentes A, Ibañez E, Señoráns FJ (2007) Screening of functional compounds in supercritical fluid extracts from *Spirulina platensis*. Food Chem 102:1357–1367
110. Mendiola JA, García-Martínez D, Rupérez FJ, Martín-Álvarez PJ, Reglero G, Cifuentes A, Barbas C, Ibañez E, Señoráns FJ (2008) Enrichment of vitamin E from *Spirulina platensis* microalga by SFE. J Supercrit Fluids 43:484–489
111. Mendiola JA, Santoyo S, Cifuentes A, Reglero G, Ibáñez E, Señoráns FJ (2008) Antimicrobial activity of sub- and supercritical CO_2 extracts of the green alga *Dunaliella salina*. J Food Prot 71:2138–2143
112. Metting FB Jr (1996) Biodiversity and application of microalgae. J Ind Microbiol 17:477–489
113. Miao X, Wu Q (2006) Biodiesel production from heterotrophic microalgal oil. Bioresour Technol 97:841–846
114. Miller HE (1971) A simplified method for the evaluation of antioxidants. J Am Oil Chem Sci 45:91–95
115. Miller NJ, Rice-Evans C, Davies MJ et al (1993) A novel method for measuring antioxidant capacity and its application to monitoring the antioxidant status in premature neonants. Clin Sci 26:265–277
116. Mišurcová L, Stratilová I, Kráčmar S (2009) Mineral contents in food products from freshwater algae and seaweed. Chem Listy 103:1027–1033
117. Mitrovic SM, Pflugmacher S, James KJ, Furey A (2004) Anatoxin-a elicits an increase in peroxidase and glutathione S-transferase activity in aquatic plants. Aquat Toxicol 68:185–192
118. Mojaat M, Pruvost J, Focault A, Legrand J (2008) Effect of organic carbon sources and Fe^{2+} ions on growth and b-carotene accumulation by *Dunaliella salina*. Biochem Eng J 39:177–184
119. Moliné M, Libkind D, del Carmen DM, van Broock M (2009) Photoprotective role of carotenoids in yeast: response to Uv-B of pigmented and naturally-occurring albino strains. J Photochem Photobiol B 95(3):156–161
120. Moreno P, Petkov G, Ramazanov Z, Garsia G (1998) Lipids, fatty acids and sterols of *Cystoseira abies-marina*. Bot Mar 41:375–378

121. Morgan KC, Wright JLC, Simpson FJ (1980) Review of chemical constituents of the alga *Palmaria palmata* (Dulse). Econ Bot 34:27–50
122. Morrice LM, MacLean MW, Long WF, Williamson FB (1983) Phorphyran primary structure. Eur J Biochem 133:673–684
123. Muñoz R, Guieysse B (2006) Algal–bacterial processes for the treatment of hazardous contaminants: a review. Water Res 40:2799–2815
124. Murakami N, Morimoto T, Ueda T, Nagai SI, Sakakibara J, Yamada N (1992) Release of monogalactosyl diacylglycerols from cyanobacterium, *Phormidium tenue*, into its growth medium. Phytochemistry 31:3043–3044
125. Narayan B, Miyashita K, Hosakawa M (2005) Comparative evaluation of fatty acid composition of different *Sargassum* (Fucales, Phaeophyta) species harvested from temperate and tropical waters. J Aquat Food Prod Technol 13:53–70
126. Nisizawa K, Noda H, Kikuchi R, Watanabe T (1987) The main seaweed foods in Japan. Hydrobiology 151(152):5–29
127. Nobre B, Marcelo F, Passos R, Beiráo L, Palabra A, Gouveia L, Mendes R (2006) Supercritical carbon dioxide extraction of astaxanthin and other carotenoids from the microalga *Haematococcus pluvialis*. Eur Foods Technol 223:787–790
128. Noda H (1993) Health benefits and nutritional properties of nori. J Appl Phycol 5:255–258
129. Norton TA, Melkonian M, Andersen RA (1996) Algal biodiversity. Phycologia 35:308–326
130. Okai Y, Higashi-Okai K (1996) Possible immonomodulating activities of carotenoids in in vitro cell culture experiments. Int J Immunopharmacol 18(2):753–758
131. Olaizola M (2003) Commercial development of microalgal biotechnology: from the test tube to the marketplace. J Biomol Eng 20:459–466
132. Onofrejová L, Vašíčková J, Klejdus B, Stratil P, Mišurcová L, Kráčmar S, Kopecký J, Vacek J (2010) Bioactive phenols in algae: the application of pressurized-liquid and solid-phase extraction techniques. J Pharm Biomed Anal 51:464–470
133. Ortiz J, Romero N, Robert P, Araya J, Lopez-Hernandez J, Bozzo C, Navarrete E, Osorio A, Rios A (2006) Dietary fibre, amino acid, fatty acid and tocopherol contents of the edible seaweeds *Ulva lactuca* and *Durvillaea antartica*. Food Chem 99:98–104
134. Orús MI, Marco E, Martínez F (1991) Suitability of *Chlorella vulgaris* UAM 101 for heterotrophic biomass production. Bioresour Technol 38:179–184
135. Osumi Y, Kawai M, Amano H, Noda H (1998) Antitumor activity of oligosaccharides derived from *Porphyra yezoensis* porphyran. Nippon Suisan Gakk 64:847–853
136. Ota M, Watanabe H, Kato Y, Watanabe M, Sato Y, Smith RL, Inomata H (2009) Fatty acid production from a highly CO_2 tolerant alga, *Chlorocuccum littorale*, in the presence of inorganic carbon and nitrate. J Sep Sci 32:2327–2335
137. Parys S, Rosenbaum A, Kehraus S, Reher G, Glombitza KW, König GM (2007) Evaluation of quantitative methods for the determination of polyphenols in algal extracts. J Nat Prod 70:1865–1870
138. Patil G, Chethana S, Madhusudhan MC, Raghavarao KSMS (2008) Fractionation and purification of the phycobiliproteins from *Spirulina platensis*. Bioresour Technol 99:7393–7396
139. Pengzhan Y, Ning L, Xiguang L, Gefei Z, Quanbin Z, Pengcheng L (2003) Antihyperlipidemic effects of different molecular weight sulphated polysaccharides from *Ulva pertusa* (Chlorophyta). Pharmacol Res 48:543–549
140. Pernet F, Trembay R (2003) Effect of ultrasonication and crushing on lipid class extraction efficiency of filter harvested planktonic samples depending on volume and storage duration. Lipids 38:1191–1195
141. Plaza M, Cifuentes A, Ibañez E (2008) In the search of new functional food ingredients from algae. Trends Food Sci Technol 19:31–39
142. Plaza M, Herrero M, Cifuentes A, Ibañez E (2009) Innovative natural functional ingredients from microalgae. J Agric Food Chem 57:7159–7170
143. Plaza M, Santoyo S, Jaime L, Garcia-Blairsy G, Herrero M, Señorans FJ, Ibáñez E (2010) Screening for bioactive compounds from algae. J Pharm Biomed Anal 51:450–455
144. Pomin VH (2010) Structural and functional insights into sulphated galactans: a systematic review. Glycoconj J 27:1–12

145. Pomin VH, Mourao PA (2008) Structure, biology, evolution, and medical importance of sulphated fucans and galactans. Glycobiology 18:1016–1027
146. Ponce NMA, Pujol CA, Damonte EB (2003) Fucoidans from the brown seaweed *Adenocytis utricularis*: extraction methods, antiviral activity and structural studies. Carbohydr Res 338:153–165
147. Prior RL, Cao G (1999) In vivo total antioxidant capacity: comparison of different analytical methods. Free Radic Biol Med 27:1173–1181
148. Qi H, Zhang Q, Zhao T, Chen R, Zhang H, Niu X, Li Z (2005) Antioxidant activity of different sulphate content derivatives of polysaccharides from *Ulva pertusa* Kjellm (Chlorophyta). J Appl Phycol 17:527–534
149. Ramazanov Z, Jimenez del Rio M, Ziegenfuss T (2003) Sulphated polysaccharides of brown seaweed *Cystoseira canariensis* bind to serum myostatin protein. Acta Physiol Pharmacol Bulg 27:101–106
150. Rao AR, Sarada R, Ravishankar A (2007) Stabilization of astaxanthin in edible oils and its use as an antioxidant. J Sci Food Agric 87:957–965
151. Riccioni G, Mancini B, Di Ilio E, Bucciarelli T, D'Orazio N (2008) Protective effect of lycopene in cardiovascular disease. Eur Rev Med Pharmacol Sci 12:183–190
152. Ródenas de la Rocha S, Sánchez-Muniz FJ, Gómez-Juaristi M, Marín MTL (2009) Trace elements determination in edible seaweeds by an optimized and validated ICP-MS method. J Food Compos Anal 22:330–336
153. Rodríguez-Bernaldo de Quirós A, Castro de Ron C, López-Hernández J, Lage-Yusty MA (2004) Determination of folates in seaweeds by high-performance liquid chromatography. J Chromatogr A 1032:135–139
154. Roginsky V, Lissi EA (2005) Review of methods to determine chain-breaking antioxidant activity in food. Food Chem 92:235–254
155. Roginsky V, Barsukova T, Hsu CF, Kilmartin PA (2003) Chain-breaking antioxidant activity and cyclic voltammetry characterization of polyphenols in a range of green, oolong and black teas. J Agric Food Chem 51:5798–5802
156. Romay CH, González R, Ledón N, Remirez D, Rimbau V (2003) C-phycocyanin, a biliprotein with antioxidative, anti-inflammatory and neuroprotective effects. Curr Protein Pept Sci 4:207–216
157. Sabhashini J, Mahipal SVK, Reddy MC, Reddy M, Rachamallu A, Reddanna P (2004) Molecular mechanisms in C-phycocyanin induced apoptosis in human chronic myeloid leukemia cell line-K562. Biochem Pharmacol 68:453–462
158. Sachindra NM, Sato E, Maeda H, Hosokawa M, Niwano Y, Kohno M, Miyashita K (2007) Radical scavenging and singlet oxygen quenching activity of marine carotenoid fucoxanthin and its metabolites. J Agric Food Chem 55:8516–8522
159. Sajilata MG, Singhal RS, Kamat MYJ (2008) Supercritical CO_2 extraction of γ-linolenic acid (GLA) from *Spirulina platensis* ARM 740 using response surface methodology. Food Eng 84:321–326
160. Sánchez-Machado DI, López-Hernández J, Paseiro-Losada P (2002) High-performance liquid chromatographic determination of α-tocopherol in macroalgae. J Chromatogr A 976:277–284
161. Sánchez-Machado DI, López-Cervantes J, López-Hernández J, Paseiro-Losada P (2004) Fatty acids, total lipid, protein and ash contents of processed edible seaweeds. Food Chem 85:439–444
162. Sánchez-Machado DI, López-Hernández J, Paseiro-Losada P, López-Cervantes J (2004) An HPLC method for the quantification of sterols in edible seaweeds. Biomed Chromatogr 18:183–190
163. Sánchez-Machado DI, López-Cervantes J, López-Hernández J, Paseiro-Losada P (2004) Simultaneous determination of thyamine and riboflavin in edible marine seaweeds by high-performance liquid-chromatography. J Chromatogr Sci 42:117–120
164. Sánchez Mirón A, Cerón García MC, Contreras Gómez A, García Camacho F, Molina Grima E, Chisti Y (2003) Shear stress tolerance and biochemical characterization of *Phaeodactylum tricornutum* in quasi steady-state continuous culture in outdoor photobioreactors. Biochem Eng J 16:287–297

165. Santoyo S, Rodriguez-Meizoso I, Cifuentes A, Jaime L, García-Blairsy Reina G, Señoráns FJ, Ibáñez E (2009) Green processes based on the extraction with pressurized fluids to obtain potent antimicrobials from *Haematococcus pluvialis* microalgae. LWT Food Sci Technol 42:1213–1218
166. Sarada R, Vindhyavathi R, Usha D, Ravinshankar GA (2006) An efficient method for extraction of astaxanthin from green alga *Haematococcus pluvialis*. J Agric Food Chem 54:7585–7588
167. Sawayama S, Inoue S, Dote Y, Yokoyama S-Y (1996) CO_2 fixation and oil production through microalga. Energy Convers Mgmt 36:6–9
168. Schaich KM (2006) Developing a rational basis for selection of antioxidant screening and testing methods. Acta Hortic 709:79–94
169. Schubert N, García-Mendoza E, Pacheco-Ruiz I (2006) Carotenoid composition of marine algae. J Phycol 42:1208–1216
170. Schuchardt JP, Huss M, Stauss-Grabo M, Hahn A (2010) Significance of long-chain polyunsaturated fatty acids (PUFAs) for the development and behaviour of children. Eur J Pediatr 169:149–164
171. Shi Y, Sheng J, Yang F, Hu Q (2007) Purification and identification of polysaccharide derived from *Chlorella pyrenoidosa*. Food Chem 103:101–105
172. Shiratori K, Ohgami K, Ilieva I, Jin XH, Koyama Y, Miyashita K, Kase S, Ohno S (2005) Effects of fucoxanthin on lipopolysaccharide-induced inflammation in vitro and in vivo. Exp Eye Res 81:422–428
173. Silberstein JL, Parsons JK (2010) Evidence-based principles of bladder cancer and diet. Curr Nutr Food Sci 6:2–12
174. Simó C, Herrero M, Neusüb C, Pelzing M, Kenndler E, Barbas C, Ibáñez E, Cifuentes A (2005) Characterization of proteins from *Spirulina platensis* microalga using capillary electrophoresis-ion trap-mass spectrometry and capillary electrophoresis-time of flight-mass spectrometry. Electrophoresis 26:2674–2683
175. Simon D, Helliwell S (1998) Extraction and quantification of chlorophyll a from freshwater green algae. Water Res 32:2220–2223
176. Simopoulos AP (1996) The role of fatty acids in gene expression: health implications. Ann Nutr Metab 40:303–311
177. Siriwardhana N, Lee KW, Kim SK, Ha JW, Jeon YJ (2003) Antioxidant activity of *Hizikia fusifonnis* on reactive oxygen species scavenging and lipid peroxidation inhibition. Food Sci Technol Int 9:339–346
178. Slavin J, Green H (2007) Dietary fibre and satiety. Nutr bull 32:32–42
179. Sloan AE (2000) The top ten functional food trends. Food Technol 54:33–62
180. Sloan AE (1999) The new market: foods for the not-so-healthy. Food Technol 53:54–60
181. Souza PH, Leao-Ferreira LR, Moussatche N, Teixeira VL, Cavalcanti DN, da Costa LJ, Diaz R, Frugulhetti IC (2008) Effects of diterpenes isolated from the Brazilian marine alga *Dictyota menstrualis* on HIV-1 reverse transcriptase. Planta Med 71:1019–1024
182. Spolaore P, Joannis-Cassan C, Duran E, Isambert A (2006) Commercial applications of microalgae. J Biosci Bioeng 101:87–96
183. Stafsnes MH, Josefsen KD, Kildahl-Andersen G, Valla S, Ellingsen TE, Bruheim P (2010) Isolation and characterization of marine pigmented bacteria from Norwegian coastal waters and screening for carotenoids with UVA-blue light absorbing properties. J Microbiol 48:16–23
184. Stanley JC, Elsom RL, Calderm PC, Griffin BA, Harris WS, Jebb SA, Lovegrove JA, Moore CS, Riemersma RA, Sanders TAB (2007) UK Food Standards Agency Workshop Report: the effects of the dietary n-6:n-3 fatty acid ratio on cardiovascular health. Br J Nutr 98:1305–1310
185. Steinke M, Mallin G, Liss PS (2008) Trophic interactions in the sea: an ecological role for climate relevant volatiles? J Phycol 38:630–638
186. Takamatsu S, Hodges TW, Rajbhandari I, Gerwick WH, Hamann MT, Nagle DG (2003) Marine natural products as novel antioxidant prototypes. J Nat Prod 66:605–608
187. Tanaka Y, Sasaki N, Ohmiya A (2008) Biosynthesis of plant pigments: anthocyanins, betalains and carotenoids. Plant J 54:733–749

188. Tasende MG (2000) Fatty acid and sterol composition of gametophytes and sporophytes of *Chondrus crispus* (Gigartinaceae, Rhodophyta). Sci Mar 64:421–426
189. Thana P, Machmudah S, Goto M, Sasaki M, Pavasant P, Shotipruk A (2008) Response surface methodology to supercritical carbon dioxide extraction of astaxanthin from *Haematococcus pluvialis*. Bioresour Technol 99:3110–3115
190. Tosh SM, Yada S (2010) Dietary fibres in pulse seeds and fractions: characterization, functional attributes, and applications. Food Res Int 43:450–460
191. Ukibe K, Hashida K, Yoshida N, Takagi H (2009) Metabolic engineering of *Saccharomyces cerevisiae* for astaxanthin production and oxidative stress tolerance. Appl Environ Microbiol 75:7205–7211
192. Verma NM, Mehrotra S, Shukla A, Mishra BN (2010) Prospective of biodiesel production utilizing microalgae as the cell factories: a comprehensive discussion. Afr J Biotechnol 9:1402–1411
193. Vismara R, Vestir S, Kusmic C, Barsanti L, Gualtieri P (2003) Natural vitamin E enrichment of *Artemia salina* red freshwater and marine microalgae. J Appl Phycol 15:75–80
194. Voutilainen S, Nurmi T, Mursu J, Rissanen TH (2006) Carotenoids and cardiovascular health. Am J Clin Nutr 83:1265–1271
195. Wang J, Chen B, Rao X, Huang J, Li M (2007) Optimization of culturing conditions of *Porphyridium cruentum* using uniform design. World J Microbiol Biotechnol 23:1345–1350
196. Watanabe F, Takenaka S, Katsura H, Zakir Hussain Masumder SAM, Abe K, Tamura Y, Nakamo Y (1999) Dried green and purple lavers (Nori) contain substantial amounts of biologically active vitamin B12 but less of dietary iodine relative to other edible seaweeds. J Agric Food Chem 47:2341–2343
197. Wiltshire KH, Boersma M, Moller A, Buhtz H (2000) The extraction and analyses of pigments and fatty acids from the green alga *Scenedesmus obliquus*. Aquat Ecol 34:119–126
198. Ye ZW, Jiang JG, Wu GH (2008) Biosynthesis and regulation of carotenoids in *Dunaliella*: progresses and prospects. Biotechnol Adv 26:352–360
199. Yukino T, Hayashi M, Inoue Y, Imamura J, Nagano N, Murata H (2005) Preparation of docosahexaenoic acid fortified *Spirulina platensis* and its lipid and fatty acid compositions. Nippon Suisan Gakk 71:74–79
200. Yun YS, Lee SB, Park JM, Lee CI, Yang JW (1997) Carbon dioxide fixation by algal cultivation using wastewater nutrients. J Chem Technol Biotechnol 69:451–455
201. Zhang QQ, Zhao T, Deslandes E, Ismaeli NB, Molloy F, Critchley T (2005) Chemical characteristic of a polysaccharide from *Porphyra capensis* (Rhodophyta). Carbohydr Res 340:2447–2450
202. Zhao T, Zhang Q, Qi H, Zhang H, Niu X, Xu Z, Li Z (2006) Degradation of porphyran from *Porphyra haitanensis* and the antioxidant activities of the degraded porphyrans with different molecular weight. Int J Biol Macromol 38:45–50
203. Zhao L, Chen G, Zhao G, Hu X (2009) Optimization of microwave-assisted extraction of astaxanthin from *Haematococcus pluvialis* by response surface methodology and antioxidant activities of the extracts. Sep Sci Technol 44:243–262
204. Zhekisheva M, Boussiba S, Khozin-Goldberg I, Zarka A, Cohen Z (2002) Accumulation of oleic acid in *Haematococcus pluvialis* (chlorophyceae) under nitrogen starvation or high light is correlated with that of axtaxanthin esters. J Phycol 38:325–331
205. Zheng W, Wise ML, Wyrick A, Metz JG, Yuan L, Gerwick WH (2002) Polyenoic fatty acid isomerise from the marine alga *Pilota ficina*: protein characterization and functional expression of the cloned cDNA. Arch Biochem Biophys 401:11–20
206. Zhu YH, Jiang JG (2008) Continuous cultivation of *Dunaliella salina* in photobioreactor for the production of β- carotene. Eur Food Res Technol 227:953–959
207. Zuliani G, Galvani M, Leitersdorf E, Volpato S, Cavelieri M, Fellin R (2009) The role of polyunsaturated fatty acids (PUFA) in the treatment of dyslipidemias. Curr Pharm Des 15:4173–4185

Chapter 36
Biogas Production from Algae and Cyanobacteria Through Anaerobic Digestion: A Review, Analysis, and Research Needs

Pavlo Bohutskyi and Edward Bouwer

Abstract Anaerobic digestion is a common process for the treatment of a variety of organic wastes and biogas production. Both, macro- and microalgae are suitable renewable substrates for the anaerobic digestion process. The process of biogas production from algal biomass is an alternative technology that has larger potential energy output compared to green diesel, biodiesel, bioethanol, and hydrogen production processes. Moreover, anaerobic digestion can be integrated into other conversion processes and, as a result, improve their sustainability and energy balance. Several techno-economic constraints need to be overcome before the production of biogas from algal biomass becomes economically feasible. These constraints include a high cost of biomass production, limited biodegradability of algal cells, a slow rate of biological conversion of biomass to biogas, and high sensitivity of methanogenic microorganisms. The research opportunities include a variety of engineering and scientific tasks, such as design of systems for algae cultivation and anaerobic digestion; optimization of algae cultivation in wastewater, nutrients recycling and algal concentration; enhancement of algal biomass digestibility and conversion rate by pretreatment; deep integration with other technological processes (e.g., wastewater treatment, co-digestion with other substrates, carbon dioxide sequestration); development and adaptation of molecular biology tools for the improvement of algae and anaerobic microorganisms; application of information technologies; and estimation of the environmental impact, energy and economical balance by performing a life cycle analysis.

P. Bohutskyi • E. Bouwer (✉)
Department of Geography and Environmental Engineering, Johns Hopkins University, 3400 North Charles Street, Ames Hall 313, Baltimore, MD 21218, USA
e-mail: bouwer@jhu.edu

J.W. Lee (ed.), *Advanced Biofuels and Bioproducts*, DOI 10.1007/978-1-4614-3348-4_36, 873

1 Introduction

People have been using anaerobic digestion processes (ADP) for centuries, but the first documented digestion plant was constructed in Bombay, India in 1859 [1]. The first usage of biogas from a digester plant was reported in 1895 in Exeter, England where biogas was used for street lighting [2]. Approximately 15 million digesters, including small farm-based digesters, are now operated in China [3, 4]. And about 12 million digesters are located in India [3, 5].

High fuel prices coupled with an increasing awareness of greenhouse gas emissions and global warming have promoted an interest in further anaerobic digestion (AD) research and industrial applications. Now, the ADP is viewed not only as a method for treatment of sewage biosolids, livestock manure, and concentrated wastes from food industry, but also as a potentially significant source of renewable fuel. The biogas gross production (Table 1) within developed countries has nearly doubled from 2000 to 2007 [6].

Different agricultural crops and terrestrial and aquatic plants are proven to be an appropriate feedstock for AD [7]. Indeed, the National Algal Biofuels Technology Roadmap 2010 noted that anaerobic digestion is an underutilized technology for algal biofuel production that "eliminates several of the key obstacles that are responsible for the current high costs associated with algal biofuels, and as such may be a cost-effective methodology" [8]. For instance, the AD of algal biomass to biogas possesses advantages compared to other biofuel sources and conversion techniques, such as:

- Higher productivity. Algae have a higher conversion efficiency of light energy to biomass compared to plants, up to 5–10% vs. 0.5–3% [9–12].
- Water quality is less critical. Wastewater, brackish water and even seawater can be used for algae culturing in addition to fresh water.
- Noncompetitive to food production. Algae can be cultivated on nonarable lands and in the ocean.
- Carbon dioxide sequestration. Algae convert carbon dioxide into biomass, and culture media can be enriched with carbon dioxide from gases exhausted from power plants or other sources.
- Elimination of several energy consuming steps. The ADP does not require drying and an extraction steps as well as a high extent of algal biomass dewatering.
- Deeper level of algal biomass utilization is possible. The ADP can convert all fractions of organic matter, including lipids, proteins, carbohydrates, and nucleic acids to biofuel.
- Partial recycling of nutrients with AD effluent. Anaerobic digestion is a natural conversion process that releases nutrients in a potentially usable and recyclable form. The supernatant liquid with higher nitrogen and phosphorus content can be used as a fertilizer for algae culturing. Moreover, the solid phase can be used as a biofertilizer in agriculture or as a livestock nutrient.
- Integration with other technologies is possible. For instance, the ADP can be used as a co-technology for algal residues utilization after biodiesel, green diesel,

Table 1 Gross production of biogas in countries (2000 and 2007)

	Biogas—gross production (TJ)	
Country/area	2000 year	2007 year
United States	123,966	183,674
Germany	23,341	100,628
United Kingdom	33,912	66,657
France incl. Monaco	6,133	16,896
Italy and San Marino	5,480	16,240
Australia	5,780	11,643
Republic of Korea	1,380	7,912
Spain	5,492	7,693
Total	205,484	411,343

bioethanol, and hydrogen production. Furthermore, a variety of organic wastes and by-products can be co-digested with algae to produce biogas.
- Environmental friendly process. No toxic materials are produced during ADP.

Nevertheless, the process of methane production from algae has several limitations that need to be overcome to become an attractive technology for producing renewable energy:

- High capital cost of algae production and AD units.
- Relatively low algae productivity. Algae growth rate is relatively limited by low efficiency of photosynthesis, photoinhibition, and carbon assimilation.
- Incomplete digestibility of algal cells. The algal biomass partially contains recalcitrant organic matter that cannot be hydrolyzed by the conventional ADP.
- Conversion rate is relatively slow. Generally, biomass residence time in the ADP varies between 10 and 30 days.
- In some cases, algal biomass has an unbalanced C:N ratio. A low ratio can lead to the accumulation of NH_4^+ in an anaerobic digester to inhibitory levels while lack of nitrogen can limit anaerobic conversion and methane production.
- High sensitivity of the ADP. Methanogenic organisms are sensitive to fluctuations of environmental and operational parameters.

This chapter provides a literature review and analysis of biogas production from algal biomass though ADP. In the first part, we describe morphological, ecological, and biochemical characteristics of cyanobacteria and three major algae groups as well as their current commercial applications. The second part provides background on ADP and focuses on the algae anaerobic digestion research in the past several decades. Finally, we discuss prospective methods for enhancement of algae production and anaerobic digestion with emphasis on metabolic manipulations, genetic engineering, algae pretreatment, co-digestion with other feedstocks, and integration of algae AD into other technological processes.

2 Algae as the Feedstock for the Anaerobic Digestion Process

Algae are a large and very diverse group of organisms ranging from simple unicellular microalgae to giant macroalgae. The morphology of macroalgae or seaweeds resembles the terrestrial plants but the biochemical composition is significantly different. The major carbon storage products in terrestrial plants are starch and fructosan [13–15] that can be easily converted to biogas. However, the main components of terrestrial plant cell walls are cellulose/hemicellulose fibers embedded into a pectin matrix and cemented together by lignin [16–18]. This lignocellulosic complex is recalcitrant to biological degradation and requires intensive chemical (acid hydrolysis, alkaline wet oxidation, ammonia fiber expansion) or thermal pretreatment (steam explosion, hot water) before biological conversion [19–22].

The major components of macroalgae are polysaccharides, algal cell wall lack lignin. The main components of cell envelopes are ulvan and xylan in green algae; carrageen, agar, and xylose in red algae; alginate and fucoidan in brown algae. Cellulose is a structural component of the cell wall in many genera, but only in some green algae is the ratio on a level comparable to terrestrial plants. The main storage polysaccharides in macroalgae are floridean starch in red algae; chlorophycean in green macroalgae; laminarin; and mannitol in brown macroalgae.

The biochemical composition of microalgae and cyanobacteria are significantly different from macroalgae. Often carbohydrates are a minor component of cell dry weight, whereas proteins and lipids account for the bulk of microalgal dry weight.

One of the challenges in AD of algae is significant variation in biochemical composition not only among different phylum or genera, but also among similar species. Biochemical composition depends on many environmental factors, such as temperature, salinity, light intensity, and nutrient availability [23–27].

2.1 Cyanophyta (Blue-Green Algae)

The Cyanophyta is a unique group of prokaryotic microorganisms and a member of a large group of photosynthetic organisms [28]. In contrast to purple and green bacteria, the photosynthetic mechanism of cyanobacteria is oxygenic and similar to the photosynthesis mechanism in plants and algae. Several filamentous blue-green algae are able to form heterocysts, which contain the enzyme nitrogenase and fix atmospheric nitrogen [29]. Cyanobacteria possess chlorophyll *a* and phycobiliproteins as part of their light harvesting antennae [30]. But cyanobacteria lack membrane-bound cell organelles (nucleus, mitochondria, chloroplast), which are defining characteristics of the Eukaryotic Kingdom [31]. Cyanobacteria are found elsewhere in marine, brackish water, freshwater, and terrestrial habitats with a variety of morphological forms: unicellular and colonial non-motile, colonial, and filamentous [32, 33]. The characteristics of Cyanophyta are presented in Table 2.

Table 2 Cyanophyta species major organic matter characteristics

Characteristic	Description	References
Nutrient reserves	Cyanophycean starch (α-1,4-glucan) as carbon and energy; cyanophycin (arginine and asparagine polymer) as nitrogen storage; polyphosphate as phosphorus storage; poly(hydroxyalkanoate)	[31, 492–496]
Cell wall organization	Multiple-layered. Envelope consists of cytoplasmic membrane and cell wall. Optional outer membrane, s-layer, sheath, capsule, and slime. Four-layered peptidoglycan (murein) is principal component. Consists of glycan backbone with peptide cross linkages	[497–504]

Table 3 Biochemical and chemical composition of selected cyanobacteria

Component	*Arthrospira maxima*	*Arthrospira platensis*	*Anabaenopsis* sp.	*Oscillatoria deflexa*
Ash	–	–	9.35	9.1
Carbohydrates	10–16	10–16	41.3	10
Protein	64–70	62–72	41.2	54.5
Lipids	6	6–7	8.1	13.8
References	[505]		[506]	[507]

Table 4 Productivity of cyanobacteria

Species	Reactor type	P_{arial} (g/m^2-day)	P_{volume} (g/L-day)	References
Arthrospira sp.	Outdoor airlift tubular undulating row (11 L)	25.4	1.15	[508]
A. platensis	Outdoor tubular undulating row (11 L)	47.7	2.7	[509]
A. platensis	Dairy wastewater anaerobic lagoon effluent (1 L)	70	0.07	[480]
A. platensis	Indoor fermenter (4 L)	–	0.17	[505]
A. maxima		–	0.16	
A. maxima	Open pond	–	0.21	[510]

Cyanobacteria are used for a variety of purposes including as a food and feed supplement due to their high protein (Table 3) and vitamin content, as a good source of fiber, and for their good digestibility. Other current and prospective applications of cyanobacteria include the production of pharmaceuticals (antiviral, antibacterial, antifungal, and anticancer compounds), enzymes, wastewater treatment, and use as a biofertilizer [34, 35]. Cyanobacterial species are characterized by high productivity (Table 4).

Table 5 Rhodophyta species major organic matter characteristics

Characteristic	Description	References
Nutrient reserves	Floridean starch (α-1,4-glucan) in cytoplasm for long-term storage. Sugars and glycosides (trehalose, floridoside, maltose, sucrose) are the primary products of photosynthesis	[511–517]
Cell wall organization	Multiple-layered. Amorphous mucilage from sulfated polysaccharides (agars and carrageenans) about 70% from dry weight	[116, 512, 518–521]
	Florideophyceae—rigid cellulose polysaccharides	
	Bangiophycidae—rigid β-1,3xylan. Outer cuticle from protein or β-1,4mannan	
	Corralinaceae and some Nemaliales calcified with $CaCO_3$	

2.2 *Rhodophyta (Red Algae)*

The Rhodophyta is a relatively well-defined group of about 6,000 algal species with several features that differentiate them from other algal divisions, such as the presence of accessory phycobilin pigments, the absence of flagella and centrioles [36]. The vast majority of red algae are marine multicellular, macroscopic species, which account for the majority of the so-called seaweeds [37]. The main habitats are nearshore and offshore zones (down to 40–60 m) in tropical and temperate climate regions while the presence of accessory pigments allow algae to grow at depths down to 200–250 m. Species with calcified cell walls are important for the establishment and support of coral reef formation. Red algae are also found in brackish and fresh water, as well as in soil [38, 39].

Porphyra species are an important food source for humans in the Asia region [40]. Several Rhodophyta species (*Gelidium*, *Gracilaria*) are an important source of agar and agarose [41]. These polysaccharides are used in many laboratories for preparing culture media and separating nucleic acids [42]. Carrageenan is widely used in the food industry as a gel forming substance and stabilizer [43] (Tables 5–7). Structural, biochemical characteristics and productivity of selected red algae species are presented in Tables 5–7.

2.3 *Chlorophyta (Green Algae)*

Chlorophyll *a* and *b* are the dominant pigments in Chlorophyta and are the source of the second name of these organisms—Green algae. The secondary pigments are carotenoids (β-carotene, prasinoxanthin, siphonaxanthin, astaxanthin) which sometimes give algae their yellowish-green and red-green colors [44]. The major habitat for green algae is freshwater although they are also found in sea or brackish water, and in soil [38, 39, 45, 46]. Chlorophyta species are unicellular or colonial motile and non-motile, filamentous, coccoid, parenchimatous, and siphonous [37, 47].

Table 6 Productivity of Rhodophyta species

Species	Reactor type	P_{arial} (g/m^2-day)	P_{volume} (g/L-day)	References
Porphyridium cruentum	Airlift tubular (200 L)	–	1.5	[522]
Porphyra	Natural population	3.6	–	[179]
Gracilaria chilensis	Outdoor tank	11.2	–	[523]
G. chilensis	Spray culture	0.5	–	[524]
G. tikvahiae (Florida)	Outdoor tank, aerated, nutrients (50 L)	12–46 (34.8^{ave})	0.06–0.21 (0.16^{ave})	[483, 525]
G. tikvahiae (Florida)	Same, AD effluent (2.4 m^3)	25	–	[483]
G. tikvahiae	Tank, aerated, nutrients (2.4–24 m^3)	22–25	–	[526]
	Pond, non-aerated (9 m^3)	5–8	–	
G. tikvahiae (Florida)	Pond (non-aerated)	9.7	–	[527]
	Pond (aerated)	11.5	–	
	Pond (large scale)	7.2	–	
	Cage culture	0–44 (13.9^{ave})	–	
G. tikvahiae (Taiwan)	Pond (<300 ha)	4.4–11.8	–	[528]
Palmaria palmata	Natural population	0.65–2.3	–	[529]
Gracilaria sp. (Florida)	Tank, nutrients	7–16	–	[179]
P. palmata	Natural population	24	–	
Hypnea musciformis	Tank, nutrients	12–17	–	
Chondrus crispus	Tank	25–30	–	
Rhodoglossum affine	Tank	12–30	–	
Iridaea cordata	Natural population	4–14	–	
I. cordata	Outdoor tank (1.4 m^3)	1.95 (20.7^{max})	–	[530]

Table 7 Biochemical and chemical composition of selected red algae

Component[a]	*C. crispus*	*P. palmata*	*G. tikvahiae*	*Gracilaria verrucosa*	*Gracilaria cervicornis*	*P. cruentum*
Water	74.1–80.9	83–90	–	–	14.66 ± 1.78	–
Ash	27.3–35.7	20.2–28.8	29–42	25–29	10.5 ± 1.6	20 ± 2.4
Carbon	24.6–30.7	30–34.9	28.1–30.8	33.8–34.1	–	–
Hydrogen	3.6–4.5	4.5–5.6	4.5–4.6	4.3–4.7	–	–
Oxygen (calculated)	32.5–33.2	32.9–35.1	27.5–30.4	27.9–33.2	–	–
Nitrogen	3.1–4.7	3.8–4.1	3.7–4.8	3.4–4.7	3.2 ± 0.4	–
Sulfur	3.8–5	0.5	–	–	–	1.41 ± 0.16
Alginate	0.6–2	0.6–3.1	–	–	–	–
Fukoidan	0.4–0.7	0.1–9.7	–	–	–	–
Carrageenan + agar	11–22.6	15.6–30	44.6–53.7	39–45	–	–
Total carbohydrates	40.5–54.9	23.1–60.9	42.5–54.7	64–75.5	63.1 ± 3.5	32.1 ± 5.6
Protein	–	–	13.3–36.2	11.9–12.3	19.7 ± 2.7	34.1 ± 4.4
Lipids	–	–	–	–	0.43 ± 0.06	6.53 ± 0.46
Chlorophyll	–	–	–	–	–	0.25 ± 0.15
Fiber	–	–	–	–	5.7 ± 0.7	0.39 ± 0.13
Cellulose	2–4.8	4–4.4	–	–	–	–
Sugars/alcohols	1–6	19.4–27.1	–	–	–	–
Polyphenols/lignin	2.2–3	2.1–2.8	–	–	–	–
C/N ratio	5.9–7.9	7.9–8.5	5.32–7.72	–	–	–
References	[531]		[121]		[532]	

[a]All data are given as a % from dry weight, water as a % from fresh weight and C/N ratio unit less

Table 8 Chlorophyta species major organic matter characteristics

Characteristic	Description	References
Nutrient reserves	Chlorophycean: mix of amylose (α-1,4-linkage) and amylopectine (α-1,4 and α-1,6 linkage) inside of chloroplast	[511, 533–540]
	Lipids	
	Polyphosphate granules	
Cell wall organization	Mostly two layered	[161, 162, 170, 541–549]
	Outer mucilage or capsule	
	Structural component—crystalline cellulose (Cladophorales), amorphous cellulose (Ulvales, Oedogoniales, coccoid algae), xylose or mannose (Caulerpales, Codiaceae, Polyphysaceae) in hemicellulose, glycoproteins (Volvocales)	
	Several microalgae (e.g., Chlorellaceae, Scenedesmaceae, Hydrodictyaceae families) have resistant trilaminar structure containing nonhydrolysable biopolymer—algaenan	
	Some marine siphonous species are calcified with $CaCO_3$	

Halophilic microalga *Dunaliella* is widely cultivated for the production of β-carotene and other human nutritional products [48]. Species from Ulvophyceae group are mostly marine macroscopic algae that are used as food in coastal regions and can be used for nitrogen removal during wastewater treatment [49] (Tables 8–10).

2.4 *Heterokont (Brown Algae, Yellow-Green Algae, Golden Algae, Diatoms, and Others)*

Heterokonts are a large and very diverse group of algae identified relatively recently that possess similar morphology, photosynthetic pigments, ultrastructural features, and genetic code [50, 51]. Several Heterokont groups of algae correspond to formerly distinct phylum, the Chrysophyta and Phaeophyta. The species are widespread in brackish water, freshwater, marine and terrestrial habitats. And chlorophyll *a* and *c* are the main photosynthetic pigments, and the main carotenoids are fucoxanthin or vaucheriaxanthin [52] (Tables 11 and 12).

Several Heterokont algae are used in mariculture. *Isochrysis galbana*, *Chaetoceros muelleri*, as well as diatoms *Skeletonema costatum*, *Nitzschia* and *Navicula* spp. are used to feed molluscs; *Nannochloropsis* is used to feed rotifers [53]. In the past

Table 9 Productivity of Chlorophyta species

Species	Reactor type	P_{aerial} (g/m-day)	P_{volume} (g/L-day)	References
Chlorella sorokiniana	Outdoor inclined tubular photobioreactor (6 L)	50	1.5	[550]
C. sorokiniana	Outdoor helical tubular (14 L)	25.2	0.9[a]	[551]
Chlorella sp. (*strain P12*)	Outdoor open thin-layer (400 L)	22.8	3.8	[552]
Chlorella sp. (*strain P12*)	Outdoor open thin-layer (2 m^3)	38.2	4.3	[553]
Chlorella vulgaris	Open pond	–	0.18	[510]
C. vulgaris	Flat-panel airlift (1 L)	17	0.56[a]	[554]
Haematococcus pluvialis	Enclosed parallel tubular (75 m^3)	13	0.05	[555]
H. pluvialis	Outdoor airlift tubular (25 m^3)	10.2	0.08[a]	[556]
Scenedesmus obliquus	Open pond	–	0.09	[510]
Dunaliella tertiolecta	Open pond	–	0.12	
Chlorella, *Scenedesmus*	Open pond, nutrients (20–80 m^2)	8.6	–	[557]
Scenedesmus	Agricultural tile drainage	10	–	[558]
Scenedesmus and *Coelastrum* (Kuwait)	High rate wastewater pond (50 m^2)	15 (30^{max})	–	[469]
Scenedesmus and *Coelastrum* (Kuwait)	High rate wastewater pond (50 m^2)	24 (38^{max})	–	[470]
T. suecica	Outdoor annular columns (960 L)	38.2	0.42	[559]
T. suecica	Outdoor flume, nutrients (48 m^2)	26.2[b]	–	[11, 12]
	Same, with foil arrays	33[b] ($44^{b})^{max}$	–	
Neochloris oleoabundans	Flat-panel airlift (1 L)	16.5	0.55	[560]
N. oleoabundans (N starvation)	Flat-panel airlift (1 L)	5.4	0.18	
Chlorococum littorale	Outdoor dome shaped (130 L)	10.95	0.095	[561]
C. littorale	Outdoor parabola shaped (70 L)	14.9	0.09	
C. littorale	Outdoor pipe shaped (70 L)	20.5	0.146	
Ulva lactuca	Tank, aerated, nutrients (0.7 m^3)	17	–	[562]
	Same, non-aerated	6.8	–	
U. lactuca	Pond (800 m^2)	7–24 (18.3^{max})	–	[563]
Ulva (Florida)	Same, nutrients (2.4 m^3)	15–25	–	[483, 564]
Ulva (Florida)	Same, AD effluent (2.4 m^3)	15–25	–	
U. lactuca and *Enteromorpha* spp.	Natural populations	0.3–1.7	–	[529]
Enteromorpha linza, *E. prolifera*, *Percursaria percursa*	Tanks (400 L), wastewater 0–40%	15^{max}	–	[565]

[a]Estimated from data given in the paper

[b]Estimated from data given in the paper using a VS/TS ratio of 0.9

several decades, diatoms were studied for the production of pharmaceuticals, health products, biomolecules, nanomaterials, and bioremediators [54]. Several diatoms and Pinguiophyceae species have large biotechnological potential due to their high content of eicosapentenoic acid [55, 56].

The brown algae (Phaeophyceae) are among the most cultivated algal species. Several brown algae were found to be good feedstock for AD. The composition of several species is presented in Table 13.

The alginate is a linear (1-4)-linked glycuronan composed of β-1,4-D-mannuronic acid and α-1,4-L-guluronic acid [57]. Mannitol is an alcohol.

Fucoidan structure varies in different algal species. Generally, it is a nonuniformly branched and sulfated polysaccharide with backbone composed of alternating 1-3- and 1-4-linked α-L-fucopyranosyl units [58, 59] (Table 14).

3 Principles of the Anaerobic Digestion Process

AD is a complex biological process performed by a consortium of anaerobic bacteria and archaea. In this section, we provide a description of the ADP biochemistry and microbiology, the influence of environmental and physicochemical parameters on process performance, and the importance of biogas composition and its application.

3.1 Biochemistry and Microbiology of Anaerobic Digestion

Algal biomass consists of a mixture of organic and inorganic matter. The organic part is composed of complex polymeric macromolecules, such as proteins, polysaccharides, lipids, and nucleic acids. The polymers appear in particulate or colloidal form. The ADP converts organic matter to the final products (methane and carbon dioxide), new biomass, and inorganic residue. Several groups of microorganisms are involved in substrate transformation and the overall process comprises multiple stages with many intermediate products. Generally, the process can be simplified to four consecutive steps: (1) hydrolysis; (2) fermentation or acidogenesis; (3) acetogenesis; and (4) methanogenesis.

The overall transformation can be described by six distinct biological processes as shown in Fig. 1 (modified from [60]):

1. Hydrolysis of colloid and particulate biopolymers to monomers.
2. Fermentation or acidogenesis of amino-acids and sugars to intermediary products (propionate, butyrate, lactate, ethanol, etc.), acetate, hydrogen, and formate.
3. β-oxidation of long-chain fatty acids and alcohol fermentation to volatile fatty acids (VFA) and hydrogen.
4. Anaerobic oxidation or acetogenesis of intermediary products, such as VFAs to acetate, carbon dioxide, and hydrogen. This reaction is performed by obligate and facultative hydrogen producing species.

Table 10 Biochemical and chemical composition of selected green algae

Component[a]	*Codium fragile*	*U. lactuca* or *rigida*	*Ulva* sp.	*Chlamydomonas* sp.	*Chlorella pyrenoidosa* (low lipid)	*C. pyrenoidosa* (lipid rich)	*Chlorella* sp.	*Chlorella* sp. (depleted residues)
Water	92.2	79.9–88.4	–	–	–	–	–	–
Ash	40.2	20.9–49.3	18.72	4.74	3.45	3.45	–	–
Carbon	19.2	18.4–35.4	38.06	45.21	47.8	67.75	53.8	44.8–47.5
Hydrogen	3.4	2.4–5	4.95	6.5	6.55	10.17	8.5	7.1–7.5
Oxygen (calculated)	35.6	27.4–37.4		38.02			29.9	46.6–47.5
Nitrogen	1.6	2.5–4.9	3.96	5.53	8.99	1.38	7.3	9.4–10.1
Sulfur	4.1	1.6–4.1	–	–	–	–	0.5	1–2.2
Alginate	<2	0.5–2	–	–	–	–	–	–
Mannitol	1.3	–	–	–	–	–	–	–
Fukoidan	0.5	4.9–8	–	–	–	–	–	–
Total carbohydrates	38.2	24.3–58.5	56.57	55.44	36.2	9.17	26.2	35.2–39.6
Protein	–	–	24.7	34.6	56	7.05	45.5	60.2–64.1
Lipids	–	–	trace	5.24	4.34	80.3	26.2	0.2–2
Chlorophyll	–	–	–	–	–	–	–	–
Cellulose	4.1	1.3–11.9	–	–	–	–	–	–
Sugars/alcohols	1.2	1.8–3.4	–	–	–	–	–	–
Polyphenols/lignin	7	1.6–12.4	–	–	–	–	–	–
C/N ratio	10	7.2–10.6	9.61	8.18	5.3	49.1	7.3	4.61–4.79
References	[531]		[506]				[436]	

[a]All data are given as a percent from dry weight, water percent from fresh weight and C/N ratio unit less

D. tertiolecta	*Nanno-chloris atomus*	*Tet-raselmis chui*	*T. suecica*	*Chlorella prototh-ecoides*	*Chlorella* sp. (CS-247)	*Stichoc-coccus* sp.	*Pyramimonas cordata*	*Pycnococcus provasolii*	*Micromonas pusilla*, tropical (temperate)
–	–	–	–	–	–	–	–	–	–
–	–	–	–	–	–	–	–	–	–
–	–	–	–	–	–	–	–	–	–
–	–	–	–	–	–	–	–	–	–
–	–	–	–	–	–	–	–	–	–
–	–	–	–	–	–	–	–	–	–
–	–	–	–	–	–	–	–	–	–
–	–	–	–	–	–	–	–	–	–
–	–	–	–	–	–	–	–	–	–
–	–	–	–	–	–	–	–	–	–
12.2	23	12.1–13.9	12	10.8	11–16.1	16.1	16.3	13.8	16.7 (14.3)
20	30	18.1–31	31	25.6	15.2–15.4	22.5	17	17.3	5.5 (17.7)
15	21	13.9–17	10	12.8	11.1–18.4	8.5	9.5	16.7	10.9 (13.3)
1.73	0.37	1.36–1.42	0.97	0.97	0.23–0.72	0.32	1.38	0.63	1.01 (1.54)
–	–	–	–	–	–	–	–	–	–
–	–	–	–	–	–	–	–	–	–
–	–	–	–	–	–	–	–	–	–
–	–	–	–	–	–	–	–	–	–
[566]					[567]				

Table 11 *Heterokonts* species major organic matter characteristics

Characteristic	Description	References
Nutrient reserves	Phaeophyceae: laminarin (β-1,3-glucan, mannitol) Xanthophyceae, Eustigmatophyceae: β-1,3-glucan, lipids Chrysophyceae: Chrysolaminarin (β-1,3-glucan with β-1,6 branches) Bacillariophyceae: Chrysolaminaran, lipids Eustigmatophyceae: oils	[38, 39, 568–573]
Cell wall organization	Phaeophyceae. Outer layer: alginic acid and fucoidan (sulfated mucopolysaccharide). Internal layer: cellulose Xanthophyceae: cellulose, glucose, uronic acid Bacillariophyceae: frustule (silica) Eustigmatophyceae, Raphidophyceae, Chrysophyceae: usually naked. Some Chrysophyceae have cellulosic, silicated, calcified, mucilage or lorica wall	[37, 39, 574–581]

Table 12 Productivity of Heterokonts species

Species	Reactor type	P_{aerial} (g/m^2-day)	P_{volume} (g/L-day)	References
Nannochloropsis sp. (spring)	Glass flat plate (440 L)	14.2	0.27	[582]
Nannochloropsis sp. (winter)	Glass flat plate (440 L)	10	0.21	
Nannochloropsis sp.	Open pond	–	0.09	[510]
Cylindrotheca closterium	Flat-panel airlift (1 L)	14	0.46[a]	[554]
Phaeodactylum tricornutum	Outdoor airlift tubular (200 L)	20	1.2	[583]
P. tricornutum	Outdoor airlift tubular (200 L)	32	1.9	[584]
P. tricornutum	Outdoor helical tubular (75 L)	40[a]	1.4	[585]
Chaetoceros calcitrans	Outdoor pipe shaped (70 L)	37.3	0.27	[561]
Ascophyllum nodosum	Natural population	5.5	–	[586]
A. nodosum	Spray culture	1.2–8 (2.8[ave])	–	[587]
Laminaria hyperborea	Natural population	1.9–13.2 (82[ave])	–	[588]
Laminaria japonica	Commercial cultivation	16.4	–	
Sargassum fluitans	Florida, short term	4.2–19.1	–	[589]

[a]Estimated from data given in the paper

Table 13 Biochemical and chemical composition of selected brown seaweeds

Component	*Macrocystis pyrifera*	*M. pyrifera*	*A. nodosum*	*L. hyperborea* (*stipe*)	*L. hyperborea* (*frond*)	*Laminaria* sp.
Water	87.5	87–89	67–82	77–89	84–87	88
Ash	38.6–44.5	34–44.3	18–24	32–37	16–37	22–37.6
Carbon	–	23.7–27	33.1–35.7	–	–	34.6
Hydrogen	–	2.8–4.1	4.5–5	–	–	4.7
Oxygen (calculated)	–	27.5–31	32.9–37.9	–	–	31.2
Nitrogen	–	1.1–1.7	2.8–3.3	–	–	2.4
Sulfur	–	0.7	1.5–2.9	–	–	1
Alginate	13–24	11.5–19.5	3.7–29	31–6	17–34	17–30
Laminarin	1	–	1.2–6.6	0.4–1	0–30	14
Mannitol	5–16	5.2–25	6.8–10.4	3.5–8.3	4–25	12
Fukoidan	0.5–2	1.2–2.1	3.8–10	2–4	–	5
Other carbohydrates	–	–	10	traces	–	–
Total carbohydrates	–	18.5–18.8	22.2–25.3	–	–	54
Protein	5–13	–	4.8–9.8	7.2–10.5	4–14	6–19
Lipids	0.5	–	1.9–4.8	0.5–0.77	–	0.9–4
Fiber	–	–	3.5–4.6	9.6–11.2	–	
Cellulose	3–8	4.7–6.4	1.6–4	–	–	3–9
Sugars/alcohols	–	12.3	1.2–2.2	–		
Polyphenols/lignin	–	4–7.8	0.5–19.1	1	–	
C/N ratio	–	13.6–23.7	10–13.9	–	–	14.4
References	[590]	[591]	[592]			[593]

All data are given as a percent from dry weight, water percent from fresh weight and C/N ratio unit less

L. saccharina spring (autumn)	*L. saccharina*	*L. agardhii*	*A. cribosum*	*A. esculenta*	*F. distichus*	*F. vesiculosus*	*S. fluitans*	*Sargassum pteropleuron*
88.7–89.2 (80.7–84.4)	82.5–87	87	77.8	78.2	76.2	80.6–81.9	86	75.1
35–38.6 (21.5–24)	17.9–35.8	47.3	30.1	26	17.5	27–28.9	39.6	23.5
–	27.5–33.9	23.8	30.5	31.9	38.1	31.2–34.5	28.3	34.8
–	3.8–5.4	2.8	4	4.7	5.1	4.3	3.68	4.51
–	30.2–39.7	23.5	32.2	33.7	35.4	30.8–32.8	27.2	–
–	2.7–4.3	2.6	3.2	3.7	3.9	2.9–3.4	1.15	0.69
–	0.3–0.4	0.4	1.5	0.7	1.4	1.5–2	–	–
23 (15)	5.9–19.2	17.8	13.3	16.8	5.8	6.1–10.8	28.3	24.5
0.16–0.21 (19–20)	0–9.1	–	–	–	–	–	–	–
4 (16)	2.5–18.3	–	1.7	4.7	6.3	5.8–11.4	4.5	3.5
–	0.1–0.9	0.1	0.7	0.5	3.1	2.5–4.3	–	–
–	–	–	14.2	–	–	–	8.3	9.2
–	14.1–39.6	13.6	14.2	28.4	28.6	14.4–21.1	–	–
–	–	–	–	–	–	–	8.6	5.1
–	–	–	–	–	–	–	–	–
–	–	–	–	–	–	–	36.5	40.6
–	2.1–6.8	8	5.5	3.2	7.3	5–5.7	–	–
–	2.3–19.4	–	6.4	3.8	11.7	1.3	–	–
–	4–9	6	17.2	9.4	12.9	5.8–6	–	–
–	6.9–10.8	9.3	9.6	8.6	9.7	10.10.9	–	–
[154]	[531]						[121]	

Table 14 Biochemical and chemical composition of Heterokont microalgae

Species, class, phylum	Chlorophyll	Proteins	Carbohydrates	Lipids	References
Bacillariophyceae, Bacillariophycophyta					
C. calcitrans	3.01	34	6	16	[566]
Chaetoceros gracilis	1.04	12	4.7	7.2	
Nitzschia closterium	–	26	9.8	13	
P. tricornutum	0.53	30	8.4	14	
Skeletonema costatum	1.21	25	4.6	10	
Thalassiosira pseudonana	0.95	34	8.8	19	
Eustigmatophyceae, Heterokontophycophyta					
Nannochloropsis oculata	0.89	35	7.8	18	[566]

All data are given as a percent from dry weight

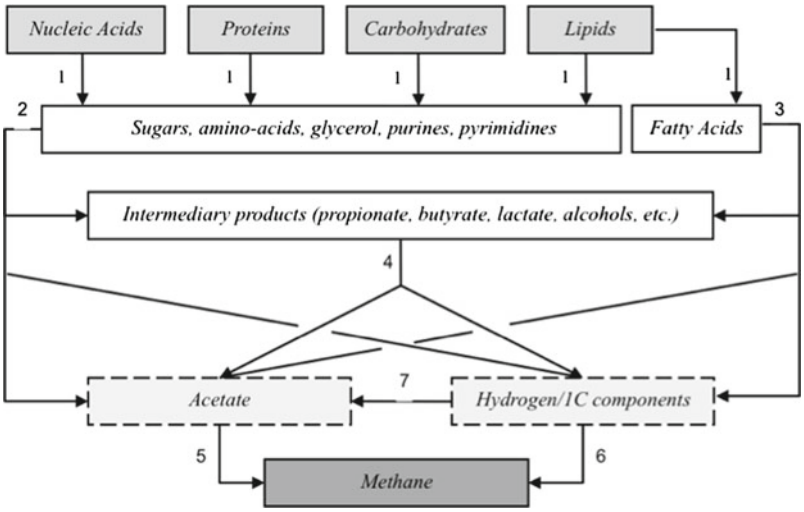

Fig. 1 Flow diagram of complex organic matter anaerobic digestion (modified from [60]), where (1) hydrolysis; (2) fermentation; (3) β-oxidation; (4) acetogenesis; (5) acetoclastic methanogens; (6) hydrogenophilic methanogens; (7) homoacetogenesis

5. Transformation of acetate into methane by acetoclastic methanogens.
6. Transformation of molecular hydrogen and carbon dioxide into methane by hydrogenophilic methanogens.

The same group of microorganisms that are primary fermenters performs the first three steps. These biological processes are sometimes referred to as acidogenesis or the acid-phase [61]. The other important biological processes in AD are:

- Conversion of a variety of monocarbon compounds (e.g., formate, methanol) to acetic acid. This reaction is carried out by homoacetogenic bacteria.
- Reduction of sulfur compounds to hydrogen sulfide by sulfur reducing bacteria.

3.2 Operational Parameters, Physicochemical Factors, and Inhibition of the Anaerobic Process

Archaea obtain a limited amount of energy from methanogenesis and possess the slowest growth rate among the anaerobic digester microorganisms. Maintaining valid environmental and operational parameters for archaea is one of the key factors for effective methane production. The main environmental factors are temperature, pH, alkalinity, and redox potential. Operational parameters, such as C:N:P ratio, the presence of essential micronutrients, organic loading rate (OLR), hydraulic (HRT) and solids retention time (SRT), and incoming salts and toxicants concentration are subject to tight control and regulation. The accumulation of certain intermediates or byproducts, such as VFAs, ammonia, and hydrogen sulfide, can lead to inhibition of methane production [62].

3.2.1 Temperature

Temperature is one of the most important environmental factors for methanogenesis. The methanogenic archaea can be classified according to the temperature ranges for maximum growth and substrate utilization rates. The optimal temperature for growth of psychrophilic organisms is between 10 and 15°C, mesophilic between 35 and 40°C, and thermophilic between 58 and 68°C [63, 64]. The rate of methane generation by psychrophilic microorganisms is significantly slower compared to mesophiles and thermophiles, and therefore the psychrophilic regime is rarely used for large-scale methane production. The methanogens are the most sensitive organisms to temperature variation. A sudden temperature change as small as 2–3°C causes an accumulation of VFAs and a decreasing methane generation rate especially at thermophilic conditions [65]. A significant temperature drop affects the activity of all anaerobic microorganisms and ceases methane production, but the microorganisms are able to recover after temperature stabilization [65–67].

3.2.2 pH and Alkalinity

The pH is another important environmental factor for the ADP. Different groups of methanogens have different ranges of optimum pH. The acidogens exhibit maximum activity at pH 5.5–6.5 while the optimum for methanogens is pH 7.8–8.2 [68]. Since the methanogens are more sensitive to pH variation, the pH in anaerobic digesters is usually maintained in the range of 7–8. Rapid inhibition of methanogens at pH higher than 8 can be caused by dissociation of NH_4^+ to the neutral NH_3 form [69]. The presence of alkalinity is an important marker of pH persistence in anaerobic digesters. The bicarbonate alkalinity buffers the fluctuations in the generation of VFAs and carbon dioxide at pH close to neutral. A stable ADP is characterized by the bicarbonate alkalinity in the range from 1,000 to 5,000 mg/L as $CaCO_3$ [70].

The ratio between VFAs to alkalinity should be in the range of 0.1–0.25. A further increase of the ratio of VFAs to alkalinity indicates possible process deterioration and requires the OLR to decrease in order to lower the VFA formation rate.

3.2.3 Nutrients

Macro- and micronutrients are required for the stable growth of anaerobic microorganisms. The approximate ratio of carbon to nitrogen and phosphate should be in the range of 75:5:1 to 125:5:1 [71]. Chynoweth reported the nitrogen limiting conditions when C/N ratio exceeded 15 during digestion of *Macrocystis* [72]. Nitrogen is an important element not only because it is necessary for the synthesis of protein and nucleic acids but also because, reduced to ammonia, it serves as a base to help maintain neutral pH. Certain macronutrients, such as iron, nickel, cobalt, molybdenum, zinc, calcium, copper, and boron, are necessary for stable AD in the mg/L level [73, 74]. The majority of metals are the principal component of the enzymes' active site. For example, copper and cobalt are constituents of B_{12}-enzyme which catalyze the methanogenesis, nickel is part of factor F_{430} found only in methanogenic bacteria, and molybdenum and selenium are subcomponents of formate dehydrogenase, which is part of the active site of hydrogenase and acetyl-CoA synthase [75].

3.2.4 Oxidation–Reduction Potential

The oxidation–reduction potential (ORP) generally is a measurement of a substance's affinity to either gain or lose electrons. In AD it reflects the availability of oxidants, such as oxygen or nitrate ions or of reductants such as hydrogen. A high ORP (>50 mV) indicates the presence of free oxygen in the anaerobic environment. An ORP between 50 to −50 mV is characteristic of an anoxic environment with nitrates and nitrites, the most favorable electron acceptors. At ORP lower than −50 mV, the environment in the digester is strongly reducing. If sulfate ions are present and the ORP is in the range from −50 to −100 mV, sulfate reducing microorganisms can outperform methanogens for hydrogen and acetate since sulfate is a more thermodynamically favorable electron acceptor. The most favorable ORP for fermentation and acid production is from −100 to −300 mV, which indicates that the strongest oxidant available is found in different organic compounds that can be reduced to a mix of acids and alcohols. Methanogenesis requires the ORP <−300 mV when carbon dioxide is used as an electron acceptor and methane is formed [76].

3.2.5 Organic Loading Rate, Hydraulic and Solids Retention Times

The OLR, HRT, and SRT are other essential characteristics of ADP. The rapid increase of OLR, especially of readily digestible substrate, causes fast acid formation, leads to alkalinity depletion and a drop in pH. The HRT determines the volume and capital cost for an AD system. The SRT influences the volatile solids (VS) reduction

and, thus the methane yield from biomass. Significant fluctuations in OLR, HRT, and SRT lead to upset of the ADP and inhibition of the methane production.

3.2.6 Toxicants

Hydrolytic, fermenting, and acidifying organisms are tolerant to the presence of oxygen but methanogens are strict anaerobes. Oxygen concentration as low as 0.1 mg/L starts to inhibit the production of methane.

High salts concentration (e.g., NaCl) can affect methane production when marine algae are used for anaerobic digestion. Nevertheless, the methane yield from green macroalgae diluted with seawater was comparable to the methane yield from a sample diluted by fresh water [77]. A shock increase in salt concentration in a fixed bacteria reactor caused inhibition only at 35 g/L. When the NaCl concentration was increased gradually, methanogens adapted to concentrations up to 65 g/L [78]. Moreover, desalination of macroalgae by heat and pressure resulted in less methane yield compared to untreated algae likely because of the loss of easily digestible organic matter [77, 79].

Heavy metals, such as lead, cadmium, copper, zinc, nickel, and chromium, are well-known toxicants for bacteria. Some algae accumulate heavy metals but their negative effect can be decreased by precipitation with sulfide compounds.

By-products, including ammonia and hydrogen sulfide, at high concentrations can be toxic for methanogenic microorganisms [62]. Generally, the main source of nitrogen and sulfur in AD is proteins, but some seaweeds have a high amount of sulfated carbohydrates. The toxicity of ammonia and sulfide is related to the presence of metals, temperature, and pH in digesters since neutral forms of ammonia and hydrogen sulfide are more toxic, possibly because they can more rapidly penetrate the cell membrane [65, 80–82]. On the other hand, other authors have reported increasing sulfide toxicity with increasing pH [83]. This discrepancy is possibly due to different mechanisms of sulfide toxicity on different species. The mechanism of sulfide toxicity is usually associated with the following factors: sulfate reducing bacteria that are able to outcompete methanogens for hydrogen and acetate [84]; denaturation of native proteins through the formation of sulfide and disulfide cross-linkage between polypeptide chains [85]; interference with the assimilatory metabolism of sulfur [86]; and the ability to remove essential metals (nickel, iron, cobalt) from the solution.

The mechanisms of ammonia toxicity are possibly associated with disruption of intracellular pH, potassium deficiency, and inhibition of a specific enzymatic reaction [87, 88]. Several studies showed that ammonia is toxic for methanogenic microorganisms at concentration 1.5–1.7 g N/L at pH 7.4 and above [89, 90]. Whereas methanogens tolerate ammonia concentration up to 3–4 g N/L at lower pH [90–92]. Moreover, microorganisms are able to acclimate to high ammonia concentration, and ADP can be stable at nitrogen concentrations as high as 5–7 g/L [93–96].

Organic acids are common intermediate products of AD but accumulation of them, especially in nonionic form, inhibits the overall process. Decline of hydrogen utilization causes accumulation of propionate, leading to failure of the acetoclastic

methanogenesis, and therefore causing acetate accumulation and a drop in pH [97]. The mechanism of inhibition by organic acids is probably the denaturation of cell proteins.

3.3 Biogas Composition, Application, and Treatment

3.3.1 Biogas Composition

Biogas is formed during AD and has two main constituents: methane (about 55–70% by volume) and carbon dioxide (30–40%). Depending on the source of the biogas, other minor components include nitrogen (<2%), hydrogen, oxygen (<1%), hydrogen sulfide (0–50 ppm), and other sulfide compounds, volatile organic compounds (VOC) 10–270 mg/m^3, and siloxanes with concentration ranging from 80 to 2,500 μg/m^3 [98, 99]. The VOC comprise aromatic and halogenated compounds. Large amounts of noxious VOC can be produced during digestion of household wastes [100, 101].

Carbon dioxide is not a harmful inert gas but the presence of carbon dioxide in biogas reduces its calorific value. The removal of carbon dioxide is an expensive process and power generation equipment commonly operates with carbon dioxide concentrations up to 40–50%.

The most abundant sulfur compound in biogas is hydrogen sulfide but other reduced sulfur chemicals (e.g., sulfides, thiols) are present as well. The main source of sulfur in biogas is degradation of sulfur containing amino-acids—cysteine and methionine. Hydrogen sulfide at concentrations higher than 300–500 ppm can form unhealthy and hazardous sulfur dioxide (SO_2) and sulfuric acid (H_2SO_4) which corrodes pipeline metal parts, storage tanks, compressors, and engines [102]. Frequently, it is necessary to install sulfur removing facilities before the biogas application. Another corrosive contaminant is ammonia (NH_3). The burning of biogas with high ammonia concentration increases the emission of nitrogen oxides to the atmosphere. Both hydrogen sulfide and ammonia are contaminants that pose a health risk.

Other compounds of concern in biogas are siloxanes—the organic polymers of silicon coming from a wide range of industrial, personal care, pharmaceutical, and other products. These organic compounds can be oxidized to silicon dioxide and accumulate on valves, gas turbines, and engines causing erosion and decreasing the operating efficiency [103].

3.3.2 Biogas Treatment

The primary treatment of biogas includes cooling, drying, and almost always removing of hydrogen sulfide. More advanced applications of biogas require upgrading it to biomethane or removing carbon dioxide. The following methods are used for the

removal of carbon dioxide from biogas: pressure swing absorption on zeolites, selective membrane separation, cryogenic separation, and biological or chemical fixation [104–106]. The typical technologies for biogas cleaning include scrubbing by solvents or an aqueous alkaline solution, absorption, and oxidation on solid sorbents, chelation, precipitation in the form of poorly soluble metal sulfides, and biological removal [105, 107, 108].

3.3.3 Biogas Utilization

The possible applications of biogas include:

- Heat or steam production via burning
- Electricity generation combined with heat and power production
- Usage as cooking gas instead of natural gas
- Usage as fuel for vehicles (upgrading to biomethane is necessary)
- Generation of electricity via fuel cells
- Production of chemicals

4 Anaerobic Digestion of Algae

Production of biogas from seaweeds and microalgae by AD was a subject of research starting in the mid-sixties [109, 110]. The first detailed large-scale study of seaweed cultivation and AD was performed in the Institute of Gas Technology by Chynoweth et al. [79, 111]. Substrate chemical composition and conversion parameters determine the amount and composition of biogas generated in the ADP. The theoretical yield of biogas can be estimated by the Bushwell equation [112].

$$\mathrm{C_cH_hO_oN_n} + y\mathrm{H_2O} \rightarrow x\mathrm{CH_4} + n\mathrm{NH_3} + (c - x)\mathrm{CO_2}$$

where:

$$x = (4\mathrm{c} + \mathrm{h} - 2\mathrm{o} - 3\mathrm{n} - 2\mathrm{s}) / 8$$

$$y = (4\mathrm{c} - \mathrm{h} - 2\mathrm{o} + 3\mathrm{n} + 3\mathrm{s}) / 4$$

The theoretical methane yield from different algae is presented in Table 15.

Lipids have the lowest oxidation state and largest theoretical methane yield, which is more than twice the methane yield from proteins, glycerol, and carbohydrates. The theoretical methane yield correlates with the average carbon oxidation state of the substrate (Fig. 2). Macroalgae with high carbohydrate content and cyanobacteria with high protein content are theoretically poorer feedstock for methane production while microalgae with high lipid content have higher potential methane yield.

Table 15 Theoretical methane yield from different algal species and biochemical compounds

Feedstock	Chemical formula	Average carbon oxidation state	Mole ratio C/N	Theoretical yield			References
				CH_4 (L/gVS)	NH_3 (mg/gVS)	CH_4 (%)	
Lipids	$C_{54}H_{82}O_6$	−1.296	–	0.97	–	66.2	–
C. pyrenoidosa (oily)	$C_{57.2}H_{103.1}O_{13.1}N$	−1.29	57.2	0.84	16.8	66.1	[506]
Scenedesmus sp.	$C_{192}H_{348}O_{62}N_{26}P_{1.7}S$	−0.760	7.38	0.64	110.3	59.5	[594]
Chlorella sp.	$C_{287.3}H_{543.7}O_{120}N_{33.2}S$	−0.71	8.65	0.59	88.5	58.9	[436]
M. pyrifera	$C_{79.6}H_{128.2}O_{46.9}N_{4.58}S$	−0.261	17.4	0.50	41.0	55.3	[79]
Anabaenopsis sp.	$C_{7.94}H_{13.46}O_{4.34}N$	−0.223	7.94	0.49	88.4	52.8	[506]
Chlorella sp. (lipids depleted residues)	$C_{121.8}H_{217.3}O_{66.6}N_{21.8}S$	−0.154	5.59	0.47	121.4	51.9	[436]
Chlamydomonas sp.	$C_{9.52}H_{16.43}O_{6.01}N$	−0.148	9.52	0.46	70.6	51.9	[506]
S. bacillaris	$C_{6.16}H_{9.83}O_{3.32}N$	−0.030	6.16	0.46	112.6	50.6	
Proteins	$C_{13}H_{25}O_7N_3S$	−0.154	3.17	0.45	152.2	51.9	–
Laminaria sp.	$C_{93.4}H_{150.7}O_{62.7}N_{5.5}S$	−0.095	16.81	0.45	39.9	39.9	[593]
C. pyrenoidosa	$C_{6.2}H_{10.2}O_{3.57}N$	−0.010	6.20	0.45	109.2	50.1	[506]
M. pyrifera	$C_{8.13}H_{14.47}O_{5.38}N$	−0.088	8.13	0.44	80.2	51.1	[79]
S. fluitans	$C_{28.8}H_{45}O_{20.8}N$	−0.014	28.77	0.44	23.07	50.2	[121]
G. verrucosa	$C_{8.48}H_{12.9}O_{5.21}N$	0.057	8.48	0.44	80.2	49.3	
A. maxima	$C_{281}H_{485}O_{167}N_{51}P_{2.3}S$	0.007	5.51	0.43	119.7	49.9	[594]
Glycerol	$C_3H_8O_3$	−0.667	–	0.43	–	58.3	–
G. tikvahiae	$C_{8.22}H_{17.21}O_{6.23}N$	−0.214	8.22	0.42	74.1	52.7	[121]
S. pteropleuron	$C_{58.9}H_{91.8}O_{46.4}N$	0.067	58.93	0.42	10.9	49.2	
Ulva sp.	$C_{39.5}H_{65.1}O_{27.9}N_{3.69}S$	0.044	10.68	0.42	60.6	49.5	[506]
A. nodosum	$C_{13}H_{25}O_7N_3S$	−0.038	11.69	0.42	54.2	50.5	[531]
M. pyrifera	$C_{102.9}H_{187.8}O_{86.7}N_{3.6}S$	−0.034	28.61	0.41	21.4	50.5	
F. vesiculosus	$C_{41.6}H_{68.9}O_{30.8}N_{3.32}S$	0.061	12.54	0.41	51.0	49.2	
Carbohydrates	$(C_6H_{10}O_5)_n$	0.00	–	0.41	–	50.0	–

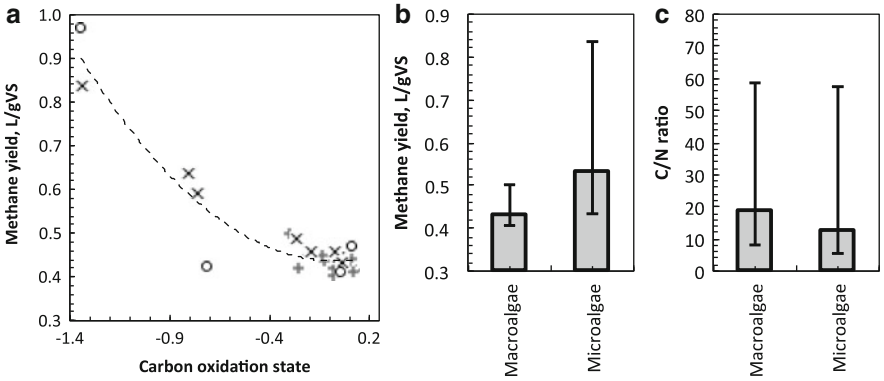

Fig. 2 (**a**) Theoretical methane yield in relation to the average carbon oxidation state. *circles*—pure compounds; *crosses*—microalgae; *pluses*—macroalgae. (**b**) Mean theoretical methane yield and (**c**) C/N ratio with maximum and minimum values (base on Table 15)

Based on this observation, increasing the lipid content in algae is a promising approach for enhancing the methane yield. Another observation is that all microalgae have C/N ratio lower than optimal range for AD and high potential level for ammonia release. In contrast, several macroalgae and oil rich microalgae have a C/N ratio that is too high and possibly require addition of nitrogen for optimal AD conditions.

4.1 Anaerobic Digestion of Macroalgae

Although the biochemical composition of algae is very different among algal groups, cellulose is a common material among many algal species. The process of cellulose biological degradation has been extensively studied in recent years. The mechanism of cellulose enzymatic hydrolysis by anaerobic bacteria is quite different from the mechanism of aerobic organisms. Anaerobic bacteria have a large multienzyme complex—cellulosome, which is attached to the cell envelope and consists of up to 11 different catalytic enzymes carried by scaffold-proteins [113, 114]. The enzymatic hydrolysis of algal cellulose is relatively slow and can be inhibited by the close association with other structural materials, such as polyphenols, fucoidan, protein, and alginate. Therefore, other specie-specific sulphonated, methylated or carboxylated polysaccharides, mannitol, proteins, and lipids usually determine the more readily biodegradable fraction of algal biomass.

4.1.1 Rhodophyta (Red Algae)

Agars and carrageenans are two sulfated polysaccharides from the red macroalgae cell wall, and are responsible for the main part of cell dry weight. Both of them have an agarose backbone composed from α(1→3) linked galactose disaccharide units, connected by β(1→4) linkages [115]. Galactose units on agars can be methylated

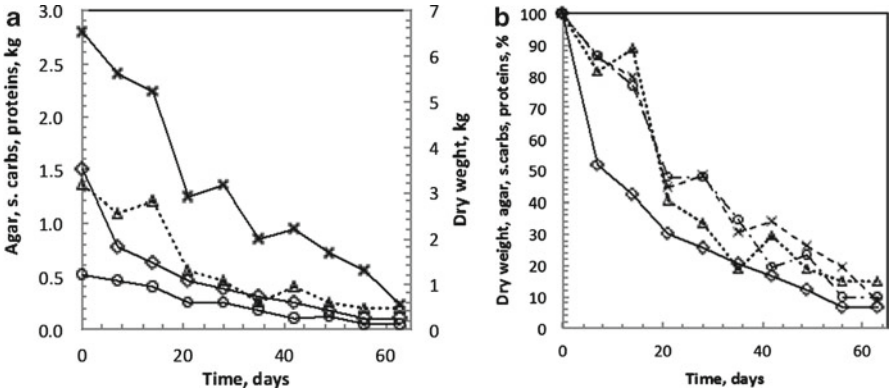

Fig. 3 Agar, soluble carbohydrates, proteins, and dry weight vs. digestion time. (**a**) kg-matter remaining in digester, (**b**) percent from initial weight. *Crosses*—dry weight; *diamonds*—agar; *triangles*—soluble carbohydrates; *circles*—proteins [119]

(up to 20%) and have few sulfate ester groups, while carrageenans can have from one to three sulfate ester groups, one for every disaccharide unit [115]. Polysaccharides have nonuniform structure that depends on algal source, life stage, and season [116]. In natural environments, several microorganisms from Gammaproteobacteria class, Bacteroidetes, and Planctomycetes phyla are able to degrade the red algal cell wall by secreting specific glycoside hydrolases—diverse agarases and carrageenases [117, 118].

Biodegradation of agar by a consortium of microorganisms from an anaerobic digester was studied on the biodegradation of *Gracilaria tikvahiae* [119]. The concentration of soluble sugars remained at the same level during the first 2 weeks and consisted mostly of agar (90–100%). Results showed that more than 50% of the agar could be fermented over the course of 3 weeks (Fig. 3). While the rest of the agar is degraded slowly and complete fermentation (more than 90%) requires more than 9 weeks, overall agar is degraded faster than the rest of the organic matter in algae. Agar in algae is a highly heterogeneous material that has different levels of biodegradability. This conclusion is supported by the results of another experiment on *G. tikvahiae* batch digestion, when less than 50% of the agar was fermented during 11 weeks [119].

AD of carrageenan was studied on the biodegradation of red alga—*Eucheuma cottonii*, which has about 61.1–72.9% of carrageenan content from dry weight [120]. About 40% of the biomass remained after 10 weeks of digestion but carrageenan accounted for 49.8–59.6% of the fraction remaining. Therefore, it is less biodegradable than the rest of the algal organic matter. The largest biogas production was observed during the first 4 weeks when the methane concentration ranged from 10 to 25%. Possible reasons for inhibition of the methanogens are accumulation of VFAs up to about 240 mM, outperformance of the methanogens by sulfate reducing bacteria, and inhibition by sulfides [120].

According to chemical composition the theoretical methane yield for *G. tikvahiae* is 0.42 L/g VS and for *Gracilaria verrucosa* is 0.44 L/g VS (Table 15). Bird et al. predicted methane yield for these species up to 0.46 and 0.48 L/g VS,

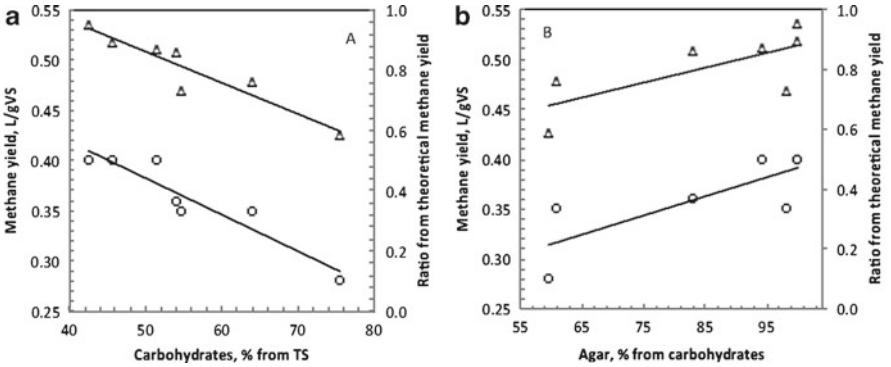

Fig. 4 (**a**) Experimental methane yield (*circles*, left axis) and its ratio from theoretical yield (*triangles*, right axis) as a function of (**a**) percent carbohydrates from TS and (**b**) percent agar from carbohydrates [121]

respectively [121]. Biomethane potential (BMP) assays provided an experimental methane yield from *G. tikvahiae* of 0.35–0.4 L/g VS added, which corresponds to about 70–95% of the theoretical methane yield [79, 121]. The methane yield from *G. verrucosa* was in the range 0.28–0.35 L/g VS, which corresponds to 58–77% of the theoretical yield. A 60-day residence time was required for *Gracilaria* conversion to biogas.

The negative correlation between methane yield and its ratio to theoretical yield from carbohydrate content (Fig. 4a) means that some carbohydrates are recalcitrant to biodegradation. Both the methane yield and its ratio to the theoretical value increased with increasing the agar fraction in the carbohydrates (Fig. 4b). Consequently, agar is possibly not the most recalcitrant material. Some carbohydrates are present in the form of fiber more resistant to biological degradation.

Limited digestibility of particular carbohydrates is supported by results obtained by Habig and colleagues [122] during AD of *G. tikvahiae* grown at different conditions. A nutrient-starved sample had about 12–25% more volatile solids, 42–74% higher carbohydrates content but also 46–59% larger neutral fiber content compared to nutrient rich and nutrient moderate samples, respectively [122]. The nutrient starved sample had a slower degradation rate and finally gave 14–17% lower methane yield compared to nutrient rich and moderate samples (Fig. 5).

The difference in substrate nitrogen concentration (5.3% of TS vs. 2.3%) was probably one of the factors responsible for the difference in methane yield during digestion of *Polysiphonia* in a batch reactor [123]. Methane yield from *Polysiphonia* collected in March was two times lower compared to algae collected in October: 0.21–0.24 L/gVS vs. 0.11–0.12 L/gVS.

The methane yield with AD of *G. tikvahiae* depends strongly on the OLR and HRT [124]. A retention time between 40 and 50 days is necessary to achieve a methane yield of 0.14–0.19 L/gVS. A lower retention time (20–30 days) resulted in a methane yield of 0.05–0.06 L/gVS likely because of recalcitrant algal components, such as agar and insoluble fiber polysaccharides (Table 16).

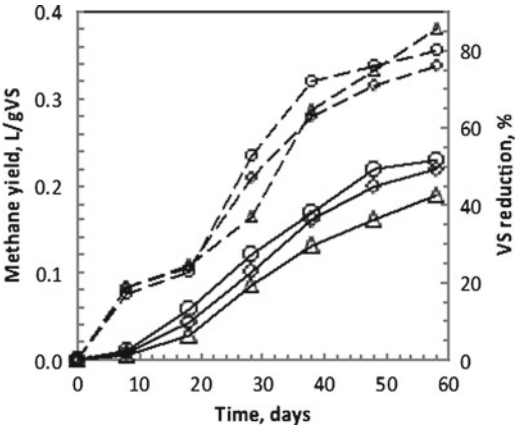

Fig. 5 Methane yield (*solid line*, left axis) and VS reduction (*dashed line*, right axis) over anaerobic digestion of *Gracilaria tikvahiae*. Influence of substrate growth regime (N, P availability). *Diamonds*—nutrient enriched; *circles*—moderate; *triangles*—starved [122]

4.1.2 Chlorophyta (Green Algae)

Ulvales, particularly *Ulva* (sea lettuce), *Enteromorpha* and *Cladophora*, are frequently considered as good feedstock candidates for AD. They are widespread all over the world [125] especially in ecological systems with high nutrient loading where it can cause the problem of eutrophication [126]. Excessive growth of *Ulva* and formation of green tides is a costly burden for many European coasts [127, 128]. Beach accumulation of tons of *Ulva* biomass is a potential feedstock for biomethane production. *Ulva* sp. has a low fraction of poorly biodegradable polyphenol materials (varies from 1 to 1.9%). The major components of *Ulva* sp. are carbohydrates (about 40–60% of cell dry weight), proteins (10–17%), and lipids (1.8–3.5%). They are considered a good substrate for AD [129]. Carbohydrates accumulate mostly as the cell envelope and consist of ulvan, cellulose, xyloglucan, and glucuronan which are responsible for up to 38–54% of the algal dry matter [130]. In contrast to cellulose, ulvan is a water-soluble sulfated polysaccharide. The structure of ulvan was carefully studied due to its possible application in food, agricultural, pharmaceutical, and chemical industries. The average composition of ulvan is rhamnose (16.8–45.0% dw), xylose (2.1–12.0%), glucose (0.5–6.4%), uronic acid (6.5–19.0%), and sulfate (16.0–23.2%) but the main repeating disaccharide is ulvanobiouronic acid that is composed of aldobiouronic acid and 4-*O*-β-D-glucuronosyl-l-rhamnose [131]. Despite the high ratio of sugars, only 8.9% of ulvan and 16.6% of *Ulva* organic matter were fermented by biota from the human colon in a study performed by Durand and coworkers [132]. The major products found were acetic, propionic, and butyric acids. The sulfate-reducing bacteria had a relatively high population compared with acetogenic and methanogenic bacteria. Since about 40% of ulvan's sulfate was reduced to hydrogen sulfide, the higher sulfate ratio is not the only reason for the poor biological degradability of ulvan. Another study reported degradation of 32, 25.9, and 50.9% of the sugars from *Ulva* after 24 h of fermentation [133]. The authors concluded that the likely reason for the high recalcitrance of ulvan is the complex chemical structure of polysaccharides that makes them poorly accessible for enzymatic attack.

The results of different AD studies with green macroalgae are presented in Table 17. The batch studies showed that the methane yield from *Ulva* sp. is in the

Table 16 Characteristics of AD of selected red seaweeds

Substrate	Reactor	T (°C)	HRT (days)	OLR (gVS/L-day)	VS red. (%)	CH_4 (L/L-day)	CH_4 (L/gTVS)	CH_4 (%)	References
G. tikvahiae (five strains)	BMP assay, (0.25 L)	35	60	–	76–95[a]	–	0.35–0.4	–	[121]
G. verrucosa (two strains)		35	60	–	58–76[a]	–	0.28–0.35	–	
G. tikvahiae (N, P enriched)	Batch (2 L)	32 ± 3	58	–	75.7	–	0.22	45.9	[122]
G. tikvahiae (N, P moderate)		32 ± 3	58	–	80.1	–	0.23	44.9	
G. tikvahiae (N, P starved)		32 ± 3	58	–	85.7	–	0.19	63.5	
G. verrucosa	Batch (0.125 L)	35	50	–	–	–	0.28	60	[595]
Polysiphonia (spring)	Batch (0.1 L)	37	35	–	37–52	–	0.1–0.12	43–44	[123]
Polysiphonia (spring, ultrasonicated)		37	35	–	43	–	0.1	34	
Polysiphonia (autumn)		37	35	–	37–52	–	0.21–0.24	48–56	
Polysiphonia (autumn, autoclaved at 121 deg.)		37	35	–	45	–	0.25	52	
Polysiphonia (spring) + primary sludge (3:1)	CSTR (4 L)	37	20	1.34–1.44	34–44	–	0.14–0.18	45–54	[123]
Polysiphonia (spring) + primary sludge (4.8:1)		37	20	2.33	54.4	–	0.129	44.5	
Polysiphonia (spring) + primary sludge (6:1)		37	20	3.09	42.9	–	0.116	43.8	
Polysiphonia (autumn) + primary sludge (6:1)		37	20	1.51	24.2	–	0.213	51.8	
Polysiphonia (autumn, autoclaved) + primary sludge (6:1)		37	20	–	30.2	–	0.245	49.1	
G. tikvahiae	Semi-continuous (2 L)	28 ± 3	20	1.65	18.2[a]	0.083[a]	0.05	36.8	[124]
		28 ± 3	30	1.1	21.2[a]	0.066[a]	0.06	39.5	
		28 ± 3	40	0.83	31.8[a]	0.12[a]	0.14	58.4	
		28 ± 3	50	0.66	39.4[a]	0.13[a]	0.19	62.7	
Gracilaria sp.	CSTR (52 L)	37	26	1.9	–	0.21[a]	0.11	–	[596]
G. tikvahiae	CSTR (2 L)	30 ± 3	10	6.4	5.6	0.064	0.01	30	[564]
		30 ± 3	15	4.2	9.1	0.168	0.04	59	
		30 ± 3	20	3.2	14.7	0.192	0.06	59	
		30 ± 3	30	2.1	26.2	0.273	0.13	66	
		30 ± 3	60	1.1	47.7	0.22	0.2	57	
Eucheuma cottonii	Batch (1 L)	20–25	70	–	60	–	–	10–25	[120]
Aegina Karnagio Kolona	Batch (1 L)	37	50	–	–	–	0.03–0.05	51	[597]

BMP biomethane potential; *CSTR* continuous stirred-tank reactor

[a]Estimated from data given in the paper using a COD/VS ratio of 1.5

Table 17 Characteristics of AD of green seaweeds

Substrate	Reactor	T (°C)	HRT (days)	OLR (gVS/L-day)	VS red. %	CH_4 (L/L-day)	CH_4 (L/gVS)	CH_4 (%)	References
Enteromorpha Iinza, *Enteromorpha intestinalis*, *Enteromorpha prohfera* and *P. percursa* (marine sediments inoculum)	Batch (2–3 L)	10	90	–	33	–	0	–	[77]
		20	60	–	34.1	–	0.004	0.11[a]	
		20	90	–	34.6	–	0.005	0.12[a]	
		25	60	–	39.1	–	0.105	0.49[a]	
		25	90	–	39.7	–	0.139	0.53[a]	
		30	60	–	48.7	–	0.168	0.56[a]	
		30	90	–	50.3	–	0.186	0.58[a]	
		35	60	–	51.9	–	0.175	0.57[a]	
		35	90	–	52.9	–	0.185	0.57[a]	
Same substrate (marine sediments inoculum, sea water, salinity 15‰)		35	60	–	42.2	–	0.143	0.55[a]	
		35	90	–	50.2	–	0.149	0.48[a]	
Same substrate (marine sediments inoculum, fresh water)		35	60	–	50.8	–	0.15	0.46[a]	
		35	90	–	59.1	–	0.189	0.65[a]	
Same substrate (filtered liquid chicken manure, sea water, salinity 15‰)		35	60	–	58.2	–	0.187	0.53[a]	
		35	90	–	60.7	–	0.198	0.53[a]	
Same substrate (filtered liquid chicken manure, fresh water)		35	60	–	57.6	–	0.154	0.43[a]	
		35	90	–	60.1	–	0.169	0.44[a]	
Same substrate (marine sediments inoculum, dewatered by pressing)		35	60	–	54.6	–	0.183	0.57[a]	
		35	90	–	58.3	–	0.201	0.57[a]	
Same substrate (marine sediments inoculum, desalted)		35	60	–	47.1	–	0.147	0.54[a]	
		35	90	–	54.2	–	0.157	0.55[a]	
Same substrate (marine sediments inoculum, desalted)		35	60	–	59.1	–	0.189	0.55[a]	
		35	90	–	63.3	–	0.209	0.56[a]	
Ulva sp., *Cladophora* sp., *Chaetomorpha* sp.	Batch, 0.7 L	35	52	–	–	–	0.48–0.55	60	[134]

Ulva sp. (non-washed)	Batch, 30 L	35	23	–	–	–	0.11	59	[129]
Ulva sp. (washed)		35	44	–	–	–	0.094	55.3	
Ulva sp. (non-ground)		35	42	–	–	–	0.145	49.2	
Ulva sp. (ground)		35	64	–	–	–	0.177	51.6	
Ulva sp. (N, P enriched)	Batch (2 L)	32±3	58	–	70.1	–	0.22	33.7	[122]
Ulva sp. (N, P moderate)		32±3	58	–	77.3	–	0.23	39.9	
Ulva sp. (N, P starved)		32±3	58	–	86.7	–	0.33	59.5	
Ulva hydrolysis juice (natural drainage)	Batch (3 L)	15	80	0.58[b]		0.029[a]	0.05[b]	56	[400]
Ulva sp.	Semi-continuous (2 L)	28±3	30	1.12[a]	41.3	0.081[a]	0.14	50.3	[124]
		28±3	40	0.85[a]	50.4	0.086[a]	0.2	59	
		28±3	50	0.68[a]	56.1	0.081[a]	0.23	60.6	
Ulva sp., *Cladophora* sp., *Chaetomorpha* sp.	SCSTR (1.2–1.6 L)	35	11–27	1.1–1.9	50–55	–	0.25–0.35	60	[134]
85% *Ulva* sp. + 15% *Gracilaria* sp. (washed, dried, ground <2 mm)	SCSTR (180 L)	35	20	1	63	0.2–0.24[a] (0.347^{max})[a]	0.2–0.24[a] (0.347^{max})	61	[137]
		35	20	2	63	0.32–0.36[a] (0.632^{max})[a]	0.16–0.18[a] (0.316^{max})	56	
85% *Ulva* sp. + 15% *Gracilaria* sp. (raw, dried, ground <2 mm)		35	15	1	54	0.168[a] (0.322^{max})[a]	0.177[a] (0.322^{max})	63	
		35	15	2	50	0.258[a] (0.444^{max})[a]	0.129[a] (0.222^{max})	58	
85% *Ulva* sp. + 15% *Gracilaria* sp. (raw, dried, ground <0.5 mm)		35	20	1	60	(0.291^{max})[a]	0.291^{max}	70	
		35	20	2	57	(0.554^{max})[a]	0.277^{max}	57	
85% *Ulva* sp. + 15% *Gracilaria* sp. (algal juice)		35	20	1	–	(0.322^{max})[a]	0.322^{max}	70	
Ulva sp. (washed, non-ground)	SCSTR (30 L)	35	20	1.7	50	0.31	0.182	50.9	[129]
Ulva sp. (washed, ground)		35	15	1.8	58.6	0.37	0.203	54.2	
Ulva sp. (washed, ground) + manure		35	15	5.3	38.8	0.93	0.174	55	
Manure (bovine)		35	15	3.5	33.7	0.63	0.18	56.6	

(continued)

Table 17 (continued)

Substrate	Reactor	T (°C)	HRT (days)	OLR (gVS/L-day)	VS red. %	CH_4 (L/L-day)	CH_4 (L/gVS)	CH_4 (%)	References
U. lactuca (ground)	CSTR (2 L)	37	20	0.67	59.2	0.098[a]	0.146	66[a]	[598]
E. intestinalis		37	20	0.67	–	0.086[a]	0.086	–	
		37	20	1.36	–	0.092[a]	0.092[a]	–	
		37	20	1.81	–	0.088[a]	0.088[a]	–	
		37	20	2.72	–	0.132[a]	0.132[a]	–	
U. rigida, *Gracilaria confervoides*, *Valonia agropila*	Semi-cont., (200 L)	35	20	–	–	–	0.15–0.3[a]	50–65	[599]
U. rigida, *G. confervoides*, *V. agropila* (washed, homogenized)	AF (5 m^3)	35	20.8	–	–	–	0.17[c]	50–58[a]	[600]
		35	12	–	–	–	0.2–0.27[c]	50–58[a]	
		35	8	–	–	–	0.17[c]	50–58[a]	
U. rigida, *G. confervoides*, *Chaetomorpha aerea*, *V. agropila* (homogenized)	SCSTR (5 m^3)	35	12	3.23[d]	–	0.65[a]	0.2[c]	–	[601]
U. rigida, *G. confervoides*, *C. aerea*, *V. agropila* liquid fraction (ground, pressed)	FB (30 L)	35	0.88	15.2	–	–	–	–	
Ulva sp. (ground)	CSTR (1 L)	37	20	0.94	–	0.04	0.043	55	[135]
Ulva sp. (ground, $FeCl_2$)	CSTR (1 L)	37	25	1.6	–	0.18[a]	0.11	46	[245]
Ulva sp. (ground)		37	25	1.85	–	0.15[a]	0.08	43	
Ulva sp. (ground, degraded)	CSTR (6 L)	37	30	1.04	–	0.30[a]	0.29	60	
Ulva sp. (ground)		37	30	1.25	–	0.24[a]	0.19	53	
Ulva sp. (ground, $FeCl_2$)		37	30	1.25	–	0.25[a]	0.2	54	
Ulva sp. hydrolysis juice (natural drainage)	UFA (1.3 L)	37	1.4	8[b]	90	3.6[a]	0.45	80	
Ulva sp. (ground)	CSTR (6 L)	30	20	1.47	–	0.29	0.198	65	[602]
Ulva sp. (ground, $FeCl_3$)	CSTR (1 L)	30	20	1.47	–	0.17	0.116	54	
Ulva sp. (ground)	CSTR (5 m^3)	35	20	1.85	–	0.28	0.149	48	[603]

Ulva sp. centrifuged filtrate	CSTR (5 m^3)	35	12	4.1	–	0.83	0.202	56	[129]
		35	18	4.81	–	1.00	0.207	69	
Ulva sp. hydrolysis juices	Fixed bed (10 L)	35	5	2	–	0.66	0.33	83	[246]
		35	2.5	4.76	–	1.49	0.313	82	
Ulva sp. hydrolysis juices (press filter)	Fixed bed (10 L)	35	10	4.16[b]	–	1.5	0.36[b]	81	[247]
Ulva sp. hydrolysis juices (natural drainage)	CSTR (1.5 L)	37	10	5.6[b]	68	1.4[a]	0.25[b]	87	[400]
		37	6	9.2[b]	53	0.92[a]	0.1[b]	85	
Sewage sludge	CSTR (1000 L)	37	14.5	1.7	28.7	0.25	0.147	61.4	[604]
U. rigida and *G. confervoides* mix + sewage sludge (81% of TS)		37	14.7	2.6	31.3	0.57	0.220	71	
U. rigida and *G. confervoides* mix + sewage sludge (83% of TS)		37	11.2	4.4	27	0.79	0.180	72	
U. rigida and *G. confervoides* mix + sewage sludge (62% of TS)		37	11.7	4.2	26.1	0.70	0.167	69.4	
U. rigida and *G. confervoides* mix + sewage sludge (60% of TS)		55	12.3	5.3	4.1	0.05	0.01	25	
Sewage sludge		55	12.3	5.5	21.2	0.70	0.128	71	
U. lactuca	CSTR (52 L)	37	26	1.9	–	0.29[a]	0.15	–	[596]
Ulva + sewage sludge (40% of TS)	CSTR	38	20	–	–	–	0.31	62	[605]

BMP biomethane potential; *CSTR* continuous stirred-tank reactor; *SCSTR* semi-continuous stirred-tank reactor; *AF* anaerobic filter; *FB* fluidized bed; *UFA* upflow anaerobic filter

[a]Estimated from data given in the paper

[b]Estimated from data given in the paper using COD/VS ratio of 1.25

[c]Estimated from data given in the paper using CH_4/biogas ratio of 0.55

[d]Estimated from data given in the paper using VS/TS ratio of 0.62

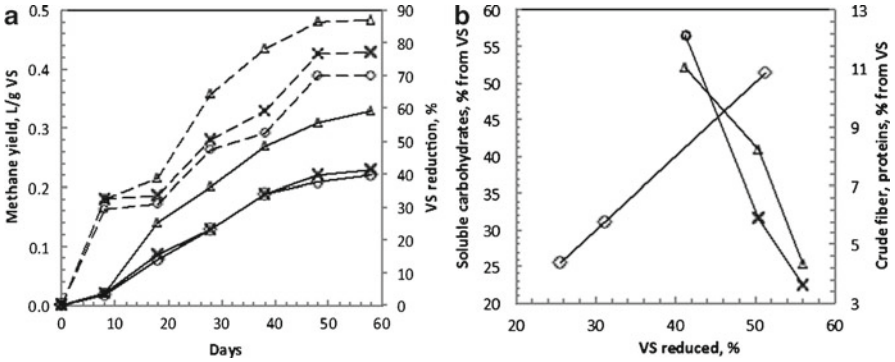

Fig. 6 Influence of *Ulva* sp. growth regime and composition on methane yield and volatile solids (VS) reduction ($T = 32 \pm 3$°C). (**a**) Time course of methane yield (*solid line*, left axis) and VS reduction (*dashed line*, right axis) during anaerobic digestion of *Ulva* sp. *diamonds*—enriched; *crosses*—moderate; *triangles*—starved. (**b**) VS reduction depending from proteins, crude fiber, and soluble carbohydrates content of *Ulva*: *circles*—proteins; *triangles*—crude fiber; *squares*—soluble carbohydrates [122]

range from 0.1 to 0.33 L/g VS [122, 129] that corresponds to 23–78% of the estimated theoretical methane yield for *Ulva* 0.42 L/g VS (Table 15). Habig reported reduction of approximately 65–87% of VS during about 60 days of fermentation [122]. Hansson observed a very high methane yield (0.48–0.55 L/g VS) for the mixture of *Ulva*, *Cladophora*, and *Chaetomorpha* [134], which is larger than the calculated theoretical methane yield for *Ulva*. As reported by the author, the possible source of methane yield overestimation can be the gas leakage from reference samples. Batch digestion of three *Enteromorpha* species and *Percursaria percursa* resulted in a methane yield 0.18–0.2 L/g VS at 90 days HRT [77].

The *Ulva* growth conditions and biochemical composition have significant influence on methane yield. The nutrient (N, P) deficient *Ulva* resulted in a 50% higher methane yield (Fig. 6a) compared to *Ulva* grown in enriched media [122]. The amount of VS degradation correlated with the soluble carbohydrate and protein ratio in the substrate (Fig. 6b). The percent of VS reduced is increasing with decreasing amount of protein and increasing amount of soluble carbohydrate content. These results suggest that for long time scales, ulvan is degradable by diverse populations of anaerobic microorganisms. The authors suggested that poor digestibility of crude fiber/cellulose is probably due to the decreasing ratio of accessible surface sites with increasing amounts of fiber. Degradation of a large amount of proteins can lead to inhibition of methanogens by ammonia. Another possible explanation of negative influence of proteins on the digestibility is formation of protein-polysaccharide complexes, which can be recalcitrant for common bacterial enzymes.

Many studies of *Ulva* digestion were done in continuously stirred-tank reactors fed in semi-continuous mode. Reduction of VS and methane yield was observed in the range from 40 to 63% and from 0.11 to 0.23 L/g VS (Table 17), respectively. The possible reasons for extreme low methane yield are inhibition of methanogens by

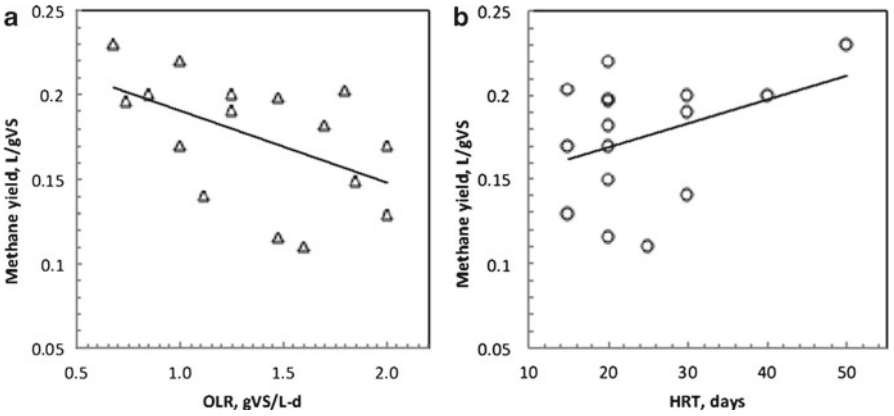

Fig. 7 Methane yield from AD of *Ulva* sp. (**a**) dependence on the organic loading rate (OLR). (**b**) dependence on the hydraulic retention time

high concentrations of sulfide, salts, and heavy metals [129, 135, 136]. Iron salts were applied in order to diminish sulfide concentrations in the digester. Alternatively, the absence of a toxicity effect on acclimated anaerobic sludge was reported at sulfide concentrations in the reactor up to 0.18–0.35 mg/L [137]. The authors suggested that the presence of sulfide was able to decrease the inhibitory effect of the metals (Al, Fe, Cu, and Zn) by the formation of insoluble salts.

The methane yield depends on the OLR and HRT. (Table 17 and Fig. 7). The overall trends are decreasing of the methane yield with increasing OLR and increasing of the methane yield with increasing HRT with a large spread in values observed for both relationships. Differences in *Ulva* composition among strains and even seasonal changes for one strain account for the observed variability [129, 131, 138]. The recommended OLR and HRT for *Ulva* AD fall in the range of 0.8–1.2 gVS/L-days and 15–20 days, respectively.

4.1.3 Phaeophyceae (Brown Algae)

The specific organic constituents of brown algae are alginic acid, laminarin, mannitol, and fucoidan (Table 11). Among these compounds, mannitol lacks polymeric structure; it is soluble, and can be easily transferred into the cell [139]. Mannitol can be utilized by anaerobic microorganisms with the formation of acetate and hydrogen as the major products, and minor production of ethanol, formate, lactate, and succinate [140]. The degradation of laminarin by anaerobic organisms was studied by inoculation of an anaerobic reactor with bacteria from the human gut [141]. The authors reported almost complete (>90%) usage of laminarin during 24 h with the formation of butyrate and other VFA. Alginate has a more complex molecular structure and usually forms a gel in algae. The alginate lyases are enzymes found to be responsible for alginate depolymerization [142, 143]. Biological degradation of soluble

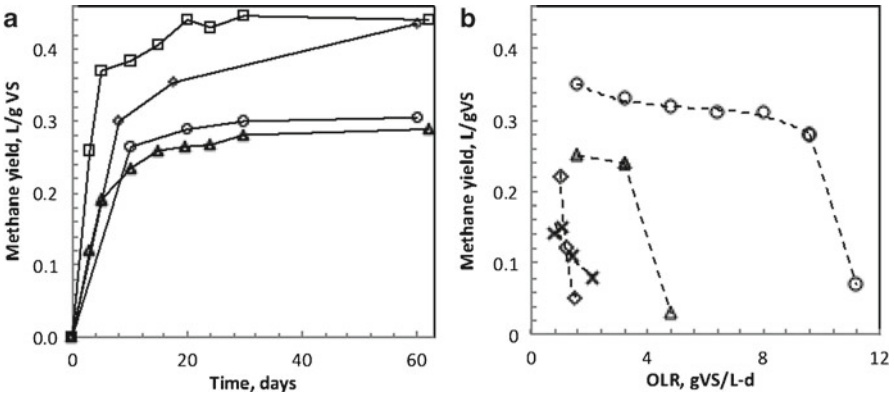

Fig. 8 (**a**) Time course of methane yield from a BMP experiment. *Circles*—*Laminaria saccharina*; *diamonds*—*Macrocystis pyrifera*; *triangles*—algin; *squares*—mannitol [79, 153]. (**b**) Methane yield from *M. pyrifera* with high mannitol content 21.5% (*circles*), low mannitol content 8.3% (*triangles*), *S. fluitans* (*crosses*), and *S. tenerrimum* (*diamonds*) depending from OLR [79]

Na-alginate gel is 6–8 times faster compared to Ca-alginate gel due to calcium cross bridging in the polysaccharides [144]. The products of alginate depolymerization are a mixture of oligosaccharides with different length [145], which are further degraded to 4-deoxy-L-erythro-5-hexoseulose uronic acid [146, 147]. The final products of alginate degradation are glyceraldehyde-3-phosphate and pyruvate [146, 147].

AD of fucoidan has not been studied in detail, but several fucoidan-degrading marine bacteria were isolated and characterized [148]. Several studies prove the possibility of AD of fucoidan containing waste sludge from alginate extraction [136, 149]. Some fucans are resistant to anaerobic fermentation possibly due to specificities of molecular structure in particular strains [148, 150, 151]. The AD of algal proteins and polyphenols and their impact on overall digestibility is an area that needs more attention. It is assumed that polyphenols associate with proteins and polysaccharides in the cell envelope that decreases their availability for biological degradation [150–152].

Brown algae are one of the most studied algal feedstocks for AD. Examined species include *Macrocystis pyrifera*, *Ascophyllum nodosum*, *Durvillea antarctica*, *Sargassum* spp., and *Laminaria* spp. According to the chemical composition, the theoretical methane yield of 0.52 L/g VS and 0.49 L/g VS were predicted for *M. pyrifera* and *Laminaria* sp. [79]. The authors reported an experimental methane yield for *M. pyrifera* of 0.43 L/g VS (82% VS reduction) but only 0.24–0.3 L/g VS (50–60% VS reduction) for *Laminaria saccharina*. The significant difference in VS reduction was explained by variability in chemical composition between these genera. *Laminaria* has a higher content of fucoidan, laminarin, and alginate but lower content of mannitol (Table 13). The ratio between experimental and theoretical methane yield among *M. pyrifera* species is highly correlated with the mannitol content [153]. Mannitol, in contrast to polysaccharides, can be easily and completely degraded by anaerobic microorganisms (Fig. 8a) [79, 153]. The methane

yield from *L. saccharina* samples harvested in spring (4.2% of mannitol and laminaran, 23% of alginate from TS) provided only 50–65% of the methane yield in comparison to *L. saccharina* samples harvested in autumn (36% of mannitol and laminaran, 15% of alginate from TS) [154].

The methane yield from *Sargassum* spp. using a BMP test showed that two species from this genus *Sargassum fluitans* and *Sargassum pteropleuron* have small potential for biomethane production [121]. All tissues added at 0.12–0.20 L/g VS exhibited a methane yield that was only 33–46% of the theoretical methane yield (Table 18). *Sargassum* species appeared to be a poor feedstock for AD possibly due to low mannitol (3.5–4.5% from TS) and a higher content of fibers (36.5–40.6% from VS) (Table 13).

The ADP in continuously stirred-tank reactors proved that *M. pyrifera* is the best substrate for methane production among brown macroalgae tested. The digester fed by the *M. pyrifera* with higher mannitol content had large methane yield and stability at higher OLR (up to 9.6 gVS/L-day) in contrast to a digester fed with *M. pyrifera* with lower mannitol content or *Sargassum* species (Fig. 8b). Using continuous reactors, the methane yield obtained for different species decreased in the following order: *M. pyrifera* (0.24–0.35 gVS/L-day), *Laminaria* sp. (0.2–0.28 gVS/L-day), *D. antarctica* (0.18 gVS/L-day), *Sargassum* sp. (0.08–0.15 gVS/L-day), *A. nodosum* (0.11 gVS/L-day).

4.2 Anaerobic Digestion of Cyanobacteria and Microalgae

4.2.1 Cyanobacteria

In contrast to many algae, the main component of cyanobacteria is proteins. They also lack a hard polysaccharide-based cell wall. These properties explain the higher digestibility of cyanobacterium species. Two genera, *Arthrospira* (*Spirulina*) and *Anabaena*, have been studied as a potential feedstock for the ADP. The BMP assay for a cyanobacterium mixture collected from Lake Dian resulted in a higher methane yield of 0.37 L/gVS (HRT 35 days) with a methane fraction of 60–65% in the biogas [155]. The methane yield during batch digestion of *Arthrospira platensis* and *Arthrospira maxima* species varied from 0.29 to 0.33 L/gVS corresponding to 68–77% of the theoretical methane yield [156–158].

Samson and LeDuy studied the digestion of *A. maxima* in a continuous reactor and concluded that *A. maxima* can be the sole substrate for stable methane production. Municipal anaerobic sewage sludge can easily adapt to the cyanobacterium feedstock, and the observed methane yield was 0.26 L/gVS at an OLR of 0.97 gVS/L-day, HRT of 33 days, and T at 30°C [159]. Despite high ammonia and fatty acids concentrations (2.5 and 2 g/L respectively), methane production was stable possibly due to high alkalinity (8 g/L) and pH of 7.55.

The incoming VS concentration, OLR, and HRT have a large influence on AD stability and methane yield with *A. maxima* (Fig. 9) [160]. The methane yield and

Table 18 Characteristics of AD of brown seaweeds

Substrate	Reactor type	T (°C)	HRT (days)	OLR (gVS/L-day)	VS red. (%)	CH_4 (L/L-day)	CH_4 (L/gTVS)	CH_4 (%)	References
S. fluitans (bladders)	BMP (0.25 L)	35	60	–	40[a]	–	0.18	–	[121]
S. fluitans (blades)		35	60	–	33.3[a]	–	0.15	–	
S. fluitans (stipe)		35	60	–	42.5[a]	–	0.2	–	
S. fluitans (whole)		35	60	–	40[a]	–	0.18	–	
S. pteropleuron (bladders)		35	60	–	46.3[a]	–	0.19	–	
S. pteropleuron (blades)		35	60	–	36.5[a]	–	0.15	–	
S. pteropleuron (stipe)		35	60	–	26.6[a]	–	0.12	–	
S. pteropleuron (whole plant)		35	60	–	35.7[a]	–	0.15	–	
Sargassum muticum	Batch (0.125 L)	35	50	–	–	–	0.01	10	[595]
M. pyrifera (ambient light)	BMP	35	60	–	82[b]	–	0.43	–	[79]
L. saccharina (ambient light)		35	60	–	58[b]	–	0.3	–	
L. saccharina (low light)		35	60	–	65[b]	–	0.24	–	
L. hyperborea	Batch (10 L)	35	30	–	–	–	0.16–0.2[c]	–	[239]
L. saccharina		35	30	–	–	–	0.22–0.23[c]	–	
A. nodosum		35	30	–	–	–	0.14[c]	–	
L. hyperborea (peeled stipe)	Batch (14 L)	35	10	–	–	–	0.014[a]	–	[144]
L. hyperborea (stipe)		35	10	–	–	–	0.065[a]	–	
L. hyperborea (peeled stipe)		35	12.5	–	–	–	0.056[a]	–	
L. saccharina (spring)	Batch (8 L)	35	15	–	–	–	0.13	60	[154]
L. saccharina (autumn)		35	15	–	–	–	0.2	60	
L. hyperborea stem alginate extraction sieve sludge	Batch (8 L)	35	32	–	–	–	0.15	60[a]	[149]
Same, flotation sludge		35	32	–	–	–	0.11	61[a]	
L. hyperborea and *A. nodosum* alginate extraction sieve sludge		35	32	–	–	–	0.09	56[a]	
Same, flotation sludge		35	32	–	–	–	0.14	67[a]	

M. pyrifera (21.5% mannitol content from TS)	CSTR (10 L)	35	50	1.6	67[b]	0.56[a]	0.35	57	[154]
		35	25	3.2	63[b]	1.06[a]	0.33	–	
		35	17	4.8	62[b]	1.54[a]	0.32	–	
		35	12	6.4	60[b]	1.98[a]	0.31	–	
		35	11[a]	8	60[b]	2.48[a]	0.31	–	
		35	10	9.6	54[b]	2.69[a]	0.28	–	
		35	8.6	11.2	14[b]	0.78[a]	0.07	–	
	NMVFR (USR) (6 L)	35	50	1.6	70[b]	0.59[a]	0.37	56	
		35	17	4.8	68[b]	1.74[a]	0.363	–	
		35	12	6.4	66[b]	2.24[a]	0.35	–	
		35	11[a]	8	66[b]	2.80[a]	0.35	–	
		35	10	9.6	64[b]	3.26[a]	0.34	–	
M. pyrifera (8.3% mannitol content from TS)	CSTR (10 L)	35	50	1.6	50[b]	0.40[a]	0.25	56	[154]
		35	25	3.2	48[b]	0.77[a]	0.24	–	
		35	17	4.8	6[b]	0.14[a]	0.03	–	
M. pyrifera (ground)	CSTR (1.5 L)	35	10	1.6	38.6	0.34	0.215	59	[79]
		35	18	1.6	50.8	0.44	0.278	58	
M. pyrifera (ground, desalted)		35	10	1.6	35.8	0.33	0.207	59	
		35	18	1.6	36.2	0.34	0.212	60	
M. pyrifera (ground control)		35	12	1.6	62.1	0.38	0.239	58	
M. pyrifera (ground, N and P added)		35	12	1.6	49.7	0.37	0.233	60	
M. pyrifera (homogenized)		35	12	1.6	44.8	0.40	0.249	61	
M. pyrifera (ground, undiluted)		35	12	1.6	63.9	0.42	0.262	59.6	
M. pyrifera (ground)		35	12	3.2	58.2	0.57	0.177	49.2	
M. pyrifera (ground, sea water added)		35	12	1.6	58.5	0.29	0.181	54	
M. pyrifera (ground, inoculum A: adopted anaerobic municipal sludge)		35	18	1.6	–	0.44	0.278	58.7	

(continued)

Table 18 (continued)

Substrate	Reactor type	T (°C)	HRT (days)	OLR (gVS/L-day)	VS red. (%)	CH_4 (L/L-day)	CH_4 (L/gTVS)	CH_4 (%)	References
M. pyrifera (ground, inoculum D: A+marine sediments)		35	18	1.6	–	0.46	0.290	52.8	
M. pyrifera (ground, inoculum E: analogous to D, developed at room T)		26	18	1.6	–	0.22	0.137	54.4	
M. pyrifera (ground, control)		35	18	1.6	50.8	0.44	0.278	58.2	
M. pyrifera (ground)		55	18	1.6	31.2	0.24	0.149	50.7	
M. pyrifera (ground)		55	7	3.2	27.3	0.43	0.134	52.1	
M. pyrifera (21.5% mannitol content from TS)	CSTR (10 L)	35	50	1.6	–	0.56[a]	0.35	57.4	[606]
	NMVFR (USR) (10 L)	35	50	1.6	–	0.60[a]	0.38	55.9	
	BFR (6 L)	35	50	1.6	–	0.60[a]	0.38	55.7	
	CSTR (50 L)	35	27	2.4	–	0.39[a]	0.16	48.2	
	NMVFR (USR) (5 L)	35	27	2.4	–	0.48[a]	0.20	47.5	
M. pyrifera	SCSTR (1.5 L)	35	18	–	–	–	0.26	59	[607]
S. fluitans	Semi-continuous (2 L)	28±3	20	2.1[a]	20.2	0.168[a]	0.08	49.5	[124]
		28±3	30	1.4[a]	27.4	0.154[a]	0.11	58.5	
		28±3	40	1.05[a]	33.3	0.158[a]	0.15	67.5	
		28±3	50	0.84[a]	40.4	0.118[a]	0.14	57.5	
Sargassum tenerrimum	Semi-continuous (5 L)	26–31	–	1.5	–	0.075[a]	0.05	60	[608]
		26	–	1.2	–	0.14[a]	0.12	60	
		26	–	1	–	0.22[a]	0.22	60	
L. hyperborea	Semi-continuous (10 L)	35	24	1.65	33.8	0.462[a]	0.28	52.8	[239]
L. saccharina		35	24	1.65	37.3	0.380[a]	0.23	0.51	
A. nodosum		35	24	1.75	25.7	0.193[a]	0.11	0.5	

M. pyrifera	Two-stage (2.5 L ASBR + 4 L UAF)	37	1 + 1	0.3[d]	–	0.033[a]	0.109[d]	65	[395]
Durvillea antarctica		37	1 + 1	0.3[d]	–	0.032[a]	0.107[d]	65	
M. pyrifera + *D. antarctica*		37	1 + 1	0.3[d]	–	0.029[a]	0.098[d]	64	
L. saccharina (spring)	CSTR (8 L)	35	–	1.5	–	0.33[a]	0.22	35–50	[154]
L. saccharina (autumn)		35	–	1.5	–	0.41[a]	0.27	35–50	
L. saccharina	SCSTR (2 L)	35	20	1	–	0.250	0.25	72	[609]
L. japonica	–	35	–	4	–	–	0.25	52	[610]
Laminaria digitata	CSTR (1 L)	37	20	1.8	52	0.558	0.31	63	[135]
Laminaria sp.	CSTR (30 m^3)	35	20	2.4[a]	–	1.2[a]	0.5	61.2	[126]
L. saccharina	SCSTR, (50 L)	37	25	1.09[a]	–	0.24[a]	0.22[a]	–	[611]
		37	25	1.64[a]	–	0.33[a]	0.2[a]	–	
L. saccharina (lime pretreated pH11)		37	25	0.6[a]	–	0.18[a]	0.297[a]	–	
L. hyperborea sieve sludge (stem alginate extraction)	Semi-continuous (8 L)	35	23	0.15	–	0.042[a]	0.28	56[a]	[149]
		35	16	0.37	45.8	0.026[a]	0.07	47[a]	
L. hyperborea flotation sludge (stem alginate extraction)		35	23	0.57	15.6	0.086[a]	0.15	60[a]	
		35	16	0.81	46.7	0.081[a]	0.1	63[a]	
L. digitata flotation sludge (from alginic acid extraction)	CSTR (6 L)	37	20	0.91	56	0.25[a]	0.28	62	[136]
		37	15	1.42	53	0.41[a]	0.29	62	
		37	10	1.81	49	0.52[a]	0.29	62	
		37	7.5	2.55	45	0.69[a]	0.27	62	

BMP biomethane potential; *CSTR* continuous stirred-tank reactor; *SCSTR* semi-continuous stirred-tank reactor; *NMVFR* non-mixed vertical flow reactor; *USR* upflow solids reactor; *BFR* baffle-flow reactor; *ASBR* anaerobic sequencing batch reactor; *UFA* upflow anaerobic filter

[a]Estimated from data given in the paper

[b]VS reduction estimated from data given in the paper using an equation $\text{VS red.} = [L(CH_4 / gVS)] / [L(CH_4 / gVS)]_{\text{theoretical}}$

[c]Methane yield estimated from biogas yield given in the paper using a CH_4/biogas ratio of 0.5

[d]Estimated from data given in the paper using total work volume 6 L and VS/TS ratio of 0.6

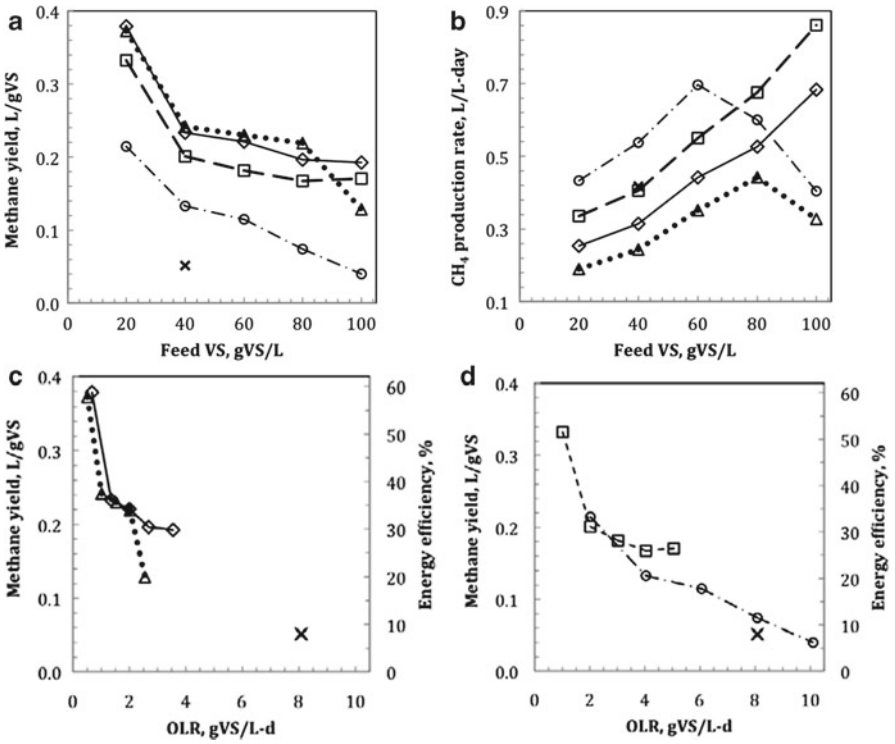

Fig. 9 Influence of the feed volatile solids (VS) concentration (**a**, **b**) and OLR (**c**, **d**) on the methane yield, volumetric productivity and energy efficiency from anaerobic digestion of *Arthrospira maxima* in semi-continuous reactors. *Triangles*—HRT 40 days; *diamonds*—HRT 30 days; *squares*—HRT 20 days; *circles*—HRT 10 days; *cross*—HRT 5 days (based on [160])

methane volumetric production rate were 0.04–0.36 L/gVS and 0.17–0.8 L/L-day, respectively. The maximum methane yield was obtained at HRT equal to 30 days, VS concentration of 20 gVS/L, and the OLR of 0.67 gVS/L-day. Despite a high concentration of ammonia (1.9–7.1 g/L) and volatile acids (up to 23.2 g/L), the methane production was stable with the exception of operation with HRT of 5 days and high feed concentration at HRT of 10 days. The average methane content of the biogas was in range of 69–71%. At high OLRs, it dropped to 46–60%, which is evidence for inhibition of methanogens. A stable ADP occurred when the alkalinity was high (7.2–29 g $CaCO_3$/L) (Table 19).

4.2.2 Microalgae

Microalgae are a very diverse group of organisms. The predominant organic constituent can vary from carbohydrates to proteins or lipids. The green microalgae were predominantly tested as possible substrate for biogas production (Table 20)

Table 19 Characteristics of anaerobic digestion of selected cyanobacteria

Substrate	Reactor	T (°C)	HRT (days)	OLR (gVS/L-day)	VS red. (%)	Conv. eff. (%)	CH_4 (L/L-day)	CH_4 (L/gTVS)	CH_4 (%)	References
Unknown cyanobacteria (Lake Dian)	BMP assay (1 L)	16–26	35	–	–	–	–	0.366	60–65	[401]
A. platesis	Batch (0.25 L)	38	35	–	–	–	–	0.293	61	[157]
A. maxima	Batch (0.12 L)	35	105	–	–	–	–	0.33	–	[158]
Arthrospira	Batch (11 L)	35	28	0.91	–	–	0.28–0.29[a]	0.31–0.32	–	[156]
A. maxima (frozen, control)	Semi-continuous (1.5 L)	35	20	2	26	–	0.38	0.19	72	[233]
A. maxima (live)		35	20	2	28.6	–	0.40	0.2	70	
A. maxima (ultrasonic)		35	20	2	23	–	0.34	0.17	75	
A. maxima (50°C, pH1)		35	20	2	0	–	0.00	0	0	
A. maxima (50°C, pH3)		35	20	2	16.6	–	0.22	0.11	64	
A. maxima (50°C)		35	20	2	28.3	–	0.40	0.2	70	
A. maxima (50°C, pH11)		35	20	2	26.6	–	0.42	0.21	73	
A. maxima (50°C, pH13)		35	20	2	12.9	–	0.18	0.09	68	
A. maxima (100°C, pH1)		35	20	2	10.1	–	0.12	0.06	60	
A. maxima (100°C, pH3)		35	20	2	20.1	–	0.28	0.14	67	
A. maxima (100°C)		35	20	2	25.8	–	0.36	0.18	71	
A. maxima (100°C, pH11)		35	20	2	27.8	–	0.44	0.22	74	
A. maxima (100°C, pH13)		35	20	2	21.4	–	0.28	0.14	73	
A. maxima (150°C, pH1)		35	20	2	4.1	–	0.04	0.02	53	
A. maxima (150°C, pH2)		35	20	2	22.2	–	0.32	0.16	70	
A. maxima (150°C)		35	20	2	24.2	–	0.36	0.18	73	
A. maxima (150°C, pH11)		35	20	2	31.9	–	0.48	0.24	76	
A. maxima (150°C, pH13)		35	20	2	8.1	–	0.16	0.08	68	

(continued)

Table 19 (continued)

Substrate	Reactor	T (°C)	HRT (days)	OLR (gVS/L-day)	VS red. (%)	Conv. eff. (%)	CH_4 (L/L-day)	CH_4 (L/gTVS)	CH_4 (%)	References
A. maxima	SCSTR (1.5 L)	15	20	2	5	5.6	0.06	0.03	54.1	[160]
A. maxima		25	20	2	20	17.6	0.24	0.12	69	
A. maxima		35	20	2	40.8	39.2	0.4	0.2	72	
A. maxima		52	20	2	6.7	6.6	0.07	0.04	53.3	
A. maxima	Semi-continuous (1.5 L)	35	20	1[a]	42.3	–	0.31[a]	0.31	74	[411]
		35	20	1.95[a]	26.2	–	0.37[a]	0.19	72	
		35	20	3[a]	24.7	–	0.51[a]	0.17	69	
		35	20	3.88[a]	24.2	–	0.62[a]	0.16	65	
90.7% *A. maxima* +9.3% sewage sludge		35	20	2.22[a]	44.2	–	0.69[a]	0.31	73	
67.3% *A. maxima* +32.7% sewage sludge		35	20	2.93[a]	38.3	–	0.82[a]	0.28	74	
50.6% *A. maxima* +49.4% sewage sludge		35	20	3.92[a]	48.1	–	1.41[a]	0.36	76	
Sewage sludge (homogenized)		35	20	1.94[a]	45.8	–	0.64[a]	0.33	73	
90.4% *A. maxima* +9.6% peat extract		35	20	2.2[a]	28.7	–	0.44[a]	0.2	71	
65% *A. maxima* +35% peat extract		35	20	3[a]	40.3	–	0.84[a]	0.28	70	
48% *A. maxima* +52% peat extract		35	20	4.13[a]	37.1	–	0.91[a]	0.22	60	
Peat extract		35	20	1.95[a]	38.5	–	0.43[a]	0.22	56	

90.7% *A. maxima* + 9.3% spent sulfite liquor		35	20	2.2[a]	34.9	–	0.55[a]	0.25	73	
66.1% *A. maxima* + 33.9% spent sulfite liquor		35	20	3[a]	12.2	–	0.15[a]	0.05	42	
50.6% *A. maxima* + 49.4% spent sulfite liquor		35	20	4[a]	8.6	–	0.12[a]	0.03	34	
Spent sulfite liquor		35	20	1.95[a]	0	–	0	0	0	
A. maxima	SCSTR (0.2 L)	55	8	2.82[a]	22.6	–	0.212[a]	0.075[b]	48.7	[158]
		55	12	1.88[a]	31.8	–	0.310[a]	0.165[b]	63.2	
		55	16	1.41[a]	30.9	–	0.190[a]	0.135[b]	57.2	
		35	8	2.82[a]	27.8	–	0.381[a]	0.135[b]	61.2	
		35	12	1.88[a]	39.8	–	0.423[a]	0.225[b]	65.6	
		35	16	1.41[a]	37.4	–	0.317[a]	0.225[b]	61.7	
A. maxima	SCSTR (12 L)	35	33	0.97	65.8	–	0.25	0.26	68–72	[159]

BMP biomethane potential; *SCSTR* semi-continuous stirred-tank reactor

[a]Estimated value from data presented in the paper

[b]Estimated from data given in L CH_4/g COD using a COD/VS ratio of 1.5

Table 20 Characteristics of AD of green microalgae

Substrate	Reactor	T (°C)	HRT (days)	OLR (gVS/L-day)	VS red. (%)	CH_4 (L/L-day)	CH_4 (L/gVS)	CH_4 (%)	References
Chlorella sp.	BMP assay (0.4 L)	37	38[a]	–	–	–	0.47[b]	–	[436]
Chlorella (residues, butanol extraction)		37	34[a]	–	–	–	0.32[b]	–	
Same + glycerol (4% of mass)		37	30[a]	–	–	–	0.34[b]	–	
Chlorella (residues chlorof./methanol extraction)		37	30[a]	–	–	–	inhib.	–	
Chlorella (residues after ACIST)		37	22[a]	–	–	–	0.26[b]	–	
Same + glycerol (4% of mass)		37	22[a]	–	–	–	0.28[b]	–	
C. vulgaris	Batch (5 L)	28–31	64	–	–	–	0.32–0.38[c]	68–76	[612]
Chlamydomonas reinhardtii	Batch (0.25 L)	38	35	–	–	–	0.387	66	[157]
Chlorella kessleri		38	35	–	–	–	0.218	65	
D. salina		38	35	–	–	–	0.323	64	
S. obliquus		38	35	–	–	–	0.178	62	
Dunaliella	Batch (11 L)	35	28	0.91	–	0.4–0.41[d]	0.44–0.45	–	[156]
Chlorella + unknown specie + *C. reinhardtii* and *Pseudokirchneriella subcapitata* at low level	Batch (0.5 L)	34	14	–	–	–	0.22	65	[237]
		34	25	–	–	–	0.28	65	
		34	45	–	–	–	0.39	65	
		41	14	–	–	–	0.22	65	
		41	25	–	–	–	0.31	65	
Same species, pretreated, $T = 80$ C	Batch (0.5 L)	41	14	–	–	–	0.18	65	
		41	25	–	–	–	0.25	65	
Same species	Plug flow	34	–	0.01	–	–	0.32	65	[237]
Scenedesmus sp. 80% and *Chlorella* sp. 20% (algae from stabilization pond)	Semi-continuous (11 L)	35	30	1.44	43.1	–	0.23–0.27[d]	61[d]	[110]
		50	30	1.44	54	–	0.31[d]	62[d]	
Scenedesmus sp. 80% and *Chlorella* sp. 20% + aluminum sulfate 90–120 mg/L (algae from stabilization pond)	Semi-continuous (11 L)	50	30	1.44	–	–	0.3–0.31[d]	61[d]	
		53	30	1.44	–	–	0.315–0.326[d]	–	
		50	22	1.44	–	–	0.303[d]	–	
		53	11	1.44	–	–	0.315[d]	–	
		53	7	1.44	–	–	0.207[d]	–	

Mix of algae (major: *Scenedesmus* sp., *Chlorella* sp.)	Semi-continuous (4 L)	35	10	2	–	0.18	0.09[d]	71.4[d]	[410]
		35	10	4	–	0.573	0.143[d]	69[d]	
		35	10	6	–	0.818	0.136[d]	68[d]	
75% mix of algae + 25% waste paper		35	10	4	–	0.968	0.24[d]	64[d]	
50% mix of algae + 50% waste paper		35	10	4	–	1.17	0.29[d]	60[d]	
25% mix of algae + 75% waste paper		35	10	4	–	0.317	0.085[d]	53[d]	
67% mix of algae + 33% waste paper		35	10	3	–	0.823	0.274[d]	67[d]	
40% mix of algae + 60% waste paper		10	10	5	–	1.607	0.321[d]	60[d]	
33% mix of algae + 67% waste paper		35	10	6	–	0.856	0.142[d]	60[d]	
Waste paper		35	10	4	–	0.452	0.324[d]	62[d]	
Tertaselmis (fresh)	CSTR (2–5 L)	35	14	2	–	0.62[d]	0.31	72–74	[609]
Tertaselmis (dry)		35	14	2	–	0.52[d]	0.26	72–74	
Tertaselmis (dry) + NaCl 35 g/L		35	14	2	–	0.5[d]	0.25	72–74	
Chlorella sp. residues after ACIST (C/N 8.53)	CSTR (4 L)	25	15	5	–	0.94	0.188	64.5	[436]
		30	15	5	–	1.135	0.227	68.3	
		35	15	5	–	1.51	0.302	67.9	
		40	15	5	–	1.54	0.308	69.2	
Chlorella sp. residues after ACIST + glycerol (C/N 12.44)	CSTR (4 L)	25	15	5	–	0.96	0.192	62	
		30	15	5	–	1.04	0.208	61.7	
		35	15	5	–	1.475	0.295	65.3	
		40	15	5	–	1.325	0.265	63.1	
Chlorella sp. (75%), *Scenedesmus* sp. (23%)	CSTR	45	20	–	–		0.43[d]	71	[109]

BMP biomethane potential; *CSTR* continuous stirred-tank reactor

[a]Methane production reached asymptotic values earlier in samples with lower HRT

[b]Estimated from data given in L CH_4/g TDS using a VS/TDS ratio of 0.9 for *Chlorella* and 0.85 for residues

[c]Estimated from data given in L CH_4/g COD using a COD/VS ratio of 1.5

[d]Estimated from data given in the paper

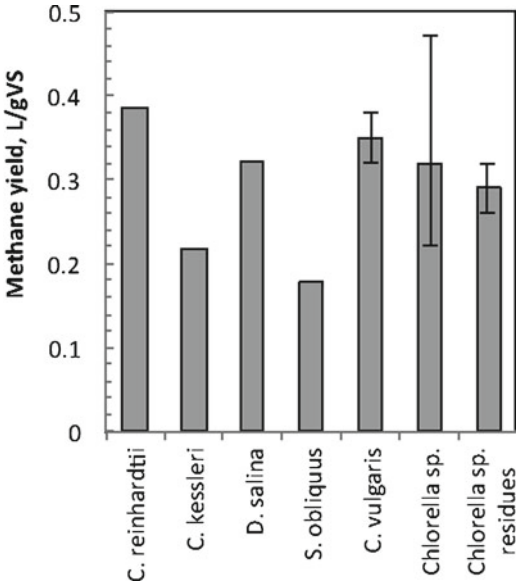

Fig. 10 Theoretical methane yield from different green microalgal species based on Table 3.6 (error bars represents calculated minimum and maximum values for each species)

because of their widespread, fast growth rate, and robustness. The BMP determined for *Chlamydomonas reinhardtii*, *Chlorella kessleri*, and *Scenedesmus obliquus* was 0.387, 0.218, and 0.178 L/gVS, respectively [157]. The amount of biogas production correlated well with the extent of algal degradation. *C. reinhardtii* exhibited a higher cell disintegration rate in comparison to *C. kessleri* and *S. obliquus*. Number of the *Chlorella* and *Scenedesmus* species as well as several other algae (e.g., *Nannochloropsis*) have resistant trilaminar membrane-like structure containing nonhydrolysable sporopollenin-like biopolymer—algaenan [161–164]. The overall cell wall structure has complex organization with three distinct layers: rigid internal microfibrillar, medial trilaminar, and external columnar (for green algae *Coelastrum*) [165]. The major algaenan functions are protection from parasites and desiccation [166]. *Chlorella* and *Scenedesmus* have internal rigid cell walls either glucose-mannose type or glucosamine-type [167–169]. In contrast, *C. reinhardtii* has a cell wall composed of proteins and glycoproteins [170–172]. Resistant cell wall retained *S. obliquus* cells undamaged after 6 months of digestion [157]. The average methane yield with different green microalgae from batch experiments is presented in Fig. 10 (error bars represents minimum and maximum values reported for each specie).

Optimal parameters reported in the literature for stable AD of a mixture of *Chlorella* and *Scenedesmus* were an OLR up to 4 gVS/L-day and an HRT greater than 11 days [110].

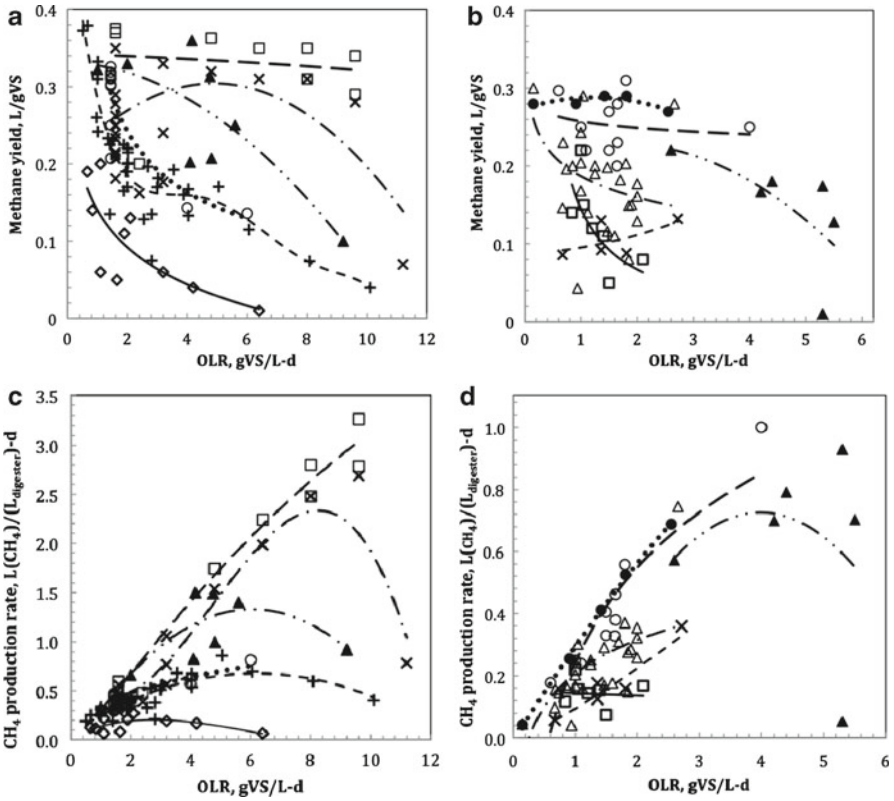

Fig. 11 Methane yield vs. OLR. (**a**, **b**) *Gracilaria*—*diamonds*, *solid line*; *M. pyrifera* (continuous stirred-tank reactor)—*crosses*, *dash dot line*; *M. pyrifera* (non-mixed vertical flow reactor)—*boxes*, *long dash line*; *Ulva* juices—*triangles*, *dash dot dot line*; *Arthrospira*—*pluses*, *short dash line*; *Scenedesmus* and *Chlorella*—*circles*, *dots line*. (**c**, **d**) *Sargassum*—*boxes*, *solid line*; *Laminaria*—*circles*, *long dash line*; *Laminaria* alginate extraction sludge—*filled circles*, *dots line*; *Ulva*—*triangles*, *dash dot line*; *Ulva* and manure—*filled triangles*, *dash dot dot line*; *Enteromorpha intestinalis*—*crosses*, *short dash line*

4.3 Comparison of Methane Yield from Different Algae

A summary of the methane yield and volumetric production rate during algal digestion in continuous reactors appears in Fig. 11. The curves drawn through the data points on each figure represent general trends for easy comparison of the nonuniform data.

Based on these data, algae as a substrate for ADP can be classified into three groups. The first group consists of algae with the methane yield larger than 0.3 L/gVS and includes brown macroalga *M. pyrifera* with high mannitol content, cyanobacterium *Arthrospira*, green microalgae *Chlorella* and *Scenedesmus*. The second group has methane yield about 0.2 L/g VS and includes brown macroalga *Laminaria* and green macroalgae *Ulva, Cladophora*, and *Chaetomorpha*. Lastly, the third group has methane yield lower than 0.15 L/g VS and includes brown macroalga *Sargassum*, red macroalga *Gracilaria*, and green macroalga *Enteromorpha*.

Another important conclusion is that AD of *M. pyrifera* is stable at values of OLR up to 10 gVS/L-day. High values of the methane volumetric production rate are achieved 2.7 L(CH_4)/L(digester)-day, reducing the required volume and the capital costs of the digester.

Finally, several methods such as application of advanced digestion reactors, co-digestion of algae with other substrates, algal hydrolysis and extraction of cellular liquids, and digestion of alginate extraction residues, significantly enhance methane yield, production rate, and the overall process efficiency.

5 Current and Prospective Methods for Algae to Methane Process Enhancement

In general, biological production of methane from algae or cyanobacteria is a two-step process. The first step is biomass production or capturing and conversion of sun light energy into new algal cells. The second step is a transformation of energy stored as biomass into a more applicable form, such as methane gas, through the ADP. Methane is easily stored, transported, and used for the production of heat or electricity. Methane can also be used as a motor fuel. The efficiency of methane production from sunlight energy relies on the performance of these coupled steps.

5.1 Algal Biomass Improvement

The performance of the biomass production step can be described by productivity per acre but the algal methane potential is controlled by algal biochemical composition. In this section, we review factors that control and limit algal productivity and methane potential. We also describe methods used for the improvement of methane production from algae.

5.1.1 Algal Productivity

Algal productivity is limited by several factors that can be classified as physical, biochemical, ecological, and operational (Table 21) [53]. Cultivation and harvesting technologies are very dissimilar for macro- and microalgae due to significant differences

Table 21 Algal productivity limitations and strategies for improving the productivity

Limitation parameter	Productivity limitation factors	Strategies to improve productivity
Physical	Light Temperature Nutrients (N, P, metals) Carbon source (CO_2, organic) O_2 concentration pH	Control of physical parameters Usage of waste-heat from power plants Usage of nutrient-rich waste-streams (domestic, agricultural, industrial wastewaters) Aeration by CO_2 rich gases (power-plant exhausted gases, biogas, alcohol fermentation gases)
Biochemical	Light harvesting efficiency RuBisCO rate and efficiency (carboxylation vs. oxygenation of ribulose-1,5-bisphosphate) Rate of carbon assimilation	Screening of naturally efficient algae Genetic engineering of photosynthetic machinery (increasing amount of secondary pigments; increasing efficiency of RuBisCO; CO_2 concentration mechanisms; reduction of photoinhibition; apoptosis elimination) Optimization of light/dark cycles
Ecological	Pathogens (bacteria, fungi, viruses) Predators (insects, zooplankton) Other algal competitors	Screening for naturally high resistant and competitive species Application of closed reactors Combined closed/open reactor operational scheme Genetic engineering of strains resistant to pathogens and predators
Operational	Mixing (hydrodynamic stress) Dilution rate Illuminated surface area/volume ratio Circulation	Design of reactor with high mass transfer coefficients and low shear stress Mathematical modeling for determination of optimal operational parameters

in physical or biochemical characteristics. Macroalgae are usually cultivated in marine nearshore and offshore zones, cages, ponds, tanks, or spray systems [173–178]. Microalgae are grown generally either in freshwater or brackish open ponds, closed photobioreactors, fermenters, or hybrid systems [179–188].

5.1.2 Enhancing Algal Digestibility by Pretreatment

Digestibility, or the amount of VS reduced (converted to biogas) during AD, is one of the most important characteristics of the feedstock. The amount of algal VS reduced varies in the range from 20 to 60% for most macro- and microalgae (Tables 16–19). Consequently, the conventional ADP is not able to convert all algal organic matter to biogas and a large fraction of energy is lost as low-value residues. Pretreatment of algal biomass is one of the strategies used for conditioning and increasing algal digestibility, methane yield, and degradation rate. Possible goals of pretreatment include:

- Disruption of cell wall
- Size reduction and increase of specific surface area of particulate biomass

- Crystallinity reduction of fiber materials (e.g., cellulose)
- Solubilization of recalcitrant and poorly biodegradable materials (e.g., hemicellulose, lignin)
- Partial hydrolysis of cell polymers
- Deactivation of toxic materials

The important requirements for pretreatment methods are to preserve the total organic matter content and to prevent the formation of inhibitory materials. Little is known about providing efficient solutions for increasing algal digestibility. A variety of pretreatment methods have been tested on waste-activated sludge (WAS), livestock manure, pulp and paper residues, and lignocellulosic biomass [21, 189–193]. Similar methods can be potentially applied for algal biomass conditioning. Methods applied for biomass pretreatment can be classified into the following groups:

- Mechanical—grinding, milling, homogenization, ultrasonic treatment, liquid shear [194–205]
- Thermal—drying, steam pretreatment, hydrothermolysis [195, 206–209]
- Chemical—acid or alkali hydrolysis, ozonation, hydrogen peroxide treatment [198, 208, 210–213]
- Biological—temperature-phased AD enzymatic treatment [195, 198, 214, 215]
- Electrical—electro-Fenton [216, 217]
- Irradiation—gamma-ray, electron-beam, microwave [218–222]
- Combination—thermochemical, wet oxidation [208, 211, 223–226]

Mechanical Pretreatment

Hydrolysis of particulate organic matter is frequently the rate-limiting step during AD [227, 228]. Mechanical pretreatment of lignocellulose materials increased the hydrolysis and methane yield by 5–25% [229] and reduced the digestion time by 23–59% [230] compared to nontreated samples. Disintegration of WAS in an agitator ball mill Model LME 50 K with fine sand balls (0.5–0.9 mm of diameter and 2.7 kg/L of density) increased chemical oxygen demand (COD) solubilization by 25–31% and enhanced biogas yield by 38% compared to nontreated WAS [231]. Mechanical pretreatment of WAS in a high-pressure homogenizer (pressure up to 600 bar) increased biogas production by 18% [195].

Ultrasonic treatment has been widely studied as a method for enhancement of WAS solubilization and methane yield. The minimum energy level required to disrupt the activated sludge cell wall is in the range of 1,000–3,000 kJ/kg TS [197, 203] or 20–30 kJ/L [197, 232]. Ultrasonic pretreatment (E_s = 40,000 kJ/kg SS) of WAS resulted in a fivefold increase in the amount of organic matter solubilization but had no influence on biogas yield [199]. Another study showed the same beneficial trend as solubilization increased by 127% at 42 kHz for 120 min [201]. Biogas and methane yields were observed to increase by 20% [201] and by 50% (for biogas) at E_s = 6,950 kJ/kg TS [197].

Mechanical pretreatment is required prior to AD of macroalgae and includes chopping (>5 mm), milling (1–5 mm), or homogenization (<1 mm). Grinding of the

Ulva did not influence the total methane yield but it increased the kinetics of hydrolysis and methane production rate [129]. The grinding of the feedstock is likely more important for continuous stirred-tank reactor (CSTR) or semi-continuous reactors where the HRT is an important operating parameter.

One study examined the influence of mechanical disintegration plus ultrasonic treatments on *A. maxima* organic matter solubilization, VS reduction, and methane yield [233]. Ultrasonic treatment (Polytron generator PT20ST, from Brinkmann Instruments) increased the soluble COD (sCOD) 3.8-fold compared to freshly harvested cyanobacteria. *A. maxima* COD solubilization increased from 21.3 to 76.7%. Surprisingly, VS reduction and methane yield were 0.9 and 0.85 times the values from fresh (not pretreated) biomass, respectively. Only hydrolytic bacteria and acidogens benefited from the larger amount of readily degradable substrate. The VFA concentration increased from 12 g/L in the digester with fresh algae to 46 g/L in the digester with pretreated algae. The lack of improvement in the methane yield might be due to the inhibition of methanogenic organisms from the high VFA concentration. Ultrasound pretreatment (19 kHz, treatment energy 1–5 Wh/L) had no influence on the methane yield from homogenized red macroalga *Polysiphonia* [123]. While the amount of biogas increased by 25–28%, the methane fraction dropped from 42–49 to 33–37%.

Thermal Pretreatment

Organic compounds organized into structurally complex parts of cells are significantly less biodegradable compared to pure compounds and simple compound mixtures, possibly due to lower accessibility to enzymes [207]. Many studies have shown that thermal pretreatment increases solubilization of particulate organic fractions and partially hydrolyzes polymeric organic molecules. The products formed during pretreatment of pure macromolecules, as well as components of primary sludge (PS) and WAS, at temperatures ranging from 130 to 220°C, was recently studied [209]. The main findings of this study are: (1) no caramelization (pyrolysis) or significant hydrolysis of starch and cellulose to mono- or dimeric reducing sugars occurred at temperatures lower than 220°C; (2) breakdown of proteins to smaller peptides is accompanied by significant ammonia release at temperatures higher than 150°C, that can lead to inhibition of methanogens; (3) unsaturated lipids are hydrolyzed mostly to VFA (acetic and propionic) while saturated lipids form long fatty acids (LFA) (valeric, capronic, heptanic); (4) amount of LCFA and products with different degrees of oxidation (aldehydes, ketones, alkanes, alkenes, alcohols) increases with increasing treatment temperature (especially for temperatures higher than 170°C). Some of these compounds can be toxic to microorganisms, especially to methanogens [62, 234].

Bougrier and colleagues classified thermal pretreatment regimes into two groups, based on their temperature range, duration, and the impact on methane (biogas) yield [196]. The first group is characterized by moderate temperature in the range from 70 to 120°C and treatment duration time from 30 min to several days. The outcome is a 20–30% increase in methane (biogas) yield. The second group is characterized by

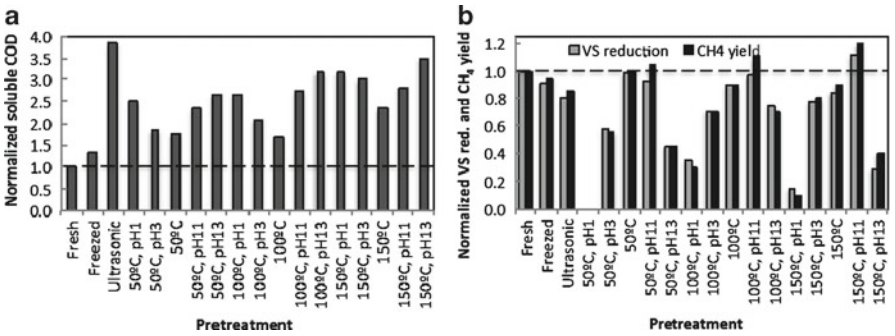

Fig. 12 Effect of freezing, ultrasonic, thermal and chemical pretreatments on: (**a**) COD solubilization of *A maxima*; (**b**) VS reduction and methane yield of *A maxima*. All data normalized to VS reduction and methane yield of fresh, living algae. CSTR volume of 2 L, HRT of 20 days, OLR of 2 gVS/L-day [233]

higher temperatures in the range of 160–180°C and shorter treatment time of 1–60 min with a 40–100% increase in biogas yield. Increasing the pretreatment temperature to 200°C reduced the bioconvertibility of all tested pure nitrogenous compounds (amino acids mix, RNA, DNA, collagen) and all tested carbohydrates (ribose, deoxyribose, glucose) and increased the toxicity. Stuckey and McCarty viewed thermal pretreatment as the sum of two separate processes: the first is the hydrolysis of complex polymeric compounds to soluble biodegradable molecules; and the second is the formation of refractory and toxic compounds from simple degradable molecules [207]. This trend was found to be true for tested amino acids, nucleotides and sugars with few exceptions (arginine, guanine, thymine). The pretreatment temperature around 170–175°C was found to be optimal for biodegradation of WAS due to formation of less biodegradable and toxic compounds at temperatures 200°C and higher [207, 235, 236].

Samson and LeDuy studied the influence of thermal pretreatment on solubilization and methane yield from cyanobacterium *A. maxima* at 50, 100, and 150°C for a 1-h contact time [233]. Thermal pretreatment at all temperatures was favorable for COD solubilization. The COD values increased by 1.8, 1.7, and 2.3 fold compared to nontreated samples (Fig. 12a). Solubilization of the COD reached 36.2%, 40%, and 50%, respectively. The levels of solubilization of thermal pretreated samples were somewhat higher than values determined for WAS. Solubilization of WAS increased from 8.1 to 17.6% (from 2.25 to 4.9 g/L) after thermal pretreatment during 30 min at 121°C [201].

The thermal treatment resulted in no benefit or inhibited the yield of methane and VS reduction (Fig. 12b). Similarly, thermal treatment of WAS during 30 min at 121°C resulted in a significant increase of COD (more than 100%). The methane yield and VS reduction increased as well and reached 135.2% and 132.1%, respectively, compared to the untreated control [201]. Pretreatment of *Chlorella* at 80°C decreased the methane production by 19% [237].

In contrast, thermal pretreatment of unicellular algae harvested from the effluent of a high-rate sewage oxidation pond at temperatures from 40 to 120°C and treatment duration of 30 min increased the methane yield [238]. The methane yield increased from approximately 0.14 to 0.17 L/gVS at 50°C and to approximately 0.25 L/gVS at 100–120°C. The methane yield increased with temperature and reached a maximum value at 100°C. The authors also reported the influence of treatment duration (from 1 to 120 h) and biomass concentration (from 3.7 to 22.5%) on methane yield at 100°C. The maximum methane yields were observed for a pretreatment duration of 8 h (0.3 L/gVS, 15% increase) and with a pretreated algae concentration of 3.7%.

Drying

The water content of macroalgae is in the range of 80–95% [79, 124, 144, 239], and centrifuged microalgae have a water content of 90–95% [157]. Biomass drying is energy intensive, but is considered if storage or transportation is necessary before AD. Drying of biomass by heating at 105°C for 24 h had a negative influence on methane yield with *C. kessleri* and *C. reinhardtii* [157]. The decrease in biogas yield from *C. kessleri* and *C. reinhardtii* compared to a nondried control were 23 ± 2.8% and 20 ± 2.7%, respectively. The authors hypothesized that easily digestible VS were lost during the drying process or became inaccessible for enzymatic attack. Consequently, AD of nondried biomass is more feasible and recommended. Technologically, it is beneficial to couple algae cultivating and AD facilities.

Chemical Pretreatment

Acidic, alkali, and oxidative pretreatment approaches have been applied to enhance the biological degradation of biomass. Pretreatment by acid reagents is commonly used for solubilization of hemicellulose and lignin compounds that make other organic materials more available for enzymatic attacks. Also, during acidic pretreatment, the hemicellulose is hydrolyzed to sugar monomers, furfural, hydroxymethylfurfural, and other products [240]. Acidic pretreatment has several possible drawbacks. First, some of the solubilized compounds can be toxic to methanogens. Second, the production of hydrogen sulfide or ammonia nitrogen instead of methane can be enhanced.

Addition of a strong alkali reagent causes solvation, saponification, alkali hydrolysis, and degradation of polymeric organic compounds. Alkali pretreatment (62.0 mEq $Ca(OH)_2$/L for 6.0 h) of the organic fraction of municipal solid waste increased the COD solubilization and enhanced methane yields up to 172% [241]. The influence of different alkaline reagents NaOH, KOH, $Mg(OH)_2$, and $Ca(OH)_2$ on solubilization of WAS has also been examined. The following levels of COD solubilization at pH 12 with the four alkaline reagents have been reported—39.8%, 36.6%, 10.8%, 15.3% [201] and 60.4%, 58.2%, 29.1%, 30.7% [225], respectively.

The effect of NaOH concentration was studied in the range from 0 to 26 g/L. COD solubilization rose significantly as the NaOH dose increased up to 5 g/L [225] or up to 7 g/L [201]. The largest biogas production or biodegradability was reported at NaOH concentrations between 4 and 10 g/L [225]. Additional amounts of NaOH led to decreasing amounts of biogas production. Based on the results from biotoxicity tests, the decrease in biodegradability was not caused by sodium toxicity, but by the formation of refractory compounds under extreme alkali conditions.

Several oxidative reagents have been tested for biomass pretreatment: ozone, oxygen, hydrogen peroxide, and peracetic acid. Hemicellulose and lignin are common targets of oxidative pretreatment. The oxidative chemical reactions include electrophilic substitution; side chain displacement; radical reactions; and cleavage of alkyl, aryl, ether, and ester linkages [242]. Disadvantages of most oxidative methods are losses of organic materials (e.g., sugars) due to the nonselective oxidation and formation of inhibitors.

The oxidative pretreatment of a wastewater sludge mixture with ozone resulted in COD solubilization from 1.3 to 29% for an ozone dose of 0.05 g/g COD and 40% at an ozone dose of 0.1 g/g COD [212]. The methane yield increased by a factor of 1.5 and 1.8, and the methane production rate increased by a factor of 1.7 and 2.2, respectively. Increasing the ozone dose (0.2 g/g COD) resulted in significant oxidation of the sludge organic fraction (about 30%), therefore decreasing the methane yield. The reactions of ozone with some chemicals, such as phenol and LCFA, can form products toxic to methanogens [243].

Biological (Hydrolytic) Pretreatment

The enzymatic hydrolysis of algal cell walls and other biopolymers is a promising alternative to energy-consuming mechanical pretreatment and chemical catalytic hydrolysis at high temperature. It has large potential to increase the digestion rate and methane yield. Treatment of WAS by carbohydrases increased the biogas yield by 13% [195]. Pretreatment with pancreatic lipases (250 units/mg protein, dose 0.25 g/L at 25°C for 5.5 h) of slaughterhouse wastewater with pork fat particles resulted in 35% hydrolysis of the neutral fat, but did not significantly increase the fat hydrolysis rate in the anaerobic reactor (sequencing batch type, 25°C) and did not influence the methane yield [244]. The authors suggested that at relatively low temperature (25°C), anaerobic oxidation of LCFA is the rate-limiting step.

Natural hydrolysis pretreatment of green macroalgae in percolators has been extensively studied [175, 245–249]. This method can be viewed as a type of two-step ADP and is discussed in the subsequent reactor design subsection.

The endo-β-1,4-glucanase from *Cellulomonas* sp. *YJ5* hydrolyzed *Chlorella sorokiniana* cell wall and caused cells lysis after 60–180 min of treatment [250]. Immobilized cellulases hydrolyzed *Chlorella* cells (reduced sugars yield 62%) and gave a twofold increase in lipids extraction efficiency [251]. Other advantages of enzymatic hydrolysis include an absence of inhibiting by-products and achievement of high selectivity [252]. While this method has a large potential, it is necessary to solve several technological blocks before it can be applied in the biofuel industry.

The major roadblocks are higher cost of enzymes production and their handling, high enzymes to substrate specificity, enormous diversity of algal cell envelope composition and structure.

Combined Methods

The simultaneous application of two pretreatment methods can potentially enhance COD solubilization, VS reduction, and methane yield. The following combination of treatment methods have been studied with WAS:

- Thermochemical (alkali-, acid-thermal pretreatment)
- Ultrasonic plus thermal
- Irradiation-assisted methods

Thermal treatment of WAS after adjustment of the pH to 12 (121°C for 30 min) led to an increase in the COD solubilization. With NaOH, KOH, $Mg(OH)_2$, and $Ca(OH)_2$, solubilization reached 51.8%, 47.8%, 18.3%, 17.1% after treatment at 121°C for 30 min [201] or 71.6%, 83.7%, 55.6%, 51.5% at 140°C for 30 min [225], respectively. Other authors reported a COD solubilization of 55% at pH 12 (NaOH) and 140°C for 30 min compared to 48% without alkali reagent [236].

Thermochemical pretreatment enhanced methane yield by 34 and 19% compared to untreated and chemically pretreated samples, respectively [201]. Combined thermochemical pretreatment of *A. maxima* had a stronger impact on increasing the amount of sCOD (Fig. 12a) [233]. A maximum solubilization value of 78% was achieved at pH 13 and temperature 150°C. In most cases, methanogenesis was inhibited compared to untreated fresh algae (Fig. 12b). At pH 11, the methane yield increased by 5%, 10%, and 20% at temperatures 50, 100, and 150°C, respectively. Overall, alkali-thermal pretreatment led to higher levels of solubilization and to larger methane yields compared to acid-thermal pretreatment. Strong inhibition of methanogens can be caused by ammonia, toxic chemicals, and/or fatty acids formed during pretreatment.

Wet oxidation is a pretreatment process when organic materials are treated by gaseous oxygen at high temperatures. It is able to convert poorly biodegradable lignocellulose to carbon dioxide, water, and carboxylic acid [253]. Newspaper biomass pretreated by wet oxidation (190°C) and fermented in a batch anaerobic reactor showed 59% lignin removal, 74–88% cellulose removal, and 59% of the total COD converted to methane [223]. A doubling of methane yield from raw yard waste after wet oxidation pretreatment was reported [254].

Microwave irradiation can be used as a volumetrically distributed heat source, and it can be applied with acid or alkali pretreatment. Microwave-assisted acid pretreatment of herbal-extraction process residue enhanced biogas production by 65, 29, and 14% compared to nontreated, acid, or microwave pretreated samples [255, 256]. Microwave-assisted alkali pretreatment of switchgrass increased the cellulase hydrolysis yield by 53% [257]. Ultrasonic treatment (42 kHz for 120 min) after thermal treatment (121°C for 30 min) had no effect on COD solubilization. Solubilization enhancement was not statistically significant—19.4% vs. 18.4% (ultrasonic only)—and was comparable with the value for single thermal pretreatment of 17.6% [201].

5.1.3 Algal Metabolic Manipulations Through Environmental Factors

The algal biochemical composition has a dramatic impact on algal biomass digestibility and methane yield (Figs. 5 and 7). Improving the extent of algal biomass biodegradability in anaerobic digesters is a critical research need.

Metabolic manipulation is an effective tool for control and influence of algal growth rate and biochemical composition. Several environmental factors, such as availability of carbon dioxide, nutrients (nitrogen, phosphorus), trace metals, silicon for diatoms, level of irradiation, salinity, and temperature affect the enzyme activity and algal biochemical profile significantly.

Generally, stress conditions (nitrogen, phosphorus, or trace metals depletion, photo-oxidative stress, and high salinity) lead to increasing cellular lipid content. Exposure to stress conditions resulted in increasing lipid content on average from 25.5 to 45.7% in green microalgae, from 22.7 to 44.6% in diatoms, and from 27.1 to 44.6% in other oleaginous algae identified as chrysophytes, haptophytes, eustigmatophytes, dinophytes, xanthophytes, or rhodophytes [258]. A major disadvantage of using metabolic methods to modify the lipid content is a decrease in the algal growth/division rate and productivity [259, 260]. This can be countered by an increase in the overall calorific value and theoretical methane potential of the algal biomass due to accumulation of more reduced lipid compounds [261–263]. Li observed the highest lipid productivity at 5 mM nitrate while the highest lipid content was observed at 3 mM nitrate [264]. Optimization of all environmental parameters is necessary to achieve the highest biomass and lipid productivity [265].

Nutrient Starvation Conditions

Many researchers have studied the response of algae to nitrogen and phosphorus limitation. The general trend for most green algae and diatoms is decreasing synthesis of proteins, polyunsaturated fatty acids, and structural polar lipids (phospholipids, glycolipids, and sulfolipids). An increasing production of carbon storage products (carbohydrates and triglycerides) is observed under nitrogen limitation [266–272].

Growth with phosphorus depletion can decrease the algal growth rate and stimulate an increase in the lipid to protein and carbohydrate to protein ratios [267, 273–277]. Phosphorus-starvation conditions negatively affect synthesis of long-chain polyunsaturated phospholipids [266].

Silicon-Deficient Conditions

Silicon is an important element for lipid metabolism in diatoms. Silicon-deficient growth conditions stimulate synthesis of more carbohydrates and triglycerides with higher ratio of saturated and mono-unsaturated fatty acids compared to cells grown in silicon rich conditions [275, 278–280]. After 4 h of silicon deficient growth, acetyl-CoA carboxylase activity increased by 100%, whereas activity of

β-(1→3)-glucan-β-3-glucosyltransferase (chrysolaminarin synthase) was reduced by 31% during the same period [275, 278–280].

Trace Metals Availability

Trace elements are important for optimal cell metabolism. *Dunaliella tertiolecta* deprivation in iron and cobalt significantly affected growth rate but simultaneously caused rapid accumulation of lipids [281]. *Botryococcus* spp. harvested during stationary phase and exposed to an iron-enriched medium stimulated lipids accumulation from 5–18 to 16–36% [282]. One *Botryococcus* species showed the highest lipid content after an exposure in nitrogen-free, but iron-enriched media with high light intensity. *Chlorella vulgaris* harvested in late-exponential growth phase and resuspended in iron-free media for 2 days followed by iron addition had a lipid content up to 57% by dry weight with 1.2×10^{-5} mol/L chelated $FeCl_3$ or three to seven fold larger compared to cells resuspended in lower iron concentrations [283].

Heterotrophic and Mixotrophic Growth

Heterotrophically cultivated cells use organic substrate(s) for carbon and energy while mixotrophically grown cells can use light and organic carbon for energy and use either organic or inorganic carbon for biomass synthesis [180, 181, 284]. Many algae can utilize various organic carbon substrates: sugars (glucose, mannose, fructose, lactose, etc.), VFA (acetate), glycerol, molasses, and organic carbon from wastewater. Under mixotrophic conditions, algae exhibit a five- to tenfold higher growth rate compared to photoautotrophic growth [285]. Species that grow mixotrophically include:

- Green algae: *C.reinhardtii* [286–288]; *Chlorella* sp. [289–293]; *Scenedesmus* [294–296]; *Tetraselmis suecica* [297]; *Platymonas subcordiformis* [298]; *Botryococcus braunii* [299]; *Micractinium pusillum* [300]; *Haematococcus pluvialis* [301–303]; *Haematococcus lacustris* [304, 305].
- Red algae: *Porphyridium cruentum* [306, 307]; *Galdieria sulphuraria* [308].
- Diatoms: *Phaeodactylum tricornutum* [256, 285, 309–312]; *Nannochloropsis* sp. [313–315]; *Navicula saprophila* [316]; *Nitzschia* [316, 317].
- Cyanobacteria: *Synechococcus* [318, 319]; *Arthrospira* [320–323]; *Nostoc flagelliforme* [324]; *Anabaena variabilis* [325].

The main disadvantage of mixotrophic growth is the high cost of organic carbon sources. Main advantages of mixotrophic growth are the elimination of light penetration limitation that allows high concentration of algae (opportunity to reduce harvesting cost), better process control, increased growth rate and production of lipids, and potential to use waste streams as an organic carbon source. One attractive solution is the coupling of wastewater treatment and algal production [326]. Another possible source of organic carbon is acetate from a modified AD system where the major products of anaerobic fermentation are acetate and hydrogen. The drawback of systems grown on waste streams is bacterial and viral contamination.

Light Conditions

Light characteristics have a significant impact on pigment content, photosynthetic activity, and lipid content [327, 328]. Generally, high irradiation inhibits the formation of polar lipids, but stimulates synthesis of storage carbohydrates and neutral lipids (usually triglycerids). Light limitation favors the production of total proteins and structural polar lipids associated with chloroplasts [258, 329–332]. *B. braunii* cultivated under continuous illumination gave the highest yield of exopolysaccharides. A light-dark cycle of 16–8 h resulted in the highest hydrocarbon yield [333]. Blue light was found to promote protein synthesis, while red light stimulated carbohydrate production [334].

5.1.4 Algal Metabolic and Genetic Engineering

Genetic technologies make use of algae as a biological factory for the production of valuable algal metabolites and recombinant proteins [335] including:

- Carotenoids [336, 337]
- Long-chain polyunsaturated fatty acids [338]
- Pharmaceutically active compounds [339, 340]
- Polysaccharides [341, 342]
- Diagnostic and therapeutic recombinant proteins [343, 344]

Originally, genetic techniques were developed for three laboratory model organisms: *C. reinhardtii*, *Volvox carteri*, and *P. tricornutum*. Recently, genetic engineering techniques have expanded to other algal species, including *Chlorella* sp. and diatoms. Sequenced genomes of algae are still limited. Green algae have only 3 genomes completed and 12 genomes are on assembly stage or in progress; diatoms have 2 completed genomes and 3 in progress. The process of sequencing 70 cyanobacterium genomes is completed and 102 genomes are on assembly stage or in progress [345].

Gene Manipulation Tools

Advanced gene manipulation tools are essential for an efficient application of genetic engineering technology, but they are still in the development stage. These gene manipulation tools include:

- Homologous gene replacement or nuclear gene targeting [346, 347]
- Inducible nuclear promoters [348]
- Gene silencing approaches [349–351]
- Gene expression regulation by riboswitches [352, 353]
- New protein tagging approaches [354]

Chloroplast Transformation Technologies

Commonly, wild-type green algae have heavily stacked thylacoids and large light-harvesting antenna complexes (LHC) acclimated for low light conditions that cause photoinhibition under high light conditions [355, 356]. To eliminate the formation of reactive oxygen species, the absorbed photons need to be released as fluorescence and waste heat. This release of energy reduces conversion efficiency of light energy to biomass [357]. One solution to increase the conversion efficiency is to reduce the LHC size and enhance light penetration to the growth media [357–360]. For example, RNA interference technology was applied to downregulate the entire LHC gene family in *C. reinhardtii* [361].

Metabolic Network Reconstruction and Simulation

A metabolic network model is a prospectively powerful tool for selection of the most suitable wild-type organism, as well as to provide direction for the genetic engineering of a more efficient mutant [362]. Combinations of knockout and added genes can be optimized for target product and/or biomass yield [363, 364]. A genome scale reconstructed metabolic network improved bioethanol production for *Saccharomyces cerevisiae* though genetic engineering and evolutionary adaptation [365, 366]. The optimal parameters of the designed bioprocess are the growth media composition, the level of irradiation, the temperature, the product yield, the physical dimensions, and the cost efficiency of the overall process [367].

5.2 Anaerobic Digestion Improvement

The main goals for improving the ADP are increasing the conversion efficiency while simultaneously decreasing capital and operational costs.

5.2.1 Inoculum Source for Anaerobic Digestion of Algae

As discussed earlier, algal biomass has specific biochemical composition and contains unique compounds, such as algin, laminarin, and fucoidan. Moreover, marine algal biomass has a high salt concentration that can affect anaerobic microorganisms. Isolation and application of microorganisms adapted for digestion of specific algae is labor-intensive but has the potential to improve algal ADP.

Generally, anaerobic sludge from a domestic sewage plant or marine anaerobic sediment is used for startup of the algal ADP. Several authors reported that anaerobic organisms adapt readily to algal biomass as a sole substrate, and the inoculum source has a minor or no effect on the final methane yield and VS reduction [77, 159, 368]. On the other hand, addition of an inoculum from marine sediments to anaerobic sewage sludge increased the initial methane production rate (Fig. 13) [77],

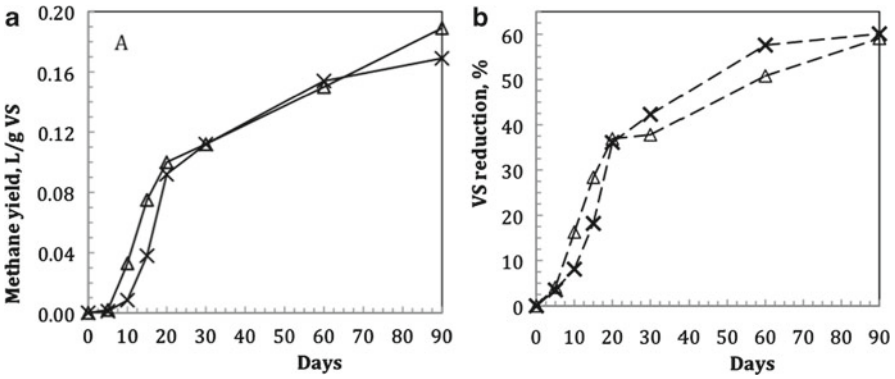

Fig. 13 Influence of inoculum source on methane yield and VS reduction [77]. *Crosses*—inoculum from manure digester; *diamonds*—mix inoculum from manure digester and marine sediments

and addition of a rumen and sewage sludge inoculum adapted to algal substrate increased biogas production and methane concentration [369]. Application of an inoculum adapted to high ammonia concentration is a possible solution to overcome the problem of ammonia inhibition. The inoculum from a piggery anaerobic pond yielded stable methane production from algae with an added ammonia-N concentration up to 3 g/L [370]. In contrast, a sewage mesophilic digester inoculum showed inhibition in methane production at an added ammonia-N concentration larger than 0.5 g/L.

5.2.2 Process Parameters and Reactor Design

Methane yield, VS reduction, OLR, and HRT are important operating parameters for the ADP. Generally, the ratios of actual to theoretically calculated methane yield and VS reduction are relatively low (typically from 0.4 to 0.6). Biodegradability is often limited by the ability of anaerobic bacteria to hydrolyze complex organic compounds as well as by the slow rate of acetogenesis and methanogenesis stages of AD. A variety of methods, including process parameters and reactor design, feedstock pretreatment and conditioning, and source and modification of anaerobic microorganisms are used to increase the AD efficiency. The general principles of digestion with non-algal feedstock can be applied to the AD of algae. Environmental parameters have a significant impact on AD performance. Optimal process design and control allow enhancing methane yield, increasing OLR and decreasing HRT.

Reactor Design

The main goal of optimal reactor design is achievement of the maximum methane yield at high OLR and low HRT in order to reduce reactor volume and capital costs. Several high-rate digester configurations were developed over the past several decades for digestion of biosolid wastes and residues. Their characteristics and

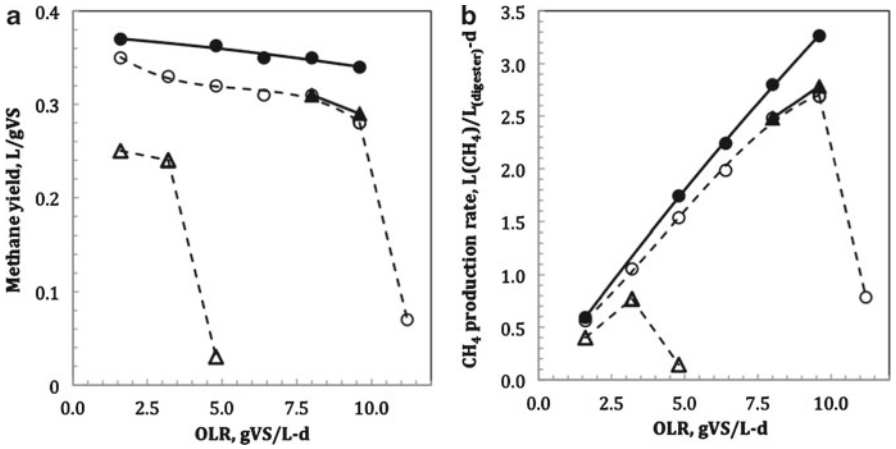

Fig. 14 Methane yield (**a**) and methane production rate (**b**) from *M. pyrifera* depending on OLR, reactor type and mannitol concentration. *Open triangles*—CSTR, 21.4% mannitol; *filled triangles*—NMVFR, 21.4% mannitol; *open circles*—CSTR, 8.3% mannitol; *filled circles*—NMVFR, 8.3% mannitol [79]

advantages and disadvantages are described elsewhere [68, 70, 371–373]. One major strategy is decoupling HRT from SRT by anaerobic sludge immobilization [374–379], granulation, and floc formation [380–387], biomass recycling [388], or membrane retention [389–391]. The methane yield and methane production in a nonmixed vertical flow reactor (NMVFR) digester were larger and more stable at higher OLR compared to CSTR (Fig. 14) [79]. Another promising approach applied for biosolids digestion is separation of the hydrolysis and acetogenesis steps from methanogenesis, a process called a two-stage system [392–394]. A two-stage anaerobic reactor system achieved stable methane production from *M. pyrifera* and *D. antarctica* with an HRT of one day for each stage [395].

A special case of the two-stage system is preliminary treatment of macroalgae in percolation reactors with natural hydrolysis and acidogenesis processes. In percolation reactors, algae are stored in a tank yielding a drained liquid product containing VFAs and ethanol as good substrates for methanogenesis [246, 248]. Legros and colleagues compared maximum OLRs for three systems: one-step CSTR, two-step CSTR, and percolator followed by upflow and fed batch digesters for liquid and solid phases, respectively. The reported maximum volumetric loads were 2.5 g VS/L-day for one-step, 4 g VS/L-day for two-step systems, 5.3 g VS/L-day for upflow reactor, and 6.3 g VS/L-day for fed batch digester (assuming COD/VS equal 1.25). A comparison of methane yield and production rate from *Ulva* and *Ulva* juices is presented in Fig. 11.

The AD of hydrolysis juices is more economically efficient compared to digestion of whole macroalgae due to lower reactor size, energy for substrate heating, grinding, and pumping [246–248]. For example, the volume of digester with fixed bacteria for digestion of hydrolysis juices is 25 times smaller compared to a CSTR digester required for whole algae [245].

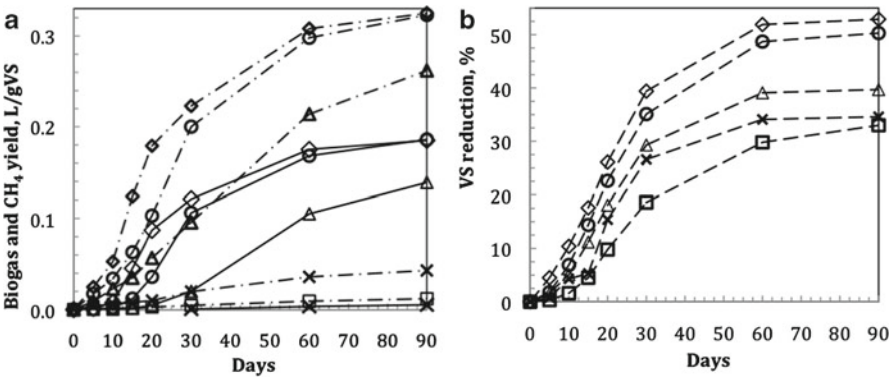

Fig. 15 Influence of temperature on anaerobic digestion of *Enteromorpha Iinza*, *E. intestinalis*, *Enteromorpha prohfera*, and *Percursaria percursa*. *Boxes*—10°C, *crosses*—20°C, *triangles*—25°C, *circles*—30°C, *diamonds*—35°C [77]

Mixing

Mixing is essential for optimal distribution of substrate, intermediate products, nutrients, and microorganisms throughout the anaerobic digester, but excessive mixing can be unfavorable for methanogenic bacteria [396–399]. Furthermore, proper mixing diminishes temperature and concentration fluctuations.

Temperature Conditions: Psychrophilic vs. Mesophilic vs. Thermophilic

Psychrophilic conditions were found to be nonfavorable for methane production from algae even when natural inoculum adapted to low temperature is used to start the AD process [77, 111, 400]. The influence of temperature on digestion of *Enteromorpha Iinza*, *Enteromorpha intestinalis*, *Enteromorpha prohfera*, and *P. percursa* in the range from 10 to 35°C is presented in Fig. 15 [77]. Insignificant methane was detected at temperatures under 25°C. The final methane yields were identical at 30 and 35°C, but the initial methane production rate was significantly higher at 35°C.

Generally, the degradation rate of biosolids is usually higher under thermophilic conditions, reducing the volume of the anaerobic digester. Furthermore, raising the temperature increases the lipid solubility in water and its availability for enzymatic attack. For example, during the digestion of a mixture of *Scenedesmus* spp. and *Chlorella* spp., a 27% higher methane yield was observed at 50°C compared to 35°C [110]. Mesophilic conditions can favor algal survival in the anaerobic digester and make them more resistant to biodegradation. This is evidenced by the low methane yield from the digestion of cyanobacteria at 22.3°C [401]. The intact *Scenedesmus* cells were detected in a digester after 6 months of incubation [157].

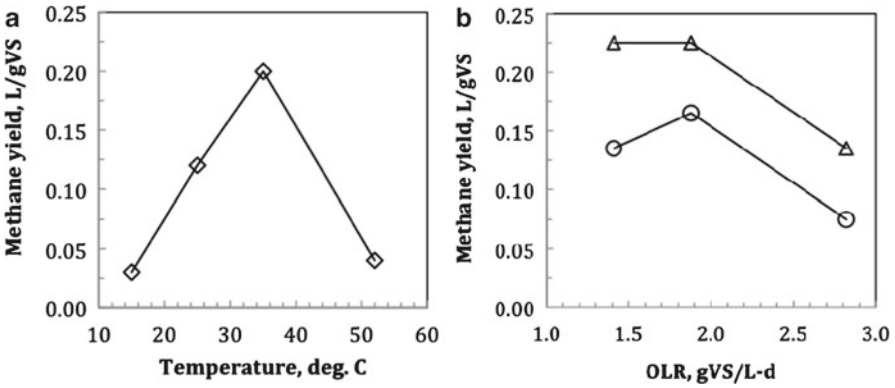

Fig. 16 Influence of temperature on the methane yield during digestion of *A. maxima* in a semi-continuous reactor. (**a**) *Solid line*, *diamonds*: HRT—20 days, OLR—2.02 gVS/L-day [160]. (**b**) *Triangles*—35°C, *circles*—55°C [158]

But, operating under mesophilic conditions is generally more stable due to lower sensitivity of mesophilic organisms to temperature and substrate variations. Moreover, toxicity from ammonia and salts increases as the temperature increases. The observed methane yield from *M. pyrifera* at thermophilic conditions was approximately two times smaller than under mesophilic conditions [402]. *A. maxima* gave 40–80% larger methane yield at mesophilic conditions compared to thermophilic regimes (Fig. 16b) [158]. The methane production from *A. maxima* was completely inhibited at 15 and 52°C (Fig. 16a) [160]. Keenan reported a similar methane yield for mesophilic and thermophilic regimes (0.312 and 0.318 L/gVS) during AD of *Anabaena flos-aquae* at OLR between 3.2 and 2.8 gVS/L-day [403].

5.2.3 Co-digestion of Algae with Other Feedstock(s)

Co-digestion of different substrates has been recognized recently as an attractive approach that has many economical, logistic, and sanitary benefits [404]. The main advantage of co-digestion is the improvement of the nutrient balance that leads to greater reduction of VS and methane yield [405]. The C:N:P ratio is an important factor for AD as discussed earlier in the chapter. Co-digestion of low nitrogen biomass (municipal solid waste, paper, sisal pulp, straw, grasses, wood wastes) with higher nitrogen wastes (sewage sludge, chicken or livestock manure, slaughterhouse, meat or fish processing wastes) can increase the loading rate and methane yield up to 60–100% [399, 406–409].

The C to N ratio varies for macro- and microalgae due to significant differences in biochemical composition. Carbohydrates are the main components of macroalgal

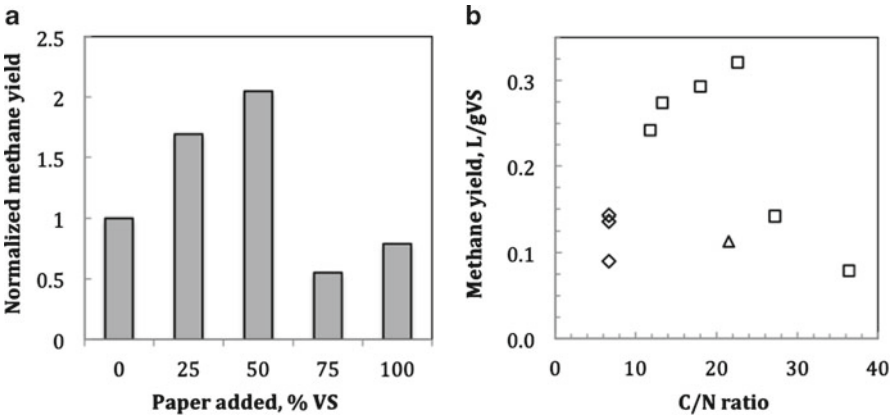

Fig. 17 (**a**) Influence of waste paper percentage on the normalized methane yield of algal biomass (*Scenedesmus* spp. and *Chlorella* spp.) at HRT 10 days and OLR 4 gVS/L-day. (**b**) Methane yield vs. biomass C:N ratio, HRT 10 days. *Diamonds*—algal biomass with varying OLR; *triangles*—waste paper with NH_4Cl and trace elements added; *squares*—algal biomass and waste paper with different ratio (based on [410])

biomass with concentrations between 50 and 70% of dry weight. Microalgae usually have a carbohydrate content in the range 10–20% while the protein content can reach 30–50% in some species. These differences in biochemical composition influence the C:N ratios and the strategies needed for co-digestion processes with macro- or microalgae.

Co-digestion of Microalgae

The C/N ratios for microalgae are in the range of 4–6. The addition of carbon rich cellulosic materials can balance the high nitrogen content. For example, addition of 25 and 50% of waste paper to a mixture of *Scenedesmus* spp. and *Chlorella* spp. resulted in a 1.59- and 2.05-fold increase in the methane yield (Fig. 17a) [410]. The optimal ratio between algal biomass (*Scenedesmus* spp. and *Chlorella* spp.) and waste paper was found to be 40% algae and 60% paper with corresponding C:N ratio equal to 22.6. The influence of the C/N ratio on the methane yield is shown in Fig. 17b. The authors also reported that paper addition stimulated cellulase activity in the anaerobic digester from 1.26 ± 0.14 mg/L-min (no paper added, C:N is equal to 6.7) to 3.02 ± 0.09 mg/L-min (50% paper, C:N is equal to 18).

Addition of *A. maxima* biomass to sewage sludge, peat extract, and spent sulfite liquor improved the VS reduction and methane yield (Fig. 18) [411]. Nutrient rich algal and cyanobacterium biomass can be added to nutrient limited waste products that cannot be digested as sole substrate.

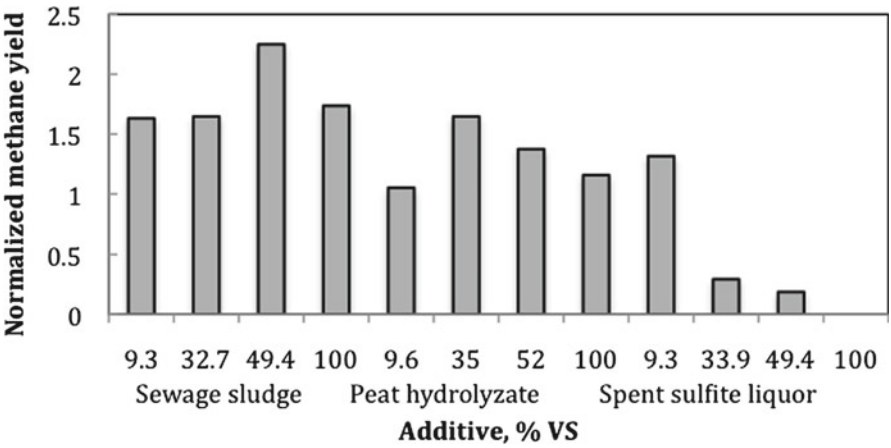

Fig. 18 Influence of added carbonaceous biomass on the methane yield from biomass mix normalized to methane yield from pure algal biomass at HRT 20 days and approximate OLR form 2–4 gVS/L-day [411]

Co-digestion of Macroalgae

The mix of Ulva and manure has a larger methane yield and production rate compared to pure Ulva biomass (Fig. 11c, d). Methane production from a mixture of alginate extraction residues and manure was lower compared to methane production from separate substrates [245]. Morand and coauthors speculated that co-digestion of different seaweeds can be problematic due to dissimilarity in digestion speeds [412]. But addition of *Ulva* to *Sargassum tenerrimum* (1–17 ratio) increased the methane yield and production rate [413].

5.2.4 Metabolic and Genetic Engineering

The application of molecular tools to microbial community structure analysis provides insight about the development of a mature microbial community, its response to changes in substrate loading rate, and the influence of environmental factors [414]. This knowledge allows us to improve the design and control of the ADP.

Metabolic and Genetic Engineering of Anaerobic Microorganisms

Classical strain improvement is an evolutionary engineering technique that has been used for decades for the production of penicillin, amino acids, and many other industrial products, but it is time consuming and has limited applications [415, 416]. Attractive opportunities exist with metabolic and genetic engineering techniques to enhance biofuel production. Studies have been conducted with several organisms

including *Escherichia coli* [417–420], *Zymomonas mobilis* [421–423], *Klebsiella oxytoca* [424, 425], and *S. cerevisiae* [426–429].

Cellulolytic *Clostridium* is one of the prospective organisms for metabolic engineering in an anaerobic digester. Hydrolysis of polymeric organic compounds is often the limiting step during biodegradation of algal biomass. Hydrolysis of algal cell walls is difficult due to its heterogeneous structure composed of carbohydrates, glycoproteins, and lipids. Guedon and colleagues applied metabolic engineering to produce a recombinant *Clostridium cellulolyticum* that exhibited 150% higher cellulose consumption and 180% larger cell dry weight in comparison to the wild strain [430]. Another possible strategy is the expression in *Clostridia* of the algal cell wall degrading enzymes from wild strains that naturally use algal biomass as a substrate. *Saccharophagus degradans* is able to degrade at least ten distinct complex polysaccharides from diverse algal, plant, and invertebrate sources and can be an outstanding source of degrading enzymes [431, 432].

5.3 Integration of Anaerobic Digestion with Other Technological Processes

The high cost of biofuel production and low efficiency of captured energy are major factors that limit the large-scale use of algae for biofuels. The integration of the ADP into the production of other high-value products (e.g., food supplements, pharmaceuticals, and clean water) from algae is likely to make AD economically attractive for biofuel generation.

5.3.1 AD Integrated into Other Algal Biofuel Production Pathways

There are several algae to biofuel conversion technologies, such as lipids extraction followed by transesterification, thermochemical hydroprocessing, phototrophic microbial fuel cell (PMFC), and algal hydrogen production. These processes generate large quantities of waste algal biomass, residues, or by-products. The ADP is a prospective technology that can convert these waste materials into valuable fuel.

Biodiesel and Green Diesel Production Processes

The ADP is widely used for processing a variety of organic residues and wastes. The AD can be integrated into many potential pathways for algal biofuels production as shown in Fig. 19 [433]. Coupling biodiesel and green diesel production processes with the ADP (Fig. 20) can improve the overall efficiency of energy recovery and reduce the final cost of biofuel [434]. Based on the theoretical calculations, the ADP can recover approximately 55–85% of the biomass energy content in a coupled biodiesel-ADP, depending on algal lipid content [263]. Similar results were achieved by the calculation of theoretical energy output from conversion of *T. suecica* [435].

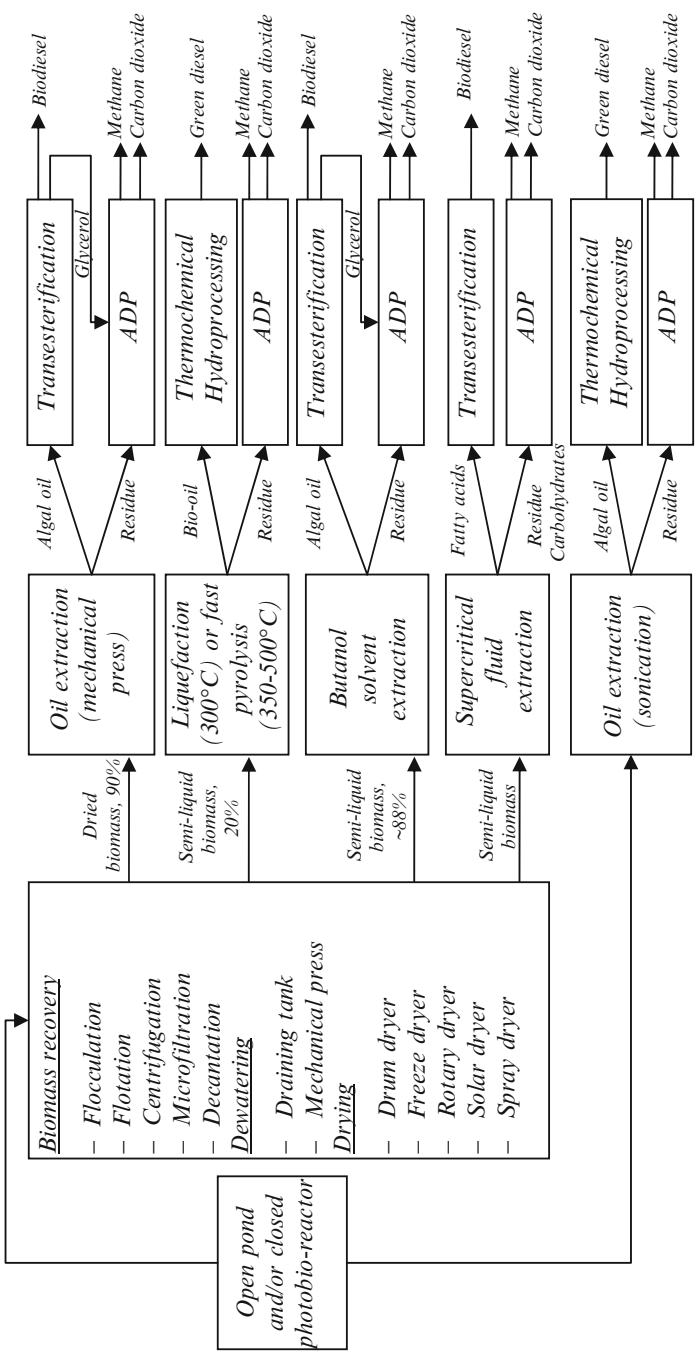

Fig. 19 The integration of anaerobic digestion process into biodiesel and green diesel production processes (based on [433])

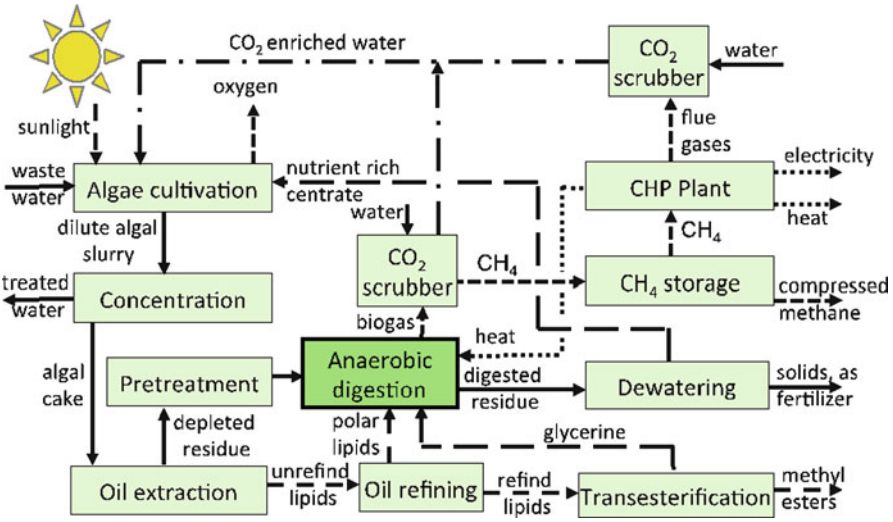

Fig. 20 Conceptual diagram for the integrated biodiesel and biogas production

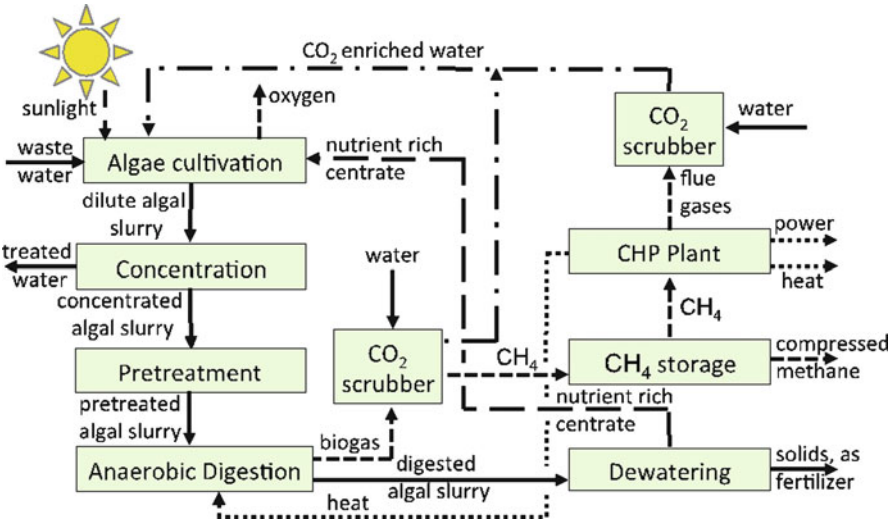

Fig. 21 Conceptual diagram for the coupling of an algal production-ADP into a carbon dioxide mitigation and waste treatment process

Simultaneous production of biogas and biodiesel gave the largest energy output, with 60% of the energy coming from biogas (Fig. 22). The authors calculated that the biodiesel-ADP reduced the biodiesel production cost by 33% and the carbon emission by 75%.

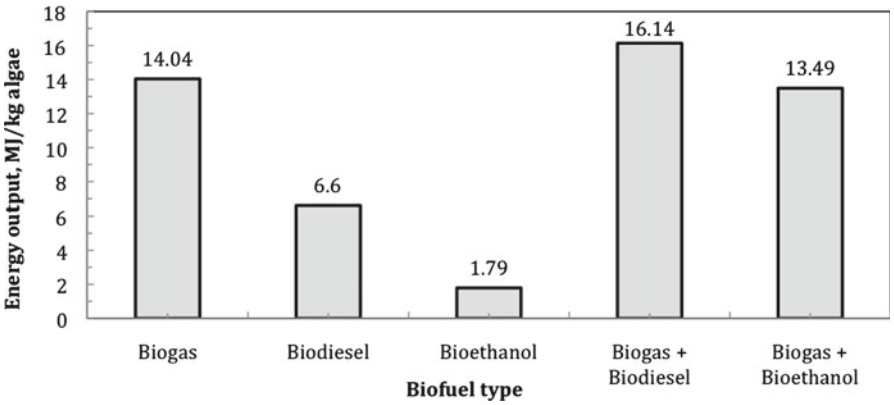

Fig. 22 Energy output of different types of biofuels with *Tetraselmis suecica* [435]

Chlorella residue from the biodiesel production process is a feasible substrate for methane production [436, 437]. Either 1-butanol as a solvent for lipid extraction or acid catalyzed in situ transesterification was recommended because application of the normal chloroform/methanol mixture inhibited methane production. The observed methane yield from algal residues was approximately 52–63% from fresh algae. Addition of glycerol as a co-substrate slightly increased the methane yield by 4–7% possibly due to a more favorable N to C balance [437].

Algal Hydrogen Production System

The ability of green algae to produce hydrogen was discovered over 70 years ago [438, 439]. Hydrogen is recognized in the US and EU as a promising future fuel [440]. While the technology of generating hydrogen from algae is far from being at the industrial scale, several laboratories are working on improving the hydrogen production efficiency by using transcriptomics, proteomics, and metabolomic data [441–443].

The ADP can be used to process surplus algal biomass into methane or hydrogen. A combined biorefinery concept has recently been proposed [157]. During the first step, *C. reinhardtii* produces hydrogen via a sulfur deprivation method. During the second step, it is digested anaerobically for methane production. The authors reported approximately 123% more biogas production from algae after the hydrogen production cycle compared to fresh algae due to the accumulation of lipids and carbohydrates during the sulfur deprivation step [443, 444].

Phototrophic Microbial Fuel Cell

Light energy can be converted into electrical energy via a PMFC [445–448]. The combination of an ADP and a PMFC in a closed loop system can produce methane and electricity [237]. In this system, algal biomass serves as a substrate for AD and provides oxygen (final electron acceptor) for the fuel cell. The liquid phase of digested biomass contains compounds and nutrients to supply electrons in the fuel cell and for subsequent use as media for algal growth. While the system failed to operate in continuous-flow mode, in batch experiments it successfully produced methane (0.32 L/gVS) and power (1.33 mW/m^2 illuminated footprint area). Possible reasons for the failure of a continuous system are low biomass concentration, high nitrate concentration, or high water circulation flow rate [237].

5.3.2 Algal Production in Waste Streams

Fertilizers and inorganic chemicals are the major costs associated with intensive algal production systems. As example, producing 1 kg of biodiesel in fresh water requires 3,726 kg water, 0.33 kg nitrogen, and 0.71 kg phosphate [449]. On the other hand, algae and cyanobacteria play a role in self-purification of water bodies and in wastewater treatment by direct assimilation of simple organic compounds [294, 450] and nutrients [451–456], removal of heavy metals [388, 453, 457–459], and finally providing oxygen for organic matter oxidation by heterotrophic bacteria. Wastewater stabilization ponds with naturally occurring algal flora are widely used in developing countries and local sewage systems [460, 461]. Closed coastal areas, such as bays, fjords, and lagoons near urban and agricultural runoffs. are potential systems for cultivation, harvesting, and utilization of macroalgae for biomethane production [177, 412]. Golueke and Oswald first suggested the combination of wastewater treatment with production of algae to yield a biofuel [109, 110, 462, 463]. Coupling the treatment of nutrient-rich wastewater with algal growth followed by conversion to methane represents a potentially attractive biofuel production process with reduced impact on the environment [464–468]. Moreover, mixotrophic microalgal growth is attractive due to induction of lipids accumulation in algal cells.

Domestic, Industrial, and Agricultural Wastewater Treatment

Removal of 95% biochemical oxygen demand (BOD), 85% COD, 90% ammonia, >65% total nitrogen, and >99% of the pathogenic indicator microorganisms from municipal wastewater can be achieved in algal ponds [469]. The effluent quality is highly variable: BOD = 10–25 mg/L and COD = 50–85 mg/L [470]. Oswald and colleagues developed and tested the Advanced Integrated Wastewater Pond System (AIWPS) [471–475]. This system consists of methane production in an advanced facultative pond, algal high rate pond, algal settling pond, and maturation pond.

This system provides a secondary effluent adequate for agricultural irrigation and has 4–5 times lower electrical power consumption per water flow compared to conventional activated sludge and extended aeration systems [476]. A conventional wastewater treatment system requires approximately one kWhr of electricity for aeration for the removal of 1 kg of BOD. In contrast, photosynthetic BOD oxidation does not require aeration but produces algal biomass that can be converted to roughly one kWh of electricity through ADP [477].

Algal Cultivation in Anaerobic Digester Effluent

Recent developments allow ADP to be applied for the treatment of a wide range of wastewaters with organic contamination. But ADP has several drawbacks particularly high organic matter and ammonium concentrations in the AD effluent. Moreover, AD has low efficiency of phosphorus removal. A similar waste liquid is generated during AD of algae. This nutrient rich anaerobic effluent can serve as fertilizer for intensive algal production.

Green microalgae (*Chlorella* and *Scenedesmus*) cultivated in diluted dairy waste anaerobic digester effluent are able to switch from phototrophic to heterotrophic or mixotrophic growth, utilize native substrates present in effluent, and increase the biomass and triglyceride production rate [478]. Ammonia removal efficiency from anaerobic treated dairy wastewater reached 96% with a mixed green algae culture [479] and 99% with *A. platensis* [480]. Aragon reported the removal of 85% BOD, 75% COD, 80% ammonia, and >97% detergents during treatment of the anaerobic effluent from an urban wastewater treatment plant by two local algae species *Scenedesmus acutus* and *C. vulgaris* [481].

A "closed" system of methane generation from light energy via algal production and anaerobic digestion was described by Golueke and Oswald [109]. The liquid phase from the digester was used as culture media for algal growth. The average methane yield was 0.44 L/gVS, the maximum energy conversion efficiency from light to biomass was 3%, and the energy conversion efficiency for the entire unit was 2%. Ras and colleagues repeated the same experiment with *C. vulgaris* as the solar light capturing organism [482]. The methane yield was 0.24 L/gVS at an HRT of 28 days and an OLR of 0.7 gVS/L-day.

Ryther compared the productivity of *G. tikvahiae* and *Ulva* sp. in media enriched by AD effluent with the productivity in a conventional mineral enrichment medium [483]. *Ulva* sp. had a similar methane yield in both media, but *G. tikvahiae* had 50–75% lower productivity in an AD effluent-enriched medium compared to a control.

5.3.3 Algal Production Integrated with Carbon Dioxide Sequestration

An attractive algal cultivation strategy is to use carbon dioxide emitted from power plants for autotrophic biomass assimilation. Such a carbon capture system with

microalgae has the following advantages compared to other carbon sequestration technologies [484]:

– Algal system does not require high purity carbon dioxide.
– Algal system produces biofuels that can be used for electric power generation.
– Some flue gas impurities (nitrogen and sulfur oxides) can be removed as well and be used by algae.

A conceptual diagram for algal production and ADP integrated into a scheme with carbon dioxide mitigation and waste treatment processes is shown in Fig. 21.

6 Economical Parameters and Energy Efficiency of Methane Production from Algae

Commercial-scale production of methane from algae requires the process to be economically feasible. Life-cycle assessment and calculation of net energy ratio (NER) are common methods to evaluate techno-economical parameters of biofuel production technology.

6.1 Algal Biomass Production

Jorquera and colleagues compared the energy life-cycle analysis for the production of microalga *Nannochloropsis* sp. in flat-plate photobioreactors (FPPR), tubular photobioreactors (TPR), and raceway ponds (RP) [485]. The NER of these systems was estimated and compared as total energy produced (energy of biomass) over the energy content of the materials, energy required for construction, and the energy required for operation. A preliminary analysis (including energy costs for pumping, mixing, and gas transfer) showed that the NER value of biomass production in the TPR is 0.2. Consequently, the energy demand is larger than the energy content of the produced biomass in the TPR. The estimated NERs for biomass production in the FPPR and RP are 4.51 and 8.34, respectively [485]. The authors also performed a detailed energy life-cycle analysis using the GaBi program and achieved NER values 4.33 and 7.01 for the FPPR and RP, respectively. This result is in agreement with data achieved for the production of *Dunaliella* biomass where raceway ponds were found to be more efficient [486]. Indeed, the production of *C. vulgaris* in raceway bioreactors is more environmentally sustainable compared to the production in air-lift tubular reactors [487].

6.2 Conversion Technologies of Algae to Biofuel

The NER values for coupled production of biodiesel and biogas (residues) from *H. pluvialis* and *Nannochloropsis* are 0.4 and 0.09, respectively, with approximately

58 and 76% of the output energy coming from biogas [488]. The sensitivity analysis showed that it is not possible to achieve an NER value larger than 1 even at most optimistic algal yield and oil content. Pumping, drying, and cell-disruption are the most energy consuming steps. Lardon et al. emphasize that integration of ADP into biodiesel production is a promising solution for external energy demand reduction and partial recycling of essential nutrients [489].

Energy output from *T. suecica* was reported for several conversion techniques (Fig. 22) [435]. Anaerobic digestion as a sole conversion technology has the largest energy output compared to biodiesel and bioethanol. Coupling of biogas production with biodiesel production gave slightly larger total energy output, and decreased the estimated biodiesel production cost from $72 to $47 per liter. But this cost is significantly larger than the current cost of petroleum-based biodiesel.

The life-cycle assessment of microalgal cultivation and biogas production shows that the NER value is equal to 1.51 for the following conditions: *C. vulgaris* is cultivated in ponds with area of 100 ha, productivity of 25 g/m^2-day, carbon dioxide supplied from biogas purification and methane combustion, and the supernatant liquid from the digester provides a portion of the fertilizers necessary for algal growth [490]. Technical parameters of the ADP include: CSTR digester, methane yield 0.292 L/gVS, OLR 1 gVS/L-day, HRT 46 days, and algal biodegradability of 56%.

Zamalloa and colleagues reviewed three scenarios of growing algae in wastewater effluent with productivity 20, 25, and 30 g/m^2-day [491]. The algal production facility utilized carbon dioxide produced during electricity production. For all scenarios, the NER values are larger than 1 and equal to 2.48, 2.67, and 3.34, respectively. This means that the energy output is larger than energy demand for algal production and anaerobic digestion. The major energy consuming processes are digester heating, mixing, algal pre-concentration, and pumping. The cost of biomass for three scenarios were $169, $138, and $117 per kg of dry weight and the levelized cost of energy were $0.232, $0.154, and $0.119 per kWh (given €1/$1 equal to 1.3652). A minimum algal productivity of 25 g/m^2-day is required in order to achieve profitability with an OLR of 18 gVS/L-day and methane yield of 0.5 L/gVA. The fermentation of at least 75% of the VS is crucial for an economically feasible process. These assumptions are relatively optimistic but can be achieved in advanced anaerobic reactors.

7 Conclusions

Cyanobacteria and algae are feasible feedstocks for biogas production through ADP. Moreover, with current understanding and technology, the anaerobic digestion of algae has the promise to be the technology that can be applied for biofuel production in the nearest future. Despite more than 60 years of research and several advantages, the technology of methane production from algae is still far from wide application at a large scale. One of the reasons for that is the vast diversity of algae and cyanobacteria. They have different cell morphology, ecology, photosynthesis biochemistry, cell structure, and biochemical composition.

Further research directions that are critical for making ADP with algae economically feasible for successful commercialization include:

- Engineering of efficient systems for algal cultivation and anaerobic digestion:
  - Design of algal production units for better light illumination, penetration, carbon dioxide dissolution, and oxygen off-take
  - Design algal harvesting and dewatering units
  - Develop methods of biomass pretreatment for greater VS reduction and higher methane yield
  - Design of anaerobic reactors with lower HRT and high SRT
  - Design of biogas upgrading systems
- Isolation and characterization of prospective natural organisms:
  - Isolation of algal strains with high production potential, biochemical composition with high colorific value, lower recalcitrance, robustness for cultivation in waste streams and to aeration by exhausted gases
  - Isolation of anaerobic bacteria responsible for digesting algal biomass in nature
- Developing and application molecular biology and genetic tools, and "omics" technologies for cyanobacteria, algae, and anaerobic organisms to target goals such as:
  - Decreasing algal photoinhibition, increasing photosynthesis efficiency and carbon dioxide uptake
  - Algal simultaneous lipid accumulation and high growth rate
  - High digestibility of algal biomass
  - Algal persistence to bacterial and viral infections
  - Development of stronger hydrolytic apparatus of anaerobic bacteria
  - Robustness of methanogens for fluctuations in environmental and operational parameters
- Integration of algal production and AD with other technologies:
  - Co-digestion with domestic, industrial, and agricultural wastes can improve the C:N:P balance
  - Algal cultivation in wastewaters containing organic carbon and nutrients
  - Co-location of algal production with carbon power plants that can be a source of carbon dioxide and waste heat
  - Application of algal anaerobic digestion with other biofuel production processes or production of high-value products from algae
- Development of information technologies:
  - For techno-economical analysis
  - Dynamic modeling of systems
  - Bioinformatics technologies
  - Metabolic networks modeling

Acknowledgments This research was supported by The Bureau of Education and Cultural Affairs of United States Department of State though an International Fulbright Science and Technology Award to Pavlo Bohutskyi.

References

1. Meynell P-J (1976) Methane: planning a digester. C.T.T. series. Prism Press, Dorchester
2. McCabe J, Eckenfelder WW (1956) Biological treatment of sewage and industrial wastes, vol 2, Anaerobic digestion and solids-liquid separation. Reinhlod, New York
3. Buysman E (2009) Anaerobic digestion for developing countries with cold climates—utilizing solar heat to address technical challenges and facilitating dissemination through the use of carbon finance. Master Thesis, University of Wageningen, Wageningen
4. Daxiong Q, Shuhua G, Baofen L, Gehua W (1990) Diffusion and innovation in the Chinese biogas program. World Dev 18(4):555–563
5. Pathak H, Jain N, Bhatia A, Mohanty S, Gupta N (2009) Global warming mitigation potential of biogas plants in India. Environ Monit Assess 157(1):407–418
6. Energy Statistics Database (2009) United Nations Statistics Division. http://data.un.org/Data.aspx?d=EDATA&f=cmID%3aBI%3btrID%3a01—EDATA. Accessed 10 July 2010
7. Gunaseelan NV (1997) Anaerobic digestion of biomass for methane production: a review. Biomass Bioenergy 13(1–2):83–114. doi:10.1016/s0961-9534(97)00020-2
8. USDOE (2010) National algal biofuels technology roadmap. U.S. Department of Energy, Office of Energy Efficiency and Renewable Energy, Biomass Program, Washington, DC
9. Wassink EC (1959) Efficiency of light energy conversion in plant growth. Plant Physiol 34(3):356–361
10. Klass DL (2004) Biomass for renewable energy and fuels, vol 1, Encyclopedia of energy. Elsevier, Oxford
11. Laws EA, Taguchi S, Hirata J, Pang L (1986) High algal production rates achieved in a shallow outdoor flume. Biotechnol Bioeng 28(2):191–197. doi:10.1002/bit.260280207
12. Laws EA, Taguchi S, Hirata J, Pang L (1988) Optimization of microalgal production in a shallow outdoor flume. Biotechnol Bioeng 32(2):140–147. doi:10.1002/bit.260320204
13. Chapin FS, Schulze E, Mooney HA (1990) The ecology and economics of storage in plants. Annu Rev Ecol Syst 21(1):423–447. doi:10.1146/annurev.es.21.110190.002231
14. White LM (1973) Carbohydrate reserves of grasses: a review. J Range Manage 26(1):13–18
15. Zeeman SC, Kossmann J, Smith AM (2010) Starch: its metabolism, evolution, and biotechnological modification in plants. Annu Rev Plant Biol 61:209–234. doi:10.1146/annurev-arplant-042809-112301
16. Knox JP (2008) Revealing the structural and functional diversity of plant cell walls. Curr Opin Plant Biol 11(3):308–313. doi:S1369-5266(08)00041-1[pii]10.1016/j.pbi.2008.03.001
17. Somerville C, Bauer S, Brininstool G, Facette M, Hamann T, Milne J, Osborne E, Paredez A, Persson S, Raab T, Vorwerk S, Youngs H (2004) Toward a systems approach to understanding plant cell walls. Science 306(5705):2206–2211. doi:306/5705/2206[pii]10.1126/science.1102765
18. Anderson WF, Akin DE (2008) Structural and chemical properties of grass lignocelluloses related to conversion for biofuels. J Ind Microbiol Biotechnol 35(5):355–366. doi:10.1007/s10295-007-0291-8
19. Gilbert HJ (2010) The biochemistry and structural biology of plant cell wall deconstruction. Plant Physiol 153(2):444–455. doi:pp. 110.156646[pii]10.1104/pp.110.156646
20. Kim Y, Hendrickson R, Mosier NS, Ladisch MR (2009) Liquid hot water pretreatment of cellulosic biomass. Methods Mol Biol 581:93–102. doi:10.1007/978-1-60761-214-8_7
21. Hendriks AT, Zeeman G (2009) Pretreatments to enhance the digestibility of lignocellulosic biomass. Bioresour Technol 100(1):10–18. doi:S0960-8524(08)00457-4[pii]

22. Balan V, Bals B, Chundawat SP, Marshall D, Dale BE (2009) Lignocellulosic biomass pretreatment using AFEX. Methods Mol Biol 581:61–77. doi:10.1007/978-1-60761-214-8_5
23. Dawes C (1986) Seasonal proximate constituents and caloric values in seagrasses and algae on the west coast of Florida. J Coast Res 2(1):25–32
24. Dawes CJ, Bird K, Durako M, Goddard R, Hoffman W, McIntosh R (1979) Chemical fluctuations due to seasonal and cropping effects on an algal-seagrass community. Aquat Bot 6:79–86
25. Dawes CJ, Guiry MD (1992) Proximate constituents in the sea-grasses *Zostera marina* and *Z. noltii* in Ireland: seasonal changes and the effect of blade removal. Mar Ecol 13(4): 307–315. doi:10.1111/j.1439-0485.1992.tb00357.x
26. Dawes CJ, Orduña-rojas J, Robledo D (1998) Response of the tropical red seaweed *Gracilaria cornea* to temperature, salinity and irradiance. J Appl Phycol 10(5):419–425. doi:10.1023/a:1008021613399
27. Marinho-Soriano E, Fonseca PC, Carneiro MAA, Moreira WSC (2006) Seasonal variation in the chemical composition of two tropical seaweeds. Bioresour Technol 97(18):2402–2406
28. Stanier RY, Cohen-Bazire G (1977) Phototrophic prokaryotes: the cyanobacteria. Annu Rev Microbiol 31:225–274. doi:10.1146/annurev.mi.31.100177.001301
29. Berman-Frank I, Lundgren P, Falkowski P (2003) Nitrogen fixation and photosynthetic oxygen evolution in cyanobacteria. Res Microbiol 154(3):157–164
30. Jordan P, Fromme P, Witt HT, Klukas O, Saenger W, Krauß N (2001) Three-dimensional structure of cyanobacterial photosystem I at 2.5 Å resolution. Nature 411(6840):909–917. doi:10.1038/35082000
31. Wolk CP (1973) Physiology and cytological chemistry blue-green algae. Bacteriol Rev 37(1):32–101
32. Cameron RE (1963) Morphology of representative blue-green algae. Ann N Y Acad Sci 108(2):412–420. doi:10.1111/j.1749-6632.1963.tb13395.x
33. Whitton B, Potts M (2002) Introduction to the cyanobacteria. In: Whitton B, Potts M (eds) The ecology of cyanobacteria. Springer, The Netherlands, pp 1–11. doi:10.1007/0-306-46855-7_1
34. Abed RMM, Dobretsov S, Sudesh K (2009) Applications of cyanobacteria in biotechnology. J Appl Microbiol 106:1–12
35. Thajuddin N, Subramanian G (2005) Cyanobacterial biodiversity and potential applications in biotechnology. Curr Sci 89(1):11
36. Kraft GT, Woelkerling WJ (1990) Rhodophyta. In: Clayton MN, King RJ (eds) Biology of marine plants. Longman, Melbourne, pp 41–85
37. Lee RE (2008) Phycology, 4th edn. Cambridge University Press, Cambridge
38. Bold HC, Wynne MJ (1978) Introduction to the algae: structure and reproduction. Prentice-Hall biological sciences series. Prentice-Hall, Englewood Cliffs, New Jersey
39. South GR, Whittick A (1987) Introduction to phycology. Blackwell Scientific, Oxford
40. Mumford TFJ, Miura A (1988) *Porphyra* as food: cultivation and economics. In: Waaland JR, Lembi CA (eds) Algae and human affairs. Cambridge University Press, Cambridge, pp 87–119
41. Armisén R (1991) Agar and agarose biotechnological applications. Hydrobiologia 221(1):157–166. doi:10.1007/bf00028372
42. Renn DW (1984) Agar and agarose: indispensable partners in biotechnology. Ind Eng Chem Prod Res Dev 23(1):17–21. doi:10.1021/i300013a004
43. Rasmussen RS, Morrissey MT (2007) Marine biotechnology for production of food ingredients. In: Steve LT (ed) Advances in food and nutrition research, vol 52. Academic, New York, pp 237–292
44. Rowan S (1989) Photosynthetic pigments of algae. Cambridge University Press, Cambridge
45. Smith GM (1955) Cryptogamic botany, vol 1. McGraw-Hill publications in the botanical sciences, 2nd edn. McGraw-Hill, New York
46. Sharma O (1986) Textbook of algae. Tata McGraw-Hill, Delhi
47. Round FE (1973) The biology of the algae, 2nd edn. St. Martin's Press, New York

48. Oren A (2010) Industrial and environmental applications of halophilic microorganisms. Environ Technol 31(8–9):825–834
49. Vandermeulen H, Gordin H (1990) Ammonium uptake using *Ulva* (Chlorophyta) in intensive fishpond systems: mass culture and treatment of effluent. J Appl Phycol 2(4):363–374. doi:10.1007/bf02180927
50. Cavalier-Smith T (1986) The kingdom Chromista: origin and systematics. Prog Phycol Res 4:309–347
51. Cavalier-Smith T, Chao EE, Allsopp MTEP (1995) Ribosomal RNA evidence for chloroplast loss within heterokonta: pedinellid relationships and a revised classification of Ochristan algae. Paper presented at the International Society for Evolutionary Protistology ISEP. Biennial meeting No 10, Halifax
52. Andersen RA (2004) Biology and systematics of heterokont and haptophyte algae. Am J Bot 91(10):1508–1522. doi:10.3732/ajb.91.10.1508
53. Borowitzka M (1997) Microalgae for aquaculture: opportunities and constraints. J Appl Phycol 9(5):393–401. doi:10.1023/a:1007921728300
54. Bozarth A, Maier U-G, Zauner S (2009) Diatoms in biotechnology: modern tools and applications. Appl Microbiol Biotechnol 82(2):195–201. doi:10.1007/s00253-008-1804-8
55. Lebeau T, Robert JM (2003) Diatom cultivation and biotechnologically relevant products. Part II: current and putative products. Appl Microbiol Biotechnol 60(6):624–632. doi:10.1007/s00253-002-1177-3
56. Hsiao TY, Blanch HW (2006) Physiological studies of eicosapentaenoic acid production in the marine microalga *Glossomastix chrysoplasta*. Biotechnol Bioeng 93(3):465–475. doi:10.1002/bit.20761
57. Gacesa P (1988) Alginates. Carbohydr Polym 8(3):161–182
58. Patankar MS, Oehninger S, Barnett T, Williams RL, Clark GF (1993) A revised structure for may explain some of its biological activities. J Biol Chem 268(29):21770–21776
59. Bilan MI, Grachev AA, Shashkov AS, Nifantiev NE, Usov AI (2006) Structure of a fucoidan from the brown seaweed *Fucus serratus* L. Carbohydr Res 341(2):238–245
60. Gujer W, Zehnder AJB (1983) Conversion processes in anaerobic digestion. Water Sci Technol 15:127–167
61. Ghosh S, Conrad JR, Klass DL (1975) Anaerobic acidogenesis of wastewater sludge. J Water Pollut Control Fed 47(1):30–45
62. Chen Y, Cheng JJ, Creamer KS (2008) Inhibition of anaerobic digestion process: a review. Bioresour Technol 99(10):4044–4064
63. Lettinga G (2001) Challenge of psychrophilic anaerobic wastewater treatment. Trends Biotechnol 19(9):363–370. doi:10.1016/s0167-7799(01)01701-2
64. Wiegel J (1990) Temperature spans for growth: hypothesis and discussion. FEMS Microbiol Lett 75(2–3):155–169. doi:10.1016/0378-1097(90)90529-y
65. Speece RE (1983) Anaerobic biotechnology for industrial wastewater treatment. Environ Sci Technol 17(9):416A–427A. doi:10.1021/es00115a001
66. El-Mashad HM, Zeeman G, van Loon WK, Bot GP, Lettinga G (2004) Effect of temperature and temperature fluctuation on thermophilic anaerobic digestion of cattle manure. Bioresour Technol 95(2):191–201. doi:10.1016/j.biortech.2003.07.013S0960852404000574[pii]
67. M-c Wu, K-w S, Zhang Y (2006) Influence of temperature fluctuation on thermophilic anaerobic digestion of municipal organic solid waste. J Zhejiang Univ Sci B 7(3):180–185. doi:10.1631/jzus.2006.B0180
68. Khanal SK (2008) Anaerobic biotechnology for bioenergy production: principles and applications. Wiley-Blackwell, Ames
69. Hansen K (1998) Anaerobic digestion of swine manure: inhibition by ammonia. Water Res 32(1):5–12. doi:10.1016/s0043-1354(97)00201-7
70. Tchobanoglous G, Burton LF, Stensel HD (2003) Wastewater engineering: treatment disposal reuse. McGraw-Hill series in water resources and environmental engineering, 4th edn. McGraw-Hill, New York

71. Eder B, Heinz S (2006) Biogas Praxis: Grundlagen, Planung, Anlagenbau, Beispiele, Wirtschaftlichkeit. Ökobuch Verlag u. Versand, Staufen
72. Chynoweth DP, Srivastava VJ, Conrad JR (1980) Research study to determine the feasibility of producing methane gas from kelp. Annual report. Institute of Gas Technology, Chicago
73. Kida K, Shigematsu T, Kijima J, Numaguchi M, Mochinaga Y, Abe N, Morimura S (2001) Influence of Ni_2^+ and Co_2^+ on methanogenic activity and the amounts of coenzymes involved in methanogenesis. J Biosci Bioeng 91(6):590–595. doi:S1389-1723(01)80179-1[pii]
74. Noyola A, Antonio TA (2005) Anaerobic thermophilic digestion of sludge from enhanced primary treatment of municipal wastewater. In: Proceedings of the Water Environment Federation, Washington, D.C., pp 8031–8042. doi:10.2175/193864705783813601
75. Fermoso FG, Bartacek J, Jansen S, Lens PNL (2009) Metal supplementation to UASB bioreactors: from cell-metal interactions to full-scale application. Sci Total Environ 407(12):3652–3667. doi:10.1016/j.scitotenv.2008.10.043
76. Gerardi MH (2003) The microbiology of anaerobic digesters. Wastewater microbiology series. Wiley-Interscience, Hoboken
77. Schramm W, Lehnberg W (1984) Mass culture of brackish-water-adapted seaweeds in sewage-enriched seawater. II: fermentation for biogas production. Hydrobiologia 116–117(1):282–287. doi:10.1007/bf00027685
78. de Baere LA, Devocht M, Van Assche P, Verstraete W (1984) Influence of high NaCl and NH_4Cl salt levels on methanogenic associations. Water Res 18(5):543–548
79. Chynoweth DP, Fannin KF, Srivastava VJ (1987) Biological gasification of marine algae. Seaweed cultivation for renewable resources. Elsevier, Amsterdam
80. Braun R, Huber P, Meyrath J (1981) Ammonia toxicity in liquid piggery manure digestion. Biotechnol Lett 3(4). doi:10.1007/bf00239655
81. Koster I, Rinzema A, Devegt A, Lettinga G (1986) Sulfide inhibition of the methanogenic activity of granular sludge at various pH-levels. Water Res 20(12):1561–1567. doi:10.1016/0043-1354(86)90121-1
82. O'Flaherty V, Lens P, Leahy B, Colleran E (1998) Long-term competition between sulphate-reducing and methane-producing bacteria during full-scale anaerobic treatment of citric acid production wastewater. Water Res 32(3):815–825. doi:10.1016/s0043-1354(97)00270-4
83. McCartney D, Oleszkiewicz J (1991) Sulfide inhibition of anaerobic degradation of lactate and acetate. Water Res 25(2):203–209. doi:10.1016/0043-1354(91)90030-t
84. Harada H, Uemura S, Momonoi K (1994) Interaction between sulfate-reducing bacteria and methane-producing bacteria in UASB reactors fed with low strength wastes containing different levels of sulfate. Water Res 28(2):355–367. doi:10.1016/0043-1354(94)90273-9
85. Conn EE (1987) Outlines of biochemistry, 5th edn. Wiley, New York
86. Vogels GD, Kejtjens JT, van der Drift C (1988) Biochemistry of methane production. In: Zehnder AJB (ed) Biology of anaerobic microorganisms. Wiley, New York, p 872
87. Gallert C, Bauer S, Winter J (1998) Effect of ammonia on the anaerobic degradation of protein by a mesophilic and thermophilic biowaste population. Appl Microbiol Biotechnol 50(4):495–501
88. Sprott G, Patel G (1986) Ammonia toxicity in pure cultures of methanogenic bacteria. Syst Appl Microbiol 7(2–3):358–363
89. Koster IW, Lettinga G (1984) The influence of ammonium-nitrogen on the specific activity of pelletized methanogenic sludge. Agric Wastes 9(3):205–216. doi:10.1016/0141-4607(84)90080-5
90. McCarty PL, McKinney RE (1961) Salt toxicity in anaerobic digestion. J Water Pollut Control Fed 33(4):399–415
91. Hendriksen HV, Ahring BK (1991) Effects of ammonia on growth and morphology of thermophilic hydrogen-oxidizing methanogenic bacteria. FEMS Microbiol Lett 85(3):241–245
92. Hobson PN, Shaw BG (1976) Inhibition of methane production by *Methanobacterium formicicum*. Water Res 10(10):849–852. doi:10.1016/0043-1354(76)90018-x
93. Hashimoto AG (1986) Ammonia inhibition of methanogenesis from cattle wastes. Agric Wastes 17(4):241–261

94. Van Velsen AFM (1979) Adaptation of methanogenic sludge to high ammonia-nitrogen concentrations. Water Res 13(10):995–999
95. Zhou H-B, Qiu G-Z (2006) Inhibitory effect of ammonia nitrogen on specific methanogenic activity of anaerobic granular sludge. J Cent South Univ Technol 13(1):63–67. doi:10.1007/s11771-006-0108-3
96. Borja R, Sanchez E, Weiland P (1996) Influence of ammonia concentration on thermophilic anaerobic digestion of cattle manure in upflow anaerobic sludge blanket (UASB) reactors. Process Biochem 31(5):477–483
97. Wiegant W (1986) The mechanism of ammonia inhibition in the thermophilic digestion of livestock wastes. Agric Wastes 16(4):243–253. doi:10.1016/0141-4607(86)90056-9
98. Rasi S, Lehtinen J, Rintala J (2010) Determination of organic silicon compounds in biogas from wastewater treatments plants, landfills, and co-digestion plants. Renew Energy 35(12):2666–2673. doi:10.1016/j.renene.2010.04.012
99. Rasi S, Veijanen A, Rintala J (2007) Trace compounds of biogas from different biogas production plants. Energy 32(8):1375–1380. doi:10.1016/j.energy.2006.10.018
100. Eklund B, Anderson EP, Walker BL, Burrows DB (1998) Characterization of landfill gas composition at the Fresh Kills Municipal solid-waste landfill. Environ Sci Technol 32(15):2233–2237. doi:10.1021/es980004s
101. Reinhart DR (1993) A review of recent studies on the sources of hazardous compounds emitted from solid waste landfills: a U.S. experience. Waste Manag Res 11(3):257–268. doi:10.1177/0734242x9301100307
102. Holm-Nielsen JB, Al Seadi T (2004) Manure-based biogas systems—Danish experience. In: Piet L, Hamelers B, Hoitink H, Bidlingmaier W (eds) Resource recovery and reuse in organic solid waste management. IWA Publishing, London, pp 377–394
103. Tower P (2003) New technology for removal of siloxanes in digester gas results in lower maintenance costs and air quality benefits in power generation equipment. In: Proceedings of the Water Environment Federation, Los Angeles, CA, pp 440–447. doi:10.2175/193864703784639859
104. Abatzoglou N, Boivin S (2009) A review of biogas purification processes. Biofuels Bioprod Bioref 3(1):42–71. doi:10.1002/bbb.117
105. Tippayawong N, Thanompongchart P (2010) Biogas quality upgrade by simultaneous removal of CO_2 and H_2S in a packed column reactor. Energy 35(12):4531–4535. doi:10.1016/j.energy.2010.04.014
106. Yang H, Xu Z, Fan M, Gupta R, Slimane RB, Bland AE, Wright I (2008) Progress in carbon dioxide separation and capture: a review. J Environ Sci (China) 20(1):14–27
107. Horikawa MS, Rossi F, Gimenes ML, Costa CMM, da Silva MGC (2004) Chemical absorption of H_2S for biogas purification. Braz J Chem Eng 21:415–422
108. Osorio F, Torres JC (2009) Biogas purification from anaerobic digestion in a wastewater treatment plant for biofuel production. Renew Energy 34(10):2164–2171. doi:10.1016/j.renene.2009.02.023
109. Golueke CG, Oswald WJ (1959) Biological conversion of light energy to the chemical energy of methane. Appl Microbiol 7(4):219–227
110. Golueke CG, Oswald WJ, Gotaas HB (1957) Anaerobic digestion of Algae. Appl Microbiol 5(1):47–55
111. Chynoweth D (1979) Anaerobic digestion of marine biomass. Paper presented at the biogas and alcohol production conference, Chicago
112. Buswell AM, Mueller HF (1952) Mechanism of methane fermentation. Ind Eng Chem 44(3):550–552. doi:10.1021/ie50507a033
113. Doi RH (2008) Cellulases of mesophilic microorganisms. Ann N Y Acad Sci 1125(1):267–279. doi:10.1196/annals.1419.002
114. Schwarz WH (2001) The cellulosome and cellulose degradation by anaerobic bacteria. Appl Microbiol Biotechnol 56(5):634–649. doi:10.1007/s002530100710
115. Rees DA (1970) Structure, conformation, and mechanism in the formation of polysaccharide gels and networks. In: Melville L, Wolfrom RST, Derek H (eds) Advances in carbohydrate chemistry and biochemistry, vol 24. Academic, New York, pp 267–332

116. Craigie JS, Correa JA, Gordon ME (1992) Cuticles from *Chondrus crispus* (Rhodophyta) I. J Phycol 28(6):777–786. doi:10.1111/j.0022-3646.1992.00777.x
117. Michel G, Helbert W, Kahn R, Dideberg O, Kloareg B (2003) The structural bases of the processive degradation of [iota]-carrageenan, a main cell wall polysaccharide of red algae. J Mol Biol 334(3):421–433
118. Michel G, Nyval-Collen P, Barbeyron T, Czjzek M, Helbert W (2006) Bioconversion of red seaweed galactans: a focus on bacterial agarases and carrageenases. Appl Microbiol Biotechnol 71(1):23–33. doi:10.1007/s00253-006-0377-7
119. Bird KT, Hanisak MD, Ryther JH (1981) Changes in agar and other chemical constituents of the seaweed *Gracilaria tikvahiae* when used as a substrate in methane digesters. Resour Conserv 6(3–4):321–327
120. King GM, Guist GG, Lauterbach GE (1985) Anaerobic degradation of Carrageenan from the red macroalga *Eucheuma cottonii*. Appl Environ Microbiol 49(3):588–592
121. Bird K, Chynoweth D, Jerger D (1990) Effects of marine algal proximate composition on methane yields. J Appl Phycol 2(3):207–213. doi:10.1007/bf02179777
122. Habig C, DeBusk TA, Ryther JH (1984) The effect of nitrogen content on methane production by the marine algae *Gracilaria tikvahiae* and *Ulva* sp. Biomass 4(4):239–251
123. Biswas R (2009) Biomethanation of red algae from the eutrophied Baltic Sea. Master Thesis, Linköping University, Linköping
124. Habig C, Ryther JH (1983) Methane production from the anaerobic digestion of some marine macrophytes. Resour Conserv 8(3):271–279
125. Guiry MD, Guiry GM (2010) AlgaeBase. World-wide electronic publication. National University of Ireland. http://www.algaebase.org. Accessed 7 Oct 2010
126. Morand P, Charlier RH, Mazé J (1990) European bioconversion projects and realizations for macroalgal biomass: Saint-Cast-Le-Guildo (France) experiment. Hydrobiologia 204–205(1):301–308. doi:10.1007/bf00040249
127. Charlier R, Morand P, Finkl C, Thys A (2007) Green tides on the Brittany coasts. Environ Res Eng Manag 3(41):52–59
128. Charlier RH, Morand P, Finkl CW (2008) How Brittany and Florida coasts cope with green tides. Int J Environ Stud 65(2):191–208
129. Briand X, Morand P (1997) Anaerobic digestion of *Ulva* sp. 1. Relationship between Ulva composition and methanisation. J Appl Phycol 9(6):511–524. doi:10.1023/a:1007972026328
130. Lahaye M, Kaeffer B (1997) Seaweed dietary fibres: structure, physico-chemical and biological properties relevant to intestinal physiology. Sci Aliments 17(6):563–584
131. Lahaye M, Robic A (2007) Structure and functional properties of ulvan, a polysaccharide from green seaweeds. Biomacromolecules 8(6):1765–1774. doi:10.1021/bm061185q
132. Durand M, Beaumatin P, Bulman B, Bemalier A, Grivet J, Serezat M, Gramet G, Lahaye M (1997) Fermentation of green alga sea-lettuce (*Ulva* sp.) and metabolism of its sulphate by human colonic microbiota in a semi-continuous culture system. Reprod Nutr Dev 37(3):267–283
133. Bobin-Dubigeon C, Lahaye M, Barry JL (1997) Human colonic bacterial degradability of dietary fibres from sea-lettuce (*Ulva* sp.). J Sci Food Agric 73(2):149–159. doi:10.1002/(sici)1097-0010(199702)73:2<149::aid-jsfa685>3.0.co;2-l
134. Hansson G (1983) Methane production from marine, green macro-algae. Resour Conserv 8(3):185–194
135. Fauchille S (1984) Digestion anaérobie de végétaux aquatiques. Institut Polytechnique de Lorraine, Nancy
136. Carpentier B, Festino C, Aubart C (1988) Anaerobic digestion of flotation sludges from the alginic acid extraction process. Biol Wastes 23(4):269–278
137. Rigoni-Stern S, Rismondo R, Szpyrkowicz L, Zilio-Grandi F, Vigato PA (1990) Anaerobic digestion of nitrophilic algal biomass from the Venice lagoon. Biomass 23(3):179–199
138. Medcalf DG, Lionel T, Brannon JH, Scott JR (1975) Seasonal variation in the mucilaginous polysaccharides from *Ulva lactuca*. Bot Mar 18(2):67–70. doi:10.1515/botm.1975.18.2.67

139. Dills SS, Apperson A, Schmidt MR, Saier MH Jr (1980) Carbohydrate transport in bacteria. Microbiol Rev 44(3):385–418
140. Forro J (1987) Microbial degradation of marine biomass. In: Bird KT, Benson PH (eds) Seaweed cultivation for renewable resources, vol 305–325. Elsevier, Amsterdam
141. Deville C, Gharbi M, Dandrifosse G, Peulen O (2007) Study on the effects of laminarin, a polysaccharide from seaweed, on gut characteristics. J Sci Food Agric 87(9):1717–1725. doi:10.1002/jsfa.2901
142. Iwamoto Y, Araki R, Iriyama K, Oda T, Fukuda H, Hayashida S, Muramatsu T (2001) Purification and characterization of bifunctional alginate lyase from *Alteromonas* sp. strain no. 272 and its action on saturated oligomeric substrates. Biosci Biotechnol Biochem 65(1):133–142
143. Wong TY, Preston LA, Schiller NL (2000) Alginate lyase: review of major sources and enzyme characteristics, structure-function analysis, biological roles, and applications. Annu Rev Microbiol 54:289–340. doi:10.1146/annurev.micro.54.1.28954/1/289[pii]
144. Moen E, Ostgaard K (1997) Aerobic digestion of Ca-alginate gels studied as a model system of seaweed tissue degradation. J Appl Phycol 9(3):261–267. doi:10.1023/a:1007953725317
145. Boyd J, Turvey JR (1978) Structural studies of alginic acid, using a bacterial poly-[alpha]-L-guluronate lyase. Carbohydr Res 66(1):187–194
146. Preiss J, Ashwell G (1962) Alginic acid metabolism in bacteria. I. Enzymatic formation of unsaturated oligosaccharides and 4-deoxy-L-erythro-5-hexoseulose uronic acid. J Biol Chem 237:309–316
147. Preiss J, Ashwell G (1962) Alginic acid metabolism in bacteria. II. The enzymatic reduction of 4-deoxy-L-erythro-5-hexoseulose uronic acid to 2-keto-3-deoxy-D-gluconic acid. J Biol Chem 237:317–321
148. Sakai T, Ishizuka K, Kato I (2003) Isolation and characterization of a fucoidan-degrading marine bacterium. Marine Biotechnol 5(5):409–416. doi:10.1007/s10126-002-0118-6
149. Kerner KN, Hanssen JF, Pedersen TA (1991) Anaerobic digestion of waste sludges from the alginate extraction process. Bioresour Technol 37(1):17–24
150. Kloareg B, Quatrano RS (1988) Structure of the cell walls of marine algae and ecophysiological functions of the matrix polysaccharides. Oceanogr Mar Biol Annu Rev 26:259–315
151. Michel C, Lahaye M, Bonnet C, Mabeau S, Barry J-L (1996) In vitro fermentation by human faecal bacteria of total and purified dietary fibres from brown seaweeds. Br J Nutr 75(02):263–280. doi:10.1017/BJN19960129
152. Scalbert A (1991) Antimicrobial properties of tannins. Phytochemistry 30(12):3875–3883
153. Fannin KF, Srivastava VJ, Chynoweth DP, Bird KT (1983) Effects of the interaction between composition and reactor design on anaerobic digester performance. Paper presented at the energy from biomass and wastes VII, Chicago
154. Østgaard K, Indergaard M, Markussen S, Knutsen S, Jensen A (1993) Carbohydrate degradation and methane production during fermentation *Laminaria saccharina* (Laminariales, Phaeophyceae). J Appl Phycol 5(3):333–342. doi:10.1007/bf02186236
155. Rui X, Pay E, Tianrong G, Fang Y, Wudi Z (2009) The potential of blue-green algae for producing methane in biogas fermentation. In: Goswami DY, Zhao Y (eds) Proceedings of ISES world congress 2007, vol I–V. Springer, Berlin, pp 2426–2429. doi:10.1007/978-3-540-75997-3_491
156. Chen PH (1987) Factors influencing methane fermentation of micro-algae. California University, Berkeley
157. Mussgnug JH, Klassen V, Schlüter A, Kruse O (2010) Microalgae as substrates for fermentative biogas production in a combined biorefinery concept. J Biotechnol 150(1):51–56
158. Varel VH, Chen TH, Hashimoto AG (1988) Thermophilic and mesophilic methane production from anaerobic degradation of the cyanobacterium *Spirulina maxima*. Resour Conserv Recycling 1(1):19–26
159. Samson R, Leduy A (1982) Biogas production from anaerobic digestion of *Spirulina maxima* algal biomass. Biotechnol Bioeng 24(8):1919–1924. doi:10.1002/bit.260240822

160. Samson R, Leduyt A (1986) Detailed study of anaerobic digestion of *Spirulina maxima* algal biomass. Biotechnol Bioeng 28(7):1014–1023. doi:10.1002/bit.260280712
161. Gelin F, Boogers I, Noordeloos AAM, Damste JSS, Riegman R, De Leeuw JW (1997) Resistant biomacromolecules in marine microalgae of the classes Eustigmatophyceae and Chlorophyceae: geochemical implications. Org Geochem 26(11–12):659–675. doi:10.1016/s0146-6380(97)00035-1
162. Gelin F, Volkman JK, Largeau C, Derenne S, Sinninghe DamstÈ JS, De Leeuw JW (1999) Distribution of aliphatic, nonhydrolyzable biopolymers in marine microalgae. Org Geochem 30(2–3):147–159. doi:10.1016/s0146-6380(98)00206-x
163. Atkinson AW, Gunning BES, John PCL (1972) Sporopollenin in the cell wall of *Chlorella* and other algae: ultrastructure, chemistry, and incorporation of 14C-acetate, studied in synchronous cultures. Planta 107(1):1–32. doi:10.1007/bf00398011
164. Burczyk J, Dworzanski J (1988) Comparison of sporopollenin-like algal resistant polymer from cell wall of *Botryococcus*, *Scenedesmus* and *Lycopodium clavatum* by GC-pyrolysis. Phytochemistry 27(7):2151–2153
165. Good BH, Chapman RL (1978) The ultrastructure of *Phycopeltis* (Chroolepidaceae: Chlorophyta). I. Sporopollenin in the cell walls. Am J Bot 65(1):27–33
166. Heslop-Harrison J (1971) Sporopollenin in the biological context. In: Brook J, Grant PR, Muir RD (eds) Sporopollenin. Academic, New York, pp 1–30
167. Takeda H (1988) Classification of *Chlorella* strains by cell wall sugar composition. Phytochemistry 27(12):3823–3826
168. Takeda H (1991) Sugar composition of the cell wall and the taxonomy of *Chlorella* (Chlorophyceae). J Phycol 27(2):224–232. doi:10.1111/j.0022-3646.1991.00224.x
169. Takeda H (1996) Cell wall sugars of some *Scenedesmus* species. Phytochemistry 42(3): 673–675
170. Goodenough UW, Heuser JE (1985) The *Chlamydomonas* cell wall and its constituent glycoproteins analyzed by the quick-freeze, deep-etch technique. J Cell Biol 101(4):1550–1568
171. Goodenough UW, Gebhart B, Mecham RP, Heuser JE (1986) Crystals of the *Chlamydomonas reinhardtii* cell wall: polymerization, depolymerization, and purification of glycoprotein monomers. J Cell Biol 103(2):405–417. doi:10.1083/jcb.103.2.405
172. Imam SH, Buchanan MJ, Shin HC, Snell WJ (1985) The *Chlamydomonas* cell wall: characterization of the wall framework. J Cell Biol 101(4):1599–1607
173. Chynoweth DP (2002) Review of biomethane from marine biomass. History, results and conclusions of the "US Marine Biomass Energy Program" (1968–1990) Gainsville: Department of Agricultural and Biological Engineering, University of Florida, pp 194
174. Santelices B (1999) A conceptual framework for marine agronomy. Hydrobiologia 398–399:15–23. doi:10.1023/a:1017053413126
175. Briand X (1991) Seaweed harvesting in Europe. In: Guiry MD, Blunden G (eds) Seaweed resources in Europe: uses and potential. Wiley, Chichester, pp 259–308
176. Kain JM (1991) Cultivation of attached seaweeds. In: Guiry MD, Blunden G (eds) Seaweed resources in Europe: uses and potential. Wiley, Chichester, pp 309–377
177. Schramm W (1991) Seaweeds for wastewater treatment and recycling of nutrients. In: Guiri MD, Bland G (eds) Seaweed resources in Europe: uses and potential. Wiley, Chichester, pp 149–168
178. Titlyanov E, Titlyanova T (2010) Seaweed cultivation: methods and problems. Russ J Mar Biol 36(4):227–242. doi:10.1134/s1063074010040012
179. Gellenbeck KW, Chapman DJ (1983) Seaweed uses: the outlook for mariculture. Endeavour 7(1):31–37
180. Borowitzka MA (1999) Commercial production of microalgae: ponds, tanks, and fermenters. In: Osinga R, Tramper J, Burgess JG, Wijffels RH (eds) Progress in industrial microbiology, vol 35. Elsevier, Amsterdam, pp 313–321
181. Borowitzka MA (1999) Commercial production of microalgae: ponds, tanks, tubes and fermenters. J Biotechnol 70(1–3):313–321
182. Carvalho AP, Meireles LA, Malcata FX (2006) Microalgal reactors: a review of enclosed system designs and performances. Biotechnol Prog 22(6):1490–1506. doi:10.1021/bp060065r

183. Chaumont D (1993) Biotechnology of algal biomass production: a review of systems for outdoor mass culture. J Appl Phycol 5(6):593–604. doi:10.1007/bf02184638
184. Lee Y-K (2001) Microalgal mass culture systems and methods: their limitation and potential. J Appl Phycol 13(4):307–315. doi:10.1023/a:1017560006941
185. Brennan L, Owende P (2010) Biofuels from microalgae–a review of technologies for production, processing, and extractions of biofuels and co-products. Renew Sustain Energy Rev 14(2):557–577
186. Day JG, Benson EE, Roland AF (1999) In vitro culture and conservation of microalgae: applications for aquaculture, biotechnology and environmental research. In Vitro Cell Dev Biol Plant 35(2):127–136
187. Vonshak A, Richmond A (1988) Mass production of the blue-green alga *Spirulina*: an overview. Biomass 15(4):233–247
188. Wagener K (1983) Mass cultures of marine algae for energy farming in coastal deserts. Int J Biometeorol 27(3):227–233. doi:10.1007/bf02184238
189. Carrere H, Dumas C, Battimelli A, Batstone DJ, Delgenes JP, Steyer JP, Ferrer I (2010) Pretreatment methods to improve sludge anaerobic degradability: a review. J Hazard Mater 183(1–3):1–15
190. Elliott A, Mahmood T (2007) Pretreatment technologies for advancing anaerobic digestion of pulp and paper biotreatment residues. Water Res 41(19):4273–4286
191. González-Fernández C, León-Cofreces C, García-Encina PA (2008) Different pretreatments for increasing the anaerobic biodegradability in swine manure. Bioresour Technol 99(18):8710–8714
192. Kumar P, Barrett DM, Delwiche MJ, Stroeve P (2009) Methods for pretreatment of lignocellulosic biomass for efficient hydrolysis and biofuel production. Ind Eng Chem Res 48(8):3713–3729. doi:10.1021/ie801542g
193. Taherzadeh MJ, Karimi K (2008) Pretreatment of lignocellulosic wastes to improve ethanol and biogas production: a review. Int J Mol Sci 9(9):1621–1651. doi:10.3390/ijms9091621
194. Baier U, Schmidheiny P (1997) Enhanced anaerobic degradation of mechanically disintegrated sludge. Water Sci Technol 36(11):137–143
195. Barjenbruch M, Kopplow O (2003) Enzymatic, mechanical and thermal pre-treatment of surplus sludge. Adv Environ Res 7(3):715–720
196. Bougrier C, Albasi C, Delgenes JP, Carrere H (2006) Effect of ultrasonic, thermal and ozone pre-treatments on waste activated sludge solubilisation and anaerobic biodegradability. Chem Eng Process 45(8):711–718
197. Bougrier C, CarrËre H, DelgenËs JP (2005) Solubilisation of waste-activated sludge by ultrasonic treatment. Chem Eng J 106(2):163–169
198. Bruni E, Jensen AP, Angelidaki I (2010) Comparative study of mechanical, hydrothermal, chemical and enzymatic treatments of digested biofibers to improve biogas production. Bioresour Technol 101(22):8713–8717
199. Climent M, Ferrer I, Del Mar Baeza M, Artola A, Vázquez F, Font X (2007) Effects of thermal and mechanical pretreatments of secondary sludge on biogas production under thermophilic conditions. Chem Eng J 133(1–3):335–342
200. Hwang K-Y, Shin E-B, Choi H-B (1997) A mechanical pretreatment of waste activated sludge for improvement of anaerobic digestion system. Water Sci Technol 36(12):111–116
201. Kim J, Park C, Kim T-H, Lee M, Kim S, Kim S-W, Lee J (2003) Effects of various pretreatments for enhanced anaerobic digestion with waste activated sludge. J Biosci Bioeng 95(3):271–275
202. Kopp J, Müller J, Dichtl N, Schwedes J (1997) Anaerobic digestion and dewatering characteristics of mechanically disintegrated excess sludge. Water Sci Technol 36(11):129–136
203. Lehne G, Muller A, Schwedes J (2001) Mechanical disintegration of sewage sludge. Water Sci Technol 43(1):19–26
204. Nah IW, Kang YW, Hwang K-Y, Song W-K (2000) Mechanical pretreatment of waste activated sludge for anaerobic digestion process. Water Res 34(8):2362–2368

205. Pilli S, Bhunia P, Yan S, LeBlanc RJ, Tyagi RD, Surampalli RY (2011) Ultrasonic pretreatment of sludge: a review. Ultrason Sonochem 18(1):1–18
206. Neyens E, Baeyens J (2003) A review of thermal sludge pre-treatment processes to improve dewaterability. J Hazard Mater 98(1–3):51–67
207. Stuckey DC, McCarty PL (1984) The effect of thermal pretreatment on the anaerobic biodegradability and toxicity of waste activated sludge. Water Res 18(11):1343–1353
208. Valo A, Carrère H, Delgenès JP (2004) Thermal, chemical and thermo-chemical pre-treatment of waste activated sludge for anaerobic digestion. J Chem Technol Biotechnol 79(11):1197–1203. doi:10.1002/jctb.1106
209. Wilson CA, Novak JT (2009) Hydrolysis of macromolecular components of primary and secondary wastewater sludge by thermal hydrolytic pretreatment. Water Res 43(18): 4489–4498
210. Goel R, Tokutomi T, Yasui H (2003) Anaerobic digestion of excess activated sludge with ozone pretreatment, vol 47. IWA, London
211. Rivero JAC, Madhavan N, Suidan MT, Ginestet P, Audic J-M (2006) Enhancement of anaerobic digestion of excess municipal sludge with thermal and/or oxidative treatment. J Environ Eng 132(6):638–644
212. Weemaes M, Grootaerd H, Simoens F, Verstraete W (2000) Anaerobic digestion of ozonized biosolids. Water Res 34(8):2330–2336
213. Zheng M, Li X, Li L, Yang X, He Y (2009) Enhancing anaerobic biogasification of corn stover through wet state NaOH pretreatment. Bioresour Technol 100(21):5140–5145
214. Ge H, Jensen PD, Batstone DJ (2010) Pre-treatment mechanisms during thermophilic-mesophilic temperature phased anaerobic digestion of primary sludge. Water Res 44(1):123–130
215. Lv W, Schanbacher FL, Yu Z (2010) Putting microbes to work in sequence: recent advances in temperature-phased anaerobic digestion processes. Bioresour Technol 101(24): 9409–9414
216. Erden G, Filibeli A (2010) Improving anaerobic biodegradability of biological sludges by Fenton pre-treatment: effects on single stage and two-stage anaerobic digestion. Desalination 251(1–3):58–63
217. Khoufi S, Aloui F, Sayadi S (2006) Treatment of olive oil mill wastewater by combined process electro-Fenton reaction and anaerobic digestion. Water Res 40(10):2007–2016
218. Eskicioglu C, Droste RL, Kennedy KJ (2007) Performance of anaerobic waste activated sludge digesters after microwave pretreatment. Water Environ Res 79(11):2265–2273
219. Eskicioglu C, Terzian N, Kennedy KJ, Droste RL, Hamoda M (2007) Athermal microwave effects for enhancing digestibility of waste activated sludge. Water Res 41(11):2457–2466
220. Kumakura M, Kojima T, Kaetsu I (1982) Pretreatment of lignocellulosic wastes by combination of irradiation and mechanical crushing. Biomass 2(4):299–308
221. Lafitte-Trouque S, Forster CF (2002) The use of ultrasound and gamma-irradiation as pretreatments for the anaerobic digestion of waste activated sludge at mesophilic and thermophilic temperatures. Bioresour Technol 84(2):113–118
222. Park B, Ahn JH, Kim J, Hwang S (2004) Use of microwave pretreatment for enhanced anaerobiosis of secondary sludge. Water Sci Technol 50(9):17–23
223. Fox M, Noike T (2004) Wet oxidation pretreatment for the increase in anaerobic biodegradability of newspaper waste. Bioresour Technol 91(3):273–281
224. Kim D-H, Jeong E, Oh S-E, Shin H-S (2010) Combined (alkaline + ultrasonic) pretreatment effect on sewage sludge disintegration. Water Res 44(10):3093–3100
225. Penaud V, DelgenËs JP, Moletta R (1999) Thermo-chemical pretreatment of a microbial biomass: influence of sodium hydroxide addition on solubilization and anaerobic biodegradability. Enzyme Microb Technol 25(3–5):258–263
226. Tanaka S, Kobayashi T, Kamiyama K-I, Lolita M, Signey Bildan N (1997) Effects of thermochemical pretreatment on the anaerobic digestion of waste activated sludge. Water Sci Technol 35(8):209–215
227. Eastman JA, Ferguson JF (1981) Solubilization of particulate organic carbon during the acid phase of anaerobic digestion. J Water Pollut Control Fed 53(3I):352–366

228. Pavlostathis SG, Giraldo-Gomez E (1991) Kinetics of anaerobic treatment: a critical review. Crit Rev Environ Control 21(5):411–490
229. Delgenes JP, Penaud V, Moletta R (2003) Pretreatments for the enhancement of anaerobic digestion of solid wastes. In: Mata-Alvarez J (ed) Biomethanization of the organic fraction of municipal solid wastes. IWA Publishing, London, pp 201–228
230. Hartmann H, Angelidaki I, Ahring BK (1999) Increase of anaerobic degradation of particulate organic matter in full-scale biogas plants by mechanical maceration. In: Mata-Alvarez J (ed) Second international symposium on anaerobic digestion of solid wastes, Barcelona, pp 129–136
231. Wett B, Phothilangka P, Eladawy A (2010) Systematic comparison of mechanical and thermal sludge disintegration technologies. Waste Manag 30(6):1057–1062
232. Gonze E, Pillot S, Valette E, Gonthier Y, Bernis A (2003) Ultrasonic treatment of an aerobic activated sludge in a batch reactor. Chem Eng Process 42(12):965–975
233. Samson R, Leduy A (1983) Influence of mechanical and thermochemical pretreatments on anaerobic digestion of *Spirulina maxima* algal biomass. Biotechnol Lett 5(10):671–676. doi:10.1007/bf01386360
234. Hanaki K, Matsuo T, Nagase M (1981) Mechanism of inhibition caused by long-chain fatty acids in anaerobic digestion process. Biotechnol Bioeng 23(7):1591–1610. doi:10.1002/bit.260230717
235. Li YY, Noike T (1992) Upgrading of anaerobic digestion of waste activated sludge by thermal pretreatment. Water Sci Technol 26(3–4):857–866
236. Stuckey DC, McCarty PL (1978) Thermochemical pretreatment of nitrogenous materials to increase methane yield. In: Biotechnology and bioengineering symposium. Stanford University, California, pp 219–233
237. De Schamphelaire L, Verstraete W (2009) Revival of the biological sunlight-to-biogas energy conversion system. Biotechnol Bioeng 103(2):296–304. doi:10.1002/bit.22257
238. Chen PH, Oswald WJ (1998) Thermochemical treatment for algal fermentation. Environ Int 24(8):889–897
239. Hanssen JF, Indergaard M, Ostgaard K, Baevre OA, Pedersen TA, Jensen A (1987) Anaerobic digestion of *Laminaria* spp. and *Ascophyllum nodosum* and application of end products. Biomass 14(1):1–13
240. Fengel D, Wegener G (1984) Wood: chemistry, ultrastructure, reactions. Walter de Gruyter, Berlin
241. Lopez Torres M, MdC EL (2008) Effect of alkaline pretreatment on anaerobic digestion of solid wastes. Waste Manag 28(11):2229–2234
242. Hon D, Shiraishi N (2000) Wood and cellulosic chemistry, 2nd edn. CRC, New York
243. Andreozzi R, Longo G, Majone M, Modesti G (1998) Integrated treatment of olive oil mill effluents (OME): study of ozonation coupled with anaerobic digestion. Water Res 32(8):2357–2364
244. Masse L, MassÈ DI, Kennedy KJ (2003) Effect of hydrolysis pretreatment on fat degradation during anaerobic digestion of slaughterhouse wastewater. Process Biochem 38(9):1365–1372
245. Carpentier B (1986) Digestion anaérobie de biomasse algale: Les résidus de l'extraction de l'acide alginique, les ulves de marées vertes. Université Pierre et Marie Curie, Paris
246. Morand P, Briand X (1999) Anaerobic digestion of *Ulva* sp. 2. Study of *Ulva* degradation and methanisation of liquefaction juices. J Appl Phycol 11(2):164–177. doi:10.1023/a:1008028127701
247. Morand P, Briand X, Charlier R (2006) Anaerobic digestion of *Ulva* sp. 3. Liquefaction juices extraction by pressing and a technico-economic budget. J Appl Phycol 18(6):741–755. doi:10.1007/s10811-006-9083-1
248. Legros A, Asinari Di San Marzano C-M, Naveau H, Nyns E-J (1982) Improved methane production from algae using 2nd generation digesters. In: Strub A, Chartier P, Schlesser G (eds) Energy from biomass. Second EC conference, Berlin. Elsevier Applied Science, London, pp 609–614

249. Legros A, di San A, Marzano CM, Naveau HP, Nyns EJ (1983) Fermentation profiles in bioconversions. Biotechnol Lett 5(1):7–12. doi:10.1007/bf00189956
250. Yin L-J, Jiang S-T, Pon S-H, Lin H-H (2010) Hydrolysis of *Chlorella* by *Cellulomonas* sp. YJ5 cellulases and its biofunctional properties. J Food Sci 75(9):H317–H323. doi:10.1111/j.1750-3841.2010.01867.x
251. Fu C-C, Hung T-C, Chen J-Y, Su C-H, Wu W-T (2010) Hydrolysis of microalgae cell walls for production of reducing sugar and lipid extraction. Bioresour Technol 101(22):8750–8754. doi:10.1016/j.biortech.2010.06.100
252. Bhat MK (2000) Cellulases and related enzymes in biotechnology. Biotechnol Adv 18(5):355–383. doi:10.1016/s0734-9750(00)00041-0
253. Bjerre AB, Olesen AB, Fernqvist T, Plöger A, Schmidt AS (1996) Pretreatment of wheat straw using combined wet oxidation and alkaline hydrolysis resulting in convertible cellulose and hemicellulose. Biotechnol Bioeng 49(5):568–577. doi:10.1002/(sici)1097-0290(19960305)49:5<568::aid-bit10>3.0.co;2-6
254. Lissens G, Thomsen AB, De Baere L, Verstraete W, Ahring BK (2004) Thermal wet oxidation improves anaerobic biodegradability of raw and digested biowaste. Environ Sci Technol 38(12):3418–3424. doi:10.1021/es035092h
255. Liu C-Z, Cheng X-Y (2009) Microwave-assisted acid pretreatment for enhancing biogas production from herbal-extraction process residue. Energy Fuel 23(12):6152–6155. doi:10.1021/ef900607f
256. Liu X, Duan S, Li A, Xu N, Cai Z, Hu Z (2009) Effects of organic carbon sources on growth, photosynthesis, and respiration of *Phaeodactylum tricornutum*. J Appl Phycol 21(2):239–246. doi:10.1007/s10811-008-9355-z
257. Hu Z, Wen Z (2008) Enhancing enzymatic digestibility of switchgrass by microwave-assisted alkali pretreatment. Biochem Eng J 38(3):369–378
258. Hu Q, Sommerfeld M, Jarvis E, Ghirardi M, Posewitz M, Seibert M, Darzins A (2008) Microalgal triacylglycerols as feedstocks for biofuel production: perspectives and advances. Plant J 54(4):621–639. doi:10.1111/j.1365-313X.2008.03492.x
259. Ratledge C (2002) Regulation of lipid accumulation in oleaginous micro-organisms. Biochem Soc Trans 30(pt 6):1047–1050. doi:10.1042/
260. Xin L, Hong-ying H, Ke G, Ying-xue S (2010) Effects of different nitrogen and phosphorus concentrations on the growth, nutrient uptake, and lipid accumulation of a freshwater microalga *Scenedesmus* sp. Bioresour Technol 101(14):5494–5500
261. Illman AM, Scragg AH, Shales SW (2000) Increase in *Chlorella* strains calorific values when grown in low nitrogen medium. Enzyme Microb Technol 27(8):631–635
262. Scragg AH, Illman AM, Carden A, Shales SW (2002) Growth of microalgae with increased calorific values in a tubular bioreactor. Biomass Bioenergy 23(1):67–73
263. Sialve B, Bernet N, Bernard O (2009) Anaerobic digestion of microalgae as a necessary step to make microalgal biodiesel sustainable. Biotechnol Adv 27(4):409–416
264. Li Y, Horsman M, Wang B, Wu N, Lan C (2008) Effects of nitrogen sources on cell growth and lipid accumulation of green alga *Neochloris oleoabundans*. Appl Microbiol Biotechnol 81(4):629–636. doi:10.1007/s00253-008-1681-1
265. Lv J-M, Cheng L-H, Xu X-H, Zhang L, Chen H-L (2010) Enhanced lipid production of *Chlorella vulgaris* by adjustment of cultivation conditions. Bioresour Technol 101(17):6797–6804
266. Harrison P, Thompson P, Calderwood G (1990) Effects of nutrient and light limitation on the biochemical composition of phytoplankton. J Appl Phycol 2(1):45–56. doi:10.1007/bf02179768
267. Kilham S, Kreeger D, Goulden C, Lynn S (1997) Effects of nutrient limitation on biochemical constituents of *Ankistrodesmus falcatus*. Freshw Biol 38(3):591–596. doi:10.1046/j.1365-2427.1997.00231.x
268. La Roche J, Geider RJ, Graziano LM, Murray H, Lewis K (1993) Induction of specific proteins in eukaryotic algae grown under iron-, phosphorus-, or nitrogen-deficient conditions. J Phycol 29(6):767–777. doi:10.1111/j.0022-3646.1993.00767.x

269. Larson TR, Rees TAV (1996) Changes in cell composition and lipid metabolism mediated by sodium and nitrogen availability in the marine diatom *Phaeodactylum tricornutum* (Bacillariophyceae). J Phycol 32(3):388–393. doi:10.1111/j.0022-3646.1996.00388.x
270. Rhee G (1978) Effects of N: P atomic ratios and nitrate limitation on algal growth, cell composition, and nitrate uptake. Limnol Oceanogr 23(1):10–25
271. Suen Y, Hubbard JS, Holzer G, Tornabene TG (1987) Total lipid production of the green ajga *Nannochloropsis* sp. QII under different nitrogen regimes. J Phycol 23:289–296. doi:10.1111/j.1529-8817.1987.tb04137.x
272. Tornabene TG, Holzer G, Lien S, Burris N (1983) Lipid composition of the nitrogen starved green alga *Neochloris oleoabundans*. Enzyme Microb Technol 5(6):435–440
273. Darley WM (1977) Biochemical composition. In: Werner D (ed) The biology of diatoms. University of California Press, Berkeley, pp 98–223
274. Heraud P, Wood BR, Tobin MJ, Beardall J, McNaughton D (2005) Mapping of nutrient-induced biochemical changes in living algal cells using synchrotron infrared microspectroscopy. FEMS Microbiol Lett 249(2):219–225
275. Lynn SG, Kilham SS, Kreeger DA, Interlandi SJ (2000) Effect of nutrient availability on the biochemical and elemental stochiometry in the freshwater diatom *Stephanodiscus minutulus* (Bacillariophyceae). J Phycol 36(3):510–522. doi:10.1046/j.1529-8817.2000.98251.x
276. Sigee DC, Bahrami F, Estrada B, Webster RE, Dean AP (2007) The influence of phosphorus availability on carbon allocation and P quota in *Scenedesmus subspicatus*: a synchrotron-based FTIR analysis. Phycologia 46(5):583–592. doi:10.2216/07-14.1
277. Stehfest K, Toepel J, Wilhelm C (2005) The application of micro-FTIR spectroscopy to analyze nutrient stress-related changes in biomass composition of phytoplankton algae. Plant Physiol Biochem 43(7):717–726
278. Enright CT, Newkirk GF, Craigie JS, Castell JD (1986) Growth of juvenile *Ostrea edulis L.* fed *Chaetoceros gracilis Schutt* of varied chemical composition. J Exp Mar Biol Ecol 96(1):15–26
279. Roessler PG (1988) Changes in the activities of various lipid and carbohydrate biosynthetic enzymes in the diatom *Cyclotella cryptica* in response to silicon deficiency. Arch Biochem Biophys 267(2):521–528
280. Vaulot D, Olson RJ, Merkel S, Chisholm SW (1987) Cell-cycle response to nutrient starvation in two phytoplankton species, *Thalassiosira weissflogii* and *Hymenomonas carterae*. Mar Biol 95(4):625–630. doi:10.1007/bf00393106
281. Chen M, Tang H, Ma H, Holland TC, Ng KYS, Salley SO (2011) Effect of nutrients on growth and lipid accumulation in the green algae *Dunaliella tertiolecta*. Bioresour Technol 102:1649–1655
282. Yeesang C, Cheirsilp B (2010) Effect of nitrogen, salt, and iron content in the growth medium and light intensity on lipid production by microalgae isolated from freshwater sources in Thailand. Bioresour Technol 102:3034–3040
283. Liu Z-Y, Wang G-C, Zhou B-C (2008) Effect of iron on growth and lipid accumulation in *Chlorella vulgaris*. Bioresour Technol 99(11):4717–4722
284. Chen G-Q, Chen F (2006) Growing phototrophic cells without light. Biotechnol Lett 28(9):607–616. doi:10.1007/s10529-006-0025-4
285. Ceron Garcia MC, Garcia Camacho F, Sanchez M (2006) Mixotrophic production of marine microalga *Phaeodactylum tricornutum* on various carbon sources. J Microbiol Biotechnol 16(5):689–694
286. Chen F, Johns MR (1996) Heterotrophic growth of *Chlamydomonas reinhardtii* on acetate in chemostat culture. Process Biochem 31(6):601–604
287. Degrenne B, Pruvost J, Christophe G, Cornet JF, Cogne G, Legrand J (2010) Investigation of the combined effects of acetate and photobioreactor illuminated fraction in the induction of anoxia for hydrogen production by *Chlamydomonas reinhardtii*. Int J Hydrogen Energy 35(19):10741–10749
288. Heifetz PB, Forster B, Osmond CB, Giles LJ, Boynton JE (2000) Effects of acetate on facultative autotrophy in *Chlamydomonas reinhardtii* assessed by photosynthetic measurements and stable isotope analyses. Plant Physiol 122(4):1439–1446. doi:10.1104/pp. 122.4.1439

289. Endo H, Sansawa H, Nakajima K (1977) Studies on *Chlorella regularis*, heterotrophic fast-growing strain II. Mixotrophic growth in relation to light intensity and acetate concentration. Plant Cell Physiol 18(1):199–205
290. Heredia-Arroyo T, Wei W, Hu B (2010) Oil accumulation via heterotrophic/mixotrophic *Chlorella protothecoides*. Appl Biochem Biotechnol 162(7):1978–1995. doi:10.1007/s12010-010-8974-4
291. Lee Y-K, Ding S-Y, Hoe C-H, Low C-S (1996) Mixotrophic growth of *Chlorella sorokiniana* in outdoor enclosed photobioreactor. J Appl Phycol 8(2):163–169. doi:10.1007/bf02186320
292. Liang Y, Sarkany N, Cui Y (2009) Biomass and lipid productivities of *Chlorella vulgaris* under autotrophic, heterotrophic and mixotrophic growth conditions. Biotechnol Lett 31(7):1043–1049. doi:10.1007/s10529-009-9975-7
293. O'Grady J, Morgan J (2010) Heterotrophic growth and lipid production of *Chlorella protothecoides* on glycerol. Bioprocess Biosyst Eng 34:121–125. doi:10.1007/s00449-010-0474-y
294. Abeliovich A, Weisman D (1978) Role of heterotrophic nutrition in growth of the alga *Scenedesmus obliquus* in high-rate oxidation ponds. Appl Environ Microbiol 35(1):32–37
295. Ogawa T, Aiba S (1981) Bioenergetic analysis of mixotrophic growth in *Chlorella vulgaris* and *Scenedesmus acutus*. Biotechnol Bioeng 23(5):1121–1132. doi:10.1002/bit.260230519
296. Shamala TR, Drawert F, Leupold G (1982) Studies on *Scenedesmus acutus* growth. I. Effect of autotrophic and mixotrophic conditions on the growth of *Scenedesmus acutus*. Biotechnol Bioeng 24(6):1287–1299. doi:10.1002/bit.260240605
297. Azma M, Mohamed MS, Mohamad R, Rahim RA, Ariff AB (2011) Improvement of medium composition for heterotrophic cultivation of green microalgae, *Tetraselmis suecica*, using response surface methodology. Biochem Eng J 53(2):187–195
298. Xie J, Zhang Y, Li Y, Wang Y (2001) Mixotrophic cultivation of *Platymonas subcordiformis*. J Appl Phycol 13(4):343–347. doi:10.1023/a:1017532302360
299. Tanoi T, Kawachi M, Watanabe M (2011) Effects of carbon source on growth and morphology of *Botryococcus braunii*. J Appl Phycol 23:25–33. doi:10.1007/s10811-010-9528-4
300. Bouarab L, Dauta A, Loudiki M (2004) Heterotrophic and mixotrophic growth of *Micractinium pusillum* Fresenius in the presence of acetate and glucose:effect of light and acetate gradient concentration. Water Res 38(11):2706–2712
301. Cai M, Shi R, Huang S, Qi A (2008) Comparison of mixotrophic and hotoautotrophic growth of *Haematococcus pluvialis* for astaxanthin production. J Biotechnol 136(suppl 1): S575–S576
302. Jeon Y-C, Cho C-W, Yun Y-S (2006) Combined effects of light intensity and acetate concentration on the growth of unicellular microalga *Haematococcus pluvialis*. Enzyme Microb Technol 39(3):490–495
303. Kobayashi M, Kakizono T, Yamaguchi K, Nishio N, Nagai S (1992) Growth and astaxanthin formation of *Haematococcus pluvialis* in heterotrophic and mixotrophic conditions. J Ferment Bioeng 74(1):17–20
304. Barbera E, Tomas X, Moya M-J, Ibanez A, Molins M-B (1993) Significance tests in the study of the specific growth rate of *Haematococcus lacustris*: influence of carbon source and light intensity. J Ferment Bioeng 76(5):403–405
305. Chen F, Chen H, Gong X (1997) Mixotrophic and heterotrophic growth of H*aematococcus lacustris* and rheological behaviour of the cell suspensions. Bioresour Technol 62(1–2): 19–24
306. Fábregas J, GarcÌa D, Morales ED, Lamela T, Otero A (1999) Mixotrophic production of phycoerythrin and exopolysaccharide by the microalga *Porphyridium cruentum*. Cryptogam Algol 20(2):89–94
307. Oh SH, Han JG, Kim Y, Ha JH, Kim SS, Jeong MH, Jeong HS, Kim NY, Cho JS, Yoon WB, Lee SY, Kang DH, Lee HY (2009) Lipid production in *Porphyridium cruentum* grown under different culture conditions. J Biosci Bioeng 108(5):429–434
308. Gross W, Schnarrenberger C (1995) Heterotrophic growth of two strains of the acido-thermophilic red alga *Galdieria sulphuraria*. Plant Cell Physiol 36(4):633–638

309. Ceron Garcia MC, Fernandez Sevilla JM, Acién Fernandez FG, Molina Grima E, Garcia Camacho F (2000) Mixotrophic growth of *Phaeodactylum tricornutum* on glycerol: growth rate and fatty acid profile. J Appl Phycol 12(3):239–248. doi:10.1023/a:1008123000002
310. Cooksey KE (1974) Acetate metabolism by whole cells of *Phaeodactylum tricornutum* bohlin12. J Phycol 10(3):253–257. doi:10.1111/j.1529-8817.1974.tb02710.x
311. Fábregas J, Morales ED, Lamela T, Cabezas B, Otero A (1997) Mixotrophic productivity of the marine diatom *Phaeodactylum tricornutum* cultured with soluble fractions of rye, wheat and potato. World J Microbiol Biotechnol 13(3):349–351. doi:10.1023/a:1018551527986
312. Fernández Sevilla JM, Cerón García MC, Sánchez Mirón A, Belarbi EH, Camacho FG, Grima EM (2004) Pilot-plant-scale outdoor mixotrophic cultures of *Phaeodactylum tricornutum* using glycerol in vertical bubble column and airlift photobioreactors: studies in fed-batch mode. Biotechnol Prog 20(3):728–736. doi:10.1021/bp034344f
313. Fang X, Wei C, Zhao-Ling C, Fan O (2004) Effects of organic carbon sources on cell growth and eicosapentaenoic acid content of *Nannochloropsis* sp. J Appl Phycol 16(6):499–503. doi:10.1007/s10811-004-5520-1
314. Xu F, Z-l C, Cong W, Ouyang F (2004) Growth and fatty acid composition of *Nannochloropsis* sp. grown mixotrophically in fed-batch culture. Biotechnol Lett 26(17):1319–1322. doi:10.1023/B:BILE.0000045626.38354.1a
315. Xu F, Hu H-H, Cong W, Cai Z-L, Ouyang F (2004) Growth characteristics and eicosapentaenoic acid production by *Nannochloropsis* sp. in mixotrophic conditions. Biotechnol Lett 26(1):51–53. doi:10.1023/B:BILE.0000009460.81267.cc
316. Kitano M, Matsukawa R, Karube I (1997) Changes in eicosapentaenoic acid content of *Navicula saprophila. Rhodomonas salina* and *Nitzschia* sp. under mixotrophic conditions. J Appl Phycol 9(6):559–563. doi:10.1023/a:1007908618017
317. Wen Z-Y, Chen F (2002) Perfusion culture of the diatom *Nitzschia laevis* for ultra-high yield of eicosapentaenoic acid. Process Biochem 38(4):523–529
318. Kang R, Wang J, Shi D, Cong W, Cai Z, Ouyang F (2004) Interactions between organic and inorganic carbon sources during mixotrophic cultivation of *Synechococcus* sp. Biotechnol Lett 26(18):1429–1432. doi:10.1023/B:BILE.0000045646.23832.a5
319. Vernotte C, Picaud M, Kirilovsky D, Olive J, Ajlani G, Astier C (1992) Changes in the photosynthetic apparatus in the cyanobacterium *Synechocystis* sp. PCC 6714 following light-to-dark and dark-to-light transitions. Photosynth Res 32(1):45–57. doi:10.1007/bf00028797
320. Andrade MR, Costa JAV (2007) Mixotrophic cultivation of microalga *Spirulina platensis* using molasses as organic substrate. Aquaculture 264(1–4):130–134
321. Chojnacka K, Noworyta A (2004) Evaluation of *Spirulina* sp. growth in photoautotrophic, heterotrophic and mixotrophic cultures. Enzyme Microb Technol 34(5):461–465
322. Mühling M, Belay A, Whitton BA (2005) Screening *Arthrospira* (*Spirulina*) strains for heterotrophy. J Appl Phycol 17(2):129–135. doi:10.1007/s10811-005-7214-8
323. Rym B, Nejeh G, Lamia T, Ali Y, Rafika C, Khemissa G, Jihene A, Hela O, Hatem B (2010) Modeling growth and photosynthetic response in *Arthrospira platensis* as function of light intensity and glucose concentration using factorial design. J Appl Phycol 22(6):745–752. doi:10.1007/s10811-010-9515-9
324. Yu H, Jia S, Dai Y (2009) Growth characteristics of the cyanobacterium *Nostoc* flagelliforme in photoautotrophic, mixotrophic and heterotrophic cultivation. J Appl Phycol 21(1):127–133. doi:10.1007/s10811-008-9341-5
325. Mannan RM, Pakrasi HB (1993) Dark heterotrophic growth conditions result in an increase in the content of photosystem II units in the filamentous cyanobacterium *Anabaena variabilis* ATCC 29413. Plant Physiol 103(3):971–977. doi:10.1104/pp. 103.3.971
326. Xin L, Hong-ying H, Jia Y (2010) Lipid accumulation and nutrient removal properties of a newly isolated freshwater microalga, *Scenedesmus* sp. LX1, growing in secondary effluent. N Biotechnol 27(1):59–63
327. Post A, Dubinsky Z, Wyman K, Falkowski P (1985) Physiological responses of a marine planktonic diatom to transitions in growth irradiance. Mar Ecol Prog Ser 25(2):141–149
328. Richardson K, Beardall J, Raven JA (1983) Adaptation of unicellular algae to irradiance: an analysis of strategies. New Phytol 93(2):157–191. doi:10.1111/j.1469-8137.1983.tb03422.x

329. Brown MR, Dunstan GA, Norwood SJ, Miller KA (1996) Effects of harvest stage and light on the biochemical composition of the diatom *Thalassiosira pseudonana*. J Phycol 32(1):64–73. doi:10.1111/j.0022-3646.1996.00064.x
330. Fábregas J, Maseda A, Domínguez A, Otero A (2004) The cell composition of *Nannochloropsis* sp. changes under different irradiances in semicontinuous culture. World J Microbiol Biotechnol 20(1):31–35. doi:10.1023/B:WIBI.0000013288.67536.ed
331. Khotimchenko SV, Yakovleva IM (2005) Lipid composition of the red alga *Tichocarpus crinitus* exposed to different levels of photon irradiance. Phytochemistry 66(1):73–79
332. Roessler PG (1990) Environmental control of glycerolipid metabolism in microalgae: commercial implications and future research directions. J Phycol 26(3):393–399. doi:10.1111/j.0022-3646.1990.00393.x
333. Dayananda C, Sarada R, Usha Rani M, Shamala TR, Ravishankar GA (2007) Autotrophic cultivation of *Botryococcus braunii* for the production of hydrocarbons and exopolysaccharides in various media. Biomass Bioenergy 31(1):87–93
334. Kowallik W (1987) Blue light effects on carbohydrate and protein metabolism. In: Senger H (ed) Blue light responses: phenomena and occurrence in plants and microorganisms, vol 1. CRC Press, Florida, pp 8–13
335. Spolaore P, Joannis-Cassan C, Duran E, Isambert A (2006) Commercial applications of microalgae. J Biosci Bioeng 101(2):87–96
336. Borowitzka MA (1988) Vitamins and fine chemicals from micro-algae. In: Borowitzka LJ, Borowitzka MA (eds) Micro-algal biotechnology. Cambridge University Press, Cambridge, pp 153–196
337. Lorenz RT, Cysewski GR (2000) Commercial potential for *Haematococcus* microalgae as a natural source of astaxanthin. Trends Biotechnol 18(4):160–167
338. Apt KE, Behrens PW (1999) Commercial developments in microalgal biotechnology. J Phycol 35(2):215–226. doi:10.1046/j.1529-8817.1999.3520215.x
339. Cannell RJP (1993) Algae as a source of biologically active products. Pestic Sci 39(2):147–153. doi:10.1002/ps.2780390208
340. Schwartz RE, Hirsch CF, Sesin DF, Flor JE, Chartrain M, Fromtling RE, Harris GH, Salvatore MJ, Liesch JM, Yudin K (1990) Pharmaceuticals from cultured algae. J Ind Microbiol Biotechnol 5(2):113–123. doi:10.1007/bf01573860
341. Geresh S, Arad S (1991) The extracellular polysaccharides of the red microalgae: chemistry and rheology. Bioresour Technol 38(2–3):195–201
342. Wijesekara I, Pangestuti R, Kim S-K (2010) Biological activities and potential health benefits of sulfated polysaccharides derived from marine algae. Carbohydr Polym 84(11):14–21
343. Potvin G, Zhang Z (2010) Strategies for high-level recombinant protein expression in transgenic microalgae: a review. Biotechnol Adv 28(6):910–918
344. Walker T, Purton S, Becker D, Collet C (2005) Microalgae as bioreactors. Plant Cell Rep 24(11):629–641. doi:10.1007/s00299-005-0004-6
345. National Center for Biotechnology Information (2010) Genome. http://www.ncbi.nlm.nih.gov/sites/genome. Accessed 22 December 2010
346. Zorin B, Hegemann P, Sizova I (2005) Nuclear-gene targeting by using single-stranded DNA avoids illegitimate DNA integration in *Chlamydomonas reinhardtii*. Eukaryot Cell 4(7):1264–1272. doi:10.1128/ec.4.7.1264-1272.2005
347. Zorin B, Lu Y, Sizova I, Hegemann P (2009) Nuclear gene targeting in *Chlamydomonas* as exemplified by disruption of the PHOT gene. Gene 432(1–2):91–96
348. Corrado G, Karali M (2009) Inducible gene expression systems and plant biotechnology. Biotechnol Adv 27(6):733–743
349. Kim E-J, Cerutti H (2009) Targeted gene silencing by RNA interference in *Chlamydomonas*. In: Stephen MK, Gregory JP (eds) Methods in cell biology, vol 93. Academic, New York, pp 99–110
350. Molnar A, Bassett A, Thuenemann E, Schwach F, Karkare S, Ossowski S, Weigel D, Baulcombe D (2009) Highly specific gene silencing by artificial microRNAs in the unicellular alga *Chlamydomonas reinhardtii*. Plant J 58(1):165–174. doi:10.1111/j.1365-313X.2008.03767.x

351. Zhao T, Wang W, Bai X, Qi Y (2009) Gene silencing by artificial microRNAs in *Chlamydomonas*. Plant J 58(1):157–164. doi:10.1111/j.1365-313X.2008.03758.x
352. Bocobza SE, Aharoni A (2008) Switching the light on plant riboswitches. Trends Plant Sci 13(10):526–533
353. Croft MT, Moulin M, Webb ME, Smith AG (2007) Thiamine biosynthesis in algae is regulated by riboswitches. Proc Natl Acad Sci U S A 104(52):20770–20775. doi:10.1073/pnas.0705786105
354. Hildebrand M (2008) Development of algal genetic tools. In: 2008 NREL-AFOSR joint workshop on algal oil for jet fuel production. NREL, Golden
355. Krause GH (1988) Photoinhibition of photosynthesis. An evaluation of damaging and protective mechanisms. Physiol Plant 74(3):566–574. doi:10.1111/j.1399-3054.1988.tb02020.x
356. Long SP, Humphries S, Falkowski PG (1994) Photoinhibition of photosynthesis in nature. Annu Rev Plant Biol 45(1):633–662
357. Prince RC, Kheshgi HS (2005) The photobiological production of hydrogen: potential efficiency and effectiveness as a renewable fuel. Crit Rev Microbiol 31(1):19–31. doi:doi:10.1080/10408410590912961
358. Kruse O, Rupprecht J, Mussgnug J, Dismukes G, Hankamer B (2005) Photosynthesis: a blueprint for solar energy capture and biohydrogen production technologies. Photochem Photobiol Sci 4(12):957–970
359. Melis A, Neidhardt J, Baroli I, Benemann JR (1999) Maximizing photosynthetic productivity and light utilization in microalgae by minimizing the light-harvesting chlorophyll antenna size of the photosystems. In: Zaborsky OR, Benemann JR, Matsunaga T, Miyake J, San Pietro A (eds) BioHydrogen. Springer, New York, pp 41–52. doi:10.1007/978-0-585-35132-2_6
360. Melis A, Neidhardt J, Benemann J (1998) *Dunaliella salina* (Chlorophyta) with small chlorophyll antenna sizes exhibit higher photosynthetic productivities and photon use efficiencies than normally pigmented cells. J Appl Phycol 10(6):515–525. doi:10.1023/a:1008076231267
361. Mussgnug JH, Thomas-Hall S, Rupprecht J, Foo A, Klassen V, McDowall A, Schenk PM, Kruse O, Hankamer B (2007) Engineering photosynthetic light capture: impacts on improved solar energy to biomass conversion. Plant Biotechnol J 5(6):802–814. doi:10.1111/j.1467-7652.2007.00285.x
362. Schmidt BJ, Lin-Schmidt X, Chamberlin A, Salehi-Ashtiani K, Papin JA (2010) Metabolic systems analysis to advance algal biotechnology. Biotechnol J 5(7):660–670. doi:10.1002/biot.201000129
363. Burgard AP, Pharkya P, Maranas CD (2003) Optknock: a bilevel programming framework for identifying gene knockout strategies for microbial strain optimization. Biotechnol Bioeng 84(6):647–657. doi:10.1002/bit.10803
364. Pharkya P, Burgard AP, Maranas CD (2004) OptStrain: a computational framework for redesign of microbial production systems. Genome Res 14:2367–2376. doi:10.1101/gr.2872004
365. Bro C, Regenberg B, Förster J, Nielsen J (2006) In silico aided metabolic engineering of *Saccharomyces cerevisiae* for improved bioethanol production. Metab Eng 8(2):102–111
366. Van Vleet JH, Jeffries TW (2009) Yeast metabolic engineering for hemicellulosic ethanol production. Curr Opin Biotechnol 20(3):300–306
367. Biagioni DJ, Bortz DM, Alber DM, Chang CH, Graf P, Jones W, Kim K (2009) Engineering of algal communities for hydrogen production. University of Colorado. http://rasei.colorado.edu/siteadmin/images/files/file_160.pdf. Accessed 22 Dec 2010
368. Chynoweth DP, Ghosh S, Klass DL (1981) Anaerobic digestion of kelp. In: Sorer SS, Zaborsky OR (eds) Biomass conversion processes for energy and fuels. Plenum Press, New York, pp 315–338
369. Espino Lopez A, Chinnasamy S, Das K, Balagurusamy N (2011) Anaerobic co-digestion of dairy manure and algal biomass for biogas production. http://www.biorefinery.uga.edu/docs/TIESgroupIIchrisposter.pdf
370. Craggs R, Sukias J (2009) Digestion of wastewater pond microalgae and potential inhibition by alum and ammoniacal-N. In: 8th IWA Specialist Group conference on waste stabilization ponds, Belo Horizonte, Brazil, 26–30 April 2009

371. Deublein D, Steinhauser A (2008) Biogas from waste and renewable resources: An introduction. Wiley-VCH, Weinheim
372. Fannin KF, Biljetina R (1987) Reactor design. In: Chynoweth D, Isaacson R (eds) Anaerobic digestion of biomass. Elsevier Applied Science, London, pp 141–171
373. Rajeshwari KV, Balakrishnan M, Kansal A, Lata K, Kishore VVN (2000) State-of-the-art of anaerobic digestion technology for industrial wastewater treatment. Renew Sustain Energy Rev 4(2):135–156
374. El-Shafie A, Bloodgood D (1973) Anaerobic treatment in a multiple upflow filter system. J Water Pollut Control Fed 45(11):2345–2357
375. Heijnen JJ, Mulder A, Enger W, Hoeks F (1989) Review on the application of anaerobic fluidized bed reactors in waste-water treatment. Chem Eng J 41(3):B37–B50
376. Switzenbaum MS, Jewell WJ (1980) Anaerobic attached-film expanded-bed reactor treatment. J Water Pollut Control Fed 52(7):1953–1965
377. Tait SJ, Friedman AA (1980) Anaerobic rotating biological contactor for carbonaceous wastewaters. J Water Pollut Control Fed 52(8):2257–2269
378. Young JC (1991) Factors affecting the design and performance of upflow anaerobic filters. Water Sci Technol 24(8):133–155
379. Young JC, McCarty PL (1969) The anaerobic filter for waste treatment. J Water Pollut Control Fed 41(5):160–173
380. Barber WP, Stuckey DC (1999) The use of the anaerobic baffled reactor (ABR) for wastewater treatment: a review. Water Res 33(7):1559–1578
381. Dague RR, Habben CE, Pidaparti SR (1992) Initial studies on the anaerobic sequencing batch reactor. Water Sci Technol 26(9):2429–2432
382. Kato MT, Field JA, Lettinga G (1997) The anaerobic treatment of low strength wastewaters in UASB and EGSB reactors. Water Sci Technol 36(6–7):375–382
383. Lettinga G (1995) Anaerobic digestion and wastewater treatment systems. Antonie Van Leeuwenhoek 67(1):3–28. doi:10.1007/bf00872193
384. Lettinga G, van Velsen AFM, Hobma SW, de Zeeuw W, Klapwijk A (1980) Use of the upflow sludge blanket (USB) reactor concept for biological wastewater treatment, especially for anaerobic treatment. Biotechnol Bioeng 22(4):699–734. doi:10.1002/bit.260220402
385. Schmidt JE, Ahring BK (1996) Granular sludge formation in upflow anaerobic sludge blanket (UASB) reactors. Biotechnol Bioeng 49(3):229–246. doi:10.1002/(sici)1097-0290(19960205)49:3<229::aid-bit1>3.0.co;2-m
386. Seghezzo L, Zeeman G, van Lier JB, Hamelers HVM, Lettinga G (1998) A review: the anaerobic treatment of sewage in UASB and EGSB reactors. Bioresour Technol 65(3):175–190
387. Sung S, Dague RR (1995) Laboratory studies on the anaerobic sequencing batch reactor. Water Environ Res 67(3):294–301
388. Hamdi M, Garcia JL (1991) Comparison between anaerobic filter and anaerobic contact process for fermented olive mill wastewaters. Bioresour Technol 38(1):23–29
389. Brindle K, Stephenson T (1996) The application of membrane biological reactors for the treatment of wastewaters. Biotechnol Bioeng 49(6):601–610. doi:10.1002/(sici)1097-0290(19960320)49:6<601::aid-bit1>3.0.co;2-s
390. Harada H, Momonoi K, Yamazaki S, Takizawa S (1994) Application of anaerobic-UF membrane reactor for treatment of a wastewater containing high strength particulate organics. Water Sci Technol 30(12):307–319
391. Lew B, Tarre S, Beliavski M, Dosoretz C, Green M (2009) Anaerobic membrane bioreactor (AnMBR) for domestic wastewater treatment. Desalination 243(1–3):251–257
392. Demirel B, Yenigün O (2002) Two-phase anaerobic digestion processes: a review. J Chem Technol Biotechnol 77(7):743–755. doi:10.1002/jctb.630
393. Ghosh S, Klass DL (1977) Two phase anaerobic digestion. US Patent 4,022,665. May 1977
394. Yu HW, Samani Z, Hanson A, Smith G (2002) Energy recovery from grass using two-phase anaerobic digestion. Waste Manag 22(1):1–5

395. Vergara-Fernandez A, Vargas G, Alarcon N, Velasco A (2008) Evaluation of marine algae as a source of biogas in a two-stage anaerobic reactor system. Biomass Bioenergy 32(4): 338–344
396. Karim K, Hoffmann R, Thomas Klasson K, Al-Dahhan MH (2005) Anaerobic digestion of animal waste: effect of mode of mixing. Water Res 39(15):3597–3606
397. Karim K, Thomas Klasson K, Hoffmann R, Drescher SR, DePaoli DW, Al-Dahhan MH (2005) Anaerobic digestion of animal waste: effect of mixing. Bioresour Technol 96(14):1607–1612
398. McMahon KD, Stroot PG, Mackie RI, Raskin L (2001) Anaerobic codigestion of municipal solid waste and biosolids under various mixing conditions–II: microbial population dynamics. Water Res 35(7):1817–1827
399. Stroot PG, McMahon KD, Mackie RI, Raskin L (2001) Anaerobic codigestion of municipal solid waste and biosolids under various mixing conditions–I. Digester performance. Water Res 35(7):1804–1816
400. Bianchi A, Randriamahefa H (1987) Méthanisation de macro-algues marines à 37 et à 15 C. University Provence, Marseille
401. Rui X, Tianrong G, Pay E, Chaofeng X (2007) Biochemical methane potential of blue-green algae in biogas fermentation progress. J Yunnan Norm Univ (Nat Sci Ed) 05. doi:CNKI:SUN:YNSK.0.2007-05-009
402. Chynoweth DP, Klass DL, Ghosh S (1978) Biomethanation of giant brown kelp *Macrocystis pyrifera*. Paper presented at the Energy from Biomass and Wastes II, Washington, DC
403. Keenan JD (1977) Bioconversion of solar energy to methane. Energy 2(4):365–373
404. Holm-Nielsen JB, Al Seadi T (1998) Biogas in Europe: a general overview. Bioenergy Department, South Jutland University Center, Denmark
405. Braun R, Wellinger A (2003) Potential of co-digestion. IEA Bioenergy Task 37 – Energy from Biogas and Landfill Gas, pp 15
406. Alvarez R, LidÈn G (2008) Semi-continuous co-digestion of solid slaughterhouse waste, manure, and fruit and vegetable waste. Renew Energy 33(4):726–734
407. Callaghan FJ, Wase DAJ, Thayanithy K, Forster CF (2002) Continuous co-digestion of cattle slurry with fruit and vegetable wastes and chicken manure. Biomass Bioenergy 22(1):71–77
408. Mshandete A, Kivaisi A, Rubindamayugi M, Mattiasson B (2004) Anaerobic batch co-digestion of sisal pulp and fish wastes. Bioresour Technol 95(1):19–24
409. Sosnowski P, Wieczorek A, Ledakowicz S (2003) Anaerobic co-digestion of sewage sludge and organic fraction of municipal solid wastes. Adv Environ Res 7(3):609–616
410. Yen H-W, Brune DE (2007) Anaerobic co-digestion of algal sludge and waste paper to produce methane. Bioresour Technol 98(1):130–134
411. Samson R, LeDuy A (1983) Improved performance of anaerobic digestion of *Spirulina maxima* algal biomass by addition of carbon-rich wastes. Biotechnol Lett 5(10):677–682. doi:10.1007/bf01386361
412. Morand P, Carpentier B, Charlier H, Mazé J, Orlandini M, Plunkett A, de Waart J (1991) Bioconversion of seaweeds. In: Guiry MD, Blunden J (eds) Seaweed resources in Europe: uses and potential. Wiley, Chichester, pp 95–148
413. Rao PS, Tarwade SJ, Sarma KSR (1980) Seaweed as a source of energy: I. Effect of a specific bacterial strain on biogas production. Bot Mar 23:599–601
414. Karakashev D, Batstone DJ, Angelidaki I (2005) Influence of environmental conditions on methanogenic compositions in anaerobic biogas reactors. Appl Environ Microbiol 71(1):331–338. doi:71/1/331[pii] 10.1128/AEM.71.1.331-338.2005
415. Cardayré SB (2005) Developments in strain improvement technology. In: Zhang L, Demain AL (eds) Natural products. Humana, Totowa, pp 107–125. doi:10.1007/978-1-59259-976-9_6
416. Yang S-T, Liu X, Zhang Y (2007) Metabolic engineering—applications, methods, and challenges. In: Shang-Tian Y (ed) Bioprocessing for value-added products from renewable resources. Elsevier, Amsterdam, pp 73–118

417. Causey TB, Shanmugam KT, Yomano LP, Ingram LO (2004) Engineering *Escherichia coli* for efficient conversion of glucose to pyruvate. Proc Natl Acad Sci U S A 101(8):2235–2240. doi:10.1073/pnas.0308171100
418. Ingram LO, Conway T, Clark DP, Sewell GW, Preston JF (1987) Genetic engineering of ethanol production in *Escherichia coli*. Appl Environ Microbiol 53(10):2420–2425
419. Kalscheuer R, Stolting T, Steinbuchel A (2006) Microdiesel: *Escherichia coli* engineered for fuel production. Microbiology 152(9):2529–2536. doi:10.1099/mic.0.29028-0
420. Ohta K, Beall DS, Mejia JP, Shanmugam KT, Ingram LO (1991) Genetic improvement of *Escherichia coli* for ethanol production: chromosomal integration of *Zymomonas mobilis* genes encoding pyruvate decarboxylase and alcohol dehydrogenase II. Appl Environ Microbiol 57(4):893–900
421. Davis L, Jeon Y-J, Svenson C, Rogers P, Pearce J, Peiris P (2005) Evaluation of wheat stillage for ethanol production by recombinant *Zymomonas mobilis*. Biomass Bioenergy 29(1): 49–59
422. JaeJeon Y, Svenson CJ, Rogers PL (2005) Over-expression of xylulokinase in a xylose-metabolising recombinant strain of *Zymomonas mobilis*. FEMS Microbiol Lett 244(1): 85–92
423. Sprenger GA (1996) Carbohydrate metabolism in *Zymomonas mobilis*: a catabolic highway with some scenic routes. FEMS Microbiol Lett 145(3):301–307. doi:10.1111/j.1574-6968.1996.tb08593.x
424. Cheng K-K, Liu Q, Zhang J-A, Li J-P, Xu J-M, Wang G-H (2010) Improved 2,3-butanediol production from corncob acid hydrolysate by fed-batch fermentation using *Klebsiella oxytoca*. Process Biochem 45(4):613–616
425. Golias H, Dumsday GJ, Stanley GA, Pamment NB (2002) Evaluation of a recombinant *Klebsiella oxytoca* strain for ethanol production from cellulose by simultaneous saccharification and fermentation: comparison with native cellobiose-utilising yeast strains and performance in co-culture with thermotolerant yeast and *Zymomonas mobilis*. J Biotechnol 96(2):155–168
426. Chu BCH, Lee H (2007) Genetic improvement of *Saccharomyces cerevisiae* for xylose fermentation. Biotechnol Adv 25(5):425–441
427. Jeffries T, Shi N-Q (1999) Genetic engineering for improved xylose fermentation by yeasts. In: Tsao G, Brainard A, Bungay H et al (eds) Recent progress in bioconversion of lignocellulosics, vol 65, Advances in biochemical engineering/biotechnology. Springer, Berlin, pp 117–161
428. Kuyper M, Hartog MMP, Toirkens MJ, Almering MJH, Winkler AA, van Dijken JP, Pronk JT (2005) Metabolic engineering of a xylose-isomerase-expressing *Saccharomyces cerevisiae* strain for rapid anaerobic xylose fermentation. FEMS Yeast Res 5(4–5):399–409. doi:10.1016/j.femsyr.2004.09.010
429. Kuyper M, Winkler AA, van Dijken JP, Pronk JT (2004) Minimal metabolic engineering of *Saccharomyces cerevisiae* for efficient anaerobic xylose fermentation: a proof of principle. FEMS Yeast Res 4(6):655–664. doi:10.1016/j.femsyr.2004.01.003
430. Guedon E, Desvaux M, Petitdemange H (2002) Improvement of cellulolytic properties of *Clostridium cellulolyticum* by metabolic engineering. Appl Environ Microbiol 68(1):53–58. doi:10.1128/aem.68.1.53-58.2002
431. Ekborg NA, Gonzalez JM, Howard MB, Taylor LE, Hutcheson SW, Weiner RM (2005) *Saccharophagus degradans* gen. nov., sp. nov., a versatile marine degrader of complex polysaccharides. Int J Syst Evol Microbiol 55(4):1545–1549. doi:10.1099/ijs.0.63627-0
432. Taylor LE II, Henrissat B, Coutinho PM, Ekborg NA, Hutcheson SW, Weiner RM (2006) Complete cellulase system in the marine bacterium *Saccharophagus degradans* strain 2-40T. J Bacteriol 188(11):3849–3861. doi:10.1128/jb.01348-05
433. Ryan C (2009) Cultivating clean energy: the promise of algae biofuels. Natural Resources Defense Council, New York
434. Chisti Y (2008) Biodiesel from microalgae beats bioethanol. Trends Biotechnol 26(3): 126–131

435. Harun R, Davidson M, Doyle M, Gopiraj R, Danquah M, Forde G (2011) Technoeconomic analysis of an integrated microalgae photobioreactor, biodiesel and biogas production facility. Biomass Bioenergy 35(1):741–747
436. Ehimen EA, Sun ZF, Carrington CG, Birch EJ, Eaton-Rye JJ (2010) Anaerobic digestion of microalgae residues resulting from the biodiesel production process. Appl Energy 88(10):3454–3563
437. Ehimen EA, Connaughton S, Sun Z, Carrington GC (2009) Energy recovery from lipid extracted, transesterified and glycerol codigested microalgae biomass. Glob Change Biol Bioenergy 1(6):371–381. doi:10.1111/j.1757-1707.2009.01029.x
438. Gaffron H (1939) Reduction of CO_2 with H_2 in green plants. Nature 143:204–205
439. Gaffron H, Rubin J (1942) Fermentative and photochemical production of hydrogen in algae. J Gen Physiol 26(2):219–240. doi:10.1085/jgp. 26.2.219
440. Abraham S (2002) Towards a more secure and cleaner energy future for America: national hydrogen energy roadmap; production, delivery, storage, conversion, applications, public education and outreach. U.S. Department of Energy, Washington, DC
441. Beer LL, Boyd ES, Peters JW, Posewitz MC (2009) Engineering algae for biohydrogen and biofuel production. Curr Opin Biotechnol 20(3):264–271
442. Nguyen AV, Thomas-Hall SR, Malnoe A, Timmins M, Mussgnug JH, Rupprecht J, Kruse O, Hankamer B, Schenk PM (2008) Transcriptome for photobiological hydrogen production induced by sulfur deprivation in the green alga *Chlamydomonas reinhardtii*. Eukaryot Cell 7(11):1965–1979. doi:10.1128/ec.00418-07
443. Timmins M, Zhou W, Rupprecht J, Lim L, Thomas-Hall SR, Doebbe A, Kruse O, Hankamer B, Marx UC, Smith SM, Schenk PM (2009) The metabolome of *Chlamydomonas reinhardtii* following induction of anaerobic H_2 production by sulfur depletion. J Biol Chem 284(51):35996. doi:10.1074/jbc.A109.003541
444. Doebbe A, Keck M, La Russa M, Mussgnug JH, Hankamer B, Tekce E, Niehaus K, Kruse O (2010) The interplay of proton, electron and metabolite supply for photosynthetic H_2 production in *C. reinhardtii*. J Biol Chem. doi:10.1074/jbc.M110.122812
445. Chiao M, Lam KB, Lin L (2006) Micromachined microbial and photosynthetic fuel cells. J Micromech Microeng 16(12):2547
446. He Z, Kan J, Mansfeld F, Angenent LT, Nealson KH (2009) Self-sustained phototrophic microbial fuel cells based on the synergistic cooperation between photosynthetic microorganisms and heterotrophic bacteria. Environ Sci Technol 43(5):1648–1654. doi:10.1021/es803084a
447. Rosenbaum M, He Z, Angenent LT (2010) Light energy to bioelectricity: photosynthetic microbial fuel cells. Curr Opin Biotechnol 21(3):259–264
448. Strik D, Terlouw H, Hamelers H, Buisman C (2008) Renewable sustainable biocatalyzed electricity production in a photosynthetic algal microbial fuel cell (PAMFC). Appl Microbiol Biotechnol 81(4):659–668. doi:10.1007/s00253-008-1679-8
449. Yang J, Xu M, Zhang X, Hu Q, Sommerfeld M, Chen Y (2011) Life-cycle analysis on biodiesel production from microalgae: water footprint and nutrients balance. Bioresour Technol 102(1):159–165. doi:10.1016/j.biortech.2010.07.017
450. Kayombo S, Mbwette TS, Katima JH, Jorgensen SE (2003) Effects of substrate concentrations on the growth of heterotrophic bacteria and algae in secondary facultative ponds. Water Res 37(12):2937–2943. doi:S0043-1354(03)00014-9[pii]10.1016/S0043-1354(03)00014-9
451. Craggs RJ, McAuley PJ, Smith VJ (1997) Wastewater nutrient removal by marine microalgae grown on a corrugated raceway. Water Res 31(7):1701–1707
452. Hashimoto S, Furukawa K (1989) Nutrient removal from secondary effluent by filamentous algae. J Ferment Bioeng 67(1):62–69
453. Mallick N (2002) Biotechnological potential of immobilized algae for wastewater N, P and metal removal: a review. Biometals 15(4):377–390. doi:10.1023/a:1020238520948
454. Nurdogan Y, Oswald WJ (1995) Enhanced nutrient removal in high-rate ponds. Water Sci Technol 31(12):33–43
455. Tam NFY, Wong YS (1989) Wastewater nutrient removal by *Chlorella pyrenoidosa* and *Scenedesmus* sp. Environ Pollut 58(1):19–34

456. Travieso L, Benitez F, Weiland P, Sanchez E, Dupeyrun R, Dominguez AR (1996) Experiments on immobilization of microalgae for nutrient removal in wastewater treatments. Bioresour Technol 55(3):181–186
457. Holan ZR, Volesky B (1994) Biosorption of lead and nickel by biomass of marine algae. Biotechnol Bioeng 43(11):1001–1009. doi:10.1002/bit.260431102
458. Leusch A, Holan ZR, Volesky B (1995) Biosorption of heavy metals (Cd, Cu, Ni, Pb, Zn) by chemically-reinforced biomass of marine algae. J Chem Technol Biotechnol 62(3):279–288. doi:10.1002/jctb.280620311
459. Tien CJ (2002) Biosorption of metal ions by freshwater algae with different surface characteristics. Process Biochem 38(4):605–613
460. Kivaisi AK (2001) The potential for constructed wetlands for wastewater treatment and reuse in developing countries: a review. Ecol Eng 16(4):545–560
461. Mara DD, Mills SW, Pearson HW, Alabaster GP (1992) Waste stabilization ponds: a viable alternative for small community treatment systems. Water Environ J 6(3):72–78. doi:10.1111/j.1747-6593.1992.tb00740.x
462. Golueke CG, Oswald WJ (1968) Power from solar energy via algae-produced methane. Solar Energy 7(3):86–92
463. Oswald WJ, Golueke CG (1960) Biological transformation of solar energy. In: Wayne WU (ed) Advances in applied microbiology, vol 2. Academic, New York, pp 223–262
464. Douskov I, Kastnek F, Maleterov Y, Kastnek P, Doucha J, Zachleder V (2010) Utilization of distillery stillage for energy generation and concurrent production of valuable microalgal biomass in the sequence: biogas-cogeneration-microalgae-products. Energy Conversion Manag 51(3):606–611
465. Kumar MS, Miao ZH, Wyatt SK (2010) Influence of nutrient loads, feeding frequency and inoculum source on growth of *Chlorella vulgaris* in digested piggery effluent culture medium. Bioresour Technol 101(15):6012–6018
466. Wang L, Li Y, Chen P, Min M, Chen Y, Zhu J, Ruan RR (2010) Anaerobic digested dairy manure as a nutrient supplement for cultivation of oil-rich green microalgae *Chlorella* sp. Bioresour Technol 101(8):2623–2628
467. Ward AJ, Kumar MS (2010) Bio-conversion rate and optimum harvest intervals for *Moina australiensis* using digested piggery effluent and *Chlorella vulgaris* as a food source. Bioresour Technol 101(7):2210–2216
468. Clarens AF, Resurreccion EP, White MA, Colosi LM (2010) Environmental life cycle comparison of algae to other bioenergy feedstocks. Environ Sci Technol 44(5):1813–1819. doi:10.1021/es902838n
469. Banat I, Puskas K, Esen I, Al-Daher R (1990) Wastewater treatment and algal productivity in an integrated ponding system. Biol Wastes 32(4):265–275
470. Al-Shayji YA, Puskas K, Al-Daher R, Esen II (1994) Production and separation of algae in a high-rate ponds system. Environ Int 20(4):541–550
471. Green FB, Bernstone L, Lundquist TJ, Muir J, Tresan RB, Oswald WJ (1995) Methane fermentation, submerged gas collection, and the fate of carbon in advanced integrated wastewater pond systems. Water Sci Technol 31(12):55–65
472. Green FB, Bernstone LS, Lundquist TJ, Oswald WJ (1996) Advanced integrated wastewater pond systems for nitrogen removal. Water Sci Technol 33(7):207–217
473. Oswald W, Green F, Lundquist T (1994) Performance of methane fermentation pits in advanced integrated wastewater pond systems. Water Sci Technol 30(12):287–295
474. Oswald WJ (1990) Advanced integrated wastewater pond systems. In: ASCE Convention EE Div/ASCE, San Francisco, CA, 5–8 Nov 1990
475. Oswald WJ (1995) Ponds in the twenty-first century. Water Sci Technol 31(12):1–8
476. Green FB, Lundquist TJ, Oswald WJ (1995) Energetics of advanced integrated wastewater pond systems. Water Sci Technol 31(12):9–20
477. Oswald WJ (2003) My sixty years in applied algology. J Appl Phycol 15(2):99–106. doi:10.1023/a:1023871903434

478. Wahal S (2010) Nutrient utilization from anaerobic digester effluent through algae cultivation. Utah State University, Logan
479. Woertz IC (2007) Lipid productivity of algae grown on dairy wastewater as a possible feedstock for biodiesel. California Polytechnic University, San Luis Obispo
480. Lincoln EP, Wilkie AC, French BT (1996) Cyanobacterial process for renovating dairy wastewater. Biomass Bioenergy 10(1):63–68
481. Aragon AB, Ros F, de Ursinos JA, Padilla RB (1992) Algal cultures with effluents from biological treatment of urban wastewaters by anaerobiosis. Resour Conserv Recycling 6(4):303–314
482. Ras M, Lardon L, Bruno S, Bernet N, Steyer J-P (2011) Experimental study on a coupled process of production and anaerobic digestion of *Chlorella vulgaris*. Bioresour Technol 102(1):200–206
483. Ryther JH (1982) Cultivation of macroscopic marine algae. University of Florida, Gainesville
484. Olaizola M, Bridges T, Flores S, Griswold L, Morency J, Nakamura T (2004) Microalgal removal of CO_2 from flue gases: CO_2 capture from a coal combustor. Proceedings of the third annual conference on carbon capture & sequestration, Alexandria, VA
485. Jorquera O, Kiperstok A, Sales EA, Embirucu M, Ghirardi ML (2010) Comparative energy life-cycle analyses of microalgal biomass production in open ponds and photobioreactors. Bioresour Technol 101(4):1406–1413
486. Huesemann MH, Benemann JR (2009) Biofuels from microalgae: review of products, processes and potential, with special focus on *Dunaliella* sp. In: Ben-Amotz A, Polle JEW, Subba Rao DV (eds) The alga *Dunaliella*: biodiversity, physiology, genomics, and biotechnology, vol 14. Science Publishers, New Hampshire, pp 445–474
487. Stephenson AL, Kazamia E, Dennis JS, Howe CJ, Scott SA, Smith AG (2010) Life-cycle assessment of potential algal biodiesel production in the United Kingdom: a comparison of raceways and air-lift tubular bioreactors. Energy Fuel 24(7):4062–4077. doi:10.1021/ef1003123
488. Razon LF, Tan RR (2010) Net energy analysis of the production of biodiesel and biogas from the microalgae: *Haematococcus pluvialis* and *Nannochloropsis*. Applied Energy 88(10):3507–3514
489. Lardon L, HeÃÅlias A, Sialve B, Steyer J-P, Bernard O (2009) Life-cycle assessment of biodiesel production from microalgae. Environ Sci Technol 43(17):6475–6481. doi:10.1021/es900705j
490. Collet P, Hèlias A, Lardon L, Ras M, Goy R-A, Steyer J-P (2011) Life-cycle assessment of microalgae culture coupled to biogas production. Bioresour Technol 102(1):207–214
491. Zamalloa C, Vulsteke E, Albrecht J, Verstraete W (2011) The techno-economic potential of renewable energy through the anaerobic digestion of microalgae. Bioresour Technol 102(2):1149–1158
492. Allen MM (1984) Cyanobacterial cell inclusions. Annu Rev Microbiol 38:1–25
493. Kromkamp J (1987) Formation and functional significance of storage products in cyanobacteria. N Z J Mar Freshw Res 21(3):457–465. doi:10.1080/00288330.1987.9516241
494. Lockau W, Ziegler K (2006) Cyanophycin inclusions: biothynthesis and applications. In: Rehm B (ed) Microbial bionanotechnology: biological self-assembly systems and biopolymer-based nanostructures. Horizon bioscience. Wymondham, England, pp 79–107
495. Shively JM (1974) Inclusion bodies of prokaryotes. Annu Rev Microbiol 28:167–187. doi:10.1146/annurev.mi.28.100174.001123
496. Stal L (1992) Poly(hydroxyalkanoate) in cyanobacteria: an overview. FEMS Microbiol Lett 103(2–4):169–180. doi:10.1016/0378-1097(92)90307-a
497. Bertocchi C (1990) Polysaccharides from cyanobacteria. Carbohydr Polym 12(2):127–153. doi:10.1016/0144-8617(90)90015-k
498. Dunn JH, Wolk CP (1970) Composition of the cellular envelopes of *Anabaena cylindrica*. J Bacteriol 103(1):153–158
499. Hoiczyk E, Baumeister W (1995) Envelope structure of four gliding filamentous cyanobacteria. J Bacteriol 177(9):2387–2395

500. Hoiczyk E, Hansel A (2000) Cyanobacterial cell walls: news from an unusual prokaryotic envelope. J Bacteriol 182(5):1191–1199
501. Jurgens UJ, Drews G, Weckesser J (1983) Primary structure of the peptidoglycan from the unicellular cyanobacterium *Synechocystis* sp. strain PCC 6714. J Bacteriol 154(1):471–478
502. Jurgens UJ, Weckesser J (1986) Polysaccharide covalently linked to the peptidoglycan of the cyanobacterium *Synechocystis* sp. strain PCC6714. J Bacteriol 168(2):568–573
503. Pritzer M, Weckesser J, Jürgens UJ (1989) Sheath and outer membrane components from the cyanobacterium *Fischerella* sp. PCC 7414. Arch Microbiol 153(1):7–11. doi:10.1007/bf00277533
504. Schneider S, Jürgens UJ (1991) Cell wall and sheath constituents of the cyanobacterium *Gloeobacter violaceus*. Arch Microbiol 156(4):312–318. doi:10.1007/bf00263004
505. de Oliveira MACL, Monteiro MPC, Robbs PG, Leite SGF (1999) Growth and chemical composition of *Spirulina maxima* and *Spirulina platensis* biomass at different temperatures. Aquaculture Int 7(4):261–275. doi:10.1023/a:1009233230706
506. Milner HW (1976) The chemical composition of algae. In: Burlew JS (ed) Algae culture: from laboratory to pilot plant. Carnegir Institution of Washington Publication, Washington, DC, pp 285–303
507. Gribovskaya I, Kalacheva G, Bayanova Y, Kolmakova A (2009) Physiology-biochemical properties of the cyanobacterium *Oscillatoria deflexa*. Appl Biochem Microbiol 45(3):285–290. doi:10.1134/s0003683809030089
508. Carlozzi P (2000) Hydrodynamic aspects and *Arthrospira* growth in two outdoor tubular undulating row photobioreactors. Appl Microbiol Biotechnol 54(1):14–22. doi:10.1007/s002530000355
509. Carlozzi P (2003) Dilution of solar radiation through "culture" lamination in photobioreactor rows facing south–north: a way to improve the efficiency of light utilization by cyanobacteria (*Arthrospira platensis*). Biotechnol Bioeng 81(3):305–315. doi:10.1002/bit.10478
510. Gouveia L, Oliveira A (2009) Microalgae as a raw material for biofuels production. J Ind Microbiol Biotechnol 36(2):269–274. doi:10.1007/s10295-008-0495-6
511. Craigie JS (1974) Storage products. In: Stewart WDP (ed) Algal physiology and biochemistry. Botanical monographs, vol 10. University of California Press, Berkeley, pp 206–235
512. Dixon PS (1973) Biology of the Rhodophyta (University reviews in botany, 4). Hafner Press, New York
513. Karsten U, West JA, Zuccarello GC, Engbrodt R, Yokoyama A, Hara Y, Brodie J (2003) Low molecular weight carbohydrates of the Bangiophycidae (Rhodophyta). J Phycol 39(3):584–589. doi:10.1046/j.1529-8817.2003.02192.x
514. Lee RE (1974) Chloroplast structure and starch grain production as phylogenetic indicators in the lower Rhodophyceae. Br Phycol J 9(3):291–295
515. Meeuse BJD (1962) Storage products. In: Lewin RA (ed) Physiology and biochemistry of algae. Academic, New York, pp 289–313
516. Brody M, Vatter AE (1959) Observations on cellular structures of *Porphyridium cruentum*. J Biophys Biochem Cytol 5(2):289–294
517. Gantt E, Conti SF (1965) The ultrastructure of *Porphyridium cruentum*. J Cell Biol 26(2):365–381
518. Arad SM, Levy-Ontman O (2010) Red microalgal cell-wall polysaccharides: biotechnological aspects. Curr Opin Biotechnol 21(3):358–364. doi:S0958-1669(10)00024-8[pii]10.1016/j.copbio.2010.02.008
519. Gretz MR, Aronson JM, Sommerfeld MR (1980) Cellulose in the cell walls of the bangiophyceae (Rhodophyta). Science 207(4432):779–781. doi:207/4432/779[pii]10.1126/science.207.4432.779
520. Siegel BZ, Siegel SM (1973) The chemical composition of algal cell walls. CRC Crit Rev Microbiol 3(1):1–26
521. O'Colla PS (1962) Mucilages. In: Lewin RA (ed) Physiology and biochemistry of algae. Academic, New York, pp 337–356
522. Rubio FC, Fernández FGA, Pérez JAS, Camacho FG, Grima EM (1999) Prediction of dissolved oxygen and carbon dioxide concentration profiles in tubular photobioreactors

for microalgal culture. Biotechnol Bioeng 62(1):71–86. doi:10.1002/(sici)1097-0290(19990105)62:1<71::aid-bit9>3.0.co;2-t
523. Ugarte R, Santelices B (1992) Experimental tank cultivation of *Gracilaria chilensis* in central Chile. Aquaculture 101(1–2):7–16
524. Pickering TD, Gordon ME, Tong LJ (1995) A preliminary trial of a spray culture technique for growing the agarophyte *Gracilaria chilensis* (Gracilariales, Rhodophyta). Aquaculture 130(1):43–49
525. Lapointe BE, Ryther JH (1978) Some aspects of the growth and yield of *Gracilaria tikvahiae* in culture. Aquaculture 15(3):185–193
526. Hanisak DM, Ryther JH (1984) Cultivation biology of *Gracilaria tikvahiae* in the United States. Hydrobiologia 116–117(1):295–298. doi:10.1007/bf00027688
527. Hanisak MD (1987) Cultivation of *Gracilaria* and other macroalgae in Florida for energy production. In: Bird KT, Benson PH (eds) Seaweed cultivation for renewable resources. Elsevier Science, Amsterdam, pp 191–218
528. Chiang YM (1981) Cultivation of *Gracilaria* (Rhodophycophyta, Gigartinales) in Taiwan. In: Levring T (ed) Tenth international seaweed symposium. Walter de Gruyter, Berlin, pp 569–574
529. Vadas RL, Beal BF, Wright WA, Emerson S, Nickl S (2004) Biomass and productivity of red and green algae in Cobscook Bay, Maine. Northeast Nat 11(sp2):163–196. doi:10.1656/1092-6194(2004) 11[163:bapora]2.0.co;2
530. Waaland JR (1976) Growth of the red alga *Iridaea cordata* (Turner) Bory in semi-closed culture. J Exp Mar Biol Ecol 23(1):45–53
531. Tompkins AN (1981) Marine biomass program. Annual report for 1980. General Electric Company, Philadelphia
532. Fuentes MM, Fernandez GG, Pèrez JA, Guerrero JL (2000) Biomass nutrient profiles of the microalga *Porphyridium cruentum*. Food Chem 70(3):345–353
533. Ball SG, Morell MK (2003) From bacterial glycogen to starch: understanding the biogenesis of the plant starch granule. Annu Rev Plant Biol 54:207–233. doi:10.1146/annurev.arplant.54.031902.134927
534. Dunstan GA, Volkman JK, Jeffrey SW, Barrett SM (1992) Biochemical composition of microalgae from the green algal classes Chlorophyceae and Prasinophyceae. 2. Lipid classes and fatty acids. J Exp Mar Biol Ecol 161(1):115–134. doi:10.1016/0022-0981(92)90193-e
535. Eixler S, Karsten U, Selig U (2006) Phosphorus storage in *Chlorella vulgaris* (Trebouxiophyceae, Chlorophyta) cells and its dependence on phosphate supply. Phycologia 45(1):53–60. doi:10.2216/04-79.1
536. Griffiths M, Harrison S (2009) Lipid productivity as a key characteristic for choosing algal species for biodiesel production. J Appl Phycol 21(5):493–507. doi:10.1007/s10811-008-9392-7
537. Huang Y, Beal C, Cai W, Ruoff R, Terentjev E (2010) Micro-Raman spectroscopy of algae: composition analysis and fluorescence background behavior. Biotechnol Bioeng 105(5):889–898. doi:10.1002/bit.22617
538. Libessart N, Maddelein ML, Koornhuyse N, Decq A, Delrue B, Mouille G, D'Hulst C, Ball S (1995) Storage, photosynthesis, and growth: the conditional nature of mutations affecting starch synthesis and structure in *Chlamydomonas*. Plant Cell 7(8):1117–1127. doi:10.1105/tpc.7.8.11177/8/1117[pii]
539. Metzger P, Largeau C (2005) *Botryococcus braunii* a rich source for hydrocarbons and related ether lipids. Appl Microbiol Biotechnol 66(5):486–496. doi:10.1007/s00253-004-1779-z
540. Wang ZT, Ullrich N, Joo S, Waffenschmidt S, Goodenough U (2009) Algal lipid bodies: stress induction, purification, and biochemical characterization in wild-type and starchless *Chlamydomonas reinhardtii*. Eukaryot Cell 8(12):1856–1868. doi:EC.00272-09[pii]10.1128/EC.00272-09
541. Adair WS, Steinmetz SA, Mattson DM, Goodenough UW, Heuser JE (1987) Nucleated assembly of *Chlamydomonas* and *Volvox* cell walls. J Cell Biol 105(5):2373–2382
542. Becker B, Perasso L, Kammann A, Salzburg M, Melkonian M (1996) Scale-associated glycoproteins of *Scherffelia dubia* (Chlorophyta) form high-molecular-weight complexes between the scale layers and the flagellar membrane. Planta 199(4):503–510. doi:10.1007/bf00195179

543. Dodge JD (1973) The fine structure of algal cells. Academic, London
544. Frei EVA, Preston RD (1961) Variants in the structural polysaccharides of algal cell walls. Nature 192(4806):939–943. doi:10.1038/192939a0
545. Huizing HJ, Rietema H (1975) Xylan and mannan as cell wall constituents of different stages in the life-histories of some siphoneous green algae. Br Phycol J 10(1):13–16
546. Huizing HJ, Rietema H, Sietsma JH (1979) Cell wall constituents of several siphoneous green algae in relation to morphology and taxonomy. Br Phycol J 14(1):25–32
547. Mackie I, Percival E (1959) The constitution of xylan from the green seaweed *Caulerpa filiformis*. J Chem Soc 30:10–15
548. Mackie W, Preston RD (1974) Cell wall and intercellular region polysaccharides. In: Stewart WDP (ed) Algal physiology and biochemistry, vol 10, Botanical monographs. University of California Press, Berkeley, pp 40–85
549. Lobban CS, Harrison PJ (1994) Seaweed ecology and physiology. Cambridge University Press, Cambridge
550. Ugwu C, Ogbonna J, Tanaka H (2002) Improvement of mass transfer characteristics and productivities of inclined tubular photobioreactors by installation of internal static mixers. Appl Microbiol Biotechnol 58(5):600–607. doi:10.1007/s00253-002-0940-9
551. Morita M, Watanabe Y, Okawa T, Saiki H (2001) Photosynthetic productivity of conical helical tubular photobioreactors incorporating *Chlorella* sp. under various culture medium flow conditions. Biotechnol Bioeng 74(2):136–144. doi:10.1002/bit.1103
552. Doucha J, Straka F, Lívansky K (2005) Utilization of flue gas for cultivation of microalgae *Chlorella* sp. in an outdoor open thin-layer photobioreactor. J Appl Phycol 17(5):403–412. doi:10.1007/s10811-005-8701-7
553. Doucha J, Lívansky K (2009) Outdoor open thin-layer microalgal photobioreactor: potential productivity. J Appl Phycol 21(1):111–117. doi:10.1007/s10811-008-9336-2
554. Pruvost J, Van Vooren G, Le Gouic B, Couzinet-Mossion A, Legrand J (2011) Systematic investigation of biomass and lipid productivity by microalgae in photobioreactors for biodiesel application. Bioresour Technol 102(1):150–158
555. Olaizola M (2000) Commercial production of astaxanthin from *Haematococcus pluvialis* using 25,000-liter outdoor photobioreactors. J Appl Phycol 12(3):499–506. doi:10.1023/a:1008159127672
556. Huntley M, Redalje D (2007) CO_2 mitigation and renewable oil from photosynthetic microbes: a new appraisal. Mitig Adapt Strat Glob Chang 12(4):573–608. doi:10.1007/s11027-006-7304-1
557. Kanazawa T, Fujita C, Yuhara T, Sasa T (1958) Mass culture of unicellular algae using the "open circulation method". J Gen Appl Microbiol 4(3):135–152
558. Beck LA, Oswald WJ, Goldman JC (1969) Nitrate removal from agricultural tile drainage by photosynthetic systems. Paper presented at the second national symposium on sanitary engineering research, development and design, Cornell University, Ithaca, 15 July 1969
559. Chini Zittelli G, Rodolfi L, Biondi N, Tredici MR (2006) Productivity and photosynthetic efficiency of outdoor cultures of *Tetraselmis suecica* in annular columns. Aquaculture 261(3):932–943
560. Pruvost J, Van Vooren G, Cogne G, Legrand J (2009) Investigation of biomass and lipids production with *Neochloris oleoabundans* in photobioreactor. Bioresour Technol 100(23):5988–5995
561. Sato T, Usui S, Tsuchiya Y, Kondo Y (2006) Invention of outdoor closed type photobioreactor for microalgae. Energy Conversion Manag 47(6):791–799
562. DeBusk TA, Blakeslee M, Ryther JH (1986) Studies on the outdoor cultivation of *Ulva lactuca* L. Bot Mar 29(5):381–386. doi:10.1515/botm.1986.29.5.381
563. Baloni WG, Florenzano A, Materassi R, Tredici M, Soeder CJ, Wagner K (1982) Mass culture of algae for energy farming in coastal deserts. In: Sturb A, Chartier P, Scheleser G (eds) Energy from biomass. Second E.C. conference, Berlin, 20–23 September 1982. Elsevier Applied Science, London, pp 291–294

564. Ryther JH, Hanisak MD (1981) Biomass production, anaerobic digestion, and nutrient recycling of small benthic or floating seaweeds. Paper presented at the Energy from Biomass and Wastes V, Lake Buena Vista, Florida, 26–30 Jan 1981
565. Lehnberg W, Schramm W (1984) Mass culture of brackish-water-adapted seaweeds in sewage-enriched seawater I. Productivity and nutrient accumulation. Hydrobiologia 116–117(1):276–281. doi:10.1007/bf00027684
566. Brown MR (1991) The amino-acid and sugar composition of 16 species of microalgae used in mariculture. J Exp Mar Biol Ecol 145(1):79–99
567. Brown MR, Jeffrey SW (1992) Biochemical composition of microalgae from the green algal classes Chlorophyceae and Prasinophyceae. 1. Amino acids, sugars and pigments. J Exp Mar Biol Ecol 161(1):91–113
568. Beattie A, Hirst EL, Percival E (1961) Studies on the metabolism of the Chrysophyceae. Comparative structural investigations on leucosin (chrysolaminarin) separated from diatoms and laminarin from the brown algae. Biochem J 79:531–537
569. Tonon T, Harvey D, Larson TR, Graham IA (2002) Long chain polyunsaturated fatty acid production and partitioning to triacylglycerols in four microalgae. Phytochemistry 61(1):15–24. doi:S0031942202002017[pii]
570. Shifrin NS (1985) Oils from microalgae. In: Ratledge C, Dawson P, Rattray J (eds) Biotechnology for the oils and fats industry. AOCS monograph, vol 11. American Oil Chemists' Society, Illinois, pp 145–162
571. Volkman JK, Jeffrey SW, Nichols PD, Rogers GI, Garland CD (1989) Fatty acid and lipid composition of 10 species of microalgae used in mariculture. J Exp Mar Biol Ecol 128(3):219–240. doi:10.1016/0022-0981(89)90029-4
572. Ben-Amotz A, Tornabene TG, Thomas WH (2004) Chemical profile of selected species of microalgae with emphasis on lipids. J Phycol 21(1):72–81. doi:10.1111/j.0022-3646.1985.00072.x
573. Opute FI (1974) Lipid and fatty-acid composition of Diatoms. J Exp Bot 25(4):823–835
574. Herth W, Zugenmaier P (1977) Ultrastructure of the chitin fibrils of the centric diatom *Cyclotella cryptica*. J Ultrastruct Res 61(2):230–239. doi:10.1016/s0022-5320(77)80090-7
575. Herth W, Zugenmaier P (1979) The lorica of Dinobryon. J Ultrastruct Res 69(2):262–272. doi:10.1016/s0022-5320(79)90115-1
576. Kristiansen J (1972) Studies on the lorica structure in Chrysophyceae. Svensk Botanisk Tidskrift 66(3):184–190
577. Nicolai E, Preston RD (1952) Cell-wall studies in the Chlorophyceae. I. A general survey of submicroscopic structure in filamentous species. Proc R Soc Lond B Biol Sci 140(899):244–274
578. Okuda K (2002) Structure and phylogeny of cell coverings. J Plant Res 115(4):283–288. doi:10.1007/s10265-002-0034-x
579. Belcher JH (1969) A morphological study of the phytoflagellate *Chrysococcus Rufescens Klebs* in culture. Br Phycol J 4(1):105–117
580. Belcher JH (1974) *Chrysophaera magna* sp. nov., a new coccoid member of the Chrysophyceae. Br Phycol J 9(2):139–144
581. Hibberd DJ (1986) Ultrastructure of the Chrysophyceae—phylogetic implications and taxonomy. In: Kristiansen J, Andersen RA (eds) Chrysophytes: aspects and problems. Cambridge University Press, Cambridge, pp 23–37
582. Cheng-Wu Z, Zmora O, Kopel R, Richmond A (2001) An industrial-size flat plate glass reactor for mass production of *Nannochloropsis* sp. (Eustigmatophyceae). Aquaculture 195(1–2):35–49
583. Acien Fernandez FG, Fernandez Sevilla JM, Sanchez Perez JA, Molina Grima E, Chisti Y (2001) Airlift-driven external-loop tubular photobioreactors for outdoor production of microalgae: assessment of design and performance. Chem Eng Sci 56(8):2721–2732
584. Molina E, Fernandez J, Acièn FG, Chisti Y (2001) Tubular photobioreactor design for algal cultures. J Biotechnol 92(2):113–131

585. Acien Fernandez FG, Hall DO, Canizares Guerrero E, Krishna Rao K, Molina Grima E (2003) Outdoor production of *Phaeodactylum tricornutum* biomass in a helical reactor. J Biotechnol 103(2):137–152
586. Vadas RL Sr, Wright WA, Beal BF (2004) Biomass and productivity of intertidal rockweeds (*Ascophyllum nodosum* LeJolis) in Cobscook Bay. Northeast Nat 11:123–142
587. Lignell A, Pedersen M (1986) Spray cultivation of seaweeds with emphasis on their light requirements. Bot Mar 29(6):509–516. doi:10.1515/botm.1986.29.6.509
588. Kelly MS, Dworjanyn S (2008) The potential of marine biomass for anaerobic biogas production: a feasibility study with recommendations for further research. The Crown Estate, Oban, Argyll
589. Lapointe BE, Hanisak MD (1985) Productivity and nutrition of marine biomass systems in Florida. In: Energy from biomass and waste IX, Lake Buena Vista, Florida. Institute of Gas Technology, Chicago, pp 111–126
590. Leese T (1976) The conversion of ocean farm kelp to methane and other products. In: Clean fuels from biomass, sewage, urban refuse, and agricultural wastes. Institute of Gas Technology, Orlando, FL, pp 253–266
591. Chynoweth DP, Fannin KF, Srivastava VJ (1987) Biological gasification of marine algae. In: Bird KT, Benson PH (eds) Seaweed cultivation for renewable resources. Developments in aquaculture and fisheries science, vol 16. Elsevier, Amsterdam, pp 285–303
592. Horn SJ (2000) Bioenergy from brown seaweeds. Doctorate, Norwegian University of Science and Technology, Trondheim
593. Reith J, Deurwaarder E, Hemmes K, Curvers A, Kamermans P, Brandenburg W, Zeeman G (2005) Bio-offshore: grootschalige teelt van zeewieren in combinatie met offshore windparken in de Noordzee. ECN, Energy Research Centre of the Netherlands, The Netherlands
594. Uziel M (1978) Solar energy fixation and conversion with algal bacterial systems. PhD thesis, University of California, Berkeley
595. Archipretre M (1981) Culture et utilisation d'algues marines: etude de methanisation. Memoire de Diplome d'Etudes Approfondies: Amélioration et transformation des productions vegetales et microbiennes. University of Science and Technology Lille, France, p 52
596. Wise DL, Augenstein DC, Ryther JH (1979) Methane fermentation of aquatic biomass. Resour Recover Conserv 4(3):217–237
597. Amon T, Kryvoruchko V, Bodiroza V, Machmuller A, Amon B (2007) Methane yield and biogas quality of *Aegina Karnagio Kolona* (seaweed). Methods (2007) Issue: February, pages: 1–8
598. Brouard F, Bories A, Sauze F (1982) Advance in anaerobic digestion of aquatic plants. Paper presented at the Energy from Biomass. 2nd EC Conference, Berlin, 20–23 Sept 1982
599. Croatto U (1982) Energy from macroalgae of the Venice lagoon. In: Strub A, Chartier P, Schlesser G (eds) Energy from biomass. Second EC conference, Berlin, 20–23 Sept 1982. Elsevier Applied Science, London, pp 329–333
600. Nicolini S, Viglia A (1985) Anaerobic digestion of macroalgae in the lagoon of Venice: experiences with a $5m^3$ capacity pilot reactor. In: Palz W, Coombs H, Hall DO (eds) Energy from the biomass: third EC conference, Venice. Elsevier Applied Science, London, pp 614–616
601. Missoni M, Mazzagardi M (1985) Production of algal biomass in Venice lagoon, environmental and energetics aspects. In: Palz W, Coombs H, Hall DO (eds) Energy from the biomass: third EC conference, Venice. Elsevier Applied Science, London, pp 384–386
602. De Waart J (1988) Biogas from seaweeds. In: Morand P, Schulte EH (eds) Aquatic primary biomass (marine macroalgae): biomass conversion, removal and use of nutrients. I. Proceedings of the first workshop of the COST48 SubGroup 3, L'Houmeau, France. Commission of the European Communities, DG XII/F Biotechnology, pp 109–110
603. Orlandini M, Favretto L (1988) Utilization of macroalgae in Italy for pollution abatement and as source of energy and chemicals. In: Morand P, Schulte EH (eds) Aquatic primary biomass (marine macroalgae): biomass conversion, removal and use of nutrients. I. Proceedings of the first workshop of the COST48 Sub-Group 3, L'Houmeau, France. Commission of the European Communities, DG XII/F Biotechnology, pp 25–28

604. Cecchi F, Pavan P, Mata-Alvarez J (1996) Anaerobic co-digestion of sewage sludge: application to the macroalgae from the Venice lagoon. Resour Conserv Recycling 17(1):57–66. doi:10.1016/0921-3449(96)88182-1
605. Rye C (1988) The use of algal for nutrient removal and as raw material for the industry with examples from Danish activities. In: de Waart J, Nienhuis PH (eds) Aquatic primary biomass (marine macroalgae): biomass conversion, removal and use of nutrients. II. Proceedings of the second workshop of the COST 48 Sub-Group 3., Zeist and Yerseke, The Netherlands, 25–27 October 1988. Commission of the European Communities, DG XII/F Biotechnology, Brussels, pp 8–11
606. Fannin KF, Srivastava VJ, Chynoweth D (1982) Unconventional anaerobic digester design for improving methane yield. In: Energy from biomass and wastes VI, Lake Buena Vista, pp 373–396
607. Ghosh S, Conrad JR, Sedzielarz FS, Griswold KH, Henry MP, Bortz SJ, Klass DL (1976) Research study to determine the feasibility of production methane gas from sea kelp. Institute of Gas Technology, Chicago
608. Tarwadi SJ, Chauhan VD (1987) Seaweed biomass as a source of energy. Energy 12(5):375–378
609. Asinari Di San Marzano CM, Legros A, Naveau H, Nyns E (1982) Biomethanation of the marine algae *Tetraselmis*. Int J Sustain Energy 1(4):263–272
610. Yokoyama S, Jonouchi K, Imou K (2008) Energy production from marine biomass: Fuel cell power generation driven by methane produced from seaweed. Int J Appl Sci Eng Technol 4:168–175
611. Troiano R, Wise D, Augenstein D, Kispert R, Cooney C (1976) Fuel gas production by anaerobic digestion of kelp. Resour Recover Conserv 2:171–176
612. Sanchez Hernandez EP, Travieso Cordoba L (1993) Anaerobic digestion of *Chlorella vulgaris* for energy production. Resour Conserv Recycling 9(1–2):127–132

Chapter 37
Gas Hydrates as a Potential Energy Source: State of Knowledge and Challenges

George J. Moridis, Timothy S. Collett, Ray Boswell, Stephen Hancock, Jonny Rutqvist, Carlos Santamarina, Timoth Kneafsey, Matthew T. Reagan, Mehran Pooladi-Darvish, Michael Kowalsky, Edward D. Sloan, and Carolyn Coh

Abstract Gas hydrates are a vast energy resource with global distribution in the permafrost and in the oceans, and its sheer size demands evaluation as a potential energy source. Here we discuss the distribution of natural gas hydrate (GH) accumulations, the status of the international R&D programs. We review well-characterized GH accumulations that appear to be models for future gas production, and we analyze the role of numerical simulation in the assessment of their production potential. We discuss the productivity from different GH types, and consistent indications of the possibility for production at high rates over long periods using conventional technologies. We identify (a) features, conditions, geology, and techniques that are desirable in production targets, (b) methods to maximize production, and (c) some of the conditions and characteristics that render GH deposits undesirable. Finally, we review the remaining technical, economic, and environmental challenges and uncertainties facing gas production from hydrates.

G.J. Moridis (✉) • J. Rutqvist • T. Kneafsey • M.T. Reagan • M. Kowalsky
Lawrence Berkeley National Laboratory, Berkeley, CA 94720, USA
e-mail: GJMoridis@lbl.gov

T.S. Collett
U.S. Geological Survey, Denver, CO 80225, USA

R. Boswell
National Energy Technology Laboratory, Morgantown, WV 26507, USA

S. Hancock
RPS Energy, Calgary, AB, Canada T2P 3T6

C. Santamarina
Georgia Institute of Technology, Atlanta 30332, GA

M. Pooladi-Darvish
University of Calgary, Calgary, Canada T2N 1N4

E.D. Sloan • C. Coh
Colorado School of Mines, Golden, CO 80401, USA

J.W. Lee (ed.), *Advanced Biofuels and Bioproducts*, DOI 10.1007/978-1-4614-3348-4_37,

Symbols, Abbreviations, and Nomenclature

ΔP	Pressure depletion (Pa)
GH	Gas hydrate
HBL	Hydrate-bearing layer
HBS	Hydrate-bearing sediment
k	Intrinsic permeability (m^2)
k_{eff}	Effective permeability (m^2)
mbsf	Meters below sea floor
MMSCF	10^6 of standard ft^3
MMSCFD	10^3 of standard ft^3/day
MSCF	$10^3$of standard ft^3
N_H	Hydration number
P	Pressure (Pa)
P_{cap}	Capillary pressure (Pa)
P_e	Hydrate equilibrium pressure at a given T (Pa)
S_H	Hydrate saturation
STP	Standard pressure and temperature
Q_M	Mass production rate (kg/s)
Q_P	Gas production rate (ST m^3/s)
Q_{avg}	Average gas production rate (ST m^3/s)
t	Time (days)
T	Temperature (K or °C)
RRR	Rate replenishment ratio
TCF	10^{12} STP ft^3 of gas
VRR	Volume replenishment ratio
WZ	Water zone

1 Introduction

1.1 Background

Gas hydrates (GH) are solid crystalline compounds in which gas molecules (referred to as guests) occupy the lattices of ice-like crystal structures called hosts. Under suitable conditions of low temperature T and high pressure P, the hydration reaction of a gas G is described by the general equation

$$G + N_H H_2O = G \bullet N_H H_2O, \tag{1}$$

where N_H is the hydration number. GH deposits occur in two distinctly different geographic settings: in the permafrost and in deep ocean sediments [91].

Naturally occurring hydrocarbon gas hydrates contain CH_4 in overwhelming abundance. Simple CH_4 hydrates concentrate methane volumetrically by a factor of 164 when compared to standard P and T conditions (STP). Such hydrates have $5.77 \leq N_H \leq 7.4$, with $N_H = 6$ being the average value and $N_H = 5.75$ the maximum one [178]. Natural gas hydrates can also contain other hydrocarbons (alkanes $C_\nu H_{2\nu+2}$, $\nu = 2$–4), but may also comprise lesser amounts of other gases (mainly CO_2, H_2S, or N_2).

Although there has been no systematic effort to map and evaluate this resource and current estimates of the in-place amounts vary widely, the consensus is that the world-wide quantity of hydrocarbon GH is vast [80, 120, 178]. Given the magnitude of the resource, the ever-increasing global energy demand, and finite conventional fossil fuel reserves, the potential of GH as an energy source demands technical and economic evaluation. The attractiveness of GH is further enhanced by the environmental desirability of natural gas, as it is an energy resource with significantly lower carbon intensity than coal, oil, or other solid and liquid fuels.

The past decade has seen a marked acceleration in GH research and development (R&D). Among the most important developments are the increasing focus of research on gas hydrate-bearing sediments (HBSs) rather than crystalline hydrate, the improvements in tools available for sample collection and analysis, the emergence of robust numerical simulation capabilities, and the transition of GH resource assessment from in-place estimates to potential recoverability [8]. A fuller understanding of the complexities of GH geological systems has emerged, including new insights into the effects of solubility, salinity and heat flow, reservoir lithology, and rates and migration pathways of both gas and H_2O [151, 167]. Additionally, critical data gaps, such as information on the mechanical and hydraulic properties of HBS, are being addressed. Significant inroads are also being made into our understanding of hydrate response under different production scenarios.

GH are often compared to coalbed gas, which was also considered an uneconomic resource in the not too distant past [21]. However, once the resource was geologically understood, the reservoir properties defined, and the production challenges addressed, coalbed gas became a viable fuel in its own right and an important part of the energy mix in the United States, where it accounts for almost 10% of the natural gas production. Past experience with other unconventional energy resources shows that the evolution of GH into a producible source of energy will require a significant and sustained R&D effort. Here we discuss the current state of this effort and of the corresponding knowledge status.

1.2 Methods of Production from Gas Hydrates

Gas can be produced from GH by inducing dissociation, which also releases large amounts of H_2O (1). The three main methods of hydrate dissociation are (1) depressurization, in which the pressure P is lowered to a level lower than the hydration pressure P_e at the prevailing temperature T, (2) thermal stimulation, in which T is

raised above the hydration temperature T_e at the prevailing P, and (3) the use of inhibitors (such as salts and alcohols), which shifts the P_e-T_e equilibrium through competition for guest and host molecules [111]. Long-term production strategies often involve combinations of the three main dissociation methods [131, 132]. Another production method involves CH_4 exchange with another hydrate-forming gas (e.g., CO_2) through a thermodynamically favorable reaction [52, 213].

2 Occurrence, Research Activities and Priorities, and Prospective Production Targets

2.1 Magnitude and Global Distribution of the Hydrate Resource

Knowledge of the occurrence of in situ GH is very incomplete, and is either based on limited direct evidence (hydrate samples) or inferred from other data. In permafrost regions, direct evidence of gas hydrate is provided by ongoing R&D programs (discussed below), and by analysis of industry 3-D seismic data and data obtained during the drilling and logging of conventional oil and gas wells. In marine environments, most of the inferences of GH occurrence are based on indirect indicators involving interpretation of relatively low-quality 2-D seismic data. Direct GH detection and characterization from marine 3-D seismic data have recently been reported by Dai et al. [32]. The use of four-component ocean bottom seismic surveys has also shown great promise [4, 14].

2.1.1 Estimates of Gas Trapped in Hydrates and Related Uncertainties

Table 1 lists several estimates of natural gas, in hydrate form, in the geosphere's GH stability zone (i.e., the P and T regime within which hydrates are stable). The maximum value (3.053×10^{18} m^3 STP of CH_4) of Trofimuk et al. [195] is based on the assumption of GH occurrence wherever a satisfactory P-T regime exists, while the minimum value (2×10^{14} m^3 STP) of Soloviev [180] accounts for limiting factors such as CH_4 availability, limited organic matter, porosity, regional thermal history, etc.

The Klauda and Sandler [80] estimate in Table 1 has received significant attention, as it is based on a state-of-the-art model that explains most known GH occurrences and offers plausible reasons for discrepancies from its predictions.

Even the most conservative estimates suggest enormous amounts of gas in hydrated form, the magnitude of which can be appreciated by comparing them to the current rate of 10^{12} m^3 STP of gas-equivalent annual energy consumption in the United States. All estimates are comparatively large relative to estimates of the conventional gas reserves of 1.5×10^{14} m^3 of methane [155]. Kvenvolden [97] indicated that his estimate of 1.8×10^{16} m^3 of CH_4 in hydrates may surpass the recoverable conventional CH_4 by two orders of magnitude, or be a factor of 2 larger than the CH_4 equivalent of the total of all fossil fuel deposits.

Table 1 Estimates of in situ methane hydrates [178]

CH_4 amount 10^{15} m^3 STP	References
3,053	[195]
1,135	[196]
1,573	[15]
120	[198]
3.1	[119]
15	[110, 109]
15	[197]
40	[99]
20	[97]
20	[107]
26.4	[51]
45.4	[64]
1	[50]
6.8	[66]
15	[111]
0.2	[180]
2.5	[120]
120	[80]

2.1.2 Geographic Occurrences

In terms of global distribution, oceanic hydrates constitute about 99% of the total GH resource [178], so that a 1% error in the ocean approximations could encompass the entire permafrost hydrate reserves [178]. Kvenvolden [98] compiled 89 hydrate sites shown in Fig. 1 [178]. At those locations, hydrates were:

1. Recovered as samples (23 locations, of which 3 in the permafrost and 20 in ocean environments).
2. Inferred from (a) Bottom Simulating Reflector (BSR) geophysical signatures (63 locations), (b) decrease in pore water chlorinity (11 locations), well logs (5 locations), and slumps/pockmarks (5 locations).
3. Interpreted from geologic settings (6 locations).

A measure of the dearth of direct knowledge on hydrates compares this meager list, which represents the entirety of the database of natural hydrates, to the huge body of information on conventional and unconventional oil and gas reservoirs [209].

Given their relative abundance, marine GH occurrences will likely be the primary targets for future R&D activities. However, given the favorable economics of conducting long-term field programs in the Arctic (as opposed to the deep water), it is expected that arctic R&D activities will also continue. Two countries, the United States and Japan, are making considerable R&D investments in the Arctic, under the reasoning that the information gained on the behavior of gas hydrate-bearing sand reservoirs can be readily transferred to the study of marine resources at a later date.

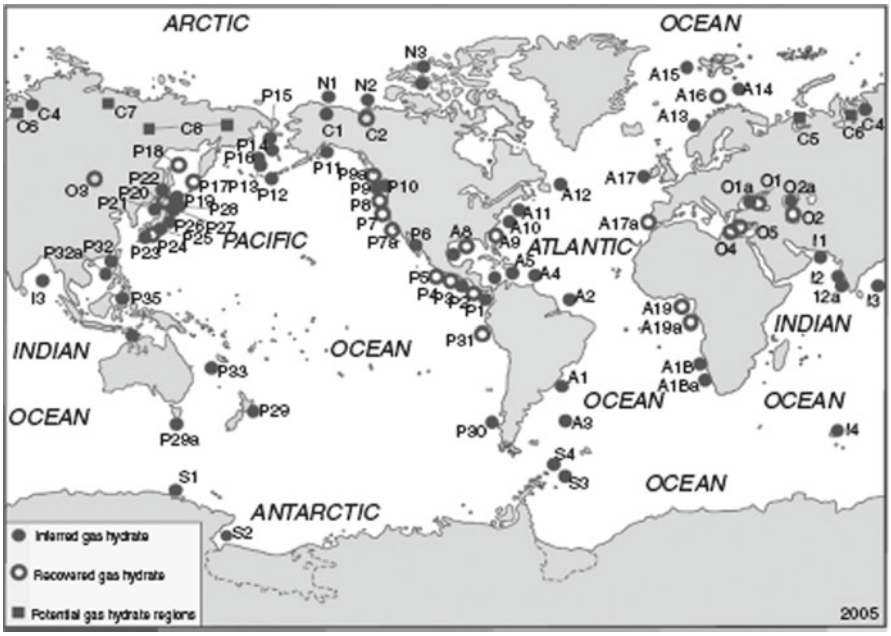

Fig. 1 Inferred (63), recovered (23), and potential (5) hydrate locations in the world [98]

2.2 Policies, Focus, Activities, and Priorities

The following review focuses on those studies that are most relevant to the assessment of gas hydrate resource potential.

2.2.1 Synopsis of Global Research Activities

Japan took a leading role in the effort to explore the potential of geologic hydrate deposits as an energy source by establishing a research program in 1995, which led to the drilling and installation of the first well in marine gas hydrate deposits in the Nankai Trough offshore Japan at a water depth of 945 m [114, 190, 199, 203]. This was succeeded by a larger multi-well exploration program [114], and is probably the most advanced program in the world in terms of proximity to commercial production. As part of this program, 36 wells were recently drilled in gas hydrate-bearing sand reservoirs at the same location [189]. Fujii et al. [47, 48] and Saeki et al. [172] described the variety of gas hydrate occurrence found in the Nankai region, and Kurihara et al. [94, 96] discussed the technical challenges and the relative economic favorability of GH in different geologic settings. Production is expected to begin around 2016. Japan has also collaborated with Canada and other nations to conduct scientific studies and production tests from GH in the Canadian Arctic. Canada has

established a large gas hydrate research and development program that resulted in the Mallik production field test [35], the most significant to-date development in the quest for gas production from hydrates (see later discussion).

In the United States, studies on GH as a resource began in 1980s, and Collett [19] conducted the first systematic assessment. He estimated the 50% probability (mean) estimate of hydrate resources within the United States at 9×10^{15} m^3 of CH_4 (with the 95% probability estimate at 3×10^{15} m^3 and the 5% probability estimate at 1.9×10^{16} m^3), i.e., the mean value indicates 300 times more hydrated gas than the gas in the total remaining recoverable conventional resources. The Methane Hydrate Research and Development Act (MHR&D Act) of Congress in 2000 authorized funding to uncover the physical nature, economic potential, and environmental role of naturally occurring GHs. Over the first 10 years of the MHR&D Act, hydrate science advanced significantly, both in terms of knowledge of natural hydrate occurrences, hydrate physical/chemical properties, and in the tools available to researchers. Researchers gained a greater understanding of the complexity of hydrate accumulations through laboratory work [40, 56, 86, 204, 215], numerical simulation analyses [88, 129, 131–134, 136, 137], and national and international collaborative field experiments [35], and began the development of the precursors to tomorrow's hydrate exploration and evaluation technologies. By 2005, it was clear that, given certain reservoir conditions, production of methane from hydrate was technically feasible and potentially commercially viable through specially tailored application of existing technologies [8]. Current research activities in the United States include laboratory experiments and simulation studies [8], in addition to field studies that focus on onshore Alaska and the offshore Gulf of Mexico (GOM)—i.e., sites of proven exploration targets in the United States [19–21]. Major federal-industry partnerships have been formed in both the GOM and on the North Slope of Alaska [20]. It is likely that the first US domestic production from hydrates may occur in Alaska because of easier access, although the possibility of first production from GHs in the GOM cannot be discounted because of pipeline capacity and easier access to markets.

The government of India is funding a large national GH program to meet its growing gas requirements. Earlier seismic data from the Indian continental margin and GH occurrences that had been accidentally discovered during drilling for conventional oil and gas resources [20] provided the impetus for a hydrate-focused scientific expedition in the summer of 2006. This expedition confirmed large GH deposits at four offshore locations, from which many hydrate-bearing cores were obtained. Most notable was the 130-m thick fractured shale occurrence in the Krishna-Godowari basin that contained GH saturations S_H previously unseen in shale-dominated reservoirs [28, 29].

China has pursued gas hydrates R&D for more than a decade [44], and conducted its initial drilling and coring program in the South China Sea in early 2007. That expedition found GH occurrences with S_H up to 40% in clay-dominated sediments at several sites [224]. As in the 2006 India expedition, these results were unexpected, and indicated that, given adequate sources of gas, hydrates are remarkably effective at filling any available pore space.

Korea has established a significant research program that aims to assess the potential hydrate resources in the Korean East Sea. Preliminary surveys conducted by the Korea Institute of Geoscience and Mineral Resources (KIGAM) between 2000 and 2004 suggest a significant potential for gas hydrate occurrence in the Ulleung Basin [146], and numerical simulation studies have raised intriguing possibilities about the production potential of these deposits [136]. In late 2007, a drilling and coring program in Korea's East Sea reported several 100-m thick occurrences [105].

Other countries (e.g., Norway, Russia, Mexico, Taiwan, Vietnam, Malaysia) have either embarked on, or are investigating the viability of, government-sponsored research programs to investigate the potential of gas production from national hydrate deposits. This list is only expected to grow. In Europe, research programs like Hydratech and Hydramed have focused primarily on scientific and environmental issues.

Recently, a growing number of deep sea drilling expeditions have been dedicated to locating marine GHs and obtaining a greater understanding of the geologic controls on their occurrence. The earliest projects were those of the Ocean Drilling Program (ODP) and the Integrated Ocean Drilling Program (IODP), including ODP Legs 164 [149] and 204 [194] and IODP Expedition 311 [162], as well as the 1998 and 2005 drilling programs conducted in the Nankai Trough by the MH21 consortium [47, 181]. More recently, the Gumusut-Kakap project offshore Malaysia [57], the Department of Energy (DOE)-sponsored drilling Legs I and II under the Joint-Industry Project in the GOM [9, 13, 166], and the India NGHP Expedition 01 [23, 28, 29], as well as those in the offshore of China [218] and South Korea [147], have continued to expand the GH knowledge base.

Given the difficulty and the large costs of conducting field studies on hydrates, significant effort is invested in international collaborative projects. The most well known (and probably the most important, in terms of knowledge generated) was the 2002 Mallik project, conducted at that site in Canada's Mackenzie Delta (Northwest Territories) by an international consortium that included seven organizations from five countries, as well as the International Continental Scientific Drilling Program. Current international collaborative projects include the Mallik 2007–2008 project [33, 37] (Japan and Canada), as well as other bilateral collaborations, e.g., US–India [27] and US–China [218].

2.2.2 Focus and Priorities

As in the case of conventional hydrocarbon production, it is logical to expect that the first gas recovery from hydrate resources will occur where there is relatively easy site access and GH are concentrated [21]. Such sites and deposits constitute the first targets on which the attempt to produce gas from hydrates must be focused.

The analysis of Boswell and Collett [10] used relative prospects for future production as the criterion to identify several key tiers of GH resource categories within the context of a *resource pyramid* (Fig. 2). At the peak of the Gas Hydrates Resource

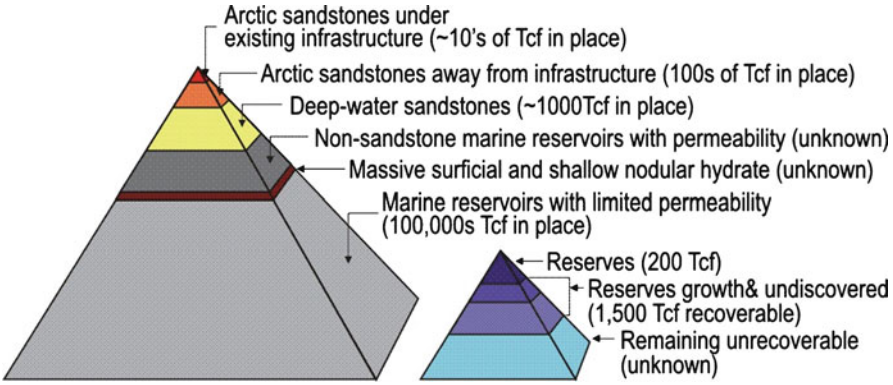

Fig. 2 Gas hydrates resource pyramid (*left*). To the *right* is an example gas resources pyramid for all non-gas-hydrate resources [10]

Pyramid (those resources that are closest to potential commercialization) are deposits that exist at high hydrate saturation S_H within quality reservoir rock under existing Arctic infrastructure (e.g., in the Eileen trend of the Alaskan North Slope), estimated to represent 9.4×10^{11} m^3 STP (=33 TCF) of gas-in-place. Modeling studies suggest that as much as 3.4×10^{11} m^3 STP (=12 TCF) of that volume may be technically recoverable. The second-from-the-top tier of hydrate resources is that of less well-defined accumulations that exist in similar geologic settings (discretely trapped, high-S_H occurrences within high-quality sandstone reservoirs) on the North Slope, but away from existing infrastructure. The current USGS estimate for total North Slope resources is approximately 1.7×10^{13} m^3 STP (=590 TCF) gas-in-place [22].

The next most challenging (third) tier of resources includes GH of moderate-to-high S_H that occur within high-quality oceanic sandstone reservoirs. The most favorable accumulations occur in the GOM in the vicinity of oil and gas production infrastructure [8]. Additional examples of this category of resource have been documented from the Nankai Trough studies offshore Japan [47] and by the IODP Expedition 311 offshore Vancouver Island [162, 163]. All subsequent tiers are considered unattractive, and major technological advancements will be needed before production from such deposits is ever to become feasible [140, 125].

2.3 Hydrate Deposits That Are Production Targets

From the previous discussion, it is obvious that hydrate deposits that are being considered as production targets must have the following attributes:

- Confirmed presence of high hydrate saturation S_H.
- Occurrence within sediments of sufficient reservoir quality.
- Site accessibility through proximity to existing infrastructure.
- Access to gas markets through pipeline availability.

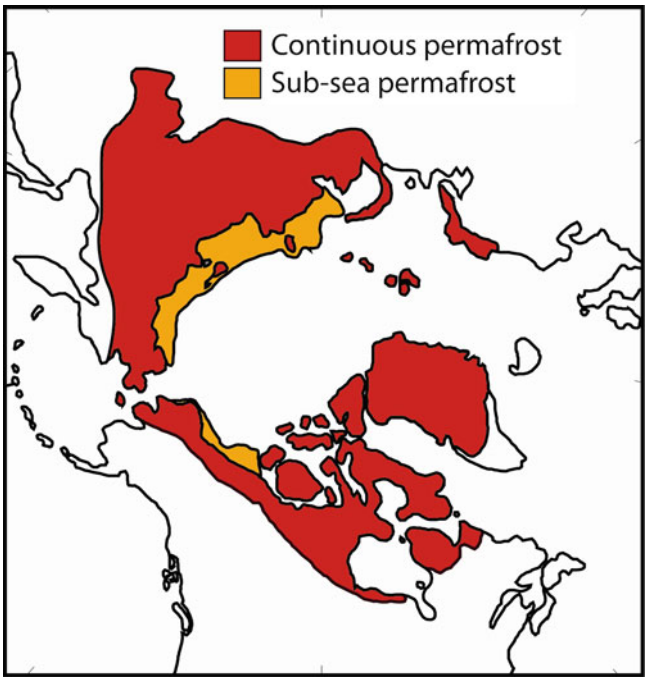

Fig. 3 Distribution of permafrost in the Northern Hemisphere [18]

Here we discuss the features and attributes of hydrate deposits that are likely targets for gas production, and we analyze the geologic and engineering factors that control their ultimate resource potential.

2.3.1 Permafrost Deposits

The discussion in this section follows closely the analysis of Collett [21], which is the most thorough treatment of the subject. Present-day permafrost underlies about 20% of the land area of the northern hemisphere. Geologic studies [122] and thermal modeling of subsea conditions [145] also indicate that *relic* permafrost [23] and GH may exist within the continental shelf of the Arctic Ocean. In practical terms, onshore and near-shore GH can only exist in close association with permafrost (Fig. 3). Because of relatively easier access, data from permafrost deposits are of better quality and represent a disproportionately large fraction of the entire hydrate database. Note that permafrost deposits represent the two top tiers of the hydrate resource pyramid of Fig. 2, indicating their relative desirability compared to oceanic accumulations. There are three permafrost deposits under consideration as first production targets.

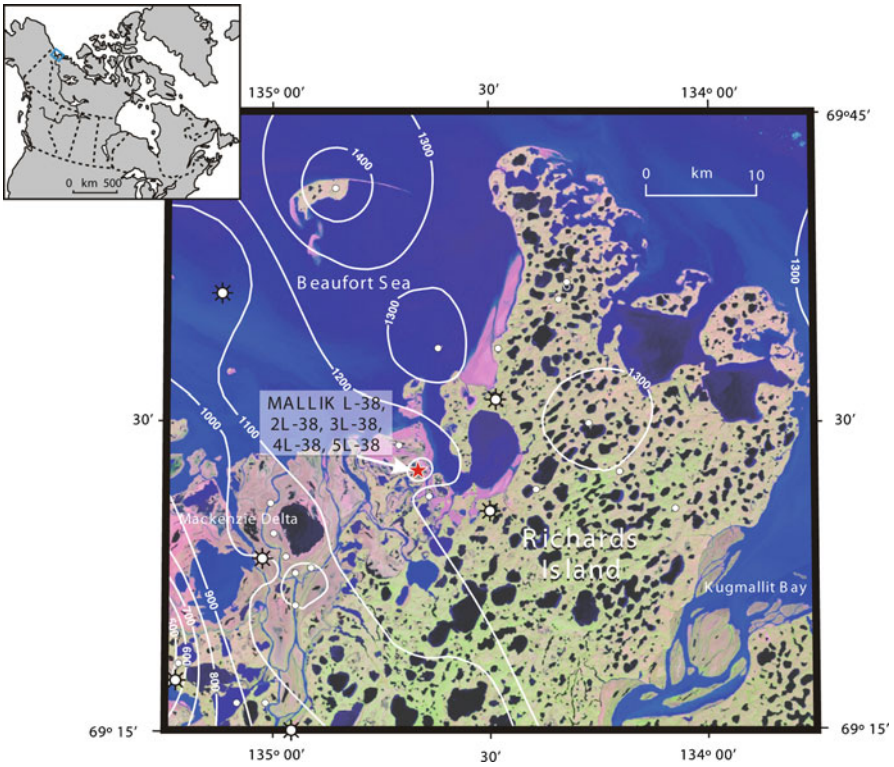

Fig. 4 Location of the wells during the 2002 field test at the Mallik site, Mackenzie Delta, Northwest Territories. Contours indicate depth to the base of the gas hydrate stability zone in meters. Symbols include *small circles* as well locations, *larger circles* with ticks are wells containing gas hydrate [35]

Mackenzie Delta, *Canada—Mallik Gas Hydrate Accumulation*. This is likely the best-characterized GH accumulation in the world. The assessment of GH occurrences in the Mackenzie Delta-Beaufort Sea area was made originally on the basis of data collected during 3 decades of conventional hydrocarbon exploration in the area [75], and was refined with data from three dedicated scientific drilling programs [34–36] that included the collection of GH-bearing core samples.

At least 10 discrete GH layers, with a total thickness of over 110 m and high S_H (occasionally exceeding 80%), were identified from well-log analysis in the 900–1,100 m interval [35, 36]. The estimates of the amount of gas in the hydrate accumulations are in the 2.8×10^{10}–2.8×10^{11} m^3 STP (=1–10 TCF) range [108, 144], making the Mallik field as one of the most concentrated GH deposits in the world. The Mallik site (Fig. 4) became the site of two recent gas hydrate production research programs: (1) The Mallik 2002 Gas Hydrate Production Research Well Program [35], and (2) the 2006–2008 JOGMEC/NRCan/Aurora Mallik Gas Hydrate Production Research Program [33, 37]. The Mallik 2002 Gas Hydrate Production

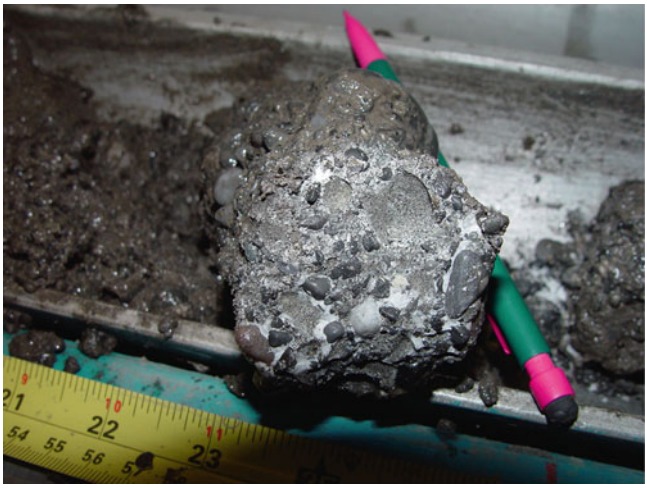

Fig. 5 Photograph of a gas-hydrate-bearing rock core from the Mallik 5L-38 gas hydrate research well. Note that the gas hydrate is the white material filling the void spaces in this conglomerate (photo courtesy of the Mallik 2002 Gas Hydrate Production Research Well Program [35])

Research Well Program involved an international consortium (comprising the Japan National Oil Corporation, the Geological Survey of Canada, the U.S. Geological Survey (USGS), the U.S. DOE, the GeoForschungZentrum-Potsdam, the Indian Ministry of Petroleum Geology and Natural Gas, Gas Authority India Ltd, and the International Continental Scientific Drilling Program), conducted the first fully integrated field study and test of production from hydrates, and yielded unique data that provided a detailed analysis of the geology, geochemistry, geotechnical, and microbiological properties of HBS [21]. Over 150 m of GH-bearing cores collected during the Mallik 2002 program provided additional insights into the macroscopic and microscopic properties of the reservoir sediments (Fig. 5). The studies originating from the Mallik 2002 test included investigations of a 5-day experiment of gas production by thermal stimulation [35], and resulted in continuous gas production at varying rates that peaked at 1,500 m^3/day (Fig. 6). These results confirmed earlier predictions that gas production from hydrates at the Mallik site by means of thermal dissociation was technically feasible [93, 95, 138].

The 2006–2008 JOGMEC/NRCan/Aurora Mallik Gas Hydra-te Production Research Program [33, 37] was a continuation of the 2002 test, and involved instrument and equipment installation, in addition to a successful short-term drawdown production test at a 12-m-thick GH section near the base of the stability zone [21, 33].

North Slope, *Alaska*, *USA—Eileen Gas Hydrate Accumulation*. The geology and geochemistry of the rocks on the North Slope of Alaska, and the subsurface temperature data needed to assess the distribution of the gas hydrate stability, are described in detail in a number of publications [7, 18]. The CH_4 hydrate stability zone in northern Alaska, as mapped in Fig. 7, covers most of the North Slope.

Fig. 6 Gas flare from the thermal gas hydrate production test in the Mallik 5L-38 gas hydrate research well (photo courtesy of the Mallik 2002 Gas Hydrate Production Research Well Program [35])

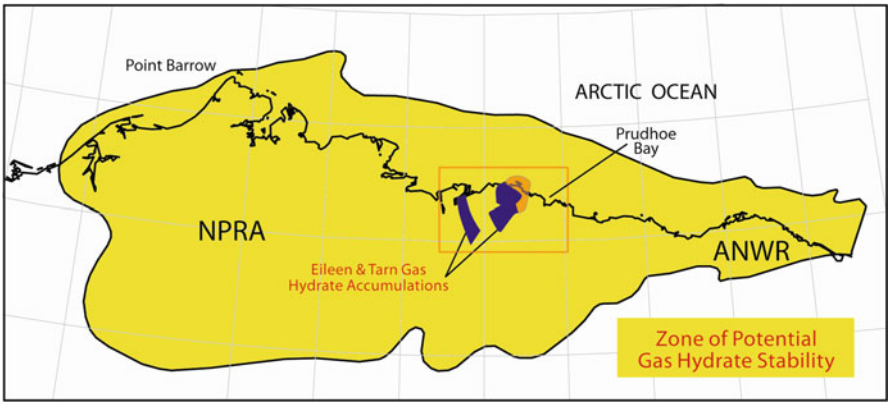

Fig. 7 Map of the Alaska North Slope gas hydrate stability zone. Also shown is the location of the Eileen and Tarn gas hydrate accumulations [18]

Analysis of downhole log data from older wells indicated hydrate occurrence in six laterally continuous sandstone and conglomerate units, which are all confined to the geographical area. The volume of gas within the Eileen Gas Hydrate Accumulation is estimated at 1.0×10^{12}–1.2×10^{12} m^3 STP [21], i.e., about twice the volume of known conventional gas in the Prudhoe Bay Field [18].

In a project aiming to determine the viability of the North Slope hydrates as an energy source [141], a well was installed in 2007 at a fault-bounded accumulation named the "Mount Elbert" to a depth of 915 m, and several analyses were conducted. Following well-log surveys, a Schlumberger Modular Dynamic Testing (MDT) was conducted in two reservoir-quality sandy hydrate-bearing sections with high S_H (60–75%). Gas was produced from GH in each of the tests. This study has yielded one of the most comprehensive datasets yet compiled [21]. The gas production data were analyzed, and were used (a) to design a long-term production test to determine reservoir deliverability under a variety of scenarios, (b) to cross-validate several numerical codes [2, 214], and (c) to analyze the project's long-term production test options.

West Siberia, Russia—The Messoyakha Field. The Messoyakha Field in the northern part of the West Siberian Basin is often used as an example of a GH accumulation from which gas has already been produced commercially. Production and geologic data have been used to deduce the GH presence within the upper part of this field [110]. Large deviations between predicted and observed pressures have been attributed to the release of gas from dissociating GH. It is estimated that about 36% (about 5×10^9 m^3 STP) of the total produced gas originated from GH [110]. Unfortunately, incomplete and/or inaccessible data from the Messoyakha field and the existence of plausible alternative theories for the pressure deviations [25, 90] do not allow the unequivocal consideration of Messoyakha as a hydrate-supported gas reservoir.

2.3.2 Oceanic Deposits

Favorable oceanic deposits are those with a high S_H in high-quality reservoirs. The challenges facing commercialization of marine GH are likely to be higher than those in the Arctic, given the higher cost deep water operations. Installed infrastructure and access to markets (e.g., in the GOM), or lack of an Arctic GH option (as is the case of India or Japan), may make this an attractive option. The oceanic deposits that serve as models for the evaluation of marine GH prospects are described below.

Offshore Japan—Nankai Trough. This area has probably experienced the largest investment and most advanced field research activity because of the intensive Japanese effort to evaluate the potential and feasibility of gas production from hydrates. Following the drilling of an exploration well in 2000 [190], a multi-well exploration program was conducted in 2004 at 16 locations in three different sites (Kumano Basin, Second Atsumi Knoll, and Offshore Tokai) that had been selected on the basis of the BSR signature [189] at water depths of 720–2,033 m (Fig. 8). A total of 32 wells were drilled, and a comprehensive evaluation was conducted. The experimental program focused heavily on the practicalities and challenges of well construction in hydrate sediments [189]. An offshore production test appears to be the next logical step [48, 96, 172, 189].

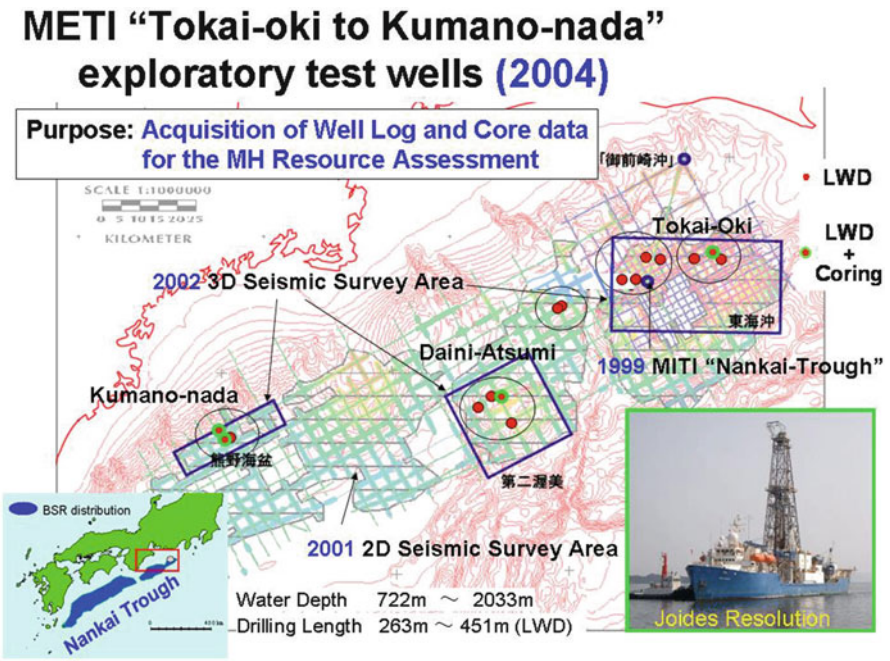

Fig. 8 The hydrate deposit areas in the Nankai Trough region offshore Japan, and the drilling sites of the 2004 Drilling Program [96]

GOM—Oligocene Frio Formation, Tigershark Deposit. Smith et al. [179] described this first documented case of high-S_H hydrate-bearing sand in the Alaminos Canyon Block 818 of the GOM (Fig. 9). Log data from an exploration well in about 2,750 m of water at the site indicated the presence of an 18.25-m thick sandy hydrate-bearing layer (HBL) (3,210–3,228 m drilling depth) at a relatively high temperature (about 21°C), with a high porosity φ (about 0.30), Darcy-range intrinsic permeability k, and with the base of the GH stability zone occurring at or slightly below the base of the hydrate [26, 179].

This deposit belongs to the third tier in the resource pyramid of Fig. 2, with initial S_H estimates ranging from 0.6 to over 0.8 [26]. Preliminary simulations with synthetic data (describing GH reservoirs under the Tigershark conditions) indicate that such systems can reach gas production rates well in excess of 2.8×10^5 m^3/day = 10 MMSCFD [131, 132].

GOM—GC955 and WR313 Deposits. The reservoirs are very recent findings that were first identified during the "Leg II" logging-while-drilling operations conducted in the deepwater GOM in April 2009 [11, 24, 142] by the GOM Gas Hydrates Joint Industry Project (JIP) [74, 115, 117, 118]. The sites for Leg II drilling of the JIP were selected based on an integrated geologic-geophysical approach designed to identify accumulations of gas hydrate at high saturation S_H (≥50%) in sand reservoirs (Fig. 10).

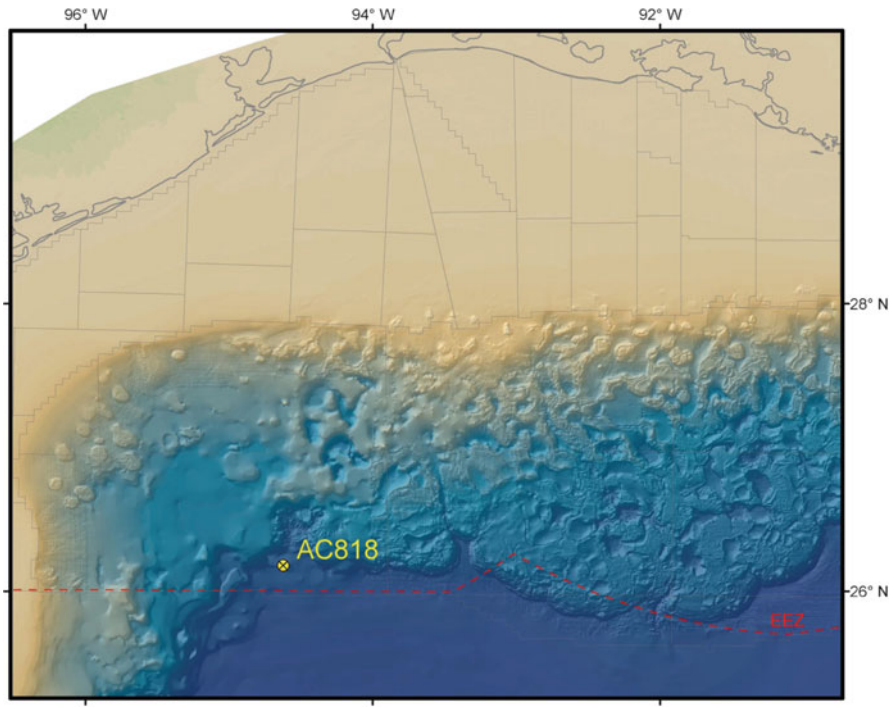

Fig. 9 Approximate location of the "Tigershark" exploratory well in the Alaminos Canyon block 818 [179]

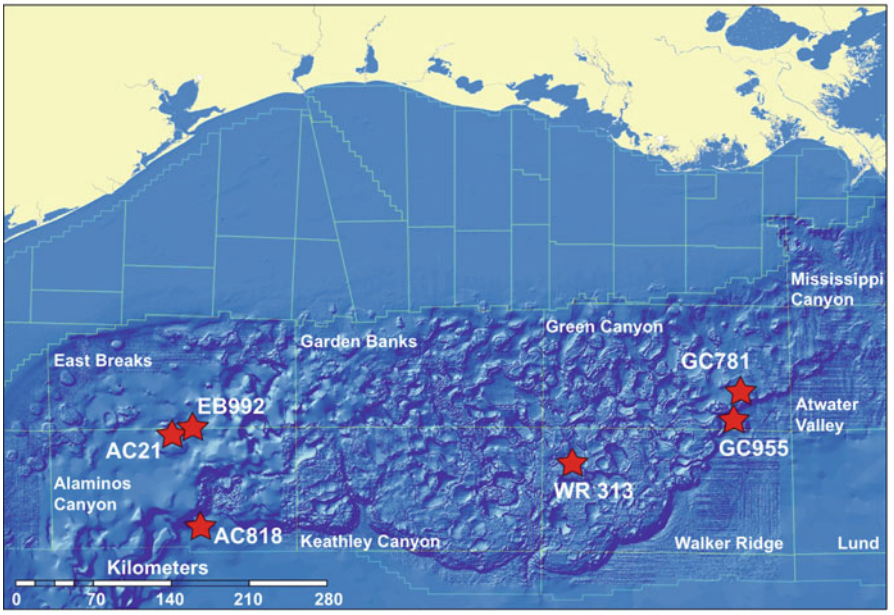

Fig. 10 Seafloor map of the Gulf of Mexico depicting the location of JIP Leg II drill sites: AC818, WR313, and GC955 [135]

The GC955 accumulation involves a sand-rich channel-levee complex at the mouth of the Green Canyon embayment. Two industry wells in the block have confirmed the presence of clean, thick sands in close proximity to the most clearly imaged channel axis. Logging results from Leg II showed a thick accumulation of gas hydrates within porous sand lithologies [54]. The drilling depth to the top of the sand unit was 389 mbsf (feet below sea floor). At the H-well location [54], approximately 100 m of GH-bearing media involved a sequence of thin horizontal sand-shale interbeds at approximately the 0.3–0.6-m scale. GH occurs in pore-filling mode in three separate zones with S_H in the 50–85% range, with no indication of free gas.

The WR313 sites are within the highly dipping eastern margin of the Terrebonne salt-withdrawal mini-basin with significant sand deposition (see [115, 117, 118, 177]). Two horizons were targeted for drilling in JIP Leg II: Well WR313 "G" and well WR313 "H" targeted the informally named "blue" and "orange" horizons, respectively. LWD data obtained at the G-well indicated a sand-rich interval with thinly interbedded sands and shales (0.3–1.5 m). The drilling depth to the top of the unit was 852 mbsf. About 12 m of GH-bearing sands within a gross interval of 21 m were identified, with S_H typically ranging from 40% to over 70%. The primary control on gas hydrate occurrence in this unit is availability of suitable reservoir conditions [9, 11]. The WR313 "H" horizon occurred approximately 140 m below the blue horizon, and consisted of two massive, clean sands with sharp bases and tops. Drilling depth to the top of the upper unit was 806 mbsf. The upper "orange" sand is 4 m thick, with S_H as high as 90% [54]; the lower unit is about 7 m thick, with S_H ranging between 35 and 80%.

3 Production Estimates and the Role of Numerical Simulation

The assessment of the production potential of hydrates requires predictions of their complex behavior. The reliability and accuracy of these predictions hinges on the following three factors: (1) the availability of robust numerical simulators that describe the dominant processes and phenomena, (2) knowledge of the parameters and relationships that quantify the physical processes (usually obtained from laboratory experiments and/or from field tests either by direct measurement or through history-matching) and the thermophysical properties of all the components of the simulated system, and (3) the availability of field and laboratory data for the validation of the numerical models. The complexity of the coupled processes involved in the dissociation reaction does not permit the use of analytical models either for direct predictions or for the verification of the numerical models except under limited conditions, i.e., at early times and after significant approximations.

Thus, the role of numerical simulation is critically important, and is practically the only tool that allows the assessment of the gas production potential of hydrates. It allows the design of laboratory and field experiments, can provide answers (or, at a minimum, general behavior trends) to very complicated problems at a very reasonable cost before necessitating substantial investments for field operations, and allows investigation of a wide range of alternative ("*what-if*") scenarios that would

be impossible to explore otherwise. Note that even if there are no field or laboratory data for code validation and only very sketchy data describing the properties and physical processes in the system, numerical simulation can provide very important insights (provided the underlying physics are correct and representative of the simulated processes) because it makes it possible to determine technical feasibility, to establish envelopes of possible solutions, to determine sensitivity to particular parameters and processes, and to identify promising target zones of hydrates for development.

3.1 Code Availability

The ability to numerically simulate the behavior of geologic hydrate reservoirs has improved substantially over the past 5 years in terms of both code availability and capabilities [8]. There are currently several numerical models that can simulate the system behavior in hydrate-bearing geologic media (e.g., [30, 68, 94, 130, 143, 152, 153, 188]). Several of these codes were calibrated against the Mallik 2002 production test data, and the data from the Mt. Elbert MDT test [2]. A code-comparison study [1, 214] indicated that most of the participating codes appear capable of simulating the behavior of hydrates and reservoir fluids during common dissociation scenarios. The current consensus is that the models generally account for the important physics of the problem, and that validation and calibration (rather than adequacy of the numerical code capabilities) will be a constraining factor in the assessment of hydrates as an energy resource [214, 2]. Additionally, while uncertainties exist in the description of properties and processes involved in numerical simulators (e.g., thermal properties of composite GH-bearing systems, relative permeability and capillary pressure, geomechanical properties related to subsidence after the dissociation of the cementing GH from the porous media, etc.), these knowledge gaps are being addressed [125, 127].

4 Gas Production Strategies

4.1 Classification of Gas Hydrate Deposits

Natural GH accumulations are divided into three main classes [124] based on simple geologic features and the initial reservoir conditions. Class 1 deposits are composed of two layers: the HBL and an underlying two-phase fluid zone containing mobile gas and liquid water [129, 125]. Class 2 deposits comprise two zones: an HBL, overlying a zone of mobile water (hereafter referred to as WZ). Class 3 accumulations are composed of a single zone, the hydrate interval (HBL), and are characterized by the absence of an underlying zone of mobile fluids. In Classes 2 and 3, the entire HBL may be well within the hydrate stability zone and can exist under

equilibrium or stable conditions. A fourth class (Class 4) pertains specifically to oceanic accumulations, and involves disperse, low-saturation hydrate ($S_H < 10\%$) deposits that lack confining geologic strata [140].

4.2 Gas Production from Class 1 Deposits

Of the three main dissociation methods, depressurization appears best suited to the conditions of Class 1 deposits because of its simplicity, technical, and economic effectiveness, and the fast response of hydrates to the rapidly propagating pressure wave [129, 125]. Hong and Pooladi-Darvish [68] applied constant-*P* depressurization at a well at the center of a GH reservoir, and analyzed the sensitivity of the continuously declining production to various properties and operational conditions. They reported that, at the end of the first year of production, about 48% of the produced gas had been replenished by hydrate-originated CH_4, thus confirming the technical feasibility of production from hydrates using conventional technology.

Moridis et al. [129] conducted a long-term (10–30 years) study of constant-rate (=0.81944 ST $m^3/s = 2.5$ MMSCFD) production from Class 1 hydrate deposits. To describe the contribution of gas released from hydrate to the production stream, they introduced the concepts of *Rate Replenishment Ratio* (*RRR*) and *Volume Replenishment Ratio* (*VRR*). *RRR* is defined as the fraction of the gas production rate at the well(s) that is replenished by CH_4 released from hydrate dissociation. *VRR* is defined as the fraction of the cumulative gas volume produced at the well(s) that is replenished by hydrate-originating CH_4. During the 30-year production period, the VRR increases continuously to a maximum of about 0.74, and the corresponding RRR is 0.54 (Fig. 11—[129]). The desirability and the great production potential of such deposits are obvious. The evolution of the S_H distribution over time is shown in Fig. 12. Production from these Class 1 deposits (a) involved conventional technologies and (b) necessitated continuous heating of the wellbore to prevent hydrate formation and plugging [129]. Note that the use of horizontal wells does not confer any practical advantages to gas production from Class 1 deposits [137].

4.3 Gas Production from Class 2 Deposits

Moridis and Reagan [131] showed that depressurization-induced dissociation appears to be the most promising gas production strategy in Class 2 deposits. They proposed new well configurations to maximize production and alleviate a persistent problem of substantial secondary hydrate (or ice) formation in a narrow zone ($r < 10$ m) around the well. Using the properties and conditions representative of the Tigershark formation and producing at an initial constant mass rate of $Q_M = 19.2$ kg/s (=10,000 BPD), Moridis and Reagan [131] showed (Fig. 13) that (a) Q_M cannot be

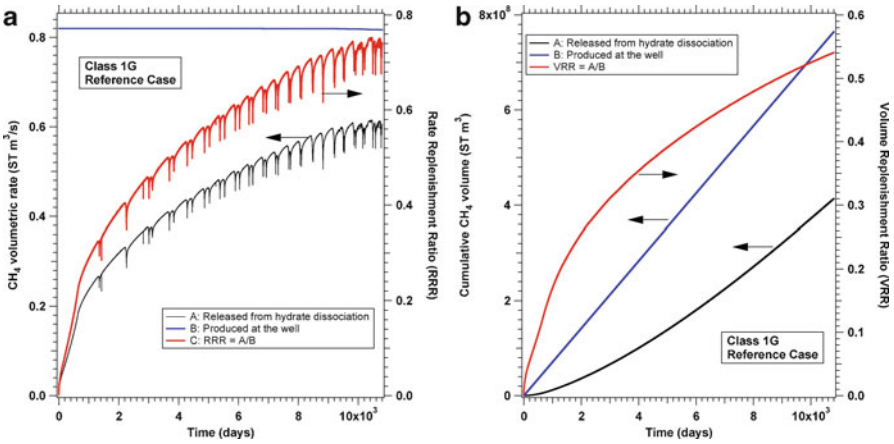

Fig. 11 Gas production from a class 1 hydrate deposit. *Left*: evolution of (a) the rate of CH_4 release from hydrate dissociation, (b) the rate of CH_4 production at the well, and (c) the corresponding rate replenishment ratio over the 30-year production period. *Right*: evolution of (a) the cumulative CH_4 volume released from hydrate dissociation, (b) the produced CH_4 volume at the well, and (c) the corresponding volume replenishment ratio over the 30-year production period [129]

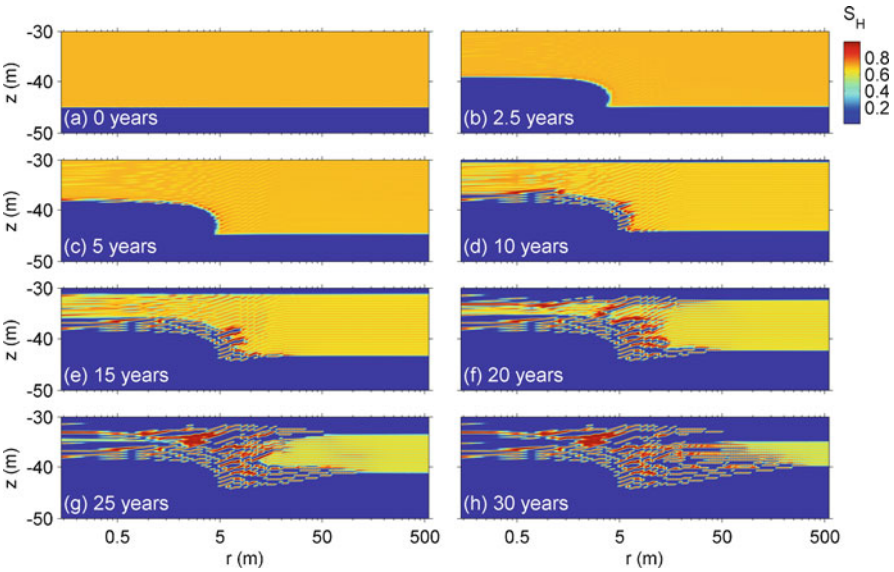

Fig. 12 Evolution of the hydrate saturation S_H distribution in a class 1 hydrate deposit during depressurization [129]

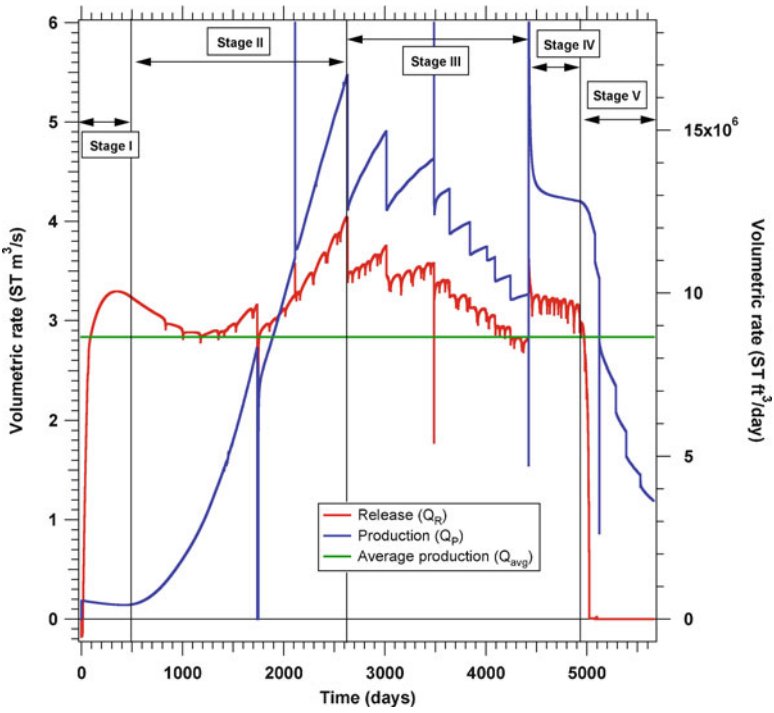

Fig. 13 Rates of (a) hydrate-originating CH_4 release in the reservoir (Q_R) and (b) CH_4 production at the well (Q_P) during production from a class 2 oceanic hydrate deposit. Several production stages and the average production rate (Q_{avg}) over the simulation period (5,660 days) are also shown [131]

maintained constant during the production period (but has to decline), (b) the gas production rate is highly variable, (c) it is encumbered by a long initial lead time during which little gas is produced, but (d) it can reach levels as high as $Q_P = 4.8 \times 10^5$ m³/day (=17 MMSCFD), with an average gas production Q_{avg} over the 5,660-day period of simulation is about 2.2×10^5 m³/day (=7.8 MMSCFD). This study showed very high recovery from hydrate deposits, although economic and geomechanical considerations may limit total recovery. Similar results were obtained from the study of an oceanic Class 2 deposit in the Ulleung Basin of the Korean East Sea [136] and (b) a permafrost-associated deposit in the North slope [133, 134], leading to the observation that Q_P on the order of several MMSCFD is attainable in Class 2 deposits despite significant differences in reservoir temperature, HBS thickness, and salinity.

The use of horizontal wells can substantially improve gas production from such deposits and reduce the initial period of low Q_P [137]. Conversely, Moridis and Kowalsky [128] determined that Q_P was too low to justify considering such accumulations as viable targets in the presence of permeable boundaries and/or with a deep WZ.

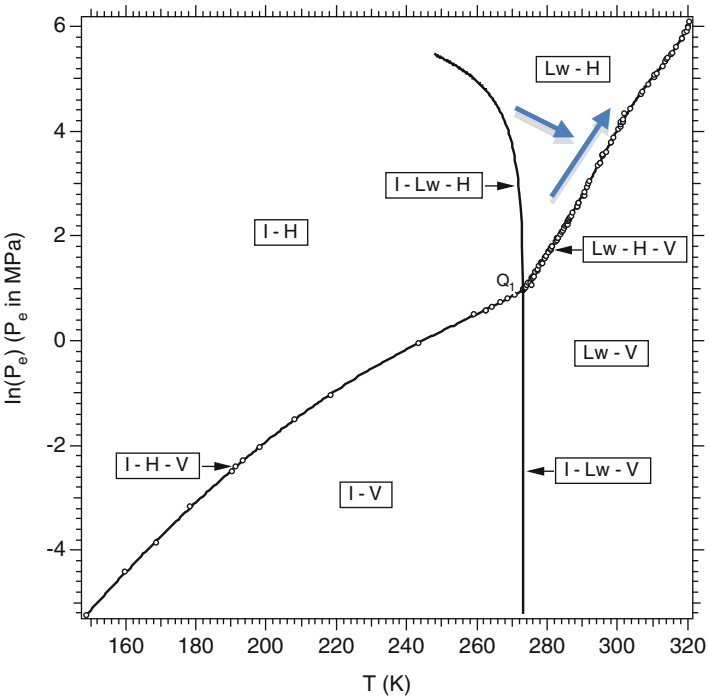

Fig. 14 Pressure-temperature equilibrium relationship in the phase diagram of the water-CH_4 hydrate system [123]. The two *arrows* show the direction of increasing thermodynamic desirability of a deposit as a production target. *Lw* liquid water; *H* hydrate; *V* vapor (gas phase); *I* ice; Q_1 quadruple point = I + Lw + H + V

4.4 Gas Production from Class 3 Deposits

Moridis and Reagan [132] indicated that production at a constant bottom-hole pressure is the most promising strategy in Class 3 hydrate deposits because it is applicable to a wide range of formation k, allows continuous and automatic rate increases to match the increasing k_{eff} (the result of the dissociation-caused reduction in S_H), and it eliminates the possibility of ice formation through the selection of a bottom-hole pressure above that at the quadruple point of hydrates (Fig. 14).

Figure 15 shows the gas production rates from a Class 3 deposit with the properties of the 18 m-thick Tigershark accumulation (see [132]) when using constant bottomhole-P depressurization. Q_p followed a cyclical pattern that includes long rising segments, followed by short precipitous drops (a behavior caused by the self-controlled formation and destruction of secondary hydrates around the well). It reached a maximum $Q_p = 4.3 \times 10^5$ ST m^3/day of CH_4 (=15 MMSCFD), with an average $Q_{avg} = 2.3 \times 10^5$ ST m^3/day (=8.10 MMSCFD) over the 6,000-day production period, and with manageable water production. These results indicated that gas can

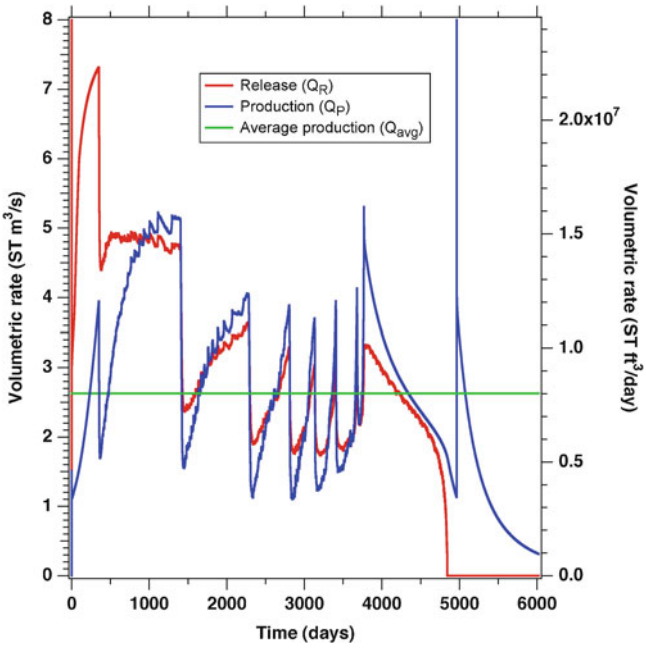

Fig. 15 *Left*: rates of (a) hydrate-originating CH_4 release in the reservoir (Q_R) and (b) CH_4 production at the well (Q_p) during constant-*P* production from a class 3 oceanic hydrate deposit. The average production rate (Q_{avg}) over the simulation period (6,000 days) is also shown [132]

be produced from Class 3 deposits at high rates over long times using conventional well technology.

5 Desirability of Potential Hydrate Targets

Although the available body of information on production from hydrates is still limited, there is sufficient information to begin identifying particular features, properties, conditions, and production methods that are linked to a higher gas production potential and increase the desirability of hydrate deposits, and to use this information to develop a set of guidelines for the selection of promising production targets.

5.1 Desirable Features and Conditions

These include the following [125]:

- Large formation k and φ, which are almost invariably associated with sandy and gravely formations that are characterized by low P_{cap}, S_{wir}, and S_{gir}, leading to relatively high permeability to gas and aqueous flow.

- Medium S_H (i.e., $30\% < S_H < 60\%$) corresponds to optimal Q_P in terms of magnitude and length of time to attain it. The effect of S_H on production is not monotonic, but a complex function of S_H and the timeframe of observation. A lower S_H has the advantage of higher k_{eff}, leading to an earlier evolution of gas and a larger initial Q_P [131, 132]. The disadvantages of a lower S_H may include a larger water production and a lower total gas production because of early exhaustion of the resource. A high S_H leads to slower evolution of gas and lower initial Q_P, but a higher maximum Q_P and total production.
- The most desirable targets can be easily identified from the inspection of the phase diagram (Fig. 14). The larger T provides a larger source of sensible heat to support the endothermic dissociation, and a larger initial P allows a larger pressure drop, leading to larger production rates. Thus, (a) hydrates that occur along the equilibrium line are very desirable, and (b) the desirability increases with an increasing equilibrium P (and, consequently, T). The production potential *decreases* as the stability of the hydrate deposit at its initial conditions *increases* (as quantified by the pressure differential $\Delta P = P - P_e$ at the prevailing reservoir T). In practical terms: we target the deepest, warmest reservoirs that are as close as possible to equilibrium conditions. In addition, the deeper reservoirs have larger overburdens and are therefore less prone to adverse geomechanical impacts.
- For reservoirs with the same hydraulic properties, S_H, and P: the warmest possible deposit is the most desirable. For reservoirs with the same hydraulic properties, S_H, and T: the reservoir with the lowest possible P is the most desirable.
- In terms of deposit classes: All other conditions and properties being equal, Class 1 deposits appear to be the most promising targets for gas production because of the thermodynamic proximity to the hydration equilibrium. Additionally, the existence of a free gas zone guarantees gas production even when the hydrate contribution is small.
- Class 2 and Class 3: Class 2 deposits can attain high production rates, but are also burdened by longer lead times of very little gas production; Class 3 deposits may yield gas earlier and can attain significant production rates, but there are indications that these are lower than in Class 2. The relative merits of these two types will likely be determined by site-specific conditions.
- All classes: The difficulties of site access notwithstanding deeper and warmer oceanic accumulations appear to be more productive than permafrost ones they can have (a) a higher T (14°C is the maximum equilibrium temperature observed in permafrost-associated deposits) and a larger sensible heat available for dissociation and (b) a higher P, increasing the depressurization effectiveness, in addition to (c) the beneficial dissociating effect of salt.
- All classes: The importance of impermeable or near-impermeable upper boundaries cannot be overemphasized.
- In terms of production method: Depressurization appears to have a clear advantage in all three classes.

5.2 Undesirable Features and Conditions

These include the following [125]:

- Class 4 deposits: Earlier studies by Moridis and Sloan [140] have indicated the hopelessness of such deposits under any combination of conditions and production practices.
- Fine sediments (i.e., rich in silts and clays), deformed fractured systems, and hydrates in veins and nodules despite high S_H, because of the geomechanical instabilities in such systems under production.
- In Class 2 deposits: Inappropriate well configurations [131].
- In Class 2 deposits: Constant-P production, because it can lead to early breakthrough and massive water production; however, such an approach can be used in a short-term flow test to determine the HBL properties [55].
- In Class 2 deposits: Deep WZ, and/or permeable overburden and underburden, can drastically reduce gas production [160]. Additionally, the use of multi-well (five-spot) systems involving simultaneous depressurization (at the production well) and thermal stimulation (through warm water injection) appears disappointing [128].
- In all Classes: Permeable upper boundaries drastically reduce production [157, 160].
- In all Classes: Pure thermal dissociation methods and/or inhibitor methods have high cost and limited (and continuously eroding) effectiveness [132].
- In all Classes: S_H that are so high that the remaining fluids are below their irreducible saturation levels. Such hydrates may not be prone to depressurization-induced dissociation.
- In all Classes: Fracturing appears to have limited effect on increasing productivity from hydrate deposits [53, 94].

6 Remaining Challenges

The concerted international effort during the last decade has led to significant progress and important advances [125, 127]. While most of the most important issues affecting gas production from geological GH systems have been addressed or are being addressed, some important issues need further attention and examination. Below we discuss the remaining challenges.

6.1 Challenges in the Analysis and Interpretation of Geophysical Surveys

This issue has been the subject of recent extensive review articles. The interested reader is directed to the papers of Bellefleur et al. [5], Dvorkin and Uden [42], Hardage et al. [62], Lee et al. [103], Inks et al. [71], and Boswell [9] for detailed

discussions. In general, the current consensus is that GH exploration is fairly well advanced when assessing deep deposits at high S_H, but challenges remain with respect to shallow hydrates and GH of complex geometries. The well-log analysis following the 2002 Mallik Test [35] still represents the state of the art in this subject. In log analysis, the approach appears to be well established for the sand reservoirs, but for grain-displacing, clay-hosted hydrates, further work is needed [102].

The current bottleneck in the state-of-practice of geophysical analysis is centered on the relationship between measured physical parameters and S_H. In particular [103, 173]:

- Electrical conductivity and Archie's Law: most applications use empirical and fitting parameters, leading to good fits to the data but uncertain predictions.
- P-wave velocity data—Biot-Gassman. The constrained modulus is strongly affected by the stiffness of the pore fluid, leading to potential error magnification in the assessment of S_H from Vp.
- S-wave velocity dependence on S_H and pore habit: proper constitutive models are needed for effective stress-dependent sediment shear stiffness and to account for the impact of hydrate on skeletal stiffness.

Laboratory-scale, borehole-scale and field-scale geophysical measurements are all conducted at different frequencies and wavelengths, hence they sense different temporal and spatial conditions, and caution is advised in the interpretation of measurements. An even bigger challenge is the need to expand to integrated geophysical analyses that include multicomponent seismic surveys [63, 174], in combination with promising EM techniques [43, 163, 201, 211, 175].

6.2 Challenges in Sampling and Sample Analysis

Sediment sampling and the interpretation of properties measured using samples are among the most challenging tasks in geo-engineering. A sample is expected (1) to represent the sediment constitution (grain size, mineralogy, and fluids), (2) to capture the statistics of the sediment characteristics, and (3) to preserve its physical properties. Unfortunately, most of these characteristics are seriously compromised in the sampling of HBS because of (a) unavoidable changes in effective stress and ensuing strains, (b) S_H changes during sample recovery, handling, and storage, and (c) discrepancies between GH feature scale and scale of sampling [127].

There are several initiatives to overcome or circumvent these difficulties. New technology developed at the Georgia Institute of Technology makes possible pressure core testing to characterize HBSs without ever exposing them outside the PT-stability field [222]. A significant effort is in progress to relate index properties to the bounds of HBS properties [31, 45, 221], and to further complement the analysis with geomechanical and geophysical testing [31, 70, 101, 113]. We can anticipate that further developments in sediment characterization will include more extensive developments in in situ testing. Finally, proper formation characterization

will combine information gathered using index-property-based bounds, reconstituted specimens, pressure cores, and in situ testing data.

6.3 Well Testing and Interpretation Issues

Well testing is a key technique that is widely employed for reservoir characterization. Well-testing and pressure transient analysis (PTA) techniques are complementary to other characterization techniques as (1) they fill a gap between the small-scale characterization based on cores and logs, and large-scale characterization based on geophysical measurements, and (2) they provide a measure of flow capacity, in contrast to static properties determined from other techniques.

In hydrate reservoirs, there are at least three reported cases of pressure transient tests that along with other techniques have been used for reservoir characterization. There has been an evolution in the techniques available for interpretation of the test results. Initially, techniques developed for conventional reservoirs were applied, ignoring temperature and phase change effects associated with hydrate dissociation. Kurihara et al. [92] determined that there is a reasonable agreement between the effective permeability k_{eff} found from application of the conventional PTA techniques, and the average k_{eff} over the dissociation zone obtained from a simulation model, but cautioned that the application of conventional PTA techniques to hydrate reservoirs is not straightforward. Gullapalli et al. [55] suggested that estimates of k_{eff} from conventional analysis could not be used because of significant uncertainties, and supported the use of hydrate-specific numerical simulators. Gerami and Pooladi-Darvish [49] developed a semi-analytical PTA technique for the interpretation of the flow (drawdown) data and parameter estimation for hydrate reservoirs that are underlain by a free-gas zone, which they verified against data from numerical simulators.

Despite the steady progress in testing and interpretation of the well-test data, significant challenges remain.

6.3.1 Theoretical Challenges

An ideal well-test interpretation solution should be *comprehensive* enough to incorporate the important mechanisms, and sufficiently *simple* to allow estimation of the controlling properties and parameters through inversion. This has been possible in the case of hydrate-capped gas reservoir [49]. Similar solutions for more prevalent GH accumulations, i.e., those that are within the hydrate stability zone and coexist with formation water, have yet to be developed. It is known whether such a complex and nonlinear problem can be simplified sufficiently to yield analytical solutions. Further complexities make the application of such solutions (even if they are possible) problematic. Thus, the strong nonlinearity of the hydrate problem renders the principle of superposition (upon which a large part of well-testing techniques are founded) inapplicable. Additionally, the concept of radius of influence may be inapplicable to GH reservoirs [127].

6.3.2 Practical Challenges

Actual well-test data from GH deposits are scarce. It is expected that our ability to interpret these tests will improve as we acquire more well-test data of longer duration [127].

6.4 Geomechanical Challenges and Well Stability Related to Production from Hydrate Deposits

The geomechanical response of HBS in general, and potential well instability and casing deformation in particular, are serious concerns that need to be addressed and understood before gas production from hydrate deposits can be developed in earnest. Deposits that are suitable targets for production often involve poorly consolidated sediments that are usually characterized by limited shear strength. The dissociation of the solid hydrates (a strong cementing agent) can degrade the structural strength of the HBS, which is further exacerbated by the evolution of expanding gas zone, progressive transfer of loads from the hydrate to the sediments, and subsidence. The problem is at its highest intensity in the vicinity of the wellbore where the largest changes are concentrated, and is further complicated by production-induced changes in the reservoir pressure and temperature. These can significantly alter the local stress and strain fields, with direct consequences on the wellbore stability, the flow and fluid properties of the system, the potential for coproduction of solid particles, and the overall gas production.

Recent coupled flow-geomechanical simulations investigated wellbore and reservoir instability during depressurization-based production from known oceanic and permafrost-related hydrate deposits [169–171]. The modeling results show that geomechanical responses during depressurization-based gas production are driven by the reservoir-wide pressure depletion, ΔP, which is in turn controlled by the production rate and pressure decline at the well. The depressurization of the reservoir causes vertical compaction and stress changes, which in most cases will increase the shear stresses within the reservoir, which in turn can induce shear failure. The effect of pressure depletion on subsidence and stress during gas production from an oceanic Class 2 deposit in Fig. 16 shows that subsidence is proportional to the magnitude of ΔP, and depends on the elastoplastic properties of the HBS. In general, subsidence will be much larger in oceanic HBS because of much larger ΔP than in the case of permafrost-associated deposits. For the example in Fig. 16, the subsidence is about 2.5 m, and is a result of compaction in the hydrate-free, relatively soft, zone of mobile water. In the case of production from permafrost deposits at Mallik and Mt. Elbert, ΔP was limited to a few MPa, resulting in a subsidence of only a few centimeters and a compaction strain of less than 1% [171]. Subsidence in this case is also reduced as a result of a relatively stiff permafrost overburden. A general observation is that subsidence occurs uniformly over a large lateral distance from the well, and may thus be less of a hazard to overlying structures.

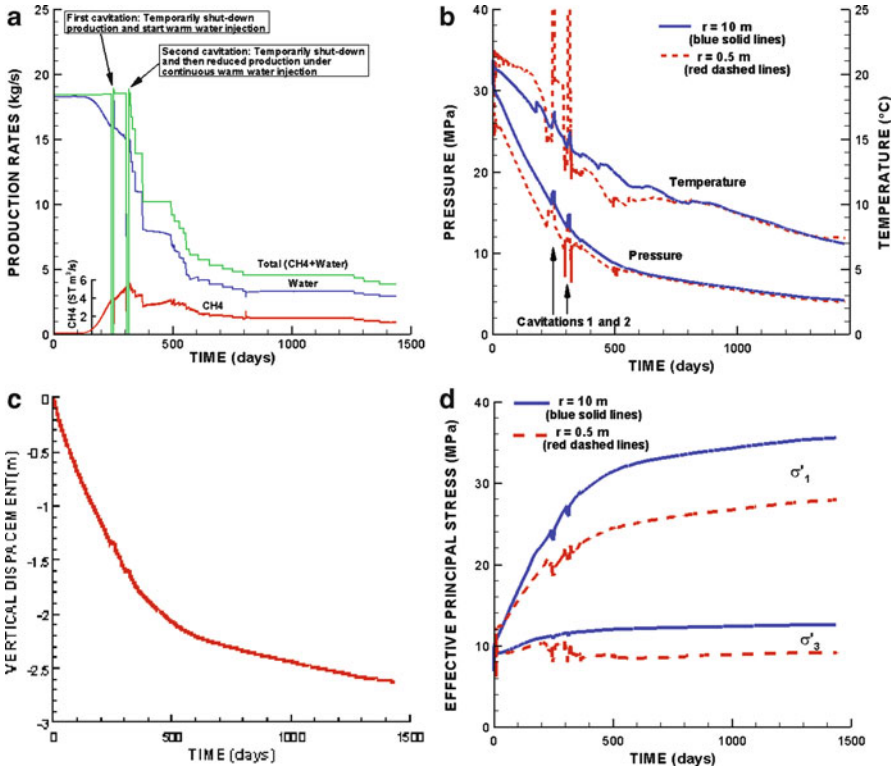

Fig. 16 Numerical simulation results of depressurization-based gas production from a class 2 oceanic hydrate deposit using a vertical production well: (**a**) production rates (CH_4, water, and total rates), (**b**) pressure and temperature, (**c**) vertical displacement (subsidence), and (**d**) maximum and minimum principal stresses [127]

Rutqvist and Moridis [170] showed that the likelihood of inducing shear failure in the reservoir (a) depends on the initial stress field and the Poisson's ratio of the host sediment, and (b) it is higher in the case of an oceanic HBS. If the stress field is initially near critical stress for shear failure, even a small pressure decline could suffice to trigger shear failure in parts of the dissociated reservoir, thus enhancing subsidence and sand production.

Stress changes and associated strain resulting from depressurization strongly affect well stability and the load on the well casing [168]. In vertical wells, the pressure depletion will generally unload the formation uniformly in a plane normal to the axis of the well, and the load on the well casing will decrease. In horizontal wells, vertical compaction of the formation acting against the upper part of the relatively stiff well casing will likely cause shear failure in the formation in that area. Such shearing of the formation can break the bonds between particles, resulting in sand production and creation of cavities around the wellbore. Several studies indicate the

difficulty of avoiding shear failure in the formation around the production intervals of the wells, and highlight the need for appropriate engineering measures to prevent solid production [127].

HBS stress changes and the vertical compaction can be substantial in oceanic HBS. Moreover, formation failure may also occur in the form of pore collapse, in which the mean effective stresses increase so much that inelastic grains slippage and rearrangement occurs. Oceanic HBS are often at the highest effective stress in their geological life, which means that their pre-consolidation pressure would likely be exceeded during depressurization-induced production. Under pore collapse, ϕ and k may be subjected to more substantial, and often irreversible, changes. Such processes and their affect on the gas production from the HBS need to be further investigated.

6.5 Challenges in Well Design, Operation, and Installation in Hydrate Deposits

Dedicated GH production wells will have to both drill and produce through and in HBS. This presents a number of unique design challenges which must be considered for both onshore and offshore GH wells including reservoir subsidence, loss of mechanical strength of the HBS along the wellbore, and development of high external pressures along the wellbore [46, 168]

Reservoir compaction greater than 5% is a consistent indicator for potential casing failures. Casing shear is the dominant failure mechanism, typically located in the overburden up to several 100 ft above the reservoir. There is typically little that can be done to prevent casing shear, other than strategic well placement. Field development economics should include a suitable budget for future well replacements if casing shear is expected. Reservoir subsidence can also result in tensile failures of the casing above the reservoir, and buckling failure within the reservoir. Tensile failures may be prevented through the use of slip joints or length expandable casing joints, placed strategically in the wellbore. Casing failures due to column buckling in the reservoir interval can be prevented by selecting heavy wall casings and by employing good cementing and solids control practices.

6.6 Challenges in Field Operations of Production from Hydrate Deposits

GH dissociation takes place in the reservoir. The transformation of the solid GH into gas and free water begins next to the well, and moves outward over time as dissociation continues. The well design must allow for the production of natural gas with variable

amounts of free water. GH wells will be more complex than most conventional and unconventional gas wells because of a number of technical challenges, including:

- Maintaining commercial gas flows with high water production rates. The water production from a GH reservoir could be highly variable, and water-to-gas ratios in excess of 1,000 bbls/MMSCF (i.e., 100 times larger than what is expected in conventional gas wells) are possible. This requires some form of artificial lift.
- Operating with low temperatures and low pressures in the wellbore to prevent hydrate formation or freezing in the wellbore and flowlines—this is critical for onshore developments producing from below thick permafrost layers. Coupled with the high water production, this requires larger wellbore, tubing, and flowlines in order to minimize friction losses.
- Controlling formation sand production into the wellbore.
- Ensuring well-structural integrity with subsidence in the reservoir and GH dissociation around the wellbore.

Technologies exist to address all of these issues, but add to development costs, especially compared to other nonconventional sources of natural gas. GH development also has one distinct challenge compared to other unconventional resources, and that is the high cost of transportation to market. Additionally, GH developments cannot be effectively drilled at the close well spacing that is used in heavy oil because of the much lower value of gas.

6.7 Challenge of Extending Production Beyond Sand Reservoirs

Currently, the greatest potential for gas hydrate production is in units of sand lithology with high intrinsic permeability [10], a condition that (a) enables the fluid and gas migration necessary for gas hydrate has to accumulate to S_H of 60% or more of pore volume, (b) allows easier transmission of destabilizing pressure and temperature pulses from wellbores, and (c) provides the pathways by which dissociated gas can be produced. It is currently not well known how large the resource of gas hydrate that exists in sand reservoirs is, but it is clearly sizeable. Current best estimates are that the in-place resources within sand reservoirs in the GOM alone likely exceed 6,000 tcf of gas. Given expected recovery efficiencies, a technically recoverable resource exceeding 1,000 tcf or more is reasonable.

However, this sand-based resource is just the tip of the hydrate resource pyramid [9]. Large volumes of in-place methane are known to exist within fine-grained sediments in locations such as the Blake Ridge [148], offshore India [27], Malaysia [57], and Korea [176, 147]. Such occurrences may be relatively common, and may occur more widely than the sand-hosted variety. Economic and environmentally sound production from such deposits clearly faces enormous technical challenges, not only because of the leanness of the resource but also because of their adverse

flow and geomechanical properties. While gas production from sandy HBS is conceivable using largely existing processes, it is clear that much more needs to be known, and perhaps fundamentally new approaches developed, to further the prospects of production from elements lower in the gas hydrates resource pyramid.

6.8 Challenges in Monitoring Production and Geomechanical Stability in Gas Hydrate Accumulations

There is an increasing need to identify suitable techniques for monitoring hydrate accumulations during production. The feasibility of remotely monitoring GH accumulations during production is only beginning to be examined. The type of geophysical measurement that has been used most successfully for exploration is surface seismic. 2D and 3D surface seismic surveys have been used extensively for mapping the distribution of GH accumulations, delineating their large-scale features and providing rough estimates of the average S_H. Advanced processing techniques can provide depth-varying S_H estimates over large areas (e.g., [30, 96, 149]), though their applicability depends on the depth and thickness of the hydrate.

In exploration surveys, little prior information is available, and the primary goal is to determine whether hydrate is present and, if so, how much. In contrast, investigations using geophysical techniques for monitoring production focus on much smaller regions in the vicinity of production wells and require higher resolution and measurement repeatability in order to image small variations in properties.

6.8.1 Challenges in Monitoring Production with Geophysical Methods

In order to use geophysical methods to monitor production from hydrate accumulations, a number of fundamental challenges must be considered. They can be summarized as follows:

Suitability of geophysical methods depends on geological setting and expected production behavior. The spatial and temporal evolution of physical properties in a hydrate accumulation differs dramatically depending on the type of the deposit and the dissociation method, thus requiring different monitoring methods. For example, the study of Moridis and Reagan [114] predicted that depressurization-induced production from the Tigershark deposit would effect changes in the HBL extending to a radius of 800 m from the production well, and including decreasing thickness of the HBL, increasing gas saturation, decreasing S_H, and the formation of free gas layers above and below the HBL. Kowalsky et al. [83] showed that such complex changes appear to be amenable to detection with time-lapse VSP measurements collected in a well 50 m away from the production well. Another study on production from a permafrost-associated hydrate accumulation in North Slope, Alaska [15] showed changes that were mostly limited to within 5 m from the production well

after 2 years of production, making the system far less ideal for VSP monitoring than in the previous case. Cross-borehole measurements may be more promising in some cases, though the spatial coverage they provide is limited to the inter-borehole region, and there is the risk of non-detection if the changes in the HBL are not pronounced [210].

Rock physics models dependence on geological setting and time-varying hydrate configuration. A considerable amount of research has been performed to determine rock physics models (the relationships between sediment properties and geophysical properties) for HBS based on theoretical considerations, laboratory experiments, and field data (e.g., [65, 100, 216]). Depending on the geological setting, GH can be distributed in a variety of ways (e.g., acting as cement between grains, acting as the matrix supporting the grains, or existing mainly in pore space), which dramatically affect the seismic and electrical properties of the sediment mixture [206]. For the purpose of geophysical monitoring at a given site, the rock physics model must be determined in advance using site-specific data such as well logging and core data. However, care must also be taken to account for the geophysical properties changes during production because the hydrate and gas saturations may move to ranges beyond those used to develop the models. It may be necessary to change models in the course of production as the hydrate conditions change, a subject that has not received much attention.

Simultaneously changing physical properties can lead to nonunique interpretations of time-lapse geophysical data. Because geophysical properties are a function of the saturations of all phases in the system, in addition to pore fluid pressures, it is difficult to uniquely attribute the change in a geophysical measurement exclusively to S_H changes. For example, during depressurization-induced production from a GH deposit, the P-wave velocity can vary due to changes in both the effective pressure and in phase saturations. As the fluid pressure decreases, the stresses and the frame bulk moduli of the sediment increase [41]. At the same time, the increases in velocity are offset by the effects of the decreasing hydrate saturation and increased gas saturation [89].

6.8.2 Coupled Modeling of Production and Geophysical Response

Given the susceptibility of particular types of hydrate deposits to geomechanical changes, and the possibility for severe stability and well stability consequences, the ability to monitor geomechanical changes by geophysical means is particularly appealing. A modeling approach that allows for the coupled simulation of hydrate production and corresponding geophysical measurements is a useful tool for constraining the interpretation of geophysical data collected during a production test and for designing appropriate geophysical surveys.

This approach was used to conduct a feasibility study for using VSP measurements to monitoring production from a submarine hydrate accumulation in the GOM [89]. The study indicated that, (a) for an incoming P-wave source, the most

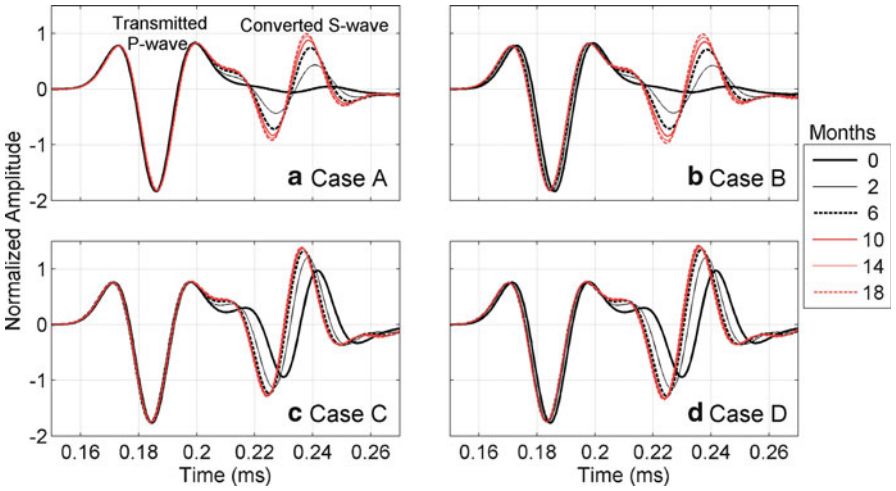

Fig. 17 Seismic signal recorded approximately 100 m below the bottom of a hydrate-bearing layer in a simulated VSP survey [89]. The horizontal component of the waveform is shown with the transmitted P-wave and converted S-wave arrivals. Waveforms are shown at six survey times (0, 2, 6, 10, 14, and 18 months after the start of production) for four different rock physics models (**a**–**d**)

reliable indicators of changing conditions in the HBL appear to be converted S-waves transmitted through the HBL and recorded below it, and reflected P-waves and converted S-waves recorded above the HBL, and (b) the response was strongly dependent on the chosen rock physics models (Fig. 17). Future improvements to this approach should include linkage to coupled flow-geomechanical codes (e.g., [170]). In addition, other types of measurements that provide complementary but lower resolution information, such as electrical and electromagnetic data, should be evaluated.

6.9 Challenges in Laboratory Investigations in Support of Gas Production Analysis

Laboratory investigations are performed on natural samples and laboratory-synthesized samples to understand the thermodynamic properties, gas composition, mechanical, electrical, thermal, and hydrologic properties of HBS. Understanding these properties is important in predicting (a) the amount of gas that can be produced from a reservoir, (b) providing "ground-truth" for geophysical and well-log measurements [23, 28, 29], (c) understanding the mechanical strength of the reservoir medium, and (d) understanding how gas will be produced.

6.9.1 Natural Samples

The results of examining and testing natural HBS cores in the laboratory environment are dependent on the quality of the collected core, and the quality of the subsampling and analysis. Gas hydrate is stabilized by elevated constituent gas pressure, as affected by the temperature and inhibitor concentration in the pore water. Drilling often requires dense muds with high ionic strength, which can alter pore water chemistry and cause hydrate dissociation (e.g., [193]). Oil-based muds can be used to minimize pore water chemistry changes [12]. Pressure coring has been used to stabilize cores at their initial reservoir pressures [23, 28, 29], and appropriate sampling equipment such as the instrumented pressure testing chamber [220–222] was developed. Field-based X-ray imaging and CT scanning, useful for understanding the core conditions and to identify representative locations for sampling and analysis, have been performed for pressurized and non-pressurized core [23, 28, 29, 67, 81].

Preserving core for later examination requires careful handling. Many measurements require briefly removing a sample from hydrate-stable conditions to transfer it into a testing apparatus. Waite et al. [205] and Kneafsey et al. [84] reported that such handling results in hydrate redistribution that affects the mechanical, flow, thermal, and electrical properties of the sample. Freezing samples in liquid nitrogen preserves the hydrate and may be the best technique for maintaining the hydrate chemistry, but that can induce extensive fracturing (caused by large thermal stresses) and affect non-chemistry measurements [84]. X-ray computed tomography (CT) can be useful in the selection of undamaged and representative parts of a GH-bearing core for sampling. Prior to testing, a preserved core needs to be returned to its natural conditions by imposing very mild thermal gradients and using materials that do not fail at the preservation temperatures (usually liquid N_2).

Because of the GH sensitivity, it can be argued than an undisturbed sample has yet to be collected. Because of the importance of such samples in the evaluation of the feasibility of gas production, the subject needs further attention.

6.9.2 Laboratory-Synthesized Samples

Many conventional laboratory investigations have been performed on laboratory-synthesized samples. These allow the flexibility of creating samples that have desired characteristics. Few laboratory-synthesized samples have been examined for uniformity, and this characteristic is often (perhaps hastily and undeservedly) assumed. Several methods are in use for making HBS, and each has its advantages and disadvantages.

Hydrate from ice. In this method, powdered ice is slowly melted in the presence of methane at the appropriate pressure and temperature [187]. As the ice melts, methane hydrate is formed. Sequential freezing and melting events can result in very high conversions to hydrate. The hydrate can then be chilled in liquid nitrogen, powdered, mixed with a selected chilled mineral medium, and compacted into a

hydrate-bearing medium. Nanoscale examination of HBS formed this way by scanning electron microscope compares favorably to natural HBS from the Mallik site [186]. HBS formed this way will typically fill pores as well as be part of the frame of the medium.

Hydrate from partially water saturated media—Excess Gas. In this method, a prescribed amount of water is uniformly added to a mineral medium, compacted into a sample vessel, and the hydrate stability conditions are exceeded [61, 87, 208]. Hydrate formed using this technique typically cements mineral grains together forming a stiff sample [208].

Hydrate from partially water saturated media—Excess Water. Using a somewhat different approach, Priest et al. [154] formed methane hydrate by placing the quantity of gas needed to form a specific amount of hydrate in a porous sample, pressurizing the sample with water, and then chilling the sample to bring it into the hydrate stability field. Their work suggests that hydrate interaction with the sediment is strongly dependent on hydrate morphology, with results indicating that hydrate formed this way is frame supporting. Additionally, natural GH may exhibit a different seismic signature depending on the environment in which it formed.

Hydrate from dissolved guest phase. In this method, water containing dissolved methane is flowed through a chilled porous medium where hydrate is formed. Although there have been some successes using this technique, it is difficult to control and time consuming [184, 185].

Micromodel studies of gas hydrates. Several studies have been performed allowing direct microscopic examination of hydrate formation, aging, and dissociation in transparent micromodels [76–78, 191, 192]. These studies show formation of hydrate with and without a gas phase, formation of dendritic hydrate crystals that age over time into particulate hydrate crystals, and faceted hydrate crystals formed at low subcooling. The presence of a water film between the hydrate and the micromodel cell walls has been observed in some tests, but not in others leading to the conclusion that hydrate may cement grains together when formed with a low degree of subcooling.

6.9.3 Thermodynamic Properties

Sloan and Koh [178] summarized (a) laboratory measurements and (b) models that provide estimates of the heat of hydrate formation and dissociation, in addition to equilibrium conditions (P, T, and inhibitor concentrations) of various states for many hydrate systems. Clarke and Bishnoi [17] and Kim et al. [79] studied the kinetics of hydrate formation and measured the activation energy and intrinsic rate constant of methane hydrate decomposition. Modeling by Moridis et al. [126, 138] has shown that dissociation kinetics plays a limited-to-no role in gas production from hydrate at the reservoir scale, but may be important in short-term laboratory studies.

Handa and Stupin [61, 202, 203] and Lu and Matsumoto (2002) investigated the effect of the properties of porous media on the hydration characteristics, and reported significant deviations between the measured hydration temperatures and those predicted from the known equilibrium curve of pure methane, i.e., temperature shifts varied from −12.3 to 8°C. The implication of these studies is that the medium properties and texture may play a defining role in hydrate equilibrium. The subject has not been fully addressed, and it has not been represented in numerical simulators, thus increasing the uncertainty of their predictions.

6.9.4 Thermal Properties

Laboratory measurements of thermal properties of methane HBS have been made by a number of researchers [56 60, 69, 126, 138, 164, 200, 204, 206, 207] Two thermal properties are important: thermal conductivity and specific heat. The specific heat of a GH-bearing medium can be computed using a mixing model and the specific heats of the components present, and does not pose a challenge. The thermal conductivity of pure methane hydrate differs from that of water by less than 10%. Although it is possible to make coarse estimates of the thermal conductivity of a hydrate bearing medium that has water and hydrate in the pore space by considering the medium to be water saturated only [165], laboratory studies have shown that GH-bearing media have higher thermal conductivity than water-saturated media [126, 138] The difference is substantial, and thus this approximation is not valid because of the paramount importance of heat transfer in hydrate dissociation.

6.9.5 Flow Properties

Flow properties of HBS have been investigated because of their importance in understanding the nature and formation of hydrate-bearing reservoirs and gas production. The main properties that are needed are (a) the formation effective permeability k_{eff} in the presence of solid phases, (b) the relative permeabilities of the aqueous and gas phases in the (potentially) four-phase system (gas, aqueous, hydrate, and ice), and (b) the relationship of the capillary pressure P_{cap} to the saturations of the fluid phases. Where the hydrate is part of the skeletal frame of the medium, the formation k_{eff} can be estimated but not measured, and hydrate dissociation will alter the structure of the medium. Moridis et al. [130] proposed two conceptual methods of handling this issue, but laboratory confirmation has not yet been attempted.

Capillary pressure and relative permeabilities in a HBS are generally dependent on the saturation of all the phases present in addition to the path (imbibition or drainage), thus they are nonunique functions and exhibit hysteresis. A simple curve can describe these relations for a system with two fluid phases, but the presence of hydrate requires a three-dimensional surface to describe them. To date, no studies have been performed covering the range of saturation values and states in HBS. Various laboratory studies have investigated the relative permeability of mobile

phases in hydrate-bearing media [73, 82, 85, 91, 121]. While these have been useful, they have produced neither sufficient nor consistent data to develop reliable quantitative relationships. No measurements of P_{cap} vs. saturation of methane hydrate-bearing sands have been published, although measurements are being made [83]. These measurements are extremely difficult because the system temperature, pressure, and volume must all be held to precisely maintain equilibrium conditions in the sample over long times while fluid is withdrawn from a sample, hydraulic equilibrium states are attained, and differential pressure is measured.

6.9.6 Mechanical Properties

A systematic study of the mechanical properties of THF-HBSs by Yun et al. [223] has yielded useful insights, but the applicability to HBS systems has yet to be demonstrated. No corresponding systematic study for methane HBS has been published, although such studies have been initiated. The mechanical strength of a number of laboratory-formed and natural methane hydrate-bearing samples has also been measured [112, 113], and Waite et al. [206] provided a summary of laboratory measurements of the mechanical properties of HBS. Studies on mechanical properties of HBS have been hampered by complex equipment needs, and the difficulties of working with methane hydrate. Data are needed particularly for hydrate saturations below 50% and for fine-grain media because much of the hydrate in oceanic deposits is present in low saturations providing risk to oil and gas operations.

6.9.7 Electromagnetic Properties

Knowledge of electrical properties of GH-bearing media is useful in hydrate prospecting and monitoring HBS undergoing changes during gas production. Either electrical conductivity or permittivity can be used to distinguish between water and non-water pore filling materials such as hydrate and gas. Electrical conductivity is dominated by the conductivity of the pore fluid; however, surface conduction must be considered for high surface area sediments [81]. Under conditions where hydrate forms or dissociates, the pore fluid conductivity will change due to freshening (hydrate dissociation) or ion exclusion (hydrate formation). Because the effect of ionic concentration is much weaker for the permittivity, this may be the more reliable indicator in many circumstances. The systematic examination of the effects of THF hydrate on the electrical properties of various media [104, 106] provided useful qualitative insights, but applicability to methane systems has not been determined. No comprehensive study has been performed for methane HBS, studies on which has been limited to measurements of electrical resistivity of a few samples [182–185].

6.9.8 Geophysical Properties: Wave Velocities and Attenuation

These are critically important in the exploration, detection, and production monitoring of GH. Compressional (P-) and shear (S-) wave speeds have been measured in a variety of medium/hydrate combinations [6, 219], but these did not involve CH_4 and the results have qualitative value for HBS studies. Waite et al. [208] measured the P- and S-wave velocities of methane hydrates in Ottawa sand at different S_H. These hydrates were formed using the excess gas method and cemented the grains of the sand, resulting in very stiff samples. No systematic tests examining P- and S-wave velocities for a variety of porous media types at a range of methane S_H and pore-filling habits have been published, but such tests are now in progress.

6.9.9 State of Laboratory Studies

Laboratory studies on natural HBS provide results that are dependent on the coring method and all the sample changes that occur prior to the measurement. In spite of these drawbacks, sampling and analysis of natural HBS provides general information on HBS reservoirs and critical site-dependant information. Laboratory studies of laboratory-synthesized HBS suffer from nonuniform samples and samples that are not fully representative of the natural environment. Specialized equipment is needed to maintain and test the samples. Hydrate laboratory researchers are striving to meet these challenges, but further development is needed.

Several types of measurements have been made on HBS over a wide range of media and saturations, particularly with THF hydrate. Studies that can convincingly validate the THF hydrate studies using methane hydrate are needed, especially at the low S_H of natural HBS. Additional studies are needed to quantify fluid flow parameters over the broad range of conditions where hydrates occur. Better understanding of the effects of fines migration and sand production as a result of hydrate dissociation is needed. These and future hydrate studies must use well-characterized specimen that possess the fundamental characteristics of natural in situ HBS including porous medium type, mineralogy, hydrate habit, uniformity, chemistry, and confinement.

6.10 Challenges in Fundamental Knowledge of Hydrate Behavior

Such challenges address the basic conceptual framework upon which theoretical and laboratory studies on the thermodynamics and flow properties of the GH systems are based.

6.10.1 Development of Universal Standards for Hydrate Sample Creation

This is an important challenge for fundamental physico-chemical hydrate research, and it first involves the establishment of a protocol to fabricate artificial hydrate samples in sediment. The second part of this challenge is to ensure that the sample is a reasonable replicate of nature. Currently the method of Spangenberg et al. [181] appears to be dominant; however, months of sample preparation time are required, and there is an urgent need for a more time-effective techniques.

6.10.2 Thermodynamic Knowledge Gaps and Time-Dependence Issues

Gibbs energy minimization methods are currently the most effective tools in determining the behavior of complex hydrates involving more than CH_4 (a subject that needs to be tackled, as such hydrates are likely in GH systems), and form the basis of the statistical thermodynamics approach in the description of the properties and behavior of such systems. Because of serious experimental difficulties, the predictions of these methods currently cannot be verified in a large part of the *P-T-X* spectrum of composite hydrates, and especially in the presence of more than one inhibitors. Additionally, time-dependent measurements are required, to establish kinetic phenomena, which are currently confounded by the addition of heat and mass transfer.

6.10.3 Multiphase Flow

Another fundamental knowledge challenge is to establish a verified transient model of multiphase flow, which is experimentally validated. Currently two-phase flow systems are fairly well established. However, a rigorous three- or four-phase transient model with experimental verification in flow loops is beyond the current state of the art. The accurate modeling and experimental validation of such phenomena in systems with coexistent of three or four of the gas, oil, water, ice, and hydrate phases will be vital to hydrate control in both energy production and flow assurance.

6.10.4 Hysteretic P-T Behavior

While the CH_4 system that is used almost exclusively in gas production study is thought to be well understood and described, an important issue (with significant implications) that has yet to be investigated is the hysteresis between the *P-T* relationships in a warming and cooling hydrate system. All predictions reported in the literature have relied exclusively on the warming *P-T* relationships, while the cooling *P-T* relationships have not even been quantified. The cooling *P-T* curve has a very different behavior (attributed to metastability) that is characterized by a long

period of very slight pressure drop during continuous cooling, followed by a precipitous drop in *P* beyond a certain point. Because cooling and secondary hydrate formation are quite common in the course of hydrate production [131, 132], such *P-T* behavior can have a significant effect on production.

6.10.5 Fast P-T-X Parametric Relationships in Composite Hydrates

Even small amounts of a second hydrate-forming gas in addition to CH_4 (a common occurrence in geologic GH deposits) can drastically alter the properties and behavior of hydrates. While statistical thermodynamics approaches [178] allow good descriptions of the composite system, these are cumbersome, slow, and unsuitable for use in numerical simulators. Thus, there is a significant need for fast parametric relationships describing the composite hydrate behavior over the *P-T-X* spectrum.

6.11 Economic Challenges of Commercial Gas Production from Hydrates

Because there are currently no unconventional developments, oil or gas, in the frontier areas where hydrates occur, and because these areas also contain significant amounts of developed and undeveloped conventional gas resources with no access to markets, GHs will have to compete with frontier conventional gas developments. This puts GHs at a distinct disadvantage compared to other unconventional gas resources (such as the booming shale-gas production in the United States) for access to the larger North American gas market. While a local market use of gas from gas hydrates may be feasible at some point, this situation appears likely to defer the timing of GH developments until sometime in the not-too-near future. Offshore GH developments may proceed sooner if the premium price required is not onerous when there is no conventional gas competition, and where security of supply is a major consideration.

The studies of Hancock et al. [59], Hancock [58], and the review study of Moridis et al. [127] were the first in-depth analyses of the economics of gas production from hydrates, and their results, while preliminary, have been encouraging. Assuming 2009 prices, it appears that (a) for onshore gas hydrates, stand-alone developments could be economic with a gas price in the upper range of historical North American prices, and (b) for offshore gas hydrates, stand-alone developments could be economic with a gas price in the upper range of what India has been paying for liquefied natural gas imports on the spot market. Thus, using the admittedly limited data from the numerical predictions of gas production in the literature [58, 59], it appears that a reasonable rate of return (i.e., 15%) can be achieved with prices in the order of $6.00–$12.00/MSCF for offshore and onshore projects, respectively (Figs. 18 and 19). However, considering the various risks and uncertainties associated with such production (well performance, geological uncertainty, reservoir characteristics,

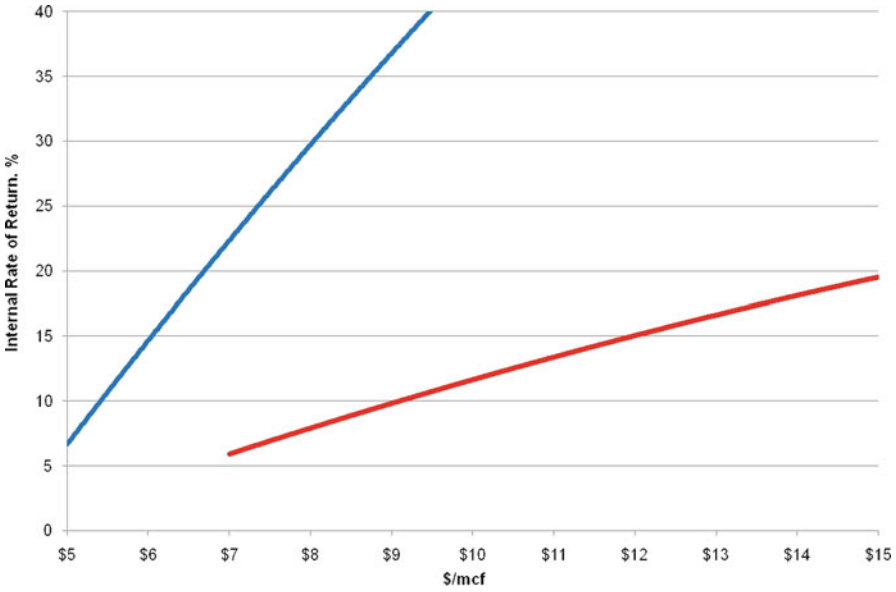

Fig. 18 Internal rate of return as a function of gas price ($/MSCF) for gas from onshore hydrates

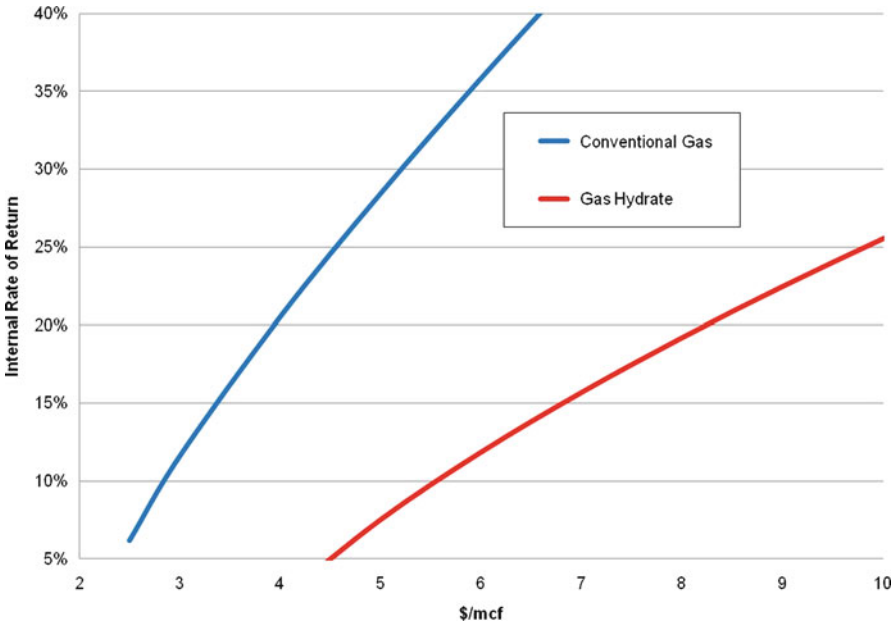

Fig. 19 Internal rate of return as a function of gas price ($/MSCF) for gas from offshore hydrates

gas-in-place, thermodynamic conditions, the absence of a long-term field test of production from hydrates, proximity to infrastructure, access to markets, uncertainty in forecasting gas prices, etc.), sustained gas contract prices in the range of $10.00–$16.00/MSCF for offshore and onshore projects respectively may be required before GH projects will proceed [127]. Given the current gas price realities, it appears that production from GH may be delayed, although unique circumstances may allow production of onshore gas hydrates for local community or industrial use, especially where there is some underlying gas. Fundamental changes in the North American gas market supply picture, as well as advances in technology may also have a significant impact on the price range required for GH development, and will inevitably affect the timing of commercial gas production from HBS.

6.12 *Environmental Challenges Associated with Gas Production from Hydrates*

A fundamental barrier to the potential utilization of methane from gas hydrates to serve future energy needs relates to our current limited understanding of the GH potential response to production activities and the associated environmental impacts. These impacts will include many issues that typically face current oil and gas exploration and production activities; including ground subsidence related to production from shallow, unconsolidated reservoirs, land and air impacts from drilling and production activities, and disposal of produced waters. Ultimately, despite the fact that GHs may be a major new source of clean-burning gas, it will remain difficult to expect public acceptance of large-scale gas hydrate production in the absence of a larger understanding of the GH role in the natural environment. This is particularly the case given the recognition that naturally occurring GH could provide a potentially deleterious feedback to ongoing climate change.

Gas hydrate is known to be an enormous storehouse of organic carbon with profound potential linkages to global carbon cycling and global climate [3, 38]. GHs are not a significant source of atmospheric greenhouses gases at present [72], but there is evidence in the geologic history attesting to the impact of methane from gas hydrate on global climates (e.g., [39]). This impact is enhanced by the powerful "greenhouse effect" of CH_4 than CO_2 (about 20 times larger) despite a short residence in the atmosphere [72]. Recent reports suggest that ongoing CH_4 releases from shallow marine gas hydrates (particularly at high latitudes) may be linked to warming climates [150, 156, 158, 159, 212], although there are limited data for confirmation.

At present, the targets of gas hydrate production research are those accumulations in the Arctic or beneath the ocean floor that are housed in deep sand reservoirs bounded by nearly impermeable boundaries. As such, they are beyond the reach of potential climate-related temperature changes and are not expected to pose an environmental hazard as sources of methane release into the atmosphere. These represent perhaps a significant resource volume, but is likely a very small percentage of the total in-place volume of methane associated with gas hydrates [9]. Thus, it is a

critical task to assess the real potential impacts associated with only this small subset of resources that occupy the peak of the total gas hydrate resource pyramid [10].

Desirable production targets involve deeper, warmer sandy GH deposits [136]. Such deposits are closer to the stability conditions (requiring less energy for dissociation) and are housed in sediments of increased mechanical strength bounded by low-permeability strata. These settings render the deposits amenable to production through standard borehole-based techniques, reduce the tendency for sand production, and are less likely to affect the integrity of the overlying sealing lithologies. Environmentally invasive approaches, such as mining of sea floor and shallow subsea-floor deposits are not a consideration. This is not only because of regulatory restrictions (as such operations would harm protected complex and poorly understood biological communities that hydrates are known to host) but also because of the economic hopelessness of such a venture (given the resource leanness of such deposits and the astronomical cost of such sea floor operations). In other words, not the targets of gas hydrate production are generally environmentally insensitive.

An issue that deserves attention is the ability of the lithologic seal overlying GH reservoirs to contain the dissociated gas, which is known to accumulate at the top of the formation [136, 131, 132]. For shallow and unconsolidated reservoirs, the possibility of failure of the top seal is a serious consideration. Therefore, all responsible production test scenarios currently envisioned include plans to actively monitor the movement of the dissociation front and of the released gas accumulation in the reservoir [217].

Gas hydrate exploration and production activities will be prone to many of the same potential environmental impacts as conventional oil and gas production. A key issue will be ground subsidence: in the marine setting, this may mean assessing the risk for seafloor failure on slopes or other issues that may compromise the integrity of sea-floor infrastructure. In the arctic, this relates to preserving the integrity of the permafrost. Careful selection of drill sites and management of production processes, such as sand control procedures, are expected to be adequate to address such issues. Another issue may be water disposal. Gas hydrate production may result in significant volumes of produced water. Although the dissociated hydrate water will be virtually fresh, there will be an inevitable mixing with formation waters that will result in the production of brackish, non-potable water, which is anoxic and potentially harmful to chemosynthetic communities if released near the ocean floor. Such water will need to be handled and disposed of properly. However, none of these issues are unique to gas hydrates—and methods are currently being employed in a variety of settings to deal with even more acute impact issues.

7 Summary

Gas hydrates are a vast resource with a global distribution in the permafrost and in the oceans. Even if a conservative estimate is considered and only a small fraction is recoverable, the sheer size of the resource is so large that it demands evaluation

as a potential energy source. Although difficulties exist, the development of hydrates into an energy source appears to have acquired its own global dynamic, with increased levels of international awareness, several national and international programs investigating the feasibility of the endeavor, and heightened levels of activity. There is a concerted international effort to determine the technical and economic feasibility of production from gas hydrates.

Production from gas hydrates faces significant challenges because of the hostile environments in which they exist. The difficulty of access, the significant cost of related work, and the need for success in the first attempt at producing gas from this unconventional source have led to the development of a rational approach to prioritize potential targets. By need and design, the first attempts to produce gas from hydrates will be limited to the few relatively well-characterized sites with proven resources.

Numerical simulation plays a critical role in the effort to assess the production potential of hydrates. While the dearth of field data has not allowed the full validation of numerical codes, the scientific consensus is that the models generally account for the important physics of the problem, and that validation and calibration (rather than adequacy of the numerical code capabilities) will be a constraining factor in the assessment of the hydrates as an energy resource. A review of the data needs for the implementation of the numerical models indicates that, while knowledge gaps exist, these are being addressed, or can be adequately addressed by sensible approximations. Sensitivity analyses can overcome the scarcity of data needed by the simulators by bounding the potential solutions. Literature review provides strong indications that gas hydrates from a variety of types of deposits (even ones considered unproductive a few years ago) can yield large amounts of gas at high rates over long periods using conventional technologies. This bodes well for the production potential of this unconventional resource.

The challenges and uncertainties facing commercial gas production from hydrates touch upon technical, economic, and environmental issues, and include (1) the assessment of in-place vs. resource vs. producible fractions of the GH resource, (2) the development and evaluation of methodologies for identifying suitable production targets, (3) the sampling of HBSs, sample analysis, and interpretation of the results, (4) the analysis and interpretation of geophysical surveys of GH reservoirs, (5) well-testing methods and interpretation of the results, (6) geomechanical and reservoir/well stability concerns in the course of gas production, (7) well design, operation, and installation appropriate for the particularities of GH systems, (8) field operations of production, (9) extending production beyond sand-dominated GH reservoirs, (10) monitoring production and geomechanical stability, (11) laboratory investigations and practices in support of gas production analysis, (12) fundamental knowledge of hydrate behavior, (12) the economics of commercial gas production from hydrates, and (13) the associated environmental concerns.

Acknowledgments The contributions of G.J. Moridis, T. Kneafsey, J. Rutqvist, M. Kowalsky, and M. Reagan were supported by the Assistant Secretary for Fossil Energy, Office of Natural Gas and Petroleum Technology, through the National Energy Technology Laboratory, under the U.S. Department of Energy, Contract No. DE-AC02-05CH11231.

References

1. Anderson BJ, Kurihara M, White MD, Moridis GJ, Wilson SJ, Pooladi-Darvish M, Gaddipati M, Masuda Y, Collett TS, Hunter RB, Narita H, Rose K, Boswell R (2011) Regional long-term production modeling from a single well test, Mount Elbert Gas Hydrate Stratigraphic Test Well, Alaska North Slope. J Mar Pet Geol 28:493–501. doi:10.1016/j.marpetgeo.2010.01.015
2. Anderson BJ, Wilder, JW, Kurihara M, White MD, Moridis GJ, Wilson SJ, Pooladi-Darvish M, Masuda Y, Collett TS, Hunter RB, Narita H, Rose K, Boswell R (2008) Analysis of modular dynamic formation test results from the Mount Elbert 01 stratigraphic test well, Milne Point Unit, North Slope, Alaska. Proc. 6th International Conference on Gas Hydrates, Vancouver, British Columbia, Canada, 6–10 July 2008
3. Archer D (2007) Methane hydrate stability and anthropogenic climate change. Biogeosciences 4:521–544
4. Backus M, Murray M, Hardage B, Graebner R (2006) High-resolution multi-component seismic imaging of deepwater gas hydrate systems. Leading Edge 25(5):578–593
5. Bellefleur G, Riedel M, Brent T (2006) Seismic characterization and continuity analysis of gas hydrate horizons near Mallik research wells, Mackenzie Delta, Canada. Leading Edge 25(5):599–606
6. Berge LI, Jacobsen KA, Solstad A (1999) Measured acoustic wave velocities of R11 (CCl3F) hydrate samples with and without sand as a function of hydrate concentration. J Geophys Res 104:15415–15424
7. Bird KJ, Magoon LB (1987) Petroleum geology of the northern part of the Arctic National Wildlife Refuge, Northeastern Alaska. US Geol Surv Bull 1778:324
8. Boswell R (2007) Resource potential of methane hydrate coming into focus. J Pet Sci Eng 56:9–13
9. Boswell R (2009) Is gas hydrate energy within reach? Science 325:957–958
10. Boswell R, Collett T (2006) The Gas Hydrate Resource Pyramid, Fire In The Ice, NETL Methane Hydrates R&D Program Newsletter. Fall 2006. http://www.netl.doe.gov/technologies/oil-gas/publications/Hydrates/Newsletter/HMNewsFall06.pdf
11. Boswell R, Collett T, McConnell D, Frye M, Shedd W, Mrozewski S, Guerin G, Cook A, Shelander D, Dai J, Godfriaux P, Dufrene R, Jones E, Roy R (2010) Gulf of Mexico Gas Hydrate Joint Industry Project Leg II: Overview of Leg II LWD Results, OTC 20560, 2010 Offshore Technology Conference, Houston, TX, 3–5 May. doi:10.4043/20560-MS
12. Boswell R, Hunter R, Collett TS, Digert S, Hancock M, Weeks M (2008) Investigation of gas hydrate bearing sandstone reservoir at the Mount Elbert stratigraphic test well, Milne Point, Alaska. Proc. 6th International Conference on Gas Hydrates, Vancouver, BC, July 6–10 2008
13. Boswell R, Shelander D, Lee M, Latham T, Collett T, Guerin G, Moridis G, Reagan M, Goldberg D (2009) Occurrence of gas hydrate in Oligocene Frio sand: Alaminos Canyon Block 818: Northern Gulf of Mexico. J Mar Pet Geol 26(8):1499–1512. doi:10.1016/j.marpetgeo.2009.03.005
14. Bunz S, Meinert J (2005) Overpressure distribution beneath hydrate-bearing sediments at the Storegga Slide on the Mid-Norwegian margin. Proc. ICGH 2005, vol 3, pp 755–758
15. Cherskiy NV, Tsaarev VP, Nikitin SP (1982). Petrol Geol 21: 65
16. Chiaramonte L, Kowalsky MB, Rutqvist J, Moridis GJ (2009) Design of a potential long-term test of gas production from a hydrate deposit at the PBU-L106 site in North Slope, Alaska: Geomechanical system response and seismic monitoring. Eos Trans AGU 90(52):Fall Meet. Suppl, Abs. OS24A-08
17. Clarke M, Bishnoi PR (2001) Determination of the activation energy and intrinsic rate constant of methane gas hydrate decomposition. Can J Chem Eng 79(1):143–147
18. Collett T (1993) Natural gas hydrates of the Prudhoe Bay and Kuparuk River area, North Slope, Alaska. Am Assoc Pet Geol Bull 77(5):793–812
19. Collett T (1995) 1995 National Assessment of U.S. Oil and Gas Resources (on CD-ROM). In: Gautier DL, Goldton GL et al (eds) USGS

20. Collett T (2004) Gas hydrates as a future energy resource. Geotimes. http://www.agiweb.org/geotimes/nov04/feature_futurehydrates.html
21. Collett T (2007) Arctic Gas Hydrate Energy Assessment Studies, The Arctic Energy Summit, Anchorage, Alaska, 15–18 Oct 2007
22. Collett T (2008) Assessment of Gas Hydrate Resources on the North Slope, Alaska, 2008, OS43F-08, AGU Fall Meeting 2008, San Francisco, CA, 15–19 Dec 2008
23. Collett TS, Agena WF, Lee MW, Zyrianova MV, Bird KJ, Charpentier TC, Houseknect DW, Klett TR, Pollastro RM, Schenk CJ (2008) Assessment of gas hydrate resources on the North Slope, Alaska, 2008. USGS Fact Sheet 2008–3073, 4. http://pubs.usgs.gov/fs/2008/3073/
24. Collett TS, Boswell R, Frye M, Shedd W, Godfriaux P, Dufrene R, McConnell D, Mrozewski S, Guerin G, Cook A, Jones E, Roy R (2010) Gulf of Mexico Gas Hydrate Joint Industry Project Leg II: Logging-While-Drilling Operations and Challenges, OTC 20452, 2010 Offshore Technology Conference, Houston, TX, 3–5 May. doi:10.4043/20452-MS
25. Collett T, Ginsburg G (1998) Gas hydrates in the Messoyakha gas field of the West Siberian Basin—a re-examination of the geologic evidence. Int J Offshore Polar Eng 8(1):22–29
26. Collett T, Lee M (2006) Well Log Analysis: Tiger Shark AC 818 No. 1, U.S. Geological Survey, internal memo
27. Collett T, Riedel M, Boswell R, Cochran J, Kumar P, Sethi A, Sathe A (2006) International Team Completes Landmark Gas Hydrate Expedition in the Offshore of India, Fire In The Ice, NETL Methane Hydrates R&D Program Newsletter. Fall 2006. http://www.netl.doe.gov/technologies/oil-gas/publications/Hydrates/Newsletter/HMNewsFall06.pdf
28. Collett TS, Riedel M, Cochran JR, Boswell R, Kumar P, Sathe AV et al (2008) Indian continental margin gas hydrate prospects: results of the Indian National Gas Hydrate Program (NGHP) Expedition 01. Proc. 6th International Conference on Gas Hydrates, Vancouver, British Columbia, Canada, 6–10 July 2008. http://hdl.handle.net/2429/1035
29. Collett TS et al (2008) Indian national gas hydrate program expedition 01 initial reports: Expedition 01 of the Indian National Gas Hydrate Program from Mumbai, India to Chennai, India; Sites NGHP-01-01 through NGHP-01-21, April 2006–August 2006, Directorate General of Hydrocarbons, Ministry of Petroleum and Natural Gas (India), Noida, India
30. Computer Modeling Group (2006) Steam, thermal, and advanced processes reservoir simulator (STARS). Online: http://www.cmgroup.com/software/stars.html
31. Dai S, Lee CH, Santamarina JC (2010) Mount Elbert sediments (with and without hydrates): characteristics, mechanical properties and geophysical parameters, submitted to Mar. Pet. Geo
32. Dai J, Snyder F, Gillespie D, Koesoemadinata A, Dutta N (2008) Exploration for gas hydrates in the deepwater northern Gulf of Mexico, Part I: a seismic approach based on geologic model, inversion, and rock physics principals. Mar Pet Geol 25:845–859
33. Dallimore SR, 2006-08 Mallik Team (2007) Community Update on the 2006–2008 JOGMEC/NRCan/Aurora Mallik Gas Hydrate Production Research Program, Northwest Territories, Canada, Fire In The Ice, NETL Methane Hydrates R&D Program Newsletter Spring/Summer 2007.http://www.netl.doe.gov/technologies/oil-gas/publications/Hydrates/Newsletter/HMNewsSpringSummer07.pdf
34. Dallimore SR, Collett TS (1995) Intrapermafrost gas hydrates from a deep core hole in the Mackenzie Delta, Northwest Territories, Canada. Geology 23:527–530
35. Dallimore SR, Collett TS (eds) (2005) Scientific Results from the Mallik 2002 Gas Hydrate Production Research Well Program, Mackenzie Delta, Northwest Territories, Canada, Geological Survey of Canada Bulletin 585
36. Dallimore SR, Uchida T, Collett TS (1999) Scientific results from JAPEX/JNOC/GSC Mallik 2L-38 gas hydrate research well, Mackenzie Delta, Northwest Territories, Canada. Geol Surv Can Bull 544:403
37. Dallimore SR, Yamamoto K (2008) Overview of the 2006–2008 JOGMEC/NRCan/Aurora Mallik Gas Hydrate Production Test Program, OS43F-06, AGU Fall Meeting 2008, San Francisco, CA, 15–19 Dec 2008
38. Dickens G (2003) Rethinking the global carbon cycle with a large, dynamic, and microbially-mediated gas hydrate capacitor. Earth Planet Sci Lett 213:169–183

39. Dickens G, O'Neil J, Rea D, Owen R (1995) Dissociation of oceanic methane hydrate as a cause of carbon isotope excursion at the end of the Paleocene. Paleooceanography 10:965–971
40. Durham WB et al (2003) The strength and rheology of methane clathrate hydrate. J Geophys Res 108(B4):2182
41. Dvorkin J, Prasad M, Sakai A (1999) Elasticity of marine sediments: rock physics modeling. Geophys Res Lett 26(12):1781–1784
42. Dvorkin J, Uden R (2006) The challenge of scale in seismic mapping of hydrate and solutions. Leading Edge 25(5):637–643
43. Edwards RN (1997) On the resource evaluation of marine gas hydrate deposits using a seafloor transient electric dipole-dipole method. Geophysics 62:63–74
44. Fan S, Zhang J, Wang J (2005) Progress of gas hydrate studies in China. Proc. ICGH 2005, vol 3, pp 1012–1021
45. Francisca FM, Yun TS, Ruppel CD, Santamarina JC (2005) Geophysical and geotechnical properties of near-surface sediments in the northern Gulf of Mexico gas hydrate province. Earth Planet Sci Lett 237:924–939
46. Freij-Ayoub R, Clennell B, Tohidi B, Yang J, Hutcheon R (2007) Casing Integrity in Hydrate Bearing Sediments. Proc. 6th International Offshore Site Investigation and Geotechnics Conference, London, UK, Sept 2007
47. Fujii T, Nakamizu M, Tsuji Y, Okui T, Kawasaki M, Ochiai K (2005) Modes of occurrence and accumulation mechanism of methane hydrate—result of METI exploration test wells "Tokai-oki to Kumano-nada". Paper 3041, Proc. ICGH 2005, vol 3, pp 974–979
48. Fujii T, Saeki T, Kobayashi T, Inamori T, Hayashi M, Takano O, Takayama T, Kawasaki T, Nagakubo S, Nakamizu M, Yokoi K (2008) Resource Assessment of Methane Hydrate in the Eastern Nankai Trough, Japan. OTC 19310, Proc. 2008 Offshore Technology Conference, Houston, Texas, USA, 5–8 May 2008
49. Gerami S, Pooladi-Darvish M (2009) An early-time model for drawdown testing of a hydrate-capped gas reservoir. SPE Res Eval Eng 12(4):596–609
50. Ginsburg GD, Soloviev VA (1995) in OTC 7693, 27th annual offshore technology conference, Houston, 1–4 May 1995
51. Gornitz V, Fung I (1994) Potential distribution of methane hydrate in the world's oceans. Global Biogeochem Cycles 8:335
52. Graue S, Kvamme B, Baldwin BA, Stevens J, Howard J, Aspenes E, Ersland G, Husebo J, Zomes D (2008) MRI visualization of spontaneous methane production from hydrates in sandstone core plugs when exposed to CO_2. SPE J 13(2):146–152. doi:10.2118/118851-PA
53. Grover T, Moridis GJ, Holditch S (2008) Analysis of Reservoir Performance of the Messoyakha Hydrate Reservoir, SPE 114375, 2008 SPE Annual Technical Conference and Exhibition, Denver, Colorado, 21–24 Sept 2008
54. Guerin G, Cook A, Mrozewski S, Collett T, Boswell R (2009) Gulf of Mexico Gas Hydrate Joint Industry Project Leg II—Green Canyon 955 Logging While Drilling (LWD): Operations and Results. http://www.netl.doe.gov/methanehydrates/JIPLegII-IR
55. Gullapalli I, Moridis GJ, Silpngarmlert S, Reik B, Kamal M, Jones E, Collett T (2008) Designing A Reservoir Flow Rate Experiment For The GOM Hydrate JIP Leg II LWD Drilling. Proc. 6th International Conference on Gas Hydrates (ICGH 2008), Vancouver, British Columbia, Canada, 6–10 July 2008
56. Gupta A et al (2006) Composite thermal conductivity in a large heterogeneous porous methane hydrate sample. J Phys Chem B 110(33):16384–16392
57. Hadley C, Peters D, Vaughan A, Bean D (2008) Gumusut-Kakap Project: Geohazard Characterisation and Impact on Field-Development Plans, IPTC 12554-MS. International Petroleum Technology Conference, Kuala Lumpur, 3–5 Dec 2008
58. Hancock S (2008) Development of Gas Hydrates. Proc. New Zealand Petroleum Conference, Auckland, New Zealand, March 2008
59. Hancock S, Okazawa T, Osadetz K (2005) A Preliminary Investigation of the Economics of Onshore Gas Hydrate Production. Proc. 7th Annual Conference on Unconventional Gas, Calgary, Alberta, Nov 2005

60. Handa YP (1986) Compositions, enthalpies of dissociation, and heat capacities in the range 85 to 270 K for clathrate hydrates of methane, ethane, and propane, and enthalpy of dissociation of isobutane hydrate, as determined by a heat-flow calorimeter. J Chem Thermodyn 18(10):915–921
61. Handa YP, Stupin DY (1992) Thermodynamic properties and dissociation characteristics of methane and propane hydrates in 70-.ANG.-radius silica gel pores. J Phys Chem 96(21):8599–8603
62. Hardage BA, Murray P, Sava D, Backus M, Remington R, Graebner R, Roberts HH (2006) Evaluation of deepwater gas-hydrate systems. Leading Edge 25(5):572–577
63. Hardage BA, Roberts HH, Murray PE, Remington R, Sava DC, Shedd W, Hunt, J (2009) Multicomponent seismic technology assessment of fluid-gas expulsion geology, Gulf of Mexico. In: Collett T, Johnson A, Knapp C, Boswell R (eds) Natural gas hydrates: energy resource and associated geologic hazards. The American Association of Petroleum Geologists Memoir 89
64. Harvey LDD, Huang Z (1995) Evaluation of potential impact of methane clathrate de- stabilization on future global warming. J Geophys Res 100(D2):2905
65. Helgerud M, Dvorkin J, Nur A, Sakai A, Collett T (1999) Elastic-wave velocity in marine sediments with gas hydrates: effective medium modeling. Geophys Res Lett 26(13):2021–2024
66. Holbrook WS, Hoskins H, Wood WT, Stephen RA, Lizarralde D (1996) Leg 164 science party. Science 273:1840
67. Holland ME, Schultheiss PJ, Roberts JA, Druce M (2008) Observed Gas Hydrate Morphologies in Marine Sediment. Proc. 6th International Conference on Gas Hydrates (ICGH 2008), Vancouver, British Columbia, Canada, 6–10 July 2008
68. Hong H, Pooladi-Darvish M (2005) Simulation of depressurization for gas production from gas hydrates reservoirs. J Can Pet Technol 44:39–46
69. Huang D, Fan S (2005) Measuring and modeling thermal conductivity of gas hydrate-bearing sand. J Geophys Res 110:10
70. Hyodo M, Nakata Y, Yoshimoto N, Ebinuma T (2005) Basic research on the mechanical behavior of methane hydrate sediment mixtures. Soils Found 45:75–85
71. Inks TL, Lee MW, Agena WF, Taylor DJ, Collett TS, Hunter RB, Zyrianova MV (2010) Seismic prospecting for gas hydrate and associated free-gas prospects in the Milne Point area of northern Alaska. In: Collett T, Johnson A, Knapp C, Boswell R (eds) Natural gas hydrates—energy resource potential and associated geologic hazards. American Association of Petroleum Geologists Memoir 89
72. IPCC (2007) Climate Change 2007: The Physical Science Basis: Intergovernmental Panel on Climate Change http://www.ipcc.ch/
73. Jaiswal NJ (2004) Measurement of gas-water relative permeabilities in hydrate systems. MS Thesis, University of Alaska Fairbanks, Fairbanks, AK
74. Jones E, Latham T, McConnell D, Frye M, Hunt J, Shedd W, Shelander D, Boswell R, Rose K, Ruppel C, Hutchinson D, Collett T, Dugan B, Wood W (2008) Scientific objectives of the Gulf of Mexico gas hydrate JIP Leg II drilling, Paper OTC-19501, 2008 Offshore Technology Conference, Houston, TX, 5–8 May
75. Judge A, Smith S, Majorowicz J (1994) The current distribution and thermal stability of natural gas hydrates in the Canadian Polar Regions, in Proceedings Fourth International Offshore and Polar Engineering Conference, Osaka, Japan, pp 307–313
76. Katsuki D, Ohmura R, Ebinuma T, Narita H (2006) Formation, growth and aging of clathrate hydrate crystals in a porous medium. Philos Mag 86(12):1753–1761
77. Katsuki D, Ohmura R, Ebinuma T, Narita H (2007) Methane hydrate crystal growth in a porous medium filled with methane-saturated liquid water. Philos Mag 87(7):1057–1069
78. Katsuki D, Ohmura R, Ebinuma T, Narita H (2008) Visual observation of dissociation of methane hydrate crystals in a glass micro model: production and transfer of methane. J Appl Phys 104(8):083514–083519
79. Kim HC, Bishnoi PR, Heidemann RA, Rizvi SSH (1987) Kinetics of methane hydrate decomposition. Chem Eng Sci 42(7):1645–1653

80. Klauda JB, Sandler SI (2005) Global distribution of methane hydrate in ocean sediment. Energy Fuel 19:469
81. Klein KA, Santamarina JC (2003) Electrical conductivity in soils: underlying phenomena. J Environ Eng Geophys 8:263–273
82. Kleinberg RL et al (2003) Deep sea NMR: methane hydrate growth habit in porous media and its relationship to hydraulic permeability, deposit accumulation, and submarine slope stability. J Geophys Res 108(B10):2508
83. Ghezzehei and Kneafsey in preparation (private communication).
84. Kneafsey TJ, Liu H, Winters W, Boswell R, Hunter R, Collett TS (2011) Analysis of core samples from the BPXA-DOE-USGS Mount Elbert gas hydrate stratigraphic test well: insights into core disturbance and handling. Mar Pet Geol 28:381–393. doi:10.1016/j.marpetgeo.2009.10.009
85. Kneafsey TJ, Seol Y, Gupta A, Tomutsa L (2008) Permeability of Laboratory-Formed Methane-Hydrate-Bearing Sand. Proc. 2008 Offshore Technology Conference, Houston, 4–8 May 2008
86. Kneafsey T, Tomutsa L, Moridis G, Seol Y, Freifeld B (2005) Methane hydrate formation and dissociation in a partially-saturated sand—measurement and observations. Proc. 5th International Conference on Gas Hydrates, vol 1, pp 213–220
87. Kneafsey TJ et al (2007) Methane hydrate formation and dissociation in a core-scale partially saturated sand sample. J Pet Sci Eng 56:108–126
88. Kowalsky MB, Moridis GJ (2007) Comparison of kinetic and equilibrium reaction models in simulating the behavior of gas hydrates in porous media. Energy Convers Manage 48(6): 1850–1863. doi:10.1016/j.enconman.2007.01.017
89. Kowalsky MB, Nakagawa S, Moridis GJ (2010) Feasibility of monitoring gas-hydrate production with time-lapse vertical seismic profiling. SPE J 15(3):634–645. doi:10.2118/132508-PA
90. Krason J, Finley PD (1992) Messoyakh Gas Field—Russia: West Siberian Basin. Amer. Assoc. Petrol. Geol, Treatise of Petroleum Geology, Atlas of Oil and Gas Fields, Structural Traps VII. pp 197–220
91. Kumar A et al (2010) Experimental determination of permeability in the presence of hydrates and its effect on the dissociation characteristics of gas hydrates in porous media. J Pet Sci Eng 70:114–122
92. Kurihara M, Funatsu K, Kusaka K, Masuda Y, Dallimore SR, Collett TS, Hancock SH (2005) Well-test Analysis of Gas Hydrate Reservoirs: Examination of Parameters suggested by Conventional Analysis for the JAPEX/JNOC/GSC et al. Mallik 5L-38 Gas Hydrate Production Research Well, in Scientific Results from the Mallik 2002 Gas Hydrate Production Research Well Program, Mackenzie Delta, Northwest Territories, Canada (ed) Dallimore SR, Collett TS; Geological Survey of Canada, Bulletin 585
93. Kurihara M, Funatsu K, Kusaka K, Yasuda M, Dallimore SR, Collett TS, Hancock SH (2005) Well-Test Analysis for Gas Hydrate Reservoirs: Examination of Parameters Suggested by Conventional Analysis for the JAPEX/JNOC/GSC et al. Mallik 5L-38 Gas Hydrate Production Test Results in Scientific Results from the Mallik 2002 Gas Hydrate Production Research Well Program, Mackenzie Delta, Northwest Territories, Canada. Geological Survey of Canada Bulletin 585, Dallimore SR, Collett T (eds)
94. Kurihara M, Funatsu K, Ouchi H, Masuda Y, Narita H (2005) Investigation on Applicability of Methane Hydrate Production Methods to Reservoirs with Diverse Characteristics. Paper 3003 Proc. 5th International Conference on Gas Hydrates, Trondheim, Norway, 13–16 June, pp 714–725
95. Kurihara M, Ouchi H, Inoue T, Yonezawa T, Masuda Y, Dallimore SR, Collett TS (2005) Analysis of the JAPEX/JNOC/GSC et al. Mallik 5L-38 Gas Hydrate Thermal Production Test Through Numerical Simulation in Scientific Results from the Mallik 2002 Gas Hydrate Production Research Well Program, Mackenzie Delta, Northwest Territories, Canada. Geological Survey of Canada Bulletin 585, Dallimore SR, Collett T (eds)
96. Kurihara M, Sato A, Ouchi H, Narita H, Masuda Y, Saeki T, Fujii T (2008) Prediction of Gas Productivity From Eastern Nankai Trough Methane-Hydrate Reservoirs, OTC 19382. Proc. 2008 Offshore Technology Conference, Houston, Texas, USA, 5–8 May 2008
97. Kvenvolden KA (1988) Methane hydrate–a major reservoir of carbon in the shallow geosphere? Chem Geol 71:41–51

98. Kvenvolden KA (2005) Personal Communication with E. Dendy Sloan, November 28, 2005
99. Kvenvolden KA, Claypool GE (1988) US geological survey open file report 88–216, 50.
100. Lee MW (2002) Biot-Gassmann theory for velocities of gas hydrate bearing sediments. Geophysics 67(6):1711–1719
101. Lee MW, Agena WF, Collett TS, Inks TL (2009) Pre- and post-drill comparison of the Mount Elbert gas hydrate prospect at the Milne Point area, Alaska North Slope. Mar Pet Geol. doi:10.1016/j.marpetgeo.2009.08.007
102. Lee MW, Collett TS (2009) Gas hydrate saturations estimated from fractured reservoir at Site NGHP-01-10, Krishna-Godavari Basin, India. J Geophys Res 114:B07102. doi:10.1029/2008JB006237
103. Lee MW, Collett TS, Inks TL (2010) Seismic attribute analysis for gas-hydrate and free-gas prospects on the North Slope of Alaska. In: Collett T, Johnson A, Knapp C, Boswell R (eds) Natural gas hydrates—energy resource potential and associated geologic hazards. American Association of Petroleum Geologists Memoir 89
104. Lee JY, Santamarina JC, Ruppel C (2008) Mechanical and electromagnetic properties of northern Gulf of Mexico sediments with and without THF hydrates. Mar Pet Geol 25(9):884–895
105. Lee C, Yun TS, Lee JS, Santamarina JC (2011) Geotechnical characterization of marine sediments in The Ulleung Basin, East Sea. Eng Geol 117:151–158
106. Lee JY, Yun TS, Santamarina JC, Ruppel C (2007) Observations related to tetrahydrofuran and methane hydrates for laboratory studies of hydrate-bearing sediments. Geochem Geophys Geosyst 8:Q06003
107. MacDonald GJ (1990) Role of methane clathrates in past and future climates. Climatic Changes 16:247
108. Majorowicz JA, Osadetz KG (2001) Gas hydrate distribution and volume in Canada. AAPG Bull 85(7):1211–1230
109. Makogon YF (1974) Hydrates of natural gas (trans: Cieslesicz WJ). Tulsa, OK, Penn Well
110. Makogon YF (1981) Hydrates of natural gas. Penn Well Publishing Company, Tulsa, p 237
111. Makogon YF (1997) Hydrates of Hydrocarbons. Penn Well Publishing Co, Tulsa
112. Masui A, Haneda H, Ogata Y, Aoki K (2005) The effect of saturation degree of methane hydrate on the shear strength of synthetic methane hydrate sediments. Proc. 5th International Conference on Gas Hydrates, Trondheim, Norway
113. Masui A, Miyazaki K, Haneda H, Ogata Y, Aoki K (2008) Mechanical characteristics of natural and artificial gas hydrate bearing sediments. Proc. 6th International Conference on Gas Hydrates, Vancouver, British Columbia, Canada, 6–10 July 2008
114. Matsumoto R, Tomaru H, Lu H (2004) Detection and evaluation of gas hydrate formation in the Eastern Nankai Trough by geochemical and geophysical methods. Resource Geol 54:53–68
115. McConnell D, Boswell R, Collett T, Frye M, Shedd W, Guerin G, Cook A, Mrozewski S, Dufrene R, Godfriaux P (2009) Proc. Drilling and Scientific Results of the Gulf of Mexico Gas Hydrate Joint Industry Project Leg II: Walker Ridge 313 Site Summary. http://www.netl.doe.gov/technologies/oil-gas/publications/Hydrates/2009Reports/WR313SiteSum.pdf
116. McConnell DR, Collett TS, Boswell R, Frye MC, Shedd W, Dufrene R, Godfriaux P, Mrozewski D, Guerin G, Cook A, Jones E (2010) Gulf of Mexico Gas Hydrate Joint Industry Project Leg II: Initial Results from the Green Canyon 955 Site, OTC 20801. Proc. 2010 Offshore Technology Conference, Houston, TX, 3–5 May. doi:10.4043/20801-MS
117. McConnell D, Kendall B (2002) Images of the base of gas hydrate stability, Northwest Walker Ridge, Gulf of Mexico, OTC-14103. Proc. 2008 Offshore Technology Conference, Houston, TX, 6–9 May. doi:10.4043/14103-MS
118. McConnell D, Zhang Z (2005) Using acoustic inversion to image buried gas hydrate distribution: Fire In The Ice (FITI) newsletter. Fall 3–5. http://www.netl.doe.gov/technologies/oil-gas/publications/Hydrates/Newsletter/HMNewsFall05_HighRez.pdf#page=3
119. McIver RD (1981) Gas hydrates. In: Meyer RG, Olson JC (eds) Long-term energy resources. Pitman, Boston, MA, pp 713–726
120. Milkov AV (2004) Global estimates of hydrate-bound gas in marine sediments: how much is really out there? Earth Sci Rev 66(3):183

121. Minagawa H et al (2005) Water permeability measurements of gas hydrate-bearing sediments. Proc. 5th International Conference on Gas Hydrates, Trondheim, Norway
122. Molochushkin EN (1978) The effect of thermal abrasion on the temperature of the permafrost in the coastal zone of the Laptev Sea: Proceedings of the Second International Conference on Permafrost, Takutsk, USSR, 13–28 July 1973, National Academy of Sciences, Washington, DC, pp 90–93
123. Moridis GJ (2003) Numerical studies of gas production from methane hydrates. SPE Journal 32(8):359–370. doi:10.2118/87330-PA
124. Moridis GJ, Collett TS (2004) Strategies for gas production from hydrate accumulations under various geologic conditions, LBNL-52568. Lawrence Berkeley National Laboratory, Berkeley
125. Moridis GJ, Collett TS, Boswell R, Kurihara M, Reagan M, Koh C, Sloan ED (2009) Toward production from gas hydrates: current status, assessment of resources, and simulation-based evaluation of technology and potential. SPE Reserv Eval Eng 12(5):745–771. doi:10.2118/114163-PA
126. Moridis GJ, Collett TS, Dallimore SR, Inoue T, Mroz T (2005) Analysis and Interpretation of the Thermal Test of Gas Hydrate Dissociation in the JAPEX/JNOC/GSC et al. Mallik 5L-38 Gas Hydrate Production Research Well, in Scientific Results from the Mallik 2002 Gas Hydrate Production Research Well Program, Mackenzie Delta, Northwest Territories, Canada. Geological Survey of Canada, Bulletin 585, Dallimore SR, Collett T (eds)
127. Moridis GJ, Collett TS, Pooladi-Darvish M, Hancock S, Santamarina JC, Boswell R, Kneafsey T, Rutqvist J, Kowalsky M, Reagan MT, Sloan ED, Sum AK, Koh C (2011) Challenges, uncertainties and issues facing gas production from gas hydrate deposits. SPE Res Eval Eng 14(1):76–112. doi:10.2118/131792-PA
128. Moridis GJ, Kowalsky M (2005) Gas production from unconfined Class 2 hydrate accumulations in the oceanic subsurface, Chapter 7. In: Max M, Johnson AH, Dillon WP, Collett T (eds) Economic geology of natural gas Hydrates. Kluwer Academic/Plenum Publishers, pp 249–266
129. Moridis GJ, Kowalsky M, Pruess K (2008) Depressurization-induced gas production from Class 1 hydrate deposits. SPE Reserv Eval Eng 10(5):458–488
130. Moridis GJ, Kowalsky M, Pruess K (2008) TOUGH+HYDRATE v1.0 User's Manual. LBNL-161E, Lawrence Berkeley National Laboratory, Berkeley, CA
131. Moridis GJ, Reagan MT (2007) Strategies for Production from Oceanic Class 3 Hydrate Accumulations. OTC 18865. Proc. 2007 Offshore Technology Conference, Houston, 30 April–3 May 2007
132. Moridis GJ, Reagan MT (2007) Gas Production from Oceanic Class 2 Hydrate Accumulations, OTC 18866, 2007 Offshore Technology Conference, Houston, Texas, USA, 30 April–3 May 2007
133. Moridis GJ, Reagan MT (2011) Estimating the upper limit of gas production from Class 2 hydrate accumulations in the permafrost, 1: concepts, system description and the production base case. J Pet Sci Eng 76:194–201. doi:10.1016/j.petrol.2010.11.023
134. Moridis GJ, Reagan MT (2011) Estimating the upper limit of gas production from Class 2 hydrate accumulations in the permafrost, 2: alternative well designs and sensitivity analysis. J Pet Sci Eng 76:124–137. doi:10.1016/j.petrol.2010.12.001
135. Moridis GJ, Reagan MT, Boswell R, Collett T, Zhang K (2010) Preliminary evaluation of the production potential of recently discovered hydrate deposits in the Gulf of Mexico, Paper OTC 21049, 2010 Offshore technology conference. Houston, Texas, 3–6 May 2010.
136. Moridis GJ, Reagan MT, Kim SJ, Seol Y, Zhang K (2009) Evaluation of the gas production potential of marine hydrate deposits in the Ulleung Basin of the Korean East Sea. SPE J 14(4):759–781. doi:10.2118/110859-PA
137. Moridis GJ, Reagan MT, Zhang K (2008) The Use of Horizontal Wells in Gas Production from Hydrate Accumulations. Proc. 6th International Conference on Gas Hydrates (ICGH 2008), Vancouver, British Columbia, Canada, 6–10 July 2008

138. Moridis GJ, Seol Y, Kneafsey T (2005) Studies of reaction kinetics of the methane hydration reaction in porous media. Proc. 5th International Conference on Gas Hydrates, Trondheim, Norway
139. Moridis GJ, Silpngarmlert S, Reagan MT, Collett TS, Zhang K (2011) Gas production from a cold, stratigraphically bounded hydrate deposit at the Mount Elbert Site, North Slope, Alaska. J Mar Pet Geol 28:517–534. doi:10.1016/j.marpetgeo.2010.01.005, LBNL-3005E
140. Moridis GJ, Sloan ED (2007) Gas production of disperse low-saturation hydrate accumulations in oceanic sediments. Energy Convers Manage 48:1834–1849
141. Mount Elbert Science Team (2007) Alaska North Slope Well Successfully Cores, Logs, and Tests Gas-Hydrate-Bearing Reservoirs, Fire In The Ice, NETL Methane Hydrates R&D Program Newsletter. Winter 2007. http://www.netl.doe.gov/technologies/oil-gas/publications/Hydrates/Newsletter/HMNewsWinter07.pdf
142. Mrozewski S, Cook A, Guerin G, Goldberg D, Collett TS, Boswell R, Jones E (2010) Gulf of Mexico Gas Hydrate Joint Industry Project Leg II: Initial Results from the Green Canyon 955 Site, OTC 20801. Proc. 2010 Offshore Technology Conference, Houston, TX, 3–5 May. doi:10.4043/20801-MS
143. National Energy Technology Laboratory (2007) The National Methane Hydrates R&D Program, Hydrate Modeling—TOUGH-Fx/HYDRATE & HydrateResSim. http://www.netl.doe.gov/technologies/oilgas/FutureSupply/MethaneHydrates/rdprogram/ToughFX/ToughFx.html#HydrateResSim
144. Osadetz KG, Chen Z (2005) A re-examination of Beaufort Sea—Mackenzie Delta Basin gas hydrate resource potential using a petroleum system approach. Proc. 5th International Conference on Gas Hydrates, Trondheim, Norway, 13–16 June 2005
145. Osterkamp TE, Fei T (1993) Potential occurrence of permafrost and gas hydrates in the continental shelf near Lonely, Alaska. Proc. Sixth International Conference on Permafrost, Beijing, China, 5–9 July 1993. National Academy of Sciences, Washington, DC
146. Park KP (2006) Gas Hydrate Exploration in Korea. Proc. 2nd International Symposium on Gas Hydrate Technology, Daejeon, Korea, 1–2 Nov
147. Park K-P, Bahk J-J, Kwon Y, Kim G-Y, Riedel M, Holland M, Schultheiss P, Rose K, UBGH-1 Scientific Party (2008) Korean national program expedition confirm rich gas hydrate deposits in the Ulleung Basin, East Sea. DOE-NETL Fire In the Ice. Spring 2008:6–9. http://www.netl.doe.gov/technologies/oil-gas/publications/Hydrates/Newsletter/HMNews.Spring08.pdf#page=6
148. Paull CK, Lorenson T, Borowski WS, Ussler W, Olsen K, Rodriguez NM, Wehner H (2000) Isotopic composition of CH_4, CO_2 species, and sedimentary organic matter within ODP Leg 164 samples for the Blake Ridge: gas source implications. In: Paull CK, Matsumoto R, Wallace P, and Dillon WP (eds) Proceedings of the Ocean Drilling Program, Scientific Results, vol 164. pp 67–78
149. Paull CK, Matsumoto R, Wallace PJ (eds) (1996) Initial Reports—Gas hydrate sampling on the Blake Ridge and Carolina Rise. Proc. Ocean Drilling Program, 164: 623, Texas A&M University, College Station, Texas
150. Paull C, Ussler W, Dallimore S, Blasco S, Lorenson T, Melling H, Medioli B, Nixon F, McLaughlin F (2007) Origin of pingo-like features on the Beaufort Sea shelf and their possible relationship to decomposing methane gas hydrates. Geophys Res Lett 34:L01603. doi:10.1029/2006GL027977
151. Paull C, Ussler W, Lorenson T, Winters W, Dougherty J (2005) Geochemical constraints on the distribution of gas hydrates in the Gulf of Mexico. Geo Mar Lett 25. doi:10.1007/s00367-005-0001-3
152. Pawar RJ, Zyvoloski GA, Tenma N, Sakamoto Y, Komai T (2005) Numerical Simulation of Gas Production From Methane Hydrate Reservoirs. Pro. 5th International Conference on Gas Hydrates, Trondheim, Norway, 13–16 June, pp 258–267
153. Phale HA, Zhu T, White MD, McGrail BP (2006) Simulation Study on Injection of CO_2-Microemulsion for Methane Recovery From Gas-Hydrate Reservoirs, SPE 100541, SPE Gas Technology Symposium, Calgary, Alberta, Canada, 15–17 May 2006

154. Priest JA, Rees EVL, Clayton CRI (2009) Influence of gas hydrate morphology on the seismic velocities of sands. J Geophys Res 114:B11205. doi:10.1029/2009JB006284
155. Radler M (2000) Oil Gas J 98(51): 121.
156. Reagan MT, Moridis GJ (2007) Oceanic gas hydrate instability and dissociation under climate change scenarios. Geophys Res Lett 34:L22709. doi:10.1029/2007GL031671
157. Reagan MT, Moridis GJ (2008) The dynamic response of oceanic hydrate deposits to ocean temperature change J. Geophys Res Oceans 113:C12023. doi:10.1029/2008JC004938
158. Reagan MT, Moridis GJ (2009) Large-scale simulation of methane hydrate dissociation along the West Spitsbergen Margin. Geophys Res Lett 36:L23612. doi:10.1029/2009GL041332
159. Reagan MT, Moridis GJ, Elliott SM, Maltrud M, Cameron-Smith, PJ (2011) Basin-Scale Assessment of Gas Hydrate Dissociation in Response to Climate Change. Proc. 6th International Conference on Gas Hydrates, Edinburgh, Scotland, UK, 17–21 July 2011
160. Reagan MT, Moridis GJ, Zhang K (2008) Sensitivity Analysis of Gas Production from Class 2 and Class 3 Hydrate Deposits, OTC 19554. Proc. 2008 Offshore Technology Conference, Houston, Texas, USA, 5–8 May 2008
161. Riedel M, Bellefleur G, Mair S, Brent TA, Dallimore SR (2009) Acoustic impedance inversion and seismic reflection continuity analysis for delineating gas hydrate resources near the Mallik research sites. Mackenzie Delta, Northwest Territories, Canada. Geophysics 74:B125. doi:10.1190/1.3159612
162. Riedel M, Collett T, Malone M, Expedition 311 Scientists (2006) Proc. IODP, 311: Washington, DC. doi:10.2204/iodp.proc.311.2006
163. Riedel M, Collett TS, Malone MJ, Expedition 311 Scientists (2006) Proc. Integrated Ocean Drilling Program, IODP 311, Washington, DC. doi:10.2204/iodp.proc.311.2006
164. Rosenbaum E, English N, Johnson J, Shaw D, Warzinski R (2007) Thermal conductivity of methane hydrate from experiment and molecular simulation. J Phys Chem B 111(46):13194–13205
165. Ruppel C (2000) Thermal state of the gas hydrate reservoir. Natural gas hydrate. In: Max MD (ed) Oceanic and permafrost environments. Kluwer, Dordrecht, pp 29–42
166. Ruppel C, Boswell R, Jones E (2008) Scientific results from Gulf of Mexico Gas Hydrates Joint Industry Project Leg 1 Drilling: Introduction and overview. Mar Pet Geo 25 doi:10.1016/j.marpetgeo.2008.02.007
167. Ruppel C, Dickens G, Castellini D, Gilhooly W, Lizzarralde D (2005) Heat and salt inhibition of gas hydrate formation in the northern Gulf of Mexico. Geophys Res Lett 32(4):L04605. doi:10.1029/2004GL021909
168. Rutqvist J, Grover T, Moridis GJ (2008) Coupled Hydrological, Thermal and Geomechanical Analysis of Wellbore Stability in Hydrate-Bearing Sediments, OTC 19672. Proc. 2008 Offshore Technology Conference, Houston, 4–8 May 2008
169. Rutqvist J, Moridis GJ (2008) Development of a Numerical Simulator for Analyzing the Geomechanical Performance of Hydrate-Bearing Sediments, paper 139. Proc. 42th U.S. Rock Mechanics Symposium, San Francisco, California, USA, June 29–July 2 2008
170. Rutqvist J, Moridis GJ (2009) Numerical studies on the geomechanical stability of hydrate-bearing sediments. SPE 126129. SPE J 14:267–282
171. Rutqvist J, Moridis GJ, Grover T, Collett T (2009) Geomechanical response of permafrost-associated hydrate deposits to depressurization-induced gas production. J Pet Sci Eng 67:1–12
172. Saeki T, Fujii T, Inamori T, Kobayashi T, Hayashi M, Nagakubo S, Takano O (2008) Extraction of Methane Hydrate Concentrated Zone for Resource Assessment in the Eastern Nankai Trough, Japan, OTC 19311. Proc. 2008 Offshore Technology Conference, Houston, Texas, USA, 5–8 May 2008
173. Santamarina JC, Ruppel C (2009) Physical properties of hydrate-bearing sediments, SEG-geophysics. In: Riedel M, Willoughby E, Chopra S (eds) Gas hydrates, part of the series investigations in geophysics
174. Sava D, Hardage B (2009) Rock-physics models for gas-hydrate systems associated with unconsolidated marine sediments. In: Collett T, Johnson A, Knapp C, Boswell R (eds) Natural

gas hydrates: energy resource and associated geologic hazards. The American Association of Petroleum Geologists Memoir 89
175. Scholl C, Mir R, Willoughby EC, Edwards RN (2008). Resolving resistive anomalies due to gas hydrate using electromagnetic imaging methods. Proceedings of the 6th International conference on gas hydrates (ICGH 2008), Vancouver, British Columbia, Canada, 6–10 July 2008.
176. Schultheiss P, Holland M, Humphrey G (2009) Wireline coring and analysis under pressure: recent use and future developments of the HYACINTH system. Scientific Drilling 7:44–50. doi:10.2204/iodp.sd.7.07.2009
177. Shedd W, Frye M, Godfriaux P, Dufrene R, McConnell D, Boswell R, Collett T, Mrozewski S, Guerin G, Cook A, Shelander D, Dai J (2010) Gulf of Mexico Gas Hydrate Joint Industry Project Leg II: Results from the Walker Ridge 313 Site. Paper OTC 20806, Proc. Offshore Technology Conference, Houston, Texas, 3–6 May
178. Sloan ED, Koh CA (2008) Clathrate hydrates of natural gases, 3rd edn. CRC Press, New York, NY
179. Smith S, Boswell R, Collett T, Lee M, Jones E (2006) Alaminos Canyon Block 818: A Documented Example of Gas Hydrate Saturated Sand in the Gulf of Mexico, Fire In The Ice, NETL Methane Hydrates R&D Program Newsletter. Fall 2006. http://www.netl.doe.gov/technologies/oil-gas/publications/Hydrates/Newsletter/HMNewsFall06.pdf
180. Soloviev VA (2002) Global estimation of gas content in submarine gas hydrate accumulations. Russian Geol Geophys 43(7):648
181. Spangenberg E, Besskow-Strauch B, Luzi M, Naumann R, Schicks JM, Rydzy M (2008) The process of hydrate formation in clastic sediments and its impact on their physical properties. Proc. Sixth International Conference on Gas Hydrates, Vancouver, BC, Canada, 5–10 July 2008
182. Spangenberg E, Kulenkampff J (2005) Physical properties of gas hydrate-bearing sediments. Proc. 5th International Conference on Gas Hydrates, Trondheim, Norway
183. Spangenberg E, Kulenkampff J (2006) Influence of methane hydrate content on electrical sediment properties. Geophys Res Lett 33:L24315
184. Spangenberg E, Kulenkampff J, Naumann R, Erzinger J (2005) Pore space hydrate formation in a glass bead sample from methane dissolved in water. Geophys Res Lett 32:L24301. doi:10.1029/2005GL024107
185. Spangenberg E, Kulenkampff J, Naumann R, Erzinger J (2005) Pore space hydrate formation in a glass bead sample from methane dissolved in water. Geophys Res Lett 32:1–4
186. Stern LA, Kirby SH, Circone S, Durham WB (2004) Scanning electron microscopy investigations of laboratory-grown gas clathrate hydrates formed from melting ice, and comparison to natural hydrates. Am Mineral 89(8–9):1162–1175
187. Stern LA, Kirby SH, Durham WB (1996) Peculiarities of methane clathrate hydrate formation and solid-state deformation, including possible superheating of water ice. Science 273(5283):1843–1848
188. Sun X, Mohanty KK (2005) Simulation of Methane Hydrate Reservoirs, SPE 93015. Proc. 2005 SPE Reservoir Simulation Symposium, Houston, TX, USA, 31 January–2 February 2005
189. Takahashi H, Tsuji Y (2005) Multi-Well Exploration Program in 2004 for Natural Hydrate in the Nankai-Trough Offshore Japan. OTC 17162, Proc. 2005 Offshore Technology Conference held in Houston, TX, USA, 2–5 May 2005
190. Takahashi H, Yonezawa T, Takedomi Y (2001) Exploration for Natural Hydrate in Nankai-Trough Wells Offshore Japan, OTC 13040. Proc. 2001 Offshore Technology Conference, Houston, Texas
191. Tohidi B, Anderson R, Clennell MB, Burgass RW, Biderkab AB (2001) Visual observation of gas-hydrate formation and dissociation in synthetic porous media by means of glass micromodels. Geology 29(9):867–870
192. Tohidi B et al (2002) Application of high pressure glass micromodels to gas hydrates studies. Proc. 4th International Conference on Gas Hydrates, Yokohama

193. Torres ME, Tréhu AM, Cespedes N, Kastner M, Wortmann UG, Kim JH, Long P, Malinverno A, Pohlman JW, Riedel M, Collett TS (2008) Methane hydrate formation in turbidite sediments of northern Cascadia, IODP Expedition 311. Earth Planet Sci Lett 271:170–180
194. Tréhu AM, Bohrmann G, Rack FR, Torres ME et al (2004) Initial Reports, Drilling Gas Hydrates on Hydrate Ridge, Cascadia Continental Margin. Proc. International Ocean Drilling Program 204. http://www-odp.tamu.edu/publications/204_IR/front.html
195. Trofimuk AA, Cherskiy NV, Lebedev VS, Semin VI et al (1973) Geol. Geofiz 2: 3
196. Trofimuk AA, Cherskiy NV, Tsarev VP (1977) The role of continental glaciation and hydrate formation on petroleum occurrence. In: Meyer RF (ed) Future supply of nature-made petroleum and gas. Pergamon Press, New York, p 919
197. Trofimuk AA, Karogodin YuN, Movshovich EB (1982) Problems of improving the conceptual base of petroleum and gas geology on the example of the concept of the "zone of oil and gas accumulation". Geologiya i Geofizika (Soviet Geology and Geophysics) 21(5): 3–10(1–7)
198. Trofimuk AA, Makogon YF, Tolkachev MV (1981) Gas hydrate accumulations—new reserve of energy sources. Geologiya Nefti i Gaza 10:15–22 (in Russian)
199. Tsuji Y, Ishida H, Nakamizu M, Matsumoto R, Shimizu S (2004) Overview of the MITI Nankai Trough Wells: a milestone in the evaluation of methane hydrate resources. Resour Geol 54:3–10
200. Turner D, Kumar P, Sloan ED (2005) A new technique for hydrate thermal diffusivity measurements. Int J Thermophys 26(6):1681–1691
201. U.S. Department of Energy (2010) Gas Hydrate Characterization in the Gulf of Mexico. http://www.netl.doe.gov/technologies/oil-gas/FutureSupply/MethaneHydrates/projects/DOEProjects/MH_5668EMCharGOM.html
202. Uchida T, Ebinuma T, Takeya S, Nagao J, Narita H (2002) Effects of pore sizes on dissociation temperatures and pressures of methane, carbon dioxide, and propane hydrates in porous media. J Phys Chem B 106:820–826
203. Uchida T, Lu H, Tomaru H, The MITI Nankai Trough Shipboard Scientists (2004) Subsurface occurrence of natural gas hydrate in the Nankai Trough area: implication for gas hydrate concentration. Resour Geol 54:35–44
204. Waite W, deMartin B, Kirby S, Pinkston J, Ruppel C (2002) Thermal conductivity measurements in porous mixtures of methane hydrate and quartz sand. Geophys Res Lett 29(24):2229. doi:2210.1029/2002GL015988
205. Waite WF, Kneafsey TJ, Winters WJ, Mason DH (2008) Physical property changes in hydrate-bearing sediment due to depressurization and subsequent repressurization. J Geophys Res 113:B07102
206. Waite WF, Santamarina JC, Cortes DD, Dugan B, Espinoza DN, Germaine J, Jang J, Jung JWT, Kneafsey T, Shin H, Soga K, Winters WJ, Yun T-S (2009) Physical properties of hydrate-bearing sediments. Rev Geophys 47:RG4003. doi:10.1029/2008RG000279
207. Waite WF, Stern LA, Kirby SH, Winters WJ, Mason DH (2007) Simultaneous determination of thermal conductivity, thermal diffusivity and specific heat in sI methane hydrate. Geophys J Int 169(2):767–774
208. Waite WF, Winters W, Mason D (2004) Methane hydrate formation in partially water-saturated Ottawa sand. Am Mineral 89:1202–1207
209. Warner HR (ed) (2007) Petroleum Engineering Handbook, vol 6. Emerging and Peripheral Technologies, Society of Petroleum Engineers, p 621
210. Watanabe T, Shimizu S, Asakawa E, Kamei R, Matsuoka T (2005) Preliminary assessment of the waveform inversion method for interpretation of cross-well seismic data from the thermal production test, JAPEX/JNOC/GSC et al. Mallik 5L-38 gas hydrate production research well; in Scientific Results from the Mallik 2002 Gas Hydrate Production Research Well Program, Mackenzie Delta, Northwest Territories, Canada, (ed) Dallimore SR, Collett TS; Geological Survey of Canada, Bulletin 585
211. Weitemeyer K, Constable S (2009) Marine Electromagnetic Methods for Gas Hydrate Characterization, Gulf of Mexico. http://www.netl.doe.gov/technologies/oil-gas/publications/Hydrates/2009Reports/NT05668_Preliminary_cruise_report.pdf

212. Westbrook G, Thatcher K, Rohling E, Piotrowski A, Palike H, Osborne A, Nisbet E et al (2009) Escape of methane gas from the seabed along the West Spitsbergen continental margin. Geophys Res Lett 36:L15608
213. White M, McGrail BP (2008) Numerical Simulation of Methane Hydrate Production from Geologic Formations via Carbon Dioxide Injection. OTC 19458, Proc. Offshore Technology Conference, 5–8 May 2008, Houston, Texas, USA. doi:10.4043/19458-MS
214. Wilder J, Moridis GJ, Wilson S, Kurihara M, White M, Masuda Y, Anderson B, Collett T, Hunter R. Narita H, Pooladi-Darvish M, Rose K, Boswell R (2008) An International Effort to Compare Gas Hydrate Reservoir Simulators. Proc. 6th International Conference on Gas Hydrates, Vancouver, BC, 6–10 July 2008
215. Winters WJ, Pecher I, Waite W, Mason D (2004) Physical properties and rock physics models of sediment containing natural and laboratory-formed methane gas hydrate. Am Mineral 89(8–9):1221–1227
216. Winters WJ, Waite WF, Mason DH, Gilbert LY, Pecher IA (2007) Methane gas hydrate effect on sediment acoustic and strength properties. J Pet Sci Eng 56:127–135
217. Yamamoto K, Nagakubo S (2009) Environmental risks of the gas hydrate field development in the Eastern Nankai Trough. Proc. American Geophysical Union Fall Meeting, San Francisco, 13–17 Dec 2009
218. Yang S, Zhang H, Wu N, Su X, Schultheiss P, Holland M, Zhang G, Liang J, Lu J, Rose K (2008) High concentration hydrate in disseminated forms obtained in Shenhu area, North Slope of South China Sea. Proc. 6th International Conference on Gas Hydrates (ICGH 2008), Vancouver, British Columbia, Canada, 6–10 July 2008
219. Yun TS, Francisca FM, Santamarina JC, Ruppel C (2005) Compressional and shear wave velocities in uncemented sediment containing gas hydrate. Geophys Res Lett, 32(10). L10609. doi: 10.1029/2005GL022607
220. Yun TS, Fratta D, Santamarina JC (2010) Hydrate Bearing Sediments from the Krishna-Godavari Basin: Physical Characterization, Pressure Core Testing and Scaled Production Monitoring, Journal of Energy & Fuels, 24;5972–5983
221. Yun TS, Narsilio GA, Santamarina JC (2006) Geotechnical characterization of Gulf of Mexico sediments. Mar Pet Geol 23:893–900
222. Yun TS, Narsilio GA, Santamarina JC, Ruppel C (2006) Instrumented pressure testing chamber for characterizing sediment cores recovered at in situ hydrostatic pressure. Mar Geol 229:285–293
223. Yun TS, Santamarina JC, Ruppel C (2007) Mechanical properties of sand, silt, and clay containing tetrahydrofuran hydrate. J Geophys Res 112:B04106
224. Zhang H, Yang N, Wu X, Su M, Holland P, Schultheiss P, Rose K, Butler H, Humphrey G, GMGS-1 Science Team (2007) Successful and surprising results for China's first gas hydrate drilling expedition, Fire In The Ice, NETL Methane Hydrates R&D Program Newsletter. Fall 2007. http://www.netl.doe.gov/technologies/oil-gas/publications/Hydrates/Newsletter/HMNewsFall07.pdf

Part VIII
Electrofuels

Chapter 38
Electrofuels: A New Paradigm for Renewable Fuels

Robert J. Conrado, Chad A. Haynes, Brenda E. Haendler, and Eric J. Toone

Abstract Biofuels are by now a well-established component of the liquid fuels market and will continue to grow in importance for both economic and environmental reasons. To date, all commercial approaches to biofuels involve photosynthetic capture of solar radiation and conversion to reduced carbon; however, the low efficiency inherent to photosynthetic systems presents significant challenges to scaling. In 2009, the US Department of Energy (DOE) Advanced Research Projects Agency-Energy (ARPA-E) created the Electrofuels program to explore the potential of nonphotosynthetic autotrophic organisms for the conversion of durable forms of energy to energy-dense, infrastructure-compatible liquid fuels. The Electrofuels approach expands the boundaries of traditional biofuels and could offer dramatically higher conversion efficiencies while providing significant reductions in requirements for both arable land and water relative to photosynthetic approaches. The projects funded under the Electrofuels program tap the enormous and largely unexplored diversity of the natural world, and may offer routes to advanced biofuels that are significantly more efficient, scalable and feedstock-flexible than routes based on photosynthesis. Here, we describe the rationale for the creation of the Electrofuels program, and outline the challenges and opportunities afforded by chemolithoautotrophic approaches to liquid fuels.

R.J. Conrado • E.J. Toone (✉)
US Department of Energy Advanced Research Projects Agency (ARPA-E),
1000 Independence Avenue, SW, Washington, DC 20585, USA
e-mail: Eric.Toone@hq.doe.gov

C.A. Haynes • B.E. Haendler
Booz Allen Hamilton, 955 L'Enfant Plaza North, SW Suite 5300,
Washington, DC 20024, USA

J.W. Lee (ed.), *Advanced Biofuels and Bioproducts*, DOI 10.1007/978-1-4614-3348-4_38, 1037

1 Introduction

Virtually all transportation—over land, air and sea—utilizes the energy stored in carbon–carbon and carbon–hydrogen bonds to provide motive force. Our use of this stored pool of solar energy can only be described as rapacious, and although the magnitude of the remaining resource is difficult to estimate, it is finite and its extraction will become increasingly complex. The USA currently consumes roughly 19 million barrels of oil per day, over 70% of which is used for transportation [58]. Nearly half the oil consumed in the USA is imported, accounting for a third of the Nation's trade deficit. In recent years, the annual cost of imported oil has exceeded $300 billion, in current dollars the equivalent of funding the entire Apollo Program twice every year.[1] Even this staggering amount significantly underestimates the true cost of imported oil, since a significant fraction of both defense and nondefense Federal spending is devoted to ensuring a stable supply of imported oil. Alternative approaches to liquid fuels are both a national and global imperative.

The sustainable production of energy-dense, infrastructure compatible liquid fuels requires the conversion of a durable form of energy—most plausibly solar radiation, but also geothermal, nuclear, or other forms of renewable energy—into stored chemical energy. The biological production of carbon-based liquid fuels requires three distinct steps: the capture of energy and transduction of that energy to a usable form by an organism; reduction of inorganic carbon to a fungible metabolic intermediate, typically in an oxidation state at or below zero; and the formation of carbon–carbon bonds to provide a fuel with convenient physical properties. Although the reduction of inorganic carbon can be achieved chemically (i.e., abiotically), the high efficiency formation of carbon–carbon bonds remains a significant challenge for the field of chemistry and purely chemical approaches to liquid fuels are not currently economically feasible at scale.

Instead, the production of liquid fuels relies primarily on terrestrial photosynthesis, in which solar radiation is assimilated through Photosystems I and II, and the captured energy is used to reduce and fix carbon through the Calvin–Benson–Bassham (CBB) cycle. In the CBB cycle, inorganic carbon is converted to glyceraldehyde-3-phosphate; although this intermediate is the source of reduced carbon for myriad products through both primary and secondary metabolism, it is primarily converted to glucose and polymerized to various structural and storage polymers. These photosynthetic products are converted to liquid fuels either fermentatively or thermally, producing a variety of fuel molecules.

The overall efficiency of this process—from solar photons to liquid fuel—depends on the nature of both the photosynthetic organism and the means of conversion,

[1] The NASA estimate, based on a Congressional Budget Office report, *A Budgetary Analysis of NASA's New Vision for Space,* found the Apollo program cost in 2005 dollars to be approximately $170 billion. The estimate includes costs for research and development; procurement of rockets, command and lunar modules; management; facilities, including construction and upgrading; and flight operations.

but is certainly less than 1%. While photosynthesis is operationally facile—plants and photosynthetic organisms are autonomous—the process competes with other forms of agriculture for resources, in particular land, fresh water and essential nutrients (NPK and trace metals). The scalable, sustainable production of liquid fuels would be greatly enhanced by the development of processes that do not share agricultural factors of production and that offer greater conversion efficiencies than those of photosynthesis.

In 2009, the US Department of Energy (DOE) Advanced Research Projects Agency-Energy (ARPA-E) created the Electrofuels program to explore nonphotosynthetic autotrophic organisms for the conversion of renewable energy to energy dense liquid fuels for transportation [2]. The approach expands the boundaries of traditional biofuels and could achieve dramatically higher overall conversion efficiencies while providing massive reductions in both arable land and water usage. If a series of technical challenges can be overcome, an Electrofuels system could have a higher utilization of refinery capacity due to feedstock flexibility and be free from fluctuations in feedstock supply and cost inherent to photosynthetic biofuels approaches. To achieve this vision, the Electrofuels program leverages foundational work in microbiology, genomics, metabolic engineering, and synthetic biology to create microorganisms that assimilate energy, fix inorganic carbon, and produce fuel molecules without photosynthesis (Fig. 1).

In this article, we describe the rationale for the Electrofuels program and consider the challenges to the economic viability of the approach.

2 Background

The USA is the global leader in the production of biofuels, in 2010 producing over 13 billion gallons of ethanol, or 9 billion gasoline gallon equivalents (GGE), from corn grain [48]. Further expansion of corn grain ethanol production is now constrained by diminishing Congressional support for government subsidies (in 2010 the Volumetric Ethanol Excise Tax credit cost taxpayers approximately $6B), growing concerns about the environmental impacts of increased corn production, and perceived impacts of converting food to fuel resources in the face of global population growth and rising food prices.

In order to address these and other issues, the Departments of Energy, Agriculture and Defense have made significant investments in advanced biofuels—biofuels derived from sustainable, nonfood resources such as agricultural residues, residues from forestry operations, food processing by-products, and municipal solid waste. In the near future, dedicated energy crops that grow on marginal or non-food-production land, including perennial grasses (e.g., switchgrass), woody species (e.g., willow), and aquatic macroalgae (e.g., *Saccharina*), will add to the supply of biomass feedstocks for the production of fuels.

Despite the many benefits offered by dedicated energy crops, the efficiency of energy capture and transduction by plants is remarkably low, calculated as the ratio

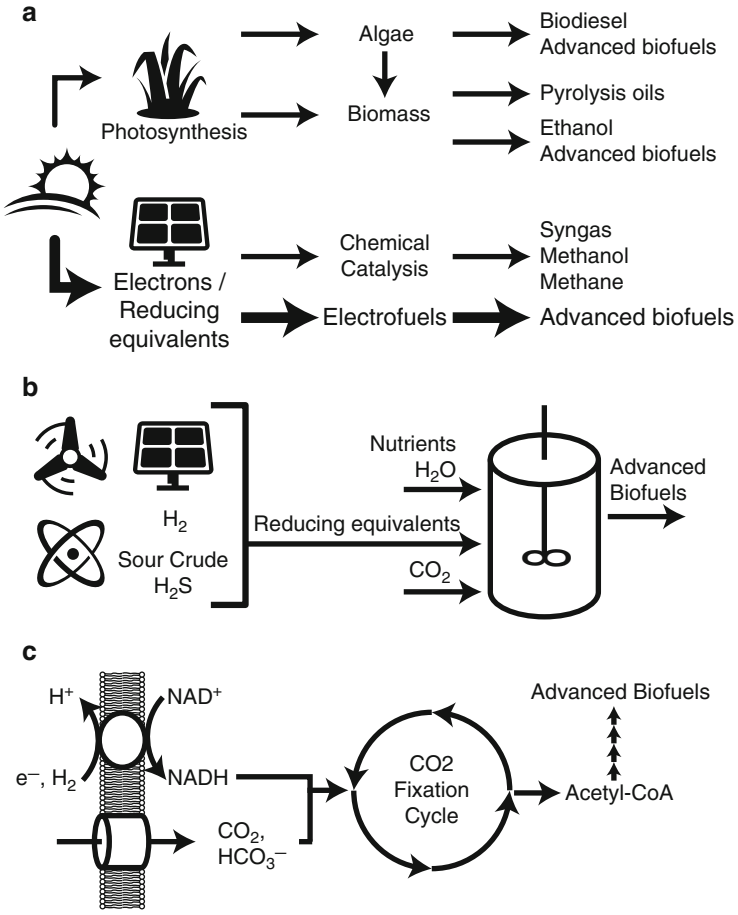

Fig. 1 (**a**) Energy conversion pathways from solar energy, with the Electrofuels pathway shown in *bold*. (**b**) The Electrofuels platform receives renewable electrons from a variety of sources, including H_2 and H_2S. CO_2, H_2O and other nutrients are fed into a bioreactor that directly produces liquid fuels. (**c**) Chemolithoautotrophs convert electrons or electron carriers into cellular reducing equivalents. Various carbon fixation cycles convert CO_2 and renewable energy into acetyl-CoA, which can be rapidly elaborated into an array of liquid fuel molecules

of incident solar radiation to stored energy in chemical bonds. Under optimized environmental conditions C4 plants can capture up to 6% of the available solar energy, while C3 plants convert a maximum of 4.5% [70]. Including in the calculation the seasonal growth of plants, the diversion of plant matter for growth, and the conversion efficiency of fixed carbon to liquid fuels, overall annual photon-to-fuel efficiency stands at 0.18% for US corn ethanol (Supp Calc 1) and 0.20% for Brazil sugarcane ethanol (Supp Calc 2). As a result, land resources are vastly underutilized, even for perennial crops. Additionally, biofuels feedstocks and energy crops have significant competition in open markets, and suffer from price fluctuations that limit the viability of this approach.

Photosynthetic microorganisms represent an alternative to terrestrial plants for the production of biofuels, and several algal and cyanobacterial approaches to fuels have also been developed for use in closed systems [30, 31, 49]. Such microorganisms offer several advantages over terrestrial plants, including genetic tractability and the ability to secrete fuel products. Genetic tractability affords the opportunity to directly engineer pathways to produce fuel without the need for secondary processing, while the ability to secrete obviates the need for harvest or biomass manipulation. Still, diurnal and annual sunlight variation makes continuous algal production difficult to control, slows microbial growth, and reduces productivity, each of which results in an increase in the cost of capital and the final fuel product. Fresh water requirements are also potentially problematic, although these concerns can be ameliorated to some extent through the use of salt-tolerant species and aggressive water capture techniques. The deployment at scale of genetically modified microorganisms also raises issues of containment, both to prevent accidental release and adventitious infection by wild-type strains.

In its broadest conception, the term "biofuels" implies the action of living organisms in one or more of the steps required to reduce inorganic carbon to an energy-dense form: the capture of energy and transduction of that energy to a usable form; the reduction of carbon from the +4 oxidation state; and the elaboration of that reduced carbon into a final fuel molecule. The diversity of the microbial world—and especially of the deep oceans—is staggering: the ocean contains 300,000 times more bacteria than there are stars in the visible universe [59, 61]. Fewer than 1% of these microbes have been identified and fewer than 0.1% of marine microorganisms have been cultured [18, 29]. This astonishing store of diversity offers tremendous opportunities for many branches of science, including energy transduction and carbon fixation.

Photosynthesis is but one of the approaches to carbon fixation found in nature; myriad life forms exist in ecological niches where both reduced carbon and light are nonexistent. Such organisms assimilate energy from other energy rich (reduced) species, including H_2, H_2S, NH_3, and reduced metals ions. A group of so-called electrotrophs are capable of accepting reducing equivalents directly as electric current [39]. Many chemolithoautotrophs use carbon fixation cycles other than the CBB cycle, including the reductive acetyl-CoA, the reductive citric acid, and 3-hydroxypropionate-4-hydroxybutyrate cycles; some of these pathways offer significant advantages over the CBB cycle [5]. Such organisms might serve as factories for the high-efficiency production of liquid fuels from renewable forms of energy.

To address these fundamental questions the Electrofuels program seeks routes to biofuels that surpass the inherent limitations of photosynthesis. At the core of the program are chemolithoautotrophic microorganisms, organisms capable of fixing and reducing inorganic carbon but that derive energy from a variety of inorganic substrates. Such microorganisms might produce renewable biofuels from solar electricity, either directly or through the agency of a soluble mediator. This solar electricity could come from photovoltaic cells that even now capture >20% of the total solar spectrum [25]; or the energy could come from other renewable

sources (hydro, wind, wave, tidal), or non-fossil-based heat (geothermal, concentrating solar, nuclear). The approaches considered under the Electrofuels program tap the enormous and largely unexplored diversity of the microbial world, and may offer routes to advanced biofuels significantly more efficient, scalable and feedstock-flexible than routes based on photosynthesis.

3 Chemolithoautotrophy and Electrofuels

The Electrofuels concept pushes the boundaries not only of traditional biofuels but of industrial biotechnology writ large, through the first demonstration of chemolithoautotrophy as a means to enable carbon fixation and the production of reduced products, including liquid fuels. Chemolithoautotrophic organisms are prokaryotes, either bacteria or archaea, capable of deriving energy from the oxidation of various reduced inorganic compounds. These organisms use inorganic carbon (CO_2 and its various hydrated forms) as their sole carbon source and are capable of growth and metabolism in the complete absence of either sunlight or reduced carbon [42]. Intriguingly, some chemolithoautotrophic bacteria have been shown to function as a biocathode, assimilating energy directly from electric current. Chemolithoautotrophs derive energy from the proton motive force generated by electron flow from a reductant (e.g., H_2, H_2S, Fe^{2+}) to an oxidant (e.g., O_2, S, CO_2). It is this energy flow that provides the driving force for the synthesis of both the ATP and reducing equivalents (NADH/NADPH) required for carbon fixation (Fig. 1c).

A large group of chemolithoautotrophs produce energy from the oxidation of molecular hydrogen:

$$2H_2 + O_2 \rightarrow 2H_2O \quad \Delta G^{\circ\prime} = -474 \text{ kJ} \tag{1}$$

Ralstonia eutropha is a relatively common soil microorganism capable of autotrophic growth on hydrogen. *Ralstonia* relies on three different [NiFe]-containing hydrogenases capable of hydrogen oxidation in the presence of oxygen [7]:

1. Regulatory hydrogenase (RH): The RH senses the presence of hydrogen and initiates the expression of both membrane-bound and soluble hydrogenases.
2. Membrane-bound hydrogenase (MBH): Found on the outer-cytoplasmic membrane, the MBH shuttles electrons from hydrogen oxidation into the respiratory pathway, creating the proton gradient necessary to drive ADP phosphorylation.
3. Soluble hydrogenase (SH): The SH generates NADH reducing equivalents by the oxidation of hydrogen and electron transfer through two flavin mononucleotides separated by a [Fe–S] cluster to NAD^+.

While all three [NiFe]-containing hydrogenases are capable of hydrogen oxidation, each activity is coupled to a unique and essential cellular function required for chemolithoautotrophic growth.

Another chemoautolithotrophic bacteria of potential use for the production of liquid fuels is *Acidithiobacillus ferrooxidans.* This microorganism recovers energy from the oxidation of ferrous iron (Fe^{2+}) in the presence of oxygen:

$$2Fe^{2+} + 0.5O_2 + 2H^+ \rightarrow 2Fe^{3+} + H_2O \quad \Delta G^\circ = -66 \text{ kJ(pH2)} \tag{2}$$

Acidithiobacillus is an acidophile, consistent with the increased stability of ferrous iron at lower pH. Evidence suggests that Fe^{2+} is oxidized outside of the cell; electrons are thought to first enter the cell through a c-type cytochrome (Cyc2) in the outer membrane, and then pass through a series of periplasmic redox carriers to a cytochrome c oxidase, which in turn drives ATP synthesis [69].

Outer-membrane c-type cytochromes may interact with metals for energy production in other bacterial species, including *Geobacter sulfurreducens.* Intriguingly, recent evidence suggests that *Geobacter* protein filaments, sometimes termed microbial nanowires, are capable of conducting electrons over long distances independent of cytochrome proteins [33]. This exciting observation suggests that naturally occurring electron-conductive biofilms might be scaled to support biofuel production.

Carbon fixation is diversified in chemolithoautotrophs. All photosynthetic organisms fix carbon through the CBB cycle, which reduces carbon dioxide to glyceraldehyde-3-phosphate (G-3-P); this intermediate is subsequently converted to five- and six-carbon sugars. The pathway requires six NADPH and 9 ATP to convert three equivalents of CO_2 into G-3-P, with a maximum efficiency 67% of the thermodynamic limit. The key enzyme of the CBB cycle is ribulose-1,5-bisphosphate carboxylase oxygenase (RuBisCO), a protein evolved for plant growth. While well suited for this purpose, RuBisCO possesses many attributes that limit its utility for the production of liquid fuels, in particular a low specific activity and a competitive reaction with oxygen [36]. In contrast, many chemoautolithotrophs use non-CBB pathways for carbon fixation. Two such pathways—the reductive acetyl-CoA, or Wood–Ljungdahl, cycle and the reductive citric acid, or Arnon–Buchanan, cycle—are more efficient than CBB, approaching the thermodynamic limit (Table 1) [28, 47]. Other non-CBB pathways, such as the recently elucidated 3-hydroxypropionate-4-hydroxybutyrate cycles use bicarbonate as the source of inorganic carbon which may improve overall CO_2 fixation kinetics relative to the CBB cycle. Further, unlike terrestrial plants that require carbon flux for complex structural carbohydrates, unicellular autotrophs use non-CBB cycle pathways to directly produce acetyl-CoA, the key intermediate for biofuel synthesis. Additionally, the 3-hydroxypropionate bicycle has no O_2 sensitivity and does not catalyze competing O_2 reactions, enabling oxidative phosphorylation for the generation of ATP. Lastly, several carbon-fixing enzymes show activities much greater than that of RuBisCO, although these enzymes have yet to be thoroughly investigated.

The Electrofuels program leverages chemolithoautotrophy and a variety of largely unexplored carbon fixation pathways as a potential platform for biofuels

Table 1 Available routes to fix CO_2 to liquid fuels and energy requirements [4, 5]

Carbon fixation cycle (CO_2 to acetyl-CoA)	Molecule produced	ATP required	e^- required (O_2/no O_2)	O_2 tolerance	Number of enzymes	Cofactor requirements	Specific activity[a] (U/mg)
Thermodynamic minimum	Acetyl-CoA	0	8/8	High	Few	None	>100
Reductive acetyl-CoA (Wood–Ljungdahl)	Acetyl-CoA	1	8.7/10	None	6	Pterin	Unknown
						Corrinoid Fe–S protein	0.77
Reductive citric acid (Arnon–Buchanan)	Acetyl-CoA	2	9.3/12	Little to none	8	Biotin	Unknown
						Thiamine	53.1
						Fe-protoporphyrin IX	
Dicarboxylate-4-hydroxybutyrate	Acetyl-CoA	5	11.3/18	Little to none	14	Thiamine	Unknown
						4Fe–4S	32.4
3-Hydroxypropionate-4-hydroxybutyrate	Acetyl-CoA	6	12/20	Some to none	13	Biotin	18
						Fe–S	
						Selenomethionine	29.6
						Vitamin B_{12}	
Reductive pentose phosphate (Calvin–Benson–Bassham)	3-Phospho-glycerate	7	12.7/22	Competing O_2 reaction	13	Thiamine	3.5
3-Hydroxypropionate bicycle	Pyruvate	7	12.7/22	High	13	Biotin	18
						Vitamin B_{12}	29.6

[a]Specific activity in units of μmol/min/mg protein for CO_2/HCO_3^- fixing reactions where multiple values represent different carbon fixing reactions

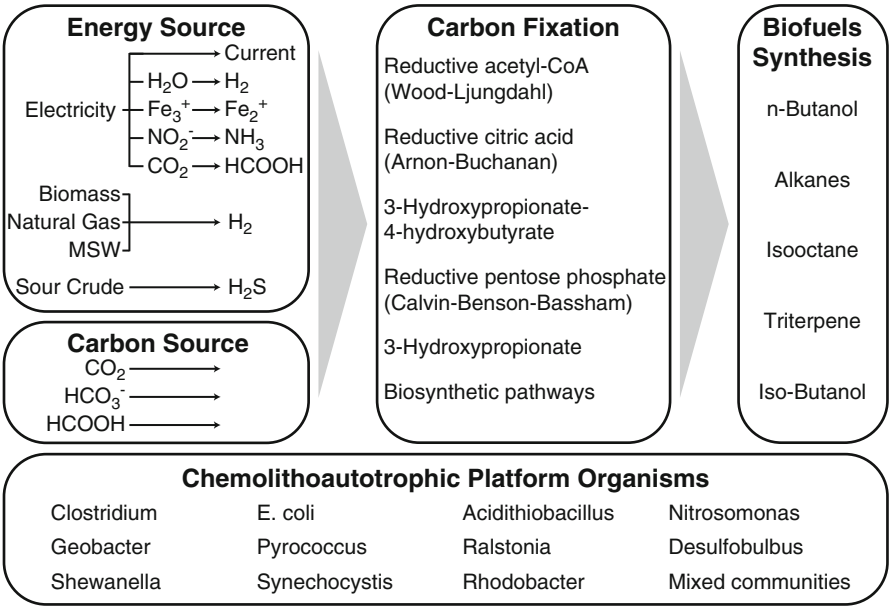

Fig. 2 Electrofuels portfolio (*MSW* municipal solid waste)

production, and is built on the thesis that chemolithoautotrophic-engineered systems can assimilate energy and fix carbon more efficiently than can photosynthetic systems. Each Electrofuels project [1] aims to demonstrate three technology modules (Fig. 2):

1. *Energy assimilation*: The efficient capture of the energy required to drive ATP synthesis and carbon fixation is a key feature of the Electrofuels program. Chemolithoautotrophic organisms capable of growth on a variety of reduced inorganic substrates are under consideration, including *Ralstonia eutropha* (H_2), *Acidithiobacillus thiooxidans* (H_2S), *Nitrosomonas europaea* (NH_3), and *Acidithiobacillus ferrooxidans* (Fe^{2+}). Electrotrophs—organisms capable of assimilating energy directly as electric current—that reduce carbon dioxide to acetate with nearly 100% Coulombic efficiency are also under evaluation [39]. The Electrofuels program also includes projects seeking to genetically engineer heterotrophic organisms such as *Escherichia coli* to function as chemolithoautotrophs. Such projects include, for example, growth and production on electrochemically produced formate.
2. *Carbon fixation*: Chemolithoautotrophs, in particular some archaea, evolved carbon fixation pathways relevant to the unique geochemical niches they occupy (Table 1). To date, five pathways that use equivalent or fewer ATP than the CBB cycle have been discovered [5]. Such pathways confer a variety of benefits to chemolithoautotrophs, including avoidance of the requirement for large quantities of an inefficient RuBisCO. Further, non-CBB pathways directly convert CO_2 to

acetyl-CoA, rather than G-3-P, an intermediate that directly feeds biofuel synthesis. Various Electrofuels projects are evaluating the characteristics of each of these pathways, as well as designed pathways not found in the natural world.

3. *Biofuel synthesis*: The Electrofuels program is designed to produce energy dense, infrastructure compatible liquids fuels, and specifies the production of fuel molecules with an energy density equal to or greater than 32 MJ/kg. A variety of fuel molecules that can either be used directly as fuels, such as butanol, or hydrocarbons that require further catalytic processing, such as alkanes, isooctane, and triterpenes, are the targets of this program. To produce such species in high yield, the Electrofuels program leverages recent advances in metabolic engineering and synthetic biology to direct carbon and energy fluxes to final fuel molecules.

In summary, the Electrofuels program considers previously unexplored pathways and organisms for the high efficiency conversion of solar energy and inorganic carbon to complex biofuels. Considering the available biochemical options and a rapidly growing toolbox for the genetic manipulation of previously intractable microorganisms, the program offers multiple options for the conversion of durable forms of energy to biofuels. In some respects, the components of a complete pathway (energy assimilation, carbon fixation, and fuel production) are "mix-and-match," and the program virtually considers more approaches than those actually constructed.

4 Challenges and Opportunities

The Electrofuels approach to biofuels represents a significant departure from photosynthetic strategies, and it is important to consider both the merits and challenges inherent to a system built around a chemolithoautotrophic platform. Here, we consider the relative advantages and disadvantages of an Electrofuels vs. a photosynthetic approach for each of the important drivers of the system, specifically the required resources and the economics of at-scale production.

4.1 Land Resources

The biochemical conversion of solar photons to liquid fuels involves many steps, each with the potential to produce losses of both energy and carbon. Plants harness energy from only a portion of the solar spectrum, and only during the growing season, which in temperate climates ranges from roughly 180 to 250 days per year. Under many conditions, plant growth is limited by access to resources other than light, in particular water, trace nutrients, and CO_2. Even the most prodigious dedicated energy crops produce harvestable biomass encompassing roughly 1% of the incident solar radiation; additional losses from agriculture and conversion

significantly reduce the usable portion of the captured energy. The primary consequence of this low efficiency is that enormous land resources are required to collect sufficient solar energy for US liquid fuel production (Table 2). Several advanced photosynthetic biofuels approaches under development claim higher solar photon utilization efficiencies, some as high as 7.2% [49], although none of these approaches have been demonstrated at scale.

Chemolithoautotrophic approaches to biofuels require land only for solar radiation collection, and can thus use nonarable land for fuel production. Any of several currently deployed technologies, for example concentrating solar or solar PV, can capture >20% of incident solar radiation energy. Coupling one of these technologies with a microorganism, up to 13% of total available solar energy could plausibly be captured in a liquid fuel (Supp Calc 4). This solar radiation can be captured year round, significantly increasing the solar yield from a given land area when compared to seasonal crops. Further, it is possible to intersperse farmland with renewable resources such as wind so that fuel production no longer competes with food production.

4.2 Water Resources

Water is a scarce resource in most of America, especially outside of the Southeast and Great Lakes states. The USA faces two macroscale drivers of water scarcity in the coming century: a growing domestic population and the continuing depletion of fossil fresh water ground reserves. Between 2005 and 2050, the US Census Bureau predicts a population increase of greater than 40% [43], increasing demands on water for domestic and commercial applications. At the same time, the US Geological Survey estimates that over 40% of agricultural fresh water and more than 30% of nonagricultural fresh water is drawn from deep aquifers that do not refresh over meaningful timeframes [26]. The magnitude of this resource, accumulated over geological time scales and currently being depleted faster than natural recharge rates, is poorly quantified nationwide.

Terrestrial energy crops grow as an open system, incurring water losses from irrigation inefficiencies [22], soil evaporation [27], and transpiration for leaf cooling and motive force for nutrient uptake; it is estimated that only 0.2–0.4% of water used in agriculture is fixed as plant matter [11, 17, 19] (Table 2). Agriculture is by far the largest source of water utilization in the USA, accounting for fully 80% of consumption from all sources [51]. Whether water is supplied by irrigation or natural rainfall, agricultural water use limits availability for other applications [34]. Similarly, open-pond algal systems suffer from evaporative losses [44], although such losses are ameliorated through the use of closed systems or salt-tolerant species [9, 24].

Several advanced biofuel systems offer the opportunity to diminish concerns surrounding water withdrawals by creating closed bioreactors that obviate water losses from evaporation and transpiration [30, 31, 49]. Closed systems facilitate complete

Table 2 Comparison of resource requirement for various approaches to biofuels synthesis

Resource requirement		Corn-to-ethanol (US)	Sugarcane-to-ethanol (Brazil)	Advanced biofuels	Electrofuels
Land (BOE/acre/yr)[a]	Solar energy	5.2[b]	7.8[c]	10.4[d]–360[e]	360–660[e]
	Wind energy	0	0	0	17–34[f]
Fresh water use (gallons H_2O/GGE)[g]	Biomass growth	3,300–4,400 [10, 68]	4,300–7,200 [35]	1.1–1,421[h,i]	1.1[i]
	Fuel processing	4–16 [10, 68]	134 [35]	1.9–9.8[h]	0–4.3 [10, 68]
Nutrients NPK (lbs/BOE)	Nitrogen (N)	0–38 [3, 8, 50, 52]	7–10 [8, 34, 37, 38]	0–58[j]	0–58[j]
	Phosphorus (P_2O_5)	0–15 [3, 8, 50, 52]	4–15 [8, 34, 37, 38]	0–8[k]	0–8[k]
	Potassium (K_2O)	0–27 [3, 8, 50, 52]	9–23 [8, 34, 37, 38]	0–3[l]	0–3[l]

[a] *BOE* barrel of oil equivalent on an energy basis
[b] Supp Calc 1
[c] Supp Calc 2
[d] PETRO FOA targets
[e] Supp Calc 5 with El Paso, Texas for reference
[f] Supp Calc 6 with North Dakota as reference
[g] *GGE* gasoline gallon equivalent on an energy basis
[h] Biomass growth on saline or brackish water: 0 g/GGE [9, 24]; cellulosic ethanol from switchgrass (no irrigation): 1.9 g/GGE (thermochemical), 5.8–9.8 g/GGE (biochemical) [68]; open-pond batch algae systems could consume 223–1,421 g/GGE fresh water [44, 62]
[i] Supp Calc 3. Upper limit includes water use from dry mill corn processing
[j] Calculations: 0-biocatalyst/woody biomass; 1.2–2.4-switchgrass; 58-algae [44]
[k] Calculations: 0-biocatalyst/woody biomass; 1–8-algae [44, 45]
[l] Calculations: 0-biocatalyst/woody biomass; 3-algae [45]

water recycle: in the limit, water is required during biofuel production only as the ultimate source of electrons during water oxidation, providing two electrons (as hydride) and molecular oxygen during CO_2 reduction. This requirement amounts to roughly 1 gal of water/gal of fuel (Supp Calc 3), plus whatever water is consumed by growing cultures. While these values are somewhat imprecise at this early stage, they will almost certainly represent a vast savings over terrestrial plants and over at least some forms of photosynthetic organisms.

4.3 NPK Resources

Similar to water resources, plants grown as open systems require significant fertilizer loads to optimize biomass yield (Table 2). Brazilian sugarcane utilizes as little as 20% of applied nitrogen [34]; the remainder is largely lost to water supplies with the attendant negative impact on the surrounding environment [14]. The requirement for nutrient complexity within soil often requires crop rotation and precludes year-over-year high biomass productivities available with closed-system bioreactors.

To the extent that growth can be separated from production, rapid CO_2 fixation is possible in an Electrofuels approach with low nutrient requirements, since relatively little biomass is produced per volume of fuel. These requirements are further diminished through nutrient recycling within the biorefinery. At least some other advanced biofuels systems also address this issue; notable examples include slow growing woody biomass (with no external nutrient requirements) and other closed system photobioreactors [49, 60].

4.4 Reducing Equivalents and Inorganic Carbon

The growth of terrestrial plants is limited by a variety of factors, depending on growth location and conditions. What is seldom limiting, however, is reductant, i.e., solar photons. Rather, plant growth is typically limited by water, nutrients, or CO_2. Likewise, an Electrofuels approach to the production of liquid fuels will be limited by a variety of factors, depending on growth conditions. Ultimately, the two factors most likely to provide insurmountable limits to production are reducing equivalents and inorganic carbon.

The approaches under consideration in the Electrofuels program utilize various means to assimilate reducing equivalents, and the limiting factor to uptake will vary as the approach. In the case of hydrogen-utilizing organisms, the aqueous solubility of hydrogen is likely to be limiting, at least under some growth conditions. Incorporated into the program are multiple efforts aimed at novel bioreactors that, at least to some extent, ameliorate these concerns. The growth of electrotrophs will ultimately be limited by the ability of organisms to assimilate electrons. The mechanisms

by which these unique species take up electrons remain unclear, and the limits to growth mandated by such processes are similarly opaque. Still, if organisms must be physically anchored to an electrode through, for example, conductive pili, then production will be limited by the accessible surface area of a highly porous electrode. On the other hand, if conduction can proceed through at least some thickness of a biofilm, the effective surface area could be multiplied manyfold, greatly increasing the potential for growth. In any event, the ability to assimilate reducing equivalents will ultimately provide a limit to fuel production.

The provision of inorganic carbon likewise presents challenges for an Electrofuels approach to fuel synthesis. Plants autonomously assimilate CO_2 from the atmosphere; while the very low concentrations of CO_2 in air limit growth, the carbon is at least free and essentially limitless. In an Electrofuels approach, inorganic carbon will be furnished at concentrations beyond that available directly from air. Such sources might include the effluent of conventional power plants, cement kilns and the like, direct mining of geologic CO_2, carbonate or bicarbonate, or CO_2 produced as a coproduct during the production of conventional biofuels from biomass, which necessarily release significant quantities of the total carbon as CO_2. The extraction of inorganic carbon from seawater may be feasible as well. While any of these approaches would decrease the Nation's dependence on foreign sources of oil, only some are carbon-neutral, while others would contribute to anthropogenic atmospheric carbon loads during combustion.

5 Cost of Electrofuels

The economic sustainability of any biofuel is dependent on the existence of a market, which is largely determined by the cost of production relative to alternative approaches. Such calculations are fraught with uncertainties regarding future costs of scarce resources and without proper assignment of various "hidden" costs, or costs not explicitly associated with or assigned to a particular fuel. To be fully comparable, such costs should include societal costs such as the military and political costs associated with the import of foreign oil and the opportunity costs associated with diverting agricultural resources to the production of fuel. Additionally, at this early stage of development the final configuration of a biofuels production facility based on a nonphotosynthetic autotrophic organism is unclear. Still, it is possible to consider at least the factors of production that will drive costs and to make at least estimates regarding limits to costs of production.

The sustainable synthesis of any liquid fuel requires inorganic carbon, hydrogen, and energy from a renewable source. In the approaches under development through the Electrofuels program a renewable source of energy is converted to either hydrogen or electricity, which in turn serves as the energy input for carbon fixation and fuel synthesis. The energy density of liquid fuels is extraordinary—gasoline contains roughly 13 kWh/kg or 34 MJ/L—and the entire electricity generating capacity of the USA represents roughly half of US oil consumption, assuming a conversion

efficiency of 65% (Supp Calc 7). Given these levels, dedicated on-site electricity generation will almost certainly be the most cost efficient design. A cost comparison of chemolithoautotrophic approaches to corn-based fuels thus turns primarily to a comparison of feedstock costs: electricity vs. corn (Fig. 3).

In recent years, a variety of factors, including a rising demand for carbon-neutral biofuels, has driven sugar costs significantly above historical levels. At the same time, advances in renewable energy production have driven down the cost of renewable electricity, especially from wind, but also from solar and other resources. Electricity costs are very low for on-site generation (Fig. 4), especially for fully depreciated installations; arbitrage opportunities may further diminish effective electricity costs by balancing electricity sales vs. fuel production. West Texas, for example, possesses a significant wind resource that is largely under-utilized at night, when electricity demand is low. This lack of demand leads to significant wind curtailment—3.9 TWh in 2009 and 2.1 TWh in 2010 of essentially "free" electricity [66]—that would have supported production of 1.5 M BOE and 0.8 M BOE in 2009 and 2010 respectively. This combination of effects leads to periods in which electricity is a significantly cheaper feedstock than sugar for the domestic production of biofuels, a trend that could amplify in the future (Figs. 3 and 4).

To project the cost of a mature Electrofuels technology, we consider an Electrofuels facility operating at the production level of a typical corn-to-ethanol facility, producing roughly 35 million GGE annually. Feedstock costs include the cost of electricity, CO_2, and water, with oxygen production considered as a coproduct when using an electricity feedstock and assuming a 65% overall energy conversion efficiency (Supp Calc 6). Wind electricity costs in the US Midwest currently range from $30 to $70/MWh [66], although these costs will diminish in the future as capital is fully depreciated. Time-of-day pricing is also especially significant for wind resources: during the cheapest 6 h of the day prices seldom rise above $20/MWh, and wind curtailment produces sustained periods of negatively priced electricity [16]. The cost of the CO_2 feedstock could approach zero where concentration and/or purification from waste streams is not necessary. Operating costs include maintenance and taxes, labor and overhead, materials and waste. The cost of capital is for the *n*th plant cost and based on capital costs for a typical corn-to-ethanol plant, using standard interest rates, construction periods, and depreciation schedules. Additional assumptions are described as footnotes to the calculations (Supp Calc 8).

Not surprisingly, the price of fuel from an Electrofuels approach is extremely sensitive to the price of the energy feedstock, and both conversion efficiencies and the choice of carbon fixation platforms are crucial. Based on realistic assumptions and a cost of electricity of even $40/MWh, the projected cost of fuel is close to $3/GGE (Table 3); at $20/MWh—the current cost of electricity in the cheapest 6 h of the day—costs drop to $2/GGE. Significant efficiency losses included our calculations include 18% from projected voltage overpotential and 14% for electricity conversion to hydrocarbon fuels. It is important to note, however, that these estimates still largely lack experimental underpinning, and more accurate estimates await additional data.

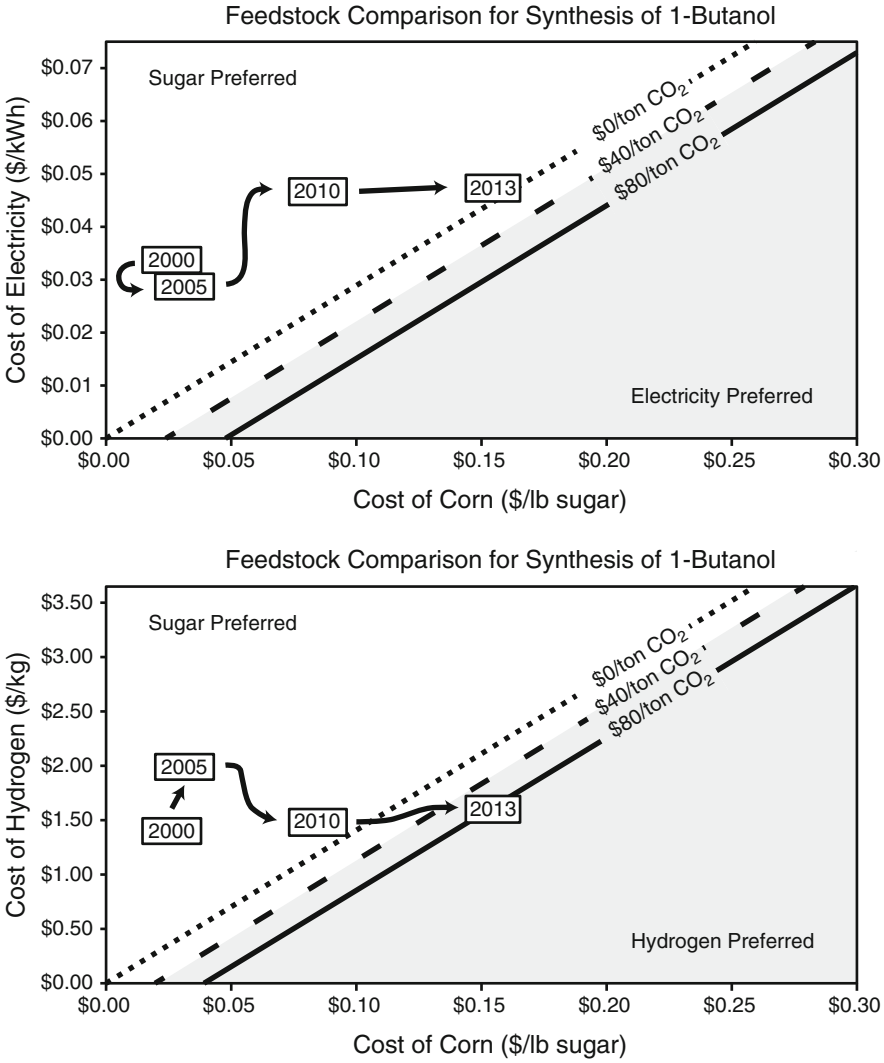

Fig. 3 Comparison of the cost of sugar vs. electricity (*top graph*) and H_2 (*bottom graph*) as feedstocks for Electrofuels production of 1-butanol. Sugar pathway: $C_6H_{12}O_6 \rightarrow 2CO_2 + C_4H_{10}O + H_2O$. Electrofuels electricity pathway: $4CO_2 + 5H_2O + 28e^- \rightarrow C_4H_{10}O + 6O_2$. Electrofuels hydrogen pathway: $4CO_2 + 14H_2 + O_2 \rightarrow C_4H_{10}O + 9H_2O$. *Solid*, *dashed*, and *dotted lines* represent the breakeven point for a sugar vs. electricity/H_2 plus CO_2 feedstock, with the *solid line* representing \$80/ton CO_2, the *dashed line* representing \$40/ton CO_2, and the *dotted line* representing \$0/ton CO_2. *Boxes* with a given year are centered on the historical annual average cost of electricity, H_2 and sugar in the US Sugar costs are calculated from the yearly average price of a bushel of US Midwest corn assuming 15.5 wt.% moisture and 76.7 wt.% starch and sugar. Electricity costs are calculated from wind electricity developed in the US Midwest. H_2 costs are calculated using the yearly average Henry Hub price of natural gas with a hydrogen production cost model. The *arrows* indicate the change in average annual price over time. Future costs are taken from corn and natural gas futures prices and electricity cost projections (sources: [12, 13, 20, 56, 57, 63–67])

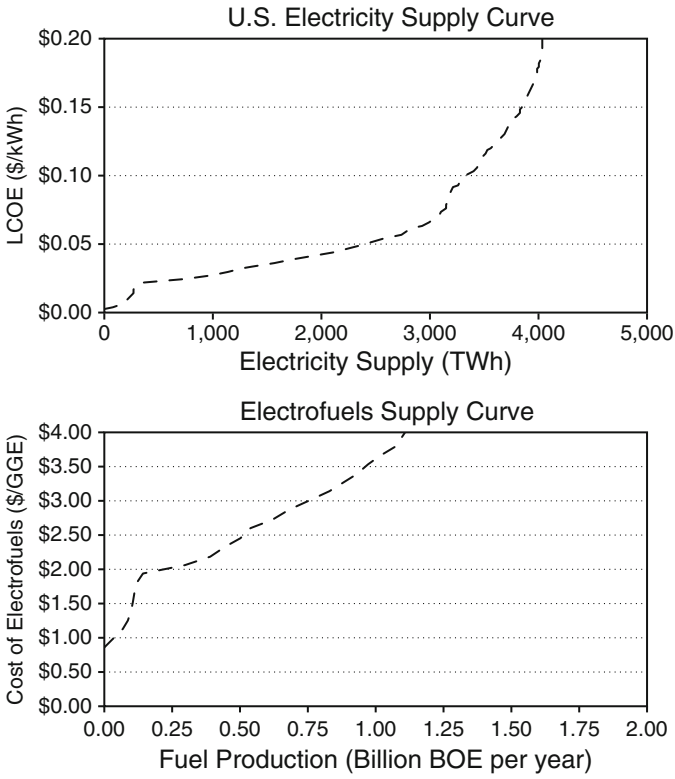

Fig. 4 Electricity supply curve (*top graph*) in the USA plotted against the LCOE, levelized cost of electricity. This supply includes the entire generation of the entire US fleet, which includes renewable and nonrenewable sources, as well as electricity produced in different locations at different times during the year. The *bottom graph* plots the corresponding supply curve of Electrofuels provided the electricity supply cost (*top graph*) and values from Table 3 (source: [47])

Both electricity and hydrogen feedstocks are clearly compatible with modern industrial infrastructure and both can supply the energy needed for an Electrofuels process (Fig. 5a). While hydrogen can be produced *via* electrolysis or perhaps from catalytic water oxidation in the future, it might also be produced from natural gas or biomass reforming, offering gas-to-liquids or biomass-to-liquids (GTL/BTL) possibilities (Fig. 5b). For example, steam reforming of industrial tail gases or low value hydrocarbons can produce hydrogen at less than $1.00/kg [32] with concomitant production of free, clean, concentrated inorganic carbon. These values would reduce feedstock costs to $1.34/GGE and overall costs to $2.25/GGE, even considering a likely increase in capital costs (Supp Calc 9).

Table 3 Major cost components of electrofuels process

Item	Base Cost	Cost ($/GGE)
Electricity Feedstock	$0.04/kWh	$2.15
Capital Cost	$2/yearly GGE	$0.45
CO_2 Feedstock	$40/ton CO_2	$0.37
O_2 Co-product	$20/ton O_2	-$0.20
Labor and Overhead	$0.15/GGE	$0.15
Maintenance and Taxes	4% of TPI	$0.09
Materials and Waste	$0.08/GGE	$0.08
Water Feedstock	$2/1000 gallons	$0.01
Total Cost	**Supp Calc 8**	**$3.09**

Item	Base Value
Cellular Energy Efficiency	100%
e- Consumed per Butanol Produced	28 e-
Delivered Voltage	1.5 V

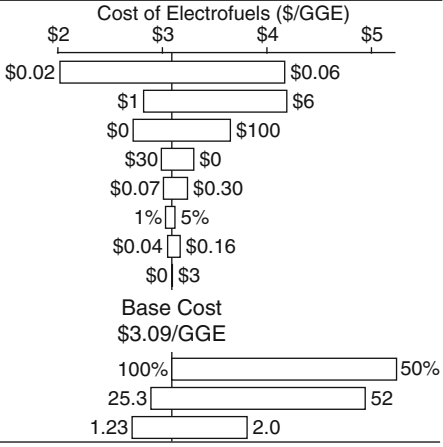

Cost components and base values are tabulated to determine the individual cost of specific components as well as the overall cost of fuel production through electrofuels. With each cost item, a sensitivity analysis is provided in the Tornado chart on the *right* to illustrate how the variation in a single parameter influences the overall cost. The *top* of the table/chart itemizes standard engineering parameters, whereas the *bottom* of the table/chart itemizes biological constraints, the latter which each of the Electrofuels projects address

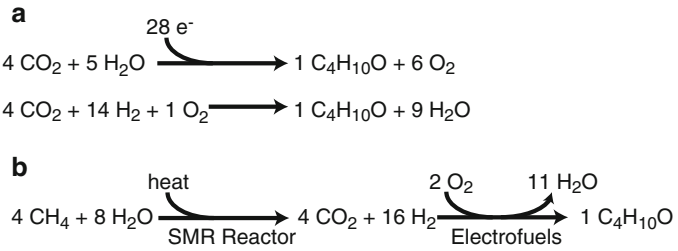

Fig. 5 (**a**) Paths to Electrofuels using either direct current or dihydrogen as the energy source. (**b**) Proposed Electrofuels pathway as a gas-to-liquids technology where methane first passes through a steam methane reformer (SMR reactor) and then through a water–gas shift reaction, before the effluent is cooled and fed to an Electrofuels reactor

6 The Challenge of Scale

Current US electricity generation (4.2×10^{12} kWh, [46]) could produce roughly 24% of the Nation's crude oil demands; the US installed base operating at 100% utilization (1.12 TW nameplate capacity, [15]) could produce roughly 55% of the Nation's crude oil demands (Supp Calc 5). The economical production of fuel at even moderate scales would require significant renewable energy feedstocks: at least 1 GW of renewable electricity would be required to synthesize 10,000 BOE/day via an Electrofuels approach (Supp Calc 5). No electrochemical process has ever approached such scales and implementation will clearly require significant advances in engineering. Still, the potential advantages of an Electrofuels platform for the production of liquid fuels through processes that avoid the constraints of photosynthetic approaches is hard to overstate; replacement of 100% of the Nation's gasoline demand using 20% efficient solar collectors could be achieved harvesting the solar resource of approximately 7,000 mi^2 of nonarable land (Supp Calc 10), an area less than 5% of the acreage currently used for corn production in the USA [54].

7 Conclusions

The Electrofuels program offers an opportunity to transform the US energy infrastructure. By converting renewable electricity at times of low demand into fungible liquid fuels, engineered chemolithoautotrophic organisms could enable further integration of wind and solar energy on the electricity grid while diminishing US dependence on foreign oil. The technical challenges remain significant, and the approach is still in its infancy. Those challenges notwithstanding the use of nonphotosynthetic autotrophic organisms offers a feedstock flexible and potentially high efficiency synthesis of liquid fuels directly from renewable energy resources, without competition for arable land or scarce water resources. Continued development of the Electrofuels program offers a hedge against future resource constraints and the costly and unpredictable supply of foreign oil.

The Advanced Research Projects Agency (*ARPA-E*). ARPA-E was created by the US Congress in 2007 to enhance our energy and economic security, strengthening national security through the way we generate, store, and use energy. ARPA-E invests in and manages the development of transformational energy technologies that hold the potential to radically shift our Nation's energy reality. Modeled after the Defense Advanced Research Projects Agency (DARPA), ARPA-E considers high-risk/high-impact routes to energy innovation. ARPA-E aims to promote the rapid development of technologies toward a point where private investment funds demonstration at scale and deployment.

Acknowledgments We thank Dr. Nicholas Cizek, Dr. Philippe Larochelle, Dr. Dawson Cagle, and Mr. Gregory Callman for their contributions to this chapter. We thank the 13 ARPA-E Electrofuels performer teams whose efforts make these goals possible.

Appendix A. Supplementary Calculations

A.1 Supplementary Calculation 1: Energy Captured by Corn-to-Ethanol

Critical values
Annual solar radiance: 4.1 kWh/m^2/day (Des Moines, IA—[40])
Corn yield Midwest: 152.8 bushels/ac-yr [55]
Corn-to-ethanol yield: 2.8 gal ethanol/bushel corn [6, 10]

Annual solar energy

$$(4.1\text{kWh/m}^2\text{/day}) \times (3.6 \times 10^6\ \text{J/kWh}) \times (4{,}047\text{m}^2\text{/ac}) \times (365\text{days/yr})$$
$$= 2.2 \times 10^{13}\ \text{J/ac - yr}$$

Annual processed fuel energy

$$(152.8\text{bushels corn/ac - yr}) \times (2.8\text{gal EtOH/bushel corn})$$
$$\times (3.785\text{L EtOH/gal EtOH}) \times (24 \times 10^6\ \text{J/L EtOH})$$
$$= 3.9 \times 10^{10}\ \text{J/ac - yr}$$

Fraction solar energy harness in ethanol fuel

$$(3.9 \times 10^{10}\ \text{J/ac - yr}) / (2.2 \times 10^{13}\ \text{J/ac - yr}) = 0.18\%$$

A.2 Supplementary Calculation 2: Energy Captured by Sugarcane-to-Ethanol

Critical values
Annual solar radiance: 5.6 kWh/m^2/day (Brazil—[21, 23])
Brazil sugarcane yield: 33.4 tons harvested/ac-yr [55]
Sugarcane-to-ethanol yield: 19.5 gal ethanol/ton sugarcane [53]

Annual solar energy

$$(5.6\text{kWh/m}^2\text{/day}) \times (3.6 \times 10^6\ \text{J/kWh}) \times (4{,}047\text{m}^2\text{/ac}) \times (365\text{days/yr})$$
$$= 3.0 \times 10^{13}\ \text{J/ac - yr}$$

Annual processed fuel energy

$$(33.4\,\text{tons sugarcane/ac - yr}) \times (19.5\,\text{gal EtOH/ton sugarcane})$$
$$\times (3.785\,\text{L EtOH/gal EtOH}) \times (24 \times 10^6\,\text{J/L EtOH})$$
$$= 5.9 \times 10^{10}\,\text{J/ac - yr}$$

Fraction solar energy harnessed in ethanol fuel

$$(5.9 \times 10^{10}\,\text{J/ac - yr}) / (3.0 \times 10^{13}\,\text{J/ac - yr}) = 0.20\%$$

A.3 Supplementary Calculation 3: Minimum Water Used by Electrofuels

Critical values

$4CO_2 + 5H_2O + 28e^- \rightarrow 1C_4H_{10}O + 6O_2$ (Electrofuels cell metabolism, $20e^-$ to convert $2CO_2$ to 2AcCoA, $8e^-$ to convert 2AcCoA to 1BuOH, assuming no diverted energy)

Minimum water use

$$(5\,\text{mol } H_2O/1\,\text{mol BuOH}) \times (18\,\text{g } H_2O/1\,\text{mol } H_2O) \times (1\,\text{mol BuOH}/74\,\text{g BuOH})$$
$$\times (1{,}000\,\text{g BuOH}/36.6 \times 10^6\,\text{J}) \times (1\,\text{L } H_2O/1{,}000\,\text{g } H_2O) \times (34.2 \times 10^6\,\text{J/L gasoline})$$
$$= 1.1\,\text{gal } H_2O/\text{gal of gasoline equivalent}$$

A.4 Supplementary Calculation 4: Solar Efficiency of Electrofuels

Critical values

$4CO_2 + 5H_2O + 28e^- \rightarrow 1C_4H_{10}O + 6O_2$ (Electrofuels cell metabolism)
Efficiency of solar panel: 20% [25]
Voltage of delivered electricity: 1.5 V [39]

Solar efficiency of electrofuels

$$(0.2\,\text{J } e^-/\text{J solar energy}) \times (1\text{C}(@1.5\text{V}) / 1.5\,\text{J } e^-) \times (6.24 \times 10^{18}\,e^-/\text{C})$$
$$\times (1\,\text{BuOH}/28\,e^-) \times (1\,\text{mol BuOH}/6.02 \times 10^{23}\,\text{BuOH})$$
$$\times (74\,\text{g BuOH/mol BuOH}) \times (36.6 \times 10^6\,\text{J}/1{,}000\,\text{g BuOH})$$
$$= 13.3\%$$
$$= 29.1\%$$

(with state of art 43.5% solar cell, [25])

A.5 Supplementary Calculation 5: Land Requirements for Fuels Production

Critical values
Electrofuels solar efficiency: 13.3% (Supp Calc 4)
Joule unlimited solar efficiency: 7.2% [49]
Annual solar radiance: 5.7 kWh/m^2/day (El Paso, TX—[40])

Land use requirements

$$(5.7\,\text{kWh/m}^2\text{/day}) \times (3.6 \times 10^6\,\text{J/kWh}) \times (4{,}047\,\text{m}^2\text{/ac})$$
$$\times (1\,\text{BOE}/6.12 \times 10^9\,\text{J}) \times (365\,\text{days/yr})$$
$$= 4{,}950\,\text{BOE/ac - yr(solar energy)}$$
$$= 660\,\text{BOE/ac - yr(Electrofuels@13.3\% Efficiency-Wood-Ljundahl)}$$
$$= 360\,\text{BOE/ac - yr(Electrofuels@7.2\% Efficiency-3 - hydroxypropionate bicycle or Calvin cycle, anaerobic)}$$
$$= 360\,\text{BOE/ac - yr(Joule Unlimited@7.2\% Efficiency)}$$

A.6 Supplementary Calculation 6: Electrofuels Production from Wind Energy

Critical values
Annual wind energy: 0.053 kWh/m^2/day (North Dakota—[41])
$4CO_2 + 5H_2O + 28e^- \rightarrow 1C_4H_{10}O + 6O_2$ (Electrofuels cell metabolism)

Electrical efficiency of electrofuels

$$(1\text{C}(@1.5\text{V})/1.5\text{J}\,e^-) \times (6.24 \times 10^{18}\,e^-/\text{C}) \times (1\,\text{BuOH}/28e^-)$$
$$\times (1\,\text{mol BuOH}/6.02 \times 10^{23}\,\text{BuOH}) \times (74\,\text{g BuOH/mol BuOH})$$
$$\times (36.6 \times 10^6\,\text{J}/1{,}000\,\text{g BuOH})$$
$$= 66.8\%$$

Land use requirements

$$(0.053\text{kWh/m}^2\text{/day}) \times (3.6 \times 10^6\ \text{J/kWh}) \times (4{,}047\text{m}^2\text{/ac})$$
$$\times (1\ \text{BOE}/6.12 \times 10^9\ \text{J}) \times (365\ \text{days/yr})$$
$$= 46\ \text{BOE/ac - yr (Wind Energy Energy)}$$
$$= 31\ \text{BOE/ac - yr (Electrofuels @ 66.8\% Efficiency-Wood-Ljungdahl)}$$
$$= 17\ \text{BOE/ac - yr (Electrofuels @ 36.0\%}$$

Efficiency-3 - hydroxypropionate bicycle or Calvin cycle, anaerobic)

A.7 Supplementary Calculation 7: Electricity Requirements for Fuel Production

Critical values

$$4CO_2 + 5H_2O + 28e^- \rightarrow 1C_4H_{10}O + 6O_2\ \text{(electrofuels cell metabolism)}$$

Voltage of delivered electricity: 1.5 V [39]
US electricity nameplate capacity: 1.12 TW [15]
US electricity generation: 4.2×10^{15} Wh/yr [46]
US annual petroleum consumption: 7.0×10^9 barrels of petroleum [15]

Electricity required to produce 10,000 BOE/day

$$(10{,}000\ \text{BOE/day}) \times (6.12 \times 10^9\ \text{J/BOE}) \times (1\text{kg BuOH}/36.6 \times 10^6\ \text{J})$$
$$\times (28\text{mole}^-/0.074\text{kg BuOH}) \times (6.02 \times 10^{23}\ \text{e}^-/\text{mole}^-)$$
$$\times (1\text{C}/6.24 \times 10^{18}\ \text{e}^-) \times (1.5\text{J}/1\text{C}(@1.5\text{V})) \times (1\ \text{day}/86{,}400\text{s})$$
$$= 1.06\text{GW}$$

Possible fuel production from current US electricity generation

$$(4.2 \times 10^{15}\ \text{Wh/yr}) \times (10{,}000\ \text{BOE/day}/1.06 \times 10^9\ \text{W}) \times (1\ \text{day}/24\ \text{h})$$
$$= 1.7 \times 10^9\ \text{BOE/yr (24\% U.S. annual consumption)}$$

Possible Fuel Production from Current US Electricity Capacity (@ 100% capacity factor)

$$(1.12 \times 10^{12}\ \text{W}) \times (10{,}000\ \text{BOE/day}/1.06 \times 10^9\ \text{W}) \times (365\text{days/yr})$$
$$= 3.9 \times 10^9\ \text{BOE/yr (55\% U.S. annual consumption)}$$

A.8 Supplementary Calculation 8: Cost of Electrofuels from Electricity

Calculations for the cost of electricity, CO_2, labor, maintenance, taxes, materials, waste, water, and value of O_2 coproduct and can be derived from base costs in Table 3, and Supplementary Calculations 1–7. The annual cost of capital is derived by numerically solving for a net present value (NPV) of zero. This can be done assuming: 3-year construction period with constant spending rate, working capital equal to 15% of the total capital investment, 20-year facility life, 5-year MARCS depreciation of capital, 10% interest rate, 2% inflation rate, 50% nameplate utilization in year 1, 75% in year 2, and 100% in years 3–20, and 10% down time in years 1–20.

A.9 Supplementary Calculation 9: Cost of Electrofuels from Natural Gas

Critical values
$4CO_2 + 14\ H_2 + O_2 \rightarrow 1C_4H_{10}O + 9H_2O$ (Electrofuels cell metabolism)
Cost of H_2: \$1/kg H_2 (on-site production; [32])
Cost of CO_2: \$0/ton (coproduced with H_2 effluent)
25% increase in the cost of capital
No O_2 coproduct
Balance of systems cost: \$0.92/GGE

Cost of feedstock

$$(14\text{mol } H_2/\text{mol BuOH}) \times (2\text{g } H_2/\text{mol } H_2) \times (1\text{kg}/1{,}000\text{g})$$
$$\times (\$1/\text{kg } H_2) \times (1\text{mol BuOH}/74\text{g BuOH}) \times (1{,}000\text{g/kg})$$
$$\times (1\text{kg BuOH}/36.6 \times 10^6\text{ J}) \times (34.2 \times 10^6\text{ J/L}) \times (3.785\text{L/gal})$$
$$= \$1.34/\text{GGE } (H_2 \text{ and } CO_2 \text{ combined cost contribution})$$
$$= \$2.25/\text{GGE (overall cost)}$$

A.10 Supplementary Calculation 10: Land Use Requirements for Electrofuels

Critical values
US daily crude oil consumption: 19,148,000 barrels/day [15]
US daily gasoline consumption: 9,034,000 barrels/day [15]
Electrofuels solar efficiency: 13.3% (Supp Calc 4)
Annual solar radiance: 5.7 kWh/m^2/day (El Paso, TX—[40])

Land use requirements

$$(19.148\times10^{6}\,\text{barrel crude oil/day})\times(6.12\times10^{9}\,\text{J/barrel crude oil})$$
$$\times(1\text{kWh}/3.6\times10^{6}\,\text{J})\times(1\text{m}^2\,\text{/day}/5.7\text{kWh})\times(1\text{ac}/4{,}047\text{m}^2)$$
$$\times(1\text{J solar}/0.133\text{J fuel})$$
$$=10.6\times10^{6}\text{ acres}$$
$$=16{,}600\text{mi}^2$$
$$=129\text{mi}\times129\text{mi (for total U.S. crude oil production)}$$

$$(9.034\times10^{6}\,\text{barrel gasoline/day})\times(42\text{ gal/barrel})\times(3.785\text{L/gal})$$
$$\times(34.2\times10^{6}\,\text{J/L})\times(1\text{kWh}/3.6\times10^{6}\,\text{J})\times(1\text{m}^2\,\text{/day}/5.7\text{kWh})$$
$$\times(1\text{ac}/4{,}047\text{m}^2)\times(1\text{J solar}/0.133\text{J fuel})$$
$$=4.4\times10^{6}\text{ acres}=6{,}950\text{mi}^2$$
$$=83\text{mi}\times83\text{mi (for total U.S. gasoline production)}$$

References

1. ARPA-E (2012) Electrofuels program. http://arpa-e.energy.gov/ProgramsProjects/Electrofuels.aspx. Accessed July 2011
2. ARPA-E (2011) Electrofuels. DE-FOA-0000206. https://arpa-e-foa.energy.gov/Default.aspx?Archive=1#d95b8b45-4738-47f6-a553-2db79c13437e. Accessed July 2011
3. ARPA-E (2011) Plants engineered to replace oil (PETRO). DE-FOA-0000470. https://arpa-e-foa.energy.gov/#bc334967-4db1-4458-9700-7371c75543cb. Accessed July 2011
4. Bar-Even A, Noor E, Lewis NE, Milo R (2010) Design and analysis of synthetic carbon fixation pathways. Proc Natl Acad Sci U S A 107(19):8889–8894
5. Berg IA, Kockelkorn D, Ramos-Vera WH, Say RF, Zarzycki J, Hügler M, Alber BE, Fuchs G (2010) Autotrophic carbon fixation in Archaea. Nat Rev Microbiol 8(6):447–460; Review
6. Bothast RJ, Schlicher MA (2005) Biotechnological processes for conversion of corn into ethanol. Appl Microbiol Biotechnol 67(1):19–25
7. Burgdorf T, Lenz O, Buhrke T, van der Linden E, Jones AK, Albracht SPJ, Friedrich B (2005) [NiFe]-hydrogenases of *Ralstonia eutropha* H16: modular enzymes for oxygen-tolerant biological hydrogen oxidation. J Mol Microbiol Biotechnol 10:181–196
8. Butler TJ, McFarland ML, Muir JP (2006) Using dairy manure compost for corn production. Texas Water Resources Institute and Texas Cooperative Extension. http://compost.tamu.edu/docs/compost/pubs/cornproduction.pdf. Accessed July 2011
9. Cellana (2011) Kona demonstration factility. http://cellana.com/production-facilities/facilities/. Accessed 20 Jun 2011
10. Christianson & Associates (2011) Biofuels benchmarking annual report 2010. http://www.christiansoncpa.com/email/Biofuels-Benchmarking-Annual-Report.aspx. Accessed 21 Jun 2011
11. Condon AG, Richards RA, Rebetzke GJ, Farquhar GD (2004) Breeding for high water-use efficiency. J Exp Bot 55(407):2447–2460
12. CME Group (2011) Corn futures. http://www.cmegroup.com/trading/agricultural/grain-and-oilseed/corn.html. Accessed 21 June 2011

13. CME Group (2011) Henry Hub natural gas futures. http://www.cmegroup.com/trading/energy/natural-gas/natural-gas.html. Accessed 9 Aug 2011
14. David MB, Drinkwater LE, McIsaac GF (2010) Sources of nitrate yields in the Mississippi River Basin. J Environ Qual 39(5):1657–1667
15. EIA (2009) Electric power annual 2009, existing nameplate and net summer capacity by energy source, producer type and state (EIA-860). http://www.eia.gov/cneaf/electricity/epa/epa_sprdshts.html. Accessed 21 June 2011
16. Electricity Reliability Council of Texas (ERCOT) (2011) Real time settlement price point display. http://www.ercot.com/content/cdr/html/real_time_spp. Accessed 2011
17. Farquhar GD, Richards RA (1984) Isotopic composition of plant carbon correlates with water-use efficiency of wheat genotypes. Aust J Plant Physiol 11(6):539–552
18. Ferguson RL, Buckley EN, Palumbo AV (1984) Response of marine bacterioplankton to differential filtration and confinement. Appl Environ Microbiol 47(1):49–55
19. Field C, Mooney HA (1983) Leaf age and seasonal effects on light, water, and nitrogen use efficiency in a California shrub. Oecologia (Berl) 56:348–355
20. Gandrik AM, Wood RA (2010) Sensitivity of hydrogen production via steam methane reforming to high temperature gas-cooled reactor outlet temperature economic analysis. INL. TEV-962. Project No. 23843
21. Goldemberg J (2008) Review. The Brazilian biofuels industry. Biotechnol Biofuels 1:6
22. Howell TA (2002) Irrigation efficiency. In: Lal R (ed) Encyclopedia of soil science. Marcel Dekker, New York, pp 736–741
23. INPE, LABSOLAR (2009) Brazil direct normal solar radiation model (10km). http://en.openei.org/datasets/node/547. Accessed July 2011
24. Joule Unlimited (2011) http://www.jouleunlimited.com/. Accessed 21 Jun 2011
25. Kazmerski L (2011) NREL compilation of best research solar cell efficiencies. http://upload.wikimedia.org/wikipedia/commons/e/ed/PVeff%28rev110408U%29.jpg. Accessed 21 Jun 2011
26. Kenny JF, Barber NL, Hutson SS, Linsey KS, Lovelace JK, Maupin MA (2009) Estimated use of water in the United States in 2005. U.S. Geological Survey Circular 1344
27. Klocke NL (2004) Water savings from crop residue in irrigated corn. In Proceedings central plains irrigation conference, Kearney, NE, 17–18 Feb 2004, pp 133–141
28. Lan EI, Liao JC (2011) Metabolic engineering of cyanobacteria for 1-butanol production from carbon dioxide. Metab Eng 13(4):353–363
29. Lee SH, Fuhrman JA (1991) Species composition shift of confined bacterioplankton studied at the level of community DNA. Mar Ecol Prog Ser 79:195–201
30. Liu X, Sheng J, Curtiss R III (2011) Fatty acid production in genetically modified cyanobacteria. Proc Natl Acad Sci U S A 108(17):6899–6904
31. Liu X, Fallon S, Sheng J, Curtiss R III (2011) CO_2-limitation-inducible Green Recovery of fatty acids from cyanobacterial biomass. Proc Natl Acad Sci U S A 108(17):6905–6908
32. Longanbach JR, Rutkowski MD, Klett MG, White JS, Schoff RL, Buchanan TL (2002) Hydrogen production facilities plant performance and cost comparisons. Final report, March 2002. The United States Department of Energy, National Energy Technology Laboratory, Pittsburgh
33. Malvankar NS, Vargas M, Nevin K, Franks AE, Leang C, Kim BC, Inoue K, Mester T, Covalla SF, Johnson JP, Rotello VM, Tuominen MT, Lovley DR (2011) Tunable metallic-like conductivity in microbial nanowire networks. Nat Nanotechnol 6(9):573–579
34. Martinelli LA, Filoso S (2008) Expansion of sugarcan ethanol production in Brazil: environmental and social challenges. Ecol Appl 18(4):885–898
35. Moreira JR (2007) Water use and impacts due ethanol production in Brazil. In: International conference: linkages between energy and water management for agriculture in developing countries. http://www.iwmi.cgiar.org/EWMA/files/papers/Jose_Moreira.pdf. Accessed July 2011
36. Maurino VG, Peterhansel C (2010) Photorespiration: current status and approaches for metabolic engineering. Curr Opin Plant Biol 13(3):249–256

37. Netafim (2011) Fertigation. http://www.sugarcanecrops.com/agronomic_practices/fertigation/. Accessed 13 Jul 2011
38. Netafim (2011) Sugar cane best practices. http://www.netafim.com/crop/sugar-cane-bio-energy/best-practice. Accessed 13 Jul 2011
39. Nevin KP, Woodard TL, Franks AE, Summers ZM, Lovley DR (2010) Microbial electrosynthesis: feeding microbes electricity to convert carbon dioxide and water to multicarbon extracellular organic compounds. mBio 1(2):e00103–e00110
40. NREL (2011) National solar radiation data base 1961–1990. http://rredc.nrel.gov/solar/old_data/nsrdb/. Accessed 21 Jun 2011
41. NREL (2011) Estimates of windy land area and wind energy potential, by state, for areas ≥30% capacity factor at 80m. http://www.windpoweringamerica.gov/wind_maps.asp#potential. Accessed 21 Jun 2011
42. Oren A (2009) Chemolithotrophy. In: Encyclopedia of life sciences (ELS). Wiley, Chichester
43. Passel JS, Cohn DV (2008) U.S. population projections: 2005–2050. Pew Research Center, Washington, DC
44. Pate R, Klise G, Wu B (2011) Resource demand implications for US algae biofuels production scale-up. Appl Energy 88(10):3377–3388
45. Patil PD, Gude VG, Mannarswamy A, Deng S, Cooke P, Munson-McGee S, Rhodes I, Lammers P, Nirmalakhandan N (2011) Optimization of direct conversion of wet algae to biodiesel under supercritical methanol conditions. Bioresour Technol 102(1):118–122
46. PLATTS (2011) World electric power plants database
47. Ragsdale SW, Pierce E (2008) Acetogenesis and the Wood-Ljungdahl pathway of CO(2) fixation. Biochim Biophys Acta 1784(12):1873–1898
48. Renewable Fuels Association (RFA) (2011) Statistics. http://www.ethanolrfa.org/pages/statistics. Accessed Jul 2011
49. Robertson DE, Jacobson SA, Morgan F, Berry D, Church GM, Afeyan NB (2011) A new dawn for industrial photosynthesis. Photosynth Res 107(3):269–277
50. Shapiro CA, Ferguson RB, Hergert GW, Dobermann AR, Wortmann CS (2003) Fertilizer suggestions for corn. University of Nebraska-Lincoln Extension, Institute of Agriculture and Natural Resources, Lincoln
51. Solley WB, Pierce RR, Perlman HA (1998) Estimated use of water in the United States in 1995, Circular 1200, U.S. Geological Survey
52. USDA (2005) Agricultural chemicals and production technology: nutrient management. http://www.ers.usda.gov/briefing/AgChemicals/nutrientmangement.htm#commercial. Accessed 13 Jul 2011
53. U.S. Department of Agriculture (USDA) (2006) The economic feasibility of ethanol production from sugar in the United States. http://www.usda.gov/oce/reports/energy/EthanolSugarFeasibilityReport3.pdf. Accessed July 2011
54. USDA (2009) 2007 census of agriculture. USDA AC-07-A-51
55. USDA (2010) National agriculture statistics service. http://www.nass.usda.gov/Data_and_Statistics/index.asp. Accessed 21 Jun 2011
56. USDA (2011) Economic research service. http://www.ers.usda.gov/data/feedgrains/. Accessed 01 Aug 2011
57. U.S. Energy Information Administration (EIA) (2011) Monthly energy review
58. U.S. Energy Informational Administration (EIA) (2011) Petroleum and other liquids data. http://www.eia.gov/dnav/pet/pet_cons_psup_dc_nus_mbblpd_m.htm. Accessed 27 Jul 2011
59. van Dokkum PG, Conroy C (2010) A substantial population of low-mass stars in luminous elliptical galaxies. Nature 468(7326):940–942
60. Vispute TP, Zhang H, Sanna A, Xiao R, Huber GW (2010) Renewable chemical commodity feedstocks from integrated catalytic processing of pyrolysis oils. Science 330(6008):1222–1227
61. Whitman WB, Coleman DC, Wiebe WJ (1998) Prokaryotes: the unseen majority. Proc Natl Acad Sci U S A 95(12):6578–6583

62. Wigmosta MS, Coleman AM, Skaggs RJ, Huesemann MH, Lane LJ (2011) National microalgae biofuel production potential and resource demand. Water Resour Res 47:W00H04
63. Wiser R, Bolinger M (2007) Annual report on U.S. wind power installation, cost, and performance trends: 2006. LBNL-62702
64. Wiser R, Bolinger M (2008) Annual report on U.S. wind power installation, cost, and performance trends: 2007. LBNL-275E
65. Wiser R, Bolinger M (2009) 2008 Wind technologies market report. NREL Report No. TP-6A2-46026; DOE/GO-102009-2868
66. Wiser R, Bolinger M (2010) 2009 Wind technologies market report. LBNL-3716E
67. Wiser R, Bolinger M (2011) 2010 Wind technologies market report. LBNL-4820E
68. Wu M, Mintz M, Wang M, Arora S (2009) Consumptive water use in the production of ethanol and petroleum gasoline. ANL/ESD/09-1
69. Yarzabal A, Brasseur G, Ratouchniak J, Lund K, Lemesle-Meunier D, DeMoss JA, Bonnefoy V (2002) The high-molecular-weight cytochrome c Cyc2 of *Acidithiobacillus ferrooxidans* is an outer membrane protein. J Bacteriol 184(1):313–317
70. Zhu XG, Long SP, Ort DR (2008) What is the maximum efficiency with which photosynthesis can convert solar energy into biomass? Curr Opin Biotechnol 19(2):153–159

Chapter 39
Engineering *Ralstonia eutropha* for Production of Isobutanol from CO_2, H_2, and O_2

Christopher J. Brigham, Claudia S. Gai, Jingnan Lu, Daan R. Speth, R. Mark Worden, and Anthony J. Sinskey

Abstract Isobutanol (IBT) can be used as a 100% replacement for gasoline in existing automobile engines, has >90% of the energy density of gasoline and is compatible with established fuel distribution infrastructure. The facultatively autotrophic bacterium *Ralstonia eutropha* can utilize H_2 for energy and CO_2 for carbon and is also employed in industrial processes that produce biodegradable plastics. Using a carefully designed production pathway, *R. eutropha*, a genetically tractable organism, can be modified to produce biofuels from autotrophic growth. Microbial

C.J. Brigham • C.S. Gai
Department of Biology, Massachusetts Institute of Technology,
77 Massachusetts Avenue, Cambridge, MA 02139, USA

J. Lu
Department of Chemistry, Massachusetts Institute of Technology,
77 Massachusetts Avenue, Cambridge, MA 02139, USA

D.R. Speth
Department of Biology, Massachusetts Institute of Technology,
77 Massachusetts Avenue, Cambridge, MA 02139, USA

Department of Microbiology, IWWR, Radboud University Nijmegen,
Heyendaalseweg 135, 6525 AJ Nijmegen, The Netherlands

R.M. Worden
Department of Chemical Engineering and Materials Science,
Michigan State University, East Lansing, MI 48824, USA

A.J. Sinskey (✉)
Department of Biology, Massachusetts Institute of Technology,
77 Massachusetts Avenue, Cambridge, MA 02139, USA

Engineering Systems Division, Massachusetts Institute of Technology,
77 Massachusetts Avenue, Cambridge, MA 02139, USA

Health Sciences Technology Division, Massachusetts Institute of Technology,
77 Massachusetts Avenue, Cambridge, MA 02139, USA
e-mail: asinskey@mit.edu

J.W. Lee (ed.), *Advanced Biofuels and Bioproducts*, DOI 10.1007/978-1-4614-3348-4_39, 1065

production of IBT can be achieved by directing the flow of carbon through a synthetic production pathway involving the branched-chain amino acid biosynthesis pathway, a heterologously expressed ketoisovalerate decarboxylase, and a broad substrate specificity alcohol dehydrogenase. We discuss the motivations and the methods used to engineer *R. eutropha* to produce the liquid transportation fuel IBT from CO_2, H_2, and O_2.

1 Introduction

Increased demand for fossil fuels along with dwindling reserve supplies reveals an immediate need for alternative fuel sources. Bio-based fuels, or biofuels, are produced from many sources of biomass. Microbially produced biofuels offer a sustainable approach to fuel production using inexpensive carbon sources, such as agricultural waste or CO_2 [1]. The availability of H_2 derived from solar-powered electrolysis will eventually increase dramatically, creating demand for microbes that use this energy source to convert CO_2 into value-added chemical compounds, including liquid transportation fuels. Ethanol has been long discussed as a biofuel since Beall et al. [2, 3] developed a method for producing ethanol from sugars using a recombinant *Escherichia coli* strain. However, ethanol is not the most suitable alcohol for biofuel use as its hygroscopicity is higher and its energy density is lower than for longer chain alcohols [4]. Isobutanol (IBT), on the other hand, can be used without gasoline-blending in existing internal combustion engines and is compatible with the existing fuel infrastructure [5]. Recently, an automobile competed in the American Le Mans racing Series running on 100% IBT [6]. Although the source of IBT was not disclosed, the American Le Mans racing Series had recently approved IBT from corn, sugarcane, and cellulosic feedstocks for use as a fuel [7].

1.1 Ralstonia eutropha as IBT Production Organism of Choice

Despite the initial successes in IBT biosynthesis with *E. coli* [4] and yeast [8] using glucose as the main carbon source, the lone published attempt to establish IBT production in a host organism that can utilize CO_2 as a carbon source, the photosynthetic cyanobacterium *Synechococcus elongates*, resulted in an IBT titer of less than 1 g/L [4]. The facultatively autotrophic Gram-negative bacterium *Ralstonia eutropha* is capable of reducing CO_2 in the presence of O_2. It has also been observed to utilize H_2, both exogenously delivered to culture vessels and produced in situ via electrolysis [9]. *R. eutropha* is a metabolically versatile bacterium that can also utilize sugars, fatty acids, amino acids, and triacylglycerols as carbon sources [10, 11]. When available in excess, carbon is typically stored by *R. eutropha* in the form of polyhydroxybutyrate (PHB), a natural polyester present in intracellular inclusion bodies [12–14]. Designing a recombinant strain of *R. eutropha* to produce IBT as opposed to PHB would require a redirection of carbon flux via the pathway shown in Fig. 1. A well-developed collection of *R. eutropha* basic biology and strain engineering tools, enumerated in Table 1, exists allowing facile

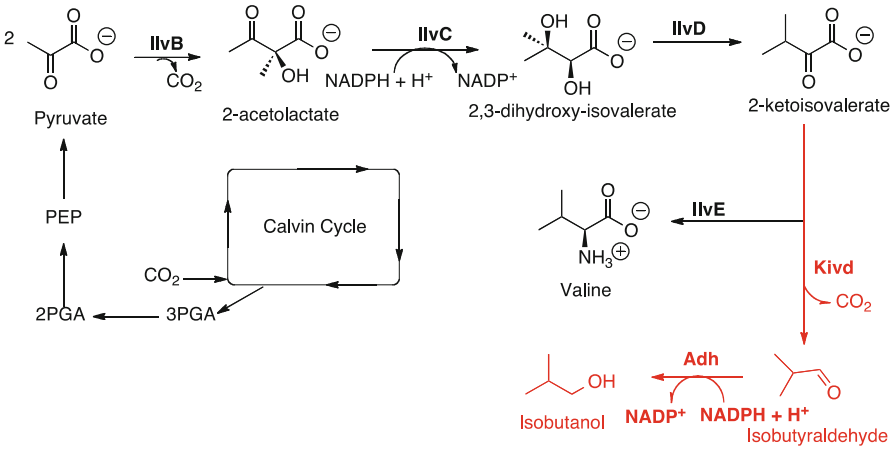

Fig. 1 Schematic diagram of the engineered isobutanol (IBT) production pathway in *Ralstonia eutropha*. Shown in *red* are the steps of the pathway that direct carbon flux away from branched chain amino acid (BCAA) biosynthesis towards isobutyraldehyde and IBT synthesis. *IlvB* acetohydroxyacid synthase; *IlvC* ketoacid reductoisomerase; *IlvD* dihydroxyacid dehydratase; *IlvE* transaminase; *Kivd* ketoisovalerate decarboxylase; *Adh* alcohol dehydrogenase; *3PGA* 3-phosphoglycerate; *2PGA* 2-phosphoglycerate; *PEP* phosphoenol pyruvate. All enzymes present in this figure are discussed in the text

Table 1 Catalog of *R. eutropha* strain engineering and culture analysis tools

Engineering/analysis tool	Research application for IBT production studies	Reference(s)[a]
Plasmid-borne gene expression	High-level expression of IBT pathway enzymes	[97]
Targeted gene deletion	Removal of genes whose products divert carbon from IBT	[98]
Microarray analysis	Identification of genes involved in CO_2 fixation and IBT production	[10]
Transposon mutant libraries	Creation of screens for product tolerance	[99]
Fermentation product analysis	GC analysis of alcohols. Test of IBT production strain. Optimize and scale-up IBT production	[100]

[a]Reference indicates an example of the technique from published literature

modification of the *R. eutropha* genome. These factors make *R. eutropha* an ideal organism for metabolic engineering to produce IBT from CO_2, H_2, and O_2.

1.2 *Engineering R. eutropha to Produce IBT: Overview and Rationale*

Autotrophic production of PHB in *R. eutropha* has been studied previously, and the fermentation parameters to maximize culture density and mitigate explosion risk

have been studied in detail [14–16]. Also, stoichiometric formulae for autotrophic biomass and PHB production have been calculated, with the latter being [14]:

$$4CO_2 + 33H_2 + 12O_2 \rightarrow C_4H_6O_2 + 30H_2O \quad (1)$$

Adapting this stoichiometry for IBT production, the overall mass balance on the gaseous inputs and liquid products would be:

$$4CO_2 + 36H_2 + 12O_2 \rightarrow C_4H_{10}O + 31H_2O \quad (2)$$

The standard free energy ($\Delta G°$) for this overall reaction is −5.0 MJ/mol IBT, which demonstrates that IBT production is not in violation of thermodynamic laws. Assuming that 50% of the electrical energy used for H_2O electrolysis ($\Delta G° = 0.237$ MJ/mol H_2O) is lost as heat, approximately ((0.237 MJ/mol H_2) × (36 mol H_2)/(0.5)) = 17.1 MJ of electrical energy are needed to produce 1 mol of IBT ($C_4H_{10}O$). As the approximate heat of combustion of IBT is 2.4 MJ/mol, the IBT production process involving a recombinant *R. eutropha* strain discussed here should be able to convert approximately 10% of the input electrical energy to transportation fuel energy. The required input H_2:O_2 ratio of 3:1 can easily be achieved via H_2O electrolysis, which produces separate H_2 and O_2 product streams that can be fed to IBT-producing *R. eutropha* cultures in any desired ratio. However, integrating the fermentation with in situ generation of H_2 and O_2 presents a reactor design challenge, which is discussed below (see Sects. 4.1 and 4.2).

When grown autotrophically, *R. eutropha* generates the energy and reducing equivalents required to drive carbon fixation by the oxidation of H_2 gas, catalyzed by hydrogenase enzymes. There are three types of hydrogenases present in *R. eutropha.* Two of these are energy conserving hydrogenases (Fig. 2): a membrane bound hydrogenase (MBH, Fig. 2a) and a soluble hydrogenase (SH, Fig. 2b). The third is a regulatory hydrogenase (RH), which serves as a hydrogen sensor [17].

Electrons generated by the MBH are directed into the respiratory chain, providing the reducing equivalents for reduction of O_2 to H_2O and the proton gradient for ATP synthesis [18]. The cytoplasmic SH directly reduces NAD^+ to NADH [19], which is necessary to drive carbon fixation via the Calvin–Benson–Bassham (CBB) cycle [20]. Because all three hydrogenases in *R. eutropha* are resistant to inhibition by ambient oxygen concentrations, H_2 oxidation can be coupled to the reduction of O_2, a rare property among microorganisms [21]. Despite the presence of a hydrogen sensor, expression of both energy-conserving hydrogenases is linked to global energy level, not the amount of available hydrogen [22]. The combination of constitutive expression and oxygen resistance allows use of the hydrogenases in aerobic processes, such as the autotrophic production of IBT.

For design of an IBT production pathway in *R. eutropha*, carbon must first be diverted from PHB biosynthesis. A deletion of the PHA synthase gene, *phaC*, abolishes PHB production [23]. However, to maximize carbon flow to IBT, the β-ketothiolase and acetoacetyl-CoA reductase genes (*phaA* and *phaB*, respectively) have also been deleted. Further optimization of carbon flow requires that many of the

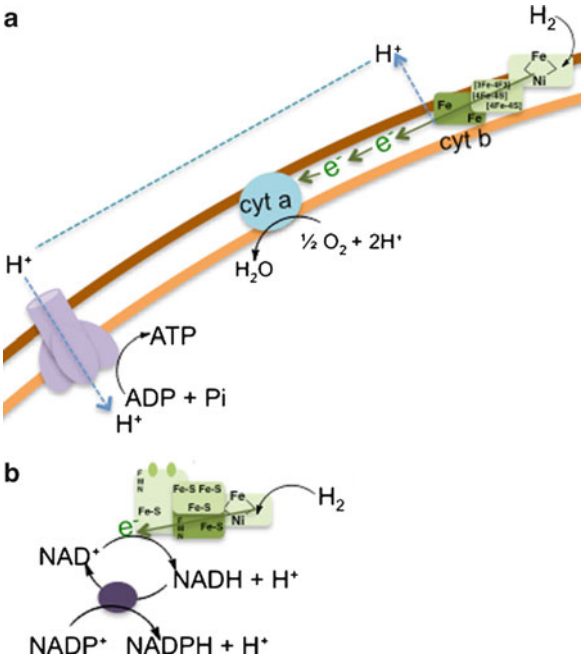

Fig. 2 Roles of membrane-bound hydrogenase (MBH) and soluble hydrogenase (SH) in *R. eutropha* during autotrophic growth. (**a**) The MBH complex (*green*) transfers electrons from hydrogen (H_2) down the electron transport chain to a cytochrome *a* (*blue*) that results in the reduction of molecular O_2 to H_2O. Alternatively, protons are pumped into the cell by the F_0F_1-ATPase (*purple*) to produce ATP. (**b**) The soluble hydrogenase splits H_2 to produce NADH + H^+ directly from NAD^+. A transhydrogenase (*dark blue*) can then produce NADPH + H^+ from $NADP^+$ and NADH + H^+. For information on the individual subunits of SH and MBH, refer to [17]

genes and enzymes needed for the IBT biosynthesis pathway (Fig. 1), most which are native to *R. eutropha*, be expressed concomitantly and that the temporal expression of the pathway is highest during "carbon storage" conditions.

The CBB cycle is used by a vast majority of autotrophic microorganisms for CO_2 assimilation, and is often coupled with photosynthesis. Ribulose-1,5-bisphosphate carboxylase/oxygenase (RuBisCO) is the key enzyme of the cycle. RuBisCO is a bifunctional enzyme that is involved both in photosynthesis and photorespiration in photosynthetic organisms. The enzyme catalyzes the initial step in the fixation of CO_2. In this reaction, one molecule of CO_2 is added to ribulose-1,5-bisphosphate, yielding two molecules of 3-phosphoglycerate (3-PGA) which can be metabolized to pyruvate or other central metabolites. When *R. eutropha* is growing autotrophically, the reducing equivalents required for the CBB cycle are generated by the oxidation of hydrogen, rather than photosynthesis. Figure 3 shows a schematic of the *R. eutropha* CBB pathway.

To enhance CO_2 fixation, organisms have developed efficient methods to acquire inorganic carbon. Carbonic anhydrase (carbonate dehydratase) enzymes play important

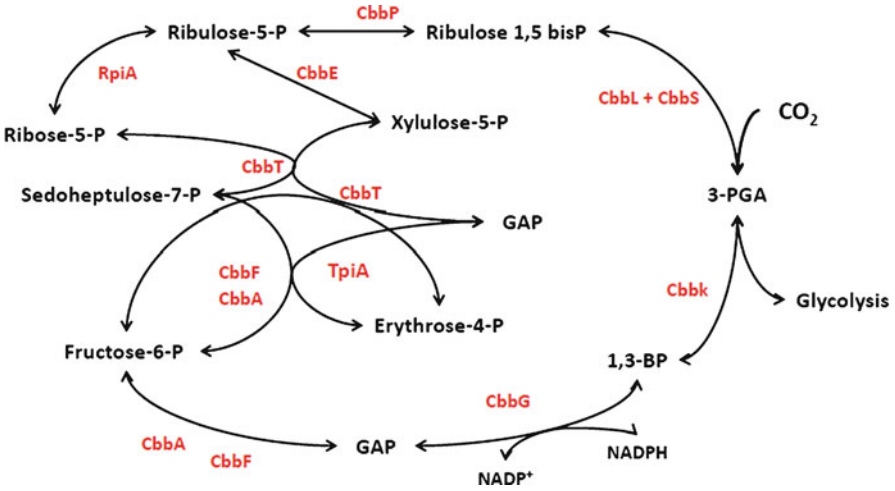

Fig. 3 Schematic diagram of the Calvin–Benson–Bassham (CBB) cycle in *R. eutropha.* Ribulose-5-phosphate is phosphorylated by the enzyme phosphoribulose kinase (CbbP). The resulting compound, ribulose-1,5-bisphosphate is then carboxylated by ribulose-1,5-bisphosphate carboxylase/oxygenase (RuBisCO) (CbbL and CbbS) The outcome of this carboxylation are two molecules of 3-phosphoglycerate (3-PGA). 3-PGA is phosphorylated by phosphoglycerate kinase (CbbK) to yield 1,3-bisphosphoglycerate (1,3-BP). 1,3-Bisphosphoglycerate is reduced by NADPH to yield $NADP^+$ and glyceraldehyde-3-phosphate (GAP) by glyceraldehyde-3-phosphate dehydrogenase (CbbG). GAP is then converted fructose-6-phosphate (F6P) by aldolase (CbbA) and fructose bisphosphatase (CbbF). The reversible reactions of the reductive pentose phosphate cycle involving erythrose-4-phosphate, fructose-6P, sedoheptulose-7P, xylulose-5P, and ribose-5-P are catalyzed by the enzymes: Transketolase (CbbT), fructose-bisphosphate aldolase (CbbA), fructose/sedoheptulose bisphosphatase (CbbF), ribulose-5-epimerase (CbbE), and triosephosphate isomerase (TpiA). Ribose-5P is isomerized by ribose-5-phosphate isomerase (RpiA) to yield ribulose-5P, which can then be put back into the cycle [27, 96]

roles in this process [24]. Carbonic anhydrases (CAs) are zinc-containing enzymes that catalyze the reversible formation of bicarbonate (HCO_3^-) from water and carbon dioxide [25]. These enzymes are important to many physiological processes as well, such as respiration, photosynthesis, transport, and autotrophic fixation of CO_2 as well as HCO_3^- or H^+ coupled ion transport, pH regulation, or carboxylation reactions. Recent work has shown that CAs are present in a wide range of metabolically diverse species from both Archaea and Bacteria, indicating that the enzyme has a more extensive and fundamental role in prokaryotic biology than previously recognized [24, 26]. Maintenance of the optimal CO_2 concentration in the *R. eutropha* cell during autotrophic fermentation avoids CO_2 limitation during carbon fixation by the CBB cycle and, in consequence, ensures optimal IBT production. The action of CAs could play a central role in this process.

The 3-PGA produced in the CBB cycle is converted into pyruvate [27], which can be utilized by the branched-chain amino acid (BCAA) production pathway to produce the intermediate ketoisovalerate (KIV) (Fig. 1). The BCAA valine, leucine, and isoleucine are synthesized by plants, algae, fungi, Bacteria, and Archaea through

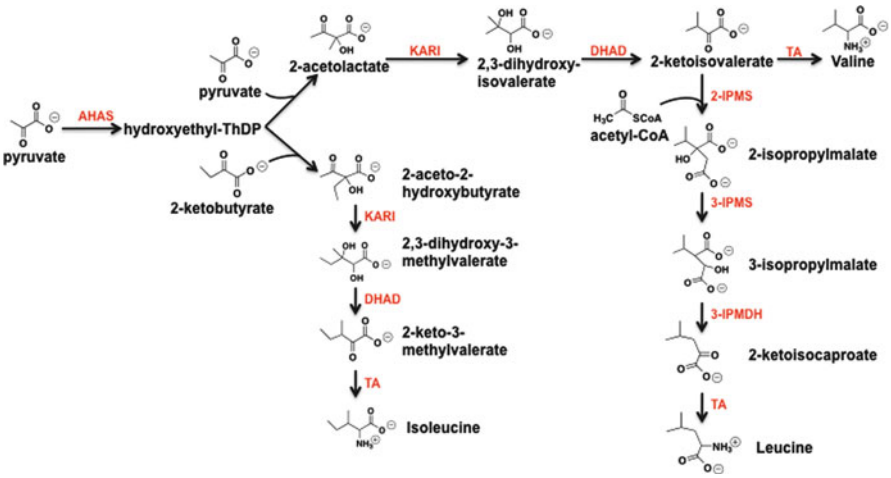

Fig. 4 Schematic diagram of BCAA metabolism in *R. eutropha*. Pyruvate is the common precursor, which is reacted by acetohydroxyacid synthase (AHAS). AHAS can also incorporate 2-ketobutyrate, allowing a branch point to isoleucine biosynthesis. Ketoacid reductoisomerase (KARI) and dihydroxyacid dehydratase (DHAD) then produce the key intermediate 2-ketoisovalerate (KIV). A transaminase (TA) produces valine from 2-KIV. The IBT production pathway competes with TA for 2-KIV. Other enzymes: *IPMS* isopropylmalate synthase; *IPMD* isopropylmalate synthase; *IPMDH* isopropylmalate dehydrogenase

a common pathway [28]. The common enzymes in BCAA biosynthesis pathways (Fig. 4) are acetohydroxyacid synthase (AHAS), ketoacid reductoisomerase (KARI), dihydroxyacid dehydratase (DHAD), and transaminase (TA). These enzymes are involved in synthesis of all three BCAAs, and their expression and activity are tightly regulated through $tRNA^{BCAA}$ repression, substrate specificity, and feedback inhibition. *R. eutropha* BCAA biosynthesis enzymes have not been studied previously. However, sequence alignment with other characterized BCAA biosynthesis enzymes from *E. coli, Corynebacterium glutamicum*, *Bacillus subtilis*, and *Streptomyces avermitilis* revealed that the *R. eutropha* enzymes are most similar to the ones from *E. coli* on the level of primary sequence.

The KIV produced in the BCAA pathway is a key intermediate in IBT production (Fig. 4). To decarboxylate KIV to isobutyraldehyde, the precursor of IBT, a heterologous enzyme must be expressed in *R. eutropha*. To accomplish this, the ketoisovalerate decarboxylase (*kivd*) gene from *Lactococcus lactis* is expressed, either on a plasmid or inserted into the *R. eutropha* genome, to allow production of isobutyraldehyde from 2-KIV (data not shown). Subsequently, an alcohol dehydrogenase (Adh) converts isobutyraldehyde to IBT. Initial assays for Adh activity in cell extracts of *R. eutropha* using isobutyraldehyde as the substrate yielded no detectable activity. Multifunctional Adh activity is repressed in *R. eutropha* during growth under ambient O_2 concentrations [29–31]. Thus, a native, constitutively expressed Adh or a heterologous Adh with substrate specificity for isobutyraldehyde is needed for the final step of IBT production. A "short-chain alcohol dehydrogenase" has

been described in *R. eutropha*, but in wild-type cells is only expressed under anaerobic conditions [31]. Thus, the enzyme must be expressed under the right conditions for use in IBT production. Additionally, heterologous Adh enzymes, such as YqhD, have shown promise for converting isobutyraldehyde to IBT. The *yqhD* gene from *E. coli* [32] has been used in previous iterations of IBT production pathways in heterotrophic organisms [4, 33].

1.3 IBT Production Conditions

Wild-type *R. eutropha* will accumulate up to 80% of its dry cell mass as the carbon storage compound PHB when it encounters nutrient stress [34]. During this stringent response, *R. eutropha* stops growth and slows down central metabolism (Brigham et al., manuscript in preparation) so that most of the intracellular carbon flux is redirected towards PHB synthesis.

Eliminating the PHB synthesis pathway from *R. eutropha* causes an overflow of the intermediate pyruvate during nutrient starvation, which is excreted to prevent toxicity [35]. Because pyruvate feeds the BCAA synthesis pathway used to generate IBT [4], nutrient starvation could be used to maximize carbon flux towards IBT.

2 *R. eutropha* IBT Production Pathway

2.1 Hydrogenase Enzymes

Hydrogenases are classified in three families, the [Fe]-hydrogenases, the [FeFe]-hydrogenases, and the [NiFe]-hydrogenases, based on their catalytic-site metal cofactors [21]. Only the NiFe hydrogenases are discussed here, as all three hydrogenases present in *R. eutropha* belong to this family [17]. Furthermore, the RH are not discussed since it does not have a role in the hydrogen metabolism of *R. eutropha* H16 [22]. As mentioned previously, the two types of energy conserving hydrogenases, MBH and SH, produce the energy and reducing equivalents supporting autotrophic growth of *R. eutropha*. Because of their oxygen tolerance, these hydrogenases in *R. eutropha* have been studied in detail (reviewed in [17, 36]).

MBH uses extracellular hydrogen to provide reducing equivalents to the respiratory chain, allowing the four-electron reduction of O_2 to H_2O. The electrons gained in oxidation of hydrogen at the NiFe catalytic site are transported through the three iron-sulfur (FeS) clusters of the electron transfer subunit to a cytochrome *b* in the membrane anchor [37]. From cytochrome *b* the electrons are directed into the quinone pool. The proximal FeS cluster, closest to the catalytic site, is critical for oxygen tolerance of the MBH, which is inferred from rapid reduction of O_2 bound to the catalytic site [38]. The required electrons for the three-electron reduction of the

peroxide radical, bound to the active site after oxidation by O_2, are transferred from the quinone pool.

The cytoplasmic SH uses intracellular H_2 to directly reduce NAD^+ to NADH, through electron transfer from its catalytic subunit, through an FeS-containing electron transfer subunit, to a flavin containing diaphorase moiety consisting of two subunits [19]. The remaining two subunits create a binding pocket for NADPH, which is required for catalytic activation of the enzyme [39]. The autotrophic growth rate of *R. eutropha* decreases twofold in an SH deletion mutant, illustrating that it is necessary to support the high reducing equivalent requirement of the CBB cycle [20]. The oxygen tolerance of the SH is thought to have a different molecular basis than that of the MBH, since it cannot access the quinone pool as rapidly. The coordination sphere of the NiFe active site is proposed to contain two additional cyanide (CN) ligands, one coordinating each metal atom [40, 41]. However, a recent study suggests that these two CN ligands are not present in situ, suggesting an alternative, yet to be elucidated, mechanism for oxygen tolerance [42].

In summary, both types of energy-conserving hydrogenase are oxygen tolerant at ambient concentrations and serve a distinct purpose in maintaining the energy balance of the cell. Optimal IBT production requires a balance of both hydrogenase activities.

2.2 Carbonic Anhydrase

Carbonic anhydrase (CA) catalyzes the reversible hydration of dissolved CO_2 via a two-step mechanism that involves an attack of zinc-bound OH^- on a CO_2 molecule loosely bound in a hydrophobic pocket. The resulting zinc-coordinated HCO_3^- ion is displaced from the metal ion by H_2O [25]. The overall reaction is as follows:

$$CO_2 + H_2O \leftrightarrow H^+ + HCO_3^- \tag{3}$$

Although this reaction occurs without CA, the uncatalyzed hydration and dehydration reactions are slow. Therefore, CA is important when the availability of CO_2 or HCO_3^- becomes limiting to a metabolic reaction [43]. Because the reaction shown in (3) involves protons, the equilibrium ratio of the two carbon forms is a function of pH. At physiological ionic strengths, CO_2 predominates at a pH of less than 6.4, and HCO_3^- is the dominant form in the pH range of 6.4 and 10.3.

Three main evolutionarily distinct families of CAs were initially identified (α, β, and γ-CAs), and recently two more CA classes, the δ and ζ classes, have been found in marine diatoms [44]. All CA families require zinc at the active site to activate the water molecule, although the γ-CAs have been shown to use iron at the active site under anaerobic conditions. However, there is no significant sequence homology between families, and they appear to be examples of convergent evolution of catalytic function.

2.2.1 Types of CA Present in *R. eutropha*

α-CA: The best-studied group of the CAs is the α-class, first described and mostly studied in mammals, but also found in other organisms [24, 26]. Most α-CAs are monomeric enzymes, with an active site zinc ion coordinated by three histidine residues. Members of this family may be involved in maintaining pH balance, in facilitating transport of carbon dioxide or bicarbonate, or in sensing carbon dioxide levels in the environment [25, 45].

β-CA: The β-class has been identified in plants, Bacteria, red and green algae, fungi, and Archaea [46, 47]. For many organisms, including *R. eutropha*, β-CA is essential for growth at atmospheric concentrations of CO_2 [47, 48]. The fundamental structure of β-CA, a dimer, is the only one known to exhibit allosteric regulation by bicarbonate ion [46].

γ-CA: The γ-CAs, which are predominantly found in Archaea, have strikingly different sequence features than the α- and β-CAs, The γ-CAs. are trimeric enzymes that contain a zinc in the active site. In an anaerobic environment, the zinc is replaced by iron as the physiologically relevant active site metal [45, 49]. *R. eutropha* is capable of growth under anaerobic conditions, and may utilize a γ-CA (see below) under these conditions.

Although the primary structure and number of subunits of the various classes of CAs are strikingly different, the metal- (in most cases zinc) coordinating site is remarkably similar at the structural level [45, 46].

Four putative CA genes were identified in the genome sequence of *R. eutropha* strain H16. Two are located on chromosome 1, and two on chromosome 2. H16_A1192 encodes a γ-like-CA/acetyltransferase, *can* (locus tag H16_A0169) and *can2* (locus tag H16_B2270) encode β-CA enzymes, and *caa* (locus tag H16_B2403) encodes a periplasmic α-CA. The presence of genes for multiple carbonic anhydrases in *R. eutropha* suggests that these enzymes play a major role in its physiology and that the function of the different types is complementary [24]. However, the exact roles of all four CA enzymes are still largely unknown. The only *R. eutropha* CA gene studied to date is *can* [48], which was identified as being essential for growth under atmospheric concentrations of CO_2. Either the presence of the other three CAs was not sufficient to support growth under ambient CO_2 concentrations, or these other CA genes were not expressed [48]. The metabolic processes in which the activity of the other three CAs plays a role remain to be identified.

Since CO_2 and HCO_3^- are both involved in a wide range of cellular processes, CAs can have different physiological roles. One role is to increase the supply of CO_2 or HCO_3^- for metabolic reactions. For example, during the carboxylation reaction of RuBisCO, which uses only CO_2, competition between CO_2 and O_2 for the active site is attenuated when the concentration of CO_2 is higher. It is mainly for this purpose that CA activity, and enhancement thereof, may be crucial for autotrophic IBT production in *R. eutropha.* Other roles CA may play include delivery of carbon to the correct location within the cell and retention of CO_2. Both of these roles are important, as CO_2 can readily pass through biological membranes and quickly leak out of

the cell. The role of CAs in transportation and retention of CO_2 is shown through the carboxysomes, or CO_2 concentration mechanism (CCM), which are important in cyanobacteria and algal carbon fixation [50, 51]. The action of CAs may also be important in pH homeostasis [43]. The roles of CA enzymes in IBT production are likely to prove important, both for concentrating CO_2 to drive the RuBisCO reaction towards carbon fixation and for increasing CO_2 tolerance.

2.3 Calvin–Benson–Bassham Cycle

Autotrophic CO_2 fixation via the CBB cycle in *R. eutropha* is genetically determined by two operons (*cbbLSXYEFPTZGKA*), one of which is located on chromosome 2 (H16_B1383 to H16_B1396) and the other on megaplasmid pHG1 (PHG416 to PHG427). The chromosomal operon (cbb_c) of the strain has a length of about 15.2 kilobase (kb) pairs comprising 13 genes. The second, highly homologous operon (cbb_p) is located on the megaplasmid pHG1 and contains only 12 genes, totaling approximately 12.8 kb. With the exceptions of the triose-3-phosphate isomerase (*tpiA*, H16_A1047) and ribose-5-phosphate isomerase (*rpiA*, H16_A2345), all enzymes of the CBB cycle are encoded in the *cbb* operons [52, 53]. The chromosomal and plasmid-borne *cbb* promoters in *R. eutropha* are functionally equivalent despite minor structural differences [54]. Transcription of all genes in either *cbb* operon depends on a single promoter upstream of *cbbL* [52, 54–56] that is subject to strong regulation [57]. Growth of *R. eutropha* under autotrophic conditions leads to high expression of the *cbb* operon genes [58]. The *cbbR* gene encodes for the transcriptional regulatory protein of the operon [55, 56]. In many organisms, the *cbbR* gene is typically located adjacent and in divergent orientation to its cognate operon. Inactivation or deletion of the *cbbR* prevents *cbb* operon transcription [55, 59]. The activating function of CbbR appears to be modulated by metabolites that signal the nutritional state of the cell to the *cbb* system. CbbR from *R. eutropha* is a sensor of the intracellular phosphoenol pyruvate (PEP) concentration. PEP increases the affinity of the activator to its operator target site, resulting in a decreased activating potential of the CbbR protein in vitro [60]. This observation suggests that the role of CbbR in *cbb* operon transcription can thus be as an activator or a repressor.

The existence of subpromoters within the operons was excluded, and premature transcription termination thus represents an important mechanism leading to differential gene expression within the *cbb* operons of *R. eutropha* [61]. There is evidence for the participation of additional regulators in *cbb* control [59].

The enzymes of the entire CBB cycle are represented in Fig. 3. Additionally, the *cbb* operons contain *cbbX* and *cbbY*, which have no known function in *R. eutropha*. However, the gene *rbcX* from cyanobacteria, located between the two RuBisCO subunit genes, is responsible for the assembling the RuBisCO holoenzyme, together with chaperones GroEL/ES [62]. The CbbX protein product presents no homology to RbcX, but has conserved domains of the AAA family proteins, ATPase proteins

that often perform chaperone-like functions assisting in the assembly, operation, or disassembly of protein complexes [63].

The structure of the RuBisCO from *R. eutropha* was published (Protein Data Base 1BXN). As in most bacteria and higher plants with form I of RuBisCO, the enzyme complex is built up from eight large subunits and eight small subunits (L8S8) [64].

Distinct residues from each subunit of RuBisCO thus comprise the active site required for both carboxylation by CO_2 and oxidation by O_2, with the two gaseous substrates clearly competing for the same active site. The specificity factor (SF) is calculated as follows:

$$\mathrm{SF} = \frac{V_{\mathrm{CO}_2} K_{\mathrm{O}_2}}{V_{\mathrm{O}_2} K_{\mathrm{CO}_2}} \tag{4}$$

In (4), V_{CO_2}, V_{O_2}, K_{CO_2}, K_{O_2} refer to the Michaelis–Menten constants of RuBisCO for the different substrates. SF defines the ratio between carboxylation and oxidation rates performed by each enzyme [65], but does not provide a direct measure of the rates, rate constants, or catalytic efficiencies of either carboxylation or oxygenation [66]. In *R. eutropha* SF = 75 [67].

The rate-limiting step in CO_2 assimilation is catalyzed by RuBisCO, which is a very poor catalyst, exhibiting low affinity for CO_2 and using O_2 as an alternative substrate. Protein engineering could potentially be used to increase RuBisCO's CO_2 carboxylation activity, thereby increasing SF [68]. However, because both CO_2 and O_2 compete for the same active site [66], a short-term strategy to enhance IBT production would be to increase the intracellular CO_2 concentration.

RuBisCO's oxygenation reaction produces one molecule of 3-PGA and one molecule of 2-phosphoglycolate [69]. The *cbbZ* gene, which encodes a phosphogycolate phosphatase on the *cbb* operon might be an evolutionary adaptation in response to the presence of the 2-phosphoglycolate produced by RuBisCO during the oxidation reaction. CbbZ would prevent the accumulation of potentially toxic concentrations of 2-phosphoglycolate and rescue part of the carbon that would otherwise be lost through the glycolate metabolism [56]. In summary, the CBB cycle will play an important role in autotrophic IBT biosynthesis by *R. eutropha* and increasing carbon flux through the CBB cycle is likely to enhance the IBT production rate.

2.4 Branched-Chain Amino Acid Metabolism and Its Role in R. eutropha IBT Production

Pyruvate produced from the CBB cycle is converted to the key intermediate α-KIV by the BCAA biosynthetic pathway. AHAS catalyzes the first step in the biosynthesis of all three BCAAs (Fig. 4). It is capable of synthesizing (2S)-acetolactate, a precursor of valine and leucine from two molecules of pyruvate and synthesizing (2S)-2-aceto-2-hydroxybutyrate, a precursor of isoleucine, from pyruvate and 2-keto-

butyrate. In most organisms, a single AHAS catalyzes both of the above-mentioned reactions, whereas in other organisms these reactions are catalyzed by separate enzymes [28]. The AHAS enzyme consists of two subunits, one being catalytic and one playing a regulatory role. No crystal structure with both subunits has been obtained to date, although individual subunits have been crystallized separately. Catalysis is believed to occur at the subunit interface, since the catalytic subunit alone has little to no activity [70]. Expression of AHAS is controlled by the amount of $tRNA^{BCAAs}$ available in the cell. High levels of $tRNA^{BCAAs}$ repress the transcription of AHAS. Additionally, AHAS activity is controlled allosterically at the activity level by its regulatory subunit, through binding of valine at the homodimer interface [71]. Combined site-directed mutagenesis and BCAA-binding studies have shown that valine binding at the homodimer interface potentially causes a conformational change resulting in a less stable complex with decreased enzymatic activity [72].

A promising approach to counter valine inhibition of AHAS can be found in *E. coli*. *E. coli* has three AHAS isozymes, each with a different substrate specificity and regulation mechanism. The sequence of *E. coli* AHAS isozyme II differs from other AHAS, and its regulatory subunit is insensitive to direct feedback inhibition by valine [70]. *R. eutropha* AHAS (IlvBH in Fig. 1) shares most sequence similarity with *E. coli* AHAS isozyme III and is also subject to allosteric feedback inhibition by pathway intermediates (dihydroxyisovalerate and ketoisovalerate; Sinskey laboratory, unpublished data) and end products (valine, leucine and isoleucine; Sinskey laboratory, unpublished data). Thus, minimizing allosteric inhibition by products and intermediates is essential to optimize IBT production in *R. eutropha*. N-terminal amino acid residues that are conserved in all valine-sensitive AHAS could contribute to the binding of valine or other BCAAs that cause allosteric feedback inhibition. These residues can be mutated to the ones that are present in the valine-insensitive AHAS isozyme II from *E. coli*. C-terminal truncation studies on the valine-sensitive *E. coli* AHAS isozyme III show decreased valine inhibition. However, the exact mechanism of inhibition alleviation is unknown, since valine and other BCAAs are hypothesized to bind only at the N-terminus of the regulatory subunit [73].

An AHAS enzyme's selectivity (R) for aceto-2-hydroxybutyrate production over acetolactate production can be calculated by the following equation:

$$R = \frac{[\mathrm{AHB}]/[\mathrm{2KB}]}{[\mathrm{AL}]/[\mathrm{P}]} \tag{5}$$

where AHB, 2KB, AL, and P represent aceto-2-hydroxybutyrate, 2-ketobutyrate, acetolactate, and pyruvate, respectively. R values for *E. coli* AHAS isozymes I, II, III, and *C. glutamicum* AHAS are 2.0, 65, 40, and 20, respectively, all of which favor the formation of AHB over acetolactate. *R. eutropha* AHAS has R value of ~45 [28].

As actetolactate is a precursor of IBT, reducing the AHAS R value would help direct carbon flow towards α-KIV, and consequently IBT. Previous mutagenesis studies on the *E. coli* AHAS II catalytic subunit revealed a tenfold reduction in R when a tryptophan residue at position 464 was mutated to lysine, glutamine, or tyrosine [74]. It is suggested that the indole ring of tryptophan interacts with the

extra methyl group on 2-ketobutyrate and stabilizes it in the active site. Site-directed mutagenesis could also be used to decrease the *R* value for *R. eutropha* AHAS.

KARI, encoded by *ilvC* in *R. eutropha*, catalyzes the formation of 2,3-dihydroxyisovalerate from 2-acetolactate and the formation of 2,3-dihydroxy-3-methylvalerate from 2-aceto-2-hydroxybutyrate (Fig. 4). KARI has similar substrate preference towards both substrates. A unique feature of its reaction mechanism is that it simultaneously catalyzes both an isomerization and a reduction reaction. Mutations in active site residues that abolished the reductase activity also eliminated the isomerization reaction, suggesting that isomerization and reduction are coupled without any intermediate. KARI requires NADPH and a divalent metal ion, in most cases Mg^{2+}, for catalysis. The metal cofactor is involved in the alkyl migration isomerization step, whereas NADPH is the electron donor for the reduction step [28]. Since KARI has no substrate bias, simple overexpression of *ilvC* is likely sufficient to provide ample precursor amounts for the production of IBT.

DHAD catalyzes the formation of ketoacids from the products of KARI. The mechanism of action is unknown, but it likely involves the dehydration of vicinal diols to ketoacids via an enol intermediate. *E. coli*'s oxygen sensitive DHAD contains a $[4Fe\text{-}4S]^{2+}$ cluster. The reaction mechanism is proposed to be similar to that of aconitase in the TCA cycle, which also involves an FeS cluster [28]. The activity, feedback inhibition and oxygen sensitivity of *R. eutropha* DHAD have not been studied. As shown in Figs. 1 and 4, the combined activities of DHAD, KARI, and AHAS convert pyruvate into the key IBT intermediate 2-KIV.

2.5 Role of a Heterologously Expressed 2-Ketoisovalerate Decarboxylase

To convert 2-KIV to isobutyraldehyde, a 2-Kivd enzyme is used. The Kivd enzyme from *L. lactis* is an uncommon enzyme with a traditional industrial role of aldehyde production for aroma development in cheese [75]. Given its activity with branched chain ketoacid substrates, this enzyme is uniquely suited to the task of bridging the BCAA production pathway to Adh to allow for heterologous IBT production [33]. The enzyme is a non-oxidative, thiamine diphosphate dependent, Mg^{2+}-dependent keto acid decarboxylase [75]. The *kivd* gene can be expressed in an active form in *R. eutropha* (Sinskey laboratory, data not shown).

2.6 Alcohol Dehydrogenase

In *R. eutropha* cells grown in the presence of O_2 under heterotrophic conditions, no detectable Adh activity is seen (Sinskey laboratory, data not shown). Adh has been assayed in *R. eutropha* grown under anaerobic conditions [31]. To ensure IBT

production under aerobic autotrophic conditions, the use of a constitutively expressed, broad substrate specificity Adh enzyme is required. A broad substrate specificity Adh has been characterized in *R. eutropha*, encoded by the *adh* gene (locus tag H16_A0757). This enzyme has been shown to exhibit activity on ethanol and 2,3-propanediol [29–31]. Constitutively expressed *adh* mutants have been isolated and characterized. These mutant strains contain alterations in the promoter region of *adh*, and in some cases have been shown to utilize short-chain alcohols for growth [29]. The Adh enzyme has recently been demonstrated to use isobutyraldehyde as a substrate to produce IBT (Sinskey laboratory, data not shown). The *R. eutropha* strains constitutively expressing *adh* can be used as parental strains to produce the IBT production strain.

E. coli alcohol dehydrogenase YqhD catalyzes the reaction between many alcohols and their corresponding aldehydes. YqhD belongs to the NADPH-dependent Adh superfamily and is subclassified as zinc-dependent long chain Adh [32]. The crystal structure of YqhD reveals Zn(II) and NADPH as cofactors for catalysis [76]. The active site contains a relative large substrate-binding pocket, which explains its ability to catalyze reactions involving both normal and branched-chain aliphatic and aromatic alcohols and their corresponding aldehydes and ketones. Using YqhD for IBT production could affect the cofactor balance. Because many native metabolic pathways require NADPH, an IBT biosynthetic pathway constructed with an NADPH-dependent enzyme could disturb the native metabolism by competing for this cofactor necessary for growth and maintenance, thus potentially resulting in slower growth or a decreased production yield. *Clostridium acetobutylicum* has two NADH-dependent Adhs, AdhE1, and AdhE2. AdhE1 is expressed under anaerobic conditions and is active towards ethanol, acetaldehyde, butanol, and butyraldehyde [77]. AdhE2 has the same substrate specificity as AdhE1, but is only expressed in high NADH/NAD^+ ratio alcohologenic cultures. AdhE2 has a conserved iron-binding motif and is hypothesized to require Fe^{2+} as a cofactor for catalytic activity [78]. The activities of AdhE1 and AdhE2 towards the reduction of isobutyraldehyde have not been explored. AdhE1 and AdhE2 are potentially advantageous for IBT production because they are both NADH-dependent and can use NADH produced directly from the oxidation of hydrogen by the soluble hydrogenase.

2.7 Cofactor Balance

The intracellular ratio of NADH to NADPH may strongly influence cell growth, metabolism, and IBT production, as key steps in the pathway require NADPH as a source of reducing potential (Fig. 1). PHB biosynthesis, the typical method for storing reducing potential in *R. eutropha* [79, 80] has been inactivated; thus an alternate method for refreshing the NADPH pool, such as the transhydrogenase reaction shown in Fig. 5a, could be needed. The *E. coli* pyridine nucleotide transhydrogenase enzyme (UdhA) has been shown to oxidize NADPH to produce $NADP^+$ while reducing NAD^+ to NADH in wild-type cells under conditions of excess intracellular NADPH [81].

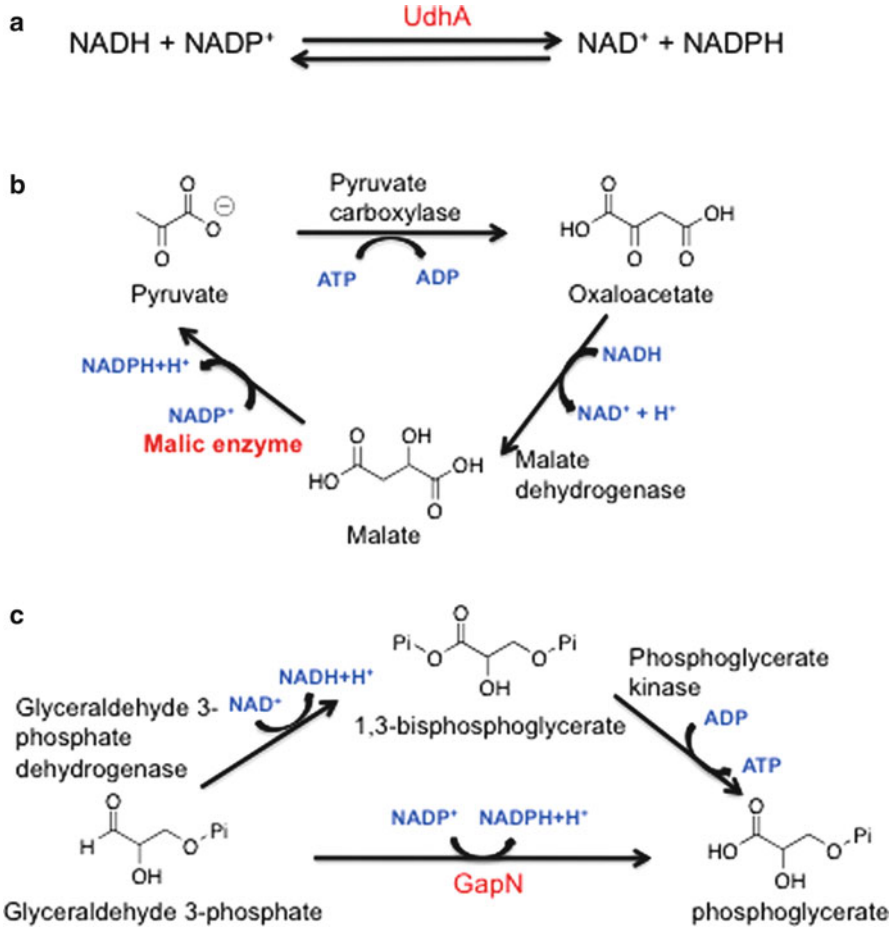

Fig. 5 Schemes for alteration of NADH/NADPH pool sizes in *R. eutropha* IBT production strain. (**a**) The use of the soluble pyridine nucleotide transhydrogenase (UdhA) can directly perform transhydrogenation to increase NADPH pool levels. (**b**) Malic enzyme (encoded by *maeA* and/or *maeB* in *R. eutropha*) can increase the NADPH pool at the expense of ATP. (**c**) The nonphosphorylating glyceraldehyde-3P dehydrogenase (GapN) produces NADPH by conversion of glyceraldehyde-3P to phosphoglycerate

The UdhA reaction occurs in an energy (ATP)-independent manner. In a heterologous *E. coli* system, the reversibility of UdhA was exploited via overexpression of the enzyme to increase NADPH availability and PHB production [82]. The increased intracellular NADPH concentration allowed a greater cofactor availability for the acetoacetyl-CoA dehydrogenase reaction [82]. A similar strategy was used in *Pseudomonas fluorescens* to increase production of hydromorphone [83]. This strategy for altering redox cofactor pool size can be used in the IBT synthesizing strain of

R. eutropha to ensure efficient activities of NADPH-requiring enzymes in the biosynthetic pathway.

In most organisms, the redox cofactor NADPH is generated via the pentose-phosphate pathway by glucose-6-phosphate dehydrogenase and 6-phosphogluconate dehydrogenase. Proteomic studies of *R. eutropha* revealed no active 6-phosphogluconate dehydrogenase under heterotrophic growth conditions [27], suggesting that *R. eutropha* synthesizes its cofactor NADPH from other pathway(s) during organoheterotrophic growth. One potential pathway involves the *maeA* or *maeB* genes, encoding malic enzyme. The malic enzyme catalyzes the conversion of malate to pyruvate and is part of a metabolic cycle that also includes pyruvate carboxylase and malate dehydrogenase (Fig. 5b). An increase in transcription of the malic enzyme gene also upregulates the transcription of both pyruvate carboxylase and malate dehydrogenase [84]. Another enzyme, nonphosphorylating glyceraldehyde 3-phosphate dehydrogenase (GapN) bypasses 1,3-bisphospho-D-glycerate in glycolysis and generates an additional NADPH from NADH, at the expense of one ATP (Fig. 5c). In order to increase the intracellular NADPH pool, *udhA* and *gapN* can be heterologously expressed in *R. eutropha* or *maeA* could be overexpressed to increase IBT production.

3 Challenges and Considerations

3.1 Carbon Sinks

As mentioned in the pathway overview, removing alternative sinks of pathway intermediates would improve the IBT yield. However, when the removal of carbon sink creates auxotrophy, supplementation of the essential nutrient will drive up the production cost. Promoter regions of genes exhibiting low-level constitutive expression during conditions permissive for IBT production have been identified based on microarray analysis of *R. eutropha* during nitrogen limitation (Brigham et al., manuscript in preparation). These promoters will be used to maintain low expression levels of genes encoding essential metabolic reactions, thus preventing auxotrophy while limiting carbon flux to alternative sinks.

The 3-phosphoglycerate (3-PGA) generated in the CBB-cycle is converted to pyruvate via glycerate-2-phosphate and PEP. Since pyruvate is the only substrate of valine synthesis, control of its concentration is essential for high IBT yield. As a key intermediate in central carbon metabolism, pyruvate concentration is tightly regulated, for example through the PEP-pyruvate-oxaloacetate node [27, 85]. The high PHB accumulation during nutrient starvation suggests that the stringent response of *R. eutropha* keeps a tight control on any sink but PHB synthesis. This notion is confirmed by the excretion of pyruvate when the PHB synthesis operon is disrupted [35]. This control of pyruvate sinks can be used to optimize IBT production using a two-stage fermentation strategy (see Sect. 4.2).

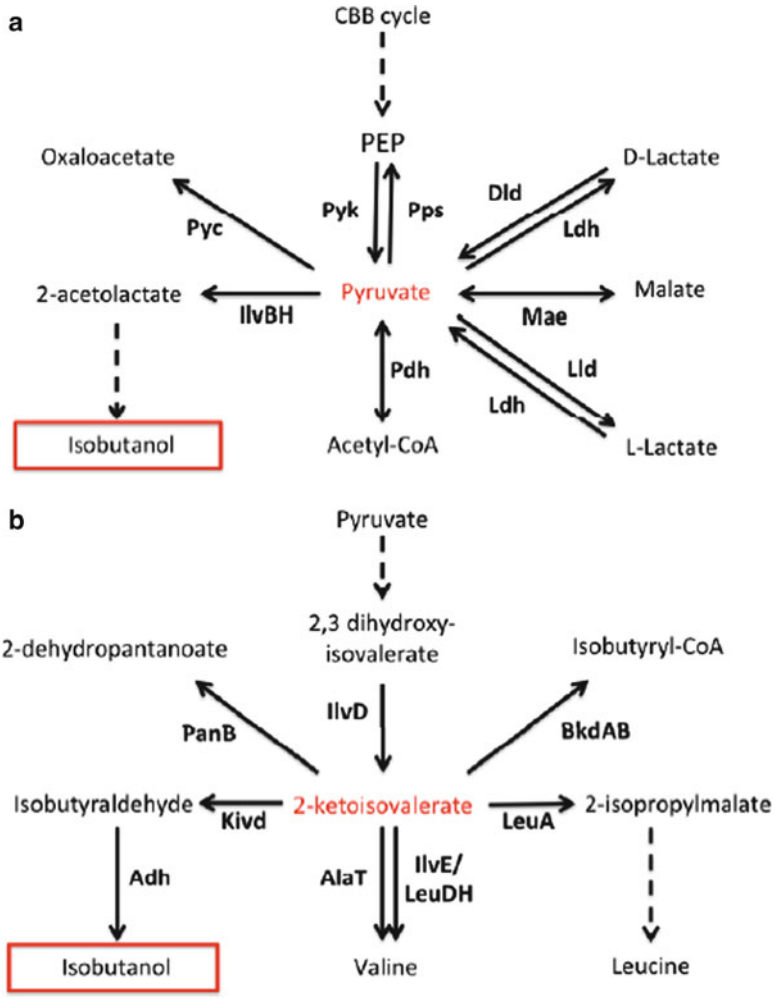

Fig. 6 Key intermediates in the IBT (*boxed in red*) production pathway and their roles in biosyntheses of other molecules. (**a**) Pyruvate and (**b**) 2-KIV. Shown in *bold* are enzymes that utilize these key intermediates as substrates

The final precursor of valine, 2-KIV, can be decarboxylated by a heterologous Kivd to yield isobutyraldehyde, the direct precursor of IBT. However, KIV is also a substrate of seven additional enzymes in *R. eutropha* (Fig. 6). To optimize the flux from KIV to IBT, alternate utilization of KIV needs to be minimized.

Of the seven enzymes representing KIV sinks, at least three are likely to be essential for survival of *R. eutropha* without auxotrophy. Isopropylmalate synthase (LeuA1, Fig. 6) is essential for leucine synthesis, BCAA aminotransferase (IlvE, Fig. 6) catalyzes the final step of valine synthesis, and 3-methyl-2-oxobutanoate

hydroxymethyltransferase (PanB, Fig. 6) catalyzes the formation of 2-dehydropantanoate, a precursor of Coenzyme A (CoA) [86]. Since use of an auxotrophic strain for IBT production would increase the cost of production, the promoter exchange strategy discussed previously could be used to minimize the activity of the above enzymes.

The remaining four enzymes representing KIV sinks can likely be deleted from the genome without auxotrophy, either because the enzyme is nonessential or has a redundant function. Leucine dehydrogenase (B0449, Fig. 6) and aminotransferase AlaT (Fig. 6) catalyze the conversion of KIV to valine and are thus redundant with BCAA aminotransferase [86]. Additionally, the second copy of isopropylmalate synthase (LeuA2, Fig. 6) will be removed from the genome to minimize the amount of protein available. Finally, 2-ketoisovalerate dehydrogenase (BkdAB, Fig. 6) is involved in valine degradation [86]. Minimizing degradation of valine will reduce the necessity to synthesize it from KIV; thus removing the genes encoding this enzyme from the genome offers two potential benefits.

3.2 Improvement of Hydrogenases

As archetypes of O_2 tolerant hydrogenases, the *R. eutropha* enzymes have been extensively studied using various spectroscopic techniques and site directed mutagenesis (reviewed in [17, 36]). Although these studies have proven that direct manipulation of the hydrogenases is possible, it has also shown the difficulty of improving activity of the enzymes. Therefore, direct manipulation of the hydrogenases to optimize the generation of energy and reducing equivalents for IBT production would be a significant challenge, and likely not a viable approach. In contrast, hydrogenase gene expression will be enhanced to assure that sufficient reducing equivalents will be available for optimal IBT yield.

To optimize IBT yield, it is important to balance the reducing equivalents generated by the SH with the ATP synthesized by the MBH. Since carbon fixation will be maximized and the IBT synthesis pathway consumes two NAD(P)H molecules for every two molecules of pyruvate reduced to IBT, the hydrogenase activity balance will be shifted towards the SH.

3.3 Enhancement of Carbonic Anhydrase

Because of the inefficiency of the enzyme, the CO_2 fixation by RuBisCO is likely the limiting step for an efficient production of IBT by *R. eutropha*. Enhancing expression and/or activity of CAs could help to increase the CO_2 concentration in the cytosol, thereby limiting the competing oxygenation reaction by RuBisCO and increasing the CO_2 flux through the CBB cycle and subsequently to IBT.

4 Outlook

4.1 Prevention of Explosive Mixtures

In most autotrophic fermentations with *R. eutropha* reported in the literature, the initial gas mixture (typically 8:1:1 H_2:CO_2:O_2) is within the explosive range for the H_2 and O_2 gas concentrations. The low aqueous solubility of both H_2 and O_2 presents challenges in making these gases bioavailable to *R. eutropha* cells [14]. As with many aerobic microbial biotransformations, the rate of gas mass transfer (dissolution) from the gas to the liquid phase represents another potential rate-limiting step.

One strategy to reduce the explosion risk during autotrophic growth of *R. eutropha* is to keep the H_2 and O_2 gas streams physically separated. This can potentially be performed by the hollow fiber reactor setup discussed in Sect. 4.2 (Fig. 7). However, for initial screening, microfermenters (bioreactors with 1 mL or less working volume, discussed in [87–90]) can be used to optimize growth and production conditions prior to culture scale-up. Risk of explosion still exists in such systems, but the small scale of the reactors would control the potential damage.

4.2 Fermentation Strategies

Unlike PHB, which is accumulated intracellularly [91], IBT is excreted from the cell (Sinskey laboratory, data not shown). Thus, continuous autotrophic IBT production is possible. A two stage approach could be used, in which the cells are first grown heterotrophically to a high cell density on the porous wall of hollow fibers. Then, the heterotrophic medium would be replaced by a nitrogen-deficient autotrophic medium to induce the stringent response and trigger rapid IBT production. The gaseous substrates would then be added, with the H_2 and O_2 being maintained on opposite sides of the fiber wall. A schematic drawing of this hollow fiber reactor setup is shown in Fig. 7.

Since no growth will be supported by the production medium, the cells will need to be periodically regenerated by brief exposure to the heterotrophic growth medium. However, the intervals on growth medium can be short since there will be no requirement to start the culture anew, thus maximizing the production time.

4.3 IBT Recovery

Like most alcohols, IBT is expected to be toxic to microbial biocatalysts. Removal of the IBT as it is formed will help avoid product inhibition and maintain high reactor productivity. Thus, in situ product recovery will be an integral part of the bioreactor design effort. Because the physical properties of IBT are similar to those of

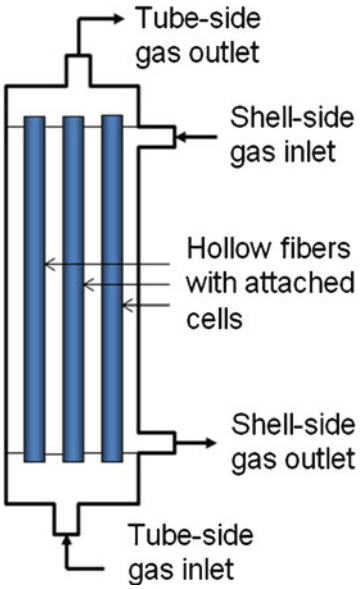

Fig. 7 Schematic diagram of reactor with hydrogen and oxygen gases maintained on opposite sides of the hollow fiber walls

n-butanol, methods developed to remove *n*-butanol from fermentation broths are also likely to work for IBT. A variety of adsorbents have proven effective at recovering *n*-butanol from fermentation broths [92–94], including polymeric resins, which adsorb *n*-butanol through hydrophobic interactions [95]. Hydrophilic polymers, like polyamides, polyurethanes and polyesters showed weak *n*-butanol adsorption. In addition, low-alumina zeolites, such as silicalite, effectively adsorb alcohols from dilute solutions. After the butanol has been adsorbed, it can be recovered from the resin by heat desorption. This desorption technique is less energy intensive (~2,000 kcal/kg alcohol) than steam stripping (~6,000 kcal/kg alcohol) or gas stripping (~5,000 kcal/kg alcohol) [93].

5 Summary and Conclusion

The nation's reliance on fossil-based fuels creates problems for the environment and our national security. The production of a renewable source of motor fuels is required. We have designed a production pathway for synthesizing IBT biofuel from CO_2, H_2, and O_2 using the genetically tractable and metabolically versatile bacterium, *R. eutropha*. The majority of the genes required for this pathway are already present in *R. eutropha*. Metabolic engineering strategies are being implemented to establish a semisynthetic pathway to produce IBT from CO_2, H_2, and O_2. This IBT production pathway has the potential to affect two high-priority environmental concerns, capture of CO_2 and production of an alternative nonfossil-based fuel.

Acknowledgments We thank John W. Quimby for critical review of this manuscript. D.S. is supported by the following foundations: Nijmeegs Universiteitsfonds (SNUF), Fundatie van de Vrijvrouwe van Renswoude te's-Gravenhage, and Dr. Hendrik Muller's Vaderlandsch Fonds. Other authors are supported, fully or in part, by the Advanced Research Projects Agency—Energy (ARPA-E) Electrofuels project. We wish to thank the ARPA-E directors and staff for their support.

References

1. Zinoviev S, Muller-Langer F, Das P, Bertero N, Fornasiero P et al (2010) Next-generation biofuels: survey of emerging technologies and sustainability issues. ChemSusChem 3:1106–1133
2. Beall DS, Ohta K, Ingram LO (1991) Parametric studies of ethanol production form xylose and other sugars by recombinant *Escherichia coli*. Biotechnol Bioeng 38:296–303
3. Ohta K, Beall DS, Mejia JP, Shanmugam KT, Ingram LO (1991) Genetic improvement of *Escherichia coli* for ethanol production: chromosomal integration of *Zymomonas mobilis* genes encoding pyruvate decarboxylase and alcohol dehydrogenase II. Appl Environ Microbiol 57:893–900
4. Atsumi S, Hanai T, Liao JC (2008) Non-fermentative pathways for synthesis of branched-chain higher alcohols as biofuels. Nature 451:86–89
5. Atsumi S, Higashide W, Liao JC (2009) Direct photosynthetic recycling of carbon dioxide to isobutyraldehyde. Nat Biotechnol 27:1177–1180
6. Fischer R, Wild S (2011) The greenest machine at Sebring: Dyson's isobutanol powered Mazda. Motor Trend Online: Motor Trend Magazine, Source Interlink Media. http://wot.motortrend.com/greenest-machine-sebring-dysons-isobutanol-powered-mazda. Accessed 21 March 2011
7. DeMeza T (2010) American LeMans Series approves renewable isobutanol fuel. Sports Car Monitor: High Gear Media. http://www.motorauthority.com/news/1043521_american-lemans-series-approves-renewable-isobutanol-fuel. Accessed 17 March 2010
8. Glassner D, Peters M, Gruber P (2009) Hydrocarbon fuels from biomass. In: 31st Symposium on Biotechnology for Fuels and Chemicals, San Francisco, CA, 12–16 May 2009
9. Schlegel H, Lafferty R (1971) Novel energy and carbon sources. Adv Biochem Eng 1:143–168
10. Brigham CJ, Budde CF, Holder JW, Zeng Q, Mahan AE et al (2010) Elucidation of beta-oxidation pathways in *Ralstonia eutropha* H16 by examination of global gene expression. J Bacteriol 192:5454–5464
11. Yang YH, Brigham CJ, Budde CF, Boccazzi P, Willis LB et al (2010) Optimization of growth media components for polyhydroxyalkanoate (PHA) production from organic acids by *Ralstonia eutropha*. Appl Microbiol Biotechnol 87:2037–2045
12. Anderson AJ, Dawes EA (1990) Occurrence, metabolism, metabolic role, and industrial uses of bacterial polyhydroxyalkanoates. Microbiol Rev 54:450–472
13. Tian J, Sinskey AJ, Stubbe J (2005) Kinetic studies of polyhydroxybutyrate granule formation in *Wautersia eutropha* H16 by transmission electron microscopy. J Bacteriol 187:3814–3824
14. Ishizaki A, Tanaka K, Taga N (2001) Microbial production of poly-D-3-hydroxybutyrate from CO_2. Appl Microbiol Biotechnol 57:6–12
15. Ishizaki A, Tanaka K (1990) Batch culture of *Alcaligenes eutrophus* ATCC 17697^T using recycled gas closed circuit culture system. J Ferment Bioeng 69:170–174
16. Ishizaki A, Tanaka K (1991) Production of poly-[beta]-hydroxybutyric acid from carbon dioxide by *Alcaligenes eutrophus* ATCC 17697^T. J Ferment Bioeng 70:254–257
17. Burgdorf T, Lenz O, Buhrke T, van der Linden E, Jones AK et al (2005) [NiFe]-hydrogenases of *Ralstonia eutropha* H16: modular enzymes for oxygen-tolerant biological hydrogen oxidation. J Mol Microbiol Biotechnol 10:181–196

18. Schink B, Schlegel HG (1979) The membrane-bound hydrogenase of *Alcaligenes eutrophus*: I. Solubilization, purification, and biochemical properties. Biochim Biophys Acta 567:315–324
19. Schneider K, Schlegel HG (1976) Purification and properties of soluble hydrogenase from *Alcaligenes eutrophus* H16. Biochim Biophys Acta 452:66–80
20. Hogrefe C, Romermann D, Friedrich B (1984) *Alcaligenes eutrophus* hydrogenase genes (Hox). J Bacteriol 158:43–48
21. Vignais PM, Colbeau A (2004) Molecular biology of microbial hydrogenases. Curr Issues Mol Biol 6:159–188
22. Schwartz E, Gerischer U, Friedrich B (1998) Transcriptional regulation of *Alcaligenes eutrophus* hydrogenase genes. J Bacteriol 180:3197–3204
23. York GM, Junker BH, Stubbe JA, Sinskey AJ (2001) Accumulation of the PhaP phasin of *Ralstonia eutropha* is dependent on production of polyhydroxybutyrate in cells. J Bacteriol 183:4217–4226
24. Moroney JV, Ma Y, Frey WD, Fusilier KA, Pham TT et al (2011) The carbonic anhydrase isoforms of *Chlamydomonas reinhardtii*: intracellular location, expression, and physiological roles. Photosynth Res 109(1–3):133–149
25. Lindskog S (1997) Structure and mechanism of carbonic anhydrase. Pharmacol Ther 74:1–20
26. Smith KS, Ferry JG (2000) Prokaryotic carbonic anhydrases. FEMS Microbiol Rev 24:335–366
27. Schwartz E, Voigt B, Zuhlke D, Pohlmann A, Lenz O et al (2009) A proteomic view of the facultatively chemolithoautotrophic lifestyle of *Ralstonia eutropha* H16. Proteomics 9:5132–5142
28. McCourt JA, Duggleby RG (2006) Acetohydroxyacid synthase and its role in the biosynthetic pathway for branched-chain amino acids. Amino Acids 31:173–210
29. Jendrossek D, Kruger N, Steinbuchel A (1990) Characterization of alcohol dehydrogenase genes of derepressible wild-type *Alcaligenes eutrophus* H16 and constitutive mutants. J Bacteriol 172:4844–4851
30. Steinbuchel A, Fruend C, Jendrossek D, Schlegel HG (1987) Isolation of mutants of *Alcaligenes eutrophus* unable to derepress the fermentative alcohol dehydrogenase. Arch Microbiol 148:178–186
31. Steinbuchel A, Schlegel HG (1984) A multifunctional fermentative alcohol dehydrogenase from the strict aerobe *Alcaligenes eutrophus*: purification and properties. Eur J Biochem 141:555–564
32. Jarboe LR (2011) YqhD: a broad-substrate range aldehyde reductase with various applications in production of biorenewable fuels and chemicals. Appl Microbiol Biotechnol 89:249–257
33. Atsumi S, Wu TY, Eckl EM, Hawkins SD, Buelter T et al (2010) Engineering the isobutanol biosynthetic pathway in *Escherichia coli* by comparison of three aldehyde reductase/alcohol dehydrogenase genes. Appl Microbiol Biotechnol 85:651–657
34. Steinbuchel A, Hustede E, Liebergesell M, Pieper U, Timm A et al (1992) Molecular basis for biosynthesis and accumulation of polyhydroxyalkanoic acids in bacteria. FEMS Microbiol Rev 9:217–230
35. Steinbuchel A, Schlegel HG (1989) Excretion of pyruvate by mutants of *Alcaligenes eutrophus*, which are impaired in the accumulation of poly(beta-hydroxybutyric acid) (PHB), under conditions permitting synthesis of PHB. Appl Microbiol Biotechnol 31:168–175
36. Lenz O, Ludwig M, Schubert T, Burstel I, Ganskow S et al (2010) H_2 conversion in the presence of O_2 as performed by the membrane-bound [NiFe]-hydrogenase of *Ralstonia eutropha*. Chemphyschem 11:1107–1119
37. Bernhard M, Benelli B, Hochkoeppler A, Zannoni D, Friedrich B (1997) Functional and structural role of the cytochrome b subunit of the membrane-bound hydrogenase complex of *Alcaligenes eutrophus* H16. Eur J Biochem 248:179–186

38. Goris T, Wait AF, Saggu M, Fritsch J, Heidary N et al (2011) A unique iron-sulfur cluster is crucial for oxygen tolerance of a [NiFe]-hydrogenase. Nat Chem Biol 7:310–318
39. Burgdorf T, van der Linden E, Bernhard M, Yin QY, Back JW et al (2005) The soluble NAD+-Reducing [NiFe]-hydrogenase from *Ralstonia eutropha* H16 consists of six subunits and can be specifically activated by NADPH. J Bacteriol 187:3122–3132
40. Happe RP, Roseboom W, Egert G, Friedrich CG, Massanz C et al (2000) Unusual FTIR and EPR properties of the H_2-activating site of the cytoplasmic NAD-reducing hydrogenase from *Ralstonia eutropha*. FEBS Lett 466:259–263
41. Van der Linden E, Burgdorf T, Bernhard M, Bleijlevens B, Friedrich B et al (2004) The soluble [NiFe]-hydrogenase from *Ralstonia eutropha* contains four cyanides in its active site, one of which is responsible for the insensitivity towards oxygen. J Biol Inorg Chem 9:616–626
42. Horch M, Lauterbach L, Saggu M, Hildebrandt P, Lendzian F et al (2010) Probing the active site of an O_2-tolerant NAD+-reducing [NiFe]-hydrogenase from *Ralstonia eutropha* H16 by in situ EPR and FTIR spectroscopy. Angew Chem Int Ed Engl 49:8026–8029
43. Badger MR, Price GD (1994) The role of carbonic anhydrase in photosynthesis. Annu Rev Plant Physiol Plant Mol Biol 45:369–392
44. Xu Y, Feng L, Jeffrey PD, Shi Y, Morel FM (2008) Structure and metal exchange in the cadmium carbonic anhydrase of marine diatoms. Nature 452:56–61
45. Tripp BC, Smith K, Ferry JG (2001) Carbonic anhydrase: new insights for an ancient enzyme. J Biol Chem 276:48615–48618
46. Elleuche S, Poeggeler S (2010) Carbonic anhydrases in fungi. Microbiology 156:23–29
47. Rowlett RS (2010) Structure and catalytic mechanism of the beta-carbonic anhydrases. Biochim Biophys Acta 1804:362–373
48. Kusian B, Sultemeyer D, Bowien B (2002) Carbonic anhydrase is essential for growth of *Ralstonia eutropha* at ambient CO(2) concentrations. J Bacteriol 184:5018–5026
49. Ferry JG (2010) The gamma class of carbonic anhydrases. Biochim Biophys Acta 1804:374–381
50. Cannon GC, Heinhorst S, Kerfeld CA (2010) Carboxysomal carbonic anhydrases: structure and role in microbial CO_2 fixation. Biochim Biophys Acta 1804:382–392
51. Kerfeld CA, Heinhorst S, Cannon GC (2010) Bacterial microcompartments. Annu Rev Microbiol 64:391–408
52. Kusian B, Bowien B (1995) Operator binding of the CbbR protein, which activates the duplicate cbb CO_2 assimilation operons of *Alcaligenes eutrophus*. J Bacteriol 177:6568–6574
53. Schaferjohann J, Yoo JG, Bowien B (1995) Analysis of the genes forming the distal parts of the two cbb CO_2 fixation operons from *Alcaligenes eutrophus*. Arch Microbiol 163:291–299
54. Kusian B, Bednarski R, Husemann M, Bowien B (1995) Characterization of the duplicate ribulose-1,5-bisphosphate carboxylase genes and cbb promoters of *Alcaligenes eutrophus*. J Bacteriol 177:4442–4450
55. Windhovel U, Bowien B (1990) On the operon structure of the cfx gene clusters in *Alcaligenes eutrophus*. Arch Microbiol 154:85–91
56. Bowien B, Kusian B (2002) Genetics and control of CO(2) assimilation in the chemoautotroph *Ralstonia eutropha*. Arch Microbiol 178:85–93
57. Kusian B, Bowien B (1997) Organization and regulation of cbb CO_2 assimilation genes in autotrophic bacteria. FEMS Microbiol Rev 21:135–155
58. Kohlmann Y, Pohlmann A, Otto A, Becher D, Cramm R et al (2011) Analyses of soluble and membrane proteomes of *Ralstonia eutropha* H16 reveal major changes in the protein complement in adaptation to lithoautotrophy. J Proteome Res 10(6):2767–2776
59. Jeffke T, Gropp NH, Kaiser C, Grzeszik C, Kusian B et al (1999) Mutational analysis of the cbb operon (CO_2 assimilation) promoter of *Ralstonia eutropha*. J Bacteriol 181:4374–4380
60. Grzeszik C, Jeffke T, Schaferjohann J, Kusian B, Bowien B (2000) Phosphoenolpyruvate is a signal metabolite in transcriptional control of the cbb CO_2 fixation operons in *Ralstonia eutropha*. J Mol Microbiol Biotechnol 2:311–320

61. Schaferjohann J, Bednarski R, Bowien B (1996) Regulation of CO_2 assimilation in *Ralstonia eutropha*: premature transcription termination within the cbb operon. J Bacteriol 178:6714–6719
62. Liu C, Young AL, Starling-Windhof A, Bracher A, Saschenbrecker S et al (2010) Coupled chaperone action in folding and assembly of hexadecameric Rubisco. Nature 463:197–202
63. Neuwald AF, Aravind L, Spouge JL, Koonin EV (1999) AAA+: a class of chaperone-like ATPases associated with the assembly, operation, and disassembly of protein complexes. Genome Res 9:27–43
64. Hansen S, Vollan VB, Hough E, Andersen K (1999) The crystal structure of rubisco from *Alcaligenes eutrophus* reveals a novel central eight-stranded beta-barrel formed by beta-strands from four subunits. J Mol Biol 288:609–621
65. Gubernator B, Bartoszewski R, Kroliczewski J, Wildner G, Szczepanik A (2008) Ribulose-1,5-bisphosphate carboxylase/oxygenase from thermophilic cyanobacterium *Thermosynechocystis elongatus*. Photosynth Res 95:101–109
66. Spreitzer RJ, Salvucci ME (2002) Rubisco: structure, regulatory interactions, and possibilities for a better enzyme. Annu Rev Plant Biol 53:449–475
67. Tabita FR (1999) Microbial ribulose 1,5-bisphosphate carboxylase/oxygenase: a different perspective. Photosynth Res 60:1–28
68. Peterhansel C, Niessen M, Kebeish RM (2008) Metabolic engineering towards the enhancement of photosynthesis. Photochem Photobiol 84:1317–1323
69. Hansen S, Hough E, Andersen K (1999) Purification, crystallization and preliminary X-ray studies of two isoforms of Rubisco from *Alcaligenes eutrophus*. Acta Crystallogr D Biol Crystallogr 55:310–313
70. Vyazmensky M, Zherdev Y, Slutzker A, Belenky I, Kryukov O et al (2009) Interactions between large and small subunits of different acetohydroxyacid synthase isozymes of *Escherichia coli*. Biochemistry 48:8731–8737
71. Chipman D, Barak Z, Schloss JV (1998) Biosynthesis of 2-aceto-2-hydroxy acids: acetolactate synthases and acetohydroxyacid synthases. Biochim Biophys Acta 1385:401–419
72. Mendel S, Elkayam T, Sella C, Vinogradov V, Vyazmensky M et al (2001) Acetohydroxyacid synthase: a proposed structure for regulatory subunits supported by evidence from mutagenesis. J Mol Biol 307:465–477
73. Mendel S, Vinogradov M, Vyazmensky M, Chipman DM, Barak Z (2003) The N-terminal domain of the regulatory subunit is sufficient for complete activation of acetohydroxyacid synthase III from *Escherichia coli*. J Mol Biol 325:275–284
74. Steinmetz A, Vyazmensky M, Meyer D, Barak ZE, Golbik R et al (2010) Valine 375 and phenylalanine 109 confer affinity and specificity for pyruvate as donor substrate in acetohydroxy acid synthase isozyme II from *Escherichia coli*. Biochemistry 49:5188–5199
75. de la Plaza M, Fernandez de Palencia P, Pelaez C, Requena T (2004) Biochemical and molecular characterization of alpha-ketoisovalerate decarboxylase, an enzyme involved in the formation of aldehydes from amino acids by *Lactococcus lactis*. FEMS Microbiol Lett 238:367–374
76. Sulzenbacher G, Alvarez K, Van Den Heuvel RH, Versluis C, Spinelli S et al (2004) Crystal structure of *E. coli* alcohol dehydrogenase YqhD: evidence of a covalently modified NADP coenzyme. J Mol Biol 342:489–502
77. Nair RV, Bennett GN, Papoutsakis ET (1994) Molecular characterization of an aldehyde/alcohol dehydrogenase gene from *Clostridium acetobutylicum* ATCC 824. J Bacteriol 176:871–885
78. Fontaine L, Meynial-Salles I, Girbal L, Yang X, Croux C et al (2002) Molecular characterization and transcriptional analysis of *adhE2*, the gene encoding the NADH-dependent aldehyde/alcohol dehydrogenase responsible for butanol production in alcohologenic cultures of *Clostridium acetobutylicum* ATCC 824. J Bacteriol 184:821–830
79. Dawes EA, Senior PJ (1973) The role and regulation of energy reserve polymers in microorganisms. Adv Microb Physiol 10:135–266

80. Schubert P, Steinbuchel A, Schlegel HG (1988) Cloning of the *Alcaligenes eutrophus* genes for synthesis of poly-beta-hydroxybutyric acid (PHB) and synthesis of PHB in *Escherichia coli*. J Bacteriol 170:5837–5847
81. Sauer U, Canonaco F, Heri S, Perrenoud A, Fischer E (2004) The soluble and membrane-bound transhydrogenases UdhA and PntAB have divergent functions in NADPH metabolism of *Escherichia coli*. J Biol Chem 279:6613–6619
82. Sanchez AM, Andrews J, Hussein I, Bennett GN, San KY (2006) Effect of overexpression of a soluble pyridine nucleotide transhydrogenase (UdhA) on the production of poly(3-hydroxybutyrate) in *Escherichia coli*. Biotechnol Prog 22:420–425
83. Boonstra B, Rathbone DA, French CE, Walker EH, Bruce NC (2000) Cofactor regeneration by a soluble pyridine nucleotide transhydrogenase for biological production of hydromorphone. Appl Environ Microbiol 66:5161–5166
84. Moreira dos Santos M, Raghevendran V, Kotter P, Olsson L, Nielsen J (2004) Manipulation of malic enzyme in *Saccharomyces cerevisiae* for increasing NADPH production capacity aerobically in different cellular compartments. Metab Eng 6:352–363
85. Sauer U, Eikmanns BJ (2005) The PEP-pyruvate-oxaloacetate node as the switch point for carbon flux distribution in bacteria. FEMS Microbiol Rev 29:765–794
86. Ogata H, Goto S, Fujibuchi W, Kanehisa M (1998) Computation with the KEGG pathway database. Biosystems 47:119–128
87. Boccazzi P, Zanzotto A, Szita N, Bhattacharya S, Jensen KF et al (2005) Gene expression analysis of *Escherichia coli* grown in miniaturized bioreactor platforms for high-throughput analysis of growth and genomic data. Appl Microbiol Biotechnol 68:518–532
88. Lee HL, Boccazzi P, Ram RJ, Sinskey AJ (2006) Microbioreactor arrays with integrated mixers and fluid injectors for high-throughput experimentation with pH and dissolved oxygen control. Lab Chip 6:1229–1235
89. Zanzotto A, Szita N, Boccazzi P, Lessard P, Sinskey AJ et al (2004) Membrane-aerated microbioreactor for high-throughput bioprocessing. Biotechnol Bioeng 87:243–254
90. Zhang Z, Szita N, Boccazzi P, Sinskey AJ, Jensen KF (2006) A well-mixed, polymer-based microbioreactor with integrated optical measurements. Biotechnol Bioeng 93:286–296
91. Kichise T, Fukui T, Yoshida Y, Doi Y (1999) Biosynthesis of polyhydroxyalkanoates (PHA) by recombinant *Ralstonia eutropha* and effects of PHA synthase activity on in vivo PHA biosynthesis. Int J Biol Macromol 25:69–77
92. Nielsen L, Larsson M, Holst O, Mattiasson B (1988) Adsorbents for extractive bioconversion applied to the acetone-butanol fermentation. Appl Microbiol Biotechnol 28:335–339
93. Qureshi N, Hughes S, Maddox IS, Cotta MA (2005) Energy-efficient recovery of butanol from model solutions and fermentation broth by adsorption. Bioprocess Biosyst Eng 27:215–222
94. Yang XP, Tsai GJ, Tsao GT (1994) Enhancement of *in situ* adsorption on the acetone-butanol fermentation by *Clostridium acetobutylicum*. Sep Technol 4:1818–1824
95. Nielsen DR, Prather KJ (2009) In situ product recovery of n-butanol using polymeric resins. Biotechnol Bioeng 102:811–821
96. Garrett H, Grisham R, Grisham C (eds) (2008) Biochemistry, 4th edn. Cangage Learning, Boston
97. Kovach ME, Elzer PH, Hill DS, Robertson GT, Farris MA et al (1995) Four new derivatives of the broad-host-range cloning vector pBBR1MCS, carrying different antibiotic-resistance cassettes. Gene 166:175–176
98. York GM, Lupberger J, Tian J, Lawrence AG, Stubbe J et al (2003) *Ralstonia eutropha* H16 encodes two and possibly three intracellular poly[D-(-)-3-hydroxybutyrate] depolymerase genes. J Bacteriol 185:3788–3794
99. Peoples OP, Sinskey AJ (1989) Poly-beta-hydroxybutyrate (PHB) biosynthesis in *Alcaligenes eutrophus* H16. Identification and characterization of the PHB polymerase gene (*phbC*). J Biol Chem 264:15298–15303
100. Gere DR, Tengrove R (1999) Fast gas chromatographic separation and detection of blood alcohol compounds for forensic methods. Agilent Technologies, Wilmington

Chapter 40
Microbial ElectroCatalytic (MEC) Biofuel Production

Steven W. Singer, Harry R. Beller, Swapnil Chhabra, Christopher J. Chang, and Jerry Adler

Abstract We are developing an integrated Microbial-ElectroCatalytic (MEC) system consisting of *Ralstonia eutropha* as a chemolithoautotrophic host for metabolic engineering coupled to a small-molecule electrocatalyst for the production of biofuels from CO_2 and H_2. *R. eutropha* is an aerobic bacterium that grows with CO_2 as the carbon source and H_2 as electron donor while producing copious amounts of polyhydroxybutyrate. Metabolic flux from existing *R. eutropha* pathways is being diverted into engineered pathways that produce biofuels. Novel molybdenum electrocatalysts that can convert water to hydrogen in neutral aqueous media will act as chemical mediators to generate H_2 from electrodes in the presence of engineered strains of *R. eutropha*. To increase the local concentration of H_2, we are engineering *R. eutropha*'s outer-membrane proteins to tether the electrocatalysts to the bacterial surface. The integrated MEC system will provide a transformational new source of renewable liquid transportation fuels that extends beyond biomass-derived substrates.

S.W. Singer (✉)
Earth Sciences Division, Lawrence Berkeley National Laboratory, Berkeley, CA 94720, USA
e-mail: swsinger@lbl.gov

H.R. Beller
Earth Sciences Division, Lawrence Berkeley National Laboratory, Berkeley, CA 94720, USA

S. Chhabra
Physical Biosciences Division, Lawrence Berkeley National Laboratory, Berkeley, CA 94720, USA

C.J. Chang
Department of Chemistry, University of California-Berkeley, Berkeley, CA 94720, USA

J. Adler
Logos Technologies, Arlington, VA 22203, USA

J.W. Lee (ed.), *Advanced Biofuels and Bioproducts*, DOI 10.1007/978-1-4614-3348-4_40, 1091

1 Introduction

Liquid transportation fuels are a critical component of the energy infrastructure of the United States. New sources of liquid fuels are required to replace petroleum-derived fuels because current supplies of petroleum are unstable and CO_2 produced by combustion of liquid transportation fuels is a significant contributor to greenhouse gas emissions. Currently, there is significant interest in transforming lignocellulosic biomass into liquid transportation fuels through hydrolysis of the biomass to monomeric sugars and fermentation to fuels, providing a carbon-neutral, renewable source of liquid fuel [20]. However, problems associated with generating engineered crops, efficient use of arable land, development of cost-effective pretreatment processes, and the cost of deconstructing enzymes still remain largely unsolved [24]. An elegant alternative to the production of cellulosic biofuels would be to transform CO_2 directly into liquid fuels, mitigating CO_2 emissions and creating a biofuel production process with the potential to be carbon-neutral [7]. Autotrophic microorganisms have evolved multiple pathways to utilize ubiquitous natural reductants to reduce CO_2 [23]. Diverting these pathways to produce liquid fuels is an intriguing opportunity to develop fuels to replace petroleum-based fossil fuels. Algal and cyanobacterial species have significant potential for generating biofuels, however these organisms absorb light inefficiently and are expensive to culture at industrial scale [17]. Chemoautotrophic organisms that use inorganic reductants ([S^{2-}, Fe(II), H_2]) or electricity have the possibility to overcome these limitations, as they may be able to reduce CO_2 more efficiently, are not dependent on available light, and may be adapted readily to industrial conditions [7]. However, these chemoautotrophic organisms, which are often isolated from extreme environments, tend to grow to low cell densities and are very difficult to manipulate genetically.

One class of chemoautotrophic bacteria, "Knallgas" bacteria that grow with H_2/CO_2 under aerobic conditions, does not have these limitations. The model species of this class, *Ralstonia eutropha*, can grow to very high cell densities (>200 g/L) and has been extensively manipulated genetically [16]. Under nutrient limitation, *R. eutropha* directs most of the reduced carbon flux generated by the Calvin cycle to synthesis of polyhydroxybutyrate (PHB), a biopolymeric compound stored in granules. Under growth with H_2/CO_2, 61 g/L of PHB was formed in 40 h, which represents ~70% of total cell weight [10]. PHB and related polyhydroxyalkonate polymers have been produced at industrial scale and marketed as Biopol™ (Monsanto) and Mircel™ (Metabolix) [16].

The PHB synthesis pathway in *R. eutropha* involves three genes expressed as an operon (Fig. 1) [15]. The gene products of this operon are PhaA, a β-ketothiolase, PhaB, an acetoacetyl-CoA reductase, and PhaC, the PHB synthase (Fig. 1). Numerous mutants have been generated that are impaired in PHB synthesis and these mutagenesis studies have demonstrated that PHB synthesis can be blocked with minimal effects on cellular function [19, 22]. An *R. eutropha* strain generated by chemical mutagenesis that is impaired in PHB synthesis has been shown to secrete large amounts of pyruvate into the medium under autotrophic conditions,

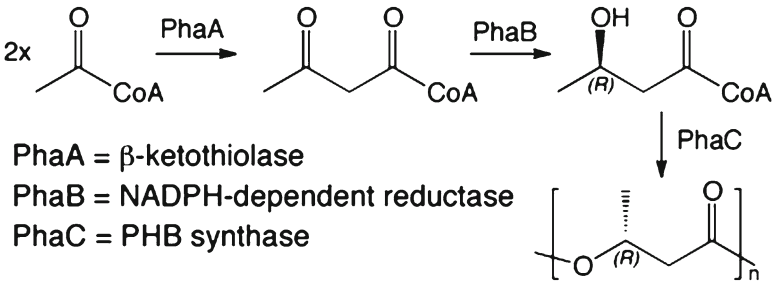

Fig. 1 Polyhydroxybutyrate (PHB) synthesis pathway in *Ralstonia eutropha*

suggesting that the mutant maintains a similar magnitude of carbon flux in the absence of PHB synthesis [4]. Metabolic engineering strategies have been successfully employed to increase carbon flux through the PHB pathway, suggesting that *R. eutropha* will be a suitable host for synthetic biology applications [5, 13].

Current efforts to produce biofuels using synthetic biology have focused on using model organisms (*Escherichia coli* and *Saccharomyces cerevisiae*) as hosts for metabolic engineering [3, 6]. These efforts have concentrated on using biomass-derived carbohydrates as the sources for renewable biofuel generation [12]. These strategies require redirection of central metabolic pathways by introduction of new pathways that redirect metabolic flux to a desired end-product. This approach has been used to produce alcohols, alkenes, and isoprenoids that may be used as liquid fuel substitutes for petroleum products [8]. Rewiring the metabolism of these model organisms so that they can utilize CO_2 as the carbon input for biofuel production would have substantial benefits in broadening the substrate scope for metabolic engineering and reducing CO_2 emissions. *R. eutropha* is an attractive host for biofuel production from CO_2 as it already has the capability for autotrophic growth, is amenable to metabolic engineering, and expresses a metabolic pathway that supports significant carbon flux.

An inexpensive source of H_2 will be essential for the effective development of *R. eutropha* as a biofuel-producing platform. For fuel production to be sensible, the method of H_2 generation must utilize methods that do not themselves consume fossil-derived energy, or draw low-carbon energy away from carbon mitigating uses. Known small-molecule metal catalysts generally require organic acids, additives, and/or solvents that are also incompatible for use with living organisms [9]. Molybdenum polypyridyl complexes (MoPy5) have been shown to be excellent catalysts for the electrochemical reduction H^+ in neutral water at rates that approach to that of hydrogenase enzymes (Fig. 2) [11]. These electrocatalysts are stable and evolve H_2 in seawater and are compatible with microbial growth media. *R. eutropha* is an ideal microbe to couple with electrocatalysis, as growth with H_2 generated in situ by an electrode has already been demonstrated [18]. Electrocatalysis will be coupled in two ways: the MoPy5 catalyst will be tethered to the electrode surface and H_2 generated at the surface will be used for chemoautotrophic growth and

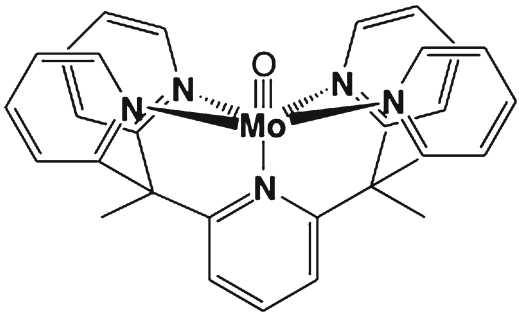

Fig. 2 Molybdenum polypyridyl-oxo catalyst for electrochemical generation of H_2 in the presence of *R. eutropha*

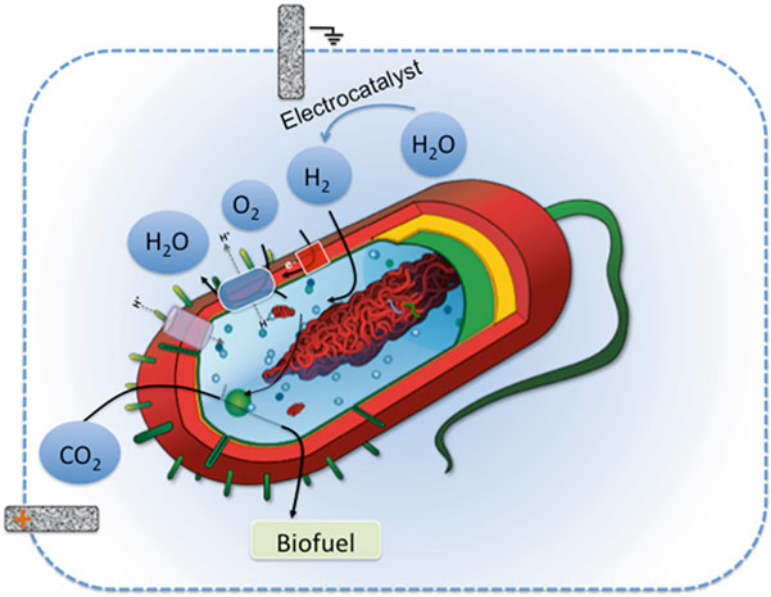

Fig. 3 Conversion of electricity and CO_2 to biofuels in a Microbial-ElectroCatalytic system with *R. eutropha* as microbial host

biofuel production by engineered strains of *R. eutropha*. In the second configuration, MoPy5 catalysts will be tethered directly to the surface of engineered *R. eutropha* strains and the strains will interact directly with the electrode surface. In this configuration, the tethered catalyst will generate H_2 at the electrode, which will be used by engineered *R. eutropha* strains for growth and biofuel production.

The integrated MEC (Microbial-ElectroCatalytic) system, the combination of a novel catalytic system to generate H_2 directly from water coupled to a chemolithoautotroph, *R. eutropha*, that is metabolically engineered to produce high titers of biofuels from H_2 and CO_2, will be a novel technology that will provide a new source of renewable liquid transportation fuels that extends beyond biomass-derived substrates (Fig. 3).

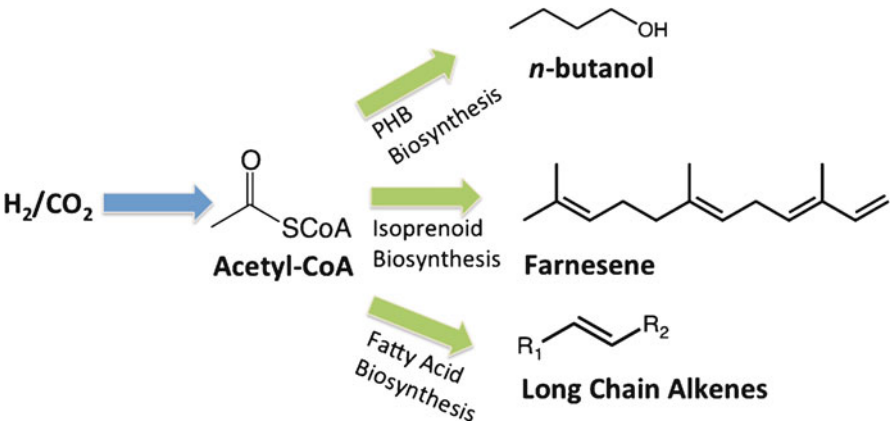

Fig. 4 Pathways for the production of biofuels in engineered strains of *R. eutropha*

2 Experimental Approach

2.1 Strain Selection and Genetic Engineering

The strain that is being used for metabolic engineering is *R. eutropha* H16 (currently classified as *Cuparividus necator*), which is a facultative chemolithoautotroph that has been extensively studied for both PHB production and chemolithoautotrophic metabolism [16]. The genome of *R. eutropha* H16 has been sequenced, demonstrating that it consists of three circular replicons: two chromosomes (4.0 and 2.9 MB) and a megaplasmid (0.45 MB), termed pHG1 [15]. *R. eutropha* H16 is capable of growing either heterotrophically on reduced carbon substrates under aerobic conditions or growing autotrophically under an atmosphere of $H_2/CO_2/O_2$.

A critical element in the success of this project will be the development of genetic tools for metabolic engineering of *R. eutropha*. Engineering of *R. eutropha* will entail successful implementation of the following elements: (1) heterologous DNA delivery; (2) compatible plasmid system for rapid construction and testing of heterologous pathways; (3) chromosomal manipulation comprising insertions and knockouts, and (4) deployment of tunable parts such as promoters, ribosomal binding sites, spacers, and terminators for precise control of heterologous genetic circuits. To ensure expression compatibility, we will perform in silico analyses of codon usage and transcript stability of all heterologous genes and parts described in this project and if necessary, commercially synthesize optimized sequences.

2.2 Biofuel Production in R. eutropha

We have chosen three potential biofuel molecules as targets for which we will metabolically engineer *R. eutropha* (Fig. 4). We have targeted three classes of biofuel

molecules: butanol, which will be derived from modifications to the PHB pathway; farnesene, which will be produced by introduction of a heterologous pathway to produce isoprenoids; and long-chain alkenes, which will be produced by modifying the fatty acid biosynthesis pathway and introducing genes for alkene biosynthesis. We have genetically modified wild-type *R. eutropha* to knock out the genes associated with the PHB biosynthesis pathway [15]. We are comparing biofuel production from plasmid-encoded heterologous pathways in the wild-type strain with production in the PHB$^-$ strains.

2.2.1 *n*-Butanol

n-Butanol has favorable properties as a gasoline blending agent and provides a valuable target to validate *R. eutropha* as a host for synthetic biology [14]. The PHB synthesis pathway in *R. eutropha* proceeds through 3-hydroxybutyryl-CoA, which is also an intermediate in the *n*-butanol synthesis pathway. Our strategy will be to divert the flux from 3-hydroxybutyryl-CoA to PHB and to redirect it to *n*-butanol. Recent work has demonstrated that high titers of *n*-butanol can be produced in *E. coli* by choosing heterologous genes judiciously and maximizing reducing equivalents available for *n*-butanol production [2]. Therefore, a detailed understanding of the expression of heterologous genes for *n*-butanol production in *R. eutropha* and the metabolic flux in *R. eutropha* PHB$^-$ mutants will be essential in achieving high titers of *n*-butanol.

Although *n*-butanol can be used directly as a gasoline replacement due to its higher energy content and lower water solubility and corrosivity relative to ethanol, it would only address short-haul ground transportation, since it could not be used to power aircraft or long-range rail and trucks. Dehydration of butanol to butylenes (C_4) and oligomerization affords C_8, C_{12} and C_{16} olefins with some disproportionation to non-oligomer C_9, C_{10}, C_{11}, C_{13}, C_{14}, and C_{15} olefins. These olefins can undergo double-bond isomerization, skeletal isomerization, cyclization and/or aromatization, forming isoalkenes, cycloalkenes, and/or aromatic products. Hydrogenation of this mixture may provide hydrocarbons suitable for use as jet fuels. We will transform the *n*-butanol obtained from H_2/CO_2 cultivation of engineered *R. eutropha* to these hydrocarbon mixtures and evaluate them as replacement for jet fuel. We are currently exploring novel catalysts for the dehydration and oligomerization of butanol to hydrocarbon mixtures that resemble jet fuel.

2.2.2 Alkenes

Aliphatic hydrocarbons are excellent biofuel targets, as they are already predominant components of petroleum-based gasoline and diesel fuels and would be compatible with existing engines and fuel distribution systems. Recently, genes for alkene biosynthesis (*oleABCD*) have been identified in multiple bacteria and the functions of these genes elucidated in in vivo and in vitro studies (e.g., [1]).

The OleABCD proteins catalyze the condensation of fatty acids to long-chain alkenes and this production is enhanced in *E. coli* by the overproduction of fatty acids. To produce long-chain alkenes in *R. eutropha*, fatty acid overproduction will be engineered into *R. eutropha* using techniques that have been used successfully in other proteobacteria [1, 21].

2.2.3 Farnesene

The isoprenoid pathway represents an important source of advanced biofuel precursors such as farnesene. Chemical hydrogenation of farnesene produces farnesane, which can serve as a diesel fuel. All terpenoids originate from the same universal precursors (isopentenyl pyrophosphate [IPP] and its isomer dimethylallyl pyrophosphate [DMAPP]), which can be generated through two known biosynthetic pathways—the mevalonate-dependent (MEV) isoprenoid pathway mostly found in eukaryotes and the deoxyxylulose 5-phosphate (DXP) pathway found in most prokaryotes. The *R. eutropha* genome encodes the DXP pathway, which generates the precursor molecules IPP and DMAPP demonstrated to be essential in prokaryotes for the prenylation of tRNAs and the synthesis of farnesyl pyrophosphate (FPP), which is used for quinone and cell wall biosynthesis [15]. While farnesene may be produced in *R. eutropha* through the manipulation of its native DXP pathway, the tight regulation of essential metabolites produced through this route may pose a significant challenge in achieving reasonable titers. For optimal production of isoprenoid-based fuel molecules, we therefore propose the incorporation of the MEV pathway, which we expect to be unregulated by this host. We will synthesize and express genes originating from distinct prokaryotic and eukaryotic sources to enable production of α-farnesene in the *R. eutropha* strains.

2.3 Optimization of Mo-Py5 Electrocatalyst

We are optimizing the chemical properties of soluble Mo-polypyridine electrocatalysts for water-to-hydrogen conversion to increase turnover frequency and stability in microbial growth media. We are also seeking improvements to minimize electrochemical overpotential for H_2 production. In particular, we are targeting the incorporation of electron-withdrawing groups at the axial and equatorial pyridine donors as well as methine bridges. Additionally, we are developing synthetic routes to more potential ligand frameworks where all the pyridines can be differentially functionalized. The overall goal is to move the reduction potentials of these complexes to more positive values, which may lead to a decrease in the overpotential for catalytic reduction of water to hydrogen. We are also testing conditions and electrode materials that will allow *R. eutropha* to grow autotrophically with H_2 generated in situ from electricity by the MoPy5 electrocatalyst.

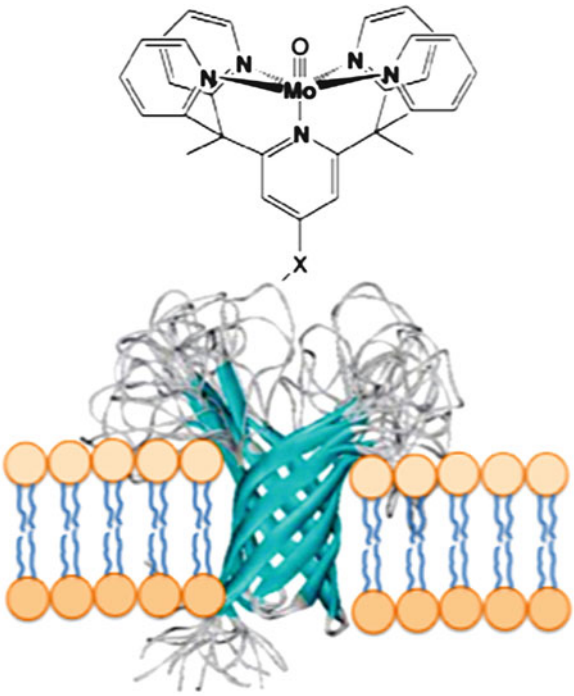

Fig. 5 Tethering of molybdenum polypyridyl-oxo catalyst to the surface of *R. eutropha* cells

As mentioned in the Introduction, we are pursuing two strategies to use these catalysts to generate H_2 electrochemically for autotrophic growth and biofuel production. These strategies involved tethering the electrocatalyst to the electrode surface and to the surface of *R. eutropha* by expressing heterologous proteins on the surface that will bind metal complexes (Fig. 5). These two strategies will be evaluated in comparison to standard methods for electrolysis of H_2O to generate H_2 and O_2 for *R. eutropha* growth.

Acknowledgments This work is funded by the ARPA-E Electrofuels program. We would also like to thank the Joint BioEnergy Institute (JBEI) for the use of its facilities and equipment; JBEI is supported by the Office of Science, Office of Biological and Environmental Research, of the U.S. Department of Energy. Work at Lawrence Berkeley National Laboratory is performed under the auspices of the U.S. Department of Energy through contract DE-AC02-05CH11231.

References

1. Beller HR, Goh EB, Keasling JD (2010) Genes involved in long-chain alkene biosynthesis in *Micrococcus luteus*. Appl Environ Microbiol 76:1212–1223
2. Bond-Watts BB, Bellerose RJ, Chang MC (2011) Enzyme mechanism as a kinetic control element for designing synthetic biofuel pathways. Nat Chem Biol 7:222–227

3. Clomburg JM, Gonzalez R (2010) Biofuel production in *Escherichia coli*: the role of metabolic engineering and synthetic biology. Appl Microbiol Biotechnol 86:419–434
4. Cook AM, Schlegel HG (1978) Metabolite concentrations in *Alcaligenes eutrophus* H-16 and a mutant defective in poly-beta-hydroxybutyrate synthesis. Arch Microbiol 119:231–235
5. Delamarre SC, Batt CA (2006) Comparative study of promoters for the production of polyhydroxyalkanoates in recombinant strains of *Wautersia eutropha*. Appl Microbiol Biotechnol 71:668–679
6. Dellomonaco C, Fava F, Gonzalez R (2010) The path to next generation biofuels: successes and challenges in the era of synthetic biology. Microb Cell Fact 9:3
7. Ferrer M, Golyshina O, Beloqui A et al (2007) Mining enzymes from extreme environments. Curr Opin Microbiol 10:207–214
8. Fortman JL, Chhabra S, Mukhopadhyay A et al (2008) Biofuel alternatives to ethanol: pumping the microbial well. Trends Biotechnol 26:375–381
9. Gloaguen F, Rauchfuss TB (2009) Small molecule mimics of hydrogenases: hydrides and redox. Chem Soc Rev 38:100–108
10. Ishizaki A, Tanaka K, Taga N (2001) Microbial production of poly-D-3-hydroxybutyrate from CO_2. Appl Microbiol Biotechnol 57:6–12
11. Karunadasa HI, Chang CJ, Long JR (2010) A molecular molybdenum-oxo catalyst for generating hydrogen from water. Nature 464:1329–1333
12. Keasling JD, Chou H (2008) Metabolic engineering delivers next-generation biofuels. Nat Biotechnol 26:298–299
13. Lee J-N, Shin H-D, Lee Y-H (2003) Metabolic engineering of pentose phosphate pathway in Ralstoniaeutropha for enhanced biosynthesis of poly-beta-hydroxybutyrate. Biotechnol Prog 19:1444–1449
14. Nielsen DR, Leonard E, Yoon SH et al (2009) Engineering alternative butanol production platforms in heterologous bacteria. Metab Eng 11:262–273
15. Pohlmann A, Fricke WF, Reinecke F et al (2006) Genome sequence of the bioplastic-producing "Knallgas" bacterium *Ralstonia eutropha* H16. Nat Biotechnol 24:1257–1262
16. Reinecke F, Steinbuchel A (2009) *Ralstonia eutropha* Strain H16 as Model Organism for PHA Metabolism and for Biotechnological Production of Technically Interesting Biopolymers. J Mol Microbiol Biotechnol 16:91–108
17. Rosenberg JN, Oyler GA, Wilkinson L et al (2008) A green light for engineered algae: redirecting metabolism to fuel a biotechnology revolution. Curr Opin Biotechnol 19:430–436
18. Schlegel HG, Lafferty R (1965) Growth of knallgas bacteria (*Hydrogenomonas*) using direct electrolysis of culture medium. Nature 205:308–309
19. Schubert P, Steinbuchel A, Schlegel HG (1988) Cloning of the *Alcailgenes eutrophus* genes for synthesis of ploy-beta-hydroxybutyric acid (PHB)and synthesis of PHB in *Eschericia coli*. J Bacteriol 170:5837–5847
20. Simmons BA, Loque D, Blanch HW (2008) Next-generation biomass feedstocks for biofuel production. Genome Biol 9(12):242
21. Steen EJ, Kang YS, Bokinsky G et al (2010) Microbial production of fatty-acid-derived fuels and chemicals from plant biomass. Nature 463:559–562
22. Steinbuchel A, Schlegel HG (1991) Physiology and molecular-genetics of poly(beta-hydroxyalkanoic acid) synthesis in *Alcaligenes eutrophus*. Mol Microbiol 5:535–542
23. Thauer RK (2007) Microbiology—a fifth pathway of carbon fixation. Science 318: 1732–1733
24. Tilman D, Socolow R, Foley JA et al (2009) Beneficial biofuels-the food, energy, and environment trilemma. Science 325:270–271

Index

J.W. Lee (ed.), *Advanced Biofuels and Bioproducts*, DOI 10.1007/978-1-4614-3348-4,